USMCA 2014

13th INTERNATIONAL SYMPOSIUM ON NEW TECHNOLOGIES FOR URBAN SAFETY OF MEGA CITIES IN ASIA

(SEIKEN SYMPSIUM 78)

ISBN4-903661-73-3

USMCA 2014
13th International Symposium
on New Technologies
for Urban Safety of Mega Cities in Asia
November 3-5, 2014
Organized by
Institute of Industrial Science, The University of Tokyo
Yangon Technological University

USMCA 2014

ICUS Report 2014-05 (serial No. 78)

the 13th International Symposium
on New Technologies
for Urban Safety of Mega Cities in Asia

November 3-5, 2014
at
Sedona hotel, Yangon, Myanmar
&
Yangon Technological University

Edited by
Eiko Yoshimoto

Organized by
Yangon Technological University (YTU)
Yangon, Myanmar
&
International Center for Urban Safety Engineering,
Institute of Industrial Science, The University of Tokyo, Japan

Sponsored by

Myanmar Engineering Society (MES), Myanmar
The Foundation for the Promotion of Industrial Science, Japan
Nippon Koei, Co., Ltd.
&
Suntac Technologies Co., Ltd.

Cooperated by

Embassy of Japan in Myanmar
Japan Society of Civil Engineers (JSCE), Japan
&
Japan International Cooperation Agency (JICA),
Myanmar Office

SYMPOSIUM ORGANISERS

CHAIRMAN and Co-CHAIRMAN
Khin Than Yu, Pro-Rector, Yangon Technological University (YTU), Myanmar
Kimiro Meguro, Director of ICUS, IIS, University of Tokyo (UTokyo), Japan

STEERING COMMITTEE
Aye Myint, Rector, YTU, Myanmar
Myint Thein, Pro-Rector, Mandalay Technological University (MTU), Myanmar
Win Khaing, President, Myanmar Engineering Society, Myanmar
Mehedi Ahmed Ansary, Bangladesh University of Engineering Technology (BUET), Bangladesh
Sudhir Misra, Indian Institute of Technology Kanpur, India
Taketo Uomoto, Chief Executive, Public Works Research Institute, Japan
Yoshiaki Nakano, Director General, IIS, UTokyo, Japan
Tsuneo Katayama, President, Real-time Earthquake Information Consortium, Japan
Wei Cheng Fan, Director, Center for Public Safety Research (CPSR), Tsinghua University, China
Worsak Kanok-Nukulchai, Rector, Asian Institute of Technology, Thailand
Yoshifumi Yasuoka, Auditor, Research Organization of Information and System, Japan

TECHNICAL COMMITTEE
Khin Than Yu, YTU, Myanmar
Nyan Myint Kyaw, YTU, Myanmar
Win Win Zin, YTU, Myanmar
Toe Toe Win, YTU, Myanmar
Myint Myint Khaing, MTU, Myanmar
Haruo Sawada, ICUS, IIS, UTokyo, Japan
Kiang Hwee Tan, National University of Singapore, Singapore
Pradeep Kumar Ramancharla, International Institute of Information Technology Hyderabad, India
Kimiro Meguro, ICUS, IIS, UTokyo, Japan
Mafizur Rahman, BUET, Bangladesh
Pennung Warnitchai, Asian Institute of Technology, Thailand
Somnuk Tangtermsirikul, Thammasat University, Thailand
Srikantha Herath, United Nations University, Japan
Taikan Oki, ICUS, IIS, UTokyo, Japan
Reiko Kuwano, ICUS, IIS, UTokyo, Japan

ORGANIZING COMMITTEE
Htay Win, Dept. of Civil Engineering, YTU, Myanmar
Cho Thin Kyi, Dept. of Civil Engineering, YTU, Myanmar
Kyaw Htun, Dept. of Engineering Geology, YTU, Myanmar
Nyein Thandar Ko, Dept. of Civil Engineering, YTU, Myanmar
Akiyuki Kawasaki, ICUS, IIS, UTokyo, Japan
Kohei Nagai, ICUS, IIS, UTokyo, Japan

SYMPOSIUM OFFICE
Yangon Technological University (YTU) &
International Center for Urban Safety Engineering (ICUS), Institute of Industrial Science (IIS),
The University of Tokyo (UTokyo)
Email: usmca@iis.u-tokyo.ac.jp

Contacts:
Eiko Yoshimoto, ICUS, IIS, the University of Tokyo, Japan
Nyein Thada Ko, Yangon Technological University, Myanmar

PREFACE

On behalf of the Organizing Institutes of the 13th International Symposium on New Technologies for Urban Safety of Mega Cites in Asia (USMCA2014), I express our sincere welcome to all symposium participants and distinguished keynote and plenary speakers.

In the Asia and Pacific-Rim regions, rapid economic development and population growth and concentration is fast accelerating the pace of urbanization. Unfortunately, the rapid expansion of infrastructure for urbanization is not adequately balanced with appropriate measures for their maintenance and management; thus, urban disasters have resulted. During the last few years, there were many big disasters in Asia and the Pacific-Rim regions, such as killer cyclones Sidr in Bangladesh (2007), Nargis in Myanmar (2008), and Aila in Bangladesh and India (2009), and Typhoon Ketsna (2009) and Yolanda (2013) in Philippines, flooding in Mongolia (2009), Pakistan (2010), Myanmar (2011) and Thailand (2011), the devastating earthquakes in Sichuan, China (2008), Sumatra (2009), Samoa (2009) and Tohoku, Japan (2011), and heat waves in Russia and Japan (2010). The number of fatalities and missing reported due to these disasters was well over 200,000. These unprecedented events show us the importance of urban safety.

The International Center for Urban Safety Engineering (ICUS) was established in 2001 at the Institute of Industrial Science (IIS), the University of Tokyo (UTokyo), with the objectives of carrying out advanced research on urban safety and implementing them towards the realization of safer cities, especially in Asia and the Pacific-Rim region, in the 21st century. For over a decade, ICUS has been actively tackling advanced researches, as well as the enhancement of networking, information collection and dissemination in order to fully realize ICUS's vision. As a part of ICUS activities, ICUS has been annually co-organizing USMCA since 2002 with its partners in the Asian region. In 2014, ICUS jointly organized the 13th USMCA in Yangon, Myanmar, with Yangon Technological University (YTU) to share their expertise, knowledge and experience in tackling the critical issues for safer cities in Asia and the Pacific-Rim region. It also provided an environment to create and reinforce collaborative networks among experts in the fields relevant to urban safety.

The symposium focused on disaster reduction, response and recovery; risk assessment; prediction and early-warning; decision-make support technologies; planning and development of urban infrastructure systems; life-cycle management of infrastructure systems; climate change mitigation and adaptation; and the application of geospatial technologies.

During the two-day symposium, 91 papers in eight parallel sessions were presented with seven keynote speeches and five plenary speeches. We also had research exhibitions in 13 booths by 11 organizations on the first day. The total number of participants was 190 from 10 countries, such as Myanmar, Japan, India, Vietnam, China, Mongolia, Sri Lanka, Singapore, Nepal, and Switzerland.

I would like to thank all the members of the Steering, Technical and Organizing Committees as well as the Symposium Secretariat for their hard work, time and effort in putting this symposium together. I would also like to thank all our sponsors for their generous support and contribution. Thanks are also due to those who have contributed towards making this symposium successful.

Kimiro MEGURO

Director of ICUS, IIS, UTokyo
(Co-Chairman of Organizing Committee, USMCA2014)

Copyright and Reprint Permission:

Photocopy of an article is permitted for authors and other researchers for their own reading and research. Abstracting and indexing of the papers are permitted but acknowledgement should be given to "The 13th International Symposium on New Technologies for Urban Safety of Mega Cities in Asia (USMCA2014)" and the authors of each specific paper. Written permission should be obtained from the publishers prior to any other type of reproduction.

Please contact:

International Center for Urban Safety Engineering (ICUS),
Institute of Industrial Science (IIS),
The University of Tokyo (UTokyo), Japan

Tel: +81-3-5452-6472
Fax: +81-3-5452-6476

2014 Program Overview

Time	***Sunday, 2 November***
17:30-19:30	*Welcome dinner at Sky Bistro*
21:00-22:00	*Registration at Sedona Hotel*

Time	***Monday, 3 November***	
07:45-08:30	*Registration (Sedona Hotel)*	
08:30-09:05	*Opening address (Mindon Room)* *WELCOME Speech (H.E. KoKo Oo, Ministry of Science and Technology)* *WELCOME Speech (Prof. Kimiro Meguro - Director of ICUS, The University of Tokyo)* *Opening Remark (H.E. Mr. Tateshi Higuchi, Ambassador of Japan to Myanmar)* *Opening Remarks (Rector of Yangon Technological University))* *Moderators: Mr. Akira Kodaka / Dr. Kaung Kyaw*	
09:05-09:35	*INTRODUCTION OF SATREPS* **Prof. Kimiro Meguro** **Prof. Khin Than Yu** *Development of a comprehensive disaster resilience and collaboration platform in Myanmar as a SATREPS (Science and Technology Research Partnership for Sustainable Development) Project* *Moderators: Mr. Akira Kodaka / Dr. Kaung Kyaw*	
09:35-10:15	*Group photo – Coffee break & Exhibitions*	
	Keynote and Plenary Speech (Mindon room)	
10:15-10:45	**Dr. Kyaw Latt** *Development Concepts of Yangon City and Major Challenges*	
10:45-11:15	**Prof. Hironori Kato** *What are critical issues of urban transportation in Yangon, Myanmar?*	
11:15-11:45	**Mr. Koji Yamada** *From the British Rangoon to a Yangon Today and a flourishing city of Yangon in 21st Century*	
11:45-12:00	**Mr. MasahikoTanaka** *Myanmar and JICA*	
12:00-12:15	**Mr. Suguru Ishiguro** *Introduction of an international cooperation program of Japan and developing countries*	
12:15-12:30	**Prof. Taikan Oki** *Lessons learnt from IMPAC-T, the First Flagship Project of SATREPS*	
12:30-12:45	**Prof. Haruo Sawada** *"Carbon Dynamics of Amazon Forest": Changes of approach brought the outcomes* *Moderators: Mr. Akira Kodaka / Dr. Kaung Kyaw*	
12:45-13:45	*Lunch at Sedona*	
	Room A	*Room B*
13:45-15:35	*Session 1 :* *Infrastructure Management 1* *Session Chairs:* *Dr. Nagai* *Dr. Nyan Myint Kyaw*	*Session 2 :* *Environmental Informatics & Urban flood: Addressing Emerging Risks* *Session Chairs: `* *Prof. Oki Daw Cho Cho Thin Kyi*
15:35-16:00	*Tea-break at Exhibition zone*	
16:00-17:30	*Session 3 :* *Infrastructure Management 2* *Session Chairs:* *Prof. Kuwano* *Dr.Toe Toe Win*	*Session 4 :* *Urban Safety & Disaster Mitigation 1* *Session Chairs:* *Dr. Numada* *Dr. Theingi Shwe*
18:30-20:00	*Symposium dinner at Sedona Hotel*	

Time	Tuesday, 4 November	
	1/2-5	Conference Room
09:20-11:00	Session 5 : Urban Safety & Disaster Mitigation 2 Session Chairs: Dr. Kato (T) Dr.Toe Toe Win	Session 6 Infrastructure Management 3 Session Chairs: Dr. Kawasaki U Htay Win
11:00-11:30	Tea-break at session area	
	1/2-5	Conference Room
11:30-13:10	Session 7 : Urban safety & Disaster Mitigation & Environmental Informatics Session Chairs: Prof. Tan Dr. Win WinZin	Session 8 : Infrastructure Management 4 Session Chairs: Dr. Nagai Dr. Nyan Myint Kyaw
13:10-14:30	Lunch at YTU	
	YTU Assembly hall	
	Keynote Speech (***)	
14:30-15:00	**Prof. Khin Ni Ni Thein** *Green Infrastructures: The Need of urban safety*	
15:00-15:30	**Mr. Tetsuro Ito** *A report of evaluation on improvement of Japanese government crisis management system on the Great East Japan Earthquake*	
15:30-16:00	**U Tin Myint** *Experience of Building Yangon City Fire Management System with GIS and GPS technologies"*	
16:00-16:30	**Prof. Taketo Uomoto** *Lessons we learn from unexpected natural hazards* Moderator: Mr. Akira Kodaka	
16:30-17:00	Closing ceremony (Assembly Hall) Young award ceremony Announcement of USMCA2015 YTU's closing speech ICUS's closing speech Moderator: Mr. Akira Kodaka / Dr. Kaung Kwaw	
18:00-	Farewell Party at Western Park by bus	

Time	Wednesday, 5 November
08:00-18:00	Excursion by bus

Contents

Keynote & Plenary Session

page

What are critical issues of urban transportation in Yangon, Myanmar? 1
Hironori KATO

The evaluation on improvement of Japanese government crisis management system on the 2011 Great East Japan Earthquake disaster 9
Tetsuro ITO

Lessons we learn from unexpected hazards 17
Taketo UOMOTO

Introduction of an international cooperation program of Japan and Developing Countries 29
Suguru ISHIGURO

Oral Sessions

TECHNICAL PROGRAMME –DAY1

PARALLEL SESSION 1: Infrastructure Management

Initiative on quality management system (QMS) for Myanmar construction company 31
Aye Mya CHO

Actual condition and trend of cavity occurrence under Japanese roads in recent years 39
Ryoko SERA, Yutaka KOIKE, Yasushi HIRONAKA Haruto NAKAMURA and Reiko KUWANO

Subsurface cavity beneath a buried sewer pipe supported by piles 49
Reiko KUWANO, Jiro KUWANO and Yikiko SAITO

Prevention of lateral movement and reinforcement of substructures on soft ground 59
Yukitake SHIOI

Optimal maintenance strategies based on BMS of a large urban expressway network in Japan 69
Yasuhito SAKAI

Case examples of surveys over architectural buildings and civil engineering structures by infrared thermography method 79
Noboru SATO

The current repair, reinforcement and seismic retrofit works of bridge for effective utilization of urban infrastructure 87
Hiroshi DOBASHI

PARALLEL SESSION 2: Environmental Informatics

A mathematical model for electric vehicle movement with respect to multiple charging-stops 97
Yudai HONMA

Travel demand forecasting for sustainable transport planning of Mandalay City 103
Khaing Zar THWIN and Kay Thwe TUN

Monitoring of land use/land cover changes in Mandalay City 105
Zin Mar LWIN, Myint Myint KHAING and Kyaw Zaya HTUN

Assessment of sedimentation and soil erosion effect on Inle Lake in mountainous region 107
Kyaw Zaya HTUN and Myint Myint KHAING

Mapping flood inundation in the Bago River Basin, Myanmar 109
Aung Myo KHAING, Akiyuki KAWASAKI and Win Win ZIN

Flood damage estimation sensitivity to spatial scale 111
Srikantha HERATH and Akinola KOMOLAFE

Numerical simulation of environmental disasters in the waterfront area under the impact of extreme events 127
Bin HE, Kyoji SASSA, Yi WANG and Srikantha HERATH

Development of flood inundation map for the Bago River Basin 129
Shelly WIN, Win Win ZIN, Akiyuki KAWASAKI and Tin MAUNG

Flood process and situation analysis in Myanmar for flood disaster preparation 137
Wang YI, Bin HE, and Srikantha HERATH

PARALLEL SESSION 3: Infrastructure Management 2

Influence of member shape on the relationship between surface defects and chloride permeability of surface concrete 139
Katsuya MITA and Yoshitaka KATO

Application of steel fiber reinforced concrete to reduce crack width of structures 149
Hoang Giang NGUYEN and Trung Hieu NGUYEN

Two-dimensional investigation on chloride ion penetration into cementitious material under freeze-thaw environment 159
Katsufumi HASHIMOTO, Hiroshi YOKOTA and Tomoyuki TANIGUCHI

Station design guidelines of Tokyo Metro for renovation 165
Masaru KUWANA, Kazuhisa KIDO, Naotsugu KOGA, Yoshihiko MUTOU, Keiji OOISHI and Shinji KONISHI

Development of asset management system -A case study tube wells of IIT Kanpur 177
Khushboo GUPTA, Onkar DIKSHIT and Sudhir MISRA

Shear failure behavior of high strength concrete beams with different shrinkage and strength development histories 185
Koji MATSUMOTO, Keisuke OSAKABE and Junichiro NIWA

Exposure test results for underground structures damaged by ASR 193
Tetsuya KOHNO, Toshiaki NAKAZAWA and Shoichi NAKATANI

Punching shear of RC elements with recycled glass as fine aggregates 199
Kiang Hwee TAN

PARALLEL SESSION 4: Urban Safety & Disaster Mitigation

History of the network plan and construction of Tokyo Metro 209
Hiroaki HASHIGUCHI and Shinsuke SHIRAKO

The transportation condition improvement to hospitals in Mandalay under seismic risks 217
Myint Myint KHAING, Hla Myo AUNG, Kyaw Zaya HTUN, Zin Mar LWIN and Takeshi KOIKE

Survey on the reach of flood evacuation information
- A case study in Nagoya City, Japan 227
Miho OHARA and Hisaya SAWANO

People with disabilities (PWD) and their functional needs during the Great East Japan Earthquake Disasters:
The results from 2013 Sendai grass-root assessment workshop of PWDs 235
Shigeo TATSUKI

International tourists as a vulnerable population during disaster events in Japan 243
Michael HENRY and Akiyuki KAWASAKI

Overview of recovery and impact of the fire accident on the metropolitan expressway 253
Shuichi YAMAGUCHI

Ten-year post-tsunami living conditions in southwestern coastal area resettlements of Sri Lanka after 2004 Indian Ocean Tsunami 263
Osamu MURAO

Expended energy based damage assessment of RC bare frame using nonlinear pushover analysis 269
Anthugari VIMALA and Ramancharla Pradeep Kumar

Analysis on disaster information dissemination process in a rural mountainous area, northeast Thailand -Comparison with heavy rain disaster in a rural mountainous area, Japan- 281
Shinya KONDO Akiyuki KAWASAKI, Miho OHARA, Akira KODAKA, Adisorn SANTHARARUK, and Kazuyoshi OTA

TECHNICAL PROGRAMME – DAY 2

PARALLEL SESSION 5: Urban Safety & Disaster Mitigation

Time delays causes in construction projects in Hanoi, Vietnam: Contractors' perspectives 291
Quoc Toan NGUYEN, Thi Hoai An LE and Bao Ngoc NGUYEN

Investigation on tendering and contracting practices of Myanmar building construction 301
Khin Su Su WAI and Aye Mya CHO

Development of mobile education system for supporting building damage assessment during large-scale earthquake disaster 311
Makoto FUJIU, Miho OHARA, Shoichiro NAKAMURA and Jyunichi TAKAYAMA

Strengthening and repairing of 5-storey RC ductile detailed structure with open ground storey 319
Swajit Singh GOUD and Pradeep Kumar RAMANCHARLA

Effect of soft storey in a structure present in higher seismic zone areas 327
Neelima V.S. PATNALA and Pradeep Kumar RAMANCHARLA

Experimental study on seismic retrofitting of masonry wall with special fiber reinforced paint 337
Kenjiro YAMAMOTO, Muneyoshi NUMADA and Kimiro MEGURO

Analysis of evacuation behavior from complex disaster based on stated preference data - Case study on Adachi-ku Senju district in Tokyo 345
Kazuyuki TAKADA, Makoto FUJIU and Takahiro KONNO

Issues and analysis of the Post-Yolanda shelter recovery process and role of international agencies 351
Tomoko MATSUSHITA

Performance evaluation of truss bridge under seismic loads 361
Nandar LWIN

Comparison of estimators of Gumbel Distribution for modelling maximum wind speed data 363
May Ei Nandar SOE and Daw Aye Aye THANT

PARALLEL SESSION 6: Infrastructure Management

Seismic behavior of traditional timber frames with through columns of townhouses in Japan 373
Hiromi SATO, Mikio KOSHIHARA and Tatsuya MIYAKE

Wind effect on structural responses of long-span suspension bridge 383
Ni Ni Moe KYAW and Kyaw Lin HTAT

Investigation on the wind effects of long-span cable - stayed bridge with H-shaped tower 395
Aye Nyein THU and San Yu KHAING

A statistical study for bi-directional seismic interaction effect in isolated bridges 407
Ji DANG, Yuki EBISAWA and Akira IGARASHI

A solution for stakeholder management in Vietnamese construction projects 417
Quan Ahn PHUNG

Evaluation of resistance of GRS coastal dikes against over-flowing tsunami current by model tests 425
Yudai AOYAGI, Kimihiro FUJII, Shouhei KAWABE, Yoshiaki KIKUCHI, Kenji WATANABE, Masatoshi IIJIMA and Fumio TATSUOKA

A study on applicability of dewatering method as a countermeasure for liquefaction 435
Yuki HORIUCHI, Toru SEKIGUCHI and Shoichi NAKAI

Evaluation of seismic performance for typical reinforced concrete buildings in downtown area of Yangon City 443
Nwe Ni MYINT

Study of atmospheric corrosion of steels in Yangon, urban location 453
Yu Yu Kyi WIN

PARALLEL SESSION 7:
Urban safety & Disaster Mitigation & Environmental Informatics

Estimation of runoff potential in Chindwin River basin using remote sensing and GIS 461
Kyu Kyu THIN and Win Win ZIN

Assessment of environmental flows requirment for the Upper Ayeyawaddy RiverBasin 471
Tin Mar LWIN , Khin Ni Ni THEIN, Win Win ZIN and Cho Cho Thin KYI

Forecasting flash flood over Daungnay ungagged watershed using GIS techniques and HEC-HMS model 481
Yin Yin HTWE and Aye Aye THANT

Climate change effects in central dry zone, Myanmar 483
Aye Myint KHAING and Win Win ZIN

Solid waste management in urban construction projects in Vietnam 493
Quan Toac NGUYEN, Mai Toac NGUYEN and Quan Ahn PHUNG

Introduction of Dye-sensitized solar cells and its application 501
Kazuteru NOMURA and Anders HAGFELDT

The integrated modelling approach for land-use change projection,
Case-study in Dak Lak, Vietnam 503
Anh Nguyet DANG and Akiyuki KAWASAKI

New mathematical model for maximizing profit of new low-cost carrier considering hub-spoke system 517
Ryosuke YABE and Yudai HONMA

Investigating socio-economic impacts of flood on the people affected by poverty:
Case study in Bago, Myanmar 525
Htoo Htoo SHWE and Akiyuki KAWASAKI

Role of news media from experiences of the 2011 Great East Japan earthquake 535
Muneyoshi NUMADA and Kimiro MEGURO

Effect of text message of mobile phone for disaster information dissemination to rural moutainous area in Thailand 545
Akira KODAKA, Akiyuki KAWASAKI, Miho OHARA and Shinya KONDO

PARALLEL SESSION 8: Infrastructure Management

Repair prioritization of reinforced concrete superstructures in mooring facilities 553
Takuho TANI, Hiroshi YOKOTA, Katsufumi HASHIMOTO and Kohichi FURUYA

An investigation on the influence of some parameters in simulation of chloride ion penetration in concrete based on truss network model 563
Punyawut JIRADILOK and Kohei NAGAI

The current practice of construction material reuse in Vietnam 573
Quan Toac NGUYEN and Ngoc B. NGUYEN

Effect of initial water content in mortar on water and moisture absorption of mortar 581
Toshiya CHIBA and Yoshitaka KATO

Influence of each seismic element on the dynamic behavior of traditional timber frames 591
Iuko TSUWA and Mikio KOSHIHARA

Effect of heterogeneity on the corrosion of rebar embedded in concrete 601
Nozomu SOMEYA and Yoshitaka KATO

Influence of magnesium ion and sulfate ion on Chloride Permeability of Concrete 609
Keigo HORI and Yoshitaka KATO

Progressive collapse analysis of reinforced concrete frame buildings 619
Su Wint YEE

Experimental study on ordinary portland cement concrete replacement by using pozzolanic materials 629
Zar Phyu TUN

Photograph

Symposium Banner

USMCA2014
13th International Symposium on New Technologies for Urban Safety of Mega Cities in Asia
November 3-5, 2014
Organized by
INSTITUTE OF INDUSTRIAL SCIENCE, THE UNIVERSITY OF TOKYO
YANGON TECHNOLOGICAL UNIVERSITY
Sponsored by
NIPPON KOEI
SUNTAC TECHNOLOGIES

At Sedona hotel on 3rd November

Reception desk at Sedona hotel

JEXWAY : Japan Expressway International Company Limited

Booths at Sedona Hotel

Public Works Research Institute,Japan
ICHARM

Public Works Research Institute, Japan

JEXWAY : Japan Expressway International Company Limited.

Japan Expressway International Company LTD., Japan

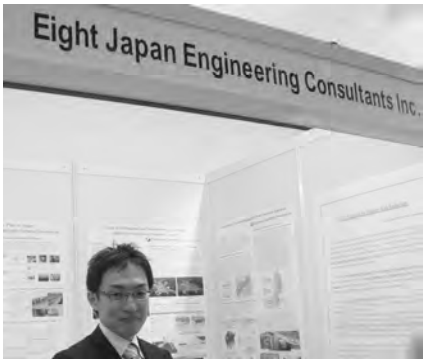
Eight Japan Engineering Consultants Inc.

Eight Japan Engineering Consultants Inc., Japan

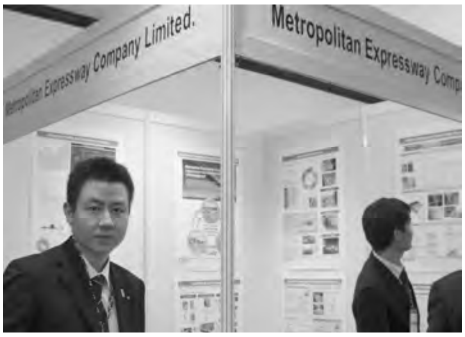
Metropolitan Expressway Company Limited.
Metropolitan Expressway Comp

Metropolitan Expressway Company LTD., Japan

TIS:The Socie cty for Thermographic Inspection of Structures

The Society for Thermographic Inspection of Structures, Japan

RC77 Research Committee for creation and promotion of new business for disasterreduction

RC77 Research Committee for creation and promotion of new business for disaster reduction, Japan

Tokyo Metro Co., Ltd., Japan

Japan Society of Civil Engineering, Jaspan

Yangon Technological University, Maynmar

International Center for Urban Safety Engineering, IIS, UTokyo, Japan

Exhibition area

Inauguration Ceremony

Welcome speech from the Ministry of Science and Technology, Mr. H.E. Dr. Ko Ko Oo

Mr. H.E. Dr. Ko Ko Oo
Ministry of Science and Technology, Myanmar

Participants of opening address

H.E. Mr. Tateshi Higuchi,
Ambassador of Japan to Myanmar

Prof. Khin Than Yu,
Pro-Rector, YTU, Myanmar

Prof. Kimiro Meguro,
Director, ICUS, IIS, Utokyo, Japan

Group photo of VIPs

Group photo at Sedona hotel on 3rd November

Key Note and Plenary Speakers

Dr. Kyaw Latt,
Advisor,
Yangon City Development Committee, Myanmar

Prof. Hironori Kato,
The University of Tokyo, Japan

Mr. Koji Yamada,
Chief Planner,
Nippon Koei Co., LTD., Japan

Mr. Masahiko Tanaka,
Chief Representative,
Japan International Cooperation Agency,
Myanmar Office, Myanmar

Mr. Suguru Ishiguro,
Manager,
Japan Science and Technology Agency, Japan

Prof. Taikan Oki,
ICUS, IIS, UTokyo, Japan

Dr. Haruo Sawada,
Visiting research Professor, Geoinformatics Center,
School of Engineering and Technology,
Asian Institute of Technology, Thailand

Prof. Kiang Hwee Tan,
Department of Civil and Environmental Engineering,
National University of Singapore, Singapore

Prof. Khin Ni Ni Thein,
Advisor,
National Water Resources Development
Committee, Myanmar

Visiting Prof. Tetsuro Ito,
ICUS, IIS, UTokyo, Japan

Mr. Tin Myint,
M.D., Suntac Technologies, Co., Ltd. Myanmar

Dr. Taketo Uomoto,
Chief Executive,
Public Works Research Institute, Japan

Second day at Yangon Technological University (YTU)

Symposium venue 2nd day (YTU main building)

Participants at 1/2-5 room

Participants at Conference room

Closing ceremony

Participants at Assembly Hall

Dr. Amod Mani Dxit,
Executive Director,
National Society for Earthquake Technology,
Nepal

USMCA2014
13th International Symposium
on New Technologies
for Urban Safety of Mega Cities in Asia
November 3.5,2014
Organized by
Institute of Industrial Science, The University of Tokyo
Yangon Technological University

Prof. Aye Myint,
Rector, YTU, Myanmar

Young-Researcher- Award recipients with Prof. Kuwano (left) and Prof. Meguro (right)
Awardees: Ms. Iuko Tsuwa, Mr. Yudai Aoyagi, Mr. Ryosuke Yabe, Ms. Su Wint Yee
and Ms. Tin Mar Lwin (from the second left to right)

Thank you presentation to YTU students

Group photo at YTU Assembly hall on 4th November

Press coverage by

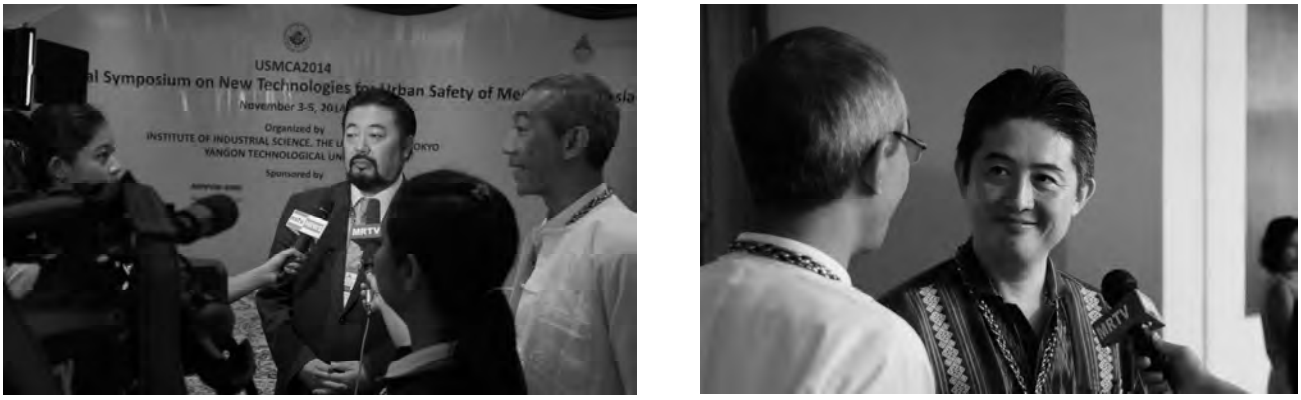

Interviews with Myanmar International TV channel

Lunch, break, banquet and farewell party

Lunch time at Sedona Hotel

Break time at Sedona Hotel

Lunch time at YTU

Dinner Reception
of
USMCA 20
10

Banquet party at Sedona hotel on 3rd November

Farewell party at Western Park on 4th November

Whole day tour Visit to Thilawa Port, Bogyoke Market, Yangon Heritage and Shwedagon Pagoda

Around Thilawa Port

Lecture from Mr. Takashi Yanai,
President and CEO of Myanmar Japan Thilawa Development Ltd.

Around Thilawa Port

Lecture from Myanmar International Terminal Thilawa staff

Group photo at Myanmar International Terminal Thilawa (MITT)

Sightseeing in Yangon City

Old port at Yangon City

Shwedagon Pagoda

Others

Myanmar
2nd November 2014
UT Alumni & USMCA
Welcome Party

Myanmar UT Alumni and USMCA2014 Welcome party at Sky Bistro on 2nd November

USMCA2014
13th International Symposium on New Technologies for Urban Safety of Mega Cities in Asia
November 3-5, 2014

ICUS staff members

Keynote& Plenary Session

What are critical issues of urban transportation in Yangon, Myanmar?

Hironori KATO[1]
[1]Dr. Eng, Department of Civil Engineering,
Graduate School of Engineering The University of Tokyo,
Japan
kato@civil.t.u-tokyo.ac.jp

ABSTRACT

This paper reported the latest traffic conditions and current problems in urban transportation of Yangon, Myanmar. The problems identified from the large-scale surveys including the Person Trip Survey are traffic congestion, long travel time, poor public transportation service, and mobility gap between high and low income individuals. The major reasons for those problems were also discussed. Although the unique transportation policies of motorcycle/bicycle ban and regulation of vehicle imports have contributed to a reduction in car usage in Yangon, their effective may be questionable in the future. An introduction of new BRT/MRT and urban growth management are strongly required for solving the transportation problems. Additionally new finance schemes such as land value capture should be also investigated for sustainable transportation investment in Yangon.

Keywords: urban transportation, large-scale survey, transportation policy, finance scheme

1. INTRODUCTION

Yangon, which is one of the largest economic cities in the Republic of the Union of Myanmar, has been experiencing rapid motorization since around 2010. They have caused serious traffic congestion at many road sections and intersections in the City, and led to significantly negative impacts on regional and local economies. Note that currently five kinds of transportation modes are available in Yangon: private car, rail, taxi, rickshaw, and bus. Although the so-called truck bus was one of the most popular public transportation options for commuters in Yangon, private cars have been recently increasing rapidly.

Although urban transportation is one of the most critical issues in Yangon City, the lack of statistical data has made it difficult for researchers and policy makers to formulate a scientific approach to them. Despite the poor availability of local data, some studies have so far challenged to analyze the transportation in Myanmar. For example, Kato *et al.* (2011) studied the feasibility of introducing bus rapid transit into Yangon City with the empirical data regarding travel behaviors and cost structure of bus operators. Zhang *et al.* (2008) analyzed the individual’s travel modal choice using both stated and revealed preference data collected in Yangon. Although they provided valuable implications to the public transportation policy in Yangon, the datasets used in their analysis were quite limited in terms of their survey scale as well as their geographical and socio-demographic coverages. This study uses the large-scale data, collected in the Project for Comprehensive Urban Transport Plan of the Greater Yangon (YUTRA) organized by the Japan International Cooperation Agency (JICA), 2013. As YUTRA's data was collected through a rigorously statistical process, which covers almost all Greater Yangon Area, it enables us to analyze holistically the latest traffic situations in Yangon. This paper reports the current problems of urban transportation in Yangon and discusses the future direction of transportation policy using the results from the large transportation surveys in YUTRA.

2. DATA COLLECTION

The YUTRA project team including the author implemented the Person Trip Survey (PT Survey) in 2013. Figure 1 shows the target area including Yangon City and a part of Thalyin, Hmawbi, Helgu, Htantabin, Twantay, and Kyauktan. This survey collected the individuals' daily travel episode, socio-economics and socio-demographics of households, their opinions about current transportation policies. The dataset contains the responses from 11,330 households, which account for 1.0 to 2.0% out of total households in the target area.

In addition to the PT Survey, the YUTRA also implemented other surveys including (1) the Cordon Line Survey that collected the data of origin-destination of trips, number of passengers, and traffic volume on 17 roads across the survey border for 16 or 24 hours; (2) the Screen Line Survey that surveyed the traffic volume and number of passengers of vehicles running through 13 roads across specific screen lines inside the survey area for 16 or 24 hours; (3) the Intersection Survey that collected the traffic volume by direction and by vehicle type, intersection queue length, signal parameters, and physical design at 19 intersections for 16 hours; (4) the Parking Survey that surveyed the dynamic change in the number of both off-road and on-road parked vehicles by vehicle type at 8 locations for 16 hours; and (5) the Travel Speed Survey that surveyed the

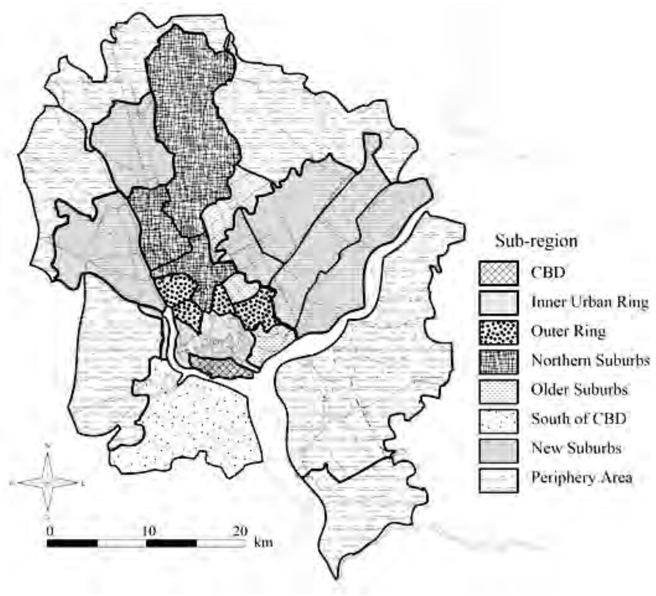

Figure 1: Map of the Study Area of YUTRA Project in Yangon

Source: JICA (2013)

travel time along 10 major roads by car during morning peak hours, daytime hours, and evening peak hours.

3. RESULTS

3.1 Modal Share

Figure 2 shows modal shares including all modes, excluding walk, and excluding non-motorized modes. The share of walking is 42.2 %, followed by bus (28.5%), bicycle (13.0 %), car/van (4.7%), taxi (4.4 %), and motorcycle (4.2%). The share of public transportation including bus, taxi, rail, and water ferry is 34.9%.

Figure 3 shows that the modal share by car ownership and by monthly household income. First, the modal share of walking is the highest in the household whose monthly household income is less than 200 US$. This is first because the workplaces of low-income individuals are located near their settlements and second because the lower-income individuals participate less in leisure activities at further places. Next, the modal share of buses in the middle income class (200-275 US$) is higher than that in other income classes for both car owners and non-car owners. The higher income car owning

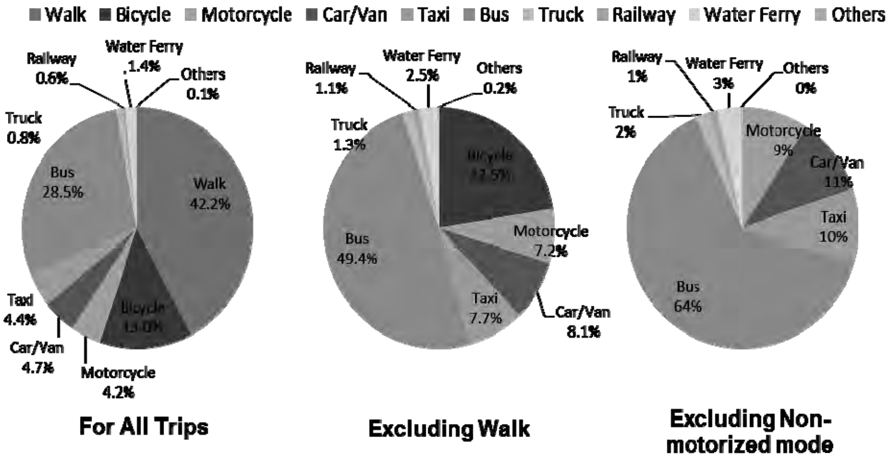

Figure 2: Modal Shares for All Trips, Excluding Walk, and Excluding Non-motorized Mode

Source: JICA (2013)

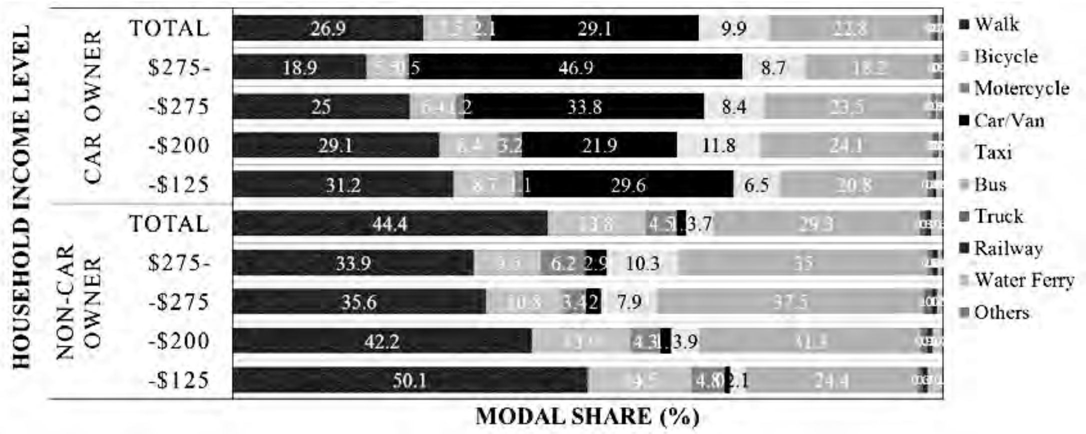

Figure 3: Modal Share by Vehicle Ownership and Household Income Level

Source: JICA (2013)

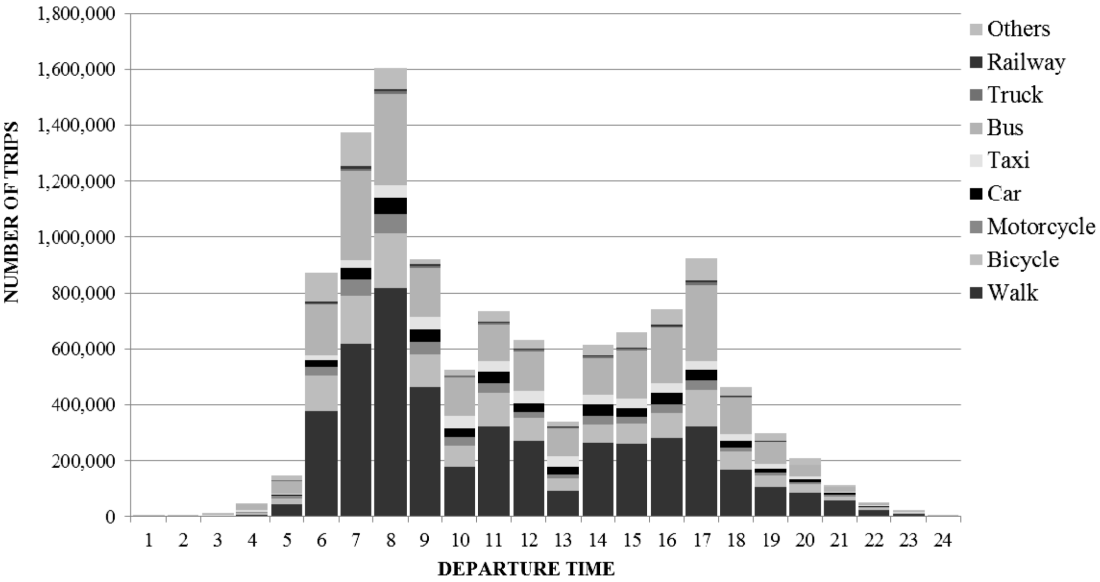

Figure 4: Distribution of Departure Time by Travel Mode

Source: JICA (2013)

households use cars and the higher income non-car owning households use taxis while the lower income households tend to walk. Finally, the modal share of buses in the car owner subgroup is 22.8%. They use public transportation services even though they own cars firstly because they use their cars not only for personal use but for commercial use such as commercial taxi services, and secondly because few household members have their own car licenses, and finally because they often do not like to spend money fueling up.

Figure 4 shows the hourly distribution of departure times by travel mode and by travel purpose. It reveals two peaks at around 7:00 to 8:00 am and at around 5:00 pm. Buses are used almost constantly throughout the day while other transportation modes are used mainly at peak hours. This shows the good provision of bus services from the early morning to the late evening.

3.2 Travel Time and Speed

Table 1 shows the distribution of travel time by travel purpose. First, this shows the most dominant travel time is 10 to 20 minutes while the average travel time is 31.6 minutes. The average travel time is much longer than its median because the tail of travel-time distribution is quite long where even over 120-minute trips were observed. Next, the average travel time for home-to-work, home-to-school, business, and private are 43.6, 24.0, 41.2, and 25.8 minutes, respectively. The long travel time for commuting trips partly reflects the long travel distance, which is caused by the current land-use pattern in Yangon. As the urban population increased, the urban area has been extended from the CBD to the north due to the geographical constraints of rivers. In addition, transportation infrastructure including highway and rail networks had also been developed to connect the CBD with the northern part of Yangon City. The main residential areas are located in the northeastern part of the City from which many commuters travel to their workplaces in the CBD.

Table 1: Distribution of Travel Time of Observed Trips by Trip Purpose

Travel Time	No. of Trips by Trip Purpose (000/day)						
	To Home	To Work	To School	Business	Private	Others	Total
-10min	688	106	227	52	310	119	1,501
-20min	1,916	298	610	146	825	321	4,116
-30min	498	129	133	64	192	95	1,110
-40min	674	218	162	100	215	100	1,469
-50min	280	137	62	55	84	45	662
-60min	125	66	24	16	29	12	271
-75min	443	204	72	74	102	50	946
-90min	144	83	21	23	35	9	316
-120min	276	121	46	42	63	21	569
120 min+	182	58	16	35	46	17	354
Total Trips	5,226	1,420	1,374	606	1,900	788	11,313
Average Travel Time (min)	32.1	43.6	24.0	41.2	25.8	25.8	31.6

Source: JICA (2013)

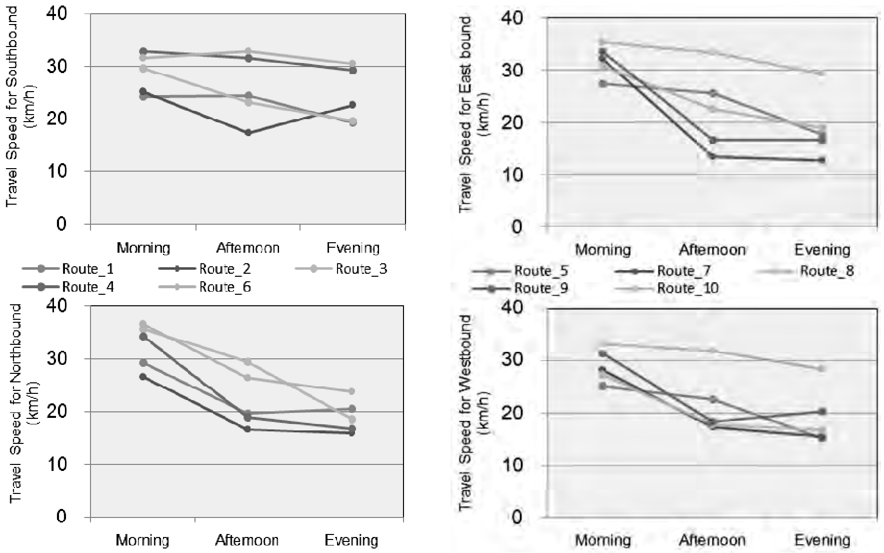

Figure 5: Travel Speeds Observed at Major Roads during Morning, Afternoon, and Evening

Source: JICA (2013)

Figure 5 shows the travel speeds observed at major roads in Yangon. This indicates that the average travel speed along major roads connecting suburbs with the CBD varies from 15 to 35 km/h. The outbound traffic from the CBD suffer from serious traffic congestion during evening peak hours while the inbound traffic to the CBD suffer from traffic congestion both during morning and evening peak hours. The inbound traffic congestion during the evening peak hours may be due to the poor traffic management and low capacity of intersections. The lower travel speed during morning peak hours also affects longer travel time of commuters.

4. URBAN TRANSPORTATION PROBLEMS IN YANGON

Urban transportation problems identified from the large-scale surveys in Yangon can be summarized as follows: “traffic congestion,” “long travel time,” “poor public transportation service,” and “mobility gap between high and low income individuals.”

Major reasons for the above problems are listed as follows:
(1) Urban travel demand has been increasing at a high growth rate along with the economic and population growth;
(2) Capacity of road network is not sufficient enough to cover the urban travel demand;
(3) Sprawling of the urban area requires the residents to travel in a long distance and this leads to longer travel time particularly for commuting from suburbs to the CBD;
(4) The facilities and infrastructure of public transportation has not been well developed, thus the individuals prefer private travel mode rather than public transportation;
(5) The gap in availability of motorized travel modes is significantly large between low/middle income classes and high income class; and
(6) Technical training and enlightenment regarding transportation is poor among drivers and pedestrians.

Although there are many similarities in the urban transportation problems of Yangon to other developing cities, the following unique issues relating to the recent history and transportation policy in Yangon should be noted. The first is that the motorcycle and bicycle ban policy has led to the public transportation oriented city where the bus was widely used in the City. Note that the motorcycle ban has been introduced into Yangon City since 2003 for reducing the number of traffic accidents in the City. The second is that the regulation of vehicle imports has reduced the car ownership in Yangon and this also contributed to a high modal share for public transportation. Note the regulation of importing foreign motorized vehicles in Myanmar was introduced a few decades ago, however, the government relaxed the regulation in 2010 in order to promote the replacement of the old motorized vehicles. The third is that the recent lift of economic sanctions from the international community has started to boost Yangon’s economy, which has escalated the traffic demand growth.

The motorcycle and bicycle ban should be respected as a challenging transportation policy. The ban has used to work well for motivating the individuals who own no car to use public transportation. The ratio of registered motorcycles to registered vehicles in the Yangon Region is significantly lower than other states/divisions in Myanmar. On the other hand, this may imply that motorcycles could be used more if the motorcycle and bicycle ban was lifted in Yangon. More individuals may request a stoppage of the motorcycle and bicycle ban policy. Interestingly, however, the local people still have a positive opinion for the current motorcycle and bicycle ban policy. The Person Trip Survey requested the respondents to answer a question: “Do you think the current limitation on the use of motorcycle in Yangon should be continued?” The results showed that 57.6% of the respondents support the regulation.

The effectiveness of motorcycle and bicycle ban could be weaker under the current situation where the vehicle import regulation has been relaxed. It is feared that this may give an incentive for high income individuals to use private cars after relaxation of the vehicle import policy. The survey also requested the respondents to answer a question: “Do you think the current limitation on the import of used vehicles should be continued?” The results show that half of the respondents disagreed with the regulation. If the urban transportation policy is determined by reflecting the opinions of local people, the motorcycle and bicycle ban should be continued while vehicle imports should be further deregulated; and this should lead to more demand of car usage in Yangon City.

5. POTENTIAL SOLUTONS TO THE PROBLEMS

5.1 Actions Required

Solutions to the urban transportation problems in Yangon are challenging because the travel demand continues to increase at a high growth rate while the capacity of implementing the appropriate transportation policies may be poor in Myanmar. Ideally, mass rapid transit (MRT) such as an underground rail system should be introduced for transporting the commuters from the suburbs to the CBD while the urban expressway network should be developed for expanding the road capacity and for bypassing the through-traffic. The Myanmar Government unfortunately does not have sufficient capacity to raise the funds for such infrastructure investment. Thus the top priority should be given the projects with high efficiency and low cost such as optimizing/upgrading existing facilities, namely: (1) bus rapid transit (BRT) into major corridors of the City to increase the traffic capacity and keep attracting people to use public transportation with better level of service, (2) improvement of the existing road/rail facilities to increase the traffic capacity and upgrade the service quality, and (3) traffic management including intersection improvement such as signal improvement and lane assignment to make full use of the road capacity.

The BRT should be well connected with a feeder service and also installed with a well-designed terminal in order to develop an intermodal transportation network where low income and/or handicapped individuals can participate in social activities. The existing bus operation should also be upgraded along with the introduction of a new BRT system where the individual-based bus operators should be restructured into a well-organized company/corporation as pointed out by Kato *et al.* (2010). However, as the BRT may not provide sufficient traffic capacity to cover the high traffic demand in Yangon City, continuous efforts to introduce MRT should be taken by the Government.

The urban sprawl should also be controlled by improving the efficiency of land-use patterns in the CBD as well as by developing strategically located satellite industrial cities so that the travel time could be reduced and the traffic congestion at the CBD could be eased.

5.2 Financial Issues

The above potential solutions could be realized through official development assistance including government-based loans or through the private sector participation in infrastructure investment projects. However, additional financial sources should be also explored by the authority/government to invest the transportation infrastructure in a sustainable way. One of them may be the value capture in transit-oriented development. The land value capture has been widely discussed as a potential tools of financing transportation infrastructure. The policy of land value capture is based on the theory that the increased value of land arising from improving the accessibility provided by transportation operators can be captured for funding or partly funding transportation infrastructures (Suzuki *et al.*, 2014). As shown earlier studies such as TCRP (2002), the value capture can take various forms. The appropriate form may depend on the governance and capacity of stakeholders including public transportation operators, land owners, urban developers, and the government. Further examination is required for finding the best financing approach to transportation investment in the context of Yangon.

6. CONCLUSIONS

This paper reported the latest traffic conditions and current problems in urban transportation of Yangon. The large-scale survey have successfully revealed the critical issues in a holistic manner. It also discussed the uniqueness of its urban transportation policies: motorcycle and bicycle ban and regulation of vehicle imports, which contributed to a reduction in car usage in Yangon. However, the effectiveness of those unique policies may be questionable due to the recent rapid changes in socio-economics and socio-demographics. Thus the introduction of BRT/MRT and urban growth control are strongly required. For sustainable transportation investment, an introduction of new funding schemes should be also investigated in addition to the conventional ODA financing and public-private partnership. They may include the land value capture relating the public transportation investment.

ACKNOWLEDGEMENTS

The surveys were implemented under the support of the Ministry of Rail Transportation, Ministry of Transport, Myanma Railways, Public Works under the Ministry of Construction, Traffic Police under the Ministry of Home Affairs, Yangon City Development Committee, and Yangon Region Government. This paper was completed on the basis of achievements in the YUTRA project organized by JICA. I sincerely thank them for their kind supports.

REFERENCES

Japan International Corporation Agency (JICA) (2013). *Draft Report of Project for Comprehensive Urban Transport Plan of the Greater Yangon (YUTRA)*, unpublished.

Kato, H., Saito, N., Inagi, A., and Myint, U. A. (2010). Regulatory framework and operational system of urban bus transportation in Yangon, Myanmar. Paper presented at the Transportation Research Board 2010 Annual Meeting, Washington D. C. (U. S.), January 2010.

Kato, H., Inagi, A., Saito, N., and Thun, P. T. T. (2011). Feasibility analysis for the introduction of a bus rapid transit system in Yangon, Myanmar. *Journal of the Eastern Asia Society for Transportation Studies*, No. 9, pp. 914–929.

Suzuki, H, Murakami, J., Y., Hong, H., and Tamayose, B. (2014). *Financing Transit-Oriented Development with Land Values: Adapting Development-based Land Value Capture in Developing Countries*, Washington, DC, USA: The World Bank Publication.

TCRP (2002). *Transit-Oriented Development and Joint Development in the United States: A Literature Review*, Research Results Digest, No.52, Transportation Research Board of the National Academies.

Zhang, J., Fujiwara, A., and Thein, S. (2008). Capturing traveler’s stated mode choice preferences under influence of income in Yangon city, Myanmar. *Journal of Transportation Systems Engineering and Information Technology*, Vol.8, No.4, pp. 49–62.

The evaluation on improvement of Japanese government crisis management system on the 2011 Great East Japan Earthquake disaster

Tetsuro Ito
Visiting Professor
Institute of industrial science, The University of Tokyo
Japan

ABSTRACT

This paper describes empirical analysis about crisis management measures. The crisis management measures was not sufficient at the time of the Kobe Earthquake Disaster occurred in January 1995, and then was improved. The Analysis is about what was the improved result actually function in the Great East Japan Earthquake Disaster occurred in March 2011. Result of the verification gets great clarity about the improvement effect of the issues that have been extracted in the previous great earthquake and improved in the Great East Japan Earthquake Disaster. On the other hand, in the field that had not been improved, it became clear that the same problem occurs again. It is important to reflect on failure and learn a lesson, and this paper shows the truth that further disasters occur at the place where the lessons are not utilized.

.

Keywords: Crisis management, Great East Japan Earthquake

1. INTRODUCTION

For enhancement of the crisis management measure it is important to continue analyzing response to actual outbreak of crisis and improving the measure. Especially in Japan, there is an issue that the system functions poorly and difficult to understand. The system is to function PDCA, such as analyzing the failure, reflecting the analysis results, assessing the reflected result and improving the measure additionally and is in order not to repeat the same mistakes.

However, as natural disaster comes to large-scale in Japan, people have understood the importance of the crisis management of the nation. In order to increase the crisis management capability of this nation, it is important to function PDCA fully and to improve continually the ability of those who manage the crisis.

The author has the experience which is working hard to secure emergency transportation as a director of Traffic Management and Control Division of the National Police Agency at the time of the Kobe Earthquake Disaster of January 16, 1995, and also spearheading the entire crisis management as the Deputy Chief Cabinet Secretary for Crisis Management, as a top of the affairs of the crisis management at the time of the Great East Japan Earthquake of March 11, 2011. From the experience at the center of the crisis management of the nation, I was keenly aware of the importance of improving the ability of person in charge of crisis management in each field.

In order to clarify the importance of the improvement of crisis management capacity of the nation, this study describes empirical analysis of the following: how to analyze the problems of the Kobe Earthquake Disaster which is the greatest crisis on record in the post-war years, how to improve the measures, and was the improved results actually function at the Great East Japan Earthquake.

2. RESPONSE OF NATIONAL GOVERNMENT AND LOCAL MUNICIPALITIES DURING THE KOBE EARTHQUAKE DISASTER

2.1 Timeline and response during earthquake

On 16th January 1995 at 5:46 am, a magnitude 7.3 earthquake occurred in the Kobe area of Western Japan. Since it was believed that the magnitude of an earthquake occurring in this region would be relatively small, many inhabitants did not think this great earthquake would occur, and their preparation was not adequate enough. Even the Japanese Government, which historically has experience and knowledge concerning large earthquakes, was also not prepared. Murayama Cabinet headed by Prime Minister Tomiichi Murayama and the National Land Agency Disaster Prevention Bureau were the concerned authority in the region. Figure 1 shows Timeline and initial response of the Government during earthquake.

At 5:55 am, the Japan Meteorological Agency announced that a seismic intensity 5 earthquake had occurred. With a seismic intensity 5 earthquake, shaking was intense enough to crack walls and pillars in old houses that did not have adequate earthquake measures, despite the fact that earthquakes with seismic intensity 5 occur every year in Japan. The Japan Meteorological Agency sent the information by fax to the concerned authority, the National Land Agency. However, there was no person on duty around the clock at the National Land Agency to collect information. As a result, a security guard of the government building received this information.

At 6:07 am, the security guard contacted officials of the National Land Agency who were at home. This was the moment that the concerned ministry came to know of the occurrence of the earthquake for the first time. At 6:13 am, the Japan Meteorological Agency announced that the earthquake was of seismic intensity 6, which had destroyed some buildings. At 6:45 am, the National Land Agency officials confirmed via a television announcement that it was seismic intensity 6.

The Secretary of the Prime Minister saw the news on the television at 7:00 am, confirmed the earthquake situation with the National Land Agency, and responded that the only answer was “there is no more information than television”. At 7:15 am, the National Land Agency queried the extent of damage with the National Police Agency and Disaster Fire Management Agency, but the response was that “information cannot be received from the local”. At 7:30 am, the secretary of the Prime Minister initially reported to the Prime Minister Murayama on the occurrence of the earthquake.

In Hyogo Prefecture, on the other hand, Governor Kaihara showed up at the prefectural government at 8:20 am. In addition at 8:26 am, Prime Minister Murayama went to the Prime Minister’s Office. By this time, over two and a half hours had elapsed since the earthquake had occurred; this was the same time attendance as usual in spite of the emergency.

At 10:04 am a regular cabinet meeting was held. The meeting determined the establishment of a disaster management headquarters of the Government headed by the Chief Commissioner of the National Land Agency, based on the Disaster Countermeasures Basic Law. However, this headquarters was not the Emergency Disaster Response Headquarters headed by the Prime Minister, which is the second biggest system of the government.

Table 1: Timeline and initial response of the Government during earthquake

5:46 am	a magnitude 7.3 earthquake occurred
5:55 am	the Japan Meteorological Agency announced that a seismic intensity 5 earthquake had occurred
6:07 am	the security guard received the fax message and contacted officials of the National Land Agency
6:13 am	the Japan Meteorological Agency announced that the earthquake was of seismic intensity 6
6:45 am	the National Land Agency officials confirmed via a television announcement that it was seismic intensity 6.
7:00 am	The Secretary of the Prime Minister saw the news on the television at 7:00 am, confirmed the earthquake situation with the National Land Agency and responded that the only answer was “there is no more information than television”
7:15 am	the National Land Agency queried the extent of damage with the National Police Agency and Disaster Fire Management Agency, but the response was that “information cannot be received from the local”
7:30 am	the secretary of the Prime Minister initially reported to the Prime Minister Murayama on the occurrence of the earthquake
8:20 am	Governor Kaihara showed up at the prefectural government
8:26 am	Prime Minister Murayama went to the Prime Minister’s Office
10:04 am	a regular cabinet meeting was held

2.2 Problems of the initial response of the Government

When an earthquake occurs, how did the government the emergency countermeasures go? As mentioned earlier, at the National Land Agency, a responsible authority when an earthquake occurs, there was no one available to collect information over a 24 hour period. Also, there was no one available to collect information to convey instruction to the Prime Minister’s office or the Cabinet Secretariat to support the Prime Minister. Only the Prime Minister, Chief Cabinet Secretary and Deputy Chief Cabinet Secretary had the privilege to organize and co-ordinate the operation of each ministry and only their secretaries could support them; therefore, nothing was done in practice. There was also legislation in the occurrence of a disaster i.e. give the Prime Minister the authority to direct each minister and the prefectural governors, but it had not been executed. For this reason, the government let each ministry independently implement emergency countermeasures. Organizing and coordinating operations of each ministry that the Cabinet should do were not executed. Coordination with other ministries was only conducted by their own judgment and only when they felt it was required. For this reason, many emergency countermeasures were lacking in organization.

2.3 Problems of the initial response of the local government

In and around the city of Kobe, damage due to the earthquake was extensive. Due to loss of power and disruption of communication lines due to radio tower collapse, communication was so poor that it was not possible to know the full extent of the damage caused by the earthquake.

The Prefectural government of Hyogo Prefecture and the Prefectural Police headquarters escaped the collapse of prefectural government buildings, although this information could not be gathered due to power outages and disrupted communications. On the other hand, Kobe City Hall, that was in the vicinity of the center of the earthquake, had been destroyed. For this reason, rescue activities, relief request to the government and the SDF were not made for a few hours after the initial earthquake.

The magnitude of the earthquake damage to housing, railroad tracks and highways was confirmed via observations from news organization helicopters. While there was no information that some areas were affected, there were also a places in those districts where most of the houses had been destroyed. However, those living in the damaged areas were unable to see the reports on TV because of power failure in the disaster area.

2.4 Problems of the relief activities

Concerning relief activities following the earthquake, relief troops including police and fire troops from across Japan and relief supplies were initially dispatched to the disaster area. However, some problems with these relief activities occurred. Firstly, the terrain of the area made access by emergency vehicles difficult. It was only possible to go to the site via the east and west because the disaster area was surrounded by sea and mountains. Three existing highways were also destroyed, and relief activities were only possible by two national roads. Moreover, one of these national roads could not be used due to collapse of the highway on it and the other national road was congested by general vehicles driven by concerned relatives of those within the disaster area. In addition, there was no reliable communication network connecting Tokyo and the disaster area.

Dispatch requests from the local government to the Self Defense Force (SDF), which is the mainstay of the relief activities, was not made quickly enough. This is because the Governor was required to request the dispatch to the SDF and the requirements for this were strict, and the SDF was not able to take any action requested by the municipality.

Regional collaboration and cross-support system of concerned bodies such as police and fire troops was not efficient enough. For this reason, after receiving a support request, each prefectural police and each municipal fire troops made a decision about which troop should go and how many troops should go. And then they ordered the troops out.

Police and fire troops that went to provide support in the disaster area had wireless communication equipment but, as the frequency of the radio wave was different, they were unable to get in touch with the headquarters and local troops within the disaster area as well as between the support teams. In addition, fire hoses were unable to be connected to fire hydrants in the disaster area due to differences in the size of calibers.

Furthermore, many problems occurred in cooperation between police, fire troops and the SDF due to not only problems in communication and terminology but also lack of knowledge between the groups.

3. IMPROVEMENT OF THE CRISIS MANAGEMENT SYSTEM

3.1 Strengthening of the country's crisis management capabilities

From the review of the Kobe Earthquake Disaster and several incidents concerning terrorist attacks after the earthquake, it was pointed out from all sides that crisis management functions were insufficient. The government decided to enhance its nationwide crisis management capabilities. The position of Deputy Chief Cabinet Secretary for Crisis Management was established so that organization and coordination of each ministry, which the Cabinet has in the Legislation of Japan, can be made to function at crisis management. It makes possible to carry out a coordinated crisis management by the government if emergency of the nation occurs such as disaster or terrorist attack [1998].

Additionally, a cabinet crisis management system composed of about 200 people was established to support the Deputy Chief Cabinet Secretary for Crisis Management. Also, the National Land Agency Disaster Prevention Bureau was moved to the Cabinet Office to provide adjustment to the measures of each ministry.

3.2 Fortification of information collecting system and risk management system at the time of emergency

To enhance emergency system in the country, following system was established:

I) To grasp the initial information in a state of emergency: (1) a 24-hour Cabinet information aggregation Center was established; (2) an early warning system to the Prime Minister was built; and (3) rapid announcement of earthquake information and transmission system was developed for the Japan Meteorological Agency.

II) To understand the extent of damage in the early stages of an earthquake: (1) an earthquake disaster information system (DIS) was established in the Cabinet Office; and (2) a Helicopter TV system was developed for police and fire authorities, the SDF and the Japanese Coast Guard etc.

III) For the establishment of a crisis management system in the Prime Minister's Office, in addition to the Deputy Chief Cabinet Secretary for Crisis Management and crisis management staff of the abovementioned: (1) a crisis management center was developed in the Prime Minister’s office for several hundreds of people working 24 hours a day; (2) crisis management accommodation was established to develop an emergency response system for crisis management personnel; and (3) to build a quick decision system by an emergency response team from director-general level of the ministries was set up.

3.3 Development of a national crisis management system

The following measures for activities in an emergency were undertaken, to make first aid measures more effective:

I) For highly reliable communication network construction: (1) central disaster prevention wireless networks in municipalities across the country were installed; and (2) communication networks from each ministry to the Crisis Management Center in the Cabinet were consolidated.

II) For the rapid dispatch of SDF requests: (1) some authority to dispatch requests was given to municipal mayors; (2) the dispatch procedure was simplified; and (3) voluntary dispatch of the SDF was improved.

III) For the construction of a wide area support system and collaboration systems between police and fire authorities: (1) wide area emergency relief teams to police were installed across Japan; (2) fire emergency relief teams were installed across the country; (3) a cooperation agreement between police and fire authorities and the SDF was established; (4) which strengthened the partnership of the authorities through partnership training; and (5) unity in wireless frequencies in case of emergency and uniform diameter fire hose was established.

4. THE 2011 GREAT EAST JAPN EARTHQUAKE DISASTER- LESSONS LEARNT FOLLOWING THE KOBE EARTHQUAKE DISASTER

On March 11th 2011, 16 years after the Kobe Earthquake Disaster, a massive earthquake hit Japan again. Massive damage caused by the earthquake shaking and the damage caused by the following tsunami, occurred over a wide area in the Tohoku region of Japan. The scale of the earthquake was large, also loss of human life and damage of buildings and facilities exceeded the Kobe Earthquake Disaster. At that time, did this country learn constructive lessons from the Kobe Earthquake Disaster?

In terms of the response to the earthquake and the tsunami, Japan applied the lessons and the reflection of the Kobe Earthquake Disaster. Firstly, quick announcement of earthquake information from the Japan Meteorological Agency and the transmission system functioned immediately. Before the earthquake shaking reached Tokyo, the Earthquake Early Warning (EEW) system, alerted immediately that the seismic intensity was seven, which was the maximum on the scale for earthquakes. The initial announcement of the tsunami height was 6 meters, but was corrected to 10 meters 30 minutes following the announcement. When the EEW predicted that height everyone must evacuate immediately.

The Cabinet Crisis Management Center also launched a system of emergency 4 minutes following the earthquake, gathered emergency teams from each ministry and discussed operations. The Earthquake Disaster Information System (DIS) also functioned and predicted the magnitude of the damage caused by the earthquake. Hundreds of crisis management staff were also gathered in a short time. In terms of the dispatch of the SDF, some went ahead to the local areas within the damaged areas before the request came out. A cabinet meeting was opened within 30 minutes of the earthquake, and it was decided to install an Emergency Disaster Response Headquarters as a maximum response organization of the government.

Radio frequencies around the country functioned. CCTV on helicopters used by each institution also started sending video images to the Prime Minister's Office. It took time to disperse rescue activities to every corner of the disaster area because it was a very wide area and damage was vast, but police and fire troops, the SDF and the Japanese Coast Guard from across the country, medical teams and road clearing teams also were dispatched to the disaster areas. Emergency relief supplies were successfully delivered to the damaged areas. Problems relating to traffic regulations or wireless networks were minimal.

5. CONCLUSIONS

This paper describes empirical analysis about what was the improved results actually function in the Great East Japan Earthquake. In conclusion, Japan applied the lessons of the Kobe Earthquake Disaster to the Great East Japan Earthquake Disaster. Taking advantage of the lessons as the wisdom of the future is the way to prevent a new devastation. However, the earthquake taught us that further disasters occur at the place where the lessons are not utilized. Among these, it has become an only major problem in emergency countermeasures against earthquake that fuel is insufficient and its transport was delayed significantly. Furthermore, it is not covered in this presentation, but, apart from this problem, accident of Fukushima Daiichi nuclear power plant that has occurred at the same time caused a serious problem indeed followed today. Both are energy-related issue under the Ministry of Economy, Trade and Industry (METI). As it turned out later, because problem of energy did not become a major issue at the Kobe Earthquake Disaster, the METI had not been taken any earthquake measures whatsoever. There would be many other problems on the Great East Japan Earthquake. To inquest and improve each single problem is the preparation for future disaster. I hope further development of research on disaster prevention.

Table 2: problems on the Great Hanshin-Awaji Earthquake and improvement on the Great East Japan Earthquake

problem	content	improvement	result
Japanese Government	・no one on duty at the National Land Agency Disaster Prevention Bureau ・lack of manpower and facilities to collect information ・lack of staff to organize and coordinate operations of each ministry by the Prime Minister	・Establishment of Deputy Chief Cabinet Secretary for Crisis Management ・Moving the National Land Agency Disaster Prevention Bureau to the Cabinet Office ・To grasp the initial information ①a 24-hour Cabinet information aggregation Center ②an early warning system to the Prime Minister ③strengthen the system for the Japan Meteorological Agency ・To understand the extent of damage ①DIS ②a Helicopter TV system ・To enhance the system ①a crisis management center in the Prime Minister’s office ②developing an emergency response system ③development of a quick decision system	・tsunami forecasting system ・The Cabinet Crisis Management Center launched a system of emergency 4 minutes following the earthquake ・gathered emergency response teams ・DIS predicted the magnitude of the damage caused by the earthquake ・CCTV on helicopters started sending video images ・crisis management staff were gathered in a short time ・installed an Emergency Disaster Response Headquarters
Local government	・collapse of government buildings ・disruption of communication lines ・breakdown of the system of knowing the damage, relief activities and dispatch requests ・difficulty of gathering staff	・development of a national crisis management system ・For highly reliable communication network construction ①install central disaster prevention wireless networks ②communication networks to the Crisis Management Center in the Cabinet ・For the rapid dispatch of SDF requests ①some authority to dispatch requests was given to municipal mayors ②simplify the dispatch procedure ③voluntary dispatch of the SDF ・For a wide area support system between police and fire ①police emergency relief teams ②fire emergency relief teams ③a cooperation agreement between police, fire and the SDF ④partnership training ⑤unity in wireless frequencies and uniform equipment was established	・voluntary dispatch of the SDF, rapid dispatch of SDF requests, dispatch of 100,000 SDF people ・activate communication network ・police and fire troops gathered from across the country ・grasp the damage from CCTV on helicopters of the SDF, police, fire and Japan Coast Guard, relief activities ・dispatch of medical teams and road clearing teams
Relief activities	・lack of roads ・lack of reliable communication network ・delay of dispatch requests ・insufficiency of support system of concerned bodies ・not-standardized equipment of relief troops ・problems in communication and terminology between relief troops		

Lessons we learn from unexpected hazards

Taketo UOMOTO
Chief Executive, Public Works Research Institute
Professor Emeritus, the University of Tokyo, Japan
uomoto@pwri.go.jp

ABSTRACT

When new construction works starts, the designers and engineers working in the field of civil engineering always try to keep the structure safe enough against expected natural hazards. The problems are that these expectations may not meet the actual hazards. Many different natural hazards are occurring every year throughout the world and some of the hazards exceed the expected level of hazards. The Great Hanshin-Awaji Earthquake happened in 1995 exceeded the expected level of ground motion and many structures were destroyed by the ground motion. In 2011, the Great East Japan Earthquake taught us the unexpected hazards caused by the Tsunami just after the earthquake. At the time of design, although these hazards were expected and considered to certain extent, the scales of the hazards expected were far smaller than the actual situation. There are similar unexpected hazards occurring elsewhere throughout the world. This paper shows examples how the engineers have to decide what to do in case of unexpected hazards, especially the case of earthquakes, tsunami, landslides caused by rainfalls, and the problem of deterioration of structures.

Keywords: engineering judgment, preparedness, earthquake, tsunami, typhoon, landslide, natural dam, deterioration, maintenance

1. INTRODUCTION

Although many hazards may occur, it is important to keep the country safe from the hazards and offer comfortable life to the people. The civil engineers are working every day to accomplish the target, but the hazards caused by nature may exceed the expected hazards. To deal with the problem, the engineers must learn from the actual hazards. Japan is a country of many natural disasters, such as earthquakes, tsunamis, typhoons, volcanic actions, liquefaction, landslides, floods, snow slides, fires, etc. To deal with these natural hazards, many attempts are being made for disaster prevention and mitigation. Figure 1 shows some of the main natural hazards happened in Japan from 2011 to 2013. From the figure, we can easily understand that the hazards are happening throughout the country.

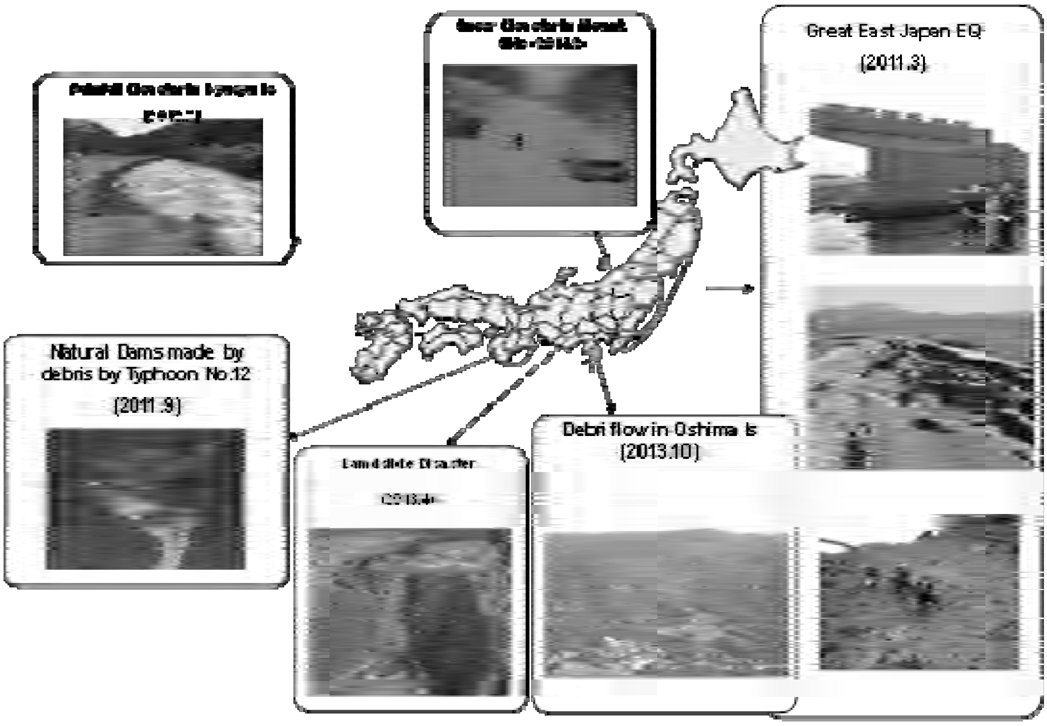
Natural Dams made by debris by Typhoon No.12
(2011.9)
Landslide Disaster
Debri flow in Oshima Is
(2013.10)
Great East Japan EQ
(2011.3)

Figure 1: Examples of natural disasters occurred in Japan (2011-2014I)

Disaster prevention and mitigation is usually planned against individual disasters as shown in Figure 2. We try to prevent and mitigate the disasters when we construct structures. But several disasters may happen at the same time; not only earthquake, but also tsunami, fire, liquefaction and even collapse of deteriorated structures. To deal with the problem, the civil engineers must learn from the disasters what is the cause of the disaster, how to prevent or mitigate the disaster against the next disasters. This paper is aimed to introduce the causes of disasters, the preventive measures and the lessons we learn from these disasters.

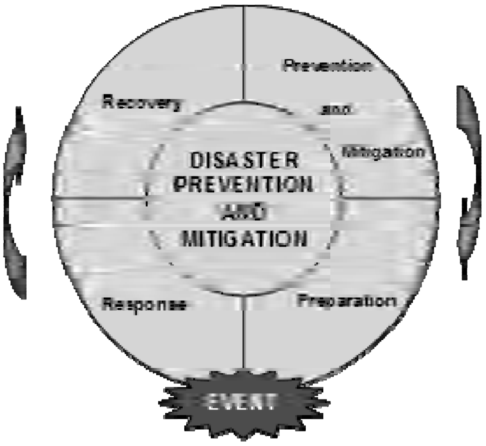
Prevention
and
Mitigation
Recovery
DISASTER
PREVENTION
AND
MITIGATION
Response
Preparation
EVENT

Figure 2: Example of disaster management cycle

2. THE GREAT HANSHIN-AWAJI EARTHQUAKE AND THE GREAT EAST JAPAN EARTHQUAKE

2.1 The Great Hanshin-Awaji Earthquake

The Great Hanshin-Awaji Earthquake took place in Hyogo prefecture in the early morning of January 17, 1995, with the Magnitude of 7.3. The strong ground motion collapsed many bridges, houses, and industrial facilities mainly in urban area. After the earthquake, fire took place in many wooden houses in the Kobe City. The number of deaths and missing of the Great Hanshin-Awaji Earthquake was 6,437 persons. The houses and bridges in the Hanshin Area were damaged by the earthquake as shown in the Figure 3. Further, wooden houses were damaged not only by the ground motion but by the fire caused by the disaster.

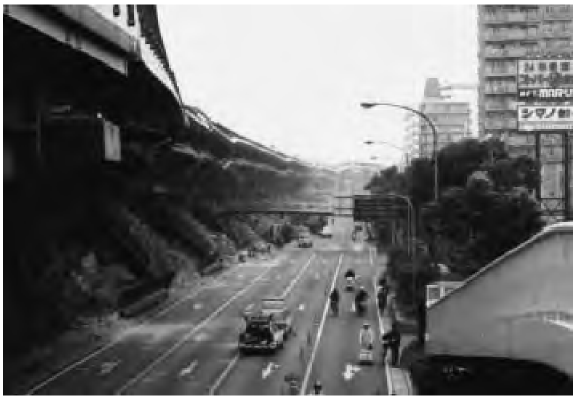

Figure 3: Destructive damage to bridges in 1995 Great Hanshin-Awaji Earthquake (MLIT)

One of the lessons we learned from this disaster is that the existing structures may not possess enough strength against seismic motions. Up till the disaster, experimental shear strength of concrete was overestimated at the time of design. To deal with the problem, we changed the design seismic forces and developed the methods to retrofit existing structures against seismic load. As a result, many structures were retrofitted after the Great Hanshin-Awaji Earthquake throughout the country. The lessons learned from the destructive damage to houses and bridges caused by the earthquake prevented the collapse of the structures by the Great East Japan Earthquake in 2011.

2.2 The Great East Japan Earthquake

On March 11, 14:46 PM, 2011, a massive scale “Great East Japan Earthquake” hit the country of Japan mostly on Pacific coast. The magnitude of the earthquake was reported as 9.0, and shook Japan from Hokkaido to Osaka City. The epicenter of the Great East Japan Earthquake was about 130km from Sanriku area (East coast of Honshu Island, facing Pacific Ocean) with the depth of 24km. The maximum JMA (Japan Meteorological Agency) Seismic Intensity was 7.0 (strongest level), and the maximum ground acceleration was more than 1,000cm/sec^2. More than one half of the whole Honshu Island and Hokkaido Island were shaken and the maximum peak ground acceleration (PGA) observed was 2,933 cm/sec^2. Furthermore, the aftershocks were also tremendous. The number of aftershocks above the magnitude of 5.0 within one month after the Great East Japan Earthquake (up till April 10, 2011) was more than 440 times. As a result, some of the structures which were not damaged much at the main shock were severely damaged to larger extent by the aftershocks. The aftershocks and the long time duration of ground motion significantly affected the damages caused by the soil liquefaction.

After the earthquake, a huge tsunami occurred. The total width of the tsunami was about 450km from north to south, and it reached most of the eastern coastal lines of Japan as shown in Figure 4. As shown in the figure, the coastal lines of north eastern part of Japan were attacked by huge tsunami. The figure is the warnings of tsunami by Japan Meteorological Agency (JMA) just after the earthquake (March 11, 16:08 PM). The estimated maximum height at the time of warning was more than 3m, but the actual height was more than 10m at some part of the coastal lines.

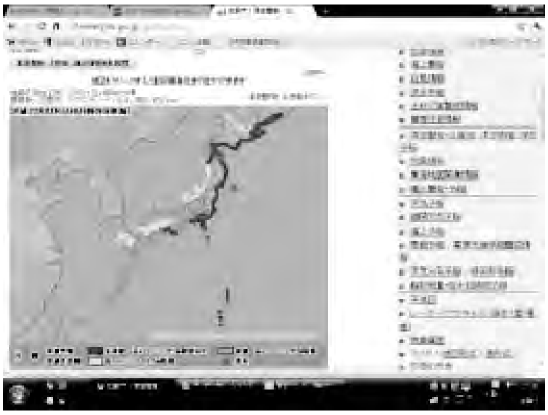

Figure 4: Warning of tsunami by JMA just after the earthquake (Internet information)

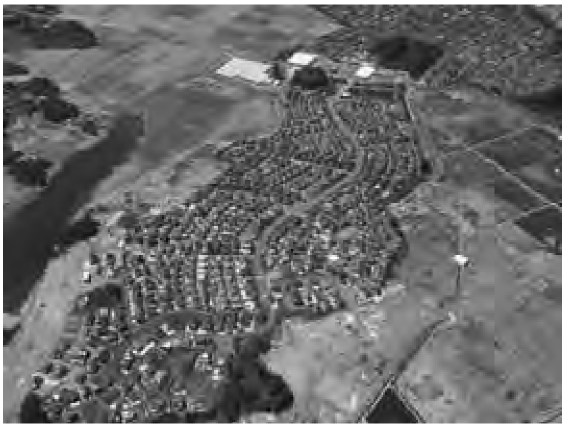

Figure 5: Houses on hilltop without damage by tsunami (Photo: PWRI)

Due to the huge tsunami, many structures located at the coastal lines were damaged and many houses were swept away. The newspapers informed that most of the houses located close to the coastal line from Iwate prefecture to Miyagi prefecture were damaged and more than 15000 people lost their lives and more than 8,000 people were missing (by June 6, 2011). The damages by tsunami were far larger than the damages caused by the seismic ground motion. Most of the houses located near the coast were swept away and only the houses located at hilltops could remain as shown in Figure 5. Due to the tsunami, the Fukushima No.1 nuclear power plant was damaged. The tsunami attacked the plant over flooding the dikes, and the sea water flooded electric power facilities shutting down the electric control of the plant. As a result, the nuclear plants became out of control, causing hydrogen explosion and melt down of the boiling water reactor (BWR).

Comparing the two earthquakes (Table 1), the main causes of the Great East Japan Earthquake were quite simple. As shown in Figure 6, original cause was the earthquake with the magnitude of 9.0. In case of the Great Hanshin-Awaji Earthquake occurred in 1995, magnitude of the earthquake was 7.3, and the damages of the structures were mostly caused by the strong ground motion (1). But in case of the Great East Japan Earthquake was followed by huge tsunami, damaging both the structures and the people (2). One of the structures was the nuclear power plant of Fukushima No.1 (3). The BWR of the power plant became out of control due to loss of electricity (both normal and temporary electric supply were not available for some time) and cooling water (4). As a result, melt down of the BWR started (5). After the hydrogen explosion, radioactive contamination spread around the surrounding area of the region. This forced the people to evacuate from the location of the power plant, and the citizens were forced to live in the evacuation area far from their residential area.

Table 1: Comparison of the Hanshin-Awaji Earthquake and the East Japan Earthquake (Data from the Cabinet Office of Japanese Government)

	Great Hanshin-Awaji Earthquake	**Great East Japan Earthquake**
Date and Time	1995/1/17 5:46 AM	2011/3/11 14:46 PM
Magnitude	7.3	9.0
Type of earthquake	Local earthquake	Subduction-zone earthquake
No. of prefectures above JMA intensity 6.0	1 (Hyogo)	8 (Miyagi, Fukushima, Ibaraki, Tochigi, Iwate, Gumma, Saitama, Chiba)
Tsunami	Several ten cm	Huge tsunami (max: above 9.3m)
Characteristic of damage	Collapse of houses and bridges, big fire occurred	Houses, bridges etc. were washed away
No. of deaths and lost	Deaths: 6,434; Lost: 3	Deaths: 15,270; Lost: 8,499
Collapsed houses	104,906	102,923
Distribution of ground motion (JMA seismic intensity above 4.0)	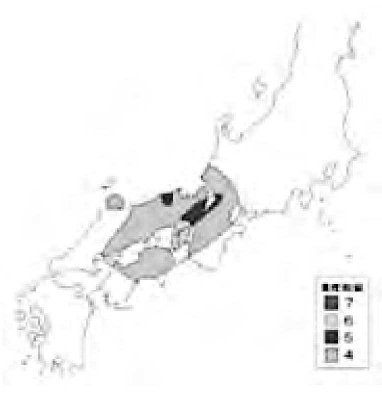	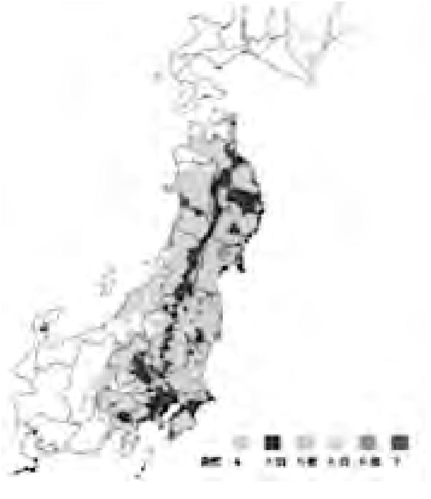

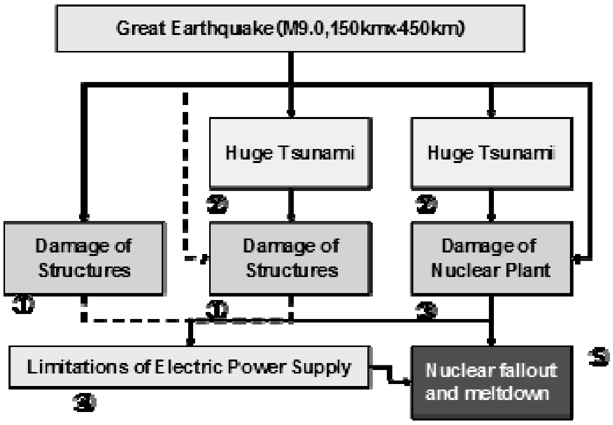
Great Earthquake (M9.0,150km×450km)
Huge Tsunami
Huge Tsunami
②
②
Damage of Structures
Damage of Structures
Damage of Nuclear Plant
①
①
③
Limitations of Electric Power Supply
③
Nuclear fallout and meltdown
⑤

Figure 6: Causes of the disaster

One of the main reasons why such a disaster occurred is that these situations were not expected even at the time of designing the structures. The expected conditions during design of structures were a large earthquake may occur during their service lives, but the attack of tsunami was considered much less in the design. Although the certain level of a large earthquake with longer return period compared to the usual structures was considered in the design of nuclear power plants, it is true that the Great East Japan Earthquake was the earthquake with very low possibility to occur. The structures constructed after 1995 or retrofitted using the modified standard specifications considering the damages by the Great Hanshin-Awaji Earthquake, did not suffer severe damages by the Great East Japan Earthquake (see Figure 7).

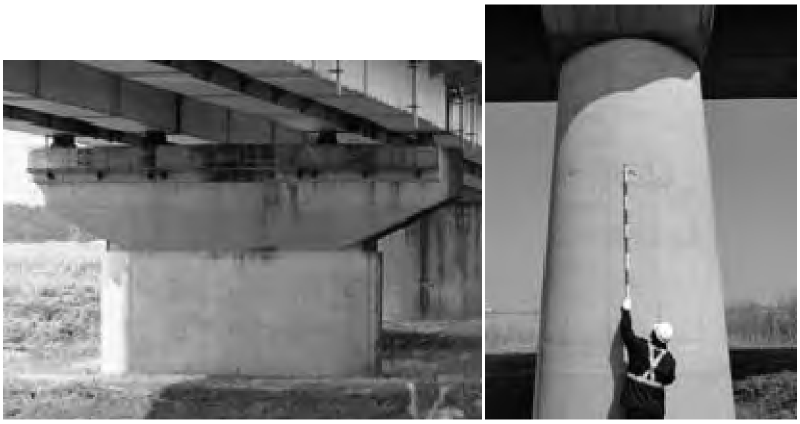

Figure 7: Bridge piers strengthened (left, no damage) and before strengthened (right, damaged) (Photo: PWRI）

But for the tsunamis, the loads were considered little on structures such as houses and bridges. This is one of the reasons why so many houses and structures were damaged (see Figure 8). The reason why the tsunami load was not considered in the design of structures is that the general concept to deal with the tsunami is to evacuate people to higher places, and it was not generally employed to design structures against the tsunami loads considering economy and limited engineering knowledge on tsunami design.

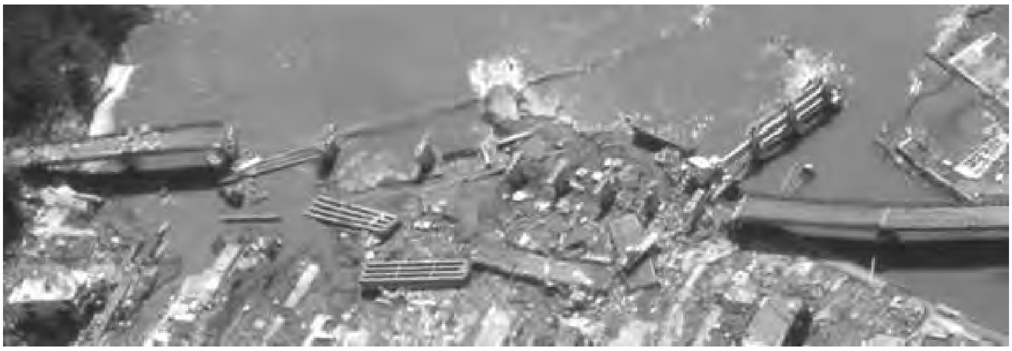

Figure 8: Bridge girders washed away from their piers by Tsunami (Photo: Tohoku Regional Bureau of MLIT)

As shown in Figure 8, many bridge girders were washed away by tsunami. Some were floated, some were turned upside down, and some had stayed as it was without any big damage. Experiments were performed to clarify the causes of these differences. And the results show that the shape of the girder made a big difference due to not only the speed of the tsunami, but also the overhanging width of the girder of the bridge (see Figure 9).

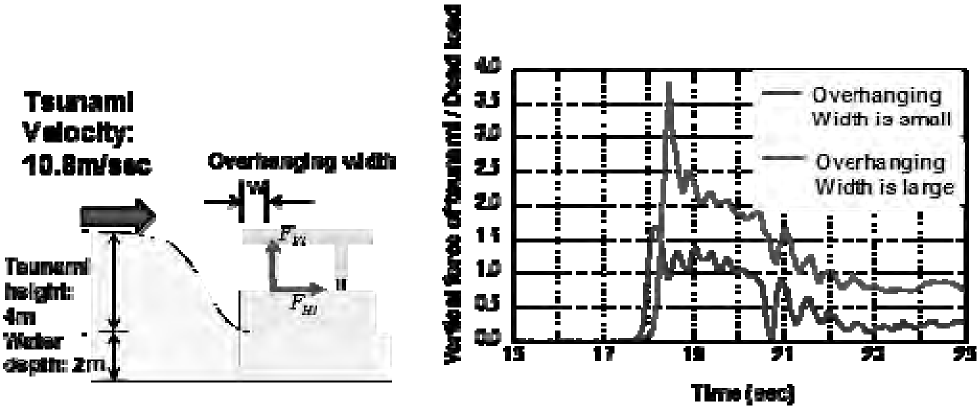

Figure 9: Experimental result of the tsunami force acting on bridge girder (Hoshikuma et al, PWRI)

3. NATURAL DAMS FORMED BY LANDSLIDES

In the year 2011, not only the earthquake but also many landslides occurred in mountainous regions of Japan. Most of the landslides occurred due to heavy rain carried by typhoons, and one of the most severe landslides was deep-seated landslides caused by the rainfalls of Typhoon No.12 arrived at Japan in September with the total amount of rainfall of 1800mm in 3 days. Total affected areas by the landslides were about 10 million square meters and total amount of collapsed debris was more than 100 million cubic meters mostly in Nara, Wakayama and Mie Prefectures. Since it is difficult to identify the vulnerable areas to deep-seated landslides caused by heavy rains and the number of such areas is so large, it is not easy to conduct preventive works in a short period of time. Therefore, the response to manage such damage becomes important.

The problems of the landslide debris are: (1) landslide debris may attack the houses and roads underneath, (2) transported landslide debris may form temporary natural dams stopping water flow of the narrow rivers, and (3) these natural dams may not be sufficient enough to resist against the ponded water pressure acting on the dam (see Figure 10). Especially where the rivers are narrow, such temporary natural dams may easily be formed by the landslide debris and may cause water flood to the people living underneath when they collapse. Actually, in case of the Typhoon No. 12, 17 temporary natural dams were formed within a few days.

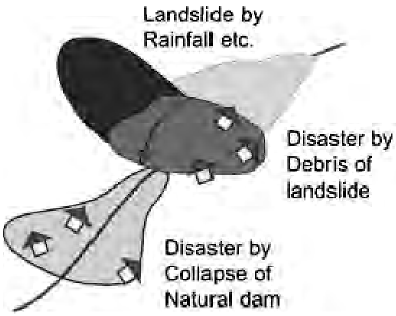

Figure 10: Schematic figure of the effect of landslide debris on a narrow river (Ishizuka et al., 2012)

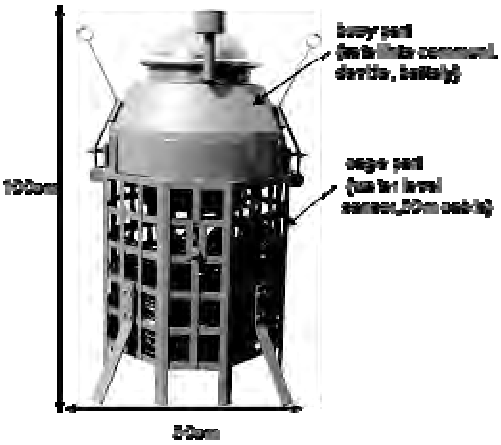

Figure 11: AcAMet used to monitor the level of accumulated water (Ishizuka et al., 2012)

To prevent further disasters, such as flood, it is important to evacuate the people living in the downstream of these rivers. But the time of the collapse cannot be estimated accurately, and it is difficult to monitor the change of the situation of the reservoir especially in deep mountains. To monitor the real time change of the water level of the reservoirs, AcAMet (Aerially-conveyable Automatic Water Level Meter: see Figure 11) was introduced and set by a helicopter. This equipment was developed by combining the water level sensor and satellite communication device. Using such a simple APF Gauge, real time monitoring of the water depth was performed, giving enough information to the public when to evacuate. The similar situation occurred in the upper reach of the city of Ambon, Indonesia, in July 2012. Although the natural dam collapsed in July, 2013 after one year, people living in the village of Negeli Lima evacuated beforehand and only a few people were affected. The collapse invaded the village and about 60% of the village was flooded and washed away. The similar device (AcAMet) was also used for real time monitoring to help the people to evacuate before the flood.

4. DETERIORATION PROBLEMS OF CONCRETE STRUCTURES

Deterioration problems are becoming another important item to consider from now on, especially in Japan with rapid new construction works being done up till today. The increases of aged structures may lose their performances with time and may cause disasters even without other disasters such as earthquakes. Figure 12 shows how rapid the annual investment for maintenance and renewal of aged structures is increasing from now on.

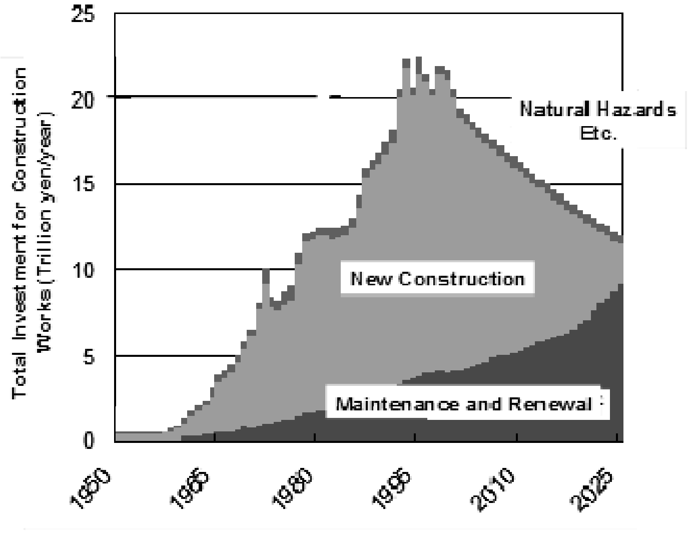

Figure 12: Investment for annual construction works (MLIT)

To deal with the problem, preventive methods have been studied in many research institutes including universities. Japan Society of Civil Engineers (JSCE) has been studying how to construct new structures and maintain existing structures from now on. “Standard Specification of Concrete Structures (Design)” and “Standard Specification of Concrete Structures (Maintenance)” were published in 2007 with the concept of (1) for new construction works, durability design must be used, and (2) for existing structures maintenance must be done keeping the required performances throughout the service life of the structure. The newly proposed performance-based durability design can be summarized as follows:

1) The concrete structure must be quantitatively checked whether the structure possesses required performance within the designed period.
2) The degree of deterioration of the structure in service for a specified cause must be specified.
3) To maintain the structure above the specified degree of deterioration, the required performance must be specified.

To examine the performance on durability, a kind of limit state design scheme was introduced for the durability of concrete structures. The equation can be written as shown in equation 1:

$$\gamma_i \cdot {}^{A_d}\!\big/_{A_{\lim}} \leq 1.0 \tag{1}$$

where, A_d is designed performance of the structure at specified time considering the specified deterioration cause, A_{lim} is limit of the performance of the structure, and γ_i is coefficient of the structure considering the importance, etc.

Generally, performance of concrete has to be verified to satisfy the required performances. Not only resistances against deterioration but also mechanical properties of concrete have to be verified throughout the service life of the structure.

Figure 13 shows an example of the calculated result for minimum cover thickness to prevent carbonation induced corrosion at different years of service for OPC concrete and BFSC concrete. As shown in the figure, the cover thickness required changes according to the type of cement to be used, water-cement ratio of concrete, years of service and exposed condition (wet or dry) of the structure to be constructed. When the structure is designed for long period of time, the cover thickness may become too large, and it is recommended to use other countermeasures such as to use Epoxy-coated bars instead of normal reinforcing bars.

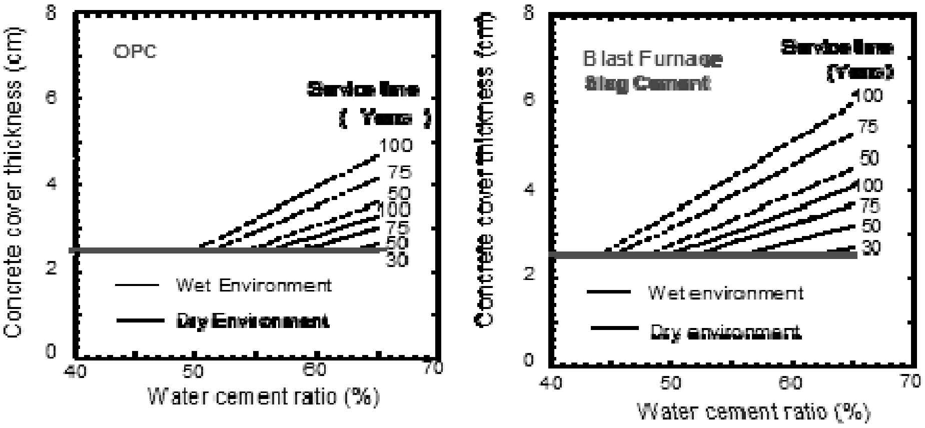

Figure 13: Calculated results of concrete cover according to JSCE Standard Specification (Concrete Committee of JSCE)

Deteriorated structures such as shown in Figure 14, need a quite large amount of fee for maintenance, and if not, the structure cannot be used safely throughout the service life. Several existing structures are already abandoned or limited for use.

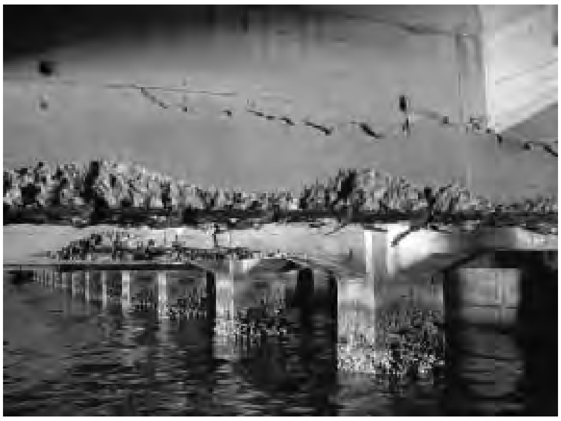

Figure 14: Deteriorated RC wharf due to chloride corrosion (Photo: Dr. Ema Kato)

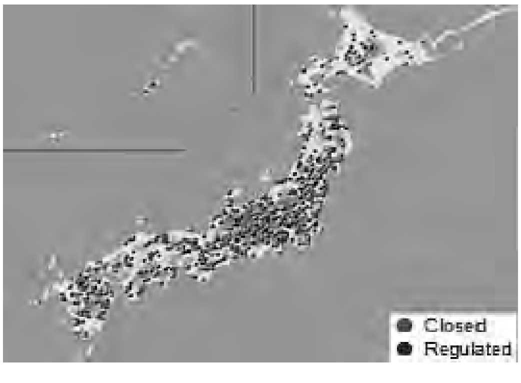

Figure 15: Location of road bridges already closed or regulated in Japan (MLIT, 2011)

Figure 15 shows the location of bridges already closed or regulated due to deterioration. Although disasters caused by deteriorated structures did not happen so often up till today, some structures caused disasters. One of the recent disasters is the collapse of tunnel ceiling happened in December 2012. The ceiling RC slabs of Sasago-Tunnel fell on to the cars running underneath in Chuo-Expressway. The running three cars were smashed and 9 people in the cars lost their lives. It was an unexpected accident for most of the drivers and passengers. The main cause of the disaster was the pull out of the adhesive anchors embedded to the tunnel roof lifting the ceiling slabs. To prevent future disasters, the ceiling RC slabs were removed from all the existing tunnels. If we do not pay much attention to the deterioration of existing structures, similar accidents may occur at any deteriorated structures in the near future.

5. CONCLUSIONS

After the earthquake, some engineers mentioned that “we did not expect to have such a large tsunami attacking the structures”. Although the available standard specifications did not mention about the design considerations when tsunami attacks the structures, the engineers must think about the safety of the people who uses the structures. It is important for the civil engineers to realize how we should keep the structures safe enough for the people or should give the information to what extent the structure can resist against any unexpected situations. To do so, it is important for civil engineers to learn from the disasters already happened and also try to estimate other disasters which may happen in the future. Usually, the civil engineers do their works to meet the available specifications trying to prevent and mitigate the disasters as much as possible. But furthermore, care is needed to anticipate what may happen if the disaster become far larger than the expected and/or with the combination with other disasters. Including the measures for evacuation, preparedness and response are the most important points to be considered even in such cases. After the Great East Japan Earthquake, lots of investigations and research works have been done. We know that any disaster may occur at any time exceeding the expected situation and scale. The civil engineers must always be careful to do their works considering the “worst case scenario” and try to keep the users of the structures safe enough at any situation.

REFERENCES

Concrete Committee of Japan Society of Civil Engineers (JSCE), 2010. *Standard Specifications for Concrete Structures -2007 “Design”.*

Concrete Committee of Japan Society of Civil Engineers (JSCE), 2010. *Standard Specifications for Concrete Structures -2007 “Maintenance”*

Hoskikuma, J., Zhang, G., Nakao, H., and Sumimura, T., 2012. *Researches on behavior of bearing supports in highway bridges under tsunami-induced force*. 28th U.S.-Japan Bridge Engineering Workshop, UJNR, Oct. 2012.

Ishizuka, T., 2013. A landslide dam in Ambon Island, Indonesia and Technical Cooperation by Public Works Research Institute. *The Sabo* 46, 20-22 (in Japanese).

Ishizuka, T., and Osanai, N., 2012. Deep catastrophic landslides and landslide dams in Japan, In *Proceedings of International Symposium on Dams for a Changing World*, 75-80.

Nakao, H., Zhang, G., Sumimura, T., and Hoshikuma, J., 2013. *Numerical assessment of tsunami-induced effect on bridge behavior*. 29th U.S.-Japan Bridge Engineering Workshop, UJNR, Nov. 2013.

Uomoto, T., 2013. *Importance of maintenance for sustainable structures*. ICCS13, Tokyo.

Introduction of an international cooperation program of Japan and Developing Countries

Suguru ISHIGURO, Ph.D.,
Japan Science and Technology Agency (JST),
Department of International Affairs

ABSTRACT

In 1995 the Diet of Japan adopted the "Science and Technology basic law" aiming to transform Japan into a science- and technology- oriented nation. Since then, Science and Technology Basic plans have, in accordance with this law, been drawn up every five year (first to 4th) and other various policies were formulated and measures have been taken.

Among such governmental efforts, one of the international research initiatives is the Science and Technology Research Partnership for Sustainable Development (SATREPS) program. The program is conducted through collaboration with the framework of Official Development Assistance(ODA)'s technical cooperation. Based on the needs of developing countries, SATREPS promote international joint research targeting global issues such as climate change adaptation, low-carbon society, bio-diversity conservation, and disaster prevention and mitigation, with an objective to utilize research outcomes in the foreseeable future.

In the symposium, the framework and current trends of SATREPS will be discussed.

Oral Sessions

Initiative on Quality Management System (QMS) for Myanmar construction company

Aye Mya Cho
Associate Professor, Civil Engineering Department,
Mandalay Technological University, Mandalay, Myanmar
amcho.civil@gmail.com

ABSTRACT

The most important focus of the construction industry is to emphasize that a project to be completed within the predetermined time, quality and cost. The implementation of quality management system (QMS) in construction industry assists improvement of the organizational management system efficiently and effectively with targeted objectives of respective company. Myanmar construction industry has been still trying to enhance its leading role to systematic set up with standardized procedure or process. Not only locally attention on it also internationally focus of it calls for inauguration of quality management system (QMS) to Myanmar companies. This leads to introduce an exemplary way of the QMS in Myanmar construction industry. The main idea of QMS is based on ISO quality family series which provide continuous improvement by using PDCA (Plan, Do, Check, Act) circle. As a short outline it includes four main categories; quality planning, quality control, quality assurance and quality improvement. Under the main considerations requirements on the QMS of a company; detail presentation of mission and vision statement of the company, method of developing the quality management, the quality policy, quality objectives, organization and responsibilities, material purchasing and supplying, control of non conformity, work procedure are presented .

Keywords: quality, quality control, quality assurance, quality improvement, objectives, policy

1. INTRODUCTION

Myanmar has started massive development in construction after the 80s of the 20th century. In the beginning there were a lot of unsystematic approaches to the implementation of construction and companies used the traditional management style under instability of some situations. Today Myanmar reforms all sectors, including the construction industry also. Construction is usually accomplished through the cooperation of the designer, the architect, the builder, site supervisors, HVAC, plumbing, electrical, and other contractors; manufacturers and suppliers of materials and components etc. Implementation of construction is done by team with smoothness of cooperation of them to meet end user's requirements. A number of constructions companies is growing and participating in the creation of the new and modernized country in abreast with others. For their long term competition with them a company requires accreditation. Here setting up the Quality Management System plays in topmost role.

2. QUALITY MANAGEMENT SYSTEM (QMS)

Quality Management System is management system to direct and control an organization with regard to quality. A fully documented QMS will ensure that two important requirements are met:

1. The customers' requirements – confidence in the ability of the organization to deliver the desired product and service consistently meeting their needs and expectations.
2. The organization's requirements – both internally and externally, and at an optimum cost with efficient use of the available resources – materials, human, technology and information.

To fulfill these requirements, the international organizations standardization points out the two considerations to be set up in an organization as follow:

1. needs to demonstrate its ability to consistently provide product that meets customer and applicable statutory and regulatory requirements, and
2. aims to enhance customer satisfaction through the effective application of the system, including processes for continual improvement of the system and the assurance of conformity to customer and applicable statutory and regulatory requirements. The followings are useful terms in QMS.
    (1) Quality: Conforming to the plans, specifications and applicable codes and standards; conformance to the requirements (i.e., meeting the owner's requirements).
    (2) Quality control (QC): Individual activities, such as inspecting and testing, by which conformance to the project specifications is validated.
    (3) Quality assurance (QA): Activities that validate the effectiveness of the quality control.
    (4) Quality management system (QMS): The people and processes in place to ensure that construction meets the owner's requirements.
    (5) Quality management program (QMP): The people and processes in place to ensure that construction meets quality requirements.
    (6) Quality management plan (QMP): The project-specific plan to ensure that quality is outlined in a quality management program.
    (7) Quality management: The application of a quality management system in managing a process to achieve maximum owner satisfaction at the lowest overall cost to the organization while continuing to improve the process.

Myanmar Construction Company has been trying to participate in ASEAN as well as international community with expected standards. This situation calls for companies to be well qualified and accredited. As consequence, companies need individual QMS in their organization. After providing general requirements mentioned above, a company requires providing documentation requirements. These requirements are set up according to the ISO Standards.

3. ISO

ISO (International Organization for Standardization) is the world's largest developer and publisher of International Standards. ISO is a non-governmental organization that forms a bridge between the public and private sectors. On the one hand, many of its member institutes are part of the governmental structure of their countries, or are mandated by their government. On the other hand, other members have their roots uniquely in the private sector, having been set up by national partnerships of industry associations. Therefore, ISO enables a consensus to be reached on solutions that meet both the requirements of business and the broader needs of society.

4. ESTABLISHMENT OF QUALITY MANAGEMENT SYSTEM IN A COMPANY

Firstly, a company should identify the general requirements and documentation requirements in the system, compromising customer requirements with its requirements and shall establish the standards of quality management system, and form it to document, implementing and maintaining it, and continually improving its effectiveness. This study presents four main categories to apply QMS in a company. These are:

(1) Quality Planning
(2) Quality Assurance
(3) Quality Control, and
(4) Quality Improvement

4.1 Quality planning (QP)

The foremost step to set up QMS is to make a plan for a quality system. In this plan a company should express its background in brief, location of the office, and field of operation, mission and vision statement by top management person. The following points are considered in the planning.

1. The director of construction company should write a clear quality policy.
2. Define the objectives of quality management system in some detail.
3. Quality manager must be appointed to direct operations**.** He or she should prepare job descriptions related to achievement of targeted quality and point out the territory of individual managerial responsibilities.
4. Recognition on QMS should be widely spreaded by compromising the needs of the customer and of the company and the system should be clearly defined, understood and operated by all internal, external and third parties.
5. Arrange for audits regularly to find out which operations areas occur potential problems and improve those.
6. Quality improvement programme (QIP) should be designed to achieve established objectives.
7. QIP implementation requires the commitment and involvement of all employees.
8. QIP should be kept to the agreed timetable (monitor progress).
9. Audit and review overall effectiveness. The practical implementation and appropriateness of the quality system should be continually compared with the objectives. A method for changes in the plan should be defined.

The organization will always need to plan and strategize activities with time bound before execution otherwise achievement cannot be measured. Therefore this position is essential for quality management system and the followings are the project manager' responsibilities;

1. Working especially with the project team to schedule activities until delivery and completion
2. Working with procurement officer and construction manager and incorporating their work scope plan into the project schedule
3. Agreeing with customer and fix milestone on project schedules
4. Setting up progress monitoring system and monitor progress on project and making alert to the project team in the case when particular activity is lagging behind
5. Fixing critical path in schedule as project required and advicing strategies to accomplish activities on critical path
6. Planning the organization's implementation of quality management system and working with management representative on review of the system
7. Writing planning and progress monitoring procedure for the continuity of system

4.2 Quality assurance (QA)

Quality assurance covers all activities from design, development, production/ construction, installation, and servicing to documentation, and also includes regulations of the quality of raw materials, assemblies, products, and components; services related to production; and management, production, and inspection processes. This should be done by quality assurance manager assigned in the company. The followings are the responsibilities to do by himself or herself.

1. Distributing roles and duties of the quality control team thereby setting up quality assurance system and reviewing construction procedure to ensure quality performance completeness
2. Overseeing the production of quality inspection plan by designating witness, review and hold points of inspection
3. Reviewing design documents and drawings ensuring that the correct revision is used in construction
4. Discussing and agreeing corrective action on non-conformance with customer representative and verification on implementation of the corrective action
5. Seeing the qualification and certification of employees and labours according to contract requirements
6. Performing surveys on suppliers for their qualification
7. Reviewing and evaluating supplier's quality program for integration into quality management system

4.3 Quality control (QC)

Quality control is a process employed to ensure a certain level of quality in a product or service. The basic goal of quality control is to ensure that the products, services, or processes provided meet specific requirements and are dependable, satisfactory, and fiscally sound. The organization laid more emphases on quality assurance and that is why this position is paramount to quality management system. The quality control engineer has the authority and responsibilities as follows;

1. To check for completeness in inspection and test reports and authenticates them

2. To work alongside QA/QC manager in the preparation of inspection and test plan on construction works and monitors its implementation
3. To review quality records and procedures and later authenticates them for QA/QC manager's approval
4. To take up the role of management representative in steering the quality management system if delegated to do so
5. To attend project quality meetings and advice improvement on quality of work
6. To work with the QA/QC manager for quality assurance of the suppliers

4.4 Quality improvement (QI)

In QMS, continual improvement enhances the organizational capabilities and flexibility to allow it to react quickly to opportunities and to make continual improvement as a permanent objective of the organization. This should be done in a company or an organization by using plan-do-check-act (PDCA) circle as shown in the Figure 1.

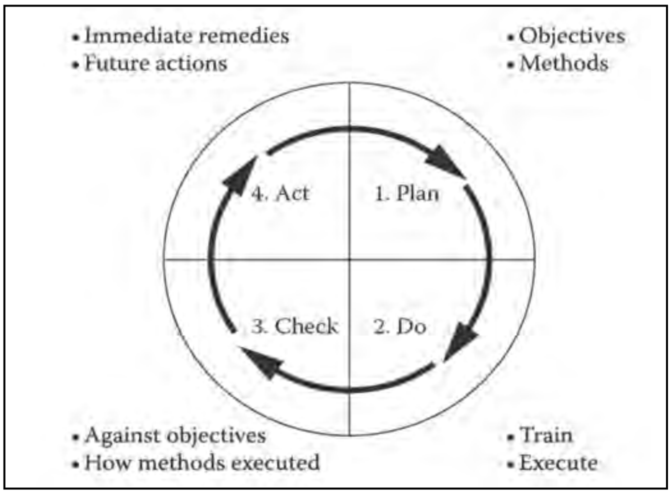

Figure 1: PDCA circle

1. Plan: Establishes the objectives and processes necessary to deliver results in accordance with customer requirements and organizations policies.
2. Do: Implements the processes.
3. Check: Monitors and measures the processes and product against policies, objectives and requirements for the product and report the results.
4. Act: Taking actions to continually improve process performance.

This PDCA circle should use at all phases of construction.

4.5 Findings of quality problems in construction

From the previous surveys, the followings are found as some problems in most of Construction Company.

1. Laying down of impracticable aim and objectives
2. Unclear identification of responsibility and authority for people in it
3. Inadequate Construction Laws and Regulations
4. Lack of awareness in principles, regulation and procedures of project
5. Quality deficiency because of management and skill requirements

6. Insufficient inspection in all parts of construction implementation
7. Extra relationships with unnecessary people in and out of the organization to operate a project
8. Lack of finding poor area of construction and upgrading it to a required level
9. Less applying management techniques to all phases of construction
10. Lack of on-job and off-job trainings

4.6 Ways to cope the problems

Myanmar Construction Industry runs for long time with limited application of international concerns. This leads to dissatisfaction of construction performance by all parties inside and outside the country. Now a day the adaptation of QMS becomes popular demand in Myanmar. The followings are important considerations to initiate QMS in the country.

1. Country-wide well known Construction Organization should be set up.
2. This organization should deliver update procedures, principles, information to all construction companies.
3. Document adequate information about company profile, field of operation, and challenges, etc.
4. Mission and vision statement should be laid down in accordance with availability of resources by company or organization.
5. Organizational structure should be established, providing adequate staff at all levels.
6. Top management team or assigned person should write required policies, manuals, and occasionally update and let all employees know them in time.
7. Top management should ask for report back from lower levels, revise old plans with new, practicable, applicable and beneficial ones
8. Accountability is required by all people at all levels of a company or an organization
9. Project manager, quality assurance manager, quality control manager, etc. should write respective policy, manual and all necessary outlines.
10. Monitoring from resources collection to the completion of construction project is required and provide close control plan for nonconformity with prescribed specifications.
11. A company or an organization must be accredited through internal and external audit.

5. CONCLUSION

Quality management system starts with commitment from the top management presented in the form of a quality policy. Although QMS is initiated by the uppermost management level, it is essential to do works in ever y steps by everybody to effectively move to targeted system implementation, compromising individual requirements and organization’s requirements.

REFERENCES

Adefolalu, O., 2013. *Developing a TQM system for a Company*, Degree Programme in Environmental Engineering.

AS/NZS ISO 9000:2006, *Quality Management Systems – Fundamentals and Vocabulary*.

AS/NZS ISO 9001:2008, *Quality Management Systems – Requirement*.

AS/NZS ISO 9004:2011, *Management for the Sustained Success of an Organization*.

Gašparík, J., 2007. Quality Management Development and Implemetation in Construction Company, 5th Research/Expert Conference with International Participations ”QUALITY 2007”, Neum, B&H, June 06-09, 2007.

Rumane, A. R., 2011. *Quality Management in Construction Projects*, Taylor and Francis Group, LLC.

Tek, O. H., Quality and Value Management in Construction, Achieving Excellence through Value-Managed Quality System (VMQS).

Actual condition and trend of cavity occurrence under Japanese roads in recent years

Ryoko SERA[1], Yutaka KOIKE[1], Yasushi HIRONAKA[2], Haruto NAKAMURA[2]
and Reiko KUWANO[3]
[1] Research-and-development center, Geo Search Co., Ltd., Japan
r-sera@geosearch.co.jp
[2] Disaster reduction department, Geo Search Co., Ltd., Japan
[3] Professor, ICUS, IIS, the University of Tokyo, Japan

ABSTRACT

Road cave-in accidents have been occurring frequently in many parts of the world in recent years. In the wake of multiple road cave-ins in Tokyo in 1988, which became a social issue known as the "cave-in syndrome", regular road cavity surveys were introduced in Japan. At present, road cavity surveys are carried out on the roads that are managed by the national and local governments as measure to prevent road cave-ins. By March 2014 more than 120,000 km of road lanes have been surveyed and more than 25,000 cavities have been found. It is well known that cavities form when soil particles wash away through breakage of degraded sewer pipes, but the frequent natural disasters in recent years, such as heavy rain and earthquakes, and the increase in underground congestion, also contribute to the formation of cavities. This paper summarizes the knowledge about the actual condition and trend of cavities that were found through regular surveys and surveys conducted in recovery efforts following earthquake disasters, and also mentions several survey examples.

Keywords: geotechnical disaster, subsurface cavity, road cave-in

1. INTRODUCTION

In Japan, road cavity surveys started in 1988, because multiple road cave-ins occurred in the Tokyo metropolitan area, which became a serious social issue known as the “cave-in syndrome”. Since then the needs for road surveys as a means to prevent road cave-ins have increased. Presently, a survey system has been established, and continues to evolve. The effectiveness of this system, which was developed by Geo Search, has been very well proven by road surveys all over Japan. The increase in the occurrence of cavities will be inevitable because of further urbanization and higher frequencies of natural disasters, and the cases that road surveys become indispensable will increase.

2. CAUSES OF CAVITY OCCURRENCE AND ITS TENDENCY

2.1 Main Causes of Cavity Occurrence

Cavities are formed by a phenomenon in which small voids expand by washout or consolidation settlement of soil particles in the subgrade. Subsurface cavities formed expand over time under the influence of various factors, some of which are shown in Table 1. When the strength of pavement exceeds its limit, a cave-in ultimately ensues. A more, detailed classification of cavity factors is shown in Table 2. In many cases, some contributing factors influencing each other cause cavities. The general tendency observed of the cavity expansion speed and direction is summarized in Table 3.

Table 1: Classification of contributing factors to the causes of cavities

Contributing Factors	**Phenomenon or Details**
Direct	Buried items, Damaged Bank Protection, etc.
Indirect	Rain Water, Ground Water, Ground, Tide, Earthquakes, etc.
External	Poor Workmanship, Excessive Traffic Loads, Vibration, etc.

Table 2: Detailed classification of contributing factors to the causes of cavities

7 Major Factors	**Details of Contributing Factors**
Washing Out of Soil around Buried Structures	Broken Pipes or Conduits or Manhole Structures or Boxes or Side Ditch, Faulty Pipe Connections, Unplugged Pipe Ends, Leakage in Water Pipes
Consolidation settlement of around Buries Structures	Lack of Backfill Compaction, Inferior Backfill, Influence of Near-by Work or Propulsion Work of Shielding Construction
Related to Large Scale Underground Structure	Remnant of Buried Structures, Water Flowing Pass around Buried Structures
Influence of Rain Water and Ground Water	Influence of Ground Water, and Rain Water Erosion
Earthquake Influence	Settlement Caused by Vibration, Liquefaction
Sucking out from Embankment	Washout of Soil and Sand from Embankment
Others or Unknown Causes	—

Table 3: Cavity expansion speed and expansion direction

Cavity Expansion Speed	**Fast**	←→	**Slow**
Expanding Phenomenon	Washout	←→	Consolidation settlement
Position	Deep (Breakage sewer pipes, etc.)	←→	Shallow (Directly under the Pavement)
Direction of Expansion	Vertical (Upward) and Horizontal	←→	Horizontal

2.2 Frequency of Cavity Occurrence

Figure 1 shows a comparison of cavity occurrence ratios by road administrator classification. The cavity occurrence ratio is defined as the number of subsurface cavities found in 1km of survey distance. This ratio is based on data of 25,642 cavities which were confirmed through the inspection surveys covering a distance 125,043 km of paved roads all over Japan, conducted by the authors from 1988 to 2013. Because of the fact that each road has its specific pavement structure, roadside attribute, and buried items, the conditions that result in cavity occurrence are not the same but depend on geographical location. Buried items are found to have many contributing factors that cause cavities. It is shown that this comparison is related to the quantity of the buried item. National roads have few buried items compared with other roads, resulting in a lower ratio. On the other hand regional roads and roads of government ordinance cities have a higher numbers of buried items such as subways and large-scale underground structures, resulting in a higher ratio.

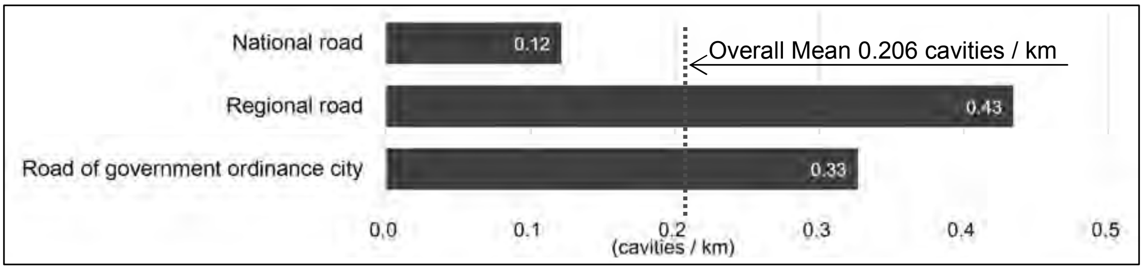

Figure 1: Comparison of cavity occurrence ratio by road administrator classification

3. CAVITIES OCCURRED UNDER NORMAL CONDITION

3.1 Causes of Cavity Occurrences under Normal Condition

Cavities that occur under normal conditions are, as shown in the Table 2, mainly related to buried items and structures underground. According to a report by the Tokyo Metropolitan Government, out of 1,018 cavities confirmed in the surveys from 2001 to 2009, 28% were caused by breakage of sewer pipes and rain water conduits, 32% were caused by inferior backfilling, and 14% were caused by congestion of buried items. It was confirmed that underground structures and items represent a major cause of subsurface cavities in city environments.

3.2 Thoughts on Factors Contributing to Cavity Expansion

Fig. 2 shows the aggregated number of cave-ins per month reported in national newspapers from 1988 to 2013. It shows that cave-ins increase in summer when asphalt becomes softer because of high road surface temperature. It is also reported that in Nagaoka City, Niigata Pref., numerous road cave-ins occurred as temperature rose and snow melted in May of the year following the 2004 Chūetsu earthquake. The paper by Koike et al. (2012) indicated that many cave-ins occurred in the years with many heavy rain days since 1995. It is assumed that the rapid expansion of cavities is caused by repetitive washout of loosened soil by rain water flowing into the underground through broken parts of underground pipes.

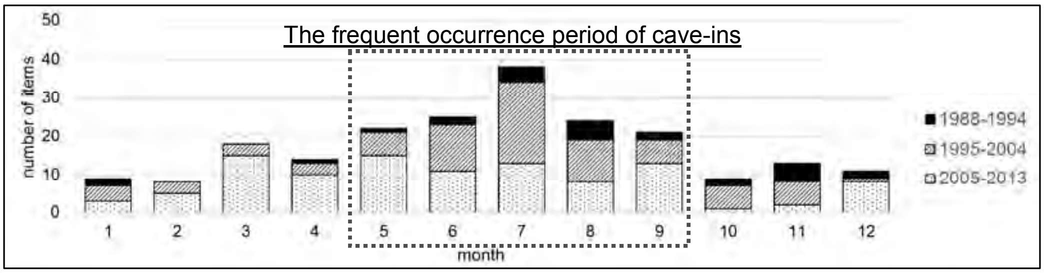

Figure 2: Newspaper reporting of cave-ins by month (throughout Japan)

3.3 An example of a Cavity Caused by a Breakage of Degraded Sewer Pipe

Figure 3 shows an example of an open-cut location to confirm a cavity caused by soil particles washout through a broken sewer pipe. The following explains how the cavity was formed.

(1) No subsidence was observed in the open-cut location at the start of cutting the asphalt pavement.

(2) After removal of the pavement, a small hole appeared.

(3) Loosened parts around the hole were dug out.

(4) Digging proceeded at intervals of about 10 cm and loose soil was confirmed at each interval.

(5) Water was poured through the loose part of the soil surface to confirm the route of water flow, and further digging revealed a ceramic sewer pipe broken at its connecting joint. This digging operation confirmed that the cause of occurrence and expanding of the cavity found was flowing out of soil and sand through a broken sewer pipe connecting joint. The ceramic sewer pipe was of an old type which is now out of use and the connecting joint was broken because of age deterioration.

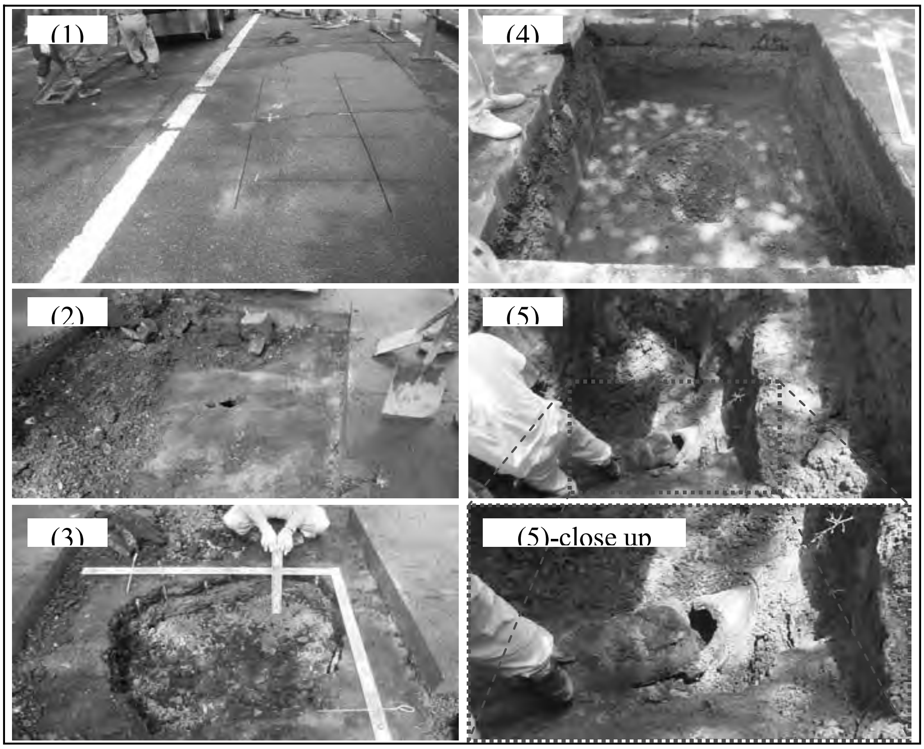

Figure 3: Open-cut investigation of a cavity caused by breakage of sewer pipe

4 CAVITIES CAUSED BY LARGE-SCALE EARTHQUAKES

For those geotechnical disasters where the damage is visible, such as landslides and slope failures, it is relatively easy to execute countermeasures. On the other hand, through investigations other studies have reported that earthquakes frequently cause invisible subsurface cavities. Once those subsurface cavities become apparent by subsidence, cave-ins, etc. countermeasures become possible. However, unrepaired cavities left unattended will surely come up to the surface as time advances. In order to ensure disaster recovery activities, subsurface cavities need to be repaired early. This chapter explains aspects of subsurface cavities with observations based on surveys carried out by the authors immediately after 4 earthquakes larger than 5+ by Japan Meteorological Agency Seismic Intensity Scale (hereinafter referred to as "I_{jma}") that occurred in 5 regional areas as shown in Table 4.

Table 4: Outline of 4 Large-Scale Earthquakes and findings about cavity occurrence

No	**Names (Date)** **Magnitude, Max I_{jma}**	**Topography or use** **Main Disasters**	**Findings about Cavity Occurrence**
1	2004 Chūetsu Earthquake (2004.10.23) M 6.8, Max I_{jma} 7	Mountains and Flats (Sand Ground) Landslide, dike and slope failure	Multiple occurrences where under I_{jma} 5 and around buried items
2	2007 Chūetsu Offshore Earthquake (2007.7.16) M 6.8, Max I_{jma} 6+	Mountains and Flats (Sand Ground) Landslide, dike and slope failure	Around the boundary of cutting and filling of embankment
3	2005 Fukuoka Earthquake (2005.3.20) M 7.0, Max I_{jma} 6-	Port Facilities Destruction of Port Facilities	Relations between section of seawall structure and cavity locations
4	the Great East Japan Earthquake (2011.3.11) M 9.0, Max I_{jma} 7	Mountains and Flats, Urban Area Tsunami, Destroyed Buildings, Road Collapse	Multiple occurrences where under I_{jma} 6 and around buried items
5		Reclaimed Land by Sand Liquefaction, Subsidence	Caused by liquefaction, thin and large areas

4.1 2004 Chūetsu Earthquake and 2007 Chūetsu Offshore Earthquake (Road Damages)

The 2004 Chūetsu Earthquake that occurred on October 23, 2004, and the 2007 Chūetsu Offshore Earthquake that occurred on July 16, 2007 devastated roads by landslides and soil avalanches. In urban areas, soil liquefaction occurred, destroying road surfaces in many locations. Figure 4 shows the I_{jma} maps of both large-scale earthquakes.

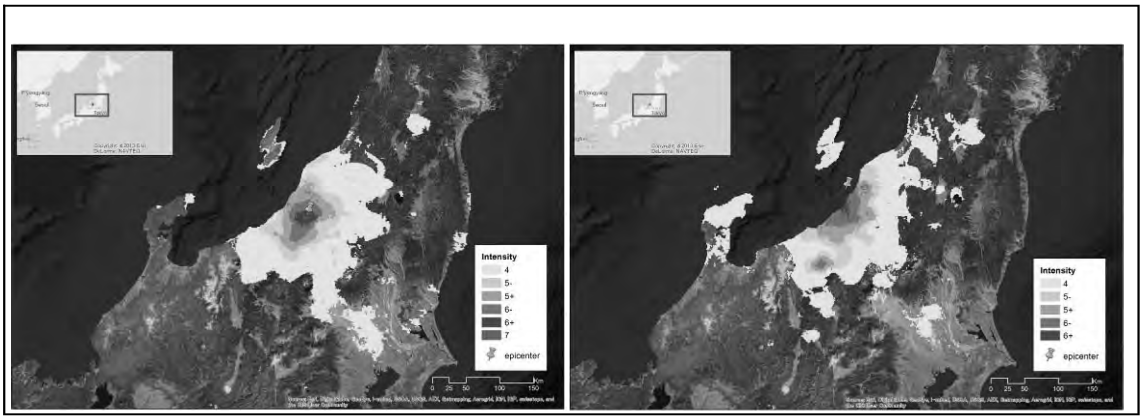

2004 Chūetsu Earthquake 2007 Chūetsu Offshore Earthquake

Figure 4: I_{jma} map of 2004 Chūetsu Earthquake and 2007 Chūetsu Offshore Earthquake

After each of the Earthquakes road cavity surveys were conducted to protect against road cave-ins. Abe et al. (2007) and Yoshikawa et al. summarized facts about what was learned from the surveys. A relation between the I_{jma} and the occurrence of cavities was identified. On roads which were stuck with I_{jma} 5+, the occurrence ratio was 2~8 times larger than normal. In addition, many cavities were found around undeground box culverts and boundaries of cutting and filling of embankment. The fruits of their study are utilized by many as a precious aid for judging the timing and methodology of emergency surveys soon after large-scale earthquakes. Figure 5 shows the typical locations demonstrating cavities that were caused by 2007 Chūetsu offshore earthquake. Cavities were found to develop discontinuously along the boundary line of cutting and filling which is running across the road. Photos of cavities taken through boreholes show that cavities that were found to be irregular in shape, as if they had been formed in sudden collapse of soil. They were different from cavities formed under normal conditions.

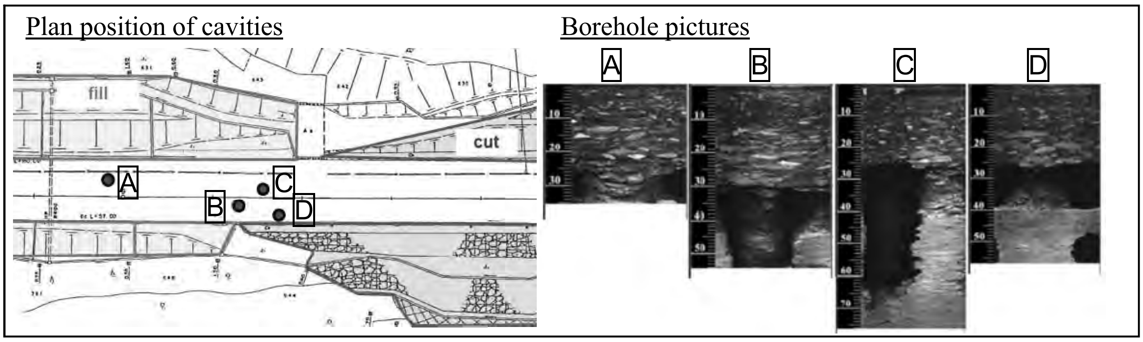

Figure 5: An example of cavities that occurred around the boundary of cutting and filling of embankment (2007 Chūetsu Offshore Earthquake)

4.2 2005 Fukuoka Earthquake (Port Facilities)

The 2005 Fukuoka earthquake of March 20, 2005 is known as one of the large-scale earthquakes. Figure 6 shows the I_{jma} map of this earthquake and a picture taken at the time of recovery work showing pier surface cave-in. Many facilities of Hakata Port were severely damaged by the quake. Liquefaction, cracks, subsidence, uplifting in the pier apron yard, bulging out of the normal lines of seawalls, and cave-ins in the backland were observed. For the purpose of ensuring safety and prevention of cave-ins,

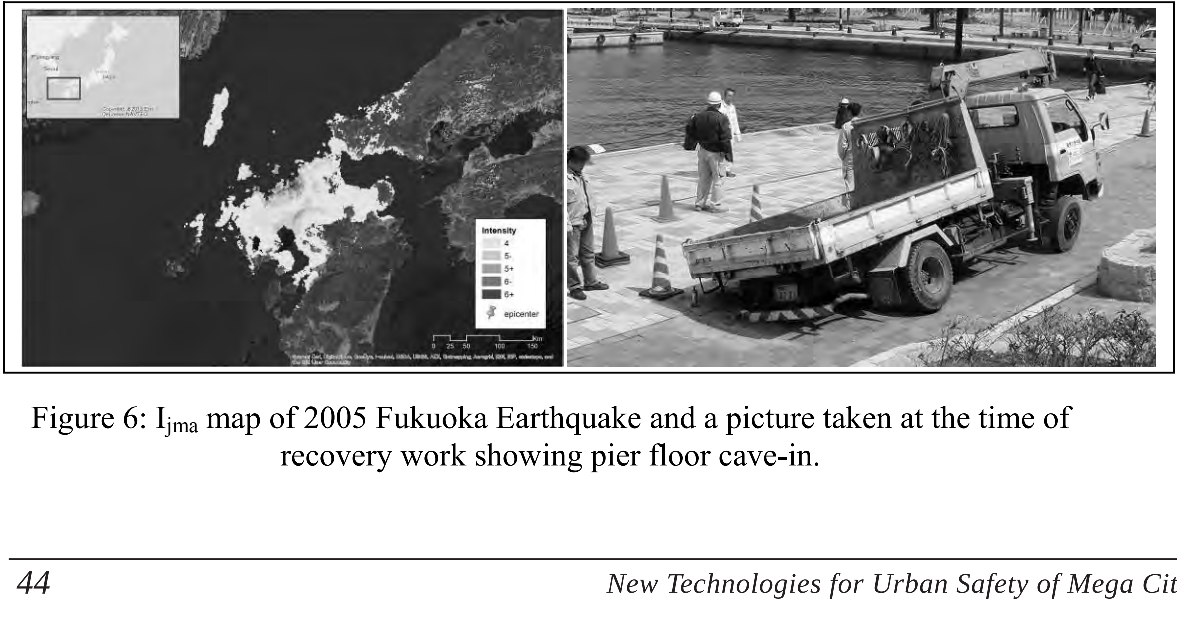

Figure 6: I_{jma} map of 2005 Fukuoka Earthquake and a picture taken at the time of recovery work showing pier floor cave-in.

cavity surveys were started. The recovery works while avoiding unfavorable influence to the cargo loading activities at the port, were completed in 2 years.

Figure 7 shows the relation between the distance from the seawall structure and cavity locations. In case of gravity type, sections where cavities were found showed that the main cause was considered to be the shifting and washout of landfill materials through joints which occurred because of inclination and slippage of the seawall. In case of sheet-pile construction, the main cause was considered to be the uneven gaps between the slab and the ground behind it because of the shifting of the seawall toward the sea.

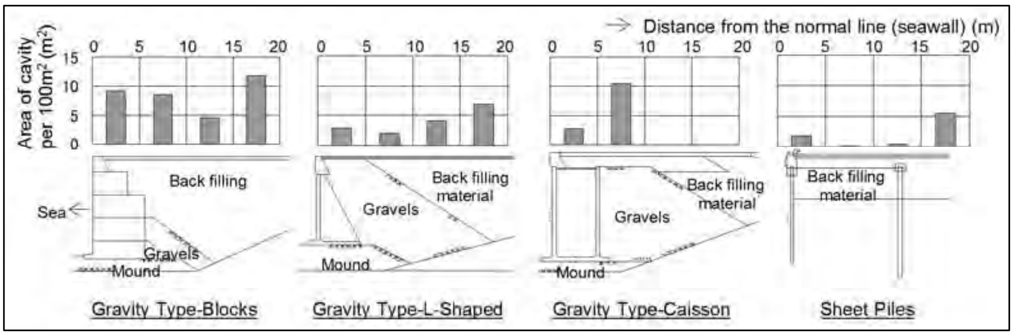

Figure 7: Cross section of seawall and the position of cavity formation (2005 Fukuoka Earthquake)

4.3 The Great East Japan Earthquake (Road Damages)

The Great East Japan Earthquake is the earthquake with the highest I_{jma} since observations began in Japan. It occurred on March 11, 2011 and recorded a magnitude of 9.0 and a maximum I_{jma} of 7. The quake-hit area spread across the Japanese main island from the North East region to the Pacific coast of Kanto region, all of which were extensively damaged by not only a Tsunami, but also by ground liquefaction and subsidence.

4.3.1 Miyagi Prefecture

In Miyagi Pref., which is the region nearest to the epicenter, I_{jma} 5+ was observed. Even 6 months after the Earthquake, more than 3,400 spots of disrupting road traffic were repaired on the roads of Miyagi Pref. By the situation mentioned above, a 5 stage survey of subsurface cavities was motivated. The survey was conducted over a period of 3 years and revealed 1,309 cavities in 1,995 km of roads. The survey was indispensable for securing traffic safety for the disaster recovery activities. Figure 8 shows the I_{jma} map of this earthquake and a picture of the survey conducted in Miyagi Pref.

According to Agatsuma et al. (2014) the cavity occurrence ratio was maximum 4.0 times and area was maximum 1.7 times as large as those under normal times. Figure 9 shows 75% of the confirmed cavities were formed in the vicinities of buried items and manhole structures. It is considered that those cavities are caused by washout of soil through broken parts and loosened by earthquake vibration. Further, heavy rains brought by a typhoon and repeating aftershocks caused large amount of rain water to flow out into the underground and the backfilling soil in the vicinities of pipes was softened.

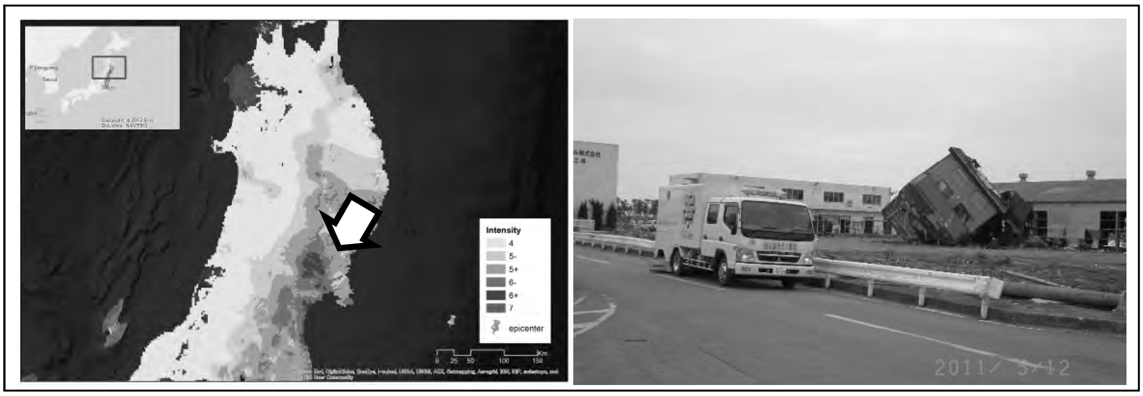

Figure 8: I_{jma} map of the Great East Japan Earthquake and a picture of survey conducted in Miyagi Pref.

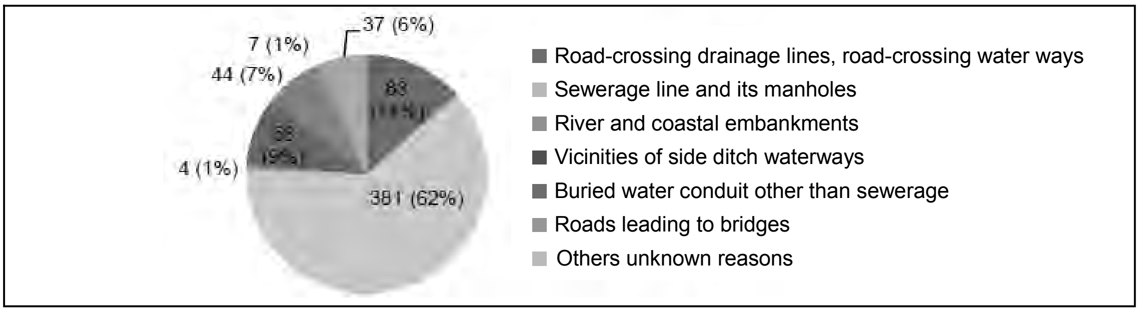

Figure 9: Places of subsurface cavities at Miyagi Pref. (the Great East Japan Earthquake)

The same report analyzes cases of cavity occurrence based on underground vibration and multiple factors. In the result, there were correlations among susceptibility to vibration, degrees of congestion of buried items and rate of sewer damage. Especially in poor subsoil, cavity occurrence ratio and area of cavity tended to be large. The follow-up observation revealed that the expansion of cavities over time and a new fact that, even after the passing of certain period from an earthquake, cavities develop depending on the status of aftershocks and underground soil conditions.

4.3.2 Tokyo Bay Coastal Areas Where Land Liquefaction Occurred

In the Tokyo Bay coastal areas, I_{jma} 5+ was observed. Soil liquefaction was confirmed

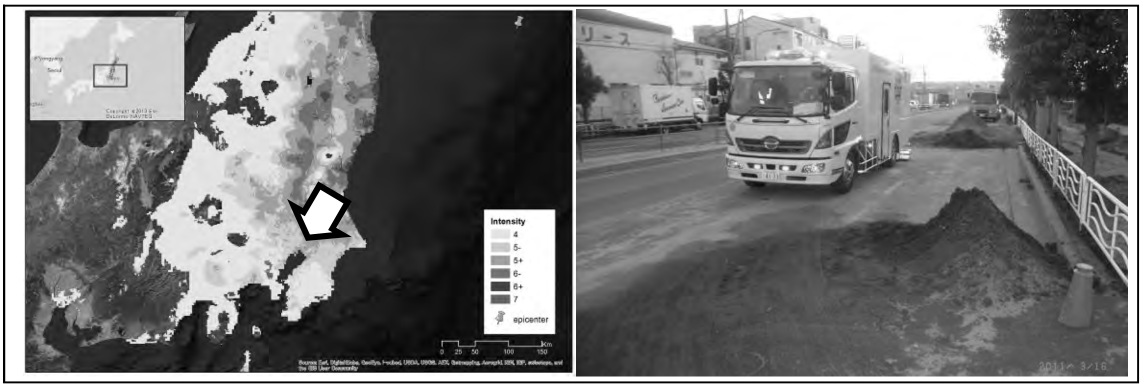

Figure 10: I_{jma} map of the Great East Japan Earthquake and picture of survey conducted in liquefied area along Tokyo Bay coast

ıt

about suspicion of subsurface cavity development. Though it was the first time that a road cavity survey in liquefied areas was conducted, the survey was carried out for the purpose of grasping the actual conditions of roads to ensure traffic safety. Sera et al. (2013) published a fact finding report about the characteristics, conditions, etc. of subsurface cavities in liquefied ground. Figure 10 shows the I_{jma} map and a picture of the survey conducted in the liquefied area along Tokyo Bay coast.

In liquefied ground, cavity occurrence ratio and area of cavity tended to be large and thickness was thinner than in normal times. Many of those cavities found showed the fact that they were formed between the pavement and subbase after the liquefaction phenomena. Figure 11 shows borehole pictures of a “string of cavities” which is one of the characteristics of liquefaction cavities. All the cavities eroded subbase in upward direction wavelike. The fact came out that cavities formed close to gaps around manholes, around the drainage systems, and under pavement joints. Kuwano et al. (2013) elucidated the mechanism of these cavity formations by experiment.

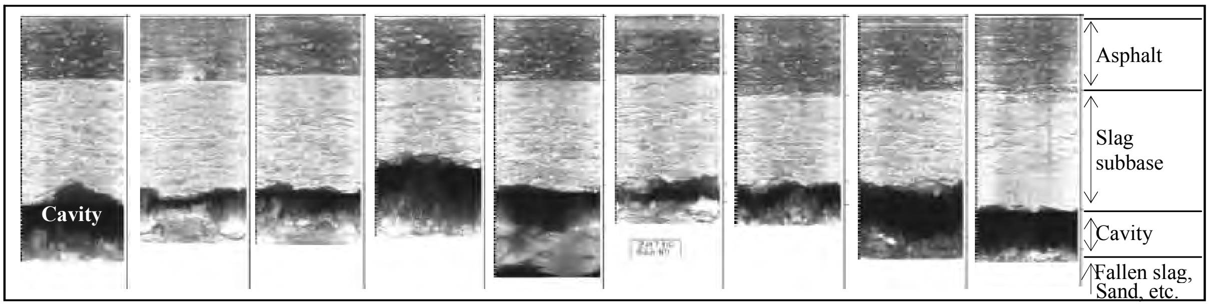

Figure 11: Borehole pictures of a string of cavities in liquefied ground (the Great East Japan Earthquake)

4.4 Summary of Occurrences of Cavities after Large-Scale Earthquakes

In all the above cases, cavities developed after the earthquakes have a tendency to become “thin but covering wide areas” and cavity occurrence ratio was higher as compared with those formed in normal times. Especially in areas which have high contents of sand in the ground, it is considered that cavity developments is susceptible to the vibration from large scale earthquakes. Table 7 below summarizes what is known from the status of cavity occurrences after large-scale earthquakes in 3 areas.

Table 7: Summarization of occurrence situation of cavity after large-scale earthquakes

Earthquakes **Occurrence situation**	**2004 Chūetsu 2007 Chūetsu Offshore**	**2005Fukuoka**	**2011 the Great East Japan**	
			Miyagi	**Tokyo bay**
Earthquakes with I_{jma} 5 or more caused more than 3 times	●	—	●	●
Multiple occurrence	●	●	●	●
Large area and thin form	●	●	●	●
Sandy ground or material of Sand were related	●	●	●	●
New cavities in the same area	●	●	●	○

*) ●: Relevant, ○: Not Investigated, but Highly Possible, —: Irrelevant

5. CONCLUSION

Table 7: Summarization of occurrence situation of cavity after large-scale earthquakes
In the future, with further urbanization and the increase of natural disasters such as earthquakes, there will be more occurrences of subsurface cavities. It is considered that the road cavity survey will become one of the indispensable means for disaster prevention and mitigation, daily road management and the security of road traffic. It is assumed that repair work becomes difficult when many cavities occur at once like after a large-scale earthquake. For the determination of the priority of repair of a huge number of cavities, Miyagi Pref. used a positioning map method for assessing of the degrees of cave-in after the Great East Japan Earthquake. This method, which consists of the depth and area of cavities, enabled to deal with the problem. Based on this assessment, cavities are classified into three steps of countermeasures to be taken: i.e. immediate repair, repair in order of priorities, and follow-up observation. Thus concrete steps for securing traffic security have been taken in a reliable way. Hereafter, with the possibilities of multiple cavity occurrences in mind, it is desired to execute a series of preventive measures against road cave-ins as a part of systematized countermeasures incorporating road surveys and practical repair methods.

REFERENCES

Abe, T., Saika, M., Kusakabe, T., Kichikawa, S., and Fujii, K., 2007. *Management of the road cave-in risk after a large earthquake using subsurface cavity survey technology*. 23rd World Road Congress of the World Road Association (PIARC).

Agatsuma, K., Tobita, Y., Sera, R., Hironaka, Y., Amari, N. and Konno, C., 2014. *Characteristics of subsurface cavities in Miyagi pref. caused by the Great East Japan Earthquake –incidence rate trend analysis-*. The Japanese Geotechnical Society special symposium – overcome the Great East Japan Earthquake, 285-293 (in Japanese).

Koike, Y. and Sera, R., 2012. *Basic Consideration on Occurrence of Sinkhole under Pavement - General Characteristics*. 47th Geotechnical Symposium, 1457-1458 (in Japanese).

Kuwano, R., Kuwano, J., Taira, S., Sera, R., and Koike, Y., 2013. *Model tests simulating sub-surface cavities formed in the liquefied ground.* New Technologies for Urban Safety of Mega Cities in Asia 2013.

Sera, R., Koike, Y., Nakamura, H., Kuwano, R. and Kuwano, J., 2013. *Survey of sub-surface cavities in the liquefied ground caused by the Great East Japan Earthquake*. New Technologies for Urban Safety of Mega Cities in Asia 2013.

Subsurface cavity beneath a buried sewer pipe supported by piles

Reiko KUWANO[1], Jiro KUWANO[2] and Yikiko SAITO[3]
[1]Professor, ICUS, IIS, the University of Tokyo, Japan
kuwano@iis.u-tokyo.ac.jp
[2]Professor, Saitama University, Japan
[3]Ministry of Land, Infrastructure and Transportation, Japan

ABSTRACT

Frequent road cave-ins happened in the area beneath which an old sewer pipe of 2m diameter was laid at a depth of 3m. The sewer pipe was supported by piles. The area was long subjected to significant ground subsidence mainly due to continuous pumping of ground water. Voids and ground loosening were considered to be formed under the foundation of pipe at a depth of 5m because the ground below the sewer pipe seemed to settle at approximately 1m while the ground above the pipe did not follow the settlement. Unlike usual subsurface cavities, the ground penetrating radar exploration technique was not effective as the pulse radar exploration was capable of detecting underground cavities up to 2m deep. Ground investigation including the surface wave survey and the ground penetrating radar exploration from a borehole was carried out to identify location and size of ground cavities and loosening.

Keywords: subsurface cavity, sewer pipe supported by piles, ground cave-in, ground loosening, ground settlement

1. INTRODUCTION

Uneven settlement was observed in the prefectural road. It caused cracks in the asphalt pavement and road cave-ins. Local government officials filled the cave and overlaying asphalt when it repeatedly happened. The subjected area is in front of a hospital, where the traffic of emergency vehicle is often expected. Local government conducted site investigation as well as laboratory tests to identify the subsurface cavities causing cave-ins. This paper describes the results of the investigation and mechanism of sub-surface cavities formation.

2. OUTLINE OF THE OBSERVED PHENOMENON

2.1 Observed phenomenon

At the suburb of Tokyo, surface deformation and frequent cave-ins occurred on one lane of the prefectural road. The damaged area is about 70m long. There is a buried sewer pipe under the lane at a depth of 2 to 4m as shown in Figure 1. Uneven settlement caused cracks and steps in the approach road to the hospital, where emergency vehicles are often passing. Asphalt overlay seemed to be repeatedly conducted at the damage of pavement. Local government became aware of the problem and started to monitor the settlement from 2011, further carrying out site investigation in 2012.

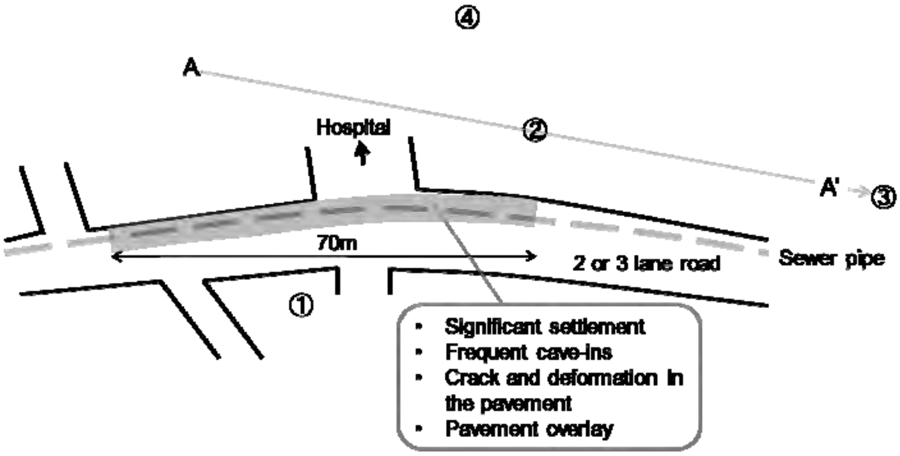

Figure 1: Location of damaged area

2.2 Possible cause for cave-ins

The major reason for the urban road cave-in is usually the failure of buried sewer pipe. Soil around the broken pipe is flown into the pipe and a cavity is formed in the ground. A subsurface cavity expands due to repeated internal erosion and eventually reaches the ground surface (Kuwano et al., 2010). However in this case, according to the observation from inside the sewer pipe, there was no sign of significant damage in the sewer pipe. The buried sewer pipe is 2m in diameter. It seems to sit on a concrete foundation supported by piles, although details are unknown because the construction was so old that no information on the foundation and the piles remained.

The area was widely subjected to the ground settlement. Judging from fences at the pedestrian road adjacent to the area, the degree of settlement can be up to 1m as shown in Figure 2. The shape of the road surface above the sewer pipe is like a horse back, curving down at both sides as shown in Figure 3. It is likely that the pile supported buried pipe did not follow the surrounding settlement and large voids were formed under the foundation of pipe. The estimated mechanism of the subsurface cavity and cave-ins are schematically shown in Figure 4.

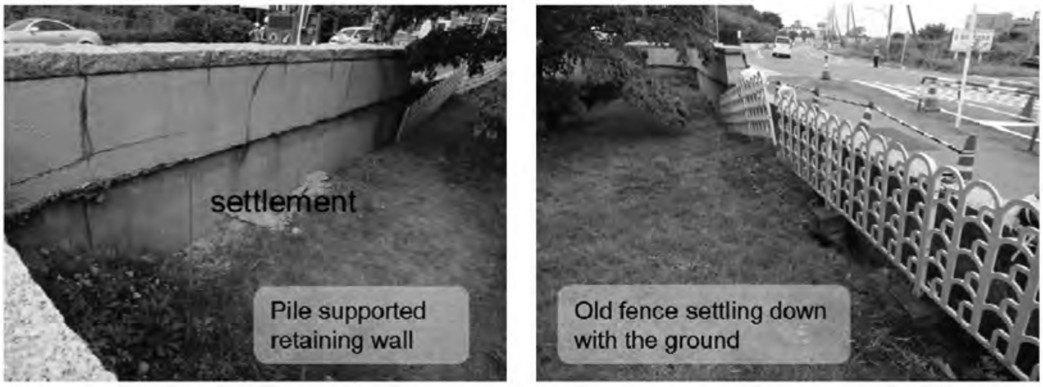
settlement
Pile supported retaining wall
Old fence settling down with the ground

Figure 2: Significant ground settlement in the area

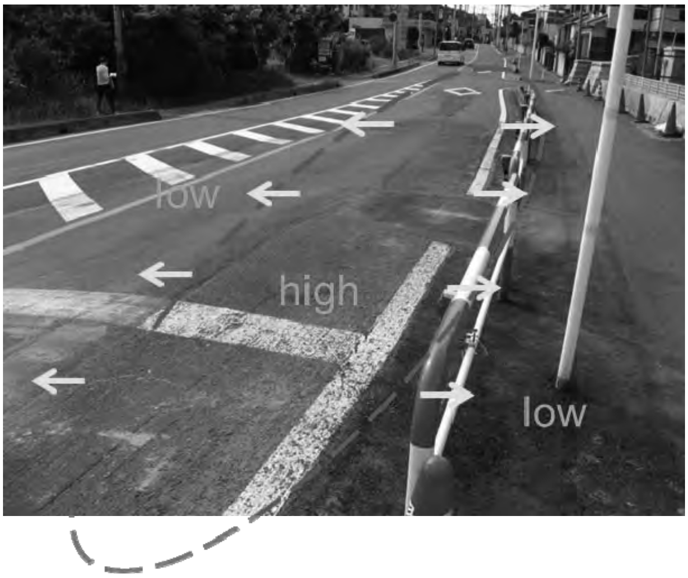
low
high
low

Figure 3: Curved surface of the road

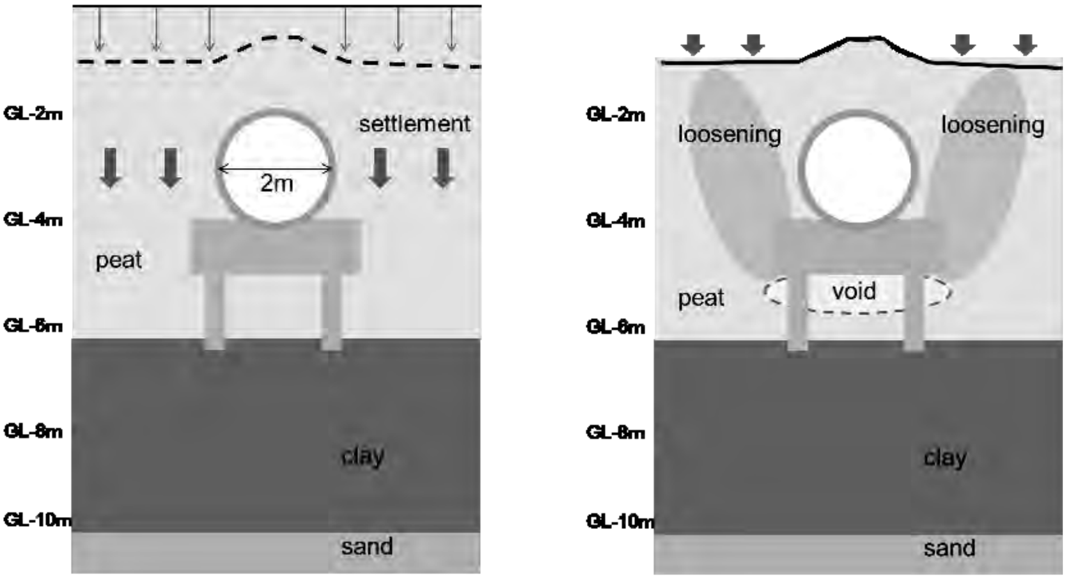
GL-2m
GL-4m
GL-6m
GL-8m
GL-10m
settlement
2m
peat
clay
sand
GL-2m
GL-4m
GL-6m
GL-8m
GL-10m
loosening
loosening
peat
void
clay
sand

Figure 4: Process of subsurface cavity formation

2.3 Site investigation

In order to determine countermeasures for the cave-ins, it is necessary to know the location, size and state of cavities. Area of ground loosening associated cavities should be also obtained. For the detection of subsurface cavities, the ground penetrating radar exploration technique is usually adapted but in this particular case it was not effective as the pulse radar exploration was capable of detecting underground cavities up to 2m deep, while suspected cavities were at larger depth. Ground investigation including the surface wave survey and the ground penetrating radar exploration from a borehole was carried out to identify the state of ground cavities and loosening. Items of investigation are shown in Table 1.

Table 1: Site investigation

	Purpose
Boring	Estimation of ground profile, measurement of ground water level
Settlement monitoring	Measurement of settlement
Sewer pipe inspection	Search for damage in a sewer pipe
Surface wave survey	Estimation of overall loosened area
Borehole radar	Detection of cavity
Soil sampling	Consolidation test to estimate further settlement

3. RESULTS OF INVESTGATION

3.1 Geological profile

Bore holes were conducted at 4 locations, 1 to 4 indicated in Figure 1. Ground profile along the road, line A-A’ in Figure 1, is presented in Figure 5. There are 3 to 5 m thick peat and 5 to 10 m thick Alluvial clay. According to the laboratory test, the consolidation yield stresses for peat and Alluvial clay exceeded effective overburden pressures.

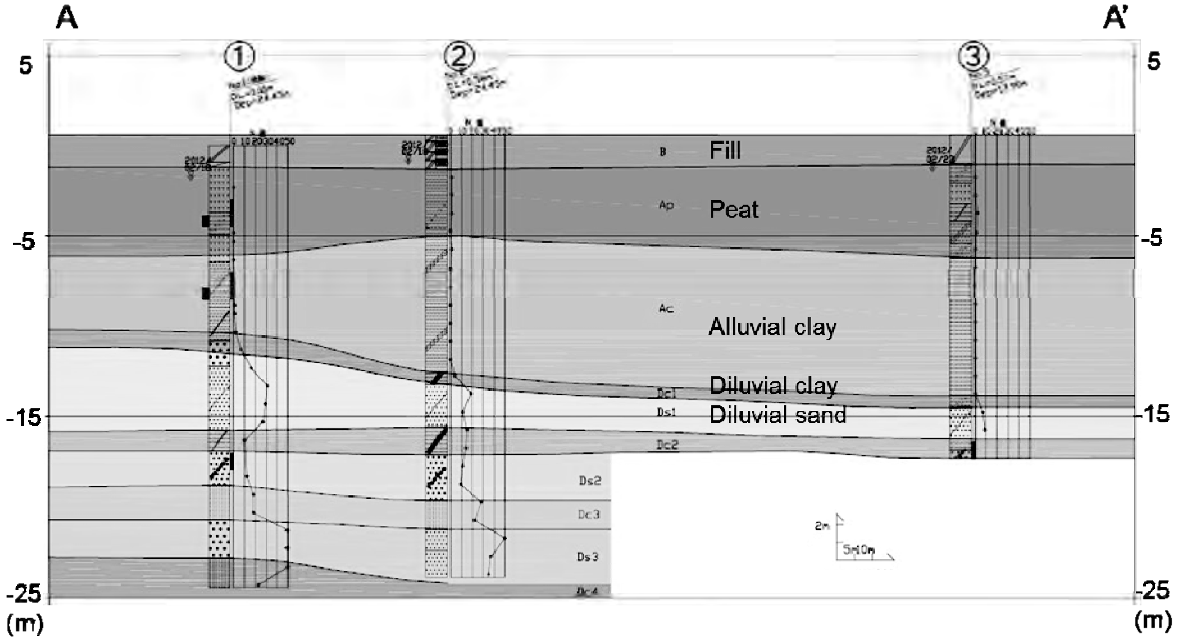
A
A'
①
②
③
5
-5
-15
-25
(m)
B
Fill
Ap
Peat
Ac
Alluvial clay
Dc1
Diluvial clay
Ds1
Diluvial sand
Dc2
Ds2
Dc3
Ds3
Dc4
2m
5m10m

Figure 5: Ground profile for line A-A' (after Sugito land development office, 2012)

3.2 Ground water

Ground water levels measured at borehole 1 to 4 from March 2012 to February 2013 are presented in Figure 6. All are in similar trend but the variation of ground water level at borehole 1 was particularly larger, about 2.5m between maximum and minimum water level. It was found that there are several points where pumping up of ground water was carried out. For example, the amount of pumping near borehole 1 in 2010 was 332m^3.

3.3 Inspection of sewer pipe

The sewer pipe was inspected from inside. No deformation of the pipe was found below the area of damaged road. However at the both ends of damaged road area, sudden change of inclination, step, crack or large settlement of the pipe was observed. These facts imply the sewer pipe was pile-supported only at certain area, about 70m long of the pipe.

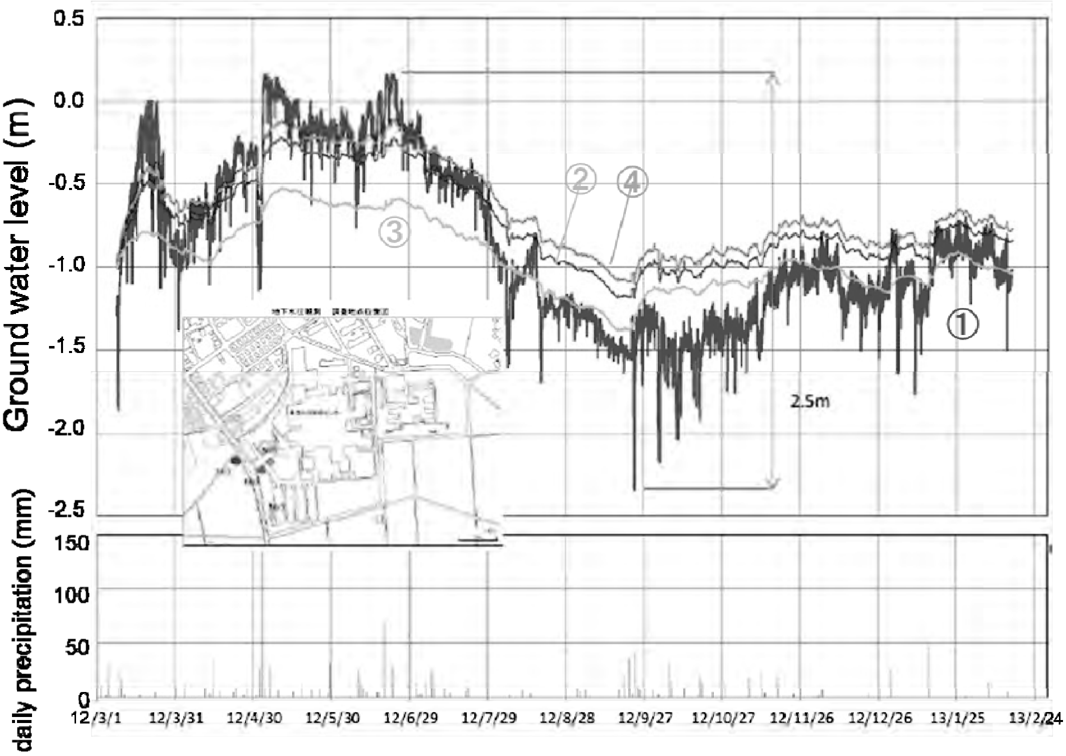

Figure 6: Variation of ground water level (after Sugito land development office, 2013)

3.4 Surface wave survey

A subsurface wave survey was conducted on eight lines, a1 to a8, indicated in Figure 7, in order to obtain the location of underground cavities and ground loosening. Lines a1 to a3 are along the road, while lines a4 to a7 are normal to the road. The profile of S wave velocities at lines a1 to a3 is shown in Figure 7. The S wave velocities are between 200 and 250 m/s. There is a layer in which S wave velocity is more than 300m/s on the surface. This is probably overlaid asphalt for the repair of damaged pavement. Areas of low S wave velocities are also observed in a1 and a2. Those are possibly loosening of the ground.

The results obtained from lines a1 to a3 are presented as S wave velocity distribution at the elevation up to GL-6m in Figure 6. GL-0.8m, GL-3.1m and GL-5m represents the depth above, at the center and below the sewer pipe respectively. Figure 8 indicates that the area of low S wave velocities is spread at GL-5.0 to 5.5m, where voids or loosened ground may exist.

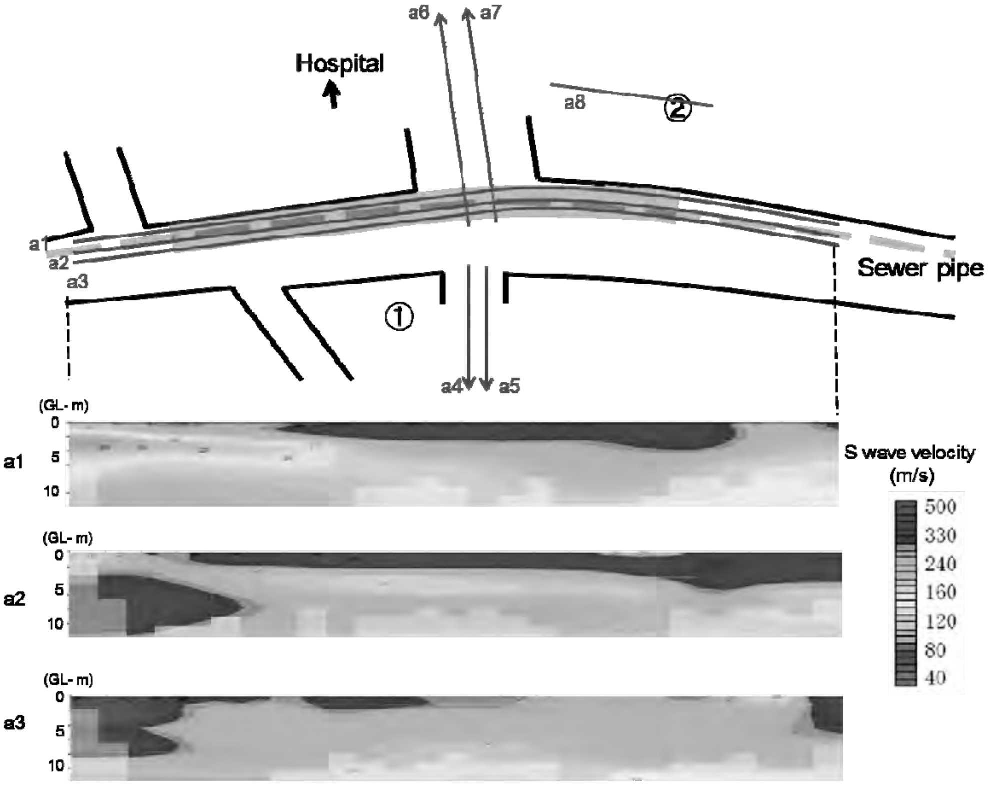
a6
a7
Hospital
a8
②
a1
a2
a3
Sewer pipe
①
a4
a5
(GL- m)
0
5
10
a1
a2
a3
S wave velocity
(m/s)
500
330
240
160
120
80
40

Figure 7: Measurement lines for surface wave survey and the results obtained for lines a1, a2 and a3 (Sugito land development office, 2012)

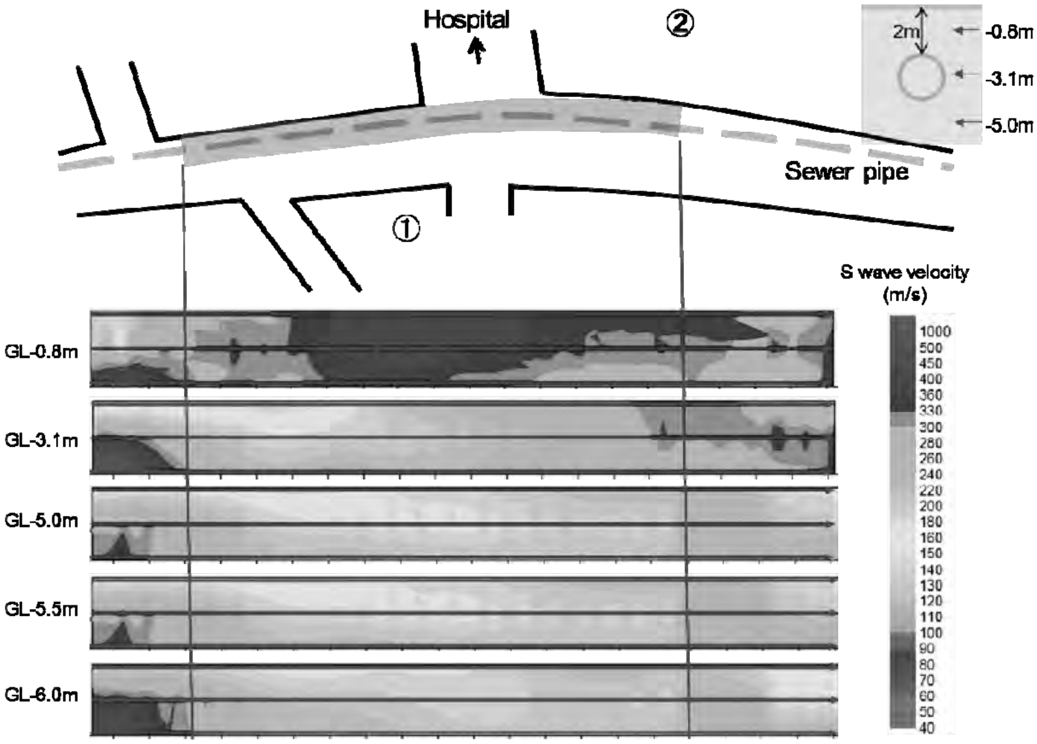
Hospital
②
2m
-0.8m
-3.1m
-5.0m
Sewer pipe
①
S wave velocity
(m/s)
GL-0.8m
GL-3.1m
GL-5.0m
GL-5.5m
GL-6.0m
1000
500
450
400
360
330
300
280
260
240
220
200
180
160
150
140
130
120
110
100
90
80
70
60
50
40

Figure 8: S wave velocity distribution at lines a1 to a3 (Sugito land development office. 2013)

3.5 Borehole radar investigation

Ground penetrating radar survey was conducted from two boreholes, B1 and B2, indicated in Figure 9. The boreholes were excavated beside the pipe foundation, 1.9m from the pipe center for B1and 1.75m from for B2. The results gave the information on the location of several characteristics points, such as ground water level, pipe center, top and bottom of foundation and tip of pile. There were some sign of ground loosening in the results obtained at B2. A 10cm thick void was also observed below the pavement at B2.

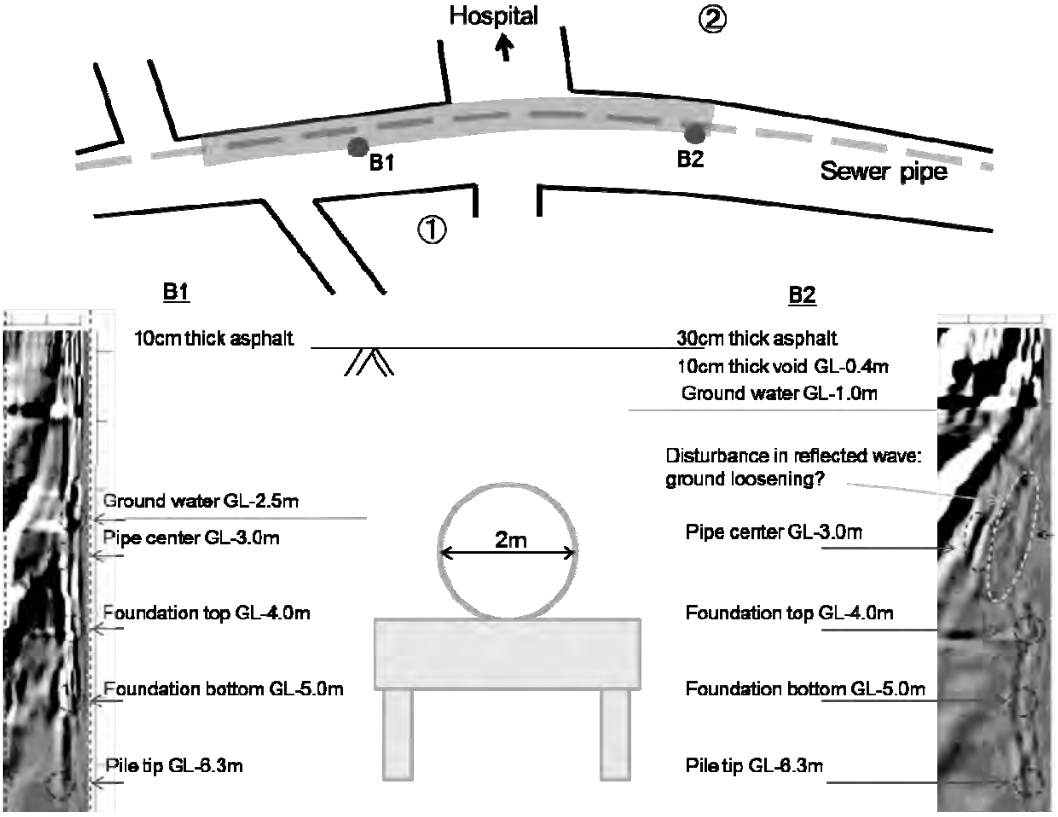
Hospital
②
B1
B2
Sewer pipe
①
B1
B2
10cm thick asphalt
30cm thick asphalt
10cm thick void GL-0.4m
Ground water GL-1.0m
Disturbance in reflected wave: ground loosening?
Ground water GL-2.5m
Pipe center GL-3.0m
2m
Pipe center GL-3.0m
Foundation top GL-4.0m
Foundation top GL-4.0m
Foundation bottom GL-5.0m
Foundation bottom GL-5.0m
Pile tip GL-6.3m
Pile tip GL-6.3m

Figure 9: Ground penetrating radar survey from boreholes (Sugito land development office, 2012)

4. SUMMARY

Frequent road cave-ins happened in the area beneath which an old pile-supported sewer pipe of 2m diameter was laid at a depth of 3m. The area was subjected to significant ground subsidence mainly due to continuous pumping of ground water. Voids and ground loosening were considered to be formed under the foundation of pipe at a depth of 5m because the ground below the sewer pipe seemed to settle at approximately 1m while the ground above the pipe did not follow the settlement. Unlike usual subsurface cavities, the ground penetrating radar exploration technique was not effective as the pulse radar exploration was capable of detecting underground cavities up to 2m deep. Ground investigation including the surface wave survey and the ground penetrating radar exploration from a borehole was carried out to identify location and size of ground cavities and loosening. It was found that the surface wave survey was helpful to obtain the approximate area of loosened ground. The inspection of the sewer pipe also indicated the section of sewer pipe which gave damage in the ground. Based on the investigation, it became possible to consider the countermeasure for the further cave-ins.

5. ACKNOWLEDGEMENTS

We greatly appreciate Dr. Sekiguchi, former director, and other staffs of Sugito Land Development office who provided valuable data set of site investigation conducted by OYO Corporation.

REFERENCES

Kuwano, R., Sato, M., and Sera, R., 2010. Study on the detection of underground cavity and ground loosening for the prevention of ground cave-in accident, *Japanese Geotechnical Journal* 5, 219-229.
Kuwano, R., Horii, T., Yamauchi, K., and Kohashi, H., 2010. Formation of subsurface cavity and loosening due to defected sewer pipe, *Japanese Geotechnical Journal* 5, 349-361.
Sugito land development office, 2012. *Document for the first meeting, June 5, 2012.*
Sugito land development office, 2012. D*ocument for the second meeting, October 15, 2012.*
Sugito land development office, 2013. D*ocument for the third meeting, March 12, 2013.*

Prevention of lateral movement and reinforcement of substructures on soft ground

Yukitake Shioi
Emeritus Professor,
Hachinohe Institute of Technology,
Hachinohe, Aomori, Japan
yshioi@blue.plala.or.jp

ABSTRACT

In Myanmar, there are many new bridges on soft ground, which are suffered dependent on the horizontal movements of substructures by the lateral flow of soft soils and the tensile force from cables of suspension bridges. The lateral flow of soft soil is caused by the weight of backfill behind the abutment. The movement of the anchorage of suspension bridge by the creep phenomenon depends on its weak foundation. These movements of substructures may cause superstructures to fall, piers to incline a large amount of compression to the beams to be inclined, spaces between beams to be lost, the seismicity to deteriorate and so on. These movements shorten the bridge's lives. It is necessary to consider a design that prevents such movement. The author indicates several methods for preventing or mitigating the lateral flow based on experiences in Japan. Furthermore, he proposes recovery and reinforcement methods for these deformed bridges. Since accidents of bridges damage the function of the entire route and require a long time and money to restore, the soundness and the long life of a bridge are very important.

Keywords: bridge, soft ground, horizontal movement, lateral flow, substructure

1. INTRODUCTION

In Myanmar, many new bridges have been constructed on four major rivers in the last 25 years, as shown in Figure 1. The main bridges are situated on soft ground along these rivers. They are suffered depending on the horizontal movements of abutment by the lateral flow of soft soils and the tensile force from cables of suspension bridges.

These movements of substructures may cause superstructures to fall, piers to incline, a large amount of compression to the beams to be induced, spaces between beams to be lost, the shoes to break, seismicity to deteriorate and so on. These movements deteriorate not only the function of bridges but also shorten their lifespan.

This paper indicates the mechanism of lateral flow on soft ground. Then, it shows measures to prevent such movement. Furthermore, it demonstrates methods for recovering and reinforcing the abutments or anchorages that were moved.

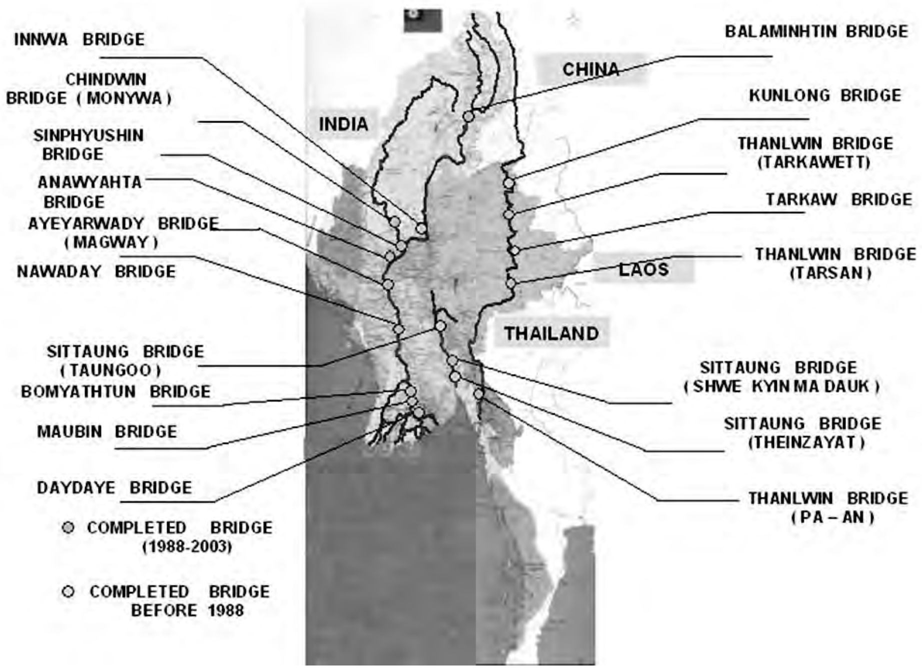
INNWA BRIDGE
CHINDWIN BRIDGE (MONYWA)
SINPHYUSHIN BRIDGE
ANAWYAHTA BRIDGE
AYEYARWADY BRIDGE (MAGWAY)
NAWADAY BRIDGE
SITTAUNG BRIDGE (TAUNGOO)
BOMYATHTUN BRIDGE
MAUBIN BRIDGE
DAYDAYE BRIDGE
◎ COMPLETED BRIDGE (1988-2003)
○ COMPLETED BRIDGE BEFORE 1988
INDIA
CHINA
LAOS
THAILAND
BALAMINHTIN BRIDGE
KUNLONG BRIDGE
THANLWIN BRIDGE (TARKAWETT)
TARKAW BRIDGE
THANLWIN BRIDGE (TARSAN)
SITTAUNG BRIDGE (SHWE KYIN MA DAUK)
SITTAUNG BRIDGE (THEINZAYAT)
THANLWIN BRIDGE (PA – AN)

Figure 1: Completed main bridges on four major rivers (after 1988)

2. MECHANISM OF LATERAL FLOW AND ITS BEHAVIORS

The phenomena of lateral flow on very soft ground take place according to the weight of distributed surcharge. In the case of bridges, abutment on soft ground moves forward and the front ground heaves up by the backfill behind despite the regular pile foundation, because soft clay under the footing causes plastic flow laterally as in Figure 2. Then, the backfill sinks gradually.

This plastic flow acts on the pile foundation equally and each single pile moves parallel and horizontally together with the clay layer, since the rigidity of long pile is not so strong. This phenomenon is a kind of equilibrium state of soft clay layer versus the change of the surrounding loads.

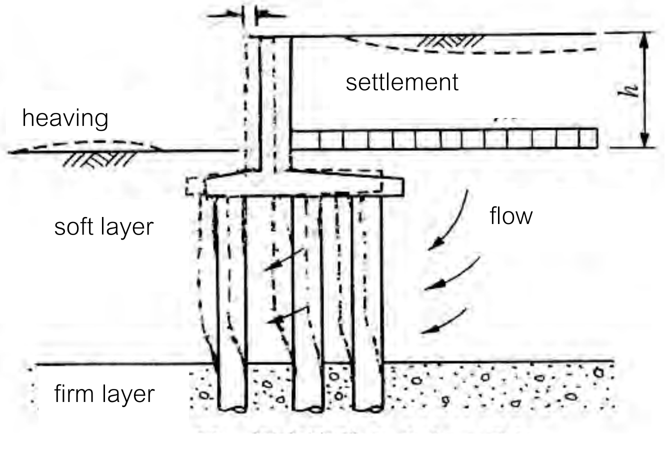
settlement
h
heaving
soft layer
flow
firm layer

Figure 2: Concept of lateral flow

To evaluate this phenomenon the following criteria is useful.

$$1.0 \geqq \lambda \cdot \gamma h/c \qquad (1)$$

Where,

λ : safety factor (1.2～1.5)
γ : unit weight
h: height of backfill
c: cohesion of soft layer

It depends on the relationship between the weight and the ground's strength. However, since the deformation of this phenomenon continues for a long time similar to the secondary settlement of soft clay, a large safety factor is preferable.

3. EFFECTS TO BRIDGES

The lateral flow of the soft clay layer damages the superstructure and the substructure of actual bridges on soft ground. The superstructure loses the interval of expand joints and its bearing shoes are damaged. Then, uncalculated large compression stresses are introduced in the beams or the slab and it encounters a dangerous situation in certain cases. In case of the substructure, since the maximum bending moment depending on lateral flow generates at the lower part of the pile where the stress is relatively small, the damage is not so fatal. However, the subsidence of the backfill resulted from lateral flow causes a gap between the bridge and the access road to disturb the comfortable running. Figure 3 shows Maubin Bridge near Bassein south-west in Myanmar. It is a four-span

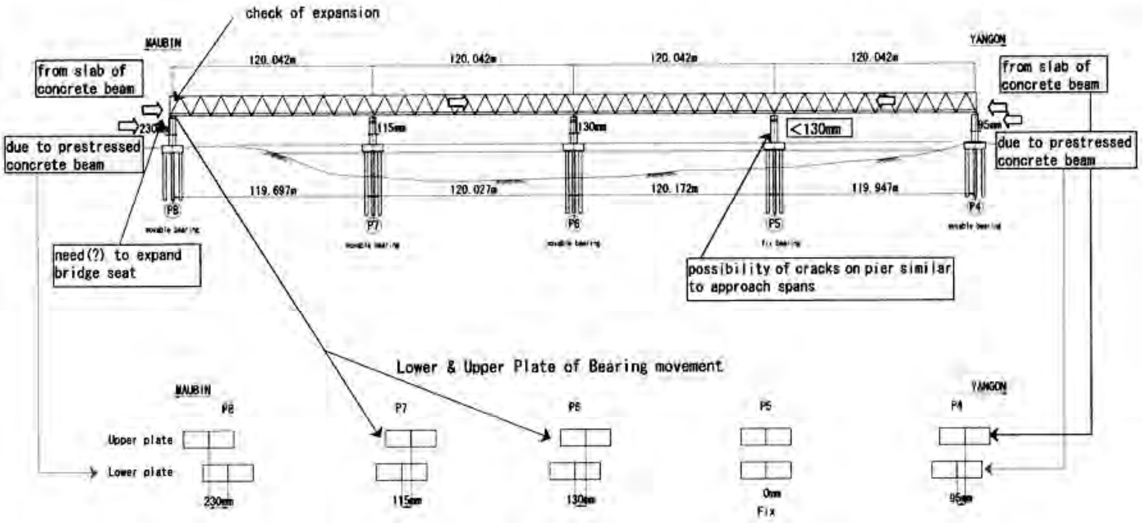

check of expansion
MAUBIN
YANGON
120.042m
120.042m
120.042m
120.042m
from slab of concrete beam
from slab of concrete beam
230mm
115mm
130mm
<130mm
95mm
due to prestressed concrete beam
due to prestressed concrete beam
119.697m
120.027m
120.172m
119.947m
P8
movable bearing
P7
movable bearing
P6
movable bearing
P5
fix bearing
P4
movable bearing
need(?) to expand bridge seat
possibility of cracks on pier similar to approach spans
Lower & Upper Plate of Bearing movement
MAUBIN
YANGON
P8
P7
P6
P5
P4
Upper plate
Lower plate
230mm
115mm
130mm
0mm
Fix
95mm

Figure 3: Lower & upper plate positions of bearing on piers of Maubin Bridge

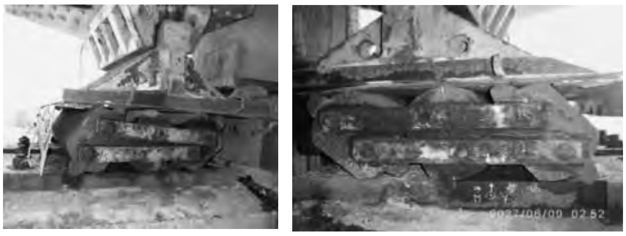

Photo 1: Deformed locker shoes on end pier

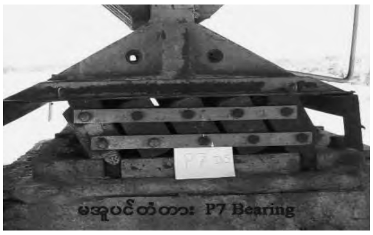

မအူပင်တံတား P7 Bearing

Photo 2: Deformed shoe on pier 7

continuous truss bridge supported by pile foundations. It receives strong horizontal force from both sides but the force from the left side exceeds the force from the right side.

The left end pier creeps forward together with the piers of approach short span bridges by lateral flow due to the backfill. The end of the truss beam end come in close contact with the parapet wall of pier through deformation of the bearing shoes in Photo 1 and the pier pushing the whole continuous truss toward the right side. Then, the bearing shoes on other piers were deformed as in shown Photo 2 and a few cracks appeared on the sidewall of the pier with the fixed shoes. Such conditions are observed in many places.

Furthermore, similar phenomena generate changes in the topography. Figure 4 shows changes to the riverbed at Thakyut Bridge site near Yangon. The topography of the riverbed at the site changed after the completion of the bridge in Figure 4. By this change, bearings on the piers on the left side moved as shown in Photo 3. The geology at the site is illustrated in Figure 5. The layer of very soft clay is deposited up to a depth of 60 meters. Thus, lateral flow occurs not only by artificial embankment but also by natural changes to the land.

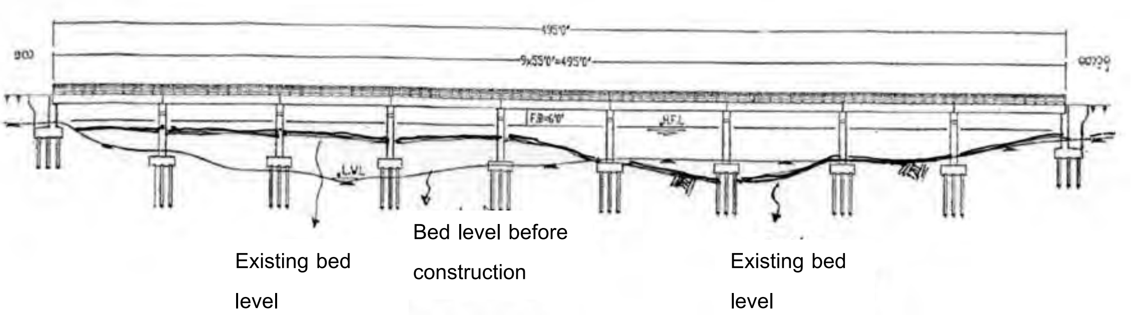

Figure 4: Thakyut Bridge site

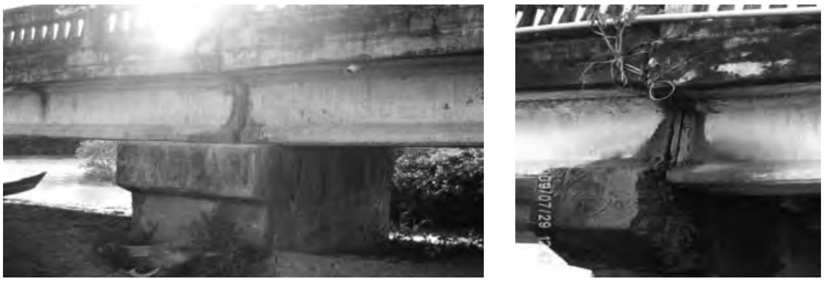

Photo 3: Displacements of beams at Thakyut Bridge

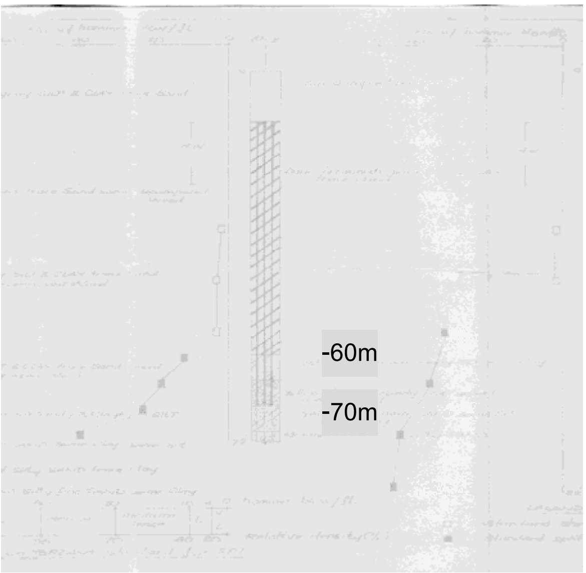

Figure 5: Geology at Thakyut Bridge

4. PREVENTATIVE MEASURES FOR DAMAGE FROM LATERAL FLOW

The orthodox method of abutment on soft ground is implementing measures that sustain the weight of the backfill and transfer its load to bearing stratum or the intermediate layer to escape the impact of lateral flow. Figure 6 indicates the method for sustaining backfill with gravel drain piles or sand compaction piles or sand drain piles via sand mats. They have three major functions. The first is sustaining power. The second is evacuating excess pore water pressure in clayey layers. The third is the horizontal shear resistance of P tan ϕ (P: vertical load in piles, ϕ : internal frictional angle in piles). In this case, although a small subsidence of road surface may occur due to the consolidation of soft clay, it is possible to recover the level of pavement easily. Instead of these sandy piles, adopting palm tree piles which are porous and have moderate strength (in Figure 7) may be considerable. Although the displacement of abutment and the heaving height decrease greatly, it is difficult to expect the complete prevention of movement by lateral flow, because a part of settling backfill not sustained by piles presses the soft soil and the pressed soft soil passes through the piles. If palm tree piles do not reach a firm layer, the weight of the backfill disperses downward from the bottom of the pile group. The impact of lateral flow may be reduced due to the deep loading level.

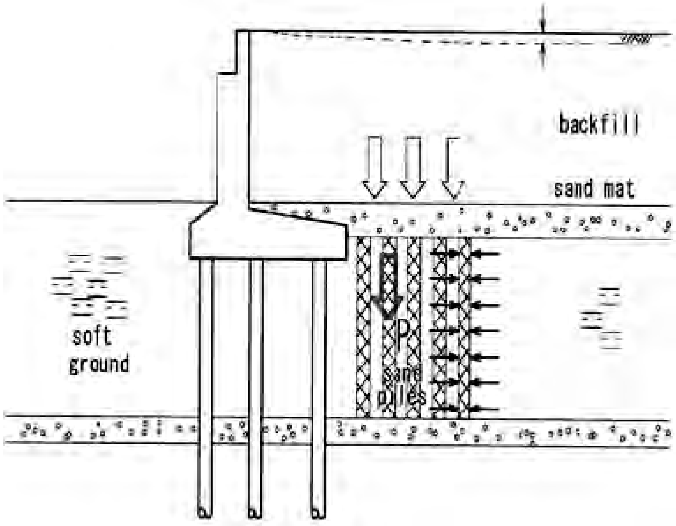
backfill
sand mat
soft ground
P
sand piles

Figure 6: An example to sustain backfill with sand

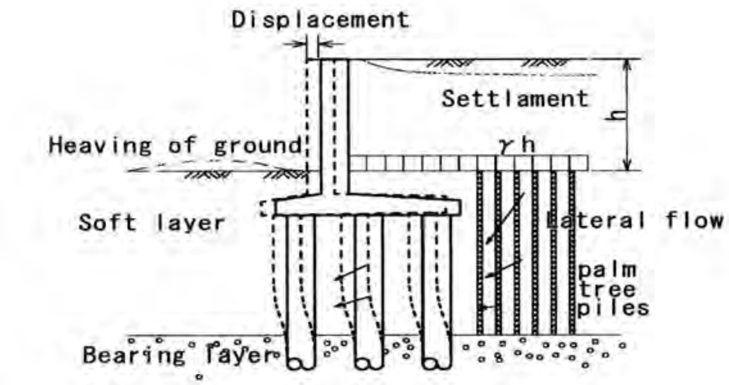
Displacement
Settlament
h
Heaving of ground
γh
Soft layer
Lateral flow
palm tree piles
Bearing layer

Figure 7: An example to sustain backfill with palm tree

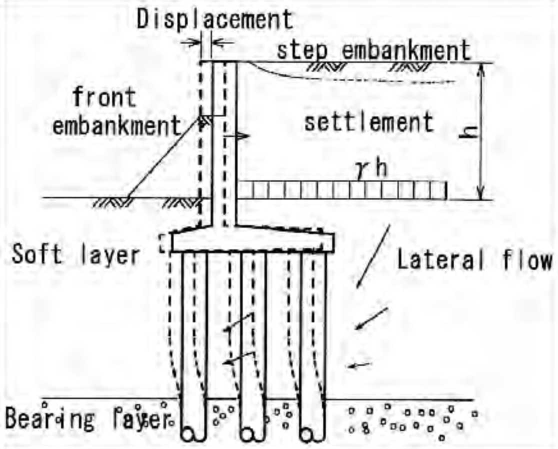
Displacement
step embankment
front embankment
settlement
h
γh
Soft layer
Lateral flow
Bearing layer

Figure 8: Front embankment and backfill

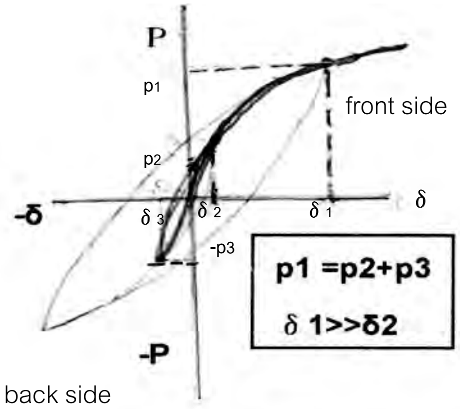

Figure 9: Hysteresis curve of soft ground

As an easy method, the precedence of the front embankment prior to the backfill is effective in Figure 8. In this case, the embankment of the backfill should be constructed step-by-step observing the surrounding deformations. The movement of soft ground is roughly illustrated in Figure 9. Firstly, soil moves to the left and lower section (backward) to the front embankment and then it goes toward the right and upper section (forward) by the backfill. The displacement δ 1 by the backfill p1 decreases to δ 2 + δ 3 and the actual displacement becomes δ 2.

5. REINFORCEMENT METHOD FOR EXISTING DEFORMED STRUCTURES

5. 1 Abutment

There are many bridges on soft ground by the lateral flow in Myanmar. They are being repaired by the method shown in Figure 10 or the expansion of the bridge seat (Photo 4). It is the correct way to clear the backfill and to reset the bearing shoes. Then, it is necessary to improve the soft ground under the backfill or to extend the superstructure as the approach viaduct up to a low height. In these cases, traffic will be stopped during construction. The way to widen the bridge seat and reset the bearing shoes is a short-term measure for the lateral flow since that movement continues for a long time as the secondary consolidation settlement of clay.

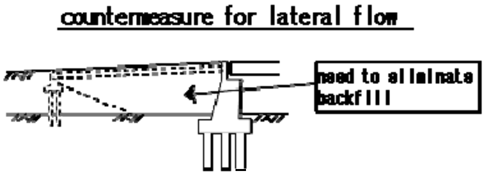

Figure 10: Eliminating backfill and extending the superstructure

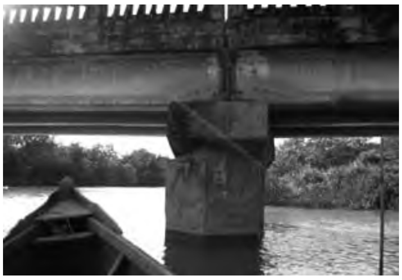

Photo 4: Expansion of bridge seat

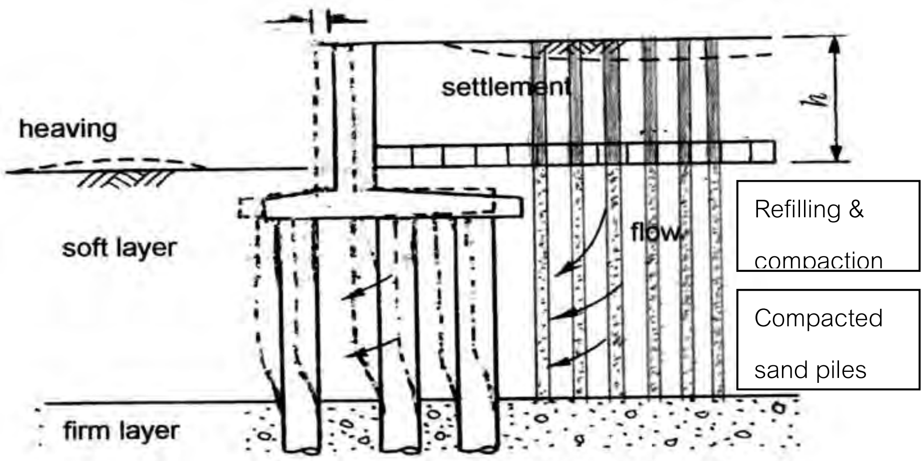

Figure 11: Recovering method for abutment that was moved by lateral flow

In order to reinforce the soft ground under the backfill without blocking traffic, there is a method to penetrate piles (gravel pile, sand compaction pile, palm tree pile, other precast piles) into the soft ground from the road surface to a relatively firm layer and to refill the holes in the backfill firmly with reliable materials. In this case, it is possible to construct them on each lane one after another. This method is applicable to stop or to decrease the continuous displacement of the abutment by lateral flow. Then, another method, known as the CCP (chemical churning pile) method, is used for the same purpose in Japan. It is a method that forms long pile in the ground with rotational nozzle of high-pressure chemicals or cement mortar. It is a little somewhat expensive.

5. 2 Anchorage of suspension bridge

The anchorages of suspension bridges on soft ground in Myanmar are constructed on cast-in-place pile foundations. Therefore, most of them suffer damage because of the horizontal displacement of anchorage due to the large tensile force of the main cable. This displacement will gradually continue for a long time and will cause the towers to lean slowly and collapse by buckling. Actually, the stiffening truss is increasing its sag at the center span. Furthermore, the increasing stress at the pile head is anxious by that displacement. Figure 12 shows side view of suspension bridge with the central span of about 250 meters, Pathein Bridge near Bassein. Photo 5 indicates that the bridge and the towers have leaned. The horizontal displacement of the left anchorage is 8 cm inward and also the right one is 12 cm inward. Now, although it is still open to traffic, early measures are required since this route is very important.

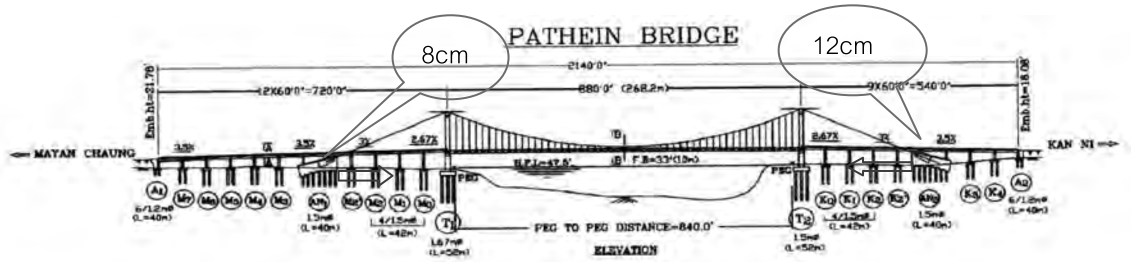
PATHEIN BRIDGE
8cm
12cm
2140'0"
12X60'0"=720'0"
880'0" (268.2m)
9X60'0"=540'0"
Emb.ht=21.78'
Emb.ht=18.08'
MAYAN CHAUNG
KAN NI
3.5%
3.5%
2.67%
2.67%
2.5%
PEG
T1
T2
A1
A2
PEG TO PEG DISTANCE=840.0'
ELEVATION

Figure 12: Side view of Pathein Bridge

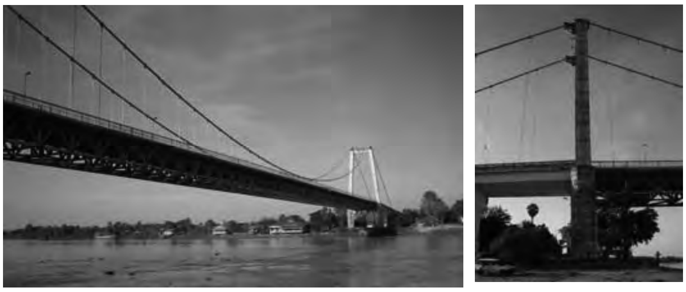

Photo 5: Pathein Bridge and its tower

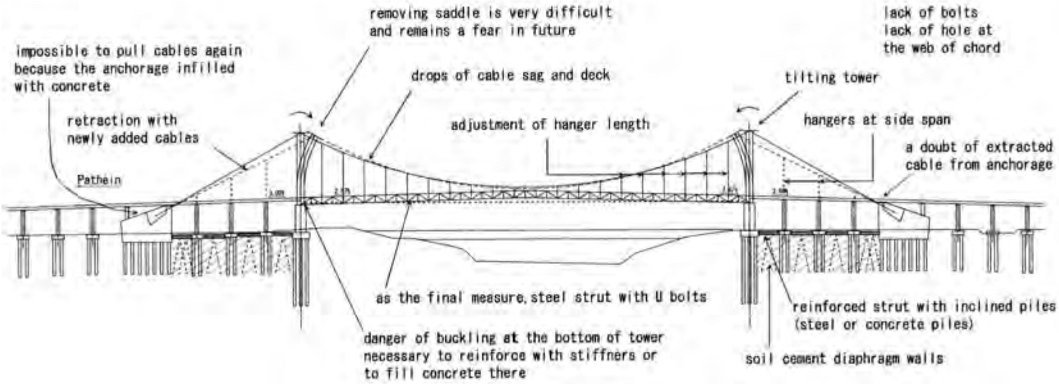
removing saddle is very difficult
and remains a fear in future
lack of bolts
lack of hole at
the web of chord
impossible to pull cables again
because the anchorage infilled
with concrete
drops of cable sag and deck
tilting tower
retraction with
newly added cables
adjustment of hanger length
hangers at side span
a doubt of extracted
cable from anchorage
Pathein
as the final measure, steel strut with U bolts
reinforced strut with inclined piles
(steel or concrete piles)
danger of buckling at the bottom of tower
necessary to reinforce with stiffners or
to fill concrete there
soil cement diaphragm walls

Figure 13: Troubles of Twantay Bridge and measures to reinforce substructure

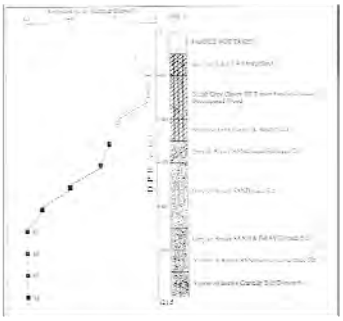

Figure 14: Geological log of Twantay Bridge

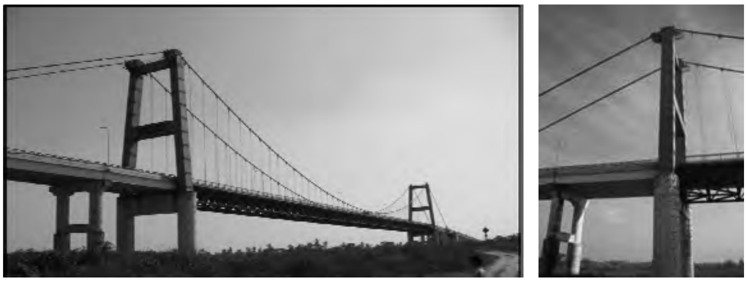

Photo 6: Twantay Bridge and its tower

Figure 13 shows the side view of a suspension bridge with the central span of about 250 meters, Twantay Bridge, near Yangon. Photo 5 indicates that the bridge and the towers have leaned. Although the horizontal displacements of the anchorage are not yet measured exactly, it has been observed that the road surface and the handrails show a gentle deflection and the towers lean slightly inward. These deformations will cause loss of the bridge's functions and will lead to the bridge collapsing. Although it is very difficult to deal with these problems, the author would like to propose several possible means for doing so. Figure 13 also illustrates troubles that the bridge is facing, and measures for restraining the displacement of the anchorage and reinforcing the structures.

One of the measures for restraining the displacement of the anchorage is a method for combining the anchorage and the piers inside, using reinforced concrete struts with inclined piles (steel or concrete piles). If it is insufficient, the diaphragm walls in the front ground up to the intermediate firm layer (Figure 14) are the best way. It can be substituted with the soil cement diaphragm wall. In case of the inclined piles in Figure 15, the pile inclined to the horizontal force is stronger than the pile inclined oppositely.
As measures related to the superstructure, the following methods can be considered; 1) the method for converting a single span suspension bridge to a three span suspension bridge and hanging the approach bridges together with the piers, 2) the method for installing inclined piles at the both sides of the moved anchorage as shown in Figure 15, 3) the method for providing additional main cables between the anchorage and the tower, and 4) the method for strengthening the stiffening truss with strong materials and to changing the present bridge to a self-anchored suspension bridge and so on.

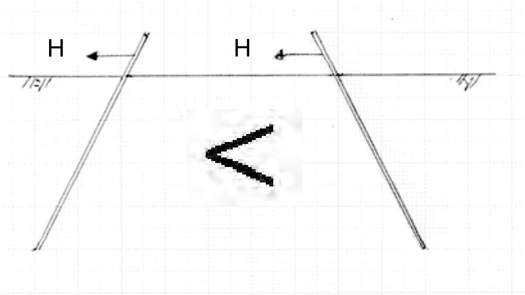

Figure 15 Comparison of inclined piles

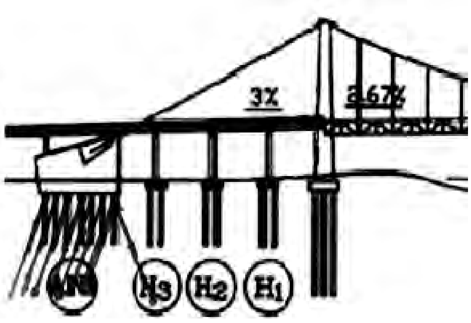

Figure 16 Reinforcement with skew piles

5. SUMMARY

The bridges on soft ground in Myanmar are suffering damage from horizontal displacement by lateral flow due to the backfill or the strong tensile force of main cables of suspension bridges. This paper explains the mechanism of lateral flow and its behavior. Then, the impact on and damage to bridges are indicated with several examples. After that, various measures are introduced to prevent and mitigate displacement by lateral flow. Similarly, measures for recovering and reinforcing structures that have already been damaged are mentioned. On the other hand, unusual cases where huge anchorages of the suspension bridges with pile foundation on soft ground moved by strong tensile force from the main cables, are pointed out. The author proposes several means to restrain those behaviors from substructure and superstructure perspectives for consideration, based on his experience. Now, Myanmar is requested to establish the design codes for bridges on soft ground and the manuals for reinforcing structures that have already been damaged.

ACKNOWLEDGEMENTS

The author expresses a great deal of gratitude to Mr. Hajime Asakura and Mr. Akira Komuro who gave him an opportunity to visit Myanmar in December, 2011.He is also very thankful for the accommodations by Mr. Han Zaw and Mr. Nay Aung Ye’ Myint who received the mission for maintaining bridges, including the author, in Myanmar.

REFERENCES

Nu, T., 2011, *Country report for comprehensive bridge engineering*, Public Works, Ministry of Construction, Myanmar.
Shioi, Y., 2013. Design methods for foundations on very soft ground, *Foundation and Soft Ground Engineering Conference*, Thu Dau Mot University ICTDMU-1, Vietnam
Shioi, Y., Oowada, A., and Swaishi, M., 2013. Reinforcement method to reduce settlement for existing pile foundations on soft ground, *Geotechnics for Sustainable Development* - Geotec Hanoi 2013, Phung (ed.). Construction Publisher. ISBN 978-604-82-0013-8, Vietnam.

Optimal maintenance strategies based on BMS of a large urban expressway network in Japan

Yasuhito SAKAI[1]
[1]Dr.Eng., Management Department,
Japan Expressway International Company Limited ,Tokyo, Japan
y.sakai.aa@jexway.jp

ABSTRACT

H-BMS (Hanshin expressway Bridge Management System) is a custom-made management tool of viaduct structures consisting Hanshin Expressway which is one of the biggest and busiest urban toll highway network in Japan. Its main features are to estimate maintenance, repair and other related costs optimized on a long-term basis with the concept of life cycle cost minimization, and to set repair work priorities by each structural element to help construct rational yearly repair planning. The system is now recognized as a part of decision-making process of structural management. H-BMS is now practiced in the construction of 5-year budget framework and concrete repair work programs in the local level. After the introduction of the system's contents, this paper shows some feedbacks from users and evaluates the system in terms of its practicality in actual management situations.

Keywords: BMS, life cycle cost ,asset management systems

1. INTRODUCTION

Since its foundation in 1962, Hanshin Expressway Public Corporation (HEPC) has built and been operating an urban toll road network in Kansai Metropolitan Area for over 40 years. The network currently expands to 259.1 km in total length and is used averagely by about 740,000 vehicles per day. In 2005, HEPC was privatized by a policy of the national government, Hanshin Expressway Company Limited (HEX) was established newly. But it is apparent that Hanshin Expressway is playing a very important role for the economic and social activities of the area as a main traffic artery supporting people's daily life in every aspect.

90% of the network is formed by viaduct structures and more than 30% are over 40 years old. The older these structures get, the more important their maintenance/repair treatment becomes in order to keep accommodating such heavy traffic. However, while the route length in service is increasing and traffic volume is steady, maintenance and repair budgets are being curtailed due to the current social and economic circumstances. Furthermore the development of more rationalized allotment scheme of the limited budget is critical as the financial condition is unlikely to be recovered in the near future. For continued proper maintenance of road structures, more effective and efficient measures need to be taken against structural aging in conjunction with future medium- and long-term plans. It is also necessary that user service be maintained at proper levels.

For these, public understanding on importance and significance of maintenance need to be further promoted.

This paper describes about, the Hanshin Expressway Bridge Management System (H-BMS). H-BMS is a maintenance management system which has functions to calculate optimal repair policies by minimizing life cycle costs, to simulate future condition state and repair costs and to determine repair priority. It uses the latest inspection data and traffic data which are stored in the Maintenance Information Management System for improving accuracy.

1. OUTLINE OF THE H-BMS

Many bridge management systems (BMS) have been constructed in recent years, modeling bridge deterioration processes from diagnostic or health evaluation results. They are designed to assist proper determination of repair and retrofit techniques and priorities for minimizing life cycle costs within limited budget. Accurate prediction of deterioration of bridge members is the key in the BMS. Deterioration process is commonly expressed using Markov transition probabilities, and a number of Markov decision models have been proposed for optimum repair strategies of civil engineering structures. For life cycle cost assessment which is the other key in the BMS, either of the two methods is available: 1) discounted present value method which evaluates life cycle cost at discounted current value; and 2) non-discounted present value method which directly evaluates life cycle cost without any discount. The discounted present value method is used in existing optimum repair models and also in the PONTIS, one of the typical BMS's in the U.S.

The Hanshin Expressway has been working on establishing a bridge management system called H-BMS for effective and efficient planning of maintenance management. In the H-BMS actual deterioration process information is integrated in the deterioration prediction through estimation of Markov transition probabilities based on the long-time accumulated inspection data of the Hanshin Expressway using multi-staged exponential hazard models. The use of multi-staged exponential hazard model allows for estimation of deterioration curves by routes and structural types. Discounted present value method is used for life cycle cost assessment. The system is also capable of simulating repair and deterioration processes of road structures with annual budget limitations taken into account.

2. PURPOSE OF THE H-BMS

The H-BMS being developed at the Hanshin Expressway has the following purposes.

i) Calculate the expenses required to maintain road structures at proper levels for an extended period.
ii) Calculate long-term changes in performance levels and costs and priorities of repair projects, and provide reference materials for maintenance management planning.
iii) Provide an explicit basis for repair plans and repair costs to support accountability.

The Hanshin Expressway has owned and operated the maintenance information management system which is road structure database since well before its privatization.

Using the asset, inspection and repair data stored in the database, the H-BMS determines condition of each structure and predicts deterioration, calculates repair and maintenance costs and priorities of repair and maintenance projects required for maintaining proper performance, and establishes budget plans and repair plans. Through ex post facto evaluation of repair and maintenance actually performed and updating of asset information, repair and maintenance policies are reviewed. This maintenance management procedure using the H-BMS can be modeled as shown in Figure 1.

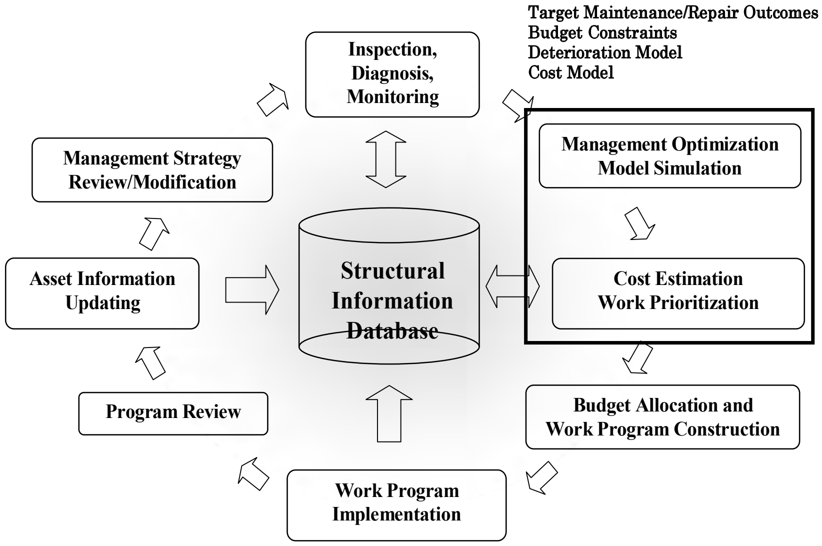
Target Maintenance/Repair Outcomes
Budget Constraints
Deterioration Model
Cost Model
Inspection, Diagnosis, Monitoring
Management Strategy Review/Modification
Management Optimization Model Simulation
Asset Information Updating
Structural Information Database
Cost Estimation Work Prioritization
Program Review
Budget Allocation and Work Program Construction
Work Program Implementation

Figure 1. New management routine of expressway structures with integration of H-BMS

Figure 1: Maintenance management procedure using the H-BMS

3. SYSTEM DESCRIPTION

The H-BMS is designed for maintenance management planning against deterioration of road structures. Structural categories included in this system are pavement, painting, expansion joints, slabs/decks, steel structures and concrete structures, and it is possible to establish maintenance management plans by structural categories. The system has been first tested with such categories that constitute large percentages of the maintenance budgets and have simple deterioration mechanisms. The following description introduces a case of pavement where the system has been most developed so far.

At the Hanshin Expressway, the system collects pavement condition data including cracking ratios by spans and by routes, average rutting depth and longitudinal roughness, using automated measuring vehicles. MCI is used as the pavement health indicator which is calculated using the following equation.

$$MCI = 10 - 1.51C^{0.3} - 0.3D^{0.7} \tag{1}$$

Here, *C* is cracking ratio (%) and *D* is rutting depth (mm). With allowable roughness in as-built management taken into account, it is assumed that cracking ratio is 0%, rutting depth is 2.0 mm and MCI is 9.5 when the pavement repair is complete.

The Hanshin Expressway developed stochastic deterioration models using the accumulated data about pavement deterioration process and carried out estimation of future pavement deterioration using the models. The deterioration process was expressed using Markov transition probabilities for its uncertainty. Multi-staged exponential hazard model15) is used to assure good precision in the probability estimation which handles inspection data from different time points at varied intervals. The parameters of the multi-staged exponential hazard model are estimated based on the inspection data, using maximum likelihood method. Markov transition matrix is derived analytically based on them, and using the Markov transition matrix, typical deterioration curves are estimated. This allows reproducing the changes in deterioration rate in relation to the pavement health, providing good consistency with logical approach. Markov transition matrix can be estimated for each section or each route of the expressway where deterioration mechanism varies. Consequently, deterioration curves are finely defined.

For the estimation using the multi-staged exponential hazard model, hazard rate was defined for the health level of each section. The following equation estimates the exponential hazard model with the hazard rates by health levels independent of time.

$$\lambda_i(y_i) = \theta_i \tag{2}$$

Here, i is health level of the member, λ_i is hazard function, y_i is a point on the time axis, and θ_i is a constant (unknown parameter). The health level needs to be expressed as a discrete value to use the Markov transition probability. For the pavement, continuous MCI values were classified by 1.0 point in the range of 5.0<MCI≤10.0 where the data exist, and the median value was taken as the typical value for the health level.

For using the multi-staged exponential hazard model, Markov transition probability is expressed as described below in accordance with the degree of deterioration.
(when the health level does not change)

$$\pi_{ii} = \exp(-\theta_i Z) \tag{3}$$

(when the health level changes by one rank)

$$\pi_{ii+1} = \frac{\theta_i}{\theta_i - \theta_{i+1}}\left\{-\exp(-\theta_i Z) + \exp(-\theta_{i+1} Z)\right\} \tag{4}$$

(when the health level changes by two or more ranks)

$$\pi_{ij} = \sum_{k=i}^{j} \prod_{m=i}^{k-1} \frac{\theta_m}{\theta_m - \theta_k} \prod_{m=k}^{j-1} \frac{\theta_m}{\theta_{m+1} - \theta_k} \exp(-\theta_k Z)(j = 1, \cdots, J) \tag{5}$$

(when the health level changes to the bottom rank)

$$\pi_{iJ} = 1 - \sum_{j=i}^{J-1} \pi_{ij} \left(i = 1, \cdots, J-1 \right) \tag{6}$$

Here, Z is inspection interval, i is health level before change, and $j(j>i+1)$ is health level after change. By estimating θ_i in the hazard function by maximum likelihood method, Markov transition matrix (7) can be estimated using equations (3) to (6).

$$\prod(Z) = \begin{bmatrix} \pi_{11}(Z) & \cdots & \pi_{iJ}(Z) \\ \vdots & \ddots & \vdots \\ 0 & \cdots & \pi_{JJ}(Z) \end{bmatrix} \tag{7}$$

As deterioration change is modeled by the hazard function, the expected time length for deterioration to reach a next level (RMD) can be expressed as follows.

$$RMD_i = \int_0^{\infty} \exp\left(-\theta_i\, y_i\right) dy_i = \frac{1}{\theta_i} \tag{8}$$

Equation (8) provides typical deterioration process. Through these processes, data are classified into some groups by factors dominating the tendency of deterioration change, and performance curves are generated. Performance curves for the pavement are generated for each slab/deck type and by routes to express different deterioration processes by traffic characteristics and road alignments. Figure 2 shows thus obtained performance curves for the pavement by slab/deck types. As shown here, pavement deterioration rate is faster on the earthworks.

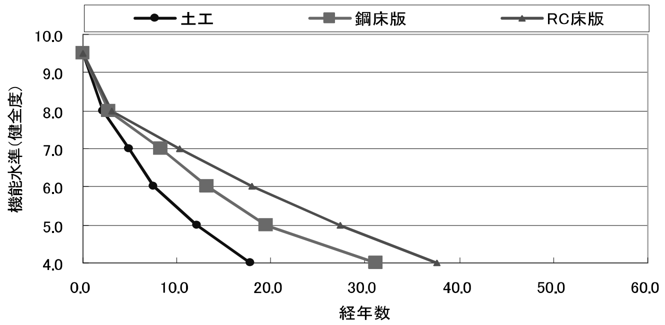

Figure 2: Pavement performance curves

4. DEFINITION OF THE OPTIMUM MANAGEMENT LEVEL

Costs required for maintaining the performance of road structures properly is evaluated by using the life cycle cost (LCC). LCC is expressed as a sum of the direct cost which is imposed on the expressway company and the external cost which is imposed on the road users:

LCC = direct cost (repair cost and maintenance cost) + external cost (vehicle operating cost and travel delay cost).

Each cost element is defined as follows:

Repair cost: repair work expenses, including expenses for traffic restriction required for road work.

Maintenance cost: expenses for routine maintenance activities including repair of potholes and correction of bumps to be carried out with the pavement deterioration (set according to MCI).

Vehicle operating cost: fuel, vehicle depreciation and other vehicle-related expenses to be imposed on road users in extra due to decrease in MCI.

Travel delay cost: loss caused to road users due to traffic congestion resulting from restriction on traffic for road work.

The travel delay cost is calculated with changes in travel time and traffic congestion condition taken into account, by using a traffic flow simulation model which has been separately developed for the traffic control system of the expressway. This model allows for a more precise reproduction of congestion and time loss by routes. A rule for repair is assumed here in which pavement repair shall be executed when the MCI value reached a certain level. That level is called a management level. The LCC required at that point is calculated for the given management level. Figure 3 shows the relationship between the management level and the LCC. The management level where the lowest LCC is reached is called the optimum management level. The time when the MCI value for the pavement reaches the optimum management level is the optimum repair time.

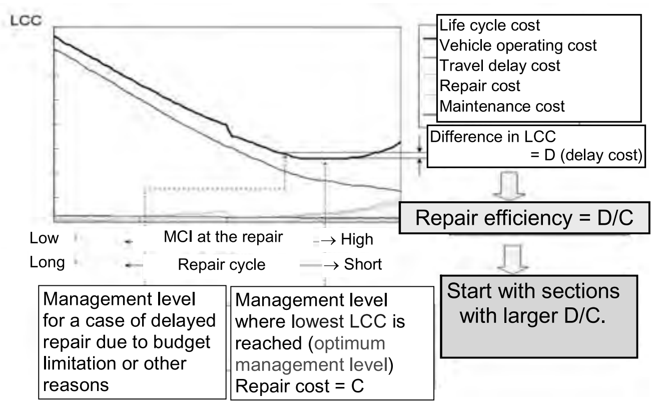

Figure 3: Determination of the optimum management level and priorities

5. DETERMINATION OF PRIORITIES

If no limitation is imposed on the pavement repair budget, it is possible to repair all locations or routes where the MCI reached the optimum management level on the annual basis, achieving the minimum LCC. However, budget is always limited, requiring prioritization of determines repair priorities according to the descending order of the ratio (repair efficiency = D/C) of the extra on the LCC due to delay from the optimum repair time (D: delay cost) against the repair cost for carrying out repair at the optimum management level (C).

LCC
Travel delay cost
Repair cost
Maintenance cost
Vehicle operating cost

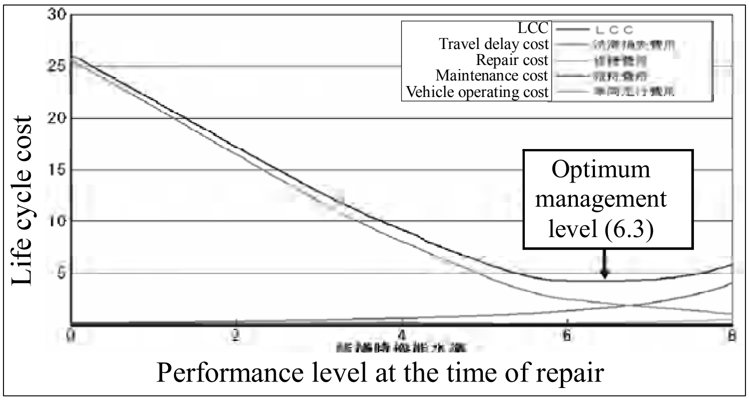

Figure 4: Optimum management level

6. RESULT OF SIMULATION

Figure 5 shows a simulated relationship between the LCC and the management level for a section of the road network for next 100 years, suggesting that repairing this section at MCI = 6.3 achieves the minimum LCC.

The H-BMS is capable of determining repair locations based on the aforementioned priorities for each year under a budget limitation which has been given exogenously as a scenario, and simulating the repair process. Figure 5 shows predicted changes in the direct cost for that section with time. There are two cases simulated here: (a) with the annual repair budget limited to "A" x 100 million yen; and (b) with an annual repair budget of "A+α" x 100 million yen (cost required for maintaining the optimum management level). In case (a), the limited repair cost leaves some pavements in poor condition as they are over the optimum repair time. Because of this, the maintenance cost for coping with them starts to increase from 2005 and reaches its limit in about 20 years. In case (b), repairs carried over from the past can be eliminated gradually, making it possible after 35 years from now to execute repairs based on the optimum management level within the annual budget limit. In addition, the total cost (maintenance cost and repair cost) for the 100 years is reduced by about 11%.

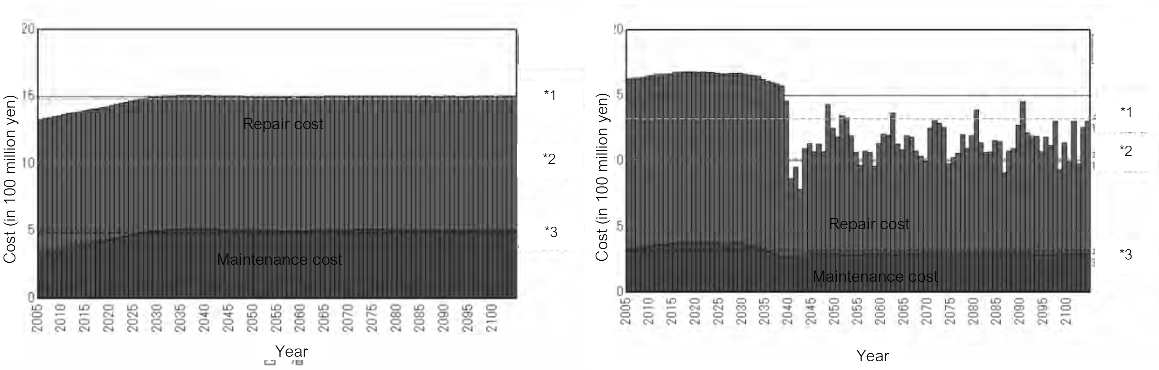

(a) Budget limit: "A" × 100 million yen/year

*1 Average total cost (1,408 million yen)

*2 Average repair cost (999 million yen)

(b) Budget limit: "A+□" × 100 million yen/year

*1 Average total cost (1,315 million yen)

*2 Average repair cost (1,006 million yen)

Figure 5: Changes in maintenance management cost

Figure 6 shows changes with time of average MCI levels for the studied section and of the lowest MCI level within that section. The (a) and (b) in this figure are those in Figure 6. In case (a) average MCI level goes down continually. Repair carryover accumulates during that period, causing the lowest performance level to decline after about 20 years. As a result, management level goes below the management limit specified by the Hanshin Expressway.

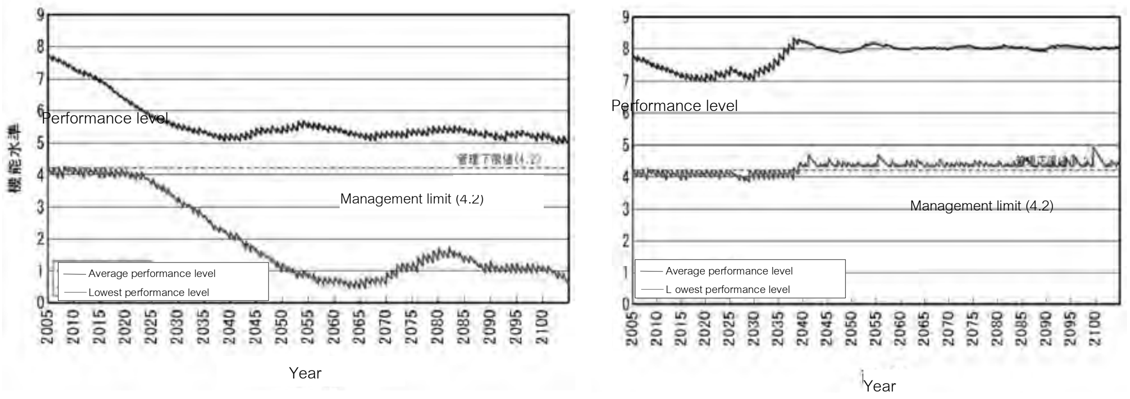

(a) Budget limit: "A" × 100 million yen/year

(b) Budget limit: "A+?" × 100 million yen/year

Figure 6: Changes in performance level

The management limit is the level that both cracking ratio and rutting depth in the pavement are ranked as damage needing to be repaired in the criteria of the Hanshin Expressway. It is about 4.2 when converted into MCI values. In case (b), average performance level is kept around the current level for an extended period, and the lowest performance level does not go below the management limit.

Consequently, it can be concluded that proper maintenance of the pavement for an extended period would be impossible with the annual budget of "A" x 100 million yen and would require the budget of "A+α" x 100 million yen every year.

7. SUMMARY

This paper introduced the H-BMS road structure management system and the logic model for routine maintenance management of the Hanshin Expressway. Of the six structural categories, the H-BMS is operated currently on pavement, painting and expansion joints as a tool for establishing annual plans of major repair projects including those requiring full closure of the entire expressway system. Its application to structural bodies (concrete structures and steel structures) is also under investigation. For the application of the logic model, constant measurement will be continued on all indicators to accumulate more data and detailed examination will be carried out for establishing management levels (management limit, optimum management level, etc.) to be used as criteria for normalization of risk.

REFERENCES

Kaito, K., Hota, K., Kobayashi, K. and Owada, K. 2005. Optimal maintenance strategies of bridge components with an average cost minimizing principles, *Proceedings of JSCE*, No. 801/I-73, 83-96.

Kobayashi, K., 2005. Decentralized life-cycle cost evaluation and aggregated efficiency, *Proceedings of JSCE*, No. 793/IV-68, 59-71.

Kobayashi, K., Ejiri, R., and Do, M., 2008. Pavement Management Accounting System, *Journal of Infrastructure Systems* 14, 159-168.

Nam, L.T., Obama, K., and Kobayashi, K. 2008. Local mixture hazard model, A semi-parametric approach to risk management system, *IEEE International conference on* Systems, Man and Cybermetrics SMC.

Sakai, Y., 2007. Practical management system of Hanshin Expressway-Logic model and BMS, 2nd International Workshop on Lifetime Engineering of Civil Infrastructure.

Sakai, Y., Arakawa, T., Inoue, Y., Furutam H., and Kobayashi, K., 2009. The development of practical asset management system for the Hanshin Expressway Network, The 4th International Conference on Structural Health Monitoring of Intelligent Infrastructure.

Sakai, Y., Arakawa, T., Inoue, Y., Furuta, H. and Kobayashi, K., 2009. The development of practical asset management system for the Hanshin Expressway Network, *The 4th International Conference on Structural Health Monitoring of Intelligent Infrastructure*, SHMII-4.

Sakai, Y., Arakawa, T., Inoue, Y., and Kobayashi, K., 2008. The development of the Hanshin Expressway Bridge Management System, *Proceedings of Information on Management*, 17, 63-70.

Sakai, Y., Arakawa, T., and Kobayashi, K., 2007. Study on HELM logic model intended for effective maintenance of expressways, *62nd Annual Conference of Japan Society of Civil Engineers*.

Sakai, Y., Inoue, Y., and Kobayashi, K., 2008. The effect of simultaneous pavement repair in urban highway network. *Proceedings of Construction Management*.

Sakai, Y., Uetsuka, H., and Kobayashi, K. 2008. *New approach for efficient road maintenance on urban expressway based on HELM*, Society for Social Management Systems.

Tsuda, S., Kaito, K., Aoki, K., and Kobayashi, K., 2006. Estimating marcovian transition probabilities for bridge deterioration forcasting, *Journal of Structural Engineering and Earthquake Engineering* 23, 241-256.

http://www.pontis.com/

Case examples of surveys over architectural buildings and civil engineering structures by infrared thermography method

Noboru SATO
President, Sankyo Co. Ltd., Tokyo, Japan
nsato@sankyo-net.co.jp

ABSTRACT

In Japan, deterioration of infrastructural objects which were built during high-growth era such as bridges, tunnels, public buildings and others are observed. It can be social issues with, for instance, debris from deteriorated concrete construct causing human suffering. At the symposium this time, several case examples are presented regarding means of deterioration survey mainly on infrared thermography method.

Keywords: non-destructive inspection, infrared thermography

1. INTRODUCTION

In order to understand deteriorated situation of massive infrastructures, many experienced engineer is needed. In the movement of increase aging structures, many companies become difficult to get experienced civil engineer due to low birth rate and longevity in Japan. Therefore, in Japanese civil engineering market, they need to work efficiency improvement and highly accurate measurement by Non- Destructive Testing (NDT) techniques.

In this symposium, we introduce some research examples by Infrared Thermography method that is one of our NDT techniques and it has comparatively high penetration in Japan. And those research examples are including the method of the infrastructure deterioration surveying that will face at South East Asia countries in near future.

2. DAMAGED STRUCTURE EXAMPLES

In this section, we introduce some examples which are the damaged structure of civil engineering and construction in Japan. Figure 1 shows the fallen concrete from the canopy top of school building. It detached itself by pushed concrete to outside due to rebar corrosion. It is due to construction defect.

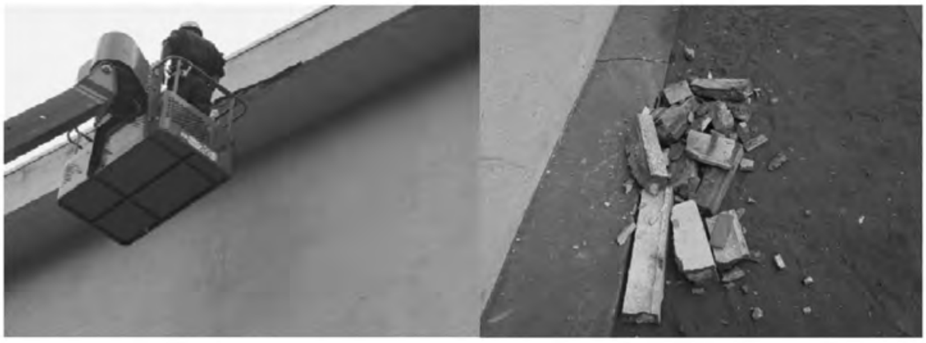

Figure 1: Surveying works and the detached concrete itself

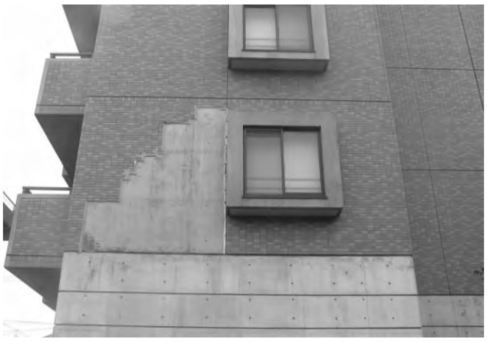

Figure 2: The case of tile detached itself

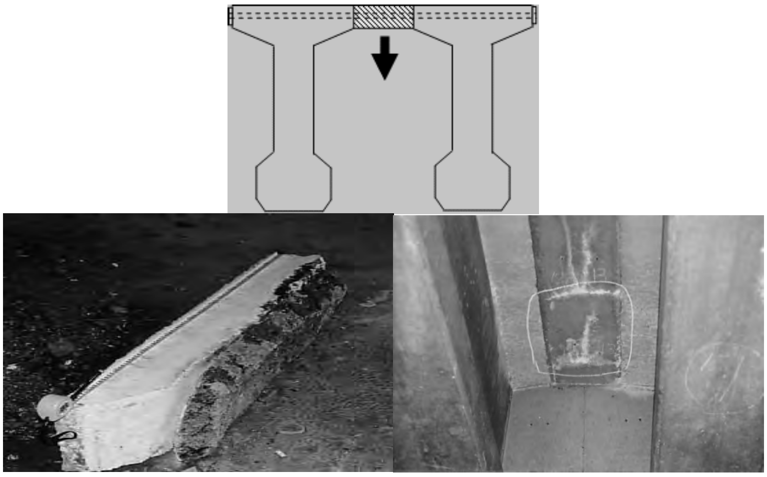

Figure 3: The case of dropped cast-in-place concrete from PC bridges

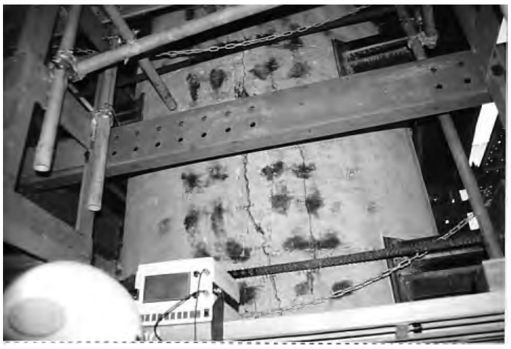

Figure 4: Cracks on highway concrete bridge pier

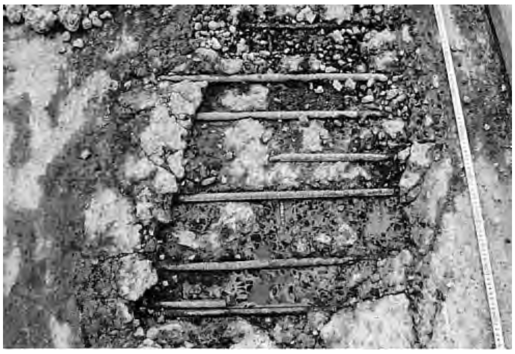

Figure 5: Degradation of road bridge floor board concrete

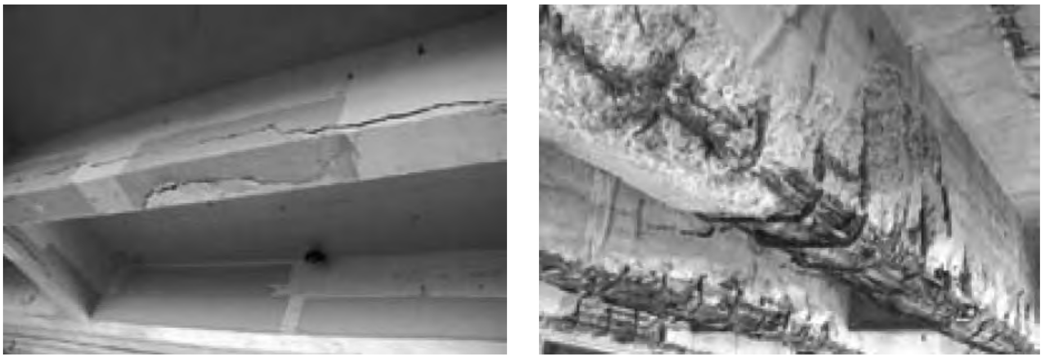

Figure 6: Degradation damage of road bridge main girder (Ministry of Land, Infrastructure and Transport website)

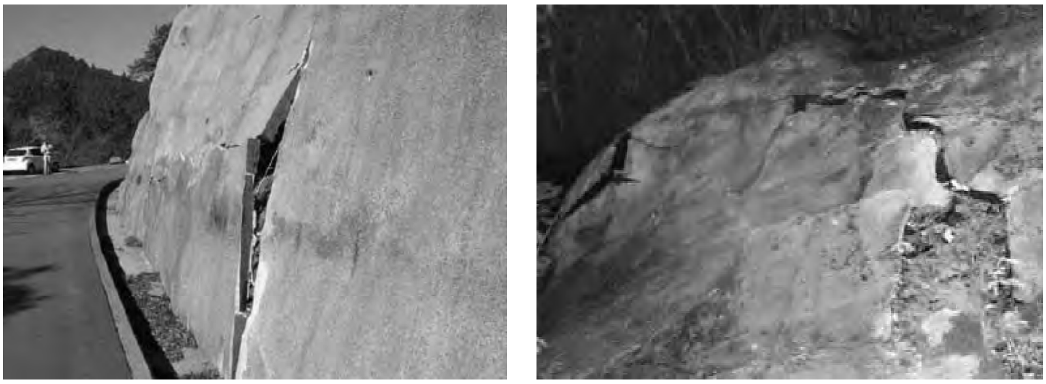

Figure 7: Degradation damage of the excavation slopes (Ministry of Land, Infrastructure and Transport website)

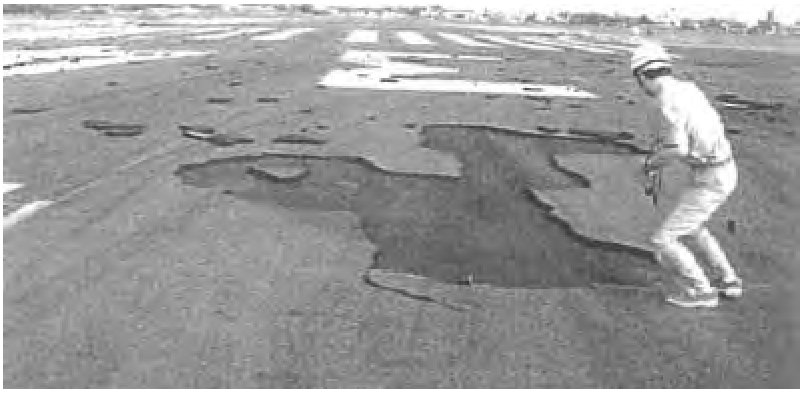

Figure 8: Pavement peeling of the airport runway ((Ministry of Land, Infrastructure and Transport website)

3. THE CASE STUDIES BY INFRARED THERMOGRAPHY METHOD

3.1 Measurement principle

The Infrared Thermography method is the techniques that gather “Void” in concrete structure from visualized object’s surface temperature distribution by Infrared Thermal Imaging Camera. Measurement principle is shown Fig.3.1. At day time, heat of sunlight transmits from concrete structure surface into inside. However, due to the insulating effect of the air layer, the defective part of surface warms faster than healthy part when there is peeling or internal voids at nearly concrete surface. This principle allows us to detect internal defects from the surface temperature distribution.

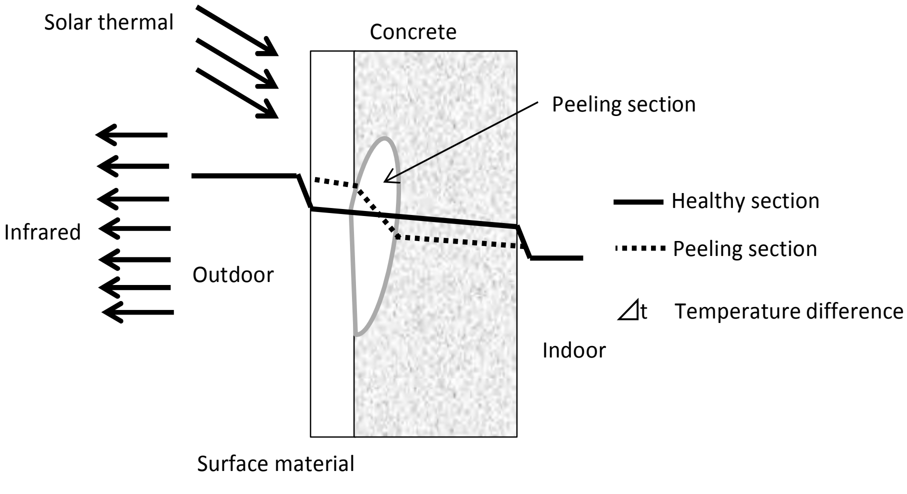

Figure 9: Surface temperature difference between the healthy part and the defective part

On the other hand, the measurement time period becomes at night, the surface temperature of the defect part becomes lower temperature against healthy part. The defect part temperature follows the outside temperature faster than the healthy part. The healthy part has higher temperature than the defect part, because accumulated heat in the deep healthy part of concrete emits longer than defect part. (Temperature of the defective part is reversed in the day and night)

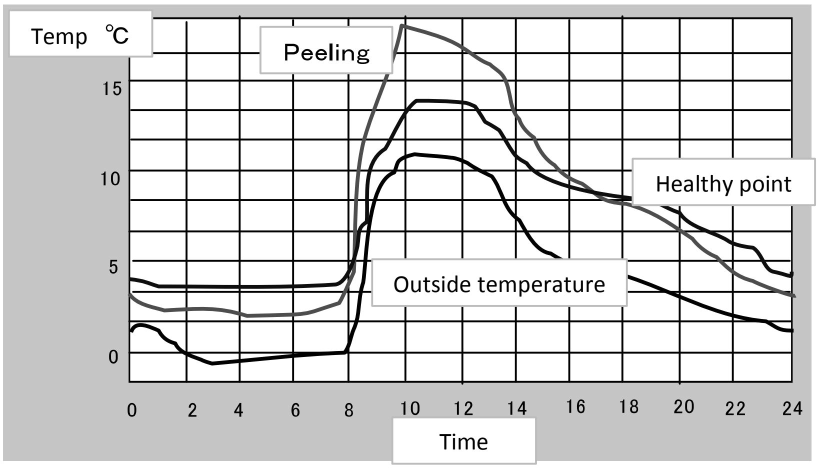

Figure 10: The process of the surface temperature of defective part and healthy part in a day

3.2 The case study of the building wall

3.1.1 The floating tiles surveying of wall

The floating tiles surveying of the wall has been conventionally performed by hammering test close to wall. However, this method takes extra cost such as temporary scaffold or vehicle for high lift work to close to wall. Infrared Thermography method is possible to study from the ground with non-contact and safety. And it is possible to obtain objective infrared images.

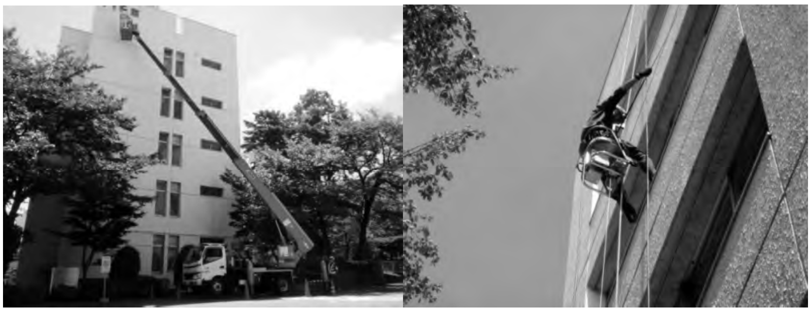

Figure 11: Conventional wall surveying

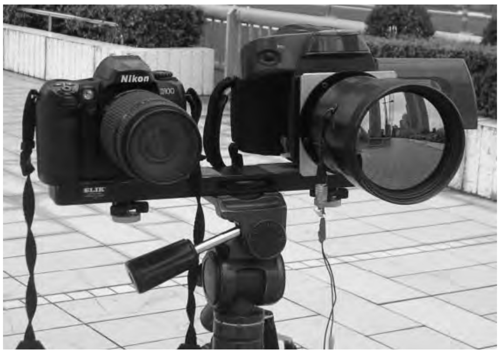

Figure 12: The survey status by infrared thermography method

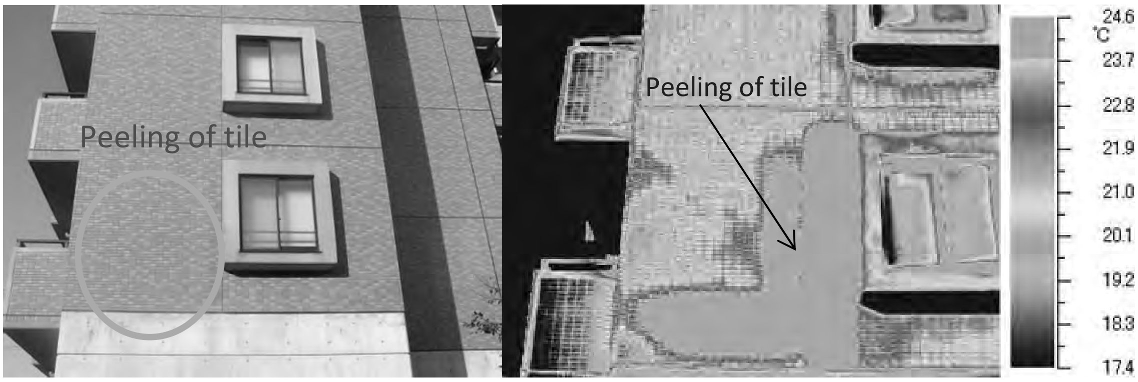
Peeling of tile
Peeling of tile
24.6
°C
23.7
22.8
21.9
21.0
20.1
19.2
18.3
17.4

Figure 13: Visible image and infrared thermal image

3.1.2 Detection of the invisible window

The opening (window) has been blocked through many years renovation. The Infrared Thermography detects the original opening easily.

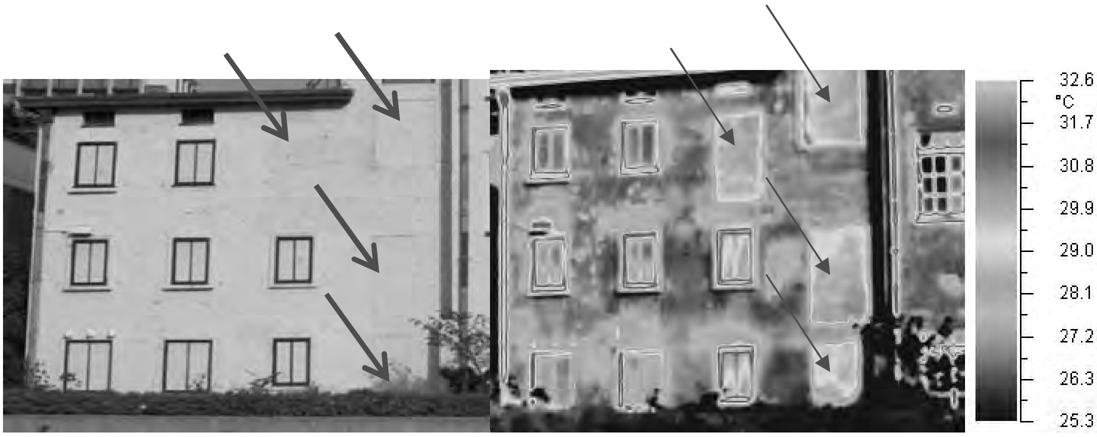
32.6
°C
31.7
30.8
29.9
29.0
28.1
27.2
26.3
25.3

Figure 14: Detection of the invisible window

3.1.3 The floating part surveying of concrete wall bridge railing

This structure has not had enough covering depth from the time of completion of construction. Then, floating part was generated at surface of concrete caused by rebar corrosion. Infrared Thermography detects the float that occurred on the wall of the road bridge. Those float parts are at risk for detached itself and hits passers under the bridge.

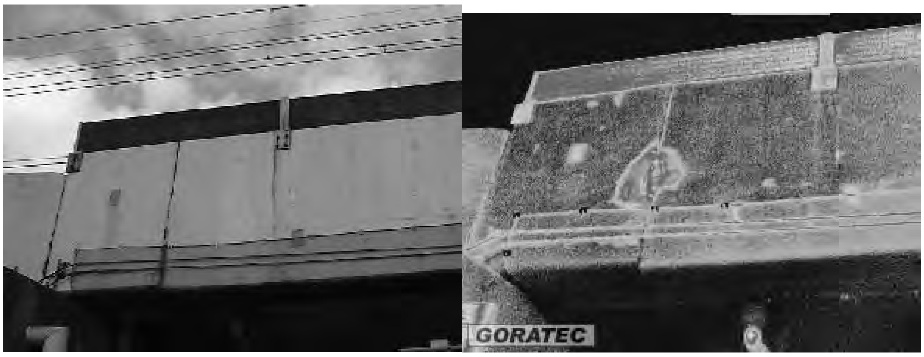

Figure 15: The float that occurred on the wall of the bridge railing

3.1.4 Cavity surveying that occurred on the back side of the excavation slope

The spray concrete of excavation slope must be integrated to the ground. However, it is at risk of caving and collapse concrete structure. It is possible to survey dangerous place like this in advance accident by Infrared Thermography method.

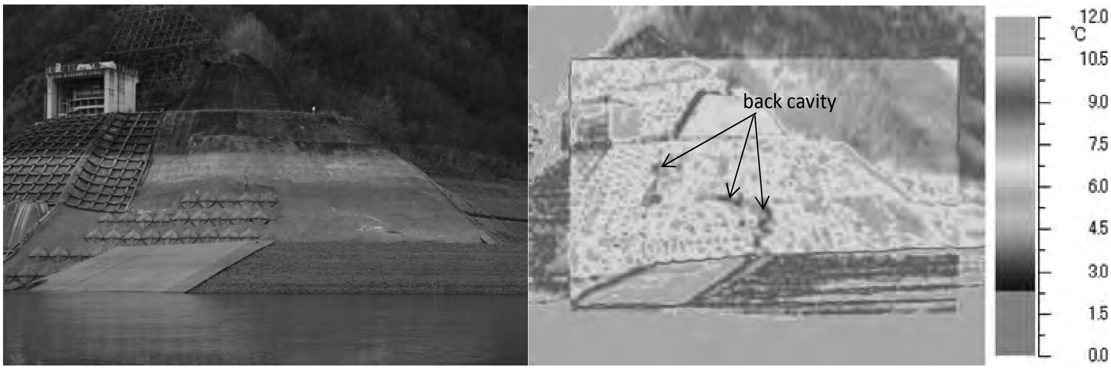

Figure 16: Back cavity detection of slope

3.1.5 Airport runway surveying

Asphalt paving of the airport runway has been constructed to many lay. However, the delamination occurs due to some reasons, and sometimes interferes with the landing of the aircraft. Previously, surveying was done with hammering test by night inspectors, but it is possible to detect high accuracy and objectively with Infrared Thermography method.

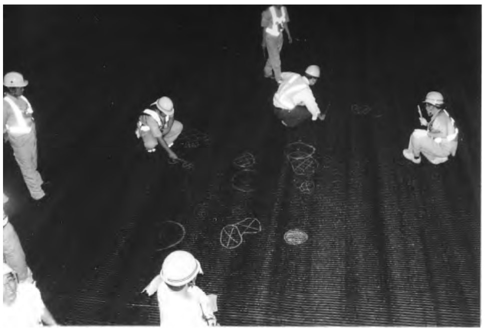

Figure 17: The hammering test by night inspector

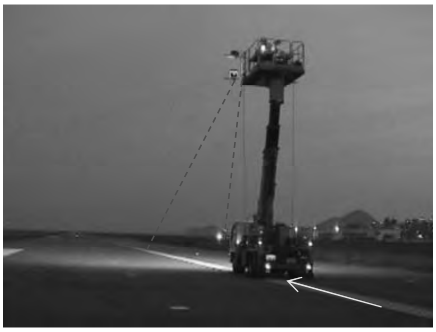

Figure 18: The inspection by Infrared Imaging Camera

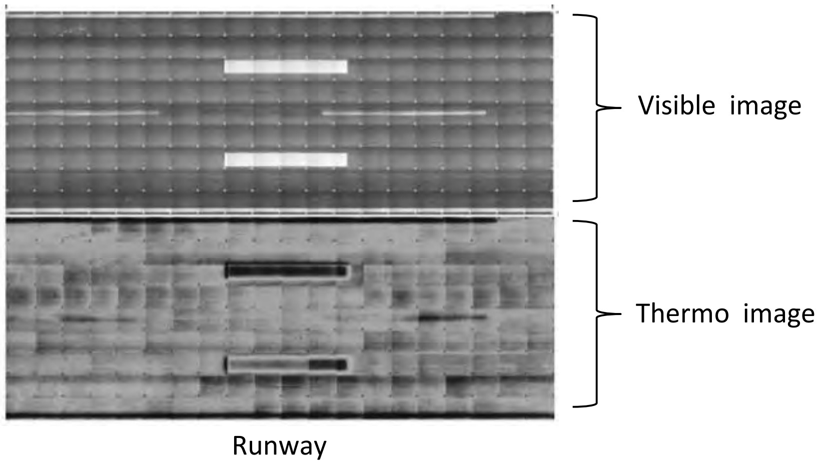

Figure 19: Case study of the runway (Combine the picture 100 m length)

4. SUMMARY

In this report, we introduced some case studies of degradations and damage case of civil engineering structure and building structures by Infrared Thermography method. Infrared Thermography method is very effective against structures that involve temperature difference between good part and bad part. Infrared Thermography method has a many potential to detect degradations and construction defect of concrete structure more than those reported cases in this time.

The degradations and construction defects might claim many lives, and become a big social problem. In recent Japanese situation, the development of various NDT techniques is required, because Japan Government makes infrastructures maintenance obligatory. About 30 years ago, in Japan, Infrared Thermography method was introduced by several companies. And it has been established applicability as a surveying technique through many trial and errors.

Today, many companies have introduced Infrared Thermography, and it becomes an active surveying market. In Southeast Asian countries at the period of high economic growth, it may face infrastructure degradation and damage problem same as Japan in the future. We desire to effective utilization of those technology that was introduced this time in the Southeast Asian maintenance market. However, we suggest that you should take enough training before survey by Infrared Thermography method, because it have applicability limit.

The current repair, reinforcement and seismic retrofit works of bridge for effective utilization of urban infrastructure

Hiroshi DOBASHI
President, Shutoko Engineering Co., Ltd., Japan
h.dobashi118@shutoko.jp
Visiting Professor, ICUS, IIS, the University of Tokyo, Japan
dobashi@iis.u-tokyo.ac.jp

ABSTRACT

The first section with 4.5km length of the Metropolitan Expressway opened in 1962 between Kyobashi and Shibaura to reduce traffic congestion in the city center. And until 1962 when Tokyo Olympic game was held, about 33km were opened. Today, the Metropolitan Expressway network plays an important role as major traffic facility that supports socio-economic activities in the Tokyo metropolitan area and it currently extends for approximately 300 km. Among those, 95% of the network is comprised of the structures such as bridges, tunnels and semi-underground structures, and 30% of the structures have passed more than 40years after opening to traffic.

In recent years, for deterioration of the urban infrastructure and a large-scale disaster such as large earthquake, appropriate operation, maintenance, retrofit and renewal works are highly required in addition to development of the infrastructures. Therefore, inspection, investigation, diagnosis for degradation and countermeasures of the structure are focused as an issue of maintenance management in order to ensure safe structures and effectively utilize existing infrastructures. In this paper, changes in seismic design criteria and seismic retrofit works for bridges are described. In addition, the repair work and reinforcement work carried out for existing damaged both steel and concrete structures are introduced.

Keywords: *urban infrastructure, maintenance management, repair and retrofit works, deterioration*

1. INTRODUCTION

The first section of the Metropolitan Expressway between Kyobashi and Shibaura was opened in 1962 to reduce the traffic congestion in the central Tokyo. Currently, the Metropolitan Expressway network extends for approximately 300 km (Figure 1). In 2011, it carried about 1 million vehicles and about 2 million passengers per day. Although the total length of the network in service is only 15% of the total length of major city roads in the Tokyo metropolitan area, it carries approximately 30% of the total traffic in terms of vehicle-kilometrage, indicating the degree of utilization. Since it carries approximately 28% of freight transportation in the area, it is considered to function approximately twice more in vehicle-kilometrage and approximately three times more in freight transportation than other major city roads. As described above, the

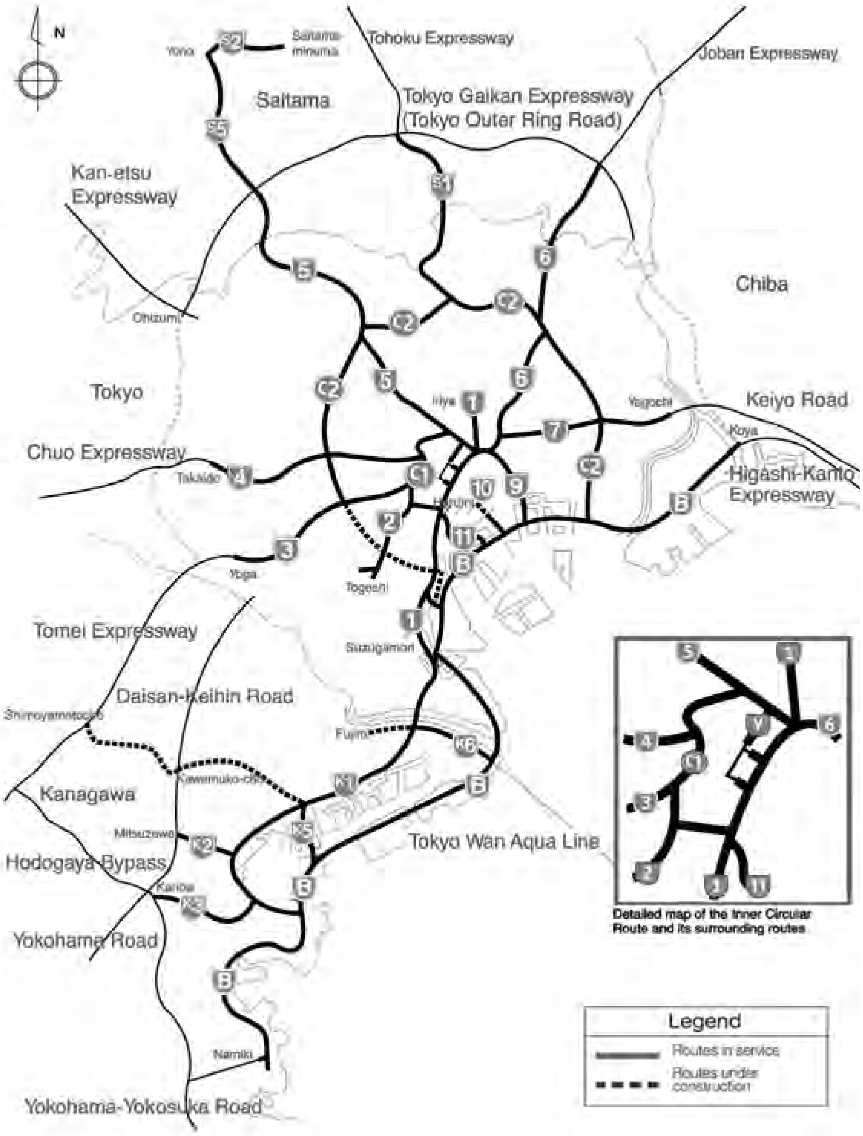
N
Yono
S2
Saitama-minuma
Tohoku Expressway
Joban Expressway
Saitama
Tokyo Gaikan Expressway
(Tokyo Outer Ring Road)
S5
Kan-etsu
Expressway
S1
6
5
C2
Chiba
Ohizumi
Tokyo
1
7
Yotsugi
Keiyo Road
Koya
Chuo Expressway
Takaido
4
C1
10
9
Higashi-Kanto
Expressway
B
2
3
11
Yoga
Togoshi
Suzugamori
Tomei Expressway
Daisan-Keihin Road
Shimoyamatocho
Fujimi
K6
K1
Kanagawa
Mitsuzawa
K2
K5
Hodogaya Bypass
Kariba
K3
Yokohama Road
Tokyo Wan Aqua Line
Namiki
Yokohama-Yokosuka Road
Y
Detailed map of the Inner Circular Route and its surrounding routes
Legend
Routes in service
Routes under construction

Figure 1: The network of Tokyo Metropolitan Expressway

Metropolitan Expressway network serves as a major traffic facility that supports socio-economic activities in the Tokyo metropolitan area, and it is a road system that is indispensable to the lifestyle of the people in the area.

Focusing on the structural features of the Metropolitan Expressway, about 95% among the networks are comprised of the structures such as bridges, tunnels and semi-underground structures, and about 30% of the structures have passed more than 40years after opening to the traffic. Therefore, deterioration of the structures has been progressed under the severe use environment with heavy and overloading traffic. The classification and elapsed years of the structures are shown in Table 1 and Figure 2.

For seismic design, seismic coefficient method was stipulated in 1926 after the Great Kanto Earthquake which was occurred in 1923. By incorporating the new findings from the earthquake that occurred after this, seismic design criteria have been revised. In recent years, the design criteria against inter-plate great earthquake have just been reviewed anew by the East Japan Great Earthquake.

This paper describes changes in seismic design criteria and seismic retrofit works for bridges. In addition, repair works and reinforcement work carried out for existing damaged both concrete and steel structures are described.

Table 1: Classification of structures

Type of structures	Accumulated length (km)	Percentage of accumulated length (%)	
Steel Girder	199.9	66%	95%
Concrete Girder	38.6	13%	
Tunnel	28.9	10%	
Semi Underground	18.5	6%	
Surface Earthwork	15.4	5%	5%
Total	301.3	100%	100%

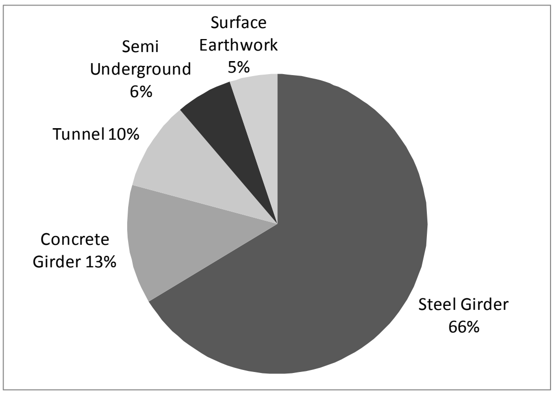

Figure 2: Elapsed years of the structures

2. CHANGES IN SEISMIC DESIGN CRITERIA

2.1 Overview of seismic design revision

Design seismic coefficient was stipulated for the first time in seismic design of Road Bridge in Japan in 1926 which was three years after the Great Kanto Earthquake. Then, with the revision of the Specification for Highway Bridges, design seismic coefficient in seismic coefficient method is embodied and has been standardized. However, important factors such as natural vibration characteristics, ductility, liquefaction of the ground, bridge falling prevention structures and etc. were not included in seismic design at that time. Horizontal seismic coefficient k_h=0.2 and vertical seismic coefficient k_v=0.1 were standard respectively. In 1971, Guideline of Seismic Design for Highway Bridges was established based on the research results of Niigata Earthquake (M7.5) which was occurred in 1964. In this guideline, modified seismic coefficient method, simple judgment method of liquefaction and bridge falling prevention structures were stipulated for the first time. In 1980, this guideline was revised as “Specifications for Highway Bridges: Part V Seismic Design”, and a verification of deformation performance to prevent brittle fracture such as shear failure of RC pier, judgment method of liquefaction by the value of F_L, dynamic analysis were introduced. In 1990, with research results on seismic response of bridges and piers, a verification method taking account of Level 2 earthquake ground motion and plastic deformation performance for RC pier were introduced. The important change was that seismic horizontal strength (L2) including ductility and dynamic strength in the plastic region was stipulated for RC pier for the first time. In 1996, based on the damage of road bridge due to the Hyogo-ken Nanbu Earthquake (M7.2), Seismic horizontal strength method was employed in earnest in addition to considering the earthquake ground motion by inland earthquakes. Furthermore, a verification method of seismic performance by dynamic analysis was introduced with aiming for specifications of performance based design in 2002. Finally, specifications are revised based on the research results of analyses of disaster case study on road bridges due to earthquake in recent years and East Japan Great Earthquake (M9.0) in 2012.

2.2 Review of Level 2 ground motion (Type I)

In seismic design for road bridges, two types of the ground motion such as Type I due to large plate boundary earthquake and Type II due to large inland earthquake as Level 2 earthquake ground motion are considered. Type I ground motion of Level 2 is

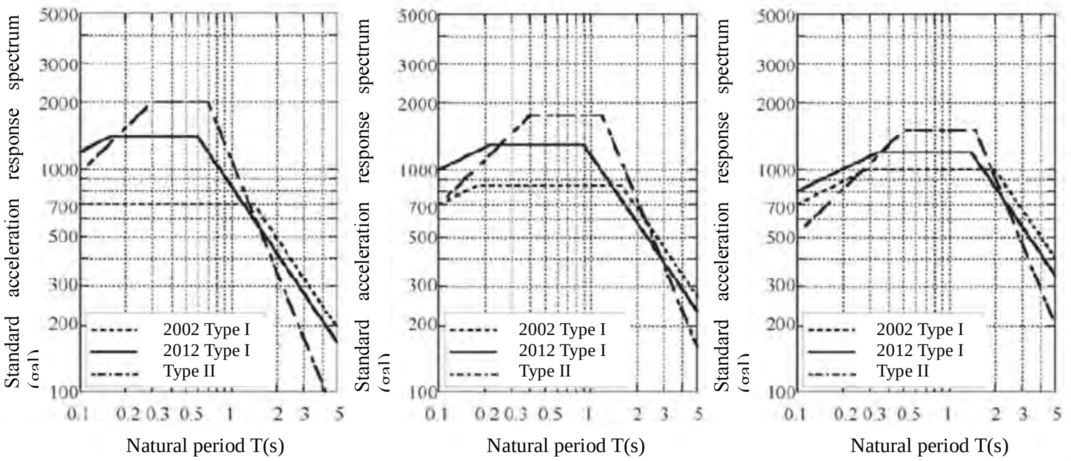

(a) Type I ground (b) Type II ground (c) Type III ground

Figure 3: Comparison of standard acceleration response spectrum

reviewed in the Specifications in 2012 since it is assumed to occur in near future Tokai, Tonankai and Nankai Earthquake which are the same plate boundary earthquake as East Japan Great Earthquake.

Comparison of standard acceleration response spectrum in between 2002 and 2012 are shown in Figure 3. Level 2 ground motion (Level 2) is determined based on the results of the ground motion generated in the Tokyo area at the Great Kanto Earthquake estimated using the attenuation formula that is advanced by a modified regression analysis and strong motion data obtained in recent years, and by the engineering judgment.

Type I ground motion is revised in 2012. Peak of the spectrum of Type I is larger than that of the ground motion of Type I in 2002 and larger than that of Type II for a long period. In addition, peak of the spectrum of Type I ground motion for the Type III ground such as soft ground of alluvium ground was set to be larger than that for Type I ground such as good ground of rock and diluvium ground in 2002. However, peak of the spectrum has been reversed in 2012. This is because that the result of estimation of the acceleration response spectra to calculate the correction factors for each ground type by using only the strong motion record with large amplitude. As a result, the peak of the acceleration response spectrum become smaller in order Type I, Type II and Type III ground.

2.3 Examples of retrofit work and results

In this section, retrofit work of RC pier is described. Failure type of reinforced concrete columns can be classified in two such as flexural failure and shear failure. Flexural failure can hold the required horizontal strength with keeping deformation performance for repeated deformation after the main reinforcement exceeds the yield stress. On the other hand, shear failure is brittle fracture of concrete before the main reinforcement exceeds the yield stress so that critical damages are occurred such as collapse and drop of bridges and large difference in level of road. In addition, flexural and shear failure which is transferred from flexural failure to shear failure after yielding of main reinforcement. To prevent above failures, retrofit work such as reinforcement of RC piers are carried out. In general, to increase ductility, flexural strength and shear

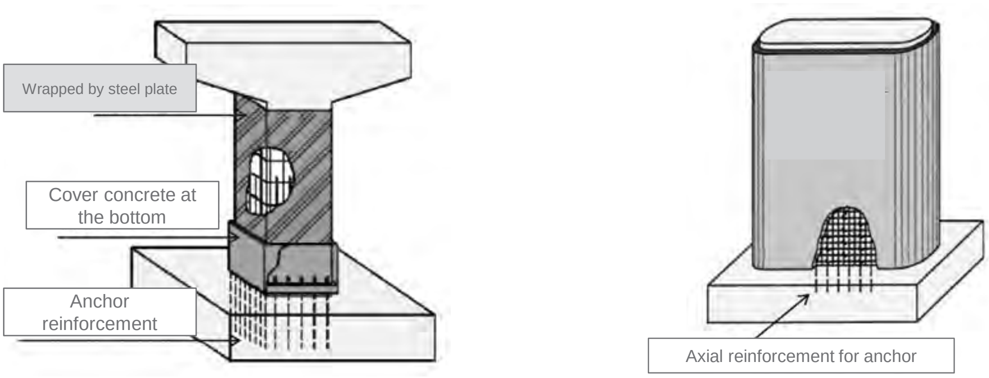

(a) Wrapped by steel plate (b) Wrapped by reinforced concrete

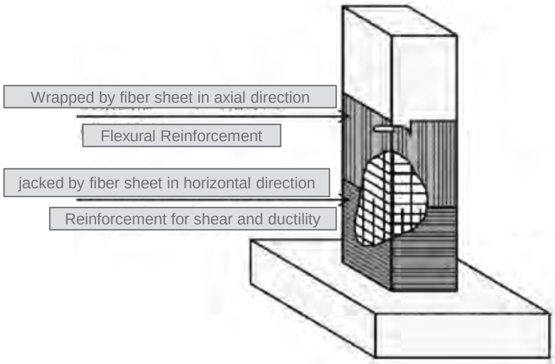
Wrapped by fiber sheet in axial direction
Flexural Reinforcement
jacked by fiber sheet in horizontal direction
Reinforcement for shear and ductility

(c) Wrapped by fiber sheet such as carbon and aramid fiber

Figure 4: 3 types of seismic reinforcement work for RC piers

strength "Wrapping Method" is used. There are three types of wrapping methods that is, wrapping with steel plate, reinforced concrete and fiber sheet shown in Figure 4.

Method by wrapping RC pier with steel plate and filling up filler such as mortar, epoxy resin between their gaps is employed in many cases when there is not enough space around pier and construction period. When flexural reinforcement is required, it is necessary to fix the footing by anchor reinforcement shown in Figure 4(a). In this case, a checking in the horizontal direction of the foundation is required. In case of shear reinforcement, it is not necessary to wrap up around the rigid zone. In case of reinforcement at the cut-off point, it may be wrapped around its reinforcing section.

Method by wrapping RC pier with reinforced concrete is employed in case that there is enough space around pier. It is necessary to unify with existing RC member and new concrete. Therefore, it is required to carry out surface treatment of the existing RC structures by chipping and etc. In case of shear reinforcement, the longitudinal reinforcements at the four corners of RC pier are arranged for the hoop ties and they are not fixed at the footing. However, in case of flexural reinforcement, they are anchored with the footing as well as above case shown in Figure 4(b).

Method by wrapping with fiber sheet such as carbon fiber or aramid fiber is employed in the case of very narrow space when shear reinforcement is required to improve ductility (Figure 4(c)). Therefore, flexural strength is not increased by this method. Shear strength of this reinforcement is calculated as the sum of contribution of concrete and reinforcement of the existing RC member, and fiber sheet. There are two failure modes depending on amount of fiber sheet reinforcement. In case of small amount of fiber sheet, tensile shear failure is occurred. In this case, shear strength is determined by the break off of the fiber sheet. On the other hand, in case of large amount of fiber sheet, shear strength is determined by the collapse of the concrete in compression zone without break off of the fiber sheet. Failure mode is transferred to the shear compression

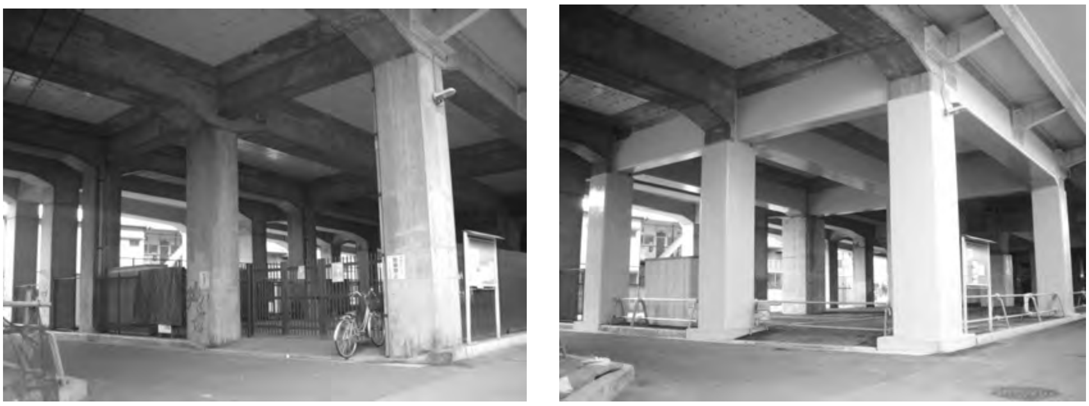

(a) Before reinforcement (b) After reinforcement

Figure 5: Seismic reinforcement of RC piers wrapped by steel plate

failure type. For this reason, the upper limit value of shear strength reinforcement is defined as 0.2%, the maximum ration of reinforcement material.

Figure 5 shows the example of seismic reinforcement work of RC piers. The piers are wrapped by the steel plate. Concrete covers the bottom of the piers and surface of the steel plate is painted.

2.4 Examples of bridge damage due to the East Japan Great Earthquake

The East Japan Great Earthquake was occurred on March 11th in 2011. The magnitude scale was 9.0, the largest earthquake recoded in Japan and maximum JMA (Japan Meteorological Agency) seismic intensity was 7 and areas with strong intensity were widely distributed. This earthquake was plate boundary type.

Figure 6 and Figure 7 show the comparison between RC piers with and without retrofit works. The different results between piers in two photos obviously have been found after the earthquake. The piers shown in Figure 6 with retrofit work were not damaged due to the earthquake. The piers in the left and right photo got the seismic intensity 6^+ and 6^-, respectively. As results of these, crucial damage was prevented by carrying out appropriate seismic strengthening.

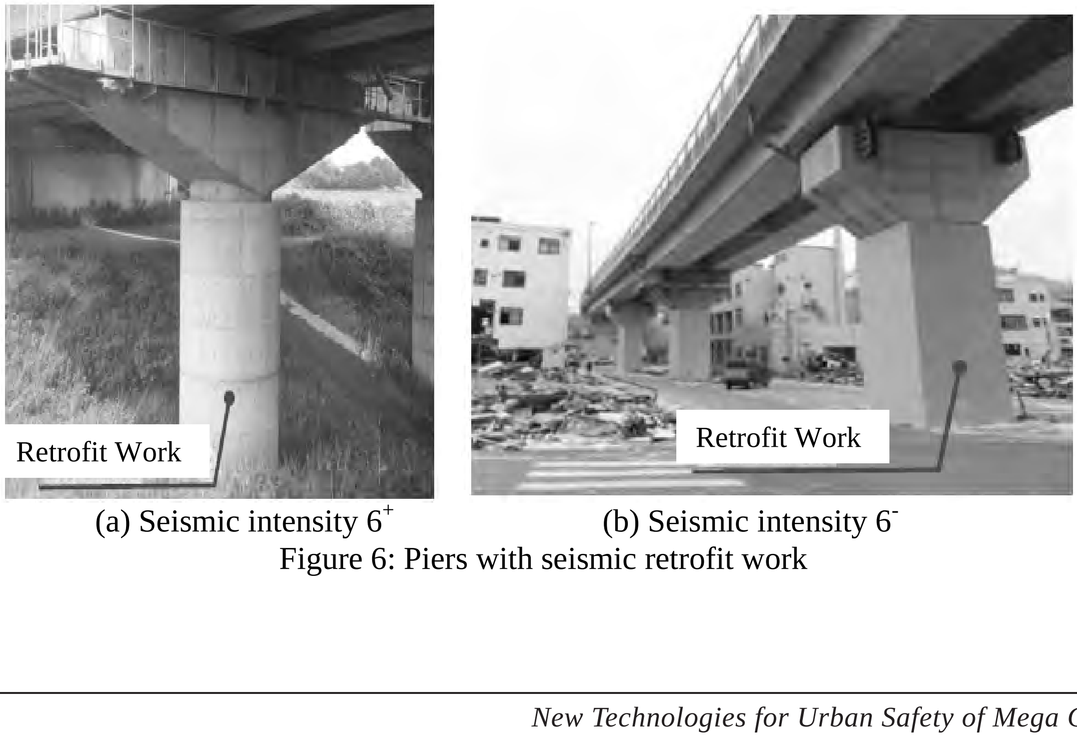

(a) Seismic intensity 6^+ (b) Seismic intensity 6^-

Figure 6: Piers with seismic retrofit work

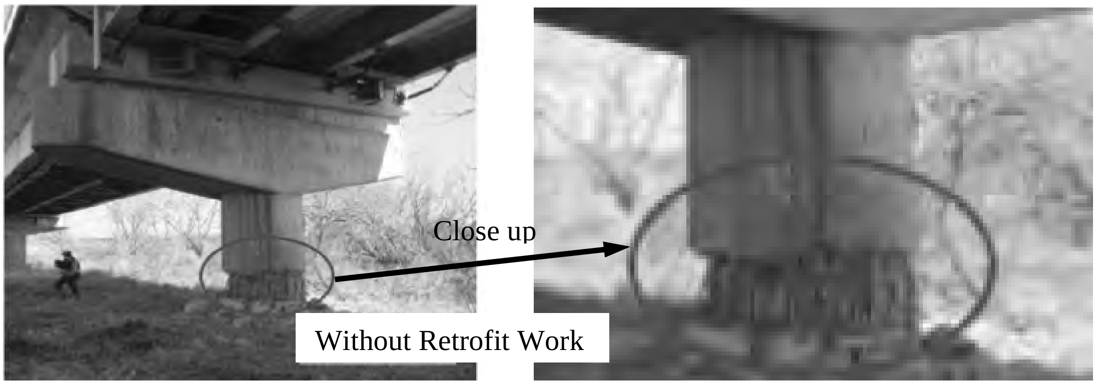

Figure 7: Pier without seismic retrofit work

3. REPAIR AND REINFORCEMENT WORKS OF BRIDGES

It is important to maintain appropriate level of performance structures should have, carrying out inspection, investigation, diagnosis and measures in-service of structures. The results of design, construction, inspection, evaluation and measures, should be recorded in a database and it is desirable to easily access to them. Especially, the records during construction and of initial inspection are very important to understand the initial situation. In addition, the records of repair and reinforcement works are essential to evaluate current situation and appropriate retrofit work. Furthermore, it is important to feed back to design and construction of new structures of a knowledge obtained during inspection, investigation and measures. In this chapter, typical examples of retrofit work of bridges are described.

3.1 Examples of the damages and retrofit works of steel structures

Among the damage of steel bridge structures of the Metropolitan Expressway, is corrosion and cracking 65% shown in Figure 8. The typical damage, their cause and countermeasures are described below.

3.1.1 Degradation of painting film and corrosion

Degradation of the painting and corrosion is caused by ultraviolet light and water leakage. In particular, rust of main girders, crossbeam, is caused by stagnant water and water leakage from the abutment and expansion joints at the end of the girders. This portion is easy to rust since the many members are connected and a space is narrowed and closed. In addition, rust around the bearing supports occurs due to rainwater and soil from the expansion joints.

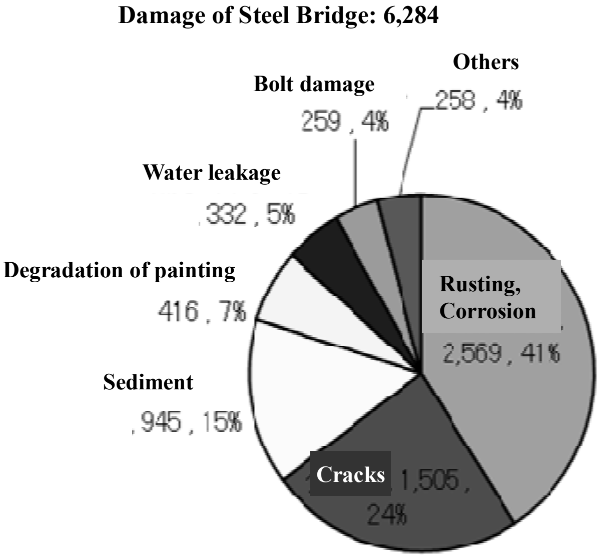

Figure 8: Typical damage of Steel Bridge

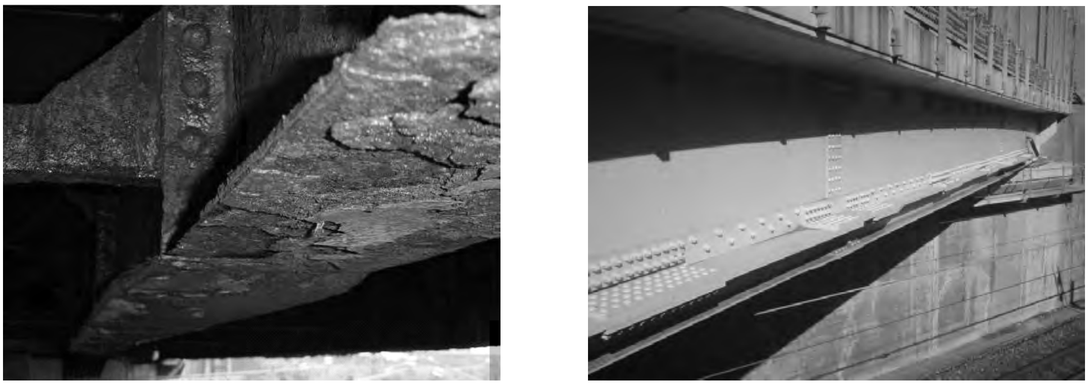

(a) Before repair (b) After repair

Figure 9: Repainting and reinforcement with stiffening plate

For the measures, it is important to eliminate the cause of such leakage and the wet environment in order to prevent corrosion. Waterproof measures such as installing waterproof layer on the surface of the RC slab and employing non-drainage structure of expansion joints.

For degradation of painting film, it is required to repaint regularly. For repainting, adhesion is important between old and new painting film. In order ensure the adhesive force, surface preparation should be carried out and the breakable layer which loses the rust effect shall be removed. In repainting, same paint system should be basically employed. However, a paint system with better anti-corrosion function such as fluororesin-based paint and polyurethane-based paint will be employed in case of extending a repainting period and not removing the cause of leakage and high floating salinity environment. In this case, weak solvent should be used not to damage old painting film or old paint should be removed. Figure 9 shows repair works such as repainting and reinforcement with stiffening plate.

3.1.2 Fatigue damage

Fatigue of steel bridge is a phenomenon that fatigue cracks occur due to repetition of large stress change at the stress concentration portion such as welded joint and are progress. There is also a risk of collapse of a bridge when fatigue cracks are progress. Therefore, a fatigue measure is an important issue in ensuring the safety of steel bridge.

The fatigue measures are classified in two countermeasures such that in-advance countermeasures to prevent occurrence of cracking, i.e. preventive maintenance and countermeasures after the crack has occurred i.e. corrective maintenance.

In order to determine the need for fatigue measures, it is necessary to diagnose and evaluate understanding the situation in which the structures are used in addition to the details of joint structures in which fatigue cracking occurs.

In this paper, typical measures as repair of fatigue damage such as a stop hole method and the mechanical repair by bolts and spliced member are introduced.

A stop hole is a circular hole which is installed in order to remove the crack tip portion. By removing the stress concentration portion with installation of a circular hole, it is possible to prevent or delay the progress of cracks. Stop Hall is generally used as emergency measures until the permanent measures are carried out or used in conjunction with other permanent measures.

Figure 10(a) shows an example that a stop hole is installed at the tip of a crack generated from the weld toe. The tip of a crack shall be completely removed by installing stop hole. Figure 10(b) shows the method of stop hole bolted with splice plate. This method is to improve the fatigue strength reducing the stress concentration of the

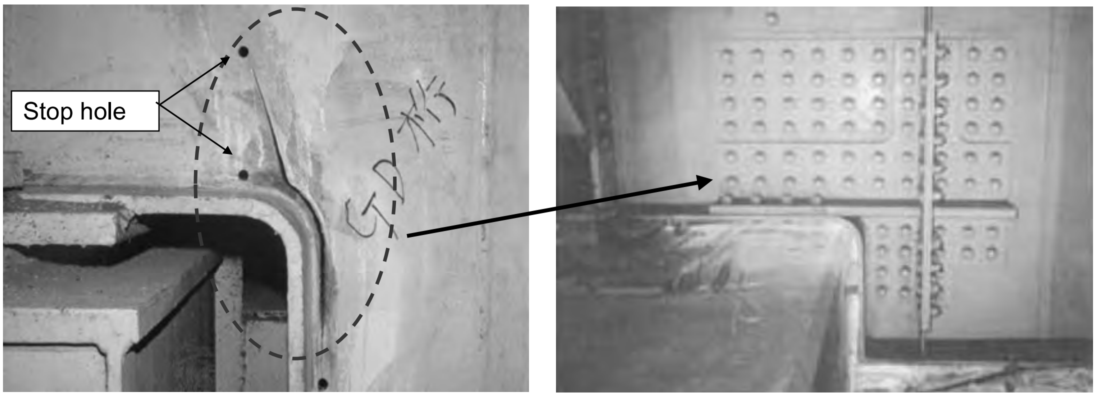

(a) Installing stop hole (b) Bolted with splice place

Figure 10 Measures for fatigue damage

crack tip by installing stop hole and being bolted tightly with splice plate around the stop hole.

3.2 Examples of the damages and retrofit works of reinforced concrete structures

Among the damage of concrete bridge structures of the Metropolitan Expressway, are crack, water leakage and free lime 46%. The main factors of deterioration of concrete structures are carbonation, salt damage, freezing damage, alkali-silica reaction, chemical erosion and fatigue of concrete slab. In this section, the typical damage of concrete slab, their cause and measures are described below.

The drying shrinkage of concrete is restricted by steel girder so that cracks are occurred perpendicular to the bridge axis. As a result of crack development due to repeated loading of wheel load, anisotropy of slab proceeds. For this reason, cracks are also occurred in the bridge axis due to the re-allocation of bending moment in the direction of the main reinforcement. Therefore, cracks at the bottom of the slab progress in two directions. By shear force and torsional vertical shear force by the repetition of wheel load, cracks in two directions are progressed to the entire lower surface of slab and developed into a hexagonal crack. Finally, peeling off and corner falling of concrete facing on cracks occurs by repeated ground-phenomenon due to opening and closing of cracks. Ultimate shear failure is occurred after local failure is induced by punching shear failure.

As the measures for fatigue cracks of concrete slab, there are several retrofit methods such as to increase thickness of upper or lower surface of the slab, to adhere steel plate or continuous fiber sheet, to install stringer and to replace the slab. Currently, carbon fiber sheet adhered in a grid shape is often used for the slab of highway bridges shown

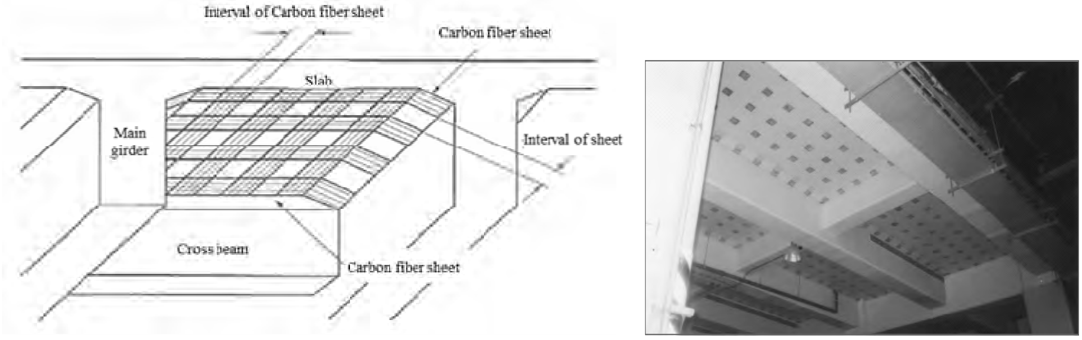

Figure 11: Carbon fiber sheet method

in Figure 11. By adhesion of carbon fiber sheet, there is an effect of restraining deflection and cracks, and improving bending strength of the slab. And if there is seepage water from the bridge surface, there is no stagnant water in the lower surface of the slab so that it does not adversely affect the slab by employing this method. It is also possible to visually inspect and observe a part of the lower surface after construction since the concrete surface is exposed between the carbon fiber sheets.

4. SUMMARY

Seismic design standards in Japan, has been revised according to the progress of research on seismic technology of bridge and the earthquake experience with past earthquakes as described in 2.2. Relatively large damage has occurred on the bridges with structural types that was designed by seismic standard older than 1990, damaged in past earthquakes and seismic design was not performed. On the other hand, the bridges designed by seismic standard after 1990 and retrofit works were carried out, were not damaged. Therefore, it is important to carry out appropriate seismic design and seismic reinforcement shown in 2.2 and 2.3. Three types of wrapping method for RC piers are introduced. As compared between the RC piers with and without retrofit work of by wrapping method, it is obvious that crucial damage was prevented by carrying out appropriate seismic strengthening.

In recent years, the importance of maintenance has been increasing with deterioration and damage of the structures. Typical damage and repair and reinforcement works of steel and concrete bridges are introduced. As for steel bridge, fatigue damage has currently become a major problem as well as corrosion. Typical measures for fatigue cracks are introduced in 3.1 and several inspection methods for detecting fatigue cracks such as ultrasonic testing (UT) and magnetic particle testing (MT) have been developed. As for concrete bridge, cracks and water leakage are major damage, especially fatigue crack of RC slab has been issued from the past. Several reinforcement works of RC slab are introduced and the one of the retrofit method which is lately employed for the Metropolitan Expressway is described. In addition, the effective measures, is the water proofing works of the top surface of slab to improve fatigue durability of concrete slab.

Based on experience of damage, deterioration and earthquake, development of new materials and further development of non-destructive inspection technology is required for carrying out effective maintenance of the structures. Furthermore, advanced infrastructure management system using ICT technology, utilizing monitoring and etc. is desired for sustainable operation and maintenance of the infrastructure.

REFERENCES

Hoshikuma, J., 2012. *Overview of the revision of seismic design standard for road bridge,* Bulletin of JAEE, No17, Japan, 57-60.

Hoshikuma, J., 2012. *Damage of Road Bridge by the Great East Japan Earthquake and further research,* Planning and Construction, No.748, Japan, 20-24.

Committee on Bridges, 2012. *Revision of Specification for Highway Bridge*, No 5, Japan Road Association, Japan, 57-59.

Niwa, J. 2012 (editor-in-chief), *Encyclopedia Sustainable Construction,* Sangyo Chosakai, Japan.

A mathematical model for electric vehicle movement with respect to multiple charging-stops

Yudai HONMA[1]
[1] Lecturer, International Center for Urban Safety Engineering,
Institute of Industrial Science, the University of Tokyo, Japan
yudai@iis.u-tokyo.ac.jp

ABSTRACT

As environmental issues become more prominent, electric vehicles (EV) have attracted an increasing amount of attention. However, the continuous cruising distance of an EV is limited to around 160 km, which is insufficient for everyday use. Battery capacity is the limiting factor in long-distance EV travel. Nissan Co., Ltd. intends to deploy rapid battery chargers for its commercial EV, the Nissan LEAF. The company will install the chargers for over 200 company dealers distributed throughout Japan. These stations enable LEAF motorists to charge their car whenever required. However, the abovementioned dealers own, at most, two rapid chargers. When multiple users converge at the station, a "queuing (or waiting)" condition is created, which may lead to the "call loss" condition. In other words, in planning the EV infrastructure, an appropriate number of chargers must be installed at each station. Therefore, the number of vehicles entering the station must be estimated. In this study, on the basis of the supporting infrastructure for widespread EV use, we propose a mathematical model for estimating the number of vehicles arriving at each charge station.

Keywords: electric vehicle, EV supporting infrastructure, multiple stops

1. INTRODUCTION

As environmental issues become more prominent, electric vehicles (EV) have attracted an increasing amount of attention. EVs have gradually become commercially available and are expected to become widely used in society. However, despite ongoing efforts to improve performance, the continuous cruising distance of an EV is limited to around 160 km, which is insufficient for everyday use (Husain, 2010). Battery capacity is the limiting factor in long-distance EV travel.

Nissan Co., Ltd. intends to deploy rapid battery chargers for its commercial EV, the Nissan LEAF, which is gaining widespread attention. The company will install the chargers for over 200 company dealers distributed throughout Japan. These stations enable LEAF motorists to charge their car whenever required (Nissan, 2014). They are located strategically, such that no region of Japan lies beyond 40 km of a rapid charge station, rendering long-distance travel by EV imminently feasible.

However, the abovementioned dealers own, at most, two rapid chargers. When multiple users converge at the station, a “queuing (or waiting)” condition is created, which may lead to the “call loss” condition. In other words, in planning the EV infrastructure, an appropriate number of chargers must be installed at each station. Therefore, the number of vehicles entering the station must be estimated.

In this study, on the basis of the supporting infrastructure for widespread EV use, we propose a mathematical model for estimating the number of vehicles arriving at each charge station. The rest of paper is organized as follows. In Section 2, a mathematical model to estimate the number of EVs arriving at each charge station is formulated, and basic properties of our model are derived. In Section 3, the model is applied to the Japanese traffic flow and road networks. Conclusion of this study and present ideas for future studies are presented in Section 4.

2. CHARGE STATION AND TRAFFIC MODEL

Set up in two dimensions, the model assumes $|O|$ trip start points (Origins) $O \in (1,\ldots,o,\ldots,|O|)$, $|D|$ trip end points (Destinations) $D \in (1,\ldots,d,\ldots,|D|)$, and $|K|$ EV charge stations $K \in (1,\ldots,k,\ldots,|K|)$ c . It further assumes that T_{od} EVs travel from an origin (o) to a destination (d) within the OD matrix. The maximum cruising distance of the EVs is L. The EVs unable to travel from “o” to “d” without charging their batteries must use one of several charge stations. Under the above assumptions, we derive the number of EVs arriving at each charge station.

Now, a directed graph $G = (V, E)$ connecting the following paths (i) through (iv) is introduced, where the distance between two points is L or less $(V = O \oplus D \oplus K)$.

(i) Origin (Start point) → Charge station
(ii) Charge station → Charge station
(iii) Charge station → Destination (End point)
(iv) Origin (Start point) → Destination (End point)

All conceivable paths of EVs traveling from the origin to destination, in the above network, are expressed on the directed graph G, and path (s) that can be expressed on the directed graph G are the only feasible paths.

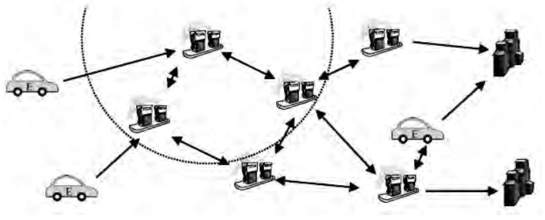

Figure 1: Idea of EV routing network

Given the above conditions and assumptions, we consider an EV moving from an origin (o) to destination (d) on the directed graph G. Many paths linking “o” to “d” are available, including one that utilizes the shortest travel time. Understandably, the path of shortest travel time will be used most frequently, and longer the travel time of a path, the less frequently it is used. To incorporate this concept into the model, we specify the probability that an EV moving from "o" to "d" will use the r th path. On the basis of the multinomial logit model, the probability is defined as

$$P_r^{od} = \frac{\exp\left[-\gamma C_r^{od}\right]}{\sum_{r\in\Phi^{od}} \exp\left[-\gamma C_r^{od}\right]} \tag{1}$$

where C_r^{od} is the cost of traveling the r th path from "o" to "d", and Φ^{od} is a set of paths from "o" to "d." In this study, C_r^{od} is the sum of link costs, and is expressed as

$$C_r^{od} \overset{\text{def.}}{=} c_{ok_1} + \sum_{l=1}^{\Lambda-1} c_{k_l k_{l+1}} + c_{k_\Lambda d} \tag{2}$$

$$C_{ok} \overset{\text{def.}}{=} \frac{d_{ok}}{v} + T \tag{3}$$

$$C_{kk'} \overset{\text{def.}}{=} \frac{d_{kk'}}{v} + T \tag{4}$$

$$C_{kd} \overset{\text{def.}}{=} \frac{d_{kd}}{v} \tag{5}$$

Here, the r th path is the following route from "o" to "d": $o \to k_1 \to k_2 \to \cdots \to k_\Lambda \to d$, d_{**} is the distance between two points, v is speed of the EV, and T is the time required for rapid battery charging.

When the set of paths Φ^{od} is a subset of the "entire conceivable paths," the network flow expressed by equation (1) is equivalent to the Markov distribution (Akamatsu, 1996)

$$p_d(j \mid i) = \exp\left[-\gamma c_{ij}\right]\frac{W_{jd}}{W_{id}}, \tag{6}$$

$$W_{id} \overset{\text{def.}}{=} \sum_{r\in\Phi^{id}} \exp\left[-\gamma C_r^{id}\right] + \delta_{id}. \tag{7}$$

where $p_d(j \mid i)$ is the transition probability of EV traveling from node $i \in V$ to node $j \in V$, and δ_{id} is the Kronecker delta symbol. W_{id} in the above equation can be obtained by the following equation (9), whose elements are given by equation (8) using the matrix A of $N \times N$:

$$a_{ij} = \begin{cases} \exp\left[-\gamma c_{ij}\right] & (\text{When the link } e_{ij} \text{ exists}) \\ 0 & (\text{otherwise}) \end{cases} \tag{8}$$

$$\{W_{ij}\} = [I - A]^{-1} \tag{9}$$

Note that the EV travel can be described by the Markov model. Next, we investigate the Markov process that reaches destination (d). When the transition matrix between nodes in the Markov process is defined by equation (10), the number (N_{id}) of EVs entering each node (while traveling towards the destination) is determined by equation (11):

$$P_d \overset{\text{def.}}{=} \left[p_d(j \mid i)\right] \tag{10}$$

$$\begin{pmatrix} N_{1d} \\ N_{2d} \\ \vdots \\ N_{|N|d} \end{pmatrix}^{\mathrm{T}} = \begin{pmatrix} T_{1d} \\ T_{2d} \\ \vdots \\ T_{|N|d} \end{pmatrix}^{\mathrm{T}} \left[I - P_d\right]^{-1} \tag{11}$$

Thus, the number (N_k) of EVs arriving at charge station k can be derived as follows (independent of destination):

$$N_k = \sum_{d \in D} N_{kd} \tag{12}$$

3. TRIAL CALCULATION BASED ON PASSENGER MOVEMENT IN JAPAN

The model described in the above sections is applied to the movement of traveling passengers in Japan (excluding Hokkaido and Okinawa), to estimate the number of EVS arriving at the charge station. Data regarding vehicles and traveling passenger movements have been extracted from the Third Inter-Regional Travel Survey (MLIT, 2010) issued by the Japanese Ministry of Land, Infrastructure, Transport and Tourism. Origin and Destination points are set by 10km mesh population data. Furthermore, travel time between two points is calculated based on the minimum road network distance (EV travel speed $v =$ 80[km/h] if highways, $v =$ 60[km/h] if metropolitan expressways, and $v =$ 30[km/h] if ordinary roads) from real road network data (Sumitomo Ltd., 2005).

Figure 1 shows the distribution of 2151 EV charge stations at which rapid chargers are currently installed (CHAdeMO Association 2014). The number of EVs arriving at the station per day is calculated. In the survey, traveling passenger movements are aggregated over the each 10km mesh (3470 meshs in total). The centers of population gravity in each meshs are set as origin and destination points, and time for rapid battery charging ($T =$ 40[min.]). The parameter γ is set to 0.1.

As evidenced from the intensity of dots shown in Figure 1 (indicating the number of EVs arriving at the charge station per day), the stations located around large cities and near arterial roads are the most frequently visited. Figure 2 is a histogram of the number of EVs arriving at the charge station per day. Approximately 63% of the 1351 stations are visited 1000 EVs per day or less (average number of EV visits 1097.2 [car/day]). In contrast, the number of EVs arriving at the busiest station is 46031.3 [cars/day], suggesting that so many chargers in the station will be needed.

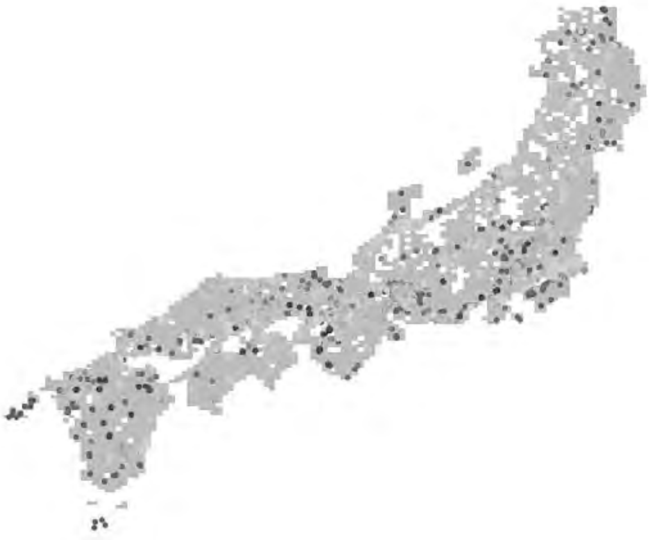

Figure 2: Number of EVs arriving at each charge station per day

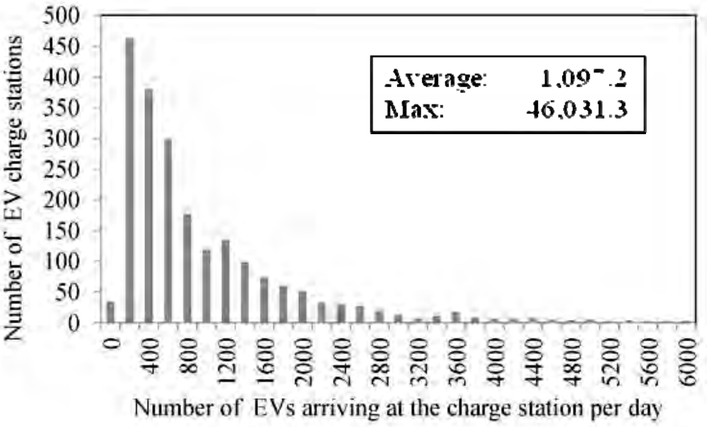

Figure 3: Histogram of the number of EVs arriving at charge stations per day

4. CONCLUSION

The waiting time at rapid-charge stations as well as the number of rapid chargers required at each station is easily determined from the Queuing Theory (M. Haviv 2013), provided that the number of EV visits at each station can be properly estimated. In addition, this model can elucidate the distribution of EVs, traveling time, and charging events (the number of times the EV will require charging), while accounting for multiple charging events in a single trip.

REFERENCES

Akamatsu, T., 1996. Cyclic flows, Markov process and transportation stochastic assignment, *Transportation Research* 30B, 369–386.
CHAdeMO Association, CHAdeMO Association HP (in Japanese): http://www.chademo.com/wp/japan/. 2014/8/31

Haviv, M., 2013. Queues: A course in queueing theory, Springer.
Husain, I., 2010. Electric and hybrid vehicles: Design fundamentals, CRC Press.
Ministry of Land, Infrastructure, Transport and Tourism, 2010. The inter-regional travel survey.
Nissan Motor Company, Nissan LEAF official Web Site, Nissan Motor Company. http://www.nissanusa.com/leaf-electric-car/. 2014/08/31.
Sumitomo Electric Industries Ltd, 2005. Japanese digital road network database.

Travel demand forecasting for sustainable transport planning of Mandalay City

Khaing Zar THWIN[1] and Kay Thwe TUN[2]
[1]Civil Engineer, Pyaeg Hlyan Moe Construction Company, Myanmar
ngengemdy1989@gmail.com
[2]Associate Professor, Department of Civil Engineering,
Mandalay Technological University, Myanmar

ABSTRACT

This paper is focus on the prediction of future travel demand of Mandalay City which is an essential task of the long-range transportation planning process to create a sustainable urban transport system of five townships known as Aung Myay Tha Zan, Chan Aye Tha Zan, Ma Ha Aung Myay, Chan Mya Tha Zi and Pyi Gyi Da Gun within the entire administrative area of Mandalay City. For a thorough understanding of existing travel pattern and identifying and analyzing of existing traffic related problems, the stepwise procedure known as four-step modeling process including four major steps: trip generation, trip distribution, mode choice, and traffic assignment is carried out. The origins and destinations of trips are determined by home interviews (for internal travel) and roadside interviews at cordon stations (for external-internal and through trips). The sample for the survey is generated using the method of stratified random sampling, with stratification. Zonal least square regression analysis is carried out for trip generation. Trip distribution is determined by using Gravity model. The modal split analysis which involves the allocation of total person trips (by all modes) to the respective modes of travel, primarily automobile and public transit is obtained by using multinomial logit model. Traffic assignment is accomplished by Equilibrium assignment. The results of this study will give a performance indicator related to environmental problems for an effective and sustainable land transport system of Mandalay city. This travel pattern developing for a multi-modal transport network will overcome the traffic congestion and delay problems occurred in Mandalay city.

Keywords: *travel demand forecasting, four-step modeling process, the elasticity of demand, origin-destination (O-D) study*

Monitoring of land use/land cover changes in Mandalay City

Zin Mar LWIN[1], Myint Myint KHAING[2] and Kyaw Zaya HTUN[3],
[1]Associate Professor, Mandalay Technological University, Myanmar
dr.zinmar80@gmail.com
[2]Associate Professor, Mandalay Technological University, Myanmar
[3]Assistant Lecturer, Mandalay Technological University, Myanmar

ABSTRACT

Land use/land cover change analysis is necessary to maintain urban environment. It also plays an important role in urban planning and managing urban resources. Due to socioeconomic factor, and increasing population density, Mandalay city has rapid urbanization and taken placed a lot of changes in land use and land cover. This study is focused on analyzing LULC changes in Mandalay city from 2004 to 2014.Changes of urban green cover is also investigated over the 10 years period. Two satellite images; Quickbird 2004 and worldview 2014 are studied to monitor land use /land cover changes, and supervised classification are done to classify different land use classes. Five land use classes are identified: urban built up, water body, vegetation cover, open-land and agricultural land. NDVI values of two images are differenced to know the changes of urban green spaces of Mandalay. Remote sensing and GIS is a cost-effective tool for monitoring and analyzing of urban LULC changes. Results show that noticeable amount of changes, especially from agricultural land to urban area are taken placed in study area.

Keywords: *land use/land cover, change analysis, remote sensing and GIS, Mandalay city*

Assessment of sedimentation and soil erosion effect on Inle Lake in mountainous region

Kyaw Zaya HTUN[1] and Myint Myint KHAING[2]
[1,2]Assistant Lecturer, Remote Sensing Department,
Mandalay Technological University, Ministry of Science and Technology, Myanmar
kyawzaya.htun@gmail.com

ABSTRACT

Inle Lake is the second largest lake in Myanmar and one of the nine key sites for sightseeing there. Inle Lake is not only a multiple purpose lake for the domicile of thirty five floating villages with approximately 90,000 people living in the vicinity of the lake but also importantly the main water source of Law Pi Ta electrical power plant which is the mainly electricity source for the whole Myanmar. Nowadays, the most obvious problem of this lake is shallowness and decreasing area of the lake. According to Movius (1939), the water level in the lake was 100 m higher than the present level. Deforestation, widespread of cultivation and soil erosion cause the three main streams in hilly region to deposit a lot of sediment in the lake. Sediment deposition mainly caused the decreasing lake area and depth. Revised Universal soil loss equation (RUSLE) was applied in conjunction with remote sensing and geographic information system technique to determine the influence of land use and land cover change (LUCC) on soil erosion potential of Inle catchment during the period 1990 to 2010 and the estimated erosion rates were compared with sediment delivery ratios. This study further demonstrates that better soil management can reduce the sedimentation load in the Inle Lake and to save from problem of shallowness and decreasing area of waterbody.

Keywords: *RUSLE, LUCC, deforestation*

Mapping flood inundation in the Bago River Basin, Myanmar

Aung Myo Khaing[1], Akiyuki KAWASAKI[2] and Win Win Zin[3]
[1]Assistant Director, Directorates of Water Resources and
Improvement of River Systems, DWIR, Myanmar
aungmyokhaing.77@gmail.com
[2] Project Associate Professor, Department of Civil Engineering,
The University of Tokyo, Japan.
[3]Associate Professor, Department of Civil Engineering,
Yangon Technological University (YTU), Myanmar

ABSTRACT

Bago river basin is at the lower part of Myanmar, mountainous in the upstream and flat in downstream, so, yearly flood occurs including urban area of Bago city. Local people and authorities are willing to reduce flood frequency and degree of destruction. Nowadays, government agencies studied causes of flood and tried to settle with structural measures. This study aims to generate flood inundation map by non-structural measures. One important data, digital elevation model, DEM, available from websites could not delineate actual stream network for the flood plain area. The 10m resolution DEM for Bago river basin was created with the elevation data of contour lines and point elevations from topographic maps and channel survey maps. The accuracy of DEM was checked by delineating the stream networks and elevation points comparing. That DEM was applied in Soil and Water Assessment Tool, SWAT, to simulate discharge. The simulated result was checked with the observed data of two stations, Zaungtu and Bago. HEC-RAS was applied to compute water surface elevation and flood inundation map was generated in HEC-GeoRAS. The simulated flood area was compared with ALOS image for the year 2006flood, 75% of flooded area was overlapped. The flood for different return periods was considered and Gumbel's distribution method was applied. Finally, flood hazard maps of different return periods were generated with HEC-GeoRAS. This flood result would support decision making for safety of local people and less damage of croplands.

Keywords: *flood inundation map, SWAT and HEC-RAS, DEM creating, Bago river basin, return period flood*

Flood damage estimation sensitivity to spatial scale

Srikantha Herath[1] and Akinola Komolafe[2]
[1] Academic Director, [2]Ph.D. Student,
Institute of for the Advanced Study of Sustainability, United Nations University
herath@unu.edu

ABSTRACT

Pre-disaster economic loss estimation is an important element in flood risk assessment and useful for mobilising investment and developing policies for flood loss prevention. With the potential increase of magnitudes and intensities of climate hazards with climate change pre-disaster loss estimation is becoming extremely important as many of the flood risk reduction decisions are made based on cost benefit analysis. From a global or regional view point it is also important to understand relative impacts on economies of countries to mobilise international support and develop response strategies under future climate scenarios. This requires a unified approach to flood damage estimation across countries and over large areal extents. There are many difficulties associated in undertaking such a task. Economic losses from floods are estimated using loss functions which relate damage to properties and content based on flood water levels. However, the classification of properties as well as approaches to derivation of these functions differ from country to country. In addition spatial resolutions used in the assessment have a direct impact on the estimation of potential flood heights as well as representation of property exposure. In this paper we investigate the sensitivity of spatial scale in estimating potential flood loss and what approaches can be taken to minimise errors arising from coarse spatial resolutions.

Keywords: flood damage, spatial resolution, loss functions, exposure

1. INTRODUCTION

The general shift of focus from flood hazard control to flood risk assessment has propelled the active involvement and interest in the flood impact assessment and economic damage estimation (Bubeck et al., 2011; Ke et al., 2012). Flood damage and loss estimation forms an integral part of flood risk assessment (Bates and De Roo, 2000). Two methods of flood damage estimation involves: i. the use of flood survey of the affected people and property to estimate the incurred damages and losses, mostly done after flood disaster; and ii. the use of stage-damage functions (Herath and Wang, 2009). Most flood damage estimation (especially in the developed countries) makes use of damage functions, formulated based on damage relationship between flood inundation characteristics to assess both after and potential future losses for different flood scenarios (Dutta et al., 2003; Islam and Ado, 2000; Ke et al., 2012; Mohammadi et al., 2014). After flood rapid damage estimations are useful for the allocation of resources for recovery and reconstruction. Understanding the potential flood damages does provide opportunity for identification of elements at risk, effective flood reduction planning, flood mitigation and control, (adaptation, awareness creation and insurance (Bubeck et al., 2011). The synthetic estimation of damages is usually developed for rapid estimation and compared with the observed (incurred) losses from the after flood survey for different damage categories such as building, infrastructures, agricultural crops. etc. (Dutta et al., 2003; Kreibich et al., 2005).

Flood damage is generally classified into two categories: the tangible and intangible damages. The tangible damages are further divided into two: direct and indirect damages. The direct damages are flood damages caused by direct or physical contact with the flood water (e.g. physical damages, loss of life) while the indirect damages are not directly connected to the flood water (e.g. trauma and loss of production and income) (Jongman et al., 2012) (Table 1). Damage and loss estimations have been derived for various categories of tangible properties such as residential, commercial and agricultural crops (Dutta and Herath, 2001; Dutta et al., 2003; Herath et al., 1999; Kreibich et al., 2005). Although the intangible damages are complex and difficult to estimate, some researchers have however attempted to simulate the losses due to loss of lives (Honghai et al., 2006).

Table 1: Flood Damage categories and examples after Dutta et al. (2003)

	Tangible		**Intangible**
	Primary	Secondary	
Direct	Structures, Contents and agriculture	Land and environment recovery	Health, Psychological Damage
Indirect	Transportation, Business Interruption	Impact on regional and national economy	

Two approaches that are usually adopted in the estimation of flood damages in urban area as explained by Su et al. (2005) are parcel-based and grid-based. The former makes use of detail information about the landuse categories, building types and dwelling types; whereas the latter approach divides the study area or region into grids of equal areas, with aggregated information from census data assigned to each cell assuming the same socioeconomic activities within the cell (Dewan, 2013; Su et al., 2005). Both approaches depend mostly on the data availability, and the spatial and temporal scales under consideration. Damage estimations are often done on micro-scale, meso-scale, and macro-scale levels. At the micro level, a detailed structural analysis of the exposure is undertaken; the types of buildings and the materials are taken into consideration in economic damage estimation. The meso scale makes use of the landuse data as the economic assets for a particular region. The macro-scale, which is more coarse and of larger units, is often used for a country and worldwide scale (Bubeck et al., 2011). Generally, flood damages are modelled based on the influence of the inundation depths. Besides the water depth factor, other flood characteristics such as velocity, sediments load, warning time and awareness, winds and duration are also incorporated in damage assessment analysis (Dutta and Herath, 2001; Herath et al., 1999; Herath and Wang, 2009). Other advocated factors by Yang (2005) cited by Chang et al.(2008) are meterological (rainfall terain) and flood prevention measures.

Damage estimation starts with the identification of the potental flood harzards and its charcteristics using various flood models. The results of the model produces flood map showing the inundated area, either as a function of its depths,velocity or duration. With the knowledge of the hazards extents, the exposure elements are identfied. Secondly, the exposure elements are classified based on the spatial characteristics; micro, meso and macro scales. Thirdly, the economic analysis of the damages are done through either survey questionaires after a particular flood events, insurance claim or construction costs. Fourthly, the stage damage curve (also called vulnerability curve) is estabilished; this is the widely accepted common method for estimating direct flood damage (Notaro et al., 2014; Smith, 1994). Stage damage curve can be constructed using either empirical or synthetic methods. The former makes use of the results of the field survey, experiences of the property owners during flood events; the later is based on the expert judgment through available data or the replacement costs of the damaged properties. Stage damage functions are developed for various categories of the exposures using different statistical fitting models (e.g polynomial, linear, square root, etc.) (Freni et al., 2010 ; Notaro et al., 2014). Lastly, the spatial layers of the hazards (inundation depths for example), exposure (property, landuse) and stage damage function can be integrated in Geographic Information Systems (GIS), normalised by the unit cost price of the exposure and the floor area to estimate the potential damages (Dutta and Herath, 2001; Herath et al., 1999) (Figure 1). Most damage simulations are done on detailed/local scale, but in order to regionally estimate damages, a larger coarse scale will be needed. The use of a larger resolution in damage estimation will have effects on the outcome of the estimated damages, hence the need to understand the impacts of the change in scale. Understanding the damages at different scales would help to level of uncertainty involved, and guide in the scaling of the estimation.

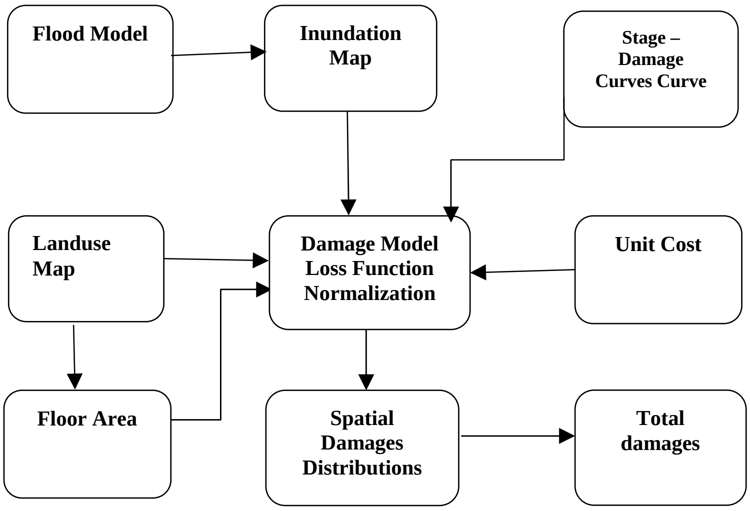
Flood Model
Inundation Map
Stage – Damage Curves Curve
Landuse Map
Damage Model Loss Function Normalization
Unit Cost
Floor Area
Spatial Damages Distributions
Total damages

Figure 1: Conceptual framework for flood damage estimation

The closeness of the estimated losses to after-flood survey losses is determined by the accuracy of the estimation processes, data inputs, and model used. The process of the estimation and the data inputs contribute significantly to the level of uncertainty involved, which can either underestimate and/or overestimate the potential damages. While a couple of processes have been evaluated for the level of uncertainty contributions, little is known about the effect of the spatial resolutions on the damage estimates. Due to multidisciplinary approaches in all stages of flood risk assessment, the introduction of some uncertainties in flood damage estimation are inevitable (de Moel et al., 2012). According to Bubeck et al. (2011) and Moel and Aerts (2011), the uncertainty in flood damage estimation comes through various sources of data inputs; the flood models used for flood hazard (mostly inundation depth) modeling, the exposure (land use), the value of the element at risk and the susceptibility of the element at risk to hydrologic conditions (depth damage function). These processes are accompanied with certain uncertainty that can overestimate or underestimate the potential damages.

Due to the complex nature of flood wave propagation processes, especially in the urban watersheds and lack or limited data for validation and calibration, some level of uncertainties are often associated with the flood damage model results (Freni et al., 2010 ; Jonkman et al., 2008; Notaro et al., 2014). Uncertainty in damage estimation is acknowledged by many researchers in trying to assess the reliability and precision of their works (Jongman et al., 2012; Ke et al., 2012). Most researches have proposed analysis of uncertainty in flood damage estimate in order to ensure reliability and confidence by the decision makers (de Moel et al., 2012). For instance, Bubeck et al. (2011) had examined the uncertainties associated with landuse characteristics and the influence of modelling approches. Furthermore, de Moel et al. (2012) examined the influence of flood and damage models on the damage estimates. The results, however, revealed substantial uncertainties, which mostly resulted from the damage curves used. But, the effect and the influence of flood depths and land-use grid resolutions on flood damage estimates need to be considered. Inundation depths, which have elevation data as an important part of its components, contribute a very large uncertainty to the loss estimates (de Moel et al., 2012; Jongman et al., 2012; Moel and Aerts, 2011). The cell size of the elevation model and grid cell as an input to flood model has strong influence on the model output, and can either under or over predict the actual flood event. The effects of resolutions on the floodplain models has been previously investigated for high resolutions (Dutta and Nakayama, 2009; Horritt and Bates, 2001; Podhorányi et al., 2013). But, the effect of a combined flood depth and land use/land cover resolution has not been given much attention. In this paper, we present, with different scenarios the influence or sensitivity of the spatial resolutions of input data on the output of the flood damage model for decision making in flood damage modeling.

2. METHODOLOGY

2.1 Study Area

Major processes in flood damage assessment were followed to analyze the sensitivity of the damage estimation to grid resolutions. Inundation maps, which produces flood depths were obtained from the existing flood model; the landuse map describing the exposure; vulnerability analysis and damage estimation modelling using Geographical Information Systems (GIS). The sensitivity analysis was done by varying the input grids resolution in NK-GIAS.

The study area for this research is Ichinomiya river basin, situated in the Chiba prefecture, Japan. The river is about 220sq.km basin and 37.3km in length. It lies within the longitude 35o18’N to 35o30’N and latitude 140o10’E to 140o25’ E (Figure 2). Topographically, the basin contains high elevation (about 155m) in the western part and lowland in the eastern part, about 2m from the mean sea level. Ichinomiya basin is frequently affected by flood resulting from intense rainfall, which often affects the lowland urban area. The basin's mean annual rainfall is approximately 1,700mm and has a uniform rainfall distribution (Dutta and Herath, 2001). In 1996, precisely between September 22 and 25, the basin experienced an extreme flood disaster caused by typhoon. According to Dutta and Herath (2001), the whole basin received about 236mm rainfall within 24hours during that period.

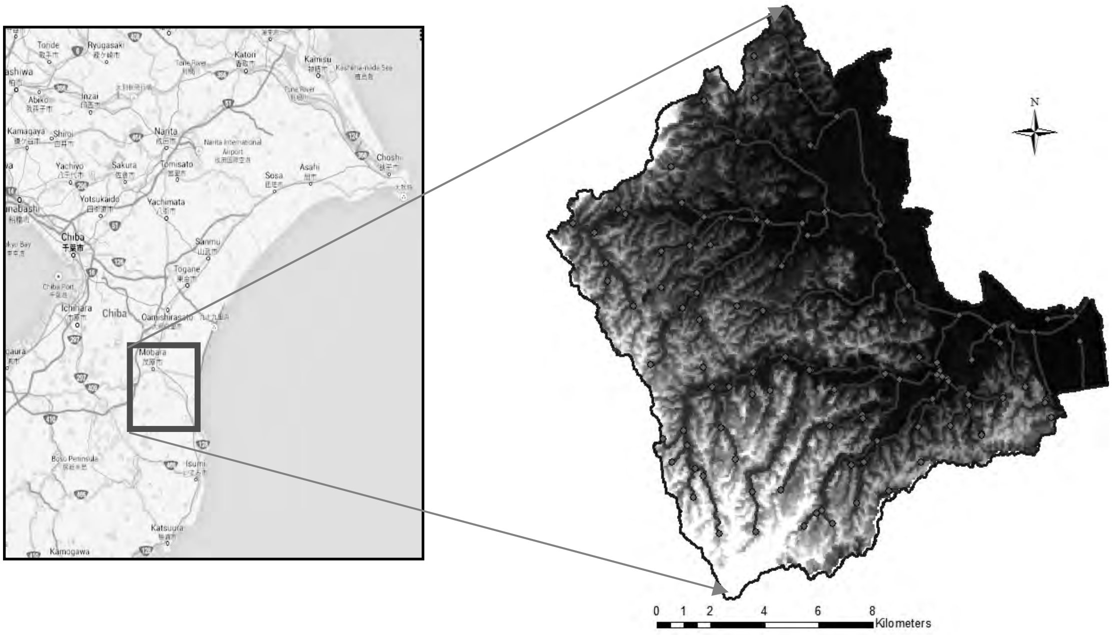
Tonde
Ryugasaki
Katori
Kamisu
Abiko
Inzai
Narita
Kamagaya
Shiroi
Choshi
Yachiyo
Sakura
Tomisato
Sosa
Asahi
Yotsukaido
Yachimata
Chiba
Sanmu
Togane
Chiba Port
Ichihara
Chiba
Oamishirasato
Mobara
Boso Peninsula
Isumi
Katsuura
Kamogawa
N
0 1 2 4 6 8
Kilometers

Figure 2: Study area (Ichinomiya river basin)

2.2 Spatial Information

2.2.1 Landuse Data

The landuse/land cover map of the basin area was derived from Landsat imagery with 30m resolution. The land cover analysis was carried out using Maximum Likelihood (ML) Supervised Classification in ArcGIS classification tool. ML is the most powerful and commonly used algorithm for image classification (Nicholas, 2005); it makes use of both variances and covariance of the class signatures to assign each cell to classes in the signature file. Training classes were generated from the existing and Google map and classification was done interactively. Generally, the basin consists of urban area, vegetation (dense and light forest), water bodies and agricultural lands. The urban area is largely situated downstream (lowlands) with flat topography; these areas are mostly vulnerable to flooding in the past, with severe damages. The vegetation areas (dense and light forests), which constitutes highest proportion of the entire coverage, serves as water shed, and are distributed mostly upstream of the study area.

2.3 Flood Information

Being the first step in flood damage estimation, hazards identification and analysis was done to using existing flood hazard map of the study area. In this paper, water depths

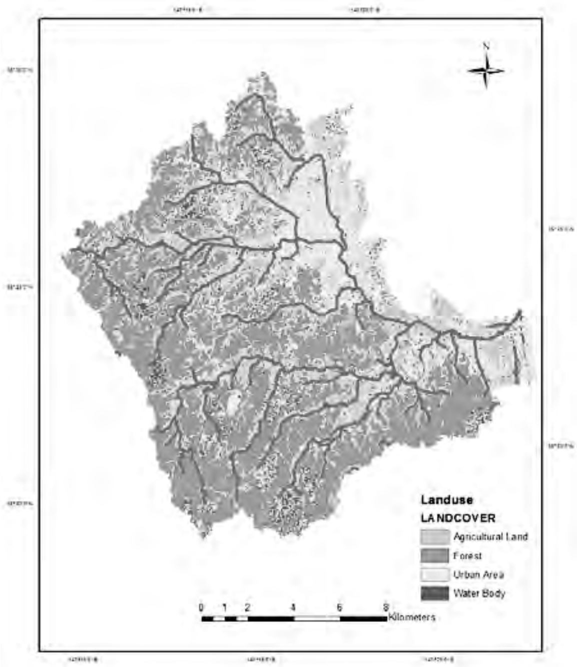
N
Landuse
LANDCOVER
Agricultural Land
Forest
Urban Area
Water Body
0 1 2 4 6 8
Kilometers

Figure 3. Landuse map of the study area derived from Landsat Image

was considered as the major factor that causes damages, and therefore forms the inputs to this damage analysis. Flood hazard was obtained from the simulation done by Dutta et al. (2003), an integrated GIS, hydrological and hydraulic model. The original vector data was 50m x 50m; it shows the simulated water depths within the floodplain in the basin. The inundation depths ranges from 0 to 5.3m, with higher water depths found in the lowlands and along the river course.

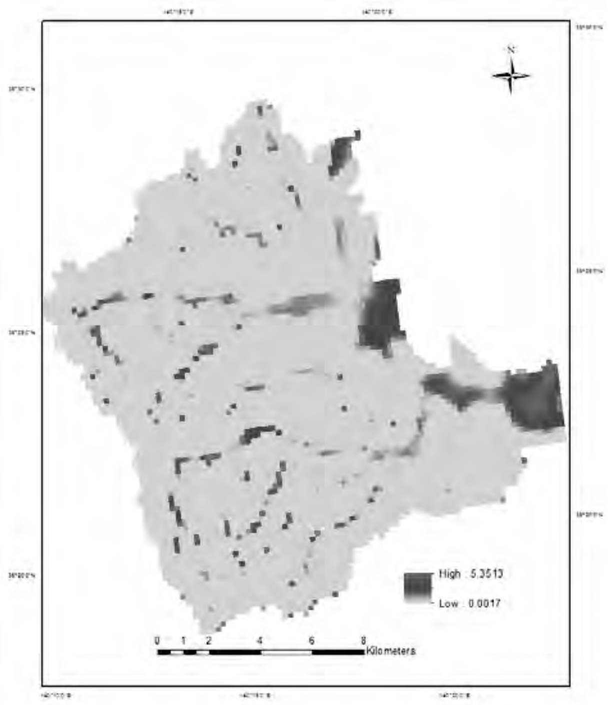
N
High : 5.3513
Low : 0.0017
0 1 2 4 6 8
Kilometers

Figure 4: Flood extent map of the study area after Dutta et al. (2003)

2.4 Damage Functions

Stage-damage function describes the relationship between flood damages and the flood water depths (Notaro et al., 2014). In this research existing stage-damage model developed by Dutta et al. (2003) was used for the estimation of flood damages in this study (Figure 5). The stage- damage curves, developed for japan was developed based on the averaged and normalized data retrieved from the Japanese Ministry of Construction, which was based on site survey (Dutta et al., 2003). Damages are categorized into five categories; industrial contents, industrial structure, residential contents, residential (non-wooden) and residential (wooden). For this research, a residential structure curve for Japan was adopted to examine the influence of spatial resolutions on the estimated results.

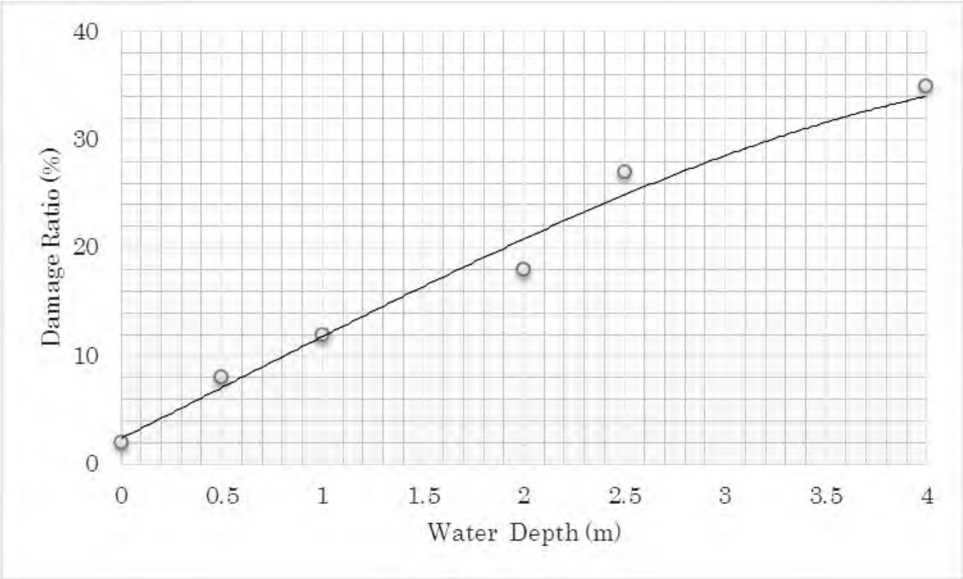

Figure 5: Japan’s flood damage function for residential structure {Dutta, 2003; Herath, 1999; Herath, 2009}

Stage - damage function was derived using polynomial model of order three (3), which describes the degree of damages as a function of flood depths with their damage coefficients (Equation 1).

$$Df = (0.0126667 + (0.0008687 * (x) - (0.000003 * (x)^2 + (0.000000004922 * (x)^3 \ldots\ldots\ldots\ldots\ldots (1)$$

Where Df is damage function expressed as a function of flood depth (x) in meter

We estimated damages based on mathematical model developed by Dutta et al. (2003) for Japan residential structure damage. The equation is a normalized damage function that considers various factors such as floor area, replaceable cost of structure and number of house unit, etc. For this research, the following equation was used:

$$\mathrm{Dr}\ (i,j) = \sum_{k=1}^{n} \{Ns\ (i,j,k) * Df\ (i,j,k) * Fa\ (i,j,k) * Cp(i,j,k\} \ldots\ldots\ldots\ldots\ldots\ldots\ldots\ldots (2)$$

Where for any grid (i,j), Ns is the number of residential building of type k, Df is the depth-damage function for each categories, Fa is the unit residential floor area for building type k and Cp in Japanese Yen is the replacement cost price.

3. ANALYSIS

Sensitivity analysis helps to gain insight into various effects of different assumption which in many ways influences the model output and could guide in the choice of model inputs. It is a simple process that involves changing of input values based on different conditions to unravel its effects on the outputs (de Moel et al., 2012; JRC, 2011; Pannell, 1997). Pannell (1997) grouped the uses of sensitivity analysis into four: (i). decision making or recommendation for decision makers, (ii). communication, (iii). increasing understanding and (iv). model development. Essentially, this study is done to understand what happens to damages at a larger scale and for decision making in the choice of input spatial resolutions in flood damage and loss modeling.

Sensitivity analysis was carried out interactively in GIS environment with varying grid resolutions as inputs to the damage estimation. Damage was estimated using NK-GIAS software. NK-GIAS (Nippon Koei-Geographic Information Analysis) is a Japanese based integrated GIS and hydrological modelling software, which is used to handle spatiotemporal data (Nippon Koei Technical report, 2011). Major grids input were: the Landuse, Floor Area, Flood depths and Cost Price. The landuse was reclassified into two; residential and others, and assigned values 1 and 0 respectively. This was resampled to various coarse resolutions (50, 100, 500, 1000 and 2000) m as in Figure 6.

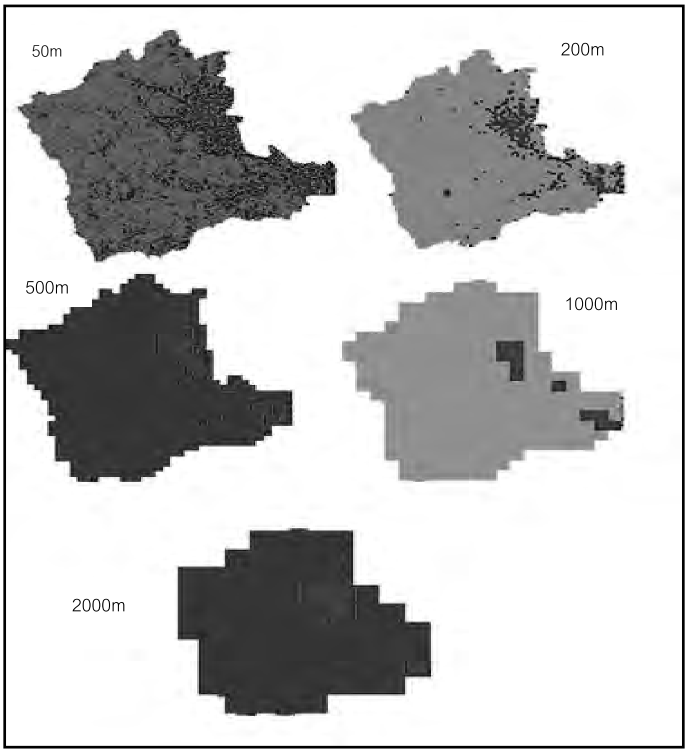

Figure 6: Different Landuse resampled grid resolutions used as inputs to the model

The flood depth was re-sampled into various spatial resolutions (200 x 200m; 500 x 500m; 1000 x 1000m and 2000 x 2000m) (Figure 5). Other layers were also resampled to the same resolutions for input into the model simulation. Damage functions for different flood depths resolutions (50, 200, 500, 1000 and 2000) m were derived with polynomial function for residential structure in equation (1) using overlay analysis in

GIS. Also, the total flood damages were simulated with the equation (2) by varying the derived damage functions grids with the landuse, cost, and floor area grids. Simulation was done with two scenarios: (i). at constant high resolution (50m) property (landuse) with increasing flood depths coarse resolutions. Since the principle of overlay allows grids of the same resolutions, the coarse flood depths were resampled back to the high resolution of the property distribution scale. (ii). at concurrent increase in the flood depths and property resolutions. The results are shown in Figures 7.

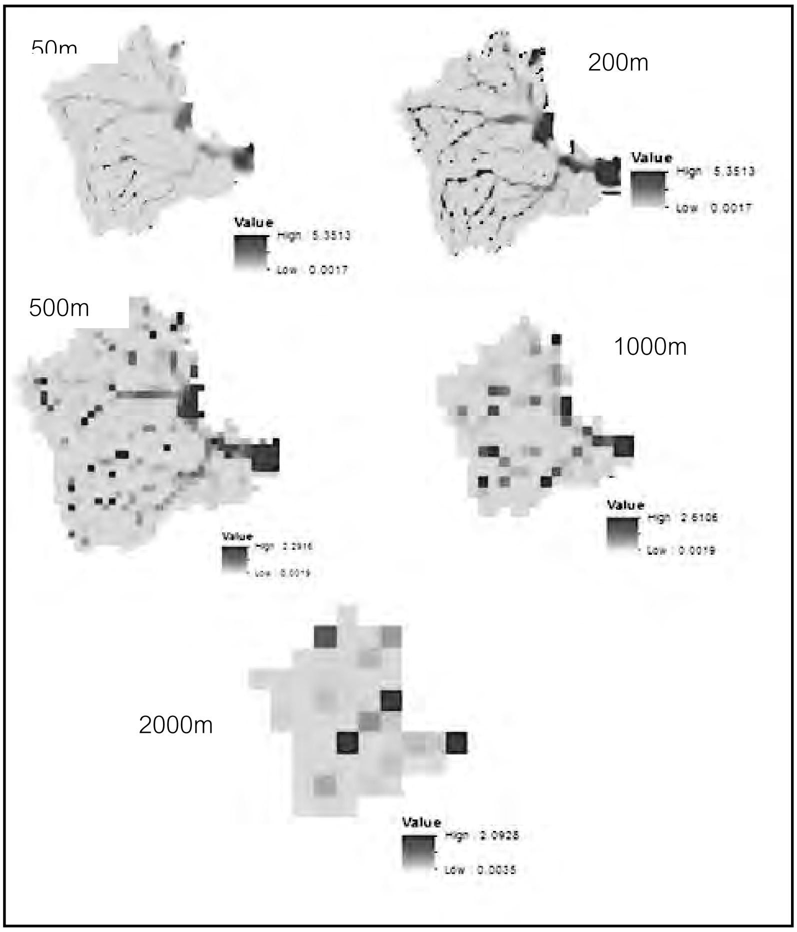

Figure 7: Flood depth resampled grid resolutions used as inputs to the model

In order to verify the authenticity of the simulated model and to determine the closeness of the simulated damages to the observed, a comparative analysis was done with the survey flood damages of the study area as reported by Dutta et al. (2003).

4. RESULTS AND DISCUSSION

Spatial resolutions in flood damage modelling impact greatly on the outputs damages. The increase in the flood depth spatial resolution (coarse layers) as shown in figures a, b and c demonstrated a large spread and flood extent with lower water heads while a decrease in grid cell sizes (high resolution) reduces the flood extent with higher water heads (Figures 6); these variations however influences the outcome of flood damage simulation.

For the first scenario, at a constant high resolution property and coarse resolution of the flood depths, the estimated damages showed a gradual increase as the resolution increases. Statistically, the total damages increase with about 10% from the 50m grid compared with the 2000m flood depth grids (Figure 6). The damage trend shown by linear model with adjusted R squared of approximately 88% as in equation (3):

$$F_{d(ij)} = 184.04x_{ij} + 5 \times 10^6 \ldots\ldots\ldots\ldots\ldots\ldots\ldots\ldots\ldots\ldots\ldots\ldots\ldots\ldots\ldots\ldots\ldots\ldots \text{(3)}$$

Where $F_{d(ij)}$ is the total flood damages in yen at any spatial scale and $x_{ij}$is the spatial resolution in meters (m)

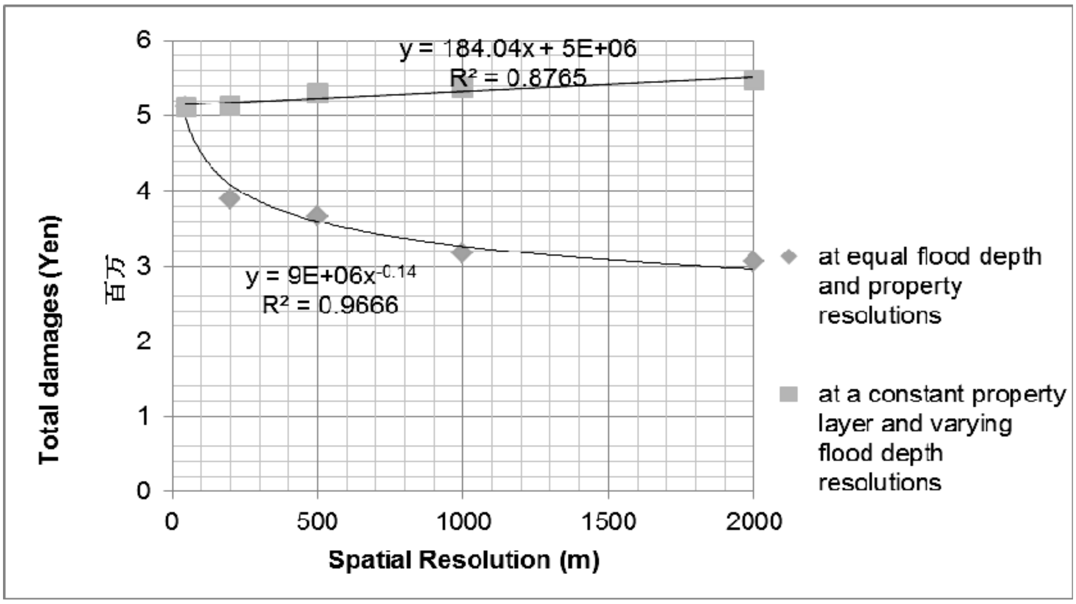

Figure 6: Variation of damage estimations with spatial resolutions (at a constant property layer and varying flood depth resolutions).

The second scenario of this analysis ensured that resolution of both grids are increased simultaneously. The result revealed an opposite side of the first scenario, with lower damages experienced, which decreases with almost 40% from 50m to 2000m (Figure 6). The trend of the results were fitted by inverse power regression model with 97% adjusted R squared as shown in figure 6. For every increase in the resolutions of both flood depths and landuse, the expected flood damages can be defined as:

$$F_{d(ij)} = 9 \times 10^6 {x_{ij}}^{-0.14} \quad \ldots\ldots\ldots\ldots\ldots\ldots\ldots\ldots\ldots\ldots\ldots\ldots\ldots\ldots\ldots\ldots\ldots\ldots \text{4}$$

Where F_(d(ij))is the total flood damages in yen at any spatial scale and x_ij is the spatial resolution in meters (m)
By using equation 4, we estimated the projected damages for different resolutions, for both 100m and 1000m resolution steps as revealed in Table 3.

Unlike the first scenarios with a constant increase in flood damages, the table shows an unequal but decrease in flood damages for both increasing steps in spatial resolutions.

Table 2: Predicted Flood damages for different spatial resolutions as defined by the first scenario’s model

Spatial Resolutions (m)	Predicted Total Damages (Yen)	Spatial Resolutions (m	Predicted Total Damages (Yen)
2100	5,386,484	**3000**	5,552,120
2200	5,404,888	**4000**	5,736,160
2300	5,423,292	**5000**	5,920,200
2400	5,441,696	**6000**	6,104,240
2500	5,460,100	**7000**	6,288,280
2600	5,478,504	**8000**	6,472,320
2700	5,496,908	**9000**	6,656,360
2800	5,515,312	**10000**	6,840,400
2900	5,533,716	**11000**	7,024,440
3000	5,552,120	**12000**	7,208,480
3100	5,570,524	**13000**	7,392,520
3200	5,588,928	**14000**	7,576,560
3300	5,607,332	**15000**	7,760,600
3400	5,625,736	**16000**	7,944,640
3500	5,644,140	**17000**	8,128,680
3600	5,662,544	**18000**	8,312,720
3700	5,680,948	**19000**	8,496,760
3800	5,699,352	**20000**	8,680,800

Table 3: Predicted Flood damages for different spatial resolutions as defined by the second scenario’s model

Spatial Resolutions (m)	Predicted Total Damages (Yen)	Spatial Resolutions (m	Predicted Total Damages (Yen)
2100	3,084,124	**3000**	2,933,902
2200	3,064,103	**4000**	2,818,085
2300	3,045,093	**5000**	2,731,409
2400	3,027,004	**6000**	2,662,572
2500	3,009,753	**7000**	2,605,726
2600	2,993,272	**8000**	2,557,466
2700	2,977,499	**9000**	2,515,640
2800	2,962,377	**10000**	2,478,806
2900	2,947,860	**11000**	2,445,950
3000	2,933,902	**12000**	2,416,335
3100	2,920,464	**13000**	2,389,409
3200	2,907,512	**14000**	2,364,746
3300	2,895,013	**15000**	2,342,015
3400	2,882,939	**16000**	2,320,950
3500	2,871,263	**17000**	2,301,334
3600	2,859,961	**18000**	2,282,992
3700	2,849,012	**19000**	2,265,776
3800	2,838,395	**20000**	2,249,564

In general, for coarse grids, the lowering of water heads causes the flood damages to be smaller while the large extent coverage increases the flood damages; these, however, compensate each other during simulation.

Comparing the observed total damages after 1996 flood event with the estimated damages from the sensitivity analysis, the results of both scenarios showed that none of the estimations are near the observed/surveyed values, except the higher resolution (50m) for first and second scenarios. This points to the fact that for a robust accurate estimates, a resampling of flood depth to high resolutions and having property distribution layer at higher resolution would be necessary (Figures 7 and 8). However, from the results, modeling damages at a large scale can achieve reasonable results, with little changes when maintaining property at a constant high resolution with increasing the resolution sizes. This is confirmed in the first sensitivity scenarios where there is a relatively small increase in damages with increase in the cell sizes compared to the second scenarios, which has a large decrease in damages.

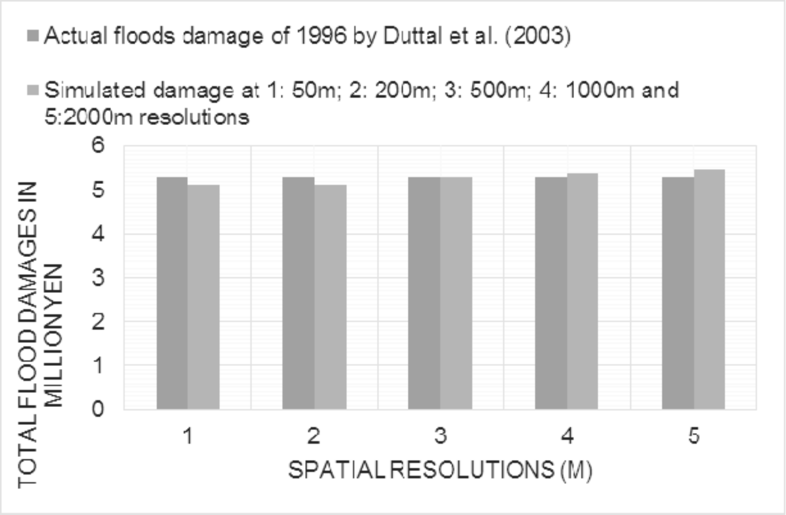

Figure 7: Comparison between the observed residential structure flood damage and the simulated flood damages at different resolutions for the first scenarios: at constant property and increasing flood depths' coarse resolutions.

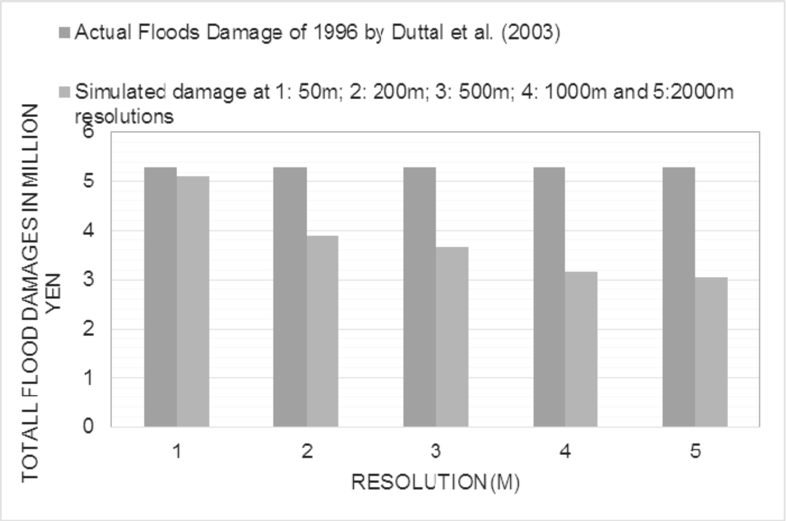

Figure 8: Comparison between the observed residential structure flood damage and the simulated flood damages at different resolutions for the second scenarios: at the same increasing resolutions of flood depths and property.

5. CONCLUSIONS

Damage estimation simulations require the integration of various spatial data layers, which are heavily dependent on the scale used to represent data. Apart from individual examination of the contributions of input data on the overall simulation results as done previously by other authors, an effort is made in this study to analyze effect of spatial resolution on flood loss estimation in order to retain original information as much as possible. This study examined the sensitivity/response of damage models to various spatial resolutions of the input data such as the flood depths and the property layers, under two scenarios: first, at a uniform increasing grid sizes for both flood and exposure information and, secondly, at a property distribution at a high resolution but flood depth at varied scales. The research reveals that it is possible to estimate pre-disaster losses close to actual losses if high spatial resolution data are used. However, as it is not possible to model floods at such a high resolution at regional scale it is inevitable to use coarser grids to model floods for regional studies. By adopting a higher resolution representation of property distribution, it is possible to retain much of the accuracy of forecasts even though the flood heights are averaged over larger grids. This result is encouraging as the computational resources required to combine coarse flood information with static high resolution property distribution to compute flood losses require much less computer resources than modeling inundation at a high spatial resolution.

REFERENCES

Bates, P. D., and De Roo, A. P. J., 2000, A simple raster-based model for flood inundation simulation: Journal of Hydrology, v. 236, no. 1–2, p. 54-77.

Bormudoi, A., Fowze, J. S. M., Hazarika, M. K., L.Samarakoon, Gunasekara, K., Kabir, S. M. H., and Mustofa, S. A., 2011, Rapid Flood Damage Estimation: A Case Study At Chandpur, Bangladesh: 3rd International Conference on Water & Flood Management (ICWFM-2011).

Bubeck, P., de Moel, H., Bouwer, L. M., and Aerts, J. C. J. H., 2011, How reliable are projections of future flood damage?: Nat. Hazards Earth Syst. Sci., v. 11, no. 12, p. 3293-3306.

Chang, L.-F., Lin, C.-H., and Su, M.-D., 2008, Application of geographic weighted regression to establish flood-damage functions reflecting spatial variation: Water SA v. 34, no. 2.

de Moel, H., Asselman, N. E. M., and Aerts, J. C. J. H., 2012, Uncertainty and sensitivity analysis of coastal flood damage estimates in the west of the Netherlands: Nat. Hazards Earth Syst. Sci., v. 12, no. 4, p. 1045-1058.

Dewan, A. M., 2013, Floods in A Megacity: Geospatial Techniques in Assessing Hazards, Risk and Vulnerability, Springer Geography, Springer Science.

Dutta, D., and Herath, S., GIS Based Flood Loss Estimation Modeling in Japan, in Proceedings Proceedings of the US-Japan 1st Workshop on Comparative Study on Urban Disaster Management, Port Island, Kobe, Japan, February 2001 2001.

Dutta, D., Herath, S., and Musiake, K., 2003, A mathematical model for flood loss estimation: Journal of Hydrology, v. 277, no. 1–2, p. 24-49.

Dutta, D., and Nakayama, K., 2009, Effects of spatial grid resolution on river flow and surface inundation simulation by physically based distributed modelling approach: Hydrological Processes, v. 23, no. 4, p. 534-545.

Dutta, D., Wright, W., Nakayama, K., and Sugawara, Y., 2013, Design of Synthetic Impact Response Functions for Flood Vulnerability Assessment under Climate Change Conditions: Case Studies in Two Selected Coastal Zones in Australia and Japan: Natural Hazards Review, v. 14, no. 1, p. 52-65.

Freni, G., La Loggia, G., and Notaro, V., 2010 Uncertainty in urban flood damage assessment due to urban drainage modelling and depth-damage curve estimation: Water Science & Technology—WST v. 61, no. 12, p. 2979 - 2993.

Herath, S., Dutta, D., and Musiake, K., Flood damage estimation of an urban catchment using remote sensing and GIS, in Proceedings International Conference on Urban Storm Drainage1999, Volume 4, p. 2177 - 2185.

Herath, S., and Wang, Y., 2009, Incorporating Wind Damage in Potential Flood Loss Estimation: Global Environmental Research p. 151-159.

Honghai, Q., Altinakar, M. S., and Youngho, J., A Decision Support Tool for Flood Management Under Uncertainty Using GIS and Remote Sensing Technology, in Proceedings The 7th Int. Conference on Hydroscience and Endgineering (ICHE-2006), , Philadelphia, USA, Sep 10 -Sep 13, 2006 2006.

Horritt, M. S., and Bates, P. D., 2001, Effects of spatial resolution on a raster based model of flood flow: Journal of Hydrology, v. 253, no. 1–4, p. 239-249.

IPCC, 2014, Climate Change 2014: Impacts, Adaptation and Vulnerability. IPCC Working Group II Contribution to AR5. Summary for Policymakers. Intergovernmental Panel for Climate Change. http://www.ipcc.ch/.

Islam, M. M., and Ado, K. S., Flood damage and management modelling using satellite remote sensing data with GIS: case study of Bangladesh, in Proceedings Remote Sensing and Hydrology 2000 (Proceedings of a symposium held at April 2000). IAHS Publ. no. 267, 2001, Santa Fe, New Mexico, USA, 2000.

Jongman, B., Kreibich, H., Apel, H., Barredo, J. I., Bates, P. D., Feyen, L., Gericke, A., Neal, J., Aerts, J. C. J. H., and Ward, P. J., 2012, Comparative flood damage model assessment: towards a European approach: Nat. Hazards Earth Syst. Sci.,, v. 12, p. Nat. Hazards Earth Syst. Sci.,.

Jonkman, S. N., Bočkarjova, M., Kok, M., and Bernardini, P., 2008, Integrated hydrodynamic and economic modelling of flood damage in the Netherlands: Ecological Economics, v. 66, no. 1, p. 77-90.

JRC, 2011, Global Sensitivity Analysis Available at: http://sensitivity-analysis.jrc.it/faq.htm.

Ke, Q., Jonkman, S. N., Rijcken, T., and Gelder, P. V., Flood Damage Estimate for Downtown Shanghai City - Sensitivity Analysis, in Proceedings Poster Presentation, the 3rd Conference of the International Society for Integrated Disaster Risk Management, Beijing, China, 7-9 September, 2012 2012.

Kreibich, H., Thieken, A. H., T. Petrow, Muller, M., and Merz, B., 2005, Flood loss reduction of private households due to building precautionary measures – lessons learned from the Elbe flood in August 2002.: Natural Hazards and Earth System Sciences, v. 5 no. 1, p. 117-126.

Moel, H., and Aerts, J. C. J. H., 2011, Effect of uncertainty in land use, damage models and inundation depth on flood damage estimates: Natural Hazards, v. 58, no. 1, p. 407-425.

Mohammadi, S. A., Nazariha, M., and Mehrdadi, N., 2014, Flood Damage Estimate (Quantity), Using HEC-FDA Model. Case Study: The Neka River: Procedia Engineering, v. 70, no. 0, p. 1173-1182.

Nicholas, M. S., 2005, Remote Sensing Tutorial, Publisher: EOS-Goddard Program Office

Notaro, V., De Marchis, M., Fontanazza, C. M., La Loggia, G., Puleo, V., and Freni, G., 2014, The Effect of Damage Functions on Urban Flood Damage Appraisal: Procedia Engineering, v. 70, no. 0, p. 1251-1260.

Pannell, D. J., 1997, Sensitivity analysis of normative economic models: Theoretical framework and practical strategies: Agricultural Economics v. 16, p. 139-152.

Podhorányi, M., Unucka, J., Bobál, P., and Říhová, V., 2013, Effects of LIDAR DEM resolution in hydrodynamic modelling: Model sensitivity for cross-sections: International Journal of Digital Earth, v. 6, no. 1, p. 3-27.

Smith, D., 1994, Flood Damage Estimation- A Review of Urban Stage -Damage Curves and Loss Functions: Water SA, v. 20, no. 3, p. 231-237.

Su, M. D., Kang, J.-L., Chang, L.-F., and Chen, A. S., 2005, A Grid-Based GIS Approach To Regional Flood Damage Assessment: Journal of Marine Science and Technology, v. 13, no. 3, p. 184 - 192.

UNISDR, 2009, Risk and Power in a Chnaging Climate: Invest today for a safer tomorrow: United Nations International Strategy for Disaster Reduction (UNIDR).

Yang L, Z. C., and Wang, Y., 2005, An effective two-stage neu- ral network model and its application on flood loss prediction.: Proc. Advances in Neural Networks, v. 3498 p. 1010-1016.

Numerical simulation of environmental disasters in the waterfront area under the impact of extreme events

Bin HE[1], Kyoji SASSA[2], Yi WANG[3]
And Srikantha HERATH[4]

[1] Key Laboratory of Watershed Geographic Sciences, Nanjing Institute of Geography and Limnology, Chinese Academy of Sciences, Nanjing, 210008, China
hebin@niglas.ac.cn
[2] International Consortium on Landslides (ICL)
[3], [4]*United Nations University (UNU)*

ABSTRACT

Waterfront is the land area alongside a body of water (ocean, river, lake), such as a harbor, dockyard, riverbank, etc. It is well known that a majority of landslides, flooding and pollution occurred in waterfront area during extreme events (e.g., heavy rainfall and earthquakes). It causes tremendous disaster to urban riverbank, port and industrial facilities. However, little attention has been paid to the environmental disaster issues in the waterfront areas. It presents the necessity of a new modelling technology for disaster risk preparedness which simulates initiation and motion of waterfront disasters, especially for urban regions. In this paper, the features and problems related to the waterfront landslide, flooding and pollution will be reviewed. The related simulation model, which was developed from the geotechnical model for the motion of landslides and flood, will be introduced. The waterfront landslides/floods are simulated for several cases of waterfront. The performance will be examined under different conditions of earthquake and rainfall. The process of progressive landslide and flood will be visualized in both two dimensions and three dimensions. The preliminary results of a computational study conducted to analyze waterfront landslide and flood for several case studies will then be presented.

Development of flood inundation map for the Bago River Basin

Shelly Win[1], Win Win Zin[2], Akiyuki KAWASAKI[3]
and Tin MAUNG[4]
[1] Master Student, Department of Civil Engineering, Yangon Technological University
zigmobridge@gmail.com
[2]Associate Professor, Department of Civil Engineering,
Yangon Technological University
[3]Project Associate Professor, Department of Civil Engineering,
The University of Tokyo, Japan
[4] Visiting Associate Professor, Department of Civil Engineering,
Yangon Technological University

ABSTRACT

Flooding is one of the major hazards in Myanmar. In this study, the Bago River basin was taken as the case study area. Flood inundation maps are needed for floodplain analysis and management. In order to perform flood inundation mapping, HEC-HMS and HEC-RAS were used as hydrological and hydraulic models, respectively. During the pre-processing of the GIS data, Digital Elevation Model (DEM) and Triangulated Irregular Network (TIN) were prepared from available contours, point elevations and surveyed cross sections data. The river geometric data was extracted by using HEC-GeoHMS and HEC-GeoRAS extension and exported to HEC-HMS and HEC-RAS model, respectively. Daily rainfall data is used for HEC-HMS calibration and validation. HEC-HMS model is used for determining the design flow hydrographs. HEC-RAS is applied to compute the water surface elevations. The observed daily water level data were used for the calibration and validation. The flow conditions for 2, 10, 50, and 100 year return periods of flood were computed in HEC-RAS model. The model result of 2006 flood inundation was verified by Advanced Land Observing Satellite (ALOS) SAR image from Japan Aerospace Exploration Agency (JAXA) of June, 2006. The flood inundation map was classified for the degree of hazard based on the flood depth. The flood hazard maps with different return periods were delineated by using HEC-GeoRAS.

Keywords: flood inundation maps, floodplain analysis and management, HEC-HMS, HEC-RAS, river geometric data, water surface elevations.

1. INTRODUCTION

During the year 2011, there were two severe floods happened in the Bago River basin in July and August. Nearly all of the rivers and creeks were over flooded and inundated paddy fields areas were 498 km^2. Thousand of households and properties were also affected and inundated duration was at least above five days (Aung, 2013).

In this study, HE-HMS and HEC-RAS were utilized as the hydrologic and hydrodynamic models which were linked to a GIS environment using HEC-GeoHMS and HEC-GeoRAS. 10 m resolution DEM developed by Khaing (2014) was used. This study contributed to develop the flood inundation maps for different return periods – 2, 10, 50 and 100 year as the future scenarios. Two statistical criteria are used to evaluate the calibrated model performance such as: Pearson's coefficient of determination (R^2) and Nash and Sutcliffe model efficiency (E_{NS}) in this research.

2. LOCATION OF THE STUDY AREA

Bago River originates from the middle mountainous region named Bago Yoma and the large portion of the river itself is within Bago Region. A small portion of the river (the outlet) is in Yangon Region where Bago River joins the Yangon River and, from there, enters the Gulf of Mottama. The basin has a catchment area of 5348 km^2, and the main river is about 331.5 km long, lying between longitudes 95°53'30"E and 96°43'30"E and between longitudes 16°43'15" N and 18°26'17" N in lower Myanmar.

The Bago River is one of the most important and useful river basins in lower Myanmar for hydropower generation, irrigation use, fisheries and navigation use. The location map of the Bago river basin with the completed structures is shown in Figure 1.

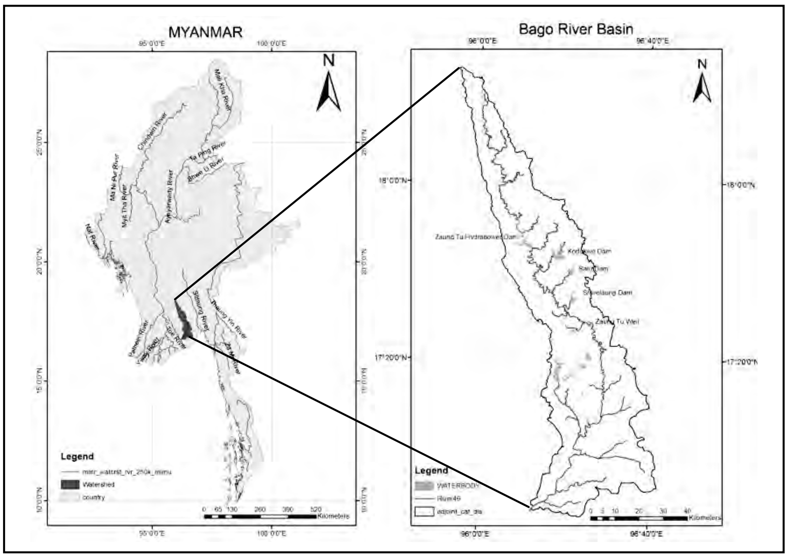
MYANMAR
95°0'0"E
100°0'0"E
N
25°0'0"N
20°0'0"N
15°0'0"N
10°0'0"N
Mali Kha River
Chindwin River
Ta Ping River
Shwe Li River
Ma Ni Pur River
Myit Tha River
Ayeyarwady River
Naf River
Sittaung River
Thaung Yin River
Pathein River
Yangon River
Legend
mmr_watrst_rvr_250k_mimu
Watershed
country
0 65 130 260 390 520 Kilometers
Bago River Basin
96°0'0"E
96°40'0"E
18°0'0"N
17°20'0"N
Zaung Tu Hydropower Dam
Kodukwe Dam
Salu Dam
Shwelaung Dam
Zaung Tu Weir
Legend
WATERBODY
River49
adjoint_cat_dis
0 5 10 20 30 40 Kilometers

Figure 1: Location map of the study area

3. METHODOLOGY AND MODEL DEVELOPMENT

3.1 Methodology

Computers models for the determination of river flood inundation mapping generally consists of four parts, these are:

(1) The extraction of geospatial data for use in the hydrological and hydraulic models (HEC-geoHMS and HEC-geoRAS). Geospatial Hydrologic Modeling extension (HEC-GeoHMS) is a software package which can be used as an

extension of the ArcGIS [USACE, 2004]. HEC-GeoRAS 4.1.1 [Ackerman, 2005], an ArcGIS extension, is adopted for post-processing of HEC-RAS output to create inundation maps for all simulations.

(2) The hydrological model which develops a design rainfall or historic rainfall events. (HEC-HMS)
(3) The hydraulic model which routes the runoff through stream channels to determine water surface profiles at specific locations along the stream network. (HEC-RAS)
(4) Flood inundation mapping and visualization (HEC-GeoRAS).

The flowchart for the methodology is shown in Figure 2.

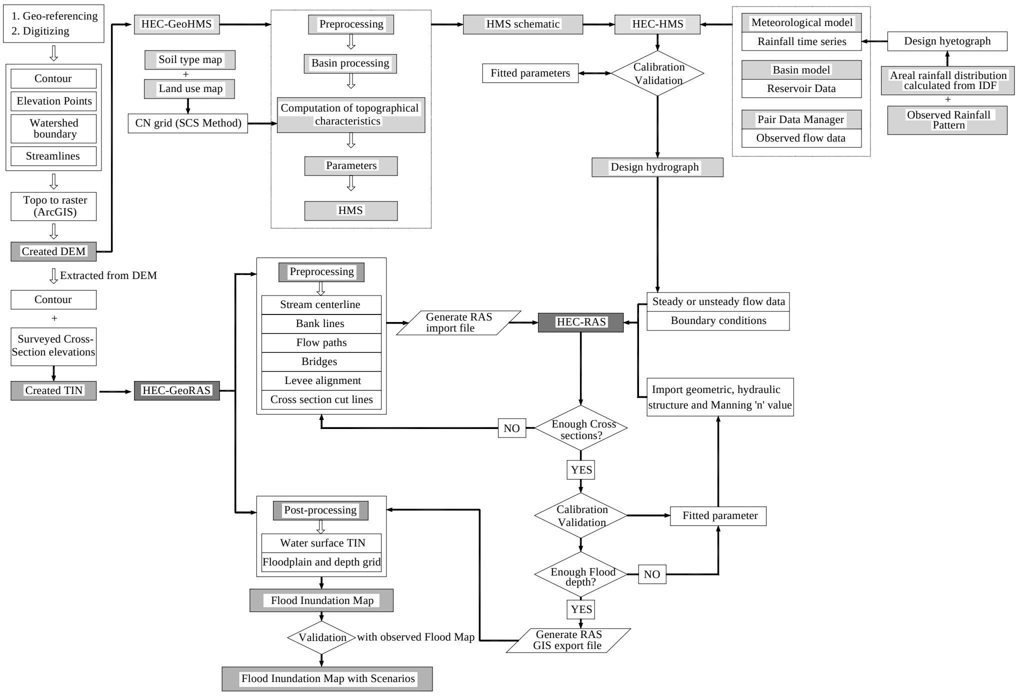
1. Geo-referencing
2. Digitizing
Contour
Elevation Points
Watershed boundary
Streamlines
Topo to raster (ArcGIS)
Created DEM
Extracted from DEM
Contour
+
Surveyed Cross-Section elevations
Created TIN
HEC-GeoHMS
Soil type map
+
Land use map
CN grid (SCS Method)
Preprocessing
Basin processing
Computation of topographical characteristics
Parameters
HMS
HMS schematic
HEC-HMS
Fitted parameters
Calibration Validation
Meteorological model
Rainfall time series
Basin model
Reservoir Data
Pair Data Manager
Observed flow data
Design hyetograph
Areal rainfall distribution calculated from IDF
+
Observed Rainfall Pattern
Design hydrograph
HEC-GeoRAS
Preprocessing
Stream centerline
Bank lines
Flow paths
Bridges
Levee alignment
Cross section cut lines
Generate RAS import file
HEC-RAS
Steady or unsteady flow data
Boundary conditions
Import geometric, hydraulic structure and Manning 'n' value
NO
Enough Cross sections?
YES
Calibration Validation
Fitted parameter
Enough Flood depth?
NO
YES
Generate RAS GIS export file
Post-processing
Water surface TIN
Floodplain and depth grid
Flood Inundation Map
Validation
with observed Flood Map
Flood Inundation Map with Scenarios

Figure 2: Flow chart of methodology

3.2 Hydrological modeling

HEC-HMS version 3.5, developed by Hydrologic Engineering Center (HEC) of the United States Army Corps of Engineers (USACE) (USACE(a), 2010) is used in this hydrologic modeling study. Only two rain-gauge and water level stations such as Bago and Zaung Tu are located in the Bago river basin. The observed daily time series of rainfall and stream flow data were used to calibrate and validate the hydrologic model.
In HEC-HMS model, there are four main components such as loss method, transform method, base-flow method and routing method. For each component, suitable method is chosen. In this study, SCS curve number and SCS unit hydrograph were selected for loss and transform method respectively. Recession and lag methods were assigned for base-flow and routing method respectively.

HEC-HMS calibration was performed for five different flood events of 2004 to 2008 using daily flow basis. HEC-HMS has an optimization feature which can be used to match the simulated flow with observed flow. It allows for multiple parameters at the same time for each sub-basin. There are 17 sub-basins for the catchment of the outlet at Tarwa. In calibration procedure, six parameters which are initial abstraction, base-flow initial flow rate, recession constant, base-flow threshold ratio and SCS lag were adjusted.

Five different events were calibrated by the optimization trial option using the peak weighted root mean square error objective function. The average of those calibrated parameters of five different flood events was used as the final calibrated parameter values. The calibration result of 2006 flood event is as shown in figure 3. The value of the coefficient of determination (R^2) was found as 0.84 and indicated a close relationship between the observed and simulated flow.

The validation process was done by these final parameter values for three events (2009, 2010, and 2011). The validation result of 2010 flood event is as shown in figure 4.

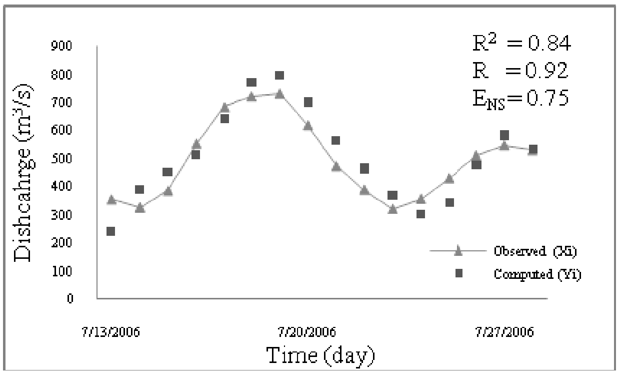

Figure 3: HEC-HMS calibration result for 2006 flood event

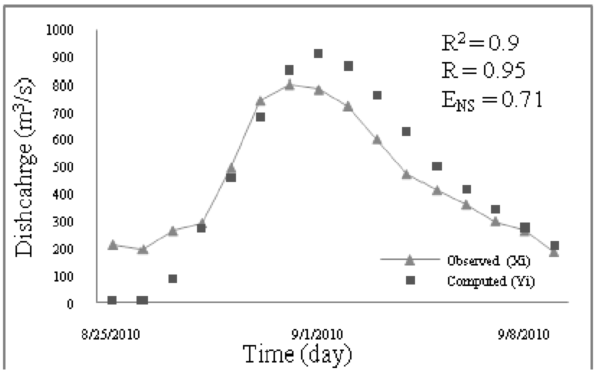

Figure 4: HEC-HMS validation result for 2010 flood event

3.3 Hydraulic modeling

HEC-RAS version 4.1, developed by HEC of USACE (USACE(b), 2010) is used in this hydraulic modeling study. Data requirements for HEC-RAS include topographic information in the form of a series of cross sections, friction parameter in the form of Manning’s n values across each cross section, and flow data including flow rates, flow change locations, and boundary conditions (Cook, 2009).

Hydraulic modeling in this study was conducted for 50 km reach of the Bago River and it started from Zaung Tu Weir to Tarwa outlet. Initially in the pre-processing, the available surveyed 48 cross sections for main channel and 1m contour lines extracted from the DEM for the flood plain were applied to develop the Triangulated Irregular Network (TIN). Then, by using HEC-GeoRAS extension in ArcGIS environment, required geometry data such as: stream centerline, main channel banks flow paths, cross sections cut lines, and levee alignment, and bridge were created. Then, these data were exported to HEC-RAS as the geometric data file.

1 D HEC-RAS model can be adequately calibrated on hydrometric data, and can then be used to make adequate predictions of flood extent when water free surfaces are extrapolated onto a high resolution DEM (Horritt, 2002).

The flow data with time series flood event simulated from HEC-HMS were used for calibrating the model. The unsteady flow condition was adopted to run this model. The manual calibration process was done for 2 different flood events (2004 and 2006). The calibrated parameters, Manning's 'n' values and slope value were adjusted by many trials of running model until the satisfactory results were produced.

The fitted Manning roughness coefficient 'n' are 0.03 and 0.045 for the channel which are different according to the nature of each cross section. And the fitted friction slope is 0.00003. Design flood hydrographs simulated from the HEC-HMS model were entered in HEC-RAS. The water surface elevation results of 2, 10, 50 and 100 year flood return periods are outputs from HEC-RAS model.

The model was validated with the two different flood events (2010 and 2011) by using the unsteady flow data option and calibration and validation results are shown in figure 5. Value of Nash-Sutcliffe model efficiency (0.6) indicates a satisfactory performance.

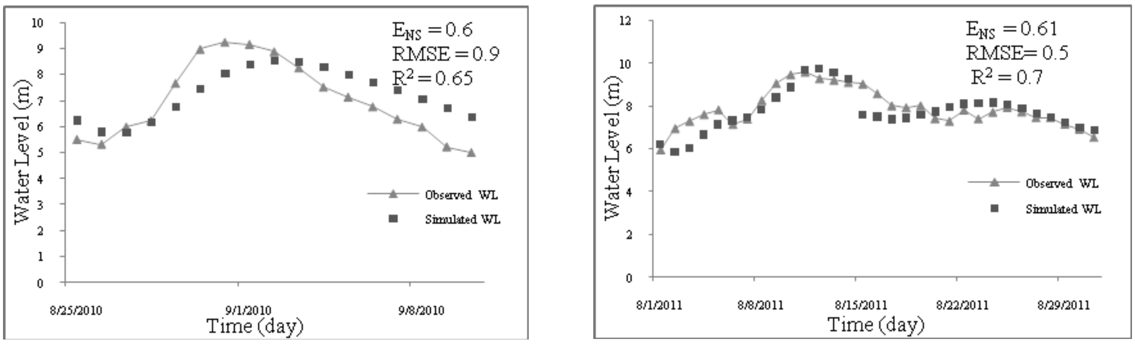

Figure 5: HEC-RAS results of 2010 and 2011 flood hydrograph

4. RESULTS AND DISCUSSION

4.1 Design flood hydrographs with different scenarios

The design rainfall hyetograph for different return periods was developed by using Intensity-Duration-Frequency (IDF) curve of Bago. The calculated design rainfall hyetographs were the inputs for HEC-HMS model. Figure 6 shows design flood hydrographs with different scenarios.

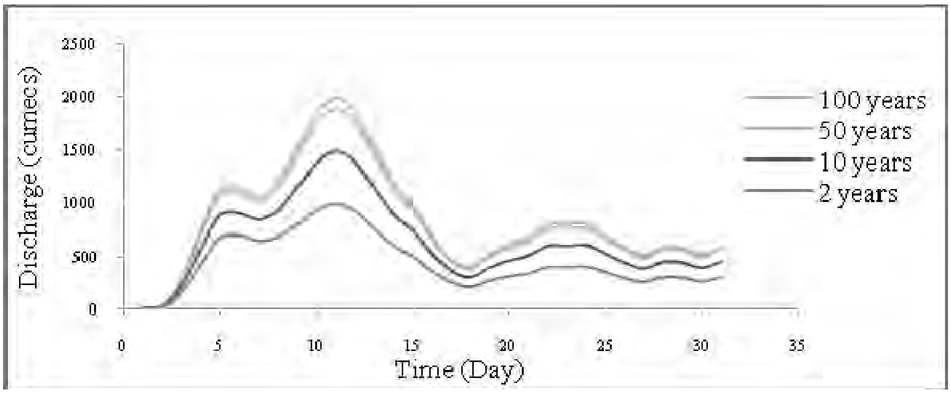

Figure 6: Design flood hydrograph with selected return periods

4.2 Flood inundation mapping

After getting the results of HEC-RAS model, the flood inundation maps for 2, 10, 50, and 100 year return periods flood were delineated by the help of HEC-GeoRAS extension. The verification process was done by the ALOS image of JAXA for 2006 flood as well as the surveyed ground GPS map of Bago urban area for 2011. Simulated inundation area for 2006 flood event by model is 51 km². Inundation area based on 2006 ALOS SAR image is obtained as 42.9 km². Difference is obtained as 18.8 %. Inundation urban area for 2011 flood event simulated by the model and observed map are 5.2 km² and 4.9 km² respectively and the difference is obtained as 6.1%.

The degree of flood hazard depth are classified as (D< 0.5 m), (0.5 <D< 2 m), (2 m <D< 4 m), (4 m <D< 6 m), (6 m <D< 8 m), and (D> 8 m). The inundation area with classified hazard depths according to 2, 10, 50, and 100 year return periods are shown in Table 1.

Table 1: Flood inundation area with classified hazard depths according to 2, 10, 50, and 100 year return periods

Water depth (m)	**Total inundation areas**							
	2 year flood		**10 year flood**		**50 year flood**		**100 year flood**	
	Area (km²)	**%**	**Area (km²)**	**%**	**Area (km²)**	**%**	**Area (km²)**	**%**
D < 0.5 m	26.45	49.58	25.65	45.09	24.9	39.27	24.7	38.53
0.5 m < D < 2 m	10.64	19.94	10.93	19.22	10.77	16.99	10.72	16.72
2 m < D < 4 m	11.26	21.11	12.4	21.80	14.06	22.18	14.17	22.10
4 m < D < 6 m	3.85	7.22	5.7	10.02	9.7	15.30	10.19	15.89
6 m < D < 8 m	1.1	2.06	2	3.52	3.16	4.98	3.41	5.32
D > 8 m	0.05	0.09	0.2	0.35	0.81	1.28	0.92	1.44
Total	53.35	100.00	56.88	100.00	63.4	100	64.11	100

4.3 Discussion

In the Table 1, the classification of flood depth areas indicates that half of the total flood areas have water depth less than 0.5 m. The total area under the water depth greater than 6 m is quite small, although it increases considerably with the intensity of flooding. By observing all maps, the depths and extents of the flood water for 2, 10, 50, and 100 year return period are increased gradually according to the recurrence interval. The most dangerous flood extents are occurred for the flow conditions of 50 and 100 year due to the maximum flow conditions as shown in figure 7.

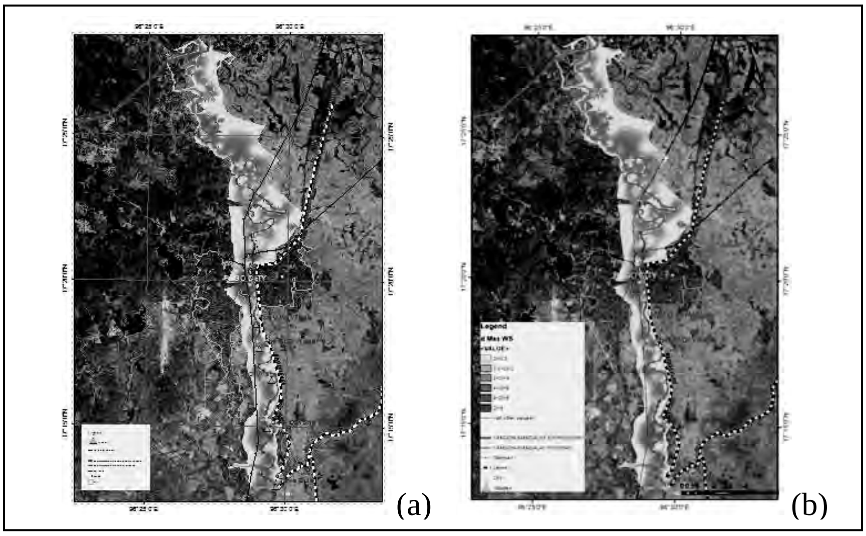

Figure 7: Flood inundation map for (a) 50 year, and (b) 100 year return period flood

5. CONCLUSION AND RECOMMENDATIONS

For considering the 50 and 100 year return period flood scenarios, the highest depth of inundation can seriously affect in the Bago City urban areas and around Bago Bridge. Most of the people in Kyauk Kyi Su quarter, Ywar Thit quarter, Mazin quarter, and Kyun Thar Yar quarter might be migrated to the flood relief center. The largest flood extent can occur in the rural areas located near the upper areas of Bago City. The downstream rural areas including the paddy fields also can be affected by the flood. It can be concluded that the inundation areas are increased according to the different return periods. And the most dangerous condition will be occurred if the 50 year and 100 year return periods of flood come.

But there are only two rainfall gauge and water level stations in the entire river basin; new automatic rain gauge stations and automatic water level recorder should be installed in the Bago river basin. The results of the model could be further improved if dense network of weather stations are available along with a good network of stream gauge data. For the more accuracy of the hydraulic model’s result, there need to survey more cross sections with closer interval. For further study, the risk assessment and vulnerability analysis with 2-D hydrodynamic models were recommended.

6. ACKNOWLEDGEMENT

First of all, the author is sincerely thankful to Dr. Nyan Myint Kyaw, Professor and Head of Civil Engineering Department, Yangon Technological University for his kind lead and guidance. The author is greatly indebted to her supervisor, Dr Win Win Zin, Associate Professor of Civil Engineering Department, Yangon Technological University, for her invaluable suggestions and careful editing this paper. The author is heartfelt thanked to Dr. Akiyuki Kawasaki, Associate Professor, Department of Civil Engineering, The University of Tokyo, for supporting to survey the cross sections. The author would like to express her special thanks to U Tin Maung, Technical Advisor, NEPS Company Ltd. and also the Visiting Associate Professor of Yangon Technological University, for his enthusiastic instructions and advices. The author is deeply grateful to the Assistant Director and the staffs of the Irrigation Department at Bago, for supplying data. The author would like to thank all the persons who have helped towards the successful completion of this paper.

REFERENCES

Ackerman, C. T., 2005, *HEC-GeoRAS: GIS Tools for Support of HEC-RAS Using ArcGIS*, Users Manual Version 4, US Army Corps of Engineers.

Aung, T. M., 2013, *Flood inundation analysis for effective countermeasures in the Bago River Basin*, ICHARM Master Paper No.67, International Centre for Water Hazard and Risk Management, Japan.

Cook, A., 2009, Effect of Topographic Data, Geometric Configuration and Modeling Approach on Flood Inundation Mapping, *Journal of Hydrology* 377, 131-142.

Horritt, M. S., 2002, Evaluation of 1 D and 2 D Numerical Models for Predicting River Flood Inundation, *Journal of Hydrology* 268, 87-99.

Khaing, A. M., 2014, *Mapping Flood Inundation in the Bago River Basin, Myanmar*, Master Thesis, Asian Institute of Technology (AIT), Thailand.

USACE., 2003, *Geospatial Hydrologic Modeling Extension (HEC-GeoHMS) User's Manual*, US Army Corps of Engineers.

USACE (a)., 2010, *HEC-HMS User's Manual Version 3.5*, Hydrologic Engineering Center (HEC), US Army Corps of Engineers.

USACE (b)., 2010, *HEC-RAS User's Manual Version 4.1*, Hydrologic Engineering Center (HEC), US Army Corps of Engineers.

Flood process and situation analysis in Myanmar for flood disaster preparation

Wang YI [1], Bin HE [2], and Srikantha HERATH [3]
[1] United Nations University, Tokyo, Japan
2768259160@qq.com
[2] United Nations University, Tokyo, Japan
[3] Professor, The Institute for the Advanced Study of Sustainability,
United Nations University, Tokyo, Japan

ABSTRACT

Myanmar is exposed to several kinds of natural hazard. In its recent history the country faced with disaster events that severely impacted its people and the overall economy of the country. These events caused significant impact on the people's livelihood, damage in the country's infrastructure systems, and sometimes a large number of fatalities. Among all the natural disasters, floods have been the most prevalent in Myanmar. Flood associated with heavy precipitation events is a recurring phenomenon across the country. Flood causes substantial damage to livestock, agricultural, roads, bridges and buildings and serious negative effects on social and economic development in the country. However, there is lack of knowledge and clear information in Myanmar regarding flood processes as well as flood characteristics analysis. The methodology and technique for a comprehensive flood process analysis and flood situation assessment in Myanmar still remains in a poor level. A good understanding of flood phenomena and their potential will allow Myanmar government to make proper advanced planning to lessen the impact of flood disaster events in the future, hence reducing the disaster risk for the country. This paper aims to analyze the flood situation and process in Myanmar from the historical events and collected hydrological information, the assessment of the currently used approach for flood monitoring and forecasting will be carried out. Furthermore, this paper will identify the current gap and possible needs for improvements of flood monitoring and disaster preparation in the different components, data observation, data collection, data processing, issuing of warning and human resources for a comprehensive and effective flood monitoring and forecast systems.

Influence of member shape on the relationship between surface defects and chloride permeability of surface concrete

Katsuya MITA[1] and Yoshitaka KATO[2]
[1] Assistant professor, Department of Civil Engineering,
Faculty of Science and Technology,Tokyo University of Science, Japan
k_mita@rs.noda.tus.ac.jp
[2] Associate professor, Department of Civil Engineering,
Faculty of Science and Technology,Tokyo University of Science, Japan

ABSTRACT

Once surface defects on a concrete structure are discovered it is then necessary to carry out repairs. However, the effect of surface defects on the permeability of surface concrete has not been studied. This study aimed to understand the influence of surface defects on the chloride permeability by intentionally producing initial defects on the surface due to different member shapes in order to vary the degree of segregation. It was observed that the surface was of uneven color and surface bubbles and sand streaks occurred due to the rapid ascent of bleeding water where the member shape was narrower in the vertical direction. Furthermore, all cases where surface defects occurred tended to have higher chloride penetration compared to the cases without surface defects.

Keywords: surface defects, chloride permeability, uneven color, surface bubbles, sand streaks

1. INTRODUCTION

Currently, to secure the durability of concrete structures, attention is being giving to improving the quality of the surface of the concrete structure. Because deterioration factor such as chloride ions, CO_2 and moisture initially penetrate from the concrete surface, its quality is important in protecting the durability of the structure. In real concrete structures, however, many initial defects may occur, such as cracks or honeycomb. There are several types of initial defects, the majority occurs in the concrete surface. Not only do these impair the appearance of the concrete structure, they also reduce the durability over time and require significant effort and cost for repair. While some initial defects can be repaired as soon as they are found, such as honeycomb and cracks, many are not recognized because they only detract from the appearance, such as sand streaks, uneven color, and surface bubbles (Figure 1), and thus repair is not required performed. Therefore, although there are many studies on the reduction method and the cause of the initial defects, the effect of initial defects has on the durability of concrete structures has not been clarified. Much of the research on the initial defects use a simple specimen, so there is no change in shape in the vertical direction when studying initial defects, even though actual concrete structures have a variety of member shapes.

In this study, in order to understand the effect of surface defects on the durability of the concrete structure, studies have been made on the effect of surface defects focusing on the salt permeability.

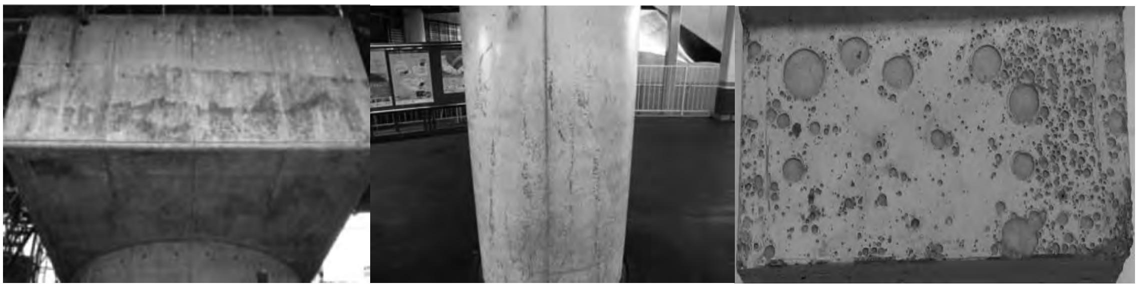
(a)Uneven color (b)Sand streaks (c)Surface bubbles,

Figure 1: Surface defects

2. EXPERIMENTAL

2.1 Material and Mix-propotion

In this study, referring to the previous studies on surface defects, the mortar of concrete surface layer portion was prepared. Ordinary Portland Cement (density 3.15 g/cm^3) and river sand (density 2.64 g/cm^3) were used. The mix proportion of mortar was W/C=55% and S/C=2.5.

2.2 Specimen

Specimen were prepared in 5 shapes as shown in Figure 2. The name of each part of the specimens is shown in Figure 3. T-shape and reversed T-shape simulate an actual structure. It was considered that, in the case of T-shape and reverse T-shape with 60º at the corner, accumulation of bleeding water could be reduced. To intentionally generate defects, L-Shape turned 45º from ground was adopted, where the inclined slope could crease a prone surface for bubbles and bleeding water could be expected in the corner. Standard prismatic specimens of 150 × 150 × 530mm were also created. After placing cement and fine aggregate in the mixer they were dry mixed for 30 seconds, then mixed again for 60 seconds after putting in the water, and finally mixed again for 60 seconds to prepare mortar. The mortar was placed into molds in two layers, and internal vibration was using for compaction. The 0 hit flow value of the mortar was 106mm. Moist curing was carried out for 7 days inside the mold, and at the age of 28 days specimens were removed from the mold and cured in the air for 7 days.

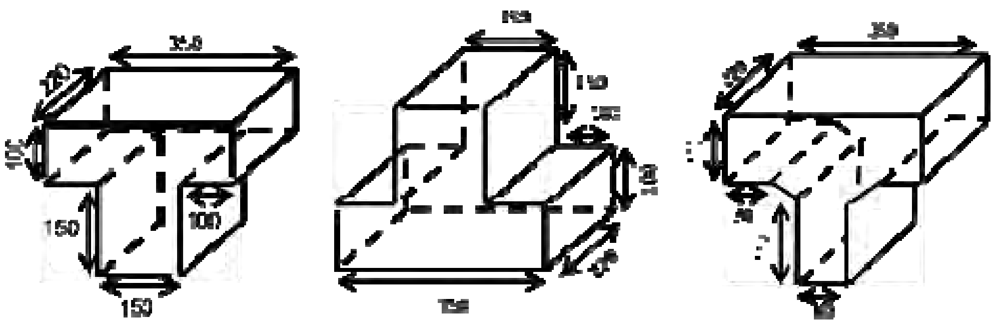
150
100
150
100
110
110
350

a)T-Shape b)Reverse T-Shape c) T-Shape with Angle 60º at corner

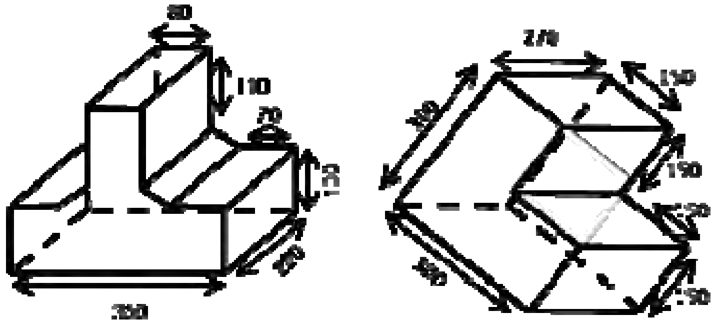
80
110
70
130
350
150
150
150
50

d) Reverse T-Shape with Angle 60º at corner e) L-Shape turned 45° from ground

Figure 2: Specimens for experiments

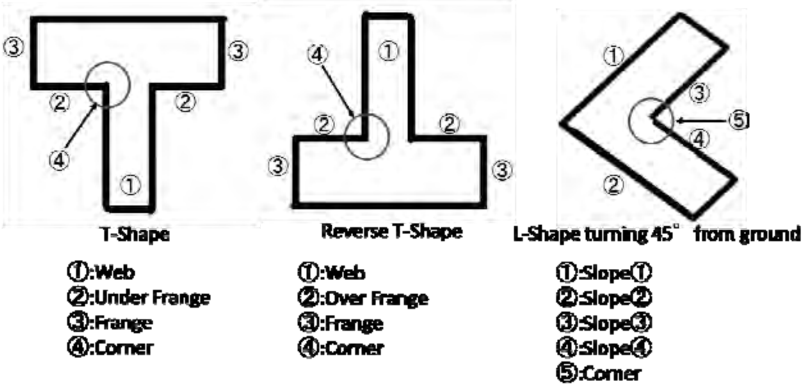
T-Shape
①:Web
②:Under Frange
③:Frange
④:Corner
Reverse T-Shape
①:Web
②:Over Frange
③:Frange
④:Corner
L-Shape turning 45° from ground
①:Slope①
②:Slope②
③:Slope③
④:Slope④
⑤:Corner

Figure 3: Name of specimens parts

2.3 Bleeding test

The bleeding test was carried out in order to compare the ease of accumulated bleeding water for each specimen shape. Following JIS A 1123, the bleeding water produced on the top surface was collected as part of the bleeding test.

2.4 Visual test

By photographing with a digital camera all aspects of the specimens after curing, the occurrence of specimen surface defects was investigated. The analysis was performed using the captured image. By converting the images to binary, the rate of occurrence of black-and-white on each side was used to calculate the area of uneven color. After calculating the total area of the defects of the target from the captured image, sand streak and surface bubbles was calculated as a percentage of the total surface area.

2.5 Salt water immersion test

After curing, specimens were immersed for 7 days in NaCl solution of 10wt%. After completion of immersion, drilling up to 3.0cm by 0.5cm depth on each side of the specimen using hammer drill, the total chloride ion content as a sample powder was measured. The sample powder was taken from the portion where sand streaks and surface bubbles and uneven color were visually observed. In the case of sand streaks, it was taken from a section of the streaked area; in the case of surface bubbles, it was taken from the center of the surface bubbles that are submerged hemispherically. In addition, samples were also taken where no surface bubbles (following, vulnerable surface) occurred. Measurement of the chloride ion content is compliant with JCI-SC4. Based on the measured values, the apparent diffusion coefficient D (cm^2/year) and surface chloride ion concentration C_0 (kg/m^3) were calculated using a theoretical solution of the diffusion equation with a constant boundary concentration, and then the number of years to steel corrosion occurrence was predicted. In compliance with the Standard Specification for Concrete Structures, the steel corrosion occurrence limit concentration was calculated to be 1.9kg/m^3 in the case of W/C = 50%. It was investigated by assuming a structure with 5cm thick cover.

3. EXPERIMENTAL RESULTS AND DISCUSSION

3.1 Bleeding test

The results of the bleeding test of each specimen are shown in Figure 4. It can be seen that the bleeding water is less in T60°, turned 45° L-sharp, and reverse T-shape as compared to the reference specimen. It was thought that it was difficult for the bleeding water to rise to the top surface and the bleeding water reservoir inside those shapes.

3.2 Visual test

The uneven color area ratio is shown in Figure 5. The sand streak and sudface bubbles area ratio is shown in Figure 6. As a result of the visual test, including the case where it is canted, sand streaks on the web and surface bubbles could be seen on the top of flange. In L-Shape turned 45º, surface bubbles on the slope① and ④ were seen. Uneven color only was observed in other shapes and the reference specimen without the other two defects. Uneven color has occurred uniformly across the entire measurement surface at around 50% uneven color area ratio. Visual observation showed that areas around the surface bubbles had turned white. It was thought that bleeding water remained in the mold interface in areas with a higher rate of white. The percentage of sand streaks was greater in Reverse T60°. Based on the results of the bleeding test and considering the previous studies, sand streaks are caused by bleeding water rapidly flowing upwards. By using the slope in a mold, it is possible that it becomes easier for bleeding water to flow. From the surface bubbles generated area ratio results, many occurred in reverse T60°. It was considered that surface bubbles occurred when bleeding water accumulates at the mold surface.

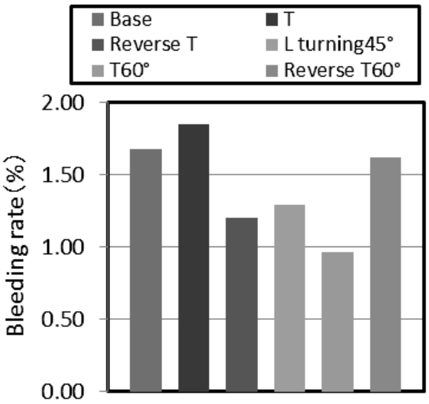

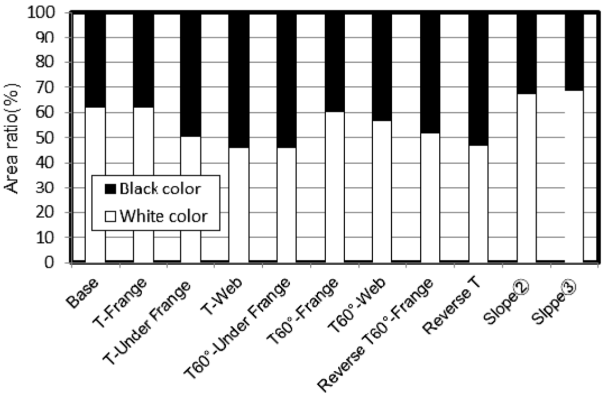

Figure 4: Result of bleeding test

Figure 5: Area ratio of unever color

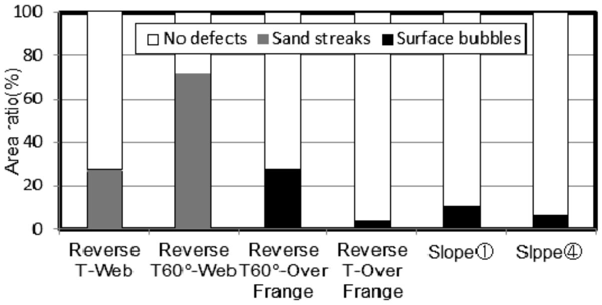

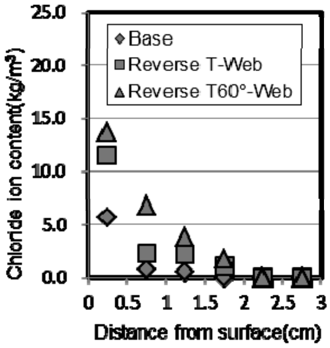

Figure 6 Area ratio of sand streaks and surface bubbles

Figure 7: Chloride ion content from sand streaks

3.3 Salt water immersion test

The chloride ion penetration properties of the sand streaks and surface bubbles are shown in Figures 7 and 8. The salt penetration properties of the vulnerable surface are shown in Figure 9. When sand streaks occurred, the chloride ion concentration was higher in any shape in the range of 0 ~ 0.5cm. It became almost the same as the base mortar, other than reverse T60º in the 0.5 ~ 1.0cm layer. In reverse T60°, degree of sand streaks was greater (the sand streaks area ratio was twice as high), and the chloride ion penetration amount was three times that of others at 0.5 ~ 1.5cm. Only the surface layer portion is likely to penetrate by sand streaks and there was little effect on the inside. However, it was considered that if the degree of sand streaks becomes large, there is an impact on chloride ion penetration of the interior. Chloride ion concentration was higher up to 0.5 ~ 1.0cm also due to surface bubbles. Surface bubbles were formed by bleeding water retained at the interface with the mold because the water-cement ratio is high and the organization of the cured body is a roughened. Chloride ion concentration at the vulnerable surface was higher than the base mortar. The vulnerable surface is laitance layer overall, and is formed by the particulate component of the cement deposited by the movement of bleeding water, and thus it is considered to have been easier to penetrate.
The salt permeability in the case when surface defects do not occur is shown in Figure 10. The results are shown for a T-shape specimen with ordinary mortar. Chloride ion concentration in the white area and the black area near the surface to 0 ~ 0.5cm was larger than the base mortar. In addition, the chloride ion concentration was higher than the base mortar in all measured surfaces. Compared to the measurement surface of the

other, the chloride ion concentration was especially high in the range of 0.5 ~ 1.0cm in the corner. It is considered that this is because the vulnerable layer is formed due to the bleeding water rise and the bleeding water is accumulated in the corner and mold interface and is unable rise to the top surface. A similar trend was also observed in other shapes, but the region of where chloride ion concentration was extremely high was not observed when it is angled in the corners.

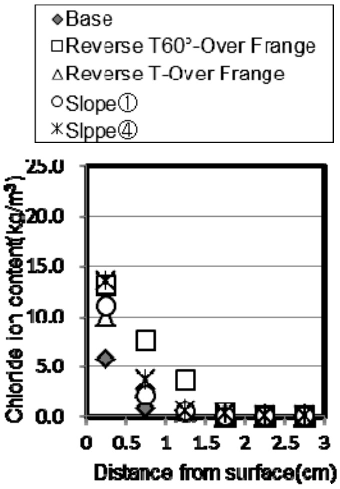

Figure 8: Chloride ion content surface bubbles

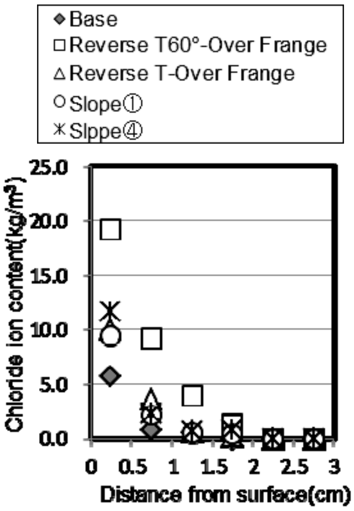

Figure 9: Chloride ion content from weak layer

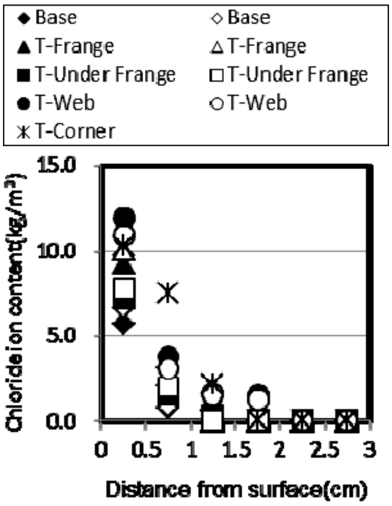

Figure 10: Chloride ion from content from no defects surface

3.4 The relationship between visual test and steel corrosion years

The relationship between the surface defect area ratio and the ratio of the steel corrosion years of surface defects for it of base mortar is shown in Figure 11. Black markers in the figure show the sand streaks and white markers show the surface bubbles. Steel corrosion years was shorter than base mortar with increasing sand streaks area ratio. It is thought that, when sand streaks are present, there is a possibility that the steel corrosion years are reduced to about half or less than the healthy cases. In the case of surface bubbles, there is a tendency that, with the increase of the area ratio, steel corrosion years are shortened roughly compared to base mortar. It is thought that there is a possibility that the steel corrosion years is reduced to less than half of the base mortar when surface bubbles are present as in the case of sand streaks. The relationship between steel corrosion year and area ratio of the black region in case of uneven color is shown Figure 12. There was no clear relationship to the steel corrosion years and black area ratio. However, the effect of the specimen shape is clear, as when compared with the base mortar, the steel corrosion occurred years had decreased in a wide range of 0.2 to 0.8 times. There is a possibility that this is due to the effect of bleeding water staying on each side of the mold. The occurrence of bleeding water leads to uneven color, but the influence of the behavior of the bleeding water has a large effect on the proportion of the black region (or white area). It is considered that the factor reduce the surface quality is by bleeding water accumulating on the mold interface. It is considered necessary to eliminate by using a water absorbent mold or permeable mold, when bleeding water easily stays in the mold interface, in order to deal with these effects.

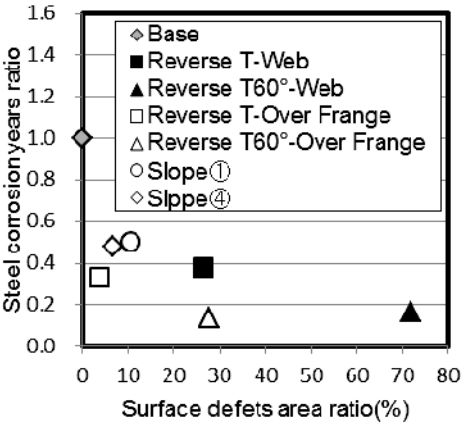

Figure 11: The relationship between steel corrosion years ratio and surface defects area ratio

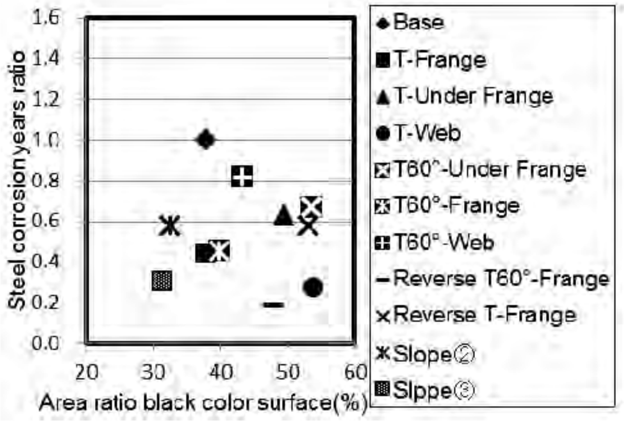

Figure 12: The relationship between steel corrosion years ratio and area ratio of black color surface

4. MEMBER SHAPE AND SURFACE DEFECTS

By the visual test of the actual structures, to figure out where it may be exposed to the progress of deterioration, the relationship between steel corrosion occurs on each side of years and surface defect-prone and bleeding water (BL water in the figure) where is likely to stay in that shape changes is shown in Figure 13. Numeric value in the figure is the magnification for steel corrosion year of base mortar. If you spread in the height direction, bleeding water is likely to move by ramping. As a result, it is considered that the surface quality is lowered in the direction of height and steel corrosion years ratio becomes smaller. It was considered that the bleeding water is likely to move to the web and put the case tilt narrowing in the height direction and the bleeding water accumulated in the the part by surface occurs has influenced.

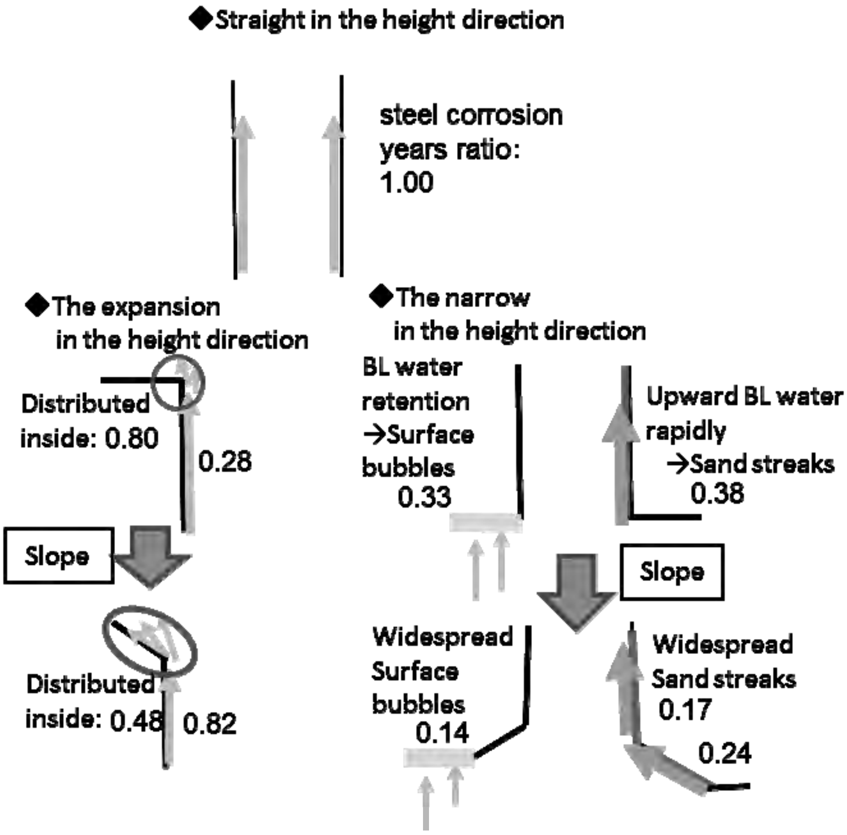
◆Straight in the height direction
steel corrosion years ratio: 1.00
◆The expansion in the height direction
Distributed inside: 0.80
0.28
Slope
Distributed inside: 0.48
0.82
◆The narrow in the height direction
BL water retention →Surface bubbles
0.33
Upward BL water rapidly →Sand streaks
0.38
Slope
Widespread Surface bubbles
0.14
Widespread Sand streaks
0.17
0.24

Figure.13 The relationship between mold shape and steel corrosion year ratio

5. CONCLUSION

As a result of this study, the following findings were obtained.

1) Including the base mortar, uneven color occurred in all specimens.

2) Sand streaks occurred on the reverse T60° and reverse T-shape. It is considered that it is likely to occur at the surface where there is a slope because bleeding water rises suddenly.

3) Surface bubbles occurred at reverse T-shape and all of the L-shape turned 45°. It is considered that air engulfed during casting rises to the mold surface and it forms due to bleeding water accumulating there.

4) If a visual inspection shows the occurrence of a defect, then the steel corrosion year tended to be faster than the base specimen.

5) Even in the surface properties of uneven color, steel corrosion year has tended to be faster than a simple shape. However, there was no clear correlation between the two.

REFERENCES

Keisaburo, K., Takashi, K., Ryuichi, C., 2012. Technical skills for acquirement of aesthetic concrete surfaces. *Report of OBAYASHI corporation Technical Research Institute* 76, 1-6.

Shigeyuki S., 2007. Devised to reduce the slope of the surface bubbles. *JCM Monthly Report* 16 5-6。

Japan Society of Civil Engineers, 2012. *Standard specifications for concrete structures,* Materials and Construction, Japan.

Katsuya, M., Yoshitaka, K., 2011. An experimental study on the effects of bleeding water on the quality of the concrete surface layer. *Proceedings of JCI Annual Conference* 33,1385-1390.

Application of steel fiber reinforced concrete to reduce crack width of structures

Hoang Giang NGUYEN [1] and Trung Hieu NGUYEN [1]
Structure testing & Construction Inspection Division,
Department of Building & Industrial Engineering,
National University of Civil Engineering, Vietnam
giangnh@nuce.edu.vn

ABSTRACT

The use of steel fiber for reinforcement has been attracted a great attention from academic and industrial parties. Various applications of this type have been using in pavements, segments, shotcrete, drainage pipes etc. This steel fiber reinforcement has shown excellent performances in crack control and load distribution due to its 3D equally distributed location. This paper presents a series of tests and analysis for different types of steel fiber in concrete samples and beams. The comparison of experimental tests of conventional and steel fiber reinforced structures are carried out. The tests show positive results and possible applications to construction structures in Vietnam where many cracks and failures of these types of conventional structures have been reported.

Keywords: steel fiber, concrete beam; reinforced concrete

1. INTRODUCTION

Vietnam is on the rapid development of its infrastructure and concrete structures have played a key role in whole process. However, many of these new structures have cracks and defects during and after construction. The presence of micro cracks in the mortar-aggregate interface is responsible for the inherent weakness of plain concrete. Many constructions have experienced such defects and needed additional reinforcements.

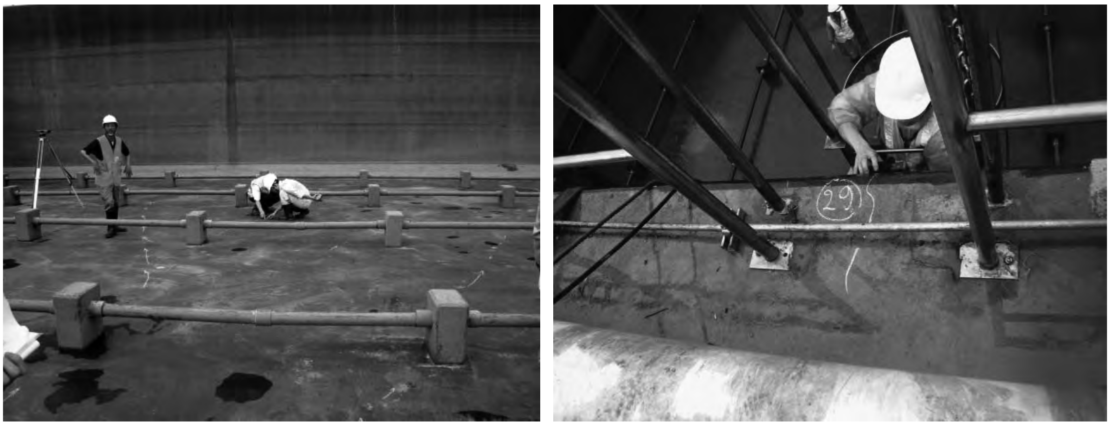

Figure 1: Cracks on Waste water pond (Thermal Power plant)

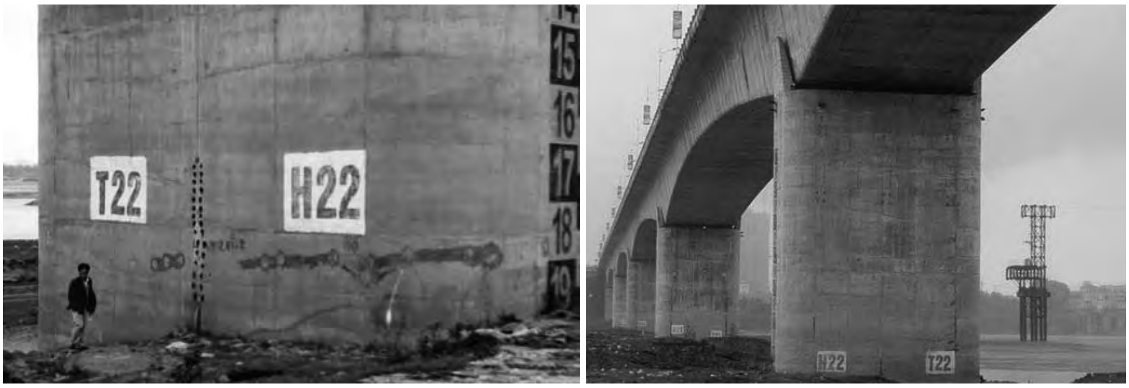

Figure 2: Cracks on Bridge abutments

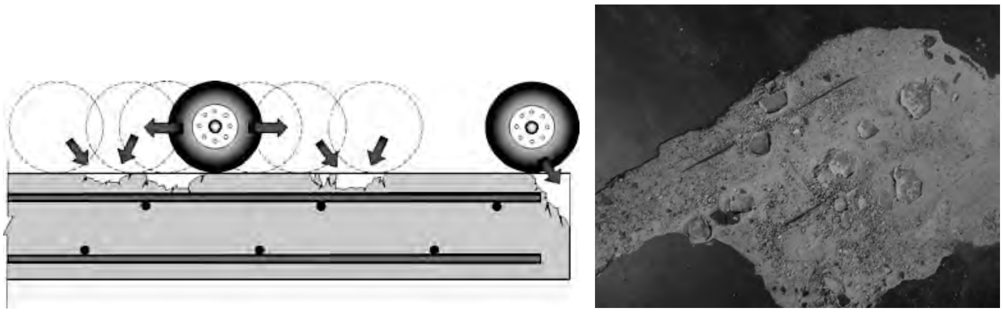

Figure 3: Failure of pavement

It is therefore a crucial issue to carry our research for a new material which could replace or strengthen current applications. Among those reinforcement methods, fibers have been studied by a number of researchers such as Shende et al. (2012) carried out a series of tests for M-40 Grade of Steel Fiber Reinforced Concrete. The results showed that with the increase of fiber in concrete, Compressive strength, Flexural strength and Split Tensile strength of steel fiber concrete also increased. Narayanan and Darwish (1987) reported the increase of shear strength attribute to steel fibers varying from 13 to 170 %. Many other researchers also have conducted research for sample of steel fiber such as (EFNARC, 2002) carried out the test to evaluate properties. Lofgren (2005) conducted research for self-compacting concrete for precast industry and other applications. It was found that Steel fibers proved to have the potential to increase the post-cracking energy absorption capacity of cement based materials, enhancing the ductile character of concrete structures behavior, mainly of those with high redundant supports (Barros and Figueiras, 1998).

In Vietnam, steel fiber has been applied in some constructions such as pavements for industrial floors, tunnel’s segments, and bridge surfaces, however, the applications have been limited. In this research, a series of experiments to test performances of steel fiber in concrete beam and pipes.

2. EXPERIMENTS

The purpose of the experiments is to compare capacity of traditional steel bar structures with steel fiber ones. The steel fiber volume types and volumes were varied to find effects of quantity on performances of structures. In this study, two types of steel fibers (FF3 and FS3N) were used. The fibers were high strength, hooked-end cold drawn produced by Maccaferri. Properties of steel fibers are shown in table 1.

Table 1: Properties of Steel Fibers

Type	Diameter D (mm)	Length L (mm)	Aspect ratio L/D	Tensile strength of the wire (MPa)	Strain at failure	Shape
FF3	0.75	50	67	> 1100	< 4%	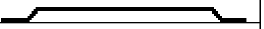
FS3N	0.75	33	44	> 1100	< 4%	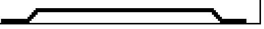

The concrete used local coarse aggregate and natural sand for mixture. The steel fiber dosage in each mix were 0, 20, 40 kg/m3 of FF3 for the elastic modulus test.

2.1 Compression test & Young Modulus

The Cylinder samples following ASTM39 Test Standard Test Method for Compressive Strength of Cylindrical Concrete Specimens for same tests at the same age of 28 days were used to evaluate compressive strength and young modulus of pure concrete and steel fiber concrete with different dosage. Compression test are shown in Figure 4.

Table 2: Concrete mixture for 1m3 of Cylinders (150 x 300)

Type	Water/cement ratio (W/C)	Water (Kg)	Cement (Kg)	Aggregate (Kg)	Sand (Kg)	Steel fiber FF3 (Kg)
M0	0.49	201.99	409.5	1258.5	649.5	0
M20	0.49	201.99	409.5	1258.5	649.5	20
M40	0.49	201.99	409.5	1258.5	649.5	40

The compressive strength is calculated as:

$$R = P / F \tag{1}$$

While: P_{max} : Maximum load (Kg); F: Cross sectional area of sample (cm^2)

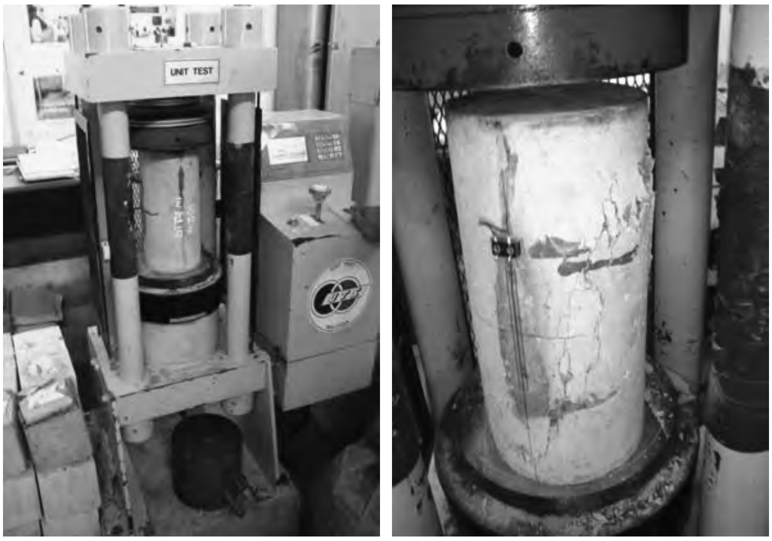

Figure 4: Concrete compression test

The results of compression tests are shown in Table 3.

Table 3: Compression test

	Traditional Concrete (kN)	**SF concrete 20kg /m3 (kN)**	**SF concrete 40kg/m3 (kN)**
P(kg)	289.5	350	502
F(cm2)	176.68	176.68	176.68
Rn(kg/cm2)	163.86	198.10	284.13

It can be observed that the steel fiber concrete increases the compressive strength of concrete with 20.9 % and 73.4 % for 20 kg/m3 and 40 kg/m3 of steel fiber respectively (Figure 5).

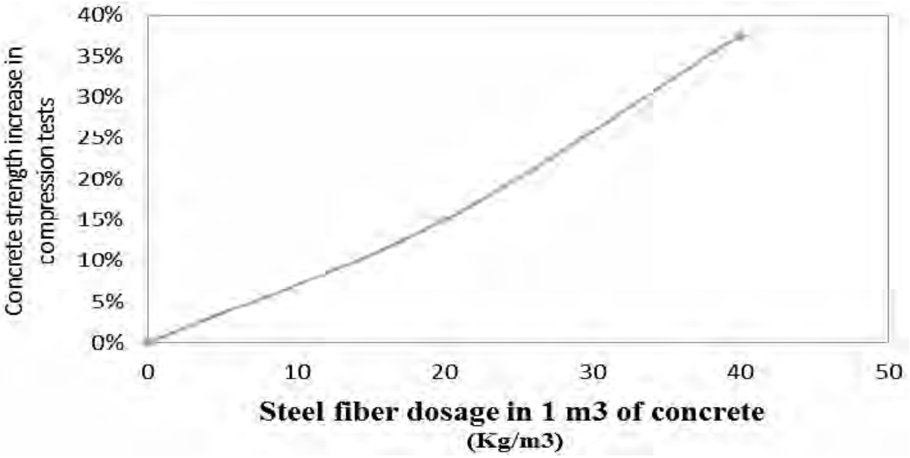

Figure 5: Increase in compressive strength of concrete

2.2 Young Modulus tests

The young modulus tests were carried out with 6 cylinder concrete samples of with 2 for each type. The concrete mixture are shown in table 4. The testing model is shown in Figure 6.

Table 4. Concrete mixture for 1m3 of Cylinders (150 x 300)

Type	Water/cement ratio (W/C)	Water (Kg)	Cement (Kg)	Aggregate (Kg)	Sand (Kg)	Steel fiber FF3 (Kg)	Steel fiber FS3N (Kg)
M0	0.49	201.99	409.5	1258.5	649.5	0	0
M20	0.49	201.99	409.5	1258.5	649.5	20	20
M40	0.49	201.99	409.5	1258.5	649.5	40	40

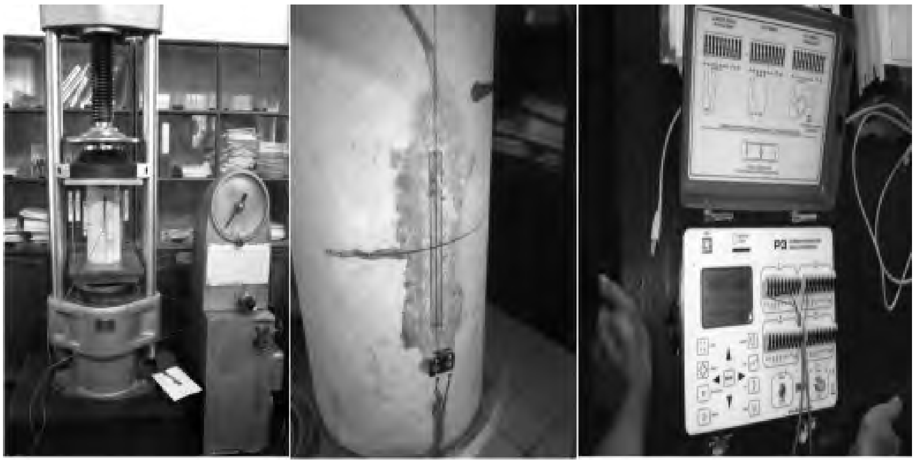

Figure 6: Young modulus test

The increase of young modulus is shown in Figure 7.

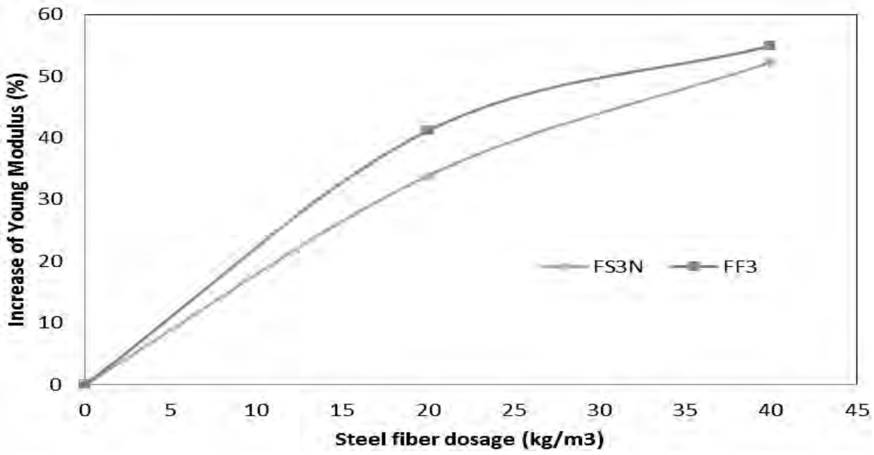

Figure 7: Elastic modulus test

It can be observed that with the increase of fiber content, the elastic modulus of concrete also increases for both cases of fiber types. With the effects of hooked end fiber, the concrete performance is increased.

2.3 Concrete bending beam tests for both conventional and steel fiber types

The reinforced concrete beams with steel bars and stirrups shown in Figure 8 were tested. Steel fiber with dosage of 0, 20 and 40 kg/m3 were added to beams. The concrete mixture of beams were similar to cylinders'. Sizes of beams: b x h x l=120 x 200 x 2000 mm. 01 beam were made for each case. The model and equipment for beam are shown in figure 9 a & b.

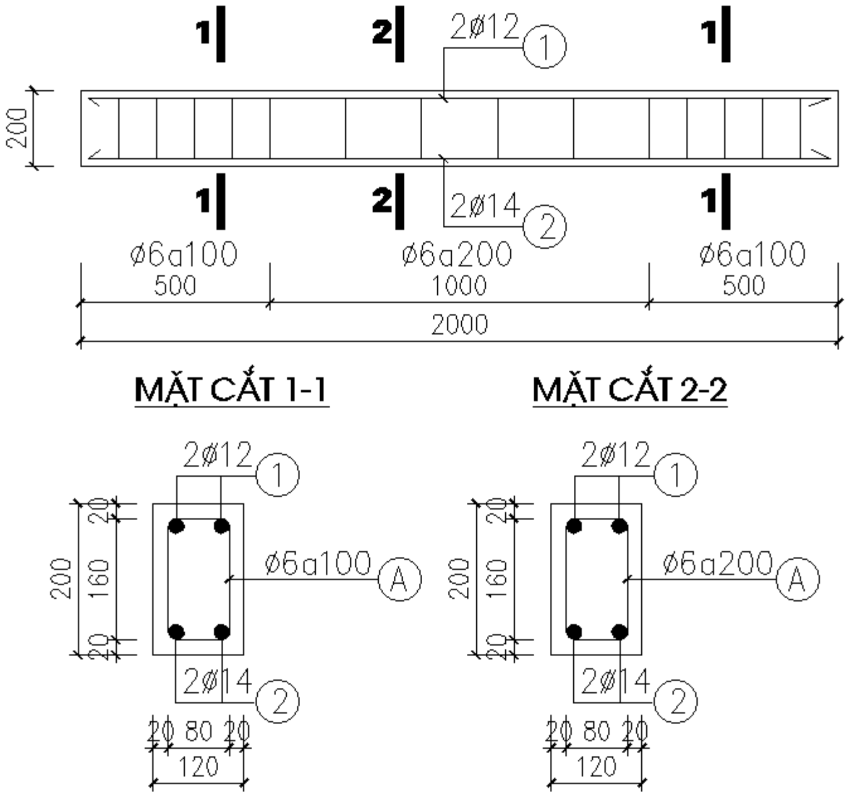
1
2
2Ø12
①
1
200
1
2
2Ø14
②
1
Ø6a100
Ø6a200
Ø6a100
500
1000
500
2000
MẶT CẮT 1-1
MẶT CẮT 2-2
2Ø12
①
20
200
160
20
Ø6a100
Ⓐ
2Ø14
②
20 80 20
120
2Ø12
①
20
200
160
20
Ø6a200
Ⓐ
2Ø14
②
20 80 20
120

Figure 8: Reinforced steel beams

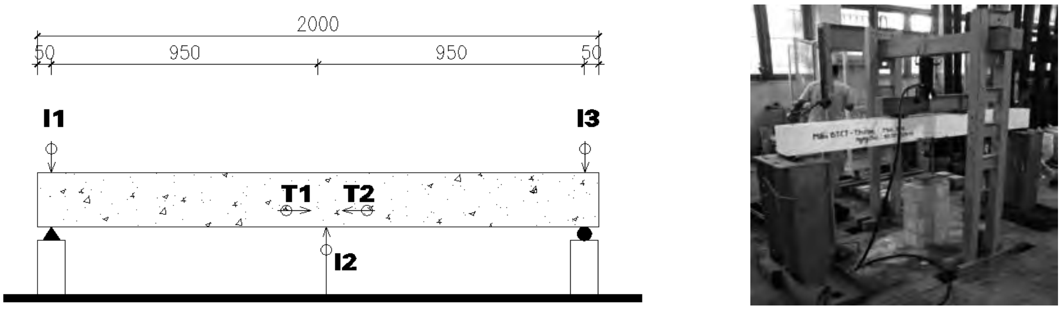
2000
50
950
950
50
I1
I3
T1
T2
I2

a) b)

Figure 9: Testing model

Indicators, LVDTs were used to determine displacements and deformation of beam at middle and 2 ends of beams. Tow indicators (I1; I3) were put at 2 ends of beam and middle part (I2) to measure displacements. Indicators (T1; T2) combined with struts were installed at tension and compression zones of beam to measure deformation and cracks.

3. RESULTS

The ultimate loads for each type of beam are shown in table 5. The ultimate load increases with the increase of dosage of steel fiber in concrete mixture.

Table 5. Ultimate loads for beam testing

Beam types	Ultimate load (kN)	Mechanism
Conventional	28	Stiffness - Bending
SF dosage 20kg/m3	30	Stiffness - Bending
SF dosage 40kg/m3	32	Stiffness - Bending

The displacement of beams were measured and shown in Figure 10 versus applied loads. It can be seen that with the increase of steel fiber dosage in concrete mixture, beam showed less displacement.

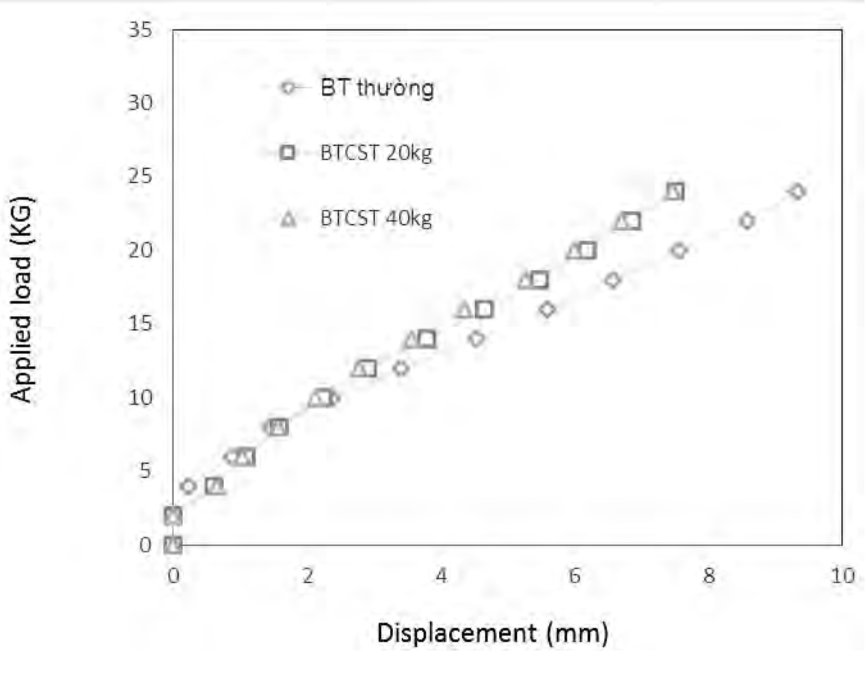

Figure 10: Displacement of beam vs applied loads

Deformation of beam for tension and compression zones were measured and plot versus applied in figure 11. As observed in figure 11, beam with less steel fiber dosage showed more deformation in both tension and compression zones.

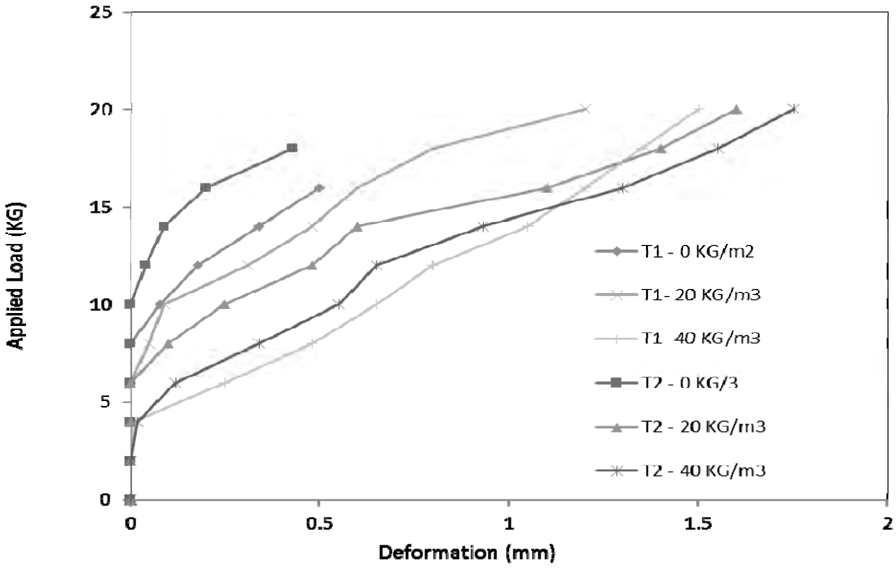

Figure 11. Beam deformation vs applied loads

Cracks appeared on the beam during the tests were recorded. The number of cracks on each beam are shown in Table 6. The crack width of beam are also shown in figure 12. It can be seen that beam with less dosage of steel fiber in concrete mixture has greater crack width under same loads in compare with other beams.

Table 6. Number of crack on beam

Concrete Types	**Number of cracks**
Conventional	11
SF dosage 20kg/m3	15
SF dosage 40kg/m3	18

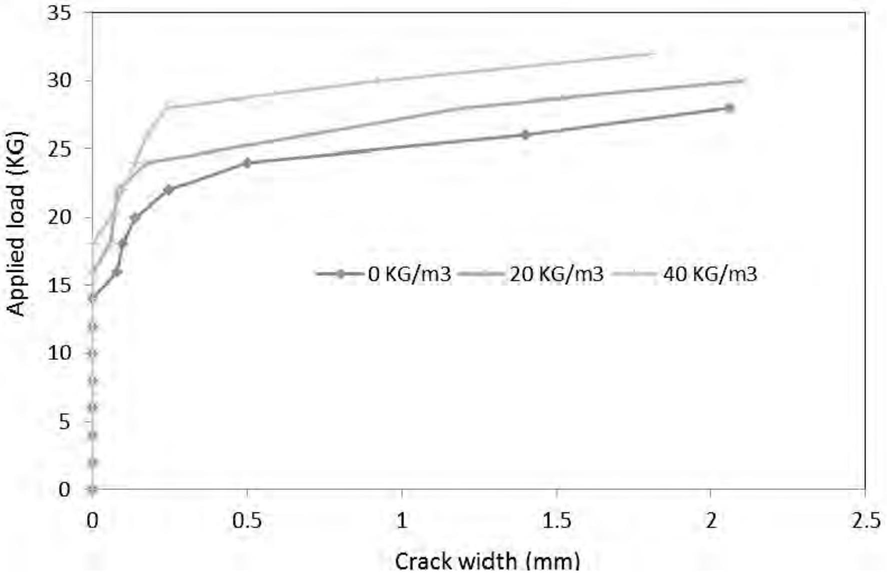

Figure 12: Crack development under applied load

As shown in figure 12, among three types of beams, crack appeared first for conventional beam (0 SF kg/m3) under load of 1600 kg. And cracks appeared for 1800 kg and 2000 kg for 20 kg/m3 and 40 kg/m3 respectively. It also can be observed that the higher of dosage of steel fiber, the higher ultimate loads the beam could sustain.

In table 6, number of crack for each type of beam after testing are shown. The conventional beam has 11 cracks then 15 and 18 for 20 kg/m3 and 40 kg/m3. It means that steel fiber contribute to transfer load evenly. Steel fiber with higher tensile strength of concrete, hooked end effect contribute to transfer load from high concentration area to adjacent zones reducing cracks. The crack width of beam with 40 kg/m3 of SF is smaller than beam with 20 kg/m3 and cracks on 20 kg/m3 is smaller than conventional beam without SF. Thus, steel fiber contribute to reduce crack width. It could be explained that when small crack appeared, steel fibers in this cracked zone absorbed energy through tensile strength. This will reduce cracks to widen as well as transfer energy to other parts.

4. CONCLUSIONS

After the series of tests and analysis, the following conclusion can be made in this research.

1. The steel fiber contributes to the increase of compressive strength of concrete. This is due to energy absorption as well as load transfer mechanism of hooked end steel fiber to increase bonding of aggregates and cement in samples.
2. Young Modulus of concrete also increases with the increase of steel fiber dosage. With effect of high strength steel fiber, concrete becomes harder.
3. Steel fiber contributes to increase of beam stiffness under applied load for bending. It also reduces cracks on beam thank to its high tensile strength to absorb energy at the cracked zones. The number of cracks on beam are higher (but crack widths are smaller) with ones with higher steel fiber dosage. Stress is more evenly distributed in beam with higher dosage of SF as well.

REFERENCES

Barros, J. A. O., and Figueiras, J. A., 1998. Experimental behaviour of fiber concrete slabs on soil. J*ournal Mechanics of Cohesive-frictional Materials* 3, 277-290.

EFNARC (2002). *Specification and Guidelines for Self-Compacting Concrete.* ISBN 0 9539733 4 4, 32.

Lofgren, I., 2005. *Fibre-reinforced Concrete for Industrial Construction.* PhD Thesis, Department of Civil and Environmental Engineering, Chalmers University of Technology, Sweden.

Narayanan, R., and Darwish, I. Y. S., 1987. Use of steel fibers as shear reinforcement. *ACI Structural Journal* 84, 216-227.

Schrader, E. K., 1971. *Studies in the behavior of fiber-reinforced concrete,* MS thesis, Clarkson College of Technology, Potsdam.

Shende, A. M, Pande, A. M, and Gulfam Pathan, M., 2012. Experimental study on steel fiber reinforced concrete for M-40 grade. *International Refereed Journal of Engineering and Science* 1, 043-048.

Two-dimensional investigation on chloride ion penetration into cementitious material under freeze-thaw environment

Katsufumi HASHIMOTO[1], Hiroshi YOKOTA[2] and Tomoyuki TANIGUCHI[3]
[1]Assistant Professor, Faculty of Engineering, Hokkaido University, Japan
hashimoto.k@eng.hokudai.ac.jp
[2]Professor, Faculty of Engineering, Hokkaido University, Japan
[3]Master's course student, Faculty of Engineering, Hokkaido University, Japan

ABSTRACT

To simulate freeze-thaw environment on the surface of concrete structure in real situation, which shows severe damage in cold region as mentioned, it is necessary to prepare experimental methodology to induce two-dimensional chloride ion penetration and icing behavior on top and side surface of concrete. The purposes of this research are 1) to prepare test methods for concrete durability under two-dimensional frost damage and chloride ion penetration and 2) to clarify chloride ion penetration behavior by Electron Probe Microscope Analyzer. Moreover, it is also targeted 3) to establish numerical method to calculate chloride ion penetration behavior under two-dimensional frost damage and chloride ion penetration. As the results, EPMA analysis showed that chloride ion concentration of thaw water and icing condition on the concrete surface influenced on chloride ion penetration depth and concentration in concrete. Additionally, prediction results on chloride ion penetration by proposed calculation method based on Fick's law in this paper showed good correlation with experimental results, although it must be further improved with consideration on diffusion coefficient alteration due to degradation degree from exposure surface.

Keywords: concrete, frost damage, chloride attack, icing condition, thaw water

1. INTRODUCTION

Concrete structures and members deteriorate and their performance will be degraded during the service life. In particular, frost damage due to freeze-thaw cycles causes deterioration of concrete structures in cold regions (Shashank, 2008). Also, chloride from deicing agents can penetrate into concrete and accelerate the deterioration due to frost damage in a freeze-thaw environment. Consequently, corrosion of reinforcing bars occurs in concrete members (Wang et al., 2014). Moreover, it has been reported that icing on the surface of concrete leads to acceleration of frost damage, which must consider the geometric conditions of the structure such as which concrete surfaces are exposed to snow cover and thaw water with chloride ion. In particular, parts of the concrete structure which have higher potential to be deteriorated by frost damage, such as bridge piers, would have chloride ion penetration two-dimensionally from the top and side surfaces of concrete. To simulate freeze-thaw environment on the surface of concrete structures considering the real environmental exposure, which shows severe damage in cold regions as mentioned earlier, it is necessary to prepare an experimental methodology to induce two- dimensional chloride ion penetration and icing behavior on the top and the side surfaces of concrete.

2. EXPERIMENTAL PROCEDURES

2.1 Materials and mix proportion

As for concrete specimens, Ordinary Portland cement (density: 3.16 g/cm^3, specific surface: 3320 cm^2/g), river sand (surface dry density: 2.71 g/m^3), and coarse aggregates (surface dry density: 2.72 g/m^3) were used for concrete specimens. Table 1 presents the mix proportion of the concrete. An air entraining agent was not used. As for mortar specimens, Ordinary Portland cement was used for casting mortar prisms. River sand (surface dry density: 2.67g/m3, fineness modulus: 2.82, maximum size: 1.7mm) was used for mortar specimens. Mix proportion of the mortar was W/C of 0.5 and S/C of 3.0. Concrete and mortar prisms, the dimensions of which were 100mm x 100mm x 400mm respectively. Test specimens were cut into the sizes of 100mm x 100mm x 100mm.

Table 1 Mix proportion of concrete

W/C (%)	**s/a (%)**	**Unit cement content (kg/m^3)**			
72	45	W	C	S	G
		220	304	831	1007

2.2 Outline of specimen

The concrete specimens were placed and exposed to an environment of immersion and freese-thaw cycles as shown in Figure 1 (A series, using 20 mm long rebars with different covers from the top) and Figure 2 (B series, using 20 mm long rebars with different covers from the side). The mortar specimens were also placed and exposed to the above mentioned environment without rebars. The specimens were demolded after 24 hours from casting, and cured in 20°C water until the age of 21 days and in air for a further 7 days. The following deterioration tests were conducted after the curing.

2.3 Freeze-thaw test and immersion test with NaCl solution

Freeze-thaw cycles of temperature history and immersion test were applied as shown in Figure 3 using 1, 3 or 5 wt% of NaCl solution in the bank on the top to simulate icing conditions. There were two test series for concrete specimens: freeze-thaw cycles for 6 days and immersion test for 1 day (Cycle 1) and immersion test for 7 days (Cycle 2). These were executed cyclically for 28, 56 and 84 days. As for mortar specimens, freeze-thaw cycles for 12 days and immersion test for 1 day were periodically-cycled till the freeze-thaw cycles reach 100 times.

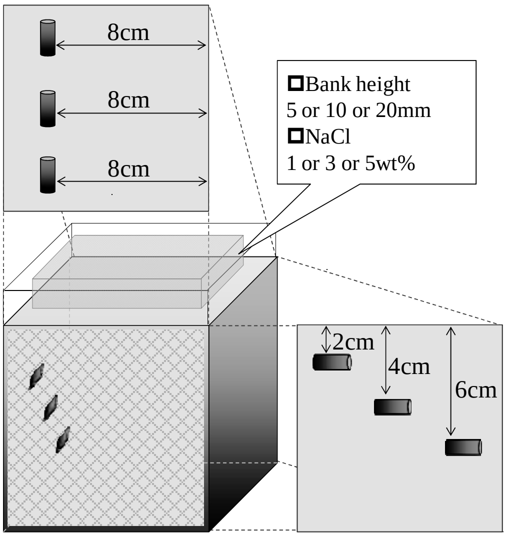

Figure 1 Geometry with different covers to rebar from the top (A series, Left)

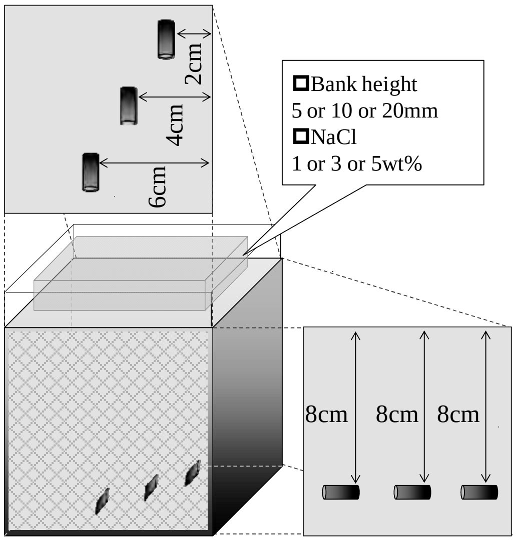

Figure 2 Geometry with different covers to rebar from the side (B series, Right)

2.4 Measurement items

In concrete specimens, chloride ion contents around 10 mm from the surface of each rebar were measured according to JIS A 1154. In mortar specimens, chloride ion penetration behavior by Electron Probe Microscope Analyzer (EPMA). The sample for EPMA was fabricated into the size of 50 x 50 x 8mm.

3. NUMERICAL METHOD ON CHLORIDE ION PENETRATION

In order to calculate two-dimensional chloride ion penetration, Fick's 2nd law of chloride diffusion was expanded to express two-dimensional chloride ion ingress as shown in equation 1 and 2.

$$\frac{\partial C}{\partial t} = \frac{\partial}{\partial x}(D_x \frac{\partial C}{\partial x}) + \frac{\partial}{\partial y}(D_y \frac{\partial C}{\partial y}) \tag{1}$$

Where,
$C(x, t)$: Chloride ion concentration (kg/m^3)
C_0: Surface chloride ion concentration (kg/m^3)
D: Apparent chloride ion diffusion coefficient (cm^2/year)

$$\begin{aligned}\frac{C(t+\Delta t)-C(t)}{\Delta t} &= \frac{C_{i,j}(t'+\Delta t')-C_{i,j}(t')}{\Delta t'} = \frac{1}{\Delta x}\left(D'_{i+1}\left(\frac{C_{i+1,j}(t')-C_{i,j}(t')}{\Delta x}\right)\right)\\ &-D'_{i-1}\left(\frac{C_{i,j}(t')-C_{i-1,j}(t')}{\Delta x}\right)+\frac{1}{\Delta y}D'_{j+1}\left(\frac{C_{i,j+1}(t')-C_{i,j}(t')}{\Delta y}\right)-D'_{j-1}\left(\frac{C_{i,j}(t')-C_{i,j-1}(t')}{\Delta y}\right)\end{aligned} \tag{4}$$

Where,
erf: Error function
$C_{i,j}(t)$: Chloride ion concentration in element (i, j) (kg/m^3)
D'_i: Apparent chloride ion diffusion coefficient in i element from the side (mm^2/year)
D'_j: Apparent chloride ion diffusion coefficient in j element from the top (mm^2/year)

Δx: Mesh size of x axis (mm)
Δy: Mesh size of y axis (mm)
$\Delta t'$: The numbers of freeze-thaw cycle

4. RESULTS AND DISCUSSION

4.1 Chloride ion concentration in thaw water

Figure 3 shows chloride ion concentration on the top of the specimens with elapsed time of freeze-thaw cycles after 0 ^{o}C. In the process, NaCl solution was concentrated, where it was found that the thaw water has been perfectly iced at 1.5 hours in the case of 1wt%-10mm (initial NaCl concentration-bank height) and 3wt%-5mm. Also in the other cases, thaw water has been iced at 2.5 hours.

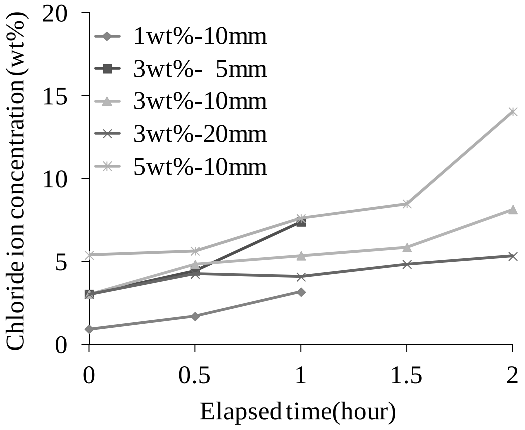

Figure 3 Chloride ion concentration in thaw-water

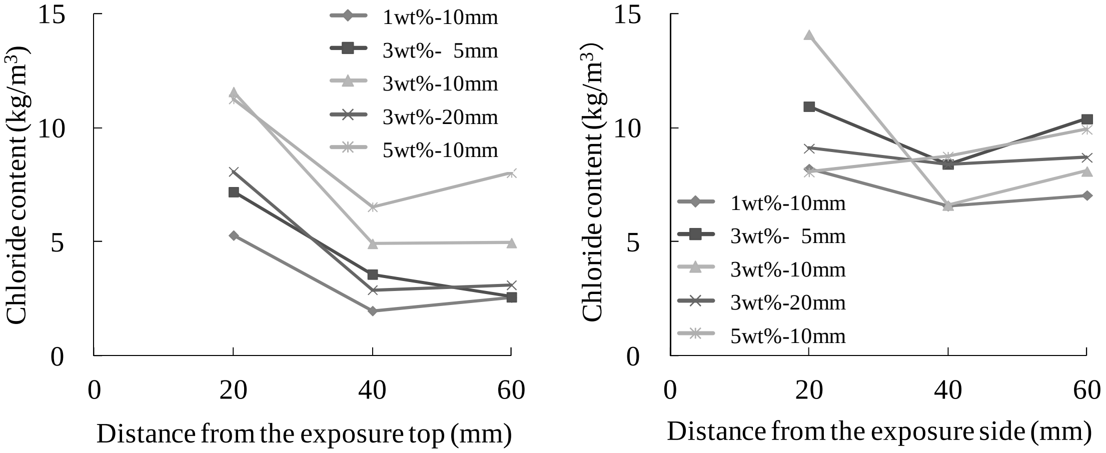

a) A series b) B series

Figure 4 Total chloride ion concentration in concrete specimens

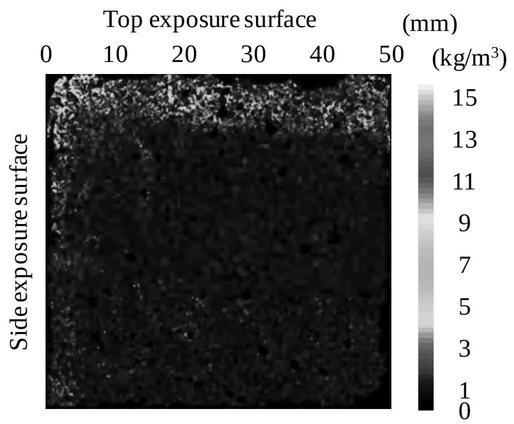

a) NaCl: 1%

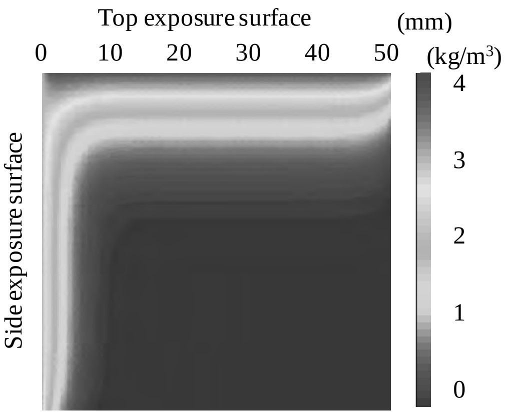

a) NaCl: 1%

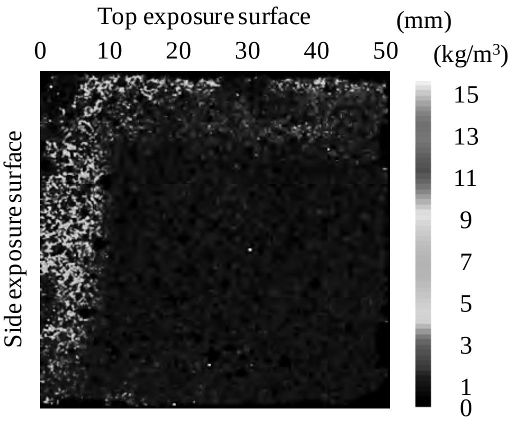

b) NaCl: 3%

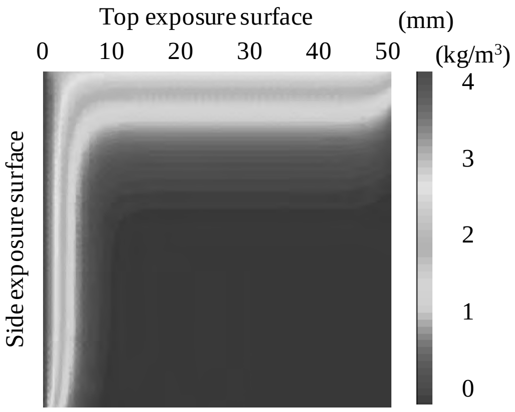

b) NaCl: 3%

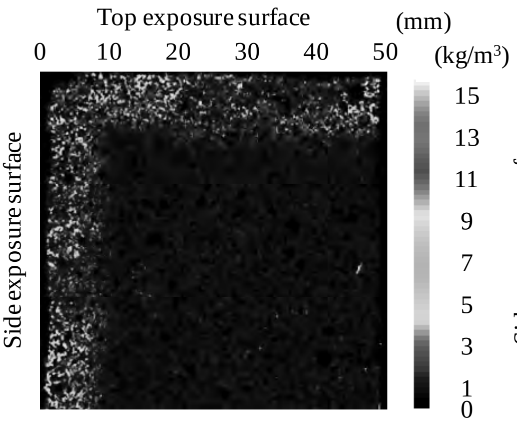

c) NaCl: 5%

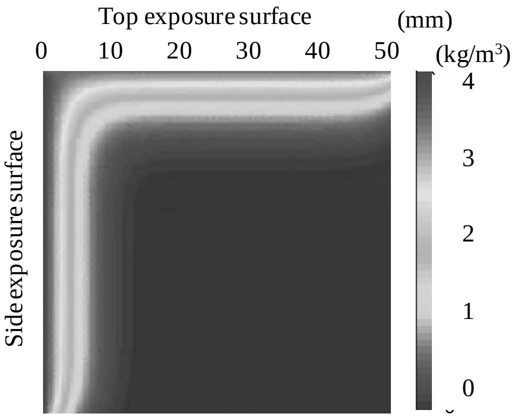

c) NaCl: 5%

Figure 5 EPMA results on chloride ion concentration of mortar specimens (Left)
Figure 6 Calculation results on chloride ion concentration of mortar specimens (Right)

4.2 Chloride ion ingress

Figure 4 shows total chloride ion concentration in concrete specimens. In comparison with Figure 4a) and b), chloride ion concentration from the top of specimen with icing formation was totally lower than that from the side of specimen without icing formation. Also, increasing tendency on chloride ion concentration from internal pat at 60mm of concrete cover to surface at 20mm of concrete cover was more remarkable in A series than B series, which means chloride ions were more concentrated in the surface area due to icing formation on the surface of concrete.

Figure 5 shows EPMA results on chloride ion concentration of mortar specimens. In any cases in this study, it was confirmed that chloride penetration depth was 10 to 15mm, which is corresponding to the experimental results. As visual inspection on the surface of mortar specimens after 100 times of freeze-thaw cycles, the case with lower concentration of initial NaCl in thaw water lead to larger scaling of top surface with icing formation, while the scaling was not observed on the side surface without icing formation.

As for chloride ion diffusivity in the EPMA results, more chloride ions were penetrated from top surface and less chloride ions from side surface in the case of NaCl 1%. In the case of NaCl 3%, more chloride ions were penetrated from side surface than top surface. Especially, the chloride ion penetration depth at 0-30mm from the top surface was larger than at 40-50mm. When NaCl 5% was used, the difference did not occur.

4.3 Evaluation on two-dimentional numerical analysis

Figure 6 shows the calculation results on chloride ion concentration of mortar specimens with using two-dimensional numerical analysis with using equation 2. Surface chloride ion concentration and apparent diffusion coefficient were set to be constant to each axis. Additionally, Δx and Δy were 1mm.

As the results of calculations, the results from calculations gave close agreement with those from experiments, where particularly the increase of chloride penetration from top with NaCl 1% and side from NaCl3%. It is necessary to put the influence of deterioration details into the numerical method, such as diffusion coefficient in each depth from surface and mechanical properties, to improve the method for more advanced discussion.

5. CONCLUSIONS

Chloride ions were more concentrated in the surface area due to icing formation of thaw water due to freeze-thaw action on the surface of concrete. On the other hand, EPMA analysis on mortar specimens showed that chloride ion concentration of thaw water and icing condition on the concrete surface influenced on chloride ion penetration depth and concentration in concrete. Additionally, prediction results on chloride ion penetration by proposed calculation method based on Fick's law in this paper showed good correlation with experimental results, although it must be further improved with consideration on diffusion coefficient alteration due to degradation degree from exposure surface.

REFERENCES

Shashank, B., 2008. Strain-temperature hysteresis in concrete under cyclic freeze-thaw conditions, *Cement Concrete Composites* 30, 374-380.

Wang, Z., Zeng, Q., Wang, L., Yao, Y., and Li. K., 2014. Corrosion of rebar in concrete under cyclic freeze–thaw and chloride salt action, *Construction and Building Materials* 53, 40-47.

Station design guidelines of Tokyo Metro for renovation

Masaru KUWANA[1], Kazuhisa KIZU[2], Naotsugu KOGA[3],
Yoshihiko MUTOU[4], Keiji OOISHI[5] and Shinji KONISHI[6]
[1] Assistant Manager, Structure Engineering Division, Tokyo Metro Co., Ltd., Japan
m.kuwana@tokyometro.jp
[2] Chief Engineer, Structure Engineering Division, Tokyo Metro Co., Ltd., Japan
[3] Manager, Structure Engineering Division, Tokyo Metro Co., Ltd., Japan
[4] General Manager, Engineering Division, Tokyo Metro Co., Ltd., Japan
[5] Deputy General Manager, Engineering Division, Tokyo Metro Co., Ltd., Japan
[6] Senior Manager, Engineering Division, Tokyo Metro Co., Ltd., Japan

ABSTRACT

Since opening the Ginza Line as the first subway in the Eastern world in 1927, Tokyo Metro has continued operations while expanding its lines. Subsequently, with the opening of the Fukutoshin Line in June 2008, the Tokyo Metro has been upgraded to include nine lines, 179 stations over a 195.1 km span of open tracks, and a daily passenger base of 6.44 million people. Tokyo Metro aims to create stations that, "all passengers can use comfortably and easily." However, many of the stations are aging, and through future renewal, in order to continually maintain stations that achieve this aim we have drawn up the "Tokyo Metro Station Design Guidelines." The guidelines consist of the following steps: "Area > Space > design concept > design guideline". For example, the order of progression is: "Concourse > accessway > smooth transit > good visibility". The guidelines indicate the Tokyo metro design concepts and design policy, and we are committed to providing customers with pleasant and attractive station spaces through the common efforts of everyone engaged in station design and construction. In this paper we will introduce the background and details of the guidelines as well as several cases from the renewal plans for the Namboku Line, Fukutoshin Line, and Ginza Line.

1. TOKYO METRO: STATION DESIGN GUIDELINES

1.1 Aims and Composition

The guidelines embody the group ideal of "Keeping Tokyo on the Move" that we uphold, and they stipulate the best designs for the stations which will be a source of Tokyo's appeal and dynamism. Tokyo Metro has established the basic idea for its designs and image that embodies these designs, and we will achieve a station design unique to Tokyo Metro and aim to increase the value of every station through sharing these perspectives and views among a broad range of people involved in the design. The guidelines integrate the "design concepts," "domain-specific concepts," and "domain-specific design guidelines" that comprise the group ideal of "Keeping Tokyo on the Move" which is the fundamental idea of the design.

1.2 Group Concept: "Keeping Tokyo on the Move"

With privatization in 2004, the Tokyo Metro group put forward its ideal of, "Keeping Tokyo on the Move" which demonstrates the group's desired attitude from a long-term perspective. This ideal is a statement of the future form that we aim for as a corporation playing a central role in the metropolitan rail network, and as a commitment to stakeholders, it will be crucial to continuously engage in various activities. In particular, stations are a crucial interface where stakeholders come into contact with the Tokyo Metro on a daily basis, and the stations play a major role as sites to achieve the group's ideal. Hence, in formulating the guidelines, based on the group's ideal we conducted investigations into the best form of station design.

Group Ideal
Keeping Tokyo on the Move

The Tokyo Metro group aims to develop the railway business as our central enterprise and thereby support the urban function of Metropolitan Tokyo.
We will maximize the city's appeal and dynamism,
and through our excellent technology and creativity,
we will provide dependable, pleasant, and better services,
and will contribute to the active daily routines of the people of Tokyo.

1.3 Design ideal "A place that enriches both Tokyo and the heart"

In order to achieve the group's ideal of "Keeping Tokyo on the Move" what role must stations play? This is the first consideration in station design.

The Tokyo Metro stations are key places of the city which extends into the far corners of Tokyo, and when considering the role of the stations we must perceive them in terms of their crucial urban function. By bringing energy to local areas and the city, and through transmitting the appeal of Tokyo to the public as the "face" of Tokyo, we aim to play a role in making Tokyo an appealing and plentiful city.

Tokyo Metro stations are also places that broaden the flow of life of the public. We perceive stations as places closely related to everyday life, and aim to enrich the hearts of every individual connected to Tokyo through providing energy and affluence to people leading a busy daily life, and creating happiness and pride in Tokyo.

In terms of the elements comprising the design ideal of "a place to enrich Tokyo and the heart," from the five perspectives of travel, life, local area, city, and society, we investigated a station format for Tokyo Metro to aim for that is not merely that of a transport hub.

1.4 Stations that Tokyo Metro aims to create

Tokyo Metro aims for the following kind of stations:

Stations are places open to usage by people in various capacities and situations regardless of age, sex, or nationality. As transportation hubs that support the public's bustle-free circulation of metropolitan Tokyo, we must achieve stress-free travel for all. We aim for stations that achieve smooth travel without delays even at peak times, that alleviate the sense of being trapped underground and the anxiety felt by elderly and disabled people, and that are able to provide a reassuring and pleasant time and space for the public as a whole.

Stations are situated within people's flow of life, and are places that link various life scenarios such as commuting to work and school, shopping, and tourism. As the "intermediary" between life scenarios, stations must be spaces that accommodate each individual in various capacities and situations. Sometimes stations will calm our passengers through providing friendly surroundings, and sometimes they will switch the moods of our users through a small surprise or discovery. We aim for stations that support the lives of our users, and that are capable of changing their day-to-day feelings.

The stations are places that welcome and send off many people, such as people living in town, commuters, and first-time visitors. As central points in the local area and town, even underground we must convey the mood of the town and create a sense of expectation for the town. Stations condense the charm of all Tokyo's various local areas and towns, and communicate that charm to the people that use them. We aim to create stations that draw people to, and develop bonds between people and the town, bringing dynamism to the local areas and towns linked to our stations.

Stations extend into the far corners of Tokyo and are essential to Tokyo as a city. To people living in and visiting Tokyo, it is necessary that stations are equipped with urban sensitivity that communicates Tokyo's individuality and characteristics. While advanced and progressive and possessing an emotive aspect conveying a sense of subtlety and warmth, stations embody the quintessence of Tokyo. Through communicating Tokyo's atmosphere and charm, we aim to create stations that raise the image of the city.

Stations are places that support society as underground network hubs that are environmentally friendly means of transportation. In order to deliver social responsibility as public amenities, stations must contribute to the maintenance and cleanup of the environment. Stations must alleviate the environmental burden through the effective usage of natural energy and enhancing maintainability and serviceability. Through environmentally friendly approaches that eliminate the burden on the environment, we aim to create stations able to take responsibility and contribute to society.

1.5 Focus areas of the guidelines

When determining the guidelines, the basic premise was shared focus areas. More specifically, the guidelines are comprised of the fundamental spaces of three areas and eight spaces.
Exit/Entrance areas: Shed space/station building space/ascending and descending space
Concourse area: Accessway space/central space
Platform areas: Ascending & descending space/platform space

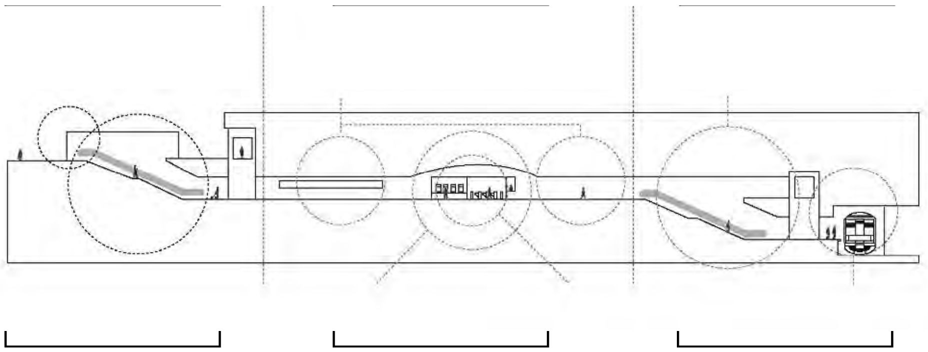

1.6 Common design guidelines

As well as design guidelines for individual areas and spaces, we determined design guidelines common to all areas and spaces that Tokyo Metro stations must fulfil. Through the guidelines we sought to create a consistent worldview for the stations overall.

Table 1: List of general common design guidelines

Design guideline	Details
Designs that convey the atmosphere of Tokyo	Structures and designs that convey a sense of Japan amidst progressiveness
	Designs that take full advantage of materials
Designs with a sense of uniformity and harmony	Advertisement arrangements with a functional beauty
	Advertising spaces and media that maintain a sense of harmony of design
Designs that maintain their charm over time	Designs that are unaffected by fashions and maintain their charm over time
Environmentally friendly designs	Use of maintainable and serviceable materials and technology
	Use of energy-efficient equipment and facilities
	Ingenuity that incorporates natural energy into the station buildings

Fukutoshin Line: Kitasando St.

Fukutoshin Line: Nishi-Waseda St.

Marunouchi Line: Shinjuku-sanchome St.

Tozai Line: Urayasu St.

Table 2: List of detailed design guidelines

Area	Space	Design concept	Design guideline
Entrance & Exit	Sheds	Spaces that have presence within the city and a sense of openness	Designs that are easily identifiable as metro stations
			Open designs that alleviate the sense of oppression and anxiety
			Design that are easy to use
	Station building	Spaces that harmonize with surrounding scenery, and that are open to the town	Designs that indicate this is a metro station
			Designs that are open to the local area
	Ascending/ descending	Spaces that provide a natural and stress-free link between the levels above and below ground	Designs that alleviate the sense of oppression and anxiety felt when descending below ground
			Designs that alleviate the stress of descending/ascending
			Uplifting designs that convey the atmosphere above ground
Concourse	Accessways	Spaces which enable	Simple designs with good

		comfortable and smooth passage	visibility
			Designs from which it is easy to ascertain the proceeding direction
			Designs that create a comfortable feeling
	Central space	Comfortable spaces which convey the atmosphere of the local area and city	Open designs without a sense of oppression
			Designs that relax and comfort
			Designs with a range of emotions
	Ticket gates	Spaces that are welcoming and friendly	Designs that do not create the stress of an entrance and exit place
			Designs from which it is easy to ascertain the proceeding direction and how to use the ticket gates
			Designs which convey a sense of warmth and hospitality
Platforms	Ascending/ descending	Spaces that enable stress-free and smooth passage	Designs that alleviate the sense of oppression and anxiety
			Designs that alleviate the stress of descending/ascending
			Designs that do not convey a sense of the monotony of ascending/descending
	Platforms	Spaces that are peaceful and calm, and provide a sense of ease	Designs which ensure good visibility and safety
			Designs that clearly identify the station name, lines and exits
			Designs that are calm and make waiting times comfortable

2. TRANSITIONS IN STATION DESIGN

Here we will introduce Tokyo Metro's station design from past to present.

2.1 Ginza Line

On the Ginza line, we considered design alterations at every station to clearly identify user stations. We changed the color of the platform walls at Tawaramachi, Inaricho and Ueno stations. At other stations we painted the walls and ceilings white to optimize lighting efficiency.

For purposes of station identification, we changed the color of advertising print holders and the body tile capping at individual stations.

2.2 Marunouchi Line

On the Marunouchi line, we changed the texture and colors of finishing materials and made individual stations easily identifiable. For the finishing materials, we selected durable and water-resistant materials, and materials with relatively high sound absorption to reduce noise.

2.3 Hibiya Line

On the Hibiya line, we further standardized facilities common to all stations. The selection conditions for finishing materials took into consideration high temperatures, high humidity, as well as fire-resistance, water resistance and durability in addition to serviceability issues and economics.

2.4 Tozai Line

On the Tozai line, with the colors of platform wall tiling we attempted a tiling method divided into a 3-color 3-step system at several stations to make all stations easily identifiable.

2.5 Chiyoda Line & Yurakucho Line

On the Chiyoda line, we altered the platform colors and wall tile sizes to make the stations easily identifiable.

2.6 Hanzomon Line

On the Shibuya to Suitengumae section, to make user stations easily identifiable we designed the platform walls characteristically using finishing materials and colors and also according to the features of the local area.

On the Suitengumae to Oshiage section, to ensure clear visibility that will lead to smooth circulation planning, in terms of creating a pleasant environment based on a consideration of a finish and color scheme plan, we implemented a bright and fun color scheme and graphics plan to create an open space that does not convey a sense of darkness or enclosure.

2.7 Namboku Line

On the Namboku line, based on the basic ideal for the vision of the Namboku line of, "a new, convenient, pleasant, and appealing subway for the 21st Century," we created a "basic plan and basic design for the Namboku line design" based on which we considered and incorporated new design profitability and an array of devices and ingenuity such as platform doors, movable benches, station colors, media-walls, ticket gates, symbol columns, ticket offices, contact corners and sheds at entrances and exits. We also installed art-walls at every station on the inside walls of the tracks and central spaces.

As three crucial design elements in making subway station spaces into appealing urban spaces, we thought up the following three considerations that are essential to the formation of the Namboku line's design image.

(1) HIGH QUALITY (2) AMENITY (3) TOTALITY

We will specifically describe the basic policy for the design of platform spaces according to the basic ideal.

Firstly, as the new subway, platform doors will be introduced to the Namboku line platforms, and we believe this will create a less conventional platform space. We attempted to establish the "image of a new space" to correspond to the introduction of platform doors, and secondly we increased the "quality of the space" in an attempt to ensure comfort. Thirdly, the platform doors will give all the stations a strong sense of uniformity, and were created to have identity and be clearly distinguishable at each station. We predicted that introducing the platform doors would make it difficult to recognize the stations from inside the carriages when checking the station signs on platforms and due to differences in the finishing materials of the stations, so we made the differences clearly recognizable through a clear-cut expression of color on the door sections of the platform doors.

On the pillars and joists of the platform doors, we used "charcoal gray" to minimize assertiveness as much as possible, and for the door sections we determined a basis of the six colors yellow, orange, red, purple, blue, and green to enable clear recognition. Furthermore for all stations on the Namboku line, we decided on and used color in a uniform order. We established this basis of six colors as the station colors and practically applied them to the platform seats, escalator belts and concourse wall surfaces. In the sections of the track closed off by the platform doors, as an extension of the platform space and in order to create a sense of "expanse" and "openness," we used a bright motif (pattern) and color scheme, and through incorporating high-quality graphic-design we created an enjoyable scene and a cheerful impression for passengers while at the same time establishing the identity of each individual station.

Namboku line: Korakuen St.

Namboku line: Ichigaya St.

Namboku line: Iidabashi St.

2.8 Fukutoshin Line

We decided on the overall concept of, "a fun station, a fun local area," for the Fukutoshin line, and as the design methods we determined the lobby space, comfortable space (large spaces and atrium), universal design, local area projection, and public art.

We zoned the approach spaces and lobby spaces inside the station building, and clearly divided the two spaces using lobby gates. We determined that the main sections of the approach spaces would be from the station entrance and exit to the lobby gates, and made them into low cost simple spaces. As for the lobby spaces, we determined that the concept for each station would be considered with an emphasis on comfort.

Inside the station building, we established large spaces with high ceilings and atrium, and planned open spaces that dispelled any sense of being trapped below ground. We planned the stations to reflect local history and culture in the concepts of each station, and artists installed public art in every station to improve their cultural value.

Fukutoshin Line: Shinjuku-sanchome St

Fukutoshin Line: Meiji-Jingumae St.

3. FUTURE TOKYO METRO STATION DESIGN

3.1 Station Design on the Ginza line and Station Renewal Plan

The Ginza line marked the 85th anniversary of opening the Asakusa to Ueno section in 2012. The current station renewal emphasizes the history of Japan's oldest subway that has linked Tokyo's towns, and simultaneously aims to solidify an image as a line incorporating and communicating advanced functionality. Based on the line's concept of a "fusion of tradition and progress," we divided the Ginza line into the five areas of the Shitamachi area (Asakusa - Kanda), commercial area (Mitsukoshimae - Kyobashi), Ginza area (Ginza), business area (Shimbashi - Akasaka-mitsuke), and the trend area (Aoyama-itchome - Shibuya). Subsequently, in tandem with revision to the station layout to improve customer convenience, while retaining uniformity of design as a line, we renovated the station to express its individuality. From this design concept, we decided to hold a design competition for each area to widely recruit various ideas contributing to improving the Ginza line’s new appeal.

First we held the "Shitamachi area" design competition and received as many as 96 works. Based on the many ideas received, in addition to the "Tokyo Metro Station Design Guidelines" we formulated the "Ginza Line Station Renewal Design Guidelines (Joint Edition)." These guidelines were created to provide guidance on steering the design policy for the Ginza line station renewal design and construction in the best direction and to ensure conformity, and also to specify basic rules on essential design considerations when advancing the design and construction of each station. However, to complement the Joint Edition of these guidelines we are also composing an area edition specific to each area.

We are currently drawing up the final design for the Asakusa and Kanda section based on the "Ginza Line Station Renewal Design Guidelines (Joint Edition)" and the "Shitamachi Edition," and are scheduled to complete the construction in 2017. In 2014 we also held a design competition for the "Commercial area" and a successful entry was selected. In future, based on the best work we will formulate the "commercial edition" and draw up a final design. Subsequently, next time we will prepare for the "Ginza area" competition followed by the "business area" and "trend area."

上野駅
伝統と未来の象徴空間
1
2
TMR0228

"Shitamachi area" Design competition winning entry Ueno St.

"Shitamachi area" detail design path Ueno St.

"Commercial area" Design competition winning entry BEST

"Commercial area" Design competition winning entry SECOND

Development of asset management system- A case study of tube wells of IIT Kanpur

Khushboo GUPTA[1], Onkar DIKSHIT[2], Sudhir MISRA[2]
[1] Research Associate, Department of Civil Engineering, IIT Kanpur, India
[2] Professor, Department of Civil Engineering, IIT Kanpur, India

ABSTRACT

With rapid growth of cities, increasing urban assets like water supply, roads, public transportation systems and power supply demands proper handling. In this research, which uses the water supply system of IIT Kanpur as a case-study, development of a web enabled water infrastructure management system (WIMS) is suggested as a possible solution for proper handling of these assets focusing on tube well as one of the component of water asset. The purpose is to initiate the design of a centralized database of tube wells which can be used for decision support, inspection planning, community need-to-know, and check for regulatory compliance. The work includes: designing of format for data collection, database creation and web based representation using open source tools to answer non-spatial queries. The system has been built in a manner that it permits upload of spatial and related non-spatial information of tube wells. It facilitates appending information related to uploaded features thereby helping to build a spatial database for tube wells. There is a need for a standard format for data collection for each and every asset existing. This would not just ease the data collection process but will also enhance the data quality. This system is built to help an organization's works department to carry out better management of water infrastructure by keeping an up to date water infrastructure database. The above research is applied in Indian Institute of Technology Kanpur (IITK) to enhance the management of water infrastructure (tube wells) by Institute Works Department (IWD).

Keywords: Urban asset management, tube well, data collection format, database creation, web enabled water information management system

1. INTRODUCTION

When we refer to an asset management system, an "asset" is a component with an independent physical and functional identity, value and service life. Maintenance, renewal and replacement of these assets is an integral part of 'managing' the assets, which can be done effectively only if an accurate and appropriate database of the assets is available (Betti, 2010). Virtual non-availability of such a database is one of the challenges faced by managers of public assets in India. The problem is compounded by the multiplicity of organizations involved in operating and maintaining the assets (Mukherjee, 2013).

Taking the case of water supply related infrastructure, developing an efficient water information management system (WIMS) which stores appropriate data for relevant assets is important for several reasons, some of which are listed below:

1. Providing a location based approach to manage operational challenges like solving complex geographical, hydrological and planning problems related to distribution of water (Garg et al, 2000).
2. New ways of acquiring water asset data and providing efficient means of processing, managing and integrating this data to meet decision making needs (Opadeyi, 2007).
3. Integrating non-spatial attribute information within the map geography, linking databases together, consolidating workflows, and presenting a common operating picture for the end user to perform water asset related spatial and non-spatial query (Kulshreshtha, 1998)
4. Handling large volume of deteriorating water infrastructure systems, particularly underground water infrastructure like tube wells, underground tanks and pipelines, which pose serious threats to the environment if they fail; as the information about the establishment and condition of these valuable assets get buried with them (Karlaftis et al., 2009; Singh, 2011).

WIMS will help a water works' manager to answer the above questions accurately and rationally, and assist in the day to day functioning of the department.

This paper focusses on the issues relating to development and management of WIMS in an urban scenario and uses the campus water supply network in Indian Institute of Technology Kanpur (IITK) as a case study. It emphasizes the need to create and maintain appropriate databases and suggests a simplified approach by developing a format for data collection considering the case of tube wells at IITK. The final objective is development of web enabled WIMS, and also explore the possibility of extending this concept to management of other urban assets such as roads and power supply systems.

2. METHODOLOGY SUGGESTED

The stages for developing the information management system for an organization's water infrastructure are as follows:

1. Understanding the existing infrastructure and availability of related information.
2. Identifying the components of water infrastructure present (e.g. drinking water, waste water and storm water pipelines, tube wells etc.).
3. Obtaining relevant information (as hardcopy, soft copy, interview, reports etc.) about these assets.
4. Interviewing the engineers and gathering the information relevant with respect to the organization's personnel for water assets.
5. Development of a data collection form (template)

2.1 Algorithm development for WIMS

The methodology used in this study is described briefly in a flow chart in Figure 1, along with the tools to be used at each step.

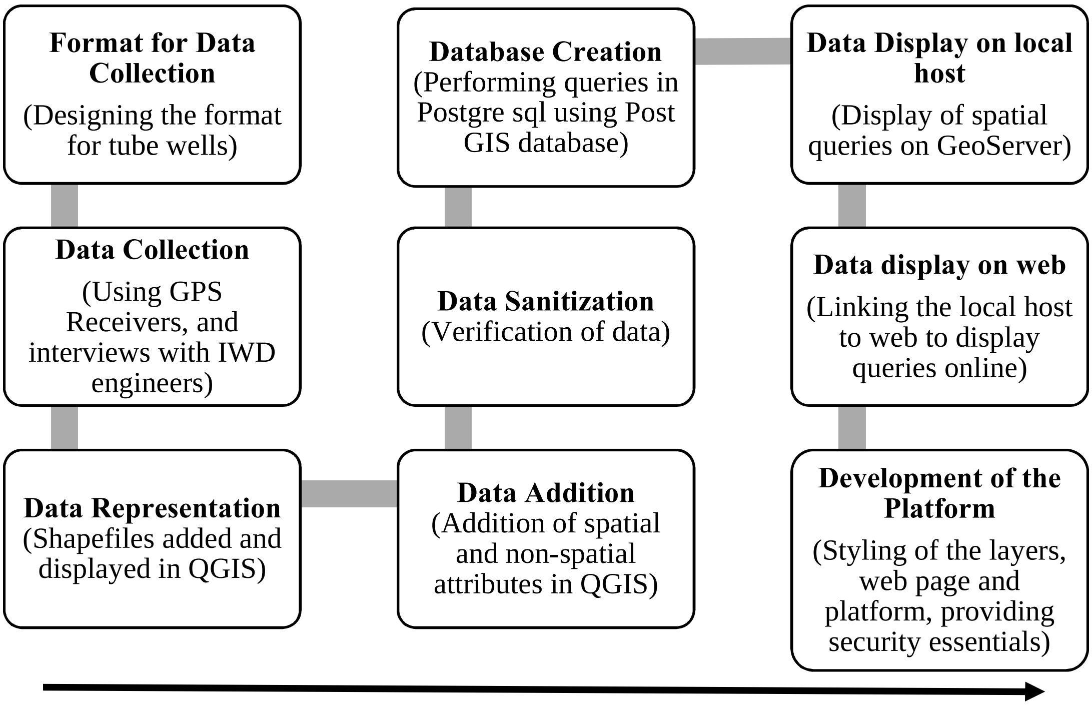
Format for Data Collection
(Designing the format for tube wells)
Data Collection
(Using GPS Receivers, and interviews with IWD engineers)
Data Representation
(Shapefiles added and displayed in QGIS)
Database Creation
(Performing queries in Postgre sql using Post GIS database)
Data Sanitization
(Verification of data)
Data Addition
(Addition of spatial and non-spatial attributes in QGIS)
Data Display on local host
(Display of spatial queries on GeoServer)
Data display on web
(Linking the local host to web to display queries online)
Development of the Platform
(Styling of the layers, web page and platform, providing security essentials)

Figure 1: Flow chart for development of Water Infrastructure Management System (WIMS)

2.2 Application of suggested methodology as a case study for water assets in IITK

The suggested methodology was implemented in the IITK campus established about 65 years ago in outskirts of Kanpur. It should be remembered that IITK is 1100 acre campus with a population of about 12000, has no ‘municipal water supply’ at present and relies completely on about 10 operational tube-wells to draw groundwater. The spread of all tube wells, working as well as abandoned in the IITK campus is described in Figure 2. The extent of campus is shown by boundary and road layers and the bullets in represent the locations of tube wells in the campus.

The system is managed completely by the engineers of the Institute Works Department (IWD). The design of data collection format for water assets involved the following steps:

1. Identifying the components of water infrastructure and the state of its management: This step involved identification and classification of these components under different heads based upon their nature. For example: Tube wells (used for extraction of water from ground)
2. Interviewing the IWD engineers to get an insight about their requirements regarding data for managing the water assets in an efficient manner.
3. Grouping these parameters under different heads to provide individual as well as overall picture of the assets. These parameters are listed in Table 1.
4. Based on these parameter heads data collection format was created.

5. Information was obtained about these assets by going through documents (such as bore log reports) with IWD related to tube wells and interviewing the IWD personnel.

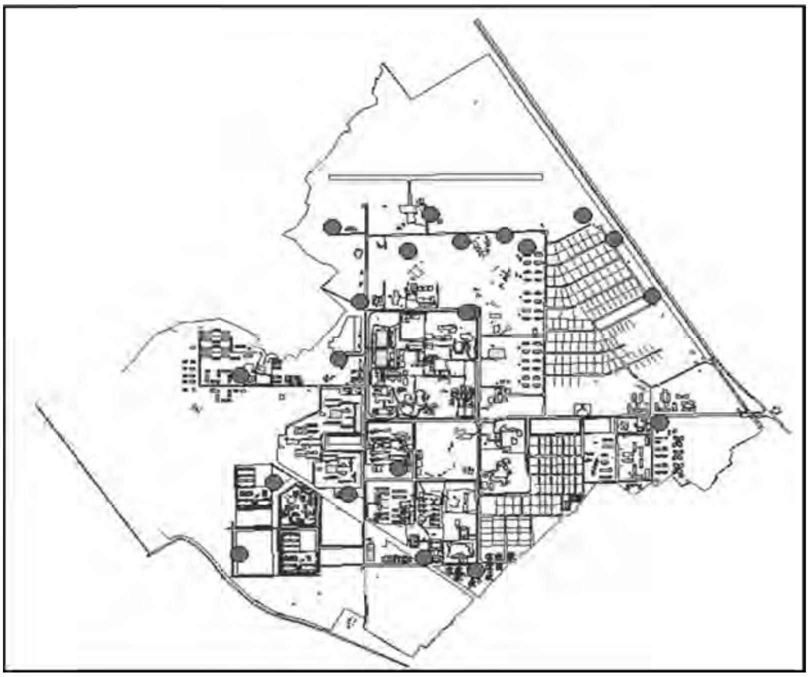

Figure 2: Tube well locations in IITK campus

2.3 Description of tools used

Relevant spatial data were collected by Trimble GPS receivers R3 and R7. The web enabled system was developed by using Quantum GIS (Quantum GIS 1.8 documentation), pgAdmin III (PostgreSQL Manual, 2006), GeoServer (Geoserver 2.0 Documentation), GeoNode (Geonode manual) and log plot utility of RockWare (for generating bore logs). A detailed description about these tools and their usage is presented in Gupta (2014).

3. RESULT AND DISCUSSION

This section describes the data collection format and different types of queries performed on data.

3.1 Description of data collection format

The data collection form consists of attributes for a tube well given in Table 1.

Table 1: Tube well attributes and their description included in data collection form

Name	**Type**	**Comment**
ID	Numeric	Unique identity number for a tube well
Tube well Name	Text	Naming convention followed
Location	Double	Coordinates in UTM projection using WGS-84 reference ellipsoid
Descriptive location	Text	Area or recognition point near which tube well is present
Type[1]	Text	On the basis of tube well depth (deep/shallow)
Condition	Text	Working condition or abandoned
Start date	Date	Year in which tube well started working.
Abandonment date	Date	Year in which tube well was abandoned
Casing Size[2]	Double	Diameter of the casing pipe
Hosing size[2]	Double	Diameter of the hosing pipe
Drilling depth	Double	Depth of bore drilled
Pipe depth	Double	Depth till which the pipe is inserted in bore
Pipe material	Text	Material of tube well pipe
Pump specifications	Integer	Power of pump in HP (horse power)
Establishment Charges[3]	Integer	Expenditure (INR) spent during establishment of tube well
Maintenance Charges[3]	Integer	Yearly expenditure on maintenance of tube well (INR)
Running Duration	Integer	Total no. of hours of drawing water in a day
Running Schedule	Text	Daily running schedule tube well
Discharge	Double	Discharge measured in liters per hour.
Electrical units consumed	Integer	Hourly consumption of electrical units consumed for running tube well
Bore log[4]	Raster	Information about lithology type existing in the bore varying with depth

Notes:

1. A tube well classified on the basis of its depth – those with depth greater than 200 m are called ‘deep’ and those with depth less than 200 m are defined as ‘shallow’.
2. A tube well casing houses the inlet, cylinder, piston valves and rising main of a "down-the-hole" type hand pump. The upper casing has a bigger diameter than the normal casing which is known as hosing. In the data set used (IIT campus), the diameter of the hosing and casing pipes are 350 mm and 250mm, respectively.
3. The cost detail is split into development and operational charges. The former consists of the all expenditure for establishment of the well, the latter includes the operational electricity charges, and repair and renewal charges.
4. Bore logs give the variation of lithology, and locations of aquifer and non-aquifer layers at different depths.

The form was used to create a database for all tube wells including functional and non-functional ones in the campus. This database formed the basis of a (local) WIMS, which provided greater insight to the asset manager and provided answers to non-spatial queries, as explained in the following paragraphs.

3.2 Analysis

Basically, to be able to answer the queries of an asset manager (AM), the information can come from the data of the tube well (discharge, etc.) and/or bore log. It should be borne in mind that it may not be possible to answer all the questions that AM may have from the overall data set created. To that extent, it may become necessary to modify the data collected from time to time. Questions that can be answered based upon tube well data include those relating to location, condition, efficiency, present value of discharge, running hours, cost details, etc. Another set of questions which arise include bore log related questions like soil profile, aquifer related information, etc. Queries relating to integration of tube well and bore log data can provide us information related to possible new locations of tube well, abandoning of deep tube wells, etc.

A number of queries, single or multiple, can be performed in a WIMS which are needed to set consciousness of saving and cost control, to make decisions on the strength of knowledge and analysis of resource utilization. The following paragraphs discuss some examples of the kinds of information that can be useful to an AM in a local WIMS.

3.2.1 Description of tube well data

From the data collected for tube wells, it can be stated that:

1. Total number of tube wells present in the campus (working or abandoned) are 22. Majorly tube wells are located towards the periphery of the campus. Out of which currently 10 are in the working condition and rest 12 tube wells are abandoned.
2. Initially, most of the tube wells built in the campus were shallow but with time all the shallow tube wells have been replaced by deep tube wells. Currently there are 12 deep tube wells and 10 shallow tube wells (working/abandoned). There is just one shallow working tube well and the others are deep tube wells.
3. The deepest bore dug is more than 400m and the shallowest bore is about is about 150m.
4. Abandoning of deep tube wells is majorly due to malfunctioning of tube well parts, like damaging of hosing pipe, inadequate screen and filter-pack selection or installation, incomplete development, screen corrosion, collapse of filter pack.
5. On the basis of establishment year of tube wells, it was realized the number of tube well currently employed for extraction of water were built after 1999. The average life span of tube wells is about 18 years.

3.2.2 Descriptive analysis on the basis of bore logs

The variation of lithology of soil with depth of drilled bore is defined as a bore log. These bore logs are generated using RockWare’s log plot utility (Rockware, 2007). Individual bore log reports (Gupta, 2014) show how the soil profile varies for a particular bore and area around that bore. The major soil types found in IITK campus are clay, morum, sand (fine to coarse), kankar clay, kankar and sand stone layer. Some layers are a combination of the above types.

Bore log reports also help in deciding the position of blind and slots to be provided in a pipe for a tube well bore. Slots are provided for the aquifer layers (medium to coarse sand, morum, gravel, sand stone layers) and blinds are provided in the non-aquifer layers of the bore (majorly clay layers). These bore logs are an important initial database requirement for performing soil profiling of the campus.

3.2.3 Information retrieved from both tube well and bore log data

There are certain aspects which need derived results using tube well and bore log data. Information related to new possible locations of tube wells require both tube well data for knowing the current locations of working tube wells and bore log data for determining the better choice for building tube wells in future based upon soil profile in respective bore logs.

Reasoning behind abandonment of tube wells, majorly shallow tube wells can be understood by integrating both the available data. The individual bore logs also gives the aquifer layer corresponding to a bore. These aquifer layer were used to study the shift of shallow tube wells to deep tube wells. On studying individual bore log reports, it was found that water in the aquifer layer existing from 100 m - 200 m below surface is almost dried up. It was observed below 200 m, aquifer layer existed deep down at about 320 m and further down. From these aquifer layers water can be extracted. Thus deep tube wells were dug and all the existing shallow tube wells on the verge of abandonment were replaced by deep tube wells.

4. CONCLUSION AND FUTURE RECOMMENDATION

This research concluded with a well-defined format to include most of the possible fields for tube wells. Based upon this format, data collected is utilized in successful development of web enabled WIMS for tube wells of IITK using open source tools. The data collection format forms the basis of creating a well-structured database for tube wells. It would solve the problem of data scarcity and will be helpful in proposing models based upon various attributes described. This WIMS provides user with easy to understand GUI. The secured platform built facilitates user to upload and append the spatial features in the form of vector layers. It gives freedom to perform spatial and non-spatial query for pipelines and tube wells. This platform also provides the facility of exporting and printing of layers and maps in various formats.

Web enabled WIMS built can be further used to develop models for cost estimation and cost comparison between different techniques. This format can be further strengthened by including the cost drivers of tube well development. The bore log information available can be modelled to obtain bore log profiling for the soil of the institute. This will require interpolation of bore log data.

ACKNOWLEDGEMENT

Work reported in this paper is a part of the research work being carried under the Obama-Singh Knowledge Initiative at IIT Kanpur in collaboration with Virginia Tech, USA. The authors are grateful for financial support from the Initiative and to Prof. Sunil Sinha for his inputs.

REFERENCES

Betti, R., 2010. *Buildings and infrastructure protection series: Ageing infrastructure*. US Department of Homeland Security.

Garg, P., Gupta, R., and Arora, M., 2000. *Analysis of Intra-District Disparities using GIS Technique*. 3rd International Conference on GIS/GPS/RS. New Delhi.

GeoNode Manual. Retrieved March 5, 2014, from GeoNode: http://GeoNode.org

GeoServer 2.0 documentation. 2012. Retrieved January 11, 2014, from GeoServer: http://GeoServer.org/display/GEOS/Welcome

Gupta, K., 2014. A web GIS for IITK water infrastructure. M Tech thesis submitted to IIT Kanpur, India

Karlaftis, M., and Peeta, S., 2009. Infrastructure planning, design and management for big events. *Journal of Infrastructure Systems*.

Kulshreshtha, N., 1998. System design and considerations in some geo information systems. M Tech thesis submitted to IIT Kanpur, India

Mukherjee, A., 2013. Archives Retrieved from Waterscapes: http://aditimukherji.wordpress.com/2012/07/13/how-many-wells-and-tubewells-in-india-no-one-really-knows/

Opadeyi, J., 2007. Road map towards effective mainstreaming of GISfor watershed management in the Caribbean. Retrieved January 13, 2014, from http://www.cep.unep.org/events-and-meetings/13th-igm-1/IWCAM-2en.pdf

PostgreSQL: Manuals. 2006. Retrieved January 15, 2014, from http://www.PostgreSQL.org/docs/manuals/

Quantum GIS user guide. Release 1.8. http://docs.qgis.org/1.8/pdf/QGIS-1.8-UserGuide-en.pdf

Rockware, 2007. Logplot user manual. colorado. https://www.rockware.com/assets/products/176/downloads/documentation/7/logplot7_manual.pdf

Singh, N., 2011. India’s water management challenge. Retrieved March 15, 2014, from http://www.eastasiaforum.org/2011/02/08/indias-water-management-challenge

Shear failure behavior of high strength concrete beams with different shrinkage and strength development histories

Koji MATSUMOTO[1], Keisuke OSAKABE[2] and Junichiro NIWA[3]
[1]Assistant Professor, Department of Civil Engineering, Tokyo Institute of Technology, Japan
matsumoto.k.ar@m.titech.ac.jp
[2]Kajima Corporation, Japan
[3]Professor, Department of Civil Engineering, Tokyo Institute of Technology, Japan

ABSTRACT

Utilization of high strength concrete has many advantages such as it can achieve high seismic performance because of the lightweight superstructures by reducing the size of the cross section as well as long span bridges and high rise buildings. In the meanwhile, one of the problems of high strength concrete is its large autogeneous shrinkage. This study focuses on the history of autogeneous shrinkage and strength development which affect the initial stress of high strength concrete beams. The objective is to investigate the effect of the combination of each history on the initial stress and shear failure characteristics of high strength concrete beams. Loading tests of high strength concrete beams, whose strength development history was varied, were conducted. As a result, the initial stress and shear cracking load can be evaluated by the strain of tensile reinforcements just before the loading test even though the autogeneous shrinkage and strength development histories are different. In addition, the structural analysis by using Rigid Body-Spring Model (RBSM) considering each history was carried out. The result of the analysis indicates that the initial stress induced by autogeneous shrinkage and the shear failure characteristics are affected by the combination of history of autogeneous shrinkage and strength development.

Keywords: high strength concrete, autogeneous shrinkage, strength development history, shear failure, RBSM

1. INTRODUCTION

High strength concrete (HSC) enables to reduce cross sectional area and increase span length of concrete bridges. On the other hand, HSC has large autogenous shrinkage in an early age. When HSC is applied to reinforced concrete (RC) structures, the deformation of concrete is restrained by inner reinforcements and measurable shrinkage stress occurs in concrete.

Kawakane & Sato (2009) have experimentally investigated the decrease in diagonal cracking strength of HSC beams without stirrups and proposed the equation for prediction of diagonal cracking strength based on the concept of the equivalent tensile reinforcement ratio which considers the effect of shrinkage. However, they do not consider the effect of history of shrinkage and strength development. The objective of this study is to investigate the effect of the combination of each history on self-induced stress and shear failure behavior of HSC beams. Loading tests of HSC beams with different strength development histories were carried out. Moreover, the discrete analysis was also carried out by using the rigid body-spring model (RBSM) considering shrinkage and strength development histories.

2. LOADING TEST OF HSC BEAMS

2.1 Experimental program

To investigate the effect of the combination of the histories on self-induced stress and shear failure behavior of HSC beams, it is desirable that the values of them at the loading test are same. According to the results of the pilot test, mix proportions of concrete were determined as shown in Table 1. Ordinary Portland cement (*OPC*) was used for OPC specimen, while high-early strength Portland cement (*HPC*) and expanding material (*EX*) were used for HEX specimen. To design all specimens to be failed in shear failure, high strength steel bars were used for the tensile reinforcements.
The outline of the specimens is shown in Figure 1. Casting and curing of concrete were carried out in the environmental chamber with a constant temperature and relative humidity of 20 degree Celsius and 60%, respectively. Sealed curing was continued just after the casting of concrete until the loading test.
Before the loading test, autogenous shrinkage of concrete and strains of tensile reinforcements were measured just after the casting of concrete until the loading test. Furthermore, compressive strength and elastic modulus of concrete were measured at the age of 0.5, 0.67, 0.83, 1, 5, 7, 14, 21 and 28 days to obtain the strength development history from the early age. Free strain and temperature of concrete were measured by the embedded gauge placed at the center of the prism specimen with 10x10x40 cm. The shrinkage strain of concrete was determined by subtracting thermal strain, which was

Table 1: Mix proportions of concrete

Name	Type of cement	G_{max} (mm)	*W*/*B* (%)	*s*/*a* (%)	Unit weight (kg/m^3)						
					W	*C*	*SF*	*S*	*G*	*EX*	*SP*
OPC	*OPC*	20	23	45	155	607	67	701	866	0	9.4
HEX	*HPC*	20	23	45	155	597	67	701	866	10	10.8

B: binder (=*C*+*SF*+*EX*), *s*/*a*: sand percentage, *SF*: silica fume, *EX*: expanding material, *SP*: superplasticizer

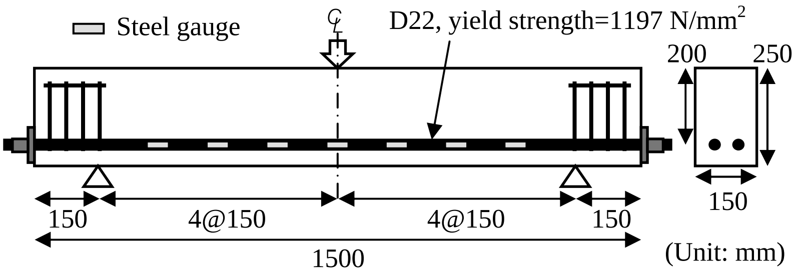

Figure 1: Outline of the specimen

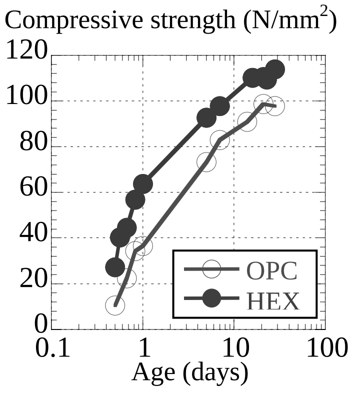

Figure 2: Compressive strength history

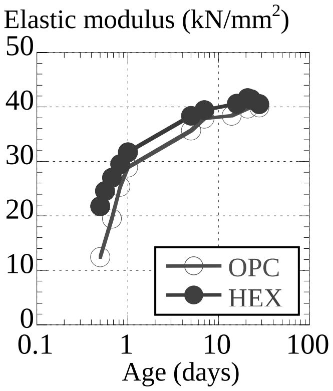

Figure 3: Elastic modulus history

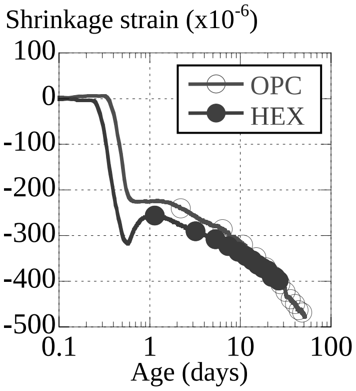

Figure 4: Shrinkage strain history

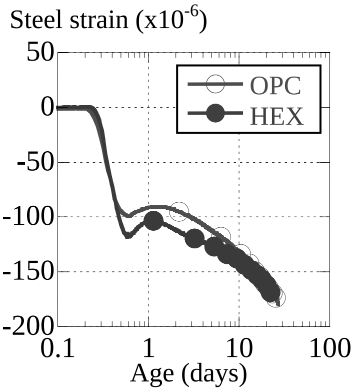

Figure 5: Steel strain history

calculated by multiplying the coefficient of thermal expansion of concrete (=10x10^{-6}/°C) to the temperature of concrete, from the measured strain.

At the loading test, mid-span and support displacements were measured by using displacement transducers and the strains in tensile reinforcements were measured by strain gauges. Three-point bending tests were conducted. Teflon sheets were inserted between the specimen and the supports to prevent the horizontal friction.

2.2 Strength development and shrinkage histories

Figures 2 and 3 show compressive strength development history and elastic modulus development history, respectively. In HEX specimen, compressive strength and elastic modulus developed earlier than OPC specimens. The difference was large in the early age and decreased with the age. As for the elastic modulus, more than 50% value at the loading test already developed at 1 day regardless of the type of concrete.

Figure 4 shows shrinkage strain history. Shrinkage strain is defined as negative value, while expansion strain is defined as positive value. In all cases, the large part of shrinkage already developed before 1 day and then gradually developed. Comparing HEX to OPC, the large shrinkage caused by high-early strength Portland cement was reduced by expanding material.

Steel strain history measured by strain gauges at the mid-span is shown in Figure 5. Compressive strain is defined as negative value, while tensile strain is defined as positive value. Nearly uniform strain distribution along the longitudinal direction of tensile reinforcements was observed in all specimens. From the comparison between OPC and HEX, the histories of them were almost same, thereby the effect of the difference of strength development history due to the cement type on steel strain was slight.

2.3 Results of the loading test

Mechanical properties of concrete at the loading test, results of the shrinkage test and the loading test are shown in Table 2. Load-displacement relationships are shown in Figure 6. At the diagonal cracking, the load clearly dropped in all cases.

To calculate the diagonal cracking load (P_c=2V_c), Eq. (1) proposed by Kawakane & Sato (2009) was used. The equation is based on the concept of the equivalent tensile reinforcement ratio and takes into account the effect of shrinkage.

$$V_c = 0.11\, E_c^{2/5}\, f_t^{1/5}\, (100p_{w,e})^{1/3}\, d^{-2/5}\, (0.75+1.4/(a/d))\, bd \qquad (1)$$

Table 2: Mechanical properties of concrete and results of the experiment

Name	Test age (day)	E_c (kN/mm^2)	f_c'	f_t	ε_{sh}	ε_s	P_c	P_{c_cal}	P_c / P_{c_cal}	$P_{\max}$ (kN)	Failure mode
			(N/mm^2)		(x10^{-6})		(kN)				
OPC	28	39.9	97.8	4.5	-407	-180	121.7	112.0	1.09	121.7	Diagonal tension
HEX	23	41.4	109.5	4.5	-390	-171	124.8	114.3	1.04	160.2	Shear compression

E_c: elastic modulus, f_c': compressive strength, f_t: tensile strength, ε_{sh}: autogenous shrinkage (+: expansion, –: shrinkage), ε_s: steel strain (+: tension, –: compression), P_c: diagonal cracking load, P_{c_cal}: calculated value of P_c, $P_{\max}$: the maximum load

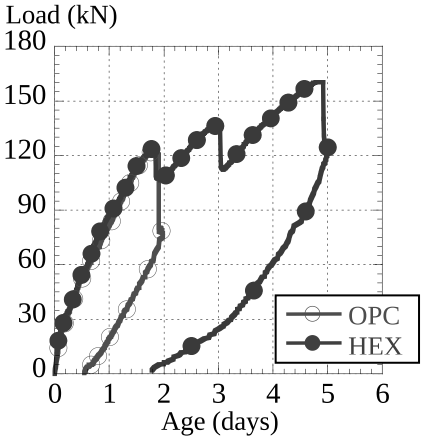

Figure 6: Load-disp. relationship

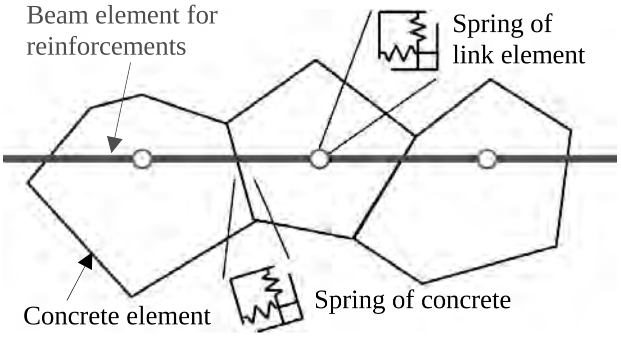

Figure 7: Outline of RBSM

where, E_c is the elastic modulus (N/mm^2), f_t is the tensile strength (N/mm^2), $p_{w,e}$ is the equivalent tensile reinforcement ratio, d is the effective depth (mm), a is the shear span (mm) and b is the web width (mm).

There was slight difference in experimental results of the diagonal cracking load as shown in Table 2. Comparing between OPC and HEX, the diagonal cracking loads of them were also almost same in spite of different strength development history.

The range of the ratio of experimental result and calculated result was from 1.04 to 1.10. Therefore, even if HSC beams have different amount of autogenous shrinkage and different strength development history, diagonal cracking load is able to be evaluated by using the steel strain caused by shrinkage within the range of this study.

3. NUMERICAL ANALYSIS

3.1 Methodology

Rigid Body-Spring Model (RBSM) (Saito & Hikosaka, 1999), which is one of the discrete analysis methods, was used. In RBSM, since cracks initiate and propagate along boundaries between elements, mesh arrangement affects the crack pattern.

To avoid such a problem, a random geometry was introduced using the Voronoi diagram. Concrete is modeled as the assemblage of rigid particles. Each element has two transitional and one rotational degree of freedom at the gravity point. The interface between two elements consists of normal and shear springs at the midpoint of the face with the stiffness k_n and k_s, respectively. As for reinforcements, discrete reinforcement model was used. Reinforcements are represented by a series of regular beam elements. The beam nodes are attached to the concrete elements through zero-length link elements.

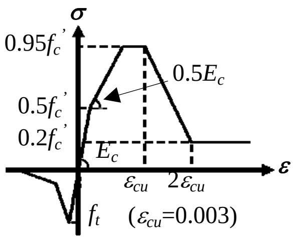

Figure 8: Tension and compression model of concrete

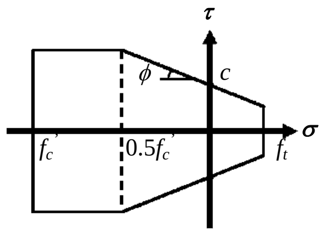

Figure 9: Mohr-Coulomb type criterion

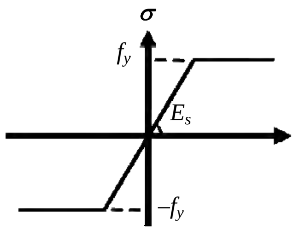

Figure 10: Reinforcement model

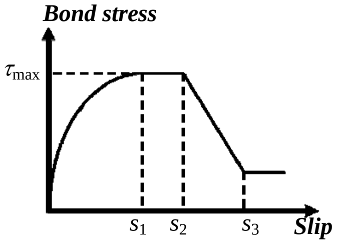

Figure 11: Bond stress-slip relationship

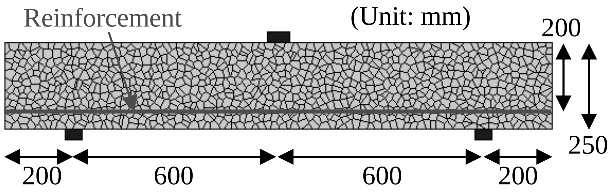

Figure 12: Analytical model

The link element consists of tangential and normal spring. Bond behavior between concrete and reinforcement is modeled using tangential spring. The outline of RBSM used in this study is illustrated in Figure 7.

3.2 Material models

Poly-linear model was used for compressive behavior and 1/4 model considering tension softening was used for tensile behavior as shown in Figure 8. The fracture energy of concrete was obtained so that the flexural strength of bending analysis of plain concrete corresponds to the experimental result of high strength concrete.

The shear strength was assumed to follow the Mohr-Coulomb type criterion as shown in Figure 9. After the shear stress reaches the yield strength, the stress moves on the yield surface until the shear strain reaches the ultimate shear strain (γ_u=4000x10^{-6}). For cracked interfaces, a softening branch was introduced after the shear stress reaches the yield strength. Moreover, the shear transferring capacity at the cracked interface changes according to crack opening. In order to take into account this effect, the shear stiffness is reduced by reduction factor (β) which is a function of normal strain.

The stress-strain relationship of reinforcements was idealized as a bilinear model as shown in Figure 10. The unloading and reloading paths follow the initial stiffness.

The bond stress-slip relationship for conventional reinforcements was modeled as shown in Figure 11 following CEB-FIP model code (1990). For the parameters in Figure 11, the values for confined concrete with good bond condition are used. The normal spring is treated as an elastic spring having elastic modulus of concrete.

3.3 Analytical model

Figure 12 shows analytical model used in this study. The average size of concrete element is 20 mm, taking into account the maximum size of coarse aggregate. To avoid the effect of mesh arrangement, the same mesh is used for all analytical cases.

Three analytical series were carried out. Series 1 is the analysis without considering the shrinkage. In series 2, autogenous shrinkage is introduced under the constant material

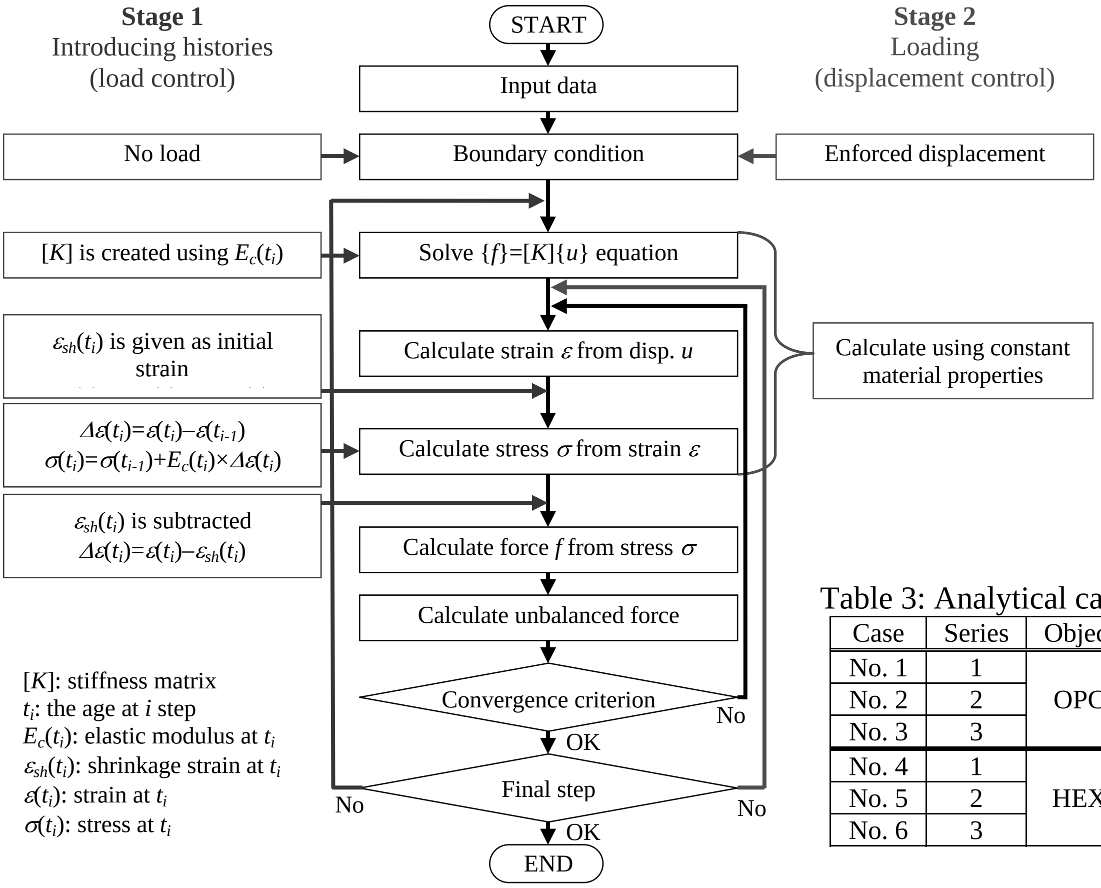
Stage 1
Introducing histories
(load control)
START
Stage 2
Loading
(displacement control)
Input data
No load
Boundary condition
Enforced displacement
[K] is created using $E_c(t_i)$
Solve $\{f\}=[K]\{u\}$ equation
$\varepsilon_{sh}(t_i)$ is given as initial strain
Calculate strain ε from disp. u
Calculate using constant material properties
$\Delta\varepsilon(t_i)=\varepsilon(t_i)-\varepsilon(t_{i-1})$
$\sigma(t_i)=\sigma(t_{i-1})+E_c(t_i)\times\Delta\varepsilon(t_i)$
Calculate stress σ from strain ε
$\varepsilon_{sh}(t_i)$ is subtracted
$\Delta\varepsilon(t_i)=\varepsilon(t_i)-\varepsilon_{sh}(t_i)$
Calculate force f from stress σ
Calculate unbalanced force
[K]: stiffness matrix
t_i: the age at i step
$E_c(t_i)$: elastic modulus at t_i
$\varepsilon_{sh}(t_i)$: shrinkage strain at t_i
$\varepsilon(t_i)$: strain at t_i
$\sigma(t_i)$: stress at t_i
Convergence criterion
No
OK
Final step
No
No
OK
END

Figure 13: Flowchart of the analysis in series 3

Table 3: Analytical cases

Case	Series	Object
No. 1	1	OPC
No. 2	2	
No. 3	3	
No. 4	1	HEX
No. 5	2	
No. 6	3	

properties (the effect of histories are not considered). Series 3 is the analysis considering shrinkage and strength development histories. Figure 13 shows a flowchart of the analysis in series 3. The developments of shrinkage and each material property such as compressive strength, tensile strength and elastic modulus are given in each time step (t_i) in the analysis. The analytical cases are shown in Table 3.

3.4 Introduction of the histories

The experimental results of each history shown in Figures 2 to 4 are used as input data. Since there is no data before 0.5 day, assuming the age when the strength begins to develop is the age when autogenous shrinkage begins to develop, the data before 0.5 day is linearly interpolated as well. The autogenous shrinkage strain is given to only normal spring of all concrete elements as initial strain.

3.5 Analytical results

3.5.1 Self-induced stress

As an example of the analytical results, the self-induced stress distribution of concrete in the case No. 6 is shown in Figure 14. It is found that the tensile stress occurred in the lower part of the beam because the reinforcement is provided. Consequently, the compressive strain occurs in the reinforcement in the analysis considering shrinkage as well as the results of the experiments. The experimental and analytical results of steel strain are shown in Figure 15. Both values are the strains measured and calculated at the mid-span, respectively.

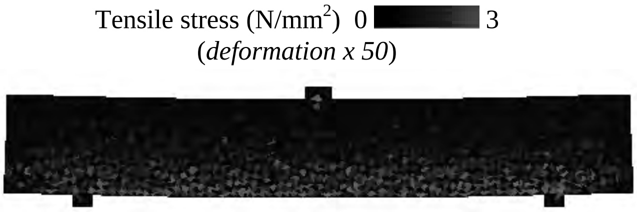

Figure 14: Self-induced stress distribution (No. 6)

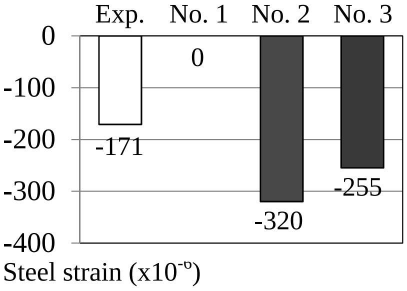

Figure 15: Steel strain caused by shrinkage

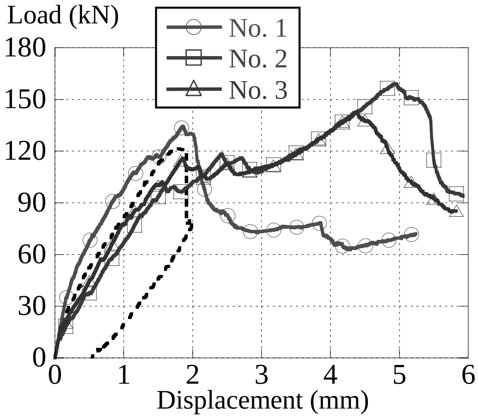

Figure 16: Load-displacement relationship (OPC)

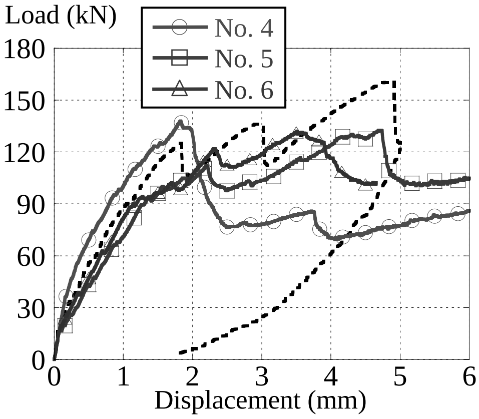

Figure 17: Load-displacement relationship (HEX)

The steel strains in the series 1 are naturally zero due to no consideration of shrinkage. The results of series 2 significantly overestimate those of experiments. This is because shrinkage is introduced under the constant material properties in series 2. On the other hand, the results of series 3 are closer to those of experiments since series 3 considers the shrinkage and strength development histories. The phenomenon that the shrinkage occurs in concrete during the material strength development can be more appropriately simulated in the series 3 by introducing the histories.

3.5.2 Load-displacement relationship

Load-displacement relationships of OPC and HEX are shown in Figures 16 and 17, respectively. Since series 2 and series 3 consider the shrinkage, flexural cracking load decreased compared to series 1. In OPC and HEX, the member stiffness of series 3 (No. 3 and No. 6) near the flexural cracking is quite close to the experimental results.

The diagonal cracking loads obtained by the experiments and analyses are compared in Figure 18. The range of the ratio of the analytical result to the experimental result in series 1 is from 1.10 to 1.12, thereby series 1 overestimates the analytical result. In series 2 and series 3, the diagonal cracking load decreased due to the effect of shrinkage. In series 2 having excessive shrinkage effect, the range is from 0.80 to 0.90, thereby series 2 underestimates the analytical result. However, the range in series 3 is from 0.93 to 0.98. The reduction of diagonal cracking road due to shrinkage can be simulated by introducing the histories to the analysis.

3.5.3 The effect of shrinkage on shear failure behavior

The stress distributions with deformation of No. 4 and No. 6 at the same load (100 kN) are shown in Figure 19. Compared to series 1, the deformation of series 3 was larger

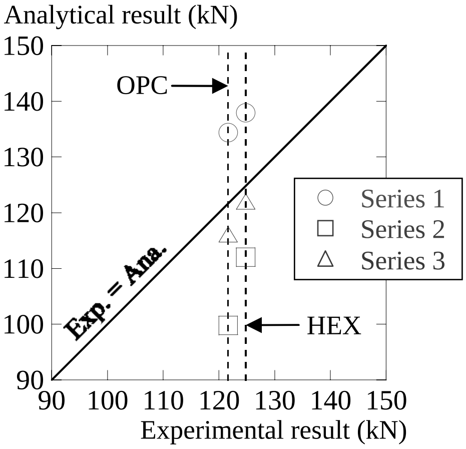

Figure 18: Diagonal cracking load

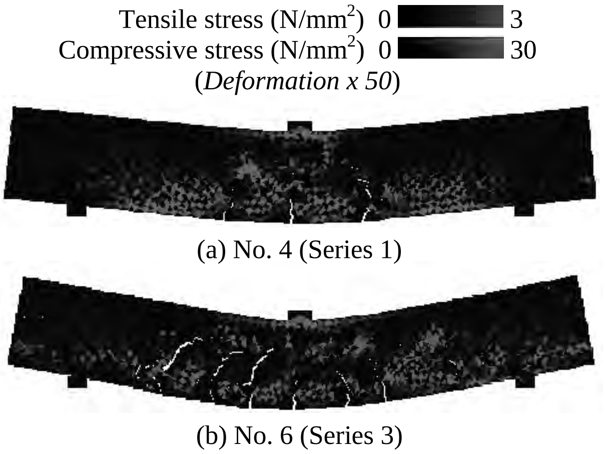
Tensile stress (N/mm^2) 0 3
Compressive stress (N/mm^2) 0 30
(*Deformation x 50*)

(a) No. 4 (Series 1)

(b) No. 6 (Series 3)

Figure 19: Stress distribution at 100 kN of load

due to the effect of shrinkage in spite of the same load. In addition, a greater number of flexural cracks with wider opening occurred and they propagated deeply towards the upper part of the beam. This result corresponds to the indication of the previous research (Kawakane & Sato, 2009). Thus, the effect of shrinkage on the shear failure mechanism can be simulated by the analysis considering the histories.

4. CONCLUSIONS

1) Even though high strength concrete have different strength development history, the diagonal cracking load can be evaluated using the steel strain caused by shrinkage.
2) The RBSM analysis result revealed that histories of autogenous shrinkage and strength development are necessary to be considered to simulate self-induced stresses.
3) The effect of shrinkage on shear failure mechanism of high strength concrete beams, such as the increase in the number and width of flexural crack and deeper crack propagation, can be analytically verified by the method developed in this study.

REFERENCES

Comite Euro-International du Beton, 1990. CEB-FIP Model Code 1990 First Draft.

Ito, H., Maruyama, I., Tanimura, M., and Sato, R., 2004. Early age deformation and resultant induced stress in expansive high strength concrete. *Journal of Advanced Concrete Technology*, 2(2), 155-174.

Kawakane, H., and Sato, R., 2009. Evaluation of shrinkage effect on diagonal cracking strength of reinforced HSC beams, *Journal of Materials, Concrete Structures and Pavements, JSCE*, 65(2), 178-197. (in Japanese)

Saito, S., and Hikosaka, H., 1999. Numerical analyses of reinforced concrete structures using spring network models. *Journal of Materials, Concrete Structures and Pavements, JSCE*, 627, V-44, 289-303.

Exposure test results for underground structures damaged by ASR

Tetsuya KOHNO[1], T. NANAZAWA[2], S. NAKATANI[3]
[1]Researcher Public Works Research Institute (PWRI), Center for Advanced Engineering Structures Assessment and Research (CAESAR), Japan
[2]Chief Researcher, PWRI, CAESAR, Japan
[3]Director, PWRI, Geology and Geotechnical Engineering Research Group, Japan

ABSTRACT

Recently, underground structures, for example footings and columns, which have degenerated due to Alkali Silica Reaction (ASR) have been discovered in Japan. In order to perform appropriate diagnosis of these structures, it is necessary to acquire a large amount of knowledge regarding underground structure degeneration caused by ASR, such as the conditions under which ASR occurs in underground structures, and the internal degradation conditions. For this reason, road administrators are unable to perform sufficient maintenance, and this constitutes a serious problem with respect to safe operation of the road network. Hence, in order to obtain the relevant knowledge, a long term exposure test has been performed under actual conditions, up to the present time, and the cracks and strain in the footings and temperature and water level in the exposure environment have been measured. In addition, we have analyzed the differences in the degradation of footings caused by the environment with respect to the water, air and underground conditions, and used the measured data to examine the reasons for these differences.

Keywords: underground structure, alkali silica reaction, exposure test, strain, crack.

1. INTRODUCTION

Recently, underground structures damaged by ASR have been reported. Some have been seriously damaged, such as the steel being fractured. Since they are underground, these structures are not generally visible. Hence, not much is known about footings damaged by ASR. Nothing is known about how ASR progresses in underground structures, or how it results in a decrease in load carrying capacity. Therefore, we conducted an exposure test in order to acquire relevant knowledge regarding footings damaged by ASR. This test was conducted under actual conditions over a long period, i.e. 6 years. We evaluated the extent of the damage occurring in the underground structures by measuring strain.

2. EXPOSURE TEST DIAGRAMS

The factors affecting damage by ASR are temperature, water and amount of reinforcing steel. Therefore, the exposure environment, scale and arrangement of the reinforcement were determined in consideration of these factors.

Figure 1 shows the details of the model. It is expected that structures damaged by ASR are those constructed before 1980. Hence, the models were designed with reference to the footings used at the time. The reinforcement used in the models was SD 295A, the ratio for the tensile reinforcement was 0.20%, and that for the compressive reinforcement was 0.05%.

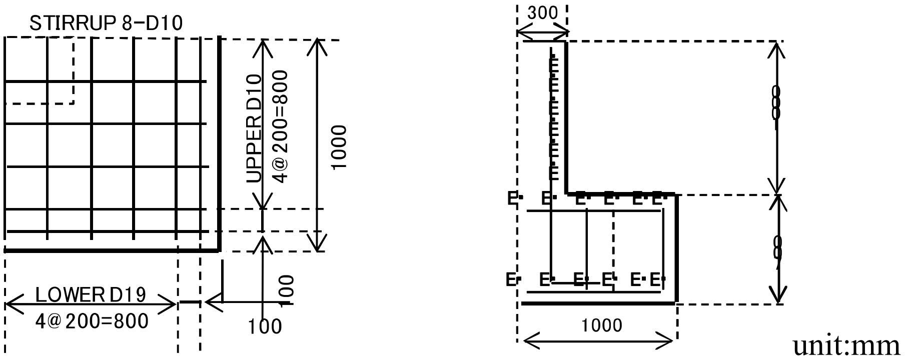

Figure 1: Drawing showing dimensions and bar arrangement of footing models (For Cases 1 and 2. Left: plane section for footing, Right: vertical section)

Three test models were used. They consisted of a pier and footing. The sizes of the footings were the same, the width and length being 2.0m and the height 0.7m. The width and length of the pier were 0.6m. The height of the pier was 1.0m in Cases 1 and 2, and 2.6m in Case 3. The cement used was ordinary Portland cement. The design strength of the concrete was 21N/mm2. The ratio of alkali reactive aggregate to non-reactive aggregate was 50:50 for the coarse aggregate, and 40:60 for the fine aggregate.

Table 1 shows the exposure test cases, and Figure-2 shows a photograph of the exposure test conditions. The test models for Cases 1 and 2 were exposed in water, and that for Case 3 was exposed underground. The groundwater level in Case 3 was around the footing, and the water level in Case 1 was changed based on the groundwater level in Case 3. The water level in Case 2 did not change. The cracks and strain in the concrete surface and reinforcement were measured.

Table 1: Exposure test cases for footing models

Case	**Exposure environment**
1	In the cistern. The water level changed between 3 levels (above the surface of the footing, halfway up the footing and around 5 cm above the bottom of the footing)
2	In the cistern. The water level did not change (was always above the surface of the footing)
3	In the ground

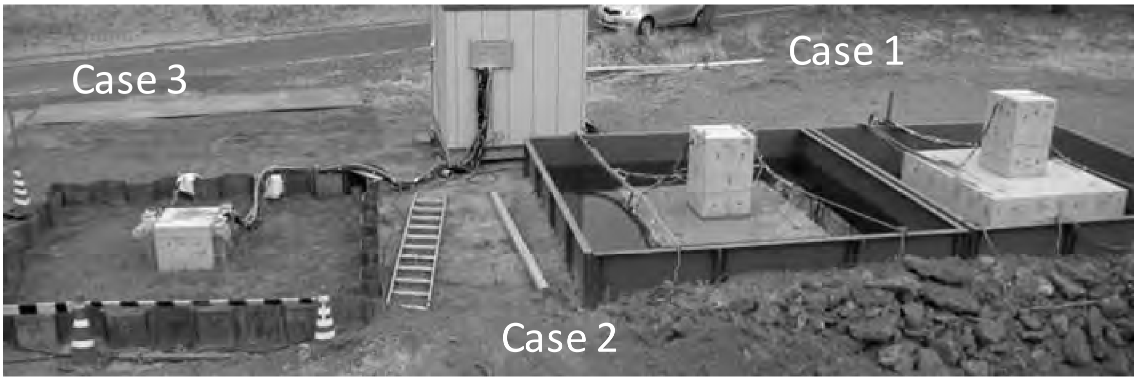

Figure 2: Photograph showing exposure test conditions

3. EXPOSURE TEST RESULTS

Figure 3 shows the variation of the groundwater level over time, and the temperature and strain in the reinforcement of the column in Case 3. Strain and temperature were measured at the same point. The groundwater level was below the bottom of the footing. The amount of reinforcement of the column does not vary with depth. Therefore, environmental conditions constitute the only reason for differences in the strain at each point.

The variation of temperature over time shows that the closer the point of measurement to the ground surface, the higher was the maximum temperature, and the lower was the minimum temperature.

The trend toward increasing strain differs depending on depth. The strain measured at GL. + 300, which is the point at which the highest temperature was measured, had reached 2000μ after around 760 days.

Conversely, the deeper the point at which the strain was measured, the later the onset of strain increase. For example, the strain measured at GL. -300 increased 1 year and 3 months after the exposure test began, and that at GL. -1200 increased at 1 year and 6 months. In addition, the deeper the point of measurement, the smaller was the increase in speed. Furthermore, the strain at GL. +300 did not increase in winter, during which the temperature became lower than 10 degrees. Conversely, at GL. -1200, the increase in speed was similar regardless of season. At this point, the temperature was close to exceeding 10 degrees. From these results, it can be seen that the trend toward increasing strain is dependent on temperature. The strain at GL-1200 decreased at 5 years and 6 months. It is thought to be due to occurring large crack on the concrete of this point.

Figure 4 shows the strain and temperature values measured in the upper steel of the footings. The temperatures measured in Cases 1 and 2 were almost the same. In contrast, the temperatures measured in Case 3 were different from those in Cases 1 and 2, both the maximum and minimum temperatures in Case 3 being lower. These results are similar to those shown in Figure 3.

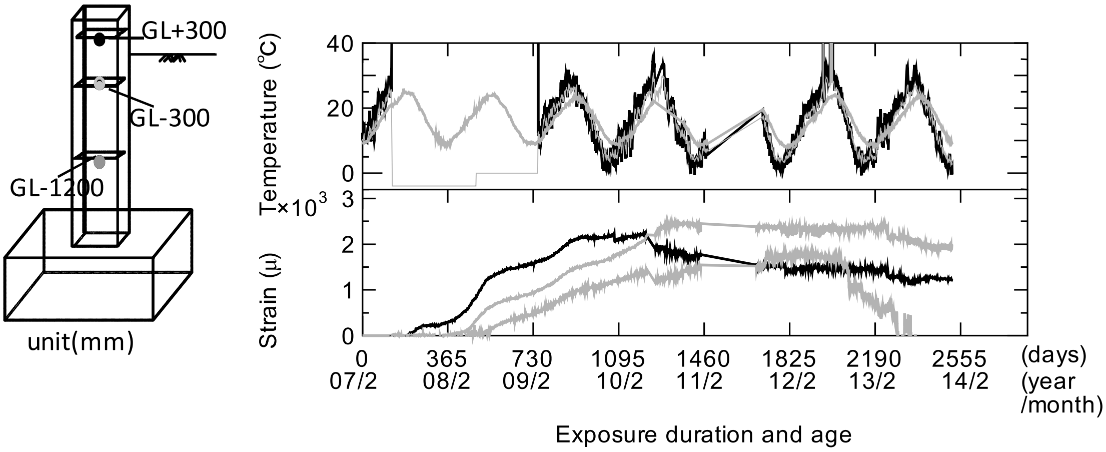

(a) Measurement points

(b) Measurement results

Figure 3: Time variation of steel strain and temperature in column

The strain results for the exposure tests show that strain values increased in all cases. However, these cases show differences in the trends that they exhibit. The strain value in Cases 1 and 2 started increasing at around 180 days. In contrast, the strain value in Case 3 started increasing at around 560 days. In addition, the speed of increase in Case 3 was similar regardless of season, but that in Cases 1 and 2 was larger in the summer when the temperature was high, and smaller in the winter when the temperature was low.

The strain values in Cases 1 and 2 converged 9 months after commencement of the exposure test. In contrast, those in Case 3 had still not converged after 2 years. However, after 4 years, the strain values in Case 3 became higher than those in Case 2. From this result, it can be concluded that the strain resulting from exposure at low temperature increases more slowly but reaches a higher final value than that resulting from exposure at high temperature.

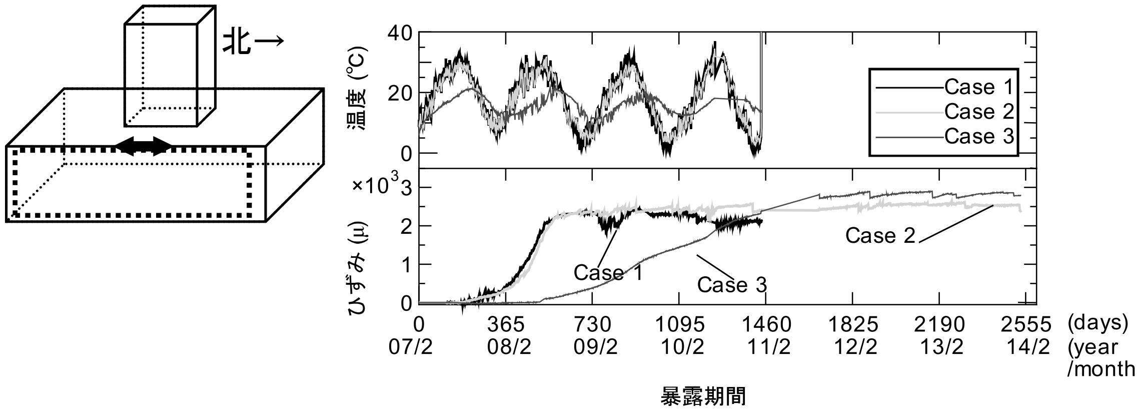

(a) Measurement points

(b) Measurement results

Figure 4: Time variation of steel strain and temperature in footings

4. CONCLUSION

We conducted an exposure test on underground structures. This was conducted in the field, over a long period. From this test, we acquired knowledge regarding ASR in underground structures, the results determining the relationship between the strain in the steel due to ASR and temperature.

Punching shear of RC elements with recycled glass as fine aggregates

Kiang Hwee TAN
Professor, Department of Civil and Environmental Engineering,
National University of Singapore, Singapore
tankh@nus.edu.sg

ABSTRACT

To address the issue of sustainability of concrete as a construction material, waste glass particles have been considered as a possible substitute for sand as fine aggregates. Previous works have indicated that use of glass particles did not cause any adverse effect on the properties of concrete at the freshly mixed state and hardened state. Durability properties were also found to be comparable or even better than concrete with natural sand as fine aggregates. Further tests revealed similar flexural and shear characteristics of beams made with waste glass or natural sand or a combination of both as fine aggregates. This paper reports the punching shear characteristics of reinforced concrete elements with waste glass as fine aggregates. Fifteen square slabs, each measuring 700 mm in side dimension and 90 mm in thickness, were supported on four sides with an effective span of 600 mm, and tested to failure under a concentrated load over a square area of side 100 mm at the center. The test parameters were concrete strength, reinforcing steel ratio, and glass-to-fine aggregate ratio. Test results indicated similar punching shear characteristics in terms of ultimate load, deflection and cracking, regardless of the percentage of glass particles as fine aggregates.

Keywords: fine aggregates, punching shear, recycled glass, reinforced concrete, sustainability.

1. INTRODUCTION

Concrete is the second most used commodity after water. It is mixed using cement, water, sand (that is, fine aggregates) and gravel (that is, coarse aggregates). The manufacture of cement results in 0.8 to 1.0 ton of CO_2 being released into the atmosphere for every ton of production, while the harvesting of sand and gravel results in deforestation and ecological damage.

Towards the sustainability of concrete as a construction material, waste glass particles have been considered as a possible substitute for sand as fine aggregates. Previous works indicated that use of glass particles did not cause any adverse effect on the properties of concrete, both at the freshly mixed state and hardened state (Tan and Du, 2013; Du and Tan, 2013, 2014). Durability properties were also found to be comparable or even better than concrete with natural sand as fine aggregates. Additionally, tests revealed similar flexural and shear characteristics of beams made with waste glass or natural sand or a combination of both as fine aggregates (Tan, 2013).

This paper reports further structural performance in terms of punching shear characteristics of reinforced concrete elements with waste glass as fine aggregates. Slabs were tested to failure under a concentrated load at the center, and the punching shear strength, and deflection and cracking characteristics are discussed herein.

2. TEST PROGRAM

2.1 Test Specimens

Fifteen square slabs as shown in Table 1, were fabricated. Each slab measured 700 mm in side dimension and 90 mm in thickness. The slabs were grouped according to the target concrete cylinder compressive strength f_c’ ((30, 45 and 60 MPa) and reinforcing steel ratio ρ_l (0.8, 1.5 and 2.0%). Each group had three specimens with glass-to-fine aggregate ratio *g*/*fa* equal to 0, 50 and 100%.

Table 1: Test specimens and parameters

Slab Designation	**f_c’ (MPa)**	**ρ_l (%)**	***g*/*fa* (%)**
30M-01	30	1.5	0
30M-02			50
30M-03			100
45L-01	45	0.8	0
45L-02			50
45L-03			100
45M-01	45	1.5	0
45M-02			50
45M-03			100
45H-01	45	2.0	0
45H-02			50
45H-03			100
60M-01	60	1.5	0
60M-02			50
60M-03			100

2.2 Materials

2.2.1 Steel reinforcement

The steel reinforcement in each specimen consisted of 13 mm diameter bars placed at a spacing of 200, 150 or 75 mm in orthogonal directions as shown in Figure 1. The bars were placed at an average effective depth of 68 mm, giving an average reinforcing steel ratio of 0.8%, 1.5% and 2.0% respectively. The bars had an elastic modulus of 193 GPa, yield strength of 480 MPa, yield strain of 0.0027, and ultimate tensile strength of 586 MPa, based on the average test results of three bar samples.

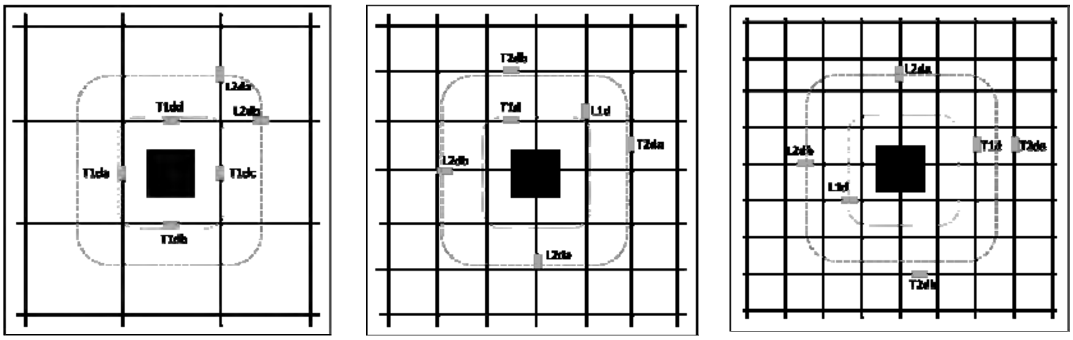

(a) ρ_l = 0.8% (grid spacing = 200 mm)

(b) ρ_l = 1.5% (grid spacing = 100 mm)

(c) ρ_l = 2.0% (grid spacing = 75 mm)

Figure 1: Reinforcement layout and instrumentation of strain guages

2.2.2 Concrete mixture

The concrete mixtures were designed according to ACI211.1 (1992) and the mixture proportions are shown in Table 2. They were designated C30, C45 and C60, with target cylinder compressive strength of 30, 45 and 60 MPa, respectively. Ordinary Portland cement was used. For each mixture proportion, natural sand and waste glass particles in three different combinations, that is, 100/0, 50/50 and 0/100 percent by mass, as fine aggregates. The waste glass particles consisted of brown and green glass in equal proportions.

The waste glass particles were obtained by separately crushing green and brown glass bottles, originally used as beer bottles, using a jaw crusher to meet the specifications of ASTM C33 (2003) for fine aggregates with a maximum of 4.75 mm. The coarse aggregates had a maximum size of 10 mm. All concrete mixtures were designed with 100 mm nominal slump, using a superplasticizer.

Table 2: Concrete mixture design

Mixture	**Content, kg/m^3**				***w*/*c***	***fa*/*c***
	Water (*w*)	**Cement (*c*)**	**Coarse Aggregate (*ca*)**	**Fine Aggregate (*fa*)**		
C30	185	378	1048	741	0.49	1.96
C45	185	487	1048	649	0.38	1.33
C60	185	578	1048	572	0.32	0.99

2.3 Fabrication of test specimens

The slabs were cast in wooden molds in batches each with six accompanying cubes for the determination of concrete cube compressive strength at the time of slab testing. The cylinder compressive strength was taken as 0.8 times the cube compressive strength. A super plasticizer was added to ensure workability. Compaction of concrete was carried out using a vibrator. The slab and cube specimens were removed from the molds after 24 hours, and then placed under wet gunny sacks for ten days and subsequently left in the laboratory under ambient conditions until the day of testing, typically 28 days after casting.

2.4 Test instrumentation and test set-up

The slabs were simply-supported on four edges with an effective span of 600 mm in both directions and subjected to a concentrated load over a square area of side 100 mm at the center. Prior to casting of the slab, electrical resistance strain gauges were installed on the reinforcing bars at distances *d* and 2*d*, where *d* is the effective depth, from the loading face, as shown in Figure 1. Linear variable displacement transducers were also used to monitor the deflection of the slab. The test set-up is shown in Figure 2.

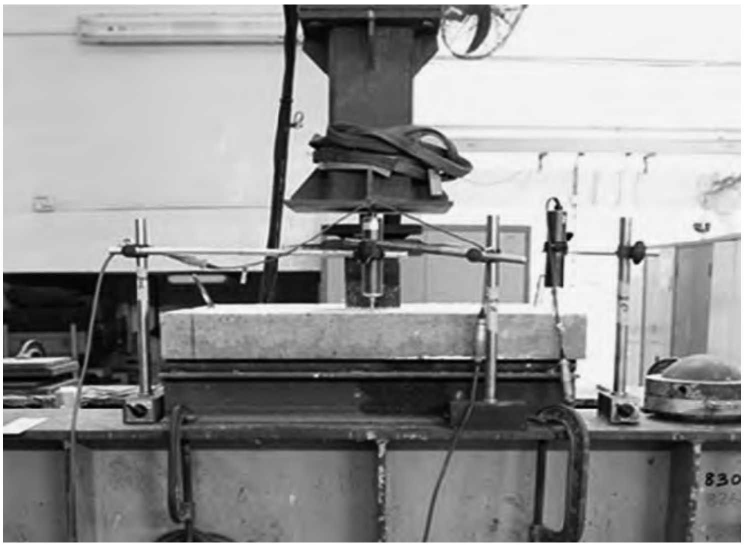

Figure 2: Test set-up

3. TEST RESULTS AND DISCUSSION

3.1 Load-deflection characteristics

The central deflections of the slabs are shown in Figure 3. The deflection initially increased linearly with the increase in applied load. For slabs with low reinforcing steel ratio ρ_l of 0.8% (Group 45L), the load-deflection curves showed a drop in slab stiffness indicating the occurrence of cracks. For other slabs, the deflection continued to increase almost linearly with the applied load up to failure.

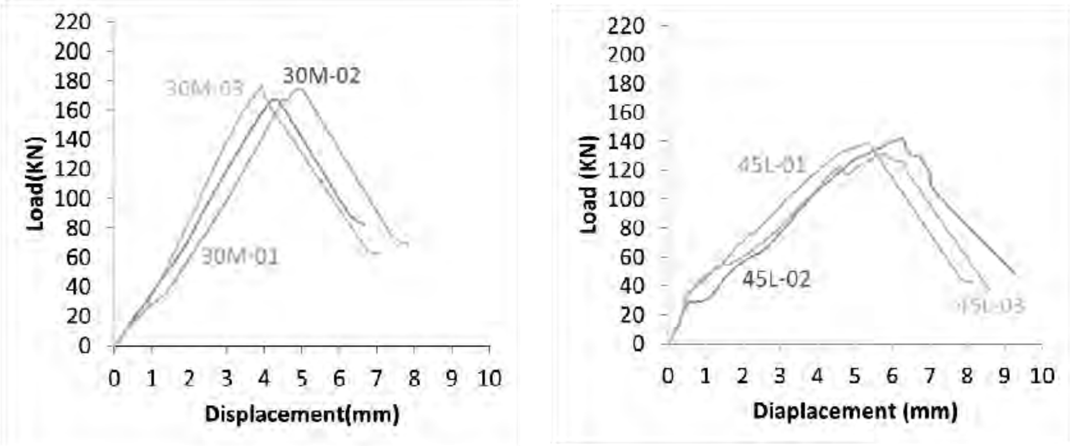

(a) Group 30M (d) Group 45L

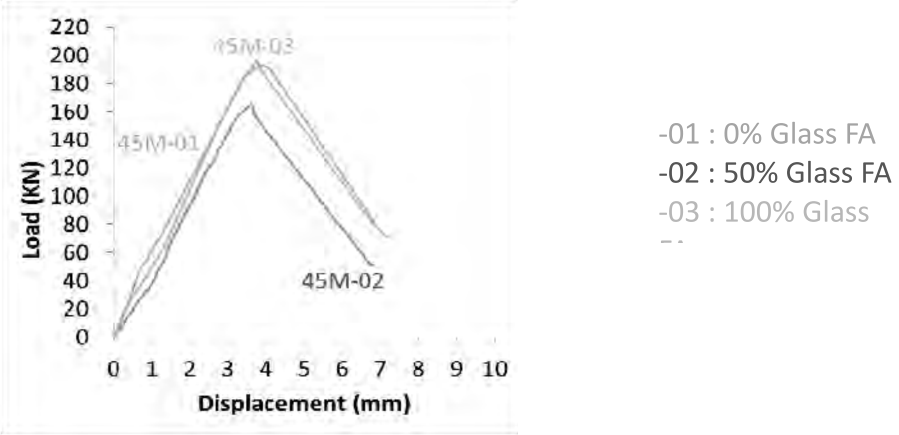

(b) Group 45M

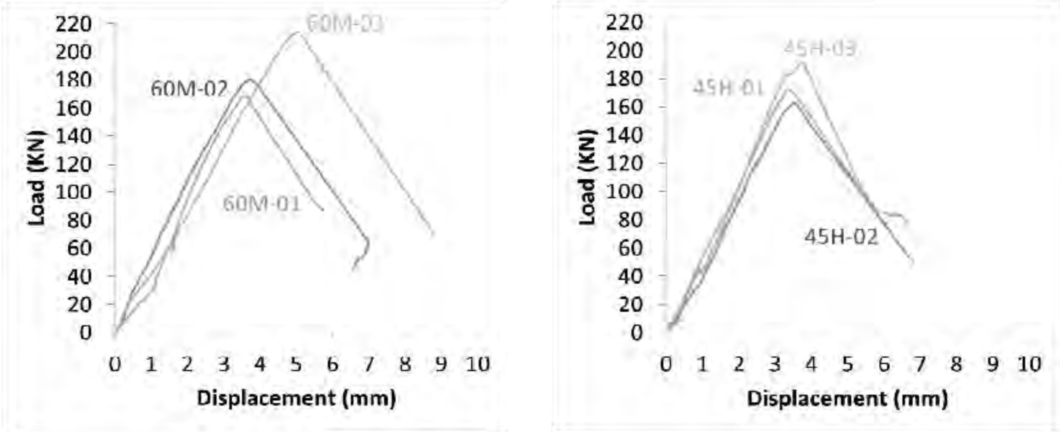

(c) Group 60M (e) Group 45H

Figure 3: Load-deflection characteristics of test slabs

The applied load dropped drastically upon reaching the maximum value, indicating a brittle mode of failure. Despite the different composition of fine aggregates, the load-deflection characteristics were almost identical up to failure for each group of slabs.

3.2 Steel strains

The development of steel strains are shown in Figure 4.

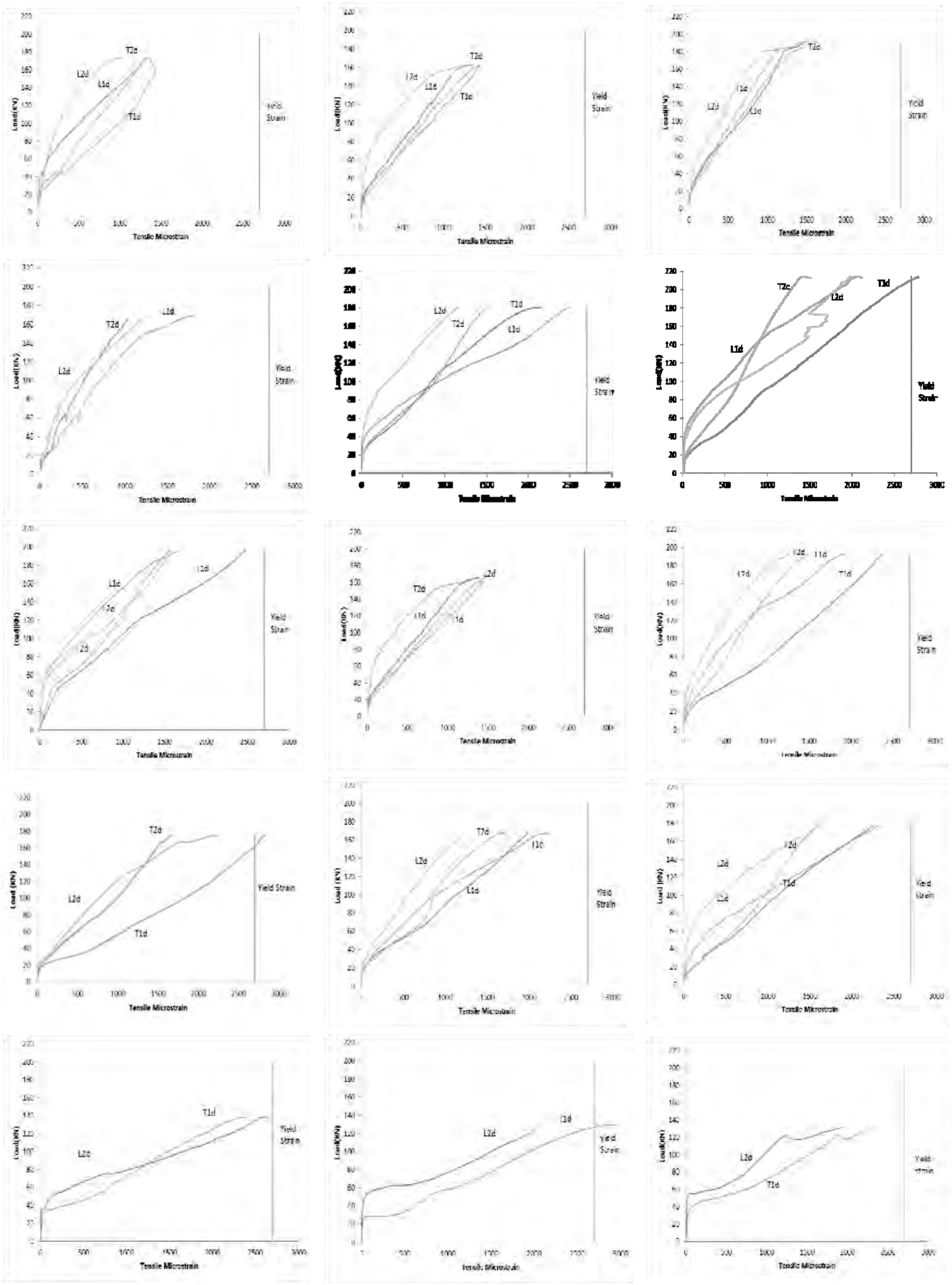

Figure 4: Load-steel strain relations (left to right: g/fa = 0, 50, 100%; bottom to top: Series 45L, 30M, 45M, 60M, 45H)

In general, the strains were higher at location *d* near the loading face, and lesser at location 2*d* further away. Also, the transverse steel strains were higher than the longitudinal steel strains at the same location.

The steel reinforcement did not yield in most of the specimens. However, for slabs with lower concrete strength (Group 30M) and lower reinforcing steel ratio (Group 45L), the steel reinforcement were near to or exceeded the yield strain of 0.0027 at failure. That is, the higher the concrete strength or reinforcing steel ratio of the slab, the lesser was the strain developed in the reinforcement.

The development of steel strains was similar in each group of slabs, that is, irrespective of the proportion of waste glass particles.

3.3 Cracking pattern

The crack patterns at the bottom face of the slab elements after they have been tested to failure are shown in Figure 5. Cracks were observed to radiate from the loading area to the edges of the slabs. The number of cracks was relatively less in slabs with smaller reinforcing steel ratio (that is, Group 45L slabs). The crack widths were larger in this group of slabs compared to other groups.

Also, the crack intensity appeared to be smaller in slabs with a larger portion of glass particles as fine aggregates.

3.4 Punching shear strength

Due to different batches of casting, the slab elements had different compressive strengths from the target values. Table 3 shows the concrete cylinder compressive strength at the time of testing the slabs, and the average value for each group of slabs. The observed punching shear strength $P_{u,test}$ is also listed. In order to compare the punching shear strength of slabs within each group, the observed value is adjusted by multiplying the value by a factor $(f_c'{}_{ave} / f_c')^{1/3}$, on the basis that the punching shear strength is proportional to the cubic root of f_c' (EN1992 2004).

The adjusted punching shear strength $P_{u,adj}$ was found to increase with higher concrete strength and reinforcement ratio, as shown in Figure 6. Also, the strength appeared to be slightly higher for slabs with a higher proportion of glass particles as fine aggregates, except for Group 45 slabs which had a lower concrete strength.

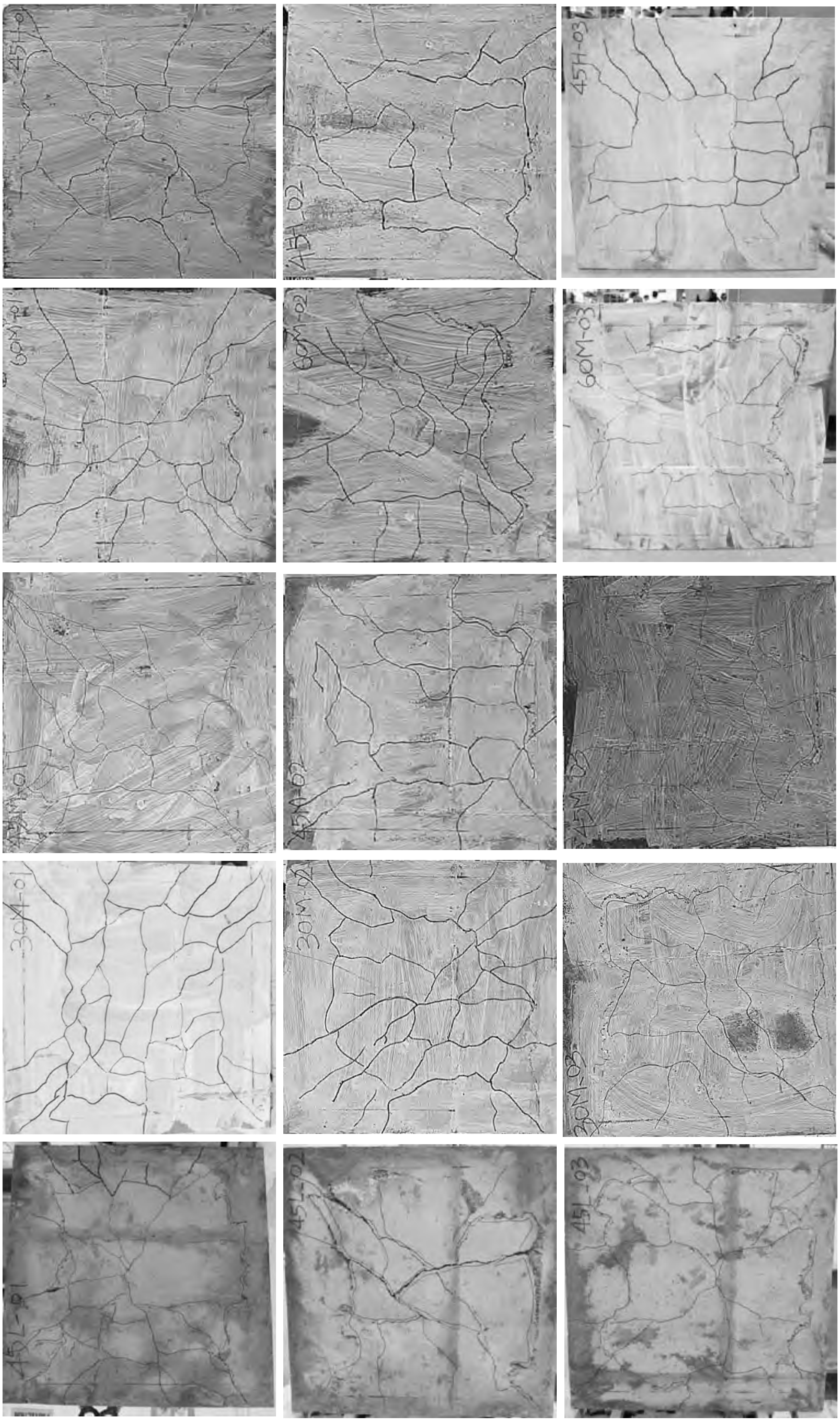
45H-01
45H-02
45H-03
60M-01
60M-02
60M-03
45M-01
45M-02
45M-03
30M-01
30M-02
30M-03
45L-01
45L-02
45L-03

Figure 5: Cracking pattern of test slabs (left to right: g/fa = 0, 50, 100%; bottom to top: Series 45L, 30M, 45M, 60M, 45H)

Table 3: Punching shear strength

Slab Designation	f_c' (MPa)	Average $f'_{c\,ave}$ (MPa)	$P_{u,test}$ (kN)	$P_{u,adj}$ (kN)
30M-01	42.6	38.2	175	156
30M-02	36.8		168	157
30M-03	35.1		177	168
45L-01	64.7	63.8	138	122
45L-02	65.0		142	126
45L-03	61.8		131	118
45M-01	53.0	44.4	196	186
45M-02	35.5		165	179
45M-03	44.8		193	193
45H-01	45.2	41.8	173	173
45H-02	35.5		163	176
45H-03	44.8		191	191
60M-01	57.5	57.0	168	170
60M-02	60.0		180	180
60M-03	53.5		214	222

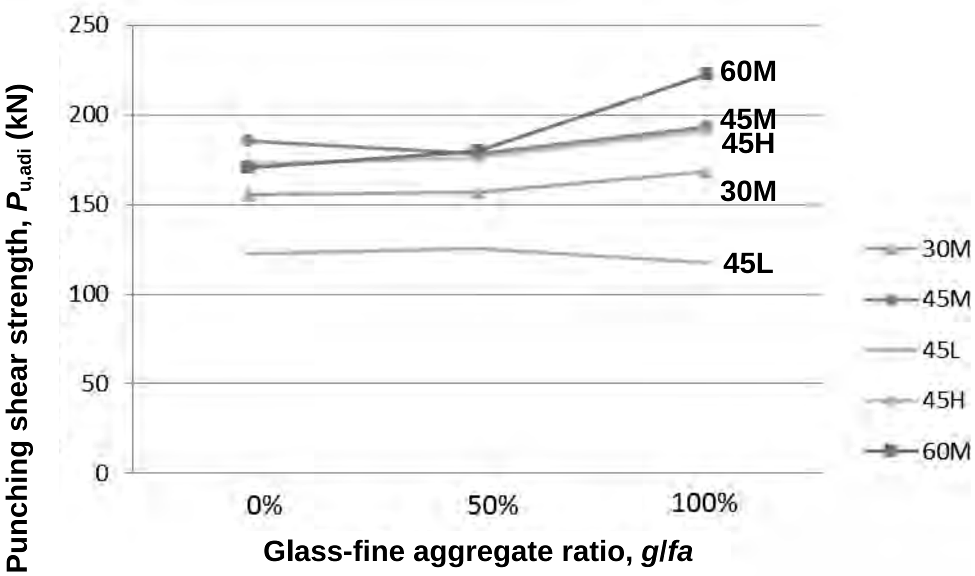

Figure 6: Effect of *g*/*fa* ratio on punching shear strength

4. CONCLUSION

The punching shear behavior of reinforced concrete slabs, with waste glass particles as fine aggregates, either partially or totally, was investigated. Test results indicated that the load-deflection characteristics, development of steel strains, and cracking pattern, were not affected with the use of waste glass particles. The punching shear strength of slab elements with waste glass particles was comparable if not higher than those without glass particles as fine aggregates. The results further attested to the viability of using waste glass particles in structural applications.

REFERENCES

ACI Committee 211, 1992. Standard practice for selecting proportions for normal, heavyweight, and mass concrete (ACI 211.1-91). *American Concrete Institution*, Farmington Hills, MI, 38 pp.

ASTM C33, 2003. Standard specification for concrete aggregates. *ASTM International*, West Conshohocken, PA, 11 pp.

Du, H. and Tan, K. H., 2013. Use of waste glass as sand in mortar: Part II – Alkali-silica reaction and mitigation methods. *Cement and Concrete Composites* 35, 118–126.

Du, H. and Tan, K. H., 2014. Concrete with recycled glass as fine aggregates. *ACI Materials Journal* 111, 47-57.

Du, H. and Tan, K. H., 2014. Effect of particle size on alkali-silica reaction in recycled glass mortars. *Construction & Building Materials* 66, 275-285.

Du, H. and Tan, K.H., 2014. Durability performance of concrete with glass powder as supplementary cementitious material. *13th International Conference on Durability of Building Materials and Components* (XIII DBMC), Sao Paulo, Brazil, September 2-5, 938-945.

EN 1992-1-1: 2004. *Design of concrete structures – Part 1-1: General rules and rules for buildings.* CEN, Brussels.

Tan, K. H., 2013. Recycled glass concrete beams under bending and shear. *12th International Symposium on New Technologies for Urban Safety of Mega-Cities in Asia* (USMCA 2013), Hanoi, Vietnam, October 9-11, *ICUS Report 73*, 219-227.

Tan, K. H. and Du, H., 2013. Use of waste glass as Sand in Mortar: Part I – Fresh, Mechanical and Durability Properties. *Cement and Concrete Composites* 35, 109–117.

History of the network plan and construction of Tokyo Metro

Hiroaki HASHIGUCHI[1] and Shinsuke SHIRAKO[2]
[1]Deputy Manager, Renovation & Construction Department, Tokyo Metro Co. Ltd., Japan
h.hashiguchi@tokyometro.jp
[2]Manager of Vertical Access Facilities Upgrade Design, Renovation & Construction Department, Tokyo Metro Co. Ltd., Japan

ABSTRACT

The first subway in Asia began running in December 1927 when service began on a 2.2 km section of Tokyo Metro's Ginza Line between Asakusa and Ueno. When the Fukutoshin Line opened in June, 2008, the Tokyo Metro network had expanded to 9 lines and 179 stations, and service covering a total of 195.1 kilometers. The network was built according to a network plan based on Japan's national transportation policy. Tokyo Metro created this plan to meet social needs, such as the need for convenient transportation in areas without service in the Tokyo Metropolitan Area. Careful consideration was given to profitability and augmentation of the area's transportation network, including existing railways. In constructing the network, every effort was made to develop technologies needed for the safest, most reliable and most economical construction methods possible. This included trial-and-error approaches to solving problems at actual construction sites. Since no two sites had construction conditions that were completely alike, Tokyo Metro has accumulated a wealth of experience in decades of subway construction. This is the foundation for Tokyo Metro's technologies. This paper introduces the changes that have taken place in public transportation in Tokyo, the transitions in the Tokyo Metro's network plan, and traces the history of subway construction.

Keywords: subway, network plan, construction

1. TRANSITIONS IN THE SUBWAY NETWORK AND CHANGES IN TOKYO METRO'S NETWORK AND STATION PLANS

1.1 Transitions in the subway plan network (characteristics and history)

(1) Emphasis on Imperial Palace southeast-bound routes and their connection to the Toden network

Tokyo's subway lines' network has been planned with focus on southeast-bound Imperial Palace since the 1920s. Building an underground high-speed railway in this area was stressed in planning due to the southeast area of Imperial Palace historically being a core district for business and commerce, and due to high demand because of the many government offices.
Although Tokyo's subway routes have a strong element being alternative routes to Toden, but also exists for long-standing riding customs and existing demand. The above-mentioned emphasis on Imperial Palace southeast-bound is due to the Toden network being deployed densely in this area.

(2) Implementation and merits of mutual direct operation

From 1948 to around 1955, each of the private railways simultaneously sought to serve central Tokyo to relieve traffic congestion. Although there were drives to have the subway operated by the metropolitan government, the advisable course of action was deemed to be promoting integrated operations under Eidan (name at that time). This was in order to avoid a chaotic network plan and causing complicated fare calculation work.

The merits of mutual direct operation include 1) reduction of transfer congestion at connecting stations, 2) passengers on directly connecting lines can be switched directly over to one's company line, and 3) passengers can travel to their final destination in the inner-city with one transfer. Due to the network's capabilities in central Tokyo, congestion rates have been equalized over every route, and mutual direct operation has proved to be tremendously effective.

(3) Changes in ideology towards relieving congestion in terminal stations

A fundamental approach of the 6th report of the Council for Urban Transport, produced in 1962, was to plan routes as to not pass through the three urban sub-centers of Ikebukuro, Shinjuku, and Shibuya, as a key measure to relieve congestion caused by transfer passengers. As urban sub-centers, these three terminal stations experienced significant congestion. After this in the 10th report of the Council for Urban Transport in 1968, the trend shifted towards focusing on passing through these three urban sub-centers, in contrast to the previous policy.

1.2 Transitions in Tokyo Metro's network and station plans

The interval at which stations are built along Tokyo Metro's routes is mostly uniform with an average of roughly 1.2 km between stations. This was determined based on the fundamental planning and design ideology that people should be able to travel to a station on foot within about 500 m (or 6 to 7 minutes). It should be noted that the emphasis was placed upon the points below in the network plan.

(1) Is the area lacking rail service?
(2) Is there local demand along the route?
(3) Will it contribute to relieving congestion other routes?
(4) Can it lead to strengthening the network for existing routes?
(5) Are there routes where mutual direct operation is possible?
(6) Are the roads of a certain width or larger?

Described below are the network plan's features and background for each route from the Marunouchi Line onwards.

1) Marunouchi Line

The Marunouchi Line was planned to a scale commensurate with its transport capacity. Since it was planned before the concept of mutual direct operation, it was planned and designed as an individual route. What is notable about the Marunouchi Line is that in addition to limiting construction funds to the initial cost, consideration was given to the distance between stations and area influenced by stations in order to meet increasing demand of the future. The line was structured in such a way that stations could be easily retrofitted at locations deemed likely to need so in the future.

2) Hibiya Line

Hibiya Line required the simplest and most economical planning and design since it was paramount that it be completed time-wise by the start of the Tokyo Olympics (opening October 10, 1964). Meanwhile, it was to be the first time to implement mutual direct operation at both ends of the route, so it was necessary to unify standards between the incoming Tobu Isesaki Line and the Tokyu Toyoko Line.

3) Tozai Line

The Tozai Line was the first time a route was envisioned as a large-scale mass transit with unprecedented characteristics as a subway such as the implementation of mutual direct operation with Japan National Railways (as it was known at the time) and operation of 10-car formations of 20 m long cars, which were the same as Japan National Railways trains. Thus, the scale of the station facilities was planned and designed while seeking to adapt to these circumstances.

4) Chiyoda Line

The Chiyoda Line has the same transportation capacity as the Tozai Line; however, the scale and configuration of the station facility was radically revised in planning and design based on experience gained with the Tozai Line. The platform configuration was planned and designed to take island type platform as its standard based on the perspective that, among other things, it allowed the area of the platform to be utilized effectively. This was because opposing separate platforms, which were commonplace up to that point, had several disadvantages such as the way that space was utilized, and the fact that imbalances in passenger loads between incoming and outgoing platforms could not be addressed.

5) Yurakucho Line

The Yurakucho Line can be broadly separated into three phases as the route was planned over the transition period to the network plan methodology. For Ikebukuro to Shintomicho in Phase 1, the plans and design directly followed the ideology of Chiyoda Line. For Wakoshi to Ikebukuro in Phase 2, there was rising awareness of issues concerning the surroundings received from residents along the railway, and measures were considered for homes along the route. For instance, weight was added to the construction to counteract vibrations. In the final Phase between Shintomicho and Shin-Kiba, the comfort of passengers became the focus. For instance, natural exhaust vents were installed in order to mitigate train wind. Construction cost increased by incorporating measures such as those mentioned above; however, the planning and design was a forerunner to the environmental measures and comfort improvements that are taken for granted today.

6) Hanzomon Line

The Hanzomon Line basically followed the ideology of Chiyoda and later lines. It was planned and designed with an emphasis placed on measures to address housing along the route and improving convenience – even more so than in the Yurakucho Line – coupled with advancing design and construction methods.

7) Namboku Line

The Namboku Line basic- ally followed the ideology of Chiyoda and later lines, but to embody the image of a 21st century rail syst- em, and as a metropolitan mass transit system, the installation of revolution- nary platform screen doors (photo-1.1), and One-man Operation were planned.

Photo-1.1: Platform screen doors

8) Fukutoshin Line

Fukutoshin Line is basically followed the ideology of the previous Chiyoda and Namboku Lines, but adopted new technologies across the entire line as a culmination of all Tokyo Metro's civil engineering and architectural technologies.

In order to enhance safety for passengers on the platform, for instance, automatic platform gates (photo-1.2), which were a signifi-cant improvement upon the screen doors adopted in the Namboku Line, were installed in conjunction with implementing One-man Ope-ration. Consideration was put into added security, and movable steps (photo-1.3), were installed at loca-tions with large gaps between the car and platform in order to pre-vent people from losing their foot-ing when embarking and disem-barking.

With respect to the station design, based on factors such as changes in the social climate and diver-sifying values, high vaulted ceil-ings and open spaces were planned to promote policies that stress comfort. Universal designs were introduced that aspire towards making the station easy-to-use for all people, without making distinctions for persons with disabilities, the elderly, and health individuals.

Photo-1.2: Automatic platform gates

Photo-1.3: Movable step

2. TOKYO METRO'S CONSTRUCTION HISTORY

2.1 Pre-1945

Miyagi Electric Railway's (currently known as the JR Senseki Line) Sendai Station was the first to open in Japan in 1925 as an underground business route. It spanned a distance of just over 200 m. Two years after this in December 1927 a 2.2 km subway route spanning between Tokyo subway Asakusa Station and Ueno Station opened to much fanfare, being hailed as "The first subway of the Orient."

The cut and cover method, typical in urban tunneling, was adopted as the standard method for constructing these railway sections. In these early days, planning concepts were heavily influenced by the design and const-ruction technology of the time. It could be said that transitions in construction technology have a pro-cess history of developing techno-logies through trial and error approa-ches to avoid obstacles such as rivers and existing structures.

Prior to 1945, pile driving was accomplished with steam hammers; soldier piles and horizontal lagging was used in earth retaining; squared timber was used in struts and intermediate pile; lumber was used in decking for road surface lining - steel material was only used in soldier pile, steel sheet pile, and girders for road surface lining.

Photo-2.1: Pile driver

2.2 Post 1945

In 1945, the Marunouchi Line sections between Ikebukuro and Ochanomizu opened. Generally the construction method used was the cut and cover method, conforming to pre-1945 technology. A noteworthy development at this time period was full-scale adoption of ready mixed concrete. The use of ready mix concrete became the standard from this point forward at sites where large quantities of concrete would be used, and ways to establish a reliable supply for concrete as well as improve quality began to be considered.

2.3 Post 1955

An era of high economic growth was entered after 1955. There was a preference towards multiple routes for subways and construction demand ballooned rapidly. At this time road traffic volume increase significantly, and automobiles grew larger - as did the burden on roads. In addition to this were a growing number of intersecting properties such as existing routes, structures, and roads. Construction depths also became progressively deeper. As a result, this was a time of remarkable development for cut and cover methods of earth retaining, since groundwater conditions also became more demanding.

Up to Hibiya Line which opened all its routes in 1964, the soldier piles and horizontal lagging method was the standard, and soldier pile remained the driven-type; however, for earth retaining in the Tozai Line and onwards, where excavation depths became increasingly deeper, column row type continuous underground walls, which have relatively large cross sections and superior water shielding properties, were employed. Initially an erection method using a single axis auger to build the reinforcement cage was utilized. Steel material also began to be used in struts, intermediate pile, and plating in the road surface lining. In addition to these, methods to provide high rigidity earth retaining were used in the Marunouchi Line; the ICOS method, which pioneered reinforced concrete continuous underground walls, was used in trial construction and an under-road type caisson method was used in sections with soft subsoil.
Meanwhile, adoption of shield tunneling methods for sections with deep excavation depth was proactively examined, and in 1957 a roof shield was used around Kokkai-gijidō-mae Station on the Marunouchi Line, which had reached an excavation depth of 22m. Then in 1964 a circular single shield was used on the inbound and outbound lanes around Kiba Station on the Tozai Line. Kiba Station became Japan's first shield tunneled station to have a one

track parallel type structure which was connected only by the shaft at both ends of the inbound and outbound platforms.

2.4 1965 to 1975

From this time there was increasing demand for environmental protection from noise and vibration, lowering groundwater levels, ground settlement and such, thus mechanized construction, no-vibration and low-noise construction, improvement of rigidity and water shielding properties, heavy load coping, and other such technological innovations were being promoted.

In the cut and cover method, moving towards column row type continuous underground walls with multiple axes, and core plates to steel material was promoted in conjunction with focusing efforts on improving power, reducing vibration, and reducing noise of the construction machines themselves, including pile drivers, backhoes and cranes. Reinforced concrete continuous underground walls with superior water shielding properties and high rigidity were among things developed to address excavation depths that grew at an accelerating pace.

Regarding shield methods, just as before some shield tunneling methods were adopted for sections with deep excavation. Coupled with this was a leveraging of the benefits of non-open cut methods, which did not requiring road surface lining and make it possible to excavate under residential areas. These methods were also adopted in constructing stations that had deep installation locations as well as for sections located under rivers or in areas of highly undulating terrain. From the Chiyoda Line onwards, Eidan Subway also gradually increased sections in which shield tunneling methods were adopted. These methods were used in roughly 20% of all routes in the Chiyoda Line, and roughly 70% of all routes in the Yurakucho Line and Hanzomon Line.

As for the change towards large diameter shields, in 1965 when construction began on the Osaka Municipal Transportation Bureau's Chou Line between Tanimachi 4-Chome Station and Morinomiya Station, the first double-track shield (with an outer diameter of 10.1 m) was used. Eidan Subway later used a 9.8 m diameter double-track shield between Kokkai-gijidō-mae and Akasaka on the Chiyoda Line, whose construction began in 1969.

Shield machines were commonly open type compressed air shield tunneling styles until around 1975. Closed type blind shield tunneling was used between Kita-Senju Station and Machiya Station on the Chiyoda Line, which began construction in 1966. However, due to reasons such as being limited in the geology it could be applied to, it was never fully adopted. Technological innovations for closed type shields, which do not require compressed air, soil stabilization or other methods to assist construction, advanced from 1975 onwards. It also became possible to adopt them in multiple track class large cross sectional tunnels as well. In closed type shields at that time, slurry pressure shield machines were commonplace. On the Yurakucho Line which started construction in 1978, between Kotake-Mukaihara and Hikawadai a 10 m class outer diameter double-track shield was employed as a slurry pressure shield - the world's largest. From this point forward slurry pressure shields were acknowledged as the standard form of closed type shields.

With regard to shield tunneled stations, Shin-Ochanomizu Station on the Chiyoda Line, which began construction in 1966, differed from Kiba Station in that it was to have a genuine island type platform installed. Thus the area between two single shield bored tunnels, was cut and expanded for all sections using a Kanzashi-beam method to complete Japan's first binocular-shaped shield tunneled station. After this, the Kanzashi-beam method was adopted for the leading and terminal edge sections of the platform in Kokkai-gijidō-mae Station on the Chiyoda Line. Nagatachō Station on the Yurakucho and Hanzomon Lines, and Mitsukoshimae Station on the Hanzomon Line adopted a roof shield to cut and open all sections. All these projects were completed by 1975.

2.5 Post 1985

2.5.1 Overview of construction technology

Around this time the principle of using the cut and cover method for station sections and shield tunneling method for areas between stations had become entrenched. For cut and covermethods that increased excavation depth further, as a general rule the highly efficient multi-axis style column row type continuous underground walls were used in hard ground, and the highly rigid reinforced concrete continuous underground walls were used in soft ground. In the Namboku Line, which began construction in 1986, a wide variety of elemental technologies linked to deep underground development in Namboku Line were employed. An inverted lining method that combined the use of reinforced concrete continuous underground walls and steel continuous underground walls was used in Kōrakuen Station to excavate to a depth of 40 m. In addition, Roppongi-itchōme Station's construction location was adjacent to an elevated two-layer structure of the Tokyo Metropolitan Expressway, as well as having topography with a 10 m difference in elevation across the transversal direction. Therefore all sections of the station were partitioned into 27 square blocks using a continuous underground wall, which also served as a buttress wall built in the transverse direction. After the blocks were filled with slurry and the ground around them stabilized, a transverse continuous underground wall method which excavates underwater was used to achieve stability in the confined water and earth pressure.

In shield tunneling methods, technologies were developed to excavate a station shield and storage track with a single shield tunneling machine.
For the station shield, a "Detachable triple shield," with the capability to change from a triple shield configuration to a double shield configuration was employed. Here, a double-track shield tunneling machine departing from the Namboku Line Shirokane-dai Station ventilation room was mounted with a slave machine at the starting edge of Shirokanedai Station, to excavate the sections of the opposing separate platforms. After transforming the tunneling machine into a triple station shield and excavating the Shirokanedai Station sections, the slave machine was detached at the terminal edge shaft.

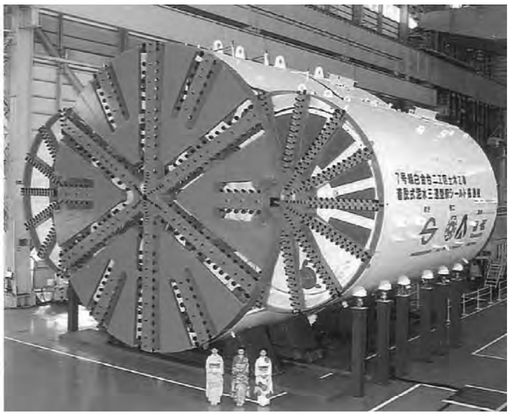
Photo-2.2: Detachable triple shield machine

For the storage track, in order to provide a return track line between the inbound and outbound lanes on the Meguro side of Azabu-Jūban Station on the Namboku Line, a three-lane sized ultra large diameter shield machine was launched from the shaft connecting the station and a "Holding-type master-slave shield" was employed, which has ability to transform into a double shield within the shaft created in the terminal edge of the return track line. Utilizing these 'cross sectional variance coping shields' made it possible to realize efficient construction and considerable cost savings.

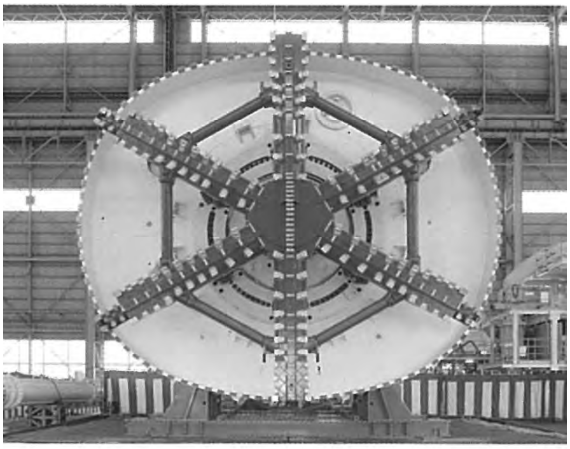

Photo-2.3: Composite circular cross-section double-track shield machine

In terms of shield formats, even in conventional large cross-sectional excavation fields dominated by slurry shields, EPB shields have made technological advances and built up a construction track record. For this reason they were used in the second phase of construction on the Hanzomon Line in three areas at sections where the geology had uniformly cohesive soil. At Kiyosumi-Shirakawa Station on the same line, triple continuous station shields were used, continuing from the work on Namboku Line. Although construction gradually progressed on the storage track and station parts, this was the first time a concrete segment was used in a shield tunneled station.

In construction on Fukutoshin Line - the last of new route construction for Tokyo Metro - while reducing the dead space of the top and bottom sections of the circular cross-section, which are spaces not used by the railway, a compo-site circular cross-section which takes advantage of the structural characteristics of circular cross-sections was adopted in the tunnel between Meiji-Jingūmae Station and Shibuya Station. As a result the reduced cross-sectional area was roughly 10% smaller than that of conventional circular cross-section double lane tunnels, making a significant contribution to reducing environmental impact.

Tokyo Metro is hopeful that the underlying logic of its network plan and construction history will serve as a useful reference in the future for progressing construction of subway development.

The transportation condition improvement to hospitals in Mandalay under seismic risks

Myint Myint KHAING[1], Hla Myo AUNG[2], Kyaw Zaya HTUN[3],
Zin Mar LWIN[2] and Takeshi KOIKE[4]
[1] Associate Professor, Mandalay Technological University, Myanmar,
drmmkhaing@gmail.com
[2] Associate Professor, Mandalay Technological University, Myanmar,
[3] Assistant Lecturer, Mandalay Technological University, Myanmar,
[4] Academic Advisor, Japan International Cooperation Agency, Japan

ABSTRACT

Mandalay city is surrounded with potential seismic risk which might be caused from the active fault lines of Sagain Fault. In the past disastrous events, many people were injured or lost under vulnerable residential buildings. Even if some people can be saved from the fallen housings, not easy access to the nearest hospitals led to loss of life. The disaster prevention activity needs two types of works, one of which is seismic reinforcement of buildings and infra-structures, and the other is related to human safety management which includes the emergent scheme in which injured people must be saved to transport to the hospitals or be led to the evacuation open spaces, intermediate scheme where evacuated people must stay at the shelters during at least 3 days with supplied emergency food and water, and long term scheme in which people have to spend inconvenient life up to recover the infrastructures. In the emergent scheme, injured people can be saved by improvement of vulnerable buildings and by increasing access to the emergency hospitals. In this study, the accessibility to the hospitals is discussed to know which factor among the hospital allocation, accessible roads and rapid transportation time is the most effective for saving the human life.

Keywords: hospital, seismic risk, fragility curves, probability of failure, human life, housing damages

1. INTRODUCTION

Myanmar is exposed to range of natural hazards such as floods, cyclone, earthquakes, drought, tsunami, etc due to its geophysical location. Among them, earthquake is one of natural hazards which threaten human lives and loss of properties. There are many cities lie on the active Sagaing Fault and all those cities have high potentials exposed to the earthquake hazard.

Since Mandalay city is surrounded with potential seismic risk from the active fault lines of Sagaing Fault, it is prone to earthquake. According to the historical records, the most significant shock is probably 23 March, 1839 event, by which very serious damages and 300 to 400 casualties resulted, and the most recent one is the magnitude 7 event shocked on 16 July, 1956, known as the Sagaing earthquake, causing several damages and about 50 deaths (Ref: Myanmar Earthquake Committee (MEC), 2012).

Seismic risk assessment is important and urgent needs to estimate potential damage in buildings and facilities including hospitals which are essential for human lives. It is also needed to improve the ways to assess various facilities under risks.

In the past disastrous events, many people were injured or lost under vulnerable residential buildings. Even if some people can be saved from the fallen housings, not easy access to the nearest hospitals led to loss of life. Lessons learnt from past earthquakes point out the needs to improve the transportation condition to hospitals to reduce human loss due to earthquake risks.

There are totally five townships in Mandalay City which are Aung Myae Thar Zan , Chan Aye Thar Zan, Mahar Aung Myae, Chan Mya Tharzi, Pyigyithakon Townships. Among them, Chan Aye Thar Zan Township is chosen to carry out seismic risk assessment since the hazard profile of Mandalay city, the high degree of vulnerability area lies in Chan Aye Thar Zan Township which peak ground acceleration (PGA) value is about 0.25g and is also highly populated commercial zone. There is only one general hospital in Chan Aye Thar Zan Township, which is called Mandalay General Hospital. In this study, that hospital is assumed to be target one to reach from each ward of that township. Remote sensing and GIS are integrated, well developed and successful tool in disaster management, and these tools are used to find out the location of hospitals and the shortest path to hospitals under seismic risks.

2. SEISMIC HAZARD MAP IN MANDALAY

One of the active fault (Sagaing Fault) runs from north to south passing through the central region. According to the historical accounts, many of strong earthquakes had occurred and felt along the Sagaing Fault and Sunda-Andaman Trench which is parallel to the Myanmar Coastal. These earthquake generators had been the focal point of many great earthquakes. The following map shows the tectonics and depths of earthquakes throughout Myanmar.

Myanmar lies on the earthquake belt of Himalayan range. The northeastern part of the Indian plate subcontinent is seismically active. It comprises of east-west extending eastern Himalaya belt, which marks the collision boundary between the under thrusting Indian plate and the Eurasia plate; approximately N-S extending Indo-Burmese Arc (IBA), which extends further southward to join the Andaman Arc and the Eastern Himalayan Syntaxes (EHS), which lies at the junction of the above two. Subduction zone occurs along the Andaman arc. The Indian (IN) plate motion with respect to Eurasia (EU) is highly oblique to the margin on the subduction zone, the right-lateral shear motion occurring along the Sumatra fault evolves northward into the rift system of the Andaman Sea. The Burma plate is thus delineated in the east by the Sumatra fault, which follows the line of arc volcanoes and the rift segments of the Andaman Sea. The right-lateral Sagaing shear fault shown in the Figure 1 is delineated in the west by the Andaman-Nicobar Trench. The seismic records show that there have been at least 15 major earthquakes bearing magnitude M ≥ 7.0 within the territory of Myanmar for the past 100 years. The seismicity in Myanmar is attributable to the following two reasons:

- The continued subduction (with collision only in the north) of the northward-moving Indian Plate underneath the Burma Platelet (which is a part of the Eurasian Plate) at an average rate of 5.5 cm/yr (5.5 Found by the author) and

- The northward movement of the Burma Platelet from a spreading centre in the Andaman Sea at an average rate of 2.5 – 3.0 cm/yr. Very large over thrusts along the Western Fold Belt resulted from the former movement, and the Sagaing and related faults from the latter movement. Intermittent jerks along these major active faults resulted in the majority of earthquakes in Myanmar.

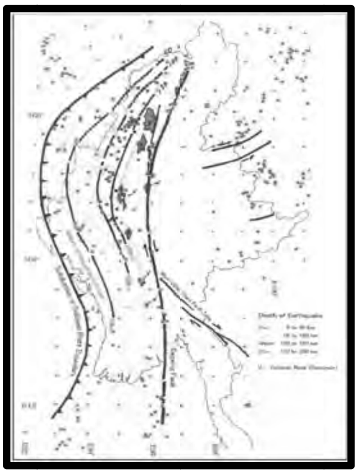

Figure 1: Map showing tectonics and depths of earthquakes

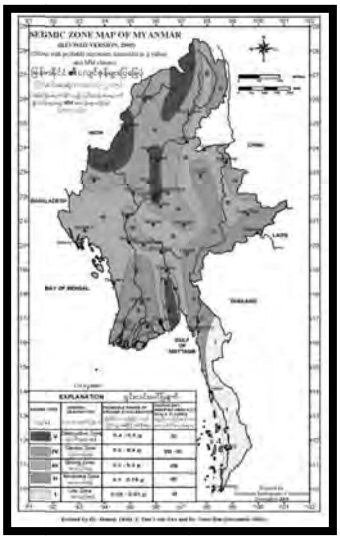

Figure 2: The seismic hazard map of Myanmar based on the deterministic data

(Source: Figures taken from the Myanmar Earthquake Committee)

The seismic hazard map of Myanmar based on the deterministic data and the probabilistic data can be described as the following diagrams.
The maximum acceleration is estimated by using the attenuation function for earthquake, (Boore, et al., 1993), (McGuire, 2004) as

$$\log(A_{\max}/g) = -0.038 + 0.216(M_W - 6) - 0.777\log R + 0.15G_B + 0.254G_C \quad (1)$$

where Amax, MW, R, GB and GC are peak horizontal ground acceleration at the ground surface, moment magnitude, hypo-central distance (km) and empirical coefficients, respectively. These two empirical coefficients are given by Table 1.

Table 1: Empirical Coefficients

Site Class	Shear Wave Velocity in Upper 30 m (m/s)	G_B	G_C
A	750	0	0
B	360-750	1	0
C	180-360	0	1

If the peak acceleration can be estimated as 90% non-exceeding level of random value, this acceleration can be expressed with its statistical moments as follows:

$$\ln A_{\max} = E[\ln A] + \Phi^{-1}(0.90)\sigma_{\ln A} = \{1 + \Phi^{-1}(0.90)\delta_{\ln A}\}E[\ln A] \qquad (2)$$

in which are mean value, standard deviation, coefficient of variation of the ground response logarithmic acceleration, ln A, and is a standard normal probability cumulative function (Ang et al., 1975) of a random variable whose mean value is zero and its standard deviation is unity.

Then, the expected ground acceleration is obtained as follows:

$$E[\ln A] = \frac{\ln A_{\max}}{1 + \Phi^{-1}(0.90)\delta_{\ln A}}, \qquad \sigma_{\ln A} = E[\ln A] \cdot \delta_{\ln A} \qquad (3)$$

So

$$\ln A_{mean} = \frac{\ln A_{\max}}{1 + \Phi^{-1}(0.90)\delta_{\ln A}}, \qquad \sigma_{\ln A} \cong \delta_A = \ln A_{mean} \cdot \delta_{\ln A} \qquad (4)$$

3. DAMAGE PREDICTION OF BUILDINGS AND HUMAN LOSS IN THE EXISTING CONDITION

(1) Structural damage estimation

Structural damage due to seismic ground motion can be evaluated by using a fragility curve which can be formulated as the conditional probability of structural failure for a given seismic intensity.

When a structure is applied by a seismic intensity *SI* which is brought by an earthquake *EQ*, the probability of structural failure can be formulated by

$$P[D_j(x_i)|EQ] = P[R_j \leq SI(x_i)] \qquad (5)$$

which is equal to the probability of damage occurrence, or fragility curve of type *j* building for a given *EQ*, and the parameters, SI, EQ, D_j, R_j, x_i are defined as follows:

SI: seismic intensity to be given by ground response acceleration of *A*
EQ: earthquake event
D_j : Damage state of type *j* building
R_j : Strength of type j building which is measured by acceleration
x_i: Location at the residential area of each ward

If all the uncertainty parameters are normal variables, equation (5) can be simply expressed as

$$P\left[D_j(x_i)\middle|EQ\right]=P\left[R_j\le SI(x_i)\right]=1-\Phi\left(\frac{R_j-A_{mean}}{\sigma_A}\right)\qquad(6)$$

The strength of Rj must be evaluated based on the ultimate limit state analysis of the structure. But in this study a rough estimation is adopted as shown in Table 2 (Roberto Miniati et al., 2014)

Table 2: Structural strength of various buildings

Type	Building type	Unit	Maximum strength in g or cm	Typical period of the building (sec)	Yield aceleration in g	Yield displacement in cm
1	Wooden	*g*	0.3	0.35	-	-
2	Brick	*g*	0.5	0.4	-	-
3	RC-low	*g*	1	0.7	-	-
4	RC-high	*cm*	10	1.8	0.7	5
	(Note) *g* means the gravity acceleration					

(2) Fragility curve estimation

Since the high-rise RC building is designed to expect an inelastic capacity, the ultimate limit criterion is given by the critical displacement. Based on the energy balance criterion (Chopra, 2012) for a structure having a perfect plastic stress-strain curve, the inelastic response displacement, d, can be converted from the acceleration as follows:

$$d(x_i)=\frac{1}{2}\left\{1+\left(\frac{A(x_i)}{A_y}\right)^2\right\}d_y\qquad(7)$$

So the corresponding mean and its standard deviation for the displacement are obtained as

$$d_{mean}=\frac{1}{2}\left\{1+\left(\frac{A_{mean}}{A_y}\right)^2\right\}d_y,\quad \sigma_d\approx\frac{d^+-d^-}{2}\qquad(8)$$

where

$$d^-=\frac{1}{2}\left\{1+\left(\frac{A_{mean}-\sigma_A}{A_y}\right)^2\right\}d_y,\quad d^+=\frac{1}{2}\left\{1+\left(\frac{A_{mean}+\sigma_A}{A_y}\right)^2\right\}d_y\qquad(9)$$

Then the fragility curve for high-rise RC building is given by

$$P\left[D_4(x_i)\middle|EQ\right]=P\left[R_4\le d(x_i)\right]=1-\Phi\left(\frac{R_4-d_{mean}}{\sigma_d}\right)\qquad(10)$$

where the strength of R_4 is a strength for high-rise building.

(3) Estimation of injured people

The expected number of injured people can be obtained as a summation of injured people in the A_k zone as follows:

$$E[HL(A_k)] = \int_{A_k} m(x) \nu_j P[D_j(x)|EQ]dx \qquad (11)$$

in which is the k-th zone, and

HL_k : number of human injured at zone k for a given EQ
$m(x)$: number of residential people at the subzone "x" in the A_k zone
ν_j : occurrence rate of injured people in the damaged type j building

In this study, the occurrence rate of injured people for 4 types of structures are simply assumed as shown in Table 3, which are roughly estimated based on the judgment by experts in Myanmar.

Table 3: Rate of injured people (%) under the damaged buildings

Type	Building type	Rate of injured people (%) under the damaged building
1	Wooden	10
2	Brick	50
3	RC-low	30
4	RC-high	40

(4) Life saving rate by hospital care at the duration time of T after the EQ occurred
When a number of human survived at zone k for a given EQ is expressed as $HS(A_k)$, the number of the survived people can be predicted by the following formula.

$$E[HS(A_k)] = \int_{A_k} HL(a) \cdot f_{HL}(a) \cdot \rho\{t(a)\}da \qquad (12)$$

in which

$f_{HL}(a)$: Probability density function of injured resident having a parameter of a which is defined in the local area A_k.
$\rho(T)$: Life saving rate by hospital care at the duration time of T after the EQ occurrence.

The duration time T is estimated by

$$T(a) = \frac{length(a)}{w_v} \times 60 \qquad (13)$$

where

$T(a)$: time from the zone A_k to the target hospital (*min*)
$length(a)$: length from the zone A_k to the target hospital (m)
w_v : walking velocity (*km/hour*)

In general, average walking speed in the free condition can be assumed to be

(Case 1) $w_v = 4\, km/hour$

But, immediately after an earthquake occurrence, traffic condition will be different from the usual condition. The walking speed must be decreased by traffic jam in such an emergency condition. So I this study, the following three cases in walking speeds are compared as access conditions.

(Case 2) $w_v = 2\,km/hour$

(Case 3) $w_v = 1\,km/hour$

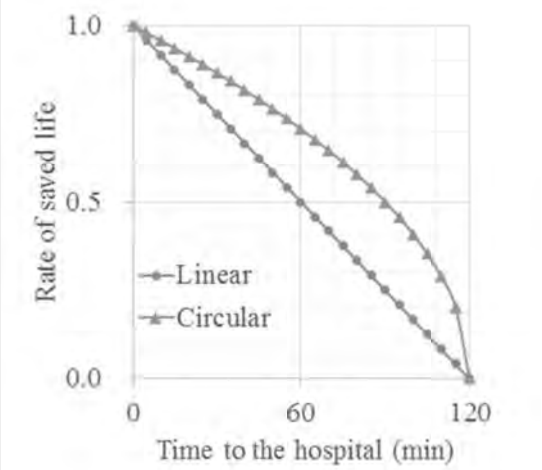

Figure 3: Rate of saving life for duration time

Life saving rate given by $\rho(T)$ reflects the efficiency of the emergency care during the conveying time to the hospital. If a careful care is applied to an injured person, this person will be possibly saved, so that the life saving rate will be increased. The circle model in Figure 3 suggests this situation.

4. DAMAGE PREDICTION OF BUILDINGS AND HUMAN LOSS IN THE REVISED CONDITION

The study area has 20 local zones shown in Figure 4. Each local zone has its own sub-zones where various housings are located. The route from the zone to the target emergency hospital is simply assumed to be given by one representative route, because the target city, which is an ancient capital, has a grid road system as shown in Figure 5. As the strategy to improve the access-ability for each site to the hospital, the following three options are proposed:

(1) If the road condition (available width, decreasing parking cars) has been improved before the earthquake, the walking velocity w_v might be increased.
The following 3 cases are evaluated: $w_v = 4km/hour, 2\,km/hour, 1km/hour$

(2) Duration time to the hospital is a key factor to save the life of injured person. Two types of critical time for life saving are assumed, linear model or circular model, as shown in Figure 3.

(3) Vulnerable building is reinforced, so that the fragility curve for residential building is improved.
By using a new R_j, the disaster prevention management effect can be evaluated by the comparison among the cases of the presenting buildings, deteriorating buildings and reinforced buildings.

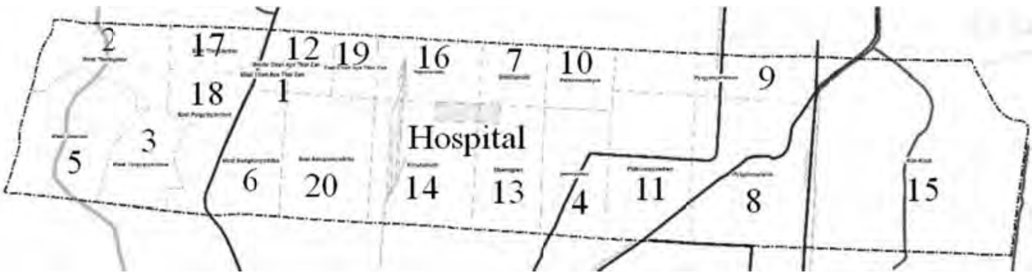

Figure 4: Site map for Location ID

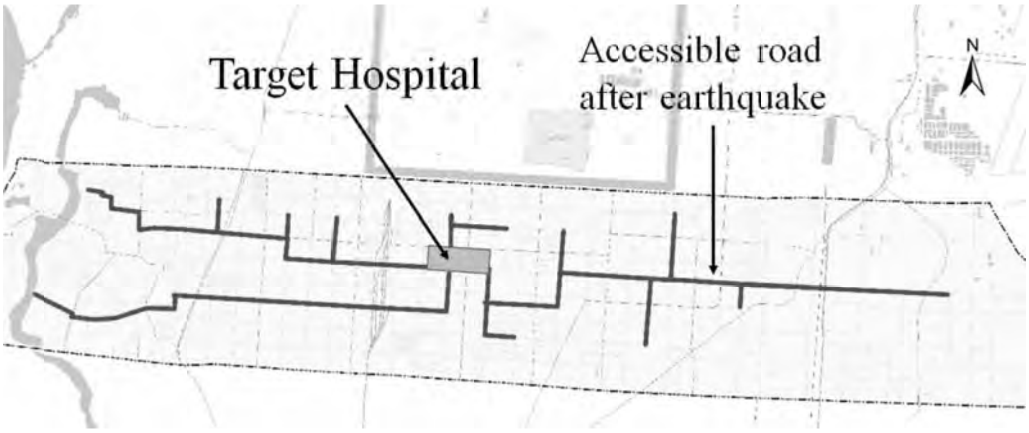

Figure 5: The route from a zone to the target emergency hospital

Table 4: Structural strengths of local buildings under the assumption of various conditions

Type	Building type	Unit	Existing strength	Deteriorated strength	Reinforced strength
1	Wooden	*g*	0.3	0.21	0.45
2	Brick	*g*	0.5	0.35	0.75
3	RC-low	*g*	1	0.7	1.5
4	RC-high	*cm*	10	7	15
	(Note) *g* means the gravity acceleration				

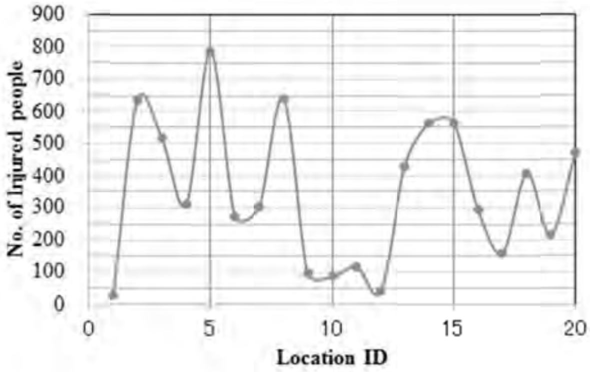

Case 1: Deteriorated strength

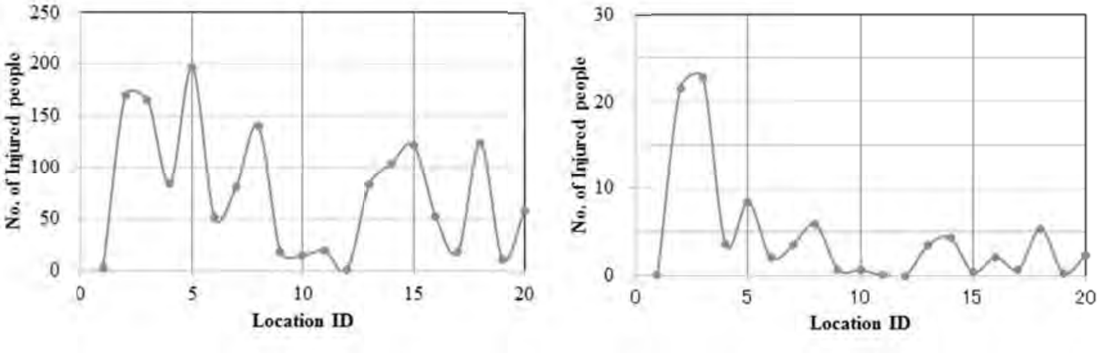

Case 2: Existing strength

Case 3: Reinforcing strength

Figure 6: Numbers of injured residences in each local zone

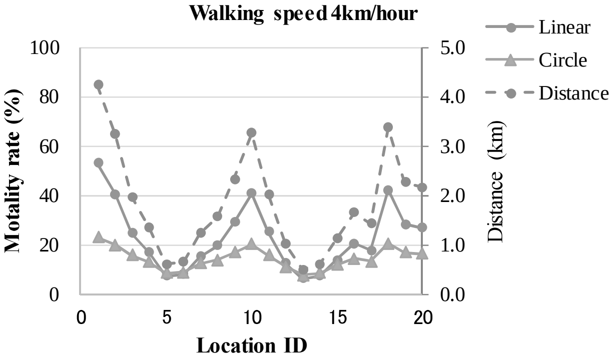

(Case 1) Walking speed 4km/hour

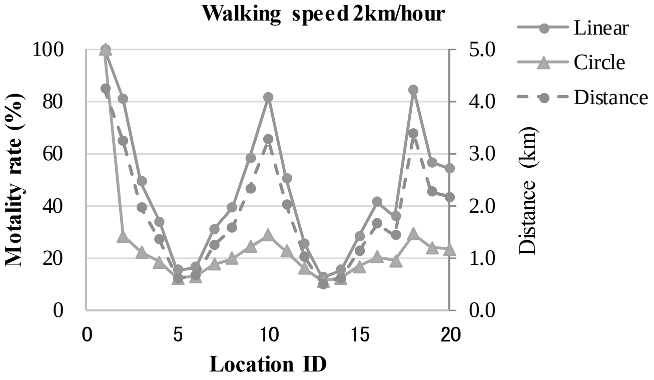

(Case 2) Walking speed 2km/hour

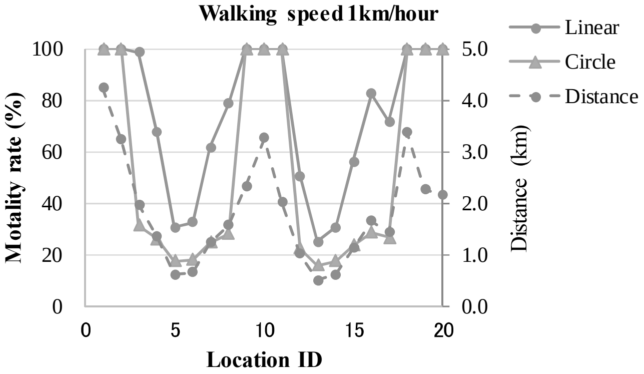

(Case 3) Walking speed 1km/hour

Figure 7. Mortality rate (%) due to walking conditions to emergency hospital from each local zone

All the local zones have a complex of wooden houses, brick houses, low RC buildings and high RC buildings. Now let assume all the strength will be deteriorated in the same rate. In Table 5, the deteriorated strength of all the structures are assumed to be 70 % of the existing ones. On the other hand, the reinforced strength is increased to be 150% of the existing ones.

In the deteriorated case, the number of injured people will be 4 times of that in the existing case. In the reinforcing case, on the other hand, the number of injured people will be 1/8 of that in the existing case. It suggests the reinforcing measures are extremely important for the reducing the injured people.

The mortality rate in this study can be defined as a ratio of dead persons per total injured persons to be conveyed from the k-th zone, A_k, to the hospital. The mortality rate curve shows the same profile with the required time by a linear model. The circular model can decrease the mortality rate in 50% than that of the linear model. It suggests that the initial emergency treatment for the injured people is more important to decrease the mortality rate.

If the traffic is congested after the earthquake, the time to emergency hospitals will be increased by slow walking speed. This effect can be shown in the Figure 7. The case of slow walking speed of 1km/hour shows 100% mortality rate in many local zones. It suggests that the access to emergency hospitals immediately after the earthquake must be obtained for the rapid transportation of the injured people.

5. CONCLUSIONS

The accessibility to the hospitals is discussed to know which factor among the hospital allocation, accessible roads and rapid transportation time is the most effective for saving the human life. According to the numerical result, the following results are obtained:

(1) By reinforcing the existing houses up to 150% of the present strength, the number of injured people can be reduced to 1/8 in the case of the existing houses.
(2) The mortality rate is directly proportional to the time from the site to the emergency hospital, which depends on the traffic conditions just after the earthquake occurrence.
(3) The numerical result suggests that the initial emergency treatment for the injured people is more important to decrease the mortality rate

REFERENCES

Roberto Miniati A.N., Pietro Capone, A., Dietrich Hosser, B.: Decision support system for rapid seismic risk mitigation of hospital systems - comparison between models and countries, International Journal of Disaster Risk Reduction 9, pp.12–25, 2014.
McGuire, Robin K.: Seismic hazard and risk analysis, EERI, 2004.
Douglas, John: Ground-motion prediction equations 1964-2010, PEER Report2011/102, PEERC, 2011.
Chopra, A. K. : Dynamics of Structures, Fourth Edition, PRENTICE HALL, 2012.
Ang, A. H.-S. and Tang, W. H.: Probability Concepts in Engineering Planning and Design, Volume I-Basic principles, Wiley, 1975.
Boore, D. M., Joyner, W. B., & Fumal, T. E.: Estimation of response spectra and peak accelerations from western North American earthquakes: An interim report. Open-File Report 93-509. U.S. Geological Survey. 70 pages, 1993.
Myo Thant, Ngwe Le’ Nge, Soe Thura Tun, Maung Thein, Win Swe, Than Myint, Myanmar Earthquake Committee, Seismic Hazard Assessment for Mandalay, Mandalay Region, March, 2012.
8. Luis E.Yamin, Alvaro I.Hurtado,Alex H.Barbat, Omar D.Cardona, Seismic and Wind Vulnerability Assessment, 5th May, 2014.

Survey on the reach of flood evacuation information - A case study of Nagoya City, Japan

Miho OHARA[1] and Hisaya SAWANO[2]
[1]Senior Researcher, International Centre for Water Hazard and Risk Management
(ICHARM) under the Auspices of UNESCO,
Public Works Research Institute (PWRI), Japan
mi-ohara@pwri.go.jp
[2]Chief Researcher, International Centre for Water Hazard and Risk Management
(ICHARM) under the Auspices of UNESCO,
Public Works Research Institute (PWRI), Japan

ABSTRACT

In Japan, flood early warnings and evacuation information are disseminated by various kinds of media such as television, radio, loudspeakers, emergency mail service to cellular phones, and the Internet. This paper proposes an index called the disaster information reach ratio (DIRR) for evaluating how widely each medium can disseminate warnings and information to the public. On 4 September 2013, Nagoya City in Aichi Prefecture, Japan, announced "evacuation preparation information" to the entire city area at 5:10 p.m. during torrential rainfall. This paper focuses on this event and calculates the DIRR using data from a questionnaire survey of people present in Nagoya City at that time. For all media, DIRR was limited to about 50% after the announcement. Among various media, emergency mail service to cellular phones had the highest DIRR. Emergency mail service was found to be an effective tool for disaster information dissemination in Japan. To evaluate how DIRR would be affected under various scenarios of future social change, a model for forecasting DIRR was developed by logistic regression analysis. Sensitivity analysis results imply that increasing the public's knowledge and experience of receiving information and upgrading own cellular phones would increase DIRR in the future.

Keywords: flood warning, evacuation information, preparedness

1. INTRODUCTION

In Japan, disaster early warnings and evacuation information are disseminated by various kinds of media such as television, radio, loudspeakers, emergency mail service to cellular phones, and the Internet. To transmit disaster warnings and information to all the people in an at-risk area, it is necessary to use media effectively by understanding the characteristics of information dissemination by each medium. This paper proposes an index called the disaster information reach ratio (DIRR) for evaluating how widely each medium disseminates warnings and information to the public. The term reach ratio is usually used in the context of advertising in order to indicate the ratio of the people in a target audience who receive an advertising message one or more times. In reference to this, DIRR is defined here as a ratio of the people in an at-risk area who successfully obtain disaster early warnings or evacuation information issued during an emergency.

On 4 September 2013, Nagoya City in Aichi Prefecture, Japan, was struck by torrential rainfall due to the effects of Typhoon No.17 and extratropical cyclone. The Nagoya Local Meteorological Observatory announced “record short-time heavy rain” after observing an hourly rainfall of 110 mm from 4:00 to 5:00 p.m. in Nagoya City. Figure 1 shows the radar precipitation maps observed at the Nagoya Local Meteorological Observatory (2013). The Emergency Operation Center in Nagoya City was established and issued “evacuation preparation information” to the entire city area at 5:10 p.m. Local governments in Japan can issue three kinds of evacuation information: evacuation preparation information, evacuation advisories, and evacuation orders. Evacuation preparation information is the information provided at the initial stage.

This paper focuses on this event and calculates DIRR using data collected by a questionnaire survey of people present in Nagoya City at the time of the announcement. Moreover, this study aims to evaluate how DIRR would be affected by future social change. This is done by using logistic regression analysis to develop a model for forecasting DIRR.

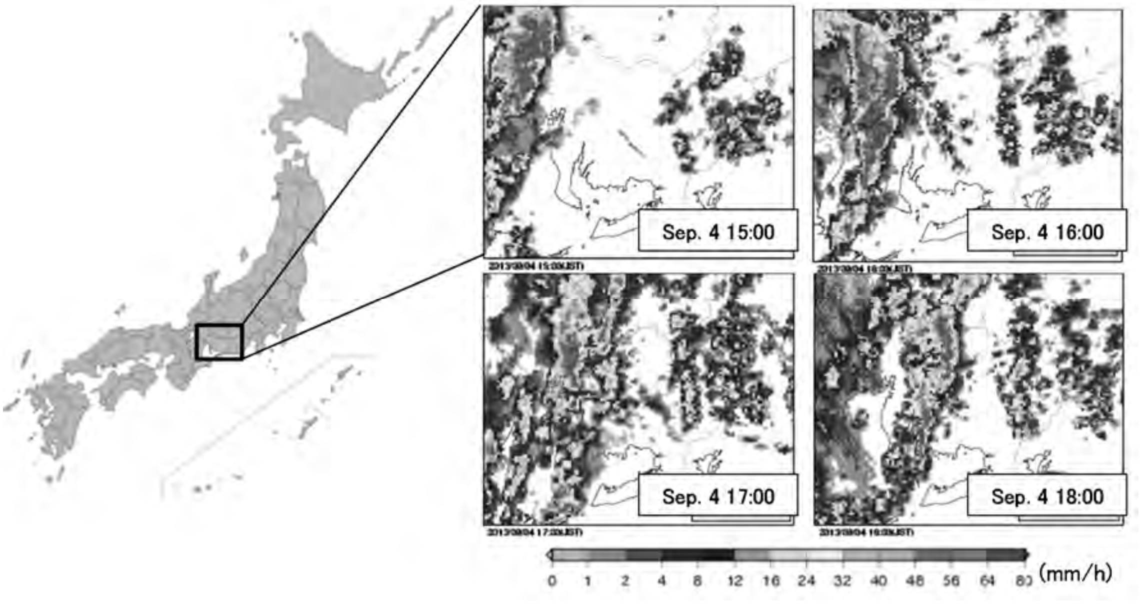

Figure 1: Radar precipitation maps

2. OVERVIEW OF QUESTIONNAIRE SURVEY

To calculate DIRR for information sent out during the torrential rain in Nagoya City, an online questionnaire survey was conducted during 13–20 December 2013. The questionnaire targets were the people aged 20-69 years who were present in Nagoya City at 5:10 p.m. when the evacuation preparation information was announced to the entire city. In an initial screening, candidates for the main survey were identified by their reported location at the time of the announcement. They were classified into three groups: group A, who were inside buildings such as houses, office buildings, shopping centers, and restaurants; group B, who were driving a motor vehicle; Group C, who were outdoors. As a result, 815 respondents were included in the main survey (425 in group A, 370 in group B, and 20 in group C). This paper focuses on the behavior of the respondents in group A. An analysis of group B has been reported by Ohara (2013).

3. QUESTIONNAIRE SURVEY RESULTS

3.1 Demographic characteristics of the respondents

Among the 425 respondents in group A who were indoors at the time of the announcement, 107 were at home; 234 were at their office or school; 50 were inside buildings other than their home, office, or school; and 34 were inside commercial facilities such as shops or restaurants (excluding underground shopping centers). The ages of the respondents were as follows: 20–29 years, 8.24%; 30–39 years, 24.7%; 40–49 years, 39.8%; 50–59 years, 21.9%; and 60–69 years, 5.41%. By a chi-squared test, no significant difference was found between the age groups and location at the time of the announcement (χ^2=15.0, p=0.243).

3.2 DIRR among the respondents

Figure 1 shows the DIRR values calculated for groups A and B. For group A, DIRR is shown by location at the time of the announcement. The figure shows both the DIRR just after the announcement and the final DIRR. The final DIRR indicates the proportion of people who received the information at any time after it was announced (not just immediately afterward); it is less than 100% because some respondents learned about the announcement from the questionnaire and were therefore not counted as having received the information.

DIRR just after the announcement was limited to about 50%. The DIRR for group B (in a vehicle) was 37%, which was lower than the DIRR for group A. This suggests that receiving disaster information is more difficult for drivers. In group A, no significant difference was found in DIRR between the four types of locations (χ^2=7.43, p=0.283). For respondents not in a vehicle, DIRR was almost the same regardless of where the respondents were located at the time of the announcement.

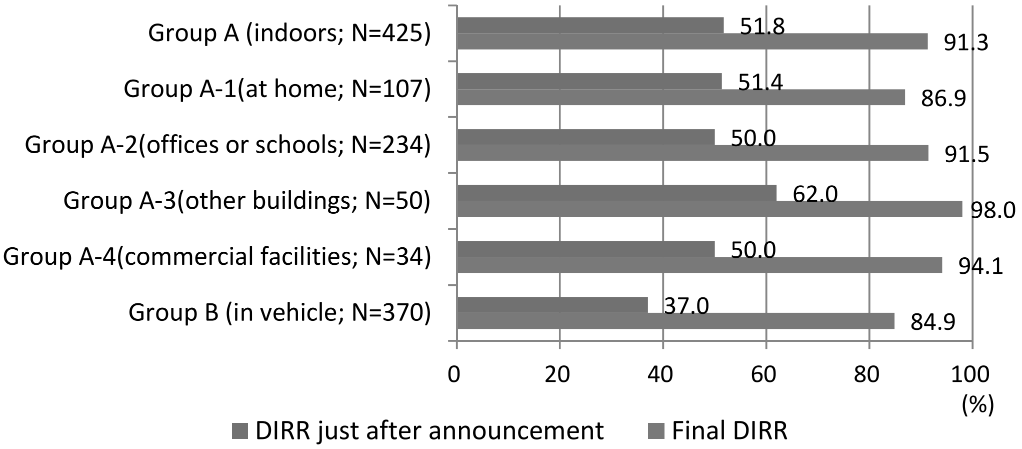

Figure 2: DIRR by location at the time of the announcement

Among respondents in group A who received the evacuation preparation information just after the announcement, 36.8% answered "All of Nagoya City is too wide an area for evacuation preparation information”, 33.2% answered "I don’t know what to do for evacuation preparation", and 30.9% answered "I don’t know where I should go during an evacuation".

3.3 DIRR by medium

Nagoya City has various media for disaster information dissemination such as loudspeakers for broadcasting disaster information, emergency mail service to cellular phones from service providers, emergency mail to cellular phones and e-mails from the city government, and the city’s website. Service providers (NTT DoCoMo, KDDI au, Softbank) can send a short emergency mail to all cellular phones inside a city under the contract between the City and them, without registration of mail address by cellular phone users. Some of older cellular phone models cannot receive such mail; however, after the experience of the Great East Japan Earthquake on 11 March 2011, this service became much more popular and was incorporated into new phones.

The City also provide another emergency mail service to cellular phones and e-mails, called “Kizuna Net Disaster Prevention Information”, which can send a short mail to users who registered their mail addresses in advance. The mail sent by this service is received regardless of whether the recipient is inside or outside the city. Also, disaster information is conveyed by the mass media such as television, radio, and Internet news sites.

Figure 2 shows DIRR just after the announcement by medium. Emergency mail service to cellular phones from service providers had the highest DIRR both as the first source of the information and as a subsequent source. This suggests that emergency mail service to cellular phones is becoming an effective tool for disseminating disaster information in Japan.

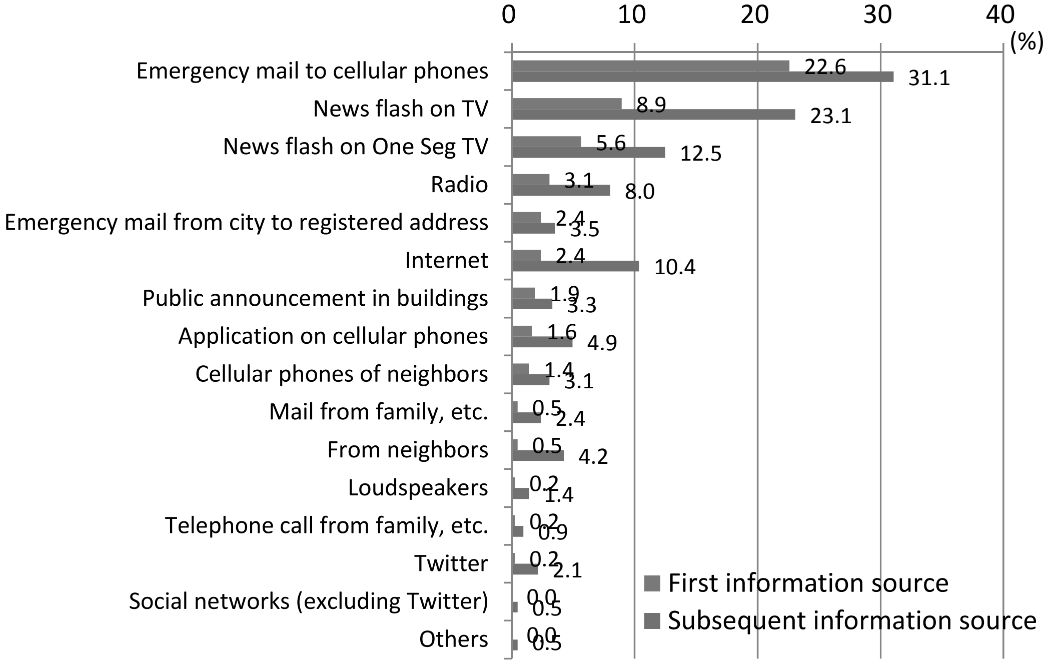

Figure 3: DIRR by medium

The media with the next highest DIRR values were, in order, news flash on television, news flash on One Seg TV (which can be watched on cellular phones), radio, emergency mail service from the city government ("Kizuna Net Disaster Prevention Information" which requires registration in advance), and the Internet. Recently, almost all local governments in Japan have a radio communication system for disaster prevention and install loudspeakers at sites within the city. In the case of the massive tsunami triggered by the 2011 Great East Japan Earthquake, loudspeakers were the most effective medium for conveying evacuation information. In the present case of the torrential rain in Nagoya City, however, loudspeakers were less effective because of the heavy rain and the environment inside buildings.

4. MODELING FOR ESTIMATING DIRR

4.1 Logistic regression analysis

The DIRR in the questionnaire survey was limited to about 50%, which means that improving the dissemination of disaster information remains an essential task. In this section, a model for forecasting DIRR was developed by logistic regression analysis in order to evaluate how DIRR would be affected by future social change.

DIRR might be affected by the various attributes of the respondents, such as their family situation, their information literacy, their psychological status, their location and the availability of media for receiving information. Here, the attributes that have an influence on DIRR were first identified by a chi-squared test. The relationships between about 50 respondent attributes and whether they received the information just after the announcement were examined by a chi-squared test. The level of significance was set at 5%. Significant relationships were found for the following attributes: age group, prior experience receiving evacuation information, knowledge of emergency mail service, prior experience receiving mails from emergency mail service, understanding evacuation preparation information, start of using current cellular phone (before March 2011 or after April 2011), having a smartphone, frequency of using mail on cellular phones, registration with Nagoya City's emergency mail service, anxiety about floods, living with family members aged greater than 75 years, having family members aged less than 12 years, and living with a family member who has a disability. Significant relationships were not observed for sex, type of building, number of floors in building, presence of basement in home, anxiety about safety of family members or houses during the heavy rain, cellular phone service provider, recognition of flood hazard map published by Nagoya City, and occupation.

Next, a model for forecasting DIRR was developed by logistic regression analysis. The explained variable was whether people received information just after the disaster. The categories of information that showed significant differences in the above analysis were tested as potential explanatory variables in "Excel Statistics 2012". Those variables found to have explanatory power were selected; these are shown in Table 1. The ratio of correct prediction with this model was 76.6%, tested by forecasting the target variable by using the model with the explanatory variables in Table 1 and comparing the result with the observed value. Taking this ratio and the values of Akaike's information criterion (AIC) and Nagelkerke's R^2 into account suggests that the chosen set of explanatory variables is appropriate.

Table 1: Obtained model of DIRR

Category	Items	Partial regression coefficient	Standard error	P Value	Definition
Information literacy	Experience receiving evacuation information	0.303	0.270	0.262	Dummy(0,1)
	Knowledge of emergency mail service	0.573	0.299	0.055	Dummy(0,1)
	Experience receiving messages from emergency mail service	0.252	0.127	0.047*	3 steps
	Frequency of using mails on cellular phones	0.359	0.139	0.010**	4 steps
	Understanding of evacuation information	0.496	0.147	0.001**	4 steps
Media	Start of using current cellular phones (before March 2011or after April 2011)	1.120	0.167	0.000**	3 steps
	At home at time of announcement	0.296	0.293	0.312	Dummy(0,1)
Family	Living with family member aged less than 12 years	0.506	0.297	0.088	Dummy(0,2)
	Living with family member aged greater than 75 years	−0.847	0.349	0.015*	Dummy(0,3)
Constant	–	−5.8922	0.8639	0.000**	
AIC=427.1, R^2=0.233, Nagelkerke's R^2=0.366					

4.2 Sensitivity analysis

Finally, a sensitivity analysis was conducted to evaluate how DIRR would be affected by future social change. By changing the values of explanatory variables in the model, their influence on DIRR was simulated.

As shown in Figure 2, DIRR just after the announcement of the evacuation preparation information was 51.8% in group A. Regarding their information literacy, 65.0% of the respondents answered that they were aware of emergency mail service to cellular phones from service providers before the heavy rain on 4 September among 425 respondents in group A. If awareness of this service were 100%, DIRR just after the announcement would increase by 5.8% in group A. This result suggests that DIRR could be increased by improving the public's knowledge through education and capacity building.

It was found that 59.6% of group A renewed their contract of using cellular phones after April 2011 among the people who answered. If this ratio were 100%, DIRR just after the announcement would increase by 7.0%. As mentioned before, some of older cellular phone models, especially those produced before 2011, cannot receive emergency mail from service provides. Therefore, it could be expected that DIRR will increase over time as new cellular phones replace older ones.

In group A, 14.7% lived with a family member aged greater than 75 years. Recently, the proportion of elderly people is increasing in Japan as the population ages and the birth rate declines. The proportion of elderly people in rural areas is further affected by depopulation as younger people move to cities. Nagoya City is one of three largest cities in Japan and is thus less affected by these trends. With respect to DIRR in rural areas, the effects of population aging should be considered since residents' behavior upon receiving disaster information is associated with whether they are elderly persons or not. In particular, if the percentage of people living with a family member aged greater than 75 years were increased by 20%, DIRR just after the announcement would decrease by 2.2%. This suggests that in rural areas today or in an aging society in the future, DIRR would be lower.

5. CONCLUSIONS

In this study, the disaster information reach ratio (DIRR) was proposed as an index for evaluating how widely various media can transmit disaster warnings and information to the public. This paper focused on the announcement of evacuation preparation information in all of Nagoya City at 5:10 p.m. on 4 September 2013 during torrential rain, and the DIRR was calculated using data collected through a questionnaire survey of people present in the city at that time.

DIRR just after the announcement was limited to about 50%. Among people who were indoors, the ratio did not differ by location. Among the various media for receiving information, emergency mail service to cellular phones from service providers had the highest DIRR. This shows that emergency mail service to cellular phones is becoming an effective tool for disaster information dissemination, and in this case, the DIRR of the emergency mail service was higher than that of loudspeakers, which are less useful during heavy rain.

To evaluate how DIRR would be affected under various scenarios of future social change, a model for forecasting DIRR was developed by logistic regression analysis. A sensitivity analysis revealed that increasing the public's knowledge and experience of receiving information and upgrading cellular phones could increase DIRR in the future.
Future studies should be conducted on DIRR in different types of disasters and in different locations. A limitation of the present study is that it considers only one type of disaster (torrential rain) in only Nagoya City, which may be representative of only urban areas. Sensitivity analysis showed the possibility that DIRR would become lower in rural areas and in an aging society. Further study of DIRR in rural area is therefore necessary. Also, the event considered here occurred around 5 p.m. on a weekday, so disasters occurring at various times of day and on various days of the week should be considered.

ACKNOWLEDGEMENT

This work was supported by JSPS Grant-in-Aid for Scientific Research(C) (KAKENHI) titled “Design of disaster information dissemination system supporting Asian farm and mountainous villages and proposal of strategy for technical assistance” (Grant Number 12345678).

REFERENCES

Ohara, M., 2014. Estimation of the effect of flood information dissemination by next-generation vehicle information and communication system, *The proceeding of the 34th annual conference of the Japan Society of Traffic Engineers*, 149-156.
Nagoya Local Meteorological Observatory, 2013, Meteorological news on torrential rain during September 4-5, 2013.

People with disabilities (PWD) and their functional needs during the Great East Japan Earthquake Disasters: The results from 2013 Sendai grass-root assessment workshop of PWDs

Shigeo TATSUKI
Professor, Department of Sociology, Doshisha University, Japan
statsuki@mail.doshisha.ac.jp

ABSTRACT

In order to identify functional needs of people with disabilities (PWD) during the 2011 East Japan Earthquake disasters, 41 impacted PWD and their supporters were invited to a grass-root assessment workshop on October 14th 2013. The workshop participants were from 16 different disability organizations for people with visual, auditory, speech, physical, mental, developmental/intellectual disabilities as well as for people with internal organ disorders and with paraplegia and quadriplegia. They were asked to report on post-it-cards what challenges and difficulties they encountered in each disaster process phase from 0 to 10 hours, 10 to 100, 100 to 1,000 and to 1,000 to 10,000hours after the 2011 disaster. Following the Total Quality Management method, the participants sorted/grouped the difficulty and challenge cards according to the affinity by themselves. Correspondence (dual scaling) analysis was introduced to analyze quantitatively the affinity association between disability categories and their corresponding difficulties. The results indicated that mobility was the critical ICF category during the first 10 hours, self-care and reasonable accommodations in attitudes of the society arose during the next 10 to 100 hours, domestic life tasks as well as utilizing services, systems and policies characterized the following 100 to 1,000 hours phase.

Keywords: people with disabilities, functional needs, the Great East Japan earthquake

1. INTRODUCTION

Japan is a country that is taking the lead in promoting evacuation and sheltering assistance for the elderly and PWD in times of disasters. In 2004, Japan experienced a series of natural disasters such as the Niigata-Fukushima flood (July), Typhoon Tokage (October), and the Niigata Chuetsu earthquake (October), in each of which higher mortality rates were recorded among the elderly and PWD. In response to these tragic results, the Japanese Cabinet Office established a committee on “Communication Disaster Information and Evacuation/Sheltering Assistance for the Elderly and Other Members of the Population during Heavy Meteorological and Other Disasters.” This committee published “Evacuation/Sheltering Assistance Guideline for People with Special Needs in Time of Disaster.” The committee continued working. So, they revised the guideline in 2006 and also published a report on the guideline in 2007. The term *saigai-jakusha* or disaster vulnerable people has been customarily used since the 1995

Kobe earthquake. The 2005 and the following committees coined the new term *saigaiji-youengosha* or “people with special needs in times of disaster.” This change was based on a paradigm shift in disability studies, from “medical model of disability” to “social model of disability” (e.g. Tatsuki, 2013).

The paradigm shift of disability studies has been made possible by the redefinition of disability by PDW themselves. The new definition of disability is based on the perspective that disability is socially constructed. The medical model of disability, an old paradigm, is a one way causal model. The individual physical condition (impairments) cause activity limitations and participation restrictions (disabilities), and these cause social disadvantages (handicaps.) The solution proposed by the medical model is medical intervention for individual impairments. The new social model, on the other hand, assumes interactive relationships between individual impairments and social factors. In other words, individual impairments do not lead to disabilities, and disabilities are caused by society when it fails to give reasonable accommodation to the needs of individuals with impairments. That being the case, society has a responsibility to relieve disabilities (e.g. Oliver, 1990; Hoshika, 2007). In the field of disaster research, only a very few studies focused on people with disabilities from this new social paradigm of disability (Tatsuki, 2013).

The International Classification of Functioning, Disability and Health (ICF) is an international standard to describe and measure health and disability based on the social model of disability (WHO, 2002). ICF was accepted by WHO in 2001 as a response to the paradigm shift in disability studies. In contrast to the International Classification of Impairments, Disabilities and Handicaps (ICIDH), ICF includes environmental factors and places more attention on the interactive relationships between individual impairments and social/environmental factors. By using ICF, it becomes possible to operationally specify what types of “special needs” the PWD experienced and more importantly what types of “functional supports” are needed in the interactive relationships between the PWD and their environment in times of disasters. This paper, therefore, proposes the term *saigaiji-seikatsu-kinou-youshiensha* or “people with functional needs in times of disasters” (Kailes and Enders, 2007) which is more operationally specific and therefore implementation-oriented rather than “disaster vulnerable people” which neglects the social interaction aspect of why disability is constructed or “people with special needs in times of disasters” which is more conceptually vague and thus less prescriptive to emergency actions.

The purpose of the current study is to collect the facts about the difficulties that the PWD experienced during the 2011 Great East Japan Earthquake Disaster and to analyze their functional needs from a social model of disabilities. The method of the study is qualitative and 41 PWD in Sendai city provided their life difficulty experiences in a TQM-style workshop and the workshop data was classified by ICF and by disaster time phase (Hayashi, 2003; Kimura et al., 2014). The “ICF category by disaster time phase” cross-tabulation table was then analyzed by dual scaling (also known as correspondence analysis) method (Nishisato, 1980), which yielded particular sets of a given disaster time phase and corresponding specific functional needs. The research findings indicated how PWD-in-environment interactions needed to be accommodated in order to support specific functional needs of PWD during each time phase.

2. METHOD

2.1 Participants

On October 14th 2013, a grass-roots assessment workshop was held in Sendai city. 41 PWD participated in the workshop and they were recruited from 16 different disability organizations catering for people with visual, auditory, speech, physical, mental, developmental/intellectual disabilities as well as for people with internal organ disorders and one for those suffering with paraplegia and quadriplegia. They were asked to report on post-it-cards what challenges and difficulties they encountered during each of the disaster time phases (Hayashi, 2003; Kimura et al., 2014) from 0 to 10 hours, 10 to 100, 100 to 1,000 and to 1,000 to 10,000 hours after the Great East Japan Earthquake. Following the Total Quality Management method that was originally introduced in life recovery assessment workshops for the 1995 Kobe earthquake survivors, ideas and opinions were sorted according to their affinity.

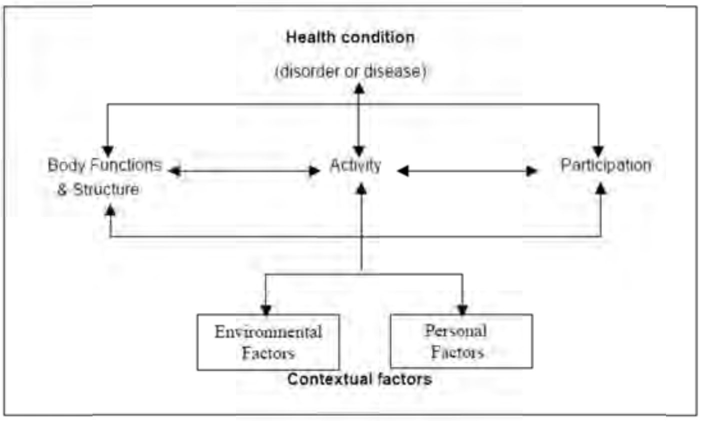

Figure 1: Conceptual diagram of ICF (Source: WHO (2002))

2.2 Instrument

ICF is a classification of health and health-related domains as shown in the Figure 1 and is the international standard to describe and measure health and disability (WHO, 2002). Based on the social model of disability, ICF views disability and functioning as outcomes of interactions between health conditions and contextual factors that include environmental and internal personal factors. ICF identifies three levels of human functioning at the level of body (physiological functioning and impairments), the whole person (activity, activity limitation participation and participation restriction), and the whole person in a social context (physical, social and attitudinal environment). As an measurement instrument, ICF postulates 4 constructs (or domains) such as Body Functions (b), Body Structure (s), Activity and Participation (d), and Environmental Factors (e), each of which is operationally defined in a hierarchical fashion (e.g., Chapter, Second level, Third level, and Fourth level). Table 1 illustrates the complete list of chapters in ICF. For this study, each statement that the workshop participants produced was viewed from the ICF framework and was coded at all four levels. For more detailed definitions of all ICF definitions, please refer to ICF illustration library (http://www.icfillustration.com/icfil_eng/top.html).

Table 1: Chapters of ICF (Source: WHO (2002))

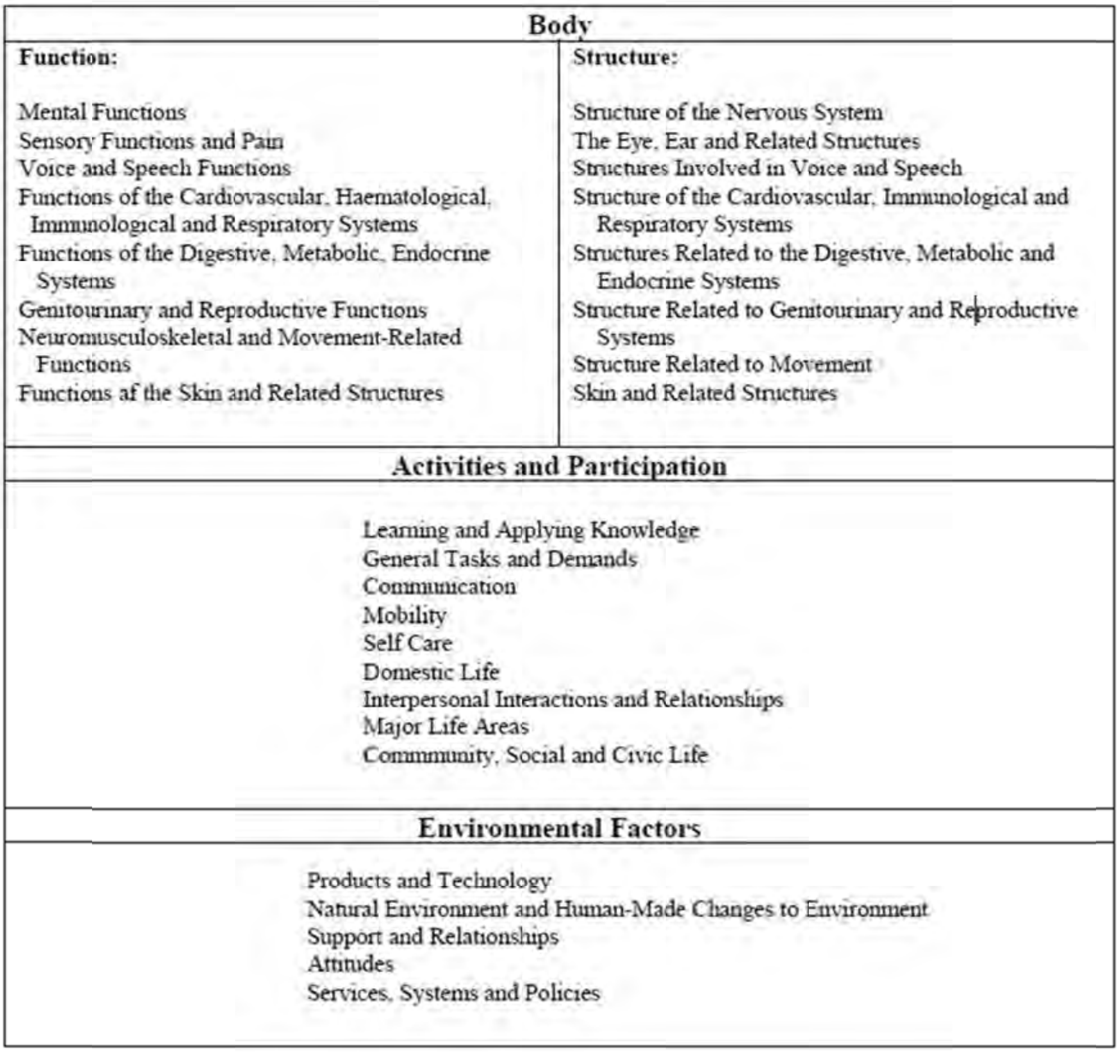

<table>
<tr><th colspan="2">Body</th></tr>
<tr><td>Function:</td><td>Structure:</td></tr>
<tr><td>Mental Functions
Sensory Functions and Pain
Voice and Speech Functions
Functions of the Cardiovascular, Haematological, Immunological and Respiratory Systems
Functions of the Digestive, Metabolic, Endocrine Systems
Genitourinary and Reproductive Functions
Neuromusculoskeletal and Movement-Related Functions
Functions af the Skin and Related Structures</td><td>Structure of the Nervous System
The Eye, Ear and Related Structures
Structures Involved in Voice and Speech
Structure of the Cardiovascular, Immunological and Respiratory Systems
Structures Related to the Digestive, Metabolic and Endocrine Systems
Structure Related to Genitourinary and Reproductive Systems
Structure Related to Movement
Skin and Related Structures</td></tr>
<tr><th colspan="2">Activities and Participation</th></tr>
<tr><td colspan="2">Learning and Applying Knowledge
General Tasks and Demands
Communication
Mobility
Self Care
Domestic Life
Interpersonal Interactions and Relationships
Major Life Areas
Commmunity, Social and Civic Life</td></tr>
<tr><th colspan="2">Environmental Factors</th></tr>
<tr><td colspan="2">Products and Technology
Natural Environment and Human-Made Changes to Environment
Support and Relationships
Attitudes
Services, Systems and Policies</td></tr>
</table>

2.3 Procedure

The workshop data was classified by ICF and by disaster time phase. This produced an “ICF category by disaster time phase” cross-tabulation table. The association among the table row and column categories was then quantitavely analyzed by dual scaling (also known as correspondence analysis) method (Nishisato, 1980), a technique for performing quantification based on the principle of internal consistency.

3. RESULTS

3.1 ICF-by-Disaster Time Phase Cross-tabulation

41 grass-roots assessment workshop participants produced 429 statements regarding their experienced life difficulties after the onset of the Great East Japan Earthquake. These statements were first categorized into one of the disaster time phases by the workshop participants themselves. They were then brought back to the laboratory and was coded in terms of ICF categories. Table 2 shows frequencies of ICF category (Chapter and Second level) by time phase. It was revealed that life difficulties that PWD

experienced peaked during the first 100 hours (about 70% of all the reported difficulties) and lasted about 1,000 hours (90 % of difficulties collected at the workshop). This suggested that PWD life difficulty experiences during the disaster time approximately corresponded to the time phase when basic functioning of the society had been impacted by the disaster until emergency relief activities helped recover the essential utility, transportation and other critical facility basic functioning that took approximately 1,000 hours.

It became clear that PWD did not experience whole range of ICF category-related difficulties equally but specific category-related difficulties were experienced more often than the other. The current study found that all the reported difficulties were classified either in the domain of Activities and Participation or Environmental Factors. The four most reported difficulties in activities and participation were in the area of “d6 Domestic Life” (30%) (e.g., acquisition of necessities, household tasks, and caring for household objects), “d5 Self-Care” (13%) (e.g., washing oneself, caring for body parts, toileting, dressing, eating, drinking and looking after one’s self), and “d2 General Tasks and Demands” (9%) (e.g., undertaking a single and multiple tasks, daily routine and holding stress and other psychological demands), and “d4 Mobility” (4%) (e.g., changing and maintaining body position, carrying, moving and handling objects, walking and moving, and moving around using transportation). Within the environment factors, the top three most reported life functioning needs were “e1 Products and Technology” (19%) (e.g., medicines, equipments for personal daily living and mobility, and products and technology for communication), “e5 Services, Systems and Policies” (13%) (e.g., utilities, services for communication, transportation, civil protection, legal and administrative applications, social security, general social support, and health), and “e3 Supports and Relationships” (8%) (e.g., family, friends, neighbors, personal care providers, strangers, health and other professionals).

Table 2: Grass-roots assessment workshop results: ICF category by disaster phase

	Disaster Time Phase				
ICF Category	**0hr - 10hr**	**10hr - 100hr**	**100hr - 1,000hr**	**1,000hr -**	**Row Total (%)**
d1Learning and Applying Knowledge	0	1	0	0	1 (0.2%)
d2 General Tasks and Demands	12	11	7	9	39 (9.1%)
d3 Communication	0	2	1	1	4 (0.9%)
d4 Mobility	13	3	0	2	18 (4.2%)
d5 Self-Care	8	31	15	3	57 (13.3%)
d6 Domestic Life	31	50	33	12	126 (29.4%)
d7 Interpaersonal Interactions and Relationships	1	0	0	0	1 (0.2%)
d8 Major Life Areas	0	0	3	1	4 (0.9%)
d9 Community, Social and Civic Life	0	0	0	1	1 (0.2%)
e1 Products and Technology	30	37	13	0	80 (18.6%)
e2 Natural Environment and Human-Made Changes to Environment	1	0	0	0	1 (0.2%)
e3 Support and Relationships	12	9	8	4	33 (7.7%)
e4 Attitudes	1	3	3	0	7 (1.6%)
e5 Services, Systems and Policies	6	25	17	9	57 (13.3%)
Column Total	115	172	100	42	429
(%)	(27%)	(40%)	(23%)	(10%)	

3.2 Correspondence Analysis of the ICF-by-Disaster Phase Cross-tabulation Table

Correspondence (dual scaling) analysis was employed to analyze quantitatively more intricate associations among ICF categories and disaster time phases by identifying the most characteristic associations of the row and column categories of the cross-tabulated data. For example, ICF category of “d4 Mobility” accounted for less than 5 % out of all the reported difficulties (i.e., 18/429). However, it accounts for more than 10 % of the ICF categories if one focuses only to the first 10 hours (13/115). This suggests that there may exist a characteristic relationship between the row category (d4 Mobility) and the column category (0hr to 10 hour). Correspondence analysis produces a two-dimensional plot (or biplot) of row and column category of cross-tabulation data where those characteristic or corresponding row and column categories are placed in proximity in usually a 2 dimensional space (Nishisato, 1980).

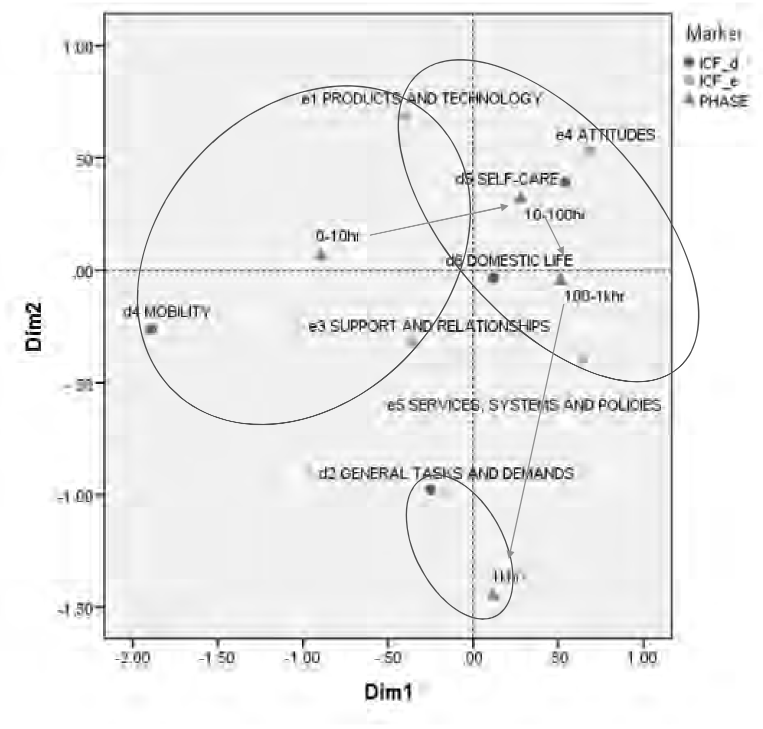

Figure 2: Corresponding analysis results of ICF-by-time phase cross-tabulated data

Note: Those categories with low frequencies (i.e., less than 1 %) were excluded from the analysis for robustness and stability of the analysis results.

The result of the correspondence analysis is shown in the above Figure2 where 1) four time phases and corresponding ICF category sets were clustered into three groups and 2) characteristic ICF and disaster time phase correspondences were revealed. First of all, the left side cluster shows the most characteristic ICF categories that appeared within the first 10 hours after the earthquake and it included “d4 Mobility”, “e1 Products and Technology”, and “e3 Support and Relationships.” The most life-threatening needs that PWD experienced in this phase were that of mobility. In normal circumstances, PWD can rely on cars, wheel chairs, and other equipments for transportation with the support from family members and their care workers. Most PWD, however, were not able to find the support from the immediate relationships and thus were not able to evacuate to nearby shelters. If they were able to elicit extra help from neighbors and even strangers for mobility support and to move to shelters, they faced life difficulties due to the lack/unavailability of “e1 Products and Technology” such as medicines, equipments for personal daily living and mobility, and products and technology for communication.

The right upper area shows the cluster consisting of two disaster time phases of 10 to 100 hours as well as that of 100 to 1,000 hours. These time phases corresponded with that of sheltering (10 to 100 hours) and of living a life when lifeline and other basic critical facilities were not functioning at normal level. The 10 to 100 hours phase was first typified by “d5 Self-Care” difficulties which included washing oneself, caring for body parts, toileting, dressing, eating, drinking and looking after one’s self either at the shelter or at their disaster affected home. These difficulties were accompanied by the continuing lack/unavailability of “e1 Products and Technology” such as medicines, equipments for personal daily living and mobility, and products and technology for communication. The life conditions of PWD were further aggravated by the lack of reasonable accommodation from “e4 Attitudes” in family members, friends, neighbors, shelter authority, personal care providers, strangers, health professionals, society and social norms.

The succeeding 100 to 1,000 hours phase was characterized by gradual re-entry into post-disaster normalcy where PWD faced daily chores associated with “d6 Domestic Life” that included acquisition of necessities, household tasks, and caring for household objects and those with “e5 Services, Systems and Policies” (e.g., utilities, services for communication, transportation, civil protection, legal and administrative applications, social security, general social support, and health).

The right lower cluster was characterized by the time phase of 1,000 hours and over and “d2 General Tasks and Demand” which mainly consisted of handling stress and other psychological demands in post-disaster recovery time.

5. CONCLUSION

This study showed how society and PWD themselves needed to handle the situation that PWD faced in each time phase. First, it is indicated that during the first 10 hours, society in collaboration with PWD and their families need to activate Mobility assistance plans that would help PWD to a nearby safer environment including the designated shelter. The evacuation assistance plan should also enumerate a list of accompanying necessity Products and Technology such as medicines, equipments for personal daily living and mobility, and products and technology for communication. Due to the fact that the participated PWD were not able to rely on regular service and care personnel for the mobility assistance, it is also important to build an alternative Support and Relationships in the neighborhood community. Second, sheltering assistance plans need to be activated in the 10 to 100 hours time phase. Such Self-Care needs as washing oneself, caring for body parts, toileting, dressing, eating, drinking and looking after one’s self are critical in this period and therefore the matching reasonable accommodations need to be arranged at every designated shelter. Third, 100 to 1,000 hours phase is characterized by gradual re-entry into post-disaster normalcy when PWD face the tasks associated with Domestic Life such as acquisition of necessities, household tasks, and caring for household objects. It is expected that a large number of disaster volunteers could be coordinated in order to respond to these needs. Third, specific needs that require expert and professional assistance also arise during the same phase for utilizing Services, Systems and Policies in utilities, services for communication, transportation, civil protection, legal and administrative applications, social security, general social support, and health. Professional volunteer and other outside experts/professionals could be mobilized to respond to these needs. Fourth, the phase over 1,000 hours is characterized by such General Tasks and Demands as handling the continuing stress and other demands in post-disaster recovery time. Traumatic stress prevention programs that focus on PWD may need to be prepared.

Last, it is essential that the above indicated solutions need to be pre-planned before the next disaster hit the society.

ACKNOWLEDGMENTS

This research was supported by RISTEX, JST.

REFERENCES

Hayashi, H., 2003. *Life saving earthquake disaster management (in Japanese)*. Iwanami, Tokyo.

Hoshika, R., 2007. *What is disability*, Seikatsu-Shoin, Tokyo (in Japanese).

Kailes, J. I., and Enders, A., 2007. A function-based framework for emergency management and planning, *Journal of Disability Policy Studies*, 17, 230–237.

Kimura, R., Tomoyasu, K., Yajima, Y., Mashima, H., Furukawa, K., Toda, Y., Watanabe, K., and Kawahara, T., 2014. Current status and issues of life recovery process three years after the Great East Japan Earthquake questionnaire based on subjective estimate of victims using life recovery calendar method, *Journal of Disaster Research*, 673-689.

Nishisato, S., (1980. *Analysis of categorical data: Dual scaling and its applications,* University of Toronto Press, Toronto.

Oliver, M., 1990. *The politics of Disablement*, Macmillan, London, UK.

Tatsuki, S., 2013. Old age, disability, and the Tohoku-Oki Earthquake. *Earthquake Spectra* 29, S403–S432.

World Health Organization, 2002. Towards a common language for functioning, disability and health: ICF The International Classification of Functioning, Disability and Health (http://www.who.int/classifications/icf/icfbeginnersguide.pdf?ua=1, accessed on October 27, 2014).

International tourists as a vulnerable population during disaster events in Japan

Michael HENRY[1] and Akiyuki KAWASAKI[2]
[1]Assistant professor, Division of Field Engineering for the Environment,
Faculty of Engineering, Hokkaido University, Japan
mwhenry@eng.hokudai.ac.jp
[2]Project associate professor, Department of Civil Engineering,
The University of Tokyo, Japan

ABSTRACT

The international tourism industry in Japan has experienced significant growth over the past 20 years – growth that is expected to continue in light of Tokyo's selection as the host city for the 2020 Summer Olympics. International tourists, however, are sensitive to issues such as safety, and Japan has a high probability of being struck by future earthquakes, which could disrupt the Olympics and severely affect the image of Japan as a tourism destination. It is thus necessary to consider international tourists in efforts to improve disaster response and resilience. This paper first summarizes historical trends in international tourism in Japan, and then identifies issues that need to be considered when addressing international tourism in disaster mitigation and response.

Keywords: international tourists; 2011 Great East Japan Earthquake; Tokyo Inland Earthquake; 2020 Tokyo Olympics; tourism economy

1. INTRODUCTION

International tourism in Japan has historically been much smaller than in other major developed countries, such as the United States or France, and has played only a small role in the development of Japan's economy. However, with the awarding of the 2020 Summer Olympics to Tokyo, the international tourism industry may be one potential area of future growth. Even before the awarding of the Olympics, the Japanese government had already announced plans to more than double the number of international tourists, from the 2012 level of 8.71 million to 20 million, by 2017 (The Asahi Shimbun, 2013).

Unfortunately, Japan's disaster hazards – which include earthquakes, tsunamis, typhoons, floods, and volcanic eruptions – are well known and threaten the image of Japan as a tourist destination. This problem was highlighted by the 2011 Great East Japan Earthquake, and the subsequent tsunami and nuclear crisis, after which there was a significant drop in international tourist arrivals. Although tourist numbers rebounded in subsequent years and even reached new milestones (as will be introduced later), disaster hazard is ever-present – including, most notably, the Tokyo Inland Earthquake, which has a 70% chance of striking within the next 30 years (Cabinet Office, 2012) and could catastrophically disrupt the 2020 Summer Olympics. Man-made disasters are also a threat, as the possibility of terrorism during the Olympics has always been high due to the event's visibility (START, 2012). As a result, host countries must prepare for a wide variety of scenarios, both natural and man-made.

One of the eight goals of the Tokyo Vision 2020, a plan developed by the Tokyo metropolitan government to clarify its future vision and policy direction, is to "achieve a sophisticated disaster resistant city and demonstrate Tokyo's safety to the world" (Tokyo Metropolitan Government, 2011). While the sub-projects of this goal focus on structural aspects such as seismic retrofitting and fire control, as well as non-structural aspects such as community disaster units and ordinances for stranded people, there is no mention of how Japan intends to address the needs of international tourists in the event a disaster strikes. It is therefore highly important that Japan include international tourists in its efforts to improve disaster resilience and response, both for the 2020 Summer Olympics and beyond. In this paper, the recent history of international tourism in Japan is first examined to understand the underlying situation and trends. Issues related to international tourists in disasters situations are then identified considering the disaster cycle, with a focus on the mitigation and emergency response phases.

2. INTERNATIONAL TOURISM IN JAPAN

2.1 Comparison at the global level

As an international tourist destination, Japan sits relatively low compared to other developed countries. As shown in Figure 1, Japan ranked 31st in the world in terms of international arrivals in 2012, and 8th in the Asian region behind developing countries such as China, Malaysia, and Thailand. In these figures, the term "international arrivals" is defined as "the number of tourists who travel to a country other than that in which they have their usual residence, but outside their usual environment, for a period not exceeding 12 months and whose main purpose in visiting is other than an activity remunerated from within the country visited" (World Bank, 2014a).

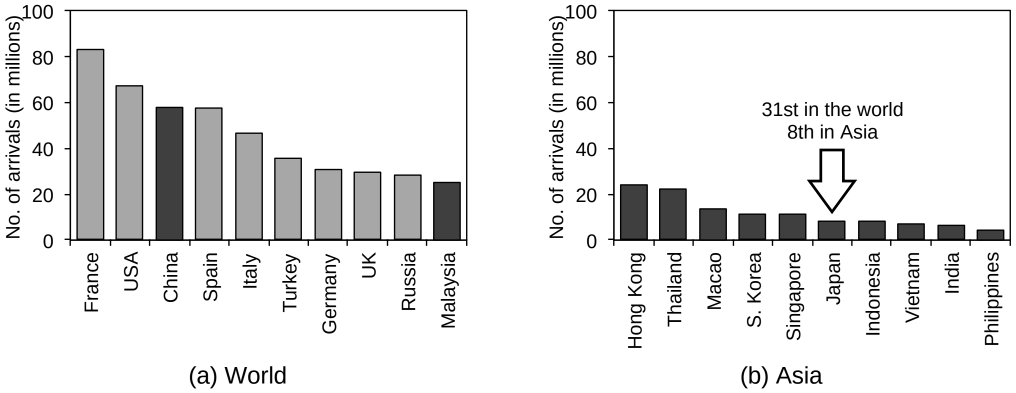

(a) World (b) Asia

Figure 1: Top-ten rankings of the number of international arrivals for the world and Asian region in 2012 (data source: World Bank, 2014a)

2.2 Trends by country of origin

Figures 2 and 3 explore the historical data on international tourists visiting Japan in greater detail. It should be noted that, unlike the previous results on the number of international arrivals, the data given in Figures 2 and 3 are for international arrivals who specified their purpose was “tourism;” therefore, these numbers are lower than the total number of international arrivals, which includes those whose purpose was “business” or “other.”

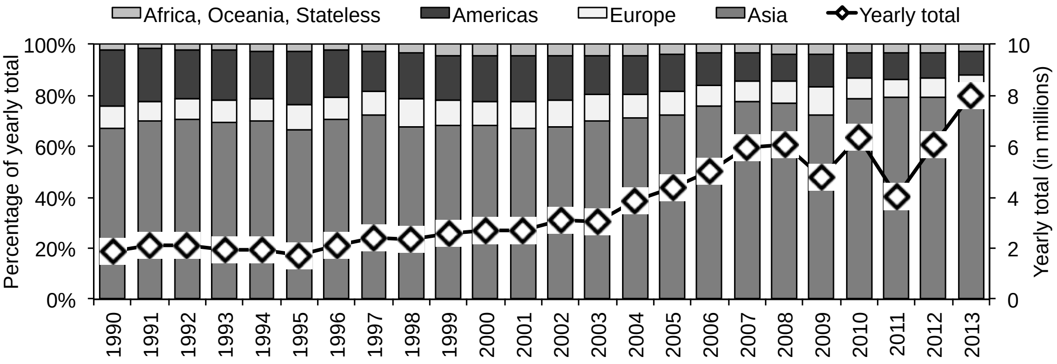

Figure 2: Total number of international tourists visiting Japan from 1990 to 2013 and the percentage share by world region (data source: JNTO, 2014; JTMC, 2014)

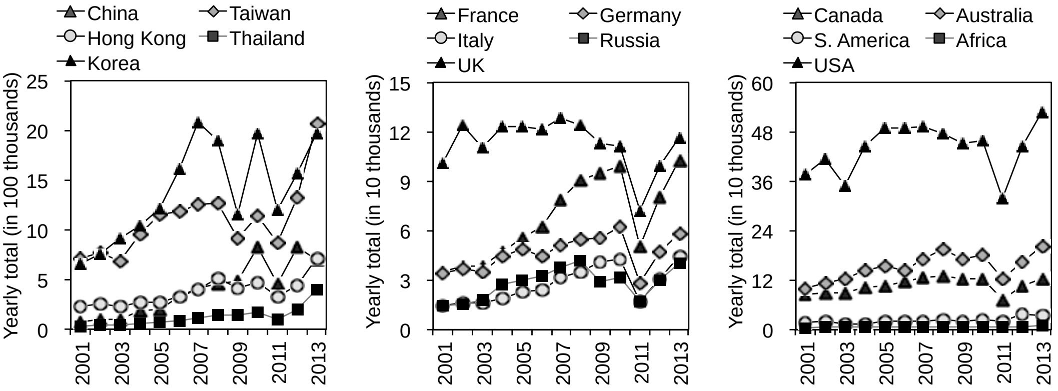

(a) Asia (b) Europe (c) Others

Figure 3: Number of international tourists visiting Japan from 2001 to 2013 by region and country of origin (data source: JNTO, 2014; JTMC, 2014)

From 1990 to 2001, the yearly total number of international tourists increased by 45%. However, between 2001 and 2008, the yearly total increased by 123% to more than 6 million international tourists. This number dropped the following year due to the financial crisis triggered in the US in 2007-2008, but recovered in 2010. In March 2011, the Great East Japan Earthquake occurred and, as a result, the yearly total dropped significantly. By 2013, however, the total number of international tourists rebounded and reached a new high that represented an increase of 96% over the 2011 value in just a two-year period.

The percentage share of international tourists coming from Asia has been steadily increasing, with a corresponding decrease in the share of tourists coming from the Americas and Europe. In 1990, 67% of international tourists were from Asia and 22% were from the Americas; however, by 2013 the percentage share from Asia increased to 81% and the share from the Americas decreased to just 9%. Over the same period, the share from Europe fluctuated but only decreased by roughly 2%.

The change in percentage share is generally not due to a decrease in tourists from North America or Europe. Rather, as shown in Figure 3, it can be understood that there has been greater relative growth in tourists from the Asian region. Tourists from South Korea and Taiwan increased by 202% and 192%, respectively, from 2001 to 2013 and, in 2013, roughly half of all international tourists were from just these two countries. Even more notable growth can be seen for China and Thailand, as the number of Chinese and Thai tourists increased by a massive 877% and 1,220%, respectively, from 2001 to 2013. Over the same 13-year period, however, tourists from the US and Canada increased by only 40% and 44%, respectively. The UK has historically been the largest European source of international tourists; however, there was only a 15% increase in UK tourists from 2001 to 2013. Other European countries have shown notably greater growth than the UK: 195% from France, 212% from Italy, and 177% from Russia.

2.3 Trends by destination within Japan

Where do international tourists go once they have arrived in Japan? The Japan Tourism Agency has been carrying out an accommodation survey quarterly from 2007 that investigates where international tourists stay during their visit. While not a direct indicator of the number of tourists visiting a prefecture or area (as tourists may conduct day trips that do not involve an overnight stay), these results give some indication of where international tourists are traveling to by means of where they are staying. From 2007 to the first quarter of 2010 (Jan. to March), the survey only collected data from accommodation facilities with 10 or more employees; however, from the second quarter of 2010 onwards, the survey was expanded to include facilities with fewer than 10 employees. In this paper, only the results for accommodation facilities with 10 or more employees are reported.

Figure 4 summarizes the percentage share of international tourists spending the night ("overnight lodgers") by region of Japan. The Kanto region, which consists of the greater Tokyo metropolitan area as well as surrounding prefectures such as Kanagawa and Chiba, hosted between 40% to 50% of international overnight lodgers from 2007 to 2013 period. The second most popular area was the Kinki region, which includes Osaka and Kyoto. This region has experienced some growth in the percentage share of international overnight lodgers, from 18% in 2007 to 23% in 2013. Other regions of Japan have only experienced small changes in their percentage share of international overnight lodgers – except for Okinawa, which has grown from 1% to 5% over the 7-year observation period.

The yearly total for international overnight lodgers for selected areas is shown in Figure 5. Although there are 47 prefectures in Japan (including Tokyo, which is designated not as a prefecture but as a metropolis), these top nine areas represent more than 75% of the yearly total of international overnight lodgers for each of the observed years. The Tokyo metropolis was the top location for international tourists to stay in 2013, followed by Osaka and Hokkaido. While all of the selected areas have shown growth over the observed period, the largest amount of growth was in Okinawa, where the number of international overnight lodgers increased by 509% in just 7 years, followed by Kyoto at 145%. Osaka, Hokkaido, and Fukuoka have also seen gains of between 49% and 63%, whereas Aichi – home to Nagoya city – only increased by 9%.

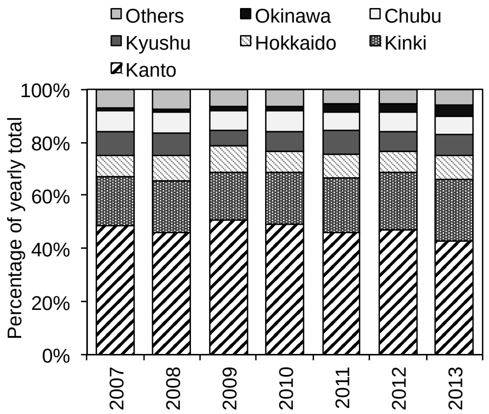

Figure 4: Percentage share of international overnight lodgers from 2007 to 2013 by region (data source: JTA, 2014a)

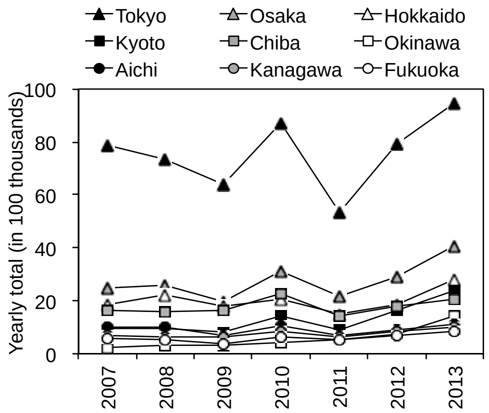

Figure 5: Number of international overnight lodgers from 2007 to 2013 for the top nine prefectures or areas as of 2013 (data source: JTA, 2014a)

2.4 Economic aspect of international tourism

In order to understand the economic aspect of international tourist-related activities, data on international tourism receipts were examined (Figure 6). This term is defined as "expenditures by international inbound visitors, including payments to national carriers for international transport" (World Bank, 2014b). The international tourism receipts as a percentage of GDP were also calculated to provide a frame of reference to the scale of tourism activities relative to the nation's total economic output.

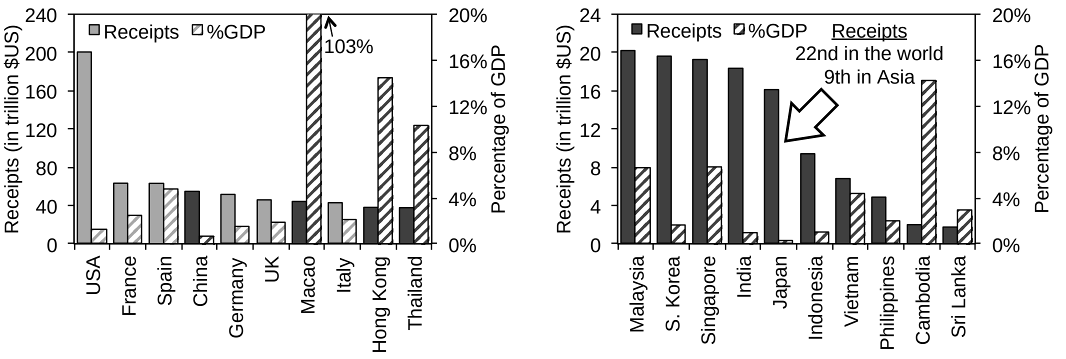

(a) World (b) Asia

Figure 6: Top-ten rankings of the receipts from international tourism (in current $US) for the world and the Asian region in 2012 and the receipts' percentage of 2012 GDP (data source: World Bank, 2014b; World Bank, 2014c)

Japan's international tourism receipts ranked 22nd in the world in 2012, and was only 8% of the receipts of the USA. China, Macao, Hong Kong, and Thailand also ranked in the top-ten globally, whereas Japan was ranked ninth in Asia. International tourism receipts were only 0.3% of Japan's GDP in 2012, which is much lower than tourist-oriented developing economies such as Thailand, Malaysia, Vietnam, or Cambodia, and still lower than similarly developed countries such as the USA, France, Germany and the UK.

Overall, international tourism is still a relatively small industry in Japan – both in terms of people and economics – compared to domestic tourism (Japanese citizens traveling within Japan). International tourists traveling in Japan contributed to only 4.6% of the domestic tourism market in 2009 (JTA, 2013), with Japanese citizen's domestic travels making up 89.5% of the market.

3. INTERNATIONAL TOURISTS AND DISASTER EVENTS

3.1 Are international tourists a vulnerable population?

The review of past and current trends in international tourism in Japan provided valuable information on who is coming to Japan and where they are going. Such information is necessary when considering how best to address the needs of international tourists as a vulnerable population before, during, and after a disaster event. However, a more fundamental question is whether international tourists actually qualify as a vulnerable population that requires special attention.

Gómez (2013) provided an overview of issues regarding international students as a vulnerable population in their study after the 2011 Great East Japan Earthquake, in which they made some comparisons between international students and international tourists. In that overview, several launching points for understanding the vulnerability of international tourists were mentioned. The first is "foreignness:" that is, international tourists are more vulnerable due to their unfamiliarity with the local language, customs, culture, and so forth. From this perspective, tourists in Japan are placed in the same category as international residents in Japan. This presumes that the category "foreigners" is homogeneous, and reflects the "us" (Japanese) and "them" (non-Japanese) mentality that is well ingrained in Japan. Previous research has demonstrated, however, that international residents in Japan are a highly heterogeneous group, and the support they may require after a disaster relies on more than assumptions based on their "foreignness" (Kawasaki et al., 2012; Henry et al., 2012; Kawasaki et al., 2013). In addition, the perception of disaster risk has been shown to vary widely even among international tourists (Seabra et al., 2013). Therefore, while international tourists may indeed be considered a vulnerable population, the basic fact of their "foreignness" is not the only factor that needs to be considered.

Another point is "transience:" that is, international tourists are only in Japan for a relatively short time, are mobile, and are less likely to have ties to the areas they are visiting or personal relationships with Japanese people. The last point is of particular importance, as it was found that having a strong support network and close ties with Japanese people was one means by which international students at Tohoku University in Sendai, Japan, coped with and responded to the 2011 Great East Japan Earthquake (Gómez, 2013). For international tourists, one method for evaluating their "local ties" may be via where they are staying, as international tourists exhibit different attitudes towards risk depending on whether they are staying at a hotel or with family or friends (Drabek, 1999).

There may be other perspectives for clarifying the vulnerability of international tourists, but the points summarized here provide some evidence in support of classifying international tourists as a vulnerable population in Japan. However, the issue is complicated by the heterogeneity of the "international" population.

3.2 Proposing measures using the disaster cycle

For improving the perception of Japan as an international tourist destination, there are several measures that can be taken that follow the spirit of Tokyo Vision 2020 to "demonstrate Tokyo's safety to the world." The disaster cycle (Figure 7) was used to identify the specific areas where action may be taken. Among these phases, it is proposed that "Mitigation" and "Emergency response" are the most relevant for international tourists. Details of these two phases will be discussed in the following sections.

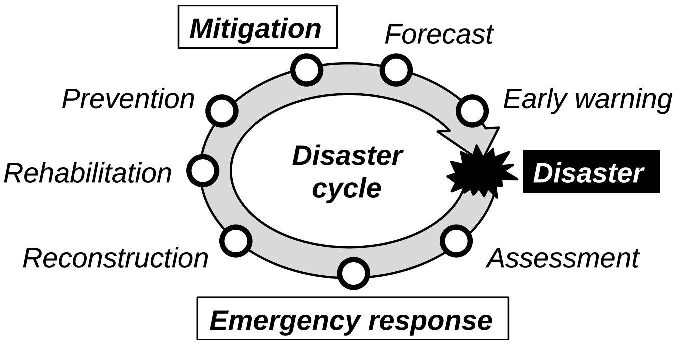

Figure 7: The disaster cycle with highlighted target phases

3.3 Resilience building in the mitigation phase

A wide variety of activities are encompassed by the mitigation phase, the goal of which is to minimize the effects of a disaster. Mitigating the effects of a disaster on international tourists can be separated into two approaches: measures that should be carried out by stakeholders in Japan, such as structural retrofitting; and measures that should be carried out by the tourists themselves, such as increasing their awareness through education. The former is already being targeted and carried, as outlined by the Tokyo Vision 2020. The latter, however, needs to receive greater consideration.

As discussed previously, disaster risk awareness varies widely among international tourists. It is thus necessary to consider how to effectively educate international tourists – taking into account their diversity – in order to build their resilience against a disaster, should one occur during their time in Japan. This is complicated by their short period of time in Japan and the desire of international tourists to get the greatest value out of their time. Educational campaigns targeting tourists interested in coming to Japan may be one possibility to address this issue; however, such campaigns may also have the negative effect of scaring away some tourists whose awareness is low. Finding an effective balance between these two aspects is therefore key to improving tourists' resilience.

3.4 Post-disaster support during the response phase

The response phase is concerned with how to provide the proper support for international tourists in a post-disaster situation. The importance of considering such support was previously observed in the aftermath of the 2004 Indian Ocean tsunami in

Thailand, when the large number of international tourists affected by the tsunami placed a huge strain on the limited local resources that were available at the time (Deebaj et al., 2011).

A first step is to understand the legal situation regarding international tourists, in order to clarify who is responsible for them and what rights they have after a disaster. For example, after the 2011 Great East Japan Earthquake, Tohoku University served as a major source of support for the affected international students (Gómez, 2013). The large number of foreign embassies active in disseminating information and giving advisories to their citizens in Japan is another example (Kawasaki et al., 2012). However, at that time the direct impact to international tourists was relatively small, as the affected areas along the Pacific coastline in the Tohoku region are not major destinations. If such a large earthquake were to occur in Tokyo itself, the number of international tourists requiring direct assistance would be much higher, and the burden carried by local governments and organizations may increase accordingly.

The dissemination of disaster information is another important point for supporting post-disaster response. Timely and relevant disaster information is necessary in order to support people’s decision making and for them to stay abreast of developing situations. Kawasaki et al. (2011) previously examined how differences in the Japanese and English language ability of international residents living in Japan at the time of the 2011 Great East Japan Earthquake affected their ability to gather information. It was found that people unskilled in Japanese could still acquire information from Japanese sources via three methods: from the national broadcaster’s (NHK) English-language translations and programs; from third-party translations of Japanese documents provided online; and by translating Japanese text themselves using translation tools. However, the quality of the first- and third-party translations is questionable and may have varied widely, thus demonstrating the importance of greater information dissemination in languages other than Japanese.

An additional point to consider regarding the implementation of support frameworks is the difference between international tourist destinations within Japan. For example, major tourist spots in Hokkaido – the third-largest destination – are generally in the countryside, with few international residents in those areas. This is in contrast to other major destinations such as Tokyo, Osaka, Kyoto, and Chiba, where the local international populations are much larger. As a result, these areas may be more experienced and better prepared for supporting international tourists after a disaster.

4. CONCLUSION

Following the intent of Tokyo Vision 2020 to create and demonstrate a safe Japan to the world, it is important to consider and prepare specific measures for supporting international tourists in disaster situations. After reviewing recent trends in international tourism in Japan, this paper proposed that consideration of international tourists should focus on the mitigation and response phases of the disaster cycle. Continued research, however, is necessary to better understand the specific needs of international tourists. The first step should be to clarify the similarities and difference between international tourists and short- and long-term international residents in Japan, as there may be overlap in these areas – specifically with regards to post-disaster support.

ACKNOWLEDGEMENT

This research was partially supported by the Japan Society for the Promotion of Science (Challenging Exploratory Research: "*Investigation on disaster information dissemination to foreigners after the great earthquake in the Tokyo metropolitan area*").

REFERENCES

Cabinet Office, Government of Japan, 2012. Counter-measures for the Tokyo metropolitan earthquake (in Japanese). http://www.bousai.go.jp/jishin/syuto/index.html (accessed Oct. 14, 2014)

Deebaj, R., Castrén, M., Öhlén, G., 2011. Asian tsunami disaster 2004: experience at three international airports. *Prehospital and disaster medicine* 26, 71-78.

Drabek, T.E., 1999. Understanding disaster warning responses. *The Social Science Journal* 36, 515-523.

Gómez, O.A., 2013. Lessons from international students' reaction to the 2011 Great East Japan Earthquake: the case of the School of Engineering at Tohoku University. *International Journal of Disaster Risk Science* 4, 137-149.

Henry, M., Kawasaki, A., Meguro, K., 2012. Foreigners' post-disaster relocation or evacuation from Japan and their disaster information gathering behavior after the 2011 Great East Japan Earthquake. *Journal of Social Safety Science* 18, 373-380 (in Japanese).

Japan National Tourism Organization (JNTO), 2014. Tourism statistics. https://www.jnto.go.jp/eng/ttp/sta/ (accessed Oct. 14, 2014)

Japan Tourism Marketing Co., 2014. Tourism statistics. http://www.tourism.jp/en/statistics/ (accessed Oct. 14, 2014)

Japan Tourism Agency (JTA), 2013. General information of tourism statistics in Japan. http://www.mlit.go.jp/kankocho/en/kouhou/general.html (accessed Sept. 8, 2014)

Japan Tourism Agency (JTA), 2014a. Accommodation survey (in Japanese). http://www.mlit.go.jp/kankocho/siryou/toukei/shukuhakutoukei.html (accessed Sept. 5, 2014)

Japan Tourism Agency (JTA), 2014b. Consumption trend survey for foreigners visiting Japan (in Japanese). http://www.mlit.go.jp/kankocho/siryou/toukei/syouhityousa.html (accessed Sept. 5, 2014)

Kawasaki, A., Henry, M., Meguro, K., 2012. Disaster information collection of foreigners after the 2011 Great East Japan Earthquake considering the difference in language ability. *Journal of Social Safety Science* 18, 381-390 (in Japanese).

Kawasaki A., Henry, M., Meguro, K., 2013. Advisories by foreign governments and the behavior of foreigners residing in Japan after the 2011 Great East Japan Earthquake. *Journal of Social Safety Science* 21, 219-227 (in Japanese).

The Asahi Shimbun, 2013. Government aims to double foreign visitor numbers by 2017. http://ajw.asahi.com/article/behind_news/politics/AJ201305110055 (accessed Oct. 7, 2014)

Seabra, C., Dolnicar, S., Abrantes, J.L., Kastenholz, E., 2013. Heterogeneity in risk and safety perceptions of international tourists. *Tourism Management* 36, 502-510.

START (National Consortium for the Study of Terrorism and Responses to Terrorism), 2012. Terrorism and the Olympics. http://www.start.umd.edu/sites/default/files/files/publications/br/TerrorismAndOlympics.pdf (accessed Oct. 14, 2014).

The World Bank, 2014a. Data: International tourism, number of arrivals. http://data.worldbank.org/indicator/ST.INT.ARVL (accessed Sept. 5, 2014)

The World Bank, 2014b. Data: International tourism, receipts (current US$). http://data.worldbank.org/indicator/ST.INT.RCPT.CD (accessed Sept. 5, 2014)

The World Bank, 2014c. Data: GDP (current US$). http://data.worldbank.org/indicator/NY.GDP.MKTP.CD (accessed Sept. 5, 2014)

Tokyo Metropolitan Government, 2011. Tokyo Vision 2020: driving change in Japan/Showing our best to the world. http://www.metro.tokyo.jp/ENGLISH/PLAN/ (accessed Oct. 10, 2014)

Overview of recovery and impact of the fire accident by the tanker truck on the Metropolitan Expressway

Shuichi YAMAGUCHI [1]
[1] Senior Director for Management
JAPAN Expressway Int. Co. Ltd., JAPAN,
mailto:s.yamaguchi.aa@jexway.jp

ABSTRACT

August 3, 2008 (Sun) 5:52, on the Metropolitan Expressway Route 5 Ikebukuro line on the northward, between Itabashi JCT and Kumano-cho JCT, a tanker truck, which was loading gasoline 16kℓ and light oil 4kℓ, was rolled over, and occurred a collision on the left side wall, and burned down. This fire caused extensive damage in the superstructure of the viaduct, pier and floor slab. This point is very important part for the road traffic and economy, connecting not only Route 5 and Center Circular Route but also the downtown Tokyo and Saitama, northern district of Tokyo. Because of this accident, expressway was stopped and heavy traffic congestion was occurred on the expressway and surface streets in Tokyo. Therefore, Large-scale and immediate recovery construction work, such as replacement of the steel girder was proceeded. Because, since during the restoration work, traffic is closed fully and partially on the expressway, severe traffic congestion continued on the roads around Tokyo and vicinity area, support team was established to serve proper information to the drivers. This paper is to report the impact of the accident on the structures and traffic, and restoration works.

Keywords: all small character (except a proper noun)

1. INTRODUCTION

The Metropolitan Expressway ("Mexway") network currently extends for almost 300km, and about 170km in Tokyo District and almost 13% of major surface streets. Compared to the rate of total road length, vehicle-kilometers is almost twice, volume of freight transport is almost three times. Mexway network serves as major traffic facility supporting socio-economic activities in the Tokyo metropolitan area.

Because of huge traffic demand, Metropolitan expressway has been heavily congested, especially daytime, on Friday, December (end of the year), March (end of the fiscal year), August (before O-bon holiday).

August 3, 2008 (Sun) 5:52, on the Mexway Route 5 Ikebukuro line on the northward, between Itabashi JCT and Kumano-cho JCT, a tanker truck, which was loading gasoline 16kℓ and light oil 4kl, was rolled over, and occurred a collision on the left side wall, and burned down. This fire caused extensive damage in the pier, etc. (digits, floor slab) and superstructure of the viaduct.

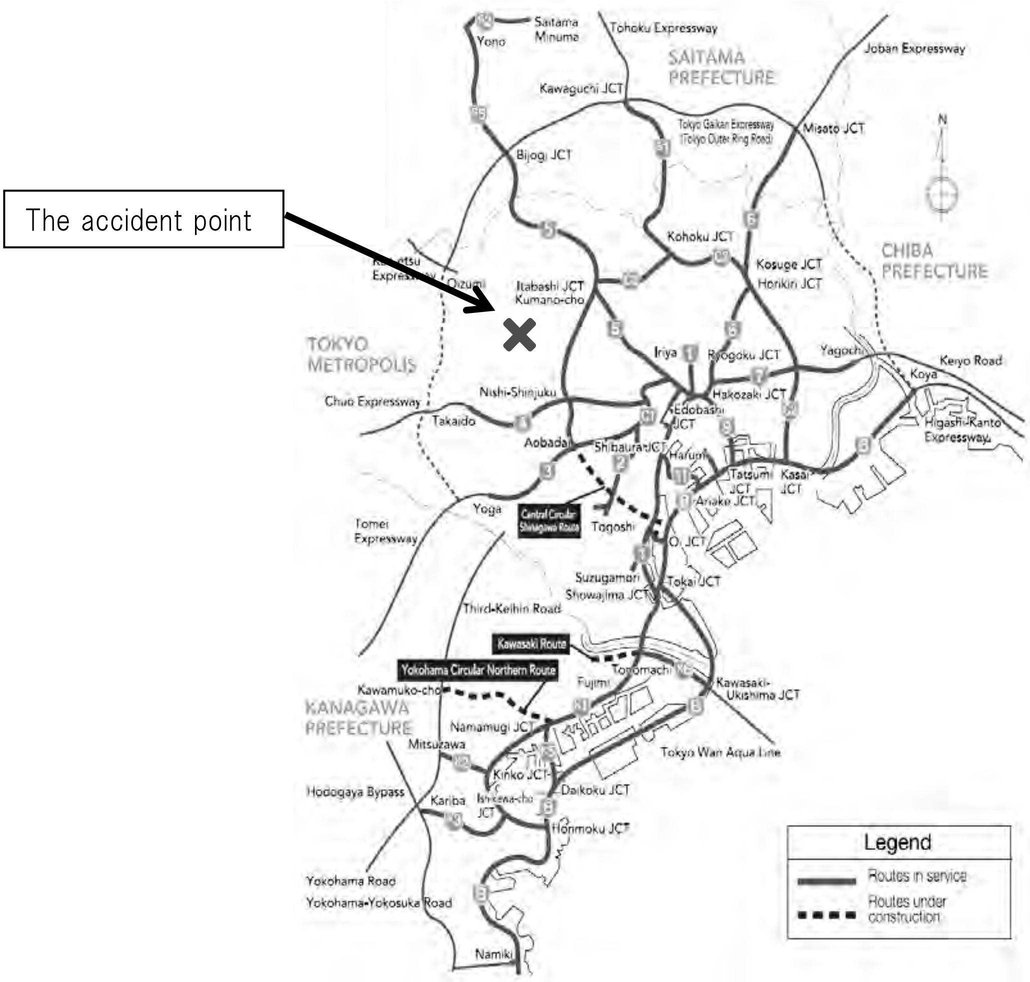
The accident point
Saitama Minuma
Yono
Tohoku Expressway
SAITAMA PREFECTURE
Joban Expressway
Kawaguchi JCT
Tokyo Gaikan Expressway (Tokyo Outer Ring Road)
Misato JCT
N
Bijogi JCT
Kohoku JCT
Kosuge JCT
Horikiri JCT
CHIBA PREFECTURE
Kan-etsu Expressway
Oizumi
Itabashi JCT
Kumano-cho
TOKYO METROPOLIS
Iriya
Ryogoku JCT
Yagochi
Keiyo Road
Koya
Nishi-Shinjuku
Hakozaki JCT
Chuo Expressway
Edobashi JCT
Higashi-Kanto Expressway
Takaido
Aobadai
Shibaura JCT
Harumi
Tatsumi JCT
Kasai JCT
Ariake JCT
Yoga
Central Circular Shinagawa Route
Togoshi
Tomei Expressway
Oi JCT
Suzugamori
Showajima JCT
Tokai JCT
Third-Keihin Road
Kawasaki Route
Yokohama Circular Northern Route
Tonomachi
Fujimi
Kawasaki-Ukishima JCT
Kawamuko-cho
KANAGAWA PREFECTURE
Namamugi JCT
Mitsuzawa
Tokyo Wan Aqua Line
Kinko JCT
Hodogaya Bypass
Kariba
Ishikawa-cho JCT
Daikoku JCT
Honmoku JCT
Yokohama Road
Yokohama-Yokosuka Road
Namiki
Legend
Routes in service
Routes under construction

Figure 1: Metropolitan Expressway Network

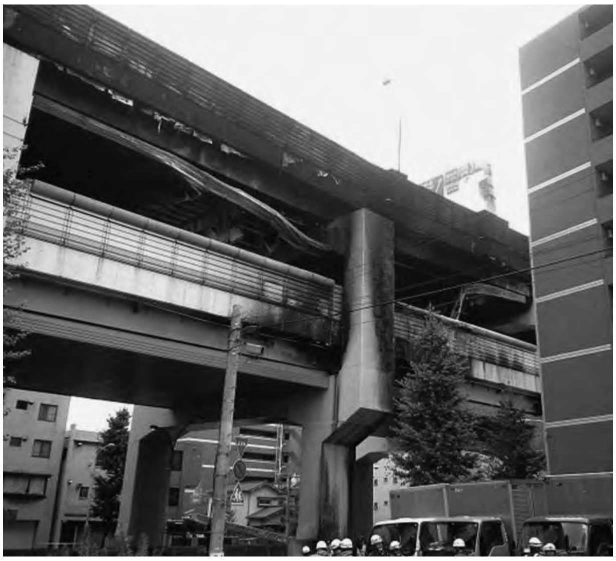

Photo 1: Burned and damaged Structures

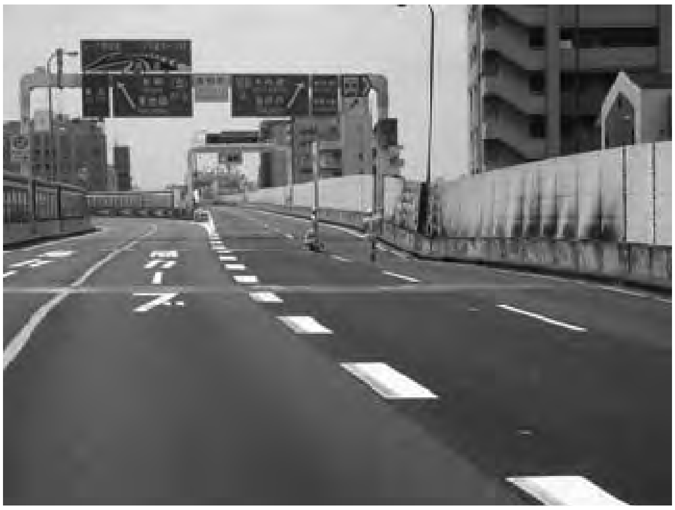

Photo 2: Waved surface by heat of the fire

2. OVERBIEW OF THE DAMAGE OF THE ACCIDENT

2.1 The damage condition of expressway

For about 90 minutes, this rolled over tanker truck had been violently burst into flames. It took more than five hours to extinguish this fire. This accident was occurred at the lower deck of the two-layer expressway viaduct.

Superstructure of this expressway is simple steel girder (6 I-beams), with lightweight concrete floor. The pier is ramen RC pier. Affected temperature for the structure is estimated to be up to about 1200 ℃, severe damage has occurred in the upper structure of the two upper span and beam of the pier at the accident location. Condition of the damage was as follows.

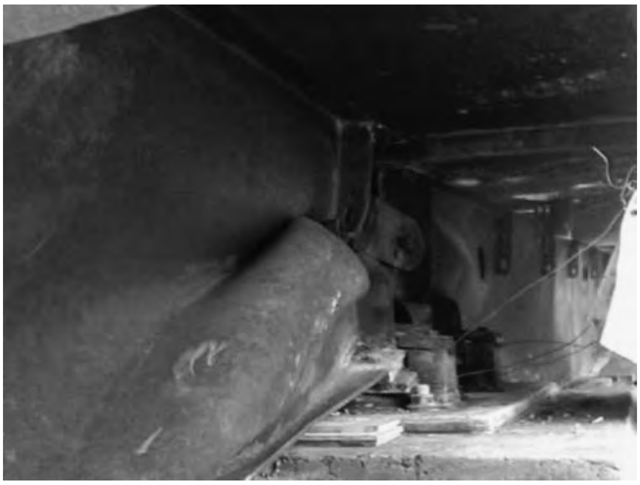

Photo 3: Damaged I- Beam

To understand the situation of deterioration and plan of the restoration work, checking deformation of the structures, physical property tests, the estimation of the heat-receiving temperature was performed. Followings are the results.

2.1.1 Upper deck

- Physical deterioration of the steel girder was significant at Beam-1 ~ Beam-3 near the fire point, because temperature of the structure was very comparatively high.
- The beam-4 ~ beam-6, which are on the contrary of the fire, were no deterioration of the material strength but deformation occurs in the whole steel beams.
- About the RC slab, near the fire, rebar exposure can be seen in a wide range but, beam-4 ~ beam-6 part away from the fire source, also seen the promotion of neutralization strength reduction, by fire rather than peeling no.
- At the next span, which is not heated by the fire, deterioration of the RC slab and the main girder is not observed.

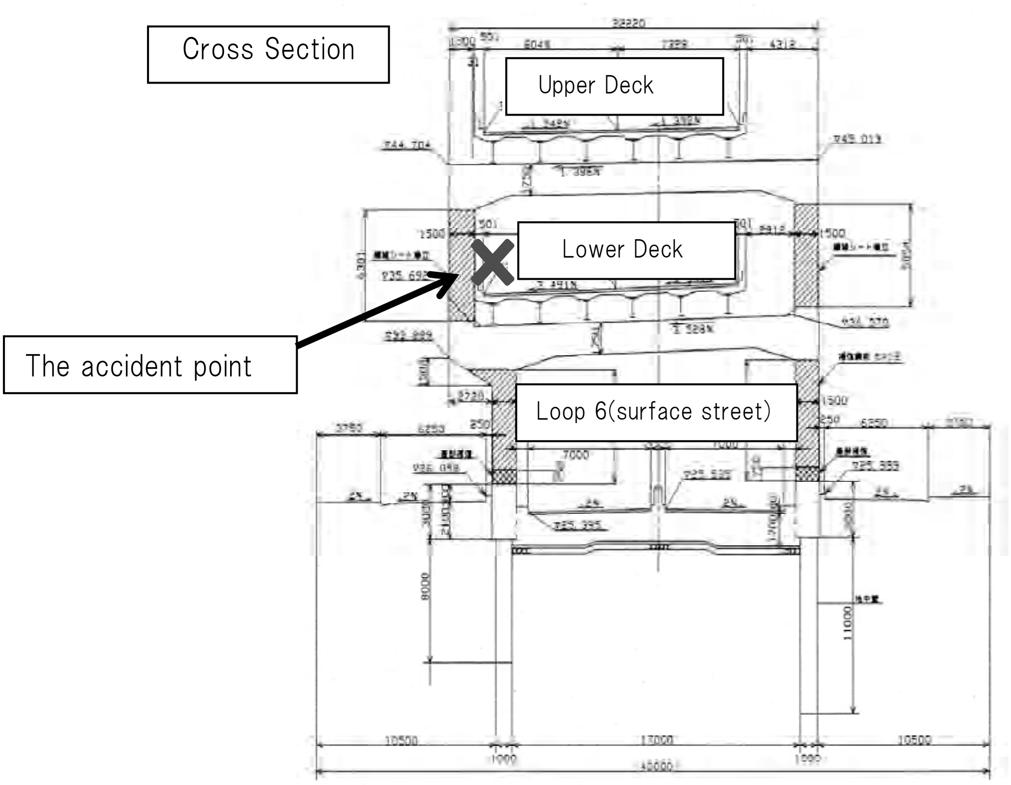
Cross Section
Upper Deck
Lower Deck
The accident point
Loop 6(surface street)

Figure 2: Cross Section of the Expressway at the Accident

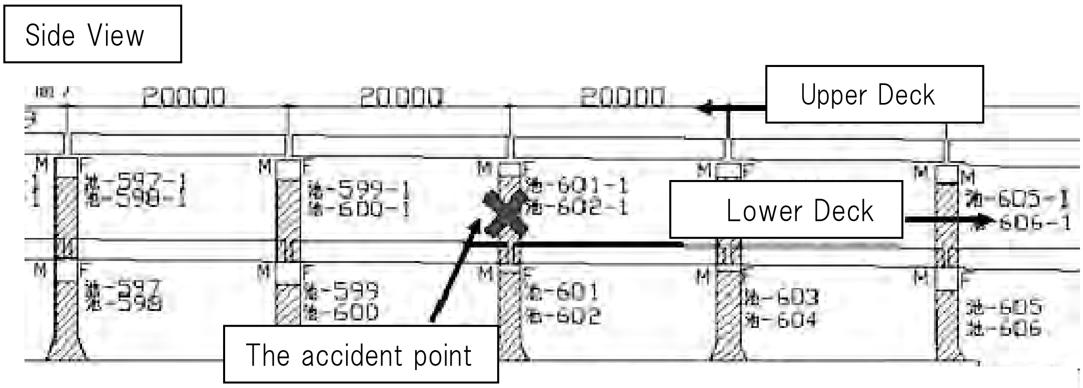
Side View
20000
20000
20000
Upper Deck
Lower Deck
The accident point

Figure 3: Side view of the Expressway at the Accident

2.1.2 Lower deck

- There is some distortion at the supporting point of Beam-1, Beam-2 near the fire. And locally, the high heat is assumed, but the deterioration of physical property is not found.
- For the RC slab, repair is required near the fire, but at other part, the promotion of neutralization and strength loss was not be found.

2.1.3 Piers

- At upper and west side cross beam, that the deterioration of the cover concrete and exposer of reinforcing bar occurred, concrete strength of the pillar and beam had dropped to about 80% of the design strength, but it was can be up to about 90% by the recover work in the future . Deterioration of reinforcement bar is not observed.

3. OVER BIEW OF THE RESTORATIN WORK

This accident had no sooner occurred, than Metropolitan Expressway Co. Ltd. ("**MEX**") immediately started the damage survey and recovery of the ruined structure, and established Recovery Committee by external experts, chairman is Dr. Ikeda Naoharu, Yokohama National University Professor Emeritus.

At the 1st Committee which was held on August 8, five days after the accident, following policy was discussed and determined.

Replace damaged two girders, near the fire point.

- Concrete piers can be used continuously with repair.
- Beam-4 ~ Beam-6 of the east part of the girder were not affected by fire, and able to use for the present.

Because replacement of all damaged girders at one time must give the great impact on the traffic of expressway and surface streets and causes heavy traffic congestion, restoration work was performed in two terms.

3.1 The first term (August 9 to September14)

As shown in Figure 4, while one lane is opened to traffic at this point, the removal and reconstruction of the beam-1 ~ beam-3 of the west halves was performed and RC pier columns and the transverse beam were restored.

This part of route five started service in 1977, and its superstructure was the steel composite girder, the floor slab has been lightweight concrete.

Basic concept of the restoration is to adopt the original structure. Furthermore, to shorten the construction period, a non-composite girder was adopted.

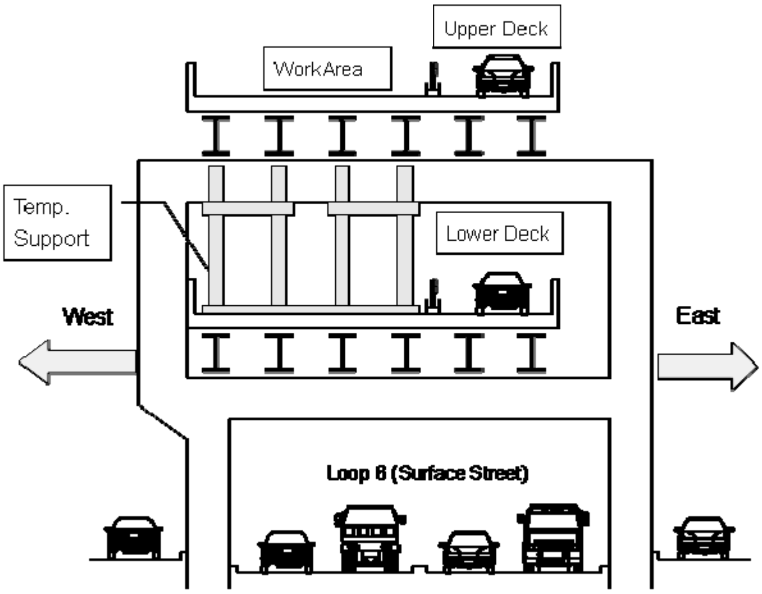
Upper Deck
WorkArea
Temp. Support
Lower Deck
West
East
Loop 8 (Surface Street)

Figure 4: Cross Section1 (During first stage restoration work)

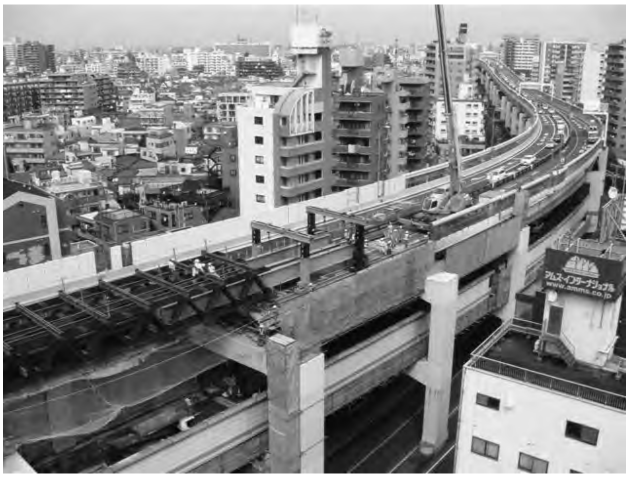

Photo 4: Restoration Work 1 (Removal of damaged girders)

Photo 5: Restoration Work 2 (Setting of New Girders by the election girder)

3.2 The second stage (October 14 - September14)

As shown in Figure 5, next step of restoration work is reconstruction of the eastern half. After the western part was opened to traffic, and the girder of eastern part was removed. The replacement of the upper slab concrete, in order to ensure integration with the deck of the western portion which is constructed in advance, was performed with the close of traffic to extinguish traffic vibration.

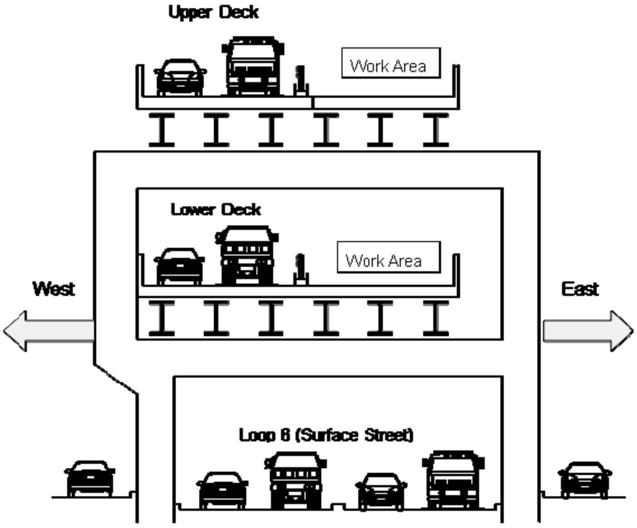

Figure 5: Cross Section 2 (During second stage of restoration work)

3.3 Information management

To keep the information of the construction work and surrounding traffic, headquarters for this reconstruction work was established to consolidate all the information about this accident, develop of this recovery plan, and to implement a proper public relations. And, “Route 5 accident emergency call center" was established to the inquiries from derivers (inquiry Total number: 1,437: maximum number of about 22,000,1 days). To collect traffic information of road network, Ministry of Land, Infrastructure and Transport, Tokyo, Tokyo Metropolitan Police Department, NEXCO East and Central presented their traffic information to the headquarters.

3.4 To Shorten the construction term

To shorten the construction term, continuous restoration work, with four times expressway full suspension of traffic, were performed. And the prefabricated high-early-strength concrete slab form, and erection with the truss girder was adopted. And the recovery policy was smoothly determined by Recovery Committee.

Finally, this part of expressway was successfully and fully opened to traffic again in October 14. Recovery work was completed in 73 days from the accident.

Photo 6: Reopened Expressway

4. TRAFFIC IMPACTS OF THIS ACCIDENT ON THE METROPOLITAN EXPRESSWAY

From August 4 to 8 (5 days of weekdays), during the traffic suspension at this point on the expressway, at the Mexway Tokyo district, a 9% drop of daily traffic volume was recorded comparing with the last week (July 28 to August 1). On the other hand, congestion was increased by about 51%. (39% at 2007, 27% at 2009)

After one lane was opened to traffic on Saturday August 9, traffic volume was a 8% drop, the traffic congestion was increased by about 25%.

Table 1: Traffic volume and Congestion Amount* of Metropolitan Expressway (Tokyo Area) before and after the accident

＊Σ (Congestion length × its Period)

	Traffic Volume (vehicles/day)	**Volume×distance (vehicles・m)**	**Congestion Amount (km・hour)**
Before Accident 28 Jul. to 1 Aug.	909,408	18,628,384	617
First period 4 Aug. to 8 Aug.	829,318	16,360,875	925
	▲9%	▲12%	+50%
Second period 20 Aug. to 26 Aug (Opened One lane)※	832,497	16,932,013	772
	▲8%	▲9%	+25%

※Considering the special impact on the traffic volume of the Bon holiday in mid-Aug.

(Amount of congestion: Length ×period, one day average, Tokyo district)

In case of this accident, because the expressway traffic between Itabashi JCT and Kumano-cho, JCT, one of the most important junction connecting Tokyo and Saitama area, was damaged and suspended, stopped traffic was detoured to another routes, between Kosuge JCT and Horikiri JCT, on Route 6. Accordingly, heavy traffic congestion was caused from this point. Moreover, additional congestion was occurred from Kumano-cho JCT to the Inner ring, and Route No. 1 and No. 3, and almost of all Mexway network. And traffic impact was greater for this time of the Bon holiday in mid-August.

Because of this accident, travel time Takaido entrance (Route 4) to Misato JCT was increased 70 minutes, from usual 61 minutes to 131 minutes at eleven AM. After the one lane release, it became 87 minutes of this route. After the release of Yamate tunnel, it becomes 53 minutes in late September, and traffic volume was almost equivalent to before the accident, the effect of Yamate tunnel as the bypass route of Inner ring has been clearly shown.

Table 2: The Amount of Traffic Congestion at MEXWAY before and after the Accident (working day, 24hours even data, 2008)

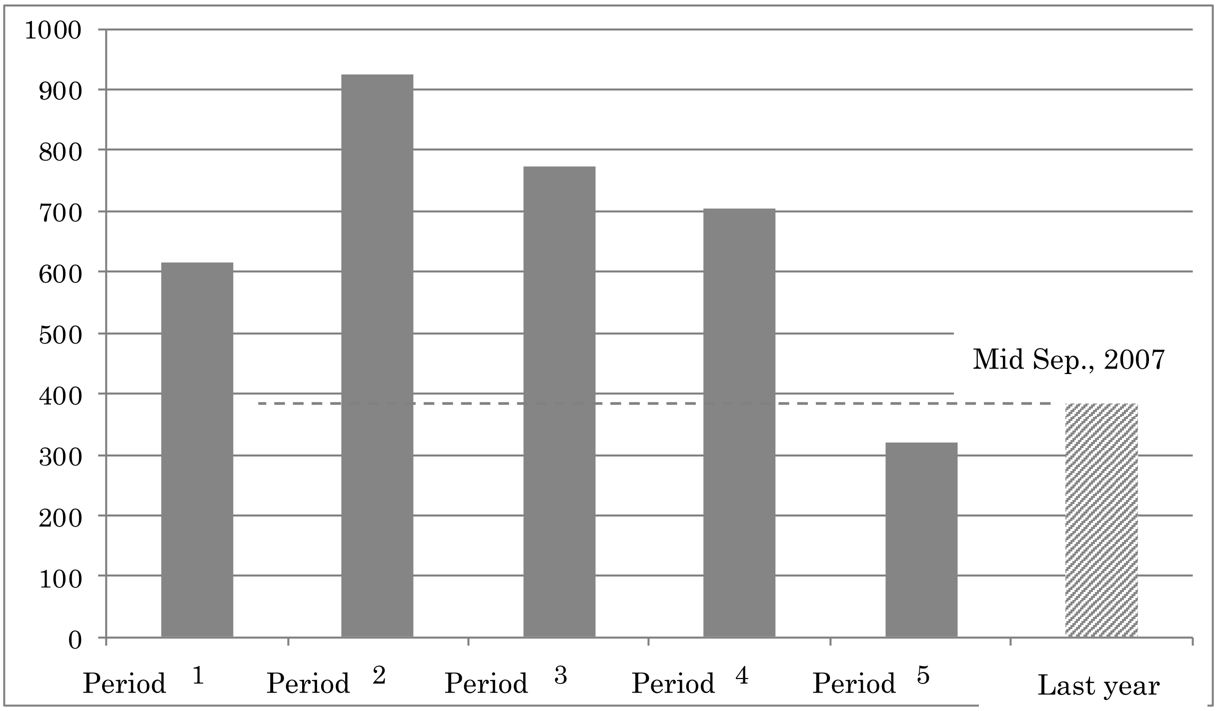

Period 1 28 Jul. - 1 Aug. (Before the Accident)
Period 2 4 Aug. - 9 Aug. (Just after the Accident)
Period 3 20 Sep. - 28 Sep. (Open of One lane)
Period 4 24 Sep. - 30 Sep.(Open of Yamate tunnel, one part of Center Circular Route)
Period 5 15 Oct. - 28 Oct. (Open of full lane, after restoration work)

On the other hand, the congestion of the surface streets and Mexway in Tokyo area were significantly increased. Furthermore, peripheral national highway, such as Route 254, 17 and 5, which are parallel to the Mexway, and arterial circular surface streets, such as Roop 7 and 6, were heavily congested.

In addition, the economic loss, which associated with this increased traffic congestion by this accident, was estimated 300 million yen per day by the Ministry of Land, Infrastructure and Transport.

5. CONCLUSION

In this accident, the importance and vulnerability of the road network, especially Mexway, had become clear. We should pay special attention to the fact that traffic accident at the critical point on the expressway, causes severe traffic congestion. In this case of the accident, fortunately big restoration work had finished in 2 month, without stopping expressway.

Furthermore, in order to increase the alternative route, more expressway network is urgently necessary, and construction of the second central ring route must be improved. (Center circler route, second expressway ring, will be completed in the end of this fiscal year.

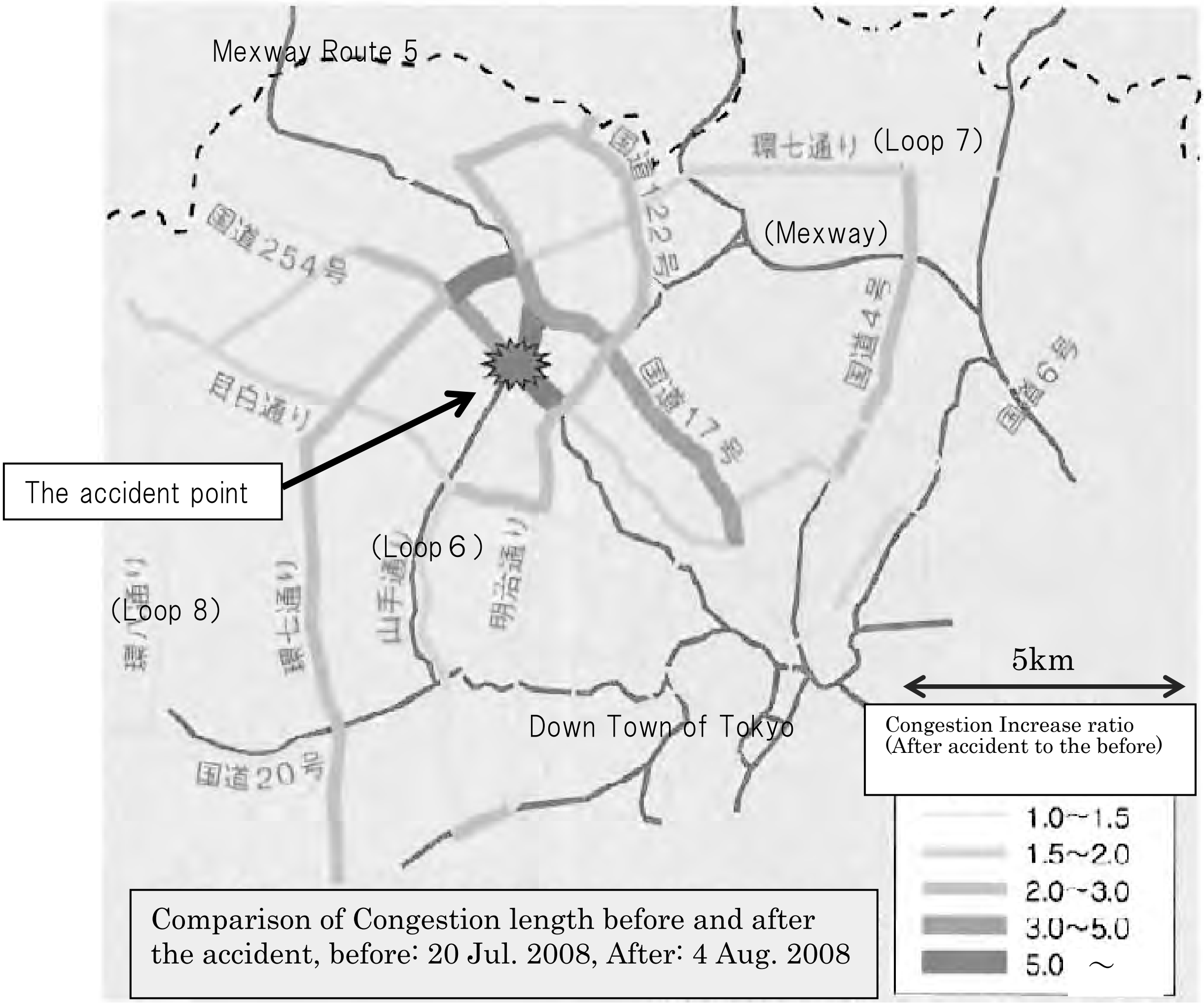
Mexway Route 5
国道122号
環七通り (Loop 7)
国道254号
(Mexway)
国道4号
国道6号
目白通り
国道17号
The accident point
(Loop 6)
山手通り
明治通り
(Loop 8)
環八通り
環七通り
国道20号
Down Town of Tokyo
5km
Congestion Increase ratio (After accident to the before)
1.0~1.5
1.5~2.0
2.0~3.0
3.0~5.0
5.0 ～

Comparison of Congestion length before and after the accident, before: 20 Jul. 2008, After: 4 Aug. 2008

Figure 6: Increase of congestion at surface streets

Also, in case of the big accident with lane stop like this, usual traffic information service is not sufficient for the driver, who must detour this accident point. In this case, supported by the Ministry of Land, Infrastructure and Transport, the Metropolitan Police Department, and Tokyo metropolitan government, Metropolitan Expressway Co. Ltd. established the supporting team, not only to control restoration work and but also to serve any necessary information. However, more useful information and early establishment of accident detouring route must be big problem.

REFERENCES

Sasaki, K., Yamaguchi, S., 2009. Overview of Recovery and Impact of the Fire Accident by the Tanker Truck on the Metropolitan Expressway Route 5. *Expressway and Automobile* 52.

Ten-year post-tsunami living conditions in southwestern coastal area resettlements of Sri Lanka after 2004 Indian Ocean Tsunami

Osamu MURAO
Dr. Engineering, Institute of Environmental Science and Engineering,
Tohoku University, Japan
murao@irides.tohoku.ac.jp

ABSTRACT

As of December 2014, ten years will have passed since the 2004 Indian Ocean Tsunami struck the coastal areas of Sri Lanka. Following the devastating event, most residents in adversely affected coastal areas moved to inland resettlements by the government's recovery policy. Following post-tsunami urban recovery processes for several years, the author conducted a field survey and questionnaire interviews about recent living conditions to residents in several resettlement districts in Southwestern Coastal Areas in the country. This paper reports ten-year post-tsunami living conditions of the residents and their tsunami risk awareness in order to consider future post-tsunami recovery strategies.

Keywords: donor, permanent housing, relocation, urban recovery, risk awareness, The Coast Conservation Act

1. INTRODUCTION

It will be one decade soon since the 2004 Indian Ocean Tsunami occurred on December 26, 2004. In Sri Lanka, where approximately forty thousand people were killed and ninety-six thousand houses were damaged by the tsunami (Department of Census and Statistics, 2005), most victims resettled in inland permanent houses supported by the national government and donors such as NGO.

Nakazato and Murao (2007) reported about the national housing reconstruction program, "Task Force for Rebuilding the Nation (TAFREN) and Tsunami Housing Reconstruction Unit (THRU) provided the framework for the following three categories of recovery housing: 1) Emergency shelters, 2) Temporary houses, and 3) Permanent houses. For the third phase, the Buffer Zone settlement is an important concept." Namely, "the 1st strip (100 m landwards on the west coast and 200 m landwards on the east coast) was defined as a *Buffer Zone* and reconstruction of affected houses in this area was regulated."

During the decade, people resettled by the policy have rebuilt individual life in various recovery processes. It is important to examine the resettlement strategy from the residents' point of view. To this end, the authors conducted a field survey in the southwestern coastal area of Sri Lanka in February 2014. This paper reports remarkable findings from the survey.

2. FIELD SURVEY

2.1 Outline

The field survey was carried out in resettlements located in the southwestern coastal area of Sri Lanka from February 8 to 11, 2014, aiming to evaluate the post-tsunami resettlement strategy implemented by the government and to clarify related problems from the viewpoints of residents through individual long-term living after relocation.
Hearing surveys were conducted living in eleven resettlements provided after the tsunami by the government in five towns –Kalutara and Beruwala in Kalutara District, Kahawa in Galle District, Dikwella in Matara District, and Hambantota in Hambantota District shown in Figure 1.

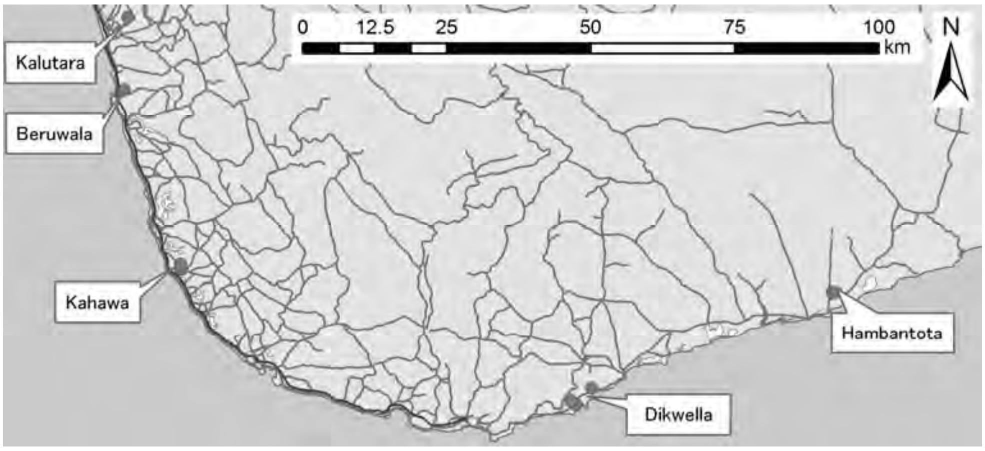

Figure 1: Object towns for field survey

2.2 Questionnaire

Gathering basic information of the individual relocation sites (name of the place, address, and construction year), the author conducted hearing surveys based on a questionnaire sheet prepared in advance. It contains following questions.

Individual Information of Interviewees:
sex, and age

Household Information:
number of families, and family structure

Conditions before Relocation:
previous address, land ownership, house ownership, number of building stories, building structure type, distance from the coastline, inundation depth, building damage conditions, and previous principal occupation for the family

Conditions after Relocation:
present condition of residential site affected by the tsunami, present condition of land ownership, individual relocation processes, date of moving in, support for relocation and donation conditions (temporary housing, permanent housing and land), present principal occupation for the family, habitation satisfaction, income satisfaction, and quality of life

Risk Recognition:
knowledge of tsunami, and feeling of relief

Evaluation of Government's Resettlement Strategies:
preferable resettlement between inland and oceanfront, and resettlement policy satisfaction

The number of interviewee became fifty-one, and total time of the interviews was eight hours and twelve minutes.

3. REMARKABLE FINDINGS

Several remarkable findings were made by the hearing surveys. This chapter reports two topics from them.

3.1 Differences caused by selection of donors

A lot of donors supplied permanent houses to the victims on inland residential sites prepared by the national government after the tsunami in Sri Lanka as well as in other countries. Quality of the provided housings, however, differed depending on donors, and the difference has seriously widened for residents as time goes by.

Figure 2 left shows a house provided by an association. The donor gave the house to the residents in December 2006, two years after the event, but construction quality was unsatisfactory. Now that seven years had passed, some parts of the house deteriorated as shown in Figure 3. Since the donor didn't give maintenance service, the residents in the area had to repair their deteriorated houses themselves. Whether they can live confortable depends on their financial conditions.

On the other hand, residents living in Tzu Chi Great Love Village in Hambantota satisfy their houses (Figure 2 right) and its environment. Tzu Chi foundation, based in Taiwan, constructed the residential site and had kept improving environmental comfortability for long-term recovery. Most residents were content with physical environment and community relationship in the village.

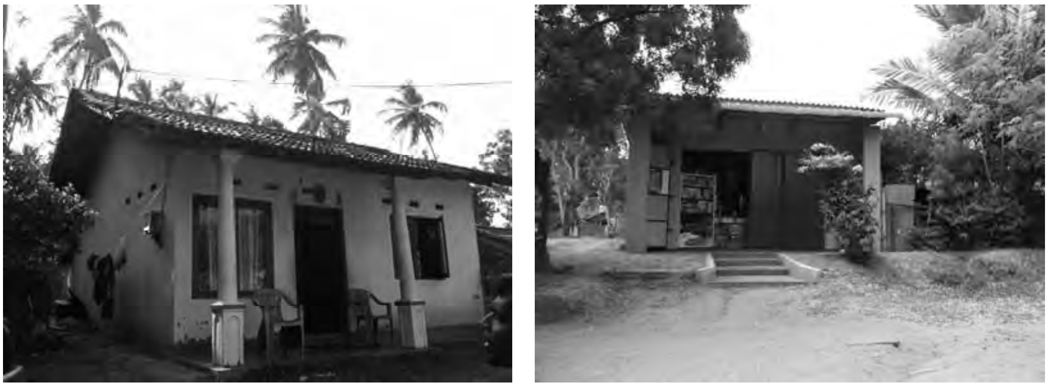

Figure 2: A house provided by an association (left) and a house provided by Tzu Chi Foundation (right)

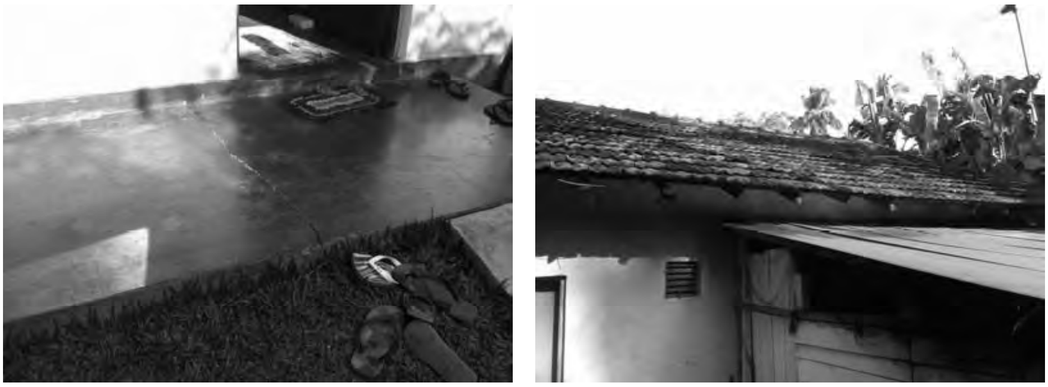

Figure 3: Crack on the floor (left) and ill-shapen roof (right)

3.2 Environmental change as time goes by

Although Tzu Chi Foundation provided this fabulous community place to the victims in Hambantota, one critical problem arose. Chinese Government started financial supporting to construct International Airport and International Ferry Terminal in Hambantota (Figure 4) some years ago, and Tzu Chi had to stop maintenance of the village. This undesirable situation was caused by an international political issue.

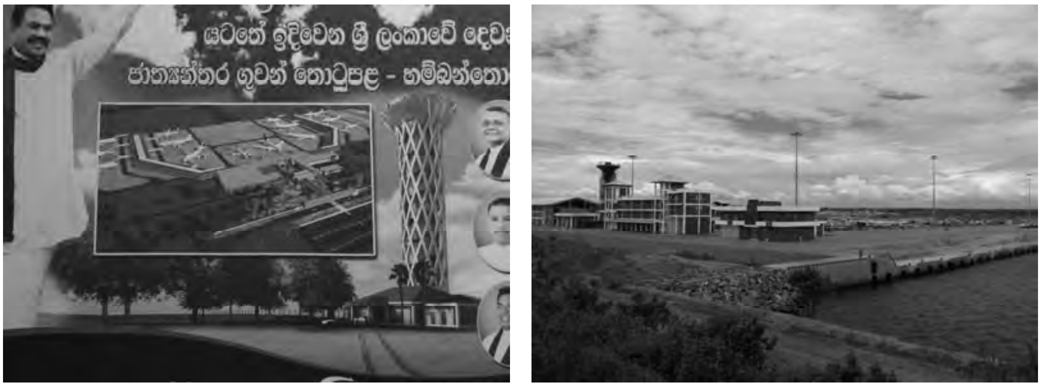

Figure 4: International Airport (left) and International Ferry Terminal (right)

4. CONCLUSION

As of December 2014, ten years will have passed since the 2004 Indian Ocean Tsunami struck the coastal areas of Sri Lanka. Following the devastating event, most residents in adversely affected coastal areas moved to inland resettlements by the government's recovery policy. Following post-tsunami urban recovery processes for several years, the author conducted a field survey and questionnaire interviews about recent living conditions to residents in several resettlement districts in Southwestern Coastal Areas in the country.

This paper reports environmental differences caused by selection of donors and problems caused by a change of supporting system as time goes by. The residents the author met in this survey were relieved living in safer inland places, but most of them were facing problems of job opportunities and income. The author would like to continue analyzing gathered information by the survey.

ACKNOWLEDGEMENTS

This research was supported by the Japan Society for the Promotion of Science (JSPS) through the Grants-in-Aid for Scientific Research No. 23404019, "Examination of Urban Recovery Plans after the 2004 Indian Ocean Tsunami and Urban Risk Evaluation of Tsunami in Asia Influenced by Global Warming." The author would like to acknowledge contribution by Mr. Navindra De Silva, and Dr. Kazuya Sugiyasu at International Research Institute of Disaster Science, Tohoku University. The author is also grateful for the cooperation of residents.

REFERENCES

Department of Census and Statistics, 2005. Census of Persons, Housing Units and Other Buildings Affected by the Tsunami, 26th December 2004.
Nakazato, H., and Murao, O., 2007. Study on regional differences in permanent housing reconstruction process in Sri Lanka after the 2004 Indian Ocean Tsunami. *Journal of Natural Disaster Science* 29, 63-71.

Expended energy based damage assessment of RC bare frame using nonlinear pushover analysis

Anthugari Vimala[1] and Ramancharla Pradeep Kumar[2]
[1]Research Scholar, Earthquake Engineering Research Centre,
IIIT-Hyderabad, India
vimala.a@research.iiit.ac.in
[2]Professor and Head, Earthquake Engineering Research Centre,
IIIT-Hyderabad, India.

ABSTRACT

Past response analyses of structures under earthquake excitations revealed that both the maximum displacement and the number of inelastic excursions cause higher damage to the structure. However, it is observed that the quantification of damage is a difficult task. In the paper, a new methodology is proposed for the quantification of damage of reinforced concrete framed structure. This method is based on the nonlinear energy dissipated by the structure along the complete displacement path. Three methods have been proposed to assess the global damage state of the structure, for any deformation level. In these proposed methods, the damage index is expressed as the ratio of nonlinear dissipated energy at an instant, to the total non-linear energy capacity of the structure. To calculate the energy, pushover curve is plotted between base shear versus displacement at C.G of external force profile, which provides consistent meaning for work done by external forces. The area under the curve represents the energy dissipated by the structure. To illustrate the proposed concept, two cases i.e., G+5 and G+9 story structures have been considered.

Keywords: Pushover analysis, expended energy, total energy, damage index.

1. INTRODUCTION

Many damage indices were proposed to quantify seismic damage sustained by complete RC frame structures, each storey in them or individual elements. Damage indices are classified broadly as local damage indices and global damage indices, the former quantify damage in individual members, at individual joints or at a particular cross-section, and the latter damage in the whole structure (Kappos, 1997). The indices used in literature are estimated combining local deformation quantities and/or some overall structure response quantities. A detailed review of damage indices is available in literature (Williams and Sexsmith, 1995; Ghobarah et al., 1999; and Padilla et al., 2009). The most widely used damage index (Park and Ang, 1985) is derived to estimate (a) local damage (member damage) using a damage function based on maximum displacement ductility and cumulative hysteresis energy, and (b) the global damage using an average of local indices, weighted by local energy absorption. This index D

takes into account both maximum plastic displacement $\delta_{\max}$ and plastic dissipated energy $\int dE$, given by:

$$D = \frac{\delta_{\max}}{\delta_u} + \frac{\beta}{Q_y \delta_u} \int dE \tag{1}$$

and is supported by a wide correlation with observed damage. But, experimental determination of parameter β is difficult.

Another damage index D_{global} (Roufaiel and Meyer, 1987) expressed global damage using deflections at roof level, as:

$$D_{global} = \frac{\delta_m - \delta_y}{\delta_f - \delta_y} \tag{2}$$

and yet another DI_μ (Powell and Allahabadi, 1988) on plastic deformations and ductility:

$$DI_\mu = \frac{u_{\max} - u_y}{u_{mon} - u_y} \tag{3}$$

In another study (Bozorgnia and Bertero, 2001), two damage indices DI_1 and DI_2 were introduced for SDOF systems in terms of displacement ductility and energy capacity on the system, as

$$DI_1 = (1 - \alpha_1)\left(\frac{\mu - \mu_e}{\mu_{mon} - 1}\right) + \alpha_1 \left(\frac{E_H}{E_{Hmon}}\right) \quad \text{and} \tag{4}$$

$$DI_1 = (1 - \alpha_2)\left(\frac{\mu - \mu_e}{\mu_{mon} - 1}\right) + \alpha_2 \sqrt{\frac{E_H}{E_{Hmon}}} \tag{5}$$

where

$\mu = \dfrac{u_{\max}}{u_y} = \text{Displacement ductility}$,

$\mu_e = \dfrac{u_{elastic}}{u_y} = \dfrac{\text{Maximum elastic portion of deformation}}{u_y} = \begin{cases} 1 & \text{for inelastic behaviour} \\ \mu & \text{for elastic behaviour} \end{cases}$

$\mu_{mon} = \text{Monotonic displacement ductility capacity}$,

$E_H = \text{Hysteretic energy demanded by earthquake ground motion}$,

$E_{Hmon} = \text{Hysteretic energy capacity under monotonically increasing lateral deformation}$

and

$0 \le \alpha_1 \le 1$ and $0 \le \alpha_2 \le 1$ are constants.

These models which include energy term need knowledge of time history response of the structure during the earthquake. Another damage model proposed (Poljanšek and Fajfar, 2008) for seismic damage assessment of RC frame structures expressed damage index DI_{PF} as a ratio of deformation demand to deformation capacity, given by:

$$DI_{PF} = \frac{u}{u_{equ}} \tag{6}$$

In general, any damage in the structure is related to inelastic deformations or inelastic energy dissipated by member or structure. Inelastic energy dissipation capacity of a structure depends on its structural configuration, yielding capacity of members and material properties of the structure. At any deformation, it is an important index that indicates the state of structural damage and reliability of the structure. Damage index for a general force-deformation relationship (Cosenza, *et al*, 2000) is expressed as the ratio of hysteretic energy capacity of the system under monotonically increasing deformation to irrecoverable hysteretic energy, given by

$$DI_H = \frac{E_H}{E_{Hmon}} \tag{7}$$

Though the damage model is energy based, to quantify the damage state of the structure, the dynamic time history response of the structure during earthquake event is needed, which is tedious and involve more calculations. Energy based damage model should be simple and require less calculations.

2. PROPOSED DAMAGE INDEX ESTIMATION APPROACH

In the present study, a new global damage estimation approach is presented for seismic damage assessment of RC frame structures, using a simple static nonlinear procedure. Damage is represented as ratio of inelastic energy dissipated at any displacement to the total inelastic energy capacity of the structure. The energy dissipated is low when lateral deformation is small, than that when lateral deformation is large. For the sake of simplicity, the proposed damage estimation approach uses inelastic displacement excursion of the structure. Static pushover analysis provides a measure of nonlinear behaviour of the structure. Two example buildings are considered in a pilot study, namely one 6-storey and another 10-storey building. 2D frames are considered and the total energy capacity of the structure estimated by performing pushover analysis using SAP2000 software. The effectiveness of proposed damage models is discussed along with the global damage state of the structure at four different displacement excursions.

In the proposed method, the total inelastic energy dissipated by frame in each incremental load step of the pushover analysis is calculated as the area under the pushover curve – base shear versus displacement of the frame at centre of gravity of external force system, which gives the real meaning of external work done or total energy dissipated by the structure. To represent the damage state of a structure in each incremental load step of the pushover analysis, a cumulative dissipated energy is used. Based on the capacity curve of a structure, the damage state of the structure can be represented in the four ranges as shown in Figure 1.

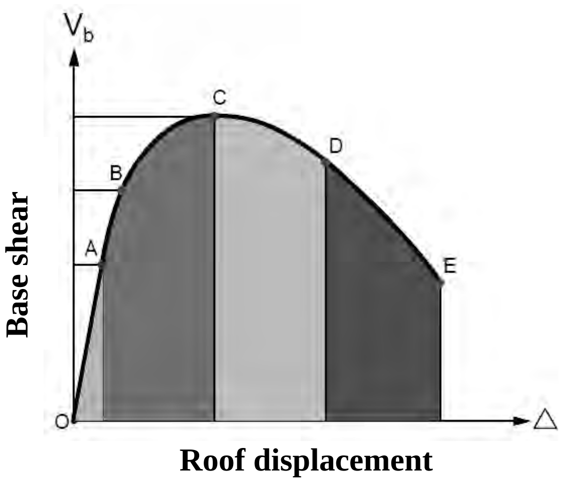

Figure 1: Damage index estimation methods critical points

Point A indicates the elastic state of the structure, point B indicates the middle stage between elastic limit and ultimate point, point C indicates the ultimate strength of the structure, point D represents the stage of the structure between ultimate point and collapse point, point E indicates the collapse stage. In the *load control region* (points O to C), the strength carrying capacity of the structure increases in nonlinear state. In the *displacement control region* (points C to E), as the displacement increases, the strength of the structure reduces. Possible damage ranges are shown in Table 1.

Table 1: Description of the behaviour of a typical structure in the whole range of nonlinear action

Range of deformation	Behaviour	State
OA	Elastic	No damage
AB	Strain hardening	Light damage
BC	Ultimate strength	Moderate damage
CD	Strength reduction	Severe damage
DE	Imminent collapse	Extreme damage and collapse

In current study, overall damage index is estimated as the ratio of dissipated energy to total energy capacity of the structure. In the present study, three methods are considered for damage estimation in RC structures, namely

$$\textit{Method 1}: \quad D_1 = \left(\frac{E - E_{ie}}{E_T - E_{ie}} \right) \times 100 \tag{8}$$

$$\textit{Method 2}: \quad D_2 = \left(\frac{E - E_e}{E_T - E_{ie}} \right) \times 100 \quad \text{and} \tag{9}$$

$$\textit{Method 3}: \quad D_3 = \left(\frac{E_L - E_{NL}}{E_{LT} - E_{NLT}} \right) \times 100 \tag{10}$$

where

E = Energy dissipated by structure at displacement level at which damage is being estimated;

E_{ie} = Initial yield energy of structure;
E_T = Total energy absorbed by structure;
E_e = Instantaneous elastic energy at displacement level at which damage is being estimated;
E_L = Linear energy at displacement level at which damage is being estimated;
E_{NL} = Nonlinear energy at displacement level at which damage is being estimated;
E_{LT} = Linear energy at maximum displacement of structure; and
E_{NLT} = Nonlinear energy at maximum displacement of structure.
All parameters of above methods are represented in figure 2.

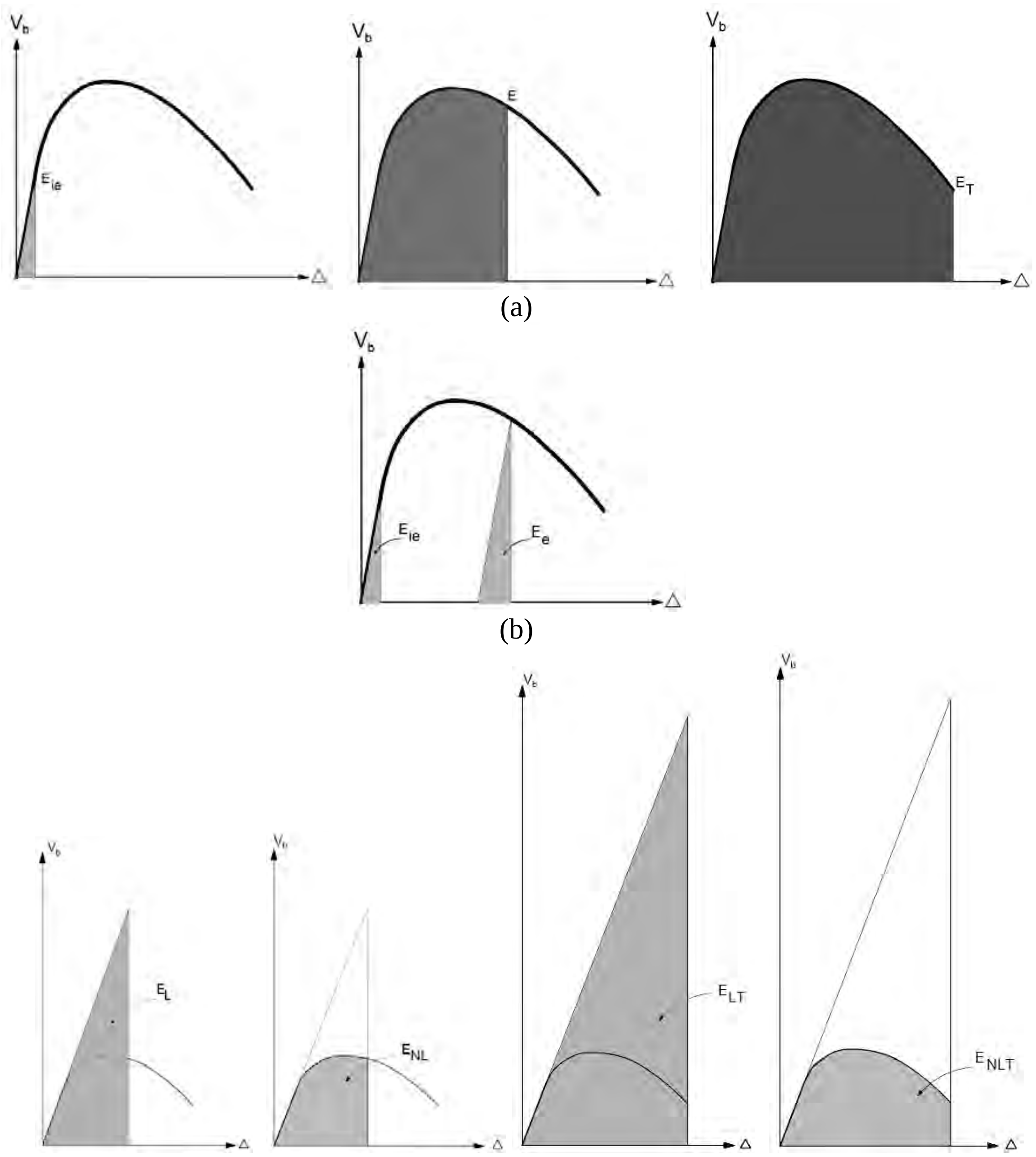

(a)

(b)

(c)

Figure 2: Parameters used for damage estimation in (a) Method 1, (b) Method 2, and (c) Method 3

3. CASE STUDY

To study the efficiency of the proposed methods, the energy dissipation is studied in two example structures, namely 6 and 10 storey RC frame buildings.

3.1 Details of the Structure

The two structures considered are to represent shear dominated building and flexure dominated building for study. These 6 and 10 story buildings are designed in accordance with the Indian codes of practice for plain and reinforced concrete (IS: 456) and for earthquake resistant design (IS: 1893(1)) . The buildings are assumed to be situated in seismic zone V of IS: 1893–2002, with a zone factor of 0.36 ground acceleration. Material properties used are: 20 MPa for concrete compressive strength and 415 MPa for steel yield strength for both longitudinal and transverse reinforcement bars. Both 6 and 10 story buildings are 15 m by 15 m in plan (Figure 3). Typical floor-to-floor height is 3m. The interior frames as shown in Figure 3 is 2D model of these buildings.

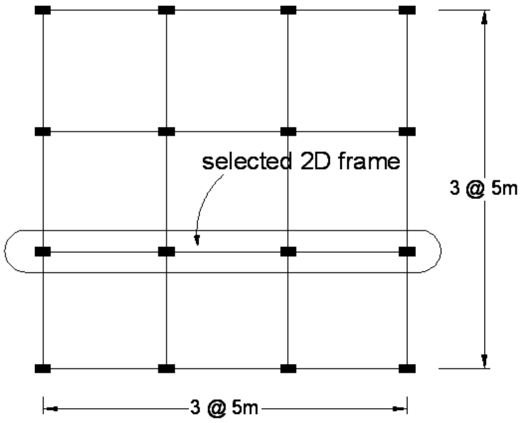

Figure 3: Plan view of 6 and 10 story buildings

The 6-story building is 18 m in elevation. All columns are 300mm x 400 mm dimensions and the amount and arrangement of longitudinal reinforcement in columns and beams are shown in Figure 4. All beams are 230 mm × 330 mm in cross section. The 10-storey building is 30 m in elevation. Column dimension, location and the amount and arrangement of longitudinal reinforcement are shown in Figure 5. All beams are 300mm×400mm and the amounts of top and bottom reinforcement of beams are shown in mm^2 in Figure 5.

3.2 Modeling

Since there is no torsional effect in the selected structures, two-dimensional (2-D) modeling is employed. A two-dimensional model of each structure is created in SAP2000 to carry out nonlinear static analysis. Beam and column elements are modeled as nonlinear frame elements with lumped plasticity by defining plastic hinges at both ends of beams and columns. SAP2000 implements the plastic hinge properties described in FEMA-356 and ATC-40. The structure is subjected to incremental lateral forces with uniform distribution along the height and the base shear versus displacement at centre of gravity of external force profile diagram is plotted to calculate the energy at any deformation. For any load pattern, if the curve is plotted with the displacement at C.G of external force system. The area under the curve represents the total seismic energy absorbed by the building which is equal to the work of seismic loads acting on the structure.

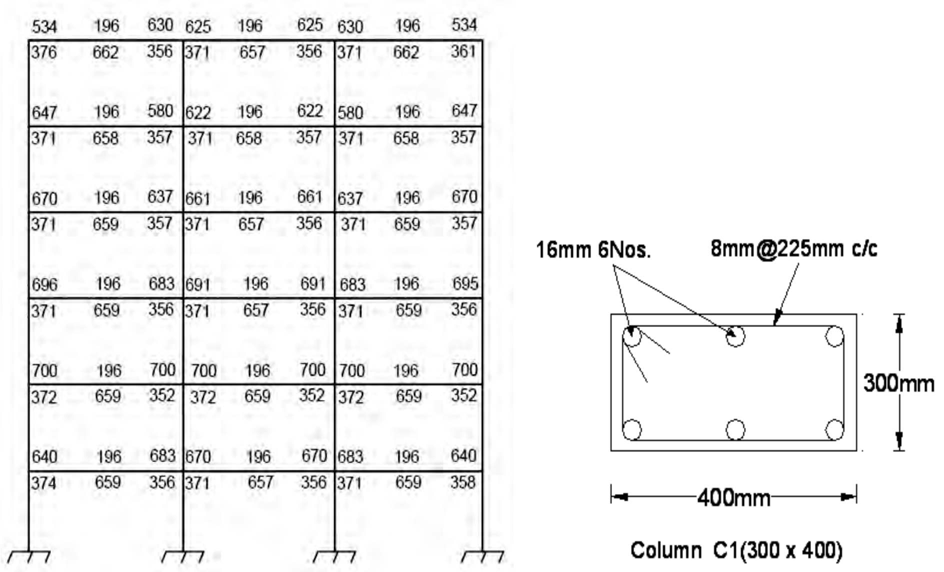
534 196 630 625 196 625 630 196 534
376 662 356 371 657 356 371 662 361
647 196 580 622 196 622 580 196 647
371 658 357 371 658 357 371 658 357
670 196 637 661 196 661 637 196 670
371 659 357 371 657 356 371 659 357
696 196 683 691 196 691 683 196 695
371 659 356 371 657 356 371 659 356
700 196 700 700 196 700 700 196 700
372 659 352 372 659 352 372 659 352
640 196 683 670 196 670 683 196 640
374 659 356 371 657 356 371 659 358
16mm 6Nos.
8mm@225mm c/c
300mm
400mm
Column C1(300 x 400)

(a) (b)

Figure 4: Details of 6-storey frame (a) Longitudinal reinforcement in beams (mm^2)
(b) Column reinforcement

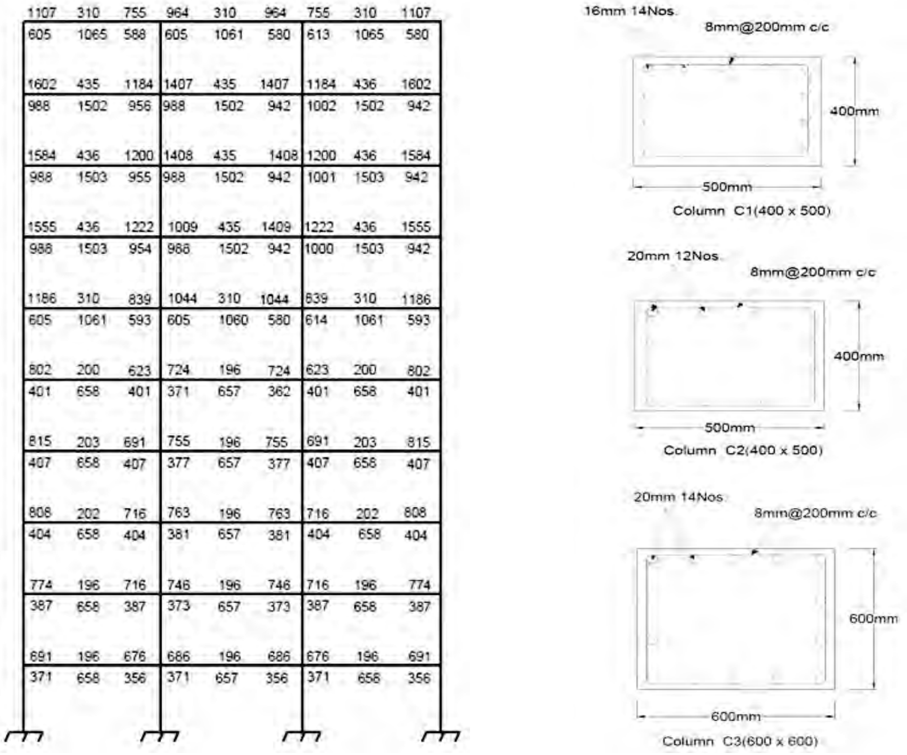
1107 310 755 964 310 964 755 310 1107
605 1065 588 605 1061 580 613 1065 580
1602 435 1184 1407 435 1407 1184 436 1602
988 1502 956 988 1502 942 1002 1502 942
1584 436 1200 1408 435 1408 1200 436 1584
988 1503 955 988 1502 942 1001 1503 942
1555 436 1222 1009 435 1409 1222 436 1555
988 1503 954 988 1502 942 1000 1503 942
1186 310 839 1044 310 1044 839 310 1186
605 1061 593 605 1060 580 614 1061 593
802 200 623 724 196 724 623 200 802
401 658 401 371 657 362 401 658 401
815 203 691 755 196 755 691 203 815
407 658 407 377 657 377 407 658 407
808 202 716 763 196 763 716 202 808
404 658 404 381 657 381 404 658 404
774 196 716 746 196 746 716 196 774
387 658 387 373 657 373 387 658 387
691 196 676 686 196 686 676 196 691
371 658 356 371 657 356 371 658 356
16mm 14Nos.
8mm@200mm c/c
400mm
500mm
Column C1(400 x 500)
20mm 12Nos.
8mm@200mm c/c
400mm
500mm
Column C2(400 x 500)
20mm 14Nos.
8mm@200mm c/c
600mm
600mm
Column C3(600 x 600)

(a) (b)

Figure 5: Details of 10-storey frame (a) Longitudinal reinforcement in beams (mm^2)
(b) Column reinforcement

In the present analysis the pushover curve is considered up to 2/3 of ultimate strength or 4% drift of the structure, whichever reach first. At any of the condition, damage in the structure is assumed to be 100%, that means the structure is no longer in serviceable condition. Pushover curves for 6 and 10 storey structure are shown in Figure 6. Defined critical points for damage assessment are represented on the pushover curves. Using three damage assessment methods, damage of 6 and 10 storey structures is calculated.

For damage estimation Method 1, the total non linear energy capacity E_T, for the structure is calculated as the total area under the pushover curve up to maximum displacement where the pushover curve is stopped . the initial elastic energy E_{ie}, is calculated as the area under the curve up to initial yield point of the structure. E is the energy dissipated by the structure up to a displacement where the damage to be calculated.

For damage estimation Method 2, the instant elastic energy E_e, is energy restored in the structure when the structure is unloaded and it is assumed that the structure come back to static position by moving parallel to initial tangent to the curve. All other parameters are calculated as given in Method 1.

For damage estimation Method 3, the damage at any deformation is estimated as the ratio of expended energy for damage to total expended energy capacity to sustain the damage of the structure. In this method, the actual non linear behavior pushover curve and imaginary linear elastic curve are drawn. At any deformation, it was assumed that if there is no damage, the structure should be in linear state. Based on this concept, at any deformation, damage causing energy which is named as expended energy is calculated and represented as a percentage of total capacity of the structure to know the damage status of the structure.

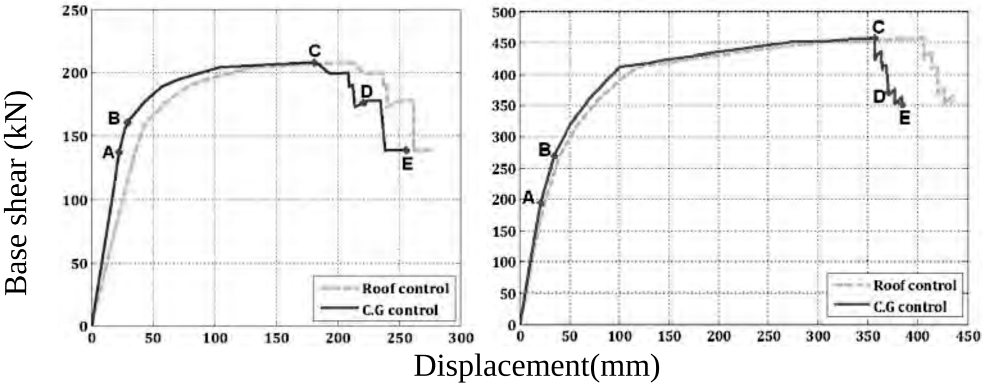

(a) (b)

(b)

Figure 6: Pushover curve up to 2/3 of Ultimate strength (a) 6 storey frame (b) 10 storey frame

Table 2: Damage in % for 6 storey structure under flexure failure

Method of Estimating Damage	**Damage at**				
	A	**B**	**C**	**D**	**E**
Method 1	0	7	70	87	100
Method 2	0	5	65	85	99.8
Method 3	0	0.5	44	71	100
Powell & Allahabadi	0	9	61	74	100

Table 3: Damage in % for 10 storey structure under flexure failure

Method of Estimating Damage	**Damage at**				
	A	**B**	**C**	**D**	**E**
Method 1	0	5	93	94	100
Method 2	0	3	87	89	97
Method 3	0	0.4	84	87	100
Powell & Allahabadi	0	8	93	95	100

To study the efficiency of proposed methods, the damage calculated at each step of pushover analysis using three methods are presented in Figure 7. The damage profile in both frames are same. From the analysis it is understood that the damage estimation by using method 3 is more appropriate. The clear meaning of damage is that the amount of non linear energy dissipated by the structure, as the method 3 represents the clear meaning of damage estimation at any deformation, and estimates the damage state of the structure as 100% at its maximum deformation capacity. Method 1 has the limit that at any deformation, the elastic energy is assumed as the initial elastic energy, but the structure may not have the same. Method 2 is also based on the assumption that at any deformation, when the structure is unloaded, it moves to static position with initial stiffness. The damage calculated at defined critical points on the pushover curve is presented in table 2 and table 3 for 6 and 10 storey structures respectively. To validate the proposed methods, damage estimated at critical points is compared with Powel and Allahbadi model, which is based on displacement ductility.

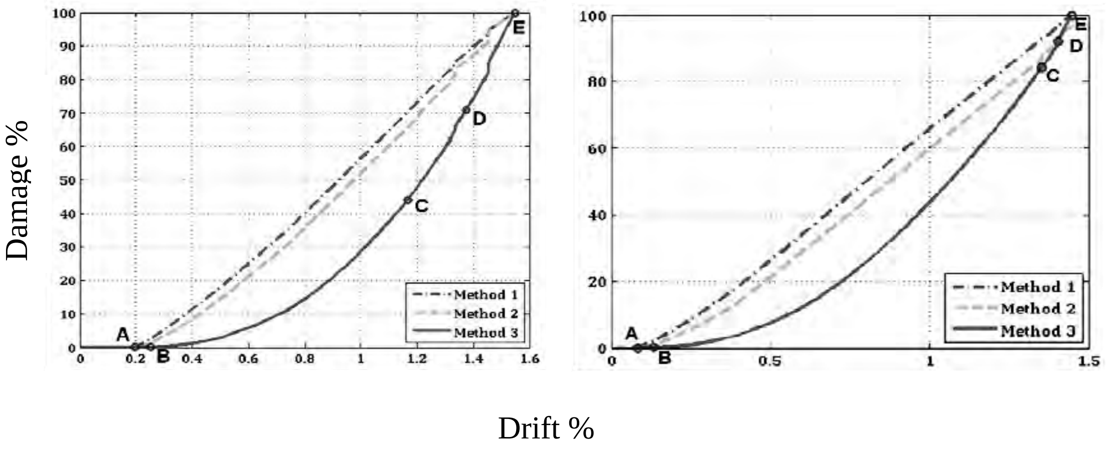

Figure 7: Damage Vs drift under flexure failure (a) 6 storey frame (b) 10 storey frame

4. CONCLUSIONS

1. The ultimate deformation capacity of the structure is found by using static nonlinear pushover analysis and for that deformation the energy capacity of the structure is calculated.
2. In the paper 3 new damage estimation methods are proposed based on energy concept. New damage estimation methods are expressed as a ratio of the nonlinear energy dissipated for any deformation to the total nonlinear energy capacity of the structure.
3. The proposed approach is very simple for quick assessment of damage state of the structure for any deformation.
4. Damage estimation method 3 is more appropriate to estimate the damage state of the structure. This method is based on the expended energy which is responsible for the damage. The deformation profile of the structure is clearly represented by damage method3.
5. Method1 and method2 lead to the less accurate result compared to method 3 because of assumptions in that approaches.

REFERENCES

Bozorgnia, Y. and Bertero, V. V., 2008. Improved shaking and damage parameters for post-earthquake applications. *Proceedings of 14th World Conference on Earthquake Engineering.*

Comartin, C. D., Niewiarowski, R. W., Rojahn, C. and California Seismic Safety Commission. 1996. ATC-40 *Seismic evaluation and retrofit of concrete buildings, Applied Technology Council,* Applied Technology Council, Redwood City, California.

Cosenza, E. and Manfredi, G., 2000. Damage indices and damage measures. *Progress in Structural Engineering and Materials* 2, 50-59.

FEMA-356., 2000. *Prestandard and commentary for the seismic rehabilitation of buildings,* Federal Emergency Management Agency, Washington.

Ghobarah, A., Abou-Elfath, H. and Buddha, A., 1999. Response-based damage assessment of structures. *Earthquake Engineering and Structural Dynamics* 28, 79-104.

Kappos, A. J., 1997. Seismic damage indices for RC buildings: evaluation of concepts and procedures. *Progress in Structural Engineering and Materials* 1, 78-87.

Kunnath, S. K., Reinhorn, A. M. and Park, Y. J., 1990. Analytical modeling of inelastic seismic response of r/c structures. *Journal of Structural Engineering ASCE* 116, 996-1017.

Murty, C. V. R. and Pradeep Kumar, R., 2013. Critical Review of Indian Seismic Code-IS1893:2002. *International colloquium on Architecture & Structure Interaction for Sustainable Development.*

Padilla, D. and Rodriguez, M., 2009. A damage index for the seismic analysis of reinforced concrete members. *Journal of Earthquake Engineering* 13, 364-383.

Park, Y. J., Ang, A. H. S. and Wen, Y. K., 1985. Seismic damage analysis of reinforced concrete buildings. *Journal of Structural Engineering ASCE* 111,740-757.

Powell, G. H. and Allahabadi, R., 1988. Seismic damage prediction by deterministic methods: Concept and procedure. *Earthquake Engineering and Structural Dynamics* 16, 719-734.

Roufaiel, M. S. L. and Meyer, C., 1987. Reliability of concrete frames damaged by earthquakes. *Journal of Structural Engineering, ASCE* 113, 445-457.

Williams, M. S. and Sexsmith, R. G., 1995. Seismic damage indices for concrete structures: A State-of-the-Art Review. *Earthquake Spectra* 11, 740-757.

Analysis on disaster information dissemination process in a rural mountainous area, northeast Thailand

-Comparison with heavy rain disaster in a rural mountainous area, Japan-

Shinya KONDO[1], Akiyuki KAWASAKI[2], Miho OHARA[3] , Akira KODAKA[4],
Adisorn SANTHARARUK [5], and Kazuyoshi OTA[6]
[1] Chief Researcher, Disaster Reduction and Human Renovation Institute, Japan
kondo2@dri.ne.jp
[2] Project Associate Professor, Department of Civil Engineering,
the University of Tokyo, Japan
[3] Senior Researcher, Global Center of Excellence
for Water Hazard and Risk Management, Public Works Research Institute, Japan
[4] Project Researcher, ICUS, IIS, The University of Tokyo, Japan
[5] Loei Fund for Nature Conservation and Sustainable Development, Thailand
[6] Civil Engineering Department, Wakayama Prefecture, Japan

ABSTRACT

In this study, for introducing a disaster information dissemination system in Japan to rural mountainous area in Thailand, the authors tried to organize the information dissemination process of leading the observation data of rainfall and river level to evacuation of residents during flood disaster, from the point of view of information management and role-sharing between related organizations. The first target area was Loei, in northeast Thailand. The second one was Kozagawa town, Southern part of Wakayama Prefecture, Japan. Kozagawa town was damaged by flood and sediment disaster caused by 2011 typhoon Talas. The authors tried to clarify the problems of the target area in Thailand after compared with the result in Japan. There were two problems, evacuation promotion of residents by districts, and sharing and observation data / forecasting and warning of the central government.

Keywords: disaster information dissemination, rural mountainous area, information management, local government

1. INTRODUCTION

Asia has achieved rapid economic growth, in the mountainous areas, there are many places that are modified to farmland is cut entirely mountain surface by large-scale land development and economy promotion measures (Qiu (2009), Ziegler (2009)). In the past to increase the resident population to the danger zone without residence experience, flood risk in the region has become significantly higher (IPCC (2007)). In these areas, poor farmers and immigrants are often living. However, governments are unable to provide adequate disaster prevention measures in the limited resources. In the future, it is necessary to measures such as early evacuation promotion by disaster information dissemination and local community. Introduction of disaster information dissemination system using a mobile phone and the Internet also can be a one of its means.

Dissemination of information and communication technologies such as mobile phones and the internet in Asian countries is expanding rapidly. And in rural and fishing villages in the mountainous areas, households that own the mobile phone are increasing. For example, according to the National Statistical Office of Thailand (2012), the internet and mobile phone penetration rate of residents of more than 6 years of age to be living in non-urban areas of Thailand in 2012, is 20.5 percent and 66.2%. In Japan, technology and scientific knowledge about the disaster experience and disaster prevention have been accumulated. Disaster information dissemination using the mobile phone and the internet has already been made. In the rural and mountainous areas, it is necessary in order to reduce human damage by future disaster to use this knowledge according to local conditions.

In this study, for introducing a disaster information dissemination system in Japan to rural mountainous area in Thailand, the authors tries to organize the information dissemination process of leading the observation data of rainfall and river level to evacuation of residents during flood disaster, from the point of view of information management and role-sharing between related organizations.

2. The disaster information dissemination process in Thailand

2.1 Overview of the investigation area

The investigation area in this study is Loei Wan Sai Sub-district of Phu Luang District at Loei Province, located in the northeastern part of Thailand (Figure 1). Disaster in the region is most the flash floods and landslides caused by torrential rain. Figure 2 shows the configuration of a local administration in this area. These are the outposts of DDPM (Department of Disaster Prevention and Mitigation) at the Loei Province office. There are eight villages in the Loei Wan Sai Sub-district. In this area, there are PAO (Provincial Administration Organization) and TAO (Tambon Administrative Organization) as local autonomy government.

2.2 Outline of survey

In this study, the authors conduct survey to organize the information dissemination process of leading the observation data of rainfall and river level to evacuation of residents during flood disaster. Specifically, the interview survey of residents of villages and the personnel of local government was carried out. And results of this interview survey and the disaster prevention plan (DPP) translated in English was organized to the information dissemination process. Table 1 is the list of persons and dates.

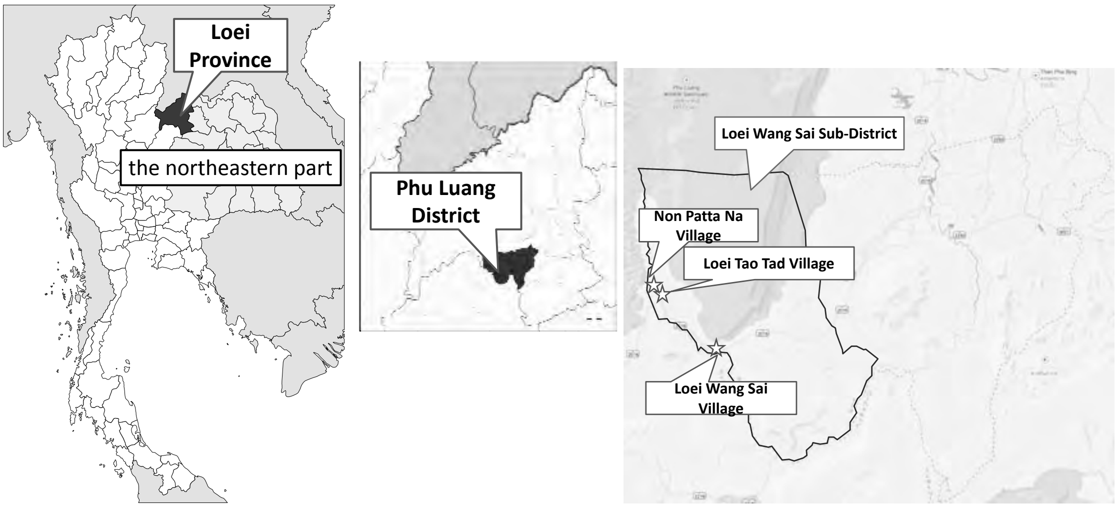
Loei Province
the northeastern part
Phu Luang District
Loei Wang Sai Sub-District
Non Patta Na Village
Loei Tao Tad Village
Loei Wang Sai Village

Figure 1: The study area in Thailand

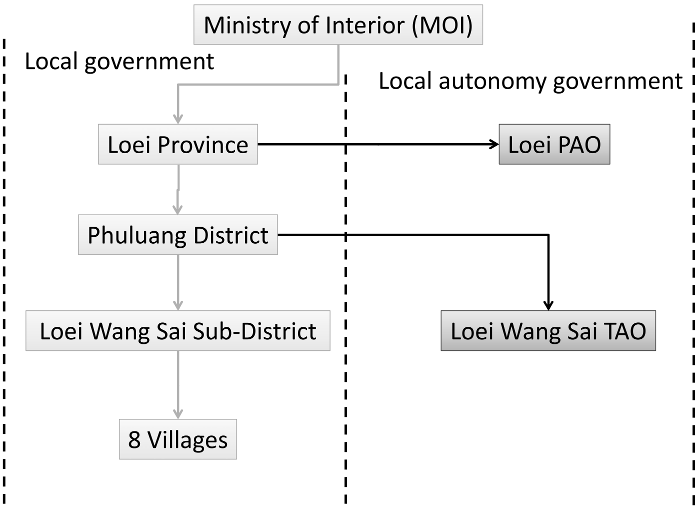
Ministry of Interior (MOI)
Local government
Local autonomy government
Loei Province
Loei PAO
Phuluang District
Loei Wang Sai Sub-District
Loei Wang Sai TAO
8 Villages

Figure 2: The configuration of a local administration in this area

Table 1: The list of persons and dates

	DPP	Persons and Dates
Loei Province	○	2012 Mar. 16: Vice-governor, Director of DDPM, Staff of DDPM, Staff of governor's office. (Total 7 people) 2012 Dec. 6: Director of DDPM, Staff of DDPM. (Total 8 people)
Phu Luang District	○	2012 Mar. 15: Director, Vice-director, Staff. (Total 9 people) 2012 Dec. 6: Vice-director.
Loei Wang Sai Sub-district	-	2012 Mar. 15: Director
Loei Wang Sai TAO	-	2012 Mar. 16: Mayor and Staff. (Total 4 people)
Village	-	2012 Mar. 15: Residents at Loei Tao Tad Village (Total 8 people)

2.3 Division of roles between the organizations

The authors organized the disaster information dissemination process on evacuation during flood in Loei Wang Sai sub-district from the point of view of the division of roles between organizations. Figure 3 shows the disaster information dissemination process in the work flow diagram. The horizontal axis indicates the relevant organizations viewed from residents as ”Central government", "Province", "District", "Sub-district", "TAO", "Residents" and "Upstream village / ranger". "Central government" includes DDPM, TMD (Thai Meteorological Department), and RID (Royal Irrigation Department). "TAO" includes Sub-district. Disaster response of "Residents" is the almost same as that of "Village". The vertical axis represents the business processes of up to evacuation of residents from the observation data of rainfall and river level as “Observation of rainfall / water level”, “Disaster / damage estimation”, “Forecasting and warning”, and “Evacuation”.

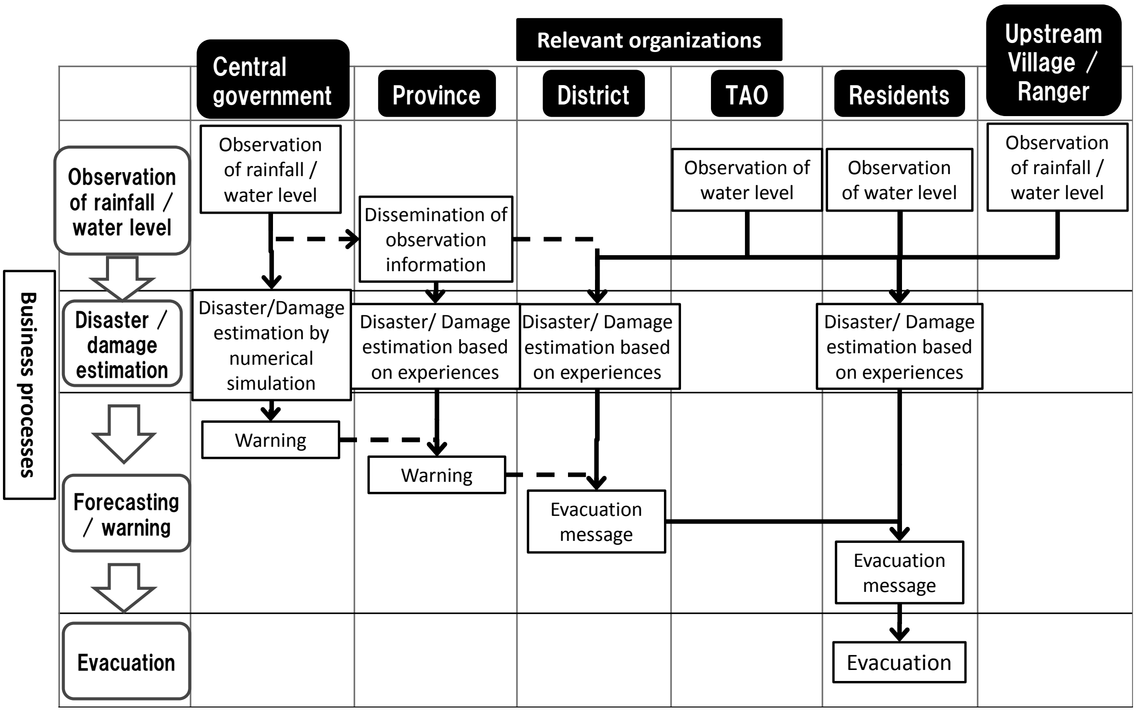
Relevant organizations
Central government
Province
District
TAO
Residents
Upstream Village / Ranger
Business processes
Observation of rainfall / water level
Disaster / damage estimation
Forecasting / warning
Evacuation
Observation of rainfall / water level
Dissemination of observation information
Observation of water level
Observation of water level
Observation of rainfall / water level
Disaster/Damage estimation by numerical simulation
Disaster/ Damage estimation based on experiences
Disaster/ Damage estimation based on experiences
Disaster/ Damage estimation based on experiences
Warning
Warning
Evacuation message
Evacuation message
Evacuation

Figure 3: The disaster information dissemination process in the work flow diagram (Loei Wang Sai district)

Information that central government, TAO, residents, upstream village and ranger has been observed is reported to district. Then, district has been issued the evacuation information to residents based on the warning information from central government and provinces. This is because district has the authority to determine the evacuation of residents according to DPP. On the other hand, residents receive the observation information from TAO, upstream village, ranger and residents. Then residents promote evacuation to other residents based on this observation information and the warning information from district. However, residents often determine the evacuation from actually see the water level of the river. Two arrows connecting central government, province and district are dotted lines. This indicates that there is a possibility of delays in communication because of two reasons below. Firstly, information from the central government has been communicated to the prefecture by fax and email. Secondly, it is necessary to approval of any stages to disseminate information.

3. The disaster information dissemination process in Japan

3.1 Overview of the investigation area

In this study, the investigation area in Japan is Kozagawa town, Wakayama prefecture (Figure 4). This municipality is located in the southern part of Kii Peninsula protruding to the south from the center of Honshu, Japan. Kozagawa town is in the mountainous area where depopulation and aging are progressing. A major industry is the primarily industry a focus on forestry. Figure 5 shows the detail of Kozagawa town. This town is located in the drainage basin of Kozagawa river. There is fear that the damage is caused by flood disaster and sediment disaster. Upstream of Kozagawa river, there is Shichikawa dam that Wakayama prefecture manages.

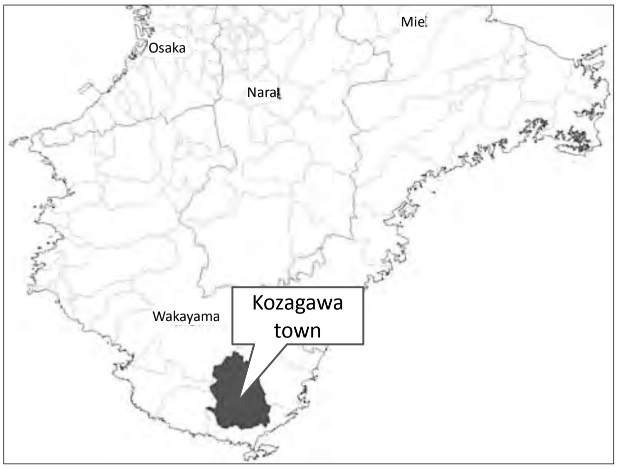
Mie
Osaka
Nara
Wakayama
Kozagawa town

Figure 4: Location of Kozagawa town

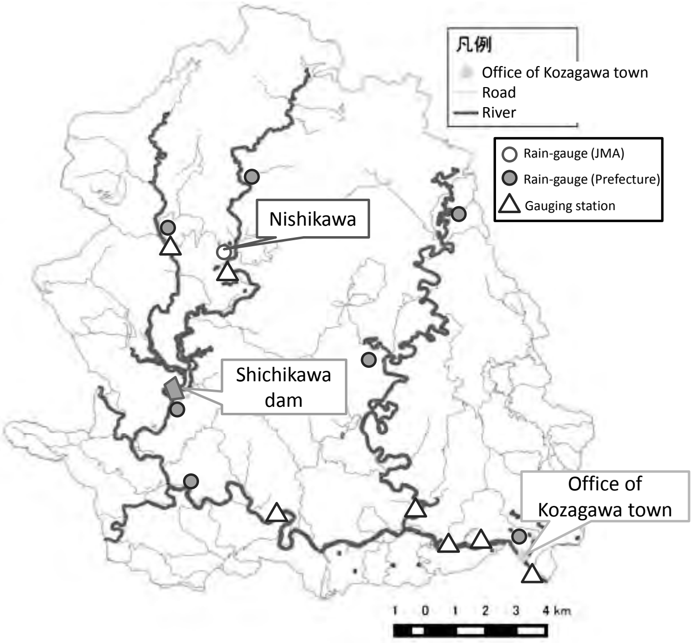
凡例
Office of Kozagawa town
Road
River
Rain-gauge (JMA)
Rain-gauge (Prefecture)
Gauging station
Nishikawa
Shichikawa dam
Office of Kozagawa town
1 0 1 2 3 4 km

Figure 5: The detail of Kozagawa town

3.2 Overview of Typhoon Talas

On 3 September, Typhoon Talas made landfall on Shikoku Island and reached the Sea of Japan on the next day after crossing Shikoku and Chugoku regions. Because Talas had a large scale strong wind area and moved very slowly, it induced moisture advection for many hours and caused the record-breaking heavy rainfall over a wide area from western to northern Japan, especially along the mountains.

Especially over a wide area of the Kii Peninsula, the total amount of the precipitation from 17 JST, 30 August exceeded 1,000 mm. The observing station at Kamikitayama-village in Nara Prefecture observed 1,652.5 mm rainfall in 72 hours, hitting the record high in Japan. The total amount of the precipitation at the station reached 1805.5 mm and precipitation amount in some areas was estimated to be over 2,000 mm. (Japan Meteorological Agency 2011). Figure 6 shows the relationship of precipitation, heavy rain warning and landslide warning information at Nishikawa, the mountainous area of Kozagawa town. Rain became heavily at early morning on 2nd September after heavy rain warning issued. Landslide warning information was also issued at 21:45 on this day at Kozagawa town. Human casualties caused by this disaster are 82 dead people and 16 missing people. In Kozagawa town, there were no direct human casualties (Fire and Disaster Management Agency (2012)).

By this disaster, there was damage to landline, mobile phone, and cable TV at Kozagawa town. Then, residents could not use Internet services. So residents could not access observation information of rainfall / river level.

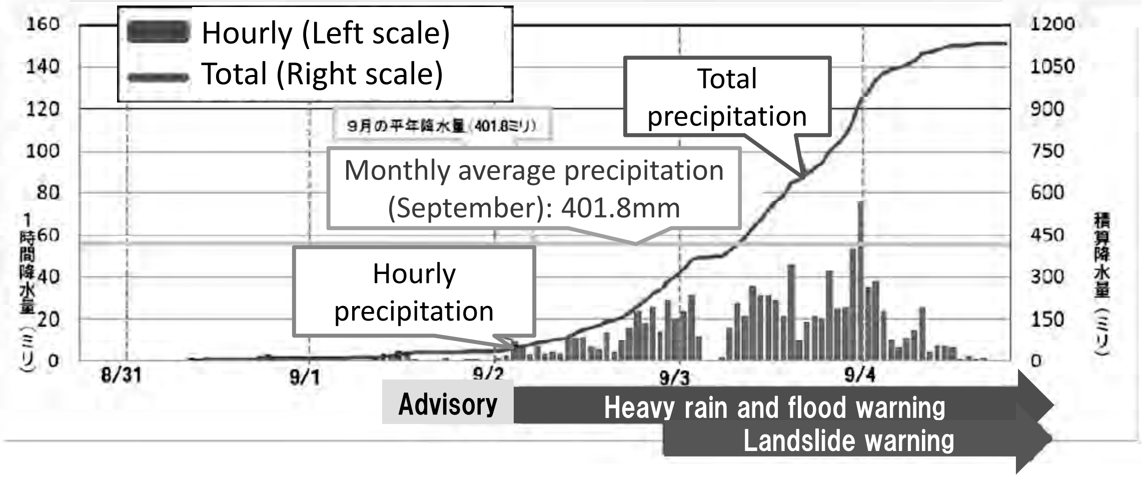

Figure 6: The relationship of precipitation, heavy rain warning and landslide warning information (Kozgawa town)

3.3 Outline of survey

In this study, the authors conduct survey the same as Loei Wang Sai Sub-district. Specifically, the interview survey of the personnel of Wakayama prefecture and Kozagawa town was carried out. And results of this interview survey, DPP of Wakayama prefecture, and abstracts of a record of this disaster (Wakayama prefecture (2013) and Kozagawa town (2011)) were organized to the information dissemination process. Table 2 is the list of persons and dates.

Table 2: The list of persons and dates

	Persons and Dates
Wakayama prefecture	2012 Jan. 10: Disaster management department staff (total 2 people)
Kozagawa town	2011 Dec. 22: Disaster management staff (1 people)

3.4 Division of roles between the organizations

The authors organized the disaster information dissemination process on evacuation during flood in Kozagawa town from the point of view of the division of roles between organizations. Figure 7 shows the disaster information dissemination process in the work flow diagram. The horizontal axis indicates the relevant organizations viewed from residents as ”Central government", "Prefecture", "Municipality (town)", "Residents" and "Dam office". "Central government" means Wakayama Local Meteorological Observatory. "Dam office" is Site office of Shichikawa Dam. The vertical axis represents the business processes of up to evacuation of residents from the observation data of rainfall and river level the same as Figure 3.

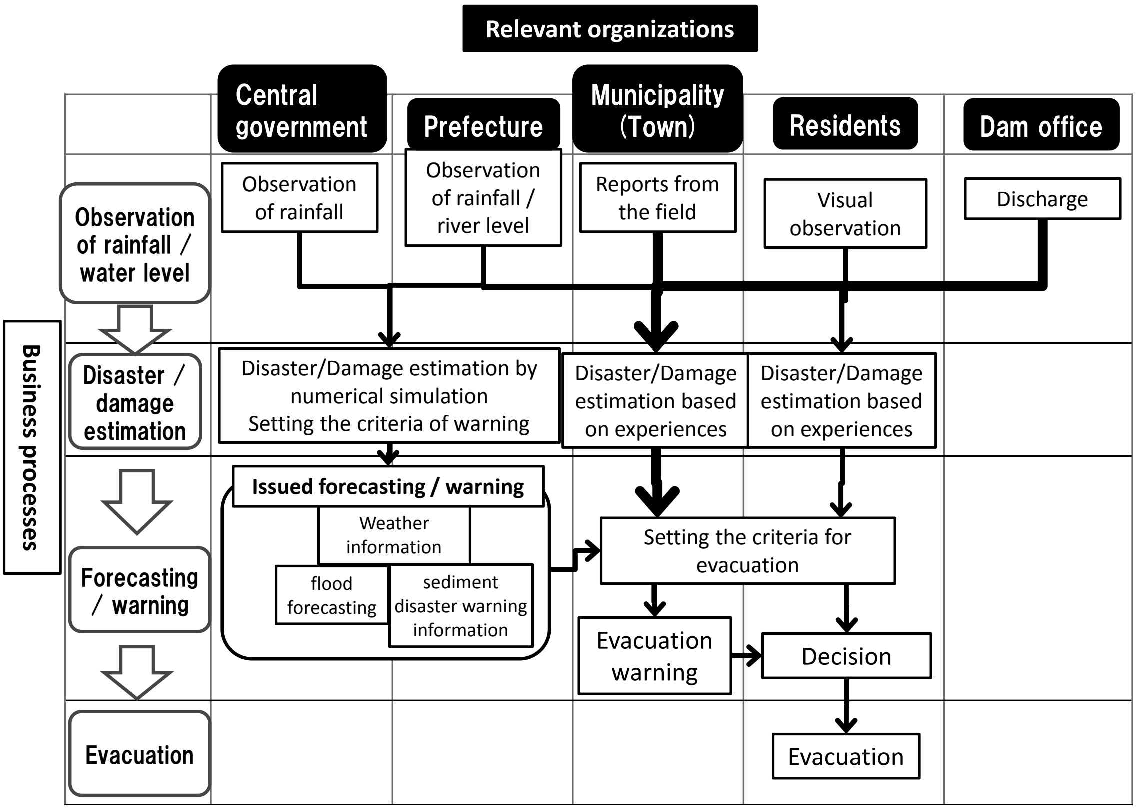
Relevant organizations
Central government
Prefecture
Municipality (Town)
Residents
Dam office
Business processes
Observation of rainfall / water level
Disaster / damage estimation
Forecasting / warning
Evacuation
Observation of rainfall
Observation of rainfall / river level
Reports from the field
Visual observation
Discharge
Disaster/Damage estimation by numerical simulation
Setting the criteria of warning
Disaster/Damage estimation based on experiences
Disaster/Damage estimation based on experiences
Issued forecasting / warning
Weather information
flood forecasting
sediment disaster warning information
Setting the criteria for evacuation
Evacuation warning
Decision
Evacuation

Figure 7: The disaster information dissemination process in the work flow diagram (Kozagawa town)

From Figure 7, each organization was estimated the disaster / damage based on the observation information of rainfall and river water level, respectively. "Central government" and "prefecture" were issued the forecasting and warning as meteorological warning, flood forecasting, and sediment disaster warning information.

"Municipality (town)" had set the evacuation criteria jointly with "residents". Kozagawa town was dispatched staff to the community. Then "residents" and staff set the evacuation criteria before sundown. Kozagawa town and “residents” had agreed to be evacuated without fear fruitless before sundown based on past experience of typhoon. As a result, evacuation of residents had been completed before the roads become unavailable in the inundation from Kozagawa river. At that time, disaster management staff of Kozagawa town had been in touch with site office of Shichikawa dam. Kozagawa town had known when Shichikawa dam discharged.

4. Challenges of the disaster information dissemination process in Thailand

In this chapter, based on the case of flood disaster in Japan which was shown in chapter 3, the disaster information dissemination during flood disaster in Loei Wang Sai sub-district is tried to evaluate. In this time, "District" in Thailand and "Municipality (town)" in Japan is the same level because they have the authority to determine the evacuation.

4.1 Share of observation information / forecasting and warning of central government

For district and residents make the decision of evacuation in early and accurately, it is necessary to get observation information as a basis. Kozagawa town grasped the observation information about rainfall / water level by local meteorological observatory and prefecture. However, in Loei province, the observation information grasped by sensor by central government has been disseminated very late by telephone and FAX. Visual observation in the field has a potential to be caught in flood. Then, observed by the sensor is desired. To estimate the disaster is not easy for the personnel of district who has poor knowledge of weather and river. The personnel of the central government with the knowledge should estimate the situation, and disseminate to district and residents as forecasting and warning.

As a solution to this problem, it is necessary to make an environment to share the observation information and forecasting / warning by Internet. Figure 8 shows the disaster information dissemination process in the work flow diagram based on this solution. By share of observation information and forecasting / warning, district and residents may increase the availability of information to determine the evacuation early.

4.2 Evacuation promotion of residents by district

Kozagawa town and “residents” had agreed to be evacuated without fear fruitless before sundown based on past experience of typhoon. Then, residents were able to evacuation before flood disaster. Kozagawa town was dispatched staff to the community. Then "residents" and staff set the evacuation criteria before sundown. There was damage to landline, mobile phone, and cable TV at Kozagawa town. Then, residents could not use Internet services. On the basis of the above, it is necessary to make an environment that district promotes residents to evacuation at Loei Wang Sai sub-district.

There are two solutions to be considered. Firstly, district encourages residents to decide whether to remain or to evacuate before the damage occurs. At normal times, district and residents should agree to be evacuated without fear fruitless. And it is necessary for district to remove the matters that residents are feeling the difficulty of evacuation.

Another is to multiplexing the means to transmitting the evacuation information to residents from district. Current means is using voice (Loud speaker, Siren, etc.). At the time of heavy rain, there is a possibility that the residents have not heard the information. Therefore, it is necessary to make an environment that district sends information in the character data, such as mobile phone short message service (SMS). If residents do not hear the voice, they confirm the information by mobile phone.

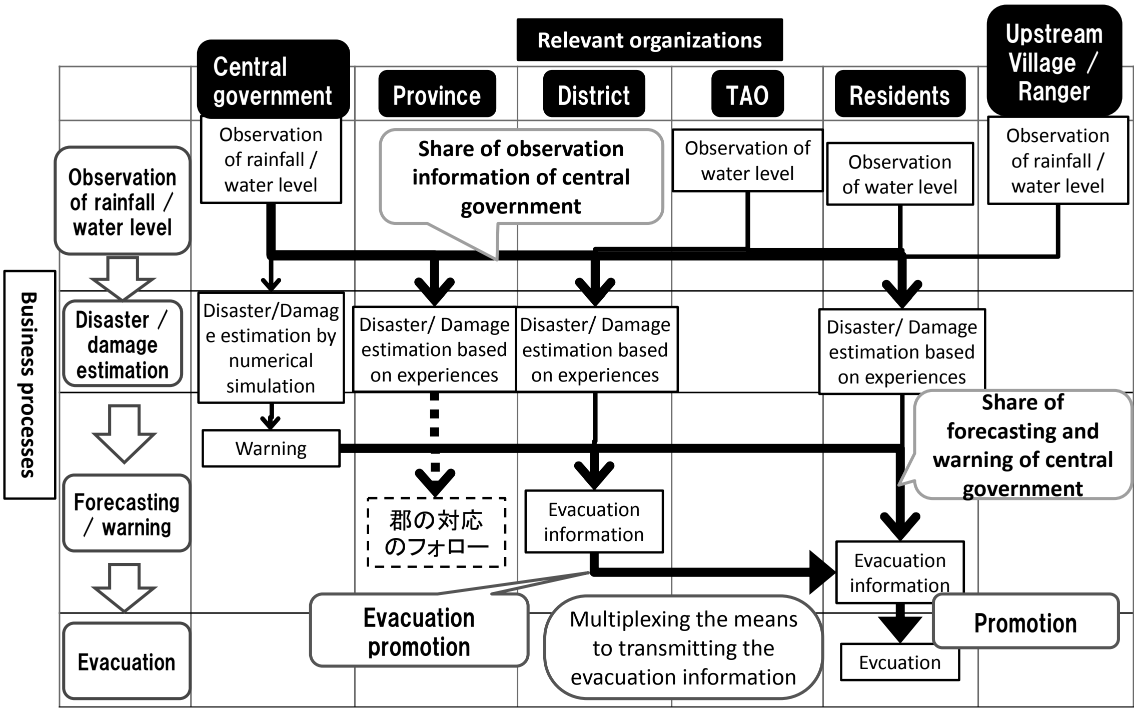
Relevant organizations
Central government
Province
District
TAO
Residents
Upstream Village / Ranger
Business processes
Observation of rainfall / water level
Disaster / damage estimation
Forecasting / warning
Evacuation
Observation of rainfall / water level
Share of observation information of central government
Observation of water level
Observation of water level
Observation of rainfall / water level
Disaster/Damage estimation by numerical simulation
Disaster/ Damage estimation based on experiences
Disaster/ Damage estimation based on experiences
Disaster/ Damage estimation based on experiences
Warning
Share of forecasting and warning of central government
郡の対応のフォロー
Evacuation information
Evacuation information
Evacuation promotion
Multiplexing the means to transmitting the evacuation information
Promotion
Evcuation

Figure 7: The disaster information dissemination process in the work flow diagram (Loei Wang Sai district, improvement plan)

REFERENCES

Qiu, J., 2009, Where the rubber meets the garden, *Nature*, 457(15), 246-247.
Ziegler, A.D., Fox, M. J., Xu, J., 2009, The Rubber Juggernaut, *Science*, 324, 1024-1025.
IPCC, 2007, Climate Change 2007, IPCC Fourth Assessment Report.
National Stastical Office of Thailand, 2012, The Information and Communication Technology Survey in Household.
Japan Meteorological Agency, 2011. *Typhoon Talas relevant information -Portal-*. http://www.jma.go.jp/jma/en/typhoon_Talas.html
Fire and Disaster Management Agency, 2012. *Disaster management of fire fighting in 2011 Typhoon Talas.(Japanese)*
Wakayama prefecture, 2013. *Abstracts of disaster management in 2011 typhoon Talas, (Japanese)*
Kozagawa town, 2011. *Kozagawa public relations magazine, (Japanese)*

Time delays causes in construction projects in Hanoi, Vietnam: Contractors' perspectives

Quoc Toan NGUYEN [1], Thi Hoai An LE [2] and Bao Ngoc NGUYEN[3]
[1]Phd Student, Lecturer, Faculty of Construction Economics and Management
hoaian102@gmail.com
[2]Master student, Faculty of Construction Economics and Management,
[3]Student, Faculty of Construction Economics and Management,
National University of Civil Engineering, Vietnam

ABSTRACT

There is an increasing number of construction activities in Hanoi, which affects to the daily life of citizen there because of noise, dust or accidents. To minimize these harms, implementation schedule of construction projects should be controlled. However, most construction projects in Hanoi to be time delays, both leading to exceeding initial time and cost budget of clients, contractors and bothering urban inhabitants' life. The paper constructed a questionnaire, basing on interview with stakeholders, which is distributed among Vietnamese contractors for identifying and evaluating the risks in terms of time in construction phase of projects in Hanoi. Results found four main groups of causing time delays: (1) by accident factors, (2) technique and management factors, (3) poor supervision and (4) government policies. Then, the paper puts forward some recommendations for the Contractors to prevent, deal with and manage time risk encountered in construction projects for carrying out safe, efficient and quality construction activities in Hanoi context, the capital of Vietnam.

Keywords: time-related risk, construction delay, construction projects in Hanoi

1. INTRODUCTION

Construction industry faces more risk than others because of its unique features such as long period, complicated processes, environment influenced, and various stakeholders [Chidambaram, Narayanan and Arazi, 2012]. Different types of risk arise at different stages in construction from preparation phase, construction phase to operation phase. These risks lead to different effects to stakeholders. From contractors' view, risks in terms of time or schedule in construction phase are most concerned. Because, if projects are time-delayed that will bring some problems to the contractors, for example, cost overrun and accompanied by building quality degradation, losing the professional reputation [Zou and Wang, 2009]. In Vietnam context, 90% [Vietnam Federation Construction, 2011] of construction projects are exceeded their planned time. Thus, effective time-risk management methods should be suggested to understand not only what kinds of risks are faced, but also how to manage these risks in construction phase. So, the paper will investigate the practice to identify and evaluate the risks causing time delays of construction in Hanoi, from contractors' perspective.

2. LITERATURE REVIEW

Around the world, many researches have been carried out on project delay problems. Typically in Vietnam, a research paper called “Risk management in oil and gas construction projects in Vietnam” was published by Emerald Group Publishing Limited in 2007 for identifying risk factors, which affect oil and gas construction projects in Vietnam and derive risk responses(Van et al., 2007); a study of Dr. Nguyen Lien Huong was published in the Vietnam Journal of Construction in No February/2002 issue, which indicated major risks in construction projects; a study of Dr. Pham Hong Luan HCMUT and M.S. Nguyen Thanh Binh UAH was published in the Vietnam Journal of Construction in the No January/2005, which shown what causes time overrun in construction projects in Vietnam; a study of Dr. Le Van Long (Institute of Construction Economics) indicated risk management issues in construction projects, was published in the Vietnam Journal of Construction in No April/2004 issue ;a study of Pham Thi Trang DUT provided a number of solutions for managing risks in construction projects through her research work in 2010. Recently, the topic was mentioned in a Master thesis of Nguyen Tien Lam (2014) in theme “Risk Management in ICON 4 Construction Company”.

Those researches, which related to the above topic, demonstrated the general content as well as some specific aspects of risk management. However, within the scope of the research works widely published which the authors found out, not seen much in-depth study of risk management in terms of time delays in construction. Thus, it is necessary to conduct a comprehensive research about time delays in Vietnam.

3. RESEACH METHODOLOGY

The research approach used for the paper included a comprehensive literature review, an online questionnaire to the contractors and a statistical analysis of the survey data. The paper uses results from a survey with respondents who are working for contractors to investigate the issues in managing risks in terms of time and schedule.

Schedule overruns occur due to wide range of factors. Usually, the most majority of project delays happen during the “construction phase”, when many unforeseen factors are always involved. So, the scope of the research is focus on time overrun causing in “construction phase”.

The questionnaire comprised of two sections. While section 1 covered general information about the respondents, section 2 carried 4 main factor groups with a total of twenty-fifth questions related risks in terms of time delay causing. The factors to be measured in the questions have been developed from interim results collected in a preliminary survey through unofficial talks with some engineers and project managers. The interviewees are requested to answer the questions according to their own experience and knowledge. 55 results of the questionnaire were received back but only 51 questionnaires are accepted to be used in the research. Moreover, authors had met some experts to interview for their suggested solutions to solve these problems.

Data analysis method

The survey focus on 2 main purposes: occurring probability and impact level of time-related risks or time delay causing. The research uses a score system from 1 to 4 representatives for rarely, usual, frequent and very frequent of factors' probability. Besides, the impact level also are assigned score 1 for low, 2 for medium and 3 for high impact level. Then, the average of occurring probabilities and impact levels are calculated to find out top time-risk in term of occurring probabilities and impact levels. Probability index: A formula is used to rank causes of delay based on frequency of occurrence as identified by the participants (equation 1):

$$(PI\ )(\%)= \Sigma(a*n/P)*100 \qquad (1)$$

Where a is the constant expressing weighting given to each response (ranges from 1 for rarely up to 4 for very frequent), n is the frequency of the responses, and P is total number of 4 main factors (25 factors) score in terms of probability.

Impact level index: The importance index of each cause is calculated as follows (equation 2):

$$(ImI)(\%)= \Sigma(a*n/I)*100 \qquad (2)$$

Where a is the constant expressing weighting given to each response (ranges from 1 for low up to 3 for high), n is the frequency of the responses, and I is total number of 4 main factors (25 factors) score in terms of impact level.

4. SURVEY DATA AND DISCUSSION

The respondents came from contractors, both public and private companies, including engineers, project managers, and consultants. Most of them (67%) work for private companies and the others work in public sectors. Their average year of work experience is 10 in the field; table 1 shows more detail of the interviewees. It can be seen that approximately 30% of respondents have worked more than 10 years in the industry, and the longest is 28 years. Moreover, the data also shows that all respondents have received tertiary education with 92% graduate degree and 8% of post graduate. The table 1 is evident that all respondents have enough experiences and knowledge to answer the section 2 of the interview. Thus, the data received back are believable to be severed the purposes of the research.

Table 1: Categories of respondents

No	Categories	No of respondents	%
1	Age group		
	Under 30	10	20%
	Over 30	41	80%
2	Work experience		
	Under 10 years	36	71%
	Over 10 years	15	29%
3	Education		
	Graduate	47	92%
	Post Graduate	4	8%
4	Type of Company		
	State-own company	17	33%
	Private company	34	67%

Table 2 below shows the projects in Hanoi area which the authors conducted to find out some reasons causing time delays.

Table 2: Categories of projects in survey

No	Name of Project	Type of project
1	National University of Economics Centre Building	Civil (Office)
2	Office building, Hai Ba Trung	Civil (Office)
3	Water supply and drainge in Gia Lam	Infrastructure
4	Pacific Building	Civil (Office)
5	Lotte Building	Civil (Office + Mall)
6	Time City Mall Project	Civil (Office +Mall)
7	Cat Linh - Ha Dong Metro Project	Infrastructure
8	345 Doi Can Building	Civil (Department)
9	Golden Place Building	Civil (Department)
10	Ministry of Foreign Affairs Head Office	Civil (Office)

The limitation of the survey is that did not cover all type of projects and number of the projects is only 10. However, these projects are likely typical and from both private and public sector.

In term of time delay causing that the respondents had feedback, they can put into 4 large groups: (1) by accident factors, (2) technique and management factors, (3) poor supervision and (4) government policies. In which, 25 time-risk causes are identified basing on information provided from participants. According to the result, group (3) is the most popular cause, being mentioned by 65,37% of the respondents. It is also the highest impact group with 61,13%. The group (1) is ranked 2nd with around 20% both occurring and impact level. The next is group (4) and the last is group (3) with similar rate both occurring probabilities and impact levels. The detail is displayed in table 3. It can be seen that the summary of percentages of all Group I + Group II + Group III + Group IV equals 100% both in terms of P.I and Im.I.

Group I: By accident factors

Because of unique features of construction industry as mentioned above, it is impacted by accident factors easily. In the survey, the participants addressed probability of causing by accident factors is around 20% and their impact level is around 20% too. In which, risk factors from natural are assigned 11% of time-delay and "bad weather" is the most popular cause. While the factors from market are occupied approximately 8% both in terms of probability and impact level with the "material price increasing" is the highest probability factor. The price of construction materials is usually changing in response to the inflation and the relationship between supplies and contractors. With regards to impact level, earthquake and economics crisis are the more influence in the group.

Table 3: Result of the survey

No	**Categories of time-related risks causing**	**P.I (%)**	**Im.I (%)**
I	**Risks posed by accident factors from external impacts**	**19,33**	**20,98**
1	***Factors from natural conditions, environment and climate***	***11,15***	***12,14***
1.1	Causing factors of geology, hydrology, topography conditions of the building site	3,61	2,64
1.2	Bad weather factors as: Heavy rain, too hot, too cold…	4,09	3,05
1.3	Disasters such as: storm, flood…	2,09	3,12
1.4	Seismic waves, earthquake…	1,35	3,32
2	***Risks posed by unexpected market fluctuations***	***8,19***	***8,84***
2.1	Material scarcity and resource restrictions	2,57	2,82
2.2	Material price increasing	3,44	2,77
2.3	Economics crisis	2,17	3,25
II	**Risks posed by technique and management factors**	**65,37**	**61,13**
3	***Risks in design and surveying***	***11,40***	***10,92***
3.1	Inadequate or insufficient site information	2,37	2,80
3.2	Design variations	9,03	8,12
4	***Unsuitable construction program planning***	***25,55***	***24,30***
4.1	Tight project schedule	7,5	7,20
4.2	Inadequate program scheduling	5,96	5,60
4.3	Insufficient of productive resources	4,25	4,00
4.4	Variations of the construction programs	7,84	7,50
5	***Risks posed by Labor factors***	***6,97***	***6,47***

5.1	Low skilled workers	3,10	3,22
5.2	Workers' awareness	3,87	3,25
6	***Causing associated with Infrastructure, Construction Occupational Safety***	***10,86***	***10,82***
6.1	Negligence of construction safety policy	3,26	2,30
6.2	Labor accidents happened on site	4,02	5,30
6.3	Infrastructure problems: supply water, electric…	3,58	3,22
7	***Risks posed by stakeholders***	***10,58***	***8,61***
7.1	Causing by the client	3,81	3,30
7.2	Causing by suppliers	3,42	2,92
7.3	Causing by subcontractors	3,36	2,39
III	**Risks posed by checking and taking over the buildings factors**	**6,74**	**8,76**
8.1	Incomplete documents	2,91	3,17
8.2	High quality expectations	3,83	5,59
IV	**Risks posed by legal - administrative factors**	**8,57**	**9,13**
9.1	Related - polices variations: interest rate, wage…	5,79	6,28
9.3	Bureaucracy of government	2,78	2,85

Group II

Group II is result from 7 key risks and it is considered the highest probability (65,37%) and its result is the most dangerous when the risks happening.

The result also shows that “Unsuitable program planning” is the most significant risk to cause time delay with the amount percentages of probability and impact level are similar (25,55% and 24,3%), and each factor in the (II.4) has alike the amounts. “Unsuitable program planning” may result from “Tight schedule”, “Inadequate program scheduling”, “Insufficient of productive resources”, “Variations of the construction programs”. It all can be responsible for lack of construction program planning knowledge of contractors. In which, “Variation of construction programs” was ranked as the most significant risk in the group because of 7,84% probability and 7,5% impact level. The next popular reason is “Tight schedule” with assigned 7,5% and 7,2%, which guess that formulating an appropriate schedule in the feasibility phase is hardly more constructive to the project delivery. “Inadequate program scheduling” often emerges in projects with a tight schedule when contractors need to be reduced some programs to meet the clients’ requirements. Moreover, uncertainty surrounds most resources (labor, material, and machine) of construction projects, which makes it impossible to accurately predict the resources required for various programs. That named “Insufficient of productive resources” which leads to time risk in projects.

The next significant main risk came from design and surveying work. “Inadequate or insufficient site information” especial soil test can affect the progress of underground work such as excavation, foundation or basement. If the work be mistake or inaccurate, this leads to design will be change after that. As the result, contractors have to revise their planning, and more or less, it affects to the project time line.

Thirdly, the contractors' abilities to communicate with stakeholder should be used as key criteria in meeting the need of time. Lack of coordination between project stakeholders may lead to change the programs. For example, the misunderstanding requirements of Clients makes contractors difficulty in approval document or checking and taking over the buildings. So, leads to late in revising and approving documents by owner causes slow payment of completed works. On the other hand, unsuccessfully of subcontractors and suppliers management also brought total 6,5% time delay causing. It may cause by poor contract management leads to occurrence of dispute between all participants.

Next, the accident on site can impede the construction progress. It may root from negligence of construction safety policy such as wearing protective tools or accident regards to electric of machines as electric welding, steel bending. It is hard to control these risks because it comes from labors' awareness. Besides, insufficient amount of skilled labor may result in delays in the construction phase. High productivity of labors and their professional is one of the keys to achieve project objective in terms of time.

Group III

Although most risks are root from technical terms, the survey found that some risk checking and taking over the buildings process. From clients' perspective, the projects outcome should be reach the need of market. So, "Incomplete documents" and "High quality expectations" usually occurs in checking and taking over the building process in order to secure quality of the project. This group is often happen when finishing the construction work and it also is the lowest probability (6,74%) and impact level (8,76%).

Group IV

These risks are normally out of the control of the contractors. The government sometimes changes the wage, quality or management polices to develop macro economics and to create a friendly environment for contractors. But, this sometimes makes the projects be frozen to adjust contract, time line and budget. The survey data addressed, from contractors' perspective, 8,57% respondents agreed that policies variation cause time overrun and 9,13% regards to impact level. This group especially is significant meanings to the public sector, where project budget and time control are under government agencies' power.

5. RECOMMENDATION SOLUTIONS

According to the survey data, list risks to cause time overrun can be identified and evaluated their impact to projects. Then, the authors suggested some solutions to handle the key risks. For example, the most significant factor, "Unsuitable construction program planning", related to the knowledge and experience of the planners. To reduce negative influence of the risk, contractors should have deeply understand of the design, client's requirements, related-polices and contractors' resources themselves to set up an informative program in order to meet the project's demands and secure the profit of the contractors. Similarly, the contractors should consider some solutions suggested below mapping out strategies which suitable with their conditions and project's context to prevent and deal with the risks in terms of time.

- Listed time-risks usually happened in projects then set up a risk countermeasures library
- Training staffs to be more professional in stakeholder communicating, more knowledge in setting up construction program planning to establish a systematic construction program scheduling
- Maintaining close and understand relationship with project managers and design team to manage variations and avoid Occurrence of dispute
- Providing safety training to on - site staff to improve their awareness of safety.
- Maintaining close relationship with local government officers

5. CONCLUSION

This research achieved its initial purposes: identifying and evaluating the time delay causing. According a survey with engineers, consultants and project managers, who own experience and knowledge of construction projects, 25 key risks were highlighted on a comprehensive assessment of their likelihood of probability and impact level on project objectives. It can be seen that, from contractors' perspectives, time delays causes both derive from internal and external factors. "Variation of construction programming" was found to have the highest impact level and probability. The factor depends on contractors' capacity especially experience and knowledge of construction program planning. From external factors, stakeholders' relationship is considered the most important one for achieving time planned.

From these result, the authors suggested some solutions to prevent time overrun. By taking care of these solutions, contractors can reduce and control the extent of time delays, contribute to carry out safe, efficient and quality construction activities in Hanoi, Vietnam. The research findings are not useful for only participants in Vietnam but others in developing countries.

REFERENCES

Alavifar, A. H., and Motamedi, S., 2014. *Proceedings of the 2014 International Conference on Industrial Engineering and Operations Management*, Bali, Indonesia, 919-929.

Bui, P. T., Pham, M. L., and Nguyen, T. L., 2014. Unpublished report, *Student Sciences Research Workshop*, National University of Civil Engineering, Vietnam.

Chidambaram, R., Narayanan, S. P. and Arazi, B. I., 2012. Construction delays causing risks on time and cost - a Critical review. *Australasian Journal of Construction Economics and Building* 12, 37-57.

Le, L. H., Lee, Y. D. and Lee, J. Y., 2008. Delay and cost overruns in Vietnam large construction projects: A comparison with other selected countries. *KSCE Journal of Civil Engineering* 12, 367-377 (in Korean).

Nguyen, D. C., Ma, X. M. and Nguyen, T. Q., 2013. Risks from in-city construction works to urban inhabitants' safety in Hanoi: the city residents' perspective. *USMCA 2013* Hanoi, Vietnam, 429-440.

Nguyen, T. L., 2014. *Master thesis in Construction Management*. Risk Management in

ICON 4 Construction Company, National University of Civil Engineering, Vietnam.

Rezaian, A., 2011. Time-cost-quality-risk of construction and development projects or investment, Iran. *Middle-East Journal of Scientific Research* 10, 218-223.

Zou, P. W. and Wang, J.Y., 2009. Identifying key risks in construction projects: Life cycle and stakeholder perspectives. *International Journal of Construction Management* 9, 61-77.

Investigation on tendering and contracting practices of Myanmar building construction

Khin Su Su WAI[1] and Aye Mya CHO[2]
[1]Phd Candidate, Civil Engineering Department,
Mandalay Technological University, Mandalay, Myanmar
khinsusuwai235@gmail.com
[2]Associate Professor, Civil Engineering Department,
Mandalay Technological University, Mandalay, Myanmar

ABSTRACT

The successful execution of a construction project is heavily impacted by making the right decision during tendering processes. Clients typically provide contractors with a set of tender documents for a bid proposal upon which a contract may be let and executed. Such tender documents often contain the information about a client's project plans so that a contractor can price it. However, in practice, tender documents are not clear, consistent and adequate. This makes the calculation of a tender programme and price for a construction project difficult. The aim of this study is to ascertain the clarity and adequacy of tender documentation in practice. This paper focuses on describing the importance of tendering and contracting practices for building construction and how the uncertainties and incomplete information can cause conflicts in construction state. To be able to do this, it is important to capture the reality of the problem. Therefore, twelve forms of tender documents from different construction organizations are analyzed to understand the quality and nature of tender documents. By discussing several issues crucial to tender preparations for building construction projects in Myanmar, this paper seeks a deeper understanding of how project manager and quantity surveyor can better standardize tender preparation work and more successfully manage in contracting processes.

Keywords: tender, contract, document, quality, standard, client, incomplete information

1. INTRODUCTION

Building construction is a highly competitive and risky business. This competitiveness is compounded where conflicting objectives amongst contracting and subcontracting firms set the stage for an adversarial and potentially destructive business relationship. The successful execution of a construction project is heavily impacted by making the right decision during tendering processes. Managing tender procedures is very complex and uncertain involving coordination of many tasks and individual with different priorities and objectives. Clients, especially those from the public sector, need broader tender evaluation criteria to complement the traditional focus on bid price. This paper describes the results and discussion of questionnaire survey concerning tendering, and contracting practices from the viewpoints of respondents in Myanmar construction industry. It also focuses on describing the importance of tendering and contracting practices for building construction and how the uncertainties and incomplete information can cause conflicts in construction state.

2. TENDERING PROCESSES IN THE CONSTRUCION INDUSTRY

Tendering is the process used by many construction clients to obtain the program and price for a project. The successful execution of a construction project is heavily impacted by making the right decision during tendering processes. Successful projects have generally started with the use of best practice tendering processes, and the benefits of such tendering practice include:

1. A clear understanding of the rights and obligations of both parties.
2. An increase in the likelihood of procuring a project to meet the required scope, time, cost and quality parameters.
3. A reduction in the likelihood of misunderstandings and disputes.

Typically, the tender process involves three distinct phases: tender preparation, tendering and tender evaluation. The commencement of the tender process is the development of the project definition and scope which will set the scene for the success of the entire process. The second step is tender selection processes. There are five main processes for the selection of tenderers. They are open or public tender, selected or approved tender, pre-qualified tender, invited tender and direct negotiation tender.

2.1 Selection methods

Once the owner determines which project delivery method and corresponding competition criteria they will use, the framework for the actual selection process has been set. There are basically three selection methods utilized for purchasing construction and construction management services:

1. Low-bid selection
2. Best-value selection (BVS)
3. Qualifications-based selection (QBS)

Each of these selection methods uses a different solicitation instrument to advertise the project. For example, low-bid selection, which is most commonly associated with traditional design-bid-build project delivery, utilizes the invitation for bids (IFB). Best-value selection utilizes a request for proposals (RFP), and qualifications-based selection employs a request for qualifications (RFQ). Each of the selection methods represents a different kind of competition, and the steps required to move through the process vary. Because the market is wide open now for any one of these methods to be utilized, it is important to be familiar with each of them.

2.2 Criteria for selection

The criteria for selection must be clearly stated in the tender documents. Such criteria need to cover the critical factors on which the success of the project is based. Typical criteria for selection include:

1. Conformity
2. Capability

   (1) Previous Experience on similar works
   (2) Financial resources
   (3) Managerial and Personnel resources
   (4) Technical resources
   (5) Current workload
   (6) Dispute Resolution record
   (7) Quality Assurance System
   (8) Environmental Compliance record
   (9) Industrial Relations record
   (10) Occupational, Health Safety & Rehabilitation record
3. Price
4. Construction Period

Hence, the criteria for selection involve both a “Price” and “Non-Price” components. Depending on the nature of the client and project, each of the above factors will have a varying weighting or priority. It is recommended that the client ensures that the criteria for selection weightings are determined prior to the opening and evaluation of tenders. It is preferable that the weightings are not disclosed to tenderers.

2.3. Tender analysis

The importance of assembling an experienced and competent tender evaluation team is critical to the success of the tender process. The team leader or chairperson should possess leadership, communication and negotiating skills as well as technical and commercial capabilities. One of the most important skills is the ability to maintain critical objectivity during the tender process. Each member of the team must be free of any conflict of interest that might undermine the objectivity of the assessment. The appointment of such a team will ensure that the most appropriate tenderer is chosen with respect to the defined criteria of selection. In major projects, each tender is likely to contain differences in the areas of design, timing, capital cost, impact, service and durability, and operating cost. Hence, a rigorous tender analysis process is required to obtain a fair comparison between individual tenders. The use of risk analysis techniques in the tender analysis process is encouraged.

2.4. Condition of tendering

In traditional design-bid-build, price is the primary criterion used to determine who will win the project. Basically, the contractor who submits the lowest price will be awarded the contract. With construction management (CM) specifically, agency CM, qualifications become the main factor in determining which CM firm will win the competition. And with at-risk CM and design-build, a combination of price and qualifications are considered when selecting the winning team. The following graphic (Figure 1) illustrates the connection between project delivery method and selection criteria.

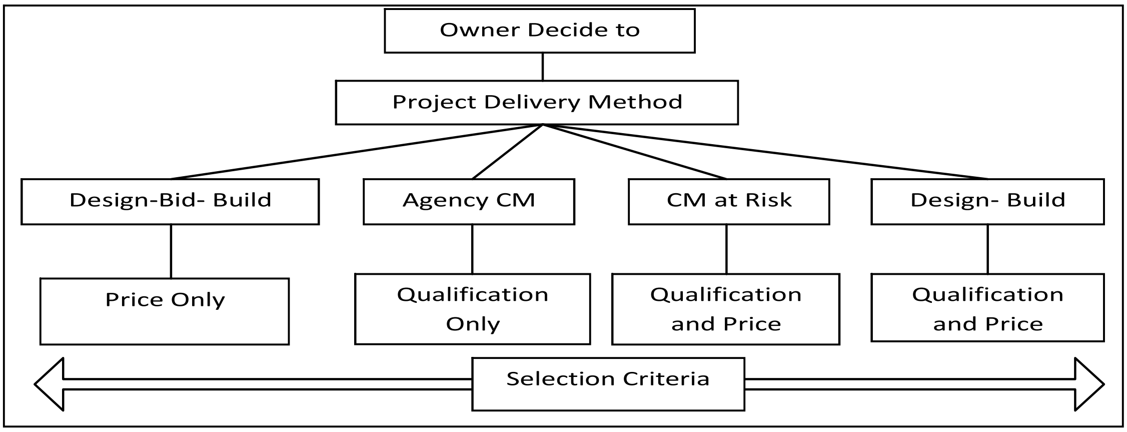

Figure 1: Connection between project delivery method and selection criteria

3. CURRENT TENDERING PRACTICES OF MYANMAR BUILDING CONSTRUCION

Tendering is one of the stages in a construction project that requires extensive information and documents exchange. Tender documents contain the information about a client's project plans so that a contractor can price it. In practice, tender documents are not always clear, consistent and adequate. This makes the calculation of a tender program and price for a construction project difficult. Several aspects of the literature in construction management indicate that the quality of tender documents is often "poor" in practice. However, there is little empirical research in the literature on the quality of tender documents used in construction and the practical implications of poor quality tender documents in construction.

Myanmar construction industry is expected with problem of construction risk as similar to global phenomenon. However, there are still less facts and figures concerned with its construction practices and no exact indication on its tendering and contracting practices. Therefore, twelve forms of tender documents from different construction organizations are analyzed to understand the quality and nature of tender documents. Letter A, B, C, D, E, F, G, H, I, J, K and L represent construction organizations. The documents include in these tender documentations are compared with tender documentation used by international construction firms and shown in (Table1). Symbol (√) represents the statement which can be seen in Myanmar building construction tender document as the symbol (-) is lack of statement. The importance of tender documentation and current tendering practices of Myanmar are discussed below.

Table 1: Tendering practices of Myanmar building construction

Description	**A**	**B**	**C**	**D**	**E**	**F**	**G**	**H**	**I**	**J**	**K**	**L**
Advertisement for bids												
Project name and description	√	√	√	√	√	√	√	√	√	√	√	√
Project location (not detail)	√	√	√	√	√	√	√	√	√	√	√	√
Owner name and address	√	√	√	√	√	√	√	√	√	√	√	√
Architect name and address	√	-	-	-	-	-	-	-	-	-	-	-
Contact information	√	-	√	√	-	-	-	-	√	√	-	√
Details of tender submission	√	√	√	√	√	√	√	√	√	√	√	√
Where to access the plans and	√	-	-	-	-	-	-	-	-	√	-	-

specs												
Project duration with anticipated start and completion dates	-	-	-	-	-	-	-	-	√	-	-	-
Bonds required	√	√	√	√	√	√	√	√	√	√	-	√
Restrictions on bidders	√	-	√	-	√	√	√	√	√	√	√	√
Project budget or anticipated price range	-	-	-	-	-	-	-	-	-	-	√	-
No; of copy require	√	-	-	-	-	-	-	-	-	-	√	-
Detail of tender submission	√	√	√	√	√	√	√	√	√	√	√	√
Agreement form	√	-	-	-	-	-	-	-	-	-	-	-
Tender form	√	√	√	√	√	√	√	√	√	√	√	√
Condition of Tendering												
Delivery method	√	√	√	√	√	√	√	√	√	√	√	√
Procurement method	√	-	-	-	-	-	-	-	-	-	-	-
Selection Criteria (P=price only, Q=qualification, B=both)	P	B	B	-	-	-	-	-	B	-	-	B
General Conditions												
Owner Responsibilities	√	-	-	-	-	-	-	-	-	-	-	-
Contractor Responsibilities	√	√	√	√	√	√	√	√	√	√	√	√
Administration of the Contract	-	-	-	-	-	-	-	-	-	-	-	-
Subcontractor Relations	√	√	√	√	√	√	√	√	√	√	-	√
Construction by Owner or Others	-	-	-	-	-	-	-	-	-	-	-	-
Changes in the Work	√	-	-	-	-	-	-	-	-	-	-	-
Time and Schedule Requirements	-	-	-	-	√	-	-	-	√	-	-	-
Payments and Completion	√	√	-	-	-	-	-	-	-	-	-	-
Protection of Persons and Property	-	-	-	-	√	-	-	√	-	√	-	√
Insurance and Bonds	-	-	-	-	-	-	-	-	-	-	-	-
Miscellaneous Provisions	√	-	-	-	-	-	-	-	-	-	-	-
Supplemental Conditions												
Soils and soil-testing information provided by the owner	-	-	-	-	-	-	-	-	-	√	-	-
Survey information provided by the owner	-	-	-	-	-	-	-	-	-	-	-	-
Materials or other services provided by the owner	-	-	-	-	-	-	-	-	-	-	-	-
Job signage requirements	-	-	-	-	-	-	-	-	-	-	-	-
Traffic control and pedestrian safety requirements	-	-	-	-	-	-	-	-	-	-	-	-
Phasing or special schedule requirements	-	-	-	-	-	-	-	-	-	-	-	-
Requirements for security	-	-	-	-	-	-	-	-	-	-	-	-
Temporary facilities and sanitation requirements	√	-	-	-	-	-	-	-	-	-	-	-
Specifications												
Technical	√	√	√	√	√	√	√	-	√	√	-	-
Materials	√	-	-	√	√	-	-	-	-	√	-	-
Standard of workmanship	-	-	-	-	-	-	-	-	-	√	-	-
Methods of installation and	-	-	-	-	-	-	-	-	-	-	-	-

erection												
Quality control and quality assurance procedures	-	-	-	-	-	-	-	-	-	√	-	-
Drawing (Depend on delivery)												
Civil	-	-	-	-	-	-	-	-	-	-	-	-
Architectural	√	√	-	√	√	√	√	-	√	√	-	-
Structural	√	-	-	√	-	-	-	-	-	-	-	-
Electrical	-	-	-	-	-	-	-	-	-	-	-	-
Mechanical	-	-	-	-	-	-	-	-	-	-	-	-
Additional information												
Environmental impact study	√	-	-	-	-	-	-	√	-	-	-	-

Construction management personnel contact owners and designers on a regular basis to inquire about upcoming projects or the status of projects already on the drawing boards. They also look for news articles and stories about facility expansions and new enterprises emerging and then follow those leads with letters of interest and company brochures. Moreover, they also notice number of copy require, detail of tender submission, agreement form, tender form and other required documents for tender submission. This is all part of the marketing effort. Without this effort to keep finding new work, a construction company cannot survive. According to studying tendering practices of Myanmar construction organizations, there are weak points in advertisement for bid. The main pessimistic point is unclear contact address of architect or engineer to inquire incomplete information of scope and drawing. Moreover, construction management personnel from contractor organization may not know where to access plans and specifications with clarity. Another point is project duration with anticipated start completion dates which can cause difficulties to construction manager in decision making in many states. In addition to project budget or anticipated price range, there is no transparency in pretender state. Since most of the tender projects are simple projects in Myanmar construction industry, project budget can be anticipated for bidding. It is the main problem for estimator or quantity surveyor. Traditional practice of Myanmar tendering style is giving contract form or agreement form to whom is awarded in competitive bidding. Therefore, construction management personnel cannot know the term and condition of contract to decide for competition of bid. To sum up most of the tendering practice of Myanmar construction organization are not transparency which can cause many risks in construction projects.

4. DISCUSSION AND SUGGESTION OF TENDERING PRACTICES FOR MYANMAR BUILDING CONSTRUCTION

To sum up, tendering practices of Myanmar building construction is not systematic and required more condition, specification and information. Myanmar construction industry needs more effective changes and upgrading activities since Myanmar is developing country. However, they are trying to be systematic tendering practice and to catch international improvement. Therefore, competitors need to consider carefully to submit tender at the time of unsystematic as well as systematic procedures of tendering practices and need to understand the behavior of tendering practices and contractor organization have to good estimator and general manger. Moreover, the decision to tender should be made by the chief estimator or general manager using the following points:

1. Is the work of a type which the contractor has experience, both in winning tenders and completing profitably? Does it conflict with the company's objectives and future workload?
2. How many contractors will be invited to tender?
3. Has the contractor the necessary supervisory staff and labour available, he may not wish to recruit untried and unknown personnel in key positions?
4. Will the estimating department have staff available with suitable expertise for the type of work to be priced?
5. Does the location of the proposed site fit the organization's economic area of operation?
6. Are there too many risks in the technical and contractual aspects of the project?
7. Will suitable documents be produced for tender purposes? A busy estimating office may give priority to work that has been measured. Poor documentation might give a clue to the standard of working documents during construction.
8. Has enough time been given to prepare a sensible estimate?
9. What will be the cost of preparing the tender? A contractor might limit the number of design and construct tenders, for example, in order to limit his exposure to cost. In the majority of cases, these costs are not recoverable.

On the other hand, the contractor needs to consider the criteria the client will use for selection. These can be:

1. Price; will the lowest price alone be the basis for selection?
2. Time; will a programme show the client that the contractor has thought about how the job can be finished on time, or ahead of time?
3. Allocation of money; will the way in which money is distributed in the priced bills help or irritate the client?
4. Method statement; would the client wish to know the methods to be adopted before accepting the offer?
5. Safety and quality; does the client expect a statement of safety or quality showing how the contractor will manage this particular contract?
6. Construction team; is the contractor proposing to supervise the job with experienced staff who will work as an effective team with the consultants?
7. Presentation; how important is an accurate, well-presented offer?

In some modern forms of procurement, clients ask for risk schedules to be submitted with tender documents. The aim is to consider which risks are best managed by each party to the main contract. An examination of the risks to be borne by the contractor may be considered at this stage. This can be divided between technical and commercial: Technical risks are dealt with by defining construction methods before costing the work. If the cost of failure is high in relation to the value of the project, it may be possible to insure against the loss, or increase the control. When uncertainties have been assessed they are priced by adding lump sums, which are a proportion of the possible losses. Commercial risks are those imposed by the form of contract and additional obligations forming part of the agreement. The most common problems arise from failure to finish by the date for completion, and commercial relationships with sub-contractors. If management feels that the contract period could be exceeded, they should consider adding a sum equal to the liquidated damages, which might be claimed. The client might wish to manage the technical risk fund and the contractor is expected to manage commercial risks. In any tender, risk management starts when the tender documents are received by identifying possible risks and allocating responsibilities to team members for managing risks and looking for opportunities. Risk management is the process associated with identifying, analyzing, planning, tracking and controlling project risks.

The decision to proceed with a tender is based on many factors including: the estimating resources available; extent of competition; tender period; quality of tender documents; type of work; location; current construction workload and conditions of contract. The role of the contractor's estimator is vital to the success of the organization. The estimator is responsible for predicting the most economic costs for construction in a way that is both clear and consistent. Although an estimator will have a feel for the prices in the marketplace, it is the responsibility of management to add an amount for general overheads, assess the risks and turn the estimate into a tender.

5. CONTRACTING IN THE CONSTRUCTION INDUSTRY

It is essential that the administration and management of contracts results in reducing risks, maximizing cost savings, minimizing claims, and improving economic return in the construction industry. These results can only be achieved through effectively managing contract risks: developing tough but fair contract documents, engaging in aggressive negotiating practices, and employing outstanding communication skills. The process of reaching a contract requires a specific sequence of steps. In taking these steps, the project manager must make a series of choices between priorities for project objectives, degrees of risk to be assumed by the contracting parties, control over project activities, and the cost of achieving selected goals. This process must first be fully understood by the project manager, then be tempered by experience, and finally be expanded into the ability to reach a contract through the exercise of negotiating and communicating skills.

5.1 Standard form of contract

Standard forms of contract exist to identify the roles and responsibilities of the parties, and their agents; and provide rules to protect and direct the parties should things go wrong. Clients have a wide choice of standard contracts for construction work, in particular the forms used for building, which cover most of the common procurement systems. The standard printed forms of contract have been developed over many years to take account of the many events which could occur during and after a construction project. Contract law will of course deal with many of the problems, but there are many matters peculiar to construction which needs clarification. Once these terms have been incorporated, they reduce the likelihood of disputes which can lead to arbitration or litigation. Contract conditions are outlined by a reference being made to the standard conditions in the tender documents, with amendments to suit the particular project.

5.2 Contract types

Just as the owner makes the decision regarding the type of project delivery to be employed, the owner also determines which contract will be utilized for the project. Generally, which form is used depends upon the type of project and the amount of risk that the owner is willing to accept. It is important that the construction manager be familiar with each type. There are seven basic types of construction contracts: lump sum, unit price, cost plus fixed percentage, cost plus fixed fee, cost plus variable percentage, target estimate and guaranteed maximum cost contract.

6. DISCUSSION AND SUGGESTION OF CONTRACTING PRACTICES FOR MYANMAR BUILDING CONSTRUCTION

Although contracting practices of Myanmar construction industry have been applicable with traditional system of contracting, there are weak points in many cases. Those weak points can cause disputes and problems lead to risk for construction industry. Since construction industry is very complex, it can involve different types of risk and uncertainty. The uncertainty in undertaking a construction project comes from many sources and often involves many participants in the project. Since each participant tries to minimize its own risk, the conflicts among various participants can be detrimental to the project. Only the owner has the power to moderate such conflicts as it alone holds the key to risk assignment through proper contractual relations with other participants. Failure to recognize this responsibility by the owner often leads to undesirable results. In recent years, the concept of "risk sharing/risk assignment" contracts has gained acceptance by the federal government. Since this type of contract acknowledges the responsibilities of the owners, the contract prices are expected to be lower than those in which all risks are assigned to contractors. Therefore, contractor should pay more attention on risk allocation and responsibilities when they entered to contracting with owner or other parties.

And then, another noticeable point for contractor is competitive bidding. Competitive bidding on construction projects involves decision making under uncertainty where one of the greatest sources of the uncertainty for each bidder is due to the unpredictable nature of his competitors. Each bid submitted for a particular job by a contractor will be determined by a large number of factors, including an estimate of the direct job cost, the general overhead, the confidence that the management has in this estimate, and the immediate and long-range objectives of management. So many factors are involved that it is impossible for a particular bidder to attempt to predict exactly what the bids submitted by its competitors will be.

Regardless of the type of construction contract selected by the owner, the contractor recognizes that the actual construction cost will never be identical to its own estimate because of imperfect information. The contractor should use different markups commensurate with its market circumstances and with the risks involved in different types of contracts, leading to different contract prices at the time of bidding or negotiation. The type of contract agreed upon may also provide the contractor with greater incentives to try to reduce costs as much as possible. The contractor's gross profit at the completion of a project is affected by the type of contract, the accuracy of its original estimate, and the nature of work change orders. The owner's actual payment for the project is also affected by the contract and the nature of work change orders.

Once a contract is reached, a variety of problems may emerge during the course of work. Disputes may arise over quality of work, over responsibility for delays, over appropriate payments due to changed conditions, or a multitude of other considerations. Resolution of contract disputes is an important task for project managers. Therefore, the mechanism for contract dispute resolution should be specified in the original contract. In order to do this, standard form of contract and standard condition of contract should be set up for Myanmar construction industry.

Moreover, construction contracts are the basis of legally binding parties to a construction project. Contracting parties and the contract administrator must clearly know their rights and obligations. Clearly, the construction process as a whole has to become more efficient, and it is important that the standard form of contract be used intelligently to support this. For clients who undertake construction projects as a regular part of their activities, the correct choice of a form of contract is more important, since the application of the principles involved may be seen as precedents in the administration of their contract. Since large sums of money are likely to be involved in these activities, it is important that the contractual arrangements should always be formal and legal from the outset of the project.

REFERENCES

Brook, M., 2006. *Estimating and Tendering for Construction Work*, Third edition.

Building and Construction Authority, 2008. *Public Sector Standard Conditions of Contract for Construction Work.*

Chinyio, E. 2011. *The Cost of Tendering*, Engineering Project Organizations Conference, Estes Park, Colorado, August 9-11, 2011.

Enshassi1, A., Mohamed, S., and Abdel-Hadi, M., 2013. Factors Affecting the Accuracy of Pre-Tender Cost Estimates in the Gaza Strip, *Journal of Construction in Developing Countries* 18, 73–94.

Evans & Peck Pty Limited, 2006. *Guidelines for Tendering*, Australian Constructor Association.

Hampson, K., and Kwok, T. *Strategic Alliances in Building Construction: A Tender Evaluation Tool for the Public Sector*, School of Construction Management, Queensland University of Technology.

Jackson, B. J., 2010. *Construction Management Jump Start* (2nd edition).

Kelly, J., and Male, S. *A Procedure for Best Value Tendering*, Glasgow Caledonian University, Glasgow.

Laryea, S. *Quality of tender documents: case studies from the UK*, School of Construction Management and Engineering, University of Reading, UK.

Robertsen, K., 2011. *Selection Criteria and Tender Evaluation: The Equivalent and Tender Price Model*, Management and Innovation for a Sustainable Built Environment, 20 – 23 June 2011, Amsterdam, Netherlands.

Rumane, A. R., 2011. *Quality Management in Construction Projects*, Taylor and Francis Group, LLC.

Tadelis, S. 2006. Incentives and Award Procedures: *Competitive Tendering vs. Negotiations in Procurement*, University of California Berkeley, Haas School of Business.

Development of mobile education system for supporting building damage assessment during large-scale earthquake disaster

Makoto FUJIU[1], Miho OHARA[2], Shoichiro NAKAYAMA[3]
and Jyunichi TAKAYAMA[4]
[1] Assistant Professor, Dept. of Environmental Design, Kanazawa University, Japan
fujiu@se.kanazawa-u.ac.jp
[2] Senior Researcher, International Centre for Water Hazard and Risk Management,
Public Works Research Institute, Japan
[3] Professor, Dept. of Environmental Design, Kanazawa University, Japan
[4] Professor, Dept. of Environmental Design, Kanazawa University, Japan

ABSTRACT

Building damage assessment is necessary for governments to issue the Victim Certificates for residents who suffered from housing damages. The process of assessment needs accuracy, quickness, objectivity and fairness because the results of assessment are used as criteria for providing public monetary supports for rebuilding of their livelihood. In Japan, several big earthquakes are expected to occur in the near future. A lot of structural damages due to these earthquakes will cause enormous needs for building damage assessment. However, there is a limit action on the number of specialists with adequate assessment skills who can access the damaged area under bad traffic conditions. Delay in building damage assessment by local governments can disturb rapid reconstruction of the damaged area. Considering these problems during large-scale earthquake disaster, authors developed the remote building damage assessment system for building damage assessment using photos of damaged house taken by residents or volunteer fire corps in damaged area. Specialists outside the damaged confirm these photos on the website and assess their damage levels. All the data used for building damage assessment is managed with GIS database on the management server located outside the damaged area under cloud condition. This kind of digital management system can contribute to enhance the accuracy and efficiency of the procedures for issuing the Victim Certificates for residents. In order to carry out the accurate assessment as a developed system, then training of assessment using these system is important. In this paper, mobile education system for supporting building damage assessment was designed and its prototype system was developed. The system for education of damaged houses was developed as smart phone. The education system for specialists to assess the damage level was developed as smart phone application.

Keywords: earthquake disaster, building damage assessment, IT system, mobile education system

1. INTRODUCTION

In Japan, several big earthquakes are expected to occur in the near future. A lot of structural damages due to these earthquakes will cause enormous needs for building damage assessment. Building damage assessment is necessary for governments to issue the Victim Certificates for residents who suffered housing damages. However, current number of human resources who are trained with the procedure of building damage assessment is not enough. The result of building damage assessment is used for issuing the victim certificate. Then, the building damage assessment during large-scale earthquake disaster requires some performances such as quickness, efficiency, accuracy, objectivity and fairness. The guidelines of general procedure for inspecting building damage and evaluating loss due to disasters were published by the Cabinet Office in 2001 and 2009. Tanaka (2008) pointed out various problems of building damage assessment such as inaccurate inspection, difficulty in quick inspection and lack of human resources with sufficient skill of assessment in past disasters.

Considering the future risk of big earthquakes, it is necessary to develop a new system which can correspond to next large-scale earthquake disaster. So far, Fujiu (2012) has proposed new remote system for building damage assessment using IT system and developed its prototype system. These systems have some features that can solve some problems pointed out at the past building damage assessments and execute building damage assessment with quickness, efficiency, accuracy, objectivity and fairness after a large-scale earthquake disaster. The proposed system consists of four sub-systems as shown in figure 1: photo uploading system used in damaged area, assessment system for supporting experts such as registered inspectors outside damaged area, e-learning system for users and Web-GIS cloud server located outside damaged area. Although the authors have already developed a prototype system, the evaluation of its effectiveness was not fully done. Then, in this research, authors conduct an operation trial to verify the usability and resolution of photos of the developed photo uploading system. This trial aims to verify applicability of photo upload system as a part of remote building damage assessment system.

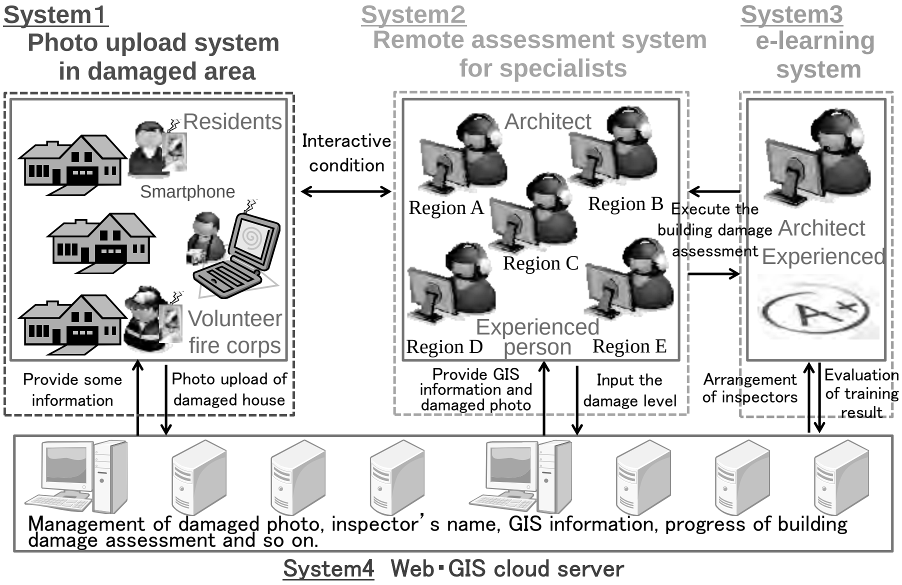
System1
Photo upload system in damaged area
System2
Remote assessment system for specialists
System3
e-learning system
Residents
Smartphone
Volunteer fire corps
Interactive condition
Architect
Region A
Region B
Region C
Region D
Region E
Experienced person
Execute the building damage assessment
Architect
Experienced
Provide some information
Photo upload of damaged house
Provide GIS information and damaged photo
Input the damage level
Arrangement of inspectors
Evaluation of training result
Management of damaged photo, inspector's name, GIS information, progress of building damage assessment and so on.
System4 Web・GIS cloud server

Figure 1: Concept of remote building damage assessment system

2. OUTLINE OF E-LEARNIG SYSTEM IN REMOTE BUILDING DAMAGE ASSESSMENT SYSTEM

After the request from residents of damaged houses, building damage assessment is executed based on building damage assessment guideline, issued by Cabinet office in Japan. Figure 2 shows the flow of building damage assessment based on the guideline. The building damage assessment has three steps; the first one is the overview judgment which is the judgment of the building damage from the overview, the second one is the inclination judgment which is the measurement of the building inclination, and the third one is the building element judgment which is the measurement of the damage level and the damage area of roof, wall and foundation. In each step, the damage ratio is calculated based on the building damage level and the building damage area. When the damage ratio reaches the standard value in each step, the damage level is decided as major damage, major-moderate damage, moderate damage or minor damage.

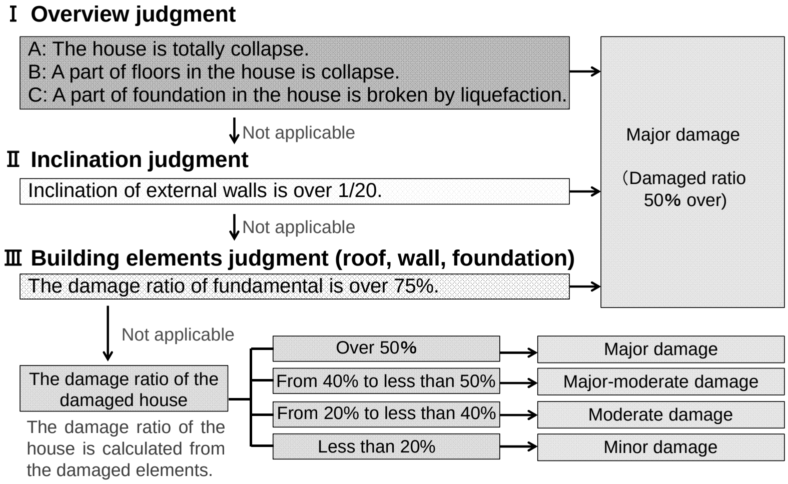
Ⅰ Overview judgment
A: The house is totally collapse.
B: A part of floors in the house is collapse.
C: A part of foundation in the house is broken by liquefaction.
Not applicable
Ⅱ Inclination judgment
Inclination of external walls is over 1/20.
Not applicable
Ⅲ Building elements judgment (roof, wall, foundation)
The damage ratio of fundamental is over 75%.
Major damage
（Damaged ratio 50% over)
Not applicable
The damage ratio of the damaged house
The damage ratio of the house is calculated from the damaged elements.
Over 50%
From 40% to less than 50%
From 20% to less than 40%
Less than 20%
Major damage
Major-moderate damage
Moderate damage
Minor damage

Figure 2: Flow of building damage assessment (Primary inspection)

Judgments of damage level and calculation method of damage area are explained in this paragraph as an example of damaged wall. Each damage level has a basic damage ratio. Figure 3 shows the relationship between damage level and basic damage ratio. The damaged wall has small and short crack as shown in Figure 3a, and the corresponding basic damage level is evaluated as 10%. The damaged wall has a long crack and small peeling off of the wall facade as shown in Figure 3b, and the corresponding basic damage level is evaluated as 25%. The damaged wall has a long crack and medium peeling off of the facade as shown in Figure 3c, and the corresponding basic damage level is evaluated as 50%. The damaged wall has peeling off of greater part of the exterior wall facade as shown in Figure 3d, and basic damage level is evaluated as 75%. The damaged wall has peeling off of almost the whole wall facade as shown in figure 3e, and the corresponding basic damage level is evaluated as 100%. The damaged area is calculated based on the decomposition method. The method is decomposition of the damaged wall to calculate the damaged area as shown in Figure 3f. The red dotted line shows the decomposition line of the damaged wall. If there is some damage in one part, the part is defined as a damaged part.

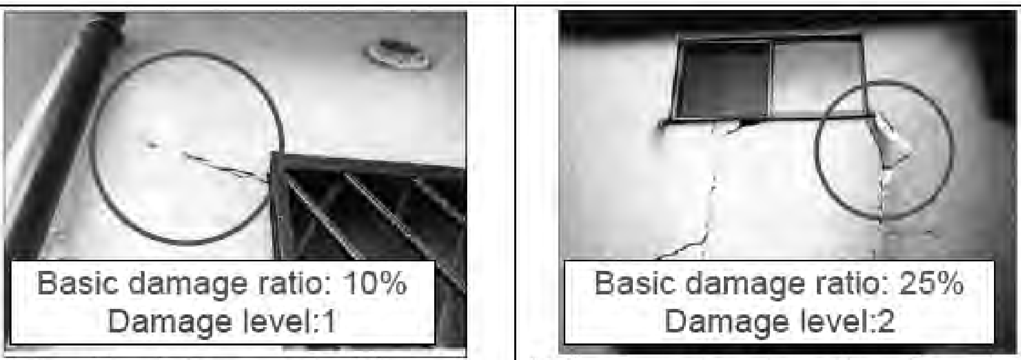
Basic damage ratio: 10%
Damage level:1
Basic damage ratio: 25%
Damage level:2

a) Small and short crack of the wall facade

b) Long crack and small peeling off of the wall facade

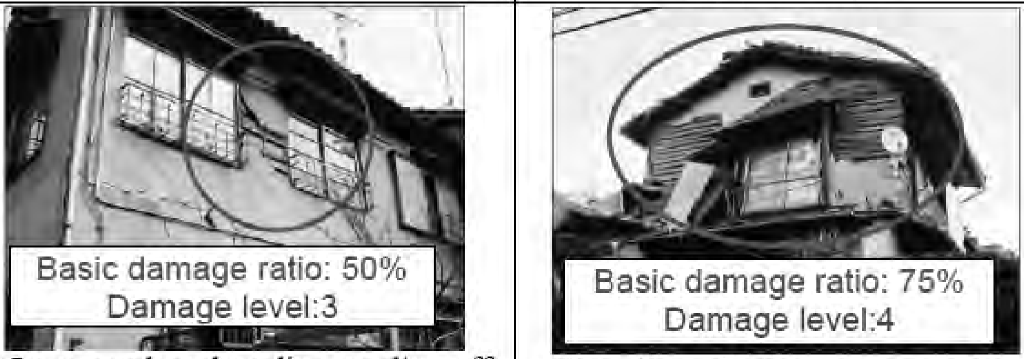
Basic damage ratio: 50%
Damage level:3
Basic damage ratio: 75%
Damage level:4

c) Long crack and medium peeling off of the wall facade

d) Peeling off of greater part of the exterior wall facade

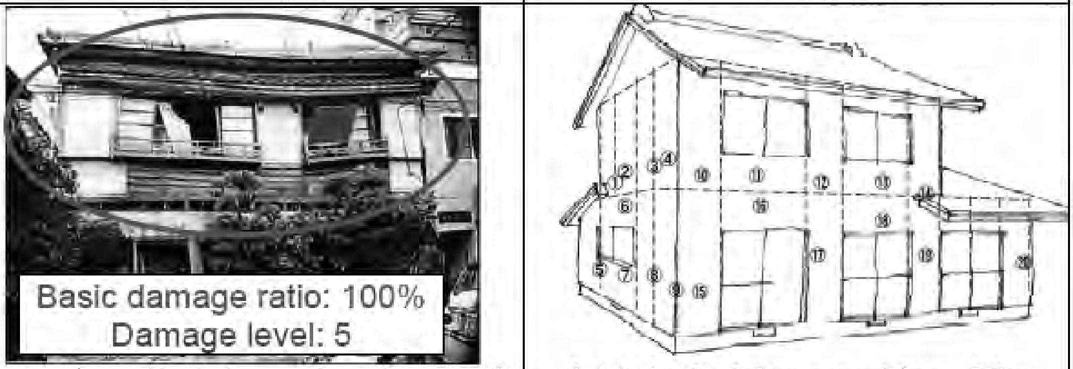
Basic damage ratio: 100%
Damage level: 5

e) Peeling off of almost the whole wall facade

f) Method of decomposition of the damaged wall to calculate the damaged area

Figure 3: Typical damage levels of walls

The damage ratio calculation has four steps: evaluation of basic damage ratio, calculation of damage ratio, calculation of sub total damage ratio and total damage ratio. The basic damage ratio is evaluated based on the damage level. The damage ratio is the value which is multiplied by basic damage level and damage area for each element, directions and damaged level as in equation (1). The sub total damaged ratio is calculated by summation of damage ratio for each element and directions as in equation (2). Finally, the total damage ratio is the value multiplied by sub total damage level and coefficient for each element as equation (3).

$$DR_{ij} = \sum_{i=1}^{n}\sum_{j=1}^{p}\sum_{k=1}^{q}\left(BDR_{ijk} \times DA_{ijk}\right) \qquad (1)$$

$$STDR_{i} = \sum_{i=1}^{n}\sum_{j=1}^{p}\left(DR_{ij}\right) \qquad (2)$$

$$TDR = \sum_{i=1}^{n}\left(STDR_{i} \times coefficient_{i}\right) \qquad (3)$$

i:Element, j:Direction, k:Damage level
DR_{ij} : Damage ratio where i,j , BDR_{ijk} : Basic damage ratio where i,j,k
DA_{ijk} : Damaged area where i,j,k , $STDR_{i}$:Sub total damage ratio where i
TDR :Total damage ratio, $coefficient_{i}$: Element coefficient

3 DEVELOPMENT OF E-LEARNING APPLICATION

3.1 Outline of e-learning application

Here, the “e-learning application for building damage assessment training” was developed. So far, human resources development of building damage assessment has been done by textbook, DVD and lecture. But these human resources development methods are limitation due to the paper based approach, and new human resources development methods are requested from government side and worked in the disaster field. In this study, “e-learning application for building damage assessment training” was developed. This application was developed for mobile phones based on Android operating system which is installed in almost all the smart phones except iPhone. The photo upload application should be installed on each Android smart phone by the users who are government officer or volunteer fire corps.

3.2 Choosing the training contents

The e-learning application for building damage assessment training can learn a great number of questions. The trainee can choose the question based on the previous result

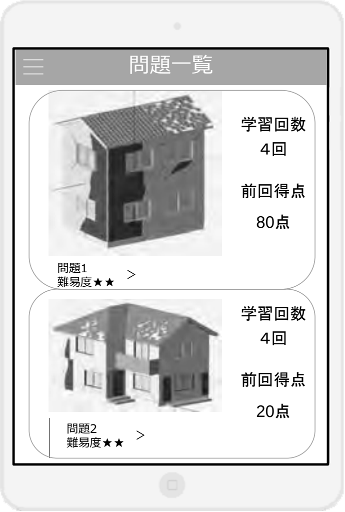

学習回数
4回
前回得点
80点

学習回数
4回
前回得点
20点

Figure 4: Question choice screen

of learning, and this application have a recommendation function which provides appropriate question based on the previous result of learning. Then, trainee can be learned effective training for building damage assessment. Figure 4 shows that question choice screen.

3.3 Training screen

Figure 5 shows that question choice screen. Firstly, trainee chose the question in the question choice screen, and question data which is “wmv” file star to download from cloud server. Then, question is displayed on the screen. The damaged building is developed 3D model house. The trainee can move aspect using slide bar, and trainee judge the damage level when the trainee finish the damage level, and final damage level calculate automatically.

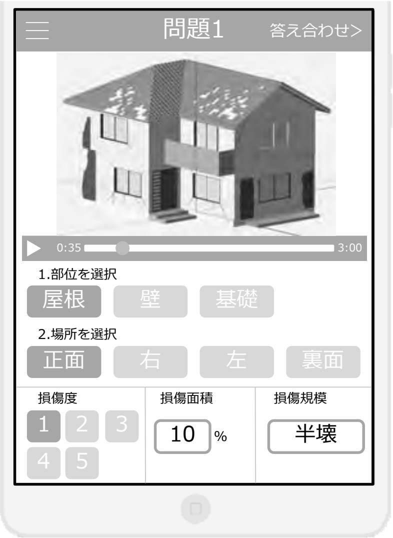

損傷度
損傷面積 10 %
損傷規模 半壊

Figure 5: Question choice screen

3.4 Confirmation of collect answer screen

The trainees finished answer the questions which are roof, wall and fundamental for each side of the damaged building, and application screen change to the answer screen (Figure 6). This application has two kinds of answer procedure. First step is answer with 3D model, Second step is detail answer without 3D model.

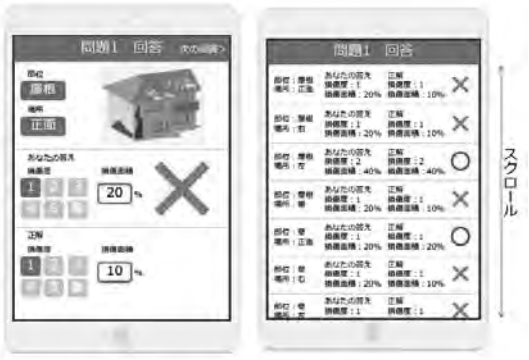

a) Case 1　　b)Case 2

Figure 6: Confirmation of collect answer screen

4. CONCLUSIONS

In this research, e-learning application for mobile smart phone as a part of remote building damage assessment system was developed. Developed application have some features which are using 3D model house, using walk through function and using two kinds of answer confirmation method. As a result of interview survey for local government, this application is effective to learn the building damage assessment before occur the earthquake disaster.

As future study, we plan to conduct more practical operation tests with some local government staffs to evaluate the effectiveness of e-learning application for mobile smart phone.

REFERENCES

Fujiu, M., Ohara, M., and Meguro, K., 2012. *Development of remote building damage assessment system during large-scale earthquake disaster*, Proceedings of the 15th World Conference on Earthquake Engineering, CD-ROM, Lisbon, Portugal.

Tanaka, S., 2008. *A Study on the building damage assessment processes for the 2007 Niigata Chuetsu Oki earthquake disaster: Kashiwazaki case study*, Proceedings of social Safety Science No.22, pp.35-38

Strengthening and repairing of 5-Storey RC ductile detailed structure with open ground storey

Swajit Singh GOUD[1] and Pradeep Kumar RAMANCHARLA[2]
[1]PhD Student, Earthquake Engineering Research Centre,
International Institute of Information Technology, Hyderabad, India
swajitsingh.goud@reasearch.iiit.ac.in
[2]Professor and Head, Earthquake Engineering Research Centre,
International Institute of Information Technology, Hyderabad, India

ABSTRACT

Reconnaissance reports of past earthquakes states that the open ground storey is one the most common problems, causing severe damage in the structural members of ground storey. In majority of the buildings, it was observed that even after proper ductile detailing, there is severe damage to the structure. This is mainly attributed to the presence soft storey. In this paper, a study is carried out to improve the seismic performance of a 5 storey open ground floor building with ductile detailing. The seismic performance is improved by: (a) providing wall infill in some portion, (b) increasing the moment carrying capacity of ground storey columns, and (c) combinations of the above two. The proposed methods can be used for new structures by incorporating the effect in design philosophy or can be implemented in the strengthening of existing structures. The performance of the structure is determined with the help of Non Linear Pushover analysis. The main parameters investigated are interstorey drift and lateral displacement. The study shows, with increase in design moments as per seismic codes for the columns having open ground storey will not improve the performance of the structure significantly. Also the open ground storey columns are severely damaged making their repairing difficult and costly. It is suggested that seismic performance of the structure can be improved more significantly by combination of constructing wall infill and higher design moments in columns; if damage occurs in wall only, it can be reconstructed and structure can be repaired easily.

Keywords: Open ground storey, pushover analysis, retrofitting, design provision

1. INTRODUCTION

Earthquake reconnaissance reports of past earthquakes shown that wall infill has significant effect on the performance of the structures. Many of the buildings which were not designed as per the seismic demand had performed satisfactorily because of infill wall. Past research done in the field of brick infill clearly shows that the stiffness and ductility of the structure increases significantly because of brick infills. On the other hand, brick infill may have negative effect introducing torsion, soft storey, weak storey and short column effects, because of irregularity in the location of brick infill horizontally and vertically. Open ground storey construction practice is most common now-a-days, preferred by Architects. As it has many functional and aesthetic advantages in multi-storeys, schools, hotels and commercial buildings. It has been recognized by structural engineers and from past earthquake surveys, that this architectural practice will do severe damage in the structural and non-structural element of the ground storey and sometimes leads to total collapse of structure (Perez, 2012).

The open ground storey as construction practice is difficult to eliminate from the architects design criteria and hence it is preferable to provide a special design criteria for such structural configuration. International seismic codes suggest that columns and beams of the floor having soft storey are to be designed for higher moments to reduce the soft storey effect. Indian seismic code IS 1893-2002 recommends a magnifying factor of 2.5 times the design forces in beams and columns obtained from analysis.

The major challenge of having damages in structures in spite of following all seismic design provisions is the difference in the analysis, design and construction. In analysis and design the modeling of the structure is done as bare frame, whereas in construction walls are provided at some locations. If wall provided does not introduce horizontal and vertical irregularity then wall infill will be advantageous, else it will lead to severe damage in structural members. Wall infill will change the force transfer mechanism in the structure and open ground storey columns will accumulate higher stresses leading to higher damage (Murty and Jain, 2000). More amount of energy will be absorbed by soft storey members, causing larger interstorey drift leading to higher deformation in ground storey columns.

In the present paper a comparative study is done between the bare frame, frame with full infill wall and soft storey model in terms of capacity, drift and time period of the structure. Designing and retrofitting method for soft storey is done by; a) increasing the moment carrying capacity of ground storey columns, b) providing wall infill in some portion, and c) combinations of the above two.

2. STRENGTHENING TECHNIQUE

Strengthening of open ground storey structures can be done at local and global level by strengthening ground storey columns and reducing the seismic demand, respectively. Local strengthening can be done by column jacketing using steel and concrete, FRP jacketing, steel caging, etc. The major disadvantage of local strengthening method is that the strengthened member will suffer severe damage during seismic events and repairing of such members will be more difficult and costly (Sahoo and Rai, 2013). Strengthening at global level can be done by using energy dissipation mechanisms like, friction dampers, metallic dampers, viscoelastic dampers and bracing elements (Soong and Dargush, 1997).

3. STRUCTURAL DETAILS

For the current study a G+4 storey building assumed to be located in seismic zone III as per IS 1893-2002 is considered. Ductile detailing provisions are considered in design as per IS 13920. Shear force demand in the ground storey column increases significantly because of soft storey effect leading to shear failure in columns. The shear failure in columns can be reduced to some extent by providing ductile detailing in columns. Figure 1 shows the considered RC frame. Typical member reinforcement details of beam and column is shown in Figure 2.

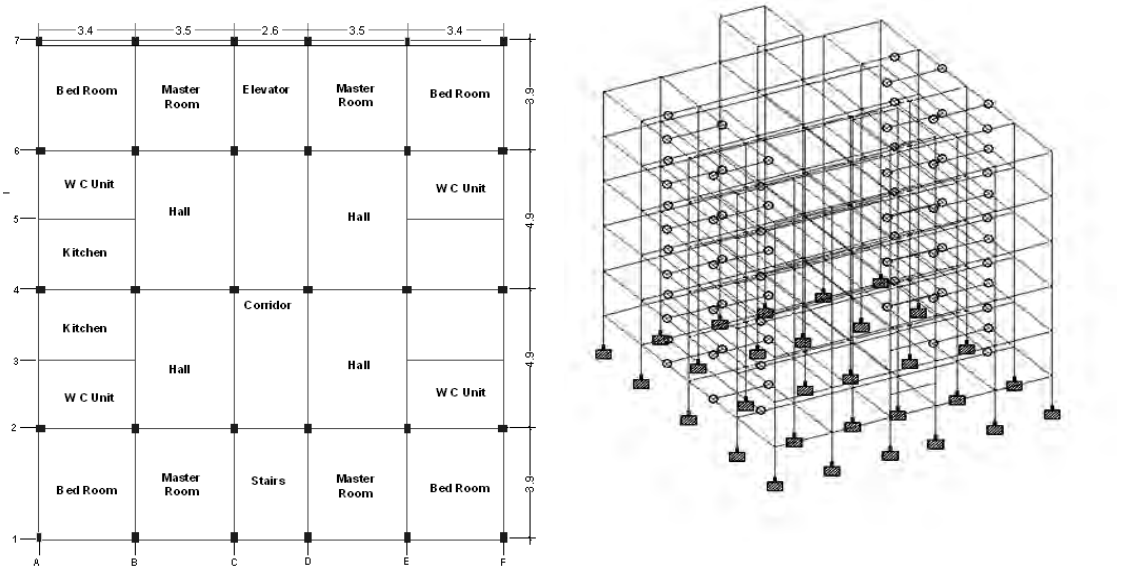
3.4
3.5
2.6
3.5
3.4
7
6
5
4
3
2
1
A
B
C
D
E
F
3.9
4.9
4.9
3.9
Bed Room
Master Room
Elevator
Master Room
Bed Room
W C Unit
Hall
Hall
W C Unit
Kitchen
Corridor
Kitchen
Hall
Hall
W C Unit
W C Unit
Bed Room
Master Room
Stairs
Master Room
Bed Room

Figure 1: Building plan with column orientation and Building Model

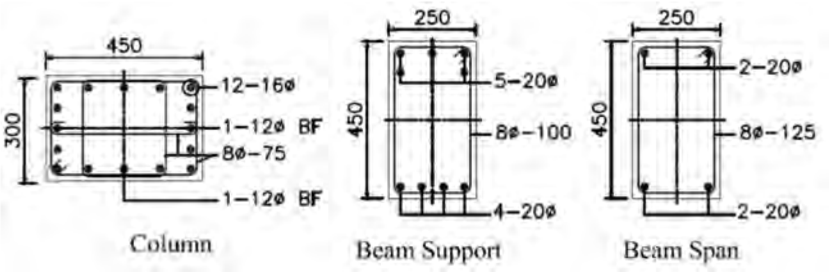
450
300
12-16ø
1-12ø BF
8ø-75
1-12ø BF
Column
250
450
5-20ø
8ø-100
4-20ø
Beam Support
250
450
2-20ø
8ø-125
2-20ø
Beam Span

Figure 2: Reinforcement detailing of column and beam

4. INFILL MODELING

Modeling of wall infill was done considering three strut model. Three strut model gives the response of the structure closer to actual behaviour of frame with infill in continuum modeling and better than single strut model (Kaushik et al., 2008). Material properties of masonry and dimensions were taken as reference (Kaushik et al., 2008).

5. PUSHOVER ANALYSIS

Pushover analyses were done for all the models considering the flexural and shear hinge in beams and columns, and axial hinge in Strut. The shear and axial hinges were defined as brittle type. Pushover analysis was performed using SAP2000 Version 15.

6. BARE FRAME, FULL BRICK INFILL AND OPEN GROUND STOREY

Linear and non-linear response of the bare frame, frame with full brick infill and open ground storey is studied in this section. Pushover curve and interstorey drift obtained in Figure 3 clearly shows the influence of brick infill on the initial stiffness and strength of the structure.

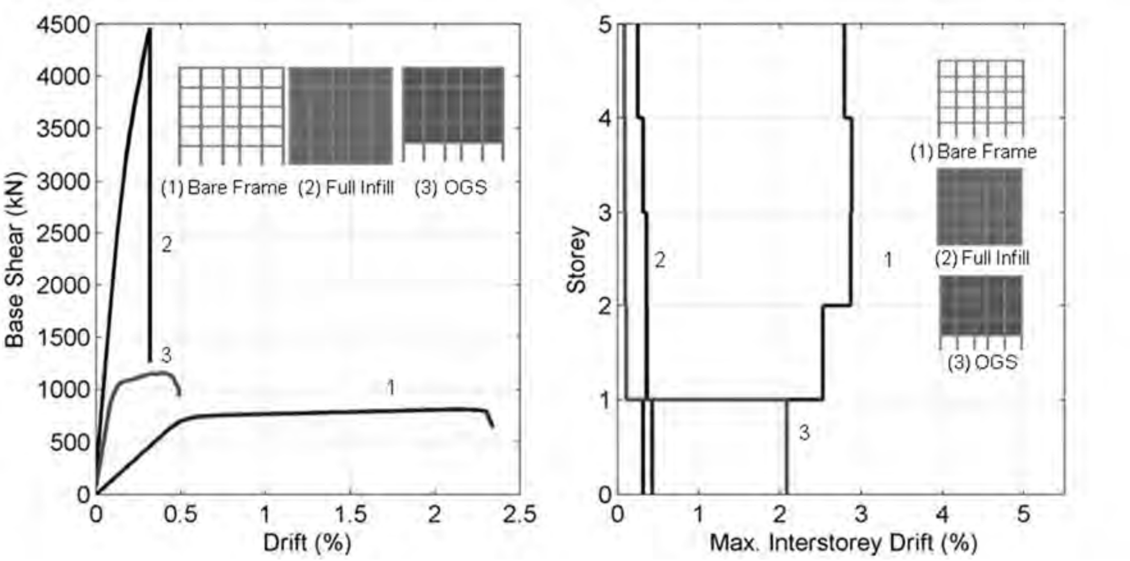

Figure 3: Pushover curve and Interstorey drift profile

The hinge mechanism in bare frame was totally different from that of open ground storey (OGS), in bare frame model hinges were well distributed in all the floors whereas in case of OGS hinges were observed only in ground floor columns. The sudden drop down in full infill frame was because of shear failure in columns of ground storey and failure of strut elements which were defined as hinge of brittle type. Interstorey drift obtained clearly shows that in OGS the deformation was concentrated in ground floor only whereas in case of full infill the deformation was observed in all floors. The change in time period (T), elastic stiffness ($K_{Elastic}$), shear force (SF), bending moment (BM), strength ($V_{max.}$), design moment (DM) and amplification factor (AF) are shown in Table 2. SF and BM of ground floor column are shown for comparison. Table 2 clearly shows significant increase in elastic stiffness and strength, and decrease in time period, SF and BM in full infill frame compared to bare frame and OGS.

7. COLUMN RETROFITTING

The OGS structure was tried to strengthen by increasing the load carrying capacity of columns of ground storey. The concept of increasing the load carrying capacity of columns can be used at the time of designing new structure by increasing the column dimensions and reinforcement or in existing structure by providing column jacketing and FRP coating to achieve the required moment of resistance. Columns of ground floor were strengthened by increasing the design moment from 2.5 to 4 times of design moments obtained from linear analysis. As per IS code (IS 1893-2002), if structure is having soft storey effect then the members of floor having soft storey need be designed for 2.5 times of the design moment. Pushover curves and Interstorey drift of building with increased column dimensions are shown in Figure 4. It was observed that by strengthening columns of ground floor as per code non linear response of structure improved, but significant changes were observed when column design moment was increased up to 4 to 5 times. Interstorey drift profile shows that even after increasing the member strength up to 5 times the deformation was concentrated in the ground floor only. Table 1 shows the changes in non linear parameters with change in moment carrying capacity of ground storey columns.

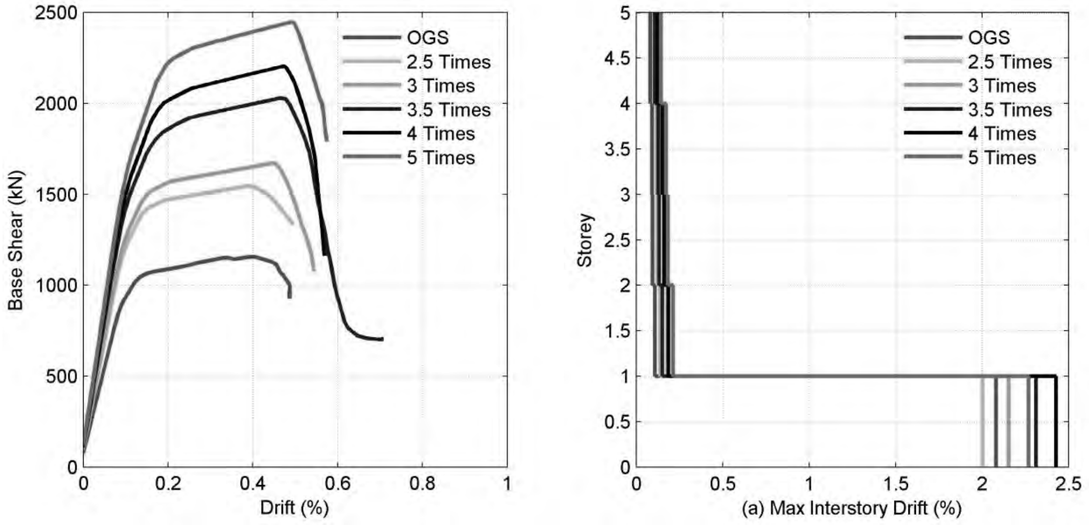

Figure 4: Pushover curves and Interstorey drift of building with column strengthening or retrofitting

Table 1: Comparison of linear and non-linear response of column strengthened frames

S. No.	DM (kN-m)	AF	Depth (mm)	Width (mm)	SF (kN)	BM (kN-m)	T (sec)	K $_{Elastic}$ (kN/m)	V $_{max}$ (kN)
1	159	1	450	300	56.5	103.5	1.03	62236	1158
2	397	2.5	550	300	54.5	92.5	0.43	78997	1548
3	475	3	575	300	54.7	96.0	0.41	82548	1671
4	557	3.5	650	300	55.0	100.0	0.39	92095	2031
5	636	4	650	350	55.1	103.4	0.38	96573	2205
6	795	5	700	350	55.2	107.38	0.36	102072	2450

8. WALL RETROFITTING

Existing structures having OGS effect can be strengthened by introducing wall in some portion of ground floor. In new structures also this concept can be used and wall locations can be changed numerically to check the maximum response. In the present study 3 probable locations of walls (Figure 5) were considered. The pushover curves and interstorey drift obtained (Figure 5) clearly shows that the nonlinear response of structure significantly depends upon the wall locations. The strength and stiffness in case 1 and case 3 were not significantly changed, but the hinges formation or deformation on the upper floor was observed more in case 3 compared to case1. Increase and decrease in interstorey drift profile was clearly observed in upper and ground floor columns, respectively. Non-linear response of case 3 was better than case 1 because, high forces were acting in interior column which were supported by walls in case 3. Response of case 2 could be more than that of case 1 and 3, if the net shear area of wall of case 2 is equal to case 1 or 3. Table 2 clearly shows significant increase in elastic stiffness and strength, and decrease in time period, SF and BM in case 1 and case compared to case 2 and OGS.

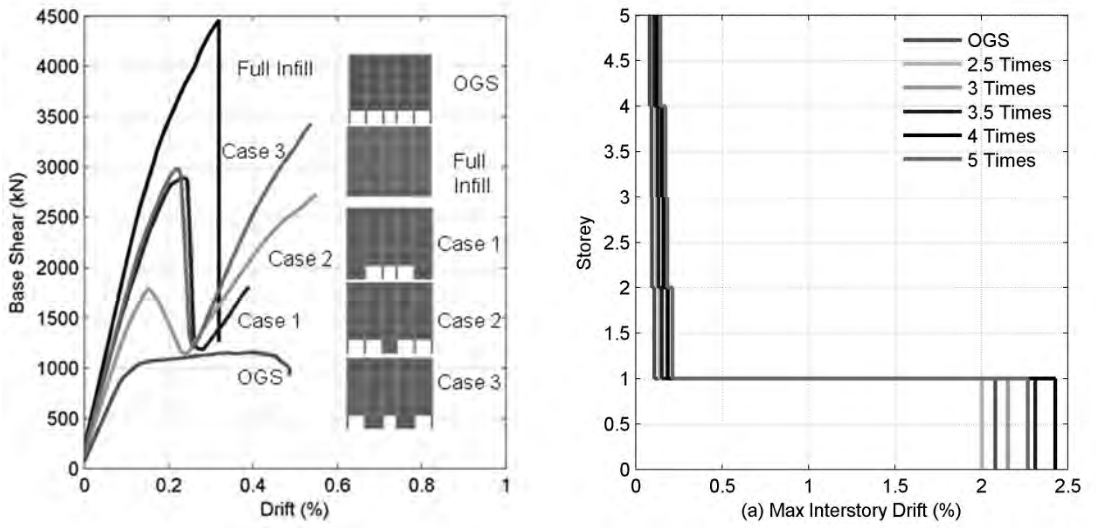

Figure 5: Pushover curves and Interstorey drift of building with wall retrofitting

Table 2: Comparison of linear and non-linear response of wall retrofitted frames

S. No.	Type	SF (kN)	BM (kN-m)	T (sec)	$K_{Elastic}$ (kN/m)	V_{max} (kN)
1	Bare Frame	56.5	103.5	1.03	9721	807
2	OGS	53.7	87.4	0.52	62236	1158
3	Full Infill	19.1	17.8	0.31	121007	4463
4	Case 1	17.5	29.0	0.36	101988	2890
5	Case 2	63.6	63.2	0.42	84669	2725
6	Case 3	40.6	33.0	0.36	103702	3430

9. COMBINED RETROFITTING

Column and wall retrofitting were done in combined retrofitting. Wall retrofitting of case 3 was only considered in combined retrofitting, as case 3 shown better response compared to other two cases. Column dimensions were increased in order to achieve the response similar to that of full infill. Figure 6 shows the pushover curves and interstorey drift obtained for combined retrofitting. It was observed that column retrofitted by design moment of 5 times and wall retrofitted with case 3 gave response closer to that of full infill. The interstorey drift profile also shows better performance of the above case. Table 3 shows the time period and stiffness of the above case was closer to full infill frame.

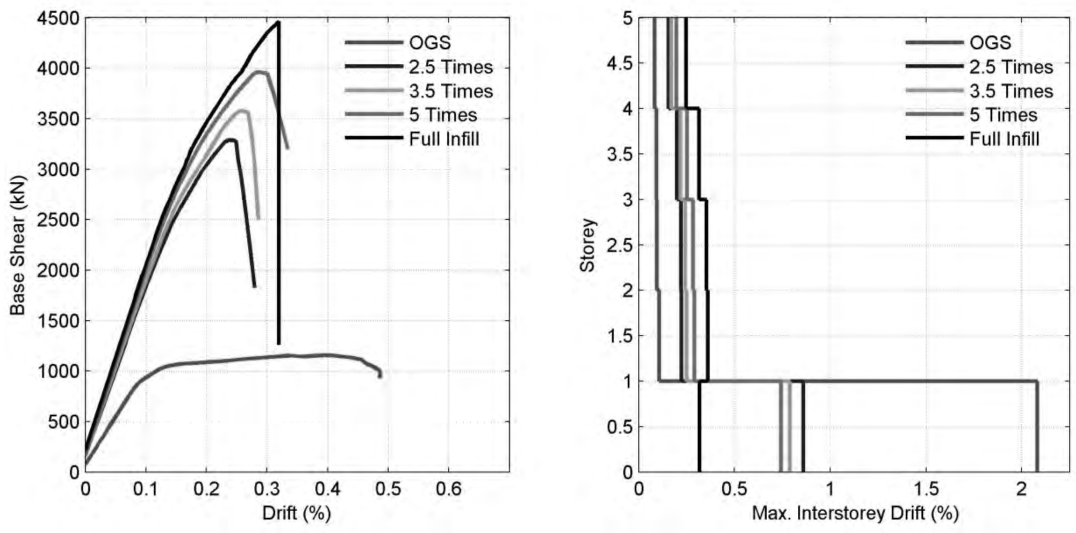

Figure 6: Pushover curves and Interstorey drift of building with combined retrofitting

Table 3: Comparison of linear and non-linear response of frames for combined retrofit

S. No.	Column Dimension	SF (kN)	AF	BM (kN-m)	T (sec)	K Elastic (kN/m)	V max (kN)
1	550 x 300	42.8	2.5	38.0	0.34	110618	3290
2	650 x 300	43.7	3.5	45.8	0.33	114527	3580
3	350 x 700	45.2	5	58.9	0.32	121185	3961

10. RESULTS

The seismic response of open ground storey structure is poor and can lead to sudden collapse of structure because of hinge formation in ground floor column. The stiffness and strength of OGS is 2.8 and 3.9 times, respectively, lesser than full infill frame. The SF and BM also in OGS are much higher compared to full infill frame.

The member level retrofitting done by increasing column capacity alone cannot improve the seismic response significantly compare to wall retrofitting and combined retrofitting (Figures 3-6).

Location of wall plays an important role in improving the seismic response, case 3 shown the better response compared to case 1 and 3 (Figure 4). Wall should be located in places where the shear stress concentration is more.

The drift pattern of frame with column retrofitting was totally different from wall retrofitting. In case of column retrofitting the damage is concentrated in ground storey only, whereas in case of wall retrofitting the damage was observed less comparatively.

11. CONCLUSIONS

The study done clearly shows that strut modeling of brick infill should be done in numerical analysis to check the exact non linear response of the structure. The response of structure will change more significantly if wall provided in structure is asymmetric. Open ground storey should be avoided as far as possible, because design provision given in seismic code shows member level retrofitting which improves the nonlinear response not much significantly. The design provisions provided in seismic codes need to be modified for design provisions of soft storey.

REFERENCES

Agarwal, P., and Shrikhande, M., 2006. *Earthquake resistant design of structures.* PHI Learning Private Limited, New Delhi, India.

Applied Technology Council (ATC)., 1996. *Seismic evaluation and retrofit of concrete buildings, ATC 40*, California.

Bureau of Indian Standards., 1993. *Indian standard ductile detailing of reinforced concrete structures subjected to seismic forces - Code of Practice, IS 13920.* New Delhi, India.

Bureau of Indian Standards., 2000. *Indian standard code of practice for plain and reinforced concrete, IS 456: 2000.* New Delhi, India.

Bureau of Indian Standards., 2002. *Indian standard criteria for earthquake resistant design of structures Part I: General provisions and buildings, IS 1893:2002.* New Delhi, India.

Federal Emergency Management Agency (FEMA)., 1997. *Improvement of nonlinear static seismic analysis procedures, FEMA 440-1997.* Washington D.C.

Jain, S. K., and Nigam, C. N., 2000. Historical developments and current status of earthquake engineering in India. *4th World Conference on Earthquake Engineering.*

Kaushik, H. B., Rai, D. C., and Jain, S. K., 2008. A rational approach to analytical modeling of masonry infills in reinforced concrete frame buildings. *14th World Conference on Earthquake Engineering.* Beijing.

Murty, C. V., and Jain, S. K., 2000. Beneficial influence of masonry infill walls on seismic performance of RC frame buildings. *12th World Conference on Earthquake Engineering.*

Perez, L. T., 2012. "Soft story" and "weak story" in earthquake resistant design: A multidisciplinary approach. *Proc. of the 15th World Congress of Earthquake Engineering.* Lisbon.

Pillai, S. U., and Menon, D., 2010. *Reinforced concrete design.* Tata McGraw-Hill Education Private Limited, New Delhi, India.

Sahoo, D. R., and Rai, D. C., 2013. Design and evaluation of seismic strengthening techniques for reinforced concrete frames with soft ground story. *Engineering Structures* 56, 1933-1944.

Soong, T., and Dargush, G., 1997. *Passive energy dissipation systems in structural engineering.* John Wiley and Sons Inc., England.

Effect of soft storey in a structure present in higher seismic zone areas

Neelima V. S. PATNALA[1] and Pradeep K. RAMANCHARLA[2]
[1]MS by Research Scholar, Earthquake Engineering Research Centre,
International Institute of Information Technology, Hyderabad, India
patnala.neelima@research.iiit.ac.in
[2]Professor, Earthquake Engineering Research Centre,
International Institute of Information Technology, Hyderabad, India

ABSTRACT

The use of unreinforced brick masonry as infill material in reinforced concrete frames is inevitable even in higher seismic zone areas. With increasing demands for architectural features in buildings, the provision of soft storey is a common practice in many multi storeyed structures throughout the world, for parking. The standard code of practice in many countries suggests higher design forces for the columns present in the soft storey. In order to understand the affect of increase in design seismic forces on the columns in a structure present in higher seismic zone areas, a study is carried out by taking pushover analysis as a tool for obtaining capacity of the structure. A comparative study between three types of arrangements; type I: structure with infill walls in all floors, type II: structure with open ground storey, type III: structure with open ground storey and columns designed for increased forces. It is observed that there is an increase in maximum load carrying capacity for the type III structure as compared to type II structure with no considerable change in behaviour of the two types of structures. It can be concluded that the increase in design forces of the columns at open ground storey may not lead to the safety as of structure type I.

Keywords: Unreinforced brick masonry (URM), multi storeyed structures, higher seismic zone areas, soft storey, pushover analysis

1. INTRODUCTION

Multi storeyed buildings gained huge popularity with the reliable applicability of reinforced concrete frames infilled with masonry walls. Out of all the kinds of masonry units used for constructing infilled walls, brick masonry is one of the oldest materials used. Due to easy construction and low cost, brick masonry is used as infill material even till date in many parts of the world. Though the presence of infill is inevitable, it is considered as a non structural element according the standard codes of practice in many countries. This leads to improper analysis of the seismic behaviour of a building as a whole. Because of increase in demand to aesthetic appearance of a building, the civil engineering details of a building have lost their importance. Open ground storey is one such detail which is mostly prevalent in the present day multi-storeyed buildings throughout the world. The presence of open ground storey in a building leads to soft storey effect. Though standard codes in some countries like India, Europe, Japan, etc., provide special clauses for the modeling the soft storey. The seismic behavior of the building with soft storey is not completely understood. Hence there is a need to verify the provisions given in different standard codes for the safety of the building with soft storey.

Significant research has been carried out in understanding the effect of soft storey on seismic performance of brick infilled reinforced concrete frames. In a similar study, Murty et al. (2000), conducted experiments on twelve single bay single storey RC frames of full scale and scaled models subjected to reverse cyclic displacement controlled loading. The main conclusions of this work were that the average initial stiffness, strength and ductility of infilled frames is 4.3 times, 70% and 4 times more than the bare frame, respectively. In order to improve the performance of soft storey buildings, Dande et al. (2013) conducted an analytical study on 12 storey symmetric building with strut modeling for infill walls. A comparative study is carried out by performing linear response spectrum analysis between the two types of retrofitting techniques; 1) by providing stiffer columns at ground floor and 2) the other by providing infill walls at the corners. It is observed that the provision of stiffer columns in the ground floor may not reduce the displacement and force demands at the open ground storey but can be reduced to some extent if infill walls are provided at the ground floor.

This paper aims at understanding the seismic behaviour of building with soft storey and tries to verify the clauses given in Indian standard code for the safety of building. A case study is carried out by performing pushover analysis on a commercial building. The comparison is made between the structure with and without soft storey and interpretations are derived.

2. NUMERICAL MODELING OF SOFT STOREY

The architectural plan and the grid line diagram of the structure are shown in Figure **1**. The structure is assumed to be present in zone IV area with high expected seismic hazard. The geometric details of the structure considered are given in the Table 1. The structure with soft storey is designed for gravity loads and seismic loads, according to the factors applicable for zone IV area as given in IS 1893-2002 and IS 456-2000.

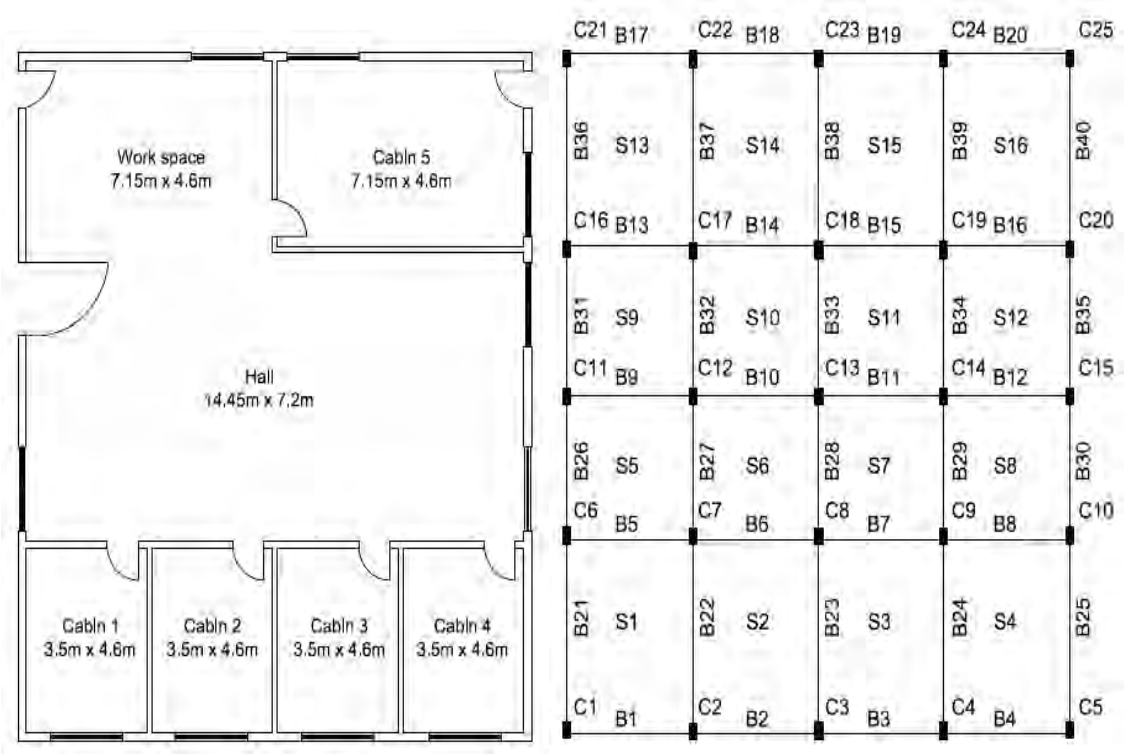
Work space
7.15m x 4.6m
Cabin 5
7.15m x 4.6m
Hall
14.45m x 7.2m
Cabin 1
3.5m x 4.6m
Cabin 2
3.5m x 4.6m
Cabin 3
3.5m x 4.6m
Cabin 4
3.5m x 4.6m
C21 B17 C22 B18 C23 B19 C24 B20 C25
B36 S13 B37 S14 B38 S15 B39 S16 B40
C16 B13 C17 B14 C18 B15 C19 B16 C20
B31 S9 B32 S10 B33 S11 B34 S12 B35
C11 B9 C12 B10 C13 B11 C14 B12 C15
B26 S5 B27 S6 B28 S7 B29 S8 B30
C6 B5 C7 B6 C8 B7 C9 B8 C10
B21 S1 B22 S2 B23 S3 B24 S4 B25
C1 B1 C2 B2 C3 B3 C4 B4 C5

Figure 1: Architectural plan and grid line marking of building

Table 1: Details of considered building

Geometric details	
1. Purpose	Commercial
2. Total plot area	24 x 22.9 m
3. Bays	4 x 4 in x & y dir
4. Floor Height	3.6 m
Loading (Seismic)	
1. Seismic Zone	IV
2. Zone factor	0.28
3. Response reduction factor	3 (Non ductile)
4. Importance factor	1
5. Base Shear	1488 kN
6. Time period in x direction	0.33 sec

3. PUSHOVER ANALYSIS

To carry out this study, four different cases are considered namely bare frame structure, structure with soft storey, structure without soft storey and structure with soft storey designed according to Indian standard code. As a first step, the pushover analysis is performed on bare frame structure and the pushover curve is shown in the Figure 2

Pushover analysis is performed by modeling the structure with and without soft storey using Applied Element Method (AEM) (Bishnu, 2004). The pushover curve obtained from AEM analysis is shown in Figure 3 and Figure 4. The propagation of crack from starting stage to the end of the analysis is shown with figures at critical locations. The location of the crack is indicated by white colored lines in the brick masonry wall and with red colored circles in reinforced concrete elements. The red colored pointers are used to indicate the location of the crack and the scope of crack propagation. For clear understanding, the sequence of cracking for the two analyses is shown in the Figure 3 and Figure 4.

The provision suggested by Indian standard code of practice for the safety of the structure with soft storey should be verified. For understanding the issue of increasing the moments and shear forces in columns, the same structure is designed for 2.5 times moments and shear forces. The increase in moments is done only in the ground floor where the structure is having open storey and the global pushover curve and the sequence of cracking in the analysis are shown in Figure 5 and Figure 8, respectively.

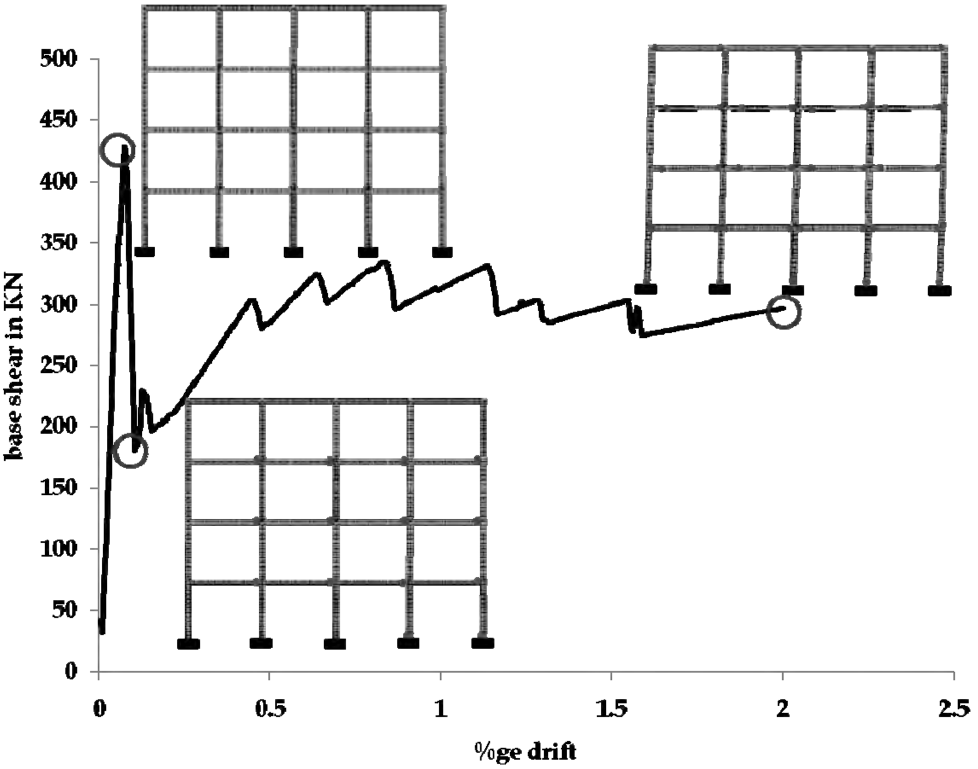

Figure 2: Global pushover curve for bare frame

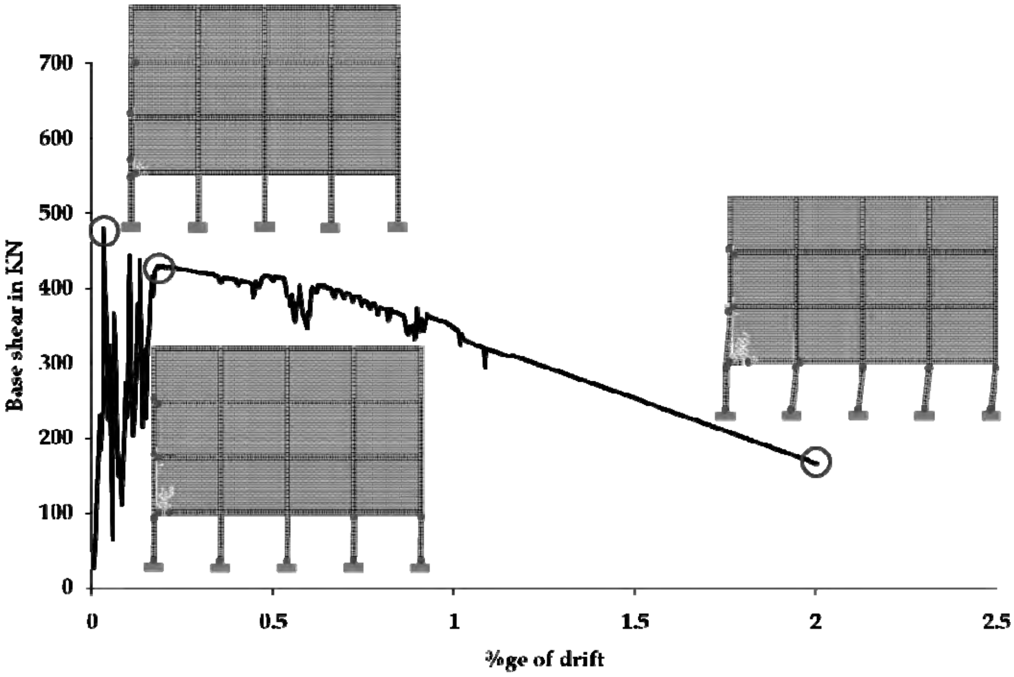

Figure 3: Global pushover curve for structure with soft storey

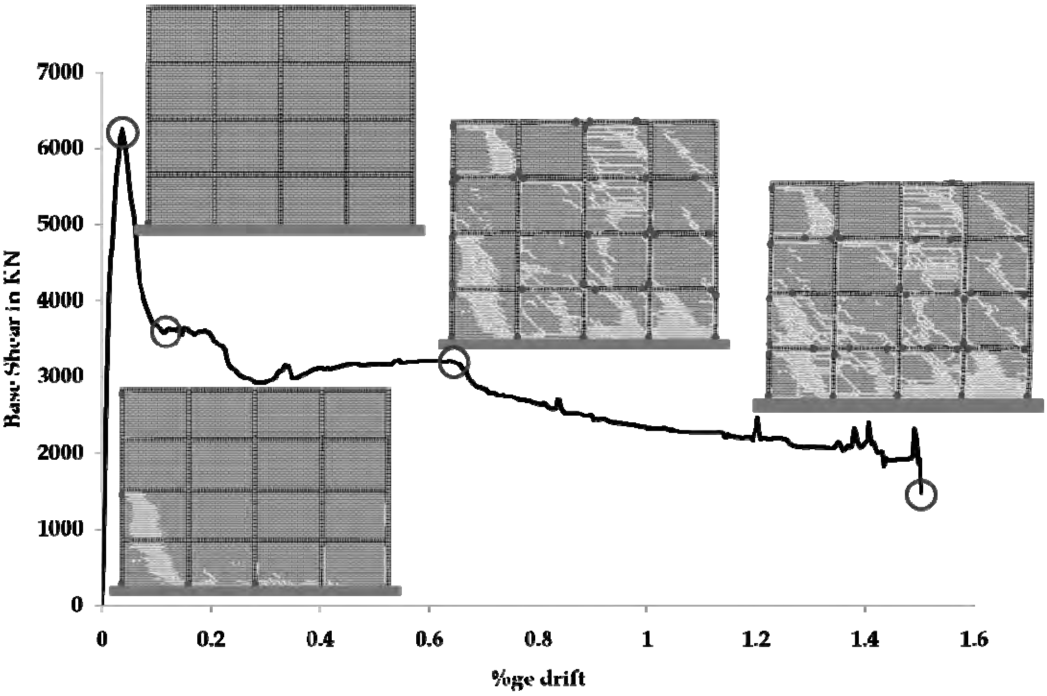

Figure 4: Global pushover curve for structure without soft storey

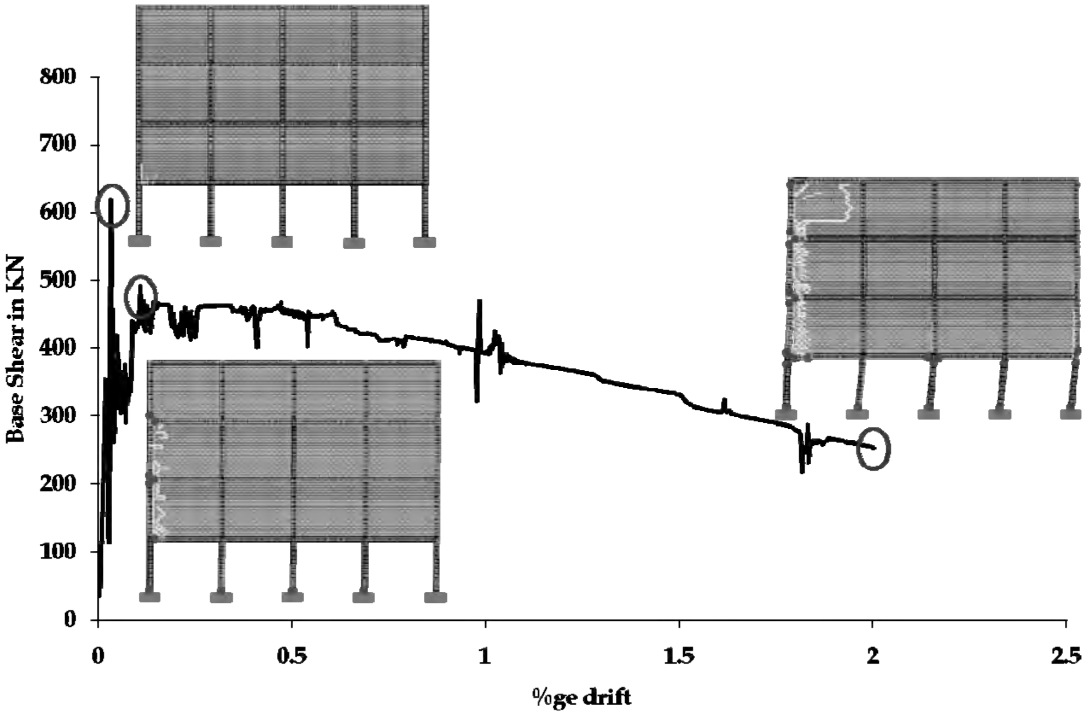

Figure 5: Global pushover curve for structure with soft storey designed for 2.5 times moments

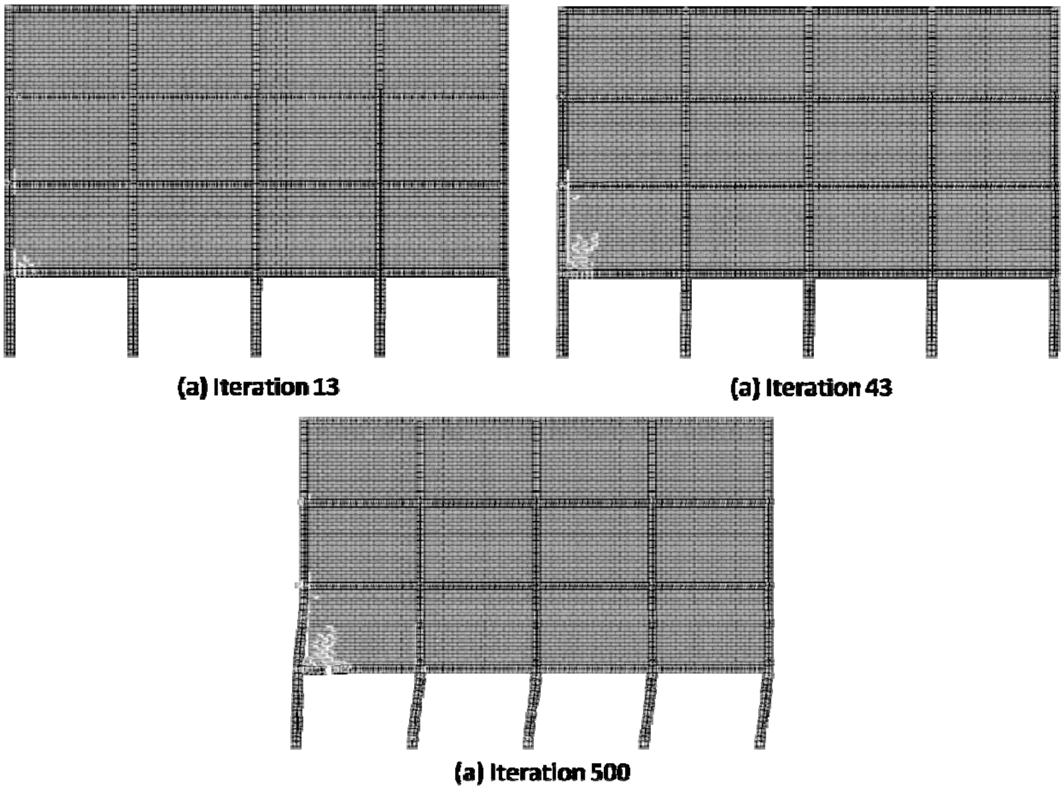
(a) Iteration 13
(a) Iteration 43
(a) Iteration 500

Figure 6: Sequence of cracking for structure with soft storey

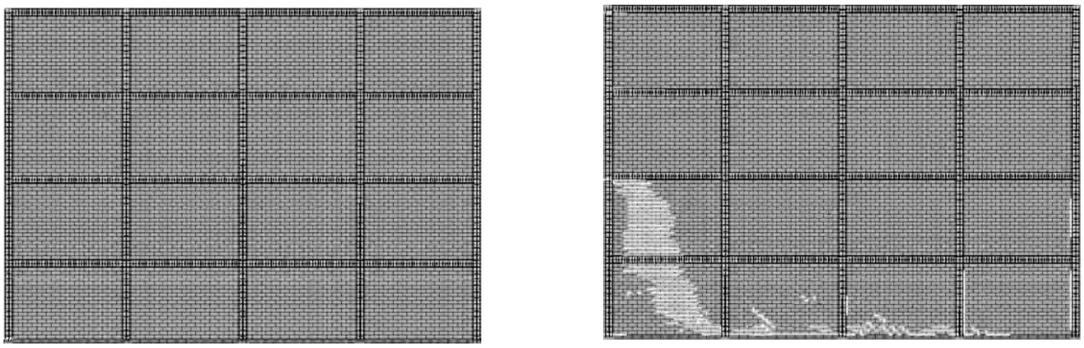

(a) Iteration 11

(b) Iteration 25

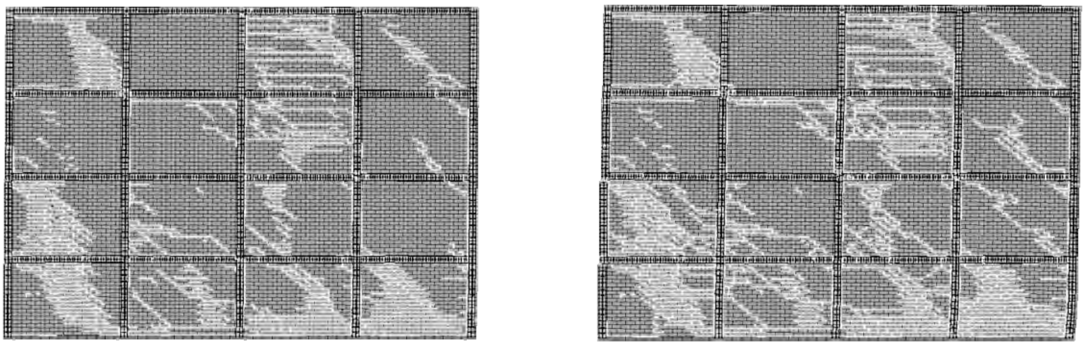

(a) Iteration 208

(a) Iteration 500

Figure 7: Sequence of cracking in structure without soft storey

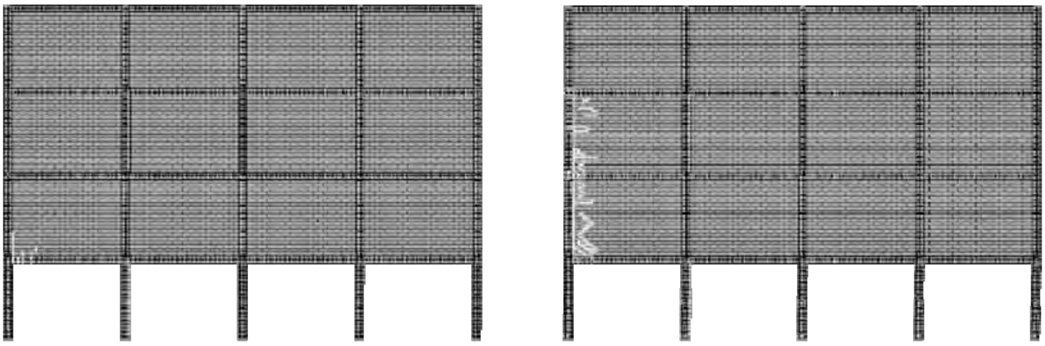

(a) Iteration 12

(a) Iteration 78

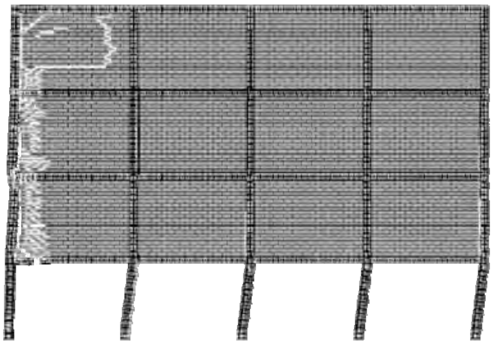

(a) Iteration 700

Figure 8: Sequence of cracking for structure with soft storey designed for 2.5 times moments

The pushover curve for bare frame structure shown in Figure 2 clearly indicates that the load carrying capacity of the soft storey is almost same as that of the bare frame. From this it can be concluded that a structure with soft storey reduces the lateral load carrying capacity to that of a bare frame without infill walls. This is serious loss because the strength and stiffness of the infill walls present in the top storeys are not at all responsible for the behaviour. With the presence of soft storey, the beneficial influence of the infill walls is completely neglected. This also causes brittle failure and easy collapse of the complete structure.

The striking observation that can be made from the curves in Figure 3 and Figure 4 is that the lateral force carrying capacity of the structure with soft storey is much less when compared to the structure without soft storey. As the walls are not present in the ground floor, the transfer of load from top of the structure (i.e., the point of application of load) to the bottom is not continuous and is breaking at the ground floor beams. Due to this, the load applied at the top of the storey is transferred only through the beam column joints at the ground floor to the ground floor columns. Hence, it can be seen that the ground floor columns which acts as a soft storey, deflects more when compared to the other floors. Proving this discussion, the infill walls in the structure without soft storey, distributed the load uniformly depending on their relative stiffness. Due to this, the crack propagated uniformly in the infill walls from top to bottom of the structure. The diagonal cracks, perpendicular to the line of application of load, in the tension zone, formed in this structure show the bending behaviour of the structure is predominant. But the cracks are visible only at the ground floor columns in the structure with soft storey effect. In addition to this, there are no cracks observed in the top floor infill walls. This indicates that the load is not transferred to any of the elements in the top storey. At the second critical point, the cracks are concentrated at the first floor wall where the sudden change in stiffness of the structure is taking place. Later at the final stage, the infill wall at the first floor got separated from the RC frame. This is caused due to the concentrated damage at the first floor.

Apart from this, another point to be observed is that, in the structure with soft storey, the ground floor columns have not deflected equally. The first column is completely straight whereas the other columns are almost reaching the collapse state. When the lateral force is acting on the structure towards positive X direction, the columns to the extreme right side are subjected to compressive forces and the columns to the extreme left side are subjected to tension forces. In addition to this, the columns in the ground floor are subjected to high lateral forces when compared to the other floors. At first floor, the tensile forces induced due to the bending behaviour of the structure are dominating the compressive forces applied at that floor. This causes columns on the left side to act rigidly to the compressive forces acting on it. On the other hand, the columns on the right side deform depending on the individual relative stiffness. This causes the difference in deformation patterns of the columns in the ground floor. The jaggerdness of the pushover curve for open ground storey structure is caused because of the spring failure which is the inherent property of the methodology used for the analysis. When the spring reaches the limit specified, an equal force on the opposite side is applied to make the net force zero. Because of irregular failure of springs in the case of soft storey structure, the curve is obtained in such a pattern.

The stiffness of the structure with and without open ground storey is varying largely and the stiffness for open ground storey structure is less when compared to the structure without open ground storey. This is because of number of effective structural elements present for resisting the lateral forces acting on the structure. Finally, the ductility of the structure which is responsible for the deformation carrying capacity of the structure is more in the case of structure without soft storey and the ductility of the soft storey structure is relatively less. On the other hand, there are no visible sudden drop in the curve for soft storey structure which can be interpreted to be more ductile when compared to the structure with all walls.

The pushover curve for structure, designed according to IS 1893, is almost similar to the pushover curve obtained for the structure with soft storey without increase in the design forces. Both the structure show similar behaviour in terms of the propagation of crack and the distribution of load throughout the structure. As the discontinuous load path is not treated in this structure also, the distribution of load is not uniform throughout the structure. Due to this, there are no cracks formed in the top storeys of the structure. This underestimates the strength of the infill walls present in the top storeys. In this structure, cracks are more concentrated in the first storey near the beam column joint where the sudden change in stiffness is taking place. But the only difference that is observed in the structures with and without increase in design moments is that the crack which is started at the first storey is not propagated to the top storey. They are concentrated more in the first storey for the structure without increase in design moments. But in the structure with increased design moments, the cracks initiated at the first storey propagated towards the top storeys. Hence the first bay which is directly subjected to the loads effects more than the other floors. With this observation, it can be concluded that the load transfer is taking place from top to bottom of the structure on one side in the soft storey structure with increased moments.

The stiffness and strength of the two structures are quantitatively shown in Table 2. From the table it can be seen clearly that the structure with soft storey has very less strength and stiffness when compared to the structure without soft storey. This is true in the case of soft storey structure designed for 2.5 times the moments and shear forces.

Table 2: Comparison of parameters

	Structure without soft storey	**Structure with soft storey**	**Structure with soft storey (2.5times)**
Initial Stiffness (kN/m)	22.87×10^5	0.86×10^5	1.58×10^5
Max Base Shear (kN)	4673	160	578

4. CONCLUSIONS

This paper aims at understanding the seismic behaviour of some special cases in Moment resisting frames with URM infilled frames. For fulfilling this objective, a RC building is considered to be present in seismic zone IV. The capacity of the structure was obtained and proper reasons were derived by observing the parameters involved in estimating the capacity and also the crack initiation and propagation patterns.

It was observed that the structure with soft storey losses greater initial stiffness and maximum strength when compared to the structure without soft storey. It was also observed that the load path from the point of application of load was not distributed properly in the structure with soft storey. Due to the improper distribution of lateral load, the structure with soft storey had very less capacity when compared to the structure without soft storey. From the structure designed according to clause given in IS 1893, it was observed that the structure had increased its maximum load carrying capacity with increase in design moments. The crack pattern had not changes much in both the cases. The assumption that the soft storey structure with increased design moments behaves as the structure with enclosed full walls is directly under question with this observation. There is no comparison between the soft storey with increased moments and the structure without soft storey. The maximum load carrying capacity and the initial stiffness is hugely varying in both the cases.

REFERENCES

Bureau of Indian Standards, 2000. *Indian Standard code of practice for plain and reinforced concrete for general building construction*, IS 456, New Delhi, India.

Bureau of Indian Standards, 2002. *Indian Standard Criteria for Earthquake Resistant Design of Structures. Part – 1 General Provisions and buildings*, IS 1893 – 2002, Part – 1, New Delhi, India.

Crisafulli, F. R., 1997. Seismic behaviour of reinforced concrete structures with masonry infills, PhD Thesis, *University of Canterbury*, New Zealand.

Dande, P. S., and Kodag, P. B., 2013. Influence of soft storey in RC frame building in earthquake resistant design, *International Journal of Engineering Research and Applications* 3, 461 – 468.

Elouli, T., Effect of infill masonry panels on seismic response of frame buildings, *The fifth Agdal Rabat Morocco, University of Mohammed*.

Kaushik, H. B., Rai, D. C., and Jain, S. K., 2008. A rational approach to analytical modeling of masonry infill in reinforced concrete frame buildings, *The 14th World Conference on Earthquake Engineering,* October 12-17, 2008, Beijing, China.

Lourenco, P. B., and Rots, J. G. 1997. Multi-surface interface model for analysis of masonry structures, *Journal of Engineering Mechanics* 123.

Murty, C. V. R., and Sudhir, K. J., 2000. Beneficial influence of masonry infill walls on seismic performance of RC frame buildings, *The 12th World Conference on Earthquake Engineering*, January 30 – February 4, 2000, Auckland, New Zealand.

Pandey, B. H., and Meguro, K., 2004. Simulation of brick masonry wall behaviour under in plane lateral loading using applied element method, *The 13thWorld Conference on Earthquake Engineering*, August 1-6, 2004, Vancouver, B.C., Canada.

Pujol, S., Climent, A. B., Rodrigueand, M. E., and Smith-Pardo, J. P., 2008. Masonry infill walls: An effective alternative for seismic strengthening of low rise reinforced concrete building structures, *The 14thWorld Conference on Earthquake Engineering,* October 12-17, 2008, Beijing, China.

Samoila, D., 2013. Masonry infill panels – analytical modeling and seismic behaviour, *IOSR Journal of Engineering (IOSRJEN)* 3, 30-39.

Experimental study on seismic retrofitting of masonry wall with special fiber reinforced paint

Kenjiro YAMAMOTO[1] Muneyoshi NUMADA[2] and Kimiro MEGURO[3]
[1]Graduate Student, Department of Civil Engineering,
The University of Tokyo, Japan, k-yama@iis.u-tokyo.ac.jp
[2]Assistant Professor, ICUS, IIS, the University of Tokyo, Japan
[3]Director/Professor, ICUS, IIS, the University of Tokyo, Japan

ABSTRACT

About sixty-percent of the total population of the world still live in masonry structures, and there have been heavy casualties in the past earthquakes due to their structural collapses. To improve seismic capacity of these weak structures, many retrofit methods have been developed. However, most of them are time-consuming and labor-intensive and can only be applied for new construction, which slows down the spread of these methods. In our research, a much easier new method applicable for both new and existing constructions was developed. The material used in this method is called 'SG-2000', special paint reinforced with glass fiber. There are two merits to use it. Firstly, it needs much shorter time and less labor to retrofit. Secondly, it has endurance to UV-ray, water, and fluctuation of temperature. An experimental study has been conducted to evaluate the performance of SG-2000 as a masonry retrofit material, and to find the best way to paint on the wall. It has been proved that the wallette coated with SG-2000 has about 14 times and 16 times larger deformation capacities in both in-plane and out-of-plane tests, respectively, than that of the unreinforced masonry wallette. We have also found some efficient ways to coat masonry walls.

Keywords: masonry, seismic retrofitting, fiber-reinforced paint

1. BACKGROUND

1.1 Masonry

There are still many masonry structures in all over the world, especially in developing countries. About sixty-percent of the total population of the world still live in masonry structures. Many masonry structures are non-engineered structures that were built by local people without any engineering background using locally available materials, such as burned or unburned bricks, some kind of blocks and stones with poor cement or mud mortar without following structural code, they are highly vulnerable to earthquakes. The bricks are so heavy, and people will be injured by their fallings. Besides, bricks and mortar that have gotten back to soil powder due to the earthquake will bury people alive. Because of these vulnerabilities, there have been heavy casualties in the past earthquakes.

1.2 Past researches for retrofitting masonry

To have an anti-seismic retrofitting of a masonry structure, it is important to improve its three abilities, "strength", "deformability", and "energy absorption capacity".

1.2.1 PP-band (Polypropylene band) method (Sathiparan, 2005)

PP-band is commonly used for packing. The method of retrofitting is only to bind masonry with PP-band in mesh shape. It is cheap, and reinforcing masonry with PP-band needs no technical high skills. Besides, this method of retrofitting masonry does not change the local style of living.

This method improves "deformability", and "energy absorption capacity" of masonry structures. Because it does not improve “strength” of the structure, it cannot avoid the early stage of destruction. It only prevents the masonry from collapse. Besides, there is another disadvantage in this method. Binding masonry with PP-band needs relatively less labor and time than other methods, but still it needs certain labor and time for real size of houses.

1.2.2 C/G-FRP (Carbon/Glass Fiber Reinforced Plastic) method

This method improves "strength" of masonry. It prevents the early stage of destruction as well as the collapse of the masonry structures. But the masonry makes a brittle fracture if the force of an earthquake gets over the strength of the parts of the building that are retrofitted with FRP. Besides, FRP is stuck to the building with epoxy bond, so when the adhesive strength of the bond is not so strong as that of FRP, it is equal to that it is not FRP but the bond that works for retrofitting. Moreover, for the real size of houses, it needs large amount of FRP that are very expensive. Therefore, this method also needs high cost, much labor and time for real size of houses.

2. PURPOSE

2.1 A new method of retrofitting masonry structures

The previous methods are simple ways to improve masonry structures’ seismic capacity. However, they all need much labor and time for real size of houses. This research was conducted to develop a new method of retrofitting masonry, which needs much less labor and time. This fact contributes to the spread of the retrofitting of masonry. The material used in this method was "SG-2000" (Figure 1), a kind of paint that is reinforced by mixing glass fiber. In this research, we conducted In-plane diagonal test and out-of-plane test to evaluate the performance of the proposed method.

3. IN-PLANE AND OUT-OF-PLANE TESTs

3.1 In-plane diagonal compression test

3.1.1 Test setup

To investigate the effects of SG-2000 to improve masonry's seismic capacity in in-plane direction, we prepared seven models that vary in the amount of paint and in the way of coating as shown in Table 1. Using these specimens, we performed in-plane diagonal compression test and compared the strength and deformability. To explore the most effective way of coating for reducing the retrofitting cost, we adopted two coating ways, full coating and mesh shape coating as shown in Figure 2. In the comparative study, the force and deformation are normalized.

The dimensions of each specimen were 277.5×282×50 mm^3 and composed of 7 brick rows of 3.5 brick each. A C/W ratio was 0.14. All the specimens were tested 28 days after construction, and 28 days after the coatings of the paint. The loading rates were 0.25 mm/min.

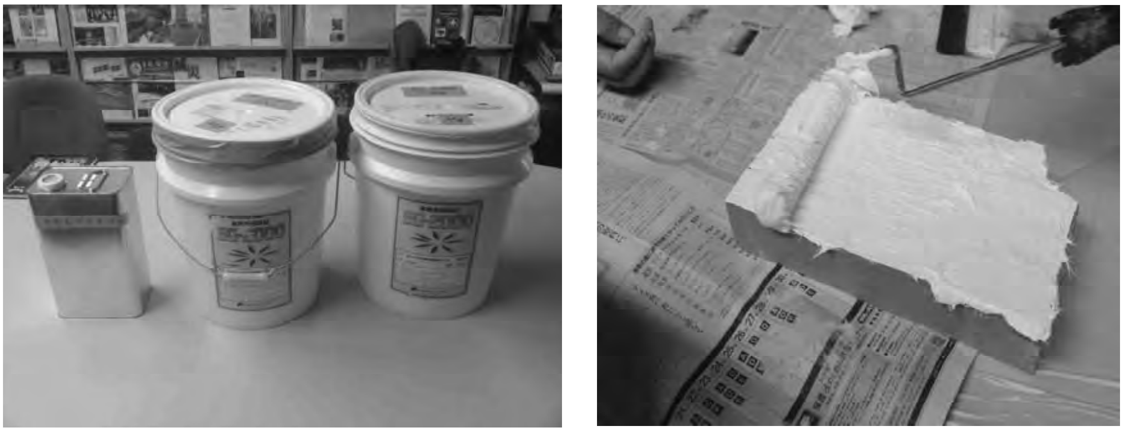

Figure 1: Paint for retrofitting (SG-2000)

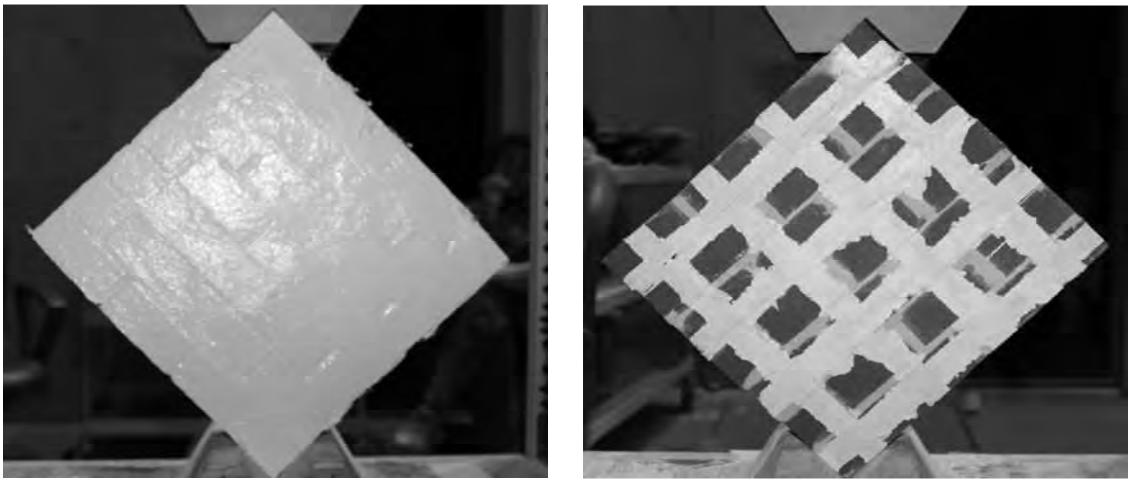

Figure 2: Full coating of both sides (left) and coating in mesh shape (right)

3.1.2 Results

Figure 3 shows the crack patterns of **URM** in 2 mm deformation and **IN-1** in 28 mm deformation. Figure 4 shows the graph of the load and the deformation in in-plane diagonal compression tests of **IN-1** and **URM**. **URM**'s stress was gradually increasing until the peak strength at 2 mm deformation, but after that the stress dropped and the specimen was broken. On the other hand, **IN-1**, fully coated in front and back side of the specimen, had the same behavior until its peak strength. However, after that, the stress was gradually decreased to zero, at 28mm in deformation. **IN-1** did not show the drop of stress, so the mechanism of breaking was safe.

Table 1: Specimens for comparative study

Name	**Coating thickness (mm)**	**The content of fiber (wt%)**	**Details of coating**
IN-1	1	1.5	Full coating of both front side and back side (see Figure 1)
IN-2	2		
IN-3	0.5		
IN-4	1	2	
IN-5	1	1.5	Full coating of front and back side without Primer, the fixing agent of SG-2000 and the wall
IN-6	1		Coating of front and back side in mesh shape, the surface area is half of the total area (equal weight to IN-3)
IN-7	0.5		Coating of both front and back sides in mesh shape, the surface area is half of the total area (half weight of IN-3) (see Figure 2)

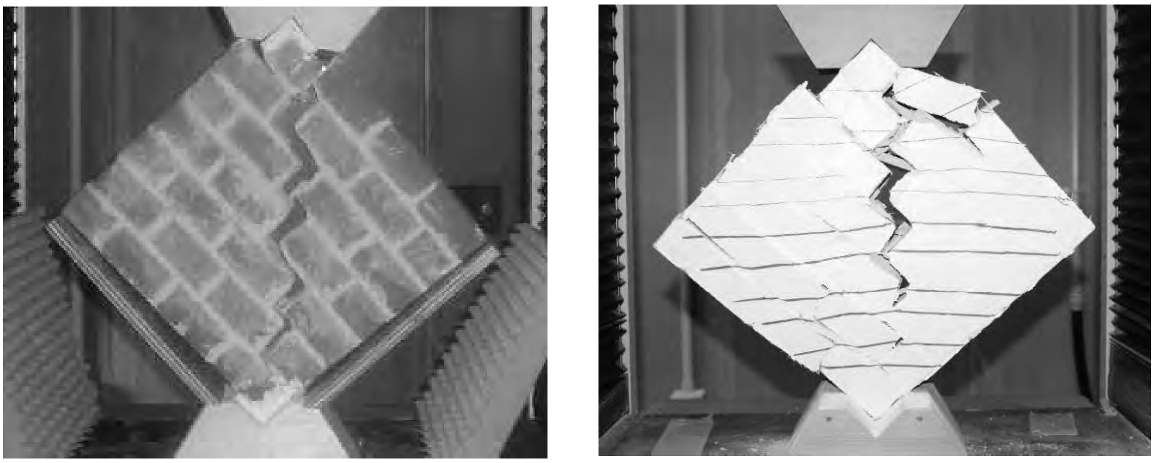

Figure 3: URM with its deformation of 2mm (left) and IN-1 with its deformation of 28mm (right)

The differences in strength between **IN-1** and **URM** were not seen, but it was seen that **IN-1**'s deformability was about 14 times as long as **URM**'s.

Figure 5 shows the normalized results of comparative studies in in-plane tests. **IN-2**, whose coating is twice thicker than **IN-1**, had twice larger deformability than **IN-1** had. **IN-3**, whose coating thickness is a half of **IN-1**, had half deformability of **IN-1**. **IN-6**, which has the same amount of paint as **IN-3**, and coated in mesh shape, had longer deformability than **IN-3** had. **IN-4**, where paint with higher amount of fiber is used, maintained its strength for longer time than **IN-1** had. **IN-5**, where the primer (the fixing agent of SG-2000 and the wall) is not used had longer deformation than **IN-1**.

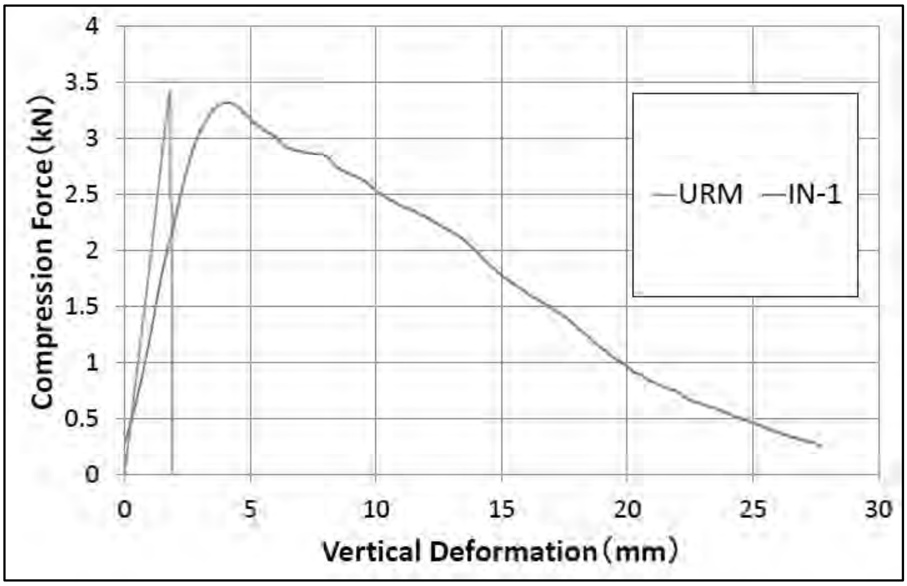

Figure 4: Comparison between URM and IN-1

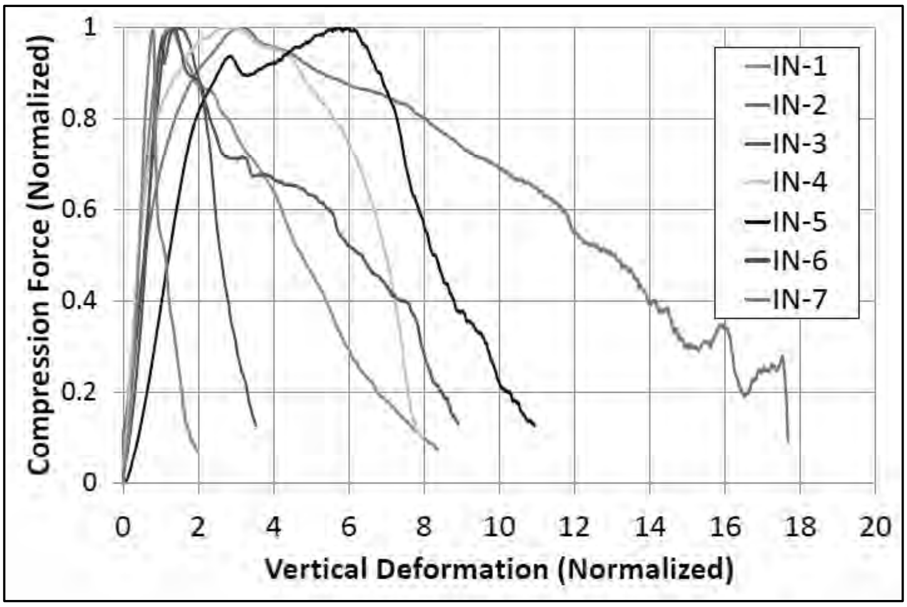

Figure 5: Normalized graph of comparative sturdy

3.2 Out-of-plane bending test

3.2.1 Test setup

To investigate the effects of SG-2000 to improve masonry's seismic capacity in out-of-plane direction, we prepared three models that vary in the amount of paint and the content of fiber as shown in Table 2. Using these models, we carried out out-of-plane bending test and compared the strength and deformability of all models. In the comparative study, the force and deformation are normalized.

The dimensions of each specimen were 475×241×50 mm^3 and composed of 6 brick rows of 6 brick each. A C/W ratio was 0.14. All the specimens were tested 28 days after construction, and 28 days after the coatings of the paint. The loading rates were 0.25 mm/min.

Table 2: Specimens for comparative study

Name	Coating thickness (mm)	The content of fiber (wt%)	Details of coating
OUT-1	1	1.5	Full coating of only under side
OUT-2	0.5		
OUT-3	1	2	

3.2.2 Results

Figure 6 shows the **OUT-1** with its deformation of 10 mm. **OUT-1**, fully coated under the specimen, prevented its stress from dropping, and the stress was gradually decreased to zero, at 16 mm in deformation. **OUT-1** did not show the drop of stress, so the mechanism of breaking was safe.

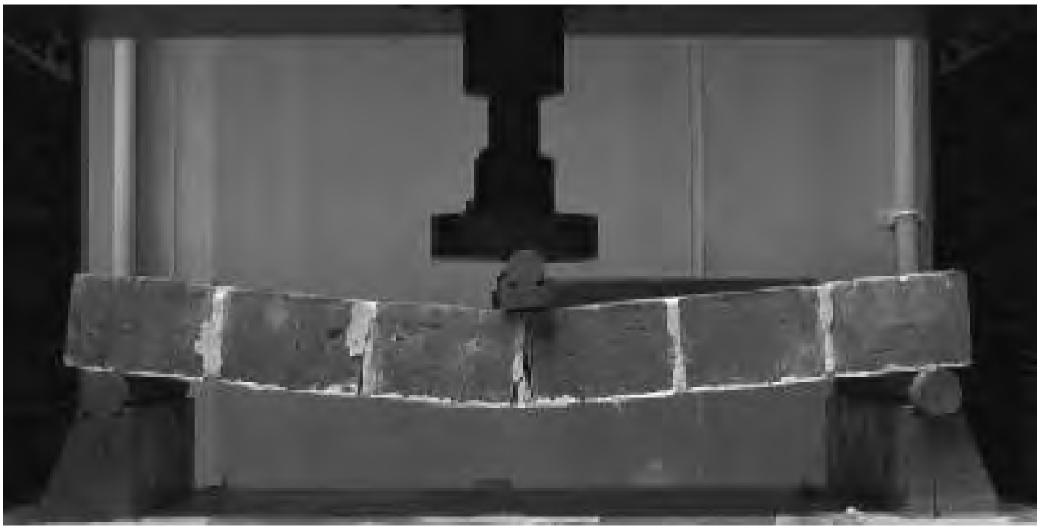

Figure 6: Out-of-plane test of OUT-1 with its deformation of 10 mm

Figure 7 shows the results of out-of-plane bending tests **OUT-1** and **URM**. It was not seen that **OUT-1** has higher strength than **URM** (reason of lower strength of **OUT-1** is use of poor mortar than **URM**), but it was observed that **OUT-1**'s deformability was about 16 times larger than **URM**'s.

Figure 8 shows the normalized results of comparative studies in out-of-plane tests. **OUT-2** and **OUT-3**, both of which have twice thicker paint than **OUT-1** has, had twice larger deformability than **OUT-1** had. **OUT-3**, where paint with higher amount of fiber is used, had almost the same curve as **OUT-1** had.

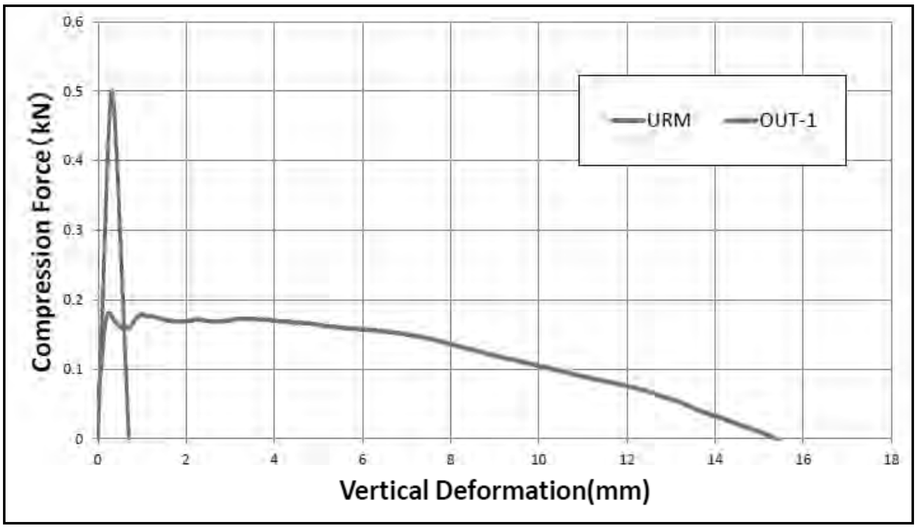

Figure 7: Comparison between URM and OUT-1

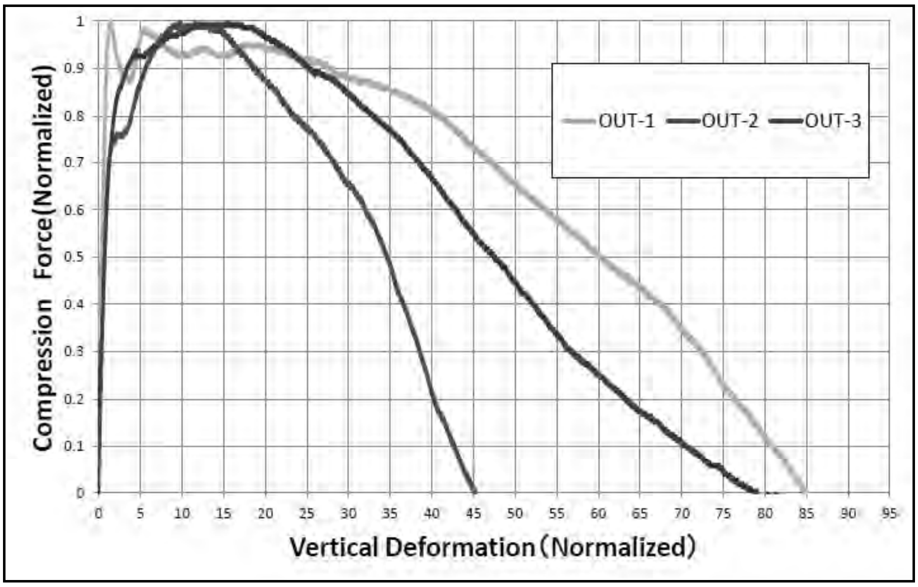

Figure 8: Normalized graph of comparative sturdy

4. CONCLUSIONS

The results of in-plane diagonal compression tests show that:

(1) SG-2000 did not contribute to the strength, but it made the wallette have larger deformability.

(2) The deformability of retrofitted wallette depends on the thickness of coating. The thicker the coating is, the larger deformation the wallette has.

(3) If coated with the same amount of paint, it is better to coat effectively in the mortar joints between bricks.

(4) The higher the content of fiber is, the longer the specimen can keep its strength, and therefore the more its energy absorption capacity becomes.
(5) For burnt brick masonry, the specimen without using primer (the fixing agent of SG-2000 and the wall) has larger ductility.

The results of out-of-plane bending tests show that:

(1) SG-2000 did not contribute to the strength, but it made the wallette have larger deformability.
(2) The deformability of retrofitted wallette depends on the thickness of coating. The thicker the coating is, the larger deformation the wallette has.
(3) In out-of-plane direction, there was no clear differences among two models that vary in only 0.5% of their content of fiber.

Future researches should be carried out to check the dynamic performance by conducting shake table tests. Also, this paint SG-2000 does not contribute to increase the strength of the structure, so it should be improved for the contribution of strength.

REFERENCES

Sathiparan, N., Mayorca, P., Nesheli, K. N., Guragain, R., Meguro K., 2005. Experimental Study on In-plane and Out-of-plane Behavior of Masonry Wallettes Retrofitted by PP-Band Meshes, *SEISAN-KENKYU* 57 (bi-monthly paper published by IIS, The University of Tokyo, Japan).

Umair, S. M., Numada, M., Meguro, K., 2012. *In Plane Behavior of Polypropylene and FRP Retrofitted Brick Masonry Wallets under Diagonal Compression Test,* 15th World Conference on Earthquake Engineering (15th WCEE), Paper No.500, e-poster, 2012.

Analysis of evacuation behavior from complex disaster based on stated preference data
- Case study on Adachi-ku Senju district in Tokyo -

Kazuyuki TAKADA[1], Makoto FUJIU[2], Takahiro KONNO[3]
[1] Professor, Tokyo Denki University, Department of Civil Engineering, Japan
takada@g.dendai.ac.jp
[2] Assistant Professor, Faculty of Environmental Design, Kanazawa University, Japan
[3] Bachelor Student, Tokyo Denki University, Department of Civil Engineering, Japan

ABSTRACT

Adachi-ku Senju district in Tokyo was selected as the investigated district of this study because Senju district has been designated by the Tokyo Metropolitan Government as the area with both high fire risk and high flood risk.
Questionnaire survey was conducted for the residents and employees in Senju district to collect the data regarding knowledge of damage estimates of Senju district, knowledge of evacuation method at big earthquake, and evacuation behavior at disaster occurrence.
As the results of aggregative analysis, it became clear that there are several problems in Senju distrct such that the employees have a tendency not to accurately understand the damage estimates and the evacuation method, both the residents and the employees have a tendency to underestimate flood risk, and some residents try to evacuate from the flood by going up the lower floor (2nd floor) of the residence under the situation that fire spread and flood are occurring at the same time. Furthermore, two kinds of evacuation behavior model were developed in this study. One is a model to explain the factor inducing evacuation and the other is a model to explain the factor to choose evacuation place under disasters. As the results of behavior model analysis, resident chose a school for evacuation destination, and height and area of destination were effected by evacuation behavior.

Keywords: evacuation behavior, complex disaster, discrete choice model

1. INTRODUCTION

Massive destruction was brought to the north-eastern region of Japan when the 2011 off the Pacific coast of Tohoku Earthquake occurred at 14:46 (JST) on March 11th, 2011. In Tokyo metropolitan area where maximum of 5-upper seismic intensity (JMA) was recorded, the earthquake suspended the transportation system such as bus and train services. On the other hand, Central Disaster Prevention Council, the supreme organization of disaster affairs in Japan, has reported that Tokyo metropolitan area has three kinds of natural mega-hazard such as M.7 class inner-plate earthquake, Tsunami and flood. Meanwhile, the number of flood disasters occurrence has increased and it is necessary to examine occurrence of the complex disaster which is over two kinds of disaster in same time. In this study, Adachi-ku Senju district in Tokyo was selected for research, which has high flood risk and building collapse risk. Then, effective countermeasures for complex disaster are required in these districts. The purpose of this study is to analyze of evacuation behavior from complex disaster based on Stated Preference Data. We have developed two kinds of models. One demonstrates the choice behavior whether they stayed in damaged area or not and the other demonstrates the choice behavior whether they evacuate vertical direction or horizontal direction.

2. Basic Analysis of Evacuation Behavior

2.1 Stated Preference Condition of Evacuation

In this study, questionnaire survey and SP survey were conducted for residents and employee in Adachi-ku Senju district in Tokyo. The residents and employee were provided some disaster condition as shown in table 1. Condition (a) was a situation that there was “Not confirm the fire, cannot confirm the smoke”. The situations of suffered people have a time for evacuation to the temporary evacuation shelter or river side evacuation space. Condition (b) was situation that there were “Spreading and expansion of the fire”, “Not walk smoothly” and “Suspension of electricity, water supply and gas supply”. The situations of suffered people have to evacuate to the evacuation shelter. Condition (c) was a situation that there was “Fear of the bank rip”. The situations of suffered people have to evacuate to the temporary evacuation shelter which does not inundate, outside of this district which does not inundate and evacuation shelter. Condition (d) and (e) was set a situation that there was the complex disaster conditions. The situation of suffered people have to evacuate to the temporary evacuation shelter which does not inundate, outside of this district which does not inundate and evacuation shelter which locate outside of riverside. Figure 1 shows that SP survey with condition (a), and Figure 2 shows that evacuation area choice analysis.

Table 1: Condition setting of Stated Preference survey

Situation	Condition(a)	Condition(b)	Condition(c)	Condition(d)	Condition(d)
	No evacuation	Gathers in evacuation area	Evacuate to outside district	Gathers in bridge area	Cannot evacuate
Flood risk	-	-	Fear of the bank rip	Fear of the bank rip	Fear of the bank rip
Fire after the earthquake	Not confirm the fire, confirm the Smoke	Fire spreading and fire expansion	-	Fire spreading and fire expansion	Spreading and expansion of the fire
Congestion of road and Sidewalk	-	Not walk smoothly	-	-	Not pass smoothly
Lifeline damage	-	Suspension of electricity, water supply and gas supply	-	Suspension of electricity, water supply and gas supply	-

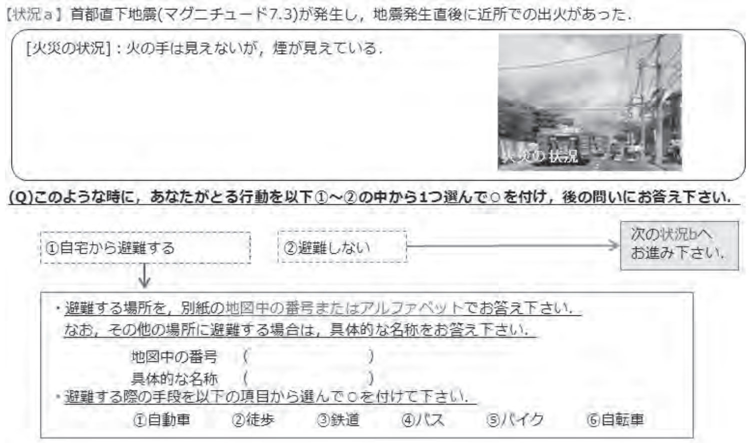

【状況ａ】首都直下地震(マグニチュード7.3)が発生し，地震発生直後に近所での出火があった．

[火災の状況]：火の手は見えないが，煙が見えている．

(Q)このような時に，あなたがとる行動を以下①～②の中から1つ選んで○を付け，後の問いにお答え下さい．

①自宅から避難する

②避難しない → 次の状況bへお進み下さい．

・避難する場所を，別紙の地図中の番号またはアルファベットでお答え下さい．
なお，その他の場所に避難する場合は，具体的な名称をお答え下さい．

地図中の番号　（　　　　　　）
具体的な名称　（　　　　　　）

・避難する際の手段を以下の項目から選んで○を付けて下さい．

①自動車　②徒歩　③鉄道　④バス　⑤バイク　⑥自転車

Figure 1: SP survey with condition (a)

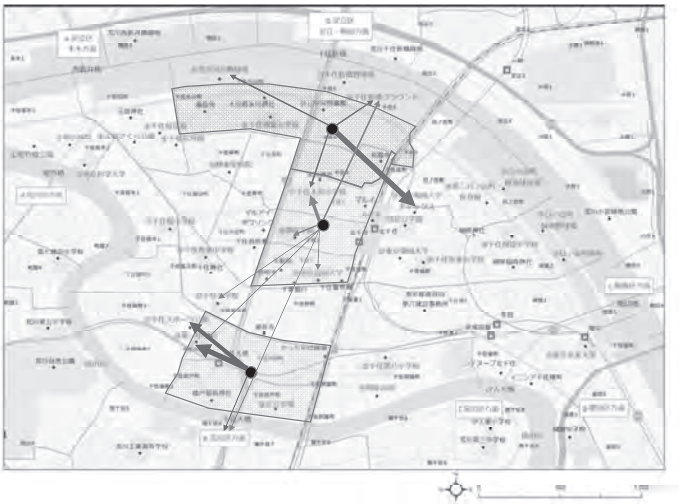

Figure 2: Evacuation area choice

2.2 Results of Evacuation Method

Table 2 shows that results of evacuation method under SP conditions. Condition (a) is high percentage of correct answer. On the other hand, Condition (b), (c), (d) and (e) is low percentage of correct answer.

A few respondents answered that suffered people evacuate to evacuation space in river side under condition (b), and almost respondent answered that suffered people evacuate to evacuation space which is elementary school and so on. Almost respondent answered that suffered people evacuate to multistory building such as department store and residential building under condition (c), and a few respondent answered that suffered people evacuate to evacuation space which is registered by Tokyo Metropolitan Government.

Moreover, same evacuation tendency confirmed under condition (d) and (e) which are complex disaster. As a result, evacuation method of suffered people is influenced by disaster conditions. But evacuation method is not recommendation method, and then improvement of understanding level of evacuation under some disaster situation is essential.

Table 2: Results of evacuation method

	Number of correct answer	Number of incorrect answer	Percentage of correct answer
Condition(a)	102	87	54.0
Condition(b)	36	189	16.0
Condition(c)	26	245	9.6
Condition(d)	44	228	16.2
Condition(e)	36	216	14.3

3. ESTIMATION OF EVCUATION BEHAVIOR MODEL

3.1 Evacuation behavior model

Table 3 shows that result of evacuation behavior model which is estimated by binary logit model. As a result of estimation of evacuation behavior model, in case of road congestion and suspension of lifeline, both of suffered residents and workers stay in suffered position.
Table 4 shows that probability of evacuation under some disaster conditions. In case of confirming the smoke, spreading the fire and road congestion, evacuation probability of residents is low.
In case of confirming the smoke and fear of the bank rip, evacuation probability of workers is high. If spreading the fire and fear of the bank rip occurred in same time, evacuation probability of residents are high.
When complex disaster such as fire and flood occurred, the possibility of isolation is high for suffered residents, and then they have high probability of evacuation.
Evacuation behavior under flood disaster may be influenced by number of stories, and then evacuation behavior model considered numbers of stories dummy variables are estimated. Depth of flood is estimated about 5.0 m in Adachi-ku Senju district in Tokyo. The estimated evacuation behavior model adopted number of stories (1・2 stories) dummy variables and number of stories (3 stories) dummy variables. As a result of evacuation model estimation, residents which live in low layer floor evacuate positively for avoiding of inundation.

Table 3: Estimated parameters of evacuation behavior model-1

Variables	Residents		Employee	
	parameter	t-value	parameter	t-value
Smoke dummy	0.225	2.057	0.099	0.736
Fire spreading dummy	0.821	6.807	0.701	1.677
Flood risk dummy	1.423	10.263	0.929	6.194
Road congestion dummy	-0.961	-4.202	-0.12	-0.439
Suspension of lifeline dummy	-0.658	-2.787	-0.065	-0.238
Initial likelihood	- 951.4		-658.8	
Final likelihood	- 233.5		-154.3	
Likelihood ratio	0.755		0.7658	
Adjusted likelihood ratio	0.749		0.7582	
Hit ratio	73.3%		74.4%	
Number of samples	1639		1080	

Table 4: Probability of evacuation behavior under some disaster conditions

Confirming the Smoke	Spreading the fire	Fear of the bank rip	Road congestion	Prob. of evacuation (residents)	Prob. of evacuation (workers)
1	0	0	0	55.6%	48.0%
0	1	0	0	69.4%	46.6%
0	1	0	1	46.5%	65.8%
0	0	1	0	80.7%	47.7%
0	0	1	1	61.4%	66.7%
0	1	1	0	90.5%	46.1%
0	1	1	1	78.4%	65.1%

Table 5: Estimated parameters of evacuation behavior model-2

Variables	parameter	t-value
Smoke dummy	0.216	1.966
Fire spreading dummy	0.640	2.013
Flood risk dummy	-1.738	-8.941
Road congestion dummy	-0.005	-0.026
Suspension of lifeline dummy	0.194	0.930
Number of stories (1･2 stories) dummy	1.684	8.964
Number of stories (3 stories) dummy	1.098	5.472
Initial likelihood	-1115.4	
Final likelihood	-1033.2	
Likelihood ratio	0.0738	
Adjusted likelihood ratio	0.0657	
Hit ratio	56.%	
Number of samples	1615	

4. CONCLUSIONS

In this study, Adachi-ku Senju district in Tokyo was selected as the investigated district of this study because Senju district has been designated by the Tokyo Metropolitan Government as the area with both high fire risk and high flood risk. Questionnaire survey as s SP survey was conducted for the residents, employees and students in Senju district to collect the data regarding the knowledge of damage estimates of Senju district, knowledge of evacuation method at the time of big earthquake, and evacuation behavior at the time of the disaster occurrence.

In this study, evacuation behavior models were developed using SP data under complex disaster conditions. It became clear that in case of road congestion and suspension of lifeline, both of suffered residents and workers stay in suffered position, and in case of confirming the smoke, spreading the fire and road congestion, evacuation probability of residents is low and in case of confirming the smoke and fear of the bank rip, evacuation probability of workers is high. If spreading the fire and fear of the bank rip occurred in same time, evacuation probability of residents are high.

When complex disaster such as fire and flood occurred, the possibility of isolation is high for suffered residents, and then they have high probability of evacuation. Moreover, As a result of evacuation model estimation considered number of stories, residents which live in low layer floor evacuate positively for avoiding of inundation.

REFERENCES

Cabinet office of Japan, Outline of Tokyo metropolitan area large-scale flood damage measures (http://www.bousai.go.jp/kaigirep/chuobou/31/pdf/31_gijiroku.pdf), 2013.
Cabinet office of Japan, Outline of large-scale earthquake disaster damage reduction countermeasures (http://www.bousai.go.jp/kaigirep/chuobou/34/pdf/34_siryo3-2.pdf), 2014.
Adachi ward office disaster council, Chapter of regional earthquake disaster prevention plan, 2012.
Tokyo metropolitan government, Regional risk measurement investigation report book, 2013.9.
Adachi ward office disaster council, the flood hazard map, 2007.
Kazuyuki TAKADA, Miho OHARA, Tomohisa YAMASHITA and Makoto FUJIU, Consciousness analysis of evacuation from complex disasters in Tokyo Senjyu district, Proceedings of Infrastructure Planning and Management, Vol.49.

Issues and analysis of the Post-Yolanda shelter recovery process and role of international agencies

Tomoko MATSUSHITA
Graduate Student, the University of Tokyo, Japan
matsu-t@iis.u-tokyo.ac.jp

ABSTRACT

Approximately four million people are said to have lost homes after Typhoon Yolanda (internationally known as Haiyan) hit the Visayan islands of the Philippines on 8th November 2013. The construction of permanent houses has started, however less than 10% of people in need of shelter are said to have received assistance for rebuilding more than half a year after the typhoon, and the majority of the affected population still live in temporary houses they build themselves using salvaged materials. More than seventy national and international humanitarian agencies are working to assist reconstruction of houses, however there are deep-rooted issues such as problems of land tenure and the lack of a comprehensive system for providing post-disaster housing, that seem to have caused the delayed reconstruction. The author will examine issues learned in the field through an on-going project "Post-Yolanda Support for Safer Homes and Settlements" implemented by United Nations Human Settlements Programme (UN-HABITAT) in the Province of Capiz, Panay Island. The recovery process and the roles of various national and international actors is evaluated in terms of approaches and effectiveness in order to create proactive suggestions for future disaster response.

Keywords: natural disaster, shelter, Typhoon Yolanda, international agency

1. INTRODUCTION

There are many guidelines about post-disaster housing readily available online thanks to the efforts by leading aid agencies such as UNHCR, IFRC, UN HABITAT and the World Bank among others (Leon, 2012; Ashmore, 2013). Even though such informative materials based on numerous case studies are extremely useful and available, we still face difficulty in every disaster because each situation is different and there is no 'one size fits all' solution to this problem, and because beyond the technical aspects of physical construction, housing involves existing social system as well as country-specific issues that requires more than just a humanitarian[1] response (Jha, 2010; Fan). In another words, short-term solutions that are often the focus of humanitarian agencies cannot address housing needs sufficiently. This problem has been recognized as the "humanitarian development gap" and is still debated to this day, with rising concern due to the growing urban population and increasing number of displaced people after disaster (Moore, 1999; Steets, 2011).

---

[1] The definition of humanitarian here refers to emergency

Two big questions emerged during the housing reconstruction project in the Philippines while the author was working as a junior shelter expert with UNHABITAT: 1) how "balanced" was the assistance that was provided to the affected populations, and 2) whether it was reaching poorest of the poor people who most desperately need help. Instead of trying to answer these rhetorical questions, the objective of this paper is to bring attention to the fact that housing reconstruction needs to take into account not only humanitarian aspects of providing housing in emergency but also a long-term, development aspect. In order to do so, this research uses case study analysis as a methodology and the authors will discuss and analyze the issues observed during the operational process of housing reconstruction project by UN-HABITAT (UNH), introducing cases from the field in the Province of Capiz and Iloilo in Region VI, the Philippines. This paper is a preparatory study for advocating a holistic approach and developing a better system to respond to post-disaster housing needs especially in the rapidly urbanizing nations with increasingly complex issues.

2. BACKGROUND: TYPHOON YOLANDA RESPONSE

2.1 Facts and status of recovery

Typhoon Yolanda, internationally known as Haiyan, made landfall on November 8, 2013, causing 6,300 deaths and affecting a total of 3.4 million families, with 16 million people in the Philippines. Nearly 1.1 million (1,127,041) houses were damaged including 548,793 totally destroyed throughout the nine affected regions of the Western Visayas (DSWD, 2013). More than half a year after the typhoon, the Regional Coverage Gap indicated a 77% gap of households that have not yet received any support (Philippines Shelter Cluster, 2014a). Eight months after the typhoon, "only 38% of assessed households reported having shelter assistance," indicating that more than 60% have not yet received assistance, according to the survey conducted across ten typhoon-affected provinces by REACH, a joint initiative of NGOs and UNOSAT (Philippines Shelter Cluster, 2014b).

2.2 Response by the National Government

On 11 November 2013, due to the massive destruction and immense effects of Typhoon Yolanda, the president declared a state of national calamity issuing Presidential Proclamation No.682 and designated the Office of Presidential Assistant for Rehabilitation and Recovery (OPARR) to oversee Typhoon Yolanda Reconstruction and Rehabilitation per Presidential Memorandum Order No.62 dated 6 December 2013 (NDRRMC, 2014). OPARR was created to carry out a coordination role of similar to that of UNOCHA in international disaster response. The national government announced it will provide 30,000 PHP cash (not yet provided) and 2 sheets of CGI (corrugated galvanized iron) roof materials per household to be used for repair although the delivery of this support has been delayed. In terms of permanent housing, the government is in the process of reviewing proposals by local governments about how to proceed strategically to assure the security of safe housing for all.

2.2.1 "No Build Zone"

The National Government has announced a so-called "No Build Zone[2]" to restrict the residents from building in the area near the coast that was considered dangerous immediately after the typhoon. Twenty-one percent of households are said to live in a no-build zone according to a survey (Philippines Shelter Cluster, 2014b). The announcement of the No Build Zone was not well received by affected people or local governments, because the national government did not provide alternative plans for relocating the affected population and therefore many residents had no choice but to stay along the coast, rebuilding their houses at the former places using salvaged materials ways considered unsafe. The "No Build Zone" announcement has caused great confusion because relocation is unrealistic for most people due to a lack of relocation area, and it also sends a wrong message that it is safe to live along the coast as long as the house is built 40 meters or more from the coastline. In fact, elevation matters more than the distance from the shore since the storm surge caused the water to rise up to 6 meters in the city of Tacloban, which caused most of the 6,300 deaths. The government recognizes the needs and is trying to address this issue of informal residents at risk living near the water while it proves to be difficult and has met great resistance from local governments and local people.

2.3 Response from the International Community

Due to the massive scale of destruction caused by Typhoon Yolanda, the United Nations announced a Level 3 (L3) declaration[3] that includes the activation of the Cluster system[4] for better coordination among actors of the same humanitarian sector (IASC, 2012). On the ground, there were many national and international agencies actively involved in the reconstruction effort throughout the entire regions of the Visayas islands in the Philippines. The Philippines Shelter Cluster was established and led by IFRC, and provided support such as setting up regular coordination meetings among shelter agencies, being a focal point with the government and providing resources including practical information on the web as well as personal consultation to discuss technical issues about construction, etc. The Shelter Cluster was later renamed the Humanitarian Shelter Working Group after the Philippines government announced that OPARR would take over the coordinating role instead.

2.3.1 Different Shelter Options by phase

The Philippines Shelter Cluster created detailed guidelines for nine shelter recovery options as shown in Table 1 (Philippines Shelter Cluster, 2014c). Among them, there are four types of housing options namely temporary shelter, bunkhouse, core houses and permanent houses with specified criteria such as the timeframe for use, size, budget and conditions of the target households. By making this type of distinction it clarifies the needs and various types of shelters required at different phases of recovery. However temporary housing often ends up becoming permanent because there is no place to move to and as a consequence many affected populations stay in undesirable conditions. This has happened in many major disasters such as in Haiti and Japan among others and its ineffectiveness has been widely recognized.

---

[2] The Philippine Water Code states "40m No build zone"

[3] Level 3 is activated when a large-scale, sudden-onset crisis occurs and it triggers the deployment of IARRM (Inter-Agency Rapid Response Mechanism) emergencies and is judged by their scale, complexity, urgency, the capacity required to respond and the reputational risk to humanitarian organisations and responders, activated by Emergency Relief Coordinator (IASC, 2012).

[4] The cluster approach was introduced as part of humanitarian reform in 2005. It seeks to make humanitarian assistance more effective by introducing a system of sectoral coordination with designated lead organizations (IASC; Steets, 2010).

Table 1. Nine options of Recovery Shelter Guidelines

Shelter options	Time frame	Size	Budget (PHP)	Condition of target household
1. Emergency Shelter Upgrade/ Replacement	6 month to 1 year	N/A	N/A	May not have clear long-term tenure over their land
2. Temporary Shelter	N/A	Minimum 3.5m^2/person, 18m^2/ family of 5	30,000-45,000	Living in high risk area, being relocated to temporary site
3. Sharing Programs	Up to 2 years	N/A	N/A	
4. Rental Support	2 years	N/A	N/A	
5. Bunkhouse Program	2 years	N/A	N/A	Facing longer displacement potential for relocation / living in high risk areas
6. Repair and Retrofit	N/A	N/A	10-18,000 (minor) 20-40,000 (major)	
7. Core House	9 years	Minimum 18m^2	60,000-110,000	Has a recognized form of tenure
8. Permanent House	Permanent	N/A	120,000-250,000	Has a recognized form of tenure
9. Settlement Planning and Development	N/A	N/A	250,000-450,000	

(Philippines Shelter Cluster, 2014c)

3. ISSUES AND ANALYSIS 1: SECURITY OF LAND TENURE

This chapter discusses issues related to land tenure which is one of the two primary concerns observed during the operational process of implementing the housing reconstruction project of UN Habitat.

3.1 Paradox in the aid reality: The more vulnerable are least likely to be assisted

It is paradoxical that the more vulnerable people are, the less likely they are to receive housing support because they are often filtered out at the process of beneficiary selection due to the lack of land tenure. It is difficult for the agencies to support informal settlers – those with no legal or formal land titles – because there is no guarantee that the landowner will let them stay after the housing is provided. The effort could come to nothing unless the house provided is independent of the land like some exceptional transferrable houses constructed in the Philippines in response to Typhoon Washi in 2012 (Hirano, 2012). In the context of the Philippines where nearly eighty percent of the population is said to be informal settlers, this creates a situation that the majority of affected population will not be entitled to the assistance that they need (USAID).

Many agencies face similar situations, being unsure of the impact of short-term interventions such as assisting informal settlers on longer-term recovery, many agencies end up leaving them out of disaster recovery (Fan). Sometimes agencies have to make trade-offs between supporting the most vulnerable (those without land and housing assets before and after natural disasters, or those in congested camps, squatting or seeking rental accommodation) and less vulnerable groups (pre- and post- natural disaster access to land and housing assets and providers of various forms of accommodation and tenure) (IASC, 2010). The diagram (Figure 1) presented by Philippines Shelter Cluster illustrates this point by indicating beneficiaries that are owners with formal rights are 'least vulnerable' and 'easiest to assist' while those renters or settlers who share land illegally are 'more vulnerable' and 'least likely to be assisted' (Philippines Shelter Cluster, 2014d). It can be said, though not applicable for all, that there is an incentive for the agencies to select 'easiest to assist' people as their target since it is more likely to achieve a "good result" by completing the work within the proposed timeframe and budget that will satisfy donors and consequently get assurance for future funding.

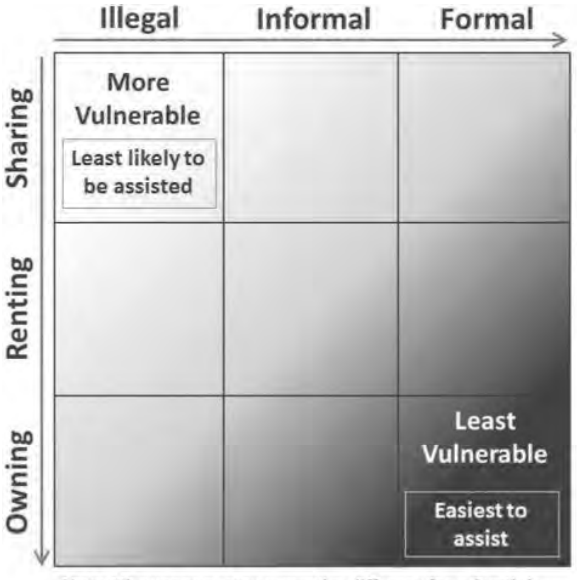

Note: The tenancy status may be different for a family's housing situation and for the land on which they stand.

Figure 1: Pre-Disaster Tenure Context in the Philippines(Philippines Shelter Cluster, 2014d)

3.2 Process of housing reconstruction by UN Habitat: From most vulnerable to less vulnerable

UNH decided to assist inland communities for their project “Post-Yolanda Support for Safer Homes and Settlements” which began in April 2014, half a year after the typhoon, because there were already a number of aid agencies concentrated in the coastal towns that were heavily hit by the storm surge and less aid agencies were present in the inland that was also damaged by strong wind and rain but not getting as much attention as coastal areas. The project had a set of criteria for beneficiary selection which included the security of land tenure among other conditions. As explained earlier, these criteria for beneficiary selection screens out the most vulnerable people from getting the assistance they need. Despite the given situation, the project by UNH demonstrated a way of transforming those vulnerable people to become less vulnerable by assisting them to gain formal ownership of the land through a series of community-level involvement.

3.2.1 The People’s Process and idea of Core House

UNH’s working method is called the “People’s Process” which puts people in the center of the process, and not only it provides housing to individual households but also it tries to engage the community as a whole to build back safer. Community participation is a crucial part of the process and would eventually enable members of the community to become less vulnerable by strengthening ties among the community to collectively tackle problems. The UNH’s project includes three main activities that are 1) to provide Core House to approximately 600 households, 2) to provide technical trainings to build safer homes and 3) to improve community infrastructure such as drainage and roads. Core House is a compact house that satisfies minimum needs of a family such as kitchen and toilet and is made to allow for expansion and building additional structures, encouraging the beneficiaries to take an initiative of completing the house as per their needs, promoting empowerment. The degree of ‘completeness’ of Core House however differs depending on who provides them and their philosophy about aids and this will be discussed later.

3.2.2 Collaboration with local organization

In order to involve affected population as a community as their objective stated, UNH collaborated with a national organization called Social Housing Finance Corporation (SHFC) to work closely with the community. SHFC assists informal settlers to gain home ownership by helping them form a Homeowners’ Association (HOA) and get loans to acquire land titles from the landowner (SHFC).

3.3 Problems observed during the assessment and effort for solution

Prior to the disaster, some of the HOAs already had some problems within their community and in the wake of Typhoon Yolanda these came to light. In some cases, the process of the reconstruction project helped solve those issues.

3.3.1 Issues with arrears

One of the common existing problems in a number of HOAs was the problem of arrears that some of the community members were delayed in their monthly payments and as a result, some of them were deprived of the opportunity to apply for shelter assistance, often not given the applications by the community leaders. This was becoming an issue since many of them were in serious need of assistance and it was evident that not giving them shelter assistance would not improve their attitude towards payment in any way. Thus the UNH team has consulted the community leaders, suggesting discussing with those in arrears to come up with a kind of agreement between them so that they can be eligible for shelter assistance in exchange for a promise that they will pay their monthly fees.

3.3.2 Lack of Community Leadership

The issue with arrears brought up another concern that is the power exercised by the community leaders. During the field assessment, some community members came up to the technical assessment team to ask why some of the most needy people in the community were not given the opportunity to apply for the shelter program by UNH. This caught the UNH staff by surprise since the applications should have been distributed equally to all members of the affected population but in fact some community leaders were making judgment as to who is eligible to apply for the UNH's project based on their records of arrears. After conducting thorough assessments and interviews, UNH communicated the message clearly to the community that it will consider all members for its project regardless of their arrear or any other condition that may concern the leaders. Another issue regarding the leadership of the community was a case where a local government official was interfering with the community matter to the point that the official was taking over the role of community leaders by managing the application submission. This was causing a lack of leadership in the community and weakening community ties. The communities with above mentioned existing issues recognized the collective responsibility and the need to cooperate with each other for the sake of mutual benefit, and tackled the issues as a community to be qualified for assistance from UNH, entailing positive outcomes in the end.

4. ISSUES AND ANALYSIS 2: COORDINATION AMONG ACTORS

This chapter discusses the other issue observed during the operation on the ground, dealing with the lack of sufficient coordination among agencies as well as with the government.

4.1 Lack of inter-agency / government coordination

Despite the fact that many national and international organizations and NGOs were actively involved in the housing reconstruction throughout the affected area, there was neither comprehensive system to effectively match agencies with affected communities nor Standard Operating Procedures (SOPs) in place from the local government side to guide agencies in selecting beneficiaries.

During an open forum led by OPARR, which succeeded the coordination function from Philippines Shelter Cluster, a number of concerns were raised among of which are (OPARR, 2014):

- Absence of coordination among NGOs and between LGUs in the local Rehabilitation and Recovery efforts.
- Overlapping of beneficiaries identified for the same service (livelihood, repair of shelter, etc.) by the different agencies including the local government unit.

- Local Government Officials prohibiting its identified beneficiaries in availing of Private Sector PPA.

What happens often in the field is that many agencies come to assist at an emergency phase immediately after the disaster and develop a relationship with the local community or local government and many organizations stay in the same area to continue their activities when the situation shifts from emergency to the subsequent recovery and reconstruction phase. Without any coordination function in place for the procurement of services, it is inevitable that overlapping of beneficiaries or other concerns expressed by OPARR would happen everywhere, due to pure luck or difference in accessibility to information and assistance.

In this absence of coordination, the Philippines Shelter Cluster that was established soon after the typhoon contributed greatly to enhance the quality of overall shelter assistance and its presence proved extremely effective serving the needs of nearly 100 agencies working in affected areas by creating a platform for agencies to interact with each other and exchange information in addition to providing up-to-date information including those from the government. Although all agencies were encouraged to take part in this inter-agency exchange, there was no obligation or penalty for not participating and it was up to the discretion of each agency. According to the interviews author conducted to some government officials and UN coordinators, there were some agencies that conducted their operation, be it construction of houses or distribution of cash, directly to the affected people without consulting or reporting to the local government or Shelter Coordinator. This was conceived as very problematic because 1) the building may not be compliant with the required level of quality to assure safety of the beneficiaries, 2) it can interfere with the activities of other actors including government in negative way and lastly 3) it can confuse the beneficiaries or even cause jealousy among the community members by creating a situation that some receive more or better assistance than others.

4.1.1 Core house: Same idea, different design

A confusion caused by a lack coordination was demonstrated in this case where one community was receiving Core House from two agencies. During the beneficiary selection process by UNH in one of the communities, it turned out that some members of the community have already committed themselves in receiving Core House from a local NGO called Iloilo People’s Habitat based in Iloilo Province. The issue was that both IPH and UNH had the same idea of providing core house in order to promote participation and empowerment, the design was different. The core house by IPH was more minimum compared to that of UNH’s, consisted of four posts and a roof while that of UNH was more complete, only a part of the wall incomplete. IPH has expressed its concern to UNH that UNH should match the design so that there will be no disparity among the people. As long as the design and specification is compliant with the government’s requirement, agencies should be able to provide services that fits their capacity and principle, however it should not create confusion or inequality to the community by their action. This problem could have been avoided if there was a central coordinating body to manage the overall distribution.

5. CONCLUSIONS AND SUGGESTION FOR THE FUTURE

This paper looked at two issues from the UN Habitat's project "Post-Yolanda Support for Safer Homes and Settlements"- how targeting beneficiaries based on their security of land tenure and the lack of sufficient coordination affect the reconstruction process. The lack of security of land tenure was causing the paradox that the more needy, vulnerable people were less likely to be assisted while the efforts of UN Habitat in its attempts to involve the affected populations as a community and empower them was effective in promoting positive change to this existing problem. The lack of sufficient coordination among the actors was causing possible overlaps and confusion while the efforts by the Philippines Shelter Cluster to provide services to fill the gaps and promote inter-agency coordination contributed to improve the quality of response to housing needs.

5.1 Suggestions

It is important to approach the problem both from the policy as well as operational level while understanding the limit of what aid agencies can and cannot do. Some suggestions from the field experiences can be useful to improve the situation.

5.1.1 Community empowerment and Land issue

The land tenure is certainly an issue to be dealt with as a development issue rather than humanitarian and it could involve a high level policy change that requires a long-term, substantial commitment by the government. While such long-term structural reform is indispensable, it should be well acknowledged that empowering the community by bringing an individual issue up to the level of common community issue was effective as demonstrated by UNH's project.

5.1.2 Agencies' role in Collaboration

Regarding the coordination issue, in author's view, what was lacking most was a comprehensive, reliable database of the affected households including basic family information and damage assessment that agencies can use while selecting beneficiaries. As described earlier, there was no system to match the agencies with communities thus each agency had to conduct its own damage assessment in an ad hoc manner which is inefficient and could be unreliable. Damage assessment should be done by the local government for good reasons however there is neither enough manpower nor knowledge / skills to do so rapidly at the time of disaster. Although many aid agencies including UNH focus on providing actual housing, some providing full house others repair kit, if some of the assistance can be used to help the local government in making damage assessment and creating a comprehensive list of affected households to be used by all involved in the housing reconstruction, it could speed up the process of reconstruction greatly.

Humanitarian development gap is a growing concern and humanitarian agencies need to pay attention to the approach in their response to housing needs. A holistic approach is needed with which the actions of all the actors including NGOs, UN organizations and local and national governments are coordinated in order to make sure the assistance is distributed in a systematic and balanced way to help the affected communities regain their livelihood and safe housing as soon as possible.

REFERENCES

Ashmore, J., and Treherne, C. 2013. *Post-disaster shelter: Ten designs*, International Federation of Red Cross and Red Crescent Societies (IFRC), Geneva.

Department of Social Welfare and Development (DSWD), 12 December 2013, *Report No. 121: Effects, services and interventions for victims of Typhoon Yolanda,* Disaster Risk Reduction and Response Operations Office (DRRROO).

Fan, L. *Shelter strategies, humanitarian praxis and critical urban theory in post-crisis reconstruction*, S78.

Hirano, S., 2012, *Learning from urban transitional settlement response in the Philippines housing land and property issues; Reflections from CRS's 2011-2012 Post-Tropical Storm Washi (Sendong) Response in Cagayan de Oro*, Catholic Relief Services, 24.

Inter-Agency Standing Committee (IASC), 2012, *Transformative Agenda: How the system responds to Level 3 (L3) emergencies*. Inter-Agency Standing Committee (IASC), *Key Messages: The IASC Transformative Agenda*.

Inter-Agency Standing Committee (IASC), 2010, *Haiti Shelter Cluster*, 2.

Jha, A. K., Barenstein, J. D., Phelps, P. M., Pittet, D., andSena, S., 2010 *Safer homes, stronger communities; A handbook for reconstructing after natural disasters*, The International Bank for Reconstruction and Development/The World Bank, Washington DC, 59.

Leon, E., Hopley, M., Lolachi, M., D'Urzo, S., and Ashmore, J., 2012. *Shelter projects 2010*, International Federation of Red Cross and Red Crescent Societies (IFRC), United Nations Settlements Programme (UN-HABITAT) and United Nations High Commissioner for Refugees (UNHCR).

Moore, J., 1999, The humanitarian development gap, *International Review of the Red Cross* 81, 103.

NDRRMC (National Disaster Risk Reduction and Management Council), 17 April 2014, *NDRRMC UPDATE - Updates regarding the effects of typhoon "YOLANDA" (HAIYAN).*

Office of Presidential Assistant for Rehabilitation and Recovery (OPARR), 2014, *Meeting Minutes 4 August 2014*.

Shelter Cluster Philippines.2014a, *Regional coverage gap – Emergency shelter and support to self recovery of shelter (09/06/14)*.

Shelter Cluster Philippines, 2014b, *Shelter sector response monitoring; preliminary findings factsheet; Typhoon Haiyan – Philippines,* p.7

Philippines Shelter Cluster, 2014c, *Recovery shelter guidelines- Shelter options*.

Philippines Shelter Cluster, 2014d, *Recovery shelter guidelines draft.*

Social Housing Finance Corporation (SHFC), http://shfcph.com.

Steets, J., 2010. *Cluster approach Evaluation 2 – Synthesis Report, IASC Cluster Approach Evaluation, 2nd Phase*, Global Public Policy Institute (GPPi).

Steets, J., 2011. *Donor strategies for addressing the transition gap and linking humanitarian and development assistance*, Global Public Policy Institute (GPPi), Berlin.

USAID, *USAID Country profile; Property rights and resource governance,* Philippines.

Performance evaluation of truss bridge under seismic loads

Nandar LWIN
Department of Civil Engineering, Mandalay Technological University,
Mandalay, Myanmar
nandarlwin.civil@gmail.com

ABSTRACT

Bridges are very important elements in the development of infrastructures because there are many obstructions in Myanmar. Among the various types of bridges, truss bridge is a commonly used as the case of easy construction, assemblage and erection panelized steel truss, and available for long span. In this study, the bridge has been built to carry combination of two highways, a railway traffic and a sideway each. Seismic demand for proposed model is determined by Time History Analysis (THA). Maximum deformation in longitudinal direction is 1.022ft at joint 462 to opposite direction, which is occurred at 2.8 seconds in 20 second duration earthquake. Self mass of this bridge model is 666.72Kip-s^2/ft and its self weight is 21451Kip. Fundamental mode is occurred at 0.576705seconds and fundamental frequency is 2.1421cycle/sec. Maximum deflection of the bridge is 0.483 ft under extremely event limit state I (EE I). The extending of seismic design is determined by performing a comprehensive seismic analysis and computing capacity-demand ratios for the components of proposed bridge. To evaluate the performance level of the proposed bridge, this study is going to emphasize a vital role of Pushover Analysis. The formation of plastic hinges along the entire bridge must be observed according to Plastic Hinge Length (PHL) method under Direct Displacement Based Design (DDBD) approach and performance level of the proposed bridge should be investigated. A collapse fragility curve of this hypothetical bridge model under different earthquakes can also be observed in this study.

Keywords: *capacity-demand ratios, performance level, pushover analysis, plastic hinge length method, collapse fragility curve*

Comparison of estimators of Gumbel Distribution for modeling maximum wind speed data

May Ei Nandar Soe[1] and Daw Aye Aye Thant[2]
[1]PhD candidate, Water Resources Engineering, Civil Engineering Department
Mandalay Technological University, Myanmar
einandarsoe2012@gmail.com
[2]Lecturer, Water Resources Engineering, Civil Engineering Department,
Mandalay Technological University, Myanmar

ABSTRACT

Estimation of maximum wind speed potential at a coastal region is very important while predicting storm surge associated with tropical cyclones to develop hazard maps, vulnerable maps and risk maps for different return periods. Assessment of maximum wind speed in a coastal region can expediently be carried out by probabilistic modeling of historical maximum wind speed data using an appropriate extreme value distribution. This paper illustrates the use of five parameter estimation Methods(Method of Moment, Probability Weighted Moment, Method of Least Square, Order Statistic Approach and Maximum Likelihood Method) of Gumbel distribution for modeling maximum wind speed data which caused storm surge propagation recorded at Rakhine coastal region. Goodness-of-Fit (GOF) tests involving Anderson-Darling (AD) and Kolmogorov-Smirnov (KS) and, diagnostic test using Root Mean Square Error (RMSE) are adopted for selection of suitable method for estimators of Gumbel distribution for modeling Maximum Wind Speed. The study shows that Method of Moment is better suited for estimation of maximum wind speed for the region under study. A comparative study of maximum wind speed of tropical cyclone for different period using five methods of Gumbel distribution is carried out and results are presented. .

Keywords: Maximum Wind Speed Estimators of Gumbel distribution, Anderson-Darling, Kolmogorov-Smirnov, Root Mean Square Error, Rakhine Coastal Region

1. INTRODUCTION

Maximum Wind Speeds, and their static and dynamic effects, need to be taken into account while considering cyclone and storm surge prediction. If the wind speed is maximal, the effect of wind on the landfall area can be critical. High winds usually cause damage to structures, vegetations, human's live and properties. Maximum wind speed estimates likely to occur for different return periods are very often important inputs for design purposes. These extreme events are also essential in the post commissioning stage, wherein the assessment of failure of structures and place and adequacy of cyclone shelters, heights and intrusion distances of storm surge need to be carried out. Most of research studies have shown that maximum wind speed of a storm is needed for designing cyclone shelters and predicting storm surge because of relation to wind speed and pressure deficiency and storm surge.

A theoretical analysis of extreme hydrological phenomena has led researchers to identify Gumbel distribution as a standard distribution for frequency analysis of recorded meteorological data and hence used in the present study. Standard analytical procedures such as Method of Moment (MOM), Maximum Likelihood Method (MLM), Method of Least Square (MLS), Order Statistics Approach (OSA) and Probability Weighted Moment (PWM) are commonly available for determination of parameters of Gumbel distribution. Number of studies has been carried out by different researchers on analyzing the characteristics of the parameter estimation methods of Gumbel distribution. Research reports indicated that MOM is a natural and relatively easy parameter estimation method. MLM is considered the most efficient method, since it provides the smallest sampling variance of estimated parameters and hence of the estimated quintiles compared to other methods. But, the method has disadvantage of frequently giving biased estimates and often failed to given the desired accuracy in estimating extremes from hydrological data.

PWM and MLS are much less complicated, and the computations are simpler. Parameter estimates from small samples using PWM and MLS are sometime more accurate than the MLM estimates for Gumbel distribution. On the other hand, OSA estimators are unbiased and having minimum variance. Since there is no general agreement in applying particular method for a region because of the characteristics of the parameters, an attempt is made to apply all five methods of Gumbel distribution for modeling MWSD of tropical cyclones recorded at Rakhine Coastal Region. GoF tests involving AD and KS are employed for checking the adequacy of fitting of the method to the recorded data. Diagnostic test involving RMSE is used for selection of a suitable method of Gumbel distribution for modeling MWSD for the region under study. In this paper, the Mean + SE values given by the suitable method of Gumbel distribution (using Goodness-of-Fit and diagnostics tests) are chosen to arrive at maximum values for the region under study. The methodology adopted in estimation of maximum wind speed using Gumbel distribution is described in ensuing section.

2. METHODOLOGY

To compute the estimators of Gumble Distribution, the following function is adopted.

2.1 Probabilistic Distribution

The Probability Density Function [PDF; f (W)] and Cumulative Distribution Function [CDF; F (W)] of Gumbel distribution is given by:

$$f(W)=\frac{e^{-(W_i-\alpha)/\beta}e^{-e^{-(W_i-\alpha)/\beta}}}{\beta} \tag{1}$$

$$F(W)=e^{-e^{(W_i-\alpha)/\beta}}, W_i, \beta>0 \tag{2}$$

Where α and β are location and scale parameters of the distribution. The parameters are computed by different methods and further used to estimate extreme wind speed (W_T) for different return periods from

$$W_T = \alpha + Y_T\beta \qquad (3)$$

The Lower and Upper Confidence Limits (LCL and UCL) of the estimated wind speeds at 95% level are computed from LCL=W_T- 1.96(SE) and UCL=W_T +1.96(SE.)
Where Y_T is the reduced variate

$$Y_T = -\mathrm{Ln}(-\mathrm{Ln}(1-(1/T))) \qquad (4)$$

and SE is the standard error.

2.2 Methods for Estimation of Parameters

In this paper, five parameter estimation methods are adopted to determine the estimators of Gumbel Distribution.

2.2.1 Method of Moment

$$\alpha = \overline{W} - 0.5772157\beta \qquad (5)$$

$$\beta = \left(\sqrt{6}/_{\pi}\right) S_W \qquad (6)$$

where $\overline{W}$ and S_W are the mean and standard deviation of the recorded MWSD.

2.2.2 Maximum Likelihood Method

$$\beta = \overline{W} - \left[\sum_{i=1}^{N} W_i \exp(-W_i/\beta) \Big/ \sum_{i=1}^{N} \exp(W_i/\beta)\right] \qquad (7)$$

$$\alpha = -\beta \log\left[\sum_{i=1}^{N} \exp(-W_i/\beta) \Big/ N\right] \qquad (8)$$

2.2.3 Method of Least Square

$$\beta = \left[\left(\sum_{i=1}^{N} W_i\right)^2 - \left(N\sum_{i=1}^{N} W_i^2\right)\right] \Big/ \left[\left(N\sum_{i=1}^{N} W_i\left(\ln(-\ln(P_i))\right)\right) - \left(\sum_{i=1}^{N} W_i\right)\left(\sum_{i=1}^{N} \ln\left(-\ln((P_i))\right)\right)\right]$$

$$\alpha = \overline{W} + \left(\left(\sum_{i=1}^{N} \ln(-\ln(P_i))\right)\beta \Big/ N\right) \qquad (10)$$

where $P_i = (i-0.44) / (N + 0.12)$ and $\ln(-\ln(P_i))$ define the cumulative probability of non-exceedance for each W_i .

2.2.4 Order Statistics Approach

The OSA estimators of Gumbel distribution are given by:

$$\alpha = r^{*}\alpha_{M}^{*} + r^{'}\beta_{M}^{'} \quad \text{and} \quad \beta = r^{*}\beta_{M}^{*} + r^{'}\beta_{M}^{'} \tag{11}$$

where r* and $r^{'}$ are proportionality factors, which can be obtained from the selected valued of k, n, n' using the relations as follows:

$$r^{*}={kn}/{N} \quad \text{and} \quad r'={n'}/{N} \tag{12}$$

Here N is the sample size containing the basic data that are divided into k sub groups of n elements each leaving n' remainders. α_{M}^{*} and β_{M}^{*} are the distribution parameters of the groups, and $\alpha_{M}^{'}$ and $\beta_{M}^{'}$ are the parameters of the remainders, if any. These can be computed from the following equations:

$$\alpha_{M}^{*}=\left({1}/{k}\right)\sum_{i=1}^{n}\alpha_{ni}\,S_{i} \quad ; \; \alpha_{M}^{'} = \sum_{i=1}^{n^{'}}\alpha_{n^{'}i}\,W_{i} \tag{13}$$

where $S_{i}=\sum_{i=1}^{k}W_{ij}\,,\quad j=1,2,3,\ldots\ldots,n$

2.2.5 Probability Weighted Moment

$$\alpha = M_{100} - 0.5772157\beta;\ \beta = (M_{100} - 2M_{101}) / \ln 2 \tag{14}$$

where $M_{100} = \overline{W}$ and $M_{101}=W_{i}(N\text{-}1)/\left(N(N\text{-}1)\right)$

Here 'i' is the rank assigned to each sample arranged ascending order.

2.2.6 Computation of Standard Error

The values of SE of the estimated maximum wind speed by MOM, MLM, MLS and PWM may be computed form Eq. (14) and given by:

$$SE=\left(\beta/\sqrt{N}\right)\left(A+BY_{T+}+CY_{T}^{2}\right)^{0.5} \tag{15}$$

The coefficient used in computation of SE by MOM, MLM, MLS and PWM are given in Table 1. The SE of the estimated maximum wind speed by OSA can be obtained from

$$SE=\left(r^{*}W_{n}+r^{'}W_{n^{'}}\right)^{1/2} \tag{16}$$

where $r^{*} = (1/k)(kn/N)^{2}$ and $r' = (n'/N)^{2}$. W_{n} and $W_{n'}$ are defined by general form as:

$$W_{n}=\left(A_{n}Y_{G}^{2}+B_{n}Y_{G}+C_{n}\right)\beta^{2} \tag{17}$$

The weight α_{ni} and β_{ni} used in determining OSA estimators, and values of A_{n}, B_{n} and C_{n} used in computing the SE for OSA, are given in AERB safety guide.

Table 1: Coefficients used in computation of SE by MOM, MLM MLS and PWM

Parameter Estimation Method	**Coefficient used in computation of SE**		
	A	B	C
MOM and MLS	1.1589	0.1919	1.1000
PWM	1.1128	0.4574	0.8046
MLM	1.1087	0.5140	0.6079

2.3. Goodness-of-Fit Tests

The AD and KS statistics are defined by:

$$AD=(-N)-(1/N)\sum_{i=1}^{N}\left\{(2i-1)\ln\left(Z_{(i)}\right)+(2N+1-2i)\ln\left(1-Z_{(i)}\right)\right\} \tag{18}$$

$$KS=Max_{i=1}^{N}\left(F_e(W_i)-F_D(W_i)\right) \tag{19}$$

Where $Z_{(i)} = F(W_i)$, for i = 1,2,3,…..,N and $W_1 < W_2 < W_3 < W_4 < W_5$……………...$W_N$. Also $F_e(W_i)$ =(i-0.44)/(N+0.12) is the empirical cumulative distribution function CDF of W_i and $F_D(W_i)$ is the computed cumulative distribution function CDF of W_i. If the values of GoF tests statistics given by the method are less than that of theoretical values at the desired significance level, then the method is accepted to be adequate for determination of parameters of Gumbel distribution for modeling MWSD.

2.4 Diagnostic Test

$$RMSE=\left[(1/N)\sum_{i=1}^{N}\left(W_i-W_i^*\right)^2\right]^{1/2} \tag{20}$$

Where W_i and W^*_i are the recorded and estimated wind speed of i^{th} observation. The method providing minimum root mean square error, RMSE, is considered as the most suitable method for estimation of maximum wind speed.

2.5. Model Performance Indicator

The correlation coefficient (CC) measures the linearity of the probability plot. It has a range between -1 and 1. Values near ±1 suggest that the observation could have been drawn from the fitted distribution. The CC is defined mathematically as;

$$CC=\sum_{i=1}^{N}\left(W_i-\overline{W}\right)\left(W^*-\overline{W}^*\right)\Big/\sqrt{\left[\sum_{i=1}^{N}\left(W_i-\overline{W}\right)^2\right]\left[\sum_{i=1}^{N}\left(W^*-\overline{W}^*\right)^2\right]} \tag{21}$$

Where $\overline{W}$ and $\overline{W}^*$ denote the average value of the observations and fitted estimation.

3. RESULT AND DISCUSSION

3.1 Estimation of Maximum Wind Speed

By adopting the methodology described above, a computer program is developed and used to estimate the maximum wind speed for different return period in Rakhine Coastal Region. The program computes the parameters of Gumbel distribution using five methods and statistical indicators such as test statistic for AD and KS, RMSE and coefficient of correlation.

Maximum wind speed data recorded at Rakhine Coastal Region for the period 1967-2010 is used to estimate the extreme wind speed for different return periods adopting five methods of Gumbel distribution. Table 2 gives the maximum wind speed estimates for different return periods together with SE given by five methods of Gumbel distribution.

Table 2: Maximum wind speed for different return periods together with SE given five methods of Gumbel Distribution for Rakhine coastal region

Return Period	**Estimated Maximum Wind Speed with SE(km/h)**									
	MOM		MLM		MLS		OSA		PWM	
	W_T	SE	W_T	SE	W_T	SE	W_T	SE	W_T	SE
2	182.1	12.7	181.8	12.4	183.74	14.3	184.3	15.1	182.4	13.8
5	208.3	18.9	207.9	17.1	213.21	21.2	213.5	21.5	210.9	19.7
10	232.1	25.5	231.6	21.9	239.87	28.7	239.9	28.2	236.6	25.8
20	254.9	32.2	254.3	26.8	265.46	36.2	265.3	35.1	261.3	32.0
50	284.3	41.2	283.6	33.4	298.52	46.2	298.0	44.3	293.3	40.2
100	306.5	48.0	305.7	38.4	323.40	53.9	322.7	51.4	317.3	46.8

3.2 Analysis Based on GoF Tests

GoF tests statistics is computed from Eqns. (18-19) using the estimators of Gumbel distribution and given in Table 3.

Table 3: Computed values of test statistics

Parameter Estimation Method	**Computed values of GoF tests for Rakhine Coastal Region**	
	AD	KS
MOM	0.4156	0.1310
MLM	0.4181	0.1285
MLS	0.3370	0.1207
OSA	0.3436	0.1297
PWM	0.3497	0.1151

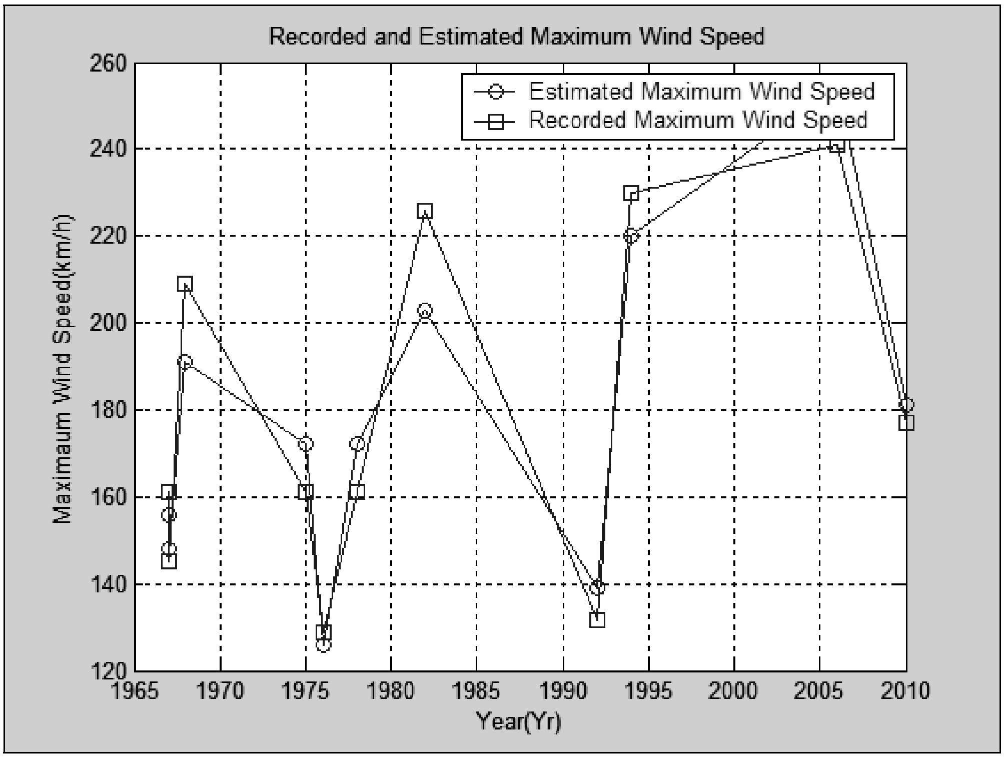

Figure 1: Plot of recorded and estimated maximum wind speed of cyclones given by Gumbel distribution (using MOM) for Rakhine Coastal Region

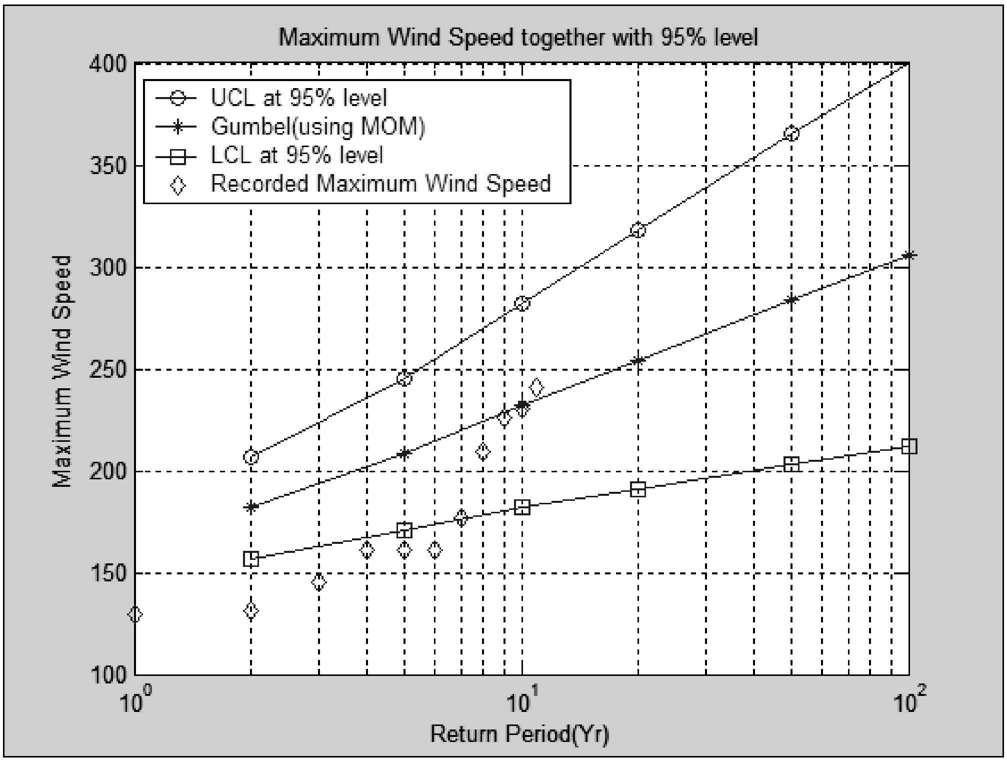

Figure 2: Plot of recorded and estimated maximum wind speed of cyclones for different return periods given by Gumbel distribution (using MOM) together with 95% confidence limit for Rakhine Coastal Region

From Table 3, it may be noted that the computed values of GoF tests statistics given by all five methods of Gumbel distribution are less than the theoretical values ($AD_{0.05}$=0.757; $KS_{0.05,11}$=0.410; $KS_{0.05,13}$=0.377) at five percent significance level, and at this level, all five methods are found to be suitable for determination of estimators of Gumbel distribution for the region under study.

3.3 Analysis Based on Diagnostic Test

The Root Mean Square Error values are computed form Eqs. (20) using the estimators of Gumbel distribution and given in Table 4.

Table 4: RMSE values given by five methods of Gumbel Distribution

Parameter Estimation Method	**RMSE(km/h)**
MOM	11.1796
MLM	11.2290
MLS	11.5542
OSA	11.4688
PWM	11.2968

From Table 4, it may be noted that, by considering the amount of variation in RMSE, MOM is defined as the best suitable method for determination of maximum wind speed for Rakhine Coastal Region since this method gives the least value of RMSE.

3.4 Analysis Based on model performance indicator

Correlation coefficients were computed from Eqns (21) and given in Table 5.

Table 5: Correlation coefficient given by five methods of Gumbel Distribution

Parameter Estimation Method	**Correlation Coefficient**
MOM	0.958140
MLM	0.958125
MLS	0.958128
OSA	0.958127
PWM	0.958128

It may be noted that the correlation coefficient (CC) between recorded and estimated wind speeds by all five methods of Gumbel distribution is almost equal as 0.9581. Figurer (1) shows the recorded and estimated maximum wind speed using Gumbel distribution (using MOM) and the plot of recorded and estimated Maximum Wind Speed of tropical cyclone by Gumbel distribution (using MOM) together with confidence limits at 95% level for different return periods in Rakhine Coastal Region are developed and presented in Figure 2.

4. CONCLUSION

The paper presents comparison of estimators of Gumbel distribution for estimation of Maximum Wind Speeds of Rakhine Coastal Region for different return periods adopting Gumbel distribution using Method of Moment, Maximum Likelihood Method Method of Least Square, Order Statistic Approach and Probability Weighted Moment. GoF tests (AD and KS) results confirm the use of five methods for determination of parameters of Gumbel distribution for modeling of MWS. The diagnostic analysis indicates that MOM is found to be an appropriate method for estimation of Maximum Wind Speeds of cyclones based on the amount of variation on RMSE. The results show that the RMSE on the estimated Maximum Wind Speed given by Gumbel distribution (using MOM) for Rakhine Coastal Region is the least (11.1796). The results also show that the CC values between recorded and estimated maximum wind speeds of five methods are nearly the same (0.958140, 0.958125, 0.958128, 0.958127 and 0.958128). The study suggests that the Mean + SE (where mean denotes the estimated maximum wind speed) values of 194.8 km/h, 227.2 km/h, 257.6km/h, 287.1 km/h, 325.5 km/h and 354.5 km/h related to 2, 5, 10, 20, 50 and 100 return periods may be adopted for prediction purposes of storm surge and risk assessment at Rakhine Coastal Region.

REFERENCES

Arora, K., and Singh, V. P., 1987. On statistical intercomparison of EVI estimators by Monte Carlo simulation, *Advances in Water Resources* 10, 87-107.

Atomic Energy Regulatory Board (AERB), 2008. *Extreme values of meteorological parameters- AERB Safety Guide* No. NF / SG / S-3.

Celik, A. N., 2004. On the distribution parameters used in assessment of the suitability of wind speed probability density functions, *Energy Conversation and Management* 45, 1735-1747.

Gumbel, E. J., 1960. *Statistic of Extremes, 2nd Edition,* Columbia University Press, New York, USA.

India Meteorological Department (IMD), 2010. *Report on availability of meteorological data*, India.

International Atomic Energy Agency (IAEA), 2003. *Meteorological events in site evaluation for nuclear power plants- IAEA Safety Guide No.Ns-G-3.4,* International Atomic Energy Agency, Vienna.

Lieblein, J., 1947. *Note on simplified estimates for Type I extreme value distribution-NBSIR 75-647*, National Bureau of Standards, U.S. Department of Commerce, Washington D.C.

Manik, D., and Datta, S.K., 1998. A comparative study of estimation of extreme value, *Journal of River Behavior & Control* 2, 41-47.

Murty, T. S., Flather, R. A., and Henry, R. F. 1986. *The Storm Surge Problem in the Bay of Bengal* 16, 195-233.

Phein, H. N., 1987. A review of Methods of parameter estimation for the extreme value type-I distribution, *Journal of Hydraulics* 9, 251-268.

Ranyal, J. A., and Salas, J. D. 1986. Estimation procedures for the type-I extreme value distribution, *Journal of Hydrology* 87, 315-336.

Rasmussen, P. F., and Gautam, N., 2003. Alternative PWM-estimators of the Gumbel distribution, *Journal of Hydrology* 280, 265-271.

Vivekanandan, N., Mathew, F. T., and Roy, S. K. 2012. Modeling of wind speed data using probabilistic approach, *Journal of Power and River Valley Development* 62, 42-45.

Zhang, J., 2002. Powerful goodness of fit test based on the likelihood ratio, *Journal of Royal Statistical Society*, 64, 281-294.

Seismic behavior of traditional timber frames with through columns of townhouses in Japan

Hiromi SATO[1], Mikio KOSHIHARA[2] and Tatsuya MIYAKE[3]
[1] Research Associate, Department of Human and Social Systems,
Institute of Industrial Science, the University of Tokyo, Japan
sato310@iis.u-tokyo.ac.jp
[2] Professor, IIS, the University of Tokyo, Japan
[3] President, Nihon System Sekkei Architects & Engineers Co., Japan

ABSTRACT

This paper presents a study of the structural performance of traditional timber townhouses in a historic town in Japan. The aim of this study was to clarify the seismic behavior of traditional timber frame with through columns in townhouses. The target area "Sawara" has many traditional timber townhouses built in from the late of 18th century to the early 20th century and these townhouses have few structural walls in the frontage direction at the first floor. In this study, the microtremor measurement and the three-dimensional analysis about five townhouses in Sawara were performed. As the results, the natural frequency of the first mode is from 2.32 Hz to 3.54 Hz by the microtremor measurement. Moreover the seismic behavior at the severe earthquake based on the Building Cord in Japan are verified and the seismic shear coefficient is clarified from 0.06 to 0.42. Finally, the result of analysis by the observation earthquake wave of the 2011 off the Pacific coast of Tohoku Earthquake is discussed in comparison with the video recording of these townhouses on this earthquake.

Keywords: traditional timber construction, microtremor measurement, seismic analysis, the 2011 off the Pacific coast of Tohoku Earthquake

1. INTRODUCTION

Japan has a long history of earthquakes and timber structures in Japan have suffered great damage caused by strong earthquakes. Old traditional timber structures suffered especially heavy damage. Besides, many of historical towns in japan have many traditional timber buildings that construction method is same in each area. These traditional buildings often have insufficient earthquake-proof performance. However, if the structural evaluation is suitable for the characteristics of their construction, the technique of earthquake-proofing suitable for those buildings can be examined. Therefor it is important to clarify a suitable evaluation method in each historical area.

In the previous study about the traditional timber frame with through columns in Japan, static tests and seismic analysis of the frame with through columns were performed and verified the relationship of wall quantity at the 2nd floor (H. Sato and M. Koshihara, 2010, H. Sato, M. Koshihara and T. Miyake, 2012, 2013 and 2014).

2. OBJECT TOWNHOUSES

2.1 Sawara district and the target townhouses

The research area of the present study is the Sawara district of Chiba Prefecture, which is located near Tokyo. The Sawara district is a historical town arranged on the riverside and contains traditional timber townhouse and storehouse with thick walls. They are built in from the late of 18th century to the early 20th century (The Sawara City, 2004). In townhouses in this area, the frontage direction of the first floor has few walls and the frames which consist of through columns. In this study, five townhouses faced on the main street were targeted (Figure 1 and 2).

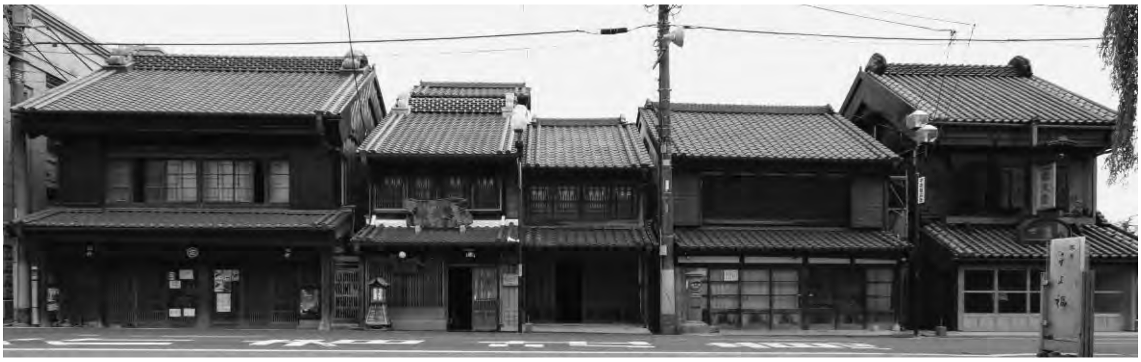

Figure 1: Facade of the target townhouses

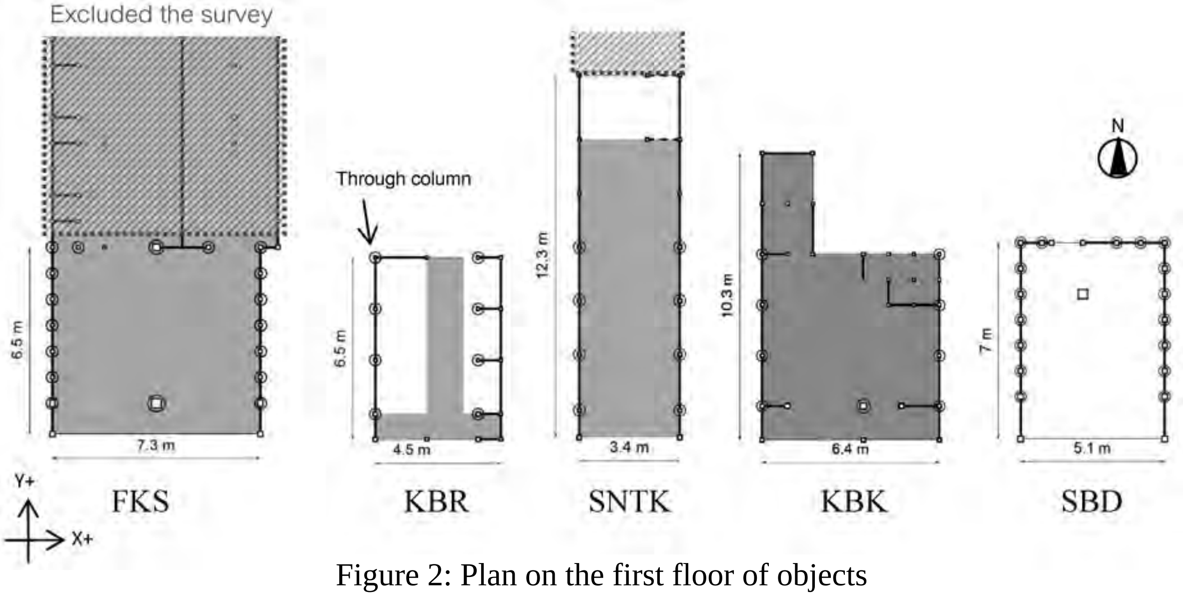

Figure 2: Plan on the first floor of objects

2.2 Previous earthquake damage

On 11 March, 2011, timber structures suffered a great deal of damage due to the 2011 off the Pacific coast of Tohoku Earthquake. This earthquake destroyed or severely damaged 289 houses in the Katori city including the Sawara district. In the Sawara district, many falls of roofing tiles, collapse of mud walls, and foundation damage were observed. The five object townhouses did not occur heavy damage, however the townhouse FKS, KBR and SBD were observed the falls of roofing because they have the very heavy roof thatched with mud and clay tiles.

2.3 Seismic diagnosis

Seismic diagnosis was performed on target townhouses based on the investigation (The Japan Building Disaster Prevention Association, 2004). The marks of the seismic diagnoses at the first floor varied from 0.03 to 0.20 in the X direction (Table 1). The mark calculated horizontal load-carrying capacity by necessary horizontal load-carrying capacity and if it was less than 1.0, the building have possibility of collapse. The seismic diagnosis on five townhouses indicated ‘high possibility of collapse’ because these townhouses on the X direction of the first floor have few bearing walls.

Table 1: Characteristics of the object townhouses

name		**FKS**	**KBR**	**SNTK**	**KBK**	**SBD**
Construction year		1895	1892	unknown	unknown	1880
Building area (m^2) [Total floor area (m^2)]		47.5 [87.1]	28.7 [51.8]	41.4 [79.7]	49.1 [91.7]	35.5 [63.3]
Number of through columns		18	8	8	9	17
Size of through columns (cm)		12	11.5	12	14.5	16.5
Mark of seismic diagnosis*,**	X	**0.06**	**0.07**	**0.03**	**0.20**	**0.10**
	Y	**0.36**	**0.16**	0.71	**0.40**	**0.51**

* at the first floor

** based on reference [5]; -1.5: Safe, 1.0-1.5: Temporarily Safe, 0.7-1.0: Possibility of Collapse, -0.7: Dangerous (High Possibility of Collapse)

3. VIBRATION CHARACHTERISTICS

In order to clarify and evaluate the fundamental vibration characteristics of the target townhouses, microtremor measurements and forced vibration tests were performed. Seven accelerograms were used in the tests, and they were set at the points indicated in figure 3. The natural frequency of vibration, the damping factor and the vibration mode of the target houses were determined.

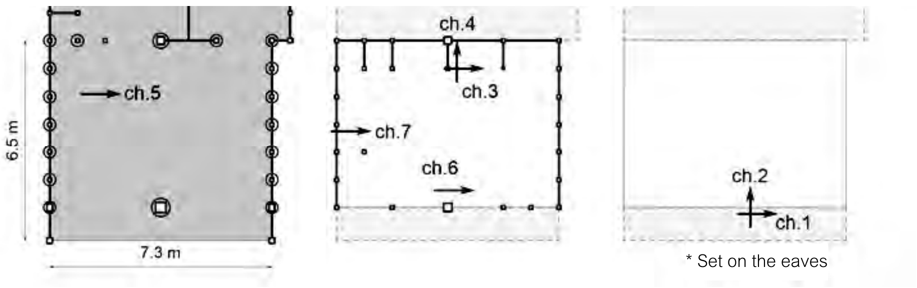

* Set on the eaves

Figure 3: Measurement apparatus (FKS, Measurement plan 2)

3.1 Fundamental vibration characteristics

The fundamental vibration characteristics of the townhouse are shown in table 2 and the transfer functions are shown in figure 4. The natural frequency of vibration of the first mode varied from 2.32 to 7.09 Hz. The natural frequency in the Y direction was approximately twice as large as that in the X direction. The damping factor was calculated from the logarithmic decrement of the free vibration waveform. The damping factor varied from 0.05 to 0.19.

Table 2: Fundamental vibration characteristics

name	direction	FKS	KBR	SNTK	KBK	SBD
Transfer function (Hz)	X	2.32	2.88	2.91	3.54	3.08
	Y	4.08	7.08	5.25	5.42	5.86
Dumping factor	X	0.05	0.05	0.04	0.07	0.06
	Y	0.06	0.05	0.19*	0.10	0.16

*only advisory

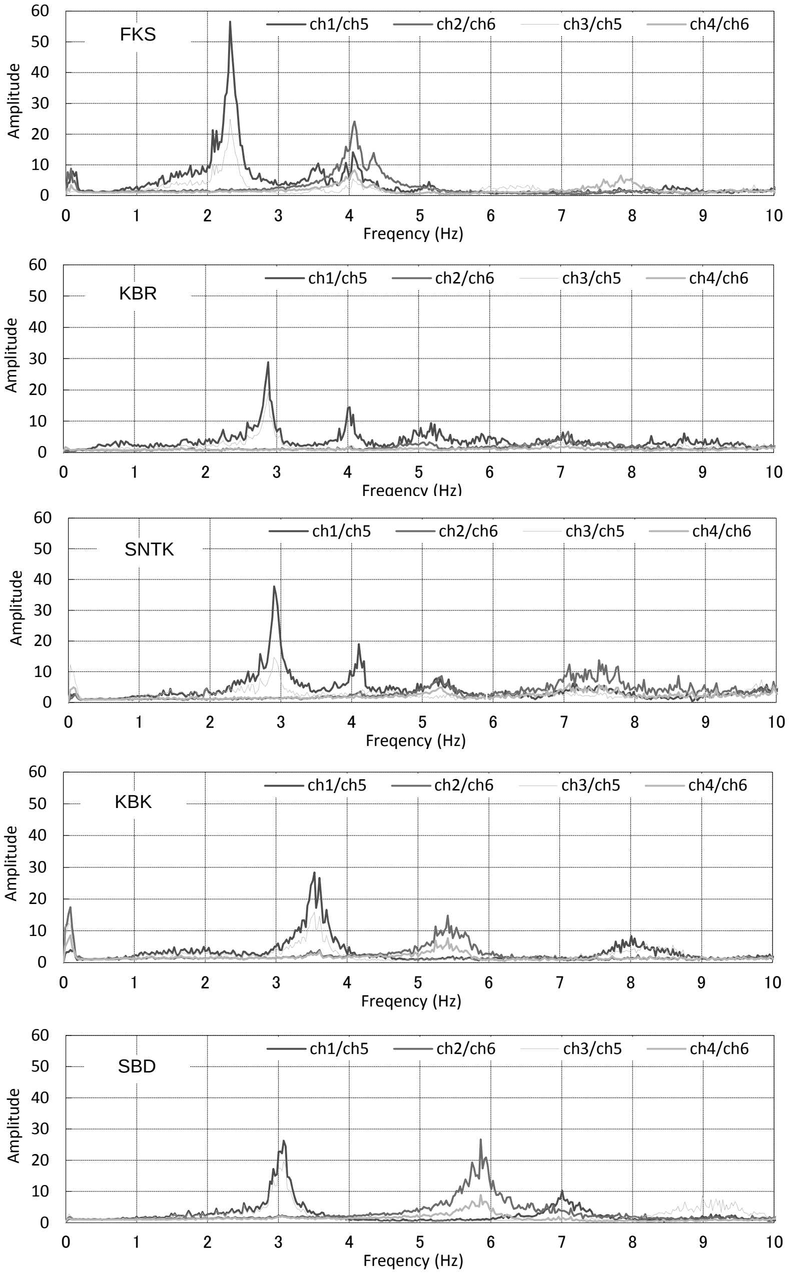

Figure 4: Transfer function

3.2 Vibration mode

The vibration modes of these houses were determined from the phase difference and the amplitude of the transfer function from the microtremor measurements, as shown in figure 5. The first vibration mode in the X direction is almost translational mode, but the displacement of the behind of the building was rather small.

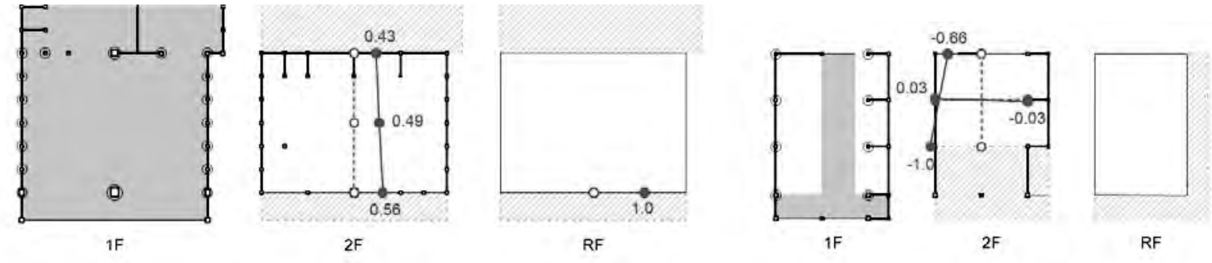

FKS (2.32 Hz) KBR (2.88 Hz)

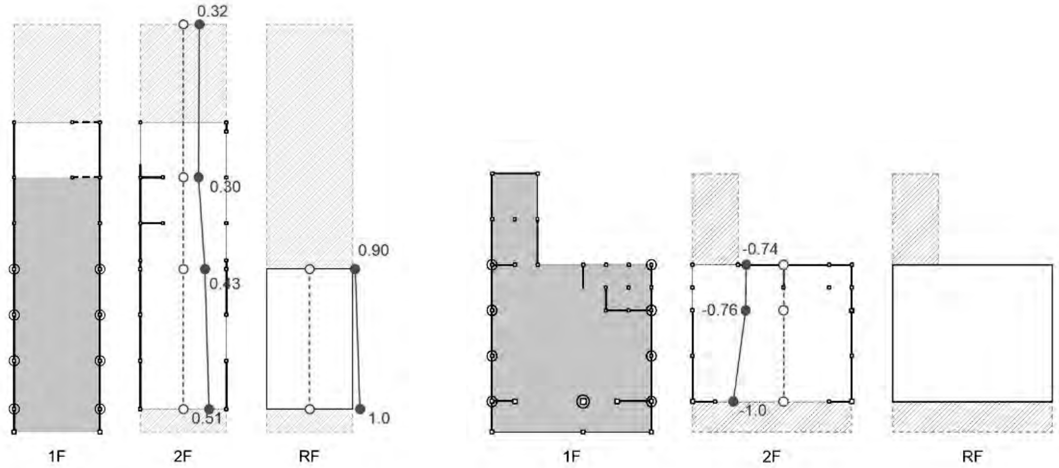

SNTK (2.91 Hz) KBK (3.59 Hz)

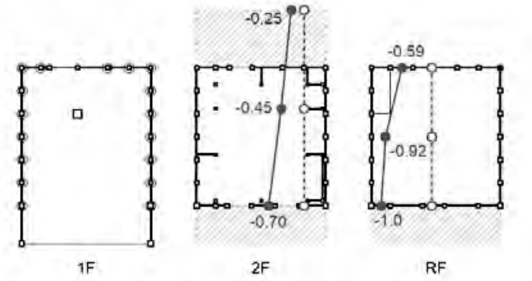

SBD (3.08 Hz)

Figure 5: First vibration modes (X)

3.3 Equivalent stiffness

The relationship between the natural frequency of vibration and the weight of traditional townhouses in this study is compared with the results of previous research (H. Maekawa and N. Kawai, 1993 and 2003, H. Maekawa, N. Kawai and A. UCHIDA, 2000), as shown in figure 6. The natural frequency of the X direction of the townhouses in the Sawara district is consistent with tendency of the previous research and that of the Y direction is higher than the overall trend. The natural frequency of the first mode of the vibration is in inverse proportion to the weight of the building (figure 7). The buildings are modelled as single-mass systems when applying the natural frequency and the weight of the building. The equivalent stiffness values of the X direction of the object townhouses calculated from this modelling varied from 3.79 to 13.30 kN/mm.

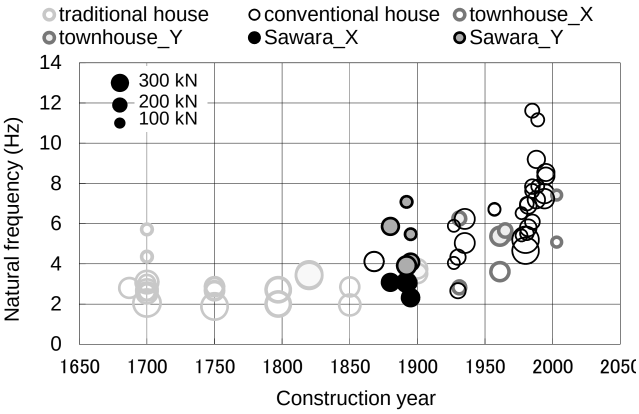

Figure 6: Natural frequency – building year relationship

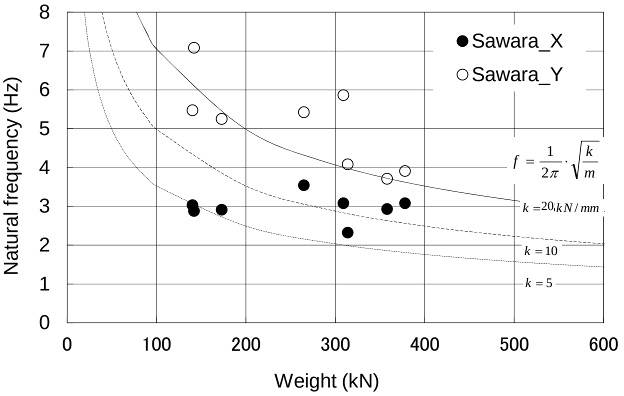

Figure 7: Natural frequency – weight relationship

4. EARTHQUAKE RESPONSE ANALYSIS

The earthquake response analyses were performed on the target townhouses.

4.1 Model of analysis

To evaluate the structural performance in detail, the five townhouses were modelled as three-dimensional frame model, as shown in figure 8. The horizontal load-resisting elements are mud walls and frames which consist of the through column and beam. The skeleton curves of the structural elements were shown in figure 9. The models of hysteresis characteristics were referenced (Architectural Institute of Japan, 2010). The roof truss was not modeled but just considered to the weight.

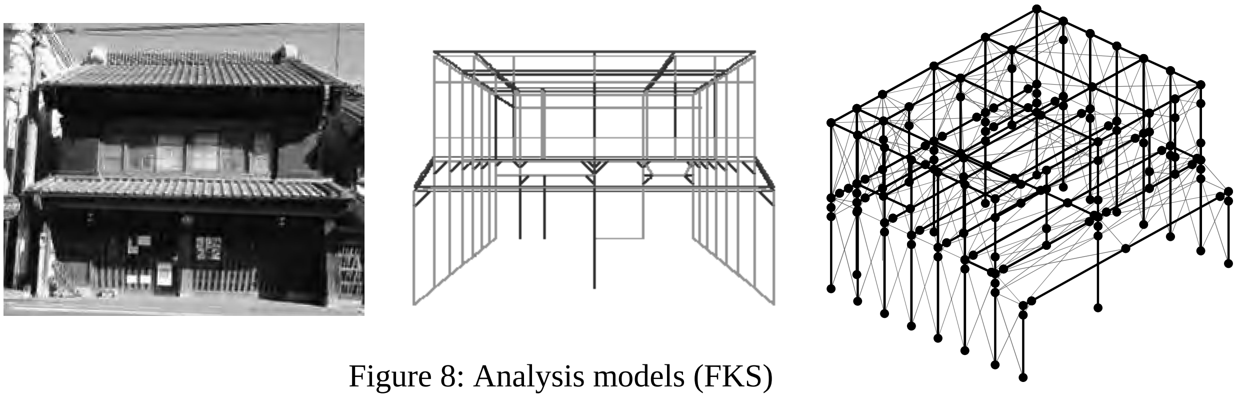

Figure 8: Analysis models (FKS)

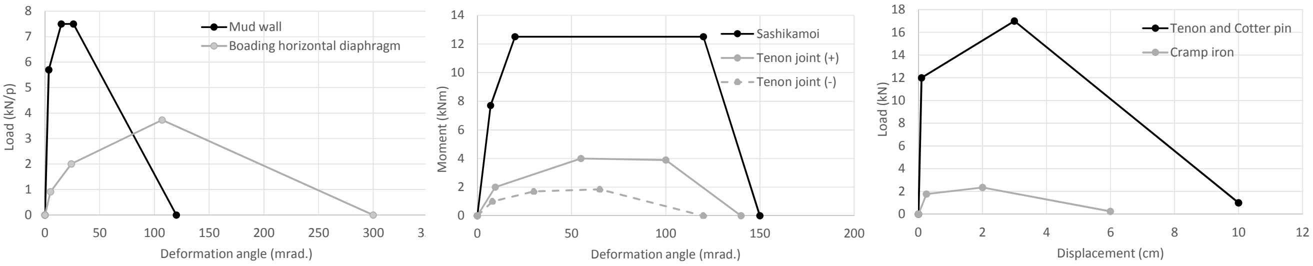

(1) mud wall and floor (2) beam-column joint (3) joint

Figure 9: Skelton curves of structural elements

4.2 Input wave

The input waves of the analysis were three simulated earthquake motions equivalent to design earthquake ground motion based on the Japanese Code and the observed earthquake wave recorded at near to the objects, as shown in figure 10. The simulated waves were modulate to the standard level using coefficient 0.85 and the input scale was changed to determine the seismic clearance of them.

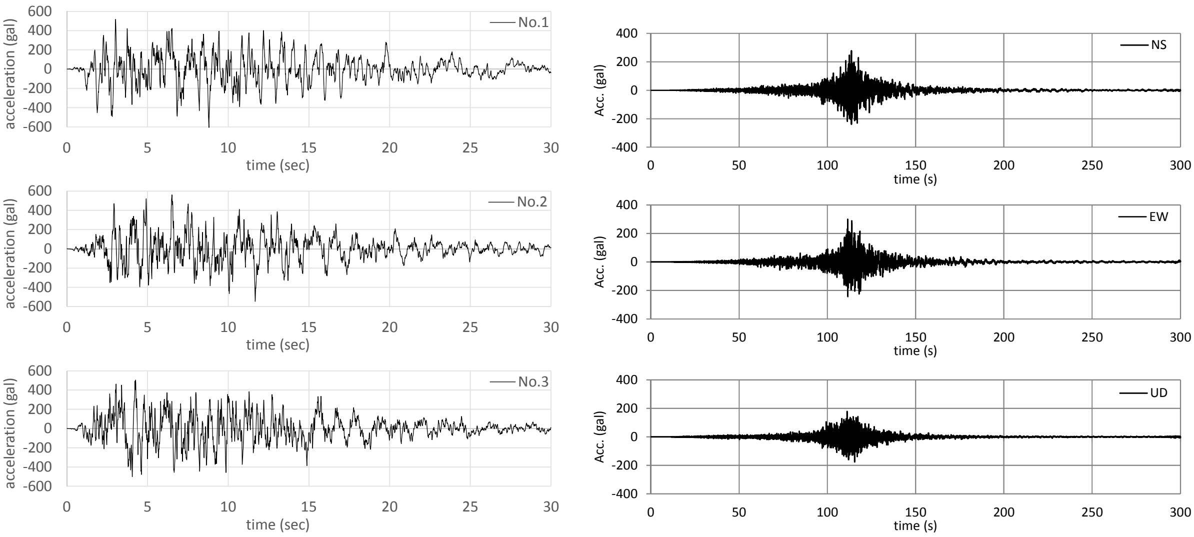

(1) Simulated earthquake wave * (2) Observation earthquake wave **

*based on the Building Standard Law in Japan

**observed at near to objects

Figure 10: Time history waveform of the input waves

4.3 Results of analysis

The earthquake response analysis of the three-dimensional frame model was performed on the five townhouses. The seismic shear coefficient (C_0) by the simulated wave varied from 0.06 to 0.42 (Table 3). Moreover, the marks of seismic diagnosis by the analysis varied from 0.5 to 1.7 and were equal to the safety clearance to large earthquake in Japan Cord. Furthermore the maximum displacement by the observed wave varied from 4.11 to 12.63 cm. The load - displacement relationship was shown in figure 11.

Table 3: Results of the analyses (X)

Input data		Value of	FKS	KBR	SNTK	KBK	SBD
Simulated wave	No.1	Maximum load* (kN)	102.7	19.1	16.2	112.9	106.2
	No.2		92.5	21.5	15.8	111.3	111.0
	No.3		92.8	19.4	16.8	108.1	110.1
		C_0^{**}	0.30	0.18	0.06	0.42	0.35
		Seismic diagnosis***	1.0	0.6	0.5	1.7	1.5
Observed wave		Maximum disp. (cm)	4.11	12.63	12.61	5.49	5.78

*at the first floor, the scale of the input wave is on the safety clearance

**the seismic shear coefficient, the maximum load divide by the weight of the building

***the max acc. of the wave on the safety clearance divide by the max acc. of the basic wave on the Japan Cord

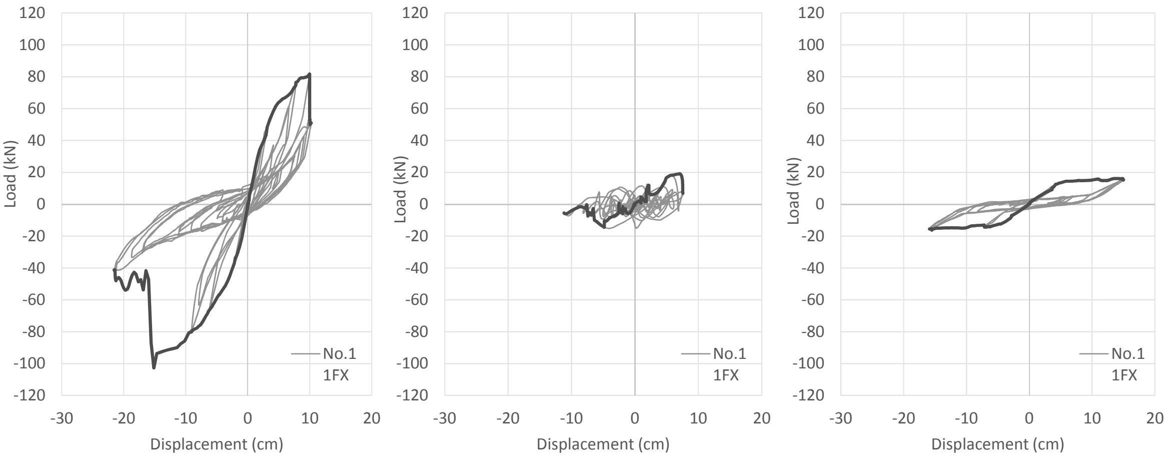

(1) FKS (input scale: 1.0) (2) KBR (input scale: 0.6) (3) SNTK (input scale: 0.5)

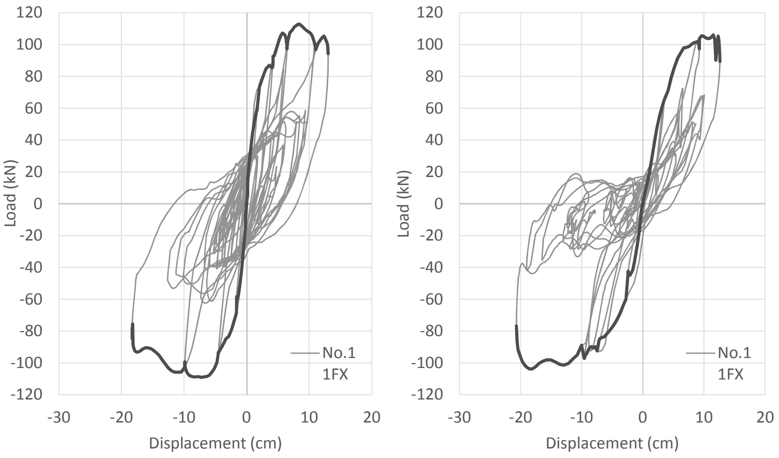

(4) KBK (input scale: 1.7) (5) SBD (input scale: 1.5)

Figure 11: Load - displacement relationship (1F-X, Simulated wave No.1)

4.3.1 Effect of the through column

Results of evaluations are compared and it verifies about the difference in evaluation methods. At first, on the seismic diagnosis of the current standard in Japan, it does not evaluate the structural performance of through column. However, the earthquake response analysis of three-dimensional frame model can evaluate the structural performance including the influence of through column in detail. As a result, it was clarified the structural performance of the traditional townhouse with through column was influenced by the number or size of through columns. The two townhouses (KBR and SNTK) have few small through columns and few mad walls in the first floor, so they don’t resist against the horizontal load. On the other hand, the three townhouses (FKS, KBK and SBD) have structural elements against the horizontal load; they have many or lather large through columns. That is the lager or many through column can become the earthquake resisting elements and their structural performance are not decided by the general seismic diagnosis just only.

Table 4: Seismic Performances on the frontage direction (X)

		FKS	**KBR**	**SNTK**	**KBK**	**SBD**
Through column	Number	18	8	8	9	17
	Size (cm)	12	11.5	12	14.5	16.5
Total weight (kN)		319	114	259	265	309
Equivalent stiffness* (kN/mm)		6.87	3.79	8.78	13.30	11.74
Structural Performance	C_0**	0.30	0.18	0.06	0.42	0.35
	Seismic diagnosis	0.06	0.07	0.03	0.20	0.10
	Seismic diagnosis***	1.0	0.6	0.5	1.7	1.5

*calculated by the natural frequency and total weight; **the seismic shear coefficient, refer to the Table 3, ***refer to the Table 3

4.3.2 Comparison with the Earthquake damage

On 11 March 2011, these five townhouses did not have severe damage. However the townhouse KBR and SNTK observed visible motion by the video recording (Townpromotion sawara, 2013). Moreover the falls of roofing observed at the townhouse KBR, SBD and FKS. In the result of the analysis, the townhouse KBR and SNTK verified large displacement. However, the roof truss and clay tile were not modeled in this study, therefore the comparison about the falls of roofing did not verified.

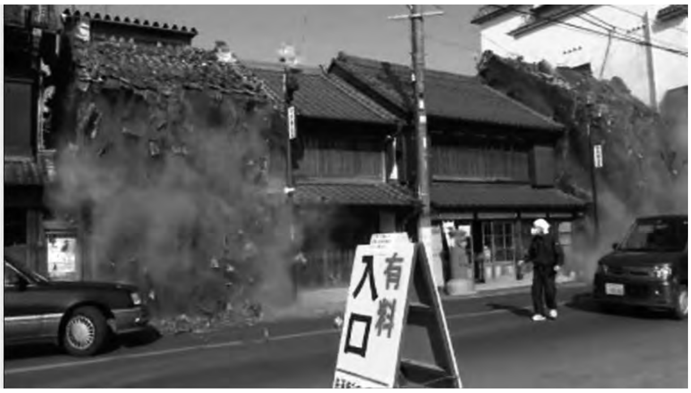

Figure 12: Earthquake damage from the video recording (townpromotion sawara, 2013)

5. CONCLUSION

The structural evaluations performed on the five townhouses with the through columns frame. There are few bearing walls in the X direction at the first floor, therefore the performance is described particularly about the X direction in this conclusion.

1. As a result of the microtremor measurement, the natural frequency were from 2.32 to 3.54 Hz and the equivalent stiffness varied from 3.79 to 13.30 kN/mm.
2. As a result of earthquake response analysis, the seismic shear coefficient (C_0) varied from 0.06 to 0.42.
3. The marks of the seismic diagnosis based on the seismic analysis varied from 0.5 to 1.7. The townhouses which have many or lager through columns were evaluate that they have higher performance than the seismic diagnosis without considering the effect of through column.

4. The analytical model in this study did not modeled with the roof truss and the clay tiles, therefore the falls of roofing regarding the seismic behavior could not verified with this models.

ACKNOWLEDGEMENT

The authors express their appreciation to the owners of the subject houses, Mr. Kawajiri of Nihon System Sekkei Architects & Engineers Co. and to members of the studies group of townhouse of the Sawara district, without whose help these experiment would not have succeeded.

REFERENCES

Architectural Institute of Japan, 2010. *Fundamental theory of timber rngineering,* 314-319.

Maekawa, H., and Kawai, N., 1993. Dynamic characteristics of traditional wooden house: Part 4: Micro tremor tests for traditional wooden house in East Japan. *Summaries of Technical Papers of Annual Meeting Architectural Institute of Japan*, C-1, 1029 - 1030.

Maekawa, H., and Kawai, N., 2003. Dynamic characteristic of traditional wooden houses: Part 8: Micro tremor measurement on Tyugoku and Shikoku District. *Summaries of Technical Papers of Annual Meeting Architectural Institute of Japan*, C-1, 449-450.

Maekawa, H., Kawai, N., and Uchida, A., 2000. Dynamic characteristic of traditional wooden buildings: Part 9: Estimation of load-displacement relationship and natural frequencies on houses. *Summaries of Technical Papers of Annual Meeting Architectural Institute of Japan*, C-1, 339-340.

Sato, H., and Koshihara, M., 2010. Horizontal load capacity of sashikamoi frame with through column. *Summaries of Technical Papers of Annual Meeting Architectural Institute of Japan*, C-1, 569-570.

Sato, H., Koshihara, M., and Miyake, T., 2012. Horizontal load capacity of sashikamoi frame with through column Part 2 Effects of seismic performance of second floor on through column. *Summaries of Technical Papers of Annual Meeting Architectural Institute of Japan*, C-1, 461-462.

Sato, H., Koshihara, M., and Miyake, T., 2013. Seismic performance evaluation of traditional timber townhouse with through column. *Summaries of Technical Papers of Annual Meeting Architectural Institute of Japan*, C-1, 505-506.

Sato, H., Koshihara, M., and Miyake, T., 2013. The structural performance of traditional frames with through columns about townhouses in Japan. *Summaries of 12th International Symposium on New Technologies for Urban Safety of Mega Cities in Asia,* 851-857.

Sato, H., Koshihara, M., and Miyake, T., 2014. Seismic performance evaluation of traditional timber townhouse with through column Part 2 Vibration characteristics. *Summaries of Technical Papers of Annual Meeting Architectural Institute of Japan*, C-1, 245-246.

The Japan Building Disaster Prevention Association, 2004, *Seismic diagnosis and reinforcement of timber house*.

The Sawara City, 2004, *Townscape of the Sawara district*

Townpromotion sawara, 2013, www.youtube.com/watch?v=R78ku1EA5ck

Wind effect on structural responses of long-span suspension bridge

Ni Ni Moe KYAW[1] and Dr. Kyaw Lin HTAT[2]
[1]Ph.D candidate, Department of Civil Engineering,
Mandalay Technological University, Myanmar
summerroseoneone@gmail.com
[2]Associate Professor, Department of Civil Engineering,
Mandalay Technological University, Myanmar

ABSTRACT

Our country, Myanmar sometime suffers the unusual storms, especially in the lower parts of the nation. Thus, a lot of bridges are necessary to design which can resist the unusual winds. So, this paper studied on the structural responses of long-span suspension bridge due to wind effect. This paper also intends to realize the effect of anchorage systems on the responses of long-span suspension bridge based on the performance of wind. In this paper, the proposed bridge is modeled with two anchorage systems. The specifications of the proposed bridge are used American Association of State Highway and Transportation Officials (AASHTO), Bridge Rules of Government of India and Japan Road Association (JRA). The proposed model is analyzed and designed by using Modeling, Integrated Design and Analysis Software (MIDAS). This paper also emphasized the deflections of the proposed bridge, the responses of the moving load analysis and the responses which are focused on the wind speeds of 100 mph and 130 mph. By conducting this research, it is hoped to fulfill the knowledge of the anchorage systems of the suspension bridge, discuss the responses under unusual wind speeds, and offer the concepts of long-span suspension bridge which can provide the future progress of our country.

Keywords: long-span suspension bridge, AASHTO, Bridge Rules, JRA, wind speeds

1. INTRODUCTION

The essential points of evolution era of civil engineering are bridges. Besides, suspension bridges are a viable structural solution to spanning long distances. It is imperative that the cable system proposed would be capable of supporting its own weight in addition to the imposed loads of the superstructure. Very long span suspension bridges are flexible structural systems. The introduction of these cable suspended structures has been profoundly enhanced by the development of new structural materials and computer methods of analysis. Suspension bridges, when well designed and proportioned, are clearly the most aesthetically pleasing of all bridges. The simplicity of the structural arrangement, with the function of each part being clearly expressed, combines with the graceful curve of the main cables, the slender suspended deck and vertical towers, to produce a naturally attractive structure. This natural grace can also make a suspension bridge a suitable choice for relatively short span footbridges, in addition to its more usual function of economically spanning long distances.

2. STRUCTURAL SYSTEM OF SUSPENSION BRIDGE

2.1 Structural components

For the vast majority of suspension bridges, it can be divided into four main components as indicated in (Figure 1):

(1) the deck (or stiffening girder);
(2) the cable system supporting the deck;
(3) the pylons (or towers) supporting the cable system;
(4) the anchor blocks (or anchor piers) supporting the cable system vertically and horizontally, or only vertically, at the extreme ends.

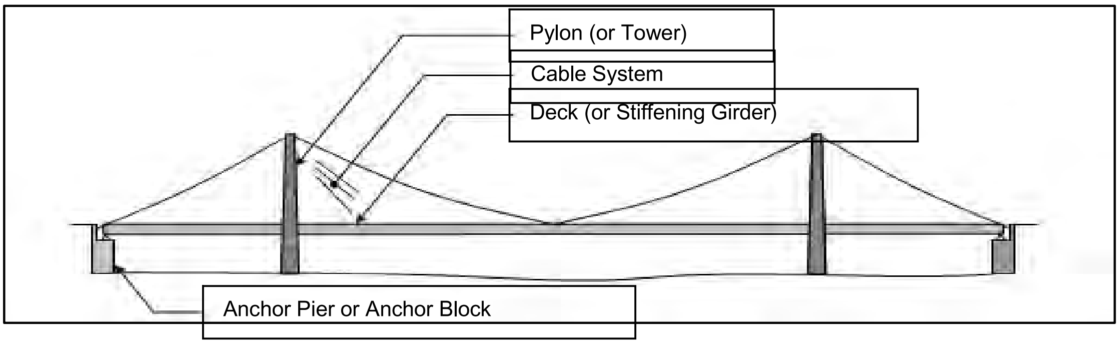

Figure 1: Main components of a suspension bridge

2.1.1 The deck (or stiffening girder)

In modern practice, the stiffening truss will be made as a space truss comprising four chords connected by four diagonal bracings: two vertical and two horizontal. On the other hand, stiffening trusses is made up of:

(1) vertical main trusses along the longitudinal direction,
(2) transverse trusses at the cross-section,
(3) floor beams and stringers and
(4) horizontal lateral bracing at the horizontal direction.

2.1.2 The cable system

The suspension system comprises a parabolic main cable and vertical hanger cables connecting the deck to the main cable. A group of parallel-wire bundled cables support stiffening girders/trusses by hanger ropes and transfer loads to towers. In most cases, the steel wire is of cylindrical shape with a diameter between 3 and 7 mm. Typically, a wire with a diameter of 5–5.5 mm is used in the main cables of suspension bridges. In the transverse direction of the bridge, a number of different solutions for the arrangement of the cable systems can be found such as

(1) One vertical cable plane
(2) Inclined cable planes

(3) Two vertical cable planes
(4) Two vertical cable planes between three separate traffic areas
(5) More than two vertical cable planes

Moreover, the following four types of cable are mainly used in suspension bridges:

(1) Helical bridge strands (spiral strands)
(2) Locked-coil strands
(3) Parallel-wire strands for suspension bridge main cables
(4) Parallel-wire suspension bridge main cables (AS method or PPWS method)

2.1.3 The pylons (or towers)

In principle, the pylon is a tower structure, but in contrast to a free-standing tower, where the moment induced by the horizontal loading (drag) from wind dominates the design, the most decisive load on a regular pylon will be the axial force originating from the vertical components of the forces in the cables attached to the pylon. These intermediate vertical structures support main cables and then transfer bridge loads to foundations. The pylons or towers of a suspension may be made up of concrete, steel or composite material. Towers are classified into rigid, flexible, or locking types. Flexible towers are commonly used in long-span suspension bridges, rigid towers for multi-span suspension bridges to provide enough stiffness to the bridge, and locking towers occasionally for relatively short-span suspension bridges. Towers are classified into portal or diagonally braced types. Moreover, the tower shafts can either be vertical or inclined.

2.1.4 The anchor blocks (or anchor piers)

The anchored system in a suspension bridge can be divided into self anchored and external anchored systems (earth anchored systems). In the self-anchored system, the horizontal component of the cable force in the anchor cable is transferred as compression in the deck, whereas the vertical component is taken by the anchor pier. In the earth anchored systems, both the vertical and the horizontal components of the cable force are transferred to the anchor block. In principle, both earth anchoring and self-anchoring can be applied in suspension bridges. In this study, the proposed suspension bridge uses the cable system of two vertical main cable plans with vertical suspenders which types are parallel wire cable (PPWS) are attached to the deck which is made up of Warren truss and X-bracing. The pylon of the bridge uses steel materials with truss type and self anchored and external anchored types are terminated at the bridge ends.

3. DESIGN APPROACH AND MODELING OF THE PROPOSED BRIDGE

3.1 Design specifications for preliminary configuration of suspension bridge

In deciding the system of the bridge, the following factors must be taken into account.

3.1.1 Span ratio

The side span length should preferably not exceed around 40% of the main span in order to provide an effective restraint to the tower top. However, the side span should not be less than 25% to 30% of the main span length.

3.1.2 Sag

For conceptual designs, the height of suspension bridge towers above the deck depend on the sag-to-span ratio which can vary from about 1:8 to 1:12. A good preliminary value is about 1:10. To this value must be added the structural depth of the deck and the clearance to the foundations to obtain the approximate total tower height.

3.1.3 Truss Depth

Stiffening-truss depths vary from 1/60 to 1/170 the span. According to the specifications described above, in the proposed bridge, side span length is 40% of main span length. Sag-to-span ration of 1:11.4 is used. The minimum depth of the stiffening truss of the proposed bridge models is 1/120 of the span.

3.2 Design loads for proposed bridge

In considering the design loads for the proposed bridge, the structures shall be designed to carry the following loads and forces to mainly focus on the performance of wind:

(1) dead load,
(2) live load,
(3) impact or dynamic effect of the live load,
(4) pretension,
(5) wind loads.

3.2.1 Dead load

In the dead load of structural materials of the proposed bridge models, the weights of the different materials are attained according to AASHTO, and Bridge Rules of Government of India.

For cables, unit weight = 84 kN/m^3
For girder and tower, unit weight = 77.09 kN/m^3
For concrete slab, unit weight = 23.56 kN/m^3
Railway rail = 90 lb/yard (0.44 kN/m)
Guardrail = 200 lb/ft (2.92 kN/m)
Asphalt 2 in thick = 9 x 2 = 18 lb/ft^2 (0.86 kN/m^2).

3.2.2 Live load

In the live load of the proposed bridge models, sidewalk loading at the edges of the bridge is involved.

Sidewalk loading, P = 32.82 lb/ft^2 (1.52 kN/m^2)

Moving loads on the specific lanes are highway loading of HS-25 according to AASHTO and railway loading of Modified Meter Gauge Train according to Bridge Rules of Government of India.

3.2.3 Impact for vehicle loading

The amount of impact allowance or increment for highway loading and coefficient of dynamic augment (CDA) for railway loading are

Impact fraction, I = 0.012
CDA = 0.157.

3.2.4 Pretension

Pretension for hanger and main cable for proposed models are:

Pretension for hanger = 2200 kN
Pretension for main cable = 12880 kN.

3.2.5 Wind Load

Wind load on the proposed bridge with two anchorage systems is considered from the wind speeds of category 2 and 3 of Saffir-Simpson Hurricane Wind Scale in (Table 1).

Table 1: Saffir-Simpson hurricane wind scale

Scale Number (Category)	Sustained Wind (mph)
1	74 - 95
2	96 - 110
3	111 - 130
4	131 - 155
5	> 155

3.3 Modeling

In the modeling of the proposed bridge, the design data used of model 1 for self anchorage system and model 2 for external anchorage system are shown in (Table 2). By using (Table 2), the following are the illustrations of proposed bridge with self anchorage model (Figure 2) and with external anchorage model (Figure 3).

Table 2: Design data used in proposed suspension bridge

Description	Model 1	Model 2
Bridge type	Suspension bridge	Suspension bridge
Total length	2160 m	2160 m
Span arrangement	3-spans arrangement	3-spans arrangement
Main span	1200 m	1200 m
Side span	480 m (each)	480 m (each)
Pylon height	180 m	180 m
Pylon type	Truss type	Truss type
Main cable plane	Two vertical planes	Two vertical planes
Number of hangers in main span	60@20 m	60@20 m
Number of hangers in side span	24@20 m	24@20 m
Main cable diameter	1.5 m	1.5 m
Hanger diameter	0.5 m	0.5 m
Sag to span ratio	1:11.4	1:11.4
Girder type	Warren truss type	Warren truss type

Girder height	10 m	10 m
Girder width	30 m, 4 m for each lane and 1 m for sidewalk	30 m, 4 m for each lane and 1 m for sidewalk
Anchorage Type	Self anchorage	External anchorage
Traffic Lane	HS 25-44, six lanes	HS 25-44, six lanes
	Modified Meter Gauge Train, one lane	Modified Meter Gauge Train, one lane

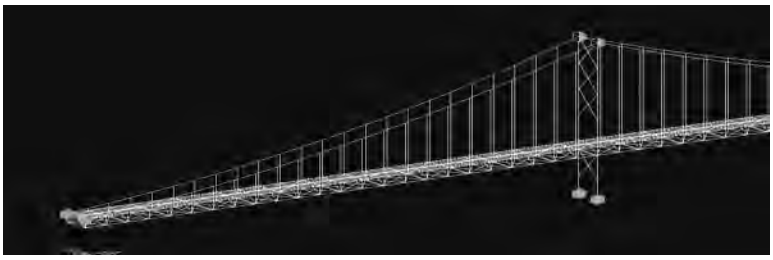

Figure 2: 3D views of support conditions for self anchorage model

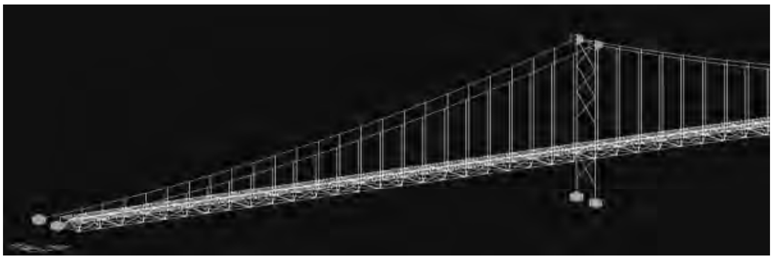

Figure 3: 3D views of support conditions for external anchorage model

4. ANALYSIS RESULTS OF PROPOSED SUSPENSION BRIDGE DUE TO SELF WEIGHT AND MOVING LOAD

4.1 Girder displacements due to self weight for self anchorage model and external anchorage model

The girder displacements due to self weight are illustrated as displacement versus bridge length. Figure 4 illustrates the girder displacement about Z-axis for self anchorage model and Figure 5 illustrates the girder displacement about Z-axis for external anchorage model.

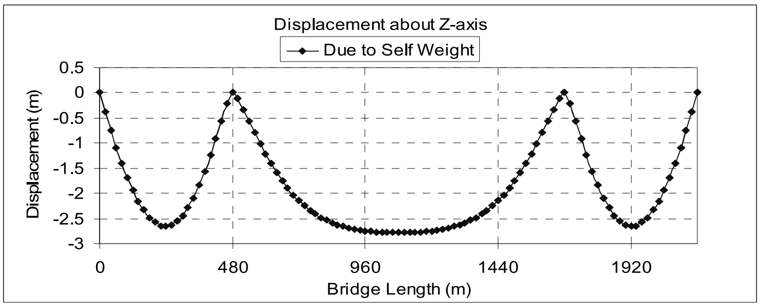

Figure 4: Girder displacement about Z-axis of self anchorage model

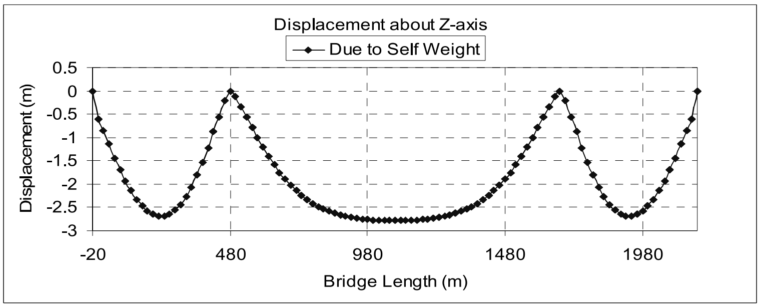

Figure 5: Girder displacement about Z-axis of external anchorage model

4.2 Girder displacements due to moving load analysis for self anchorage model and external anchorage model

Figure 6 shows girder displacement about Z-axis for self anchorage model and Figure 7 shows that for external anchorage model. The displacements also called deflections of the girder for each model are obtained from these figures.

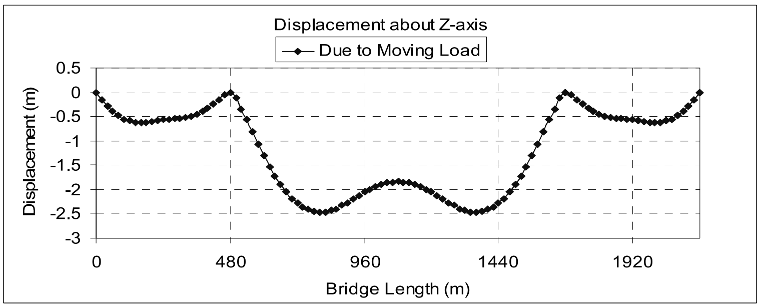

Figure 6: Girder Displacement about Z-axis of self anchorage model

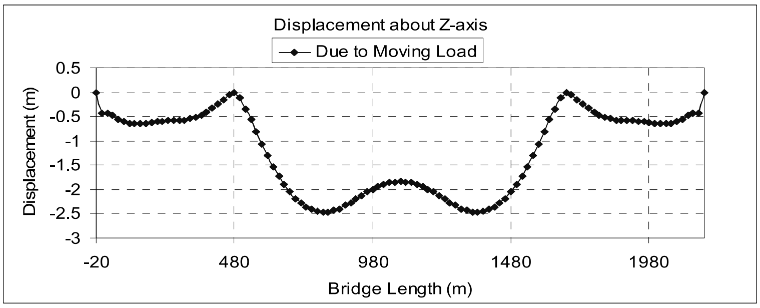

Figure 7: Girder Displacement about Z-axis of external anchorage model

4.3 Checking of Deflection for Moving Load

Allowable deflection of proposed suspension bridge = 1200/350
= 3.43 m
Maximum deflection due to moving load of self anchorage system = 2.464028 m
Maximum deflection due to moving load of external anchorage system = 2.464075 m

Maximum deflections of proposed self and external anchorage bridge modes lies within the allowable limit of 3.43 m. So, it can be said that the proposed self and external anchorage bridges are in the satisfactory condition.

5. ANALYSIS RESULTS OF PROPOSED SUSPENSION BRIDGE DUE TO WIND LOAD

Girder forces due to wind loads are revealed with respective forces which occur along the bridge length in proposed self anchorage bridge models. (Figure 8) reveals responses such as axial force along the bridge length, shear about Y-axis along the bridge length, shear about Z-axis along the bridge length, torsion along the bridge length, moment about Y-axis along the bridge length, moment about Z-axis along the bridge length of self anchorage system due to two different wind speeds is revealed.

Also in proposed external anchorage bridge model, girder forces due to wind loads are revealed with respective forces which occur along the bridge length. (Figure 9) reveals responses such as axial force along the bridge length, shear about Y-axis along the bridge length, shear about Z-axis along the bridge length, torsion along the bridge length, moment about Y-axis along the bridge length, moment about Z-axis along the bridge length of external anchorage system due to two different wind speeds is revealed. These two wind speeds (100 mph and 130 mph) are selected from the category 2 and 3 of Saffir-Simpson hurricane wind scale.

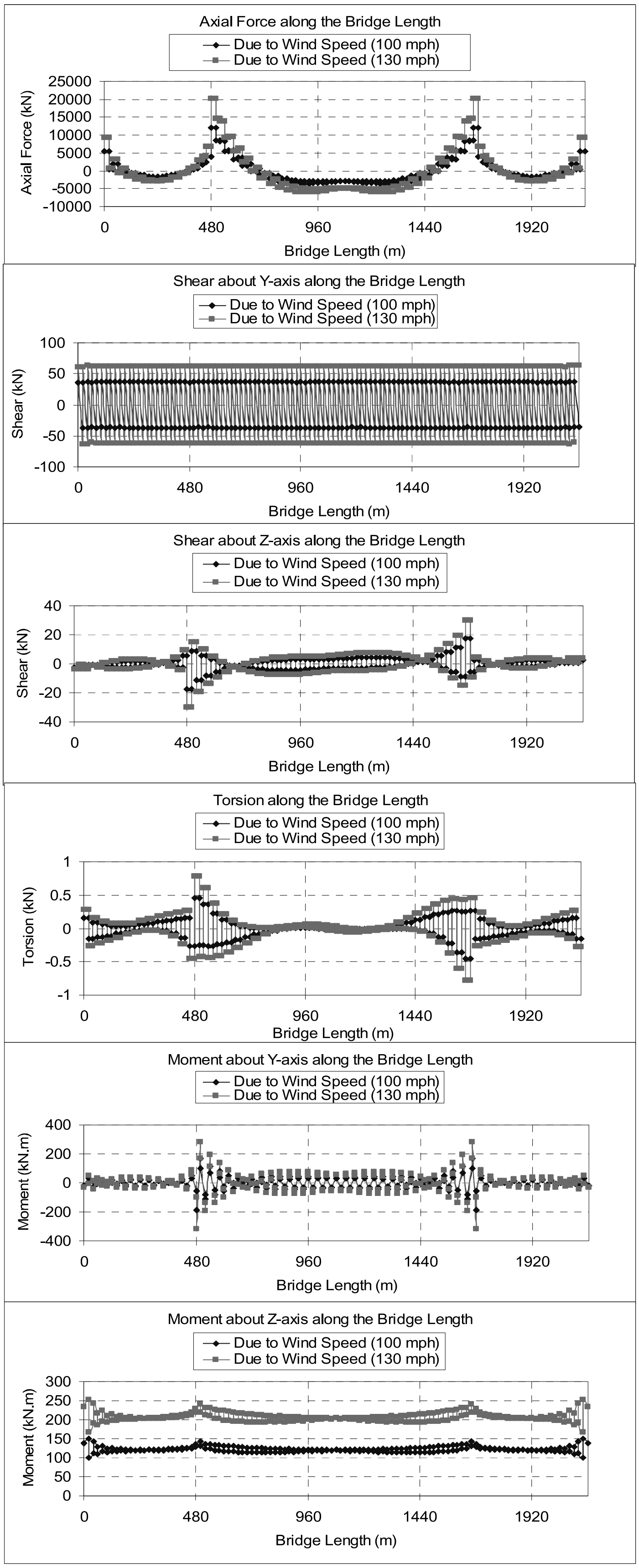

Figure 8: Responses of self anchorage system due to 100 mph and 130 mph

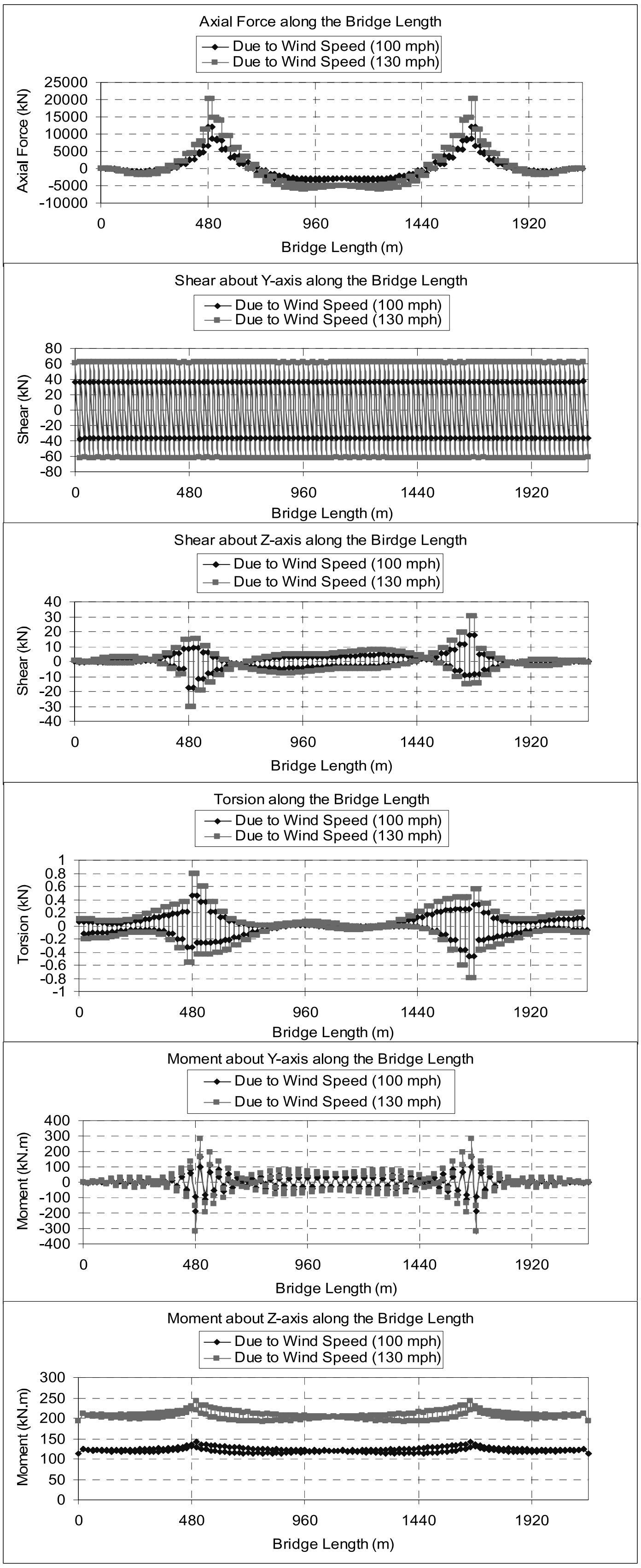

Figure 9: Responses of external anchorage system due to 100 mph and 130 mph

6. DISCUSSIONS AND CONCLUSIONS

Only self weight condition under linear static analysis of proposed models, the value of displacement about Z-axis of self anchorage system is not nearly the same with that of external anchorage system. But, the maximum deflection of self anchorage system of 2.78425 m and the maximum deflection of external anchorage system of 2.78495 are with in the limit of the allowable deflection of the proposed bridge of 3.43 m.

In moving load analysis, as in only self weight condition, the displacement of girder about Z-axis of the external anchorage model is less than those of self anchorage model. In checking of deflection, the maximum deflection of external anchorage model, 2.464075 m and the maximum deflection of self anchorage model, 2.464028 m are less than the allowable deflection, 3.43 m.

Under wind load conditions, the response configurations of the self anchorage model and the external anchorage model are similar. The differences are occurred at axial force of 100 mph (11987.05 kN) and axial force of 130 mph (20274.76 kN) of self anchorage structure which is greater than those of 11986.71 kN and 20274.76 kN of external anchorage structure; shear about Y-axis of 100 mph (37.39 kN) and shear about Y-axis of 130 mph (63.24 kN) of self anchorage structure which are greater than those of 37.15 kN and 62.84 kN of external anchorage structure. Moreover, moment about Y-axis of self anchorage structure (188.89 kN.m at 100 mph and 319.66 kN.m at 130 mph) is greater than that of external anchorage structure (188.79 kN.m at 100 mph and 319.49 kN at 130 mph). All maximum values for 100 mph, 130 mph of moment about Z-axis of self anchorage model (149.75 kN.m, 253.26 kN.m) is greater than that of external anchorage model (142.7 kN.m, 241.36 kN.m).

REFERENCES

American Association of State Highway and Transportation Officials, 2002. *Standard Specifications for Highway Bridges*, 17th Ed.
Buick, D., and Graham, O., 2003. *Steel Designers' Manual*, The Steel Construction Institute, 6th Ed.
Chen, W. F and Duan, L., 2000. *Bridge Engineering Handbook*, CRC Press LLC.
Gimsing, N. J., 2012. *Cable Supported bridges; Concepts and Design*, John Wiley & Sons, 3rd Ed.
Gimsing, N. J., 2000. *Cable Supported bridges; Concepts and Design*, John Wiley & Sons, 2nd Ed.
Government of India, Ministry of Railways (Railway Board), 2008. *Bridge Rules (IN SI UNITS)*, Research Designs and Standard Organisation, Lucknow -226011, 2nd Ed.
Hany, J. F., 1999. Wind and Earthquake Response in Very Long Span Cable-Stayed and Suspension Bridges, *Journal of Civil Engineering*, 55-62.
Japan Road Association., 1987. *Specifications for Highway Bridges*, English Ed.
Ryall, M. J, Parke, G. A. R and Harding, J. E., 2000. *The Manual of Bridge Engineering*, Thomas Telford.

Investigation on the wind effects of long-span cable-stayed bridge with H-shaped tower

Aye Nyein THU[1] and Dr. San Yu KHAING[2]
[1]Ph.D candidate, Department of Civil Engineering,
Mandalay Technological University, Myanmar
rhythmangel11@gmail.com
[2]Associate professor, Department of Civil Engineering,
Mandalay Technological University, Myanmar

ABSTRACT

This paper intends to investigate on the wind effects of long-span cable-stayed bridge with H-shaped tower. The two main purposes of this article are to know the structural behavior of long-span cable-stayed bridge and study the structural responses under wind load condition. Cable-stayed bridges have become very popular over the last 40 years because of their economy, structural efficiency and aesthetics. But long-span bridges can be influenced by various natural hazards. Therefore, it is very important to consider the effects of wind and earthquake on the kinds of long-span bridges. And then, the wind-resistant designs of long-span bridges started around late 1950s and early 1960s. So, 2400 ft main span superstructure of long-span cable-stayed bridge is analyzed and designed by using SAP 2000 version 14 software and specifications of American Association of State Highway and Transportation Officials and Japan Road Association. It is analyzed and designed under linear static condition and moving load conditions. Moreover, it is especially emphasized in the wind effects of long-span cable-stayed bridge with H-shaped tower with the values of wind speed 100 mph and 130 mph. This study provides the results of cable tension forces, bridge forces, truss girder displacement, support reactions and so on.

Keywords: wind effects, long-span cable-stayed bridge, H-shaped tower, SAP 2000 version 14 software, wind speed

1. INTRODUCTION

The cable-stayed bridge has been developing rapidly since World War II, and becomes one of the most competitive types of bridges for main span ranging from 300 to 600 meters. The cable-stayed bridge form has a fine-looking appearance and fits in with most surrounding environments. The structural systems can be varied by changing tower shapes and the cable arrangements. The configurations of cable-stayed bridge are stiffening girder, cable system, towers and foundations. The stiffening girder is supported by straight inclined cables which are anchored at the towers. These pylons are placed on the main pier so that the cable force can be transferred down to the foundation system. Nowadays, cable-stayed bridges are increasingly built because they can span distance far longer than any other kinds of bridge.

2. MAIN COMPONENT PARTS OF THE SUPERSTRUCTURE OF CABLE-STAYED BRIDGE

In the superstructure of cable-stayed bridges, there are five components that must consider. They are cables, cable system, pylon, stiffening girder or truss, cable anchorage and connection.

2.1 Cables

Cables are the most important elements of a cable-stayed bridge. They carry the load of the girder and transfer it to the tower and the back-stay cable anchorage. Cables are tension members. Types of cable may consist of locked coil , helical or spiral strands (prefabricated), bar bundles, parallel wire strand, new parallel wire strand (prefabricated), parallel strand.

2.2 Cable system

2.2.1 Cable arrangement

Three basic arrangements for the longitudinal layout of the stay cables are shown in Figure 1. They are radial system, harp system and fan system.

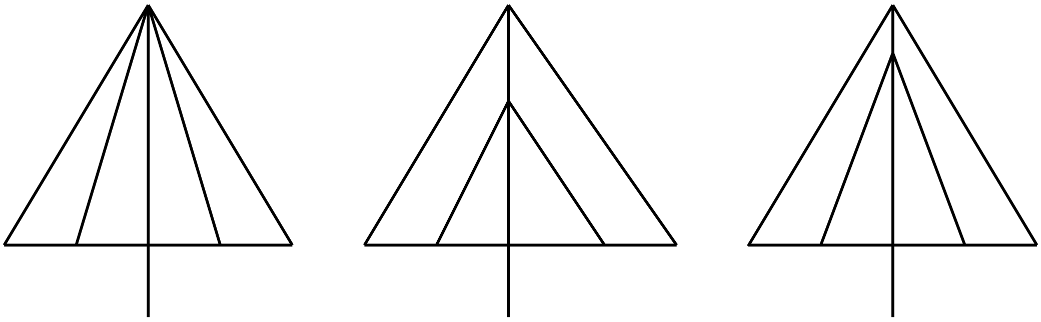

(a) Radial (b) Harp (c) Fan

Figure 1: Configuration of longitudinal cable arrangement

2.2.2 Number of cable planes

The transverse cable layout may be arranged single plane system, double plane system and triple plane system. The three basic transverse cable configurations are shown in Figure 2.

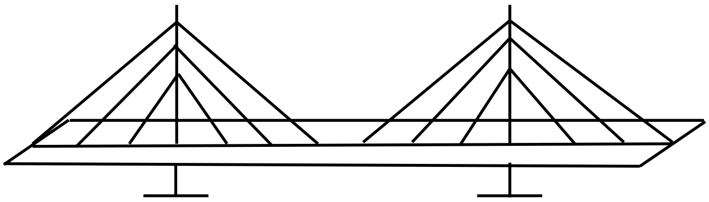

(a) Single plane

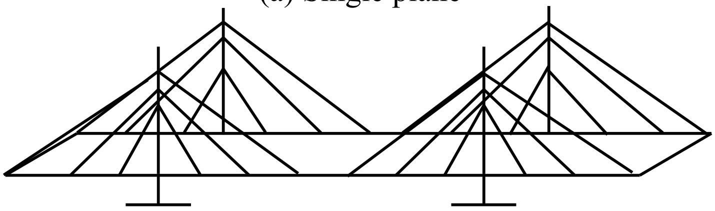

(b) Double plane

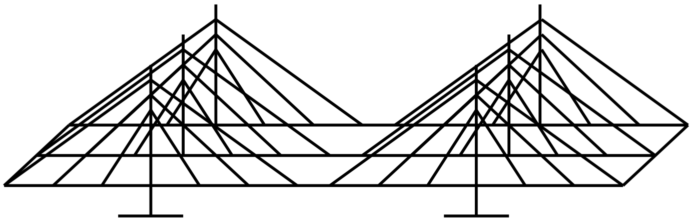

(c) Triple plane

Figure 2: Configuration of transverse cable arrangement

2.2.3 Span arrangement

There are three basic span types. They are two spans; symmetrical or asymmetrical: three spans: and multiple spans.

2.3 Tower or pylon

The towers are the most visible elements of a cable-stayed bridge. Therefore, aesthetic considerations in tower design are very important. The design of the pylon must adapt to the various stay cable layouts. The primary function of the pylon is to transmit the force arising from anchoring the stays and these forces will dominate the design of the pylon. Many varied types of pylon have been developed to support both the vertical and inclined stay layouts. These include H-frame, A-frame and inverted Y-frame pylons.
In this cable-stayed bridge, portal-type (H-shape) pylon is used. The two legs of the pylon are interconnected by a horizontal strut at the top. This type is convenient with a pure fan system. If the pylon legs are leaning in the regions where the cables are to be attached, the horizontal strut should not be positioned at the top. Radial or harp system was not convenient. The H-towers are the most logical shape structurally for a two-plane cable stayed bridges. The tower is steel.

2.4 Stiffening girder or truss

In modern practice, the stiffening truss will be made as a space truss comprising four chords connected by four diagonal bracings, two vertical and two horizontal.

2.4.1 Arrangement of floor beams and stringers

The floor beams at the nodes are supplemented by stringers spaced to give the deck adequate support in the transverse direction. This arrangement was preferred in earlier days when the bridge deck act independently of the truss and might still be a favorable solution if the deck is made as a concrete slab with composite action the stringers, the floor beam, and the top chords of the main trusses.

2.4.2 Bracing system

The bracing systems used in stiffening trusses are generally the same as found in other trusses with constant depth. Three bracing systems for the vertical main trusses are Warren truss, Pure warren truss and Pratt truss.

2.4.3 Horizontal lateral bracing

For the horizontal lateral bracing a symmetrical configuration will generally be applied. Systems of horizontal lateral bracing are X-bracing, diamond bracing and K-bracing.

2.5 Cable anchorage and connection

In cable supported bridges, the structural connections between elements of the girder and the pylon can be designed by principles generally known from other type of structure. The structural connections are those which the element of the cable system is attached to the stiffing girder and the pylons.

2.5.1 Connection between cable and pylon

(1) External anchorages
(2) Internal anchorages
(3) Anchorage by hooking

2.5.2 Connection between cable and girder

When designing a cable-supported bridge, it is very important to follow thoroughly the transmission of forces from the cables into the stiffening girder.

3. STRUCTURAL SPECIFICATIONS OF CABLE-STAYED BRIDGE WITH H-SHAPED TOWER

Structural specifications of proposed bridge with H-shaped tower are described in Table 1. The general arrangement of cable-stayed bridge is shown in Figure 6.

Table 1: Structural specifications of proposed bridge with H-shaped tower

Structural Specifications	**H- Tower Model**
Type of Bridge	Cable-Stayed Bridge
Total length of Bridge	4800 ft
Span arrangement	3-spans arrangement
Main span, Lm	2400 ft
Side span	1200 ft (each)
Height of Pylon	740 ft
Pylon	H-type

Cable system	Fan type
No. of cables (each main span)	40 @ 60 ft
No. of cables (each side span)	20 @ 60 ft
Cable Diameter	6 in
Cable plane	Double plane
Height of truss	30 ft
Traffic	HS 20-44, four lanes
Girder width	56 ft
Type of truss	Warren truss

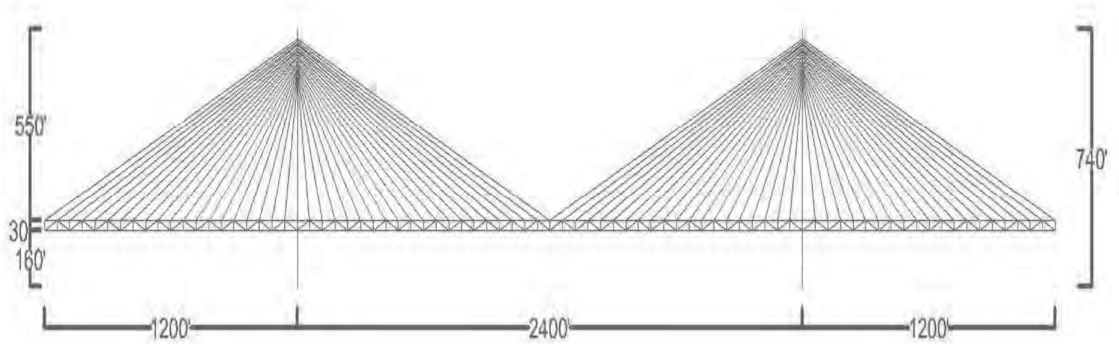

Figure 6: General arrangement of cable-stayed bridge

3.1 Cable tension force

Cable tension force can be calculated from reaction force and the angle between cable and girder. Cable tension forces and cable lengths for H-shaped tower model is described in Table 2.

Table 2: Cable tension forces and cable lengths for H-shaped tower model

Cable No.	**Cable Length (ft)**	**Tension Force (lb)**	**Cable No.**	**Cable Length (ft)**	**Tension Force (lb)**
1	1307.82	13036220	21	410.41	1500788.4
2	1250.52	12587630	22	429.12	2562182.5
3	1193.51	12131075	23	455.109	3454541
4	1136.84	11665958	24	487.213	4251512
5	1080.56	11191598	25	524.309	4984119
6	1024.74	10707218	26	565.417	5669132
7	969.462	10211913	27	609.725	6316906
8	914.814	9704629	28	656.585	6934400
9	860.92	9184118	29	705.49	7526575
10	807.933	8648888	30	756.042	8097123
11	756.042	8097123	31	807.933	8648888
12	705.49	7526575	32	860.92	9184118

13	656.585	6934400	33	914.814	9704629
14	609.725	6316906	34	969.462	10211913
15	565.417	5669132	35	1024.74	10707218
16	524.309	4984119	36	1080.56	11191598
17	487.213	4251512	37	1136.84	11665958
18	455.109	3454541	38	1193.51	12131075
19	429.12	2562182.5	39	1250.52	12587630
20	410.41	1500788.4	40	1307.82	13036236

3.2 Load considerations

The applied loads on superstructure are dead loads, moving load, wind load with values of wind speed 100 mph and 130 mph.

3.2.1 Dead load

The following weights of materials are applied on superstructure of proposed bridge.

Unit weight of steel - 490 lb/ft^3
Unit weight of concrete - 150 lb/ft^3
Unit weight of guardrail - 200 lb/ft
Unit weight of asphalt, 2 in - $9 \times 2 = 18$ lb/in^2

3.2.2 Moving load

HS 20-44 truck is considered for moving load case based on AASHTO specifications.

3.2.3 Wind load

The wind load shall consist of moving uniformity distributed loads applied to the exposed area of the structure. There are five tropical cyclone categories according to Saffir-Simpson Hurricane Wind Scale based on a hurricane’s sustained wind speed. Tropical cyclone categories are described in (Table 3).

Table 3: Tropical cyclone categories

Scale Number Category	Wind Speed (mph)
1	74 - 95
2	96 - 110
3	111 - 130
4	131 - 155
5	> 155

3.3 Analysis results due to own weight

3.3.1 Girder displacement due to own weight

The displacements about X- axis are shown in Figure 7. We can see that the displacement about X- axis is exactly zero at mid span. The displacements about Y-axis are also shown in Figure 8 and the displacements about Y-axis are symmetric.

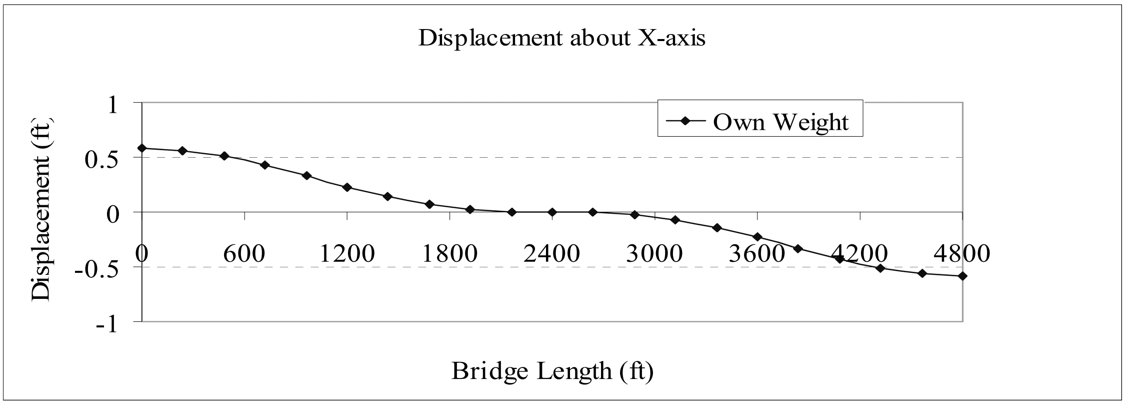

Figure 7: Displacement about X-axis

Figure 8 illustrates displacement about Z-axis due to own weight. The maximum vertical displacement (2.61 ft) occurs at mid span.

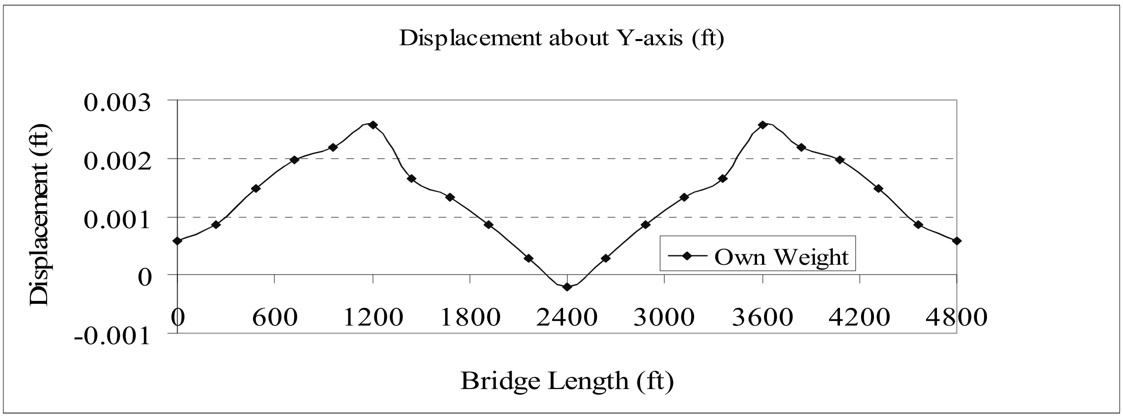

Figure 8: Displacement about Y-axis

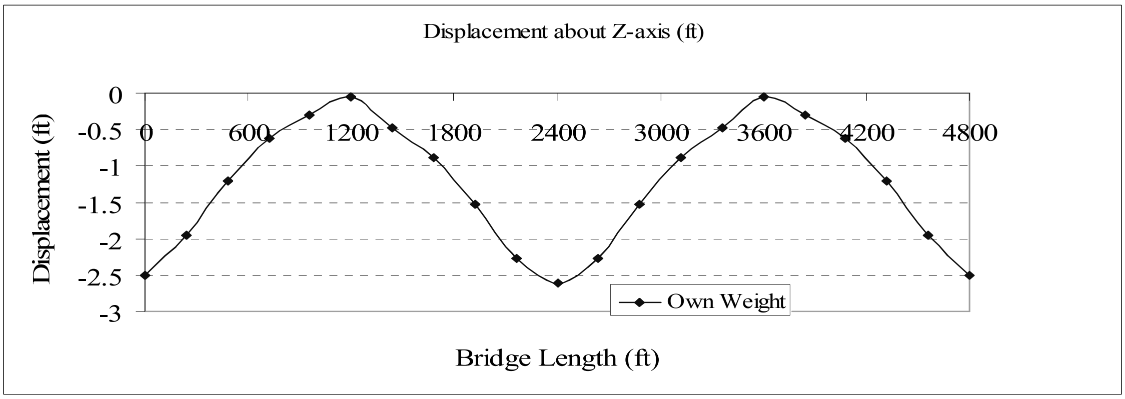

Figure 9: Displacement about Z-axis

3.3.2 Deflection check due to own weight

Allowable deflection, δ_{all} = L/400
= 731.52/400 = 1.83m
= 6 ft
Maximum deflection due to self weight = 2.613 ft < 6 ft
So, it is satisfied.

3.3.3 Deflection check due to moving load

Allowable deflection, δ_{all} = L/400

= 731.52/400 = 1.83m

= 6 ft

Maximum deflection due to self weight = 4.71 ft < 6 ft

Therefore, it is satisfactory condition.

4. ANALYSIS RESULTS DUE TO WIND LOAD

From results due to wind load, the values in maximum wind speed (130 mph) are optimum. The values of axial force for three basic wind speeds such as 100 mph, 130 mph are shown in Figure 10. For these wind speeds, the maximum values of axial forces are found at mid span whereas minimum values occur at tower supports.

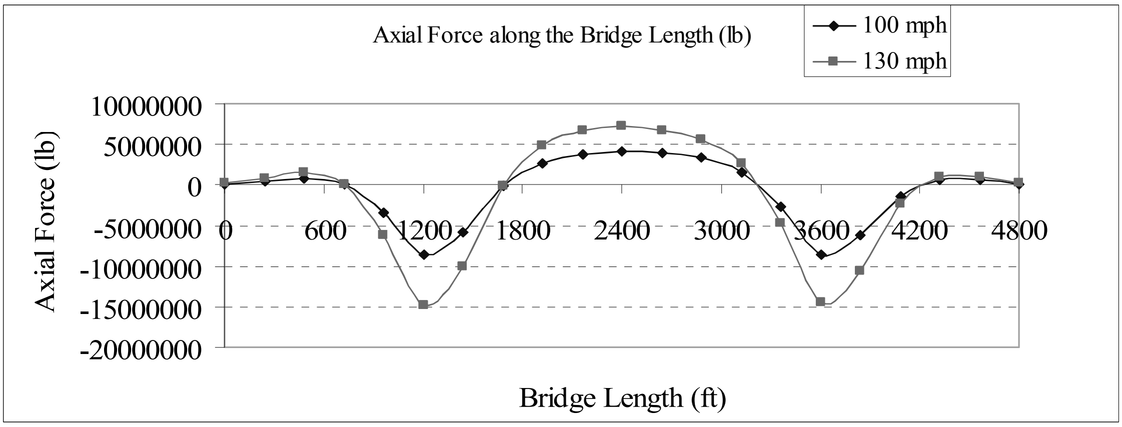

Figure 10: Axial force due to wind load along the bridge length

The maximum values of bridge forces are found at mid span whereas minimum values occur at tower supports in both shape tower models. The maximum values of vertical shear and horizontal shear for wind load condition are shown in Figure 11 and Figure 12.

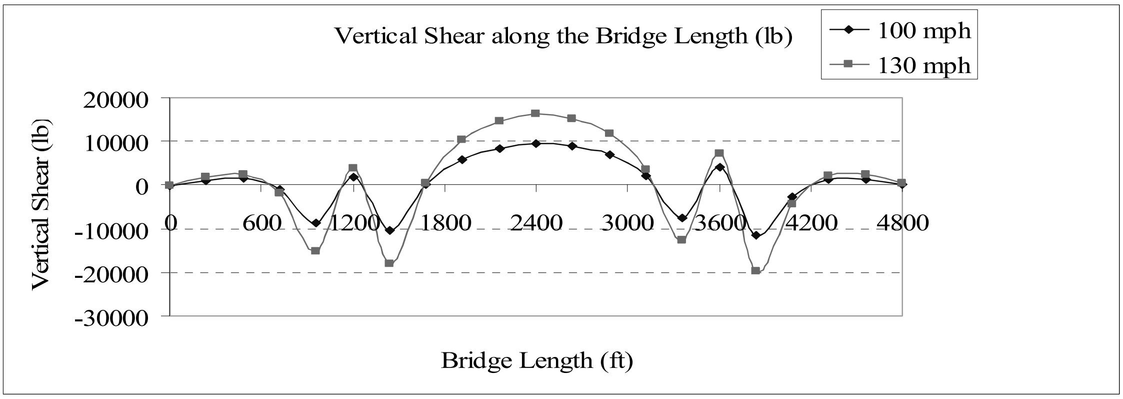

Figure 11: Vertical shear due to wind load along the bridge length

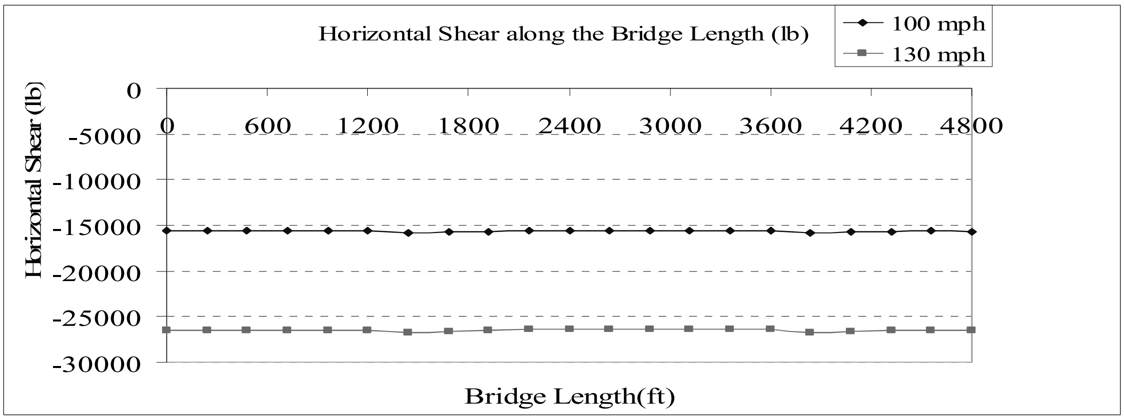

Figure 12: Horizontal shear due to wind load along the bridge length

Figure 13 illustrates the values of torsion for three kinds of wind load condition. The minimum values of torsion are found at tower supports and maximum values occur at mid span.

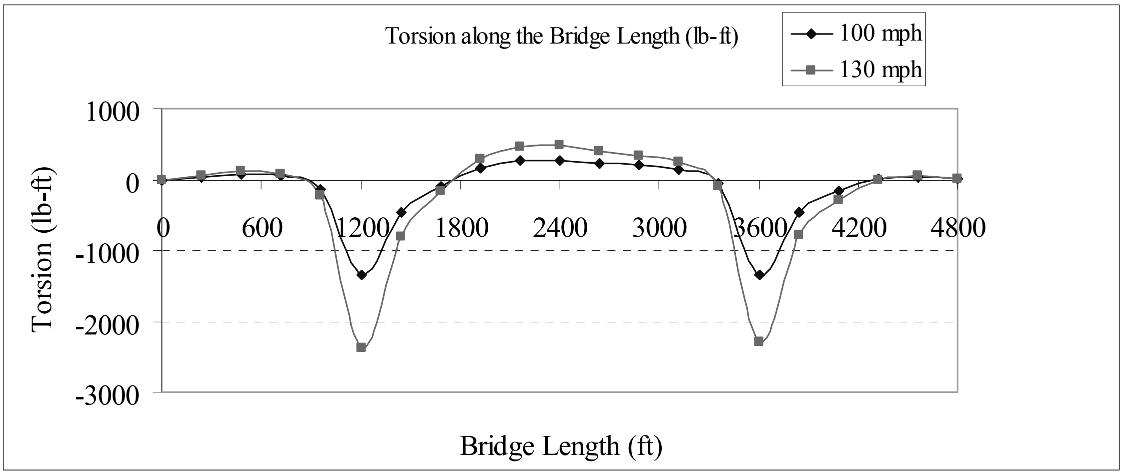

Figure 13: Torsion due to wind load along the bridge length

In addition, maximum values of vertical moment and horizontal moment for three types of wind load conditions are also shown in Figure 14 and Figure 15.

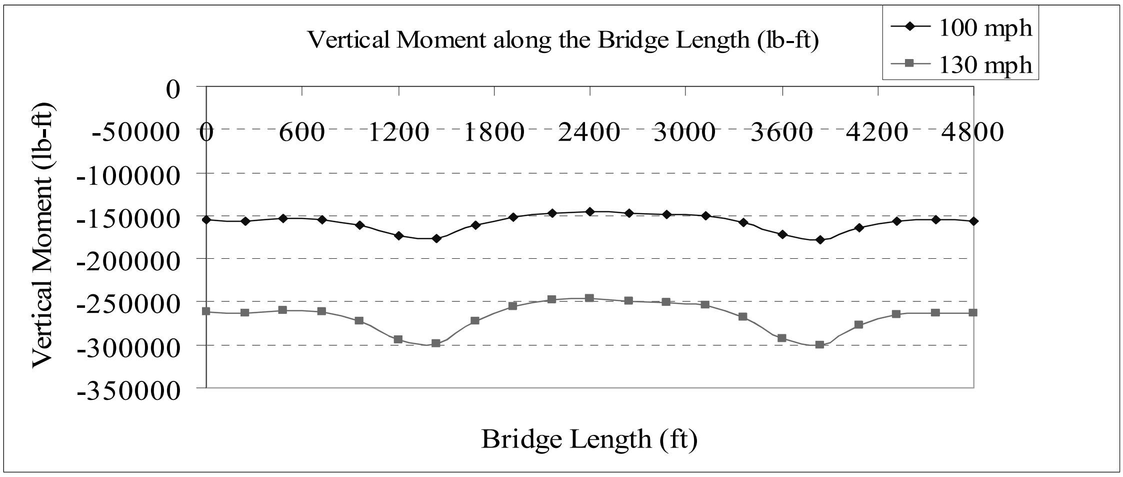

Figure 14: Vertical Moment due to wind load along the bridge length

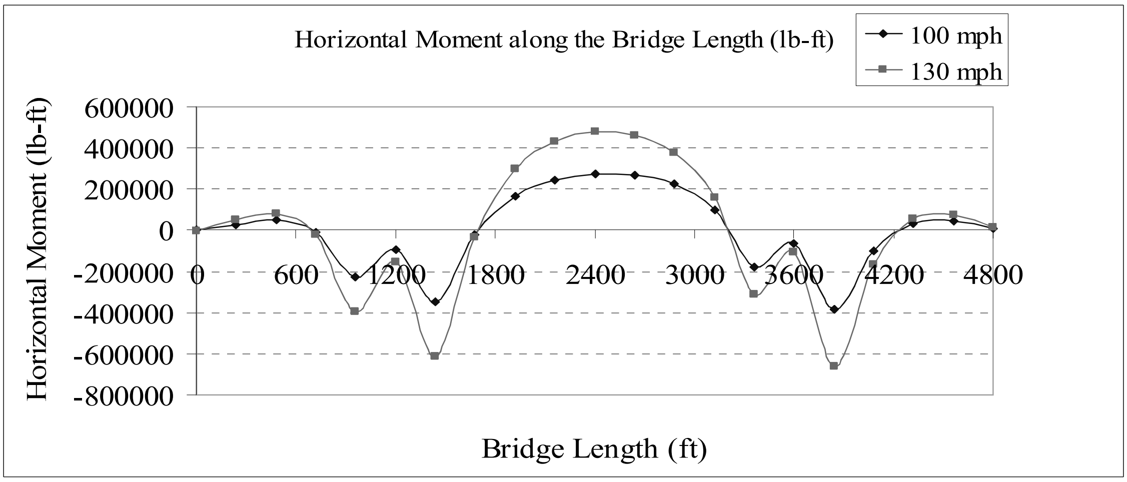

Figure 15: Horizontal Moment due to wind load along the bridge length

5. DISCUSSIONS AND CONCLUSIONS

In this study, the 2400 ft main span cable-stayed bridge is analyzed by using SAP 2000 software. Therefore, this study would give some knowledge of analysis and design of three-span cable-stayed bridge with H –shaped tower and for the way how to use SAP 2000 software. The maximum values of bridge forces are found at mid span whereas minimum values occur at tower supports in both shape tower models. The maximum values of axial force for H –tower model are (4131.47 kip) for 100 mph and (7192.16 kip) for 130 mph. The maximum values of vertical shear, (9.38 kip) for 100 mph, (16.28 kip) for 130 mph can be seen at 2400 ft from bridge start distance or at mid span. The maximum values of horizontal shear, (15.8 kip) for 100 mph, (26.76 kip) for 130 mph can be seen at 1440 ft from bridge start distance. The maximum values of torsion, (274.65 lb) for 100 mph, (480.42 lb) for 130 mph are found at 2400 ft from bridge start distance. The maximum values of vertical moment, (176.26 kip-ft) for 100 mph and (299.47 kip-ft) for 130 mph are found at 2160 ft from bridge start distance. The maximum values of horizontal moment, (275.74 kip-ft) for 100 mph, (480 kip-ft) for 130 mph occur at mid span.

REFERENCES

American Association of State Highway and Transportation Officials., 2002. *Standard Specifications for Highway Bridges*, 17th Ed.

Buick, D and Graham, O., 2003. *Steel Designers' Manual*, The Steel Construction Institute, 6th Ed.

Chen, W. F and Duan, L., 2000. *Bridge Engineering Handbook*, CRC Press LLC.

Gimsing, N. J., 2000. *Cable Supported bridges; Concepts and Design* 2nd Ed, John Wiley & Sons.

Gimsing, N. J., 2012. *Cable Supported bridges; Concepts and Design* 3rd Ed, John Wiley & Sons.

Government of India, Ministry of Railways (Railway Board)., 2008. *Bridge Rules* 2nd Ed *(IN SI UNITS)*, Research Designs and Standard Organisation, Lucknow -226011.

Japan Road Association., 1987. *Specifications for Highway Bridges*, English Ed.

Ryall, M. J, Parke, G. A. R and Harding, J. E., 2000. *The Manual of Bridge Engineering*, Thomas Telford.

Walther, R., 1999. *Cable Stayed Bridges* 2nd Ed, Thomas Telford.

A statistical study for bi-directional seismic interaction effect in isolated bridges

Ji DANG[1], Yuki EBISAWA[2], and Akira IGARASHI[3]
[1] Assistant Professor, Graduate School of Science and Engineering,
Saitama University, Japan
dangji@mail.saitama-u.ac.jp
[2] Graduate Student, Graduate School of Engineering,
Tokyo Institute of Technology, Japan
[3] Professor, Disaster Prevention Research Institute, Kyoto University, Japan

ABSTRACT

The bi-directional nonlinear interaction effect of bridge structures has been omitted in the current seismic design approach. The differences in hysteretic behavior of High Damping Rubber (HDR) bearings and responses of isolated bridges are found to be depending on the bi-directional ground motions' uncertainties. In this study, Incremental Dynamic Analysis (IDA) was conducted for evaluation of the bi-directional earthquake interaction effect of isolated bridges. A recently developed hysteresis model, the Modified Park-Wen (MPW) model, was applied to simulate the restoring force of high damping rubber bearings under bidirectional deformation and a number of earthquake records were used to obtain the uncertainty of phase difference of seismic inputs. The IDA curves and fragility curves obtained from these analyses suggest that the bi-directional earthquake interaction is likely to increase the structural displacement response. Furthermore, the difference between the directions of maximum seismic input and maximum response is found to be the main cause of underestimation in assessment of seismic response of isolated structures using the unidirectional approach.

Keywords: Incremental Dynamic Analysis, bi-directional interaction, phase difference

1. INTRODUCTION

From the 1990s, the use of elastomeric bearings started in highway bridges as replacement of steel roller bearings. In the 1995 Kobe Earthquake, these bridges survived with only relatively minor damage in contrast to severe damage experienced by bridges with conventional steel bearings (Japan Society of Civil Engineering, 1996). Natural Rubber (NR) bearings, Lead Rubber Bearing (LRB) and High Damping Rubber Bearings (HDRBs) have been widely used for seismic isolation practice for highway bridges thereafter. At the time of the Great East Japan Earthquake, although a few cases of fracture of rubber bearing were reported, performance of most of the isolated bridges is mostly adequate as expected (Earthquake Engineering Committee of JSCE, 2011).

The HDRBs appear to be the most important seismic isolation device for highway bridges applied in reconstruction and retrofitting in the foreseeable future, due to the lack of other effective measures. As the preparation for the next major seismic event in Japan that can be disastrous in the near future, performance based seismic design for highway bridges has been continually improved since the 1995 Kobe Earthquake. The nonlinear time history analysis is generally used in practice for bridge design incorporating seismic isolation concept. The bi-linear model and equivalent linearization techniques are used to present the nonlinear character of rubber bearings.

However, the bi-directional nonlinear interaction effect of bridge structures has been neglected in the current seismic design practice. This is because of the lack of reliable models of bi-directional nonlinear interaction effect between structural nonlinear response components. The behavior of bridge columns is assumed based on the loading tests of the structural components under constant vertical force and cyclic uni-directional horizontal loading. The data for nonlinear hysteresis character of elastomeric bearings as well as bridge columns under bi-directional loading have not been available. To avoid the problem, continuous girder bridges with constrained transverse displacement of the elastomeric bearings have been widely employed for the ease and convenience of the design process, and a conservative isolation design method has been used for curved girder bridges.

Recently, the bi-directional interaction effect in the restoring force-displacement hysteretic behavior and seismic response were experimentally studied by conducting both quasi-static loading and pseudo-dynamic loading tests (Iwata, 1998; Murakoshi 2013). Increase of the hysteretic damping of HDRBs and consequent seismic response changes were found in the results of those experimental studies.

Furthermore, these differences in hysteretic response are dependent on the bi-directional loading patterns and input accelerograms. Only very limited cases of seismic input can be tested experimentally. To clarify the seismic response behavior of the isolated bridges, the amplitude and the number of input accelerograms are the important keys to evaluate the measure of statistical correlations between the bi-directional components of the nonlinear seismic response of structures.

In this study, the Incremental Dynamic Analysis (Vamvatsikos and Cornell, 2002) of isolated bridges using a large number of input accelerograms is conducted. A recently proposed numerical model for bi-directionally loaded HDRBs is used to simulate the complicated hysteretic behavior of the elastomeric bearing under bi-directional deformation.

The seismic responses of the isolated bridges under uni- and bi-directional ground motion input are compared by the average IDA curves. The likelihood of collapse or failure of the isolated bridges neglecting the bi-directional effect is estimated using probability concepts including the fragility curves and interval estimation. Finally, seismic performance design recommendations and simple modified equations are proposed.

2. NUMERICAL STRUCTURAL MODEL

A benchmark bridge is hypothesized for the numerical model established for the analysis. The bridge is represented by a two-mass 4-DOF model. The bridge piers are assumed to behave in undamaged elastic range and expressed by linear springs in the two directions. The bi-directional nonlinear behavior of the rubber bearing is taken into account with the Modified Park-Wen model.

2.1 Numerical bridge model

The benchmark bridge representing a typical viaduct, shown in Figure 1, consists of a superstructure, bearings and substructure. In this study, the deformation of the substructures, such as the piers and abutments, is simply considered to be linear elastic. The superstructure and the substructure are assumed to be modeled as the two concentrated masses. Thus, the bridge structure can be considered as a two-mass system shown in Figure 2.

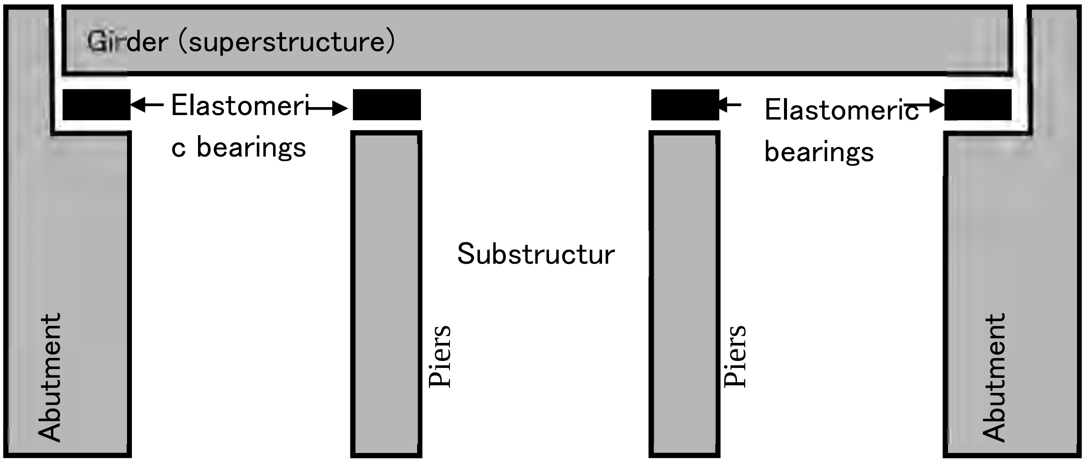
Girder (superstructure)
Elastomeri
c bearings
Elastomeric
bearings
Substructur
Abutment
Piers
Piers
Abutment

Figure 1: Layout of the benchmark bridge

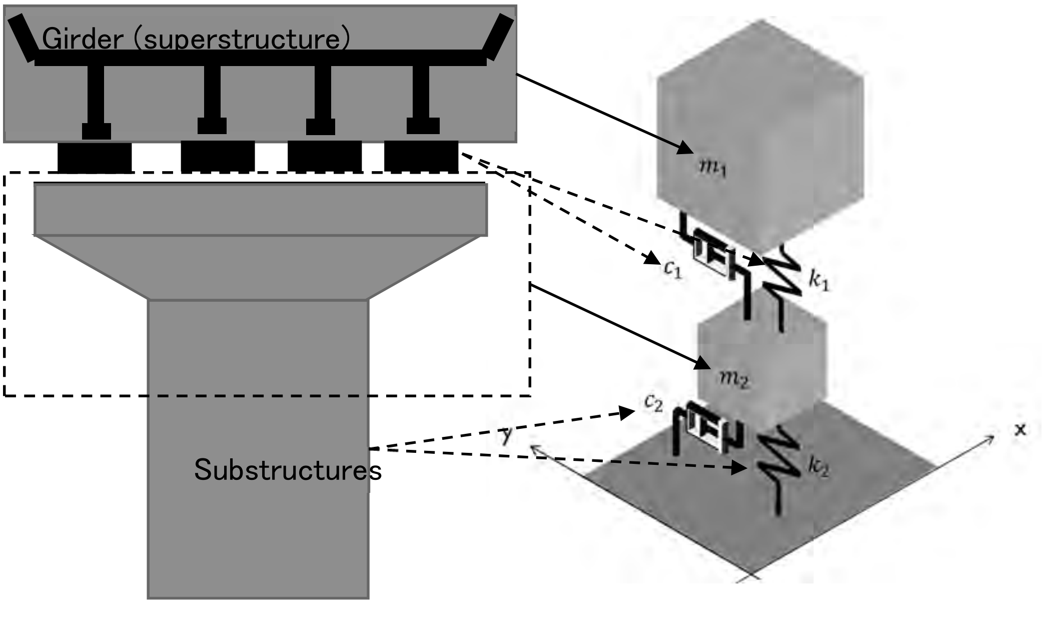
Girder (superstructure)
m_1
c_1
k_1
m_2
c_2
k_2
y
x
Substructures

Figure 2: Bi-directional two-mass 4-DOF model for isolated bridges

As can be seen in the figure, the top mass point m_1 represents the concentrated mass corresponding to superstructure, and mass point m_2 represents the half of the tributary mass of the piers. The restoring force and damping due to deformation of the elastomeric bearings are represented by the stiffness k_1 and viscous damping coefficient c_1, and that of the piers are expressed by k_2 and c_2. The elastomeric bearings and piers here are assumed to be replaced with a bi-directional nonlinear elasto-plastic model to express the complicated bi-directional hysteresis behavior of HDRBs in the nonlinear time-history analysis.

The bi-directional hysteretic restoring force model for the bearings is calibrated by quasi-static loading test results. Test specimens for the tests are high damping rubber bearing (HDR-S bearings) of a square cross-section of 160mm×160mm, with a total rubber thickness of 40mm(=4×10 mm). The specimens were loaded under a constant vertical pressure of $p = 6$ MPa. The plan and elevation dimensions of elastomeric bearings used in the benchmark structure are considered as 4 times larger than the specimen, with a cross-section of 640mm × 640mm and total rubber thickness as 160mm. Thus, in accordance with the similitude law, the superstructure mass weight for all bearings with the number of N_b should be as follows.

$$m_1 = N_b \times p \times A_b \times S^2/g \tag{1}$$

where A_b (=640mm×640mm) is the cross-section area of the elastomeric bearing, S is the scale factor 4, and g represents the gravity acceleration.

The mass of the substructure is empirically chosen to be 1/2 times m_1, and the tributary mass is assumed to be 1/3 of the mass of substructure.

$$m_2 = \frac{1}{2}\frac{1}{3}m_1 \tag{2}$$

The deformation of the substructure is considered to be within the elastic range, so that the restoring force can be expressed by the bi-directional linear spring of stiffness k_2.

$$k_2 = (m_1 + m_2)(2\pi/T_f)^2 \tag{3}$$

where T_f represents the natural period of the bridge structure with the condition of fixed connection between the superstructure and the substructure. Since typical regular bridge structures without isolation have natural periods ranging from 0.2 to 1.5s, T_f is specified as 0.5 s for the benchmark structure.The Rayleigh damping assumption is used for calculation of c_1 and c_2 , so that the modal damping ratio of all natural modes are 0.05.

2.2 Bi-direction model for HDRBs

Modified Park-Wen (MPW) model (Dang 2013) has been proposed and experimentally verified recently for high-damping-rubber bearings under bi-directional loading. The proposed MPW model can be expressed by the following equations.

$$\begin{Bmatrix} F_x \\ F_y \end{Bmatrix} = \alpha K \begin{Bmatrix} u_x \\ u_y \end{Bmatrix} + (1-\alpha)K(1+b\varepsilon^2)\begin{Bmatrix} Z_x \\ Z_y \end{Bmatrix} \tag{4}$$

$$\dot{Z}_x = A\dot{u}_x - \beta|\dot{u}_x Z_x|Z_x - \gamma\dot{u}_x Z_x^2 - \beta|\dot{u}_y Z_y|Z_x - \gamma\dot{u}_y Z_x Z_y \tag{5}$$

$$\dot{Z}_y = A\dot{u}_y - \beta|\dot{u}_y Z_y|Z_y - \gamma\dot{u}_y Z_y^2 - \beta|\dot{u}_x Z_x|Z_y - \gamma\dot{u}_x Z_x Z_y \tag{6}$$

$$\varepsilon = \frac{\sqrt{u_x^2+u_y^2}}{h} \tag{7}$$

where F_x and F_y are the restoring forces, u_x and u_y are displacements, Z_x and Z_y represent the plastic components, corresponding to the x and y components, respectively. The Symbol K denotes the initial elastic stiffness, αK is the second stiffness, which is also the loading history independent elastic component stiffness for elastomeric. The $(1-\alpha)K = (1-\alpha)f_0/u_0$ part presents the critical force normalized by the yield displacement u_0. Constant A is generally equal to unity, and the maximum limit of Z_x and Z_y are the yield displacement u_0, which is determined by the parameters β and γ defined as the following equation.

$$Z_x, Z_y < Z_n = u_0 = \sqrt{\frac{A}{\beta+\gamma}} \tag{8}$$

where Z_x and Z_y are defined by the implicit differential equations (5) and (6). They can be easily obtained numerically by computing the step-by-step incremental displacements $\Delta u_x (=\dot{u}_x dt)$ and $\Delta u_y (=\dot{u}_y \Delta t)$ either in static displacement loading analysis or time history simulation. However, the displacement increment Δu_x, Δu_y in each step should be sufficiently small to allow accurate calculation of the increments of Z_x and Z_y, which are $\Delta Z_x (= \dot{Z}_x \Delta t)$ and $\Delta Z_y (= \dot{Z}_y \Delta t)$.

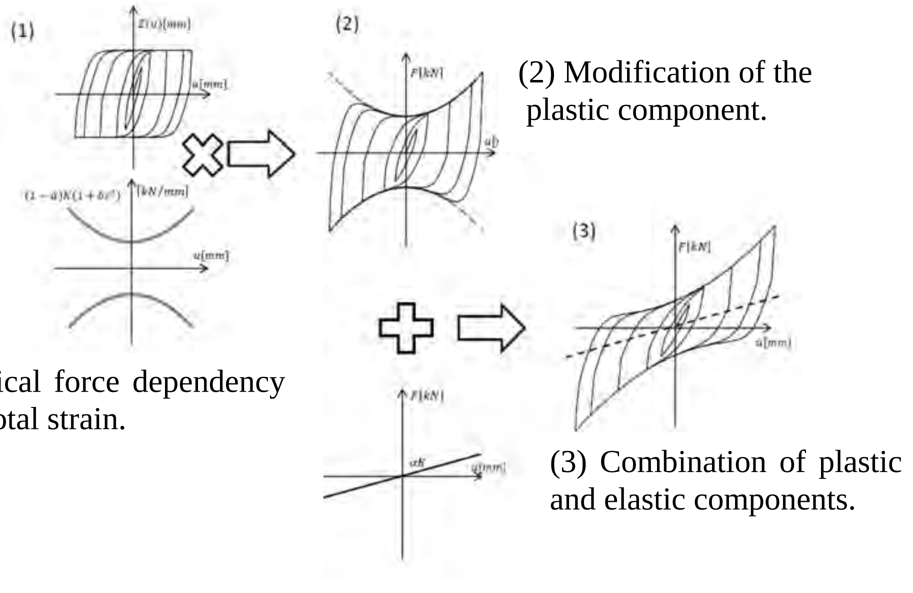

(2) Modification of the plastic component.

(1) Critical force dependency on the total strain.

(3) Combination of plastic and elastic components.

Figure 3: Constitutive rules for Modified Park-Wen model

The displacement increment limit for each step of $u_0/10$ should be regarded as sufficiently small. If the displacement increment is larger than $u_0/10$, division of the step to small multiple sub-steps is necessary. The symbol ε denotes the total horizontal shear strain of the rubber bearing under bi-directional loading, and h is the total rubber thickness.

The modifier term $b\varepsilon^2$ expresses the change of the critical force due to the bi-directional shear deformation. This is a highly simplified representation of the assumptions of rubber bearing's bi-directional interaction and the square term is used to approximate the relationship between the critical force and the shear strain level. The constitutive rules of the proposed model are illustrated in Figure.3.

Comparison of the test result, the original Park-Wen model, and the MPW model are illustrated in Figure. 4, in which the advantage of using the MPW model is clearly shown. The analysis results using the bi-linear model and the MSS-bilinear model are found to be similar to that of the PW model shown in the figure, while they are greatly deviated from the experimental result, which is most effectively approximated by the MPW Model.

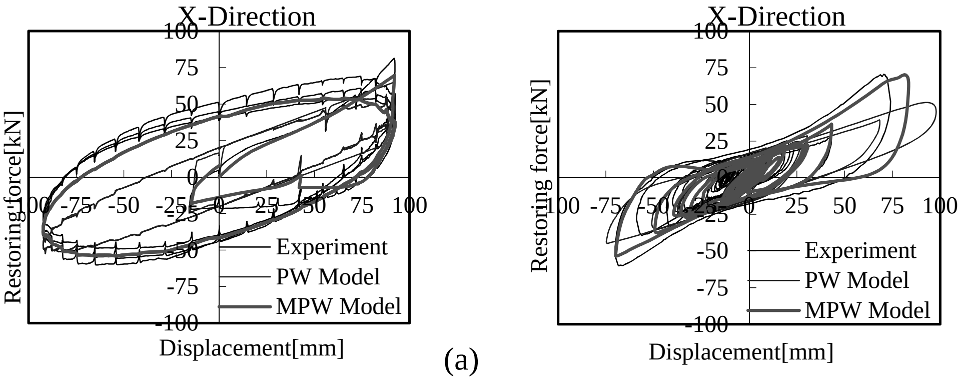

(a) (b)

Figure 4: Comparison of MPW model with original Park-Wen model by (a) circular bi-directional loading and (b) hybrid-simulation (pseudo-dynamic test) loading

3. INCREMENTAL DYNAMIC ANALYSIS

Seismic response of complicated nonlinear systems, such as an isolated bridge structure with bi-directional interactions, is greatly influenced not only by the ground motion intensity but also by uncertainty due to the randomness of phase character. To evaluate the statistical distribution of the seismic performance of isolated bridge structures under uni- and bi-directional earthquake excitation, both the uncertainty of the input ground accelerograms and that of the intensity level of the input should be taken into account. For this purpose, the Incremental Dynamic Analysis (IDA) approach is used as an effective method to conduct this kind of seismic performance evaluations.

3.1 Outline of analysis procedure

Following calculation approach was used to perform IDA in this study.

1) Select a reference earthquake accelerogram a_g which satisfies appropriate conditions.
2) Prepare the input accelerogram a_λ by scaling a_g by an intensity factor λ.

$$a_\lambda = \lambda \times a_g \tag{9}$$

3) Conduct nonlinear time-history analysis for the structural model using the input a_λ to find the structural response.

4) Increase λ to obtain increased input a_λ and repeat 2) and 3) until the failure of the structure.
5) Determine the relationship between the input earthquake intensity and the maximum nonlinear structural response.

3.2 Definition of intensity indices

The intensity of the input ground motion is evaluated on the basis of PGA (Peak Ground Acceleration) in this study. The PGA for the earthquake records containing two orthogonal directions is calculated as their peak vector norm as the following expression:

$$PGA_{2D} = max\left(\sqrt{a_{NS,n}{}^2 + a_{EW,n}{}^2}\right) \tag{10}$$

The input accelerograms are generated with the specified PGA which is increased from 100 cm/s^2 at the interval of 100 cm/s^2 until the structural collapse. The maximum response of the uni-directional loading case is evaluated by the absolute peak value of the response time history. On the other hand, the maximum response of the bi-directional input analysis is defined as the peak length of the displacement vector.

$$d_{NS,max} = max\left(d_{NS,n}\right),\ d_{EW,max} = max\left(d_{EW,n}\right) \tag{14}$$

$$d_{2Dmax} = max\left(\sqrt{d_{NS,n}{}^2 + d_{EW,n}{}^2}\right) \tag{15}$$

The collapse of structure is defined as the situation such that the response of the rubber bearing reaches 250% shearing strain. Therefore, the ultimate response strain of rubber bearings is defined as the following expression.

$$urr = d_{max}/2.5h \tag{16}$$

4. ANALYSIS RESULTS

The IDA curves representing the relationship between the increased intensity of input ground motion and their consequent nonlinear response of the structures obtained by uni-directional and bi-directional accelerograms using 100 sets of earthquake records of major earthquakes (Mw>6, PGV>50kine). The average curves are shown in Figure 5.

It can be seen from the figures that the IDA curves for uni-directional loading take higher values than that for bi-directional loading. This implies that the seismic response of the structure evaluated by conventional analysis based on the uni-directional loading may be overestimated.

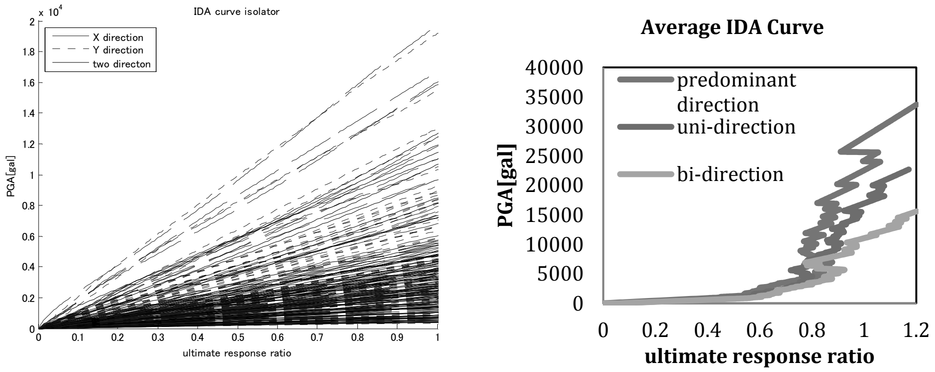

Figure 5: Analysis results: IDA curves for 100 sets of earthquakes and Average IDA curves

The response ratio α is defined as follows to measure the difference of structural response between uni- and bi-directional loadings.

$$\alpha = d_{2Dmax}/d_{1Dmax} \tag{17}$$

The response ratio of cases which have response near to level 1 and level 2 performance demand are plotted with its wave number in Figure 6 (a). The probability of the response ratios A exceeding a ratio level α P(A>α) is calculated by the proportion of cases which resulted a ratio A that larger than α. The exceedance probability and the 95% confidential level are plotted in the Figure 6 (b). These statistical estimation plots reveal that the likelihood of the situation such that the response amplitude assessed by analysis using uni-directional loading is smaller than that using the bidirectional loading case for the same PGA is about 62% to 77%. And responses of both levels of the response performance show similar results. This implies that there are about 70% possibility that a bi-directional seismic loaded isolated bridge may fail, which means response larger, the uni-directional based design.

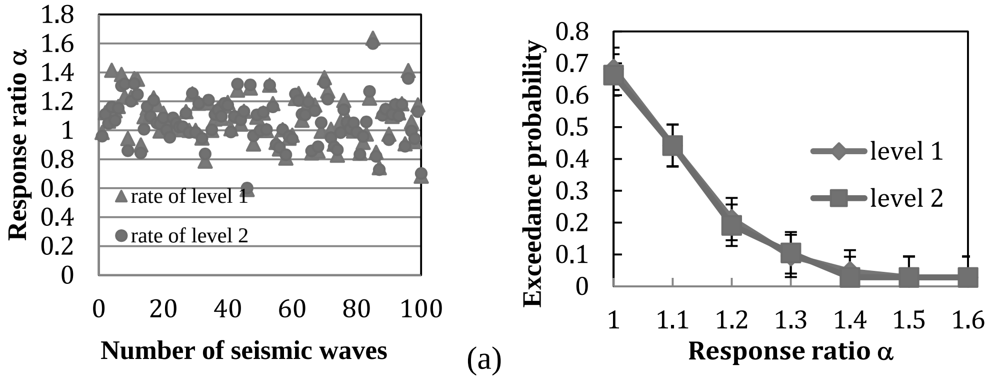

(a) (b)

Figure 6: (a) Response ratios and (b) its exceedance probability

$$P(L - R > 0) = 66\% \tag{18}$$

Here, L is the response of structure due to uni-directional analysis, R is the deformation design limit.

The probability paper for estimation of the possibility distribution of response ration α can be obtained by reorder the number of cases by ranging them in order of response ratio, as can be seen in Figure 7, as well as its estimation of Possibility Density Function (PDF). The number of cases which imply the cumulative possibilities increase the response ration linearly, approximately. The linear regression estimation fits the relation in the figure well, this implies that the possibility distribution of response ratio α can be represented by a normal distribution with an average (expected value) μ=1.1 and deviation σ=0.11.

Thus a safety factor C can be introduced to low down the possibility of failure of convenient uni-directional design, due to the normal distribution estimation of response ratio $\alpha \sim$N(1.1, 0.11). Thus, a proper safety factor for a desire design reliability can be calculated by following equation.

$$P(CL - R > 0|C = x) = \Phi(X < (x - 1.1)/0.11) \tag{19}$$

For example the reliability of 90% need to use a safety factor C=1.3. $P(CL - R > 0|C = 1.3) = \Phi(X < (1.3 - 1.1)/0.11) = 90\%$. Here $\Phi(x)$ represent the standard normal distribution.

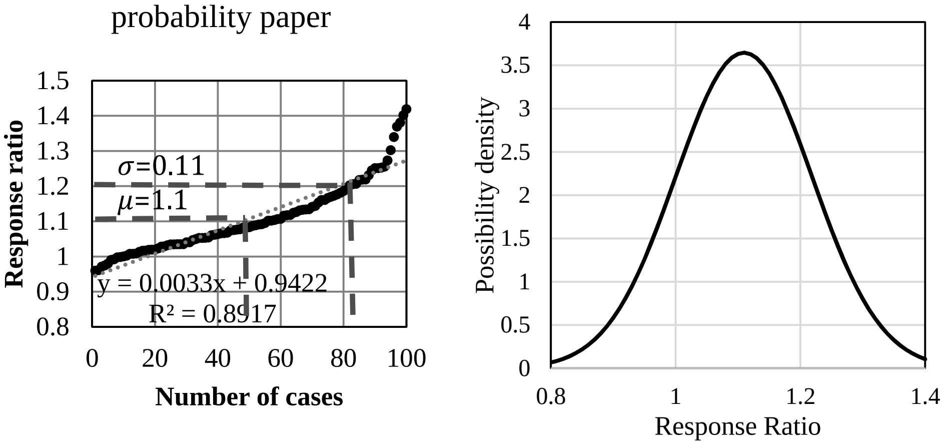

Figure 7: Probabilistic distribution estimation of response ratio α

Proportion of the number of cases such that the angle between the directions of maximum seismic input and the maximum response is greater than π/20 is as much as 75% of all cases. Based on this observation, the difference of the directions of excitation and structural response may be regarded as a major reason for the increase of the response assessed by analysis using the bi-directional excitation. It can be seen in Figure 8 that the radian angle of difference in predominant directions of input earthquake and structure response is also following a normal distribution with μ=0.26π and deviation σ=0.16π.

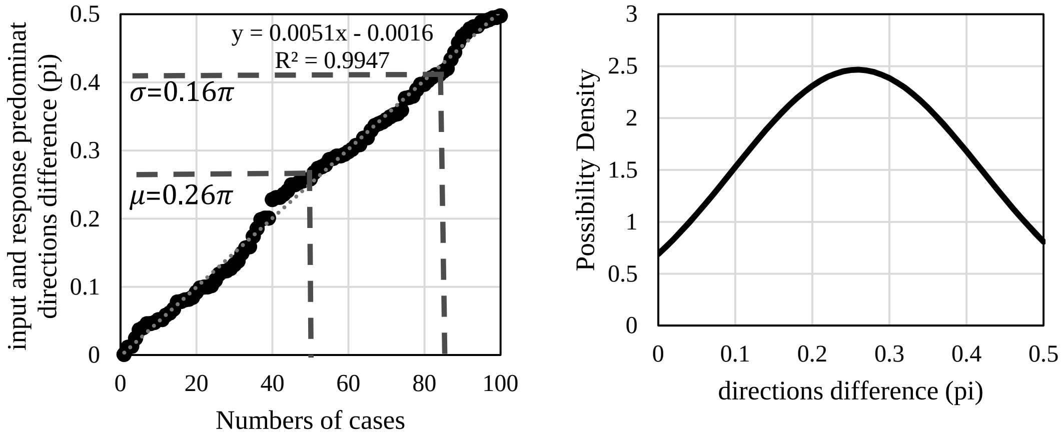

Figure 8: Probabilistic distribution estimation of direction difference

CONCLUSIONS

The IDA curves and fragility curves for a typical bridge with seismic isolation are obtained by nonlinear time history analyses under unidirectional and bi-directional excitations using a model of the bi-directional hysteretic behavior of the elastomeric bearing. The results indicate that the bi-directional earthquake interaction tends to increase the seismic response and the associated bearing displacement. A simplified design method to use a safety factor to increase the design reliability of uni-directional analysis based design. The difference of the directions of excitation and structural response under the bi-directional excitation may be a reason for the overestimate of the response assessed by unidirectional analysis.

REFERENCES

Earthquake Engineering Committee of JSCE, 2011. Emergency Damage Reconnaissance Report of Tohoku Earthquake.

Dang, J., Igarashi, A. and Murakoshi, Y., 2013. Nonlinear numerical hysteresis model for bi-directionally loaded elastomeric isolation bearings. *Proc. 2nd International Symposium on Earthquake Engineering*, No.2, 131-140.

Iwata, S., Iemura, H., Aoki, T., Sugiyama, K. and Uno, Y. (1998). Hybrid earthquake loading test (pseudo-dynamic test) of bi-directional base isolation bearing for a large pedestrian bridge. *Proc. of the 10th Earthquake Engineering Symposium* 10-1, 207-212 (in Japanese).

Japan Society of Civil Engineering, 1996. Reconnaissance Report of Hanshin-Awaji Great Earthquake Vol.1 damage of civil engineering structures (Bridges) (in Japanese).

Murakoshi, Y., Igarashi, A., Dang, J. and Ito, T., 2013. Bi-Directional Experimental Hybrid Simulations of Elastomeric Isolation Bearings for Validation of Hysteretic Modelling, *Proc. 15th World Conference on Earthquake Engineering*.

Park, Y. J., Wen, Y. K. and Ang, A. H-S., 1968. Random Vibration of Hysteretic Systems under Bi-directional Ground Motions, *Earthquake Engineering & Structural Dynamics* 14, 543-557.

Vamvatsikos, D. and Cornell, C. A., 2002. Incremental Dynamic Analysis. *Earthquake Engineering & Structural Dynamics* 31, 491-514.

A solution for stakeholder management in Vietnamese construction projects

Quan A. PHUNG[1]
[1]Project Management and Law Division,
Faculty of Construction Economics and Management,
National University of Civil Engineering, Vietnam
anhquan26@gmail.com

ABSTRACT

In recent decades, stakeholder management – a special perspective of management – has become implanted in managers' and planners' mind. It is expected to become an increasingly important management aspect. In Vietnam, there are some problems in stakeholder management in construction projects like low level of vision sharing among management team, lack or limited application in applying stakeholder management processes, and weakness in managers' ability and stakeholder management strategies. All of them lead to an ineffective management style in projects and cause negative impact when troubles from stakeholders appear. From these inspected causes, this paper is to suggest a practical lean construction based solution for the top managers to apply to solve their current problems and to improve effectiveness in construction companies and project management. The paper discussed on six main reasons for this current situation; they are silo information system, management process, human HR training quality, internal – external working environment, measurement and evaluating method, and top management cause. Based on these causes, the thesis puts forward a solution and recommendations for the top managers to apply some stakeholder management processes, which expected to solve their current problem and increase effectiveness of construction project management.

Keywords: stakeholder management, project management, Vietnam, construction and civil engineering.

1. INTRODUCTION

No one can deny that a construction project requires the involvement among a number of parties – stakeholders. This involvement, on the one hand, is the cooperation of consultancy, capital, human resource, machines, technology, information and others from different stakeholders (for example: authorities, partners, customers, distributors, suppliers, and consultant groups); on the other hand, there is a mutual affection between internal stakeholders of the project. Therefore, the success of a project depends on the way of managing these people and organizations. One thing that must be noticed is that the complexity of stakeholders in the modern economy when globalization and cooperation are becoming more and more popular. It means that relationships among individuals and organizations in constructing operation have turned to be more complicated. Many researchers investigated and recognized that stakeholder management is an important factor of civil engineering and management (Yang, 2010). However, management of stakeholders and their relations does not meet the required level (Rowlinson et al., 2010). One of keys reasons for the gap is that managers and their teams did not follow a possessive, systematic and official stakeholder management (Karlsen, 2002). Therefore, how to manage stakeholders effectively is still a question mark to all project managers.

Regardless of managers' attempts, the result of this research shows that there are three main weaknesses behind the unprofessional working styles in Vietnamese construction projects. Those weaknesses cause unexpected impact to image, competitiveness, profit and other benefits of projects. The output will not change if everything stands still. It is high time to apply a more effective and efficient method of managing stakeholder in construction project. It is convinced that appropriate management of stakeholders will improve performance and operations of the project, strengthen competitive advantage in the market, enhance relations with partners (suppliers, contractors and subcontractors) in sustainable way and long term orientation. It is also believed to improve working environment for staffs and workers of construction projects, and enrich shareholders and owners.

2. METHODOLOGY

This research followed a traditional research approach. Initially, the paper has started from the fact. An investigation on the real conditions of Vietnamese construction projects will help to find out their problems. In order to do that, this research makes use of results from a survey on the people who are working in Vietnamese construction projects. The questionnaire used in the survey includes 33 questions which required the respondents to answer the questions based on their own experience. 59 results of the questionnaire were received back from various fields in construction, types and sizes of projects, and positions of interviewees. Collected data then was transcribed, coded, and analyzed with SPSS software. After the problems are recognized, the literature then is reviewed in order to find out relevant knowledge, researches, and best practices to solve the problems of the projects that have been applied on over the world. Finally, based on knowledge and experience from various sources of research reference of which the three most important are PMBOK (Project Management Institute, 2013), Stakeholder Cycle Methodology (Bourne, 2009), and Turner's model (Turner, 2009), the solution was integrated, and modified to overcome three main weaknesses of Vietnamese construction project. This solution was proposed by taking all advantages and best practices of the global researches, which was adjusted to be suitable with particular condition of Vietnamese construction projects and management style.

3. DEFINITIONS

3.1. Stakeholder

The term "stakeholder" was used the first time in 1963 by the Stanford Research Institute's Long Range Planning Service (Thorpe and Holt, 2008), then many theories and definitions were developed by experts and researchers in the world. From 1963, the academic world have seen different definition of “stakeholder”, Friedman and Miles (2006) summarized 55 definitions of “stakeholders” in their book named “Stakeholder: Theory and Practice”. To sum up, we can conclude that stakeholders are individual or organization (like customer, sponsors, contractors, or public) who involved in or be under influence, and they can make a remarkable impact (directly or indirectly) to the operation and result of the project. It is worthy to notice that their impact can be in both sides (positive and negative). Therefore, management should be wise to take advantage of good impacts as well as prevent and minimize bad ones.

3.2. Stakeholder Management

Stakeholder management, in some publications, has been created with labels such as ‘social responsibility manager’, ‘community manager’, and ‘environmental manager’ (Miles et al., 2002). Like the term of stakeholders, there are lots of definitions proposed for the term of stakeholder management. It can be understand as “essentially stakeholder relationship management as it is the relationship and not the actual stakeholder groups that are managed”(Friedman and Miles, 2006). Forward a practical approach, PMI defines stakeholder management as a continuous chain of processes. It includes processes of identifying the stakeholder; analyzing their expectations and result impact on the project; and developing reasonable management plan for engagement. Moreover, as mentioned in PMBOK, this institute stated that stakeholder management should focus on “continuous communication with stakeholders” to comprehend “their needs and expectations” and to manage related issues and conflicts (Project Management Institute, 2013). This definition can cover almost all of aspects in stakeholder management.

4. CURRENT STATUS OF THE STAKEHOLDER MANAGEMENT IN VIETNAMESE CONSTRUCTION PROJECTS

4.1. A behavior analysis of managers

In the first part of the questionnaire, there are some questions about the importance of 14 key stakeholders in construction projects. Each of the stakeholders is evaluated on a Likert scale with five levels of importance: code 01 is the lowest level, and code 05 means the highest one. The classification of them is based on cluster analysis by dendrograms using Ward Method in non-hierarchical clustering. By this method, elements (records) are combined together based on the similarity of them. The rescaled distance cluster combines diagram shows that tradeoffs between the distance and the number of clusters, 3 clusters are reasonable. They are:

- ***Cluster 1:*** Managers in this group can be named as “subjectivism”, they gave low grades for 14 stakeholders, and the average grade they gave is 2.38, it ranges from 1.73 to 3.20 over maximum level of 5.
- ***Cluster 2:*** They are in the “neutral” group with the average grade for these stakeholders is 3.25 (Ranged from 2.30 to 4.45)
- ***Cluster 3:*** They can be called as “caution” group. Managers in this group are highly appreciated key stakeholders, the average grade is 4.21 with minimum point is 3.67 and maximum value is 4.86, much higher than the two previous groups.

Interestingly, the “caution” cluster tends to be more successful in managing stakeholders. They can realize connections between stakeholders with higher rate and predict better troubles. Besides, these managers prefer to use negotiation when facing with stakeholders, in other words, they try to avoid passive reactions when solving problems with stakeholders. As a result, 21 managers in this group experienced a better ability to preventing trouble and creating a good opportunity for the project. Moreover, the caution group can estimate better the attitude of stakeholder (whether they support or oppose the project).

Table 1: Outstanding abilities of "caution" cluster

No.	Ability to	Cluster 1	Cluster 2	Cluster 3
1	Realize connections between stakeholders	60.0%	75.0%	81.0%
2	Predict troubles from stakeholders	80.0%	75.0%	92.5%
3	Solve problem by negotiation	6.7%	20.0%	28.6%
4	Solve problem by passive reactions	86.7%	75.0%	66.7%
5	Complete the mission	95.3%	85.0%	73.4%

4.2. Three main problems in stakeholder management: An exploration

4.2.1. Low level of vision sharing among staffs

Stakeholder management is mainly implemented in a decentralized method. It means that different managers or staffs take roles on stakeholder management independently. In 59 results of the survey, there is 63.8% and 66.1% of the questioned managers manage their internal and external stakeholders in this way. Moreover, the idea of using a common or formal method to connect staffs is less popular than informal ones. In fact, the types of forms, tables and diary is used limitative (45.6% of result use them), and there are only 17.5% of projects using professional tools and software to manage their stakeholders. The communication between staffs (who are responsible for stakeholder management) is mainly carried out via meetings (87.7% of answers) and interpersonal communication (54.5%) without or limited in recording as a document like memorandum of understanding. As a result, the lack and insufficiency of shared-vision tools lead to a paradox in storing and retrieving stakeholder information. Up to 78% of them agree that they are in troubles of retrieving and using stakeholder information regularly. The reason for this problem is the lack of a methodological method to store useful information about stakeholders. Moreover, each staff uses their own way to store their information.

4.2.2. Lack or limited application of stakeholder management processes and its effects

In fact, almost all of these projects have not had an effective method to manage their stakeholders. Only a small number of the projects use a simple method in their management processes, but it is not clear in all the time. For instance, in stakeholder analysis, there are three main issues: ineffectiveness; limited application in determining stakeholders’ attributes; and in storing and updating information about stakeholders. Firstly, making a full list of stakeholders is still used, but not effective because of limitation in staffs’ skills. In detail, 76.2% of respondent stated that they have made a prediction about that list, but 52.5% of them often get into troubles when they cannot develop a full list of stakeholders. Secondly, only determining stakeholders' expectations is not enough to evaluate them and to decide the priority of who should be managed more closely than others. Besides, predicting stakeholders' expectation is also at a low level of efficiency. Only 15.3% of the staffs can estimate reasonably. This can be understood when information resource is limited and there is lack of continuous tracking for stakeholders in the operations of the project. Thirdly, although a list of stakeholders is recognized as an important process of almost all of the stakeholder management methods, this list is not usually stored as formal documents. Up to 45.8% of surveyed staffs answered that there is no formal document about the list leading to another issue where changes in characteristics of stakeholders (power, influence, interest, requirement and others) will not be managed as a whole. Furthermore, the task of responsibility assignment separates this list into small parts, but there is no tool to manage them in an integrated list. This work pours into the top managers, who run it as their own experiences. The result is that some stakeholders can be forgotten, no crosscheck and hard to updating this list on time. Only 23.7% of staffs can update this list timely then the list is normally insufficient.

In terms of developing stakeholder management plan, it is cursory. Top managers mainly assign tasks to employees and let them do the work independently by their own experience. No general strategy is agreed by the whole staffs. This unthoughtful preparation will surely create troubles for the implementing stage. As the result, troubles often occur in stakeholder communication, up to 85% of respondents admitted that they have difficulties in communicating with stakeholders; 63% of respondents recognized that the most important cause of this problem is the insufficient agility in receiving and processing information related to the concerned stakeholders. Even in the projects using a common form to manage stakeholders' relations, they did not finish all the required content in the form correctly and completely. In addition, 44.4% of staffs in those projects think that the forms are outdated and should be updated and adjusted. Another problem in communication is the passive role of project in solving stakeholder related issues. To explain it, we can start from spare preparation, which leads to weaknesses in preventing the troubles and push project in a passive situation when they cannot anticipate future actions. As a result, staffs normally wait for problems happen and try to solve them instead of finding a way to avoid them right at the beginning.

4.2.3. Limited ability of managers

Building strategies to manage stakeholders is not an advantage of managers in Vietnamese construction projects. To hypothecate this, a small survey is conducted to examine whether the staffs can develop appropriate strategies for different types of stakeholders or not. This survey based on a very popular model in identifying stakeholders – power/interest grid. Particularly, 59 interviewees were instructed about the use of the model and tested to allocate 14 main stakeholders in the construction industry in that grid. Almost all of the allocations are similar to each other and 79.3% of them answered that this model is easy to apply. After they understand the model, questions about choosing strategies for 4 main types of stakeholders in this model were given to staff. Appropriate and accurate strategies are adapted from general principles to manage each group of stakeholder stated by Johnson et al. (2005). The result shows unappreciated selections of strategies. In details, 71.4% of interviewees did not choose the suitable strategy for "keep satisfied" group (who have high power but low interest). For the other three groups, the rates of wrong selections are 66.7%, 57.9% and 42.1%.

4.3. Discussion about causes of the Problems

From the ideal of Ishikawa cause and effect analysis (Fishbone analysis) and the 6 Ms (used in manufacturing industry), this paper summarize causes for the problem into six types.

- ***Silo and enterprise information system:*** The common causes in this group are sending information is not sufficient and not timely, timely to accessing necessary data, unclear method to send information to stakeholders, data is saved separately in different ways, managed by different people and updated lately, or cannot be updated.
- ***Management process:*** In management, managers did not make a full list of stakeholders, they faced with limitation in evaluating stakeholders' attributes, unclear priority criteria for classification of stakeholders in term of strategy development, did not use methodology strategy to manage and communicate with stakeholders. Moreover, mistakes in evaluating stakeholders' expectations, requirements and importance lead to failure in gaining support, to bear negative reactions of stakeholders. All of them lead them to a passive role in solving stakeholder problems.
- ***Human resources quality and policies:*** Staffs are weak in negotiation and professional skills and top managers assigned responsibility inefficiency.
- ***Internal working environment:*** This group expresses for lack of common form to communicate among staffs, lack of reference and standard guidance for staffs to implementing processes and no measurement mechanism for evaluating results of stakeholder management.
- ***Top Management:*** Top managers are one of significant causes for problems when they are afraid of change, and affected by group interest and underground problems in the project. Moreover, they were stuck on limited budget.
- ***External stakeholder relationships (external environment):*** Beside the subjective causes, the complexity of stakeholders is another reason for problem when the stakeholder list can be changed over time and number of stakeholders can be very high, and then managing them is difficult.

5. PROPOSAL OF A STAKEHOLDER MANAGEMENT PROCESSES

This paper proposes an integrated and improved stakeholder management model. Based on three practical models of Project Management Institute (2013), Stakeholder cycle methodology of Bourne (2009), and Turner's stakeholder management process (Turner, 2009), a chain of processes was created by taking advantages of the two models, and adapted to focus on solving the current situation in Vietnamese construction projects. These three models are chosen because of they follow a logical and practical process approach. The proposed processes will be graphed by the program of Business Process Model and Notation (BPMN) because it supports a logical and understandable graph, and it is a good tool to present the formalization process for business activities. In this model, there are four main groups and one ancillary group of processes: (1) Identifying stakeholders (Identification), (2) Developing stakeholder management strategies (Building strategy), (3) Managing stakeholder's engagement (Engagement management), and (4) Controlling communication with stakeholders (Control); and an ancillary process of data storing (5). All five groups of process will be carried out during operations of activity or project as many repeating cycles till the corporation activity/project end. The use of four main stages (group of processes) is adapted common points of the three models to create a closed management cycle. In each of stages, processes were considered to join in proposed model in terms of ability of practical application, logical order and combination, advantages of related tools & techniques. Moreover, the balance between costs of management and benefits are also taken into account for the selection, reconstruction of the proposed processes. This proposal expected to give the managers a friendly and not complex model to apply when all processes are clear and reduced all the theoretical and unnecessary requirements, these processes are shown step by step, with detailed information to implement. Moreover, the main idea to apply this model is continuously monitored and control; it will help the team to be more flexible with changes in context.

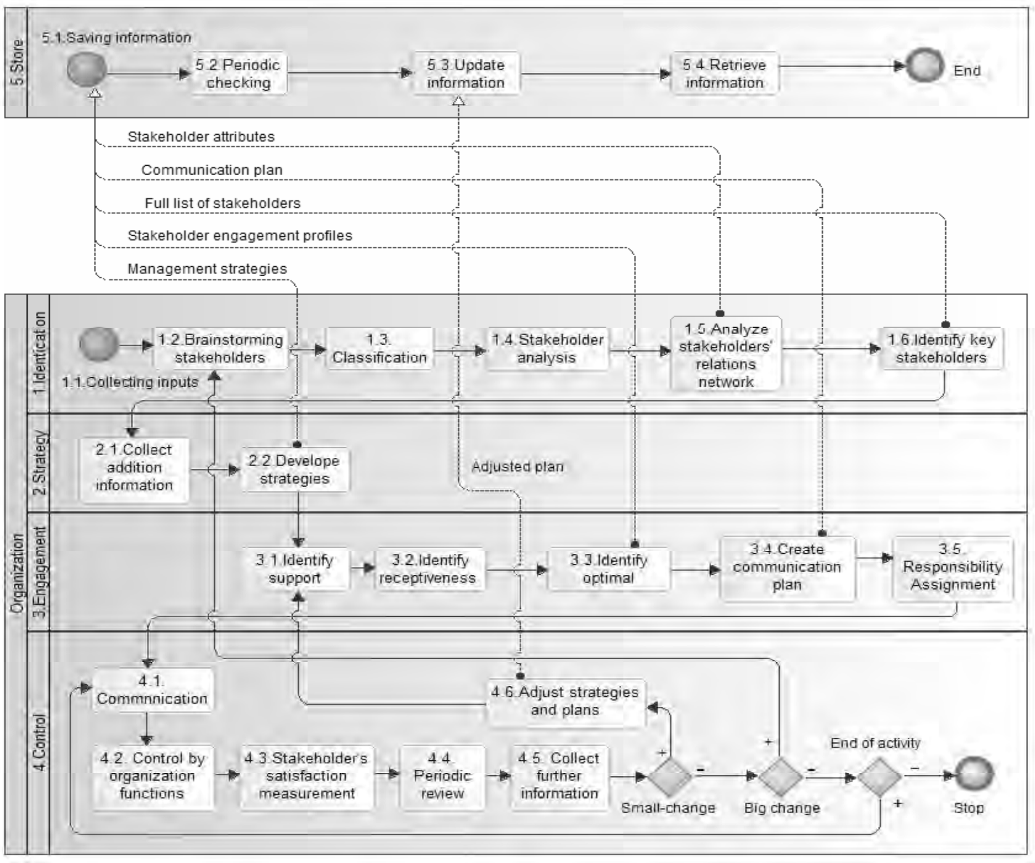
5.Store
5.1.Saving information
5.2 Periodic checking
5.3 Update information
5.4 Retrieve information
End
Stakeholder attributes
Communication plan
Full list of stakeholders
Stakeholder engagement profiles
Management strategies
Organization
1.Identification
1.2.Brainstorming stakeholders
1.3. Classification
1.4.Stakeholder analysis
1.5.Analyze stakeholders' relations network
1.6.Identify key stakeholders
1.1.Collecting inputs
2.Strategy
2.1.Collect addition information
2.2.Develope strategies
Adjusted plan
3.Engagement
3.1.Identify support
3.2.Identify receptiveness
3.3.Identify optimal
3.4.Create communication plan
3.5. Responsibility Assignment
4.Control
4.1. Commnnication
4.6.Adjust strategies and plans
4.2. Control by organization functions
4.3.Stakeholder's satisfaction measurement
4.4. Periodic review
4.5. Collect further information
Small-change
Big change
End of activity
Stop
+
-

Figure 1: Proposed processes of stakeholder management

- ***In stage 1:*** The analysis of stakeholder's relations network is divided into a dependent process to stress on the mutual affection among stakeholders. Moreover, in the end of this stage, the process of identify key stakeholders will help managers focus on important stakeholders and its output of a full list of stakeholders will be shared among all related managers and staffs.
- ***In stage 2:*** Before the strategies are created, it is necessary to collecting more new information or updating data to eliminate the risk that our strategies would be developed based on out-of-date information.
- ***In stage 3:*** Processes 3.1 to 3.3 are inherited from stakeholder cycle methodology with evaluation of support, receptiveness and optimal engagement of stakeholders. After understanding all these important features, the communication plan and control plan have big chance to write into detail one. In order to finish this stage, a

responsibilities allocation is added. Although it is not mentioned clearly in the three models, it is very important in terms of performance management and control.

- ***In stage 4:*** When the other models only control stakeholder by communication, I believe that it is a big mistake because communication is not enough to control stakeholders; they should be control through organization functions as well. It means that the project can influence their stakeholder by the affection of resources management, which is control directly and indirectly by the organization functions. Then, the process of "control by organization functions" is added to the model. Furthermore, the measurement of stakeholders' satisfaction is another new contribution of this model; it is followed by a balanced tool to implement.

6. CONCLUSION

Stakeholder management is obviously expressing its important role with the change of the economy in a new era and the complex of projects and activities that carried out by projects. The research on context and solution bring to managers in Vietnamese construction projects three main contributions. Firstly, it helps the managers to understand more about their stakeholders, their common weaknesses in Vietnamese construction projects, and to appreciate the careful attitude when solving problems of and manage their stakeholders. Secondly, after investigation on current management style of Vietnamese construction projects, the result shows three main weaknesses that need to be improved. Thirdly, the research proposed a solution of a detail management process.

REFERENCE

Bourne, L., 2009. *Stakeholder relationship management: A maturity model for organisational implementation*. Gower.

Friedman, A. L., and Miles. S., 2006. Stakeholders: Theory and practice. *Oxford University Press*

Johnson, G., Whittington, R., and Scholes, K., 2005. *Exploring corporate strategy - Text and Cases*, 7th edition.

Karlsen, J. T., 2002. Project stakeholder management. *Engineering Management 14*, 19.

Miles, S., Hammond, K., and Friedman, A. L., 2002. *Social and environmental reporting and ethical investment*. London, United Kingdom.

Project Management Institute. (2013). *A Guide to the Project Management Body of Knowledge* - 5th edition (pp. 391–415).

Rowlinson, S. M., Tuuli, M. M., and Koh, T., 2010. Stakeholder management through relationship management. *Performance Improvement in Construction Management, 173-193. Spon Press, London.*

Thorpe, R., and Holt, R., 2008. *The SAGE Dictionary of Qualitative Management Research*.

Turner, J. R., 2009. *The handbook of project based management - Leading strategic change in organizations*. McGraw-Hill.

Yang, J., 2010. A framework for stakeholder management in construction projects, The Hong Kong polytechnic university, 11–12.

Evaluation of resistance of GRS coastal dikes against over-flowing tsunami current by model tests

Yudai AOYAGI[1], Kimihiro FUJII[2], Shouhei KAWABE[3], Yoshiaki KIKUCHI[4],
Kenji WATANABE[2], Masatoshi IIJIMA[5] and Fumio TATSUOKA[4]
[1]Graduate student, Dept. of Civil Engineering, the University of Tokyo, Japan
y-aoyagi@iis.u-tokyo.ac.jp
[2]Railway Technical Research Institute, Japan
[3]National Agriculture and Food Research Organization, Japan
(Formerly, Tokyo University of Science)
[4] Professor, Tokyo University of Science, Japan
[5] Integrated Geotechnology Institute Limited, Japan

ABSTRACT

A great number of fill-type coastal dikes fully collapsed by deep overtopping tsunami current of the 2011 Great East Japan Earthquake and could not function as expected at many places. In this study, by using the following several different small models of coastal dikes arranged in a channel circulating water, the method to increase the resistance of coastal dike was studied: A) conventional embankment type coastal dike with the upstream slope sprayed with cement slurry; B) both slopes are covered with a model of soil bags; C) the crest of the embankment of model B was stabilized by using compacted gravelly soil; D) the backfill is reinforced with geosynthetic layers and the soil bag models were wrapped-around with reinforcement (GRS coastal dike); and E) the crest of model D was stabilized in the same manner as employed in model C. As a result, models D & E exhibited high resistance against erosion: i.e., the progress of the erosion was delayed by reinforcing the backfill with geosynthetic layers. The improvement of the crest of the embankment in models C & E increased the resistance against the erosion starting from the crest.

Keywords: coastal dikes, geosynthetics, tsunami

1. INTRODUCTION

The Great East Japan Earthquake generated a massive tsunami in the northwestern Pacific Ocean on March 11, 2011. The serious damage by the 2011 Great East Japan Earthquake includes: 1) damage to a great number of old soil structures due to strong shaking in a very wide are; 2) soil liquefaction, in particular in young reclaimed lands; and 3) damage by great tsunami. The tsunami run-up height reached 40m in some coastal areas (The 2011 off the Pacific coast of Tohoku Earthquake Tsunami Information). A great number of coastal dikes collapsed by deep overtopping tsunami current and totally lost their function as a tsunami barrier at many places (Figure 1). A great number of wooden residential houses and reinforced concrete buildings were

washed away. More than 340 bridges lost their girders or approach fills or both (Kosa, 2012). The number of dead and missing is 18,500, most by tsunami.
Therefore, tsunami barrier dikes should survive deep over-flowing tsunami current.

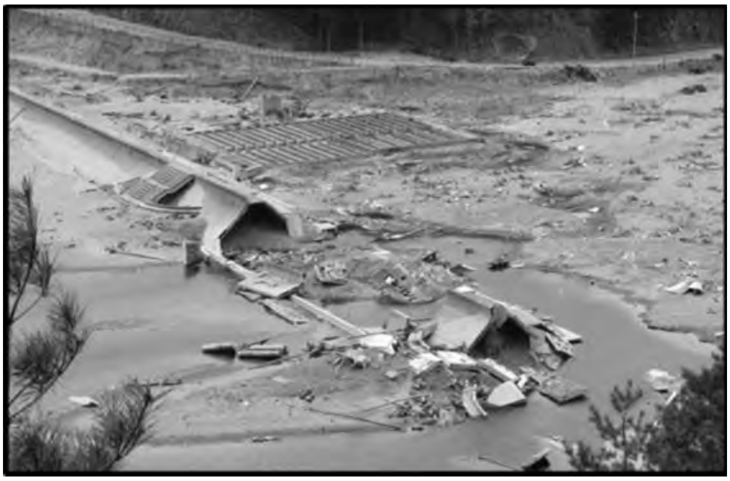

Figure 1. A typical fill-type coastal dike that fully collapsed by tsunami, Aketo, Tanohara, Iwate Prefecture (courtesy of Koseki, J., Univ. of Tokyo)

Based on this lesson, a reinforced soil dike with geogrids, Geosynthetic-Reinforced Soil (GRS) coastal dike, has been proposed as a new construction method (Figure 2). This is composed of continuous concrete facing connected to the geogrid layers reinforcing the backfill. The advantageous features of this type are as follows:

1) A very high seismic stability of GRS retaining walls (RWs) having full-height rigid facing has been validated by their very high performance during the 1995 Kobe Earthquake and the 2011 Great East Japan Earthquake (e.g. Tatsuoka et al. 1998, 2012). With slopes more gentle than the near vertical wall face of these GRS RWs, this type of GRS coastal dike should have a very high seismic stability, definitely much higher than the conventional type shown in Figure 1.
2) With the proposed GRS coastal dike, the ground in front of the toe of the down stream slope should be protected against scouring with a concrete slab or another relevant means. Even if some amount of scouring takes place, the facing on the downstream slope can maintain its stability much better than the conventional type. Besides, the facing has a high resistance against lift up by over-flowing tsunami current. Even if the facing is lost, the resistance of the reinforced backfill against erosion is higher than the unreinforced backfill of conventional type coastal dikes.

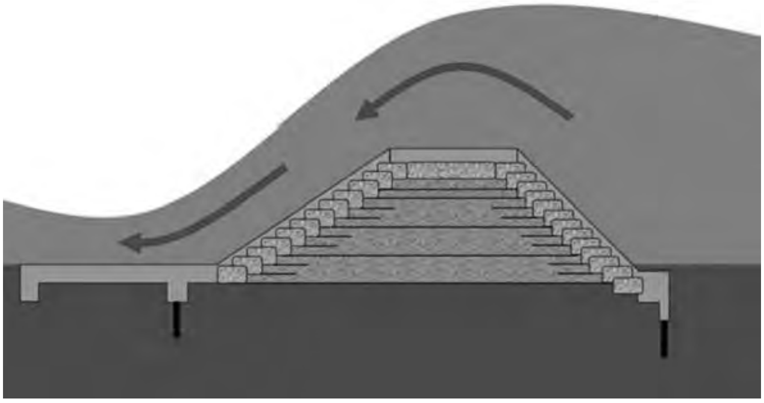

Figure 2. Geosynthetic-Reinforced Soil (GRS) coastal dike

In previous studies, wave pressure, erosion, penetration and scouring are main causes of collapse. However, wave pressure caused by tsunami, and the others cause by long time over-flowing tsunami current. Therefore, it is important to improve coastal dikes against long time over-flowing tsunami current. This study was conducted to evaluate the resistance of GRS coastal dikes (Figure 2) against over-flowing tsunami current using several small-scale models of coastal dikes arranged in a circulating water.

2. EXPERIMENT

Figure 3 shows the model test configuration (Aoyagi et al., 2014). To produce as much as long-period over-flowing tsunami current, a channel circulating water was used. The over-topping tsunami current was produced by using four submersible pumps. Figure 4 shows the quantity of flows after the start of over-flowing tsunami current. Five models shown in Figure 5 and explained below were tested. The considered model scale in

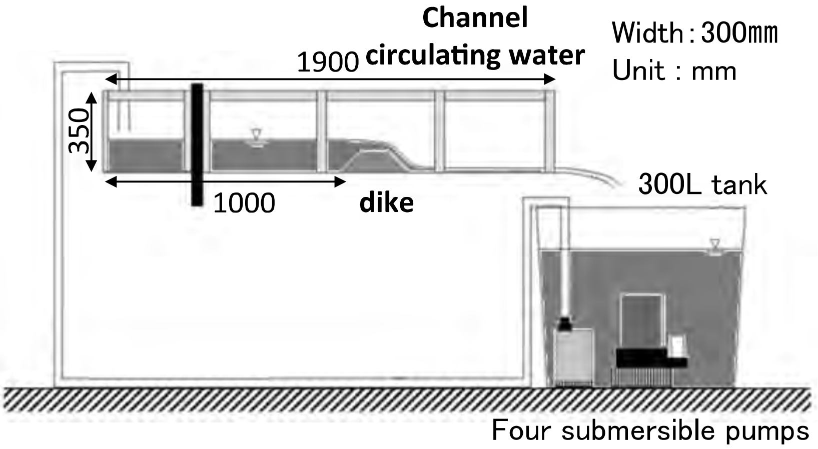

Figure 3. Model test configuration

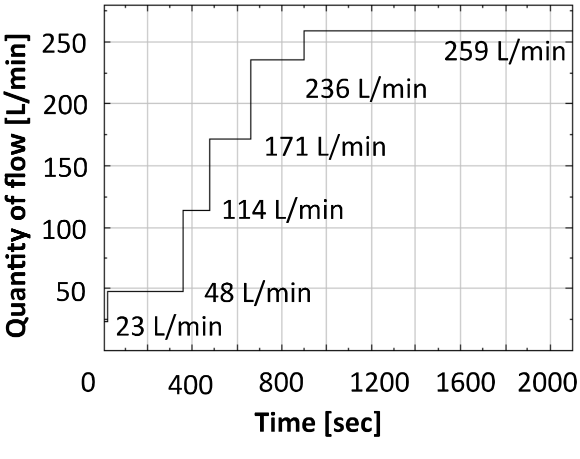

Figure 4. Quantity of flows after the start of over-flowing tsunami current

Length is 1:50: i.e. the simulated prototype dike is 5m-high and the initial height of the simulated tsunami is from 1.2m to 3.2m. The model dikes were produced by compacting moist Silica sand mixed Bentonite at the optimum water content (w=15%) to degree of compaction D_c=95% by the standard Proctor.

Model 1 (Figure 5a):
This is a model of the conventional fill-type dike without concrete facing and reinforcement layers. Upstream slope was sprayed with cement slurry.

Model 2 (Figure 5b):
This is a model of the conventional fill-type dike with a model of soil bags. The unreinforced backfill is the same as model 1. Both slopes are covered with a model of soil bags that have trapezoid shapes. The soil bags made of gravel adding mortar and are not connected to each other.

Model 3 (Figure 5c):
The crest of the embankment of the model 2 was stabilized by using compacted gravelly soil. As the gravelly soil Chiba gravel under 4.75mm diameter (ρ_d=2.0g/cm^3) is used.

Model 4 (Figure 5d):
This is a model of GRS coastal dike (Figure 2). The backfill is reinforced with geosynthetic layers and the soil bag models were wrapped-around with reinforcement. The backfill of the same fill-type as model 1 was reinforced with five layers of a polyproylene geogrid with an aperture of 1.3 mm.

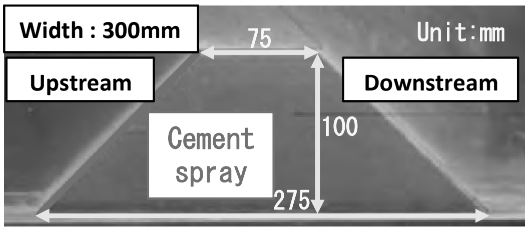

a) Model 1

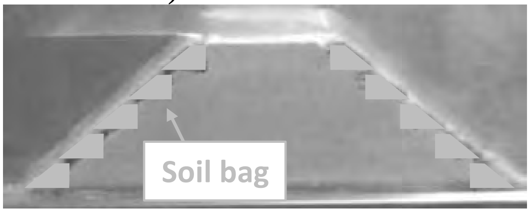

b) Model 2

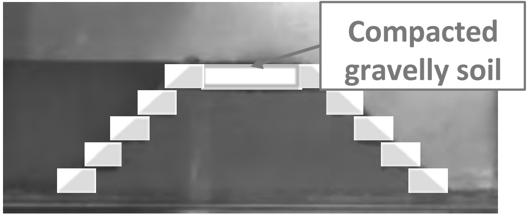

c) Model 3

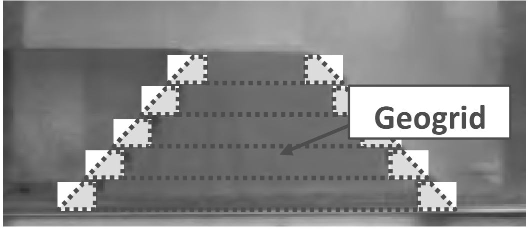

d) Model 4

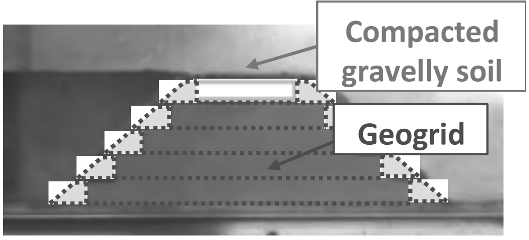

e) Model 5

Figure 5. Coastal dike models

Model 5 (Figure 5e):
The backfill was reinforced as model 4 and the crest was covered with the compacted gravelly soil as used model 3.

3. TEST RESULTS

Figures 6-10 show the behaviors of models 1-5 during the over-flowing tsunami current tests.

Model 1 (Figure 6; a model of the conventional fill-type coastal dike):

By the attack of the over-flowing tsunami current, model 1 fully collapsed by very fast erosion of the backfill starting from the downstream slope. It was reconfirmed that the erosion in the upstream slope is much slower than in the downstream slope under otherwise the same conditions. This model completely collapsed for about 50 seconds.

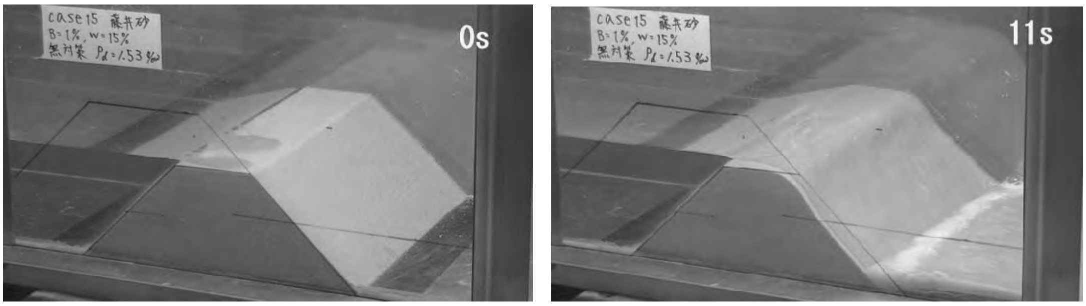

a) t=0 seconds since start of over-flowing b) t=11 seconds

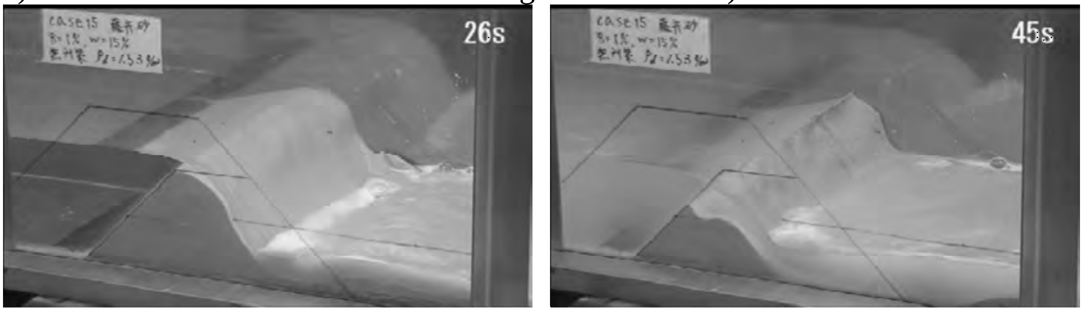

c) t=26 seconds d) t=45 seconds

Figure 6. Model 1

Model 2 (Figure 7):

The start of backfill erosion delayed by covering the up- and down-stream slopes. However, once the sand bags on the downstream slope were lost, then very fast erosion started. Model 2 also fully collapsed by the over-flowing tsunami current. Although this model survived the over-flowing tsunami current better than model 1 due to a resistance against erosion, it completely collapsed for about 90 seconds.

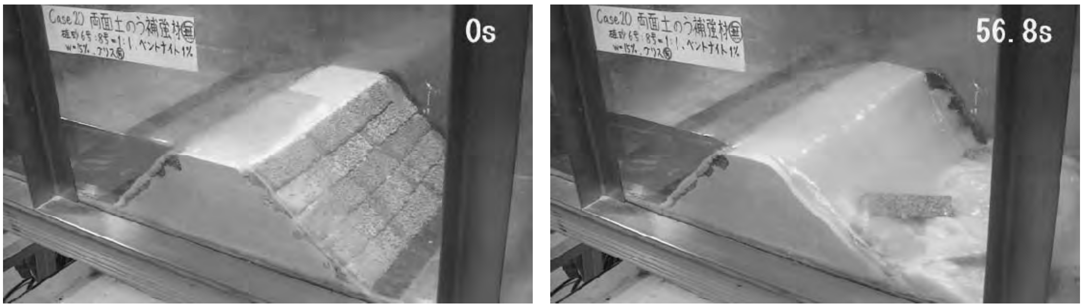

a) t=0 seconds since start of over-flowing b) t=56.8 seconds

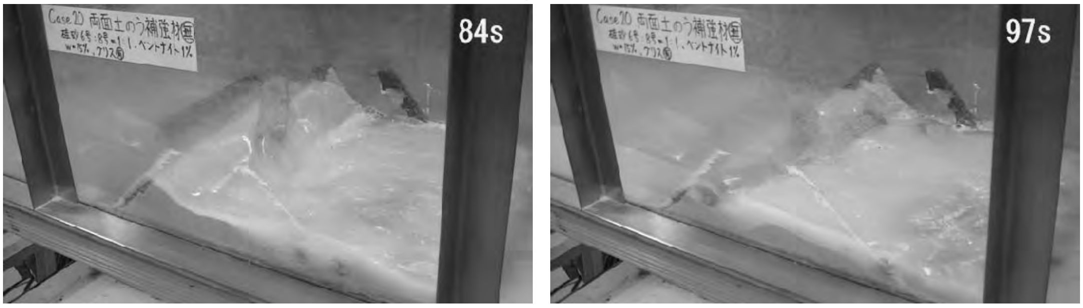

c) t=84 seconds d) t=97 seconds

Figure 7. Model 2

Model 3 (Figure 8):

As seen from Figure 8, this model fully collapsed by the following process: 1) As seen from Figure 8b, the bottom soil bag of the downstream slope was first washed away triggered by erosion of the backfill immediately behind. 2) As seen from Figure 8c, fast erosion of the backfill started from the downstream slope. 3) As seen from Figure 8d, the full-section of the dike was finally lost. However, Figure 8 shows that the improvement of the crest of the embankment increased the resistance against erosion starting from the crest. This model survived the over-flowing tsunami for 440 seconds.

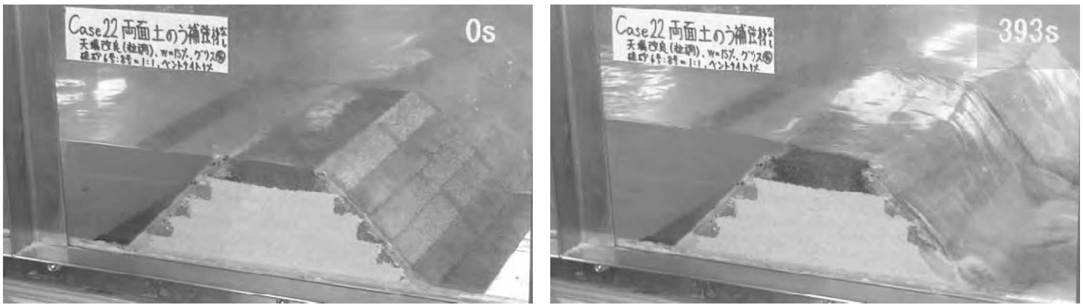

a) t=0 seconds since start of over-flowing b) t=393 seconds

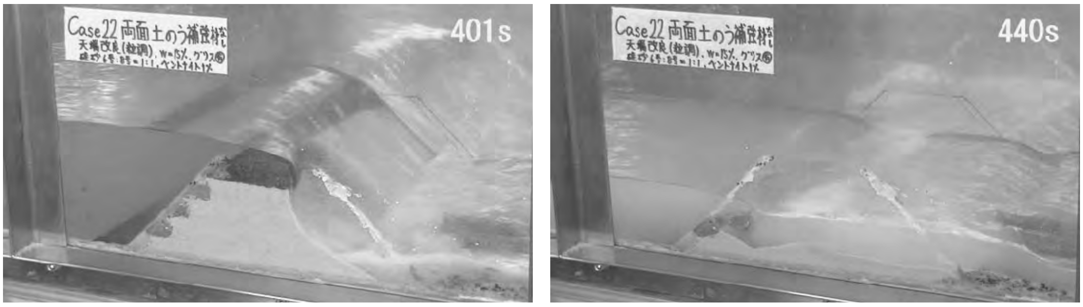

c) t=401 seconds d) t=440 seconds

Figure 8. Model 3

Model 4 (Figure 9; a model of the Geosynthetic-Reinforced Soil coastal dike):
The collapse took place more slowly by some better resistance of the reinforced backfill against erosion. The erosion took place one soil layer by one soil layer. Therefore, it is easy to reconstruct after the over-flowing tsunami current. Although this model survived the over-flowing tsunami current better than models 1-3 due to a higher resistance against erosion, this model survived for 860 seconds.

Model 5 (Figure 10):
Figure 10 shows the behavior of model 5. The model survived very well the over-flowing tsunami current without exhibiting any significant erosion of the backfill. The improvement of the crest of the embankment increased the resistance against erosion starting from the crest. This model survived for 1750 seconds.

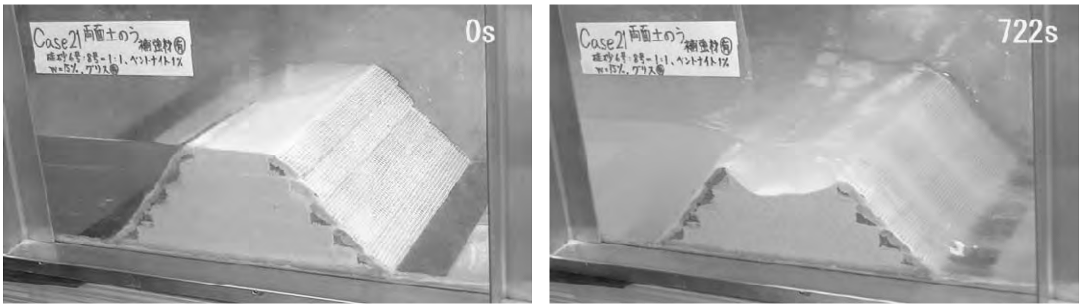

a) t=0 seconds since start of over-flowing b) t=722 seconds

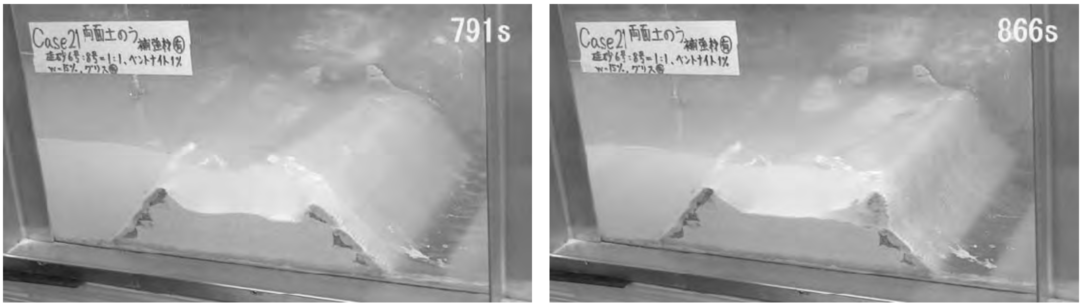

c) t=791 seconds d) t=866 seconds

Figure 9. Model 4

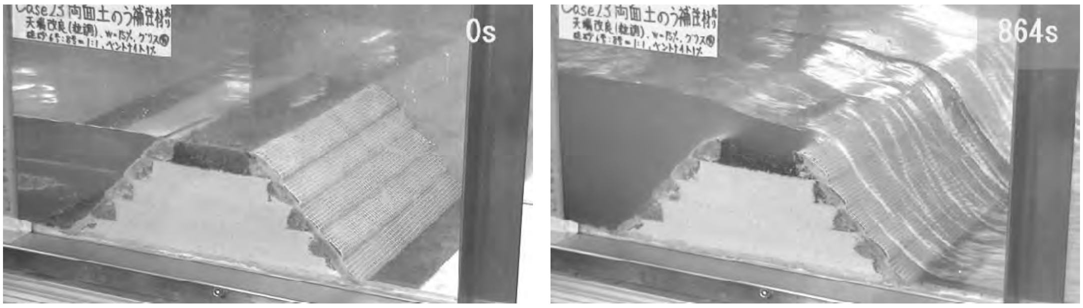

a) t=0 seconds since start of over-flowing b) t=864 seconds

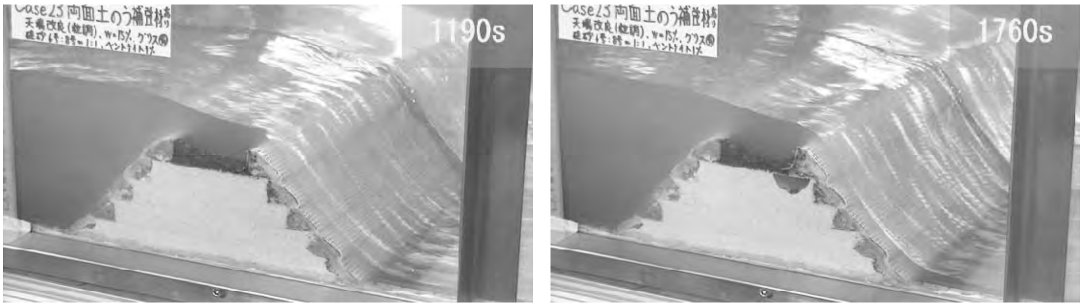

c) t=1190 seconds d) t=1760 seconds

Figure 10. Model 5

4. CONCLUSIONS

The following conclusions with respect to the stability of fill-type coastal dike against the over-flowing tsunami current can be drawn from the test results presented above:

1. When the backfill was not reinforced and not covered with facing, very fast erosion of the backfill started from the downstream slope and the full cross-section was quickly lost.
2. The rate of backfill erosion decreased by reinforcing the backfill with geogrid layers.
3. The start of backfill erosion delayed by covering the up- and down-stream slopes. However, once the sand bags on the downstream slope were lost, then very fast erosion started.
4. Geosynthetic-Reinforced Soil (GRS) coastal dike exhibited high residence against erosion. And the erosion took place one soil layer by one soil layer.
5. The improvement of the crest of the embankment increased the resistance against erosion starting from the crest.

The stability against over-flowing tsunami current of the models was evaluated by the retention ratio of cross-sectional area seen from the side (Figure 11). For the over-flowing tsunami current, models 4-5 exhibit a higher retention ratio of cross-sectional area than models 1-3. The process of fast erosion with models 1-2 are readily seen from a significantly decreasing rate of the retention ratio. Model 5 exhibited essentially no loss in the cross-section. Model 4 also exhibited good performance against the over-flowing tsunami current.

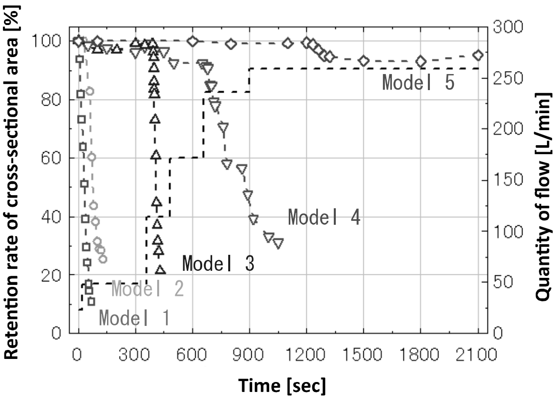

Figure 11. Retention of cross-sectional area after the start of over-flowing tsunami current

REFERENCES

Kosa, K., 2012. Damage analysis of bridges affected by tsunami due to Great East Japan Earthquake. *Proc. International Sym. on Engineering Lessons Learned from the 2011 Great East Japan Earthquake*, March, Tokyo, Japan, 1386-1397.

Tatsuoka, F., Koseki, J., Tateyama, M., Munaf, Y. and Horii, N., 1998. *Seismic stability against high seismic loads of geosynthetic-reinforced soil retaining structures*, Proc. 6th Int. Conf. on Geosynthetics, Atlanta, 1, 103-142.

Tatsuoka, F., Tateyama, M., and Koseki, J., 2012. GRS structures recently developed and constructed for railways and roads in Japan, *Proc. Second International Conference on Transportation Geothehnics*, IS-Hokkaido, Miura et al., eds., 63-84.

Tatsuoka, F., Hirakawa, D., Nojiri, M., Aizawa, H., Nishikiorim H., Soma, R., Tateyama, M. and Watanabe, K., 2009. A new type integral bridge comprising geosynthetic-reinforced soil walls, *Geosynthetics International* 16, 301-326.

The 2011 Tohoku Earthquake Tsunami Joint Survey (TTJS) Group, 2014. (http://www.coastal.jp/ttjt/), *The 2011 off the Pacific coast of Tohoku Earthqukake Tsunami Information*.

Yamaguchi, S., Yanagisawa, M., Kawabe, S., Tatsuoka, F., Nihei, Y., 2013. *Evaluation of the stability of various types of coastal dyke against over-flowing tsunami current,* Design and Practice of Geosynthetic-Reinforced Soil Structures, October, Italy, 572.

Yamaguchi, S., Yanagisawa, M., Uematsu, Y., Kawabe, S., Tatsuoka, F., and Nihei, Y., 2012, Experimental evaluation of the stability of GRS coastal dyke against over-flowing tsunami, *Proc. 47th Japan National Conference on Geotechnical Engineering*, 1809-1810.

A study on applicability of dewatering method as a countermeasure for liquefaction

Yuki HORIUCHI[1], Toru SEKIGUCHI[2] and Shoichi NAKAI[2]
[1]Graduate student, Dept. of Civil Engineering, the University of Tokyo, Japan
y-hori@iis.u-tokyo.ac.jp
[2]Professor, Chiba University, Japan

ABSTRACT

Dewatering method with sheet pile enclosure is one of the liquefaction countermeasures. It is economical and highly effective for reclaimed land. Chiba City government, in Japan, conducted the demonstration test of this proposed method in Mihama ward. In the present study, the centrifugal model test was performed based on the demonstration test and this method was confirmed to be effective. It was observed that sheet piles restricted pore water dispersion, which may enlarge structure settlement but it also restricted ground movement, which reduced structure tilting. In addition, applicability of this method in Mihama ward was considered. Ground structure model which is usually used for an earthquake hazard map was improved and the suitable areas to apply the proposed method were identified, considering from three points of view. The measure should be applied to the location with high risk of liquefaction. The place needs an enough thick cohesive soil layer to prevent groundwater influx. The depth of the cohesive soil layer should not be too deep to reduce construction costs of sheet pile. The results show Mihama ward has complex ground structure, and finally the application map was produced as an example.

Keywords: liquefaction, centrifugal model test, groundwater revel, geologic map

1. INTRODUCTION

A number of houses built in the reclaimed land in the coast of Tokyo Bay were damaged due to liquefaction at Great East Japan Earthquake. A countermeasure for the liquefaction was considered and Chiba City government conducted the demonstration test of dewatering method in Mihama ward. The proposed method is to pumping up the groundwater within the area surrounded by the sheet pile enclosure to lower the ground water level, as shown in Figure 1.

In the present study, the centrifugal model test was performed simulating the proposed method and effectiveness of this measure was examined. In addition, applicability of this measure in Mihama ward was considered. The ground structure model which is usually used for an earthquake hazard map was improved and the suitable areas to apply the proposed measure were considered.

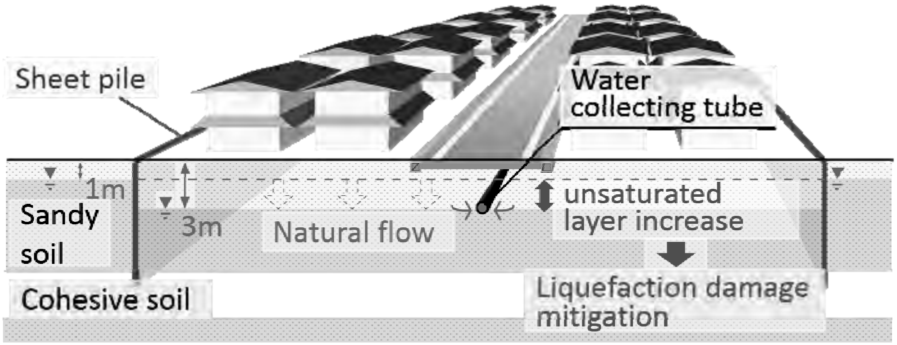
Sheet pile
Water collecting tube
1m
Sandy soil
3m
Natural flow
unsaturated layer increase
Cohesive soil
Liquefaction damage mitigation

Figure 1: The concept of the dewatering method with sheet pile enclosure

2. EFFECTIVENESS OF THE PROPOSED MEASURE IN MIHAMA WARD

2.1 Overview of the model test

Table 1 presents test cases. Case 1 and Case 1’ simulated original ground conditions.

Figure 2 illustrates location of the measuring sensors in Case 3 as real size. Inner size of shear box was 770mm × 470mm × 370mm. The model ground was prepared using No.7 silica sand and 5% of kaolin clay (Dr≒35%) by air pluviation and pore fluid of silicon oil. Water pressure gauges were set at depth of 2, 4 and 6m. The structure model of detached two stories house was put in the center of ground surface. The size of the structure foundation was 4.5m square and depth of footing was 0.5m. The mean contact pressure of the structure was 21.8kPa. The left side of the structure was heavier than the right side. The contact pressure of the left side was 25.9kPa and that in right side was 17.9kPa, respectively.

Figure 3 shows the input wave.

Figure 4 is the photo of model and shaking table set in the centrifugal equipment. 30g was applied on the model and when the value of all the gauges stabilized in 30g field, input wave was applied.

Table 1: Test cases

Test cases	Groundwater level (G.L.)	Sheet pile
Case 1	–1m	Not exist
Case 1’	–0.5m	
Case 2	–3m	
Case 3	–3m –1m (Inside of sheet pile)	exist

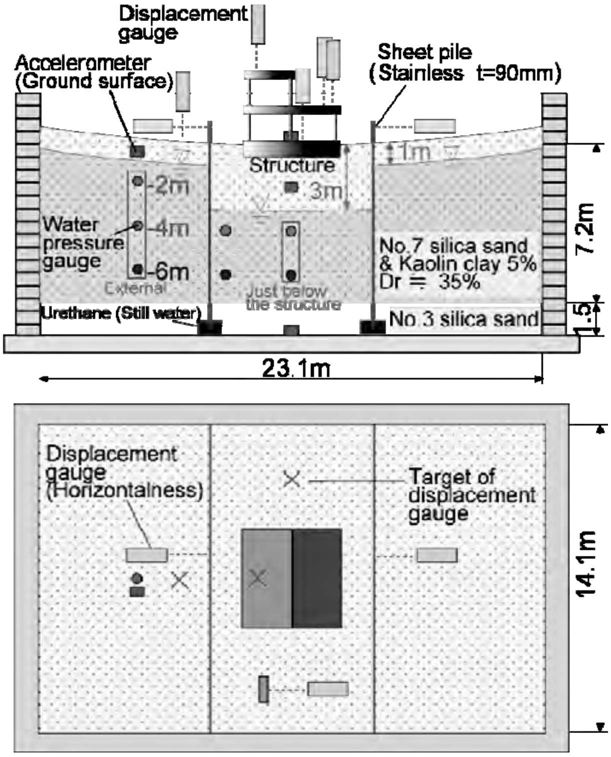
Displacement gauge
Accelerometer (Ground surface)
Sheet pile (Stainless t=90mm)
Structure
1m
3m
-2m
-4m
-6m
Water pressure gauge
External
Just below the structure
No.7 silica sand & Kaolin clay 5% Dr ≒ 35%
Urethane (Still water)
No.3 silica sand
7.2m
1.5
23.1m
Displacement gauge (Horizontalness)
Target of displacement gauge
14.1m

Figure 2: Instrument layout drawing,
the upper part: Cross section
the lower part: A plane figure
Case 3, converted size

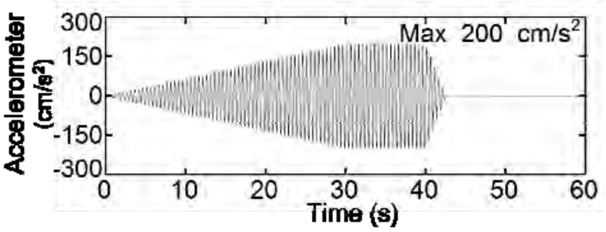

Figure 3: Target of input wave

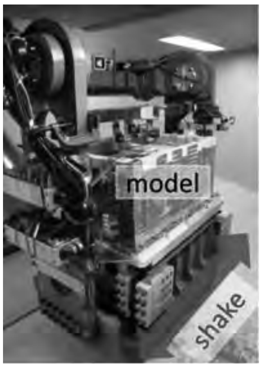

Figure 4: model and shaking table

2.2 Results of the tests

Figure 5 illustrates the overview of test cases. Figure 6 presents the time history of input wave, acceleration of ground surface, acceleration of structure, excess pore water pressure ratio of just below the structure and external ground. In those figures, converted values based on the similarity rule are presented. The acceleration of ground surface and structure reduced when liquefaction occurred at some depth. The excess pore water pressure ratio of just below the structure was small by effective vertical stress increment in comparison with external ground. As for the excess pore water pressure ratio of external ground, the layer of –2m in Case 1 and Case1’ liquefied but the layer of –4m in Case 2 didn’t liquefy nevertheless both were the same 1m below of groundwater level. This result suggests that non-liquefaction layer was increased more than the unsaturated layer by dewatering.

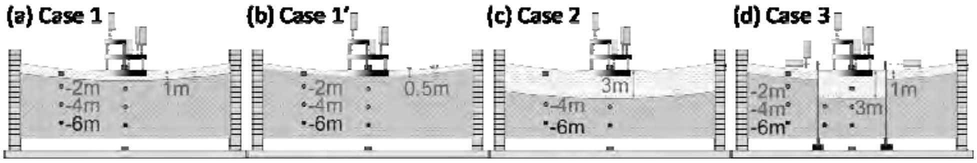

Figure 5: Overview of a test case

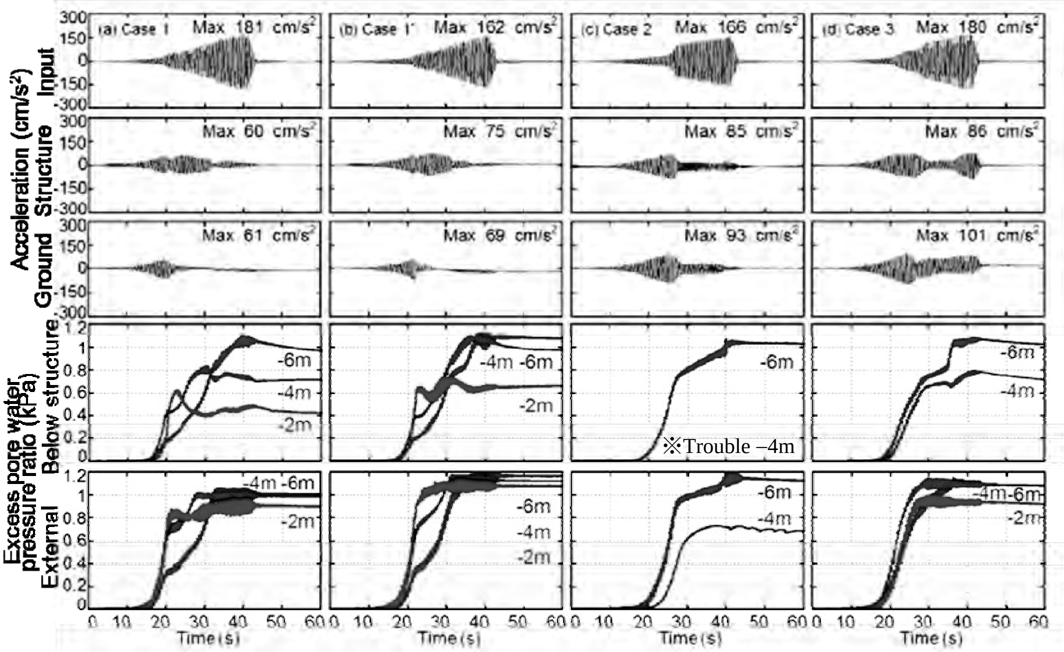

Figure 6: Time history of acc. wave and excess pore water pressure

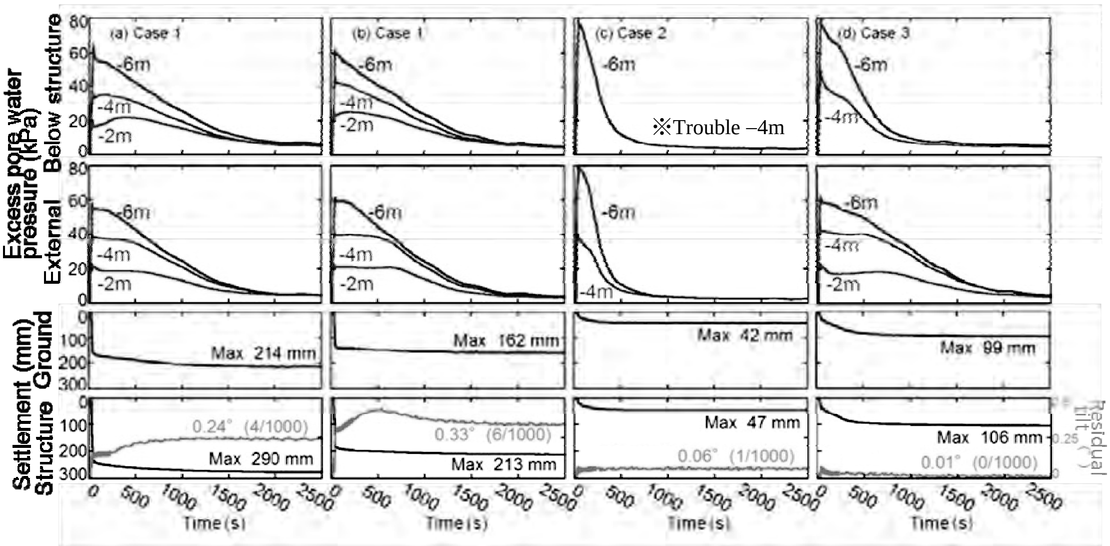

Figure 7: Time history of excess pore water pressure, ground settlement, structure settlement and tilting

Figure 7 shows the long time history of the excess pore water pressure of just below the structure and external ground, ground settlement, structure settlement and tilting. As groundwater level was lower, dispersion time of excess pore water pressure was decreasing and settlement was also decreasing. As for the excess pore water pressure of just below the structure, dispersion time for Case 3 was longer in comparison with Case 2. Settlement seemed to increase due to the prevention of the dissipation of water pressure by the sheet piles. The structure tilting of Case 2 and Case 3 was as small as 1/1000 or less. The constraint effect of the sheet pile reduced the structure tilting of Case 3 in comparison with Case 2.

Figure 8 shows ground surface after the experiment of Case 1 and Case 2. The sand boiling was observed in the edge of the box and near the structure in Case 1.

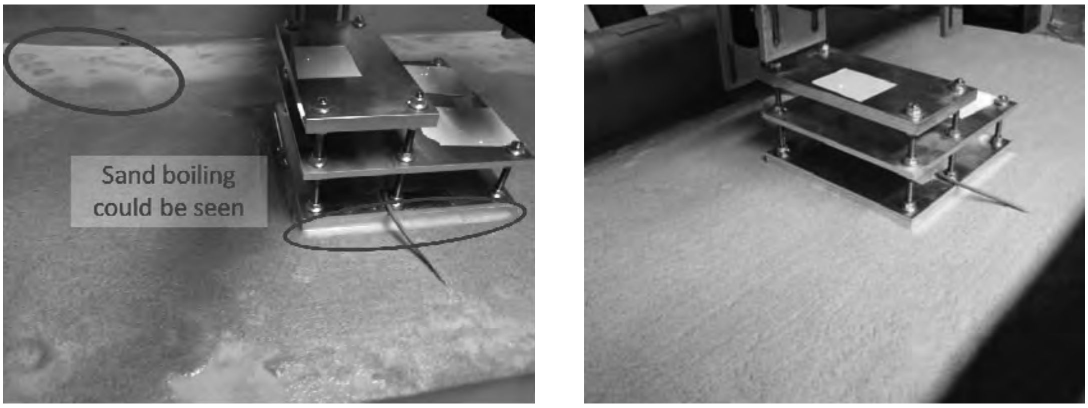

Figure 8: Appearance after the experiment, left: Case 1, right: Case 2

3. APPLICABILITY OF THE PROPOSED MEASURE IN MIHAMA WARD

3.1 Geological structure of Mihama ward

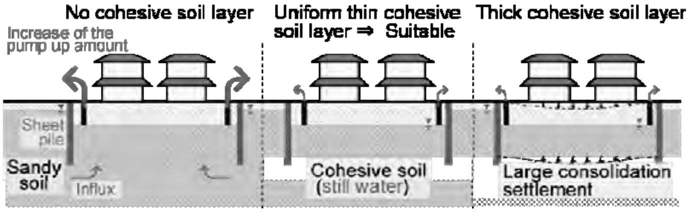
No cohesive soil layer
Increase of the pump up amount
Uniform thin cohesive soil layer ⇒ Suitable
Thick cohesive soil layer
Sheet pile
Sandy soil
Influx
Cohesive soil (still water)
Large consolidation settlement

Figure 9: The difference due to the thickness of cohesive soil

As shown in the Figure 9, lowering the water table within the enclosed area, sheet piles should be constructed from ground surface to cohesive soil layer. Then the cohesive soil layer should exist in order to prevent groundwater influx. However, the cohesive soil layer should not be too thick because it may cause excessive settlement due to consolidation. Therefore cohesive soil layer of appropriate thickness is necessary for the proposed measure.

To consider the applicability of the proposed measure in Mihama ward, the geological structure of Mihama ward should be examined. The cross section of the ground along the lines A-A' to G-G' in Figure 10 was reconstructed by the ground structure model proposed by Murakata et al. (2009). The two long cross section lines, A-A' and B-B', parallel to the coastline of

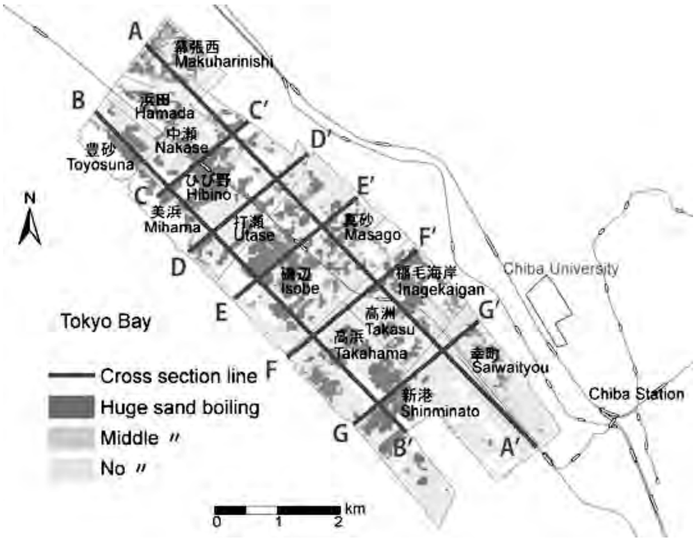
A
幕張西 Makuharinishi
B
浜田 Hamada
中瀬 Nakase
C'
D'
豊砂 Toyosuna
ひび野 Hibino
E'
C
美浜 Mihama
打瀬 Utase
真砂 Masago
F'
N
D
磯辺 Isobe
稲毛海岸 Inagekaigan
Chiba University
Tokyo Bay
E
高洲 Takasu
G'
高浜 Takahama
幸町 Saiwaityou
Cross section line
F
Huge sand boiling
Middle 〃
No 〃
新港 Shinminato
Chiba Station
G
B'
A'
0 1 2 km

Figure 10: The distribution of sand boiling in Mihama ward and positions of cross section line

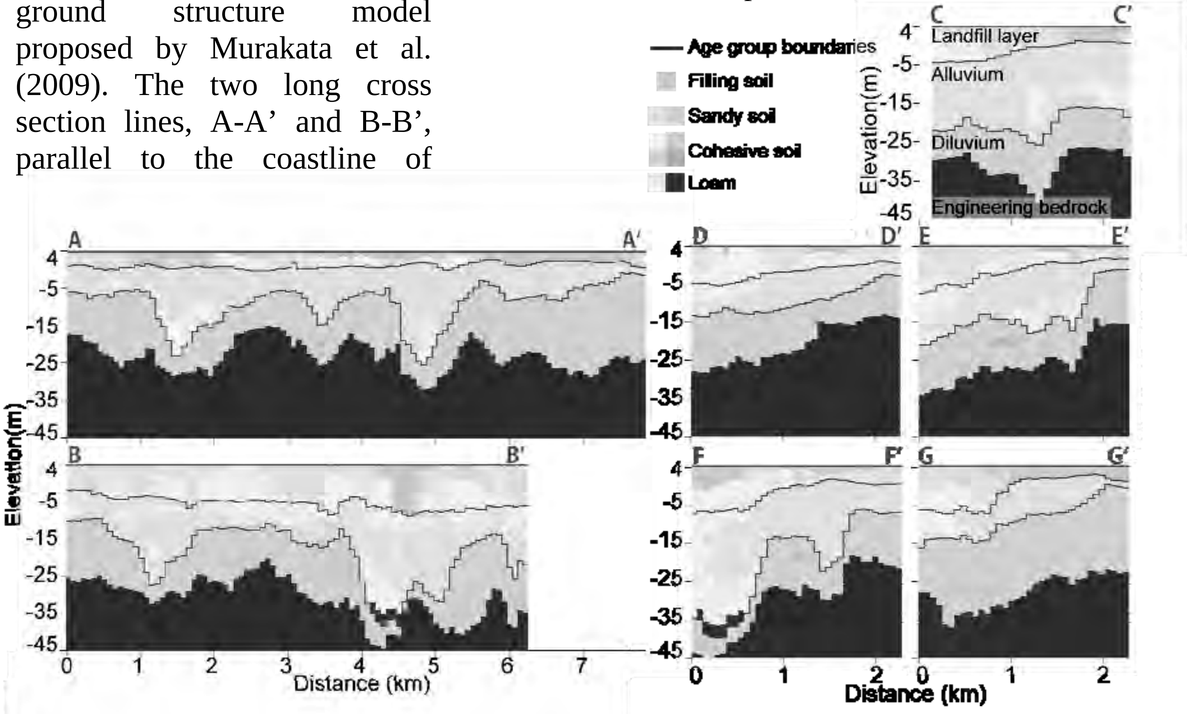

Figure 11: Geological cross section, left: long lines, right: short lines

Tokyo Bay and the five short lines, C-C’ to G-G’, perpendicular to the coastline were shown. The distribution of sand boiling damages due to Great East Japan Earthquake was also presented.

Figure 11 illustrates the cross sections. The geological features and age group boundaries were indicated. In long lines, A-A’ and B-B’, the drowned valley was observed. In short lines, it is found that the sandy soil layer spread below the observed sand boiling. The thick cohesive soil layer was observed in near the coast. The uniform and thin cohesive soil layer was observed in the middle of D-D’ and F-F’. It is indicated that Mihama ward has a complex geological structure.

3.2 Applicability of the proposed measure in Mihama ward

The suitable areas to apply the proposed measure were identified, considering from three points of view. The location should be of high risk of liquefaction. The place needs cohesive soil layer of enough thickness to prevent groundwater influx as shown in the Fig.9. The cohesive soil layer should not be too deep to reduce construction costs of sheet pile. These geological features were computed quantitatively using improved ground structure model. Figure 12 shows the distribution of the shallowest cohesive soil layer, of those thickness and upper boundary. A very thin cohesive soil layer of less than 1.5m was neglected. A cohesive soil layer was not observed in Saiwaicho and northeast of Masago. In addition, thick cohesive soil layer was observed near the coast areas such as southwest of Isobe. These areas were not suited for the proposed measure. On the other hand, middle of Shinminato was not suited for the measure because the cohesive soil layer was too deep. In this way, it was possible to catch the complexity of the geological structure which was not captured in cross sections.

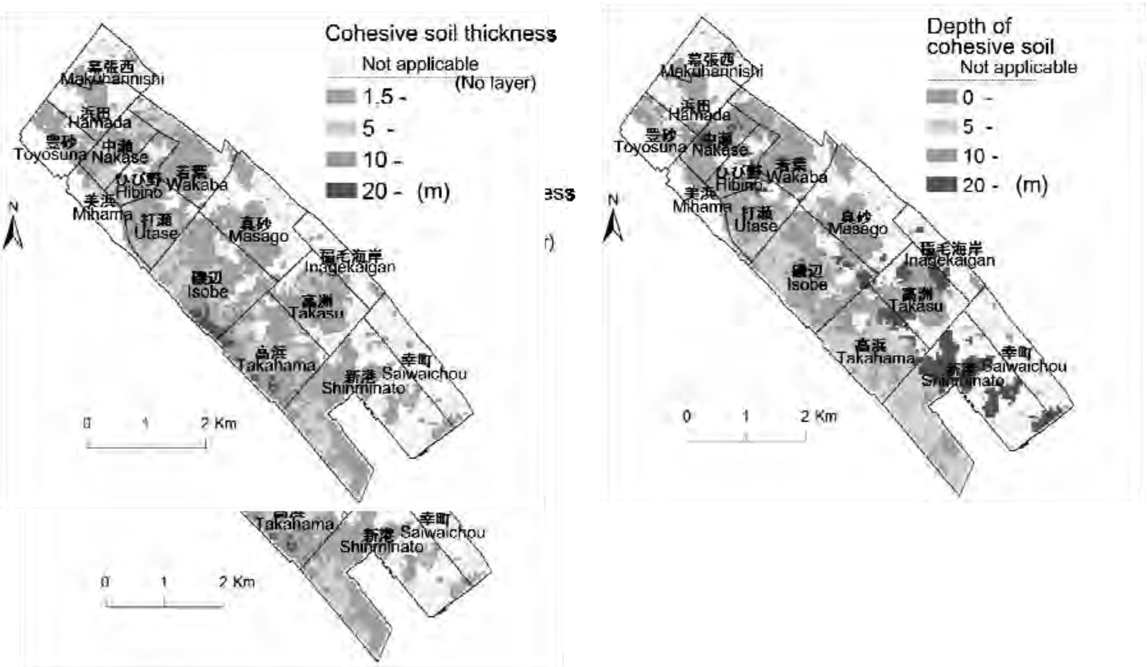
Cohesive soil thickness
Not applicable (No layer)
1.5 -
5 -
10 -
20 - (m)
Depth of cohesive soil
Not applicable
0 -
5 -
10 -
20 - (m)
N
幕張西 Makuharinishi
浜田 Hamada
豊砂 Toyosuna
中瀬 Nakase
ひび野 Hibino
若葉 Wakaba
美浜 Mihama
打瀬 Utase
真砂 Masago
稲毛海岸 Inagekaigan
磯辺 Isobe
高洲 Takasu
高浜 Takahama
新港 Shinminato
幸町 Saiwaichou
0 1 2 Km

Figure 12: The distribution maps, left: cohesive soil thickness, right: sandy soil thickness

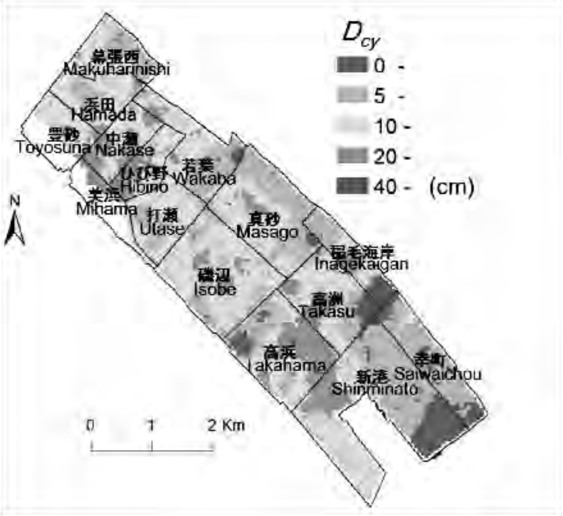
D_{cy}
0 -
5 -
10 -
20 -
40 - (cm)
幕張西 Makuharinishi
浜田 Hamada
豊砂 Toyosuna
中瀬 Nakase
ひび野 Hibino
若葉 Wakaba
美浜 Mihama
打瀬 Utase
真砂 Masago
稲毛海岸 Inagekaigan
磯辺 Isobe
高洲 Takasu
高浜 Takahama
新港 Shinminato
幸町 Saiwaichou
N
0 1 2 Km

Figure 13: The distribution map of D_{cy}

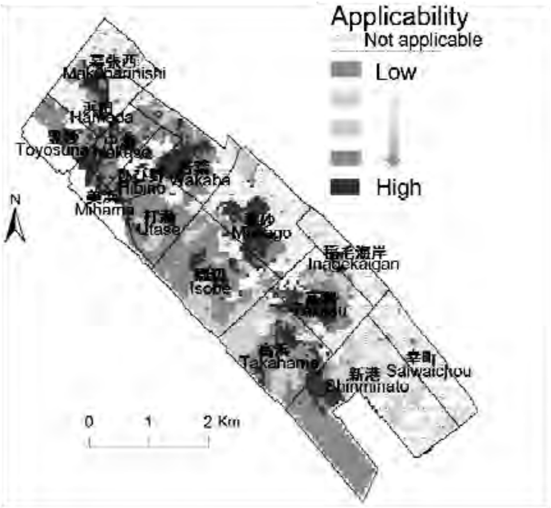
Applicability
Not applicable
Low
High
幕張西 Makuharinishi
浜田 Hamada
豊砂 Toyosuna
中瀬 Nakase
ひび野 Hibino
若葉 Wakaba
美浜 Mihama
打瀬 Utase
真砂 Masago
稲毛海岸 Inagekaigan
磯辺 Isobe
高洲 Takasu
高浜 Takahama
新港 Shinminato
幸町 Saiwaichou
N
0 1 2 Km

Figure 14: The applicability map

Figure 13 illustrates the distribution map of D_{cy}, settlement expected due to liquefaction. In a lot of areas, value of D_{cy} was more than 10 cm, which corresponds to the location of sand boiling (Fig.10). D_{cy} was estimated in each mesh in the same way as the geological features.

Figure 14 shows the distribution map of applicability of the proposed measure as an example. In the evaluation, following factors were taken into account.

a) Consolidation settlement,
b) Depth of cohesive soil layer,
c) D_{cy}

a) and b) reflected the efficiency of the construction and c) represents liquefaction risk. Consolidation settlement was calculated roughly in each mesh as one-dimensional vertical calculation when the groundwater level was dropped from −1m to −3m. Only plastic deformation was considered in landfill soil and alluvium soil. The increase of vertical effective stress due to groundwater drawdown was considered following the concept of Yasuda (2013). Required soil parameters for calculating ground conditions was determined based on the literature and the report of demonstration test in Mihama ward. Southwest of Masago and Takahama and middle of Isobe were found to be fit to the proposed measure.

4. CONCLUSION

A series of centrifugal model tests simulating the dewatering method was performed and the proposed measure was confirmed to be effective. The result suggests the following findings.

・Non-liquefaction layer was increased more than the unsaturated layer by dewatering.

・By dewatering, dissipation of excess pore water pressure was accelerated, which reduce settlement. The structure tilting became 1/4 or less compared to original condition.

・By the sheet pile, settlement increased due to the delay of the dissipation of excess pore water pressure. On the other hand, the structure tilting became smaller due to the constraint effect.

In addition, applicability of the proposed measure was indicated as a distribution map using improved ground structure model in Mihama ward.

REFERENCES

Architectural Institute of Japan, 2001. Building foundation structure design guidelines.

Steel pipe pile, steel sheet pile Technology Association, Steel sheet pile standard, http://www.jaspp.com/index.html.

Geotechnical Society, 1990. Commentary with the methods of the soil test, 121.

Murakata, K., Sekiguchi, T. and Nakai, S., 2009. Evaluation of ground motion amplification characteristics based on the ground model that takes into account the geological cross section, *Japan Association for Earthquake Engineering Competition*, 210-211.

Sekiguchi, T., and Nakai, S., 2012. Influence of surface ground structure that gave the liquefaction damage in Mihama ward, Chiba city, *Japan Association for Earthquake Engineering Papers* 5, 21-35.

Sekiguchi, T., and Nakai, S., 2012. Relationship of landfill ground structure and liquefaction damage distribution in Mihama ward, Chiba city, *Architectural Institute of Japan Collection*, 469-470.

Yasuda, S., 2013. Features of damage and countermeasures of housing land, road and the lifeline, *GeoKanto 2013, Special Session.*

Evaluation of seismic performance for typical reinforced concrete buildings in downtown area of Yangon City

Nwe Ni MYINT
PhD Student, Department of Civil Engineering,
Yangon Technological University
nwenimyint28@gmail.com

ABSTRACT

The purpose of this study is to evaluate seismic performance for generic archetypal Reinforced Concrete (RC) buildings in downtown area of Yangon. Most of the buildings in downtown area of Yangon are regular both in plan and in elevation and designed for gravity loads only. These buildings have limited lateral resistance and are susceptible to story mechanisms during earthquake loading. Seismic performance level of buildings are essential to assess the seismic vulnerability of Gravity Load Design (GLD) RC buildings in Yangon. The variable parameters are the number of storeys and the level of seismic design, in terms of design Peak Ground Acceleration and design ductility level. Plastic hinge is used to represent the failure mode in the beams and columns when the member yields. The pushover analysis is performed using ETABS software to assess Life Safety performance under seismic effects. Base shear versus tip displacement curve of the structure, called pushover curve, is an essential outcomes of pushover analysis for two actions of the plastic hinge behavior, force-controlled (brittle) and deformation-controlled (ductile) actions. Seismic structural capacity values will be selected corresponding to the performance levels or damage states as specified in FEMA-356.

Keywords: seismic performance, seismic vulnerability, peak ground acceleration, pushover analysis

1. INTRODUCTION

Earthquakes cause significant human suffering and damage to build environment that includes buildings, water, gas, power supply, and transportation systems. This study is concerned with assessment and evaluation of seismic performance for buildings in the downtown region of Yangon. Yangon City, the largest economic center of Myanmar, has about 5.14 million population (2011) and is experiencing rapid urbanization. This current rapid urbanization is putting more pressure on the existing old infrastructures in Yangon City and concerns for the deterioration of its urban environment are growing. Estimates of structural capacity to disaster are of direct value to those making decisions including engineers, city planners, emergency services, and also for optimizing the allocation of resources for maintenance, repair, and rehabilitation of buildings.

1.1 Seismic hazard in yangon region

Most of Myanmar's urban cities developed in the proximity of active seismic sources and are at risk of experiencing earthquake events. Among the many seismic sources in Myanmar, the Sagaing and Kyaukkyan faults produced significant earthquakes in the past. Yangon is located 35km from the west of the Sagaing fault and on the southern spur of NNW-SSE trending Bago anticlinal ridge. Based on the seismicity and the previous records, Yangon region is assumed as low to medium seismicity region. The most significant earthquake in this region is the Bago earthquake on 5th May, 1930 with the magnitude of 7.3. This earthquake caused 500 casualties and great destructions in Bago and considerable damages and 50 deaths were recorded in Yangon.

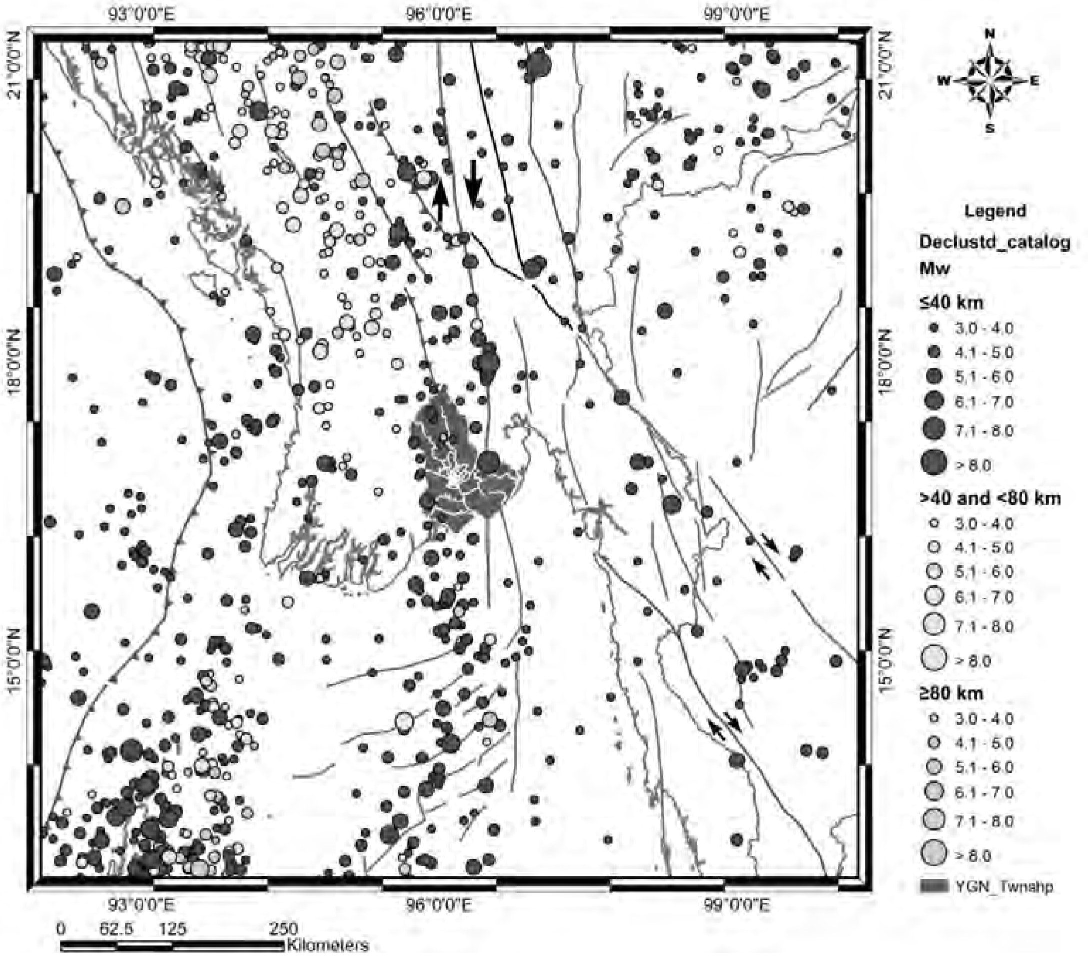
93°0'0"E
96°0'0"E
99°0'0"E
21°0'0"N
18°0'0"N
15°0'0"N
N
S
W
E
Legend
Declustd_catalog
Mw
≤40 km
3.0 - 4.0
4.1 - 5.0
5.1 - 6.0
6.1 - 7.0
7.1 - 8.0
> 8.0
>40 and <80 km
3.0 - 4.0
4.1 - 5.0
5.1 - 6.0
6.1 - 7.0
7.1 - 8.0
> 8.0
≥80 km
3.0 - 4.0
4.1 - 5.0
5.1 - 6.0
6.1 - 7.0
7.1 - 8.0
> 8.0
YGN_Twnshp
0
62.5
125
250
Kilometers

Figure 1: The seismicity of Yangon Region
(Data Source – ANSS earthquake catalog, 1963 –2009)

Table 1: Some records of earthquakes in Yangon and surrounding areas

Date	Location	Magnitude and/or brief description
1568	Yangon	Collapsed of the upper part of the Shwedagon Pagoda
1661	Yangon	Fell down of Htee (umbrella) with Magaik (pillar of umbrella) of the Shwedagon Pagoda
1664	Yangon	Fell down of Magaik of the Shwedagon Pagoda
1668	Yangon	Collapsed of the topmost portion of the Shwedagon Pagoda and falling down of Htee
27 Dec. 1927	Dedaye	M_L=7;Severe destruction of building in Yangon including extending to Dedaye, Tharrawaddy, Maubin and Pyapon districts (felt over 5000 square miles)
9 Sept. 1970	Dedaye	Hits of moderate intensity and some damage in Yangon

Source: Seismic sources in Myanmar by Seismotectonics Research Division

1.2 Building inventory

Generic buildings are defined by structural geometry, typical structural components and methods of design. Low- and mid-rise reinforced concrete (RC) frame buildings represent a common type of construction in downtown area of Yangon and this region has higher population than others.

In this study, the building data in downtown area collected by YCDC are used for the classification of buildings based on the structural type, number of stories. There are six townships in downtown area: Pazundaung, Botahtaung, Kyauktada, Pabedan , Latha and Lanmadaw .In these area, the building types are masonry and reinforced concrete and the number of stories are in the low-rise to mid-rise stories range. Based on the number of stories, buildings are classified as low-rise (1 to 5 story) and mid-rise (6 to 12 story). Based on this inventory data, 3stories, 5stories, 6 stories, 8 stories and 12 stories RC frame buildings are selected to represent the generic GLD RC frame buildings in the study area.

2. NONLINEAR STATIC ANALYSIS

Nonlinear static (pushover) analysis is used to quantify the resistance of the structure to lateral deformation. In general, a sequence of inelastic static analysis is performed on the structural model of the building by applying a predefined lateral load pattern which is distributed along the building height. The lateral forces are then monotonically increased until it becomes unstable and reaches the collapse state (force controlled) or its roof displacement reaches the predetermined limit (displacement controlled).

Nonlinear static analysis procedures include the capacity spectrum method (CSM) that uses the intersection of the capacity (pushover) curve and a reduced response spectrum to estimate maximum displacement; the displacement coefficient method that uses pushover analysis and a modified version of the equal displacement approximation to estimate maximum displacement; and the secant method that uses a substitute structure and secant stiffness.

Two key elements of a performance-based design procedure are demand and capacity. Demand is a representation of the earthquake ground motion. Capacity is a representation of the structure's ability to resist the seismic demand. The performance is dependent on the manner that the capacity is able to handle the demand. In other words, the structure must have the capacity to resist the demands of the earthquake such that the performance of the structure is compatible with the objectives of the design.

The nonlinear analysis of a structure is an iterative procedure and in this study, ETABS software is used and it have features to perform nonlinear static analysis. It has built-in defaults for ACI 318 material properties and ATC-40 and FEMA 273 hinge properties. Also it has capability for inputting any material or hinge property.

2.1 Structural Capacity

In general, structural capacity is defined as the maximum displacement, force, velocity, or acceleration that a member or a system can withstand without failure, or more specifically, without exceeding a prescribed performance level. The inter story drift capacity corresponding to the desired performance level is used as the structural capacity. The capacity values are considered corresponding to different performance levels as specified in FEMA-356 (2000) and those computed from nonlinear pushover analysis. The inter story drift capacity value described for different performance levels according to FEMA-356 (2000) are: Immediate Occupancy (IO), Life Safety (LS), and Collapse Prevention (CP). In this study for low- and mid-rise GLD RC frame buildings reduced drift capacity values of 1%, 2%, and 4% of the story height are used for IO, LS, and CP performance levels, respectively. These drift values are selected based on the approximate member level rotations for vertical elements suggested in FEMA-356 (2000).

Table 2: Structural performance levels specified in FEMA-356 (2000)

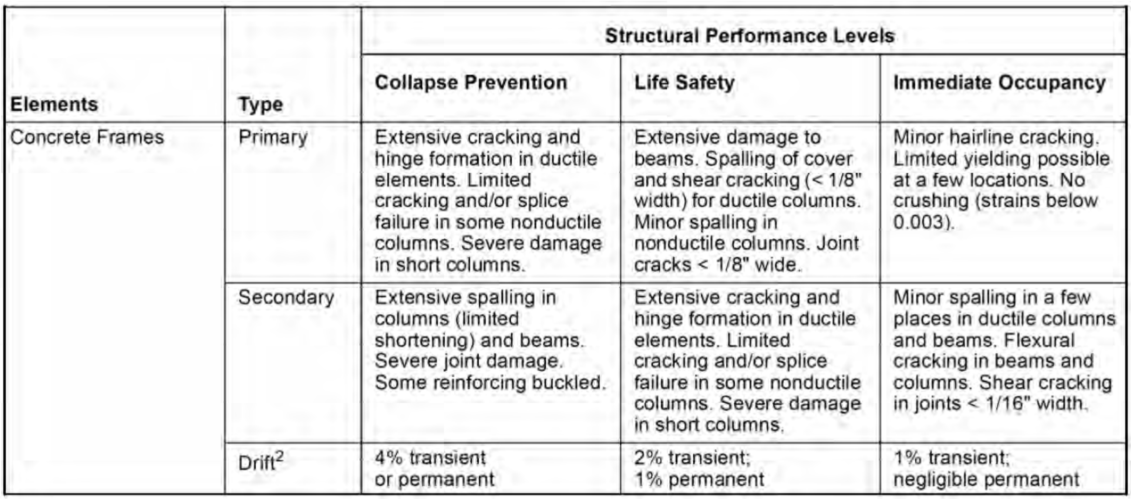

Elements	Type	Structural Performance Levels		
		Collapse Prevention	**Life Safety**	**Immediate Occupancy**
Concrete Frames	Primary	Extensive cracking and hinge formation in ductile elements. Limited cracking and/or splice failure in some nonductile columns. Severe damage in short columns.	Extensive damage to beams. Spalling of cover and shear cracking (< 1/8" width) for ductile columns. Minor spalling in nonductile columns. Joint cracks < 1/8" wide.	Minor hairline cracking. Limited yielding possible at a few locations. No crushing (strains below 0.003).
	Secondary	Extensive spalling in columns (limited shortening) and beams. Severe joint damage. Some reinforcing buckled.	Extensive cracking and hinge formation in ductile elements. Limited cracking and/or splice failure in some nonductile columns. Severe damage in short columns.	Minor spalling in a few places in ductile columns and beams. Flexural cracking in beams and columns. Shear cracking in joints < 1/16" width.
	Drift^2	4% transient or permanent	2% transient; 1% permanent	1% transient; negligible permanent

2.2 Nonlinear Hinge Property

In the present study, the nonlinear hinge properties as assigned in ETABS model are calculated as described in the following:

1. Axial load-bending moment (P-M) interaction surface:

P-M interaction surface determines the load at which a reinforced concrete section of the beam or column becomes inelastic and forms a hinge. For a given section geometry, material and reinforcement, P-M interaction surface are calculated according to ACI code (2002).

2. Moment-plastic rotation (M- θ_p) relation:

M- θ_p relation for a member section consists of plastic rotation and corresponding moments as ratio of yield moment .This relation affects the behavior of a section once a hinge forms there. Plastic hinge length required for this calculation was based on FEMA guidelines.

3. SELECTED CASE STUDIES AND ANALYSIS

In this study, pushover analysis will be carried out, modeling three-dimensional frame buildings using ETABS Software. Most of the buildings in downtown area of Yangon City are rectangular in shape and the sizes are generally (25ftx 50ft) and (25ftx40ft) in some streets. The building types are one unit apartment or two unit apartment in one floor. Floor to floor height is 9ft or 10ft for typical floor and varies from 10ft to 17ftfor ground floor. In this report, 3stories with one unit apartment and six stories with two unit apartment had been analysed for ground motion of 0.3g & 0.4g. These building are some existing generic residential buildings and the structural components are modelled according to the permitted drawings for construction by Yangon City Development Committee (YCDC). These models are analysed with live load of 40 psf for occupants, 20psf for roof and 15psf for finishing. Material strengths are f'_c=3000 psi and f_y=40000 psi. Data preparation for analysis and design are according to Uniform Building Code 1997 and ACI 318-99. Depending on the time period of the structure, 4 percentage of building height with nonlinear response was used as target displacement in the pushover analysis.

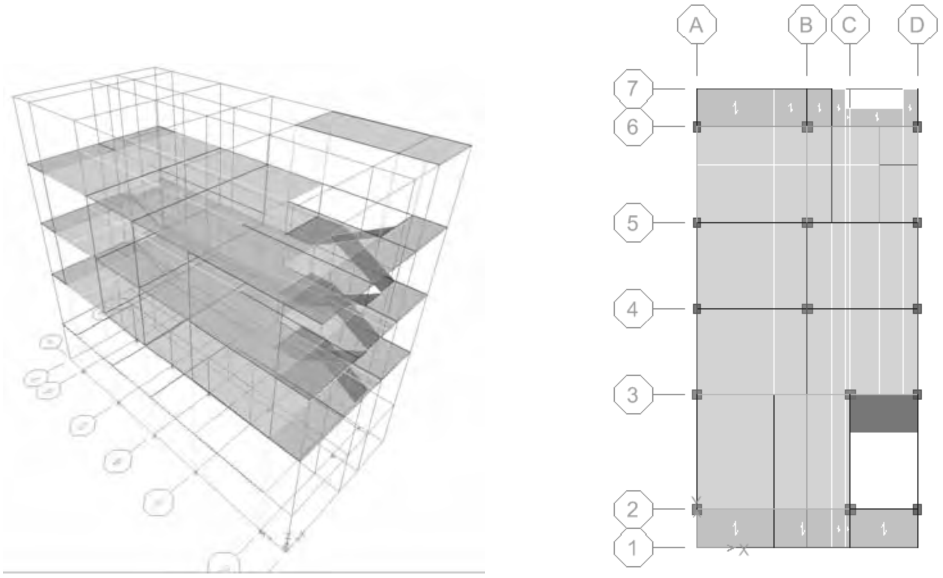

Figure 2: 3D View and Floor Plan of Structural Model for 3stories with 1unit apartment

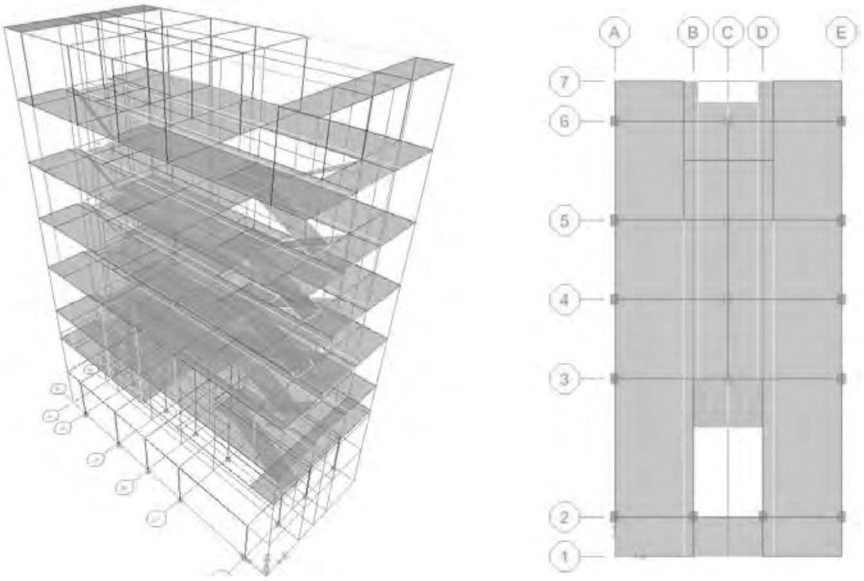

Figure 3: 3D view and floor plan of structural model for 6 stories with 2 unit apartment

3.1 Defining hinge properties

There are three types of hinge properties in the software: Default hinge property, User defined hinge property and generated hinge property. Only default hinge property are assigned to the frame elements. Default hinge properties are as per ATC-40 and FEMA 273.Moment and shear (M & V) hinges are considered for beam element and axial with biaxial moment (P-M-M) hinges are considered for column element

3.2 Defining static push over cases

For push over analysis, the gravity loading is applied as PUSH 1 and subsequently lateral displacement or lateral force is used as PUSH 2 in sequence to derive capacity curve and demand curve. It starts from previous pushover case as PUSHDOWN for gravity loads is considered for lateral loading as PUSH 2.

3.3 Pushover analysis results

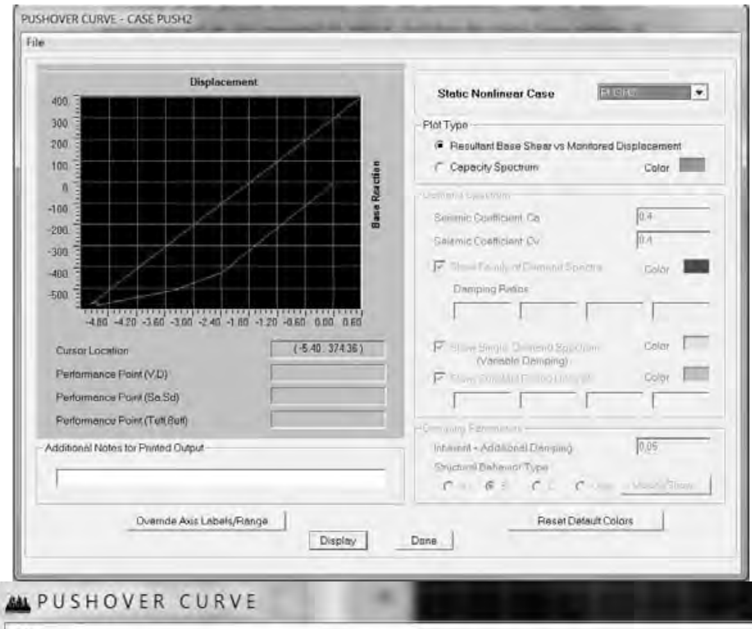
PUSHOVER CURVE - CASE PUSH2
File
Displacement
400
300
200
100
0
-100
-200
-300
-400
-500
-4.80
-4.20
-3.60
-3.00
-2.40
-1.80
-1.20
-0.60
0.00
0.60
Base Reaction
Performance Point (V,D)
Performance Point (Sa,Sd)
Performance Point (Teff,Beff)
Additional Notes for Printed Output
Damping Ratios
(Variable Damping)
Structural Behavior Type
Override Axis Labels/Range
Reset Default Colors
Display
Done

Static Nonlinear Case: PUSH2

Plot Type
● Resultant Base Shear vs Monitored Displacement
○ Capacity Spectrum

Cursor Location: (-5.40 , 374.36)

Seismic Coefficient Ca: 0.4

Seismic Coefficient Cv: 0.4

Inherent + Additional Damping: 0.05

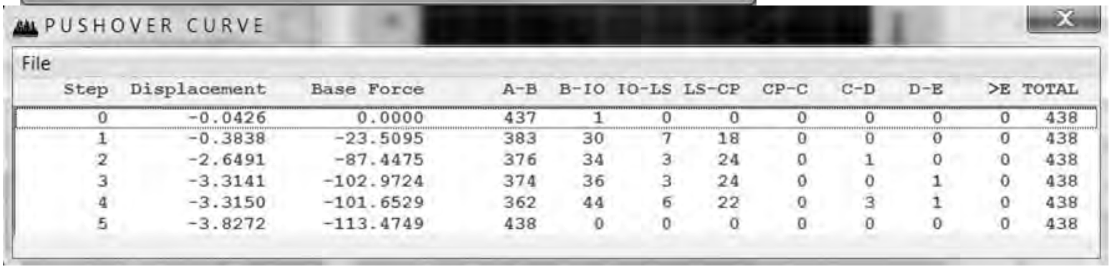

```
PUSHOVER CURVE
File
  Step  Displacement     Base Force      A-B  B-IO  IO-LS  LS-CP  CP-C   C-D   D-E   >E  TOTAL
   0       -0.0426         0.0000        437    1     0      0      0     0     0     0    438
   1       -0.3838       -23.5095        383   30     7     18      0     0     0     0    438
   2       -2.6491       -87.4475        376   34     3     24      0     1     0     0    438
   3       -3.3141      -102.9724        374   36     3     24      0     0     1     0    438
   4       -3.3150      -101.6529        362   44     6     22      0     3     1     0    438
   5       -3.8272      -113.4749        438    0     0      0      0     0     0     0    438
```

Figure 4: Pushover curve for 3 stories building with 1 unit apartment

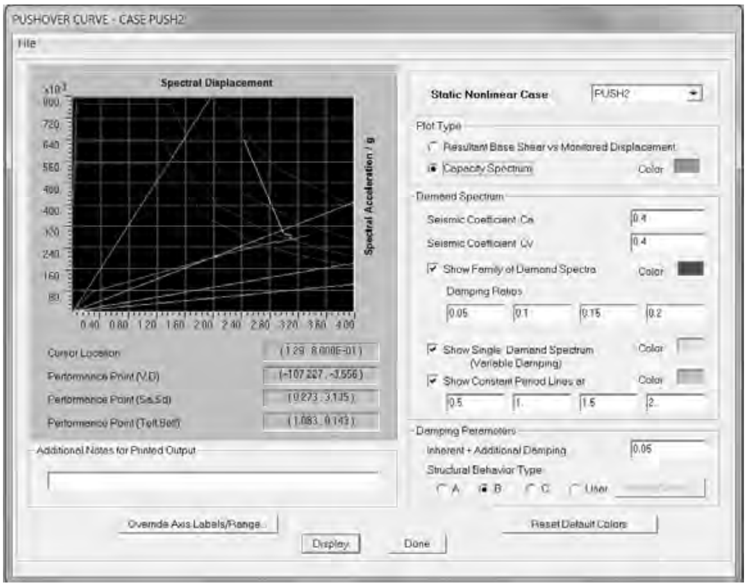
PUSHOVER CURVE - CASE PUSH2
File
Spectral Displacement
x10⁻³
900.
720.
640.
560.
480.
400.
320.
240.
160.
80.
0.40 0.80 1.20 1.60 2.00 2.40 2.80 3.20 3.60 4.00
Spectral Acceleration / g
Override Axis Labels/Range...
Display
Done
Reset Default Colors

Static Nonlinear Case: PUSH2

Plot Type
○ Resultant Base Shear vs Monitored Displacement
● Capacity Spectrum

Demand Spectrum
Seismic Coefficient Ca: 0.4
Seismic Coefficient Cv: 0.4
☑ Show Family of Demand Spectra
Damping Ratios: 0.05 0.1 0.15 0.2
☑ Show Single Demand Spectrum (Variable Damping)
☑ Show Constant Period Lines at: 0.5 1. 1.5 2.

Cursor Location: (1.29, 8.000E-01)
Performance Point (V,D): (-107.227, -3.556)
Performance Point (Sa,Sd): (0.273, 3.135)
Performance Point (Teff,Beff): (1.083, 0.143)

Damping Parameters
Inherent + Additional Damping: 0.05
Structural Behavior Type: ○ A ● B ○ C ○ User

Figure 5: Capacity spectrum for gravity plus earthquake for 3 stories building with 1 unit apartment

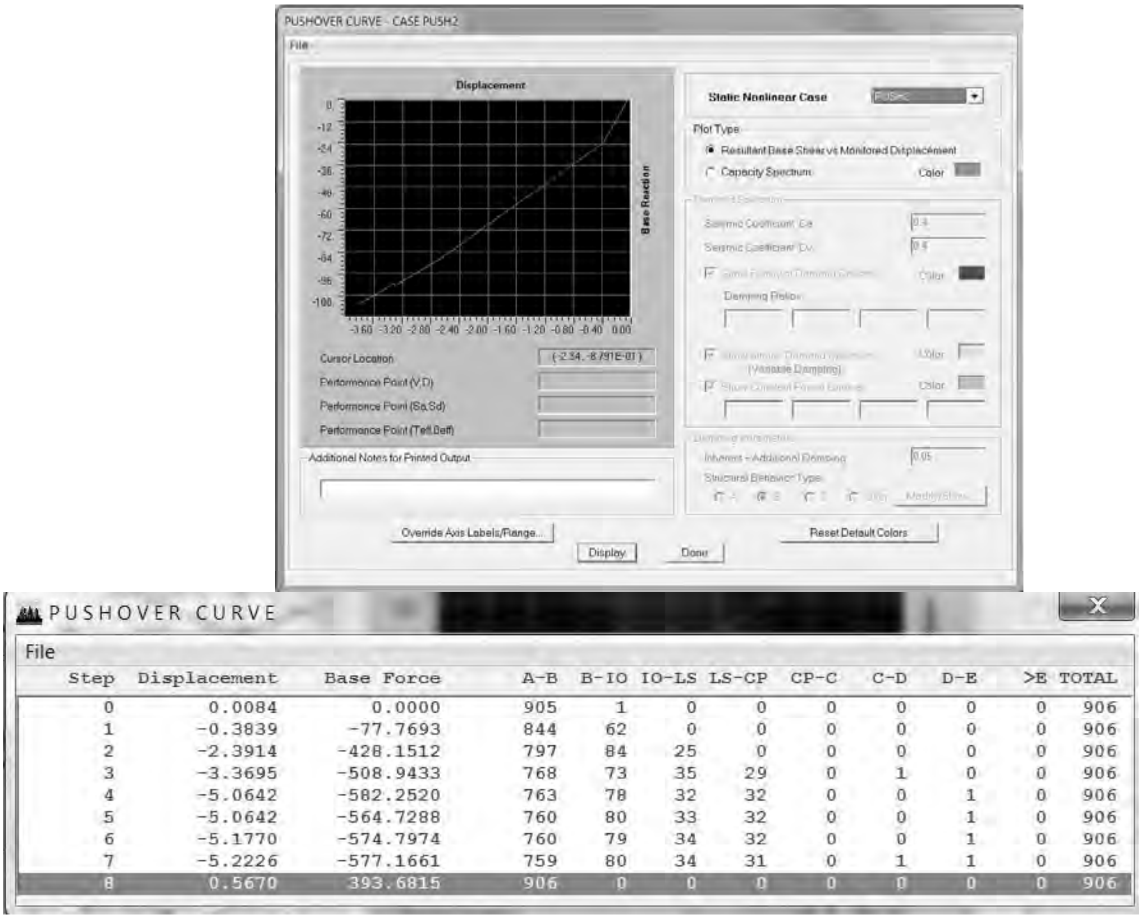
PUSHOVER CURVE - CASE PUSH2
File
Displacement
0.
-12.
-24.
-36.
-48.
-60.
-72.
-84.
-96.
-108.
-3.60 -3.20 -2.80 -2.40 -2.00 -1.60 -1.20 -0.80 -0.40 0.00
Base Reaction
Override Axis Labels/Range...
Display
Done
Reset Default Colors
PUSHOVER CURVE
File

Plot Type
● Resultant Base Shear vs Monitored Displacement
○ Capacity Spectrum

Cursor Location: (-2.34, -8.791E-01)

```
  Step  Displacement     Base Force      A-B  B-IO IO-LS LS-CP  CP-C   C-D   D-E   >E TOTAL
     0        0.0084         0.0000      905     1     0     0     0     0     0    0   906
     1       -0.3839       -77.7693      844    62     0     0     0     0     0    0   906
     2       -2.3914      -428.1512      797    84    25     0     0     0     0    0   906
     3       -3.3695      -508.9433      768    73    35    29     0     1     0    0   906
     4       -5.0642      -582.2520      763    78    32    32     0     0     1    0   906
     5       -5.0642      -564.7288      760    80    33    32     0     0     1    0   906
     6       -5.1770      -574.7974      760    79    34    32     0     0     1    0   906
     7       -5.2226      -577.1661      759    80    34    31     0     1     1    0   906
     8        0.5670       393.6815      906     0     0     0     0     0     0    0   906
```

Figure 6: Pushover curve for 6 stories building with 2 unit apartment

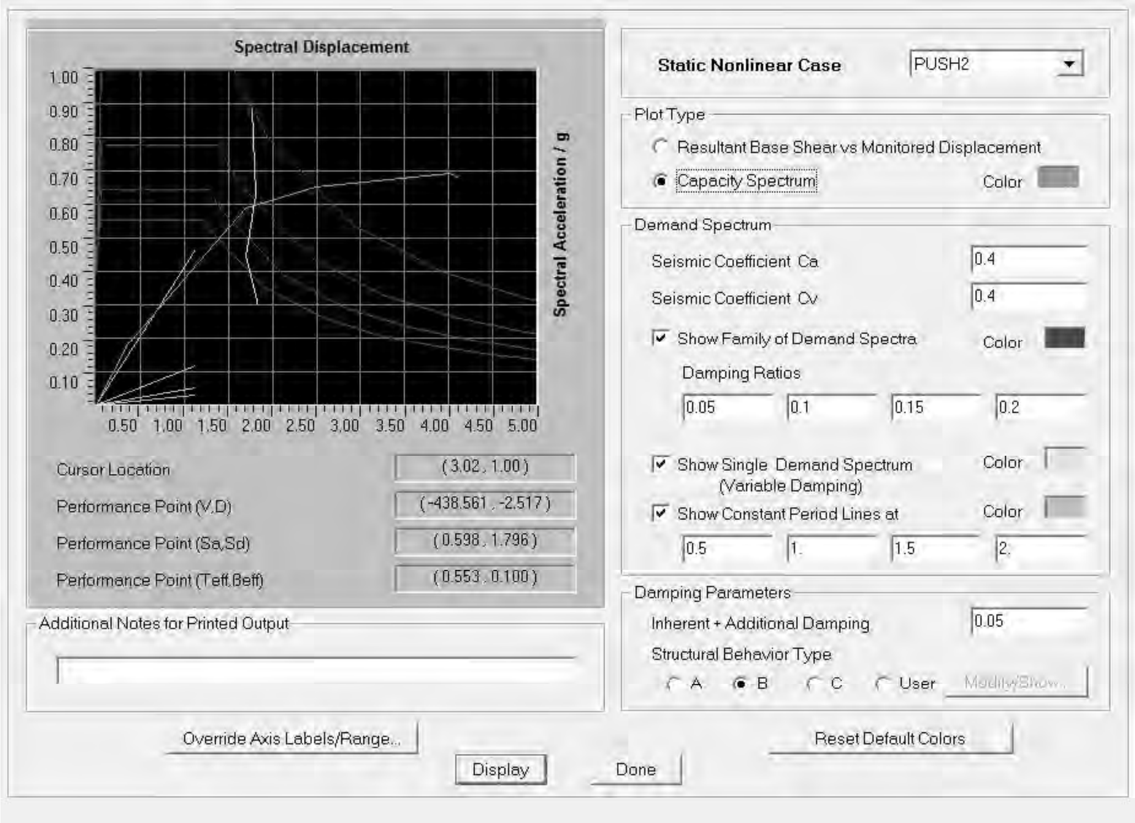
Spectral Displacement
1.00
0.90
0.80
0.70
0.60
0.50
0.40
0.30
0.20
0.10
0.50
1.00
1.50
2.00
2.50
3.00
3.50
4.00
4.50
5.00
Spectral Acceleration / g
Color
Color
Color
Color
Modify/Show...
Override Axis Labels/Range...
Reset Default Colors
Display
Done

Cursor Location (3.02 , 1.00)
Performance Point (V,D) (-438.561 , -2.517)
Performance Point (Sa,Sd) (0.598 , 1.796)
Performance Point (Teff,Beff) (0.553 , 0.100)

Additional Notes for Printed Output

Static Nonlinear Case PUSH2

Plot Type
○ Resultant Base Shear vs Monitored Displacement
● Capacity Spectrum

Demand Spectrum
Seismic Coefficient Ca 0.4
Seismic Coefficient Cv 0.4
☑ Show Family of Demand Spectra
Damping Ratios 0.05 0.1 0.15 0.2
☑ Show Single Demand Spectrum (Variable Damping)
☑ Show Constant Period Lines at 0.5 1. 1.5 2.

Damping Parameters
Inherent + Additional Damping 0.05
Structural Behavior Type ○ A ● B ○ C ○ User

Figure 7: Capacity spectrum for gravity plus earthquake for 6 stories building with 2 unit apartment

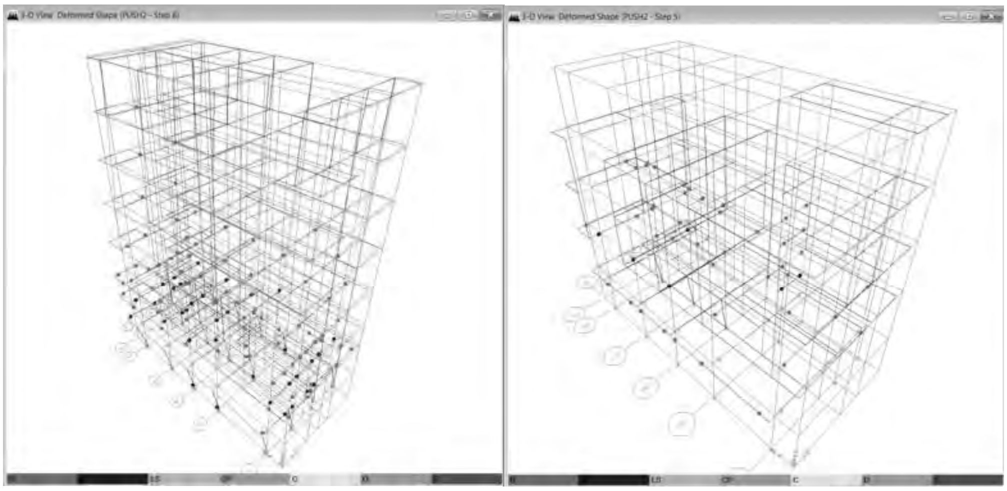

Figure 8: Plastic hinge Patterns at gravity plus earthquake for 3 stories building and 6 stories building.

4. DISCUSSION AND CONCLUSION

This study intended to apply the capacity design principles in seismic resistant design of structures. By applying the capacity design concept, the performance of buildings during a severe earthquake can be known. Potential structural deficiency in RC frame due to earthquake can be estimated by the nonlinear pushover procedure. The procedure showed that the frame is capable of withstanding the presumed seismic force with some significant yielding at several beams. The structure can be economically designed for a friction of the estimated elastic seismic design forces, while maintaining the basic safety performance objective.

From the results for two types of case studies, it can be seen that performance point of frame structure without seismic design is within elastic range. Sequence of formation of plastic hinges (yielding) in the frame members can be clearly seen in the beams only. The building clearly behaves like the strong column-weak beam mechanism. Lateral deformations at the performance point are required to be checked against the deformation limits of ATC-40 for safety of people against seismic force. It can be seen that building with symmetric frames have more seismic capacity than unsymmetrical buildings.

REFERENCES

Applied Technology Council (ATC.), 1996. *Seismic evaluation and retrofit of concrete buildings*, ATC-40 Report, Redwood City, California, USA.

ETABS User’s Manual, *Integrated building design software,* Computer and Structures Inc. Berkeley, USA.

Federal Emergency Management Agency (FEMA)., 1997. *NEHRP guidelines for the seismic rehabilitation of buildings*” FEMA-273.

Kadid, A. and Boumrkik, A., 2008. Pushover analysis of reinforced concrete frame structures. *Asian. J.Civ. Engrg, (Building and Housing)* 9, 75-83.

Reston, Virginia Uniform Building Code: UBC, 1997, *International Conference of Building Officials*, Whittier, Calif.

Srinivasu and Rao, P., 2013. Non-linear static analysis of multi-storied building. *International Journal of Engineering Trends and Technology* 4.

Thant, M., 2012. *Probabilistic seismic hazard assessment for Yangon Region, Myanmar*, the 5th AUN/SEED-Net, Regional Conference on Geo-Disaster Mitigation in ASEAN, September 2012, Manila, Philippines.

Study of atmospheric corrosion of steels in Yangon, urban location

Yu Yu Kyi Win
[1] Ph.D Student, Department of Civil Engineering, Yangon Technological University
yuyukyiwin@gmail.com

ABSTRACT

Corrosion is a degrading process and it is the main degradation problem in building industry in the world. Corrosion cannot be defined without a reference to environment. All environments are corrosive to some degree. Among the various types of corrosion, the corrosion that occurs in the atmosphere is known as atmospheric corrosion and it accounts for more failure than other types of corrosion. Models for predicting the corrosion rate of metals in the atmosphere are useful for judicious selection of materials concerning the durability of metallic structures, determining the economic costs of damages associated with the degradation of materials, and acquiring knowledge about the effect of environmental variables on corrosion kinetics. So, predictions of corrosion rates in structural elements are important to be considered. The present study concentrates on the prediction of atmospheric corrosion rates of structural steel in Yangon, Urban location based on ISO 9223. The atmospheric variables (pollutants and meteorological variables) are recorded every month. The pollutant data of sulfur dioxide and chloride are measured by JIS Z 2382 and the meteorological data are collected by data logger. The corrosivity classification is made according to ISO 9223 by evaluating the important atmospheric variables, such as Time of Wetness, CL^- *and* SO_2*. The corrosion rate is then predicted based on ISO 9223. Based on the atmospheric data obtained, the total time of wetness, chloride, and sulfur dioxide up to now are 3226 hours, 0.245* $mg/(dm^2 \cdot d)$ *and 0.118* $mg/(dm^2 \cdot d)$*, respectively. So, according to ISO 9223, the corrosivity categories for Yangon area may be* C_3 *and thus the predicted corrosion rate may be 201-400* g/m^2*.year.*

Keywords: ISO 9223, atmospheric corrosion, pollutant data, meteorological data

1. INTRODUCTION

The term “atmospheric corrosion” means the attack on metal exposed to the air as opposed to metal immersed in a liquid. Atmospheric corrosion is mainly an electrochemical process that occurs in the presence of thin film electrolytes formed on the metal surface. The attack proceeds by balancing anodic oxidation reaction, which involves the dissolution of the metal in the electrolytic film, and cathodic reactions, involving the oxygen reduction reaction. There are several factors that influence the rate of corrosivity. These are: temperature, time of wetness, pollution by sulfur and airborne salinity. Corrosion effects of other pollutants (ozone, nitrogen oxides, particulates) also influence the corrosivity and can be evaluated as yearly corrosion loss, but these factors are not considered decisive in the assessment of corrosivity according to international standard, ISO standard 9223, which considered only temperature, time of wetness, sulfur and airborne salinity for estimation of corrosivity. As far as the corrosivity of atmospheres is concerned, EN 12500 defines five outdoor environments on the basis of the presence of corrosive agents in the air, namely: rural atmosphere, urban atmosphere, industrial atmosphere, marine atmosphere, and marine industrial atmosphere. The conditions comprising the makeup of the atmosphere are very complex and continually changing. The atmosphere can contain acid rain, chloride salts, nitrogen compounds, ammonia, sulfur dioxide, hydrogen sulfide, carbon dioxide and other industrial contaminants. Climatic factors affecting atmospheric corrosion are items such as; solar radiation, relative humidity, air chemistry, particles carried by the atmosphere (sand, soil, dust), air temperature, rain and winds

2. METHODOLOGY

2.1 Collecting of meteorological and pollutant data

[1]. Meteorological Data

Meteorological Data; such as temperature, rainfall, and humidity of location are recorded by one month time interval by data logger, and shown in Figure 1. From these data, time of wetness is calculated according to ISO 9223. According to ISO 9223, time of wetness can be calculated as hours per year when relative humidity greater than 80 percent and temperature greater than 0°C.

[2]. Pollutant Data

The pollutant data of chloride and sulphur dioxide are obtained by using dry gauze and lead dioxide cylinder methodology, according to JIS Z 2382, and shown in Figure 2, and Figure 3, respectively.

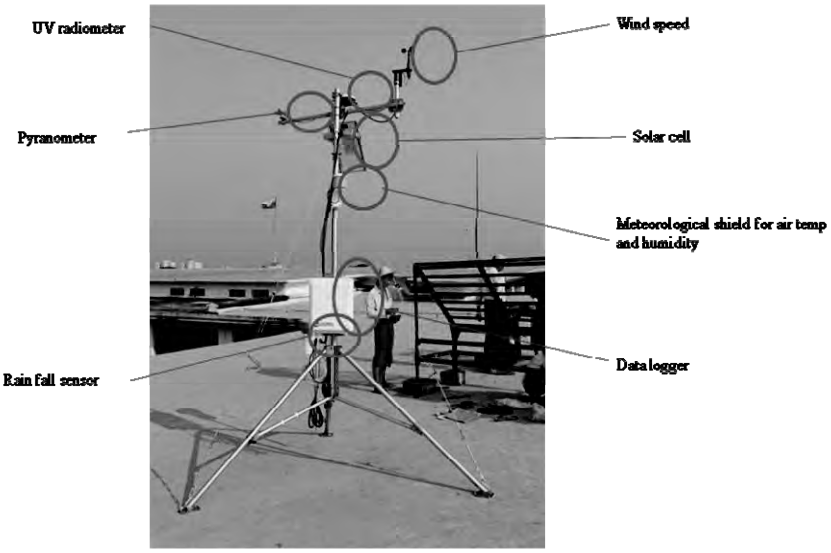

Figure 1: Weather monitoring system

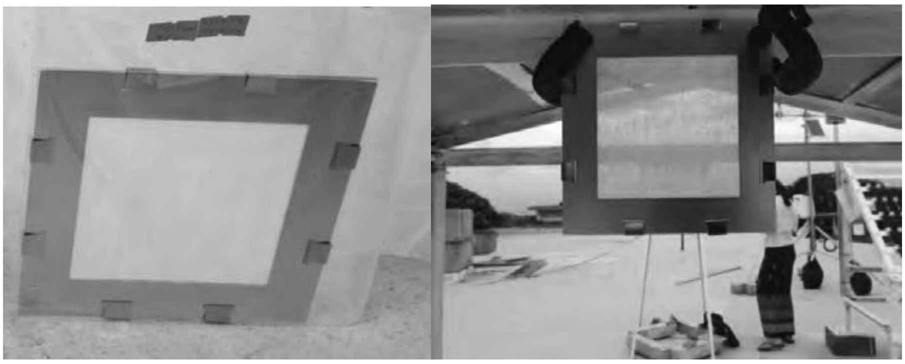

Figure 2: Testing for chloride with dry gauze methodology

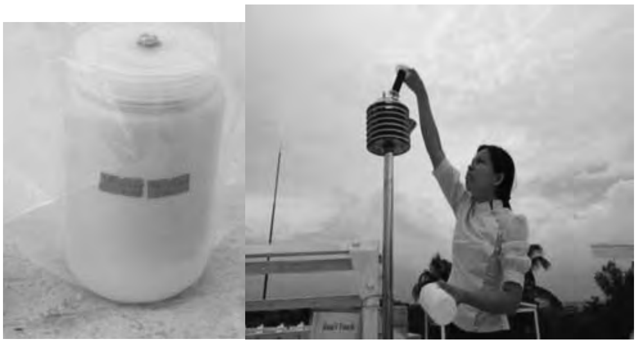

Figure 3: Testing for sulfur with cylinder methodology

2.2 Prediction based on ISO 9223

The ISO corrosivity classification from atmospheric parameters is based on the simplifying assumption that the time of wetness (TOW) and the levels of corrosive impurities determine the corrosivity. Only two types of corrosive impurities are considered, namely, sulfur dioxide and chloride. Practical definitions for all the variables involved in calculating an ISO corrosivity index follow.

1. Time of wetness. Units: hours per year (h.year^{-1}) when relative humidity (RH)>80 percent and t >0°C

TOW	≤ 10	$T1$
10	$< \text{TOW} \leq 250$	$T2$
250	$< \text{TOW} \leq 2500$	$T3$
2500	$< \text{TOW} \leq 5500$	$T4$
5500	$< \text{TOW}$	$T5$

2. Airborne salinity. Units: chloride deposition rate (mg.m^{-2}.day^{-1})

$S \leq 60$	$S1$
$60 < S \leq 300$	$S2$
$300 < S$	$S3$

3. Industrial pollution by SO2. Two types of units are used:

Concentration ($\mu g.m^{-3}$), PC

PC ≤ 40	P1
$40 < PC \leq 90$	P2
$90 < PC$	P3

Deposition rate ($mg.m^{-2}.day^{-1}$), P_D

$P_D \leq 35$	P1
$35 < P_D \leq 80$	P2
$80 < P_D$	P3

ISO 9223 Corrosivity categories of atmosphere

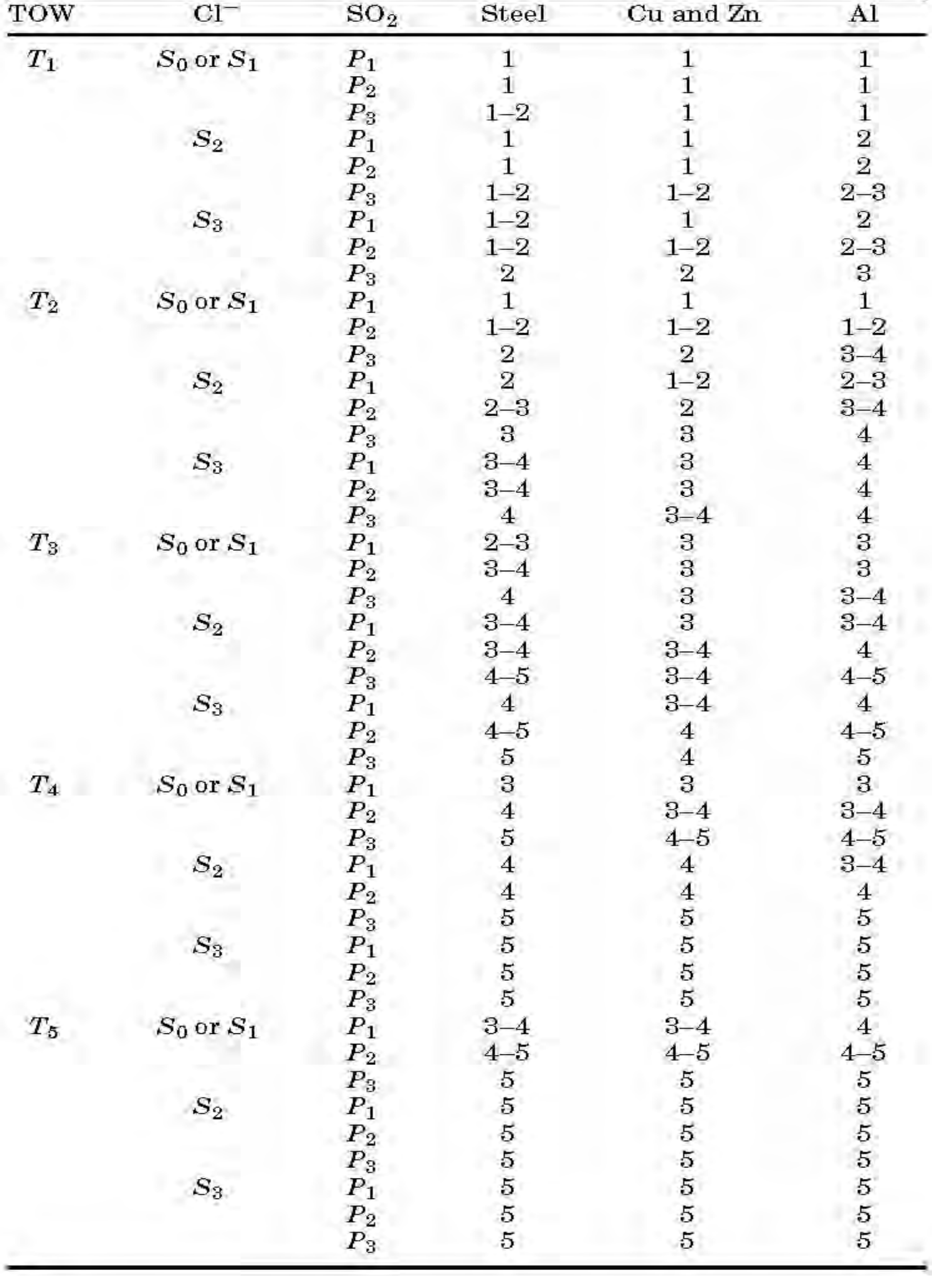

TOW	Cl^-	SO_2	Steel	Cu and Zn	Al
T_1	S_0 or S_1	P_1	1	1	1
		P_2	1	1	1
		P_3	1–2	1	1
	S_2	P_1	1	1	2
		P_2	1	1	2
		P_3	1–2	1–2	2–3
	S_3	P_1	1–2	1	2
		P_2	1–2	1–2	2–3
		P_3	2	2	3
T_2	S_0 or S_1	P_1	1	1	1
		P_2	1–2	1–2	1–2
		P_3	2	2	3–4
	S_2	P_1	2	1–2	2–3
		P_2	2–3	2	3–4
		P_3	3	3	4
	S_3	P_1	3–4	3	4
		P_2	3–4	3	4
		P_3	4	3–4	4
T_3	S_0 or S_1	P_1	2–3	3	3
		P_2	3–4	3	3
		P_3	4	3	3–4
	S_2	P_1	3–4	3	3–4
		P_2	3–4	3–4	4
		P_3	4–5	3–4	4–5
	S_3	P_1	4	3–4	4
		P_2	4–5	4	4–5
		P_3	5	4	5
T_4	S_0 or S_1	P_1	3	3	3
		P_2	4	3–4	3–4
		P_3	5	4–5	4–5
	S_2	P_1	4	4	3–4
		P_2	4	4	4
		P_3	5	5	5
	S_3	P_1	5	5	5
		P_2	5	5	5
		P_3	5	5	5
T_5	S_0 or S_1	P_1	3–4	3–4	4
		P_2	4–5	4–5	4–5
		P_3	5	5	5
	S_2	P_1	5	5	5
		P_2	5	5	5
		P_3	5	5	5
	S_3	P_1	5	5	5
		P_2	5	5	5
		P_3	5	5	5

ISO 9223 Corrosion Rate after one year exposure predicted for different corrosivity classes

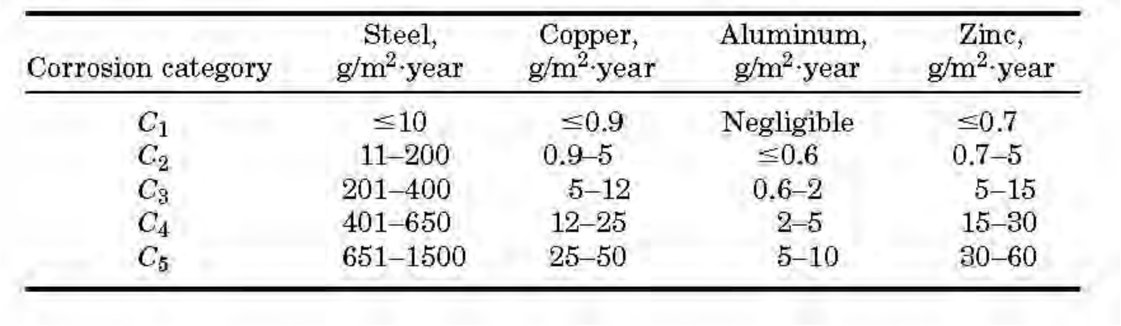

Corrosion category	Steel, g/m^2·year	Copper, g/m^2·year	Aluminum, g/m^2·year	Zinc, g/m^2·year
C_1	≤10	≤0.9	Negligible	≤0.7
C_2	11–200	0.9–5	≤0.6	0.7–5
C_3	201–400	5–12	0.6–2	5–15
C_4	401–650	12–25	2–5	15–30
C_5	651–1500	25–50	5–10	30–60

3. RESULTS AND DISCUSSION

3.1 Meteorological data of Test Sites

The meteorological data, temperature, and relative humidity, from March, 2014 to September, 2014 are shown in Table 1, and the variation of these is shown in Figure 4 and Figure 5, respectively. Time of wetness is calculated according to ISO 9223. The variation of time of wetness is also shown in Figure 6.

Table 1: Meteorological data of the test site

Site	Time	Avg, T, ·C	Avg, RH, %	TOW
YTU	18.3.14~22.4.2014	29.88101	68.27274	329
	23.4.2014~22.5.2014	29.86671	75.39856	361
	23.5.2014~22.6.2014	28.08754	87.46431	573
	23.6.2014~22.7.2014	26.94331	92.18743	641
	23.7.2014~22.8.2014	26.54154	94.60301	703
	23.8.2014~22.9.201	26.96366	90.59358	619

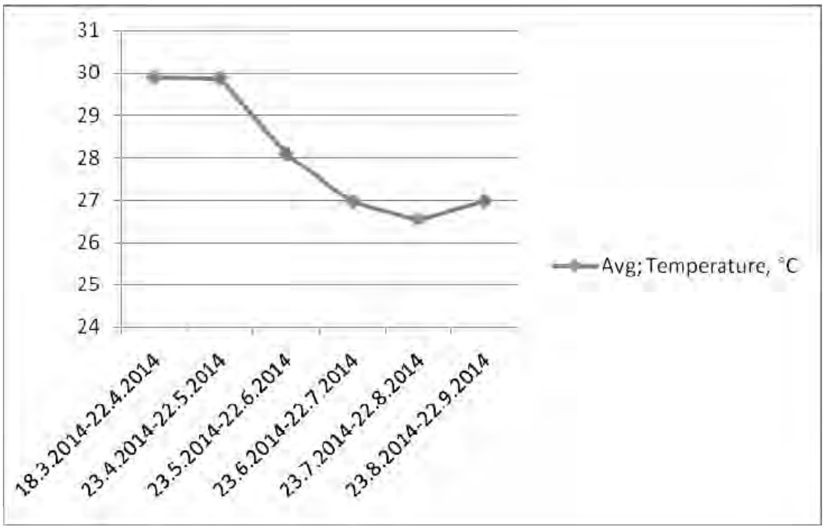

Figure 4: Average temperature of the site

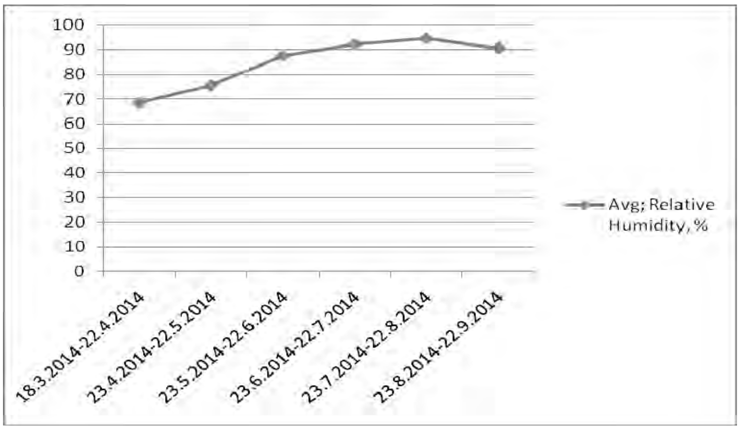

Figure 5. Average relative humidity (%) of the site

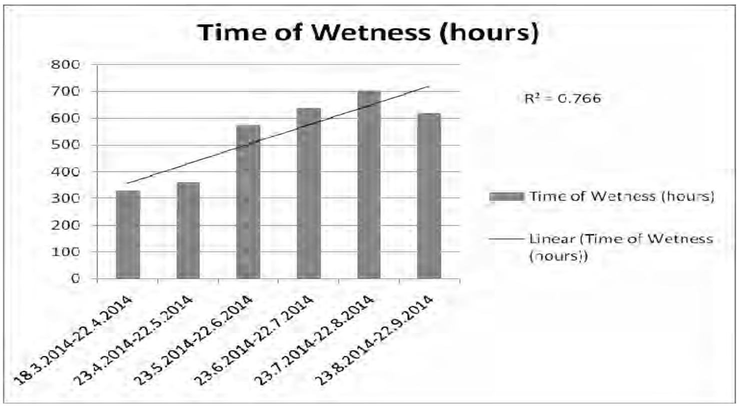

Figure 6: Variation and trend line for time of wetness

3.2 Pollutant data of Test Sites

The pollutant data, chloride and sulfur dioxide, obtained for March, 2014 and April, 2014 is shown in Table 2, and Table 3 and their variations are shown in Figure 10. The calculation of pollutant data is based on JIS Z 2382.

Table 2: Chloride data of the test site

Test period			**3/18-4/22**	**4/22-5/22**	**5/22-6/22**	**6/22-7/22**	**7/22-8/22**
Interval (days)	t	d	35	30	31	30	31
Amount of chloride ion on dry gauze	C_1	mg/l	43.0	47.2	51.9	20.5	25.1
Amount of chloride ion in blank test	C_2	mg/l	0.2	0.2	<0.1	<0.1	<0.1
Amount of airborne sea salt	R (NaCl)	NaCl· mg/(dm^2·d)	0.050	0.065	0.069	0.028	0.033

Table 3: Sulphur Dioxide data of the test site

Test period			**3/18-4/22**	**4/22-5/22**	**5/22-6/22**	**6/22-7/22**	**7/22-8/22**
Interval (days)	t	d	35	30	31	30	31
Weight of BaSO4 from PbO2 cylinder	W_1	mg	4.1	2.4	2.9	2.2	2.0
Weight of BaSO4 of blank test	W_2	mg	<1	<1	<1	<1	<1
Amount of SO2 deposition	S	mg SO_2/ (dm^2·d) （PbO_2	0.032	0.022	0.026	0.020	0.018

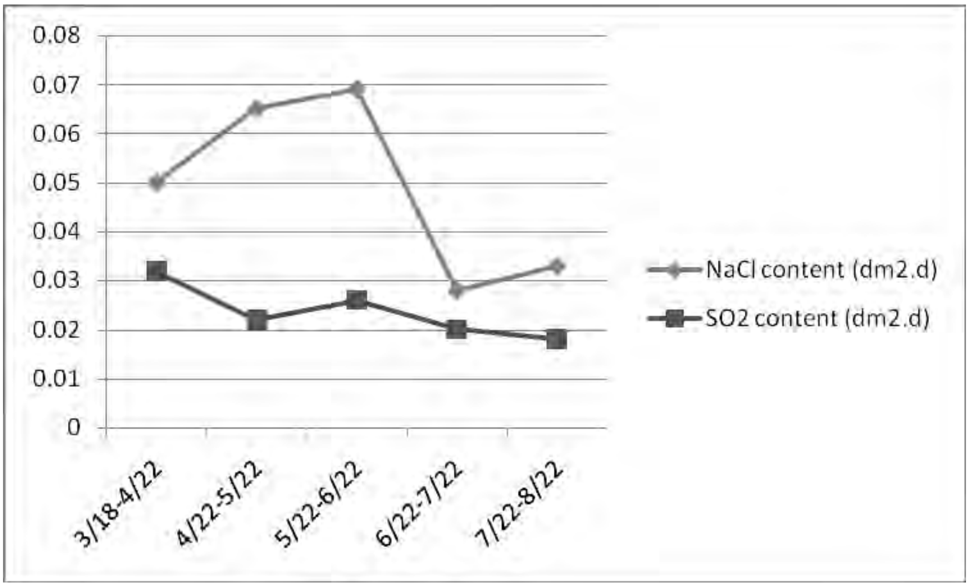

Figure 10: Variation of pollutant data, chloride and sulfur dioxide

3.3 Discussion

The present study intended to predict the rate of corrosion for steel under particular atmospheric condition by using ISO 9223 methodology. The atmospheric corrosion rates of steel after one year exposure in Yangon (urban) atmosphere will be made. The atmospheric variables (pollutants and meteorological variables) are also recorded every month. Now, the meteorological data for temperature and relative humidity for six months were obtained and the pollutant data for chloride and sulfur dioxide were obtained for five months. Time of wetness is calculated from temperature and relative humidity, according to ISO 9223. The prediction of corrosion rate will be made based on ISO 9223 by evaluating the important atmospheric variables, such as Time of Wetness, CL^- and SO_2.

4. CONCLUSION AND RECOMMENDATIONS

From the obtained meteorological data, all of the temperatures obtained yet are above 0°C, and the different is not very large (between 26°C to 29°C). From the obtained relative humidity, the relative humidity of greater than 80% was selected for this research to calculate time of wetness according to ISO 9223. The trend for relative humidity is slightly increased. Time of wetness had an increasing trend and the R^2 value is 0.766. It can be clearly seen that time of wetness; main indicator for corrosion is mainly depended on the relative humidity because times of wetness and relative humidity have nearly the same increasing trend. On the contrast, the effect of temperature on time of wetness is not so much. So, for Yangon, relative humidity is the main contributor for corrosion, from meteorological point of view. For pollutants, total chloride and sulfur dioxide for five months is 0.245 $mg/(dm^2 \cdot d)$ and 0.118 $mg/(dm^2 \cdot d)$, respectively and thus the amount is very small. Based on the atmospheric data obtained, the total time of wetness, chloride, and sulfur dioxide up to now are 3226 hours, 0.245 $mg/(dm^2 \cdot d)$ and 0.118 $mg/(dm^2 \cdot d)$, respectively. So, according to ISO 9223, the corrosivity categories for Yangon area may be C_3 and thus the predicted corrosion rate may be 201-400 g/m^2.year.

For recommendation, the actual corrosion rates of commonly used structural steels should be found and then compare with the ISO 9223 results. By correlation between actual corrosion rates and atmospheric variables, the corrosion rates for each type of steel should be formulated. The prediction of corrosion rates for long term should be made by using linear bilograthmic law. The testing should be done not only in urban area, but also in other area, such as industrial, marine, and rural, and then comparison between them should be made.

REFERENCES

Roberge, P. R., 2000. *Handbook of corrosion engineering*. The McGraw-Hill Companies, Inc., New York.
Roberge, P. R., 2008. *Corrosion engineering principles and practice*, New York.
ISO 9223: Corrosion of metals and alloys—*corrosivity of atmospheres— classification.*
Japan International Standard; *JIS Z 2382*, JIS, Editor. 1987.

Estimation of runoff potential in Chindwin River Basin using remote sensing and GIS

Kyu Kyu Thin[1] and Win Win Zin[2]
[1] M.E, Yangon Technological University
[2]Associate Professor, Yangon Technological University
kyukyut9@gmail.com

ABSTRACT

The integration of Geographic Information System (GIS) and remote sensing data extracted from earth observation satellites with additional collateral data of the study area, provides a powerful tool in estimation of runoff. Chindwin river basin is chosen as case study area. In this study, runoff potential was analyzed by two methods: the SCS curve number method and the Index method. The parameters such as land cover, soil type, rainfall, area of the catchment and slope are considered. Landcover map was prepared using LANDSAT images with supervised classification method. The slope map was generated from Digital Elevation Model (DEM) of 30 meter spatial resolution by using ArcGIS. Generally, flat and gently sloping areas promote infiltration and less runoff potential, and steeply sloping grounds encourage runoff and little or no infiltration. The landuse pattern – arable land, grass land, forest or cultivated area, greatly affect runoff. The soil classes used for the runoff potential are based on the hydrologic property of FAO classification. All point and polygon data were converted to grid. In index method each of the class in the thematic layers was qualitatively described and reclassified by assigning numbers starting from 1 up to 5. Numbers were assigned based on runoff potentiality of each class in layers. The higher the number is the better runoff potentiality is. Runoff potential of a catchment that is a crucial design parameter for water harvesting systems.

Keywords: GIS, Remote Sensing, Runoff Potential, SCS Curve Number Method, Index Method

1. INTRODUCTION

Surface runoff, or simply runoff, refers to all the waters flowing on the surface of the earth, either by overland sheet flow or by channel flow in rills, gullies, streams, or rivers. Surface runoff is a continuous process by which water is constantly flowing from higher to lower elevations by the action of gravitation forces. Small streams combine to form larger streams which eventually grow into rivers. In time, rivers carry their flow into the ocean, completing the hydrologic cycle. Rainstorms generate runoff, and its occurrence and quantity are dependent on the characteristics of the rainfall event. Apart from these rainfall characteristics, there are number of catchment specific factors, which have a direct effect on the occurrence and volume of runoff. This includes soil type, land cover, slope, rainfall intensity, duration of rainfall, catchment shape and area of the catchment. Remote sensing and geographic information systems are modern scientific tools for the determination, assessment and modeling of environmental characteristics and processes. In this study, remote sensing images were used in large scale to determine the land cover for the study area. Geographical information systems allow the linkage and interrelation with other data which are important to determine runoff potential. Remote sensing can derive information about objects on the surface of the earth without physically coming into contact. The objective of this research is to estimate the runoff potential of the study area based on the integration of satellite images, topographic data, rainfall and soil data. This integration will be implemented through the use of spatial databases and geographic information systems (GIS).

2. DATA USED IN THIS STUDY

The land use and land cover map was prepared using Landsat ETM and ETM+ satellite images with a resolution of 30m. Digital Elevation Model (DEM) with 30 m resolution of the study area was obtained from USGS (US Geological Survey). The soil information was downloaded from FAO soil map of the world at 1:5,000,000 scale.

3. STUDY AREA

Chindwin river is the largest tributary of Ayeyarwaddy river. The Chindwin river, which is originated in the northern border mountains and the Kumon ranges in Kachin state, flows down through the Hukawng valley, Hkamti, Tamanthi, Homalin, and Mawlaik to the southwest along the eastern edge of the 2000-3800 m high Rakhine Mountains with repeating numerous bends. The river changes its course at Kalewa to the southeast, crossing a number of vast plains and finally joins the Ayeyarwaddy river at the east of Pakokku via Mingin, Kani, Shwezaye narrow and Monywa. Location of study area is shown in Figure 1. The Chindwin River has the catchment area of 115,300 km^2 with the gap of 130 m between the confluence and the Hukawng Valley. Length of the river is approximately 1046 km. Wide and thickly developed river terraces are frequently seen on the both banks along the river, sometimes stretching more than a mile wide across the river.

The Chindwin river is naturally configured with tremendous segments of rivulets, streamlets and tributaries and it could of be ranked as the largest tributary of the Ayeyarwaddy river. The source of the entire river system approximately falls at 97.00 degree Eastern longitude and 25.50 degree Northern latitude being having an elevation of about 2134 meters in the Kumoon range within the northern Kachin state of "Myanmar". The upper segment of Chindwin river is alternatively known as Tanai Hka that flows in north direction in its upper reach before entering into the Hukaung valley. Very clearly, rapids and waterfalls could often be seen along the river stretch within the 850 km water course from the origin to Mawlaik. After that, the system alters its direction and runs West-North-West and the directional aspect changes to the South while traversing for approximately 1200 km before joining with the Ayeyarwaddy river near Myingyan, being situated at 26 km upstream of Pakokku.

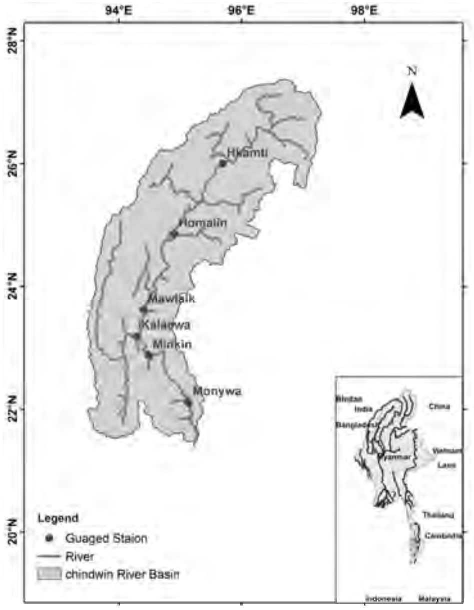

Figure 1: Location of Study Area

4. LITERATURE REVIEW

Factors effecting runoff are storm characteristics, meteorological characteristics, basin characteristics and storage characteristics. Steep rocky catchments with less vegetation will produce more runoff compared to flat tracts with more vegetations. If the vegetation is thick greater is the absorption of water, so less runoff. Catchments located at higher altitude will receive more precipitation yield greater runoff. The land use pattern – arable land, grass land, forest or cultivated area, greatly affect runoff. The runoff potential can be determined through two different methods: One method included the SCS method, the other one comprised the indexing method in this study. Within the index method the various parameters for runoff generation were identified according to their importance to runoff generation. A data layer in the raster format was made for each parameter. The layers within this study include: slope, soil texture, land cover, rainfall and area of the catchment. Here an attempt was made to identify features (land cover) using remote sensing image interpretation. One form of classification is the spectral one which includes unsupervised classification or supervised classification, neural network classification and the classification tree, statistical procedure within a decision making environment. Geographic Information Systems (GIS) are computer based tools that store, analyze, and retrieve, manipulate large amounts of spatial data. They are spatial; data-base management techniques. Originally these tools were developed to ease cartography, but are being used these days for inventory analysis estimation, planning and modelling. GIS may be either raster-based or vector-based. A raster-based GIS is more storage efficient than a vector-based GIS. The larger the coverage the greater the storage spaced used by vector-based GIS. The processing speed of a vector-based GIS is slower and can be an important consideration if extensive spatial processing is needed for a watershed model. GIS improves the ability to incorporate spatial details beyond the existing capability of watershed models. With much better resolution of terrain-streams and drainage areas, the ability to delineate more appropriate grid layers for a finite element watershed model is enhanced.

5. METHODOLOGY

This research was accomplished by using ENVI 4.2 and Arc GIS 10. In this study, LANDSAT ETM and ETM+ (30 m resolution) from the years 2009 images and DEM (30 m resolution) developed from USGS was applied in this study. Spatial baseline database (soil, slope, rainfall) were prepared in GIS. The different polygons in the thematic layers were labeled separately and then they were registered. In the final thematic layer initially each one of the polygons were qualitatively visualized into five categories and then in terms of their importance with respect to runoff potential and suitable weights have been assigned. Finally thematic layers were converted into grid by only considering the related weight and then integrated and analyzed, using weighted aggregation method. The grids in the integrated layer were grouped into different runoff potential by a suitable logical reasoning and conditioning. The runoff potential map was generated and then reclassified by GIS into low, medium and high. The SCS method is based on the empirical assumption that the ratio of actual to initial runoff is equal to the ratio of actual retention to potential retention.

5.1 Implementation Program:

- Satellite and ancillary data acquisition, processing and analysis of satellite data
- Development of landcover
- Preparing spatial baseline database in GIS
- Spatial data analysis and developing of appropriate model relating with meteorological characteristics and basic characteristics which influence the runoff potential of the study area.
- Develop runoff potential map by overlaying all the thematic layers in GIS.

5.2 Land Cover

In this study, supervised classification with Maximum Likelihood method and Minimum Distance are used to develop the land cover map. Land cover map is shown in Figure 2.

Table 1: Weightage of Land cover For Runoff Potential

Land cover	Score
Evergreen forest	1
Mixed forest	2
Woody Savannas	3
Croplands	4

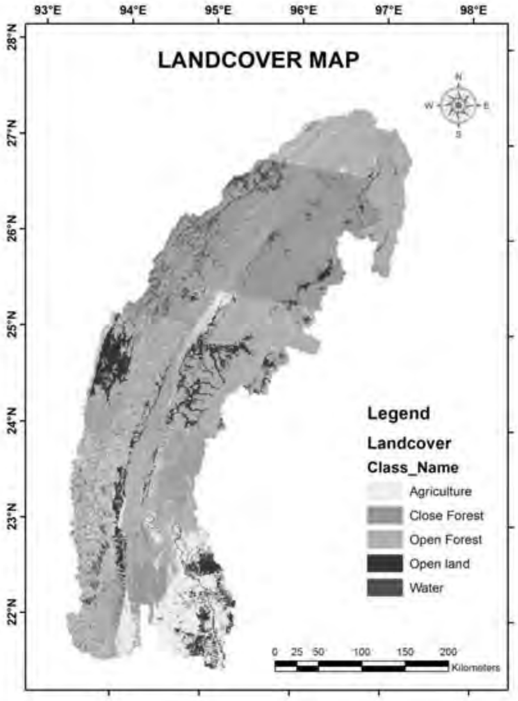
93°E
94°E
95°E
96°E
97°E
98°E
28°N
27°N
26°N
25°N
24°N
23°N
22°N
LANDCOVER MAP
N
W
E
S
Legend
Landcover
Class_Name
Agriculture
Close Forest
Open Forest
Open land
Water
0 25 50 100 150 200
Kilometers

Figure 2: Land Cover Map of Chindwin River Basin

5.3 Slope

Generally, flat and gently sloping areas promote infiltration and less runoff potential, and steeply sloping grounds encourage run-off and little or no infiltration. The area has a steeply slope; it supports high discharge of overland flow and low rate of infiltration. Therefore, runoff potentiality is expected to be greater in the steeply sloping area. Steeply topography then will give more chance for runoff potential. The slope map was generated from digital elevation model of 30 meter spatial resolution by using Arc GIS and it is shown in Figure 3.

Table 2 : Weightage Of Slope For Runoff Potential

Slope	Description	Score
0 ° - 7 °	Almost Flat	1
7 ° - 14°	Undulating to rolling	2
14 ° - 21 °	Hilly Disserted	3
21 ° - 28 °	Steep Dissected	4
28 ° - 35 °	Very steep	5

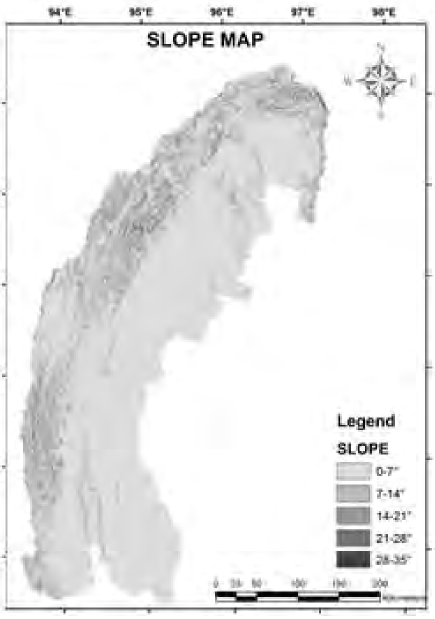
94°E
95°E
96°E
97°E
98°E
SLOPE MAP
27°N
26°N
25°N
24°N
23°N
22°N
N
W
E
S
Legend
SLOPE
0-7°
7-14°
14-21°
21-28°
28-35°
0
25
50
100
150
200
Kilometers

Figure 3: Slope Map

5.4 Rainfall

Precipitation and evaporation are the two fundamental phases in the hydrological cycle which involves processes in the atmosphere and at the earth's surface/atmosphere interface. It plays an important role in the hydrologic cycle which controls runoff potential. Knowing the nature and characteristics of precipitation, we can conceptualize and predict its effects in runoff, infiltration, evapotranspiration, and water yield. Therefore, for hydrologic analyses it is important to know the areal distribution of precipitation. Several areal precipitation estimation techniques are currently used for averaging precipitation depths collected at ground stations. In this study, Isohyetal method was applied to estimate the areal precipitation over the entire basin.

Table 3. Weightage of rainfall for runoff potential

Criteria	Classes(mm)	Weight
Rainfall	729-2295	1
	2295-2297	2
	2297-3820	3
	3820-3931	4
	3931	5

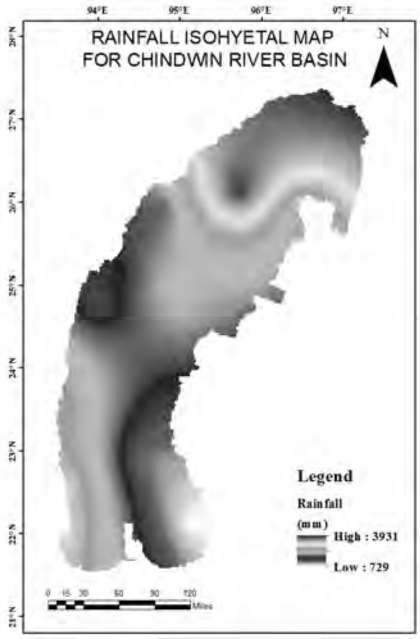
94°E
95°E
96°E
97°E
RAINFALL ISOHYETAL MAP
FOR CHINDWIN RIVER BASIN
N
28°N
27°N
26°N
25°N
24°N
23°N
22°N
21°N
Legend
Rainfall
(mm)
High : 3931
Low : 729
0
15
30
60
90
120
Miles

Figure 4: Isohyetal Map of Chindwin River Basin

5.5 Soil Type

The physiography of soil plays on important role on runoff potential and loss through infiltration. The type of soil and permeability affects the water holding and infiltrating capacity of soil. The soil classes used for the runoff potential are based on the hydrologic property of FAO classification of soil FAO. In the study area there are about 6 types of soil classes. These are gleysols, luvisols, vertisols, acrisols, cambisols and lithosols. The following table lists soil types defined by the FAO together with a brief description of the characteristics of each soil family.

Table 4. FAO Soil Legend

Symbol	Soil Type	Comment
GL	Gleysols	Unless drained, are saturated with groundwater.
CM	Cambisols	Soil with slight profile development that is not dark in colour.
AC	Acrisols	Acidic soils with a layer of clay accumulation. This class consists only of clays with low cation exchange capacity.
LV	Luvisols	Soils with strong accumulation of clay in the B-horizon and not dark in colour. These soils have clays with high cation exchange capacity.
I	Lithosol	Thin soils over rock.
VR	Vertisols	Clayey soils that form deep and wide cracks when dry.

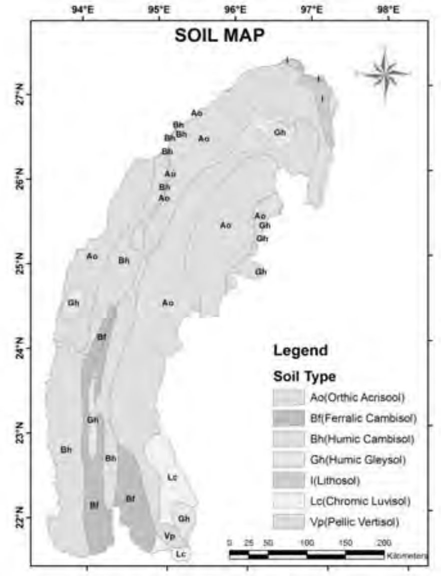
94°E
95°E
96°E
97°E
98°E
27°N
26°N
25°N
24°N
23°N
22°N
SOIL MAP
Ao
Bh
Gh
Bf
Lc
Vp
Legend
Soil Type
Ao(Orthic Acrisool)
Bf(Ferralic Cambisol)
Bh(Humic Cambisol)
Gh(Humic Gleysol)
I(Lithosol)
Lc(Chromic Luvisol)
Vp(Pellic Vertisol)
0 25 50 100 150 200
Kilometers

Figure 5: Soil Map of Chindwin River Basin

Table 5. Weightage of Soil Type For Runoff Potential

Soil Type	Score
Gleysols	1
Cambisols	1
Acrisols	2
Luvisols	2
Lithosol	3
Vertisols	4

5.5 CN Value

A low curve number means that water easily infiltrates into the soil, leaving less for runoff. A high curve number means the water is not captured by the land surface, but instead turns into runoff. Popularity of the method mainly comes from the dimensionless number CN which is tabulated for various soil types and conditions (SCS 1972; USDASCS 1985). To account for the spatial variability of soil moisture, the original USDA procedure adjusts the CN value on the total rainfall of 5 preceding days. The storage volume can be calculated based on CN grids.

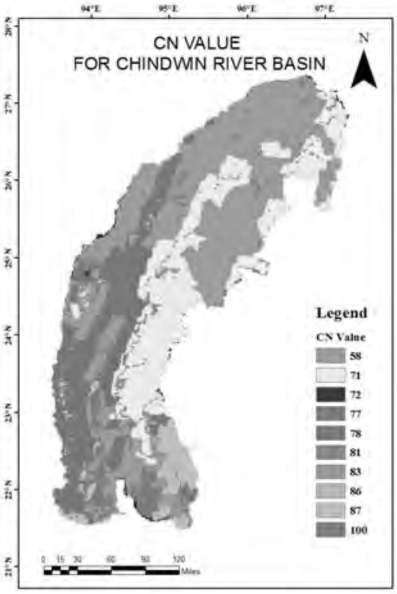
94°E
95°E
96°E
97°E
CN VALUE
FOR CHINDWIN RIVER BASIN
N
Legend
CN Value
58
71
72
77
78
81
83
86
87
100
0 15 30 60 90 120
Miles

Figure 6: CN Map of Chindwin River Basin

5.5 Runoff Potential Using Index Method

The thematic layers include rainfall, land cover, soil type and slope. All point and polygon data were converted to grid. Each of the class in the thematic layers was qualitatively described and reclassified by assigning numbers starting from 1 up to 5. Numbers were assigned based on runoff potentiality of each class in layers. The higher the number is the better runoff potentiality is. Figure 7 shows the runoff potential map for Chindwin river basin using index method.

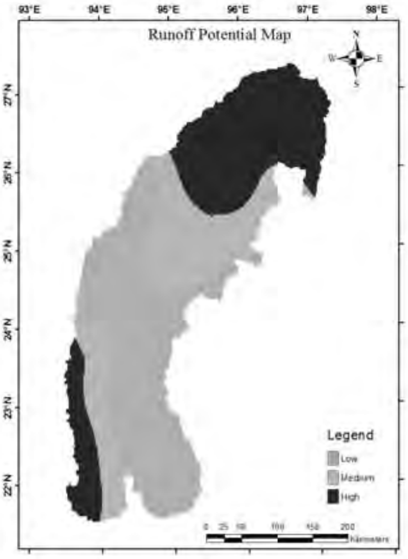
93°E
94°E
95°E
96°E
97°E
98°E
Runoff Potential Map
N
W
E
S
27°N
26°N
25°N
24°N
23°N
22°N
Legend
Low
Medium
High
0 25 50 100 150 200
Kilometers

Figure 7: Runoff Potential Map Using Index Method

5.6 Runoff Potential Using SCS Curve Number Method

The Soil Conservation Service Curve Number (SCS-CN) method is simple, well acclaimed and produces better results. This method takes into account major runoff producing watershed characteristics, like soil type, land use and antecedent moisture conditions (AMCs) to estimate the loss and runoff volume which can be obtained from the optical and microwave remotely sensed data. The calculation process was done using the geographical information system analysis by ArcView. Figure: 8 shows the resulting map of potential runoff for the study area. Maximum potential runoff is around 151 mm in upper part of the Chindwin basin.

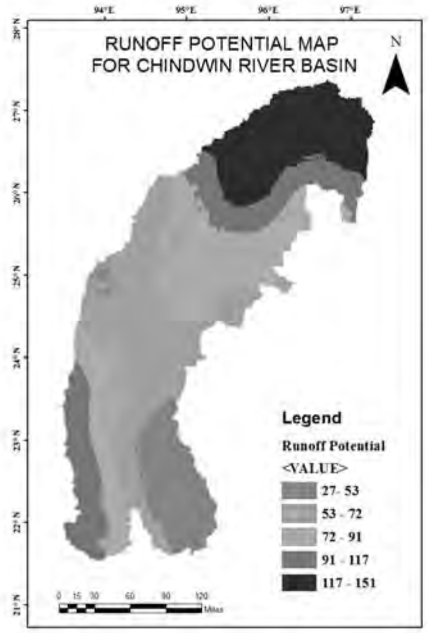

Figure 8: Runoff Potential Map Using SCS Curve Number Method

6. CONCLUSIONS

In this study, runoff potential of Chindwin river basin is estimated integration with GIS. Three classes such as low, medium and high potential were identified by index method and the runoff potential was quantitatively classified by using SCS curve number method too. A weighted overlay model was implemented using five different effective weighted parameters such as land cover, slope, soil type, rainfall, area of the catchment. Satellite data has been proven to be very informative and useful for surface runoff study, especially in detecting surface features and characteristics such as land use and land cover. Spatial thematic maps of the above parameters were prepared in a GIS and runoff potential map was obtained by algebraic summation of these effective weighted parameters. Runoff potential of a catchment that is a crucial design parameter for water harvesting systems.

REFERENCES

Aye, M. N. 2001. *Flood regionalization using rainfall and basin characteristics of*

Chindwin catchments, Ph.D Thesis, Yangon Technological University, Myanmar.

Chang, K-T., *Introduction to geographic information systems* 4th ed., Tata McGraw-Hill.

Maidment, D. R., and Mason, D., *An analysis of a methodology for generating watershed parameters using GIS*, The University of Texas, Austin, TX 78712-4497.

Maung Win Min Oo, 2013. *An integrated approach of remote sensing and GIS for the groundwater potential*, Ph.D Thesis, Yangon Technological University, Myanmar.

Musa, K A., Juhari Mat, A., and Abdullah, I. 2000. Groundwater potential zoning in Langat basin using the integration of remote sensing and GIS. *The 21st Asian Conf. on Remote Sensing, Taipei* (Taiwan).

Longley, P. A., Goodchild, M. F., Maguire, D. J., and Rhind, D. W., *Geographic information systems and science* 2nd ed., John Wiley and Sons, Ltd

Oberle, A., 2004. *GIS-based identification of suitable areas for various kinds of water harvesting in Syria.*

Assessment of environmental flows requirment for the Upper Ayeyawaddy River Basin

Tin Mar LWIN[1], Khin Ni Ni THEIN[2],Win Win ZIN[3], Cho Cho Thin KYI[4]
[1]Ph.D. Candidate, Dept. of Civil Engineering, Yangon Technological University,
tinmarlwin001@gmail.com
[2]Visiting Senior Professor and National Water Resources
Committee Member
[3]Associate Prof., Dept. of Civil Engineering, Yangon Technological University
[4]Associate Prof., Dept. of Civil Engineering, Yangon Technological University

ABSTRACT

The natural flow of the tributaries of Ayeyawaddy river have been altered due to the construction of the water infrastructures. . The flow alterations affect some or all components of stream health: ecosystem and physical alteration of the river. Many hydropower dams have also been planned on the Upper portion of the main stem of the Ayeyawaddy river to fulfill the hydropower requirement for the socio-economic development of the country. For the Upper portion Ayeyawaddy river, balancing the requirement of water of the aquatic environment, environmental flow, and other uses is becoming critical to safeguard as the healthy river. This study aim to assess the river health impact points of the Upper Ayeyawaddy River Basin by using Dundee Hydrological Regime Assessment Method (DHRAM) tool based on daily hydrologic data and also attempt to consider environmental flow requirements for the Upper Ayeyawaddy River Basin at unmodified flow condition by applying hydrological method for sustainable development based on integrated water resources management (IWRM) approach.

Keywords: Dundee Hydrological Regime Assessment Method (DHRAM), environmental flow, hydrologic alteration, Integrated Water Resource Management (IWRM)

1. INTRODUCTION

The Ayeyawady river flows from north to south of Myanmar. It is the country's largest river (about 1350 miles or 2170 km long) and the most important commercial waterway, with a drainage area of about 413,000 km². There is a saying that "Ayeyawady is Myanmar", which reflects the fact that the total area of the Ayeyawady River Basin is nearly 61% of the total land area of Myanmar. It is rich in natural resources particularly forests, land and water resources in addition to biodiversity. Large part of the Water-Energy-Food security of Myanmar depends upon that ecosystem. Therefore ecosystem of the Ayeyawady River Basin and the entire river system play a crucial role as the lifeline of Myanmar populace. Achieving sustainable development of these resources is vital to the country and the sustainability of water-energy-food security in Myanmar is of paramount importance. Environmental flows refer to water provided within a river, wetland or coastal zone to maintain ecosystems and the benefits they provide for people and the environment. In other words, environmental flows are effectively a balance between water resources development and the need to protect freshwater-dependent ecosystems. There is abundant hydropower potential, mainly on the upper portion of the Ayeyawady river. Hydropower stations and dams are currently being planned to fulfill the electricity requirement for the social and economic development of the country. The hydropower dams have been already constructed on the tributaries of the Ayeyawaddy river. The study of environmental flow for Upper Ayeyawady River Basin aims to minimize the adverse impact of water infrastructure development project on aquatic ecosystems. Therefore, environmental flow is an urgent and important need to protect the Ayeyawady's river and it will also support in the development of integrated water resources management in Myanmar.

2. GENERAL DESCRIPTION OF STUDY AREA

2.1 Physiography

The Ayeyawady River Basin is situated at 15º 30' ~ 28º 50' north latitude and 93º 16'~98º 42' east longitude. The river has two source rivers. The eastern source originates at the southwest foot of Boshula Mountains within Chayu Country of Tibet Autonomous Region in China, which is called Jitaiqu in Tibet Autonomous Region and Dulongjiang in Yunnan Province. It flows into Myanmar via Maku of Gongshan Country in Yunnan Province, China and is then named as May Kha River. The western source river, the Mali Kha River, originates from the northern mountainous region of Myanmar. The confluence (Myitsone in Myanmar language) is situated at a place approximately 45 km north of Myitkyina, where the two branches converge. From there, it is called the Ayeyawady River. It traverses the entire Myanmar from the north to the south, flowing through the mountainous region in the north, the arid region in central Myanmar and the delta area in the south.

2.2 Climate condition

The Ayeyawady River Basin lies in Asia southwest monsoon zone, where the climate is effectively affected by the southwest monsoon. There are three seasons in a year. From March to May, it is a hot season. From June to October, it is a wet season. From November to February, it is a cool season. The average air temperature in January, the coldest month ranges from 20ºC to 25ºC. The average air temperature in April, the hottest month, ranges from 25ºC to 30ºC.

There is abundant rainfall in the basin with an annual rainfall of 2,000~4,000 mm in the north and the delta, and 600~1,000mm in the plains at the middle stream of the river. The maximum rainfall usually occurs in July. Whenever the rainy season comes, the southwest monsoon is dominant, which brings abundant rainfall resulting in swift water rising and floods. When the dry season comes, the river water level drops. A lot of tideland and islets are outcropping and the river drops. In the Bhamo region in the upstream of Ayeyawady River, the width of the river is less than 500m in the hot season, while it reaches over 3 km in the rainy seasons. The variation of the water level is around 10 m in a whole year. The average annual rainfall in Machanbaw and Putao (within Myanmar) is approximately 4,000 mm. The average annual rainfall in Myitkyina is 2,314 mm, 1,8000 mm in Bhamo and 1,510 in Katha.

3. DATA USED

Environmentally acceptable flow regimes should mimic natural patterns of flow variability in a river (Richer et al., 1997; Hughes and Hannart, 2003). The natural flow variability is best described by time series of daily discharges. In the Upper Ayeyawady River Basin, there are three hydrological stations, namely, Myitkyina, Katha and Sagaing. The daily mean discharge data of these stations were obtained from the Department of Hydrology and Meteorology (DMH). The available data length for these stations are_ Myitkyina station(1970-2011), Katha (1966-2011) and Sagaing (1966-2011). According to DWIR, the catchment area for Myitkyina is 41, 803 Sq. Km, Katha is 77, 942 Sq. Km and Sagaing is 117, 900 Sq. Km respectively. The river basins and river system of Myanmar is shown in Figure 1 and the location Map of Upper Ayeyawady River Basin and its hydrological stations are shown in Figure 2. The location of proposed dam sites and constructed dam site are also shown in Figure 3.

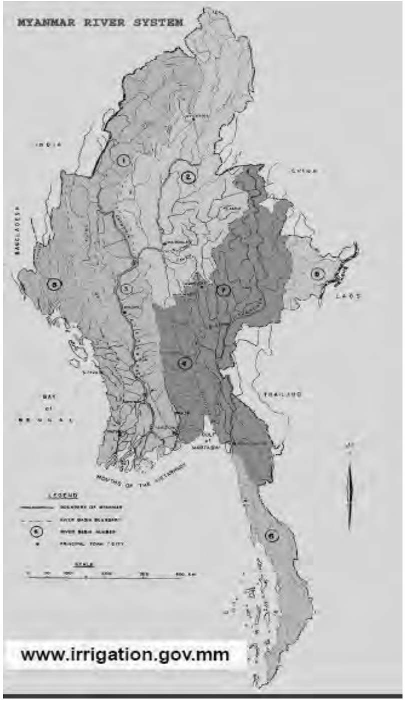
MYANMAR RIVER SYSTEM
INDIA
CHINA
BANGLADESH
LAOS
THAILAND
BAY OF BENGAL
LEGEND
www.irrigation.gov.mm

Figure 1: Major river basins in Myanmar

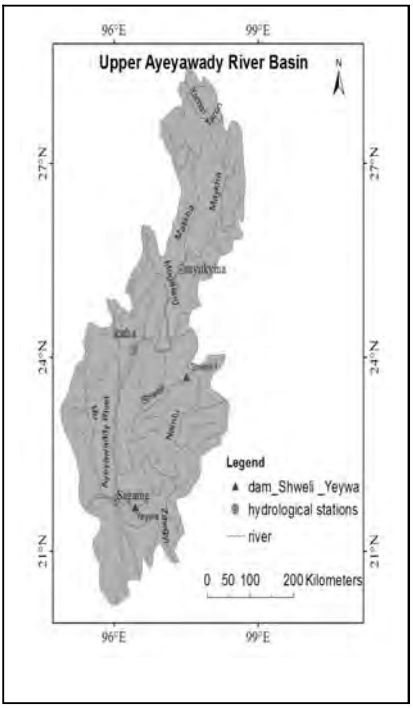
96°E
99°E
Upper Ayeyawady River Basin
N
27°N
24°N
21°N
Myitkyina
Katha
Shweli
Sagaing
Yeywa
Legend
dam_Shweli _Yeywa
hydrological stations
river
0 50 100 200 Kilometers

Figure 2: Catchment area of Upper Ayeyawady river basin

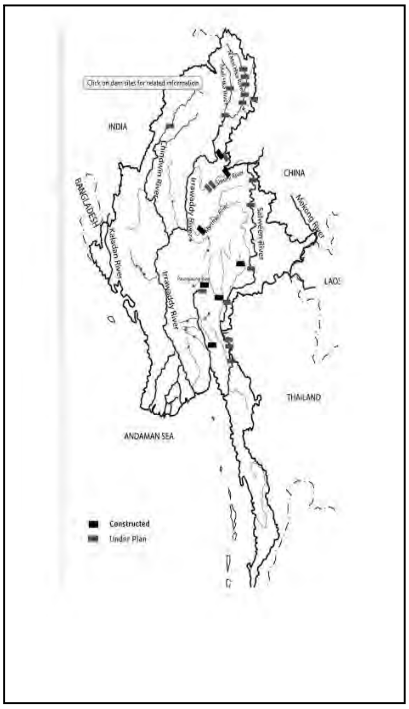
Click on dam sites for related information
INDIA
CHINA
BANGLADESH
LAOS
THAILAND
ANDAMAN SEA
Constructed
Under Plan

Figure 3: Proposed and constructed dams location in Myanmar

3. METHOD AND ANALYSIS

Five groups of hydrologic parameters,(1) maginitude of monthly water condition, (2) magnitude and duration of annual extremes, (3) Timing of annual extremes, (4) Frequency and duration of high and low pulses and (5) Rate and frequency of change in conditions, are influenced on both river health and ecosystem. The mean and coefficient of these five groups of hydrologic paramenters are generated by using Indicator of Hydrologic Alteration (IHA) software based on daily flow data. The total impact point of river health is calculated by comparing the percentage difference of mean and coefficient of variation of these five groups of hydrologic parameters of pre-alteration and post-alteration flow data periods by using DHRAM (Dundee Hydrological Regime Assessment Method) tool. There is no risk to stream health if the total impact point generated by DHRAM tool is zero. If the total impact points range from 1 to 4, the river health is low risk. For the moderate risk of river, the total impact points range from 5 to 10. The total impact points for high risk of river range from 11 to 20. The river health can be defined as server risk if the total impact points range from 21-30. The river health of Upper Ayeyawaddy river basin is assessed at Myitkyina, Katha and Sagaing stations based on daily flow data by using IHA-DHRAM approach.

There are many techniques and methods being applied to assess the environmental flows requirements. These methods can be classified into four categories_ hydrological method, hydraulic rating methods, habitat simulation and holistic methods. The methods differ in scope of application and data requirements. The approach to assess environmental flow for the Upper Ayeyawady river basin was developed by using hydrological method. Tennant method describes a threshold of 10 percent of mean annual flow reserved for aquatic ecosystem was considered to be the lowest limit for environmental flow considerations. Fair/good habitat conditions could be ensured if 35 percent of the mean annual flow is allocated for environmental purpose. Allocation in the range of 60 to 100 percent of mean annual flow represents an environmental optimum. Historical daily mean discharge data of Myitkyina, Katha and Sagaing stations was collected from Department of Hydrology and Meteorology (DMH). Mean annual flow for each discharge station is analyzed from the historical daily mean flow data. The seasons for Tennant's method are categorized as high flow season for the months of May to October, and low flow season for the months of November to April for the study area.

Global Environmental Flow Calculator (GEFC) was developed by International Water Management Institute (IWMI) to link the flow and ecology condition based on flow duration curve approach method. Environmental management class (EMC) based on flow duration curve approach is based on mean monthly flow data. There are six ecological classes in this method such as Class A- natural, Class B- slightly modified, Class C – moderately modified, Class D – largely modified, Class E –seriously modified and Class F – critically modified Environmental flow requirement for each ecological class are determined by the lateral shift of the original reference FDC – to the left, along the 17 percentage points on the probability axis: 0.01, 0.1, 1, 5, 10, 20, 30, 40, 50, 60, 70, 80, 90, 95, 99, 99.9 and 99.99. The higher the EMC, the more water will need to be allocated to the ecosystem or conservation and more flow variability will need to be preserved.

FDCs are hydrological tools that are used to represent the percentage of time flows that are equaled or exceeded for a particular river location. Q95 and Q90 flows are most often used as low flow indices the government literature and academic sources.

4. RESULTS

The pre-alteration period and the post-alteration period of Myikyina, Katha and Sagaing stations are divided by based on the change point of cumulative curve of rainfall and water level on slope line. After drawing the cumulative curves for each station, the change point of cumulative curve for Katha station starts at 1979 and for the Sagaing station starts at 1975.

There is no change point of cumulative curve for Myitkyina station. Therefore, pre-alteration period and post-alteration period for Myitkyina station is assumed as (1970-1990) and the post-alteration period for Myitkyina station is assumed as (1991-2011). The former periods of change points (1966-1979) is regarded as pre-alteration period for Katha station and the later periods of change points (1980-2011) is regareded as post-alteration period. The pre-alteration period for Sagaing station is (1966-1975) and the post-alteration period for Sagaing station is (1976-2011). The five groups of hydrologic parameters are caluculated by using IHA software based on these pre- and post-alterations periods. DHRAM tool calculated the percentage difference of mean and coefficient of variation of five groups hydrologic paraments to assess the river health of Myitkyina, Katha and Sagaing stations. By using DHRAM, the estimated impact points for river health at Myitkyina station is 3 (low risk of impact), Katha station is 4 (low risk of impact) and the Sagaing station is 5 (moderate risk of impact).

The amount of environmental flows requirement at gauging stations of the upper Ayeyawady river basin by using GEFC software is summarized in Table 1. The GEFC software describes the amount of environmental flows requirement as a percentage of mean annual runoff. The mean annual runoff calculated by GEFC software is for 159718 million cubic meter, 160,146 million cubic meters and 233,334 million cubic meters respectively in Myitkyina, Katha and Sagaing stations. These can also be shown as flow rates in three gauging stations, 5065 cumecs in Myitkyina, 5078 cumecs in Katha and 7399 cumecs in Sagaing. The shifting flow duration curve for each ecological class developed by GEFC software is depicted in Figure 4 to 6. Flow duration curve is based on daily mean discharge. In this study 50 percentile flow for high flow season and 90 and 95 percentile flows for the low flow season is being considered as require Environmental Flow as shown in Table 2 and Figure 7 to 9.

The mean annual flow analyzed from historical mean daily discharge data for Myitkyina is 5155 cumecs, Katha is 5178 cumecs and Sagaing is 7609 cumecs. The environmental flows requirement for the upper Ayeyawady river basin for wet and dry seasons based on Tennant method is described in Table 3 and 4.

Table 1: Environmental flows requirement for the gauge stations of Upper Ayeyawaddy river basin by global environmental flows calculators

Station name	**Environmental Flow Requirement (% of MAR)**					
	Class A	**Class B**	**Class C**	**Class D**	**Class E**	**Class F**
Myitkyina	82.5	65.4	51.5	40.7	32.7	27
Katha	78.9	58.7	42.4	30.3	21.9	16.2
Sagaing	78.1	57.8	41.9	30.3	22.1	16.6

Table 2: Environmental flows requirement for the guage stations of Upper Ayeyawaddy river basin based on flow duration method by using daily mean

Station	**50th percentile flow (cumecs)**	**90th percentile flow (cumecs)**	**95th percentile flow (cumecs)**
Myitkyina	3607	1493	1289
Katha	2812	1003	842
Sagaing	4342	1604	1217

Table 3.Environmental flows requirement for the guage stations of Upper Ayeyawaddy river basin in wet season based on Tenant method

Narrative description of flows	**Myitkyina m^3/s**	**Katha m^3/s**	**Sagaing m^3/s**
Flushing or maximum	10310	10356	15218
Optimum range	3093-5155	3106.8-5178	4565.4-7609
Outstanding	3093	3106.8	4565.4
Excellent	2577.5	2589	3804.5
Good	2062	2071.2	3043.6
Fair or degrading	1546.5	1553.4	2282.7
Poor or maximum	515.5	517.8	760.9
Severe degradation	0-515.5	0-517.8	0-760.9

Table 3: Environmental flows requirement for the guage stations of Upper Ayeyawaddy river basin in dry season based on Tenant method

Narrative description of flows	**Myitkyina m^3/s**	**Katha m^3/s**	**Sagaing m^3/s**
Flushing or maximum	10310	10356	15218
Optimum range	3093-5155	3106.8-5178	4565.4-7609
Outstanding	2062	2071.2	3043.6
Excellent	1546.5	1553.4	2282.7
Good	1031	1035.6	1521.8
Fair or degrading	515.5	517.8	760.9
Poor or maximum	515.5	517.8	760.9
Severe degradation	0-515.5	0-517.8	0-760.9

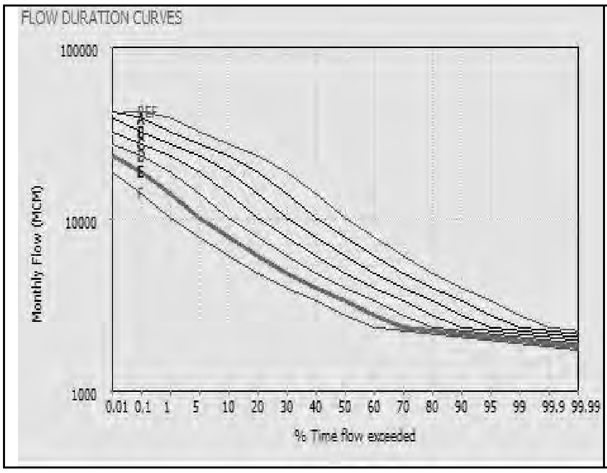

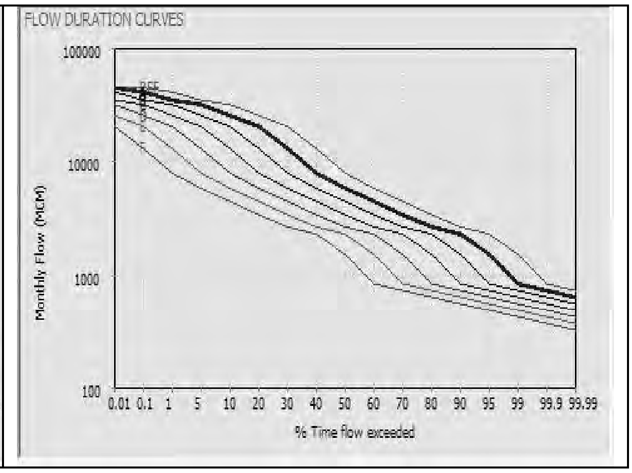

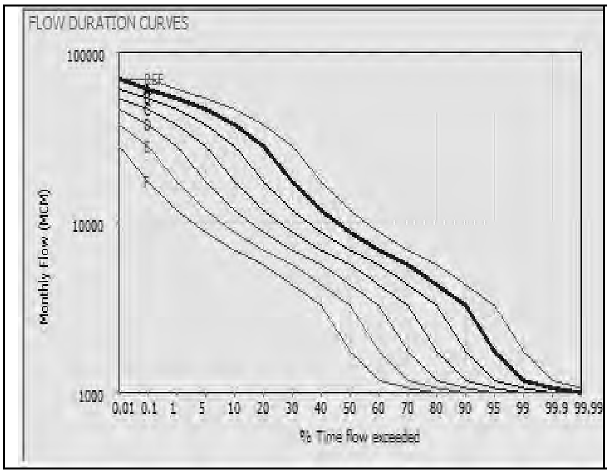

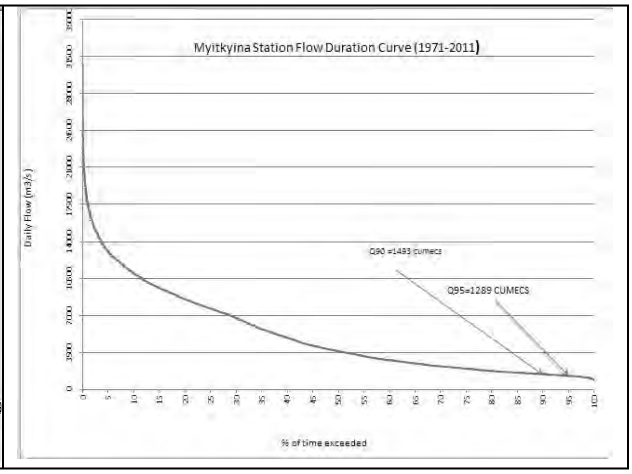

Figure. 6 Environmental flow duration curve for Sagaing discharge station by GEFC

Figure. 7 Daily flow duration curve for Myitkyina discharge station

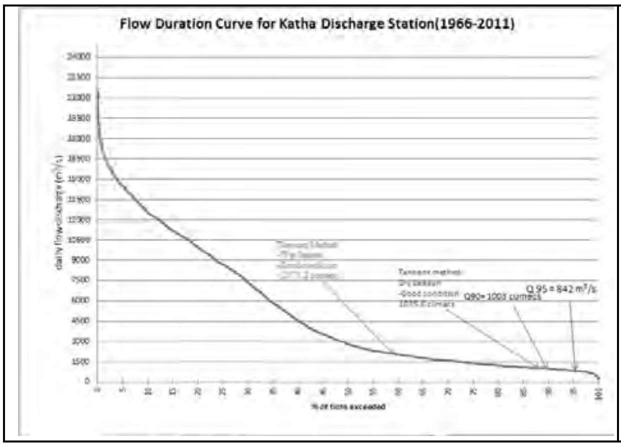

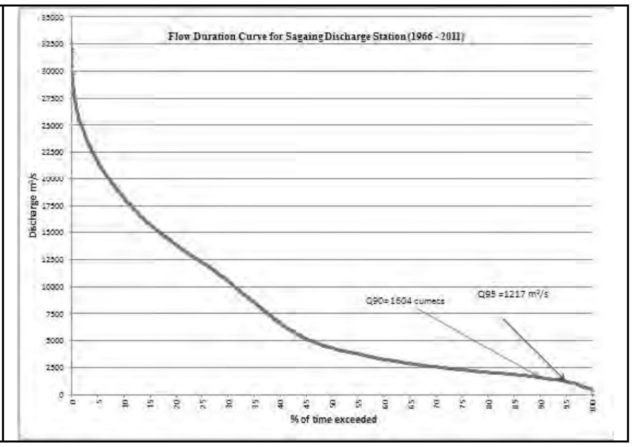

Figure 8 Daily flow duration curve for Katha discharge station

Figure 9 Daily flow duration curve for Sagaing discharge station

5. CONCLUSION

Although there is no dam along the main stem of the Ayeyawaddy river, many dams had already been constructed and have been planned to construct at the tributaries of the Ayeyawaddy river. To study whether the construction of dam at the tributaries affects on the main stem, the river health assessment is carried out on the Upper portion of the Ayeyawaddy river.The river health is assessed at the guaing stations of Upper Ayeywaddy river basin: namely Myitkyina, Katha,and Saginaing stations, by using IHA-DHRAM approach based on daily flow discharge data. The river health assessment at the Myitkyna and Katha stations is low risk of impacts and the moderate risk of impact is occurred at Sagaing station. This is seem to be that the hydropower dam at the upper portion of the Ayeywaddy river above Myikyina guaging station are under planning state and there are not many dams near Katha guaging station. Near Sagaing gaugin station, hydropower dams, Yeya and Shwe Li dams, have already been constructed at the tributaries, Myitnge river and Shweli river, of the Ayeyawaddy of the river near Sagaing station and the total catchment area of these tributaries rivers is about 30 % of the Upper Ayeywaddy river basin. Since construction of dam at the tributaries of the river can also impact on the main stem of the river, environmental flow requirements should be assessed not only at the adjacent downstream of the dam site but also on the main stem of the river. The environmental flow requirement for the upper Ayeyawady river basin at three gauging stations is calculated based on hydrological analysis method. Those include six Environmental Management Class based on the flow duration curve approach by applying Global Environmental Flow Calculator (GEFC), flow duration curve method and Tennant method. GEFC and Tennant method describe the linkage between flow and ecological discharge while the flow duration curve describes the percentage of time that the specified daily discharges are equal or exceeded during a given period of record. The ecological class and the flow obtained by GEFC and Tennant method determined the confidence limits of the flow amount by using a daily flow duration curve. The environmental flow requirement for moderately modified condition of Class C calculated by GEFC and Tennant's method of wet season of good ecological condition exceeded the 50th percentile flow of the daily flow duration curve. The dry season of good ecological condition by Tennant's method exceeded the 90th percentile flow of the daily flow duration curve. According to the hydrological method based on daily discharge data, the conservation of 50th percentile (for wet season) and 90th percentile (for dry season) of the daily flow duration curve at the Myitkyina, Katha and Sagaing stations will maintain the good ecological conditions.

Most of the Myanmar's river basin, including the upper Ayeyawady river basin, there was no assessment made so far to determine the environmental flow requirement. The main purpose of this study is to simulate the environmental water allocation prospects in the country and the results suggest that river ecosystem could be maintained in a reasonable state with existing data based on hydrological method. This study should be seen as a step towards the development of more detailed environmental flow tool in the field of environmental flow assessment for the Myanmar's river basins.

REFERENCES

Acreman, M. and Dunbar, M. J., 2004. Defining environmental river flow requirements - a review. *Hydrology & Earth System Sciences* 8. 861-876.

Brown, C. and King, J., 2003. Environmental flow assessment: Concepts and methods. *Water Resources and Environment*, Technical Note C.1., World Bank, Washington D.C.

Dyson, M., Bergkamp, G., and Scanlon, J., 2004. *Flow: The essentials of environmental flows*. IUCN, Gland, Switzerland and Cambridge, UK.

Korsgaard, L., 2006. *Environmental flows in integrated water resources management: linking flows, services and values*. Ph.D Thesis, Institute of Environment and Resources, Technical University of Demark. Available Online, from http:///www.er.dtu.dt

Mullick, M. R.A., Babel, M.S. and Perret, R., 2010. *Flow characteristics and environmental flow requirements for the Teesta River, Bangladesh*. In: The Proceedings of International Conference on Environmental Aspects of Bangladesh. University of Kitakyushu, Japan, September 4, 159-162.

Meijer, K., 2006. *Human Well-Being Values of Environmental Flows*. Ph.D thesis. Delft University, Delft, The Netherlands.

Poff N. L., Allan J. D., Bain M. B., Karr J. R., Presteegard K. L., Ritcher B. D., Sparks R. E., and Stromberg, J. C., 1997. The natural flow regime. *Bioscience* 47, 769.

Postel, S., and Richter, B., 2003. *Rivers of life. Managing water for people and nature*. Island Press, Washington D.C.

Ramakar Jha, Sharma, K. D., and Singh, V. P. 2008. Critical appraisal of methods for the assessment of environmental flows and their application in two river systems of India. *KSCE Journal of Civil Engineering* 12, 213-219.

Ritcher, B. D., Baumgartner, J. V., Braun, D. P. and Powell, J., 1997. How much does a river need? *Freshwater Biology* 37, 231-249.

Smakthin, V. U., Shilpakar, R. L., and Hughes, D. A., 2006. Hydrology-based assessment of environmental flows: an example from Nepal. *Hydrol. Sci. J.* 51, 207-222.

Smakhtin V. U. and Anputhas, M., 2006, *An assessment of environmental flow requriments of Indian river basin*, International Water Management Institute, Colombo, Sri Lanka, 42 (IWMI, research report 107).

Tharme, R. E., 2003. A global perspective on environmental flow assessment: Emerging trends in the development and application of environmental flow methodologies for rivers. *River Research and Applications* 19, 397-441.

Tennant, D. L., 1976. Instream flow regimes for fish, wildlife, recreation and related environment resource. *Fisheries* 1, 6-10.

US Environmental Protection Agency, 2011. An approach for estimating stream health using flow duration curves and indices of hydrologic alteration. Agri Life Reasearch and Extension, Texas A&M system.

Vogel, R. M. and Fennessey, N. M., 1995. Flow duration curves II: A review of applications in water resources Pplanning. *Journal ofthe American Water Resources Association* 31, 1029-1039.

Forecasting flash flood over Daungnay ungagged watershed using GIS techniques and HEC-HMS model

Yin Yin HTWE[1] and Aye Aye THANT[2]
[1]PhD research candidate, Department of Civil Engineering,
Mandalay Technological University, Mandalay, Myanmar
yinyinhtwe.civil@gmail.com
[2]Lecturer, Department of Civil Engineering,
Mandalay Technological University, Mandalay, Myanmar

ABSTRACT

This study reveals forecasting flash flood over Daungnay ungaged watershed using GIS techniques and HEC-HMS model. The flash flood forecasting is one of the most important challenges for research in hydrology as flash floods are considered natural disasters that can cause casualties and demolishing of infrastructures. In this study, Remote Sensing and GIS Techniques are used to develop Digital Elevation Model and to extract watershed and its drainage network for Daungnay creek. There are 17 sub-basins (10 upstream sub-basins and 7 downstream sub- basins) in this watershed. The Soil Conservation Service (SCS) curve number (CN) method and synthetic dimensionless unit hydrograph (UH), and Muskingum stream routing applied in HEC-Hydrological Modeling System (HEC-HMS) to formulate flood characteristic for the study area. Storm frequency is considered as input data for meteorologic model component in HEC-HMS. Each sub-basin is modeled with its own parameters. The respective curve number for each sub-basin is determined from the landuse map and hydrologic soil map. Landuse map is classified from landsat satellite image in ENVI software. Muskingum Stream routing method is used to predict the changing magnitude of flood as a function of time at the points along the watercourse for various design return periods. Routing time step is assumed to be 15 minutes. The discharge data from the rainfall-runoff model utilizing HEC-HMS is used to produce maps for run-off volume and flood discharge.

Keywords: *flash flood forecasting, digital elevation model, Daungnay watershed, HEC-HMS, Arc-GIS*

Climate change effects in central dry zone, Myanmar

Aye Myint KHAING[1] and Win Win ZIN[2]
[1] Ph.D Student, Department of Civil Engineering, Yangon Technological University
ayemyintkhing410@gmail.com
[2]Associate Professor, Department of Civil Engineering,
Yangon Technological University

ABSTRACT

This research evaluates the possible effects of climate change on meteorological variable of central dry zone of Myanmar. These variables are important indicators of climate change. One of the commonly used tools for detecting change in climatic and hydrologic time series is trend analysis. Annual rainfall data was analyzed in order to detect climate change. The physical impact of climate change in relation to water resources through the analysis of water availability, water demand and the supply situation are determined. The growing water scarcity due to climate change will pose a serious threat to food security, poverty reduction and protection of the environment. In this study, the Mann-Kendall non-parametric test, which is widely used to detect trends, was applied. The change per unit time was estimated by applying Sen's estimator of slope. It is important to investigate present and probable future climatic change patterns and their impacts on water resources so that appropriate adaptation strategies may be implemented.

Keywords: climate change, trend analysis, non-parametric test, Mann-Kendall, Sen's slope.

1. INTRODUCTION

Particularly, identification of trends in long-term runoff is one of the important themes in hydrologic science (NRC 1991). The reason is that the long-term runoff analysis is an important tool for detecting any modification in hydrological systems (Chang, 2007). Climate variability has relevant importance on the hydrology and water resources availability in the world. Changes in temperature and precipitation patterns as consequence of the increase in concentrations of greenhouse gases may affect the hydrology process, availability of water resources, and water use for agriculture, population, mining industry, aquatic life in rivers and lakes, and hydropower. One of the most important impacts of climate change is on hydrology, which results in changes in river flows and regional water resources. Climate change is expected to intensify the global hydrological cycle resulting in major impacts on regional water resources. A change in the total amount, frequency, and the intensity of precipitation will directly affect the amount and timing of runoff and intensity of floods and droughts.

Trend detection in hydrological data has become increasingly popular in connection with climate change (Hamed, 2008). Trend analysis has been widely used to evaluate the potential impacts of climate change in hydrologic time series throughout the world, including the US, Western Europe, Canada, and Western Britain (Hamed, 2008). Climate change also causes trends not previously experienced or detected, which provide new challenges. In recent year, with growing concerns about the impacts of climatic changes (IPCC, 2007), researchers have employed various statistical and stochastic techniques to identify trends and shifts in hydrological series at different temporal scales of aggregation.

Changes in precipitation and streamflow characteristics directly impact hydrology, water resource management, agricultural practices and ecosystems. Therefore, it is vital to investigate the climate change impact on spatial and temporal rainfall characteristics to facilitate better water management practices and strategy. One of the commonly used tools for detecting changes in climatic and hydrologic time series is trend analysis. In this study, the Mann-Kendall non-parametric test, which is widely used to detect trends, was applied. The change per unit time in a time series having a linear trend was estimated by applying a simple non-parametric procedures namely Sen's estimator of slope. Trend detection is an active area of interest for both hydrology and climatology in order to investigate climate change scenarios and enhance climate impact research.

Therefore, it is vital to investigate the climate change impact on precipitation and streamflow characteristics to facilitate better water management practices and strategy. In this study, the time series data refer to the period mostly from 1967 to 2013. The methodology adapts statistical approach in order to detect possible changes in time series. The Mann-Kendall test is a non-parametric test for detecting trends in time series data. This test is widely used for analysing environmental data, including precipitation data (Partal and Kahya, 2006), streamflow data, and water quality data. This method is simple and robust and can cope with missing values and values below a detection limit. Linear regression is another simple and good approach to detecting trends in monthly precipitation and discharge data.

The data network used in this study consists of twelve stations of Central Dry Zone of Myanmar. This paper examines the possible effects of climate change on meterological variables in Central Dry Zone of Myanmar.

2. LOCATION OF THE STUDY AREA

The Dry Zone is one of the most climate sensitive and natural resource poor regions in Myanmar. The dry zone lies between latitudes 19° 20" and 22° 50" north and longitudes 93° 40"and 96° 30" east, stretching across the southern part of Sagaing Division, the western and middle part of Mandalay Division and most parts of Magway Division. It is situated in the rain shadow area of the Yakhaing Yoma and obtains most of its rainfall from the southwest monsoon. The zone covers approximately 54,390square kilometers and represents about 10% of the country's total land area. The present population in the Dry Zone is estimated at 18 million people. It constituted 34% of the country's total population. The population density is 123 people per square kilometer, making it the third most densely populated region in Myanmar. Across the Dry Zone, water is scarce, vegetation cover is thin, and soil is degraded due to severe erosion. The region is characterized by low annual rainfall that ranges between 508 and 1016 mm per annum with high variability and uneven distribution. The monsoon rain is bimodal with a drought period during July when dry desiccating winds blow from the south. The undulating land, composed mainly of sandy loam with low fertility, is subjected to severe erosion under rain and strong winds. The average mean temperature in the Dry Zone is about 27˚ C and the temperature often rises to about 43˚ C in the summer period. This dry environment with its other natural limiting factors has led to conditions of growing food insecurity and severe environmental degradation.

The major economic activities in the Dry Zone are subsistence farming and small agricultural crops such as paddy, sesame and groundnut. Agricultural productivity is low and the farmers are heavily dependent on products from the natural forest especially fuel wood, pole, post and fodder to support their living and livestock. Many landless people are working as seasonal farm labourers, migrating to urban regions during non-planting time to find temporary employment. Location of study area is shown in Figure 1.

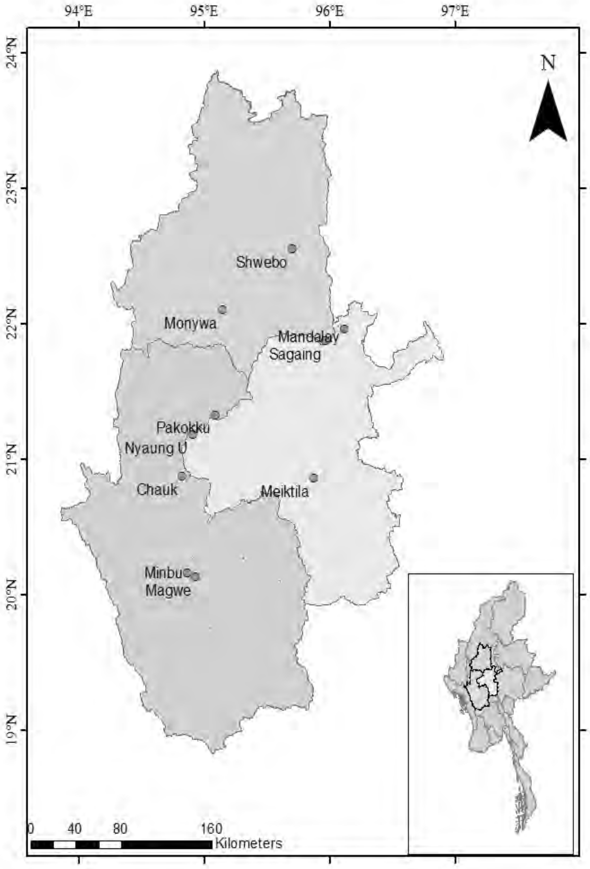

Figure 1: Location map of the study area

3. METHODOLOGY

The steps involved in analysing are as follows:

1. The first step was to choose the variables to be studied. Rainfall and temperature variables were used, as they tend to reflect an integrated response of the catchment area as a whole.

2. The second step was to choose the stations that have sufficient long time records of data.
3. The third step was to check for the present of trends in the data. This was done using the Mann-Kendall non-parametric test.
4. The fourth step was to determine the significance of the detected trends. This was accomplished utilizing a permutation procedure. It was also necessary to define a global, or field, significance level, reflecting the correlation structure that exists in the data set.

3.1. Tests for Trends

There are many tests for trend identification. They are as follows:

1. Mann-Kendall test,
2. Sequential Mann-Kendall test,
3. Seasonal Kendall test,
4. Spearman's Rho test,
5. Sen's T test, and
6. Linear Regression test.

In this study, Mann-Kendall test was applied. This test was found to be an excellent tool for trend detection by other researchers in similar applications (Hirsch et al., 1982).

3.1.1 Mann-Kendall Test

The time series of all the hydrologic variables were analysed using the Mann-Kendall non-parametric test for trend. (Mann, 1945) originally used this test and (Kendall, 1975) subsequently derived the test statistic distribution. The Mann-Kendall test is based on the null hypothesis that a sample of data is independent and identically distributed, which means that there is no trend or serial correlation among the data points. The alternative hypothesis is that a trend exists in the data. First, the statistic defined by variable S was computed. It is the sum of the difference between the data points for a series {x_1,….., x_n} which come from a population where the random variables are independent and identically distributed shown in the following equations:

$$S = \sum_{k=1}^{n-1} \sum_{j=k+1}^{n} \operatorname{sgn}\left(x_j - x_k\right) \qquad (1)$$

$$\operatorname{sgn}(x_j - x_k) = \begin{cases} +1 \text{ if } (x_j - x_k) > 0 \\ 0 \quad \text{if } (x_j - x_k) = 0 \\ -1 \text{ if } (x_j - x_k) < 0 \end{cases} \qquad (2)$$

Mann (1945) and Kendall (1975) determined that the statistics S is normally distributed when $n \geq 8$ allowing for the computation of the standardized test statistics Z which represent an increasing or decreasing trends respectively. For the statistical trend test used in this study, a 5-percent level of significance was selected. The 5- percent level of significance indicates that a 5-percent chance for error exists in concluding that a trend is statistically significant when in fact no trend exists.

$$z = \begin{Bmatrix} \frac{S-1}{\sqrt{Var(S)}} \text{if} \quad S > 0 \\ 0 \qquad\quad \text{if} \quad S = 0 \\ \frac{S+1}{\sqrt{Var(S)}} \text{if} \quad S < 0 \end{Bmatrix} \tag{3}$$

Where Var(S), the variance of the data point is given by,

$$Var(S) = \frac{1}{18}\left[n(n-1)(2n+5) - \sum_t t(t-1)(2t+5) \right] \tag{4}$$

Where m is the number of tied (i.e., equal values) groups in the data set and t is the number of data points in the i^{th} tied group. Under the null hypothesis, the quantity z defined in the following equation is approximately standard normally distributed even for the sample size n = 10. The positive values of S indicate upward trends whereas negative S value indicate downward trend.

The slope of the data set can be estimated using the Thiel/Sen Approach. This equation is used instead of a linear regression because it limits the influence that the outliers have on the slope (Hirsch et al., 1982). To normalize the slopes calculated for streams of different size, the mean flow value of each parameter and station was used to find a percent change in flow rate.

$$\beta = \text{Median}\left[\frac{X_j - X_i}{j - i} \right] \quad \text{For all } i < j \tag{5}$$

Mann-Kendall approach requires the data to be serially independent. Serial correlation indicates the relation between a data point and its adjacent point. If the data are positively serially correlated then the Mann Kendal approach by itself tends to overestimate the significance of a trend. If, on the other hand, the data have a negative serial correlation, then the significance of the trend is underestimated. To correct the serial correlation in the data, a form of pre-whitening of the sample has been used (Yue et al., 2002).

$$Y_t = X_t - \beta t \tag{6}$$

Where X_t is the series value at time t, β_t is the slope and Y_t is the detrended series. When the trend is removed from the data, then an estimate of the lag-1 sample serial correlation using the detrended series is calculated using Equation 3.13. The use of an autoregressive AR (1) model is justified due to the weak serial correlation present in most hydrological time series. The lag-one serial coefficient is calculated after the trend was removed in order to preserve the initial trend.

$$r_k = \frac{\frac{1}{n-k}\sum_{t=1}^{n-k}\left(Y_t - \overline{Y}_t\right)\left(Y_{t+k} - \overline{Y}_t\right)}{\frac{1}{n}\sum_{t=1}^{n}\left(Y_t - \overline{Y}_t\right)^2} \tag{7}$$

If lag-one serial correlation coefficient (r_k) is not significant at 5% significance level, then the Mann-Kendall test is applied to the original time series. Otherwise, it is removed from Y_t as:

$$Y'_t = \overline{Y}_t - r_1 Y_{t-1} \tag{8}$$

This procedure is known as the Trend-Free Pre-Whitening (TFPW) procedure. The third step is to add the trend back to Y'_t by using Equation 3.14 and then the Mann-Kendall test is conducted on this new series.

$$Y = Y'_t + \beta t \tag{9}$$

Kendall’s tau is an alternative non-parametric statistic that can be used to test for trend (Hirsch et al., 1982; Hirsch and Slack, 1984). This statistic can be calculated as the number of possible pairs of years for which the ordering of the years is the same as the ordering of the annual summary statistics (the lower annual statistic occurs in the earlier year) less the number of possible pairs of years with the reverse ordering. If there is no trend and all observations are independent, then all rank orderings of the annual statistics are equally likely, this result is used to compute the statistical significance of the tau statistic. Adjustments for tied annual summary statistics are described in the cited articles. Adjustments of Kendall’s tau for seasonality (Hirsch et al., 1982) and serial dependence (Hirsch and Slack, 1984) have been proposed and investigated in the context of water quality data analysis. A seasonally adjusted Kendal’s tau (Hirsch et al., 1982) allows for different annual means and trends in different calendar months by adding up the 12 Kendall’s tau statistics from each month. The null distribution of this statistic (when there are no trends) calculated assuming values from different calendar months are independent. The null distribution calculated assuming values in different months can be correlated. Both papers include calculations of the power of these tests for simulated data. The power of the seasonal and serial dependence adjusted by Kendall’s tau is greater than the power of the simpler seasonal dependence adjusted by Kendall’s tau if there is serial dependence, but is less in the independent case.

Kendall’s tau test of trend is related to the Theil-Sen non-parametric slope estimator, which gives an estimate of the assumed linear trend. This estimator is the median of all possible ratios of the change in the annual summary statistic from one year to a later year divided by the number of years separating the two values. If the trends differ by calendar month, then the same calculation can be applied to the monthly summary statistics by only considering ratios for values in the same month, i.e., that differ by an exact multiple of 12 months (Hirsch et al., 1982).

3.2 Sen’s Estimator of Slope Method

If a linear trend is present in a time series, then the true slope (change per unit time) can be estimated by using a simple non-parametric procedure developed by (Sen 1968b). The slope estimates of N pairs of data are first computed by

$$Q_i = \frac{x_j - x_k}{j - k} \text{ for } i=1,\ldots, \qquad (10)$$

Where x_j and x_k are data values at times j and k (j>k) respectively. The median of these N values of Q_i is Sen’s estimator of slope. If N is odd, then Sen’s estimator is computed by

$$Q_{med} = Q_{(N+1)/2} \qquad (11)$$

If N is even, then Sen’s estimator is computed by

$$Q_{med} = [Q_{N/2} + Q_{(N+2)/2}]/2 \qquad (12)$$

Finally, Q_{med} is tested by a two-sided test at the 100(1-α) % confidence interval and the true slope may be obtained by the non-parametric test.

4. RESULTS

Hydroclimatologists are concerned with analyzing time series by concentrating on differences in 30-year normals along the whole period of records. This is why the period of 30-year is assumed to be long enough for a valid mean statistic. It also amounts to describing hydroclimatic time series as non-stationary with local periods of stationary (Kite, 1991). The selection of stations in a climate change research is substantial at the initial step and that a minimum record length of 25 years ensures validity of the trend results statistically (Burn and Elnur, 2002). The length of data set in this study, mostly 46 years, suffices the minimum required length in searching evidence of climatic change in hydroclimatic time series. The majority of rainfall and temperature records include observations of 46 years spanning from 1967 to 2013. Daily rainfall and temperature data of the selected stations were taken from the Department of Meteorology and Hydrology (DMH). Table 1 and 2 show the results of Mann-Kendall test for selected stations. Sen's slope results for total rainfall are shown in Table 3.

Table 1. Mann-Kendall test results for total rainfall

Station	Tau	Test Statistic-Z	Trend Direction
1. Magway	0.28	2.736	Upward
2. Mandalay	-0.06	-0.578	Downward
3. Meikhtila	0.11	1.07	Upward
4. Minbu	-0.053	-0.499	Downward
5. Sagaing	-0.030	-0.284	Downward
6. Shwebo	-0.102	-1.103	Downward
7. Monywa	-0.101	-0.954	Downward
8. Pakokku	-0.051	-0.496	Downward
9. NyaungU	0.065	0.616	Upward

Table 2. Mann-Kendall test results for maximum rainfall

Station	Tau	Test Statistic-Z	Trend Direction
1. Magway	0.053	0.512	Upward
2. Mandalay	0.069	0.663	Upward
3. Meikhtila	0.009	0.076	Upward
4. Minbu	-0.009	-0.078	Downward
5. Sagaing	-0.137	-1.335	Downward
6. Shwebo	0.019	0.18	Upward
7. Monywa	-0.038	-0.368	Downward
8. Pakokku	0.121	1.143	Upward
9. NyaungU	0.018	0.166	Upward

Table 3. Sen's slope results for total rainfall

Station	Slope Value
1. Magway	3.5
2. Mandalay	-4.06
3. Meikhtila	-3.84
4. Minbu	-0.09
5. Sagaing	-3.06
6. Shwebo	-3.526
7. Monywa	-3.32
8. Pakokku	-1.703
9. NyaungU	1.890

5. DISCUSSION AND CONCLUSION

Changes in a time series can occur steadily (a trend), abruptly (a step-change) or in a more complex form. It may affect the mean, median, variance or other aspect of the data. Trend has various statistical methods for detecting trend, step change, differences in means or medians between two data periods and randomness in hydrological time series data. The Mann-Kendall method was applied to know the existence of trends in streamflow and precipitation time series. All the trend results in this research have been evaluated at 10%, 5% and 1% level of significance to ensure an effective exploration of the trend characteristics of the study region. The study period is mostly from 1967 to 2013. Significance level indicates the trend’s strength and Sen’s slope estimator indicates the magnitude of the trend. Sen’s estimator of slope was employed to figure out the change per unit time of the trends observed in all runoff time series, where a negative sign represents a downward slope and a positive sign indicates an upward one.
In this study, the time series of temperature and precipitation in central dry zone during the period 1967-2013 were tested for gradual trend and abrupt change at the annual total and maximum scales. The results of Mann-Kendall test showed some strong significant decreasing trends in the annual total rainfall. The largest negative was occurred in Minbu station. Sagaing station indicated negative trend in annual maximum rainfall. A noticeable increase in the total rainfall was observed mostly in Magway station.

6. ACKNOWLEDGEMENT

First of all, the author is sincerely thankful to Dr. Nyan Myint Kyaw, Professor and Head of Civil Engineering Department, Yangon Technological University for his kind lead and guidance. The author is greatly indebted to her supervisor, Dr Win Win Zin, Associate Professor of Civil Engineering Department, Yangon Technological University, for her invaluable suggestions and careful editing this paper. The author is heartfelt thanked to Daw Cho Cho Thin Kyi, Associate Professor, Department of Civil Engineering, Yangon Technological University. The author would like to thank all the persons who have helped towards the successful completion of this paper.

REFERENCES

Chang, H., 2007. Comparative stream flow characteristics in urbanizing basins in the Portland metroplitan area. *Hydrological Processes* 21, 211-222.

Hamed, K. H., 2008. Trend detection in hydrologic data: The Mann-Kendall trend test under the scaling hypothesis. *Journal of Hydrology* 349, 350-363.

IPCC. 2007. *Climate Change 2007: The Physical Science Basis*. Contribution of Working Group I to the Fourth Assessment Report of the Intergovernmental Panel on Climate Change. Cambridge University Press: Cambridge, UK.

Kite, G., 1991. *Looking for evidence of climatic change in hydrometeorological time series*. Western Snow Conference, April 12-15, Washington to Alaska.

NRC (National Research Council). 1991. *Opportunities in the Hydrologic Sciences.* National Academy Press, Washington, D.C.

Partal, T., and Kalya, E., 2006. Trend analysis in Turkish precipitation data. *Hydrological Process* 20, 2011-2026.

Solid waste management in urban construction projects in Vietnam

Quan T. NGUYEN[1], Mai T. Nguyen[2], Quan A. PHUNG[3]
[1,3] Project Management and Law Division,
Faculty of Construction Economics and Management,
National University of Civil Engineering, Vietnam
nguyenquan.nuce@gmail.com
[2] Vietnam Green Building Council

ABSTRACT

Construction waste accounts for a large amount of waste in urban areas all over the world as well as in Vietnam. Aiming to find out more proper solutions for managing this type of waste, this paper looks into the practice of construction waste management in urban construction project in Vietnam. Using both secondary data available in published materials and primary data from a survey with 56 respondents as construction practitioners, this paper points out the application of six popular approaches in waste management in urban construction projects in Vietnam: disposal, process, recycle, reuse, reduce and prevent in different level of popularity. It also reviews relevant regulations and laws for construction waste management in Vietnam as supporting factor for promoting modern methods for construction waste management. The roles of different stakeholders in urban construction projects such as owners, contractors and construction management etc. are also investigated in terms or their responsibility for waste management as well as cost bearing for implementing activities for construction waste management.

Keywords: sustainable construction, construction waste, 3R, polluter pays, urban environment protection

1. INTRODUCTION

Construction industry in Vietnam plays a significantly important role in Vietnam in many aspects. Recently, when the Government committed for promoting and implementing sustainable development, the construction industry cannot stand out. In terms of sustainable construction, waste handling becomes the biggest issues, since the industry consumes a huge amount of energy and natural resources. As a developing country, Vietnam is a little behind the developed countries in construction waste management. This paper looks into the practice of construction waste management and then the implications of the issues in urban areas in Vietnam.

2. CONSTRUCTION WASTE MANAGEMENT: A BRIEF LITERATURE REVIEW

Waste is defined as "an object" that currently "no longer has any beneficial use" (NSCC, 2007). "Construction waste" is used to call waste generated from construction activities. Construction wastes are classified using different criteria such as their properties, sources etc. They are also categorized based on construction stages (Katz and Baum, 2011), which generate different amount of waste. The most popular construction waste include excavated soil & dust, green waste (bushes, grass), broken bricks, surplus concrete, surplus mortar, steel & metal, wood, plastic, glass (NSCC, 2007) and other waste from catering or other activities.

There are a lot of methods to manage waste in general as well as construction waste. Among them, the most popular approaches include the following six approaches (in order of increasing priority): disposal, process, recycle, reuse, reduce and prevent. However, the application of these approaches varies from country to country. There are barriers for construction waste management that are categorized into five groups (Yuan et al., 2011): lacking of relevant laws and regulations; the underdevelopment of recycling markets; low understanding of construction waste management; in sufficient economic incentive and lack of proper skills.

3. RESEARCH APPROACH

This paper applies a triangular research approach. Data used are both secondary from relevant reports and primary collected in an empirical survey. Relevant laws and regulations and other governmental documents are also analyzed when applicable. Before the main survey, a preliminary survey was carried out in order to collect information for designing the questions of the main survey. Respondents for the main survey were recruited with a convenient approach, in which potential respondents were introduced to the researchers by existing respondents.

4. SOLID WASTE AND CONSTRUCTION SOLID WASTE IN VIETNAM

4.1 Concepts

In Vietnam, waste is defined as solid, liquid or gaseous substances that are disposed of from production, business, service provision, citizens' living activities or other activities. Construction solid waste includes solid debris and waste discharged from construction projects. Popular types of construction solid waste in Vietnam include mortar, broken tiles, concrete, pipes, roof sheets etc. coming from demolition, innovation of existing construction projects or building new projects.

4.2 Classification of construction solid waste

Generally, solid wastes in Vietnam are classified by origin into: urban solid waste, construction solid waste, rural solid waste, industrial solid waste and waste from hospital and health services. Waste (from here, we use the word "waste" with the meaning of “solid waste”) are also categorized into unhazardous and hazardous waste. In construction, wastes are also put into similar groups. Unhazardous waste include soil and mud from excavation and other earthwork, wasted construction materials, etc. (Vietnamese Government, 2007). Hazardous or dangerous wastes include contaminated construction and demolition waste, such as soil excavated from polluted areas, construction materials containing solid substance or asbestos, disposing hazardous substance etc. as listed in Decision 23/2006/QĐ-BTNMT (MONRE, 2006).

5. THE PRACTICE OF CONSTRUCTION WASTE MANAGEMENT IN VIETNAM

5.1 A review on relevant regulations and laws

There are a number of regulations and laws that have been issued for the purpose of managing waste in general and construction waste in particular. The Law on Protection of the Environment has reserved a full chapter (Chapter 8) for waste management (Vietnamese Congress, 2005). Decree 59/2007/ND-CP proposed regulations for solid waste management. Chapter 5 in this Decree has presented 9 technologies for handling solid waste for the reference of waste handlers. Decision 23/2006/QĐ-BTNMT has put out the list for hazardous waste. Decision 1447/2005/QD-BXD was accompanied with “Action Program for protecting construction environment” presenting the objectives of the industry for managing solid waste. Apart from those, there are circulars, guidelines and Vietnamese standards on waste classification and management that need to be consulted as well. Significantly important standards as listed in Table 1.

Table 1: Significantly important standards on waste management

No	Code of the standards	Standards
1	TCVN 7469: 2005	Safety for radiation. Measurement of active level of solid waste to be considered as not radio-active to recycle, reuse or dispose of.
2	TCVN 7629:2007	Threshold for hazardous waste
3	TCVN 6705:2009	Unhazardous waste. Classification
4	TCVN 6707:2009	Hazardous waste. Symptoms and warning signs
5	TCVN 6696: 2009	Solid waste. Hygienic landfill sites. General requirements on environment protection
6	TCVN 6706: 2009	Hazardous waste. Classification

That is to say, there are lots of regulations and laws in Vietnam on waste management in general and waste in construction in particular and they are sufficient for managing construction waste. However, those regulations are far from completely effective in practice since the lack of the obedience by the industry stakeholders e.g. the classification of waste at sources is not done as the Law on Protection of the Environment requires. Some regulations are still impractical and need more guidance to be applied in the practice. Selected regulations do not force the industry to apply but encourage, then do not attract proper attention from the practitioners.

5.2 Construction waste generation in urban areas in Vietnam

According to statistic figures, construction waste in urban areas in Vietnam accounts for from 10-15% or the urban waste. More details, in 2009, there were approximately 1000 tons and 2000 tons of construction waste being generated daily in Hanoi and Ho Chi Minh City, the two largest cities in the country, respectively (MONRE, 2011) and the figures reached 2000-3000 tons for Hanoi (MONRE, 2013) and more than 1000 tons for Ho Chi Minh City in 2013 (DONRE, 2013). In urban areas in a smaller province of Tien Giang, the amount of construction waste generated in a day has reached 40 tons in 2010 (MONRE, 2011). In the next few years, the rate of waste generation is estimated to significantly increase due to the renovation and development of old public housings in large cities in Vietnam.

Despite of the huge amount of construction waste, especially in urban areas, waste handling is still a problem in Vietnam. The rate of solid waste collection is only 83.5% in urban areas, 50-60 in towns and 20-30% in rural villages (Khoa, 2013). In Hanoi, URENCO, the state-run enterprise that is in charge of waste collection can only collect about 790 tons/day, other bodies collect 600 tons/day (MONRE, 2013), leaving the rest uncollected. In other large cities like Da Nang, Hai Phong, Can Tho, there is the same problem with construction waste management. Solid waste in urban areas in Vietnam now is mostly subject to disposal by landfilling, but the collection capacity is too low that there are still lots of waste uncollected. What is more, the mass media have repeatedly reported many cases of solid waste being disposed of illegally on pavements, roads in areas with low population density. The practice leads to the need of solutions for more effective management of construction waste in the country.

5.3 An investigation on construction waste in Vietnam urban construction projects

A survey conducted for the research with 56 respondents was carried out in late 2013. Among the survey participants, there are people from investors/owners, main construction contractors, subcontractors, material suppliers and even civil servants in construction industry. The classification of the survey respondents is presented in Table 2. Though the sample size is not large, the sample covers a variety of respondents' type, ensuring its representativeness.

Table 2: Survey respondents' classification

No	Classification	Number of respondents	Percentage
I	*Type or organizations*		
1	Investors	18	32.14%
2	Main contractors	18	32.14%
3	Subcontractors	6	10.71%
4	Material suppliers	1	1.79%
5	Civil servants	2	3.57%
6	Others/ Unanswered	11	19.64%
II	*Working experience*		
1	Less than 5 years	30	53.57%
2	From 5-10 years	16	28.57%

No	Classification	Number of respondents	Percentage
3	More than 10 years	7	12.50%
4	Unanswered	3	5.36%
	Total	56	100%

Table 3 shows the survey results in terms of type of construction waste they have observed in the sites and the management approaches used in handling the waste. According to the results, the most recognized waste is excavated soil and mud. Other types of waste have also been repeatedly mentioned by most of the respondents (from about 90% or greater). Generally speaking, the approaches applied are suitable for the types of waste. All of six waste management approaches have been applied in construction in Vietnam.

Table 3: Types of construction waste and management approaches

Types of waste	**Frequency**	**%**	**Waste management approaches**					
			(1)	**(2)**	**(3)**	**(4)**	**(5)**	**(6)**
(A) Excavated soil & dust	55	98.21%	41	5	1	8	0	0
(B) Green waste (bushes, grass)	52	92.86%	31	5	4	11	0	1
(C) Broken bricks	53	94.64%	21	2	6	24	0	0
(D) Surplus concrete	53	94.64%	19	3	5	14	8	4
(E) Surplus mortar	52	92.86%	16	1	6	16	11	2
(F) Steel & metal	53	94.64%	5	6	16	19	6	1
(G) Wood	51	91.07%	3	2	11	20	12	3
(H) Plastic	52	92.86%	15	3	12	10	4	8
(I) Glass	50	89.29%	18	4	4	8	8	8
(K) Others	13	23.21%	0	6	0	3	3	1
Total			169	37	65	133	52	28

Notes on waste management approaches: (1) Disposal, (2) Process, (3) Recycle, (4) Reuse, (5) Reduce, (6) Prevention.

There are about 30 plants all over Vietnam for handling solid waste in operation with local and imported technologies. The most popular technologies include disposing of (burial), composting and burning (Manh Cuong 2013). This explains the figures that Disposal is the most popular approaches in waste management approaches applied for construction waste, as in Table 3. Disposal is the first choice of practitioners in construction in Vietnam, regardless of their working positions. This reflects the fact that the conditions for handling waste in Vietnam is limited. Almost the waste collection sites in Hanoi use landfilling method, but about 85-90% of the landfill sites are not hygienic and in danger of pollution (Thanh Tram 2009). In addition, landfilling consumes large areas of land and it needs long time for the waste to dissolve. Therefore, the industry should promote more the application of 3R in solving construction waste.

Because only a limited amount of construction waste is organic, most of construction wastes are unable to be burnt or composted, burning is not considered as a suitable method for construction waste, as well as composting. That is why recycling has been applied less in practice than disposal and reuse (Table 3). The imported technologies seem to be improper to Vietnam since wastes in Vietnam have not been classified properly at sources. However, a significant number of applications was put on Reuse as in Table 3, making it the second selection of the industry. Project stakeholders have thought of saving construction materials by finding ways to use again surplus materials or usable waste such as wood, metal and broken bricks. Attracting far less number of choices, Reduce was mentioned only 52 times in Table 3. Broken bricks, concrete, wood and mortar are among the type of waste that people tend to apply the reduce approach most. The figures show that some of the construction practitioners have made efforts to plan for reducing the waste in their projects. Process and Prevention are the ones getting the least applications in the respondents' projects. It seems that construction practitioners have got difficulties in getting equipped with proper equipment or technology for processing the waste as well as effective method for preventing waste in their projects.

Regarding responsibilities of each stakeholder in handling waste on construction sites, the contractors have been most appointed to bear the biggest responsibility for handling the waste issue (Table 4). The second position is for professional waste treatment enterprises, but the significance is very far from that of contractors. Only one survey respondent chose the owner and no one selected the consultants/construction management as the ones who are in charge of handling construction waste on site.

Table 4: Responsibility allocation in terms of managing construction waste

Body in charge of waste issues on construction sites	**Total of choice**	**Waste management approaches**					
		(1)	**(2)**	**(3)**	**(4)**	**(5)**	**(6)**
Contractors	84	23	6	15	14	15	11
Investors/Owners	1	1	0	0	0	0	0
Construction Management	0	0	0	0	0	0	0
Professional waste management enterprises	11	5	0	2	2	2	0

Notes on waste management approaches: (1) Disposal, (2) Process, (3) Recycle, (4) Reuse, (5) Reduce, (6) Prevention.

The survey results show that almost all of the construction project stakeholders agree that it is the contractors' responsibilities to solve construction waste issues. The implication emerged from this for waste managers is to focus on this type of organizations for better waste management. However, attention should also be paid on owners and construction management. The owners have lots of direct benefits such as cost savings in reusing waste. Construction management is in charge of the whole construction phase, so they need to bear some responsibilities as well. The related emerging issue is which body should bear the cost for waste management. Figures in Table 5 show that the owners and the contractors are the ones who should be responsible for the cost, but the owners have been selected by more respondents. That is to say, the figures support the "polluter pays" principle in dealing with environmental issues. Nevertheless, the figures also show that it depends on each construction project's conditions to decide who should bear the cost for waste handling. This may lead to the fact that everybody wants to shift the responsibility to another stakeholder, if there is no particular agreement or regulation.

Table 5: The selection on body in charge of paying for waste handling

Body in charge of paying for waste handling on construction sites	**Total of choice**	**Waste management approaches**					
		(1)	**(2)**	**(3)**	**(4)**	**(5)**	**(6)**
Contractors	38	11	3	5	6	7	6
Investors/Owners	52	14	4	11	9	9	5
Construction Management	0	0	0	0	0	0	0
Professional waste management enterprises	0	0	0	0	0	0	0

Notes on waste management approaches: (1) Disposal, (2) Process, (3) Recycle, (4) Reuse, (5) Reduce, (6) Prevention.

6. CONCLUSIONS

The construction industry in Vietnam have a rather good understanding on the issues of construction waste since the country adopted sustainable development as its official trend, that is why there are lots of relevant regulations and laws being issued recently. Then construction waste gradually attracts more and more attention of project stakeholders. Construction waste accounts for a large percentage of waste in large cities in Vietnam and leads to big handling problem. Six approaches for construction waste management have been applied in construction projects in Vietnam, but they are different in the level of popularity. Disposal of waste, the lowest level in the waste management approaches, is the most popular method to be used in construction projects in Vietnam. Luckily, the next popular method is reuse, which is considered as at a higher level of waste management that brings benefits to not only the contractors but also the owners. Recycling waste is not popular due to the lack of localized technologies and the habit not to classify waste on construction sites. There is also waste reduction as well as prevention activities carried out on sites, but the practice is not very popular. Conforming to the principle of "polluter pays", it is recognized by the research results that the contractors should be responsible for waste management but the cost responsibility should be shared both the owners and the contractors.

However, in comparison to developed countries, there are not proper quantitative criteria for waste in general and construction waste in particular. This practice, as well as the limited application of high level waste management approaches are among the important barriers that Vietnam need to overcome in order to solve the construction waste issues and to achieve its objectives of 90% of urban waste are handled, 60% of which would be collected for reuse or recycle purposes in 2025, as stated in the Decision 2149/QD-TTg dated 12th December 2009.

REFERENCES

DONRE., 2013. Ten years for developing and improving the system for managing solid waste in Ho Chi Minh City. Retrieved 2013 (http://www.donre.hochiminhcity.gov.vn/thong-tin-hoat-dong/lists/posts/post.aspx?Source=/thong-tin-hoat-dong&Category=C%C3%B4ng+ta%CC%81c+qua%CC%89n+ly%CC%81+m%C3%B4i+tr%C6%B0%C6%A1%CC%80ng&ItemID=2968&Mode=1).

Katz, A., and Baum, H., 2011. A novel methodology to estimate the evolution of construction waste in construction sites, *Waste management* 31, 353-358.

Khoa, K., 2013. *The rate of solid waste collection is only 20-30% in rural areas*, Hanoi Moi Newspaper.

Cuong, M., 2013. Contributions to the draft of the Decree as a replacement for Decree 59 on solid waste management. Construction Newspaper Hanoi, http://www.baoxaydung.com.vn/.

MONRE., 2006. Decision 23/2006/QD-BTNMT on the publication of hazardous waste list dated 26th December 2006. 23/2006/QD-BTNMT. Ministry of Natural Resources and Environment.

MONRE., 2011. Report on the national environment 2011 on solid waste. Hanoi.

MONRE., 2013 News from the website.

NSCC., 2007. Reduce, Reuse, Recycle Managing your waste. London.

Tram, T. 2009 "90% of the landfill sites are not proper sites." Dan Tri Newspaper.

Vietnamese Congress., 2005. Law on Protection of the Environment. 52/2005/QH11. Vietnam. 52/2005/QH11.

Vietnamese Government., 2007. Decree No. 59/2007/ND-CP on Solid Waste Management dated 09 April 2007. 59/2007/ND-CP. Vietnamese Government.

Yuan, H., Shen, L and Wang, J. 2011. Major obstacles to improving the performance of waste management in China's construction industry. *Facilities* 29, 224-242.

Introduction of Dye-sensitized solar cells and its application

Kazuteru Nonomura[1] and Anders Hagfeldt[2]
[1]Researcher, Swiss Federal Institute of Technology (EPFL), Switzerland
kazuteru.nonomura@epfl.ch
[2]Professor, Swiss Federal Institute of Technology (EPFL), Switzerland

ABSTRACT

Solar cells is one of the energy sources to cover the electricity in the world. Solar cells have some advantages compared to other energy sources due to its environmentally friendly characteristics. Especially, it is a large advantage that it is not necessary to transfer electricity from the generation site to the consuming places. The challenges in the current solar cell technologies are the stability and the efficiency. For the top solar cell like used in a space project, the efficiency of over 40% have been achieved. However, in a market, the efficiency is less than 10% or so. Moreover, the cost of electricity generated by solar cells is higher than the one generated from other sources. The reasons for the high cost are the cost of the material and the preparation process. For example, silicon solar cells, most well-known solar cell and the most introduced in the society, have a limitation in the materials and it requires a high purity of the materials.

Dye-sensitized solar cell is one of the challenges to solve these. Dye sensitized solar cell is a solar cell which can generate electricity by using metal oxide semiconductor, pigments and electrolyte. Although the efficiency and the stability need to be improved further, the environmentally friendly characteristics are enhanced. The choice of the materials are huge and the color of the solar cells can be tuned. In this presentation, dye-sensitized solar cell is going to be introduced and its practical applications will be shown.

Keywords: *solar cells, dye-sensitized solar cells, renewable energy,*

The integrated modelling approach for land-use change projection, Case-study in Dak Lak, Vietnam

Anh Nguyet DANG[1] and Akiyuki KAWASAKI[2]
[1] Research Associate, School of Environmental Engineering and Management,
Asian Institute of Technology, Thailand.
dang@ait.ac.th
[2] Project Associate Professor, Department of Civil Engineering, School of
Engineering, the University of Tokyo, Japan

ABSTRACT

With the rapid socio-economic changes, Vietnam has experienced huge land conversions which causes negative impacts on both natural ecosystem and human living environment. In Dak Lak, the province possess the largest area of natural forest in central highland of Vietnam, competition among forest conservation, agricultural development and urbanization have been increasingly a pressing issue. For this reason, appropriate land-use planning is required for sustainable development in this province and broadly Vietnam. In this light, the aim of our study is to develop an integrated model for land-use changes projection with the case study in Dak Lak. Our model integrates System Dynamic (SD) and GIS-based model in order to combine the strength and overcome the limitation of each single modelling technique. SD model can comprehensively examine the interactions between land-use change process and non-spatial driving factors (economic development, policy, technology, and population) but it cannot deal with a mass of spatial data. While GIS –based model has superior power of storage, retrieval and presentation of spatial information for complex land-use allocation process however this model cannot appropriately work with non-spatial driving factors. The output of SD model is the land-use demand of Dak Lak from 2015 to 2030. GIS-based model was used to allocate these land-use demand to the most suitable location of each land-use type and produce land-use change projection maps in future. We employed backward method to validate result of GIS-based model by comparing model-based land-use map in 2010 with actual land-use map in 2010. In addition, we also compared model-based land-use projection map in 2020 and land-use planning map in 2020 obtained from Dak Lak province's authority for further discussion. The outcome of our integrated model would support land-use planner and policy makers for better land-use planning and managements.

Keywords: land-use change model, integration approach, System Dynamic, GIS

1. INTRODUCTION

Half of the Earth's ice-free land surface has been transformed by humankind and most of the rest is managed for human purposes over the past 10 millennia or so (Global Land Project, 2005a). Land-cover changes are caused by both natural processes and human activities. However, large percentages of land-cover changes of the recent past up to present are due to the changes of land-use purposes (Briassoulis, 2000; Turner et al., 1999). Changes in land-use have increasingly put the negative impacts on water cycle (Sterling et al., 2012; Swartz et al., 2003), soil environment (da C Jesus et al., 2009) to bio- diversity (Hof et al., 2011; Seto et al., 2012). These changes, ultimately, contribute to regional and global climate change through affecting the balance of greenhouse gas fluxes and surface Aledo effect (Cai et al., 2004; Chhabra et al., 2006; Pielke, 2005; Rindfuss et al., 2004; Steffen et al., 2004). Land-use change, therefore, increases the vulnerability of people to socio-economic and environmental issues (Lambin et al., 2001; Wu et al., 2014). Nevertheless, with the continuous increase of world population, land-use change is an unavoidable process and sustainable land-use management have become ever more important to human (Global Land Project, 2005b).

The issues of land-use change have attracted interest among a wide variety of researchers (Lambin et al., 2003; Ronneberger, 2006). At first, most land-use change research was focused on land-cover conversions (e.g., deforestation, urbanization) by a simple comparison of successive land-cover maps (Irwin et al., 2001). Over past few decades, land-use change models has emerges as a mean for better understanding of land-use dynamics which help to address why, how, when and where the changes occurred (Müller, 2003; Verburg et al., 2004a; Verburg et al., 1999). Through land-use model, the user can test hypotheses, make predictions and evaluate scenarios for land-use planning and policy. Due to the complexity of land-use change process, previous researches demonstrated that no singer model is capable of capturing the whole range of land use change’s characteristic (Briassoulis, 2000; Lambin et al., 2000; Verburg et al., 2004a). Accordingly, integration modelling approach, which combines different modelling techniques has been widely used (Michetti, 2012; Upadhyay et al., 2006; Verburg et al., 2009a). This approach explicitly deals with temporal and spatial dynamics, and achieves a higher level of multidisciplinary. Examples of integrated land-use models are CLUE-GTAP (Britz et al., 2011), IMAGE-GTAP LEI (B. Eickhout et al., 2008; van Meijl et al., 2006; Verburg et al., 2009b), IIASA-LUC (Fischer et al., 2001), KLUM-GTAP (Ronneberger et al., 2009), IMPACT (Rosegrant et al., 2002), IMAGE (Letourneau et al., 2012; Strengers et al., 2004). IAM (Matsuoka et al., 2001) and LandSHIF (Alcamo et al., 2011) etc.

The dimension of integration is not the same in different models. Take the integration of CLUE-GTAP as an example, they are two independent models CLUE and GTAP combined together. GTAP - the economic based model- was used to calculate changes in demand for areas of land use while a spatially explicit land use change model (CLUE-s) was used to translate these demands to land use patterns (Verburg et al., 2008). The models of IMAGE-GTAP LEI, IIASA-LUC, EPIC-IFPSIM or KLUM-GTAP employ the similar operation of integration.

Another group of integrated model including AIM, IMPACT, IMAGE and IIASA LUC in which the integration is defined as the combination of sub-model adopted from a wide range of disciplines. However, almost models of this group, are not specifically developed for land use studies. IAM was designed to study impacts on the market and on greenhouse gas emissions of land-using sectors rather than on land-use change prediction (Matsuoka et al., 2001). The IIASA-LUC, IMAGE, IMPACT models are specific for agriculture sector (Strengers et al., 2004). Although these models incorporates many sub-systems, interactions and feedbacks, it has become complex to operate and, above-all, difficult to parameterize due to the high data requirements for most countries (Fischer and Sun 2001).

Review from the previous land-use change models shows that although previous integrated model are very advanced, they are still a black box to user. While working with the operational models, it is quite difficult for user to understand what behind the model operation. In addition, using the operational models may also limit the scope of study because each model was built for a specific purpose and some just can be used for analyzing the change of one or two land-use types. For this reason, our purpose of this study is to develop an integration methodology which combine System Dynamic (SD) and GIS-based model for project land-use change with the case study in Dak Lak Province, Vietnam. In our study, land-use changes in Dak Lak is projected in the period 2015-2030. In the first step, SD model was used to estimate the land-use demand of Dak Lak from 2015 to 2030. GIS-based model was then employed to allocate these land-use demand to the most suitable location of each land-use type and produce land-use change projection maps in future. The results map was validated by backward method. This newer approach is expected to increase the transparency of land-use change modelling process which is the limitation of previous land-use change model. In addition, the integration of SD and GIS-based model will be demonstrated as the robust method which is able to seize the complicated interactions among the factors as well as deal with the spatial scale issues.

2. STUDY AREA

Dak Lak is located in the Center High Land of Vietnam. The total area is 13,125.4 km^2, the total population in 2012 was 1.796 million. With the potential for economic development, recently, Dak Lak has witnessed the significant increase of population due to immigration from other provinces. The province has also attracted more domestic and foreign investment. Increasing population and investment create a growing demand for agricultural land, especial for cash crop (coffee, rubber, sugar-cane) and forest products, which leads to a degradation of forest quality and a decrease in forest cover in the recent history of Dak Lak. Consequently, Dak Lak is facing the intense changes in land-use especially for infrastructure and agriculture development.

Although there were several researches of land-use change carried out in Dak Lak province and Mekong river region, which encompassed Dak Lak, there has not been any comprehensive study on land-use change in the whole province. Problems still remain which mentioned in previous researches in Dak Lak and Mekong river region. Firstly, the previous studies pointed out the limitation of including economy and policy factors in land use change measurement The research of Müller et al. (2004) put effort to examine the complexity of natural, social and economic issues in two district (Lak and Krong Bong) of Dak Lak, but only two factors, policy and technology, were taken into account. Both Takamatsu et al.(2014) and Ty et al (2012) built land-use change models however they could not cover socio-economic driving factors . Our research is expected to fill the gap in land-use research in Dak Lak in particular and Mekong river basin in general. It can contribute as the technical assistance for the policy makers and planners in Dak Lak to address future land use change. Based on that, they can develop land-use planning and management strategy for sustainable development in Dak Lak province, Vietnam.

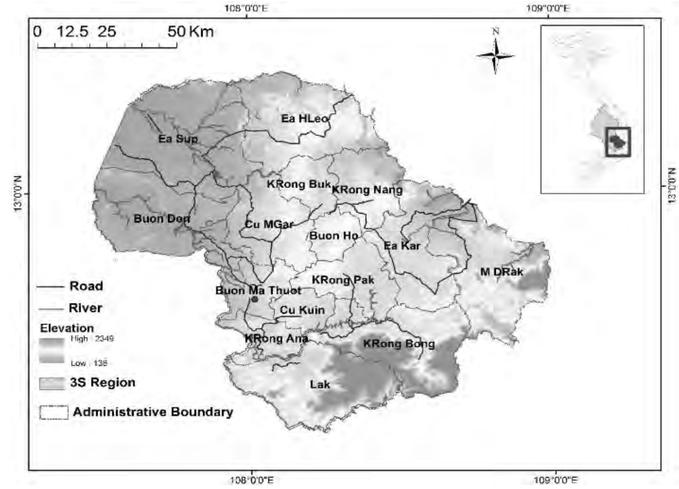
108°0'0"E
109°0'0"E
13°0'0"N
0 12.5 25 50 Km
N
Ea HLeo
Ea Sup
KRong Buk
KRong Nang
Buon Don
Cu MGar
Buon Ho
Ea Kar
M DRak
Buon Ma Thuot
KRong Pak
Cu Kuin
KRong Ana
KRong Bong
Lak
Road
River
Elevation
High : 2349
Low : 138
3S Region
Administrative Boundary

Figure 1: Study area

3. DATA AND METHODOLOGY

3.1 Data

Both non-spatial data and spatial data were used. The non-spatial data are social-economic statistical data in different years were obtained from Dak Lak Statistics Yearbooks (2004-2012). As there was a change of administrative boundary in 2004, hence, we chose to start using data from 2004 to avoid inconsistence within data. The social-economic statistical data includes data of population, labor forces, agriculture and forestry, economic, investment and construction, trade and price etc. In addition, we collected planning reports from Department of Environmental and Natural Resources of Dak Lak province as well as reports from Asian Development Bank (ADB) and Mekong River Commission (MRC).

Spatial data includes two land-use map (2005, 2010) of Dak Lak province; Digital Terrain Model raster data (resolution 30 m); soil map; road map; river map and province boundary obtained from Department of Environmental and Natural Resources of Dak Lak province; the population density raster (resolution 1000 m) from website of NASA.

3.2 Methodology

This study built an integrated SD and GIS-based model to account for the structure of land-use change processes in Dak Lak. The SD model was used to comprehensively examine the interaction among non-spatial driving factors (economic development, policy, technology, population) and quantify the demand for land-use types as a whole without spatial consideration. (Heistermann et al., 2006; Kok et al., 2001; Verburg et al., 2008). SD is able to deal with temporal heterogeneity, i.e. fundamental changes in driving forces or processes through time related to a change in system properties. The GIS-based model which has superior power of storage, retrieval and presentation of spatial information for complex land-use allocation process is occupied for the actual allocation of land-use. This combination can help to utilize the strengths and minimize the weaknesses of individual model.

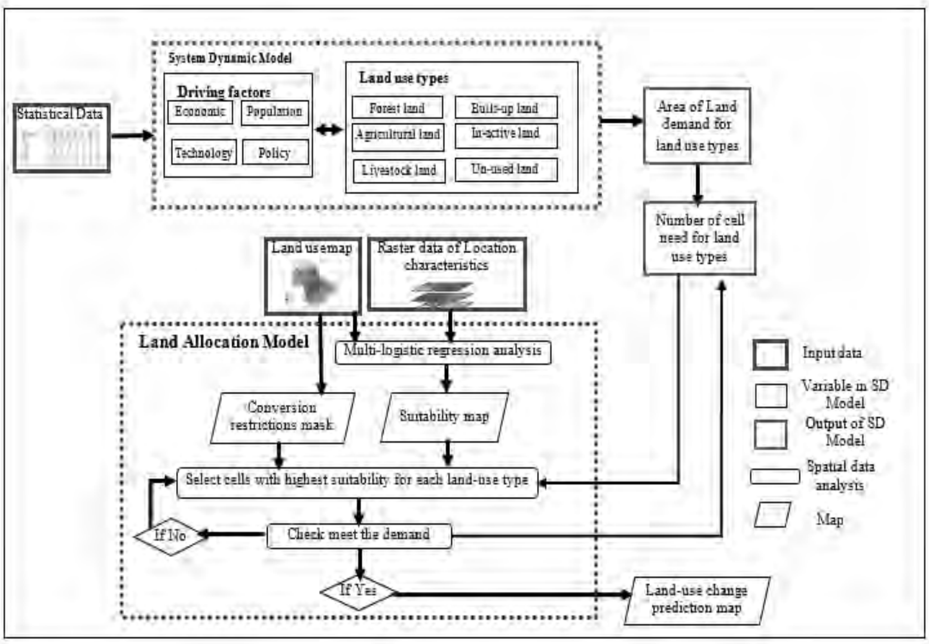
Statistical Data
System Dynamic Model
Driving factors
Economic
Population
Technology
Policy
Land use types
Forest land
Built-up land
Agricultural land
In-active land
Livestock land
Un-used land
Area of Land demand for land use types
Number of cell need for land use types
Land use map
Raster data of Location characteristics
Land Allocation Model
Multi-logistic regression analysis
Conversion restrictions mask
Suitability map
Select cells with highest suitability for each land-use type
If No
Check meet the demand
If Yes
Land-use change prediction map
Input data
Variable in SD Model
Output of SD Model
Spatial data analysis
Map

Figure 2: General framework for land-use change prediction model

3.2.1 System Dynamic model for land-use demand

Land-use is constantly changing in response to dynamic interaction between driving factors and feedbacks from land-use change to these driving factor which can be categorized as natural variability, economic and technological factors (e.g. rural income, agricultural productivity), demography (e.g. population growth, immigration), institution, culture and globalization related factors (Lambin et al., 2003). The potential application of System Dynamic (SD) in land-use model was demonstrated in previous studies (Han et al., 2009; Liu et al., 2013; Voinov et al., 1999). On the base of analyses on driving factor, the structure of SD was drawn with the causality functions and feedback loop between a large numbers of socio economic and policy variables (Han et al., 2009; Liu et al., 2013; Voinov et al., 1999). Once a systems of land-use change is constructed, what-if scenarios can be explored more easily than with other modeling approaches that are not systems oriented (Veldkamp et al., 2001).

In this research, STELLA was used to designed stock and flow diagram according to the causal loop diagram of SD model and automatically generate the corresponding equations based on the designed stock and flow diagram. STELLA is chosen because it is well-documented and has a very intuitive graphic user interface and can be used to develop from simple to very complex models

Based on the availability of data and classification of driving forces, this study simplified the major components of systems and grouped these components into 5 sub-systems: 1) a land-use system, 2) a population and labor forces system, 3) economic system, 4) policy system and 5) technology system. These sub-system are consistent with the groups of causal factors that affect LUCCs in Dak Lak that are population growth, economic development, technology innovation and policy. The interactions of these subsystems are shown in Figure 3

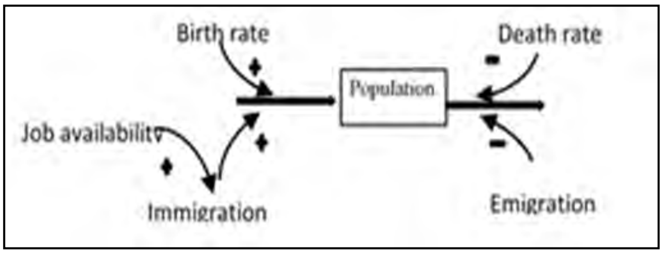
Birth rate
Death rate
Population
Job availability
Immigration
Emigration
+
+
+
-
-

Figure 3: The interactions of subsystems

Figure 4 displays the structure of the population subsystem. The total population change depends on factors such as: birth rate, mortality rate, immigration and emigration rate. Population change affect agricultural activities, demand for housing which cause changes in built-up land and agricultural land.

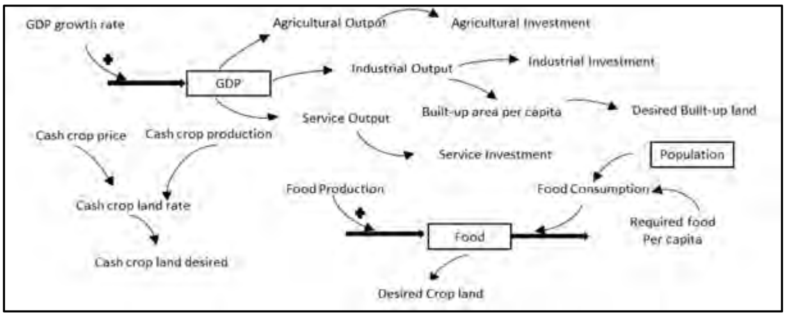
GDP growth rate
Agricultural Output
Agricultural Investment
Industrial Output
Industrial Investment
GDP
Service Output
Built-up area per capita
Desired Built-up land
Cash crop price
Cash crop production
Service Investment
Population
Food Production
Food Consumption
Cash crop land rate
Required food Per capita
Food
Cash crop land desired
Desired Crop land
+
+

Figure 4: Structure of population subsystem

The major component in land-use subsystem are 6 land-use types: agricultural land, livestock land, forest, built-up land, un-used land and inactive land. We defined the inactive land as lake, reservoir and protected area. The changes of each land-use type are influenced by other land uses as well as, population information, gross domestic product, demand for cash crop production and food crop production, re-forestation policy, average life of land which are obtained from population subsystem, economic subsystem, policy subsystem and technology sub system (See Figure 5).

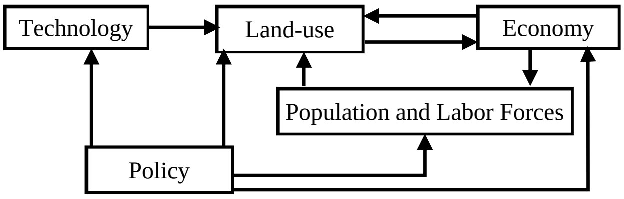
Technology
Land-use
Economy
Population and Labor Forces
Policy

Figure 5: Structure of land-use subsystem

Dak Lak economic depend mostly in agricultural activities that why economic subsystem includes cash crop, food crop and livestock subsystem. Figure 6 illustrates the influence of economic on the output of agricultural, industrial and services industry. GDP is considered a major economic actor resulting from agricultural, industrial and service, which affect investment in agricultural activities, construction of built-up area, afforestation, livestock raise as well as job availability.

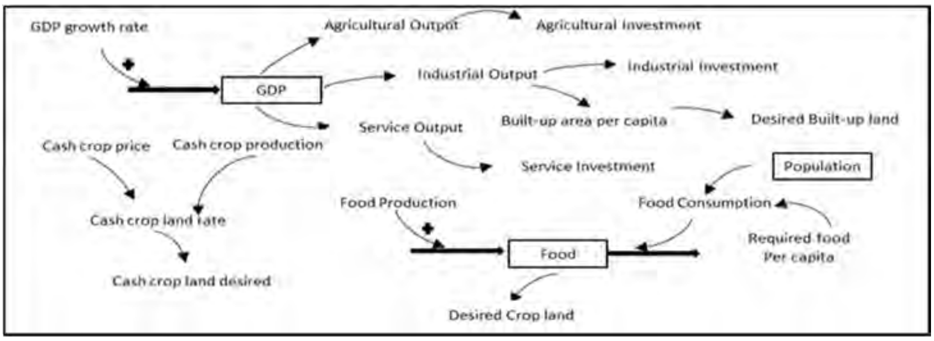
GDP growth rate
Agricultural Output
Agricultural investment
GDP
Industrial Output
Industrial investment
Built-up area per capita
Desired Built-up land
Service Output
Cash crop price
Cash crop production
Service investment
Population
Cash crop land rate
Food Production
Food Consumption
Required food Per capita
Food
Cash crop land desired
Desired Crop land

Figure 6: The interactions within economy subsystem

3.2.2. GIS based land-use changes allocation

For the allocation model, the driving factors was translated into suitability or preference maps, which are a key component of the allocation. Such suitability maps can be created using theory or expert knowledge of the land-use system, empirical analyses or rules based on neighboring cells (Verburg et al., 2004b). Using this suitability and the magnitude of change, an allocation algorithm will then allocate the claims in the best suited areas. This allocation algorithm can be a simple cut-off value that selects the most suitable locations, but can also be a more sophisticated algorithm that takes the competition between different land uses into account (Lambin et al., 2006).

In this study multi-logistic regression was used to indicate the probability of a certain grid cell to be devoted to a land use type given a set of potential driving factors. Based on GIS dataset, logistic regression model was constructed to determine the relation between land-use types and a set of potential driving factors. Six predictor variables were compiled in our regression model: slope, elevation, population density, soil type, distance to road, and distance to river.

After logistic regression analysis was successfully executed, the land allocation model will be built based on eight steps are required to accomplish: (1) Create suitability map to find the best suited location of the expansion of different land-use type; (2) Create a mask of un-changed area includes lake, reservoir and protected area; (3) Allocate cell to future built-up land where there is no conflict of suitability between built-up land and other land-use type; (4) examine whether needed allocate additional cells to future built-up land where results show built-up land suitability values are in conflict; (5) Create a 2030 remaining land mask to account or the cell allocated for future built-up land in step 1-2; (6) Allocate remaining cells to future agricultural use where results show agriculture suitability values are not in conflict and greater than livestock land suitability value; (7) Allocate remaining cells to future livestock land suitability where results show conservation collapsed preference values are not in conflict and greater than agriculture and urban collapsed preference values; (8) Allocate all remaining cell to either agriculture or livestock land where results show collapsed preference values are in conflict (moderate and major) but the normalized preference values for agriculture and conservation respectively greatest (Hart, 2008).

4. RESULTS

4.1. Projected land demand

The SD model was used to project the demand or land use type during 2004-2030. Based on the local statistical social-economic information form 2004-2012, related macroeconomic planning and policies at provincial level, variable setting of population increase, economic growth, technology development, forestry recovery and marketing have been designed in the next 26 year from 2004. Then according to the combination of these settings, a future social economic scenario is defined and their demand for land-use change be projected. The time run for SD model simulation is from 2004-2030 with yearly time step. The data 2004 were used to calibrate the model to specify model parameters and variables setting. The data of 2005-2010 was use to validate the model to evaluate its ability of projection.

Table 1: Projected land-use demand in 2020 and 2030 (Thousand ha)

Land-use type	**2020**	**2030**
Forest	655.2	646.9
Agricultural land	491.1	501.8
Livestock land	0.568	0.709
Built-up land	101.5	107.8
Unused land	52.3	43.5

Table 2: Validation of land-use demand (Thousand ha)

		2005	**2006**	**2007**	**2008**	**2009**	**2010**
Forest	Projected result	668.5	667.7	666.8	666.0	665.2	664.3
	Actual data	665.0	602.5	598.6	600.0	624.6	637.5
Agricultural land	Projected results	479.9	474.4	475.5	476,.7	477.8	480.0
	Actual data	477.4	478.2	478.9	487.1	479.0	487.0
Livestock land	Projected results	0.327	0.325	0.342	0.359	0.376	0.393
	Actual data	0.325	0.323	0.308	0.229	0.389	0.455
Built-up land	Projected results	92.3	92.8	93.4	93.9	94.5	95.1
	Actual data	91.8	95.5	100.8	101.4	102.0	105.0
Unused land	Projected results	59.8	65.6	64.7	63.8	62.9	62.0
	Actual data	59.5	68.2	61.3	56.3	60.9	66.0

4.2 Projected Land allocation

4.2.1 Results of multi-logistic regression

The result of multi-logistic regression analysis determine the relations between land-use type and a set of land-use change driving factors. Theses formulas were then used to evaluate the suitability of certain grid cell. The ROC characteristic is a measure for the goodness of fit of a multi-logistic regression which is similar to R- square statistic in Ordinary Least Square regression. A complete random model gives a ROC value equal of larger than 0.5; a perfect fit results in a ROC value of 1.

(1) Forest = 6.12 – 1.66**Population density* + 0.84**Slope* - 0.54**Inverse distance to river* + 0.27* *Inverse distance to road* -0.67**Soil Fertility* - 0.62**Elevation (ROC:0.88)*
(2) Agricultural Land= - 4.27 + 0.99* *Population density* - 0.70**Slope* - 0.13* *Inverse distance to river* - 0.37* *Inverse distance to road* + 0.52* *Soil Fertility* + 0.63* *Elevation (ROC:0.84)*
(3) Livestock Land = -8.98 - 0.39* *Population density* - 0.13**Slope* + 0.03* *Inverse distance to river* - 1.02* *Inverse distance to road* + 0.55* *Soil Fertility* + 0.48* *Elevation (ROC:0.72)*
(4) Built-up Land = -4.42 + 0.49* *Population density* -0.52**Slope* +0.33* *Inverse distance to river* - 0.47* *Inverse distance to road* + 0.27* *Soil Fertility* + 0.26* *Elevation (ROC: 0.78)*
(5) Unused Land = -4.97 - 0.20* *Population density* + 0.18*Slope + 0.57* *Inverse distance to river* + 0.62* *Inverse distance to road* + 0.13* *Soil Fertility* - 0.56* *Elevation (ROC: 0.70)*

From the logistic-regression results, we can found the specific characteristics of each land-use type in Dak Lak. Forests are mostly at higher slope and lower elevation. The soil in forest has high fertility that explains for the reason why many forest land has been converted to agricultural purpose. As for Agricultural land, soil type is the one of the most important factor. Cultivation is carried out at highland plain therefore we can observe the negative relation between agricultural land and slope and the positive relation between agricultural land and elevation. Built-up land is close to the road, high population density and developed in plain area of the highland. This can be explain by negative coefficient of slope, positive coefficient of population density and elevation.

4.2.2 Land-use distribution in 2030

After conducting suitability map, the cell with highest suitability for specific land-use will be assigned to corresponding land-use type using ArcGIS Modeler Builder. Figure 7 shows the simulated land-use in 2030. Table 4 compares actual land-use distribution and simulated land-use in 2010. The Kappa statistic was employed to evaluate the accuracy of the model. Kappa statistic uses confusion matric to compare the ground truth data with land-use model results. In our case, land-use map in 2010 collected from Department of Natural Resources and Environment Dak Lak is compared with the land-use map conducted from our integration model.

The model was used to simulate land-use change in 2020 and compared with planned land-use map obtained from Dak Lak administrators. Our simulation result relatively close to the province land-use plan with Kappa value of 0.75.

Table 3. Comparison of actual land-use (2010) and projected land-use (2010) by model and Kappa value

Kappa value	2010	**Legend**
	0.87	Legend ☐ Forest ░ Agriculture ■ Grassland ▨ Built-up land ▩ Un-used land ■ Water
Actual land-use	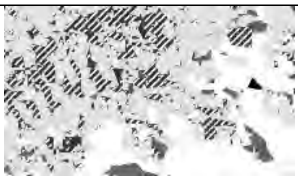	
Projected land-use by model	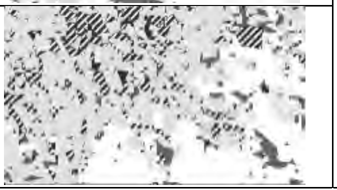	

Table 4. Comparison of planned land-use (2020) and projected land-use (2020) by model and Kappa value

Kappa value	2020	**Legend**
	0.75	Legend ☐ Forest ░ Agriculture ■ Grassland ▨ Built-up land ▩ Un-used land ■ Water
Actual land-use	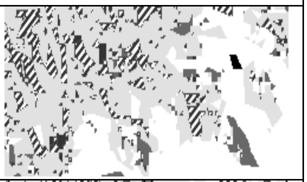	
Projected land-use by model	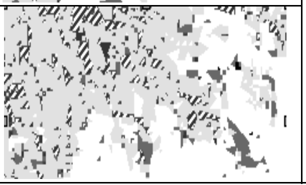	

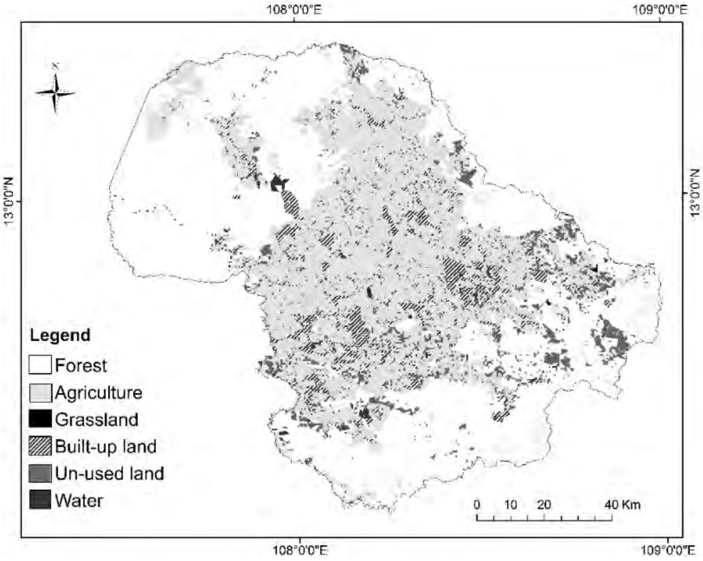
108°0'0"E
109°0'0"E
13°0'0"N
13°0'0"N
Legend
Forest
Agriculture
Grassland
Built-up land
Un-used land
Water
0 10 20 40 Km
108°0'0"E
109°0'0"E

Figure 7: Projected land-use in 2030

5. DISCUSSION AND CONCLUSION

5.1 Discussion

Modeling involves making trade-offs between realism, precision and generality (Wainger et al., 2007). The more precisely a model captures a particular system, the less likely it can be applied to another area (generality). As for the demand model with SD, the selection of factors and modeling the integration among factors depends on the practical socio-economic circumstance of Dak Lak. To apply the model for other study area, the selection of factors have to be revised and modify in the model.

In addition, a challenge in any land-use change projection researches is the accuracy assessment. In order to improve the application ability of our model, participatory approach could be involved in the steps of selecting driving factors and model validation. If the combination of SD, GIS-based and participatory approach is successfully applied, the uncertainty of our proposed model can be reduced.

The demand – driven approach in our model could helps modelling process in close conjunction with clients (clients could be stakeholders such as decision-makers). Clients can contribute to create a satisfactory balance among the social, economic, environmental and institutional components of a specific problem.

5.2 CONCLUSION

This paper accounted for such perspective that combination or integration of existing land-use modelling technique could improve land-use change scenario analysis. Through our research, the integration approach has demonstrate the ability to accelerate the strengths of SD model and GIS-based model to characterize the land-change dynamic in a more realistic manner with a case study in Dak Lak province during the period of 2004-2030. The SD model help to predict the demand for each land-use type. The GIS based model limits of including social-economic factors but can allocate the land-use demand determined by SD model. By changing value of different factor in SD, the planners or decision makers could create different scenario, then accordingly, could see how it affects land change dynamic through GIS-based model. With it transparency characteristic, our model can be a useful tool to analysis the complex land-use change process.

Acknowledgements
The authors wish to thank Mr.Pham Tan Ha, GIS expert at Department of Environmental and Natural Resources of Dak Lak province, for his support during our project.

REFERENCES

Alcamo, J., Schaldach, R., Koch, J., Kölking, C., Lapola, D., and Priess, J., 2011. Evaluation of an integrated land use change model including a scenario analysis of land use change for continental Africa. *Environmental Modelling & Software 26*, 1017-1027.
Eickhout, B., van Meijl, H., and Tabeau, A. E. S., 2008. The impact of environmental and climate constraints on global food supply. Economic analysis of land use in global Climate Change Policy.Routledge, New York.
Briassoulis, H., 2000. *Analysis of land use change: Theoretical and modeling approaches.* Retrieved from http://www.rri.wvu.edu/WebBook/Briassoulis/contents.htm 12 Feb 2012.

Britz, W., Verburg, P. H., and Leip, A., 2011. Modelling of land cover and agricultural change in Europe: Combining the CLUE and CAPRI-Spat approaches. *Agriculture, Ecosystems & Environment 142*, 40-50.

Cai, M., and Kalnay, E., 2004. Climate (communication arising): Impact of land-use change on climate. *Nature 427*, 214-214.

Chhabra, A., Geist, H., Houghton, R., Haberl, H., Braimoh, A., Vlek, P. G., Patz, J., Xu, J., Ramankutty, N., Coomes, O., and Lambin, E., 2006. Multiple Impacts of Land-Use/Cover Change. In: Lambin, E., and H. Geist (Eds.), *Land-Use and Land-Cover Change* (pp. 71-116): Springer Berlin Heidelberg.

da C Jesus, E., Marsh, T. L., Tiedje, J. M., & de S Moreira, F. M. (2009). Changes in land use alter the structure of bacterial communities in Western Amazon soils. *ISME J, 3*(9), 1004-1011.

Fischer, G., & Sun, L. (2001). Model based analysis of future land-use development in China. *Agriculture, Ecosystems & Environment, 85*(1–3), 163-176.

Global Land Project. (2005a). Annual report. IGBP Report No. 53/IHDP Report No. 19.IGBP Secretariat, Stockholm.64.

Global Land Project. (2005b). Science Plan and Implementation Strategy. IGBP Report No. 53/IHDP Report No. 19.64.

Han, J., Hayashi, Y., Cao, X., & Imura, H. (2009). Application of an integrated system dynamics and cellular automata model for urban growth assessment: A case study of Shanghai, China. *Landscape and Urban Planning, 91*(3), 133-141.

Hart, D. (2008). Smart Land-Use Analysis: The LUCIS Model: Land-Use Conflict Identification Strategy. *Journal of the American Planning Association, 75*(1), 89-89.

Heistermann, M., Müller, C., & Ronneberger, K. (2006). Land in sight?: Achievements, deficits and potentials of continental to global scale land-use modeling. *Agriculture, Ecosystems & Environment, 114*(2–4), 141-158.

Hof, C., Araujo, M. B., Jetz, W., & Rahbek, C. (2011). Additive threats from pathogens, climate and land-use change for global amphibian diversity. *Nature, 480*(7378), 516-519.

Irwin, E. G., & Geoghegan, J. (2001). Theory, data, methods: developing spatially explicit economic models of land use change. *Agriculture, Ecosystems & Environment, 85*(1–3), 7-24.

Kok, K., Farrow, A., Veldkamp, A., & Verburg, P. H. (2001). A method and application of multi-scale validation in spatial land use models. *Agriculture, Ecosystems & Environment, 85*(1–3), 223-238.

Lambin, E. F., & Geist, H. J. (2006). *Land-Use and Land-Cover Change: Local process and global impacts*: Springer Berlin Heidelberg.

Lambin, E. F., Geist, H. J., & Lepers, E. (2003). Dynamics of land-use and land-cover change in tropical regions. *Annual Review of Environment and Resources, 28*(1), 205-241.

Lambin, E. F., Rounsevell, M. D. A., & Geist, H. J. (2000). Are agricultural land-use models able to predict changes in land-use intensity? *Agriculture, Ecosystems & Environment, 82*(1–3), 321-331.

Lambin, E. F., Turner, B. L., Geist, H. J., Agbola, S. B., Angelsen, A., Bruce, J. W., Coomes, O. T., Dirzo, R., Fischer, G., Folke, C., George, P. S., Homewood, K., Imbernon, J., Leemans, R., Li, X., Moran, E. F., Mortimore, M., Ramakrishnan, P. S., Richards, J. F., Skånes, H., Steffen, W., Stone, G. D., Svedin, U., Veldkamp, T. A., Vogel, C., & Xu, J. (2001). The causes of land-use and land-cover change: moving beyond the myths. *Global Environmental Change, 11*(4), 261-269.

Letourneau, A., Verburg, P. H., & Stehfest, E. (2012). A land-use systems approach to represent land-use dynamics at continental and global scales. *Environmental Modelling & Software, 33*(0), 61-79.

Liu, X., Ou, J., Li, X., & Ai, B. (2013). Combining system dynamics and hybrid particle swarm optimization for land use allocation. *Ecological Modelling, 257*(0), 11-24.

Matsuoka, Y., T. Morita, & M. Kainuma. (2001). Integrated Assessment Model of Climate Change: The AIM Approach. In T. Matsuno & H. Kida (Eds.), *Present and Future of Modeling Global Environmental Change: Toward Integrated Modeling* (pp. 339–361): Terrapub.

Michetti, M. (2012). Modelling Land Use, Land-Use Change, and Forestry in Climate Change: A Review of Major Approaches. *FEEM Working Paper No. 46.2012; CMCC Research Paper No. 133.*

Müller, D. (2003). *Land-use change in the Central Highlands of Vietnam: A spatial econometric model combining satellite imagery and village survey data.* (Doctoral thesis), Georg-August University of Göttingen. Retrieved from http://ediss.uni-goettingen.de/handle/11858/00-1735-0000-0006-AB5C-0

Müller, D., & Munroe, D. K. (2004). *Tradeoffs between rural development policies and forest protection: spatiallyexplicit modeling in the Central Highlands of Vietnam.* Paper presented at the American Agricultural Economics Association Annual Meeting, Denver, Colorado.

Pielke, R. A. (2005). Land Use and Climate Change. *Science, 310*(5754), 1625-1626.

Rindfuss, R. R., Walsh, S. J., Turner, B. L., Fox, J., & Mishra, V. (2004). Developing a science of land change: Challenges and methodological issues. *Proceedings of the National Academy of Sciences of the United States of America, 101*(39), 13976-13981.

Ronneberger, K., Maria, B., Francesco, B., & Richard , T. (2009). KLUM@GTAP: Spatially explicit, biophysical land use in a computable general equilibrium model In T. W. Hertel, S. K. Rose & R. S. J. Tol (Eds.), *Economic Analysis of Land Use in Global Climate Change Policy* (pp. 304-338). New York: Routledge.

Ronneberger, K. E. (2006). *The global agricultural land use model KLUM : a coupling tool for integrated assessment.* (Doctor), University of Hamburg, Hamburg, Germany.

Rosegrant, M., Meijer, S., & Cline, S. (2002). International model for policy analysis of agricultural commodities and trade (IMPACT): Model description *International Food Policy Research Institute. Washington D.C,* 28

Seto, K. C., Güneralp, B., & Hutyra, L. R. (2012). Global forecasts of urban expansion to 2030 and direct impacts on biodiversity and carbon pools. *Proceedings of the National Academy of Sciences, 109*(40), 16083-16088.

Steffen, W., Sanderson, A., Tyson, P. D., Jäger, J., Matson, P., Moore, Oldfield, F., Richardson, K. S., Schellnhuber, H. J., Turner, & Wasson, R. J. (2004). *Global change and the Earth system: a planet under pressure*: Springer.

Sterling, S., Ducharne, A., & Polcher, J. (2012). The impact of global land-cover change on the terrestrial water cycle. *Nature Climate Change, advance online publication.*

Strengers, B., Leemans, R., Eickhout, B., Vries, B., & Bouwman, L. (2004). The land-use projections and resulting emissions in the IPCC SRES scenarios scenarios as simulated by the IMAGE 2.2 model. *GeoJournal, 61*(4), 381-393.

Swartz, C. H., Rudel, R. A., Kachajian, J. R., & Brody, J. G. (2003). Historical reconstruction of wastewater and land use impacts to groundwater used for public drinking water:Exposure assessment using chemical data and GIS. *J Expo Anal Environ Epidemiol, 13*(5), 403-416.

Takamatsu, M., Kawasaki, A., Rogers, P., & Malakie, J. (2014). Development of a land-use forecast tool for future water resources assessment: case study for the Mekong River 3S Sub-basins. *Sustainability Science, 9*(2), 157-172.

Turner, B. L., Skole, D., Sanderson, S., Fischer, G., Fresco, L., & Leemans, R. (1999). Land-Use and Land-Cover Change; Scinece/Research Plan. HDP Report No.7.Stockholm and Geneva.

Ty, T., Sunada, K., Ichikawa, Y., & Oishi, S. (2012). Scenario-based Impact Assessment of Land Use/Cover and Climate Changes on Water Resources and Demand: A Case Study in the Srepok River Basin, Vietnam—Cambodia. *Water Resources Management, 26*(5), 1387-1407.

Upadhyay, T. P., Solberg, B., & Sankhayan, P. L. (2006). Use of models to analyse land-use changes, forest/soil degradation and carbon sequestration with special reference to Himalayan region: A review and analysis. *Forest Policy and Economics, 9*(4), 349-371.

van Meijl, H., van Rheenen, T., Tabeau, A., & Eickhout, B. (2006). The impact of different policy environments on agricultural land use in Europe. *Agriculture, Ecosystems & Environment, 114*(1), 21-38.

Veldkamp, A., & Lambin, E. F. (2001). Predicting land-use change. *Agriculture, Ecosystems & Environment, 85*(1–3), 1-6.

Verburg, P., Eickhout, B., & Meijl, H. (2008). A multi-scale, multi-model approach for analyzing the future dynamics of European land use. *The Annals of Regional Science, 42*(1), 57-77.

Verburg, P., & Overmars, K. (2009a). Combining top-down and bottom-up dynamics in land use modeling: exploring the future of abandoned farmlands in Europe with the Dyna-CLUE model. *Landscape Ecology, 24*(9), 1167-1181.

Verburg, P., Schot, P., Dijst, M., & Veldkamp, A. (2004a). Land use change modelling: current practice and research priorities. *GeoJournal, 61*(4), 309-324.

Verburg, P. H., de Koning, G. H. J., Kok, K., Veldkamp, A., & Bouma, J. (1999). A spatial explicit allocation procedure for modelling the pattern of land use change based upon actual land use. *Ecological Modelling, 116*(1), 45-61.

Verburg, P. H., de Nijs, T. C. M., Ritsema van Eck, J., Visser, H., & de Jong, K. (2004b). A method to analyse neighbourhood characteristics of land use patterns. *Computers, Environment and Urban Systems, 28*(6), 667-690.

Verburg, R., Stehfest, E., Woltjer, G., & Eickhout, B. (2009b). The effect of agricultural trade liberalisation on land-use related greenhouse gas emissions. *Global Environmental Change, 19*(4), 434-446.

Voinov, A., Costanza, R., Wainger, L., Boumans, R., Villa, F., Maxwell, T., & Voinov, H. (1999). Patuxent landscape model: integrated ecological economic modeling of a watershed. *Environmental Modelling & Software, 14*(5), 473-491.

Wu, W., Verburg, P., & Tang, H. (2014). Climate change and the food production system: impacts and adaptation in China. *Regional Environmental Change, 14*(1), 1-5.

New mathematical model for maximizing profit of new low-cost carrier considering hub-spoke system

Ryosuke YABE[1] and Yudai HONMA[2]
[1]Master course student, Department of Industrial and Management System Engineering,
School of Creative Science and Engineering, Waseda University, Japan
ryabe@toki.waseda.jp
[2]Lecturer, International Center for Urban Safety Engineering,
Institute of Industrial Science, the University of Tokyo, Japan

ABSTRACT

Recently, numerous low-cost carriers (LCCs) have been established and have become popular as a new style of airline service. In Japan, Peach Aviation began business as an LCC in 2012. However, while it is true that some airline companies are suffering from a slump in business, Peach Aviation has succeeded because it set up a hub airport at Kansai International Airport and runs many cash-cow routes. To establish a new LCC, consideration of airline networks is most important for success. Therefore, in this study, we propose a mathematical model to optimize the airline network, flight volume, and number of aircrafts for maximizing a new LCC's profit supposing a hub-spoke style network, and solve the model as a mathematical programming problem. First, we investigate the case of a single-hub network, and subsequently consider a two-hub network. It was determined that, when both Narita and Kansai International Airports are chosen as hub airports, a new LCC's profit is maximized.

Keywords: low-cost carrier, LCC, hub-spoke, airline network, single-hub, two-hub

1. INTRODUCTION

Recently, many airlines that offer low fares by simplifying services have been established and are referred to as low-cost carriers (LCCs); this has resulted in a greater number of transportation choices for travelers. When a new LCC is founded, it is essential for the LCC to consider optimum routes. From this viewpoint, in this study, we consider an LCC that has newly entered the domestic airline network in Japan. We evaluate the optimal airline network with simultaneous consideration of flight volume and number of aircrafts that will maximize the new LCC's profit. In particular, we consider a hub–spoke network used by many LCCs.

An earlier study by Sohn, called "A linear program for the two-hub solution problem," is considered as a fundamental basis for the present study. Sohn discussed the means to formulate and obtain an exact solution for the problem of which link between a spoke airport and a hub airport should be connected when the location of the hub airport is given to minimize transportation cost. Sohn's model indicated that every spoke airport must be connected to a hub airport. In our model, however, it is possible, under optimum conditions, that some spoke airports are not connected to any hub airport. Furthermore, Sohn considered a comparatively simple objective function involving strictly the minimization of transportation cost; the model did not include the parameters of airline volume or number of aircrafts. Many differences exist therefore between Sohn's model and the model proposed in this study. In what follows, we propose an optimal airline network to maximize a new LCC's profit, and apply the model to Japan's domestic airlines.

2. PROPOSED MODEL

In this section, we assume a new LCC that gains access to Japan's domestic airline network, and simultaneously determine the optimal network, flight volume, and number of aircrafts that maximize the new LCC's profit.

2.1 Network model

First, we suppose a total of I hub airports indexed by i ($i = \{1, 2, \ldots, I\}$) and a total of $J - I$ spoke airports indexed by j ($j = \{I+1, I+2, \ldots, J\}$). In the proposed network model, the hub airport is given and each spoke airport can be arbitrarily connected to other hub airports resulting in a hub–spoke network (which suggests that we assume a multiple allocation model). Within the proposed network, hub–hub connections are possible but spoke–spoke connections are not allowed. As such, in this network model there are

$$I \times (J - I) + \binom{I}{2} \tag{1}$$

possible flight links.

In this study, we propose flight volumes R_{ij} from a given hub airport to each hub–spoke airport and number of aircrafts A as decision variables. Additionally, we suppose a hub–spoke network, so that R_{ij} = 1 indicates a single service trip both outward and homeward between airports i and j. Furthermore, in this study, we suppose that the same aircraft can be used in any flight.

2.2 Profit calculation for the new LCC

In this study, we consider both income and cost to maximize the profit of the new LCC. First, fare income and incidental business income are considered for the total income. Incidental business income is earned by charging food/drink or seat assignments. This income, given by the parameter β (%), is attached to the fare income. When the fare for link i is Y_i (Yen) and the number of embarkations between airports i and j is m_{ij}, the total income *REV* is formulated as given by Eq. (2).

$$REV = (1+\beta)\sum_{i=1}^{I} \sum_{j=i+1}^{J} \left\{ Y_{ij} \left(m_{ij} + m_{ji} \right) \right\} \tag{2}$$

By calculating the summation in (2), every link in (1) is considered.

Next, the costs of airport use (C_i^H and C_j^S, Yen/year), sales management (K, Yen/year), aircraft (M, Yen/year), fuel and employment (f, Yen/flight·minute), and traveling, maintenance, and shipping (L, Yen/flight) are considered. The parameter L also includes the cost to employees for airport use.

When t_{ij} is the traveling time between airports i and j, and Q is 365 (days), the total expenditures *COST* is formulated as given in Eq. (3).

$$COST = \sum_{i=1}^{I} C_i^H + \sum_{j=I+1}^{J} b_j C_j^S + \sum_{i=1}^{I}\sum_{j=i+1}^{J} e_{ij}K + AM + Q\sum_{i=1}^{I}\sum_{j=i+1}^{J} R_{ij}\left\{f\left(t_{ij}+t_{ji}\right)+2L\right\} \tag{3}$$

Furthermore, e_{ij}, in the above equation, indicates whether there is more than one flight between airports i and j, where e_{ij} = 0 for no flight and e_{ij} = 1 for more than one flight. Additionally, b_j indicates whether a spoke airport is placed at airport *j*, where b_j = 0 when airport j is not used and b_j = 1 if airport j is placed as a spoke airport.

2.3 Proposed model

Under the above assumptions, the proposed formulation for maximizing the new LCC profit is given by Eqs. (4)–(16).

$$\max \quad REV - COST \tag{4}$$

$$\text{s.t.} \quad \sum_{i=1}^{I}\sum_{i=j+1}^{J}\left\{R_{ij}\left(t_{ij}+t_{ji}+2\theta\right)\right\} \le TA \tag{5}$$

$$m_{ij} \le n_{ij} \quad \forall i, j \tag{6}$$

$$m_{ij} \le QGR_{ij} \quad \forall i, j \tag{7}$$

$$m_{ji} \le n_{ji} \quad \forall i, j \tag{8}$$

$$m_{ji} \le QGR_{ji} \quad \forall i, j \tag{9}$$

$$R_{ij} \le 99 e_{ij} \quad \forall i, j \tag{10}$$

$$\sum_{i=I+1}^{J} e_{ij} \le I b_j \quad \forall j \tag{11}$$

$$0 \le m_{ij} \quad \forall i, j \tag{12}$$

$$R_{ij} \in \{0,1,2,\cdots\} \tag{13}$$

$$A \in \{0,1,2,\cdots\} \tag{14}$$

$$e_{ij} \in \{0,1\} \tag{15}$$

$$b_j \in \{0,1\} \tag{16}$$

In the above equations, T indicates the maximum operation time (minutes), θ indicates the shuttle time (min), n_{ij} indicates the predicted number of people traveling in an airplane between airports i and j, and G indicates the number of seats in an aircraft. Incidentally, the coefficients of determination of this mathematical programming are R_{ij}, A, e_{ij}, and b_j.

3. METHOD OF PARAMETER ASSIGNMENTS

To calculate revenues and costs, we must assign a value to each parameter. In this section, we describe the parameter setting method employed.

3.1 Method to set predicted number of people using airplane, n_{ij}

To assign a value to n_{ij}, we use data from the “Domestic Passenger Record per each route and month” and “Inter-Regional Travel Survey” produced by the Ministry of Land, Infrastructure, Transport and Tourism.

The Domestic Passenger Record contains data regarding the number of people for each route among existing airlines and the total number of all airlines for each route in 2012. The Inter-Regional Travel Survey contains the number of people traveling by airplane between arbitrary prefectures in 2010. We use these data based on the rule above to set n_{ij}.

3.1.1 If an existing LCC is already in service

If the new LCC obtains a route wherein an existing LCC is already in service, we ascertain the number of people using that route and divide that number by the number of competing LCCs. In this case, we do not consider an increase in demand.

3.1.2 If only a legacy carrier is in service

When only a legacy carrier is in service, we ascertain the number of legacy carrier customers on that route and consider an increase in demand owing to the new LCC service. We subsequently employ a logit model to calculate the rate of LCC use. Finally, we multiply the number of legacy carrier customers including the assumed increase in demand by the obtained rate of LCC use.

3.1.3 If any carrier is not in service

Because Inter-Regional Travel Survey data indicate air traffic between arbitrary prefectures, we first mete out airports to each prefecture. We already calculated the rate of LCC use for each route by the logit model, and we calculate an average for each airport. Then, we multiply the number of travelers derived from the Inter-Regional Travel Survey by the average from the logit model for each airport and arrive at a value for n_{ij}.

3.2 Fare, Y_{ij}

If an existing LCC is in service between airport i and airport j airport, we use this value for Y_{ij}. We ascertain this value from each LCC’s homepage and use an average over one month. If an existing LCC is not in service, we employ the relationship given by Eq. (17) below, where *distance* is the air travel distance between airports to establish Y_{ij}.

$$Y_{ij}(calc.) = 872.96 \times distance^{-0.731} \tag{17}$$

3.3 Cost of airport use C_i^H and C_j^S

From data derived from Skymark Airlines Inc., one of Japan’s largest LCCs, the cost of airport use consists of payments to employees and airport rental fees. The number of employees is proportional to the flight volume; therefore, we calculate the payments to employees per flight by dividing Skymark’s total payments to employees by Skymark’s total flight volume over a period of one year. This value is included in L, the cost of which changes depending on flight volume.

On the other hand, rental fees do not depend on flight volume but on land value or airport size. It is not feasible to determine land values around each airport; therefore, we assume that this fee depends only on the airport size, which we assume depends on the number of people using the airport. We then calculate C_i^H and C_j^S by comparatively allocating costs using the past record of the 14 airports used by Skymark.

To consider airports other than these 14 airports, the airport size is considered. We already calculated the airport use cost for these 14 airports, and we employ a rate based on these 14 airports in accordance with the relative size of the other airports to calculate C_i^H and C_j^S.

3.4 Other parameters

To calculate the cost of sales management *K* on a per flight basis, we divide Skymark's cost of sales management by 22, which is the number of flight links in the Skymark airline network. Next, Skymark has 18 Boeing 737 aircrafts, and we divide Skymark's cost of aircrafts by 18 to calculate the cost of aircraft *M* on a per aircraft basis. Furthermore, we calculate the cost of fuel and employment f per minute from Skymark data. Finally, we calculate traveling, maintenance, and shipping cost *L* on a per flight basis from Skymark data.

In a working paper by the Ministry of Land, Infrastructure, Transport and Tourism, there is a comparison between the unit costs of Skymark and Air Asia for many of the parameters used here. We can use comparisons between the various parameterized costs of the two airlines to establish a rate by which we can appropriately scale each cost for a new LCC. Additionally, for the type of aircraft, we assume the Boeing 737-800 with 189 seats, which is popular with LCCs, to be the standard aircraft. Therefore, for the number of seats in an aircraft, we assume $G = 189$.

4. EXAMPLE CALCULATIONS

In this section, we provide a specific calculation using our profit maximization model for a new LCC given in Section 2, and the method of parameter assignment given in Section 3 in the case of a domestic airline network in Japan.

4.1 Setting target airport

There are more than 100 airports in Japan, but in this study we restrict our investigation to the Narita Airport and 15 other airports, and attempt to obtain an exact solution by employing a branch and bound approach using Mathematica 9. It is not possible to consider all airports owing to limitations in calculational resources. Therefore, we chose a hub airport that is ranked in the top 15 based upon the number of incoming and outgoing passengers. Additionally, we chose Narita, Shin-Chitose, Fukuoka, Kansai, Naha, and Chubu as possible hub airports.

4.2 Value of each parameter

The parameters we must consider are the cost of airport use $C_i^H = C_j^S$, aircraft M, fuel/employment f, and traveling/maintenance/shipping L. Furthermore, we set the shuttle time θ = 30 min and the maximum operation time for each aircraft $T = 600$ (min). Tables 1 and 2 below list the parameters used in the calculations.

Table 1: Values for the various parameters used in the calculations

Airport Use	**(Yen/Year)**	**Table-2**
Traveling	(Yen/flight)	81,994
Maintenance	(Yen/flight)	17,226
Shipping	(Yen/flight)	12,996
Salary	(Yen/flight)	30,364
Aircraft	(million yen/year・craft)	406
Sale Management	(million yen/route)	25
employment	(Yen/minute)	444
Fuel	(yen/minute)	5,187

We also calculated cost of airport use (rental fee) $C_i^H = C_j^S$; the results are listed in the table below.

Table 2: Cost of airport use (Rental fee; million yen)

Airport	Narita	Shin-Chitose	Naha	Fukuoka	Chubu	Kansai
Rental fee	131	572	508	505	164	185
Airport	Kagoshima	Sendai	Hiroshima	Kumamoto	Miyazaki	
Rental fee	162	88	78	97	91	
Airport	Kobe	Matsuyama	Nagasaki	Komatsu	Oita	
Rental fee	86	80	92	69	50	

4.3 Results of single-hub calculations

First, we list the results of single-hub calculations, where I = 1, in Table-3.

Table 3: Results of single-hub calculations (million yen)

Hub	**Profit**	**Revenue**	**Cost**	**Number of Aircraft**
Narita	1,481	13,794	12,313	7
Chubu	1,171	12,196	11,025	6
Fukuoka	1,011	8,320	7,309	4
Kansai	880	4,661	3,781	2
Shin-Chitose	846	7,690	6,845	4
Naha	75	10,781	10,706	6

From Table-3, the new LCC's profit is maximized when Narita Airport is the chosen hub airport. Table-4 below shows which airports best serve as spoke airports and the respective flight volumes from Narita.

Table 4: Flight volumes from Narita to various spoke airports (flights)

Spoke	**Kansai**	**Chubu**	**Fukuoka**	**Shin-Chitose**	**Naha**
Flight Volume	0	0	0	0	0
Spoke	Kagoshima	Sendai	Hiroshima	Kumamoto	Miyazaki
Flight Volume	2	0	3	2	1
Spoke	Kobe	Masuyama	Nagasaki	Komatsu	Oita
Flight Volume	1	0	1	3	1

It should also be noted that, wherever we set a hub airport, numerous links connect to small airports in rural areas. The reason for this is related to the cost of airport use (rental fee), in that the rental fee for a small airport in a rural area tends to be considerably smaller than that for a large airport in an urban area. While there are many more travelers between large airports, the rental fee has a greater effect.

4.4 Results of two-hub calculations

Subsequently, we list the results of two-hub calculations, where I = 2, in Table-5.

Table 5: Results of two-hub calculations (million yen)

Hub pair	**Profit**	**Revenue**	**Cost**	**Aircraft**
Narita-Chubu	3,209	31,826	28,616	16
Narita-Fukuoka	2,748	25,899	23,151	13
Narita-Shinchitose	2,689	27,495	24,806	14
Narita-Kansai	2,673	22,347	19,674	11
Chubu-Fukuoka	2,522	20,703	18,181	10
Shinchitose-Fukuoka	2,329	20,342	18,013	10
Kansai-Fukuoka	2,130	18,432	16,302	9
Shinchitose-Chubu	2,000	16,469	14,468	8
Shinchitose-Kansai	1,996	12,981	10,985	6
Narita-Naha	1,930	26,566	24,636	14

As shown in Table-5, profit is maximized when Narita and Chubu International Airports are chosen as the hub airports. Flight volumes from Narita and Chubu International Airports are listed in Table-6 below.

Table-6 Flight volumes from Narita and Chubu International Airports (flights)

	Narita	**Chubu**	**Fukuoka**	**Shin-Chitose**	**Kansai**	**Naha**
Narita	×	0	3	1	1	0
Chubu	0	×	3	5	0	3
	Kagoshima	Sendai	Hiroshima	Kumamoto	Miyazaki	Kobe
Narita	2	0	3	3	2	1
Chubu	2	1	0	0	1	0
	Matsuyama	Nagasaki	Komatsu	Oita		
Narita	1	1	3	1		
Chubu	0	0	0	0		

Similar to the case of the single-hub calculations, numerous links connect to small airports in rural areas, and, again, the rental fees affect the results. In fact, the primary reason that the top two most profitable hub airport pairs are Narita-Kansai and Narita-Chubu is that these three airports are the top three airports based on the number of incoming and outgoing passengers with the lowest rental fees.

5. Conclusion

In this study, we consider a new LCC that has gained access to Japan's domestic airline network, and establish an airline network that maximizes the new LCC's profit. We consider a hub–spoke network that numerous existing LCCs presently use, and we investigate a multi-hub network using simultaneous decision of flight volume and number of aircrafts.

Furthermore, we found that rental fees profoundly affect connection choices. As such, it would be most beneficial to establish more accurate rental fees to increase the accuracy of our calculations because the top three airports based on the number of incoming and outgoing passengers with the lowest rental fees were chosen for hub airports as a result.
A source of inaccuracy in our calculations, which could be rectified in the future, is the use of 2012 data. Use of 2013 data would allow for more accurate calculations if the data were disclosed to the public.

REFERENCES

Ministry of Land, Infrastructure, Transport and Tourism, Cited 30 Apr 2014. Domestic Passenger Record per each route and month, www.mlit.go.jp/k-toukei/index.html
Ministry of Land, Infrastructure, Transport and Tourism, Cited 30 Apr 2014. Theinter-regional travel survey:
www.mlit.go.jp/sogoseisaku/soukou/sogoseisaku_soukou_fr_000016.html
Sohn J., Park S., 1997. A linear program for the two-hub solution problem, *European Journal of Operational Research* 100, 617-622.
Sohn J., Park S., 2000. The single allocation problem in the interacting three-hub network, *NETWORKS* 35, 17-25.
Skymark Airlines Inc., Cited 30 Apr 2014. Skymark official HP, www.skymark.co.jp

Investigating socio-economic impacts of flood on the people affected by poverty: Case study in Bago, Myanmar

Htoo Htoo Shwe[1] and Akiyuki KAWASAKI[2]
[1]Senior Sub-Assistant Engineer (Civil), Irrigation Technology Center (ITC),
Irrigation Department, Myanmar
hs.htoohtooshwe@gmail.com
[2]Project Associate Professor, Department of Civil Engineering,
University of Tokyo, Japan

ABSTRACT

The study is aimed to analyze differences in impacts of flood between poor household and non-poor household by investigating the social and economic standard of people living in flood affected area with those living in non flood affected areas. A field survey was carried out in 196 households in 13 wards of Bago city, Myanmar for year 2010 and 2011 flood. By the 2010 year poverty line and their own point of view, 52% of poor people and 48% of non poor people lived in the field survey area. Cross tabulation was used to describe statistical findings such as frequency, percentage, and average of assessment of socio-economic status focusing on gender, age group, income, households' attendance on disaster risk reduction training. Geographic Information System (GIS) was used to visualize the place of flood affected zone with their spatial characteristic and demographic characteristic according to their location such as housing location from the river bank, surface slope, elevation, and flow accumulation. Based on this study, it is revealed that the poor people are more likely affected. The effects are studied with reference to age group, income level, landholding size, housing location, accesses to school and road. There are high direct and indirect costs on poor people compared with their average family income. The extents of flood impacts on poor people are more than that of non-poor. The results of this study would indicate local people and policy maker to be considered flood mitigation actions in order to alleviate the poverty more and those will support also for further flood risk managements.

Keywords: poverty line, socio-economic impacts, flood mitigation, GIS

1. INTRODUCTION

The runoff generating from rainfall combine existing water and pass through any waterway or drainage, or become flooding when those water is over-capacity of water channels. Huge flood causes danger to human and their properties. The poverty and disaster are linked (Fothergill and Peek, 2004). In developing countries, poverty causes community getting more vulnerability to disasters and reducing its coping capacity and increasing disaster risk again because of low education, cost of education and less chance to join school. Socioeconomic status of people are taken into consideration in many disaster management researches how people with different socio-economic prepare for and respond to natural hazard risks and how much impacted differentially before, during and after. Socio-economic impacts are such as direct damages to house, more expenditures and low income, transportation disability, and water sanitation valves damage, and time losses etc. The poverty is taken into account on the lack of access to the factors: safe water and sanitation, health care, nutrition, job vacancy, education opportunities, transportation, and electricity (David Singleton, 2003). Poverty is defined as a deficit below some lowest amount level of resources, which is termed the poverty line (Kyaw, 2006).To ensure development and sustainable poverty alleviation, risk reduction into poverty reduction should be integrated to mitigate the community's vulnerability to natural hazards by assuring productivity, job opportunities and improving stabilized incomes and consumption. Myanmar suffers annually from flood disasters caused by heavy rainfalls of monsoon season (June to October). Approximately 60% of Myanmar people are farmers and fishermen who are highly vulnerable to floods and cyclones. Currently, there is very few poverty studies related with disaster management in Myanmar because the statistics of observation on the impact of flood disaster and understanding of poverty are inadequate. Therefore, policy maker, civil society, private sector may be failed to draw plan and design for reducing flood disaster and ameliorate the impact of flood on households, and poverty alleviation. The general objective of this study is to recommend the approach of poverty alleviation by flood mitigation. It aims to assist in decision making for operation, maintenance, rehabilitation and modernization of water infrastructures for flood mitigation measures by developing integrated GIS-based spatial characteristic maps of flooded places and flood impacts which could be used as a tool for imagination of hypothesis and scenario to draw flood disasters mitigation plans for the study area. This study assesses the adverse effects of flood disaster before and after flood for the year 2011 and 2012, to study the socio-economic impacts of the flood events and to propose flood mitigation interventions from socio-economic point of view to alleviate the poverty of the study area.

2. DESCRIPTION OF STUDY AREA

Bago region is located in the southern central part of the country between 46°45'N and 19°20'N and 94°35'E and 97°10'E. Bago region produces paddy second most in Myanmar after Ayeyarwaddy Region and thus possess a strong agro-based economic and densely populated. Location of the study site is shown in Figure 1. The study site is, Bago Township which area is 7,830 km^2, with a population of 220,000. It is located near Bago river bank and is flooded in every year due to its geographically lowland area to assess the flood inundated place. Heavy

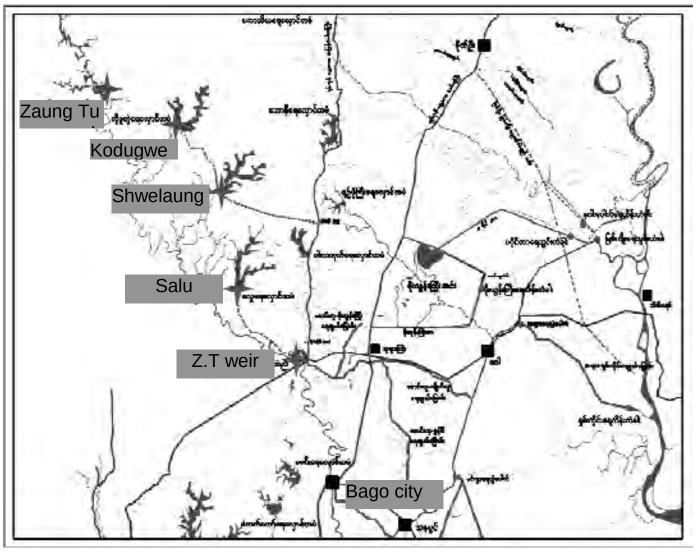

Figure 1: Reservoir networks upstream of Bago

rainfall in the Bago river catchment and high tide from the downstream of the river cause floods during the months of July and August. The flood reaches Bago city's danger level annually. Bago river is averagely 60 m wide and 5 m deep. Catchment area is 2680 km^2 and its annual inflow is 3530 x 10^7 m^3. The maximum river water level in rainy season is 8.60 m above mean sea level and its' danger level is 9.10 m. In flooding time, approximately 3.2 km of Yangon-Mandalay highway and railway in the Bago was flooded over 1 m and it causes transportation disabilities. Some areas of the city were flooded with a depth of 1.5 m. Severe floods occurred in 2011 and its' water level was 9.60 m. It was the highest new record during last 47 years. In 2012, Irrigation Department constructed Kodugwe, Salu and Shwelaung dams upstream of the Bago river (Figure 1) in order to maintain some extents of flood protection.

3. DATA USED

DEM (Digital Elevation Model) data of 90-m resolution downloaded from hydroshed website was used for GIS analyses. Field survey was carried out to investigate the relation between poverty alleviation and flood mitigation except information on health and nutrition due to people's limited knowledge on the health issues. Flood and damage data before and after flooding were collected through questionnaire and also from local authorities for the year 2011 and 2012. The focus region includes both the flood-affected wards and not comparatively affected wards. Data collection for households was done using random sampling procedures. The general questionnaire are mainly related to the respondents' age, sex, education, occupation, housing details, income, asset, sources of water, and flood related problems of inundated depth and duration. The questionnaire covered impact of floods on different occupational group, coping mechanisms, household activities during and after floods. Quantitative information on population of the villages, per capita income, and water level during flood was obtained from focus group discussion.

4. METHODOLOGY

The research was carried out by the following methodological framework.

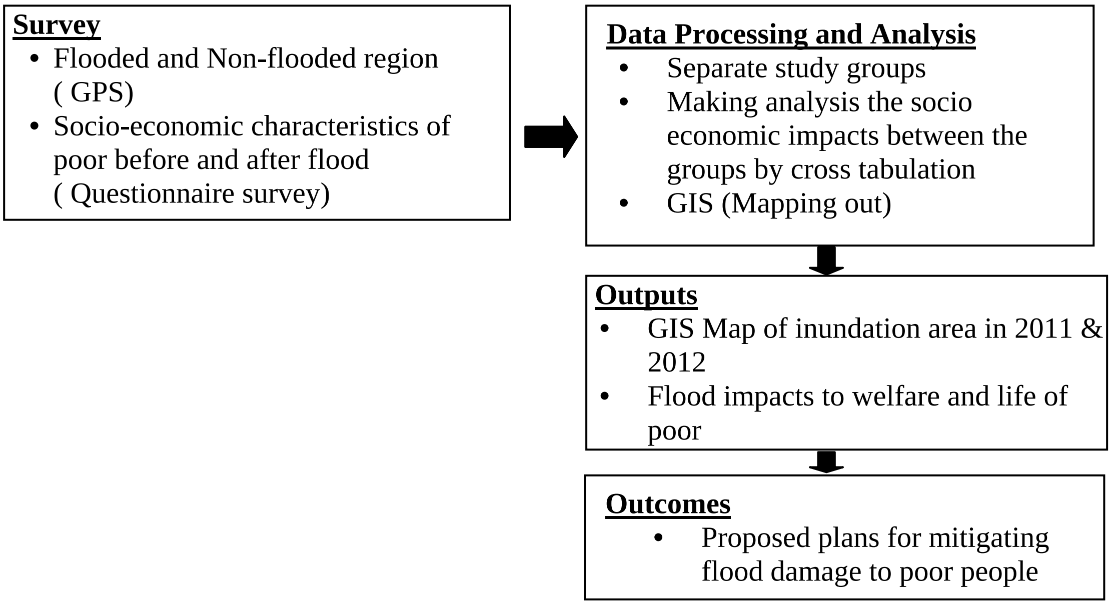
Survey
Flooded and Non-flooded region (GPS)
Socio-economic characteristics of poor before and after flood (Questionnaire survey)
Data Processing and Analysis
Separate study groups
Making analysis the socio economic impacts between the groups by cross tabulation
GIS (Mapping out)
Outputs
GIS Map of inundation area in 2011 & 2012
Flood impacts to welfare and life of poor
Outcomes
Proposed plans for mitigating flood damage to poor people

Figure 2: Framework of the study

In this study, poor people are defined on the basic of income and their self view on their wealth status through questionnaire sheet and country poverty line for 2010. The Ministry of National Planning and Economic Development in Myanmar provided the total year poverty line is about 376,151 kyats (431 USD) by 2010 year poverty line (MNPED, at el, 2011). Flooded or non-flooded households were surveyed by coordinating with the administrative office of wards. The respondents in the study area are identified into four groups: (1) poor and flood (PF), (2) poor and non-flood (PNF), (3) non-poor and flood (NPF), and (4) non-poor and non -flood (NPNF) based on flood inundation depth and flood duration, characteristics of people who suffered flood impacts, and damage cost due to flood.

Direct damaged cost will cover all costs immediately used after flood such as repairing houses, fences, and other damages. Total damaged cost is the combination of direct damaged cost and cost because of disabilities and also consideration of loss accesses. In this study, the indirect cost was mainly calculated on income difference of respondent before and during flood. Average daily income is generated from field survey by dividing the monthly household income with 30 days. And finally indirect cost is calculated by multiplying the daily income and flood duration in day.

Cross tabulation is applied to find out frequency and statistic of the variables of respondents: education, occupation, location, age, geometry, distance from river bank, total damage cost. Locations of households observed with GPS were input to GIS maps using Arc GIS 10.1 for spatial characteristics. Tabular information of analytical impacts, flood characteristics on study groups are linked to the developed GIS maps.

5. RESULTS AND DISCUSSION

5.1 Demographic condition of the study area

Demographic condition is obtained from field survey through questionnaire sheets. The sample number of each analysis was not being same and it depended on the respondent's feed backs. Average family size of study area is about 5 and for the whole country is about 4 (minimum) and 5 (maximum). The fieldwork is carried out on 178 households to know the gender distribution and age distribution of household-headed. It is obliviously seen that most of households-headed are males 65% who get the main income for the whole family. Female household-headed 35% is less than male household head and most of them is housewife. In study area most of the household headed are in lower education standard. On occupation status, poor people are daily wages while non poor people are doing business. In housing status, poor household types are made of thatch roof and Bamboo, medium house are brick masonry and wooden house with zinc roofing. Most of rich people live in reinforced concrete and brick masonry houses. In the survey, 136 households own their houses, and only 11 households are tenant. There are 134 separate type houses but only 7 are attached type houses. In flood affected areas, the lowest floor level of houses are ranging from 1.2 m to 2.5 m. Common water supply systems are tanks, earthen pots, public ponds, pipe line or tube wells. In some places, people who has no own pumps or wells have to buy water with 700 kyats/day even on non-flood period. From field survey results, it was found that poor is 52% and non-poor is 48%, flooded is 55% and non-flooded is 45%.

5.2 Flood Impacts

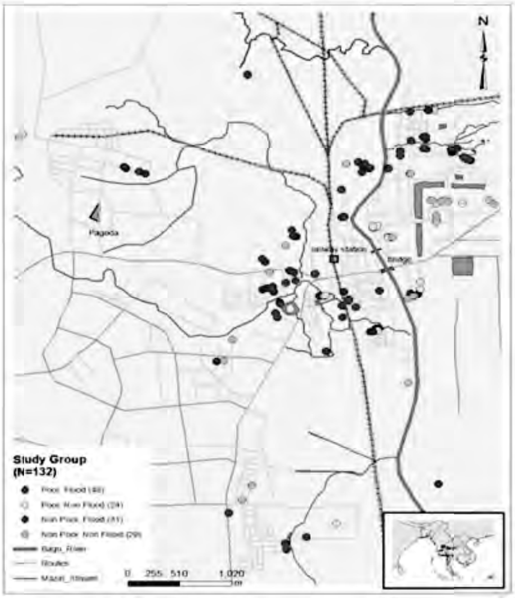

Figure 3: Distributions of PF, PNF, NPF and NPNF

Flood inundation depth and flood duration, flood affected household characteristics and damaged costs are studied for four groups: (1) poor and flood (PF), (2) poor and non-flood (PNF), (3) non-poor and flood (NPF), and (4) non-poor and non -flood (NPNF). The distribution of those groups is shown in (Figure 3).

Flood Depth and flood duration affected on poor and non-poor in 2011 and 2012 are shown in (Figure 4.1- 4.4). It was found that maximum flood depth and duration affected on poor more than non-poor. By comparing 2011 and 2012 flood events, flood depth decreased in 2012 while flood duration was longer than in 2011.

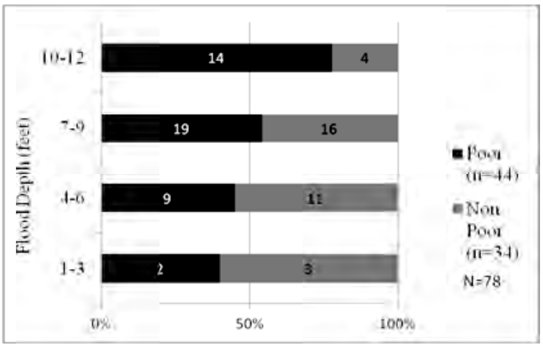

Figure 4.1 Flood depth affected on poor and non-poor in 2011

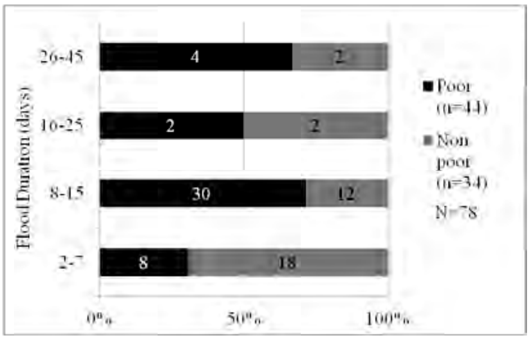

Figure 4.2: Flood duration affected on poor and non-poor in 2011

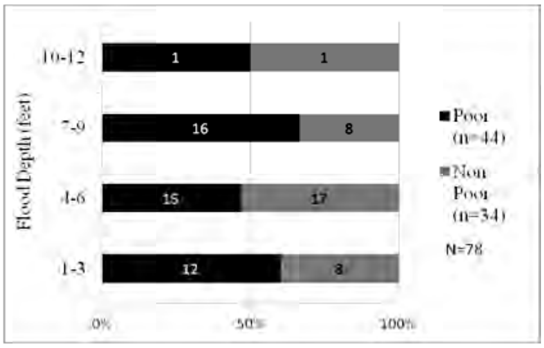

Figure 4.3: Flood Depth affected on poor and non-poor in 2012

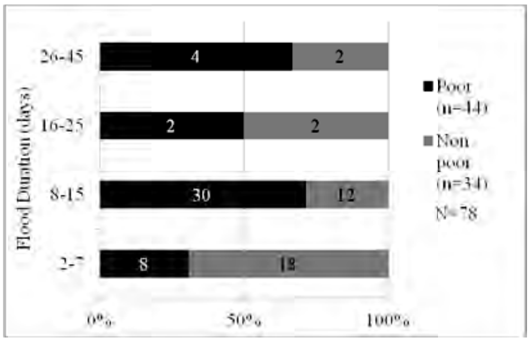

Figure 4.4: Flood Duration affected on poor and non-poor in 2012

In (Figure 5.1 and 5.2), education and occupation status of four groups are shown. It was found that 44% of PF are illiterate than the other three groups and 62% of PF are labor and daily wages. Thus PF suffer impact of floods and they have to find alternative jobs for daily income during flood period.

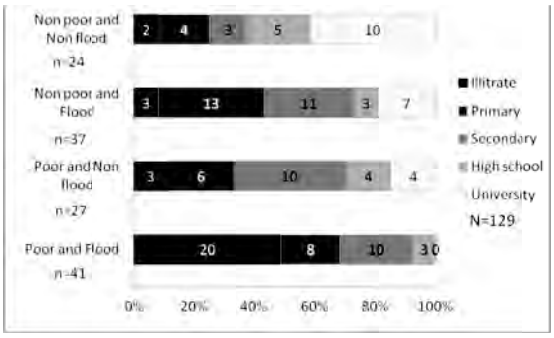

Figure 5.1: Household distributions with the education status of poor and

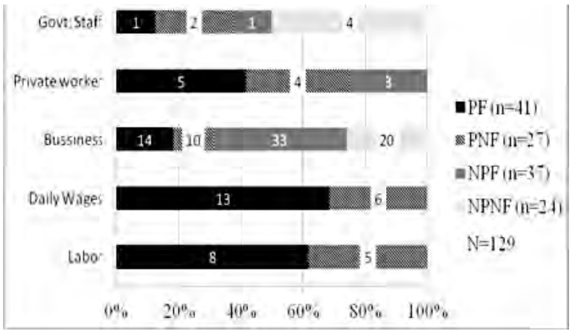

Figure 5.2: Household distributions with the occupation status of poor and flooded

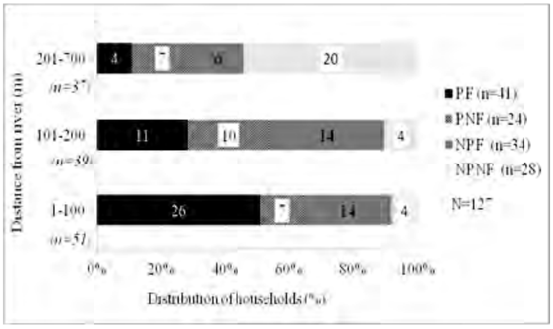

Figure 5.3 Household distributions with the distance to river

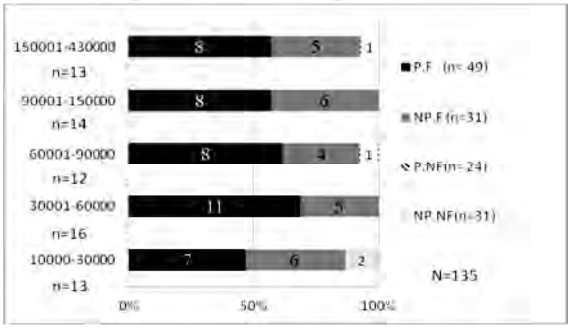

Figure 5.4 Damaged costs for flood impacts

Figure 5.3 shows household distribution in relation with distance from the river. It is obliviously seen that more than 90% of household within 100m distance from river bank is poor household. Figure 5.4 shows the damaged cost of respondents affected by flood. Poor people have more damaged cost than non poor. The amount of maximum cost is 430,000 Kyats (495 USD) in 2011. Most poor people had two time of damage cost than non poor people.

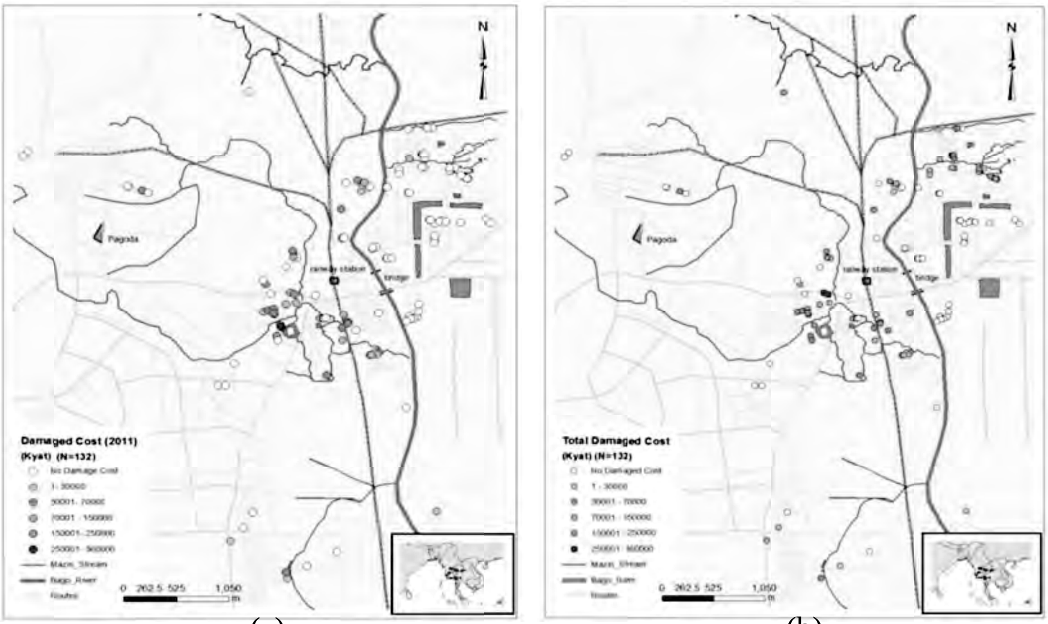
N
Pagoda
railway station
bridge
Damaged Cost (2011)
(Kyat) (N=132)
No Damage Cost
1 - 30000
30001 - 70000
70001 - 150000
150001 - 250000
250001 - 360000
Main_Stream
Bago_River
Routes
0 262.5 525 1,050
m
N
Pagoda
railway station
bridge
Total Damaged Cost
(Kyat) (N=132)
No Damaged Cost
1 - 30000
30001 - 70000
70001 - 150000
150001 - 250000
250001 - 360000
Main_Stream
Bago_River
Routes
0 262.5 525 1,050
m

(a) (b)

Figure 5.5: (a) Comparison of damaged costs and (b) total damaged cost for flood

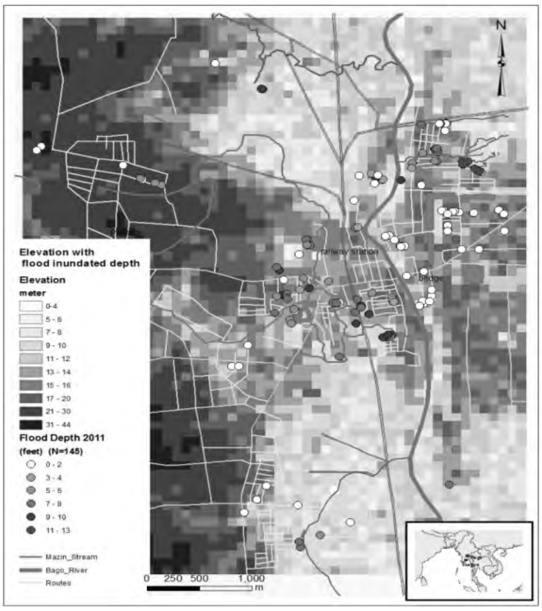

Figure 5.6: Elevation with flood inundated depth

Figure 5.5 shows the comparison of the household distributions affected by direct damaged cost and total damaged cost. It can be seen in the (Figure 5.5 a) that poor live at the left side of Bago river have low direct damage cost however they have high total damaged cost due to the addition of indirect damage cost from disabilities of roads and electricity affected by longer flood duration (Figure 5.5 b). The developed GIS spatial characteristics map (Figure 5.6) shows that poor live at the left side of the river are in higher elevation so that they are resilient to direct damage at flood depth up to 4 feet (1.22 m) shown in orange circles.

About one fourth of total respondents (36:135) could not go to school during the floods and the ratio of disabilities of poor student and non-poor students is found to be (23:15). About half of respondents (72:135) could not access roads and electricity during the flood and poor people could not use longer than non poor people. Over one fourth of total respondent's (30:135) loss accesses more than 16 days. Moreover, in the case of water sanitation system, 36 households is affected their daily use water sanitation system due to flood. In the case of flood information, 52 households out of 196 did not get enough early information about flood for preparedness and evacuation and 26 households didn't get the sufficient information.

The respondents have experiences in preparedness before floods and respondness after the floods. They have different ways in preparedness and respondness according to their financial status and locations of households. The study investigated the coping strategy on PF, PNF, NPF, and NPNF from the aspects of physical, social and economical in flooded and non-flooded areas before, during and after the floods (Figure 5.7).

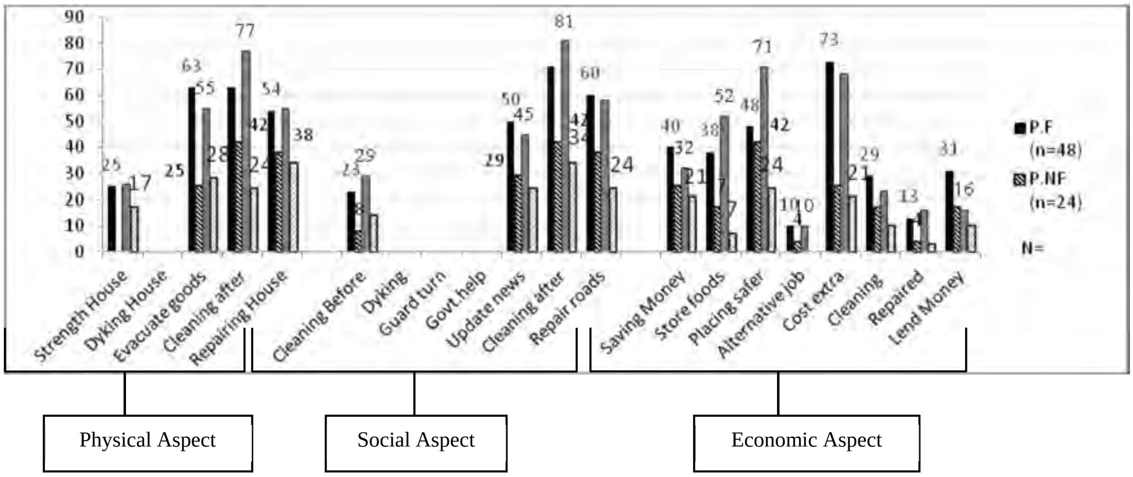

Figure 5.7: Preparedness and respondness of respondents with specific item on flood

Among the four groups, it can be seen that PF are more affected by floods in physical, social and economical aspects strengthening houses before flood, evacuating goods during flood, lend money for extra costs of recovery process such as repairing houses after floods. NPF are the second most affected by floods. But they still have high recovery process for direct damage. Thus, it is necessary to consider land elevation, floor levels of houses and distance from the river for flood mitigation plans.

In case of flood impacts on farmlands and livestocks, paddy yield is decreasing about 50% due to flood in these years. Most area of Bago is unban and only sub-urban along highway is the farmland outside city area. They are facing problem for agriculture in lack of water at summer time and heavy water on rainy time. They have no monthly income and monthly expenditure is about averagely 180,000 kyats. The majority of farmer families are depending on yearly income from farmland. Low yearly income by flood affected to the farmers lowering living standard more and more. They can grow only one season starting about Nov or January only but not in rainy season because of flooding waters. The damaged cost on farming case includes the loss of farmlands (low production) and recovery cost for farmland to be use in coming season. The average damaged cost of farmers is 1,857,066 kyats and 1,817,353 kyats for 2011 and 2012 respectively.

5.3 Proposed Flood Mitigation Measures

In the focus group discussion, some people in flooded wards have their own thinking for reducing the impacts of flood. They would like to report to local authorities about their difficulties due to flood and they hope to mitigate the floods as much as possible because of extra cost in transportation and evacuation, and income loss due to work absence during the flood. On the other hand, the farmers would like to get better drainage and irrigation system, improved flood protection works and to strengthen the existing dykes and embankments for rice cultivation in rainy season. The farmer presented their flood mitigation plans for their farmlands and they hoped to be implemented in future. Most of the farmers in Mekone ward, would like to strengthen the existing hydraulic structures and bridges across Thae Phyu Chaung and Mazin Chaung because narrowing drainage gates and low height bridges disturb water flow and make flood traps in the farmlands. The administrative people of Pinse ward would like the stream to be dredged out and to be widen near the ward because water flows into the ward and farmlands from the narrow stream.

The respondents in the most critical flood area in Bago city mentioned that hydraulic structures construction to slow down the water flowing speed around Kyun Thar Yar ward and Kalyarni ward because they could not go outside from their home during flood time even though by boat and it is too dangerous around Kalyarni ward.

We developed a GIS flood mitigation measures map based on flood depths, land gradients, streams across the wards and outcomes from focus group discussion. Flood mitigation approaches should be strengthening the existing embankment or construction new embankment or hydraulic structure around Mazin stream, lateral of Bago river. And early warning system will be reduced some extent the flood impacts (Figure 5.8).

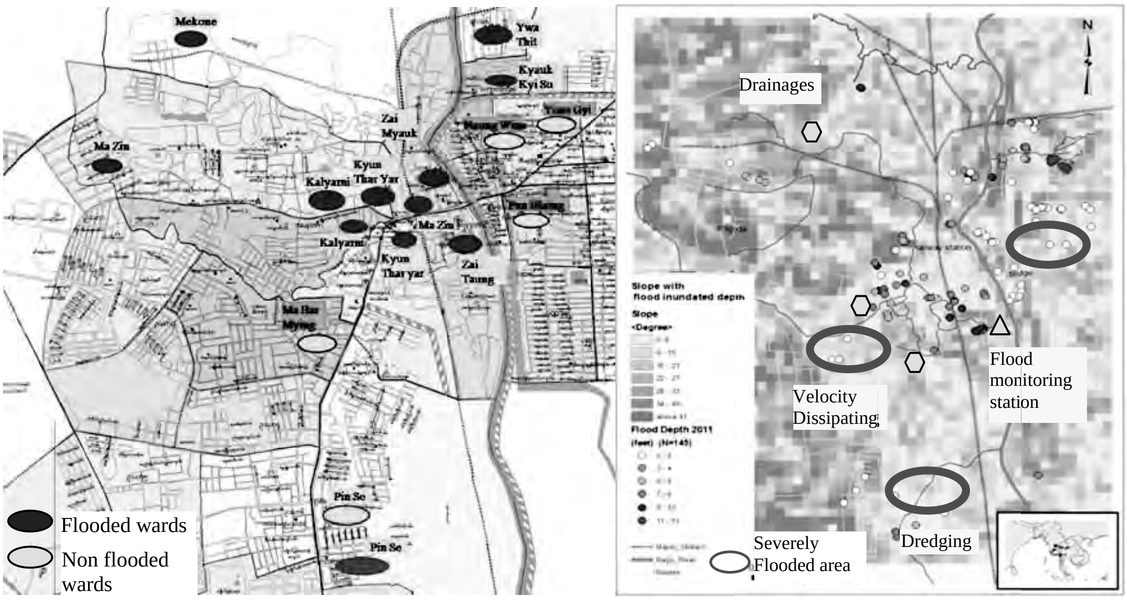
Mekone
Ywa Thit
Kyauk Kyi Su
Zai Myauk
Ma Zin
Kyun Thar Yar
Kalyarni
Ma Zin
Kalyarni
Kyun Thar yar
Zai Taung
Ma Har Myaing
Pin Se
Pin Se
Flooded wards
Non flooded wards
Drainages
Flood monitoring station
Velocity Dissipating
Severely Flooded area
Dredging
N

Figure 5.8: Study wards and proposed GIS based flood mitigation measures map

6. CONCLUSION AND RECOMMENDATION

6.1 Conclusion

Demographic characteristics of the study area Bago city, Bago Region, Myanmar are examined. The difference of flood impacts among four groups of poor flooded, poor non flooded, non poor flooded, and non poor non flooded people are analyzed. The flood impacts are assessed in terms of social, economic, physical aspects.

The results show that the whole area of Bago city is not inundated even in the severe floods. Floods annually occur in the same places in July and August. However, Irrigation Department carried out flood mitigation works by constructing dams in the upstream of the Bago River in the year 2012. By means of those mitigations, flood areas and flood inundation depths were reduced to some extents and high flood water levels were lower than in year 2011.

Majority of poor people are illiterate and having only primary education level and hence, they have limitation to access to disaster related information and risk reduction programmes. Then they are relatively more suffered by flood. However, non poor people who have multiple sources of income and higher education are less affected by flood than poor people. Poor people have more direct and indirect costs while the non poor people have direct cost only. Poor and flooded people group who live in near river bank are daily wages labor and lower education than non poor. Poor people lost nearly twice than non poor people and they are affected by flood impacts and consequences not only during and after the floods, but also they have preparation costs before floods.

6.2 Recommendations

The study would like to recommend that poor people live in inundated area which is close to river with low elevation. Thus, poor people were more flooded than non-poor people, but their economic damage would be less than non-poor because of low income and fewer properties. Absolute economic loss of poor people would be small but the relative economic loss and social impact of poor would be larger than that of non-poor. Flood mitigation works should be planned in order to alleviate poverty on basic of the combination of economic improvement, knowledge improvement and also in infrastructure works. In the case of poor people, they can have flood impacts by unfavorable spatial characteristic of their locations. Even if their economic was improved and they are likely to be suffered flood impacts with their low education and less matured than non poor people.

This study would likely to upgrade the interest of stakeholders on economy of poor people. Single occupation may suffer flood impact more than multiple occupations and own business. Multiple occupations can increase not only income but also living standards. Training, education and public awareness are needed to reduce flood impacts. Public knowledge on practical preparedness measures at the household level is needed so that the communities can implement on their own. Therefore, it can be reduced social and economic impacts and improve preparedness plans in the affected area for the future floods. The study is recommended to assist reliable information database for policy makers, civil societies, private sectors to imagine how to reduce flood and the socio-economic impacts on households and for the understanding of poverty alleviation by flood mitigation. It is recommended to do nationwide survey on flood impacts and to speed up the poverty alleviation actions by flood mitigation.

ACKNOWLEDGEMENT

I would like to express my sincere gratitude to my advisor, Professor Dr. Akiyuki Kawazaki, and Professor Dr. Sutat Weesakul, Professor Dr. Damien Jourdain for their guidance, comments and precious suggestions, close supervision. And I would like express my deep appreciation to Director U Zaw Min Htut, Deputy Director U Kyaw Lin Oo and Assistant Director Dr. Aung than Oo from Irrigation Department for their guidance, encouragement and kind supports throughout the study. Deeply appreciations and thanks are conveyed to my research donor, Swedish International Development Cooperation Agency (SIDA). Special thanks are conveyed to the Director General, Deputy Director General of Irrigation Department, Ministry of Agriculture and Irrigation, the Republic of the Union of Myanmar. Finally I would like to express my thanks to all who help and encourage me within my study period, and the authors, the publishers of all books I referenced in my study.

REFERENCES

Kyaw, D., 2006. *Rural poverty analysis in Myanmar - A micro level study in the dry zone,* PhD Thesis, Asian Institute of Technology.

Fothergill, A., and Peek. L. A., 2004. Poverty and disasters in the United States: A review of recent sociological findings. *Natural Hazards* 32, 89–110

Messner, F. and Meyer, V., 2005. *Flood damage, vulnerability and risk perception - challenges for flood damage research*.

MNPED, UNDP, SIDA, 2011. *Integrated Household Living Conditions Survey in Myanmar*, (2009-2010), Technical Report, 53.

Singleton, D., 2014. *4th Brunel International Lecture, Poverty alleviation- The role of the engineer*, Institute of Civil Engineer (ICE), accessed the website in October, 2014.

Role of news media from experiences of the 2011 Great East Japan earthquake

Muneyoshi NUMADA[1] and Kimiro MEGURO[2]
[1] Lecturer, ICUS, IIS, The University of Tokyo, Japan
numa@iis.u-tokyo.ac.jp
[2] Professor, ICUS, IIS, The University of Tokyo, Japan

ABSTRACT

News media reported the conditions of the damaged areas. Information disseminated by mass media is still considered as major information source to understand the damage, social trend and the activities in affected areas. The important roles of mass media are mainly two functions in terms of before and after the hazard attacks. After the disaster occurs, huge amount of digital data of the Earthquake is provided by the highly-developed digital data technology. But the method and technique for analysis of these huge digital data are not developed sufficiently. This paper proposes a running spectrum technique for text data and analyzing changes of disaster phase during the disaster management cycle. Impact analysis of the disaster has been performed by using Fukushima Minpo newspaper for its verification. The result shows the dynamic characteristics of the disaster. As the time interval B becomes longer, the analysis data is used from wide range period along with the smoothing effect. When observing different time intervals B, fewer keywords have been ranked in the longer time intervals of B. The proposed technique is a powerful tool to analyze effectively the huge amount of digital data for the effective and efficient disaster response and management.

Keywords: mass media report, disaster information, Tohoku earthquake, running spectrum analysis

1. INTRODUCTION

Three years have passed since the 2011 Great East Japan earthquake. The impact of this earthquake caused long-term problems during recovery and reconstruction not only in damaged areas but also all over Japan. People, governments and researchers have been trying to solve these problems for the future society. Mass media (news media) reported the conditions of the damaged areas during the 2011 Great East Japan earthquake. Even with the development of social network technology, information disseminated by mass media is still considered as major information source to understand the damage, social trend and the activities in affected areas.

However one of the major problems of mass media during disaster situations is the focus on particular areas with easy access or with shocking events. Therefore, it is difficult to understand the total picture of the disaster. The important roles of mass media are mainly two functions in terms of before and after the hazard attacks. After the disaster occurs, huge amount of digital data of the Earthquake is provided by the highly-developed digital data technology. Huge amount of digital information related to the Earthquake has been published by newspapers, wire agencies and TV stations. The volume of information has exceeded that of past disasters because the tools by using to send out information have dramatically changed; Internet-based platforms are now widely used as popular sources for news updates. The contents covered include many different kinds of events and problems that were caused simultaneously by the earthquake. Reports on regional damage induced by the earthquake, tsunami and economic problems in the Tokyo metropolitan area, Fukushima nuclear power plant accident and much other information spread out at the same time.

Cloud computing technology can evaluate more and more digital contents that produced and stored in the digital world. This new innovative environment and incorporating powerful delivery data system enable us to use information more easily for different purposes. However, the quality of data analysis technique in the disaster management field is far from enough. Efficient tool boxes are needed to analyze important events out of the vast amount of information. Furthermore, the trends within a certain time frame and the changes occurring in the disaster management phase can be observed.

Some algorithms in literature evaluation method suggest using association rules such as TF-IDF (Term Frequency - Inverse Document Frequency) (Lindsay, 1995; Srinivasan, 2004), Z-score (Yetisgen-Yildiz, 2006) and Mutual Information Measure (MIM) (Wren, 2004). The association rules and TF-IDF are based on term co-occurrence frequencies, while Z-Score and MIM are based on term co-occurrence probabilities (Meliha, 2009). The characteristics of disaster-related-information change or shift in accordance with each disaster management cycle phase, “which are namely damage mitigation, preparedness, prediction and early warning, damage assessment, emergency disaster response, recovery, and reconstruction/restoration”. When handling this kind of information with characteristics that depend on time-changing, it is necessary to make analysis within a certain time span. Therefore, we propose a dynamic analysis technique of literature with considerations on time series to offer proper and appropriate responses. This paper shows the overview of proposed techniques. News from the newspaper of Fukushima Minpo has been used for its verification. The proposed technique is a powerful tool to effectively analyze the huge amount of digital data, thereby responding to the upcoming society with growing volume of information.

2. RUNNING SPECTRUM ANALYSIS OF TEXT DATA

2.1 Running Spectrum Analysis

Running spectrum analysis is a method widely used in the seismic ground motion analysis for understanding the wave characteristics in time and frequency domain. It is an approach that shifts a time interval of analysis points to conduct analysis within a certain time frame. In our research, the target is further expanded to the literature field. It can be seen in Figure 1 that moving-average method which is widely used to smooth short-term data fluctuations in time series is applied for dynamic analysis. The time interval B is defined as the calculating range for smoothing the data fluctuations.

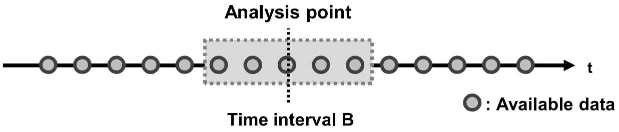

Figure 1: Time interval B of moving average method.

2.2 Flow of text data running spectrum analysis

Figure 2 shows the flowchart diagram of running spectrum analysis on text data proposed in this research. Firstly, Japanese Kanji letters, Katakana letters, numbers and alphabets are extracted from the documents separately as keywords. For this purpose, we have developed an "extract-keyword-program (EKP)". The EKP can extract each keyword individually and accurately. For example, “hinan” (“evacuation” in English) and “hinansya” (“evacuee” in English) are identified as different keywords within the same document. The EKP can also count the frequency of appearance within one certain day or all the days during the specified period. Users can freely reset the period depending on purposes. Secondly, keywords are reviewed and analyzed. The weights of all extracted keywords are calculated respectively. Suggested algorithms for keyword analysis are: Clustering, TF-IDF, LSI (Latent Semantic Indexing), and Co-occurrence. Our proposed system can choose the most suitable weighing approach according to the purposes and requirements of each user. In this paper, we have used TF-IDF (Term Frequency-Inverse Document Frequency) in the time span B. TF-IDF is a statistical measurement method to evaluate the degree of importance of a specified keyword in a document among a collection of numerous documents. The importance level is determined by the frequency and distribution within the collection of all documents (Meliha, 2009).

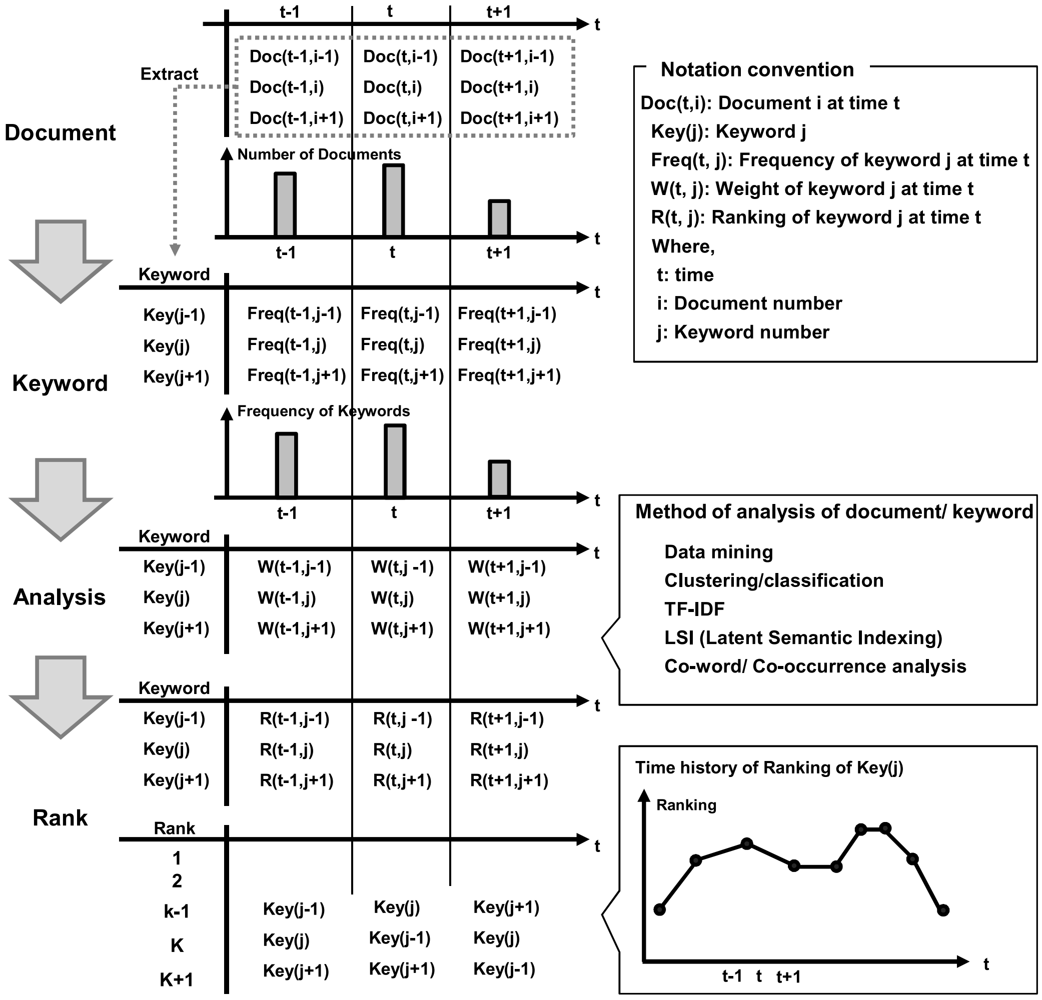
t-1
t
t+1
t
Extract
Doc(t-1,i-1)
Doc(t,i-1)
Doc(t+1,i-1)
Doc(t-1,i)
Doc(t,i)
Doc(t+1,i)
Doc(t-1,i+1)
Doc(t,i+1)
Doc(t+1,i+1)
Document
Number of Documents
Notation convention
Doc(t,i): Document i at time t
Key(j): Keyword j
Freq(t, j): Frequency of keyword j at time t
W(t, j): Weight of keyword j at time t
R(t, j): Ranking of keyword j at time t
Where,
t: time
i: Document number
j: Keyword number
Keyword
Key(j-1)
Key(j)
Key(j+1)
Freq(t-1,j-1)
Freq(t,j-1)
Freq(t+1,j-1)
Freq(t-1,j)
Freq(t,j)
Freq(t+1,j)
Freq(t-1,j+1)
Freq(t,j+1)
Freq(t+1,j+1)
Frequency of Keywords
Method of analysis of document/ keyword
Data mining
Clustering/classification
TF-IDF
LSI (Latent Semantic Indexing)
Co-word/ Co-occurrence analysis
Analysis
W(t-1,j-1)
W(t,j -1)
W(t+1,j-1)
W(t-1,j)
W(t,j)
W(t+1,j)
W(t-1,j+1)
W(t,j+1)
W(t+1,j+1)
R(t-1,j-1)
R(t,j -1)
R(t+1,j-1)
R(t-1,j)
R(t,j)
R(t+1,j)
R(t-1,j+1)
R(t,j+1)
R(t+1,j+1)
Rank
Time history of Ranking of Key(j)
Ranking
1
2
k-1
K
K+1
Key(j-1)
Key(j)
Key(j+1)
Key(j)
Key(j-1)
Key(j+1)
Key(j+1)
Key(j)
Key(j-1)
t-1 t t+1

Figure 2: Flowchart diagram for running spectrum technique.

To apply TF-IDF for the running spectrum analysis, TF-IDF value is calculated as:

$$TF \cdot IDF(t,j) = TF(t,j) \times IDF(t,j) \tag{1}$$

Where,

$$TF(t,j) = \frac{Kj(t)}{K(t)} \tag{2}$$

$$IDF(t,j) = \log \frac{T(t)}{Tj(t)} \tag{3}$$

Where Kj(t) is number of occurrence of keyword (j), K(t) is total number of occurrence keywords in the time interval B, Tj(t) is number of literatures which includes keyword (j) and T(t) is total number of literatures in the time interval B.

Thirdly, after the evaluation of the importance of each keyword in certain time interval B, all keywords are ranked according to its weights.

3. CASE STUDY OF FUKUSHIMA MINPO NEWSPAPER

3.1 Newspaper data

Fukushima Minpo is a local newspaper with circulation of 250 thousand copies per day and the largest in Fukushima Prefecture (Fukushima minpo co.). Newspaper repeatedly reports on nuclear power plant accidents as the company office is located near the site. Figure 3 shows news report archives from March 2011 to May 2012, analyzing articles by the running spectrum approach described above. Figure 3 includes the reports about not only nuclear plant accidents but also earthquake, tsunami, and damages to analyze all impacts of this disaster.

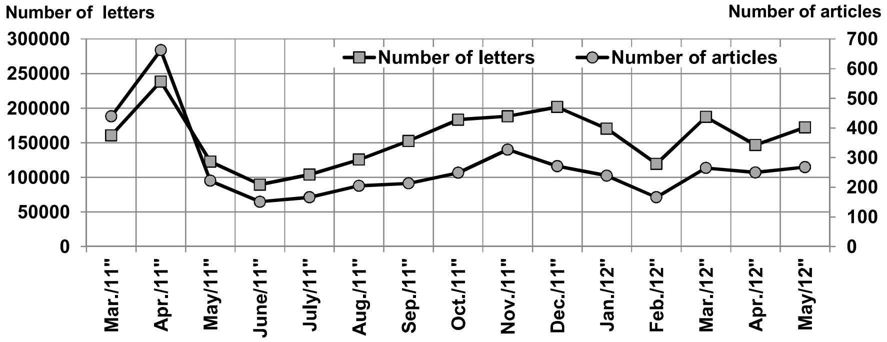

Figure 3: Archives of Fukushima Minpo newspaper

3.2 Extracting keywords

Figure 4 shows the number of keyword items and its frequency. Total of 67,881 different keywords have been extracted. For example, Frequency is shown as “1” in 44,022 items (64.85% of the total), indicating that the keyword appears only one time. Most newspaper articles report the name, gender and age of those dead or injured, therefore the number of keywords with only one-time appearance equals the number of items. Figure 5 represents keywords with high frequency. “Refuge” is listed as the most frequently used keyword with 1,696 appearances, followed by “residents” with 1,614 times over the period from March 2011 to May 2012. Because both tsunami and nuclear plant accidents induced the emergency evacuation and long-term evacuation to the people, refuge and residents are frequently used. Keywords related to nuclear power accidents such as “decontamination”, “nuclear power plant accident”, “influence”, “radioactive material”, “children”, “dose of radiation” etc. are ranked high. In this study, one-letter words have been omitted because the keyword often has no meaning by itself at alone and therefore should be interpreted within idioms, phrases and contexts.

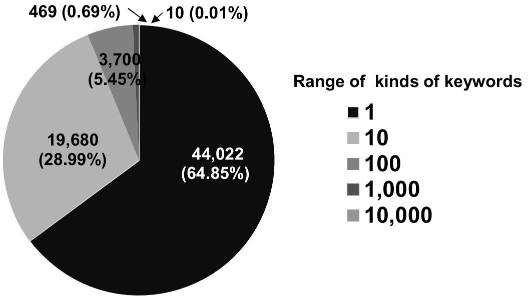

Figure 4: The number of keyword items and its appearance within a certain range.

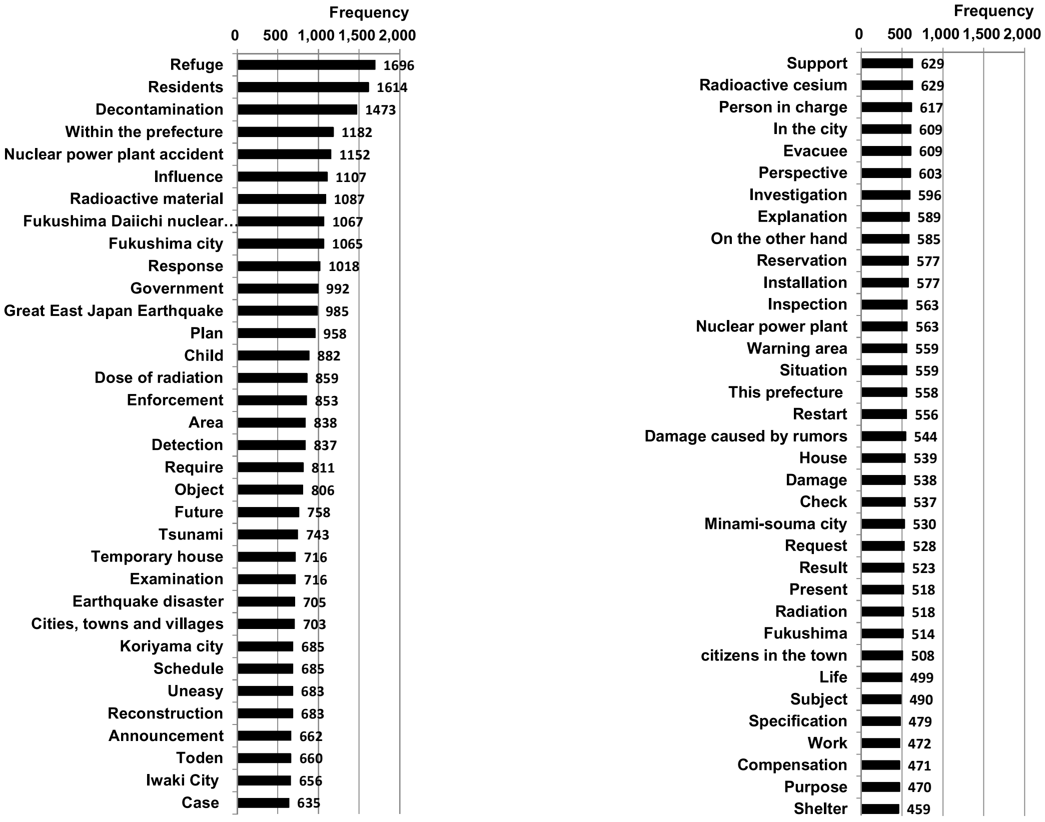

Figure 5: List of Keywords and its appearance frequency (high frequency part).

3.3 Results of running spectrum analysis

All keywords are given the rank respectively according to the weighting algorithm on daily or monthly level by proposed method. We get to understand which keywords received attention at the time and tracing down the hottest keywords changing with the circumstances of the moment.

(1) Time-chart of the top ranked keywords: Table 1 shows the time chart of the top three ranked keywords having top ranking in a day in March 2011 as a sample period for B =3, 7 and 31 days respectively due to space limit of paper.

Table 1: Time chart of keyword ranking

		B=3			B=7			B=31		
		1	2	3	1	2	3	1	2	3
2011/3/11	Keyword	Fukushima city	Tsunami	Center	Tsunami	Evacuation	Disaster victim	Evacuation	Refuge	Response
	TF-IDF	0.015884	0.015884	0.015884	0.018549	0.017122	0.014268	0.011379	0.008302	0.007007
2011/3/12	Keyword	Tsunami	Center	Evacuation	Koriyama city	Disaster victim	Evacuation	Evacuation	Refuge	Response
	TF-IDF	0.015694	0.015694	0.013079	0.012868	0.012433	0.010568	0.010424	0.007525	0.006362
2011/3/13	Keyword	Center	Generating	Offer	Disaster victim	Koriyama city	Evacuation	Evacuation	Refuge	Acceptance
	TF-IDF	0.007838	0.006532	0.006532	0.010186	0.007478	0.007099	0.009608	0.006706	0.005774
2011/3/14	Keyword	Koriyama city	Disaster victim	Suffering a calamity	Disaster victim	Evacuation	Koriyama city	Evacuation	Refuge	Acceptance
	TF-IDF	0.013906	0.008126	0.005794	0.004954	0.004817	0.004578	0.008486	0.005925	0.005415
2011/3/15	Keyword	Koriyama city	Debris	Business	Debris	Acceptance	Activity	Evacuation	Refuge	Acceptance
	TF-IDF	0.004075	0.003943	0.003943	0.003477	0.003367	0.003134	0.007612	0.005316	0.005158
2011/3/16	Keyword	Business	Work	Part	Pregnant	Debris	Niigata prefecture	Evacuation	Acceptance	Refuge
	TF-IDF	0.003505	0.002804	0.002804	0.004234	0.003024	0.003024	0.006876	0.004736	0.004668
2011/3/17	Keyword	Directions	Woman	Blanket	Pregnant	Numerical value	Detection	Evacuation	NPPA	Acceptance
	TF-IDF	0.002985	0.002985	0.002985	0.003366	0.002512	0.002476	0.005918	0.004135	0.004135
2011/3/18	Keyword	Pregnant	Citizen	Niigata prefecture	Last spring	Detection	Citizen	Evacuation	Acceptance	NPPA
	TF-IDF	0.004228	0.003020	0.003020	0.002930	0.002916	0.002287	0.005239	0.003820	0.003747
2011/3/19	Keyword	Detection	Pregnant	Postponement	Last spring	Citizen	Detection	Evacuation	Acceptance	NPPA
	TF-IDF	0.003803	0.003803	0.003260	0.002767	0.002754	0.002046	0.005153	0.003757	0.003433
2011/3/20	Keyword	Last spring	Goods	water supply	Citizen	Restart	Holding	Evacuation	Acceptance	NPPA
	TF-IDF	0.002857	0.002711	0.002449	0.002561	0.002292	0.002167	0.004497	0.003283	0.003125
2011/3/21	Keyword	Student	Successful applicant	Citizen	Citizen	Postponement	Holding	Evacuation	NPPA	Acceptance
	TF-IDF	0.004139	0.003726	0.003312	0.002103	0.002103	0.001896	0.003873	0.002961	0.002885
2011/3/22	Keyword	Difficulty	Aizuwakamatsu	Holding	Holding	Last spring	Postponement	Evacuation	Election	NPPA
	TF-IDF	0.002421	0.002421	0.002118	0.001622	0.001622	0.001523	0.003244	0.002655	0.002600
2011/3/23	Keyword	Postponement	Holding	Life in refuge	Student	Holding	Last spring	Evacuation	Election	Acceptance
	TF-IDF	0.001976	0.001874	0.001606	0.001690	0.001598	0.001598	0.003221	0.002636	0.002519
2011/3/24	Keyword	Holding	Large scale disaster	Life in refuge	Student	Holding	Last spring	Evacuation	Election	Acceptance
	TF-IDF	0.001555	0.001333	0.001333	0.001740	0.001646	0.001646	0.003200	0.002619	0.002503
2011/3/25	Keyword	Restoration	Tokyo metropolitan	Large scale disaster	Student	Holding	Election	Evacuation	Election	Acceptance
	TF-IDF	0.001899	0.001625	0.001625	0.001907	0.001804	0.001704	0.002723	0.002609	0.002493
2011/3/26	Keyword	Attendance	Tomioka	Tokyo metropolitan	Election	Reservation	Holding	Election	Acceptance	Detection
	TF-IDF	0.003176	0.002117	0.002117	0.002433	0.001899	0.001778	0.002573	0.002458	0.002356
2011/3/27	Keyword	Radioactive material	Tomioka	Sea water	Election	Reservation	Acceptance	Election	Acceptance	Detection
	TF-IDF	0.004758	0.003569	0.003569	0.002681	0.002053	0.001967	0.002539	0.002426	0.002325
2011/3/28	Keyword	Acceptance	Investigation	Residents	Attendance	Acceptance	Radioactive material	Election	Acceptance	Detection
	TF-IDF	0.006747	0.003680	0.003169	0.002556	0.002283	0.001886	0.002553	0.002440	0.002338
2011/3/29	Keyword	Reservation	Fukushima	Accident	Hotel	Victim	Japanese style hotel	Election	Acceptance	Postponement
	TF-IDF	0.002896	0.002896	0.002779	0.004085	0.003682	0.003156	0.002503	0.002392	0.002222
2011/3/30	Keyword	Temporary back-home	Inside Shelter	Accident	Victim	Hotel	Japanese style hotel	Election	Postponement	Acceptance
	TF-IDF	0.002826	0.002826	0.002711	0.004175	0.003578	0.003227	0.002442	0.002418	0.002334
2011/3/31	Keyword	Victim	Hotel	Restart	Victim	Hotel	Japanese style hotel	Postponement	Election	Acceptance
	TF-IDF	0.005895	0.005359	0.003751	0.004514	0.003870	0.003490	0.002508	0.002360	0.002214

Taking a look at the B=3 cases, frequently used keywords in this emergency period immediately after the quake include “tsunami”, “evacuation”, “disaster victim” and “debris”, “Blanket” was another important word since the earthquake occurred during the winter season and blankets were strongly required by the evacuees.

On March 19th, due to worries about the spread of radiation from the nuclear power plant accident, the word “pregnant” was seen for the first time. On March 30th, “temporary home return” was ranked top. This was when the evacuees who had to leave their hometown for fear of radiation and were allowed to pay a brief visit home just to bring their valuables. The B=7 case, which is similar to the B=3 case, covers the time when the earthquake hit. Keywords described as emergency terms such as “tsunami”, “evacuation” and “debris” is seen. On March 16th and 17th, “pregnant” was ranked top indicating the serious concerns of radiation by pregnant women as in the B=7 case. As for B=31, “evacuation” and “refuge” were the most used keywords for some days during emergency period. From March 22nd, “election” was ranked high because the nationwide local elections in April were also another issue of attention.

(2) Effect of different time interval B: Comparing the short and long time intervals in terms of “B” , top ranked keywords change day by day in B=3 (in which the target time interval days are shorter). On the other hand, some specific keywords, such as “evacuation”, “refugee”, “acceptance” and “election”, tend to be ranked higher in the longer time intervals. Therefore, because the time interval B becomes longer, the analysis data is used from wide range period along with the smoothing effect. The characteristics of the duration effect of time interval B can be explained by how many kinds of keywords were ranked No.1 at least once as shown in Figure 6.

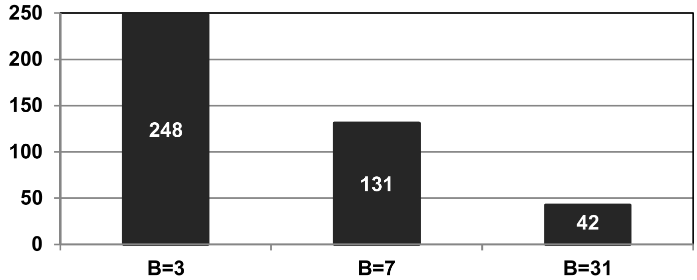

Figure 6: Comparison of items of keywords ranked No.1.

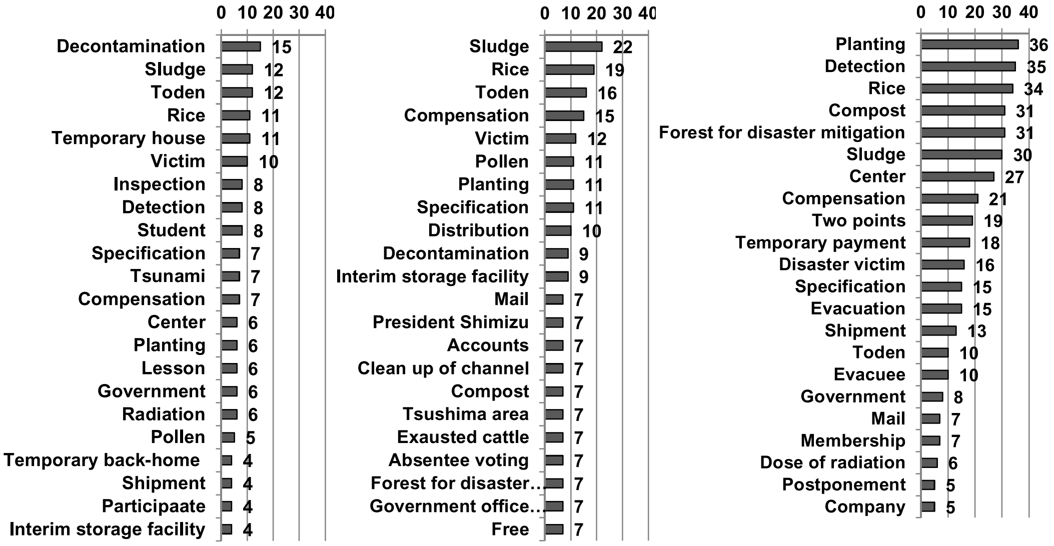

(a) B=3 (b) B=7 (c) B=31

Figure 7: Keywords ranked as No.1 and its frequency.

When observing different time intervals B = 3, 7 and 31 days, fewer keywords have been ranked in the longer time intervals of B. For example, the B=31 case shows only 42 kinds of keywords ranked No.1 while the B=3 case shows as many as 248.

(3) Keywords ranked No.1: Figure 7 shows the keywords which were ranked No.1, and how many times the keyword has reached the No.1 position. The most frequently ranked as No.1 include: "decontamination" with 15 times for B=3 days, "sludge" with 22 times for B=7 days and "planting" with 36 times for B=31 days.

Table 2: Time-history of keywords that ranked as No.1 with its frequency

		B=3		B=7		B=31	
Year	Month	Keyword	Number of No.1	Keyword	Number of No.1	Keyword	Number of No.1
2011	3	Center	3	Last spring	3	Evacuation	15
		Pregnant	2	Student	3	Election	5
		Tsunami	2	Pregnant	2	Postponement	1
	4	Student	3	President Shimizu	7	Disaster victim	12
		Move in	3	Danger	4	Evacuee	5
		Vegetables	2	Move in	4	Request	5
	5	Japan Agriculture	3	Temporary payment	5	Temporary payment	18
		Temporary back-home	3	Toden	5	Government	8
		Temporary payment	3	Japan Agriculture	4	Toden	5
	6	Sludge	3	Sludge	7	Sludge	19
		Temporary house	3	Clean up of channel	7	Company	5
		Clean up of channel	3	Measurement	5	Temporary back-home	2
	7	Specification	4	Specification	9	Specification	15
		Participate	3	Shipment	4	Shipment	13
		Ratio of adjustment	3	Beef cattle	4	Farmhouse	3
	8	Student	3	Sludge	3	Compensation	11
		Specification	3	Compensation	3	Evacuee	5
		Pension for survivor	2	Announcement	3	Refuge	5
	9	Reconciliation	3	Two points	6	Two points	16
		Prime minister Noda	3	Compensation	5	Compensation	6
		Mediation	3	Guardian	4	Temporary place	4
	10	Rice	3	Rice	7	Forest	23
		Landslide	3	Forest	7	Two points	3
		Forest for disaster mitigation	3	Interim storage facility	4	Compensation	3
	11	Wild boar	3	Compost	7	Compost	22
		Compost	3	Absentee voting	7	Forest	8
		Absentee voting	3	Government office	7	-	-
	12	Golf course	3	Tsushima area	7	Rice	13
		Sludge	3	Bark	6	Compost	9
		Recycle	3	Membership	6	Membership	7
2012	1	Decontamination	6	Toden	7	Rice	21
		Hanami Yama mountain	3	Rice	4	Planting	5
		Government	3	Decontamination	4	Donation	2
	2	Rice	4	Victim	7	Planting	29
		Subsidy for reconstruction	3	Pollen	6	-	-
		Planting	3	Subsidy for reconstruction	5	-	-
	3	Free	3	Accounts	7	Center	27
		Area where is difficult to return	3	Distribution	7	Planting	2
		Distribution	3	Free	7	Iodine	1
	4	Exhausted cattle	3	Mail	7	Detection	12
		Mail	3	Exhausted cattle	7	Mail	7
		Personnel	3	Pollen	4	Exhausted cattle	5
	5	Cherry blossom	3	Sludge	7	Detection	23
		Sludge	3	Yanagisawa	7	Sludge	8
		Subsidy	3	Buying credit	4	-	-

From this result, we can see that specific keywords were constantly listed high for the longer B due to the effect of soothing.

Table 2 shows the time-history of keywords that remained No.1 for a month. By reviewing this table, the timeline of events are observed. Unfortunately, only the top three are shown in this table due to the limitation of paper space even though many keywords remained in the No.1 position for a month. Focusing on the B=31 case, keywords of the months in chronological order at the top are observed. “Evacuation” was the most important keyword in March 2011, followed by “disaster victim” (April), “temporary payment” (May), “sludge” (June), “specification” (July), “compensation” (August), “two points” (September), “forest for disaster mitigation” (October), “compost” (November), “rice” (December). Moving onto 2012, “rice” (January), “planting” (February), “center” (March) and “detection” (April and May). By following the top keywords, the outline and the stream of this complex disaster despite them intertwined problems and difficulties.

⑷Trend of each keyword: This system also analyze the trend of specific keywords that a system user might take interest. For example, focusing on the top ranked keyword “planting” in Figure 7 (c), the trend of its ranking is presented as seen in Figure 8. The nuclear power plant accidents have given the impact to the planting of rice in the rice fields. The case B=3 shows high discontinuity, while continuity is clearly shown in B=31 due to the soothing effects. From around October 2011, the problems related to “planting” constantly emerge as shown in the B=31 case.

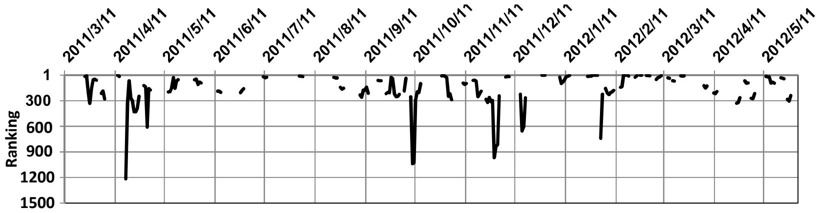

(a) B=3 case

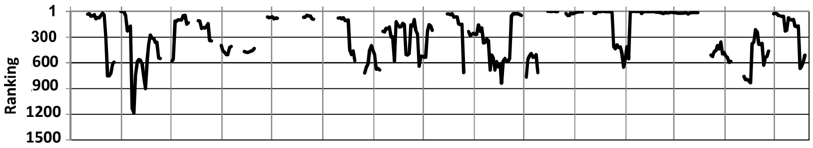

(b) B=7 case

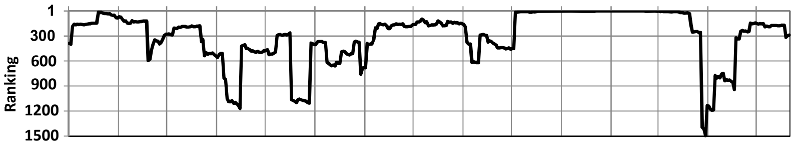

(c) B=31 case

Figure 8: Time history of ranking of “Planting”.

4. CONCLUSIONS

Running spectrum system for analyzing text data in the advanced society having digital data is proposed in this paper. The news reported by Fukushima Minpo newspaper is used for the verification of the technique and analyze of the impact of nuclear power plant accidents in Japan. The result shows the dynamic characteristics of the nuclear power plant accidents. As time goes on, more digital information on natural disasters will become available. Then, the proposed technique serves efficiently and effectively to analyze huge amount of digital information, thus providing appropriate understanding of the impact of the nuclear power plant accidents.

REFERENCES

Fukushima-Minpo Co, Tohoku earthquake reports [Online], http://www.fukushimaminponews.com/ about.html (accessed June 28, 2012)

Wren., J.D., 2004. Extending the mutual information measure to rank inferred literature relationship. *BMC Bioinformatics* 5, 145.

Yetisgen-Yildiz, M., and Pratt, W., 2006. Using statistical and knowledge-based approaches for literature based discovery. *Journal of Biomedical Informatics* 39, 600–611.

Srinivasan., P., 2004. Generating hypotheses from MEDLINE. *Journal of the American Society for Information Science and Technology* 55, 396-413.

Lindsay, R.K., and Gordon, M. D., 1999. Literature based discovery by lexical statistics. *Journal of the American Society for Information Science and Technology* 49, 674-685.

Effect of text message of mobile phone for disaster information dissemination to rural mountainous area in Thailand

Akira KODAKA[1], Akiyuki KAWASAKI[2], Miho OHARA[3]
and Shinya KONDO[4]
[1]Project Researcher, ICUS, IIS, The University of Tokyo, Japan
akira@iis.u-tokyo.ac.jp
[2]Project Associate Prof., Dept. of Civil Engineering, The University of Tokyo, Japan
[3]Senior Researcher, International Centre for Water Hazard and
Risk Management (ICHARM) under the Auspices of UNESCO,
Public Works Research Institute (PWRI), Japan
[4] Chief Researcher, Disaster Reduction and Human Renovation Institution, Japan

ABSTRACT

As one of the major Information Communication Technology, mobile phone has been taking a significant role for disaster risk reduction during the time of emergency situations by warning the public with text-based features. The role becomes more important to the area where less improvement of infrastructure to mitigate disaster damages is expected due to lack of human and material resources. Rural mountainous areas are very places where mobile phone has great potential to be used for warning the public as its penetration rate has been increasing rapidly. However, the effect of the text-based features of mobile phone is still unknown in those areas. Here we show that Short Message Service (SMS), one of the features, would be able to warn the public in a rural mountainous area accurately and promptly. Furthermore, we found that SMS has an effect of information propagation that content of the message is transferred from recipients to others even to those who do not receive the message. Our results demonstrate the usefulness of mobile phone for strengthening and stabilizing current dissemination system in the area, sound-based using loudspeaker and siren, by multiplexing channel of communication and information representation. We anticipate our research to be a basis for further analysis on the effect of text-based features of mobile phone for warning the public. For example, propagation of the contents of SMS among the public could be visualized in chronological order. Furthermore, accuracy of disseminated information should be examined when the hearsay information is continued to be transferred person-to-person.

Keywords: mobile phone, disaster information dissemination, rural mountainous area, Short Message Service

1. INTRODUCTION

Mobile phone, one of the representative of Information Communication Technology (ICT), has been developed rapidly and taking an important role in disaster information gathering, distribution, and sharing at the time of crisis. Besides, it has become popular in all over the world. Mobile phone subscribers including multiple ownerships reached at 93.1% of world population in 2013. The percentage is expected to increase up to 95.5% by 2014 worldwide and 87.6% in developing countries (International Telecommunication Union: ITU, and the World Bank). It would appear that Short Message Service (SMS) standardized by Global System for Mobile Communications (GSM) has high potential to be used as a media to warn public in developing countries where available media including internet are limited. However, there is little research has been done that investigates actual effect of mobile phone used as a media to disseminate disaster information in rural mountainous areas.

On the other hand, mobile phone business in Thailand has been in transition period that carriers start providing variety of services drastically after December 2012. To total population of approximately 67 million, the number of mobile phone subscribers has reached around 92 million including multiple subscriptions as of 2013 (ITU). Smart phone and a tablet have become popular among people in urban areas, yet second-generation mobile phone called 2G has still been used mainly in rural areas.

Therefore, this paper aims to investigate a possibility of the SMS to be a media to warn the public at rural mountainous areas in Thailand by conducting interview with relevant local government and questionnaire surveys with villagers. To that end, result of questionnaire survey in need and importance for developing public warning in the area are summarized. Subsequently, future challenges to analyze the effect of mobile phone for warning the public are discussed.

2. STUDY AREA AND METHODOLOGY

2.1 Study area

In this research, Phuluang district, Loei province, located in northeastern Thailand (Figure 1) was chosen as a study area since there is surrounded by mountains at 600 to 1,500 meters high and many rural communities exist in there. Majority of residents are farmers and many of them cultivate farm lands on mountain surfaces to grow cash crops such as maze, cassava, rubber trees, and so forth.

Thai rural mountainous areas lag significantly behind of communication infrastructures development. Villages are sporadic around intermountain areas with lower population density. Thus, many villages are inaccessible to communication services. For disaster information dissemination, there are three types of media are utilized mainly: loudspeaker, walkie-talkie, and mobile phone. Since sudden disasters such as flash flood and land slide due to heavy

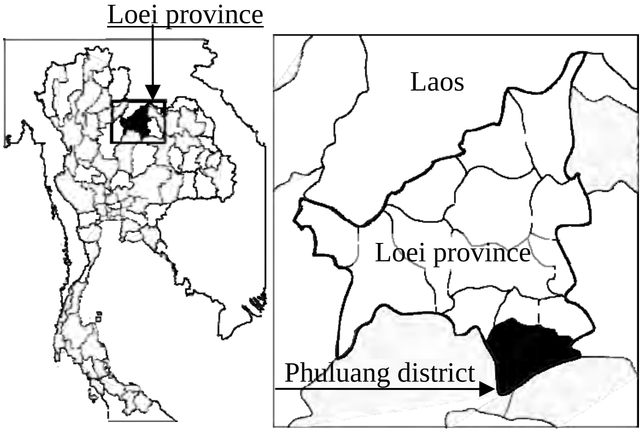

Figure 1: Study area

rain are the most major in this area, prompt communication is highly required.

2.2 Questionnaire survey

Questionnaire survey with villagers was conducted covering three villages. First two villages, Non Phattana (NP) and Loei Taw Tad (LTT), are designated as flood- and landslide-prone areas assigned by Department of Disaster Prevention and Mitigation (DDPM) Last one, Loei Wang Sai (LW), has a monitoring point of rainfall and water level of Loei River, a major River at the province, measured by a Mr. Warning, a volunteer trained by DDPM. The survey was started from April 6, 2011 for four days. Total of 300 questionnaires, 100 in each questionnaire, are corrected. Face-to-face interview method was adopted considering misconception due to low information literacy, and little penetration rate of a fixed-line phone, fax, and internet.

Furthermore, to make the result of the survey able to compare to the disaster awareness in Japan, the questionnaire was made referring to the one used in Annual national survey on disaster awareness conducted by the Center for Integrated Disaster Information Research (CIDIR), The University of Tokyo. The questionnaire therefore was made in Japanese firstly, and translated to English, and then lastly to Thai.

3. RESULT OF QUESTIONNAIRE SURVEY

3.1 Characteristics of the sample

Although respondents were chosen to be equally distributed in ages and gender to avoid bias of the sample's characteristics, male to female ratio resulted in two third since many males worked away from home for a long period. Majority of the respondents at 75% of the total are farmers: 64% and 11% of them are full- and part-time workers respectively (Figure 2). They are mainly growing rice and cash crops including cassava, and maze. Respondents tend to live with relatively larger family size made up of 55% of them who are living with more than five people (Figure 3).

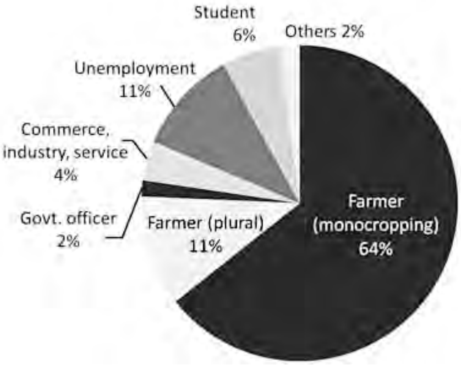

Figure 2: Occupation (N=300)

3.2 Awareness to disaster risk

3.2.1 Overall disasters

The question was made to figure out what type of matters respondents are worried in daily life. A result is shown in Figure 4 by classifying the degree of anxiousness into five levels. Respondents cited "Politics" and "Crime" as the least anxious matters. The sum of percentages of "Not at all" and "Somewhat" on each matter was 61% and 58% respectively. Meanwhile, the

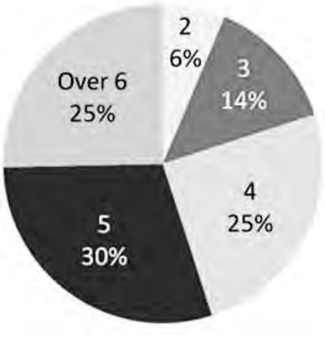

Figure 3: Family size (N=300)

percentage of “Natural disaster”, sum of “Very anxious” and “Anxious”, was 66%, the second-most anxious matter after “Market price of agricultural crops” of 78%. When score is given to each level of anxiousness (five to “Very anxious”, and one to “Not at all”), “Natural disaster” is 3.8. The value is almost equal to the one in Japan of 3.9, which was obtained by the “Annual national survey on disaster awareness” in 2011 with 3,000 samples.

A result of the same question in each type of “Natural disaster” is summarized in Figure 5. “Flood” was cited the most by the 67% of respondents as they feel very anxious followed by “Land slide” of 36%. The score of the “Flood”, 4.08, marked higher than the one of Japan of 3.17. On the other hand, “Earthquake” which marked higher score in Japan resulted in lower for villagers in Thailand.

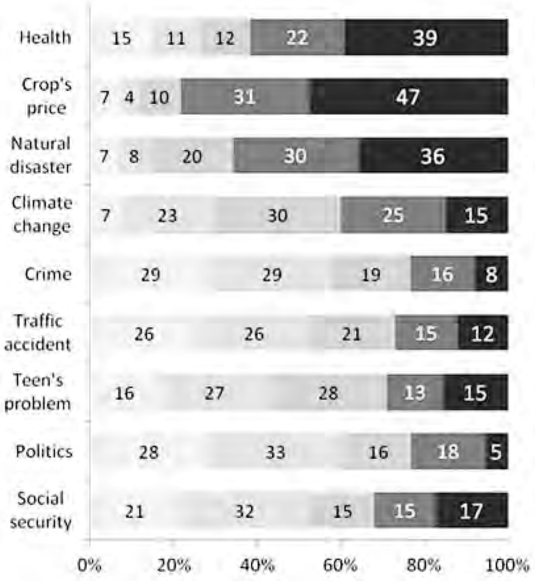

Figure 4: Awareness to issues (N=300)

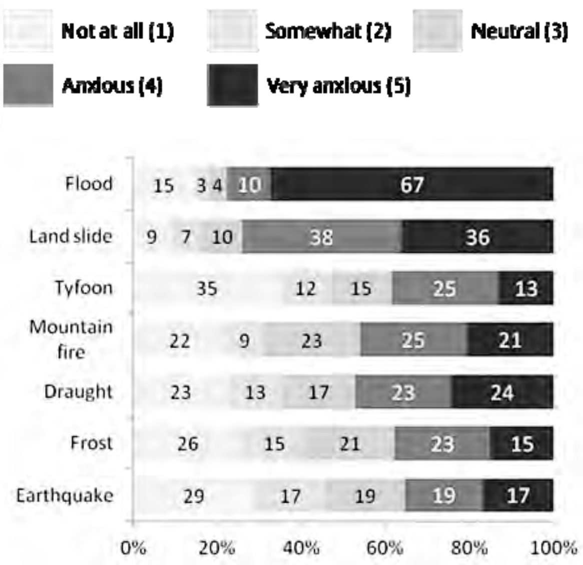

Figure 5: Awareness to disasters (N=300)

3.2.2 Flood

The result of a question, whether a river close to their homes, Loei River in this survey, is flood-prone or not, is summarized in Figure 6. 27% and 36% of respondents residing in NP and LTT village respectively cited “Strongly agree”. The percentages exceed 80% for both residents when the value of “Agree” is added while the percentage at LW village stays lower at 69%. These results would be correlated with an influence of respondents’ past disaster experiences; only 39% of respondents in LW had been affected by a flood disaster(s) yet those of NP and LTT were at 76% and 66% respectively. Figure 7 shows a comparison between the situations of flood damage that the respondents have actually affected, and

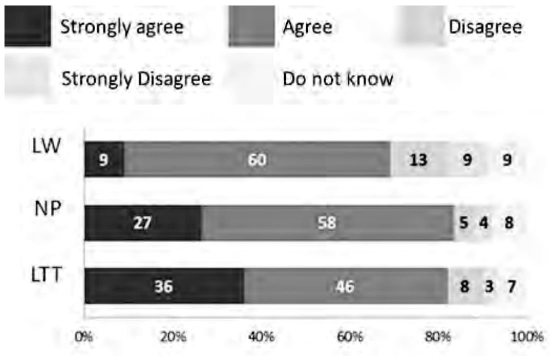

Figure 6: Awareness to flood (N=300)

weather they recognize the situation as flood damage or not. For past disaster experience, “Damage of agricultural crops” and “Damage of homes and belongings” were cited at higher rates by 35% and 32% respectively. It could be seen that the percentage of the respondents who recognize a situation as flood damage is lower than the one of those who actually experienced it. In other words, the respondents tend to recognize the situation that they have experienced as flood damage; e.g. out of 35% of respondents who had “Damage of agricultural crops”, 31%, approximately 80% of 35%, have faced same situation in the past. On the other hand, among the respondents who have never been damaged by flood, 98% of them cited “Do not know” for a situation that they recognize it as flood damage. Therefore, it would be appeared that respondents’ risk awareness depend on their past flood experience.

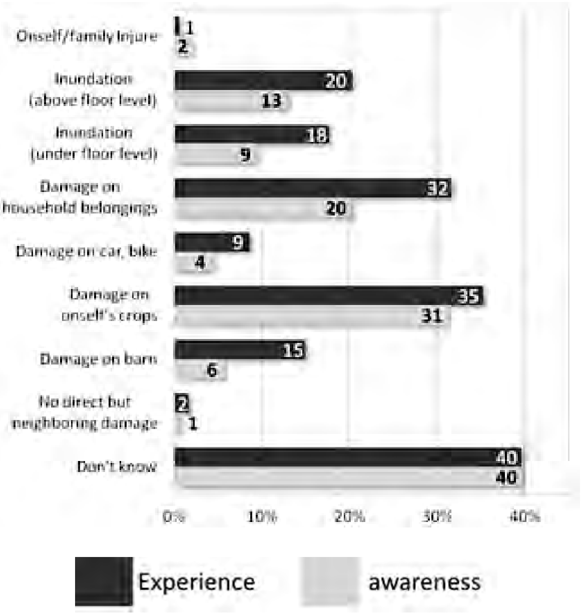

Figure 7: Disaster experiences and awareness (N=300)

3.3 Media for disaster information dissemination

For disaster information dissemination, media preferred by the respondents to be used is summarized in Table 1. Most-cited media was “Loudspeaker” at 91.3% followed by “Television” of 30%; the reason for the result would be because the speaker is used for announcements of their daily activities. On the other hand, mobile phone (SMS) was cited only at 0.7% of the respondents.

Table 1: Media preferred to receive disaster information (N=300)

Type of media	Percentage
Loudspeaker	91.3%
Television	30.0%
Radio	17.3%
Mobile phone (call)	4.3%
Internet	1.3%
Mobile phone (SMS)	0.7%
Direct contact (face-to-face)	0.7%

3.4 Mobile phone ownership rate

Understandably, mobile phone is required to receive SMS messages. Figure 8 shows mobile phone ownership rate of the respondents by age group. In this paper, phone is simply classified into two types for descriptive purposes: Smart phone which has internet accessibility, and

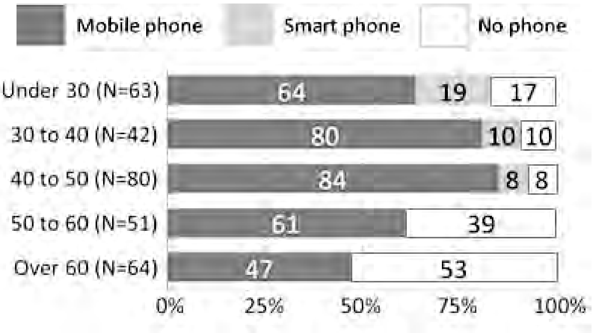

Figure 8: Mobile phone ownership rate (N=300)

mobile phone which doesn't. Age group of "from 40 to less than 50" has mobile phone the most at 84% followed by "from 30 to less than 40" of 80%. On the other hand, the rate is relatively low in the group of "50 to less than 60" and "more than 60" at 61% and 47% respectively. For the rate of smartphone, the younger age groups the higher ownership rate of smartphone: 8% at "from 40 to less than 50", 10% at "from 30 to less than 40", and 19% at the "less than 30".

3.5 Mobile phone reception

As same as the mobile phone ownership, strength of mobile phone reception should be known to ensure SMS message to be received properly. Since majority of respondents are farmers working at their farm land in day time, strength of mobile phone reception was asked for both at their homes and farm land. Since an antenna station is located near LW village and reception was fairly available at both places, 100% at home, and 74% at farm land are strong enough. Reception at both places is weak that 62% and 40% of respondents cited "No reception" at their home and farm land respectively.

3.6 Information propagation

It is known that the warning message has a diffusion effect that a person who received it would apprise others the content even to those who do not received the message (Ohara, 2012). Figure 9 shows the result by family size weather the respondents would apprise others the contents of SMS or not if they are assumed to be received the message. In every group, sum of "Family (oral)", and "Relatives, acquaintances, and friends (oral)" cited over 80%. "Others" cited by 98% of responses was village leader, and the smaller family sizes cited at the higher rate on him.

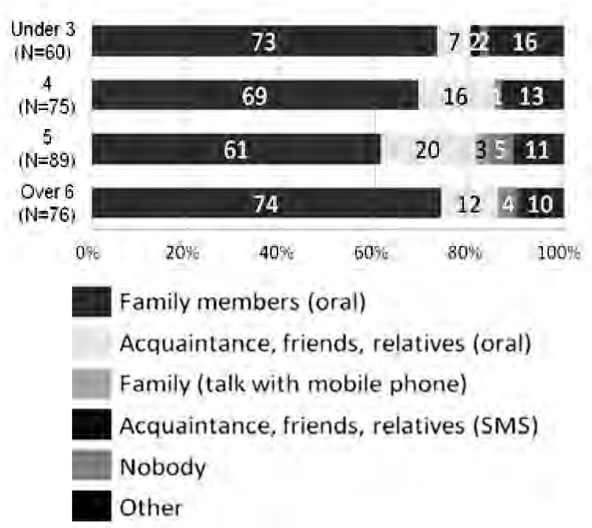

Figure 9: Information propagation by size of family (N=300)

4. DISASTER INFORAMTION DISSEMINATION BY SMS MESSAGE

4.1 SMS messaging to mass mobile phone users

There are two types of messaging services to deliver SMS message to mass mobile phone users: Service-Cell Broadcast (SMS-CB), which delivers multiple mobile phone users who are in specific area. Meanwhile, Bulk Messaging sends message to selected users by registering their mobile phone numbers in advance.

Currently, three leading mobile phone operators named Advance Info Service PLC (AIS), Total Access Communication PCL (dtac), and True Corporation PCL (TRUE) are providing the service to send SMS to multiple users; AIS and dtac provide both services whereas True provides only Bulk messaging. They target mainly to corporate purposes yet unfamiliar with public uses. SMS-CB is used for sending welcome and promotion messages and only available at limited places such as a conference center, and exhibition where an antenna is installed. Therefore, Bulk SMS would be useful for rural mountainous areas since it only requires internet access for use.

4.2 mobile phone use in remote areas

By National Broadband Policy enacted in November 2010, internet access has been developed preferentially to local government offices, schools, and important communities even in rural mountainous areas. Therefore, Bulk messaging service can be used technologically in those areas if a local government is assumed to take a role for dispatching SMS messages.

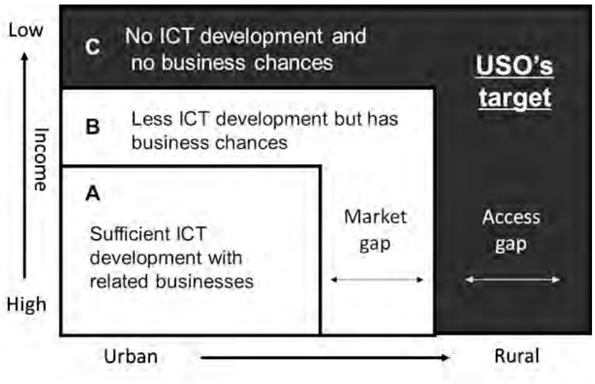
Low
Income
High
C No ICT development and no business chances
B Less ICT development but has business chances
A Sufficient ICT development with related businesses
Market gap
Access gap
USO's target
Urban
Rural

Figure 10: Target area of USO

Moreover, National Broadcasting and Telecommunications Commission (NBTC), regulatory and supervisory agency in broadcasting and Telecommunication sectors in Thailand, leads Universal Service Obligation (USO) that promotes communication services to remote areas where information access is limited (see Figure 10). Every telecommunications carrier who has acquired a business license from NBTC is required to accomplish for USO projects. The three leading carriers have acquired the license in use of 2.1GHz frequency at the same time on December 2012 from NBTC and been able to receive a support from USO fund for their projects. Although NBTC is conditioning the project such as how to examining a way of monitoring assessment and competitive bidding system, there is a high possibility in the future that USO projects would expand mobile phone service area to where a reception is currently not available.

5. DISSCUSSION

It would appear that SMS has high potential to be a mean for disaster information dissemination at rural mountainous areas in Thailand as number of subscribers and service area of mobile phone increase. Although, communication infrastructures of internet access have been developing and Bulk SMS is technologically available, its introduction to the public should be taken into account carefully.

At the time of 2011 Thai Great Flooding, Flood Relief Operations Center (FROC) announced disaster information to public starting from 11th Oct. 2011 through SMS services asking all mobile phone operators. However the attempt had been faced opposition from the public and stopped 23th of the month with only four SMS messages in total. Feedbacks were “useless”, “not functioning as early warning”, and so forth. The contents had less sense of emergency such as calling for volunteer and operating report.

On the other hand, current information dissemination system in rural mountainous areas uses mainly loudspeaker. If that is unusable due to blackout, handy siren will be used instead. Therefore, there is a challenge that disaster information would not be transferred clearly, or reached to villagers in a worse situation because the information is sound-based and gets radio disturbance with heavy rain. In addition, majority of houses are corrugated-roofed which creates intense noise when it's pelted by heavy rain.

SMS is a text-based feature that can redeem loudspeaker and strengthen the current system of the rural mountainous areas to warm the public. Positive results from the questionnaire survey were also obtained that ownership rate and service area of mobile phone would be increasing in the future. Moreover, we found that villagers tend to transfer information obtained from SMS to others, especially family members, even to those who do not receive the message. However, as villagers preferred loud speaker rather than SMS to obtain disaster information, usefulness and effectiveness of the SMS should be demonstrated to prove an actual effectiveness of the SMS to be introduced into current disaster information system of rural mountainous areas.

6. CONCLUSION

Characteristic of Thai is generally considered as they do not worry about risk of flood disaster referred to as being “Sabai” and little research figures degree of the anxiousness. In other words, even if the SMS system is possible to be installed, it would not be socially utilized, or not accepted in the worth case, by local people in the areas. However, this research clarified that they concern flood damage seriously if there is a threat that their agricultural crops get damaged. Furthermore, it could be seen that SMS has possibility to strengthen current disaster information dissemination system, sound-based using loudspeaker and siren, at rural mountainous areas by multiplexing channel of communication and information representation. To examine further possibility of the SMS introduction, actual experiment sending SMS to observe whether the message is spread and propagate among villagers.

REFERENCES

International Telecommunication Union, ICT STATISTICS, http://www.itu.int/en/ITU-D/Statistics/Pages/default.aspx.

The World Bank, Mobile cellular subscriptions (per 100 people).
http://data.worldbank.org/indicator/IT.CEL.SETS.P2

The Center for Integrated Disaster Information Research (CIDIR), The University of Tokyo, 2011. Annual national survey on disaster awareness.

Kawasaki, A., Kondou, S., Ohara, M., Komori, D., Kodaka, A., Kaewmoracharoen, M., Shrestha, S., Ninsawat, S., and Sunthararuk, A., 2013. Disaster information dissemination system in rural and agricultural mountainous area in Thailand Part 1 - Project outline-. *Seisan Kenkyu* 64, 505-508.

Ohara, M., Kawasaki, A., Kondo, S., and Tanaka, A., 2012. A Survey on Information Dissemination by Area-mail during Storm Disaster due to Typhoon Talas in September 2011-Quick Report on Survey in Miki-cho, Kagawa Prefecture. *Seisan Kenkyu* 64, 553-556.

Repair prioritization of reinforced concrete superstructures in mooring facilities

Takuho TANI[1], Hiroshi YOKOTA[2], Katsufumi HASHIMOTO[3]
and Kohichi FURUYA[4]
[1]Master's course student, Faculty of Engineering, Hokkaido University, Japan
tanitakuho@eng.hokudai.ac.jp
[2]Professor, Faculty of Engineering, Hokkaido University, Japan
[3]Assistant Professor, Faculty of Engineering, Hokkaido University, Japan
[4]Bureau of Construction, Tokyo metropolitan government, Japan
[5]Institute of Construction Management, Service Center of Port Engineering, Tokyo, Japan

ABSTRACT

In Japan, since many concrete structures were constructed in 1960s, the number of concrete structures with severe deterioration has been increasing. Although huge budgets are usually required to repair such deteriorated structures, budgetary restrictions are generally imposed. Therefore, this study discussed the prioritization on repair procedure to repair deteriorated structures based on the net present values (NPV). There are few studies for effective prioritization of harbor concrete structures. In this study, five superstructures of mooring facilities are focused on as a model case and their prioritization procedures are evaluated. In this study, deterioration progress of superstructures in mooring facility was simulated by using the Markov-chain process. Transition probabilities in the process were obtained with using the Monte Carlo simulation. After simulating the deterioration, the NPVs of each facility in the planned service life (50 years) were calculated from repair costs and benefits under budgetary restrictions. As the results, the NPV increased as annual budgets increase in spite of combination of repair scenarios, and the increase in annual budgets reduced the dispersion of NPV in the scenarios*. In addition, the more NPV was expected for the facility having higher benefit under a preventive maintenance strategy was set at the higher repair prioritization.*

Keywords: maintenance strategy, mooring facilities, NPV, prioritization, budgetary restriction

1. INTRODUCTION

In Japan, the number of infrastructures has been built in 1960s. It is essential to establish lifecycle management strategies in order to ensure performance of an existing structure. Although huge budgets are usually required to repair such deteriorated structures, budgetary restrictions are generally imposed. Therefore, it is difficult to repair all infrastructures in a short period.

Considering this situation, there is a need for the efficient and effective maintenance strategy to decrease the cost for repair and replace. Conventionally, the maintenance strategy that determined the prioritization procedure of repair by only deterioration condition is usually used. However, when there are budgetary restrictions, so it is out of order that repair the facility that having low benefits. It is required to establish the maintenance strategy considering the repair costs and benefits. Concrete is used for infrastructures commonly, and there are many researches that focuses on the prioritization procedure of repair for concrete structures. However, there are few researches that have focused on the prioritization procedure of repair for port facilities. Long-term performance of port facilities are affected by environments such as wave, chlorides and so on. Therefore, this study discusses the prioritization procedure of repair and most efficient annual budget based on the net present value (*NPV*). Five mooring facilities were investigated in this study as a model case and their prioritization procedure and annual budget were evaluated.

2. OUTLINE

2.1 Data of facilities subject to this study

In this study, five mooring facilities (W1~W5) in Y port were focused on as a model case. Y port plays an important role in Japan. Table 1 shows the data of facilities subjected to this study.

Table 1: Data of target facilities

		W1	W2	W3	W4	W5
Constructed year		1988	1981	1976	1994	2005
Structural type		Open-pile	Open-pile	Open-pile	Open-pile	Open-pile
Depth (m)		14	12	12	12	14
Length (m)		280	240	240	300	330
Number of members (beam & slab)		966	732	626	1010	-
Elapsed year from survey		17	24	28	16	-
Proportion of probability	*d*	0.64	0.67	0.70	0.88	-
	c	0.34	0.28	0.30	0.04	-
	b	0.01	0.05	0.00	0.00	-
	a	0.00	0.00	0.00	0.08	-
Start *DP*		1.63	1.52	1.48	1.09	-

2.2 Deterioration prediction

Deterioration progress of mooring facilities was predicted by using the Markov-chain model in this study. A Markov process is a random process to simulate the present state, in which the future states are independent of the past. A Markov chain is a process that consists of a finite number of states and the transition probabilities P_x, where P_x is the probability of moving from the state to other state. Furthermore, it is assumed that infrastructure assets can deteriorate only one state at a time. For simplicity, the transition probability in this study is assumed to be identical in each state (Kato et al. 2009).

The Markov-chain model is represented in Equation 1. Once the transition probability is determined, the deterioration progress can be simulated at any elapsed year *t*.

$$\begin{pmatrix} d \\ c \\ b \\ a \end{pmatrix} = \begin{pmatrix} 1-P_x & 0 & 0 & 0 \\ P_x & 1-P_x & 0 & 0 \\ 0 & P_x & 1-P_x & 0 \\ 0 & 0 & P_x & 1 \end{pmatrix}^t \begin{pmatrix} 1 \\ 0 \\ 0 \\ 0 \end{pmatrix} \tag{1}$$

Where *d~a* are the proportions of probability remaining in respective grades, P_x is the transition probability and *t* is the elapsed year.

The deterioration point (*DP*) is defined to describe the overall degree of deterioration. DP can be calculated by using Equation 2 in which factors of 4, 3, 2, and 1 are taken for weighting the grade of condition. Those factors are temporarily determined because the constant transition probability is applied in every Markov chains and required further investigation in the future.

$$DP = 4\times a + 3\times b + 2\times c + 1\times d \tag{2}$$

Where *d~a* are the proportions of probability remaining in respective grades and *DP* is the overall condition grade that is a discrete index (1.0~4.0).

2.3 Setting the transition probability (P_x)

In this study, the probability density function was used for predicting the deterioration progress because of accurate transition probabilities (P_x) of Y port's facilities were unknown. The probability density function was got from the investigation for 56 open-piled marginal wharves in Japan, and the distributions of transition probabilities conform with the log-normal distribution for open-piled marginal wharves (Furuya et al. 2011). Figure 1 shows the distribution and its parameters. P_x was taken from the distribution by using the Mersenne Twister (Matsumoto and Nishimura 1998) for predicting the deterioration progress.

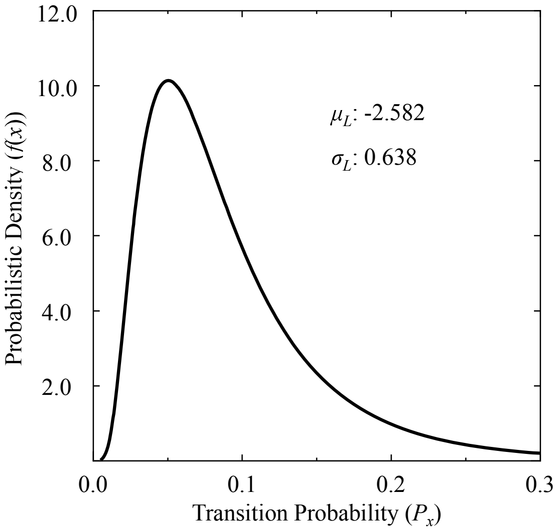

Figure 1: Probability density function, *f*(*x*) and its parameters

2.4 Calculation method of repair costs

Repair methods were set by considering the deterioration condition. Based on the *DP*, number of repairs and unit prices of each repair method according to repair costs of each facility were calculated. 3 types were set for repair methods, preventive maintenance (Type P), corrective maintenance (Type C1~C4), and replacement (Type R). Table 2 shows the number of repair percentage of concrete surface area for each facility and range of *DP* which is suitable for each repair method.

Table 2: Repair method and range of *DP*

Type		Repair method	Range of *DP*
P	Preventive maintenance	Surface coating (100%)	$1.7 \le DP < 2.0$
C1	Corrective maintenance	Patch repair (small: 80%) +Surface coating (100%)	$2.0 \le DP < 2.3$
C2		Patch repair (small: 60%, large: 20%) +Surface coating (100%)	$2.3 \le DP < 2.6$
C3		Patch repair (small: 20%, large: 60%) +Surface coating (100%)	$2.6 \le DP < 3.0$
C4		Patch repair (large: 80%) +Surface coating (100%)	$3.0 \le DP < 3.5$
R	Replacement	Replacement	$3.5 \le DP \le 4.0$

Surface coating is taken place overall concrete surface of facility as preventive maintenance (Type P). Surface coating prevents chloride penetration which causes rebar corrosion, therefore this method should be applied before the rebar corrosion starts. In terms of the material deterioration mechanism, range of *DP* for preventive maintenance was set at $1.7 \le DP < 2.0$. It is assumed that if surface coating is taken place at first time in the planned service life (50 years), transition probability becomes the half (Yamaji et al. 2004).

Patch repair and surface coating are taken place as corrective maintenance (Type C1~C4). Range of *DP* for corrective maintenance was set at $2.0 \le DP < 3.5$. However, deterioration condition depends on the proportions of deteriorated members. Consequently, in this study, 4 repair methods (C1~C4) were set for corrective maintenance. Each method was different from number of repair percentage as shown Table 2.

Replacement is taken place when value of *DP* is $3.5 \le DP \le 4.0$.

Table 3and 4 show the unit price for each repair method and concrete surface area & volume of each facility. In this study, repair costs were calculated from the unit price and concrete surface area or volume.

Table 3: Unit price of repair

Repair method		**Unit**	**Unit price (Yen)** **Slab & Beam**
Preventive maintenance	Surface coating	$/m^2$	15,000
	Temporary structure fee		9,000
Corrective maintenance	Surface coating		13,500
	Temporary structure fee		9,000
	Patch repair (small)		75,000
	Patch repair (large)		115,000
Replacement	Replacement	$/m^3$	300,000

Table 4: Concrete area and volume

	W1	**W2**	**W3**	**W4**	**W5**
Area (m^2)	6,912	7,364	8,021	8,664	17,568
Volume (m^3)	2,482	2,731	2,149	3,748	12,730

2.5 Calculation method of benefits

Benefits of each facility were estimated by given step. Figure 2 shows the schema of benefit calculation method. In this study, benefits were calculated only by considering the effect of cost for transportation (land transportation, sea transportation and transit time). Delivery area, transportation course and overseas port were set from type and amount of cargo for each facility. Transportation costs were calculated in two cases, which one is the case that the facilities in Y port are used and the other is the case that the alternate port's facilities are used. Finally, benefits were calculated from the difference from transportation costs between the cases.

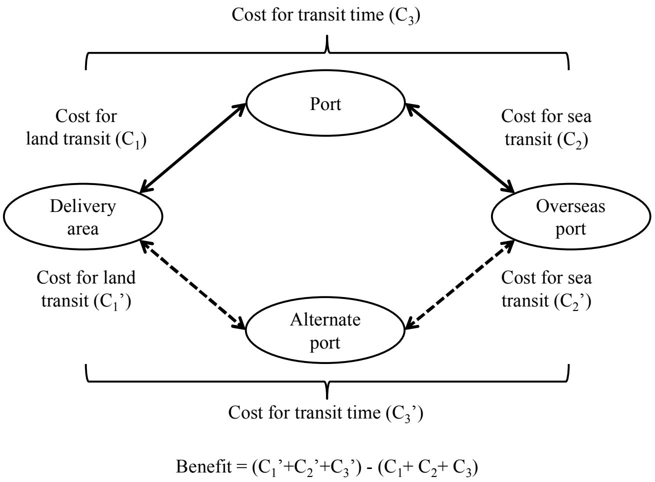
Cost for transit time (C_3)
Port
Cost for land transit (C_1)
Cost for sea transit (C_2)
Delivery area
Overseas port
Cost for land transit (C_1')
Cost for sea transit (C_2')
Alternate port
Cost for transit time (C_3')
Benefit = (C_1'+C_2'+C_3') - (C_1+ C_2+ C_3)

Figure 2: Schema of benefit calculation

3. DETERMINATION METHOD OF PRIORITIZATION PROCEDURE BY USING THE *NPV*

3.1 Calculation method of *NPV*

The *NPV* of each facility in the planned service life (50 years) was calculated from the repair costs and the benefit by using Equation 3.

$$NPV = \sum_{n=1}^{50} \frac{B_n - C_n}{(1+r)^n} \tag{3}$$

Where n is the elapsed year, B_n is the benefit at n-th year, C_n is the cost at n-th year and r is the social discount rate (4% in this study).

Basically, it is assumed that facilities are repaired by using preventive maintenance method, which means that facilities are repaired at *DP*=1.7 because it is supposed that the repair costs are increased when corrective maintenance method or replacement is applied. However, it is assumed in this study that the facility which has the higher priority is repaired earlier if the repair of some facilities are coincidental. In addition, it is presumed that no benefit can be expected during $DP \geqq 3.0$.

3.2 Budgetary restriction, repair scenario and benefit during the repair

It is assumed that there are annual budgetary restrictions (0.05, 0.1, 0.15, 0.2, 0.25, 0.3, 0.35 and 0.4 billion yen in this study). Therefore, repair may not be completed in one year. Repair scenarios were set every conceivable pattern. In this study, 5 facilities were focused, where 120 (=5!) scenarios were considered. *NPV* was calculated in all scenarios. It is assumed that the benefits are reduced during the repair period and the reduction depends on the repair method. In this study, 0%, 30%, 50% and 70% reduction with Type P, C1, C2 and C3 are presumed, respectively. No benefit can be expected during the repair with Type C4 and R.

3.3 Calculation method of *NPV* by using the Monte Carlo Simulation

The *NPV* was calculated by using the transition probability (P_x) which is resampled in the distribution 1,000 times under the condition shown in Figure 1. *DP* in first year is estimated by using the result of the visual inspection (Table 1). The most efficient and effective repair scenario was investigated by comparing the *NPV*s in all scenarios. In addition, the most suitable annual budget can be estimated by calculating the *NPV* under the some annual budgets.

4. RESULTS OF CALCULATION FOR REPAIR COSTS AND BENEFIT

Table 5 lists the results of calculation for repair costs of each facility. In this study, unit price is the same in all facilities, therefore repair costs depend on the concrete surface area or volume. Comparing Table 4 and 5, the repair cost of larger facility is higher. Especially, W5 is the largest facility in all facilities, and the repair cost of W5 is highest of all facilities. In addition, the repair cost of Type R was the highest of all repair methods at W4 and W5. However, the repair cost of Type C4 is the highest of all facilities at W1, W2 and W3. The Type with the highest cost of all repair methods is different in each facility because calculation method parameters are different. The repair costs of Type P, C1, C2, C3 and C4 depend on the concrete surface area of each facility, but that of Type R depends on the concrete volume of each facility.

Table 6 lists the type of cargo, cargo volume per year and benefit of each facility. From the table, the cargo volume of W1 is the largest of all facilities and the cargo volume of W2 is the smallest of all facilities. Similarly, the benefit of W1 is the largest of all facilities and the benefit of W2 is the smallest of all facilities. However, the cargo volume of W3 is larger than that of W4 and W5, and the benefit of W3 is smaller than that of W4 and W5 due to the difference of transportation method. It was assumed that the cargo of W3 is transported by using trailer, while the cargo of W4 and W5 is transported by using container. The transportation cost using trailer is lower than the transportation cost using container. As the result, the transportation cost of W3 and the difference between the cases became small.

Table 5: Repair costs (billion yen)

	W1	**W2**	**W3**	**W4**	**W5**
P	0.17	0.18	0.19	0.21	0.42
C1	0.57	0.61	0.66	0.1	1.45
C2	0.63	0.67	0.73	0.78	1.59
C3	0.74	0.78	0.85	0.92	1.87
C4	0.79	0.84	0.92	0.99	2.01
R	0.74	0.82	0.64	1.12	3.82

Table 6: Type of cargo, cargo volume and benefit

	W1	**W2**	**W3**	**W4**	**W5**
Type of cargo	Coal	Coil	Cars	Containers	Containers
Cargo volume per year (thousand ton)	2,774	175	1,329	1,230	1,274
Benefit per year (billion yen)	5.74	0.18	0.75	2.82	4.12

5. INFLUENCES OF ANNUAL BUDGET ON THE *NPV*

Figure 3 shows the average and variation coefficient of *NPV* which were calculated in all repair scenarios under any annual budgets. Scenarios were classified as follows: the scenario which W1 is the highest priority was classified into Group 1. Similarly, the scenario which W5 is the highest priority was classified into Group 5. Also, the average of *NPV* in the Group is shown in Figure 3, where the average of *NPV* increases as that of the annual budget. The average *NPV* when the annual budget is 0.4 billion yen is 286 billion yen. This value is 41 billion yen larger than the average *NPV* when annual budget is 0.05 billion yen. It is observed that there are large reductions of benefit in the cases where annual budgets are small because repairing period becomes long as decrease of the annual budget. In addition, the repair costs are decreased as increase of the annual budget because preventive maintenance can be applied to the repair of facilities. Furthermore, variation coefficient of *NPV* decreases as increase of the annual budget. It means that average *NPV* varies widely in the cases where annual budgets are small. This trend is noticeable when annual budget 0.05, 0.1 and 0.15 billion yen, where variation coefficients are 0.044, 0.027 and 0.022, respectively. In cases where annual budgets are small, the facilities which have low priority cannot be repaired. Thus, no benefit can be expected from such facilities. Consequently, there is a difference between each scenario. On the other hand, usual benefit can be expected in cases where annual budgets are large because repair period tends to be short. Variation coefficient becomes less than 0.015 in all cases when annual budgets are more than 0.2 billion yen.

In each group of the Figure 3, the average of *NPV* varies widely in the cases where annual budgets are small. Especially, the difference between maximum and minimum value of average *NPV* in each Group is 10 billion yen when annual budget is 0.05 billion yen. The difference between maximum and minimum value of average *NPV* in each Group decreases as an increase the annual budget.

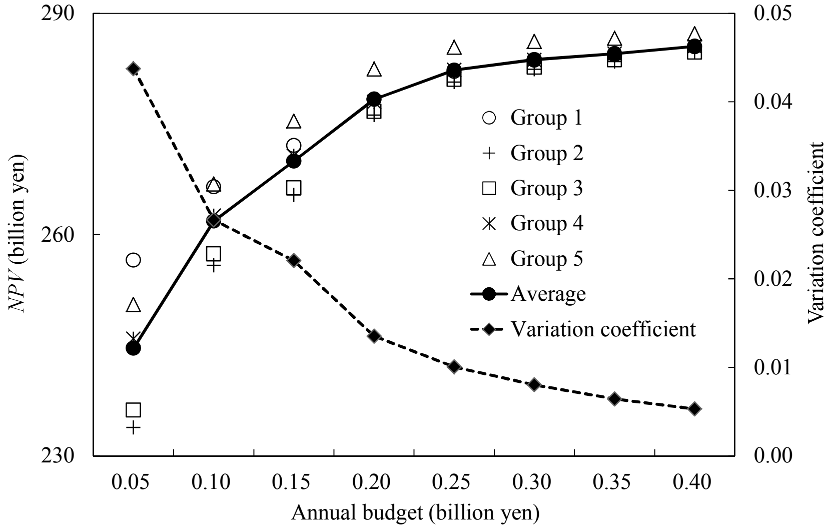

Figure 3: Average and variation coefficient of *NPV*

6. MOST EFFICIENT REPAIR PRIORITIZATION PROCEDURE

Figure 4 shows the average *NPV* in each Group for each annual budget. The average *NPV* of Group 1 is the largest of all Groups when annual budget is 0.05 billion yen and the average *NPV* of Group 5 is the largest of all Groups when annual budget is more than 0.1 billion yen. Group 1 and Group 5 are the groups that W1 and W5 have the highest priority. From the table 6, W1 is the largest benefit of all facilities and W5 is the second largest benefit of all facilities. In addition, the average *NPV* of Group 2 is the smallest of all Groups. When the preventive maintenance is applied, high priority facility can be repaired at an early time and no loss of benefit is expected during the planned service life. Therefore, it is estimated that average *NPV* becomes high in cases where the facility with large benefit has high priority.

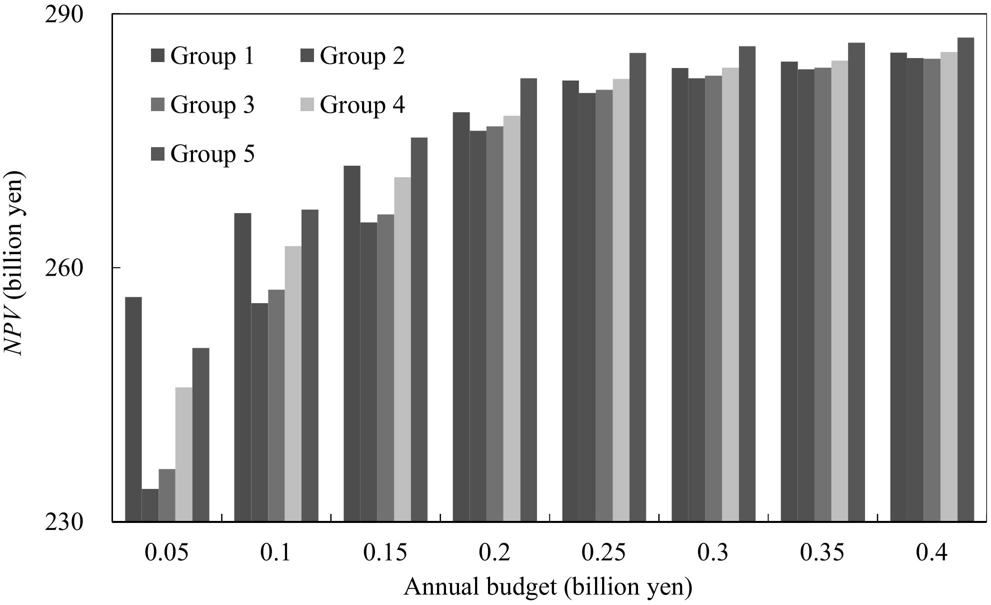

Figure 4: Average *NPV* in same Groups

7. CONCLUSIONS

The following conclusions are drawn in this paper.

1) Repair scenario should be carefully assessed because average *NPV* varies widely in the cases where annual budgets are small.
2) When any facilities are under maintenance, the preventive maintenance should be applied to the facility with the largest priority during the planned service life.
3) Average *NPV* tends to become larger in the scenario that the facility with larger benefit is on high priority at any annual budget.

8. ACKNOWLEDGMENT

The authors would like to express their appreciations to port office, Mr Hirinao Takahashi during the calculation of benefit. Also, the authors would like to express their appreciations to Shinichiro Miyai and Takeshi Hyodo, Institute of Construction Management, Service Center of Port Engineering for his help during the calculation of *NPV*.

REFERENCES

Kato, E., Iwanami, M. and Yokota, H., 2009. *Development of life cycle management system for open-type wharf*. Report of the Port and Airport Research Institute 48.

Furuya, K., Yokota, H., Hashimoto, K. and Hanada, S., 2011. *Reliability of Deterioration Based on Markov Model for Mooring Facilities*. Journal of Japan Society of Civil Engineers, Ser. F4 Vol.67, I_159-I_168.

Matsumoto, M. and Nishimura, T., 1998. Mersenne Twister: a 623-dimensionally equidistributed uniform pseudorandom number generator. *ACM transactions on modeling and computer simulation* 8, 3-30

Yamaji, T, Komure, K. and Hamada, H., 2004. *Durability of 15-years Old Concrete Specimens with Surface Coating under Marine Environments*. Report of the Port and Airport Research Institute 43.

An investigation on the influence of some parameters in simulation of chloride ion penetration in concrete based on truss network model

Punyawut JIRADILOK [1] and Kohei NAGAI [2]
[1] Master course student, Department of Civil Engineering
The University of Tokyo, Japan
[2] Associate Professor, International Center for Urban Safety Engineering
Institute of Industrial Science, The University of Tokyo, Japan

ABSTRACT

Many reinforced concrete structures are exposed to the marine environments which result in chloride ion penetration, subsequently decreasing in structural capacity due to a corrosion of steel. Therefore, an estimation of chloride ion penetration in concrete is important for maintenance of the structures. This study aims to verify the accuracy of chloride penetration simulation under saturated condition. In this study, a truss network which represents the chloride penetration is introduced based on Fick's 2nd law. The chloride penetration profiles are varied due to the influent parameters, for example, length or cross section area which converted from effective area of truss element. The effect of related parameters, namely, element meshing size, time step interval, influence of dimensions and spatial element arrangement, are investigated on the numerical simulation by varying each parameter under control condition. Mesoscale modelling of the chloride diffusion in single crack are then simulated to verify the applicability for future study, i.e., the application with chloride diffusion in crack concrete based on RBSM model. The study discusses about the optimum setting and influence for each parameter in chloride penetration profiles prediction, which would be beneficial for the future study of the chloride diffusion simulation.

Keywords: chloride ion penetration, truss network model, crack width, Fick's 2nd law

1. INTRODUCTION

Nowadays, There are many reinforced concrete infrastructures which exposed to the marine environment, these lead to the deterioration of the structure. The main reason is chloride ion ingression causes the corrosion of reinforcing steel. Therefore, a precise prediction of chloride ingession profiles is crucially benefited to the maintenance and renovation of the structures. Presently, studies on the chloride diffusion in concrete gains a lot of attention in the research community. A number of studies tried to simulate the chloride ion ingress into concrete by system of truss element model with governing equation developed from Fick's 2nd law, namely, a study done by Nakamura (2006) or Wang and Ueda (20011) and so on. However, each inputted parameters, like element size or time step interval, are various in each studies, and the effect of those parameter are not clarify yet. Hence, in this study, we want to verify the influent of each parameter that related in Fick's 2^{nd} law. The numerical simulation based on truss network model and governing equation based on Fick's 2^{nd} law are carried out to predict chloride ion penetration profile. 1D and 2D meso-scale truss model with varying in influent parameters are proposed. Several parameters relating to the accuracy of chloride penetration prediction are investigated. Further, the simulation with single crack is done to study the applicability of combining the truss network for chloride ingression with the RBSM model (Nagai et al., 2004) that can well simulate the crack pattern of concrete structure under the real working load condition in the future.

2. SIMULATION MODEL

2.1. Truss network model

In this chloride penetration simulation meso-scale model, concrete is treated as a heterogeneous material. Specimen is meshed into meso-scale element having average sizes from 0.5×0.5 mm^2 to 15.0×15.0 mm^2 as an input value to see the effect of meshing scale. The element center is spatially random in square grid of element size. The chloride transportation is represented by assembly of one dimension pipe element system which assembles into truss network. The chloride ingress in concrete is presented by concentration at element nodes which linked together with the truss network that have coefficient depend on phase and length between nodes it's linked. The initial condition and boundary condition is set to simulate the behavior of concrete exposed to the chloride environment which focusing on the time dependent diffusivity. By setting of the element size, number of elements in X, Y direction and boundary condition, the simulation in both one dimension and two dimensions can be done. (Figure 1) In two dimension model, a node is randomly allocated in square grid of inputted element size using random number generator. Then, truss network is generated to link a node with it adjacent node for simulating the path of chloride ion transportation. (Figure 1(b))

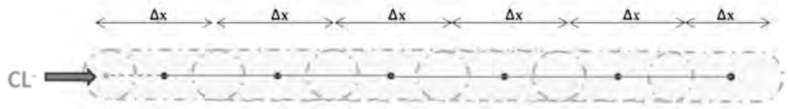

(a) Truss model in one dimension

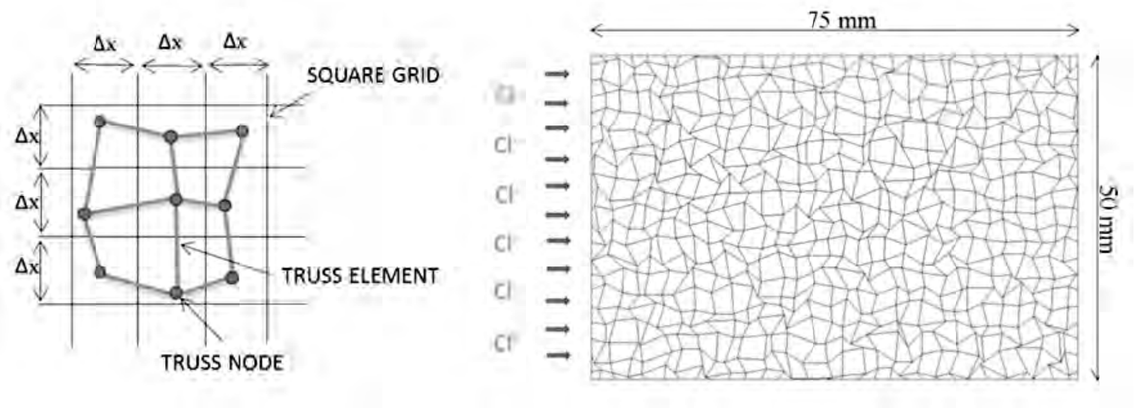

(b). Setting of truss system (c) Truss network in two dimension

Figure 1: Truss model in one and two dimensions

2.2 Chloride diffusion model and governing equation

In this model, the scope of study is limited to case of water saturation only. Hence, the convection or capillary suction transportation from different moisture content is not considered. The chloride ion transportation is simulated to move through "pipe" system that linked from node to node. The assembly of the truss system governing by Fick 2^{nd} law (Poulsen E, Mejlbro L,2006) is applied for the whole domain.

$$\frac{\partial C}{\partial t} = D\frac{\partial^2 C}{\partial x^2} \tag{1}$$

Here, C is the chloride content, t time, D the chloride diffusion coefficient, and x the spatial coordinate.

For this kind of Fick's 2^{nd} law problem, the boundary conditions and initial condition are usually set as $C(0,t) = C_s$ (constant) and $C(x, t_0) = 0$ when t_0 is initial time.
By using the Galerkin approach (RW. Lewis, P. Nithiarasu, KN. Seetharamu, 2004), Fick 2^{nd} law is converted into the following system of linear equation and applies to the whole domain.

$$\mathrm{M}\frac{\partial \mathrm{C}}{\partial \mathrm{t}} + \mathrm{KC} = \mathrm{f} \tag{2}$$

where, M is the element mass matrix, K the element diffusion matrix, and f the forcing vector. The $\frac{\partial C}{\partial t}$ indicates a time derivative. In this simulation, the forcing vector representing the chloride flow outward the specimen boundary are set to be zero, which mean no flux boundary conditions. The mass matrix and diffusion matrix is expressed as following:

$$\mathrm{M}=\frac{AL}{6\omega}\begin{bmatrix}2 & 1\\1 & 2\end{bmatrix},\ K = \frac{AD}{L}\begin{bmatrix}1 & -1\\-1 & 1\end{bmatrix} \tag{3}$$

Here, L is the element length, A element cross sectional area, and D is diffusion coefficient, which is set to be $1.971\mathrm{x}10^{-2}$ mm^2/h for concrete, as proposed by Oh and Jang(2004). ω is a correction parameter for conversion the volume of element to volume of truss element due to the overlap area of adjacent truss element. Considering mass transfer to several directions from one node, there are overlap zone of calculated truss area. (Figure 2)

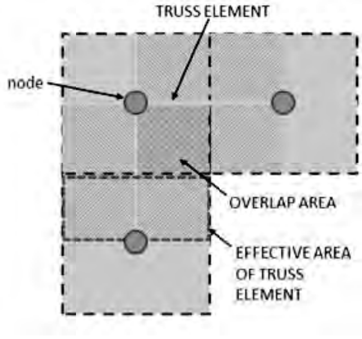

Figure 2: Definition of overlap area

The parameter ω is used to correct the errors in calculation of volume of truss element from the volume of voronoi cell, due to the overlap area of adjacent element. It is expressed as (Nakamura et al., 2006):

$$\omega = \frac{\sum_{i=1}^{n} A_i L_i}{V_{real}} \tag{4}$$

Where i= element number, n= total number of elements, A_i =effective area of each truss, L_i = length of each truss element and V= volume of the structure. Therefore, ω is set to 1 and 2 for one dimension and two dimensions respectively.

For estimating the value of chloride concentration depending on time, the implicit method, Crank Nicolson approach, is adopted. The above system is converted into the following matrix form.

$$\left(M + \frac{1}{2}\Delta t K\right) C^{t+1} = \left(M - \frac{1}{2}\Delta t K\right) C^{t} \tag{5}$$

$$\begin{bmatrix} \frac{2AL}{6\omega} + \frac{\Delta t DA}{2L} & \frac{AL}{6\omega} - \frac{\Delta t DA}{2L} \\ \frac{AL}{6\omega} - \frac{\Delta t DA}{2L} & \frac{2AL}{6\omega} + \frac{\Delta t DA}{2L} \end{bmatrix} \begin{bmatrix} C_i^{t+1} \\ C_J^{t+1} \end{bmatrix} = \begin{bmatrix} \frac{2AL}{6\omega} - \frac{\Delta t DA}{2L} & \frac{AL}{6\omega} + \frac{\Delta t DA}{2L} \\ \frac{AL}{6\omega} + \frac{\Delta t DA}{2L} & \frac{2AL}{6\omega} - \frac{\Delta t DA}{2L} \end{bmatrix} \begin{bmatrix} C_i^{t} \\ C_J^{t} \end{bmatrix} \tag{6}$$

where Δt is the time step interval, C^{t+1} is chloride concentration at next time step. Then, by solving the set of above equation, the chloride ingression profiles depending on the time parameter can be obtained.

2.3 Analytical solution of Fick's 2nd law in error function form

To predict the chloride ingression with focusing on time dependent diffusivity and set boundary condition

By using the error function solution to Fick's 2nd law, Equation.1 can be converted to the following form, which can predict chloride concentration in term of penetration distance and time dependent(Jens Mejer Frederiksen et al.,2008).

$$\mathrm{C(x,t)} = C_s\left[1 - erf\left(\frac{x}{\sqrt{4D_c t}}\right)\right] \tag{7}$$

where *Cs* = chloride concentration at surface, *x* = distance from exposed surface, D_c = chloride diffusion coefficient and *t*= time.

The equation 7 is appropriate for check the chloride ion penetration in cementitious material by varying the diffusion coefficient as the materials. However, in the real structure which concrete has cracks from the working load, only this equation is not enough to predict the chloride ion penetration.

3. SIMULATION RESULTS

3.1 Comparison the simulations results with the analytical solution of Fick's 2nd law

In order to verify the simulation model from Equation 5, the Equation 7 was used to comparing the results. The simulations which set similar condition in 1dimension and 2 dimensions are performed. The simulation conditions are set as following. The average truss element length is 2.5mm. The diffusion coefficient is set to be 0.01971 mm^2/hour. The time step interval is 1 hour per step. Chloride concentration at surface is 5×10^{-3} g/ cm^2 Total time of penetration is 52 weeks. ω are set to be 1 in one dimension and 2 in two dimensions. The results of the simulations are shown in following figure.

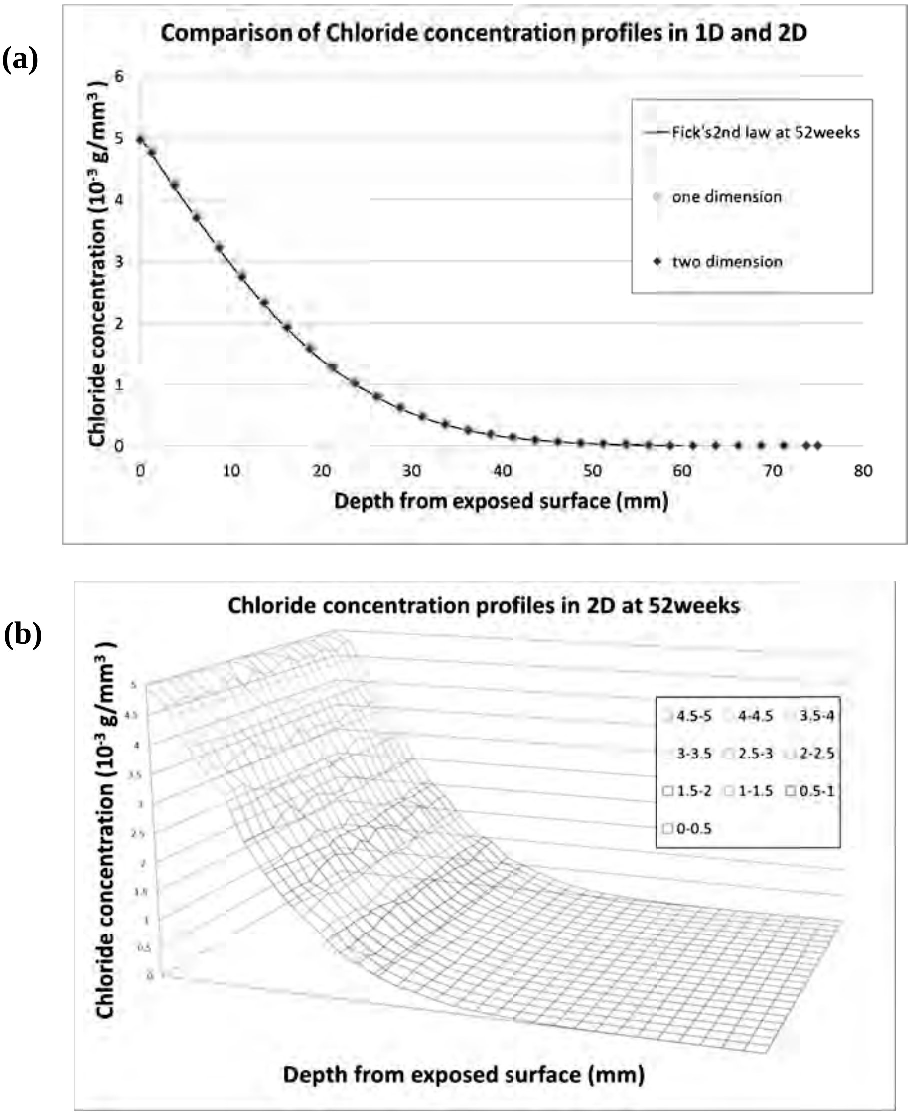

Figure 3: Comparison of chloride concentration in one and two dimension (a), Chloride concentration profiles in two dimension (b)

From the simulation results, the chloride penetration profiles from truss network model provided a similar trend line with the analytical solution of Fick's 2nd law in both one dimension and two dimensions. The results confirm the correctness of governing equation (Eq. 5) and correction parameter ω.

3.2 Effect of time step interval

The input time step interval Δt values are varied from 0.1hour to 168 hours, while the other parameter are set to be same, as 2.5×2.5 mm^2 of average meshing size and 0.01971 mm^2/hour of diffusion coefficient, for observing the effect of time step interval on the accuracy of model. The results is shown as following graph (Figure 4)

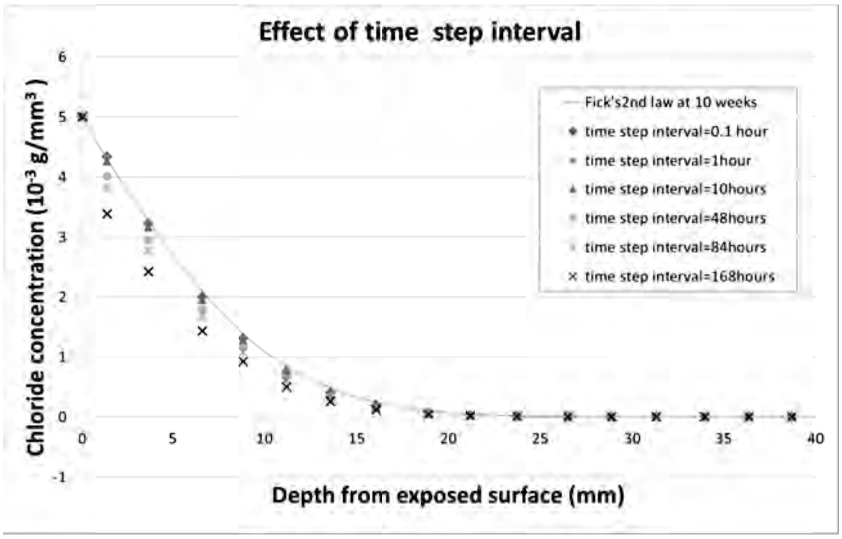

Figure 4: Effect of time step interval on chloride penetration profiles

From Figure 4, it shows that the smaller time step interval makes the chloride ions concentration profiles more closely to the trend of analytical solution of Fick's 2nd law. In case of Δt smaller than 1 hour, the graph is close to the analytical solution and no significant difference can be observed. In case that Δt is very large, e.g. time step interval larger than 48hours, the chloride penetration profile significantly decrease, and show big different from the analytical solution of Fick's 2nd law.

3.3 Effect of element meshing size

For study the effect of meshing size, the specimen of 50×75 mm and 150×150mm is meshed to element average size of 0.5×0.5, 2.5×2.5, 5.0×5.0, 10.0×10.0 and 15.0×15.0 mm^2 as show in Figure 5(a), (b), (c) and (d) respectively. The model is then simulated the chloride penetration at 5 weeks. The results is shown as following graph (Figure 6)

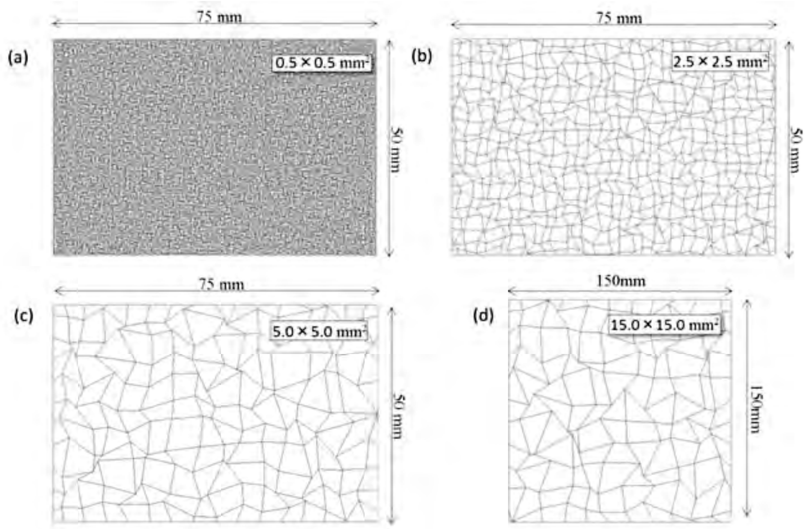

Figure 5: Truss network of specimen of 50×75mm and 150×150 mm at different meshing size

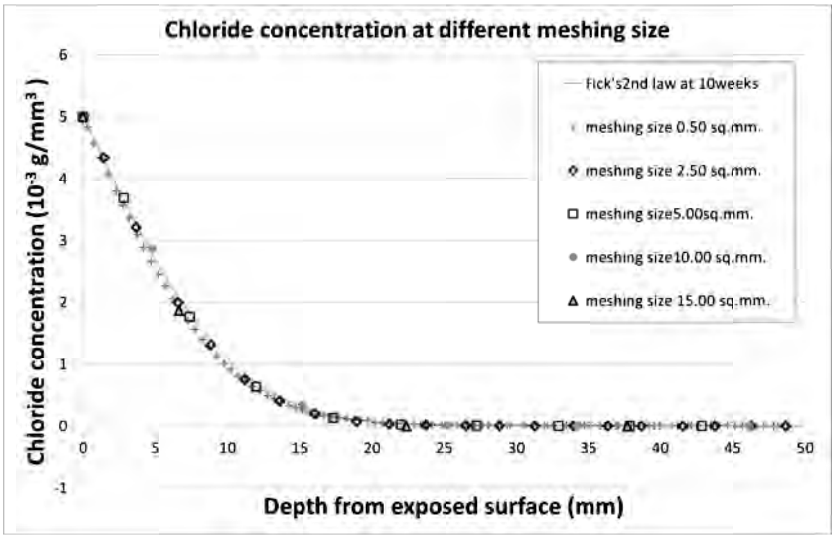

Figure 6: Effect of time step interval on chloride penetration profiles

The simulation results in Figure 6 show that Chloride penetration profile giving the similar trend even the meshing is larger.

3.4 Effect of random reahing and regular meshing

In two dimension model, regular meshing model and random meshing model has been generated for study the effect of element arrangement. (Figure 7)

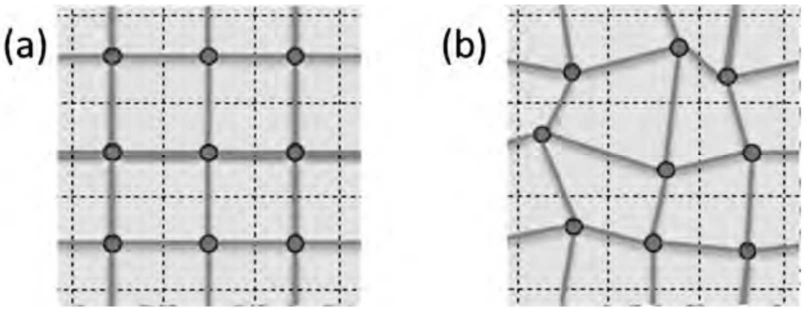

Figure 7: Regular meshing and random meshing truss arrangement

In two dimension model, a node is randomly allocated in square grid of inputted element size using random number generator. The simulation conditions both in regular meshing and random meshing are set as following. The average truss element length is 2.5mm. The diffusion coefficient is set to be 0.01971 mm^2 /hour. The time step interval is 1 hour per step. Chloride concentration at surface is 5×10^{-3} g/ cm^2 Total time of penetration is 10 weeks. The simulation results are shown in Figure8.

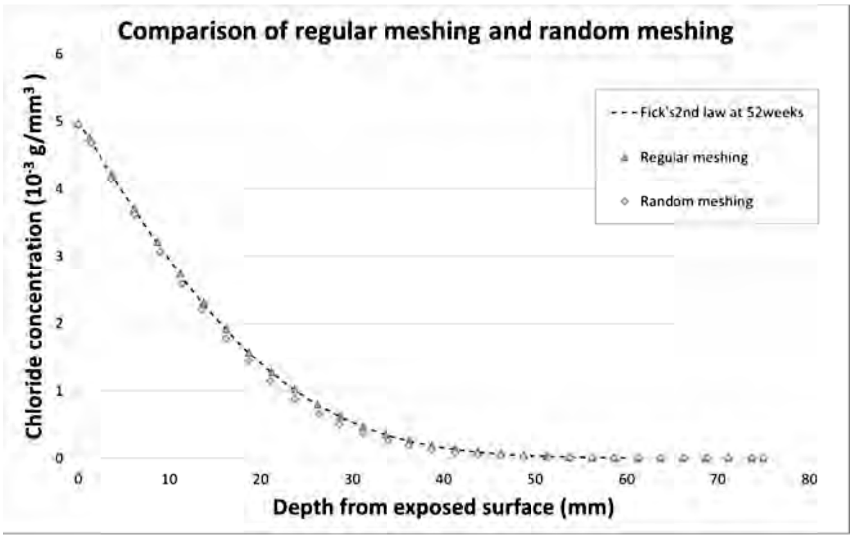

Figure 8: Chloride penetration profiles of regular meshing and random meshing truss arrangement

In case of regular meshing, the chloride penetration profile is perfectly match with the analytical solution of Fick's 2nd law. While, in case of random meshing, the chloride profile slightly oscillate around the analytical solution. From the overall picture, there are no significantly different in trend between regular meshing and random meshing.

3.5 Simulation with single crack

For verify the applicability of the truss network with the cracked concrete in the future study, the simulation of single crack specimen has been simulate. The specimen of $50\times75\text{mm}^2$ with a singlecrack of 30 mm depth and 50 μm and 80 μm width was presented to see the chloride peretration through crack by truss model.(see Figure 9)

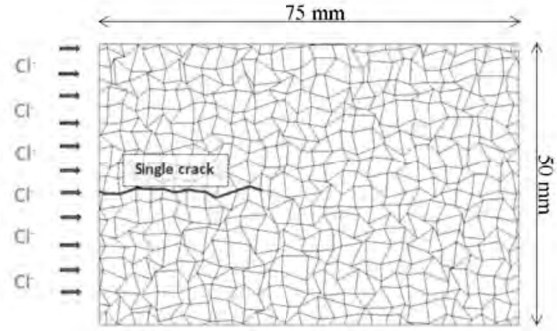

Figure 9: Single crack modeling

To calculate the diffusion coefficient through crack D_{crack} in cement-based materials, the following experimaltal bilinear equation,proposed by Djerbi (2008), is used.(Eq.8 and 9)

$$D_{crack} = 2\times10^{-11}w - 4\text{x}10^{-10}\ (\text{m}^2/\text{s}) \quad \text{for } 30\ \mu\text{m} \le w < 80\mu\text{m} \qquad (8)$$

$$D_{crack} = 1.4\times10^{-9}\ (\text{m}^2/\text{s}) \quad \text{for } w \ge 80\mu\text{m} \qquad (9)$$

Figure 10 show the chloride penetretion profile of single cracked specimen at 1 day, 1week and 12 weeks of specimen with single carck of 50μm and more than 80μm, respectively.

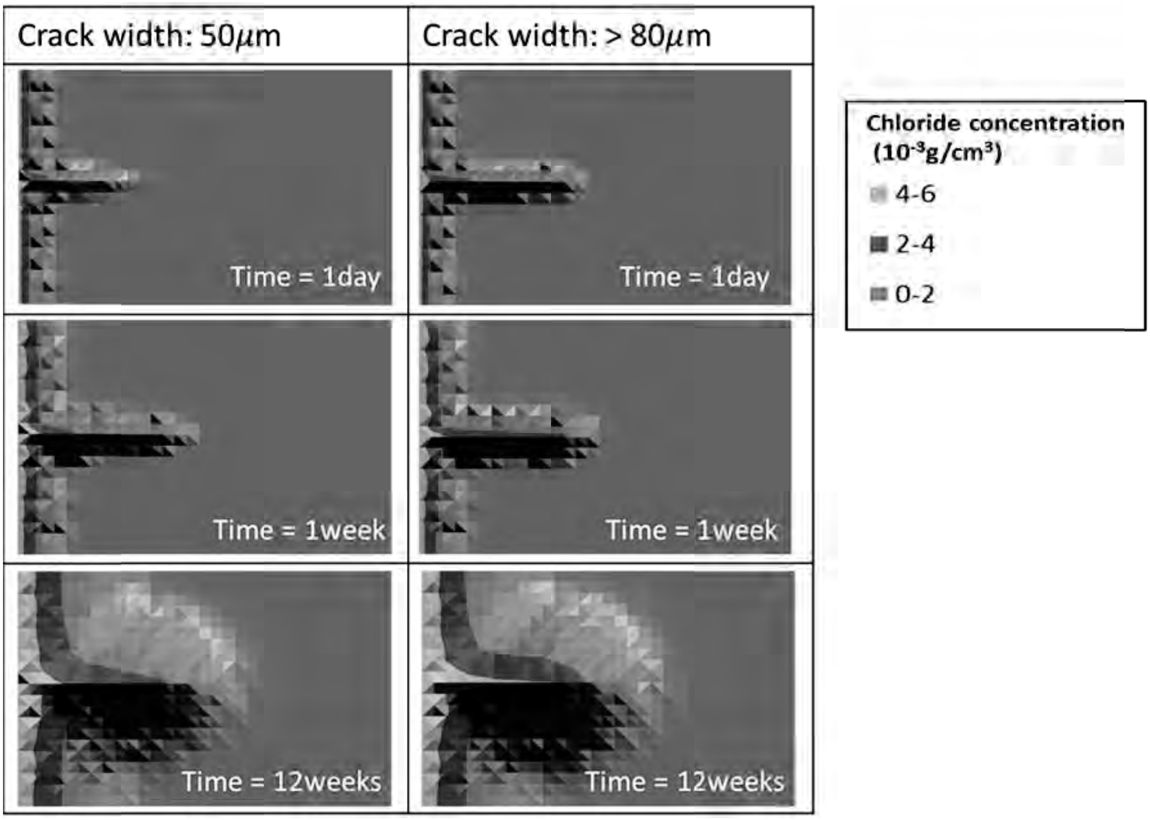

Figure 10: Chloride penetration profiles of single crack specimen

From the results, the chloride penetration through crack is faster comparing with that ingress from surface. Not only increasing the maximun penetration depth, but the chloriod ion concentraion in the area perpendicular to the crack also increase due to the higher diffusivity. Based on this results, the truss model can possibly apply with the other numerical simulation like RBSM for simulation of chloride penetration in cracked concrete.

4. CONCLUSIONS

From the results of simulation investigating the influence of each parameter and simulation of chloride penetration through single cracked specimen, the following conclusion are made.

1. The simulation results give a same tendency with the analytical solution of Fick's 2^{nd} law.
2. The fineness of meshing and time step interval relate to the accuracy of simulation. The more fineness meshing and smaller time step interval provide the better trend of chloride ion penetration profiles. However, too small meshing size results in higher calculation time and memory usage. Hence, in this study the model is generally set the time step interval equal to 1 hour per step, and average meshing size equal to

2.5×2.5mm^2, because the setting of meshing size and time step interval smaller than this value do not show significantly different in simulation results.

(3) Chloride penetration profile from the random meshing arrangement gives a similar trend with regular mesh and the analytical solution of Fick's 2nd law by error function solution.

(4) From the simulation of chloride penetration through single crack model and the random meshing element arrangement, these show the possibility in adaptation of the truss network model with another numerical simulation which can predict crack width directly, namely, RBSM model (K.Nagai et al., 2004) that can calculate the fracture of the structure correctly. Then, the simulation of chloride penetration into cracked concrete can be performed, consequently.

REFFERENCES

Djerbi, A., Bonnet, S., Khelidj, A. and Baroghel-Bouny, V., 2008. Influence of traversing crack on chloride diffusion into concrete. *Cement and Concrete Research,* 877-883.

Dousti, A., Rashetnia, R., Ahmadi, B., and Shekarchi, M. 2013. Influence of exposure temperature on chloride diffusion in concretes incorporating silica fume or natural zeolite. *Construction and Building Materials* 49, 393–399.

Frederiksen, J. M., Mejlbro, L., and Nilssom, L-O., 2008. *Fick's 2nd law-Complete solutions for chloride ingress into concrete-with focus on time dependent diffusivity and boundary condition*, Report TVBM-3146 Lund2008.

Lewis, R. W., Nithiarasu, P., and Seetharamu, K. N., 2004. *Fundamentals of the finite element method for heat and fluid flow*. John Wiley & Sons, New York.

Nagai, K., Sato, Y., and Ueda, T., 2004. Mesoscopic simulation of failure of mortar and concrete by 2D RBSM. *Journal of Advanced Concrete Technology* 11, 359-374.

Nagai, K., Sato, Y., and Ueda, T., 2005. Mesoscopic simulation of failure of mortar and concrete by 3D RBSM. *Journal of Advanced Concrete Technology* 11, 385-402.

Nakamura, H., Srisoros, W., Yashiro, R., and Kunieda. M., 2006. Time-dependent structural analysis considering mass transfer to evaluate deterioration process of RC structures. *Journal of Advanced Concrete Technology* 4, 147-158.

Poulsen, E., and Mejlbro, L., 2006. *Diffusion of chloride in concrete: theory and application*, Taylor & Francis, New York.

Šavija, B., Pacheco, J., and Schlangen, E., 2013. Lattice modeling of chloride diffusion in sound and cracked concrete. *Cement & Concrete Composites* 42, 30–40.

Srisoros, W., Nakamura, H., Yashiro, R., and Kunieda, M., 2007. Analysis of crack propagation due to thermal stress in concrete considering solidified constitutive model. *Journal of Advanced Concrete Technology* 5, 99-112.

Wang, L., Soda, M., and Ueda, T., 2008. *Simulation of chloride diffusivity for cracked concrete cased on RBSM and truss network model. Journal of Advanced Concrete Technology* 6, 143-155.

Wang, L., Soda, M., and Ueda, T., 2011. Mesoscale modelling of the chloride diffusion in cracks and cracked concrete. *Journal of Advanced Concrete Technology* 9, 241-249.

The current practice of construction material reuse in Vietnam

Quan T. NGUYEN[1], Ngoc B. NGUYEN[2]
[1] Project Management and Law Division,
Faculty of Construction Economics and Management,
National University of Civil Engineering, Vietnam
nguyenquan.nuce@gmail.com
[2] Faculty of Construction Economics and Management,
National University of Civil Engineering, Vietnam

ABSTRACT

Reusing material is a measure for resource-saving which is considered important in sustainable development as well as in sustainable construction management worldwide. This approach leads to the reduction in the amount of construction waste, energy and raw materials, and then contributes to sustainable construction as well as sustainable development. In Vietnam, in history, re-using demolition materials in new houses was already applied by Vietnamese people long time ago when they built their own homes in order to reduce cost, but the practice was spontaneous and has not been considered widely as important. Aiming to explore the current practice of re-using construction materials in the construction industry in Vietnam, a survey has been conducted with respondents from academic institutions and the industry. The paper points out that this practice can be found in a variety of types of construction projects, but is most popular with private houses. The materials to be commonly reused are limited to materials such as steel and metal, brick and aggregate and wooden materials. The rate of using those materials is relatively low in projects, mostly below 10%. The paper then presents three groups of solutions for promoting and developing this practice to a wider application. It is believed that the local and governmental authorities need to act first, then other stakeholders in construction will follow.

Keywords: sustainable construction, reusable materials, construction material reuse, reclaimed construction materials, construction demolition

1. INTRODUCTION

Reusing material, together with reducing and recycling, is an important strategy for sustainable development as well as sustainable construction. Long time ago, in Vietnam, people spontaneously used spare material and demolition material in building new houses. Recently, with commitment from the Government for dissemination and implementation of sustainable development in which sustainable construction is a key pillar, the reduction of energy and natural resources used for construction activities has become more and more important. Since construction waste is considered a serious problem in large cities (Begum et al., 2006), in recent times emerged the importance of construction waste minimization, which includes several approaches such as reduction, reuse and recycle of materials. Among the three approaches, reuse is considered to be good both in decreasing environment pollution and in cost savings because of the reduction of the amount of new materials to be used (NSCC, 2007) as well as the amount of waste. Using exploratory approach, this research paper investigates the current practice of construction material reuse in Vietnam based on the results from a survey with construction practitioners. The concerning aspects include material types and sources, reuse percentages, suppliers for reused materials as well as solutions for promoting the reuse of materials in the construction industry in Vietnam.

2. REUSING CONSTRUCTION MATERIALS AS AN APPROACH IN SUSTAINABLE CONSTRUCTION WORLDWIDE

2.1 Construction materials and waste

Construction materials are solids and fluids which comprise facilities in construction. The most frequently used materials include steel, aggregate, concrete, masonry, asphalt, and wood, then aluminum, glass, plastics, and fiber-reinforced composites (Mamlouk and Zaniewski, 2011). Waste is defined as “an object” that currently “no longer has any beneficial use” (NSCC, 2007). Construction materials may become waste if they are the surplus or rejected materials delivered to the sites or results of the demolition of existing structures. This type of construction waste contributes to the huge amount of solid waste that large cities need to deal with. However, since they are still in the original form or just need a slightly process to be back in their original form, it is advised to try reusing them until they have no value instead of disposing them after they have been used once (NSCC, 2007).

2.2 Reuse, reduce and recycle

Reduce, reuse and recycle are three processes that are advised to be used in a professional environmental project plan (PMI, 2007). These approaches are concerned with better resource efficiency in different ways. Reduce means the elimination of waste generation if it is possible, by reducing the amount of materials brought to sites in the first place. Reuse is defined as “making use of materials in their original state on the same site or at other sites”. Recycle is considered as “turning materials into new products for other purposes” (NSCC, 2007). Though all of these can contribute to further reducing the demand on natural resources, they are only three of six levels in waste management (in order of increasing priority): disposal, process, recycle, reuse, reduce and prevent.

3. RESEARCH APPROACH

In order to understand the practice of construction material reuse in Vietnam, a survey with a convenient approach for respondent recruitment was conducted. The questionnaire was designed and converted into a Google form, then the link to the form was sent to online professional construction networks. The printed questionnaires were also distributed to potential respondents using “snowball” method. Only respondents that have experienced or observed projects with construction materials reused were recruited. 173 questionnaires had been filled and sent back, among which there are 150 good completed ones that have been interpreted and analyzed. Respondents completed these 150 questionnaires come from a variety of job positions in the construction industry, from organizations as investors, contractors, consultants and even training institutions.

4. RESULTS AND DISCUSSIONS

4.1 Origin and sources of construction materials for reuse

There are three major sources for supplying reused construction materials for construction projects in Vietnam, as the survey results reveal: the demolition contractors, the waste traders, and self-provision. Table 1 demonstrates the sources of reused construction materials in terms of suppliers in the survey respondents' construction projects. The figures shows that, most of projects that reused construction materials procure material for reusing from demolition contractors (70.67%), about a half of them used the reused construction materials that they have generated, while just a third of them buy from waste traders. The reasons behind the choice could be explained by further analysis with the respondents' perception of quality of this type of material.

Table 1: Suppliers for reused construction materials

Suppliers for reused construction materials	Total of choices	%
Demolition contractors	106	70.67%
Waste traders	50	33.33%
Self-provision	75	50.00%

In terms of the origin of this type of material, nearly 80% of the projects mentioned in the survey used reused materials from demolished construction projects. More than three quarter of the projects tried to make use of the surplus materials due to exceeding order or materials being considered as wastage in normal conditions. Greater than a half of the projects (61.33%) accept materials collected from the demolition job of unaccepted components on the same site. Figures from this table cross-explain why most of the projects mentioned in the surveyed have bought construction materials for reuse from demolition contractors and there are a half of them could have reused materials generated be themselves on sites.

Table 2: Suppliers for reused construction materials

Origin of reused construction materials	Total of choices	%
Materials from demolished construction projects	119	79.33%
Materials collected from demolition of unaccepted components on the same site	92	61.33%
Surplus/wasted materials on the same site	114	76.00%
Others	9	6.00%

There are several major types of materials to be reused in the surveyed projects, as in Table 3. According to the respondents, the most popular material to be reused is steel or metal, with nearly 90% of the projects having used. This is understandable because steel and rebar can be used for many activities and structured on sites, especially if there is a welding machine. The next popular material is brick and aggregate. This type of material need no or very little processing job to be used again, it explains the figures. Wooden materials can also be easily reclaimed in lots of construction activities, like in falsework for structures or even to be burnt for heat or fire. That is why nearly two-third of the projects has experienced reusing wooden materials. Surprisingly, there are 24 out of 150 respondents claimed that they have observed projects reusing concrete mortar/masonry mortar. It is not easy to re-use concrete/masonry mortar due to the fact that this type of material become hard very fast and have limited use in hard form. The project management team may need a contingency plan to use the surplus concrete mortar right away when the ordered volume seems not to be used all for the currently executing components.

Table 3: Types of materials to be reused

Types of materials to be reused	**Total of choices**	**%**
Steel and metal materials	113	88.67%
Brick and aggregate	103	68.67%
Concrete/masonry mortar	24	16.00%
Wood	97	64.67%
Plastic	2	1.33%
Finishing materials	2	1.33%

According to the survey results, the reuse of construction materials has been observed in several types of construction projects, such as private houses, high-rise/multi-story buildings, infrastructure and industrial projects. Among those types of projects, private houses have been mentioned the most, with 71.33% (Table 4). In history, Vietnamese people had often made use of reusable construction materials for their houses for cost savings, and the modern citizens now have inherited this good tradition. In addition, quality is not very difficult to control in private houses; that is why householders allow the use of this type of material more easily.

Table 4: Types of projects reusing reused construction materials

Types of projects	**Total of choices**	**%**
Private houses	107	71.33%
High-rise/multi-story buildings	64	42.67%
Infrastructure projects	62	41.33%
Industrial projects	65	43.33%

Other types of construction projects attract nearly the same number of choice regarding the use of reused construction materials. The percentages are rather high, more than 40%, promising a new market for this type of material in the near future.

Another aspect that needs to be investigated is the percentage of reused materials in a typical construction project (Table 5). About one fourth of the projects have employed approximately 10-29% reused materials. This rather high percentage is explained by the high rate of private houses being observed and reported in the survey. However, the survey results show that the rate of reused material in total amount of material used for a project is mostly less than 10% with more than one fifth of projects in the survey have used very limited amount of 3% and less.

Table 5: The rate of reused materials in projects

Percentage of reused material from total amount of material	**Total of choices**	**%**
<3%	33	22.00%
3- less than 10%	55	36.67%
10 – 29%	40	26.67%
30 – 49%	8	5.33%
50% and greater	10	6.67%
Unanswered	4	2.67%

When being asked about the quality of reused materials in comparison to new materials, most of the respondents (82%) agreed that this type of material is relatively low quality than the new ones. Only 27 respondents (18%) argued that the two types have the same level of quality. The figures explain that in most cases (66.67%), this type of material was used for unimportant structures in the projects. Though there are 43 respondents admitted that they have observed this type of material to be used for main project components, this can be explained by the number of observes in private houses in the survey, as shown in Table 4. The reasons the respondents have revealed for the state of low quality for reused materials include: being deformed, being mixed with other substance, being affected/corroded by the environment, incorrect processing and having no suitable equipment or technology to convert back to the original state, etc. That is to say, reused materials in construction have been recognized widely, but considered low quality and are only suitable for certain types of projects and components.

5. PROPOSED SOLUTIONS FOR PROMOTING CONSTRUCTION MATERIAL REUSE IN VIETNAM

Respondents who are not for the use of reused construction materials agreed on three major barriers as reasons for this practice as shown in Table 6. That is to say, the consumers’ perception of low quality of this type of material is the greatest barrier that people have to overcome. The next, as being very popular in Vietnam, is legal and regulation issues.

Table 6: Reasons for not using reused construction materials

Reasons	**Total of choices**	**%**
Legal issues in construction processes	23	15.33%
No relevant regulations	38	25.33%
Worry on quality	95	63.33%
Others	7	4.67%

In order to promote the larger use of reusable construction materials, several solutions have been nominated by the survey respondents. The solutions can be grouped into the following categories:

(1) Solutions on quality assurance of reusable materials: developing specific regulations, standards and guidance for classification and preservation of this type of materials, establishing quality tracking, controlling and accrediting systems to ensure that this type of materials is legally accepted and properly used in construction projects;
(2) Solutions on developing markets for reusable materials: propagating the benefits of using this type of materials to investors, contractors, construction-related students and the whole society in terms of sustainable development, setting up mechanism for establishing collection and distribution points, professional traders, connecting different geographical areas and construction stakeholders to widen the markets
(3) Solutions on enhancing the reusability of wasted materials: developing specific standards and specification for designing using this type of materials, investing on suitable technologies for demolition to minimize the negative impacts to materials, conducting research to apply new materials that are more durable, have higher quality and suitable for multi-use.
That is to say, almost all of the proposed solutions need the involvement of the local and central authorities. Other stakeholders in construction do not seem to recognize their roles in maximizing the reuse of construction material. Therefore, the first step should be taken is to carry out campaign on establishing and developing markets for reusable materials (group 2 above) in order to get stakeholders in construction involved in promoting the reuse of this type of materials. Then, the stakeholders in turn will put pressure back to the local and governmental authorities to get them enable and develop the markets. Other groups of solutions then will be applied gradually.

6. CONCLUSIONS

The construction market in Vietnam has accepted the reuse of construction material from demolition and even construction waste but reusable, since long time ago. However, only some popular types are made use in construction projects but for some specific component and structures, though the application can be found in a variety of projects. Apart from private houses where the households could make full decision on everything, including the type of material used, in other types of projects, the regulations on quality assurance limit the use of this type of materials. Therefore, the reuse of this type of material only limited in several popular and easily-reusing types of materials such as steel and metal, brick and aggregate and wood. The rate of using those materials is low, less than 10% in most of the case. In order to develop the use of this type of material to support sustainable construction and sustainable development of the country, it is firstly the job of local and governmental authorities to establish and develop markets for this type of material, then get other construction stakeholders in. Other stakeholders then will automatically play their necessary roles for promotion of construction material reuse for the country.

REFERENCES

Begum, R. A., Siwar, C., Pereira, J. J., and Jaafar, A. H., 2006. A benefit–cost analysis on the economic feasibility of construction waste minimisation: the case of Malaysia. *Resources, Conservation and Recycling* 48, 86-98.
Mamlouk, J. P. and Zaniewski, M. S., 2010. *Materials for civil and construction*

engineers. New Jersey, Upper Saddle River: Pearson Prentice Hall.

NSCC (2007). *Reduce, Reuse, Recycle Managing your waste*. London.

PMI (2007). *Construction Extension to the PMBOK Guide Third Edition*, Newtown Square, Pennsylvania: Project Management Institute, Inc.

Effect of initial water content in mortar on water and moisture absorption of mortar

Toshiya CHIBA[1] and Yoshitaka KATO[2]
[1]Master student, Department of Civil Engineering,
Graduate School of Science and Technology, Tokyo University of Science, Japan
toshiya1350@gmail.com
[2]Associate Professor, Department of Civil Engineering,
Faculty of Science and Technology, Tokyo University of Science, Japan

ABSTRACT
Deterioration mechanisms of concrete structures, such as salt damage, alkali-aggregate reaction and drying shrinkage, are closely related to the water present in the concrete. It is believed that clarifying the water movement in concrete can contribute to more precise prediction of the deterioration of concrete structure, and thus understanding the basic nature of water transport is very important. In this study, the saturation distribution in concrete was estimated using the moisture diffusion coefficient obtained from the water and moisture absorption test with varying levels of initial saturation of the mortar. The results of the water absorption test showed that the moisture diffusion coefficient as the gas phase is small in the low-saturation region, but the moisture diffusion coefficient as the liquid phase is large in the high-saturation region. Then it was possible to reproduce more accurately the saturation distribution in the mortar by setting appropriately the saturation boundary of the low-saturation region and the high-saturation region.

Keywords: water movement, saturation, moisture diffusion coefficient, mass transfer

1. INTRODUCTION

Reinforced concrete structures are widely used for infrastructure, but it is necessary to improve the durability of both new and existing structures. It is known that the durability of a concrete structure is closely related to the water content of its concrete. For example, the alkali aggregate reaction is a chemical reaction between alkali hydroxide in the pore solution with reactive aggregate. The gel formed by this reaction expands upon absorbing water and causes cracking of the concrete and rebars breakage. Consequently, the durability of concrete structures is greatly affected by the alkali aggregate reaction (Sekino, 2009), and hence the water content within the concrete internal affects the speed of deterioration. It has also been reported that the water content of concrete affects the speed of neutralization and that moisture around the rebars greatly affects the corrosion mechanism (Yamamoto, 2001). In order to quantitatively grasp the deterioration of concrete structures, it is important to understand the water movement properties of the concrete.

Regarding past studies on water movement in concrete, many studies have elucidated the shrinkage due to drying (Sakata, 1981; Kobayashi, 1995; Akita, 1994). Most studies have focused on the movement of water vapor inside the concrete. However, actual structures in the environment are affected by drying, moisture absorption and water absorption, so it is necessary to consider the combined liquid phase and vapor phase water movement inside the concrete.

Akita et al. experimentally studied water movement in the drying process, moisture absorption process and water absorption process (Akita, 1990). They modeled the water movement as a diffusion phenomenon, and confirmed that it can be expressed as the diffusion of water vapor in the moisture absorption process and drying process. However, it was reported a large difference between the analytical and experimental values in the water absorption process. In practice, in the water absorption process, the diffusion phenomenon caused by the movement of water vapor in the gas phase and that caused by water movement in the liquid phase by capillary force are complexly mixed and so cannot be easily represented. Therefore it is necessary to consider the water movement of the water absorption process in greater detail.

Many studies on water movement in concrete used specimens in the absolutely dry state by oven drying at 105ºC before conducting experiments on water absorption and moisture absorption. However, actual concrete structures are not in the absolutely dry state because the surrounding environment is repeatedly undergoing drying, moisture absorption and water absorption. So, in order to accurately predict water movement inside a concrete structure, it is necessary to understand the water movement in consideration of the water content of the concrete before the water and moisture absorption test.

In this study, water and moisture absorption tests were conducted using specimens in which the water content had been adjusted in order to examine the effect of initial saturation on water movement in concrete. By using non-linear analysis of one-dimensional and experimental results, the diffusion coefficient and the analytical values of saturation distribution were collected, and the method of calculating the diffusion coefficient taking into account the boundary saturation and the water content of a mortar specimen was examined.

2. EXPERIMENTAL OUTLINE

2.1 Material and specimens

The cement used in this study was ordinary Portland cement (symbol C, density 3.15 g/cm3). The aggregate used was Yamanashi Fujikawa river sand (symbol S, density 2.61 g/cm3). The mix proportion is shown in Table 1. The prepared specimens were rectangular columns (4 × 4 × 16 cm).

Table 1: Mortar mix proportions

W/C(%)	**S/C**	**(kg/m^3)**		
		W	**C**	**S**
50	2.3	254	508	1169

2.2 Water and moisture absorption test

The specimens were demolded and cured for 91 days in water to allow hydration to advance sufficiently. Then, the specimens were sealed with tape on the four sides except for one face for water and moisture absorption. In this study, with reference to the method of Maruyama et al., mortar specimens were cut using a precision cutter as shown in Fig. 1 at intervals of 7.5 mm, 10 mm, and 30 mm before starting the test (Maruyama 2011). Then, by combining them, the water and moisture absorption test was started. The absolutely dry weight of the specimens cut by the precision cutter were measured and the saturation of each element was also measured. The degree of saturation of the mortar specimen was adjusted so as to approach 0% (A), 25% (B), 50% (C) and 75% (D). The saturation of each element of the specimen adjusted for initial saturation are shown in Fig. 2. The figure shows that the measured and set saturation generally matched.

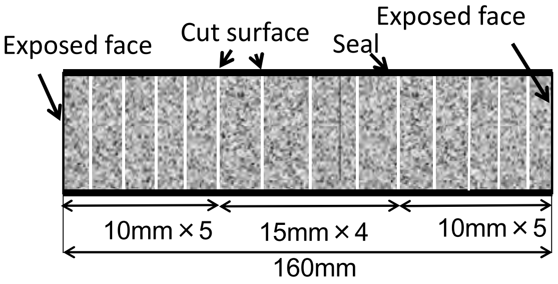

Figure 1: Sample preparation

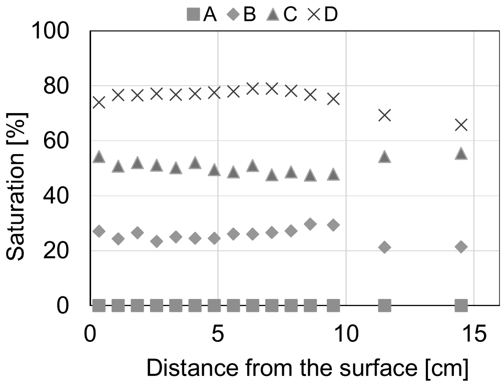

Figure 2: Adjustment of the initial

The situation of the water absorption test after adjusting the saturation in mortar is shown in Fig. 3. The mass of each element was measured at 2 hours, 6 hours, 1 day, 3 days, 7 days and 14 days from the start of water absorption using an electronic balance with an accuracy of 0.0001 g. In a similar way, the moisture test was conducted after adjusting the initial saturation. Then, the mass of the specimens placed in a high-humidity environment was measured at 3 days, 7 days, and 14 days. The high-humidity environment was created by constant condensation in a sealed vessel filled with water. The saturation (R_i) of each element was determined by Equation (1).

$$R_i(\%) = \frac{W_i - W_{i(dry)}}{W_{i(sat)} - W_{i(dry)}} \times 100 \tag{1}$$

Where $W_{i\,(sat)}$ is the saturation weight of the specimen (g), $W_{i\,(dry)}$ is the absolutely dry weight of the specimen (g), W_i is the weight of specimen after the test (g).

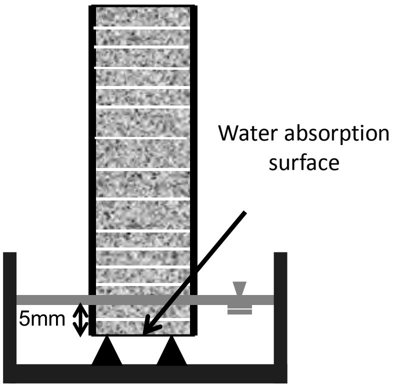

Figure 3: Water absorption test

3. ANALYSIS METHOD

In this study, it is considered that water movement can be expressed by the nonlinear diffusion equation of one-dimensional by using Equation (2).

$$\frac{\partial R}{\partial t} = \nabla\left(D(R)\nabla R\right) \tag{2}$$

Where D(R) is the diffusion coefficient ($\mathrm{cm^2/day}$), R is the saturation of the specimen.

The diffusion coefficient (D(R)) can be expressed as Equation (3) used to Boltzmann variable (λ) shown in Equation (4).

$$D(R) = -2 \cdot \left(\frac{\partial \lambda}{\partial R}\right)_{R=R_2} \int_{R_e}^{R_2} \lambda dR \tag{3}$$

$$\lambda = \frac{x}{2\sqrt{t}} \tag{4}$$

Where λ is the Boltzmann variable ($\mathrm{cm/s^{1/2}}$), x is the distance from the surface (cm), t is the period of moisture absorption and water absorption (day), R_2 is the any degrees of saturation (%), R_e is the initial saturation (%).

In order to use the Equation (3), it is necessary to obtain an approximate expression by the regression relationship between R and λ. In this study, a hyperbolic Equation (5) was used with reference to the method of Akita et al..

$$R = 100\left\{-f + a/(\lambda + b)^2\right\} \tag{5}$$

Where a, b, and f are factors used by the approximate expression.

4. RESULTS AND DISCUSSION

Fig. 4 shows the results of the moisture absorption test using the specimens adjusted for the initial saturation. Considering the difference of initial saturation, it is confirmed that water movement occurred in specimen A, B and C, which was in the absolutely dry state. Water movement in the gas phase can be considered as a diffusion phenomenon of simple water vapor. So it is considered that the moisture movement increased with greater difference in the water content of the mortar inside and the external environment. The results of the water absorption test are shown in Fig. 5. Comparing A, B, and C, the higher the initial saturation of specimens, the more the saturated elements tend to be in an area away from the water absorption surface. It can be seen that the water absorption progresses. It is considered that the water absorption progresses by the initial saturation because the intermolecular force of water molecules is activated. However, the trend in D was not observed, as explained later.

In accordance with the analysis method described in Chapter 3, the diffusion coefficient was calculated from the measurement results of Fig. 4. The relationship of the diffusion coefficient and saturation is shown in Fig. 6. The diffusion coefficient of low initial saturation is larger than that of high initial saturation immediately after starting each moisture absorption test. The diffusion coefficient of initial saturation 75% was not calculated because the moisture transfer could not be observed.

Similarly, the relationship of saturation with diffusion coefficient using the water absorption test results in Fig. 5 is shown in Fig. 7. In this study, the diffusion coefficient was calculated according to the analysis method of Akita et al. (Akita, 1990). Unlike the relationship of diffusion coefficient and saturation in the moisture absorption test, the relationship of D-R changes depending on the number of days of water absorption. This means that the water movement cannot be expressed as the diffusion. However, it is possible to consider the physical phenomenon of the water absorption process, by focusing on the saturation when the diffusion coefficient increases rapidly in Fig. 7.

Saturation when the diffusion coefficient changes rapidly shows the boundary of the slow movement by water vapor in the low-saturation region and rapid movement by liquid water in the high-saturation region. In this study, this is referred to as boundary saturation. The boundary saturation of Fig. 7 is obtained from the approximate expression of the relationship of saturation and Boltzmann variable. Looking at the results of Fig. 7, boundary saturation when the diffusion coefficient sharply rises is low in the short-term water absorption time of 2 h and 6 h. This is considered to be due to rapid movement of liquid water by capillary force. The value of the diffusion coefficient in D is small compared to A, B, and C, and confirming that the movement of the water is low. It is considered that the driving force of the water movement is reduced because of the difference in the internal saturation and the saturation near the surface is small. It is believed that if the initial saturation state is too high, there is action to slow down the water absorption, because the driving force of the water movement is reduced.

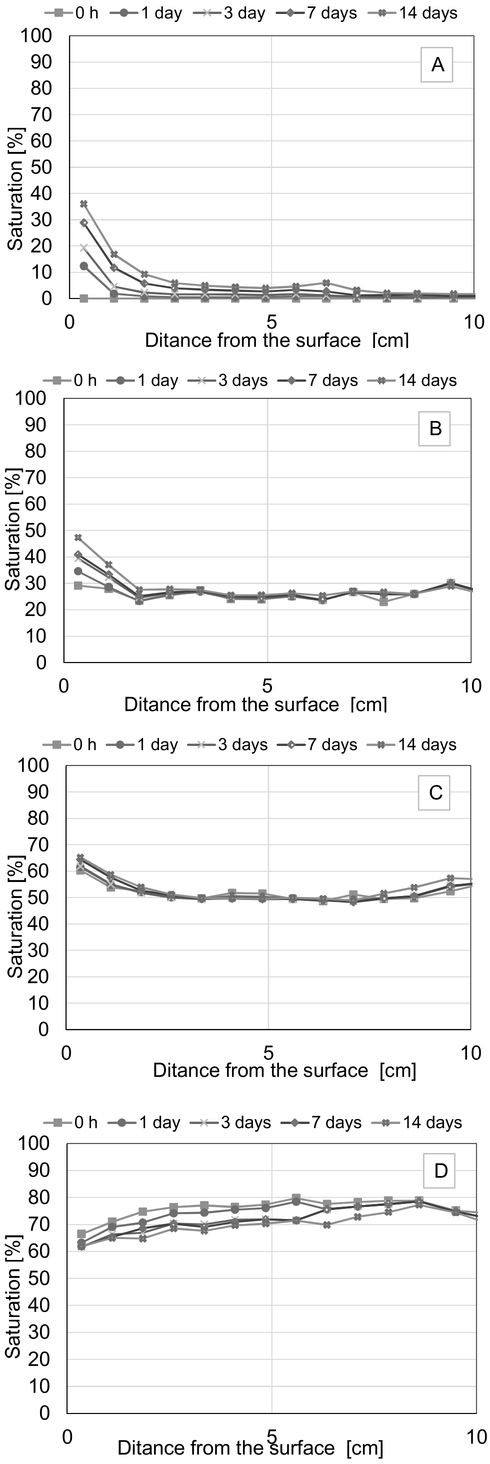

Figure 4: Results of moisture absorption test

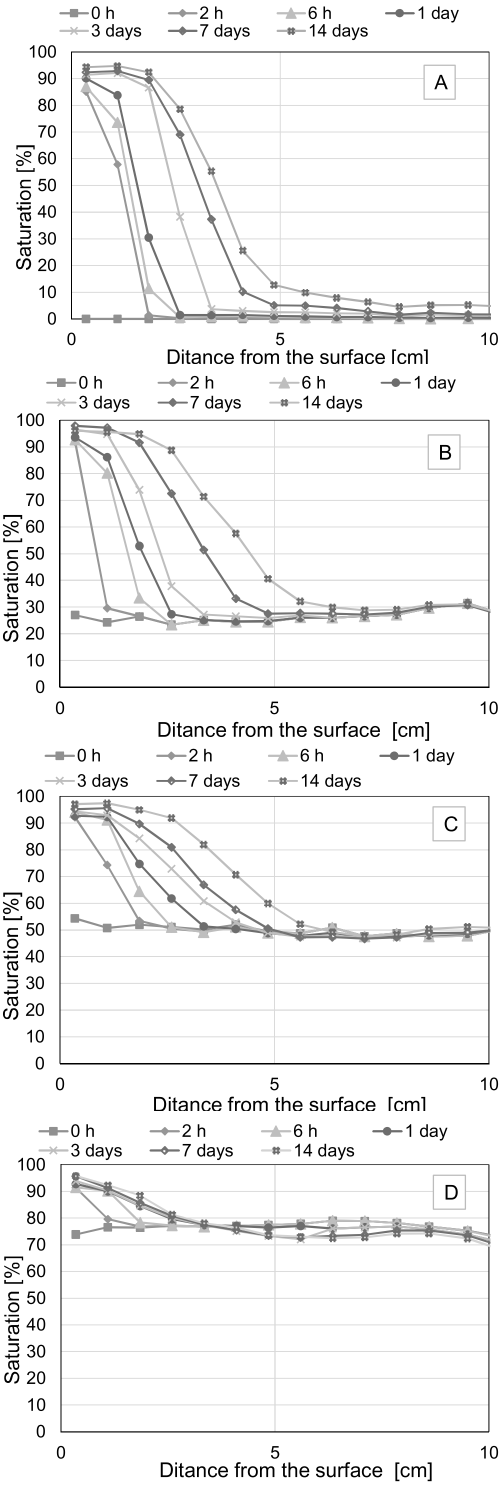

Figure 5: Results of water absorption test

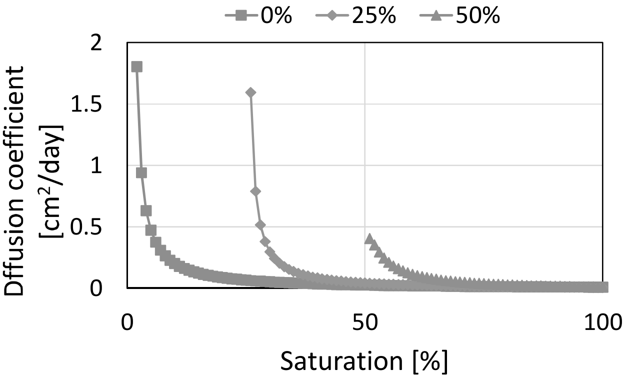

Figure 6: Relationship of D-R of moisture absorption test

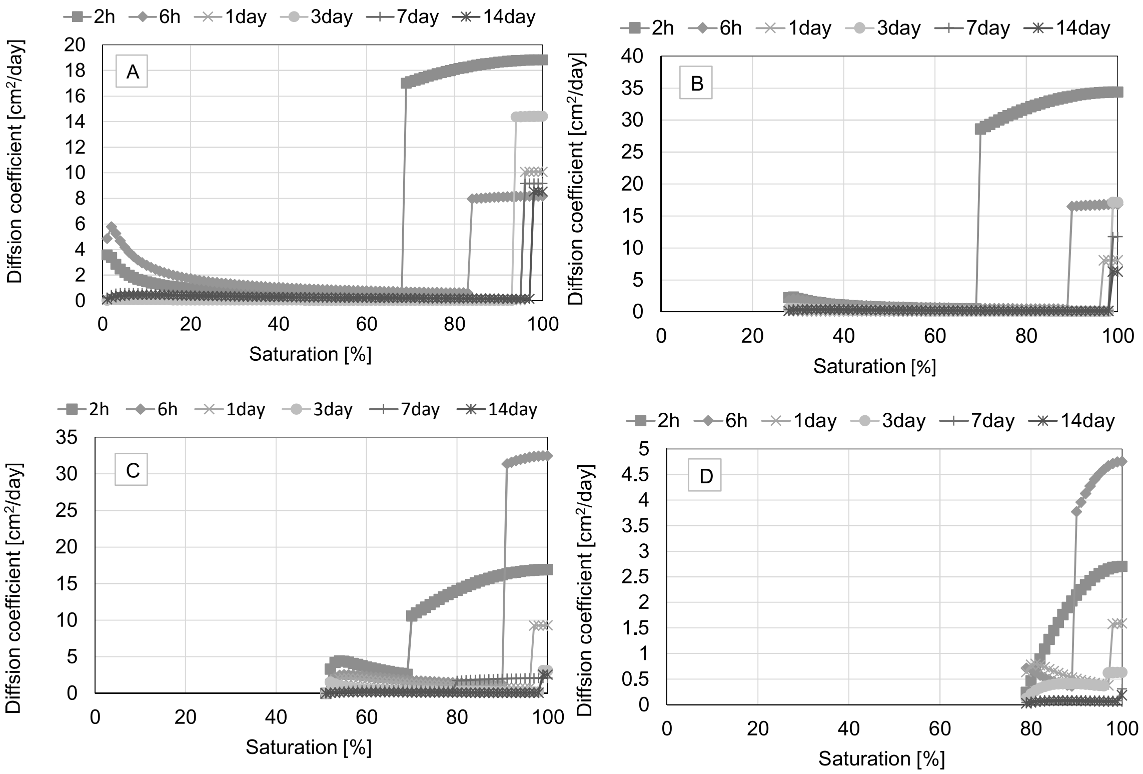

Figure 7: Relationship of D-R of water absorption test

A comparison of the experimental values with the analysis values calculated by using the diffusion coefficients obtained from the results of Fig. 7 - A are shown in Fig. 8. In the analysis, the diffusion coefficient obtained for each water absorption day was used. For example, when calculating the analysis value up to 1 day from the start of water absorption, the analyzed data is calculated using the diffusion coefficients obtained from the experimental results of 0–2 h, 2 h–6 h, and 6 h to 1 day. The analytical values of non-initial water absorption are higher than the experimental values.

In this study, the analytical values were not calculated appropriately. Perhaps the saturation boundary used to approximate the experimental values was not appropriate. It is considered from the experimental value to be a smooth gradient change point.

However, the cause is suspected to be because of using the intersection of the approximate expression. The movement of liquid water by capillary phenomenon dominates immediately after starting the water absorption test. As the number of days of water absorption progresses, water vapor diffusion occurs from the front of the meniscus. It is considered that the form of water movement gradually changes, and that boundary saturation also continuously changes.

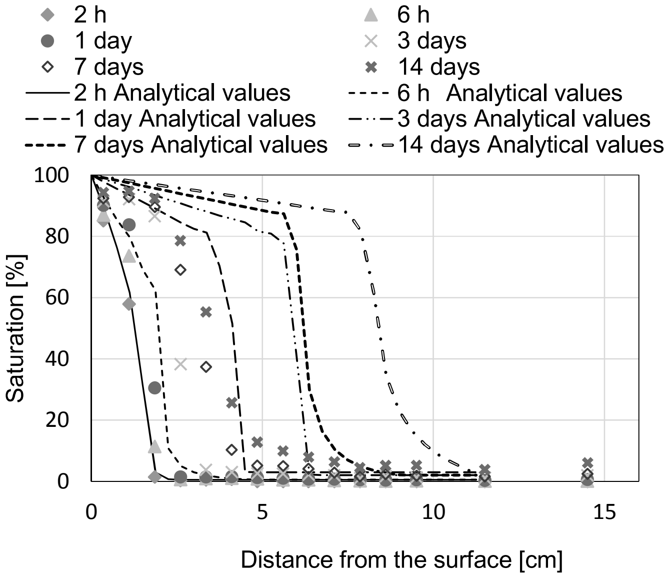

Figure 8: Comparison with the analytical value with the experimental value

The saturation boundary at a particular time was calculated by inverse analysis from experimental values such as in Fig. 9. The time-dependent temporal change of the saturation boundary was considered. The temporal change of the boundary saturation obtained when calculating the analysis values in Fig. 9 is shown in Fig. 10. A significant difference in the initial saturation was not observed, but the saturation boundary was smaller with fewer water absorption days. Equation (6) is an approximate expression of the relationship between water absorption in days and boundary saturation obtained by inverse analysis in Fig. 10.

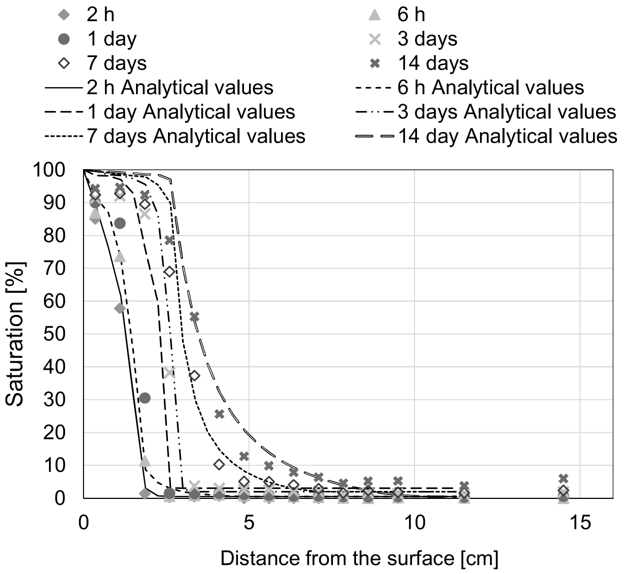

Figure 9: Comparison with the experimental value with the analytical value considering the saturation boundary

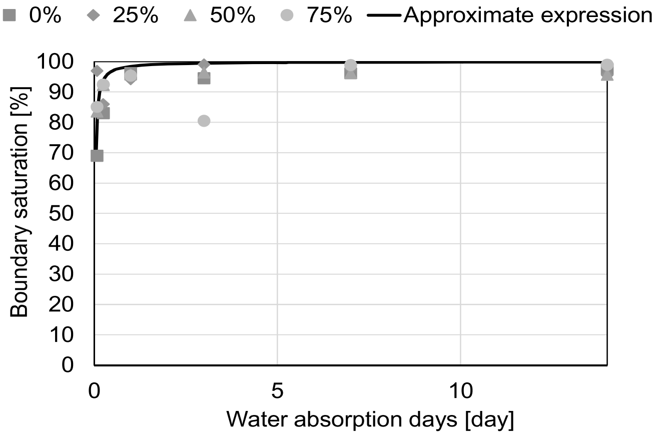

Figure 10: Relationship of water absorption days and boundary saturation

$$R_b = \frac{-1.53}{t} + 100 \tag{6}$$

Where R_b is the boundary saturation (%), t is the water absorption days (day).

It is considered that the movement of liquid water by capillary force was prominent when the boundary saturation was small and reduced over time. Temporal change of the boundary saturation is different from the result of Akita et al. (Akita, 1990). But, in this study, the data of the initial water absorption was used, and it is observed that the rapid movement of liquid water by capillary force occurred.

5. CONCLUSIONS

The results of this study are summarized as follows.

1) Water absorption tests using mortar specimens with adjusted initial saturation showed that the initial saturation affects the speed of moisture and water absorption.

2) As a result of using the boundary saturation obtained by inverse analysis from the experimental values, it was found that the boundary saturation increases over time. It is considered that the movement of liquid water by capillary force affects the initial water absorption. Thereafter, the action of capillary force becomes weaker and water absorption slows down.

REFERENCES

Akita, H., Fujiwara, T., and Osaka, Y., 1990. Water movement mortar due to drying and wetting, *Proceedings of the Japan Society of Civil Engineers* 13.
Akita, H., Fujiwara, T., and Osaka, Y., 1994. An analytical method of moisture transfer within concrete due to drying, *Journal of Materials, Concrete Structures and Pavements* 23, 101-110.
Kobayashi, T., Yamada, K., and Yamamoto, T., 1995. Fundamental study on development of drying shrinkage and strength due to water movement in concrete, *Japan Concrete Institute* 17, 633-638.
Maruyama, I., Igarashi, G., and Kishi, N., 2011. Fundamental study on water transfer in Portland Cement past, *Journal of Structural and Construction Engineering* 76, 1737-1744.
Sakata, K., and Kuramoto, O., 1981. A study on the water diffusion and shrinkage in concrete by drying. *Proceedings of the Japan Society of Civil Engineers* 312, 142-145.
Sekino, K., Tsuyuki, N., and Yoshimoto, M., 2009. Study on inhibitor of alkali-aggregate reaction, *Cement Science and Concrete Technology* 63, 408-413.
Yamamoto, K., Ikasa, H., Koga, I., and Masuda, Y., 2001. An experimental study on effects of the moisture condition of concrete on steel corrosion, *Japan Concrete Institute* 23, 535-540.

Influence of each seismic element on the dynamic behavior of traditional timber frames

Iuko TSUWA[1] and Mikio KOSHIHARA[2]
[1]Engineer, The Japanese Association for Conservation
of Architectural Monument, Japan
tsuwa@bunkenkyo.or.jp
[2]Professor, Institute of Industrial Science, the University of Tokyo, Japan

ABSTRACT

Traditional timber structures such as temples and shrines in Japan are preserved and utilized actively and used by general public. Thus even traditional buildings need sufficient aseismic performance. Many traditional timber buildings are built by the knowledge and experiences of carpenters. However we need to quantitatively evaluate the earthquake-resistant performance of traditional timber structures in order to understand their seismic capacity. Recently researches about the evaluation of seismic capacities in traditional frames or structural elements are increasing. However it is not clarified how a whole frame is evaluated with the existing evaluation method about seismic elements. In addition, it is not sufficiently clear how seismic elements behave in a whole frame. In this paper, we developed three dimensional models of some kinds of traditional timber frames including Kumimono used in temple and shrines and conducted the parametric dynamic analysis focused on the combination way of seismic elements. The purpose of this paper is to examine the dynamic characteristics of seismic elements in a whole traditional timber frame.

Keywords: traditional timber structure, Kumimono, earthquake response analysis, non-linear dynamic behavior

1. INTRODUCTION

We conducted shaking table tests with three kinds of specimens as shown in Figure 1. The picture in Figure 1 shows Specimen 2 on a shaking table. The wall stiffness of Specimen 1, 2, 3 became higher in this order, in order to understand the effectiveness of wall stiffness on vibration characteristics. The details of the experimental method were presented in USMACA 2011, 2013. In this paper, we improved an analysis model based on shaking table test results. The model was developed with the springs of earthquake resistant elements. We also made improvements in modelling of restoring force characteristics of each structural element. Parametric analysis was conducted in which a column base condition and the strength of a wall was changed. The analysis results were compared with experimental results. The effectiveness of each structural element on the seismic behavior of a whole frame was discussed.

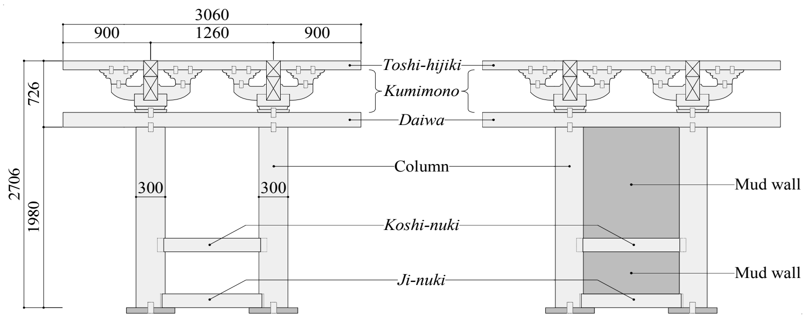
3060
900
1260
900
726
2706
1980
300
300
Toshi-hijiki
Kumimono
Daiwa
Column
Koshi-nuki
Ji-nuki
Mud wall
Mud wall

Specimen 1 Specimen 2

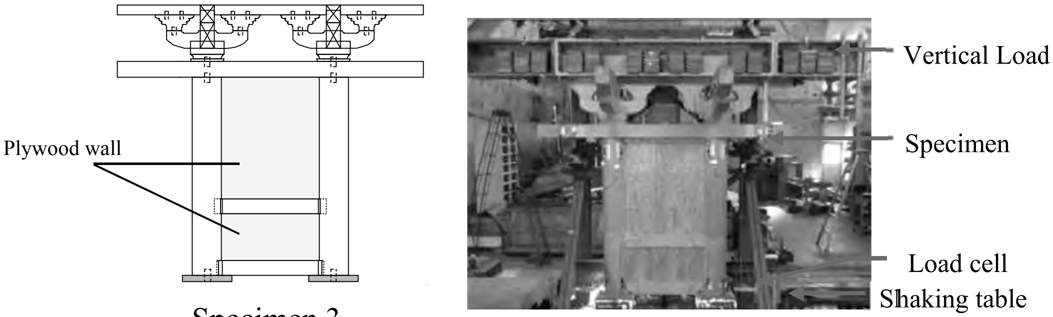
Plywood wall
Vertical Load
Specimen
Load cell
Shaking table

Specimen 3

Figure 1: Experiment in a previous research

2. ANALYSIS MODEL

2.1 Outline

We developed three-dimensional analysis model. Each seismic element was modeled as rotation, shear or compression and tension springs as shown in Figure 2. Modeled elements were the rotation spring of column, the rotation spring of column-*Nuki* joints, the shear spring of walls, shear and compression and tension springs of *Kumimono*. It was assumed that a column base went up.

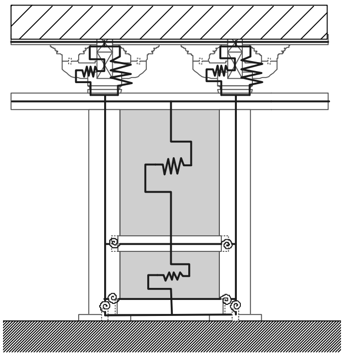

Figure 2: Analysis model

2.1 Modelling of structural elements

We set each restoring force characteristic of seismic springs based on shaking table tests and previous researches. Table 1 shows the characteristics. We modeled the hysteresis curves of *Koshinuki*-column joints, *Kumimono* and mud walls from the results of shaking table tsets. A *Jinuki*-column joint was set by a previous theory of Inayaama, 1992. The restoring force characteristic of plywood wall was determined by the shear force of surface bars and nails as shown in the previous research of Murakami et al, 2006. The characteristic of *Koshi-nuki* joints was improved in this time and was different with our previous paper. We also made improvements in the spring model of a column base. We show the details next.

A column has a resistance force to rocking because columns have a large diameter in this experiment. Therefore we set a rotation spring at the column base. In addition, the uplift of column was also seen at the column base in some tests of Specimen 3. On the other hand, the column base did not go up in the tests of Specimen 1 and 2. In our previous research, we individually set the column condition in analysis. However the specification of a column base was same in every specimen. The column put on a base stone. There was a wooden dowel between a column and base stone. Therefore any specimen could go up at a column base. For this reason, the analysis model of every specimen needs to have a same condition at a column base. The uplift of a column base and a rotation spring by rocking were included in every specimen.

Next we consider the restoring force characteristic of a column. The property is usually defined by previous researches of Ban 1942 and Kawai, 1972 as shown in Figure 4. The characteristic includes an effect called the p-δ effect. It is a phenomenon that vertical loads act in a direction increasing horizontal displacement in association with the increase of displacement. An analysis soft called *Wallstat* used in our research has the p-δ effect contributing to a whole building in an analysis. Accordingly the p-δ effect is counted doubly when we use the property of previous researches (AIJ 2013). Therefore we used the restoring force characteristic as shown in Figure 5 (b). The characteristic was calculated by subtracting the p-δ effect from the original property as shown in Figure 5. The hysteresis characteristic was nonlinear elastic. Additionally the fluctuation of vertical loads was also included in a simulation.

2.2 Verification of analysis model

2.2.1 Analysis method

The input wave of each specimen was an acceleration wave on a shaking table gained from the experimental results inputting the wave of level 2 provided by Building Center of Japan. Figure 6 shows the original wave. The maximum acceleration of the original wave was 355.66 gal. Viscous damping factor was 2.0 % of a stiffness-proportional damping. We used an improved analysis soft called wallstat ver2.0.1 (Nakagawa, 2010).

Table 1: Some comments on tables

Element	**Restoring force characteristic**
Koshinuki-column joint 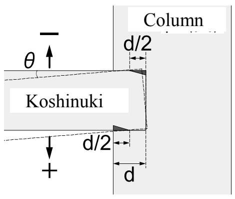 Column d/2 θ − Koshinuki d/2 + d	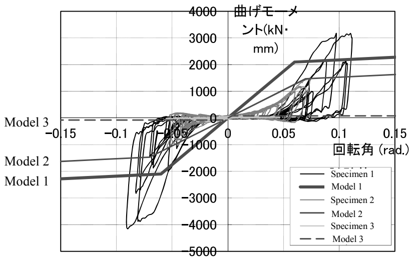
Jinuki-column joint 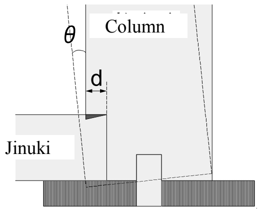 θ Column d Jinuki	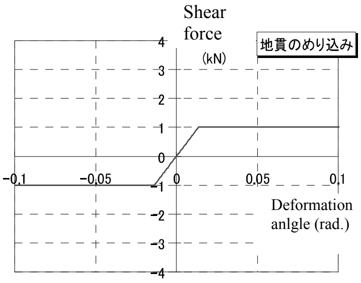
Kumimono 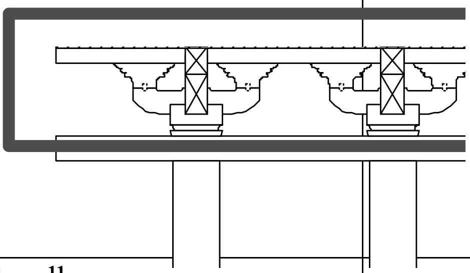	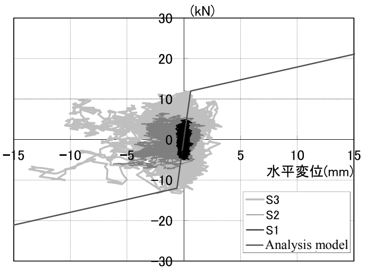
Mud wall 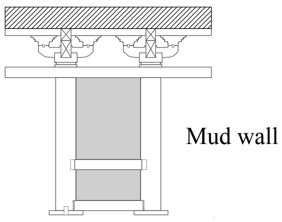 	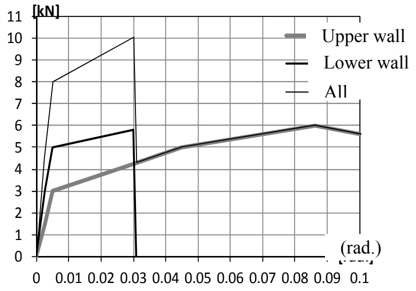
Plywood wall 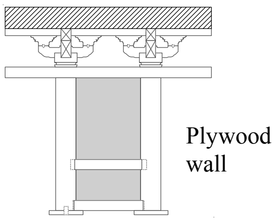 Plywood wall	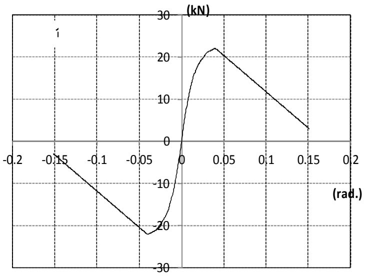

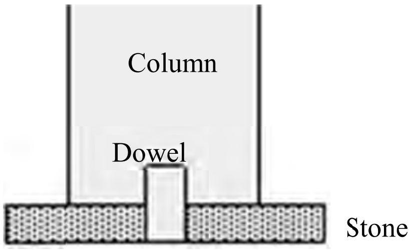

Figure 4: The specification of a column base in all specimens

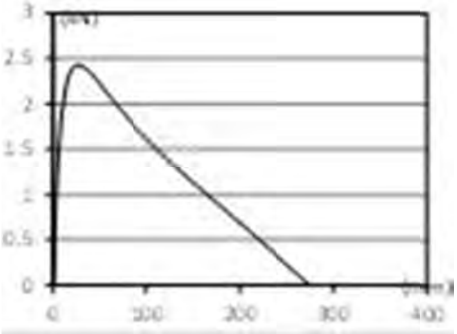

(a) The characteristic of a previous research

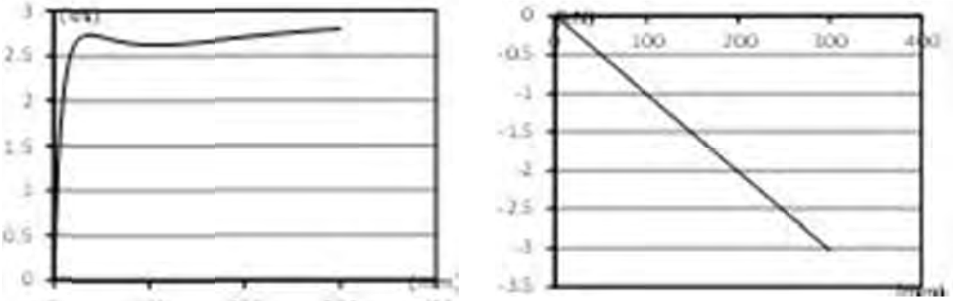

(b) The characteristic of this research

(c) p-δ effect

Figure 5: Analysis model

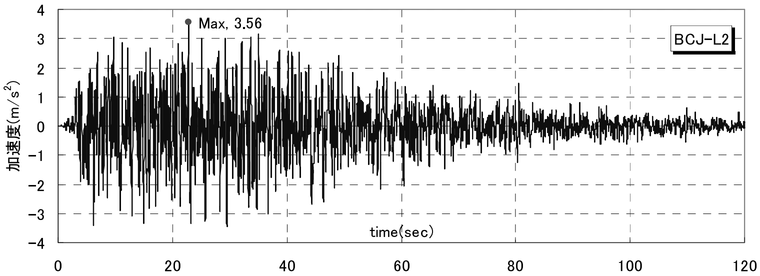

Figure 6: Original input wave

2.2.2 Comparison with experimental results

We compared the analysis results to shaking table test ones. The load displacement relationship of whole frames in all specimens was described in Figure 8. Analysis results almost corresponded with experimental results in any specimen. The maximum horizontal displacement and shear force at the top of a frame were almost same.

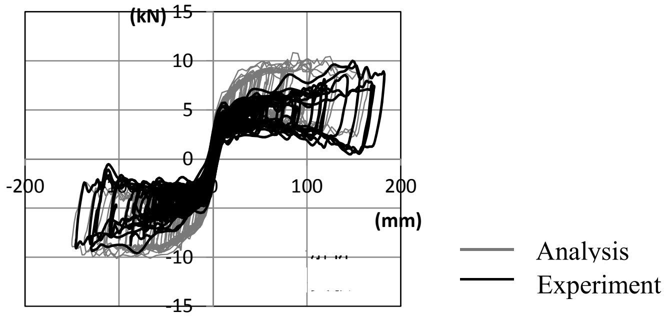

Specimen 1

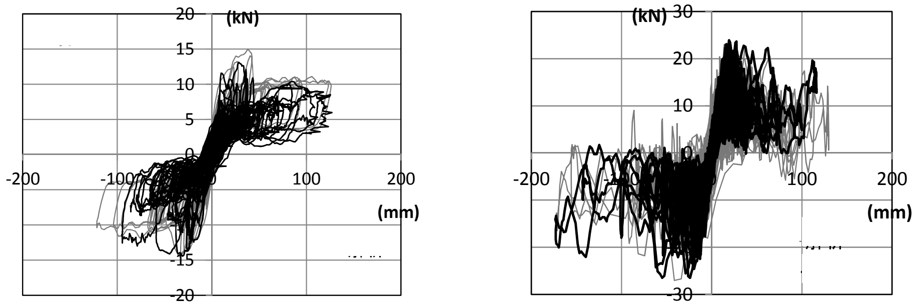

Specimen 2

Specimen 3

Figure 7: The relationship between load and displacement of all specimens

3. PARAMETRIC ANALYSIS

3.1 The influence of columns base condition

In the experiment of Specimen 3, a column base went up. However in the experiment of the other specimens, specimen 1 and 2, the uplift of a column base was no seen. In this paragraph, we consider the difference of seismic behavior depending on the condition of a column base.

We made a model (Model A) changed the condition of a column base in Specimen 3. We assumed that a column base in the analysis model of Specimen 3 did not go up. The other condition of analysis models was same. The analysis model of Specimen 3 calls Model 3.

The analysis results of Model A were compared with ones of Model 3. Figure 8 shows the relationships between load and displacement about a whole frame and *Kumimono*. The displacement of a whole frame in Model A was smaller than Model 3. The maximum load of Model A was larger than Model 3. The shear displacement of *Kumimono* in both models was almost same. Figure 9 described the seismic behavior at the maximum horizontal displacement of a top in a frame. The seismic behavior was a different tendency in both specimens. In Model A, the parts of *Kumimono* deformed by shearing independently of a wall frame. On the other hand, *Kumimono* deformed with a wall frame in Model 3.

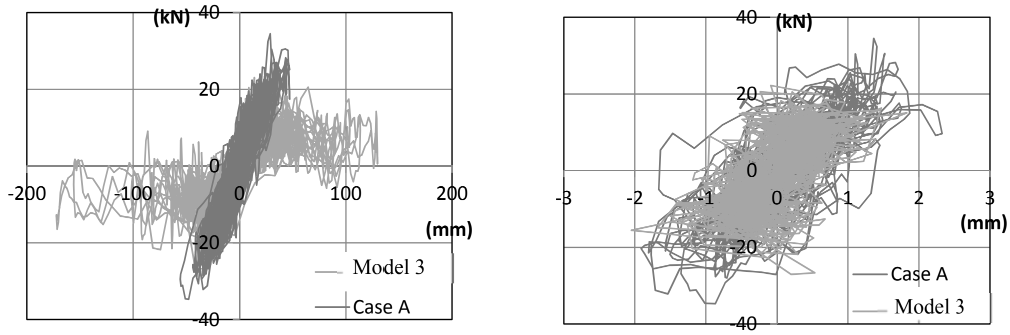

Whole frame

Kumimono

Figure 8: The relationship between load and displacement of all specimens

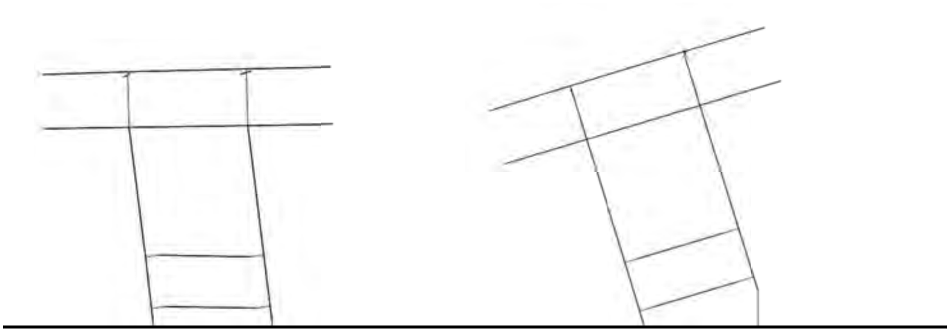

Case A

Model 3

Figure 9: The relationship between load and displacement of all specimens

3.2 The influence of wall strength

In the experiment of Specimen 2, the collapse of mud walls was observed and the shear force of the whole frame in Specimen 2 decreased around 50mm deformation. In this paragraph, we analyzed with the model having high strength mud walls in order to examine the influence of the wall strength on the seismic behavior of a frame. The analysis model of Specimen 2 shows Model 2. The model of this new analysis calls Case B.

The horizontal displacement of a frame top in Case B became smaller than Model 2 as shown in . It almost halved. The displacement of *Kumimono* in Case B was larger than Model 2. The form of the load displacement relationship of Case B was swollen. The rotation angle at a *Koshinuki* column joint in Case B was smaller than Model 2 as shown in Figure 10.

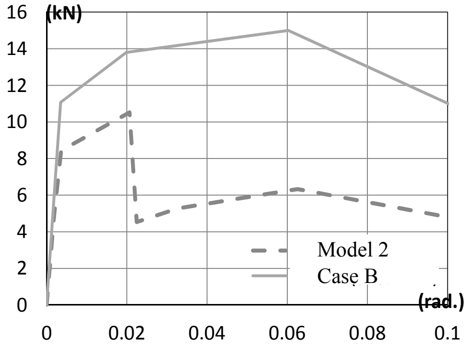

Figure 10: The restoring force characteristic of a mud wall

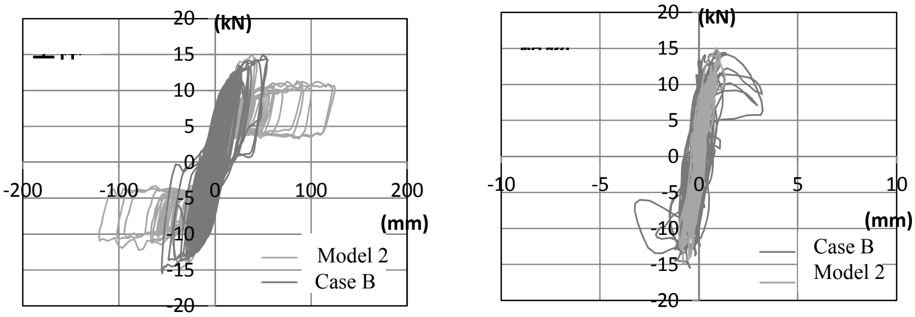

Figure 11: The restoring force characteristic of a mud wall

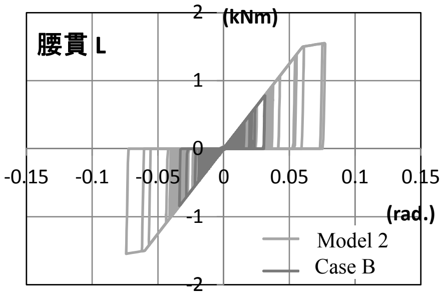

Figure 12: The restoring force characteristic of a mud wall

4. CONCLUSIONS

The analysis model of three kinds of timber frames was improved. We examined the effect of a column base condition and the strength of a wall on the seismic behavior of frames.

When the uplift of a column base is not allowed like the case of Case A, the shear resistant force of a wall was effective. The shear deformation of a whole frame became smaller. When mud walls have high strength like Case B, the tendency of seismic behavior was similar to Case A. The horizontal displacement of a whole frame in Case B became smaller compared to Model 2. On the other hand, one of

Kumimono was larger in the case of Case B. It can be seen that the shear deformation at the parts of Kumimono become larger when the shear force of a part of frame under Kumimono is high.

REFERENCES

AIJ, 2013, *AIJ Standard for the structural calculation of traditional wooden buildings by the calculation method of response and limit strength*, pp.71 (in Japanese).

Ban, S., 1942. A study on the determination of the stability about main hall structures, Vol. 3: a mechanical study on the Japanese Traditional Frame, 1, the stability restoring force of a column. *Papers of annual meeting of Architectural Institute of Japan,* March, 252-258 (in Japanese).

Inayama, M., 1991. The theory of compression perpendicular to the grain in wood and its application, Dissertation of the University of Tokyo (in Japanese).

Kawai, N., 1992. A study on the structural stability of traditional timber structures, *Report of the Building Center of Japan*, March (in Japanese).

Murakami, M., and Inayama, M., 2006. Formulae to predict the elastic and plastic behaviour of sheathed walls with any nailing arrangement pattern, *Journal of structural and construction engineering* 519, 87-94 (in Japanese).

Nakagawa, T., and Ohta, M., 2010. Collapsing process simulations of timber structures under dynamic loading III: Numerical simulations of the real size wooden houses. *Journal of Wood Science* 56, 284-292.

Tsuwa, I., 2014. The difference of seismic behavior by the combination way of earthquake resistant elements in traditional timber buildings, - an example of fifth storied pagoda-, Dissertation of the University of Tokyo (in Japanese).

Tsuwa, I., and Koshihara, M., 2009. Shaking table tests of traditional timber frames including Kumimono - Modeling of horizontal resistance force -, USMCA 2009.

Tsuwa, I., and Koshihara, M., 2011. A study on the effect of wall stiffness on the vibration characteristics of traditional timber frames including *Kumimono*, USMCA 2011.

Tsuwa, I., and Koshihara, M., 2011. Modeling and earthquake response analysis of traditional timber frames including Kumimono, USMCA 2103.

Effect of heterogeneity on the corrosion of rebar embedded in concrete

Nozomu SOMEYA[1] and Yoshitaka KATO[2]
[1]Doctoral Student, Department of Civil Engineering,
Graduate School of Science and Technology, Tokyo University of Science, Japan
someya0910@yahoo.co.jp
[2]Associate Professor, Department of Civil Engineering,
Faculty of Science and Technology, Tokyo University of Science, Japan

ABSTRACT

In this study, corrosion of steel reinforcement (rebar) was induced in concrete with varying chloride ion concentrations and varying material permeability, and the effect of heterogeneous chloride ion exposure on the rebar corrosion was examined. When the chloride ion concentrations in the two halves of the specimen were 10% and 0%, the corrosion current density in the portion with 10% tended to increase and became around $2.0\mu A/cm^2$*, whereas in the portion with 0% the corrosion current density became around* $0.8\mu A/cm^2$*. For the corrosion reaction, the 10% portion became the anode and the 0% portion became the cathode. The results also confirmed the tendency of localized corrosion in the rebar under the heterogeneous exposure.*

Keywords: corrosion, heterogeneous, chloride ion concentrations, varying material permeability

1. INTRODUCTION

Patching repair of polymer cement mortar (hereafter PCM) is used to repair reinforced concrete structures that have deteriorated due to chloride induced corrosion. In this case, the half-cell potential of the unrepaired part is lower than that of the repaired part, because the potential in the patched area is noble (cathode) with a lower chloride ion concentration and the not-patched area is less noble (anode). As a result, a corrosion circuit current occurs again owing to the difference in potential between the patched area and not-patched area. Re-deterioration within the not-patched area around the patched area is known to occur in existing structures1) (see Fig. 1).

Macrocell corrosion generally causes severe corrosion, and so has a major influence on structures. In order to measure the actual macrocell corrosion current passing through steel bars, a segmented steel bar is used2). However, the existing structures are shunted with other rebars, and so it is difficult to measure only the electric current of the point where macrocell corrosion occurs.

In this study, the macrocell corrosion of steel rebar was induced in concrete with varying chloride ion concentrations and varying material permeability, and the effect of heterogeneous chloride ion exposure on the rebar macrocell corrosion was examined by electrochemical measurements.

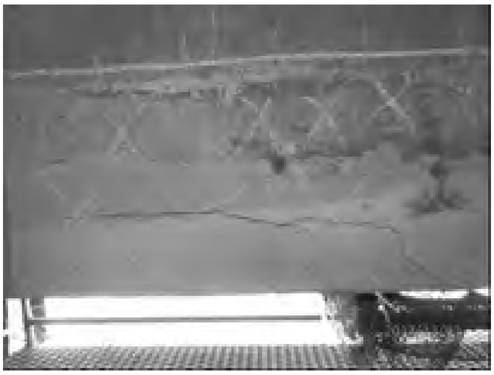
Figure 1: Macrocell corrosion

2. EXPERIMENTAL

2.1 Specimens

Corrosion of steel rebar was induced in concrete with varying chloride ion concentrations and varying material permeabilities, and the effect of heterogeneous chloride ion exposure on the rebar corrosion was examined. Concrete was made with ordinary Portland cement (density: 3.15 g/cm^3, Blaine fineness: 3320 cm^2/g). The fine aggregate was river sand (density: 2.64 g/cm^3, fineness modulus: 2.75) while the coarse aggregate was crushed sandstone with Gmax of 20 mm (density: 2.72 g/cm^3, fineness modulus: 6.61).

The concrete mix proportion is shown in Table 1. The slump of fresh concrete was 10±2.5 cm and the air content was 4.5±1.5%. The PCM was made with premixed polymer cement mortar and water, using 25 kg of premixed polymer cement mortar and 3.5 kg of water. The chloride ion concentrations in the specimen were 0% and 10% by weight of water (chloride ion concentration of concrete unit volume 0 and 16.5 kg/m^3). The steel rebar (SS400) was 16 mm in diameter and 250 mm in length, and the embedded area of the electrode was 125.6 cm^2. The rebars were integrated electrically through connection with lead wires.

The specimen is illustrated in Fig. 2. Corrosion of steel rebars was induced in concrete with the chloride ion concentration in the two halves of the specimen being either 10% or 0% (hereafter NaCl 0–10%) and the material permeability in the two halves of the specimen was OPC or PCM (hereafter OPC-PCM). Specimens including steel rebar prisms of 100×100×400 mm with a concrete cover of 20 mm were prepared. The specimens were demolded and cured for 14 days in water, then coated with epoxy resin except for the surface to be exposed to the immersion solution.

The specimens with chloride ion concentrations were cured for 14 days in NaCl 10% water. The specimens were exposed to 14 cycles of wet-dry exposure, consisting of submersion in NaCl 10% water for 3 days followed by drying for 4 days per cycle.

Table 1: Concrete mix proportions

W/C (%)	s/a (%)	(kg/m^3)				AE (C*%)	Ad (C*%)
		W	C	S	G		
60	45	165	275	835	1051	0.35	0.3

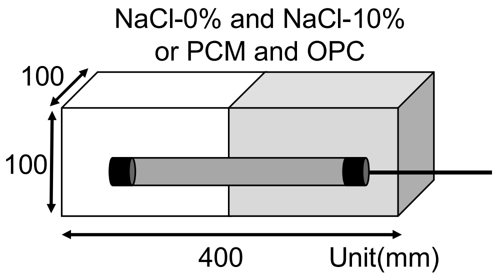
NaCl-0% and NaCl-10%
or PCM and OPC
100
100
400
Unit(mm)

Figure 2: Test specimens

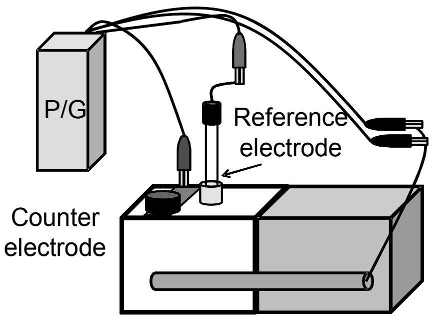
P/G
Reference electrode
Counter electrode

Figure 3: Measuring device

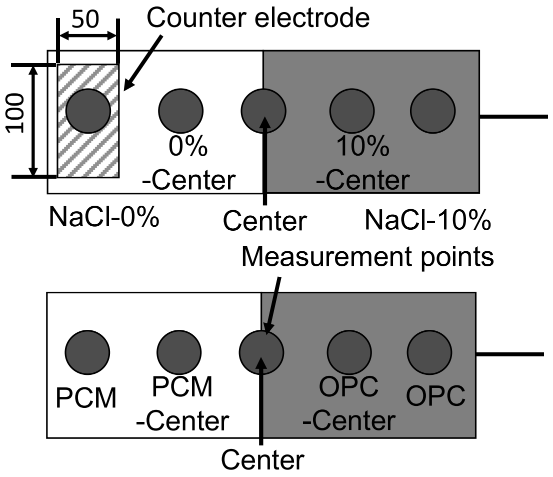
50
Counter electrode
100
0%
-Center
10%
-Center
NaCl-0%
Center
NaCl-10%
Measurement points
PCM
PCM
-Center
OPC
-Center
OPC
Center

Figure 4: Measurement points

2.2 Measurement

Potentiometric titration, potential and polarization curves were measured. Stainless steel of 100×50 mm was used as a counter-electrode. The ionic contact with Ag/AgCl (SSE) used as a reference electrode. Measurements were conducted using a potentio-galvanostat (P/G) and FRA, as shown in Fig. 3. Location and abbreviation of the measurement points are shown in Fig.4.

(1) Potentiometric titration
The total amount of chloride ions contained in the concrete samples was measured by potentiometric titration according to JIS A.1154. The concrete samples were collected from mortar at varying distances from the exposure, up to 40 mm, using the drill method every 5 mm.

(2) Half-cell potential
The half-cell potential was measured at the time of measuring the polarization curve.

(3) Polarization curves
The scan was started at the half-cell potential to the cathodic limit, and was conducted in the anodic direction until reaching the anodic limit. In addition, the polarization curve excluding the resistance of the concrete was obtained by considering the decrease in voltage. As a results, the cathodic curve and anodic curve were obtained.
The relationship between electric current and voltage for the anode and cathode can be expressed by Equation (1). Then, the coefficients in Equation (1) were calculated using

the measurement results. The corrosion current can be obtained from the point of intersection of the two lines.

$$\eta = a + b \log i \tag{1}$$

Where, η: Overvoltage (mV), i: Current density (μA/cm^2), a, b: Fixed number peculiar to an electrode reaction, (mV) (mV/decade),

3. RESULTS AND DISCUSSIOn

3.1 Total chloride ion concentration

The measurement results of the total chloride ion concentration in W/C = 60%, OPC, and 14 cycles of wet-dry exposure are shown in Fig. 5. When looking at the region of 20 mm, the chloride ion concentration was 2.07 kg/m^3. The C_{lim} of W/C = 60% in this experiment is 1.6 kg/m^3, following the 2012 JSCE Standard Specification for Concrete Structures[4)]. This result suggests that corrosion occurred in the concrete cover of 20 mm.

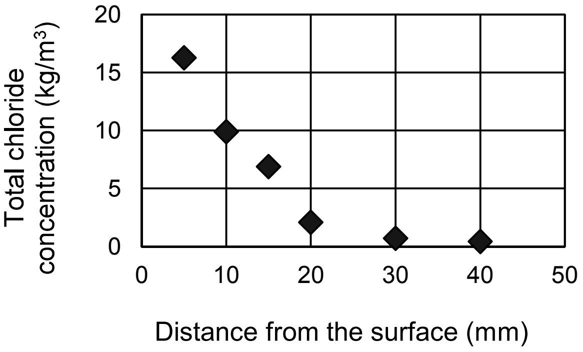

Figure 5: Chloride penetration profiles in concrete

3.2 Half-cell potential

Figures 6 and 7 show the evolution of the half-cell potential. Figure 6 shows that NaCl 0–10% shifted to slightly less noble in the range of −500 to −600 mV. After 10 cycles, stable potential readings were close to −400 mV. This study focused on the stable potential values below −500 mV after about 8 cycles. From the ASTM Standard Test Method[5)] (E ≤ −230 mV vs. SSE), it is thought that the corrosion of rebars has a probability of more than 90%.

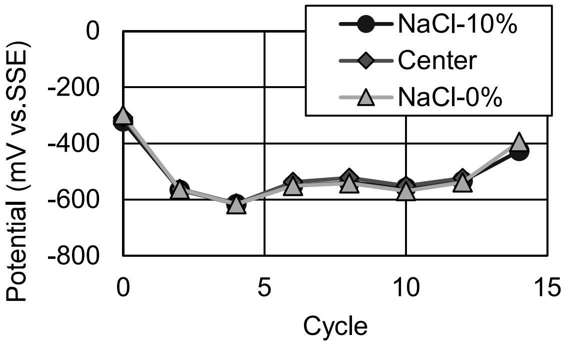

Figure 6: Half-cell potential (NaCl 0-10%)

Figure 7 shows the results for the evolution of half-cell potential looking at OPC-PCM. In this figure, the experimental results show that the OPC-PCM shifted to slightly less noble in the range of −300 to −400 mV. From the ASTM Standard Test Method[5)] (E ≤ −230 mV vs. SSE), it is thought that the corrosion of rebars has a probability of more than 90%.

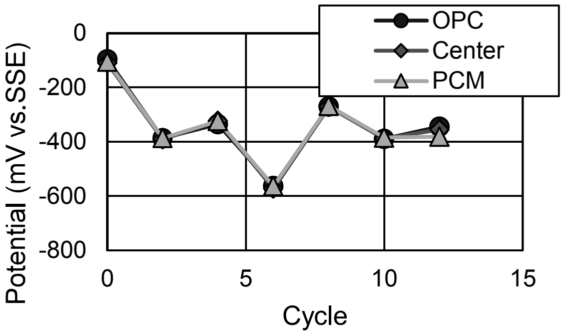

Figure 7: Half-cell potential (OPC-PCM)

Figure 8 shows the results of the half-cell potentials for the locations of the measurement points after 14 cycles. The half-cell potential of NaCl 0–10% of the measurement point locations of 250 mm and 350 mm was −395 mV and −427 mV. The half-cell potential difference became around 30 mV. It is thought that NaCl 10% at the measurement point location of 350 mm presents a more negative half-cell potential than the passive measurement points and therefore corrosion of rebars is expected. The half-cell potential difference between maximum and minimum in the case of OPC-PCM was around 40 mV. And the half-cell potential at the center part shows the most negative value. This result confirmed that the corrosion of steel rebars was induced in concrete with varying chloride ion concentrations and varying material permeability, but it is difficult to judge the corrosion point.

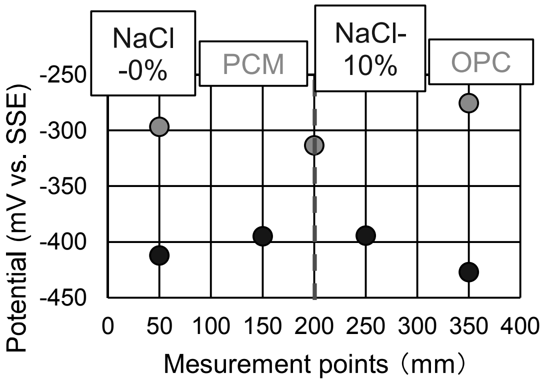

Figure 8: Half-cell potential（NaCl 0-10%，OPC-PCM，14cycle）

3.3 The corrosion current density

Next, from the half-cell potential results, the stable potential values after about 8 cycles are considered. Figures 9 and 10 show the results of the evolution of corrosion current density. Figure 8 shows that the corrosion current density of NaCl-0% remained in the range of 0.8–2.0 μA/cm^2. However, the corrosion current density of 10%-Center increased and decreased and reached 4.2 μA/cm^2. The corrosion current density 0%-Center and 10%-Center at cycle 14 were 2.0 μA/cm^2 and 0.8 μA/cm^2, respectively. Regarding the corrosion reaction, the NaCl-10% and the 0%-Center at 14 cycle became the anode and the cathode. The results also confirmed the tendency of localized corrosion in the rebars under heterogeneous exposure. From CBE[6)] (1.0 μA/cm^2 ≤ corrosion current density), it is thought that the corrosion of rebars was severe.

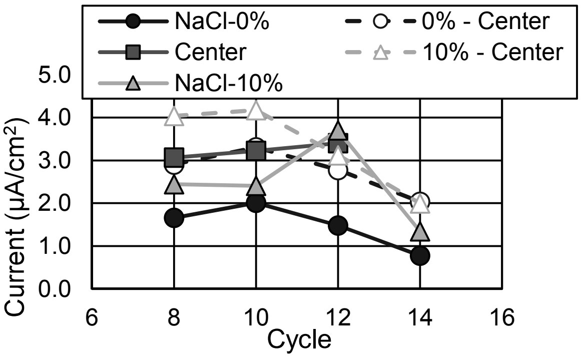

Figure 9: Corrosion current density (NaCl-0%)

Figure 10 shows the OPC-PCM when the corrosion current density became around 1.3 μA/cm^2. The OPC-Center at 14 cycle of the corrosion current density became around 1.2 μA/cm^2. This result suggests that for concrete with Cl$^-$, the maximum value of macrocell corrosion was located in the joint and its surrounding. Because the difference of the corrosion current density was small, it is necessary to perform further measurements in future.

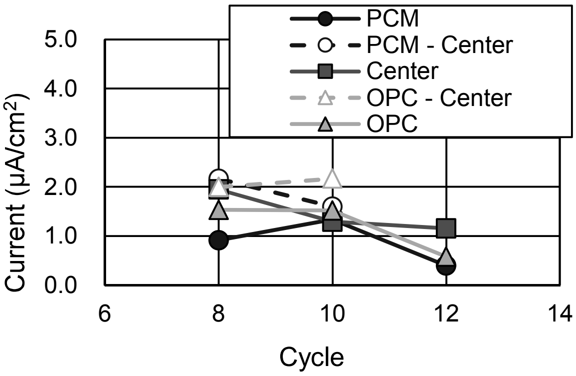

Figure 10" Corrosion current density (OPC-PCM)

Figure 11 shows the results of the corrosion current density at the locations of measurement points after the 14th cycle. When the chloride ion concentrations in the two halves of the specimen were 10% and 0%, the corrosion current density of the portion with 0% (50 mm) was around 0.8 µA/cm^2. The corrosion current density of the portion at 150 mm and 250 mm was around 2.0 µA/cm^2. The results also confirmed the tendency of localized corrosion at the joint and its surrounding. The difference in corrosion current density of OPC-PCM was around 1.1 µA/cm^2. It followed that corrosion progressed near the edge part. The results also confirmed the tendency of localized corrosion in the rebars under heterogeneous exposure.

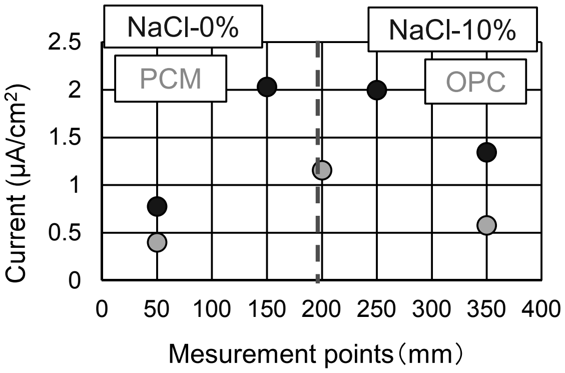

Figure 11: Corrosion current density
（NaCl 0-10%，OPC-PCM，14cycle）

4. CONCLUSION

In this study, corrosion of steel rebars was induced in concrete with varying chloride ion concentrations and varying material permeability, and the effect of exposure to heterogeneous chloride ions on rebar corrosion was examined.

(1) The potential difference of NaCl 0-10% and OPC-PCM was around 30 to 40 mV. This result confirmed that corrosion of steel rebar was induced in concrete with varying chloride ion concentrations and varying material permeability, it was difficult to judge the corrosion point.
(2) When the chloride ion concentrations in the two halves of the specimen were 10% and 0%, the corrosion current density in the portion with 10% tended to increase

and became around 2.0 μA/cm^2, whereas that in the portion with 0% became around 0.8 μA/cm^2. For the corrosion reaction, the 10% portion became the anode and the 0% portion became the cathode. The results also confirmed the tendency of localized corrosion in the rebar under heterogeneous exposure.

REFERENCES

ASTM C 876-91, Reapproved 1999. Standard test method for half-cell potentials of uncoated reinforcing steel in concrete, *Annual Book of ASTM Standards* Vol.03.02, 457-462.

CBE Bulletin No. 243, 1998. *Strategies for testing and assessment of concrete structures affected by reinforcement corrosion*.

Japan Society of Civil Engineers (JSCE). 2012. *Standard specifications for concrete structures -2012, Design*.

Katsuya, T. Takehiro, M. Manabu, I., and Toshiharu, K., 2012. Study on repaired concrete by electrochemical Inspection under marine environment for 10 years. *Proceeding of the Japan Concrete Institute* 34, 1750-1755 (in Japanese).

Shigeyoshi, N. Nobuaki, O. Atsurou, M., and Shinichi, M., 1996. The experimental study on corrosion mechanism of reinforced concrete at local repair part. *Proceeding of Japan Society of Civil Engineers (JSCE)* V-32, 109-119 (in Japanese).

Shiro, H. 2012. Electrochemistry for surface engineers. Maruzen Shuppan (in Japanese).

Influence of magnesium ion and sulfate ion on Chloride Permeability of Concrete

Keigo HORI[1] and Yoshitaka KATO[2]
[1]Master Student, Department of Civil Engineering,
Graduate School of Science and Technology, Tokyo University of Science, Japan
j7613618@ed.tus.ac.jp
[2]Associate Professor, Department of Civil Engineering,
Faculty of Science and Technology, Tokyo University of Science, Japan

ABSTRACT

In this study, the effect of seawater ions on the chloride permeability of concrete was experimentally studied by focusing on SO_4^{2-} and Mg^{2+} during immersion in sulfate solutions containing NaCl and $MgCl_2$. The results of chloride ion penetration tests showed that chloride penetration was suppressed in all solutions except NaCl solution. The specimens were immersed in a solution containing a large amount of Mg^{2+}, and suppression of chloride ion penetration due to the formation of brucite suggested that up to 56 days immersion, however, the suppressive effect tended to be reduced at 126 days of immersion. When it was immersed in a solution containing SO_4^{2-}, chloride ion permeability was reduced due to the influence of the void filled with gypsum dihydrate.

Keywords: chloride permeability, sulfate attack, magnesium ion, amount of calcium hydroxide

1. INTRODUCTION

Japan is an island country surrounded by the sea, and therefore many concrete structures are in environments where salt damage may occur due to the penetration of chloride ions from seawater. It is necessary to consider the durability of these concrete structures against salt damage. To evaluate durability, it is important to understand the penetration of chloride ions into concrete (Taketo and Yoshitaka, 2007).

Many studies on the penetration of chloride ions in concrete have focused on only chloride ions (Yuji, 2001). However, the seawater contains various ions such as Mg^{2+} and SO_4^{2-}, so it is necessary to consider the effects of these ions on the penetration of chloride ions.

Coexisting ions in seawater cause an electric effect and deterioration of hardened cement paste, which means that Mg^{2+} and SO_4^{2-} react with CH or C-S-H, and generate brucite and gypsum dihydrate (Yoshida, 2010). Moreover, in natural diffusion, since chloride ions moves together with positive ions, if the diffusion velocity of a cation is larger, the diffusion velocity of chloride ions will also become large (Matsuda, 2005).

To examine the effect of sulfate attack on chloride ion permeability, previous studies used a solution prepared by adding ($MgSO_4$, Na_2SO_4, $CaSO_4$, K_2SO_4) sulfate and NaCl, and performing an immersion test. The solution except $CaSO_4$ caused penetration of chloride ions to be promoted compared with NaCl. It is believed that this is due to sulfate attack, but it is not possible to prove this phenomenon.

This study examined the effects of ions in seawater on the chloride ion permeability of hardened cement paste by immersion tests. Using the distribution of chloride ion concentration obtained from these tests, and the effect of ions in seawater on the chloride permeability was experimentally studied.

Figure 1: Example of salt damage

2. EXPERIMENTAL OUTLINE

2.1 Material and Specimens

Cement used in the experiment is ordinary Portland cement (symbol C, density 3.15 g/cm^3). Aggregates used in the experiment are river sand of Yamanashi Fujikawa production (symbol S, density 2.60 g/cm^3) and crushed stone of Chichibu, Saitama Prefecture production (symbol G, density 2.72 g/cm^3). The mix proportion is shown in Table 1. Specimen was column specimens with φ10 × 12.5cm (see Figure 2).

Table 1: Concrete mix mixture proportion

W/C(%)	**(kg/m^3)**				
	W	**C**	**S**	**G**	**Ad**
50	175	350	795	1001	2.10

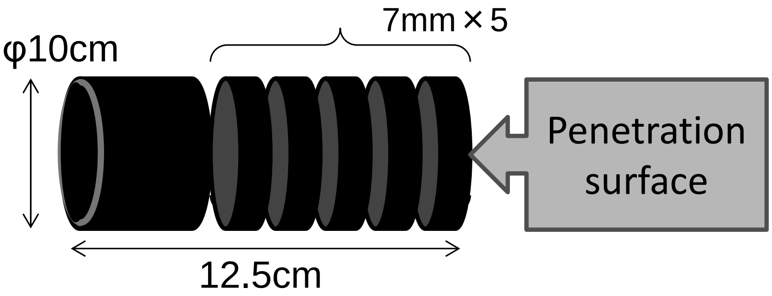

Figure 2: Specimen shape and size

2.2 Experimental conditions

The specimens were cured for 28 days in water after demolding of specimen, and were coated with epoxy resin except the surface to be exposed to the immersion solution. The specimens were then immersed in NaCl aqueous solution or one of five kinds of mixed solution for 28, 56 or 126 days. Many studies have examined the influence of ions in sea water on hardened cement and the diffusion of chloride ions. Cations such as Na^+ and Mg^{2+} affect the diffusion coefficient of chloride ions (Kondo, 1974). The depth to which Mg permeated was defined as the "deterioration depth", and it has been suggested that the depth could be used as an index of the deterioration of concrete (Yamaji, 2007). Therefore, in order to grasp the influence of seawater ions on the chloride permeability of concrete, we focused on Na^+, Mg^{2+}, Cl^-, and SO_4^{2-}. Five kinds of solution were created by combining these; the kind of solution and the concentration of each ion are shown in Table 2.

Table 2: Each ion concentration in the mixed solution

	Cl^-	**Na^+**	**Mg^{2+}**	**SO_4^{2-}**
NaCl(A)	1.90	1.90	-	-
$MgCl_2$(B)		-	0.95	-
$NaCl+Na_2SO_4$(C)		2.09	-	0.10
$NaCl+MgSO_4$(D)		1.90	0.10	
$MgCl_2+MgSO_4$(E)		-	1.04	
Artificial seawater(F)		1.62	0.19	

2.3 Potentiometric titration

An amount of total chloride ion and soluble chloride ion contained in the concrete sample were measured by the potentiometric titration according to JCI-SC4. Concrete sample was collected from part of mortar that the distance from the surface of exposure is the region 0–7mm, 7–14mm, 14–21mm, 21–28 mm and 28–35mm. Cutting image of a specimen is shown in Fig. 2.

2.4 TG-DTA

The specimens were immersed in the various solutions and differential thermal analysis (TG-DTA) measurements were performed, and CH and gypsum dihydrate were quantitatively analyzed. It was quantified that the gypsum dihydrate changed weight from 130 to 160°C, and CH from 450 to 500°C. In order to eliminate the influence of the aggregate, cement paste of the same water-cement ratio was used for the samples.

3. RESULTS AND DISCUSSIONS

3.1 Total chloride ion concentration

The results of measuring total chloride ion concentration after immersion for 126 days in each solution are shown in Fig. 3. The chloride ion concentration in the region of 0–7 mm is larger in the order of NaCl, $MgCl_2+MgSO_4$, $MgCl_2$. In the other solutions (artificial seawater, $NaCl+Na_2SO_4$, $NaCl+MgSO_4$), chloride ion penetration was small. In the region of 7–14 mm, penetration of $NaCl+MgSO_4$ was larger than that of $MgCl_2$;

the result differed from that in the surface layer. Next, in the region of 14–21 mm, $MgCl_2+MgSO_4$ exceeded NaCl, but it was not a significant difference compared with the other solutions. By using the chloride ion concentration distribution shown in Fig. 3, the apparent diffusion coefficient (D_a) and surface chloride ion concentration (C_0) were calculated from a theoretical solution of the diffusion equation of Fick under the condition of constant surface concentration. From the result, the number of years up to the limit concentration (C_{lim}) that causes steel corrosion was estimated, and the ease of penetration of chloride ions was compared. C_{lim} in OPC50 of this experiment was 1.9 kg/m^3, which complies with the Standard Specification for Concrete Structures of 2012. The number of years taken to reach C_{lim} in 5 cm cover concrete was calculated, and the results were as shown in Table 3. NaCl, $MgCl_2$, and $MgCl_2+MgSO_4$ reached C_{lim} earlier than the other solutions.

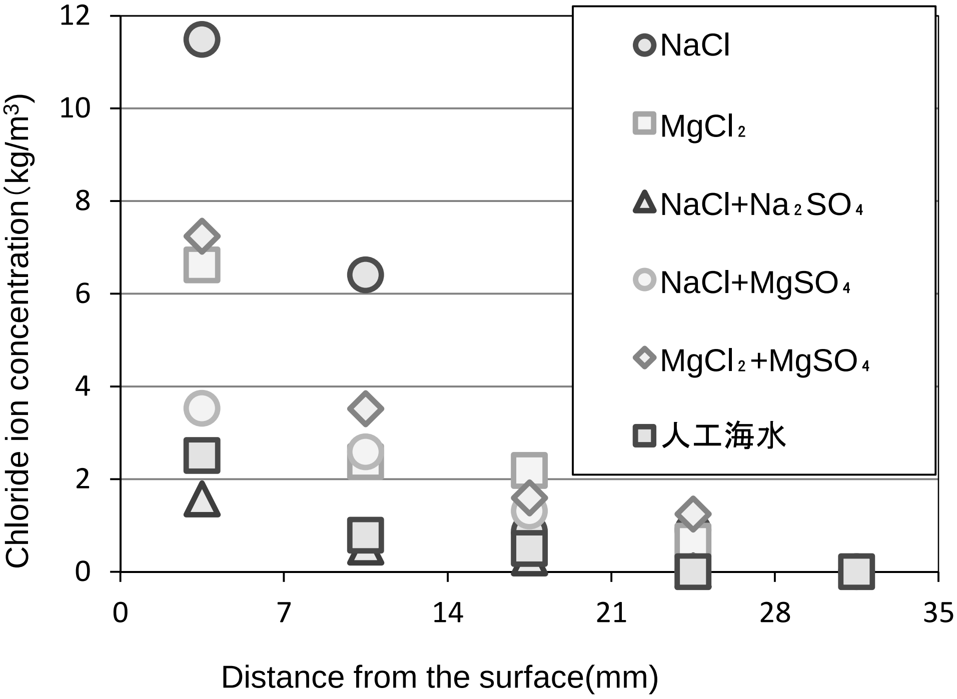

Figures 3: Chloride ion concentration distribution (immersion age = 126 days)

Table 3: Calculation result

Kinds of immersion solution	Diffusion coefficient D_a(cm^2/year)	Surface chloride ion concentration C_0(kg/m^3)	Times (year)
NaCl	1.84	15.8	2.82
$MgCl_2$	2.07	8.62	4.03
$NaCl+Na_2SO_4$	2.18	1.37	343
$NaCl+MgSO_4$	3.15	4.72	5.67
$MgCl_2+MgSO_4$	2.47	9.12	3.20
Artificial seawater	1.27	3.54	25.8

3.2 TG-DTA

Figure 4 shows an example of differential thermal analysis using cement paste. The sample specimen was immersed for 91 days in $MgCl_2$+$MgSO_4$. The thermal change curve and the weight change curve are shown in Fig. 4. The peak of 130–160°C of the thermal change curve was considered to be due to drying of gypsum dihydrate. Calcium hydroxide was dehydrated at 450–500ºC, and its chemical reaction was as shown in Equation (1). The weight loss measured by TG-DTA was due to dehydration from CH, so the measured weight loss was considered as the amount of CH.

$$Ca(OH)_2 \rightarrow CaO+H_2O \tag{2}$$

The specimens subjected to differential thermal gravimetric analysis were NaCl (A), $MgCl_2$ (B), MgCl+$MgSO_4$ (E), Artificial seawater (F), and fresh water.

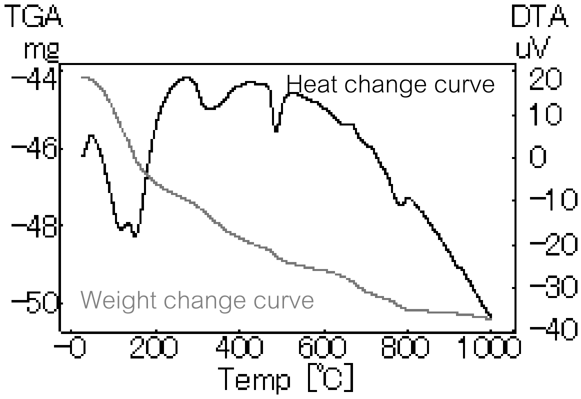

Figure 4: Example of differential thermal analysis

3.2.1 Changes in the amount of CH

The amount of CH per cement paste is shown in Fig. 5. Figure 5 (a) shows the amount of CH after immersion for 28 days; there was no significant change in the amount of CH in any solutions. When immersed for 56 days (Fig. 5(b)), $MgCl_2$+$MgSO_4$ (E) and artificial seawater (F) showed small amounts of CH compared with the other solutions. When immersed for 126 days (Fig. 5(c)), $MgCl_2$ (B) and $MgCl_2$+$MgSO_4$ (E) showed very small values. Next, the variation over time in the amount of CH for each solution was examined. The variation over time when immersed in $MgCl_2$ (B) is shown in Fig. 5 (d). When immersed for 91 days, the amount of CH decreased, and the quantity per cement paste was 3.7%. In $MgCl_2$+$MgSO_4$ (Fig. 5(e)), similarly, the amount of CH decreased over time, and was about 4.8% at 91 days. The change in time of artificial seawater (F) (Fig. 5(f)) could not be checked.

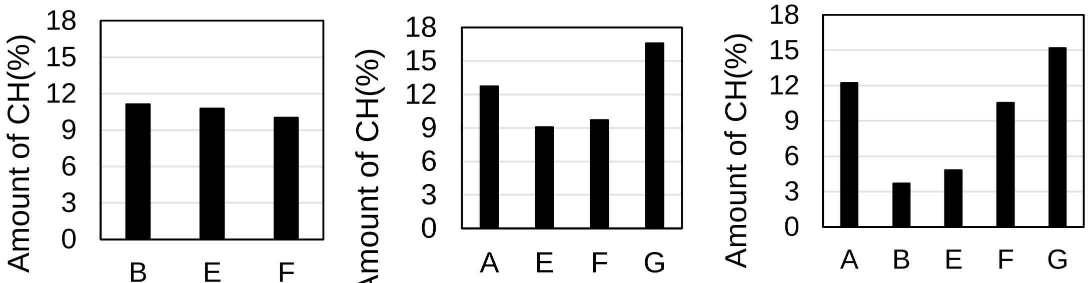

(a) Materials age 28 days

(b) Materials age 56 days

(c))Materials age 91 days

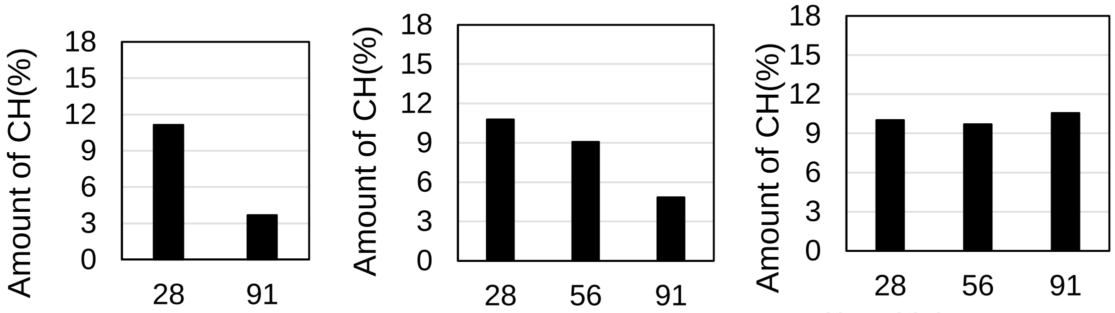

(d) $MgCl_2$

(e) $MgCl_2$+$MgSO_4$

(f) artificial seawater

Figure 5: Amount of CH per cement paste

3.2.2 Changes in the amount of gypsum dihydrate

The amount of gypsum dihydrate per cement paste is shown in Fig. 6. The result for immersion for 91 days is shown in Fig. 6 (a).The average value of gypsum dihydrate in all cases is about 18%, amount of gypsum dihydrate of $MgCl_2$+$MgSO_4$ (E) is about 22%, showing larger values than the other solutions. The variation over time when immersed in $MgCl_2$+$MgSO_4$ (E) is shown in Fig. 6 (b). The amount of gypsum dihydrate increased with increase of immersion period.

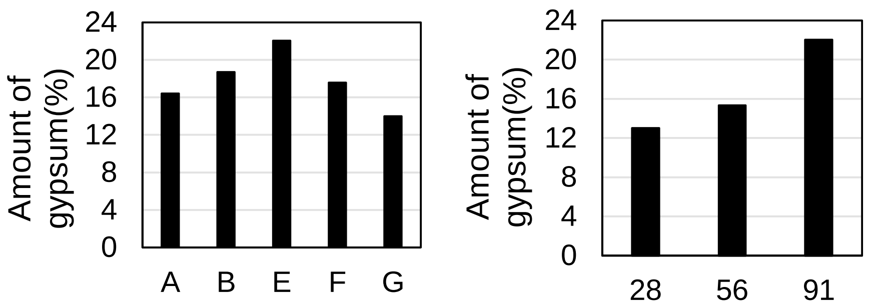

(a) 材齢91日

(b) $MgCl_2$+$MgSO_4$

Figure 6: Amount of gypsum dihydrate per cement paste

3.3 Influence of ions in seawater

Using the result of chloride ion concentration and TG-DTA, each solution was compared in terms of the influence of ions in seawater. NaCl was compared with $MgCl_2$ in order to consider the influence of cations (Fig. 7). To consider the influence of the amount of Mg^{2+}, $NaCl+Na_2SO_4$, $NaCl+MgSO_4$, and $MgCl_2+MgSO_4$ were compared (Fig. 8). To consider the influence of SO_4^{2-}, NaCl and $NaCl+Na_2SO_4$ were compared (Fig. 9).

From the result of Fig. 7, the amount of chloride ion penetration of NaCl was large. To maintain the electro-neutral condition, the same number of cations moved when the chloride ions diffused due to the concentration gradient. If the diffusion coefficient of cations is low, the penetration of chloride ions is suppressed by the electric field (Matsuda, 2005). The diffusion coefficient of Mg^{2+} is smaller than that of Na^+, and so suppression the penetration of chloride ions. From Fig. 8, the amount of penetrated chloride ions increased with the increase in the amount of Mg^{2+}. As the reason for this, ion penetration suppression effect has been demonstrated in the generation of brucite by the action of Mg^{2+} in the early stages, but the increase of gypsum dihydrate and the disappearance of CH progresses over time, affecting the pore structure. It can be surmised that the amount of chloride ion penetration increased due to the reduction of the suppressive effect.

Figure 9 shows that the penetration of chloride ions was suppressed with the solution containing SO_4^{2-}. From the measurement results of TG-DTA, the amount of gypsum dihydrate increased over time in the case of the solution containing SO_4^{2-} (Fig. 6(e)). The resulting volume expansion is expected to have a void filling effect in the initial stage, thus suppressing the chloride ion penetration of a solution containing SO_4^{2-}.

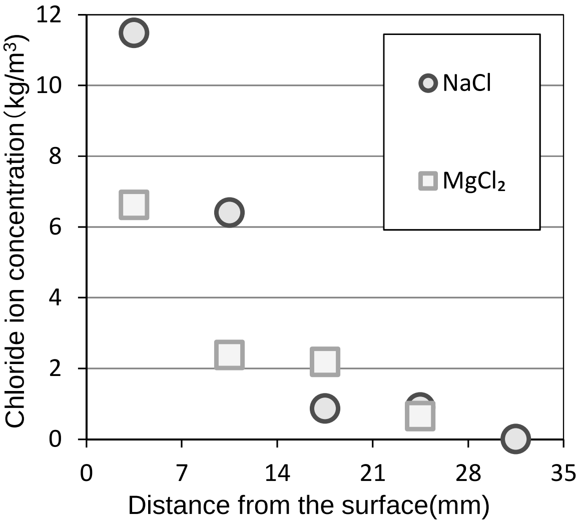

Figure 7: Influence of cation

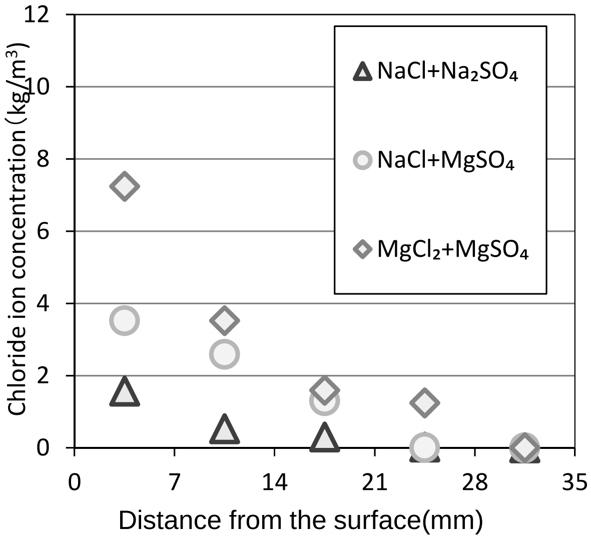

Figure 8: Influence of amount of Mg^{2+}

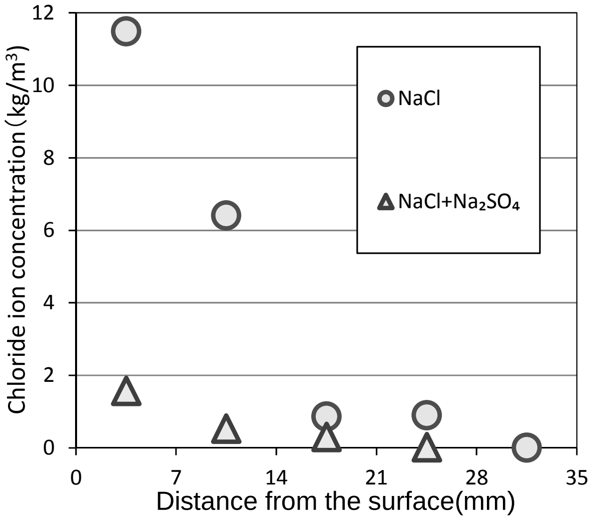

Figure 9: Influence of SO_4^{2-}

Regarding the two kinds of solution, NaCl and $MgCl_2$+$MgSO_4$, which showed quick penetration of chloride ions, the variation over time of chloride ion concentration is shown in Fig. 10 (NaCl) and Fig. 11 ($MgCl_2$+$MgSO_4$). With these solutions, the amount of penetration of chloride ions increases rapidly between 56 days and 126 days of immersion. For these two solutions, the calculation results of C_0, D_a, and T are shown in Table 4. T in NaCl indicates a relatively small value at all immersion periods, but indicates a large value until 56 days in $MgCl_2$+$MgSO_4$, and was smaller at 126 days. There are two reasons why T increased to 56 days of age. One is the effect of ion penetration suppression by brucite, and the other is the void filling effect due to the generation of gypsum dihydrate. However, it can be inferred that the amount of chloride ion penetration is increased by the reduction of suppressive effect to 126 days of immersion.

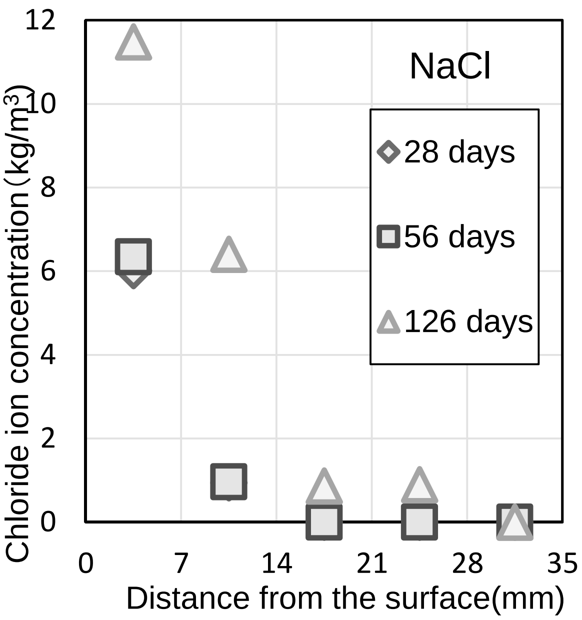

Figure 10: Chloride concentration distribution (NaCl)

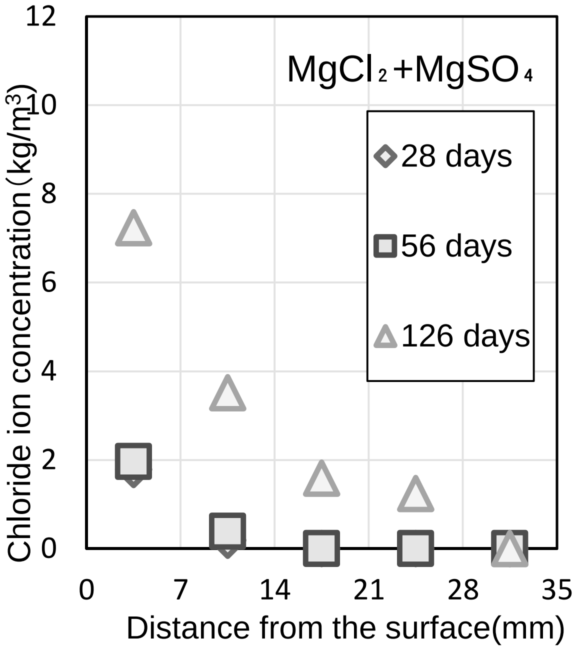

Figure 11: Chloride concentration distribution ($MgCl_2$+$MgSO_4$)

Table 4: Calculation results of C_0, D_a, and T

	28 days	**56 days**	**126 days**
C_0(NaCl)	10.5	11.2	15.8
C_0($MgCl_2$+$MgSO_4$)	3.39	3.26	9.12
D_a(NaCl)	2.48	1.22	1.84
D_a($MgCl_2$+$MgSO_4$)	1.98	1.47	2.47
T(NaCl)	2.80	5.45	2.82
T($MgCl_2$+$MgSO_4$)	18.6	28.2	3.20

4. CONCLUSIONS

The chloride ion penetration properties of specimens immersed in various solutions were examined, and the following results were obtained.

1) With all solutions other than NaCl solution, penetration of chloride ion was suppressed. A strong suppressive effect was demonstrated with the solution containing SO_4^{2-}. The solution containing a large amount of Mg^{2+} showed reduced suppression effect from 56 to 126 days of immersion.
2) Mg^{2+} and SO_4^{2-} reacted with the cement hydrate, and these reactions caused the formation of gypsum dihydrate and consumption of CH.

In future, the impact on cement hydrate and electrical effects of ions in seawater should be examined.

REFERENCES

Chiba, T., Mita, K., and Kato, Y., 2013. *Influence of coexistent ions in seawater on the chloride permeability of concrete*, New Technologies for Urban Safety of Mega Cities in Asia, No.34.

Hidetoshi, E., 1988. Study on protection against corrosion and corrosion of rebar in concrete using the artificial seawater. *Japan Concrete Institute* 10, 499-504.

Kazusuke, K., 2011 *Deterioration diagnosis method of the concrete structure by coring*, Morikita Shuppan (in Japanese).

Kouki, M., 2005. Influence of cations on the diffusion of chloride ions in the mortar. *Japan Society of Civil Engineers* 28, 2.

Natsuki, Y., 2010. *Deterioration of concrete due to crystal formation of sodium sulphate*, Tokyo Institute of Technology dissertation.

Renichi, K., 1974. Ion diffusion of hardened cement paste, *Cement technology annual report*, 58-61.

Taketo, U., and Yoshitaka, K., 2007. *Materials design of concrete structures*. Ohmsha (in Japanese).

Toru, Y., 2007. A study on the degradation index and simple deterioration situation of concrete that has been immersed in seawater for long term, *Port and Airport Research Institute Technical Report*, No.1150.

Yuji, T., 2001. Experiments on the chloride ion penetration mechanism of cement paste. *Japan Concrete Institute* 23, 505-510.

Progressive collapse analysis of reinforced concrete frame buildings

Su Wint YEE
Ph.D Student, Department of Civil Engineering, Yangon Technological University
suwintyeeko@gmail.com

ABSTRACT

The reinforced concrete frame buildings with simple geometry are considered to study progressive collapse analysis for the fact that these buildings are remarkably more than the total number of steel structures in Yangon City, Myanmar. The progressive collapse of a building is initiated when one or more critical load carrying members are removed by man-made or natural hazards. It is a situation where local failure of a primary structural component leads to the collapse of adjoining members, which in turn leads to additional collapse. Hence, the extent of total damage is disproportionate to the original cause. Although historical data indicate that the risk of progressive collapse in buildings is very low, loss of life and severe injuries would be significant when a fully occupied multi-story building sustains a large partial or total collapse. The nonlinear static analysis (pushdown analysis) by Sap2000 software simulation is used to capture initial yielding and gradual progressive plastic behavior of elements and overall building response under column removal excitations in this study. According to limitations in GSA guidelines, the structure damaged by the removal of structural members will be analyzed to state the condition that it can survive or not from the progressive collapse due to a hazard condition. A three-story reinforced concrete frame is analyzed with and without flooring and also a six-story without flooring is considered. Then analysis results, significant deflections and progressive collapse assessment of these frames are presented for various progressive collapse cases. The study of the performance and collapse of a structure for abnormal loading conditions of natural or man-made hazard would help to improve design consideration and planning for disaster preparedness, mitigation and resilience of infrastructures in a city.

Keywords: progressive collapse, reinforced concrete, Sap2000, pushdown analysis, GSA guidelines.

1. INTRODUCTION

The design philosophy of structures subjected to abnormal loads is to prevent or mitigate damage, not necessarily to avoid the collapse initiation from specific cause. Whereas resistance to progressive collapse is primarily an issue of gravity load-carrying capacity, the design of elements (beams, columns) also depends on demands from seismic or wind actions. For structural members, the larger load-bearing capacity due to more severe gravity load actions considered in design, the higher capacity to prevent progressive collapse.

Progressive collapse is defined as a situation where local failure of a primary structural component leads to the collapse of adjoining members, which in turn leads to additional collapse. Thus, “progressive collapse” is an incremental type of failure where in the total damage is out of proportion to the initial cause.

The concept of progressive collapse can be illustrated by the famous 1968 collapse of the Ronan Point apartment building (Fig. 1). The structure was a 22-story precast concrete, bearing wall building. A gas explosion in a corner kitchen on the 18th floor blew out the exterior wall panel and failure of the corner bay of the building propagated upward to the roof and downward almost to ground level. Thus, although the entire building did not collapse, the extent of failure was disproportionate to the initial damage.

Immediately following the Ronan Point collapse, some countries, such as the U.K. and Canada adopted some form of regulatory standards to address prevention of progressive collapse. In the 1980s, design standards in the U.S. began to incorporate requirements for “general structural integrity” to provide nominal resistance to progressive collapse.
The General Services Administration (GSA) of United States of America published “Progressive Collapse Analysis and Design Guidelines for New Federal Office Buildings and Major Modernization Project” in 2000. The method discussed in the GSA publication is normally used for buildings 10 stories above grade and less, but can be applied to taller buildings.

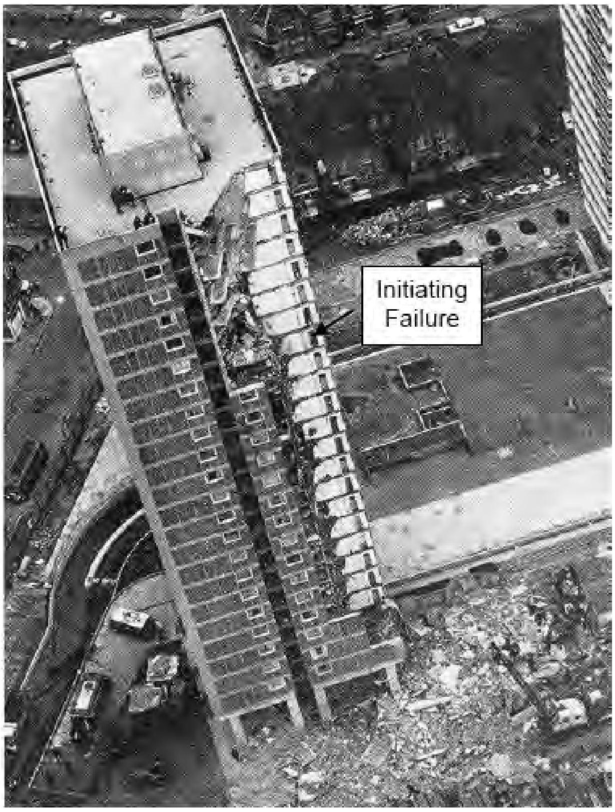

Figure 1: Ronan Point collapse: a gas explosion on the 18th floor resulted in a progressive collapse

2. METHODOLOGY AND MODEL DEVELOPMENT

2.1 Progressive Collapse Assessment According to GSA Guidelines

2.1.1 Exterior Consideration

a) Case one: Analyze for the instantaneous loss of a column for one floor above grade (1 story) located at the corner of the building.

b) Case two: Analyze for the instantaneous loss of a column for one floor above grade (1 story) located at or near the middle of the short side of the building.

c) Case three: Analyze for the instantaneous loss of a column for one floor above grade (1 story) located at or near the middle of the long side of the building.

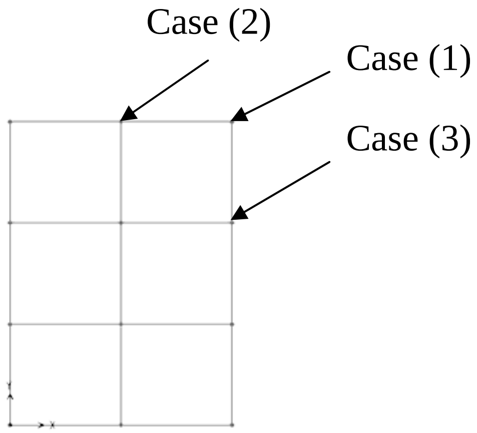

Figure 2: Plan view of exterior consideration for progressive collapse analysis

2.1.1 Interior Consideration

a) Case four: Analyze for the instantaneous loss of a column that extends from the floor of the underground parking area or uncontrolled public ground floor area to the next floor (1 story). The column considered should be interior to the perimeter column lines.

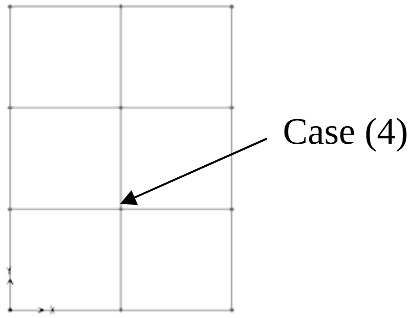

Figure 3: Plan view of interior consideration for progressive collapse analysis

2.2 Pushdown Analysis

Steps for creation model in pushover analysis are-

i. The basic model is analyzed and designed under normal design load condition without pushdown data.
ii. Define properties and acceptance criteria for the hinges. Default hinge properties are based on average values from ATC 40 and FEMA 356.
iii. Locate the hinges on the model.
iv. Define the pushdown load cases. Typically, the first pushover load case is used to apply gravity load and then subsequent lateral pushover load cases are specified to start from the final conditions of the gravity pushover. In this study, 2DL + 0.5LL will be applied vertically with force control for progressive collapse analysis.
v. Run the static nonlinear pushdown analysis.
vi. Review the pushdown displaced shape and sequence of hinge formation on step-by-step. Hinges appear when they yield and are color coded based on their state.
vii. Joint displacements, frame member forces and state at each step can be obtained for selected elements.

2.3 Input Data for Analysis

f'_c = 2500 psi & f_y = 40000psi
Beam Size = B9x12
Column Size = C12x12
Unit weight of concrete = 150 pcf
4-1/2inch thick Brick wall = 50 psf
Superimposed Dead Load on floor = 20 psf
Typical Floor Live Load =40 psf
Normal load combination = 1.4 DL + 1.7LL
Abnormal load combination = 2DL + 0.5LL
Column Spacing = 12ft

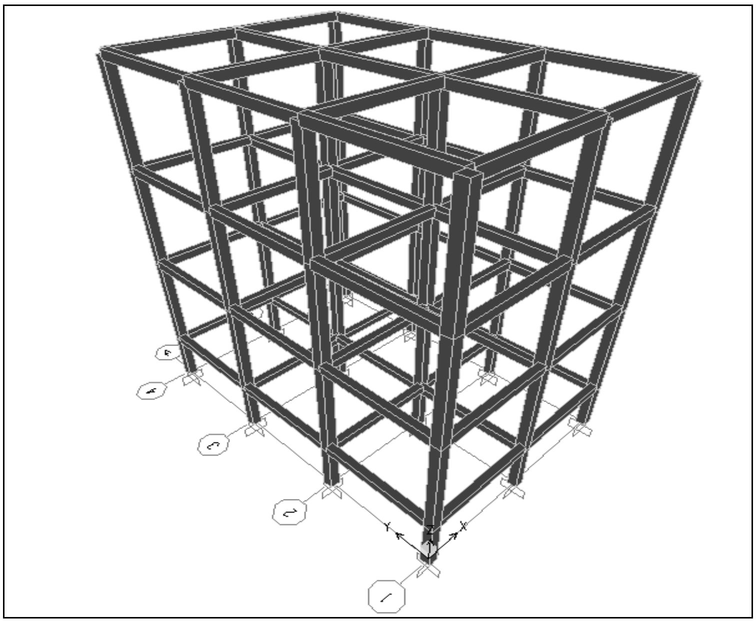

Figure 4: Three-story reinforced concrete frame model

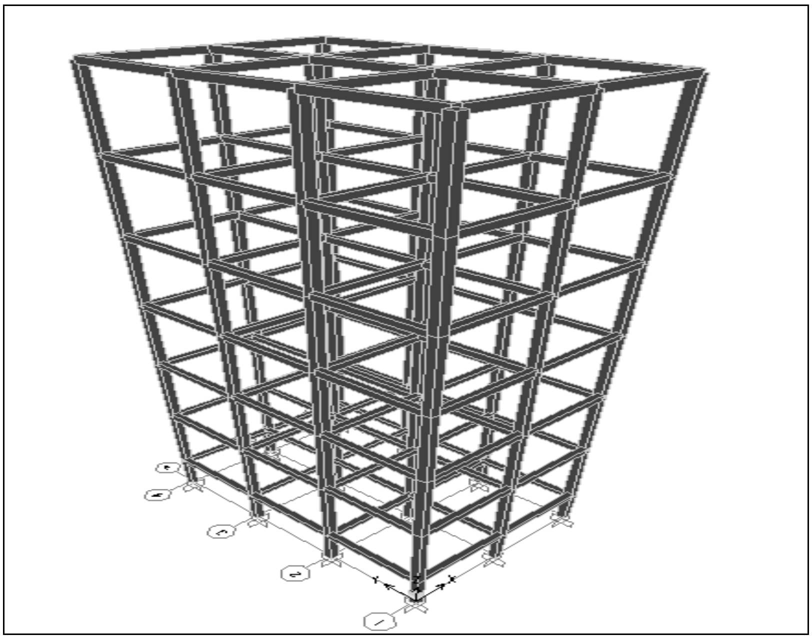

Figure 5: Six-story reinforced concrete frame model

3. RESULTS AND DISCUSSION

3.1 Significant Displacements

The significant displacements of joints which are above the removed column are almost same and severe for all floors. They are shown in Figure 6, Figure 7 and Figure 8 for each step of analysis and cases of the frames.

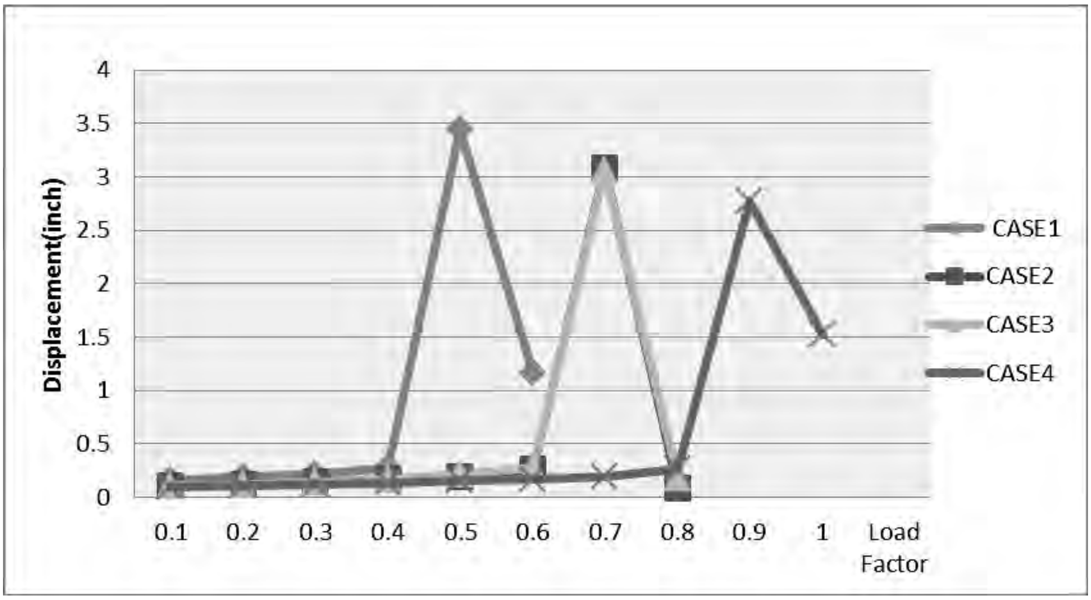

Figure 6: Significant deflections of a joint for four cases in three-story frame without flooring

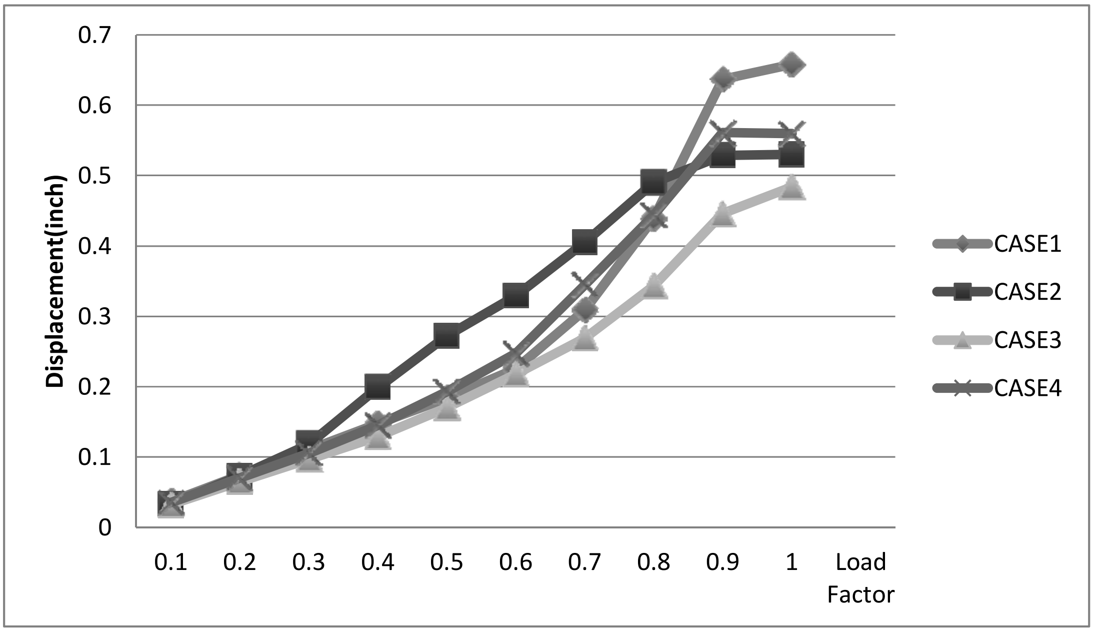

Figure 7: Significant deflections of a joint for four cases in three-story frame with flooring

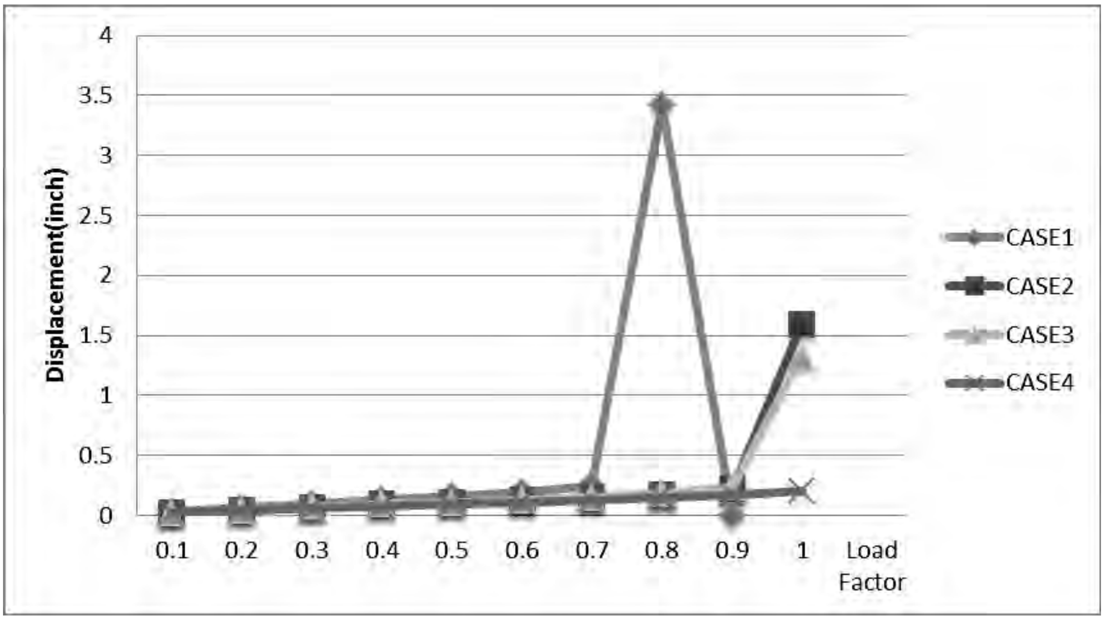

Figure 8: Significant deflections of a joint for four cases in six-story frame without flooring

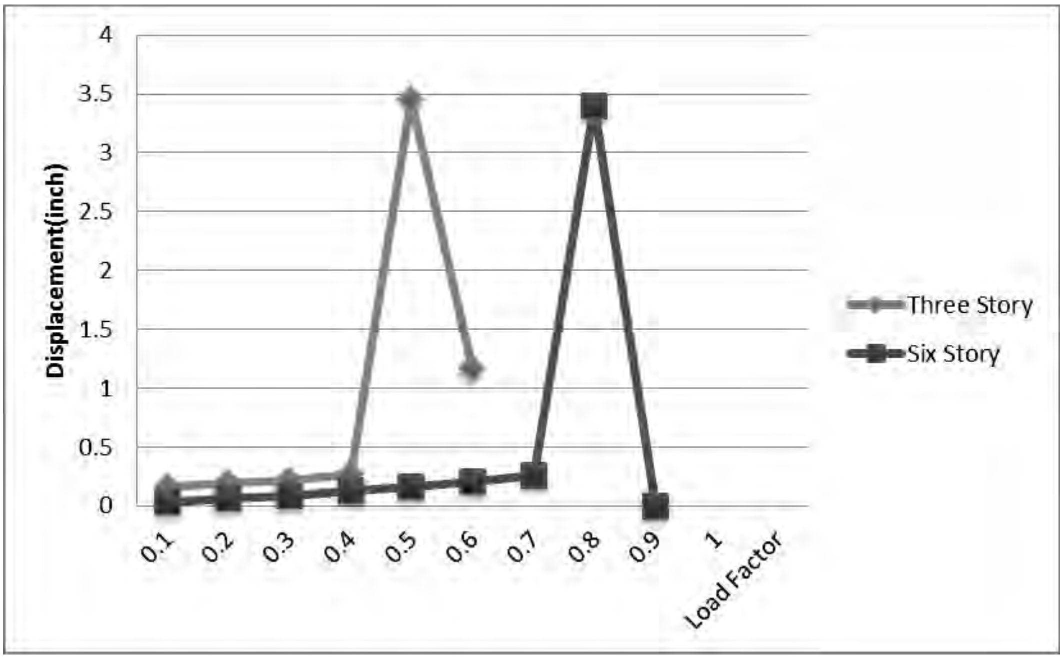

Figure 9: Comparison of significant deflections of a joint for only case (1) in three and six-story frames without flooring

3.2 Number of hinges

The numbers of hinges in each step of analysis for three-story frame without flooring and six-story frame without flooring are shown in Figure 10 and Figure 11. Only yield hinges are found in the analysis for all cases in three-story frame with flooring.

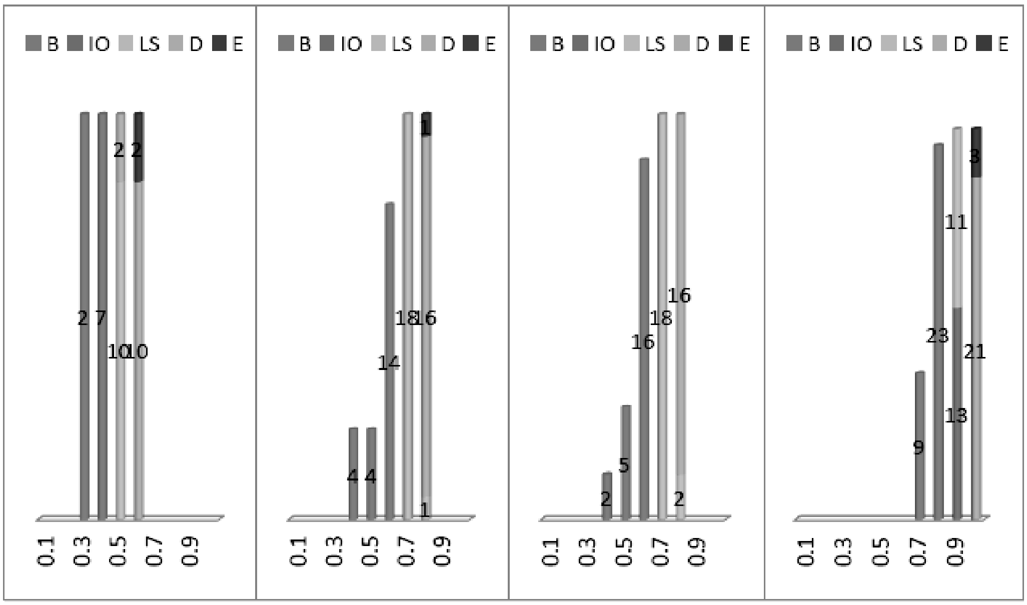

Figure 10: Number of hinges for three-story without flooring cases (1, 2, 3 & 4)

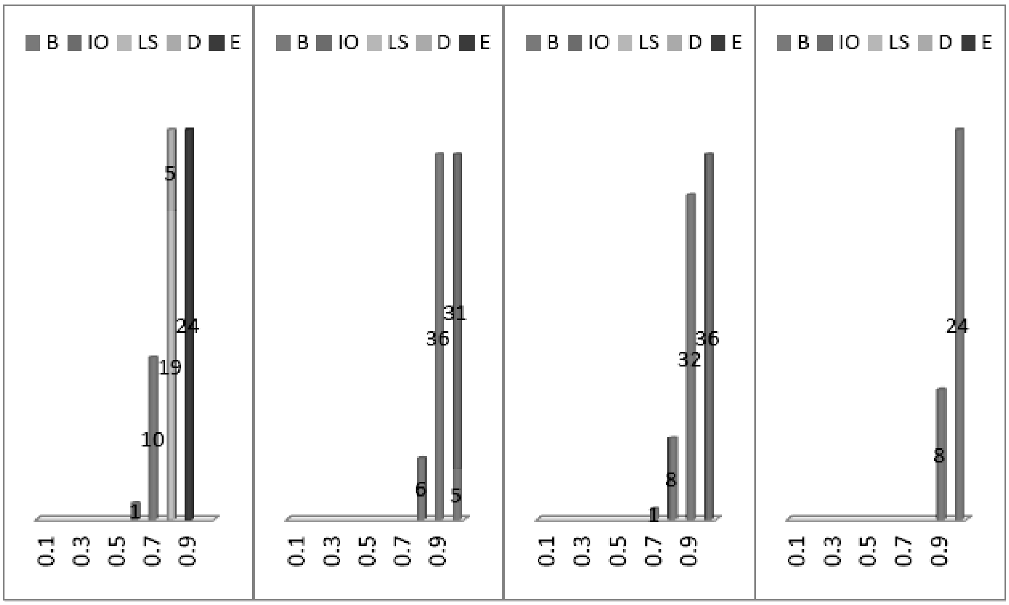

Figure 11: Number of hinges for six-story without flooring cases (1, 2, 3 & 4)

3.3 Discussion

In pushover analysis, the full load combination is applied as specified. The load combination is known and the structure is expected to be able to support the load in the elastic range and hence, force control is used in this progressive collapse analysis. Displacement control should be used for applying lateral load to the structure in considering earthquake, or for any case where the magnitude of the applied load is not known in advance, or when the structure can be expected to lose strength or become unstable. In the analysis with displacement control, pushover curve of monitored displacement and base shear of the global response of the structure can be obtained but not in the analysis with force control.

Ductile behavior of the frame is found in models with floor while non-ductile failure occurs in models without flooring. Although the amount of deflections are nearly same, the amount of load at which failure occurs are different for case (1) in three and six story frames without flooring. In the three story frame without floor, collapse hinges are found in half of the total load while nearly four fifth of the total load in the six story frame. Moreover, no collapse hinges are found in the cases except case (1) for six story frame without flooring.

4. CONCLUSION AND RECOMMENDATIONS

The corner column removal case is the most severe case among the three exterior columns considered and the second is the middle column removal in the short direction. There is a great difference in comparing frames with and without floor. Progressive collapse potential in frames with slab is much less than that without slab floor. Therefore, horizontal tie force and distribution of gravity load are important in considering progressive collapse of the frame. Moreover, the more the numbers of story, the less deflection values and progressive collapse potential of the reinforced concrete frames.

For further study, high-rise reinforced concrete frames with various widths to height ratios should also be analyzed and designed considering progressive collapse potential.

REFERENCES

Applied Technology Council ATC-40, *Seismic evaluation and retrofit of concrete building*, Volume 1, California 94065.

Federal Emergency Management Agency (FEMA), *Pre-standard and commentary for the seismic rehabilitation of buildings*, Building Seismic Safety Council, Washington, D.C.

Habibullahand, A., and Pyle, S., 1998. *Practical Three Dimensional Nonlinear Static Pushover Analysis*, Structure Magazine.

National Institute of Standards and Technology, Technology Administration, U.S. Department of Commerce, *Best practices for reducing the potential for progressive collapse in buildings*.

Nilson, A.H. and Winter, G., 1997. *Design of Concrete Structure*, 12th edition, McGraw Hill Co. Inc..

The U.S. General Services Administration, *Progressive Collapse Analysis and Design Guidelines for New Federal Office Buildings and Major Modernization Projects*, 2003.

Rajendra R. Joshi and Abhay A. Kulkarni, *Progressive Collapse Assessment of Structure*.

Sarosh H., Lodi Aslam, F., Khan, M. R. A., and SelimGunay, M., *A Practical Guide to Nonlinear Static Analysis of Reinforced Concrete Buildings with Masonry Infill Walls*.

Shankar Nair, R. *Progressive Collapse Basics*.

Experimental study on ordinary portland cement concrete replacement by using pozzolanic materials

Zar Phyu TUN
[1]Ph.D Student, Department of Civil Engineering, Yangon Technological University
zptmmn@gmail.com

ABSTRACT

This paper presents experimental study on ordinary Portland cement concrete replacement by using pozzolanic materials. Materials used in experiments are Hlaing river sand, Myan aung river stones, elephant cement, normal water and natural pozzolan from Pupa. In this paper, physical properties of cement, fine aggregate and coarse aggregate that are used in concrete mix design were tested. Specific gravity test, consistency test and setting time test of cement and compressive strength test of cement mortar were carried out. Then specific gravity test, unit weight test and seieve analysis tests were carried out for both fine and coarse aggregate. After that mix design for various proportion of conventional concrete were calculated according to ACI 211 and trial tests were made. Depending on compressive strength results, the appropriate concrete mix designs for conventional concrete were selected. Finally, pozzolanic materials were replaced by changing the percentage of cement content and select the mix proportion that gains target strength with the most cement replacement.

Keywords: compressive strength, pozzolanic materials, mix design, conventional concrete, cement replacement.

1. INTRODUCTION

When Portland cement is produced there is a significant amount of CO_2 emitted from the calcination of limestone. If the amount of CO_2 emitted can be reduced a system is considered to be “more green”. Less cement in concrete would make concrete “more green”. One method to reduce the amount of cement in concrete is to use a pozzolan (Dunstan, 2011). Pozzolan is a siliceous or siliceous and aluminous material that in itself possesses little or no cementitious value but that will, in finely divided from and in the presence of moisture, chemically react with calcium hydroxide (lime) at ordinary temperatures to form compounds having cementitious properties (ACI). Pozzolans are effective at lowering the mortar’s heat of hydration, which improve its workability and durability. They can also improve concrete and mortar resistance to both sulfate attack and alkali-silica reaction (ASR), which makes it beneficial to use in large concrete projects such as bridges and dams (Gibbons, 1997; Tsimas et al., 2005; Hossain and Mol, 2011), as well as in the restoration of historic and monumental masonry structures as a restoration mortar (Moropoulou et al., 1998).The results presented in this paper form part of an investigation of locally available natural pozzolanic material for the development of green concrete.

2. METHODOLOGY

2.1 Materials

Ordinary Portland Cement (OPC) complies with the requirements of the ASTM C 150 and the natural pozzolan used in this investigation was compared with the requirements of natural pozzolan (Class N) outlined in ASTM C 618. The chemical and physical properties of OPC and natural pozzolan are given in Table 1. Table 2 presents the comparison of local natural pozzolan with Class N of ASTM C 618. It can be seen that the total content of silicon, aluminum and iron oxides are 77.3, which is higher than the minimum requirement prescribed in ASTM C 618 of Class N. Sulfur trioxide and loss on ignition are much lower than the upper limit of ASTM. It is evident that the local natural pozzolan conforms with the requirements of ASTM C 618 and, hence, can be used as a partial replacement for the production of concrete. Grading limit of fine and coarse aggregates were in accordance with ASTM C33. Both the fine and coarse aggregates were air-dried before use. The water used in mixing looked clean and free from any visible impurities.

Table 1: Chemical and physical analysis of OPC and natural pozzolan

Chemical constituent	**OPC**	**Natural pozzolan**
SiO_2 (%)	23.58	52.39
Al_2O_3 (%)	4.35	16.49
Fe_2O_3 (%)	4.35	8.42
CaO (%)	63.21	10.65
MgO (%)	1.51	6.34
SO_3 (%)	1.28	0.34
Loss on ignition ((%)	0.97	2.26
Fineness- Blaine(cm^2/g)		3500-4100

Table 2: Comparison of local natural pozzolan with Class N of ASTM C 618

Description	**Composition (%)**	
	Local natural pozzolan	**Requirements as per ASTM for Class N**
Silicon dioxide (SiO_2), aluminum oxide (Al_2O_3) and iron oxide (Fe_2O_3)	77.3	Min. 70.00
Sulfur trioxide (SO_3)	0.34	Max. 4.00
Available alkalies	Nail	Max. 1.5
Loss on ignition ((%)	2.26	Max. 10.00

2.2 Test procedures

Mixing was done in revolving drum mixer in accordance with ASTM C192. Compressive strength was measured using 150mm cubes in accordance with BS 1881.

The slump test was carried out in accordance to ASTM C143. Demoulding was done after 24 hours and the specimens immersed in a curing tank to cure for strength gain. Curing improves both the physical and mechanical properties of concrete. The compressive strengths were determined by crushing concrete cubes at 3,7,14 and 28 days of curing. Before crushing, the concrete cubes were removed from the curing tank and placed in open air in the laboratory for about two hours. The results presented here are the average of three tests. Six different mixes were used for selecting the control mix of grade 35. The control mix was produced using OPC only as binder and then the natural pozzolan replacements were selected at 10%, 15%, 20%, 25% and 30% as a partial cement replacement by weight of cement content. The details of mix propotions are shown in Table 3and 4.

Table 3: Concrete mix details

	Cement (kg)	**Coarse aggregate (kg)**	**Fine aggregate (kg)**	**Water (kg)**
G35 I	11.63	22.38	12.57	4.5
G35 II	9.56	22.38	14.3	4.5
G35 III	9.21	22.38	17.73	3.6
G35 IV	8.78	22.38	17.84	4.4
G35 V	8.34	22.38	19.28	4.3
G35 VI	7.9	22.38	20.03	4.7

Table 4: Concrete mix details with pozzolan replacement

Percentage replacement (%)	**Cement (kg)**	**Pozzolan (kg)**	**Coarse Aggregate (kg)**	**Fine Aggregate (kg)**	**Water (kg)**
0	11.63	0	22.38	12.57	4.5
10	10.46	1.16	22.38	12.57	4.5
15	9.88	1.88	22.38	12.57	4.5
20	9.3	2.33	22.38	12.57	4.5
25	8.72	2.91	22.38	12.57	4.5
30	8.14	3.76	22.38	12.57	4.5
35	7.56	4.07	22.38	12.57	4.5

3. RESULTS AND DISCUSSION

3.1 Slump test and compressive strength of OPC concrete

The results of slump test are presented in Table 5. The variations of compressive strength of OPC are presented in Table 6 and Fig 1. According to slump test results, it falls within a range of 25mm and 100mm, specified by ACI. As shown in Figure 1, the maximum compressive strengths for 3-days (31.34 MPa), 14-days (39.42 MPa) and 28-days (43.09 MPa) can be seen at G35 I and maximum 7-days strength (32.78 MPa) can be seen at G35 II. According to ACI 318-11, the required cube compressive strength for

Grade 35 is 43 MPa and thus Grade 35 I was chosen as control mix for pozzolanic replacement.

Table 5: Slump test result of OPC concrete

	Grade					
	G35 I	G35 II	G35 III	G35 IV	G35 V	G35 VI
Slump (mm)	50	87.5	25	25	25	25

Table 6: Compressive strength of OPC concrete (MPa)

Age at testing	**G35 I**	**G35 II**	**G35 III**	**G35 IV**	**G35 V**	**G35 VI**
3-days	31.34	28.09	21.00	25.42	19.06	12.82
7-days	31.84	32.78	27.58	28.16	24.73	18.48
14-days	39.42	37.76	30.25	27.16	26.57	22.05
28-days	43.09	37.17	32.57	28.68	29.26	23.95

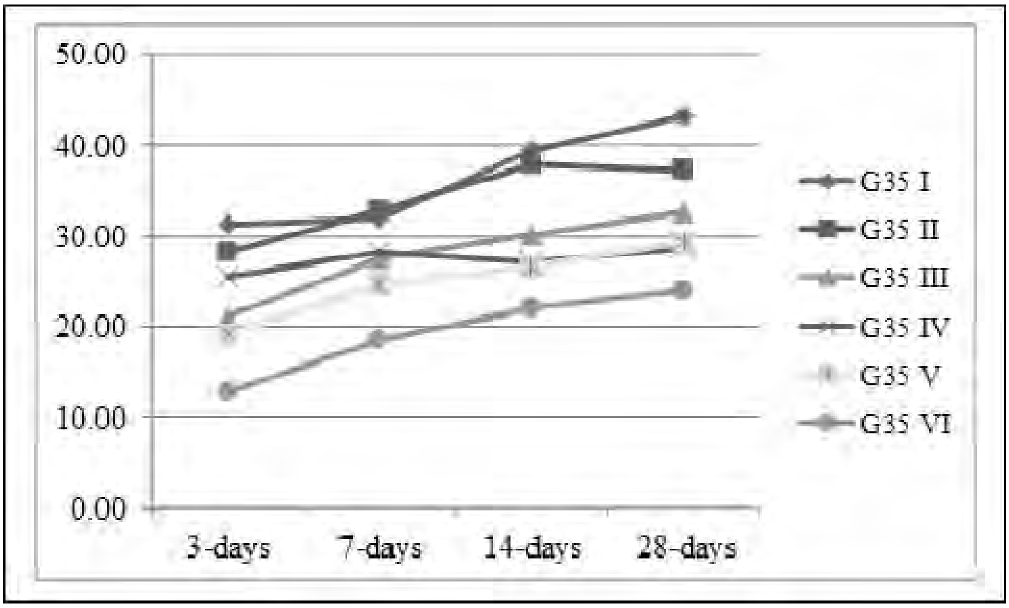

Figure 1: Variations of compressive strength of OPC

Table 5: Slump test result of pozzolan replacement concrete

	Percentage replacement (%)						
	0	**10**	**15**	**20**	**25**	**30**	**35**
Slump (mm)	50	43	40	38	34	33	30

From the results of Table 5, it can be seen when the replacement of pozzolan increases, the slump of concrete decreases. Since the quality of water remains the same for all mixes, the water demand increases with the pozzolan replacement increases and thus decreases the slump.

Table 6: Compressive strength of pozzolan replacement concrete (MPa)

Age at testing	**Percentage replacement (%)**					
	0	**10**	**15**	**20**	**25**	**30**
3-days	31.34	30.86	31.57	33.79	27.81	25.34

5. CONCLUSION AND RECOMMENDATIONS

The natural pozzolan conforms to the requirements of ASTM C618 and can be designated as class N. From this research, it can be seen as the replacement of pozzolan increases, the slump of concrete decreases.

REFERENCES

American Concrete Institute (ACI), 2010, Farmington Hills, Michigan.

Dunstan, E. R. Jr., 2011. How does pozzolanic reaction make concrete “Green”. *World of Coal Ash (WOCA)*, May 9-12, 2011 Denver, CO, USA.

Gibbons, P., 1997. Pozzolans for lime mortars, *The Conservation and Repair of Ecclesiastical Buildings*. Available online: http://www.buildingconservation.com/articles/pozzo/pozzo.htm.

Hossain, K. M. A., and Mol, L. 2011. Some engineering properties of stabilized clayey soils incorporating natural pozzolans and industrial wastes, *Construction and Building Materials* 25, 3495-3501, 2011.

Moropoulou, A., Maravelaki-Kalaitzaki, P., Borboudakis, M., Bakolas, A., Michailidis, P., and Chronopoulos, M., 1998. Historic mortars technologies in Crete and guidelines for compatible restoration mortars. *Journal of the European Study Group on Physical, Chemical, Biological and Mathematical Techniques Applied to Archaeology* 55, 55-72.

Tsimas, S., and Moutsatsou-Tsima, A., 2005. High-calcium fly ash as the fourth constituent in concrete: Problems, solutions and perspectives. *Cement and Concrete Composites* 27, 231-237, 2005.

International Center for Urban Safety Engineering
Institute of Industrial Science, The University of Tokyo
4-6-1 Komaba, Meguro-ku,
Tokyo 153-8505, Japan
Tel: +81-3-5452-6472
Fax: +81-3-5452-6476
http://icus.iis.u-tokyo.ac.jp
E-mail: icus@iis.u-tokyo.ac.jp

Myanmar International
Terminals Thilawa